



UK Atomic
Energy
Authority

UKAEA-R(18)004

February 2018

Michael Fleming
Jean-Christophe Sublet
Jiri Kopecky

Integro-Differential Verification and Validation, FISPACT-II & TENDL-2017 nuclear data libraries

“© COPYRIGHT UNITED KINGDOM ATOMIC ENERGY AUTHORITY 2018”

“This document is intended for publication in the open literature. It is made available on the understanding that it may not be further circulated. Extracts or references may not be published prior to publication of the original when applicable, or without the consent of the UKAEA Publications Officer.”

“Enquiries about Copyright and reproduction of this document should be addressed to UKAEA Publications Officer, UKAEA, Culham Science Centre, Abingdon, Oxon, OX14 3DB, U.K.”

Email: publicationsmanager@ukaea.uk

Integro-Differential Verification and Validation, FISPACT-II & TENDL-2017 nuclear data libraries

**Michael Fleming
Jean-Christophe Sublet¹
Jiri Kopecky²**

February 2018

UK Atomic Energy Authority
Culham Science Centre
Abingdon
Oxfordshire
OX14 3DB

¹ IAEA Nuclear Data Section
Vienna International Centre, A-1400 Vienna, Austria

² Juko Research
Kalmanstraat 4, 1817 HX Alkmaar, The Netherlands



Contact Dr Michael Fleming
UK Atomic Energy Authority
Culham Science Centre
Abingdon
Oxfordshire
OX14 3DB
United Kingdom

Telephone: +44 (0)1235-466884
email: michael.fleming@ukaea.uk
website: <http://fispact.ukaea.uk>

Disclaimer

Neither the authors nor the United Kingdom Atomic Energy Authority accept responsibility for consequences arising from any errors either in the present documentation or the FISPACT-II code, or for reliance upon the information contained in the data or its completeness or accuracy.

Acknowledgement

This work was funded by the RCUK Energy Programme under grant EP/P012450/1.

Special thanks are due to A. Koning and D. Rochman in building the TENDL libraries. The authors would like to gratefully acknowledge the work of M. Pillon, Y. Ikeda and F. Maekawa for their work and efforts in sharing the experimental data used in this report. We would like to thank R. A. Forrest, A. Klix, S. P. Simakov, P. Bém, M. Honusek and E. Šimečková for their previous validation work.

CCFE is the fusion research arm of the United Kingdom Atomic Energy Authority.

CCFE is certified to ISO 9001 and ISO 14001.

Executive Summary

Studies of the radioactive properties of nuclear devices, including future power stations, rely upon calculations of the neutron-induced activation-transmutation of materials. In order for trust to be placed in the results of such calculations it is necessary that the inventory code and the data libraries are verified and validated. This is done by comparing the predictions of the code system with activation measurements made on materials relevant to nuclear technology in well-characterised neutron fields. Cases where the ratio of results from Experiment (E) and Calculation (C) are close to 1 generally serve as validation of the code/data system, for the energy range covered.

A series of irradiations of various materials in several complementary neutron fields have been carried out over several decades. Analyses of the results have produced integrated effective cross-sections attributed to various nuclear interactions. Neutron spectra calculated for each experiment can be convolved over energy with library cross-sections for comparison with experimental results.

For the present validation exercise the latest version of FISPACT-II is used. Analysis of all experimental data enables effective cross sections to be calculated and these are presented in tabular form as well as plots of the C/E ratio. A graph showing the TENDL cross section as a function of neutron energy is plotted for each reaction, along with experimental data extracted from the EXFOR database. Using these graphs, an assessment can be made to determine if the reaction is validated or if re-evaluation of the TALYS parameters responsible for TENDL is required. These assessments will be used with other information to enable improvements to be made to future TENDL libraries.

FISPACT-II provides the functionality of an inventory code with full access to the TALYS-based Evaluated Nuclear Data Library (TENDL). It also retains legacy compatibility with the European Activation File (EAF). While several similar reports were published for the EAF library, it is no longer under development as TENDL provides a more robust methodology for building a more complete nuclear data file. This report provides more than an updated version of the previous integral validation reports; the TENDL library contains more complete, replicable total/pathway data, as well as variance and covariance data, all calculations have been performed using the new FISPACT-II code and every effort has been made to ensure that this document is as self-contained and reproducible as possible.

Contents

Contents	7
1 Introduction	8
2 Validation methodology	9
3 Integral data experiments	15
3.1 Japan Atomic Energy Agency data	15
3.2 Technische Universität Dresden data	17
3.3 Forschungszentrum Karlsruhe data	18
3.4 Frascati Neutron Generator data	18
3.5 Jülich Nuclear Physics Group data	23
3.6 National Physics Institute Řež data	23
3.7 Californium-252 spontaneous fission data	24
4 Code and libraries	30
5 Comparison of results	32
5.1 Boron	53
5.2 Nitrogen	54
5.3 Oxygen	56
5.4 Fluorine	57
5.5 Neon	59
5.6 Sodium	60
5.7 Magnesium	64
5.8 Aluminium	68
5.9 Silicon	72
5.10 Phosphorus	78
5.11 Sulfur	82
5.12 Chlorine	86
5.13 Argon	90
5.14 Potassium	91
5.15 Calcium	96
5.16 Scandium	102
5.17 Titanium	106
5.18 Vanadium	114
5.19 Chromium	120
5.20 Manganese	128
5.21 Iron	134
5.22 Cobalt	143
5.23 Nickel	152
5.24 Copper	164
5.25 Zinc	175
5.26 Gallium	183

5.27 Germanium	186
5.28 Arsenic	190
5.29 Selenium	195
5.30 Bromine	198
5.31 Rubidium	200
5.32 Strontium	202
5.33 Yttrium	208
5.34 Zirconium	215
5.35 Niobium	223
5.36 Molybdenum	234
5.37 Ruthenium	254
5.38 Rhodium	257
5.39 Palladium	262
5.40 Silver	266
5.41 Cadmium	270
5.42 Indium	273
5.43 Tin	283
5.44 Antimony	299
5.45 Tellurium	301
5.46 Iodine	303
5.47 Caesium	307
5.48 Barium	309
5.49 Lanthanum	318
5.50 Cerium	323
5.51 Praseodymium	326
5.52 Neodymium	328
5.53 Samarium	332
5.54 Gadolinium	337
5.55 Terbium	342
5.56 Dysprosium	346
5.57 Holmium	355
5.58 Erbium	360
5.59 Thulium	368
5.60 Ytterbium	369
5.61 Lutetium	373
5.62 Hafnium	377
5.63 Tantalum	386
5.64 Tungsten	398
5.65 Rhenium	415
5.66 Osmium	425
5.67 Iridium	426
5.68 Platinum	427
5.69 Gold	428
5.70 Mercury	439
5.71 Thallium	441

5.72 Lead	445
5.73 Bismuth	451
6 Discussion	457
References	470
A Pathway analysis	470
A.1 Technische Universität Dresden data	470
A.2 Forschungszentrum Karlsruhe data	478
A.3 Frascati Neutron Generator data	491
A.4 Japan Atomic Energy Agency data	502
A.5 Jülich Nuclear Physics Group data	509
A.6 National Physics Institute Řež data	510
B Actinide data	518

1 Introduction

Studies of nuclear technology rely on calculations of the activation-transmutation of materials arising from the operation of nuclear devices or plants that produce neutrons or other particles. Such calculations are then fed into studies of the operations, possible accident scenarios, exposure doses to plant workers and the eventual decommissioning of nuclear facilities. The calculations are performed using an inventory code which requires as input large amounts of nuclear data: neutron-induced cross sections for targets covering the whole periodic table, radioactive decay data such as half-lives and decay energies and the biological effects of radionuclides on humans. The requirement of completeness of the dataset forces library evaluators to draw from both models and experiments. Thus for some reactions the cross section has been well measured and the uncertainty is small (or simply acceptable), while for others there may be little or no experimental measurements and the data are based entirely upon model code calculations.

Legacy libraries have been built in a patchwork fashion, where periodic evaluations add or modify the data related to a subset of nuclides/reactions/applications. This has resulted in gradual improvement of the libraries which have matured over several decades, but can leave gaps for certain applications where missing data result in simulation inaccuracy. The TALYS code system is a collection of nuclear modelling software which is based on an entirely different methodology [1]. Instead of gradually adding new data and improving the data through periodic evaluations, TALYS takes a set of physical parameters and produces a complete library. In each year since 2008 a complete library version is published as the TALYS-based Evaluated Nuclear Data Library (TENDL) [2, 3]. The feedback from users and validation exercises directly informs the models and parameters which are responsible for the whole library, rather than an isolated nuclide.

In order for trust to be placed in the results of calculations, it is necessary that the inventory code and the data libraries are validated. By this it is meant that the predictions of the code system are compared with measurements made on materials relevant to nuclear technology in well-characterised neutron fields. The ratio between effective cross-sections that are determined from experiment (E) and calculation (C) give an indication of agreement. Due to uncertainties in the measurements and errors in the data libraries a range of C/E values is typically found for any one reaction, underlining the need for analysis of the experimental parameters and possible methods of error introduction. As a result, some abnormal C/E values may not be sufficient to convince evaluators to modify data and these will remain anomalous until additional data become available.

By considering a large range of materials it is possible to cover a wide range of reactions, although it must be noted that with the current facilities, which produce a relatively weak source of neutrons, it is only possible to validate reactions on stable or long-lived targets that give products with short to medium half-lives. Additionally,

the measurement of the effective cross-sections for specific reactions in mixed materials (such as steels and alloys) can be challenging due to competing reaction pathways, overlapping gamma energies or counting rates.

When differing experimental data of sufficient quality becomes available, validation reports are essential vehicles for informing evaluators of discrepancies. Appropriate cross section modifications can be made with confidence if integral results in several complementary neutron spectra are available and if adequate experimental differential data exist. An evaluator may either renormalise the cross section over the entire energy range to get a better fit to the measurements or renormalize over particular energy regions. With a technological library such as TENDL the process instead involves careful parameter modification to retain a consistent library. Improvement of data libraries is therefore an additional outcome of the validation process. Only when all available measurements on all relevant materials can be accurately reproduced by the calculations, can it be said that the library is validated. Until then new integral measurements will continue to be required to provide feedback and improve the quality of the nuclear data libraries.

The present validation report utilises the updated FISPACT-II code [4, 5]. Effective cross-sections are calculated through the collapse of experimental neutron spectra and compared with reference values. The Japanese Atomic Energy Agency (JAEA) Fusion Neutron Source (FNS) total decay heat experiments [6] have been completed re-analysed using TENDL-2017 and published in a companion validation report [7].

2 Validation methodology

The production of an activation library which satisfies the various incident-neutron energy and materials requirements of the fission and fusion energy communities has involved many nuclear data experts. The previous FISPACT-II versions relied upon the European Activation File (EAF), which was the subject, in its continually evolving form, of several integral validation efforts [8, 9, 10, 11]. Various contributors within the experimental and nuclear data communities provided comparisons between experimental and calculated heat or activity. By isolating a decay period where one nuclide dominating the measurement, the production of a specific radionuclide would be determined and the C/E ratio could be used to calculate the effective cross-section for the reaction responsible for that product. The experimental cross-sections published in the 2007 report [11] are used for our validation, except the values from the FNS experiments and FNG decay heat measurements.

This led to the development of a modern system for V&V, which covered not only the legacy EAF-format data, but the re-developed FISPACT-II code and its capability to handle international-standard ENDF-6 data formats, notably including TENDL-2014 [12]. The results showed that the TENDL library at that time [13] had already improved to the point of surpassing the EAF evaluation methodology.

The validation of TENDL-2017 with the measurements from the JAEA FNS experiments has been recently done in another CCFE report [7] and the results are included for this analysis. Note that the Jülich and spontaneous ^{252}Cf fission data are not based upon analysis done using FISPACT-II and are drawn directly from their sources.

A more recent set of validation reports using a similar methodology have been produced for FENDL-3.0/A and other major libraries [14, 15, 16]. These have introduced additional integral measurements from Maxwellian-averaged cross sections (MACS) and resonance integrals. These data are considered in a separate report [17].

Neutron spectra

The validation of nuclear data for exotic and/or high-energy threshold reactions (above 1 MeV) presents several challenges to both experimentalists and theorists. Fully characterising the neutron flux from a 14 MeV source down to thermal energies has been done with a host of complementary techniques, including stochastic/deterministic modelling, multi-foil activation and unfolding. Even with the most impressive experiments cited in this report, fluxes were calculated using Vitamin-J 175 or 211 group structures which possess a notoriously coarse thermal energy treatment¹. In many cases this may hide a poorly known low-energy flux and in some cases large variations in published flux bin values² explicitly indicate that the flux is not well-characterised enough for purposes such as this validation exercise. The following sections contain summaries of all the experimental campaigns whose integral data is cited. Every cut or modification of neutron flux data is made clear in the appropriate section.

For all fluxes, one consistent modification has been made in converting the data into the considerably finer CCFE 709 multi-group using the FISPACT-II convert module. The TENDL data used by FISPACT-II is processed into this multi-group and provides a more robust collapse calculation than with legacy multi-group structures. In order to deal with the one 1E-5 to 1E-1 Vitamin-J group, a physically realistic³ 1E-2 cutoff was made and the excluded neutron population was shifted into the collection of 1E-2 to 1E-1 bins. Unfortunately this must remain a constant, featureless thermal spectrum since there is no additional information available.

Multiple-pathway measurements

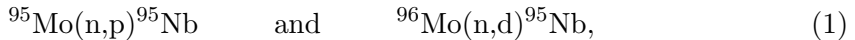
Integral data experiments often cannot extract data for a specific reaction rate due to the multiple reaction pathways which contribute to a specific nuclide production. This

¹Specifically, five bins below 1 eV with one bin for 1E-5 to 1E-1 eV. An experiment with poor knowledge of the thermal spectrum produces no trustworthy data for non-threshold reactions.

²Even fluxes with alternating zero and non-zero neutron populations per group in a course 175 structure.

³Of course a truly physical flux would depict the Maxwellian distribution, but this report will simply use the cutoff to prevent overestimation in reactions with large thermal cross-sections.

can be the result of multiple stable isotopes in a natural sample, isomer production and (potentially unknown) sample impurities, for example. Consider the reactions



which will both invariably contribute to any measurement of the product ^{95}Nb . Many elements possess multiple stable isotopes and mixed materials, such as steels and alloys, can have many reactions from multiple elements/isotopes leading to the same measured nuclide. When the incident neutron energies climb above the many thresholds in the 30–200 MeV range, a surprising number of multi-particle and spallation reactions become available. A previous EAF/EASY report [11] contained the reaction



which has no EXFOR entries [18]. The six nucleons contained within those two ejected particles can clearly be combined in other ways, such as (n,npa), and this represents one of numerous pathways. These reactions suffer from rarely possessing any experimental measurement and *near total absence* from the major nuclear data libraries⁴. In TENDL a separate MT=5 is used to store the total for ‘other’ 30+ MeV cross-sections whose product break-down is stored in the MF=10 ‘yield’ file. These contain the 30+ MeV continuation of other cross-sections, as well as a multitude of other reactions⁵. When using FISPACT-II, the total reaction is processed as (n,O).

For many product nuclides there exists a single pathway which dominates the production in a given experiment. In these cases the effective cross-section

$$\bar{\sigma} = \frac{\sum_g \phi_g \sigma_g}{\sum_g \phi_g}, \quad (3)$$

where group-wise summation over g is implied, can be calculated using FISPACT-II and directly compared with the corresponding experimental result. If there exists some set of pathways with non-negligible contribution to the production of that nuclide, it is not possible to isolate individual reactions without assumptions which would quite possibly invalidate the result. One significant advantage with TENDL is the use of physical parameters to guide where pathways exist, rather than a patchwork of experimental results. As indicated by the pathway tables in Appendix A, TENDL identifies a substantial number of higher-energy reactions which would otherwise be forgotten.

The identification of missing reactions using legacy libraries relies upon the *mos maiorum* philosophy, where data contained within old libraries becomes accepted and arguments must be made for its modification. This hides the weaknesses of the data being used and slows (or prevents) its improvement. It often also results in misconceptions about the quality of nuclear data amongst users. Without the capabilities

⁴In part due to energy cut-offs which fall below the thresholds. See Figure 13 for a summary of the reactions considered in this report.

⁵Note that the pathway breakdown **is not** included in this file, while TALYS **does** calculate each pathway. This is a deliberate choice in the structure of TENDL at 30 MeV.

of a code system such as TALYS, to produce high-energy libraries and validate them against experiments is achieved using the legacy approach where reactions are added and adjusted by hand. This has the advantage of being able to directly alter data to fit experiment, but ultimately results in the separation of data from physics. While nuclear data and nuclear physics are indeed not equivalent, nuclear data must be informed and shaped by nuclear physics to address current and next-generation problems.

The use of data taken from the measurement of a nuclide with multiple reaction pathways introduces several subtleties. While codes such as FISPACT-II will generate % pathway contributions from each possible reaction, the accuracy of this allocation depends entirely on the accuracy (and inclusion) of the cross-sections which are the subject of the validation. When attempting to validate cross-sections with legacy libraries, the *fundamentally incomplete* nature of their data prevents a trustworthy pathway analysis. The completeness of TENDL enables an allocation of reaction pathways which, although still dependent on the cross-sections, will consider each reaction whether or not an evaluator has decided to add data for it or not – completely eliminating this flaw.

An important distinction must be made for those integral values which are taken from experiments where the measured nuclide has multiple reaction pathways. While EXFOR datapoints are juxtaposed with the TENDL cross-sections, these are not directly related to the C/E integral values – even in the same energy region. This caveat is important for those EXFOR entries which are truly made without the contamination of multiple reactions and where integral values (often from steels or alloys) are made with non-negligible contributions from multiple nuclides/reactions. For cases where multiple isotopes contribute with different reactions or multiple reactions with the same target (such as the (n,d) and (n,np) reactions), the distinction between the integral and differential data may however not be very precise. The $^{96}\text{Mo}(\text{n,np})^{95m}\text{Nb}$ reaction serves as a good example, where the Q -values for it and $^{96}\text{Mo}(\text{n,d})^{95m}\text{Nb}$ are -9.30 and -7.07 MeV, respectively. The most recent (and impressively robust) paper outlining molybdenum cross sections below 20 MeV only includes a value for $^{96}\text{Mo}(\text{n,X})^{95m}\text{Nb}$ [19]⁶. An enriched sample was used to isolate those reactions from the stronger $^{95}\text{Mo}(\text{n,p})^{95m}\text{Nb}$, but a brief survey of the EXFOR entries for these reactions reveals considerable variation in the data and (more fundamentally) in the analysis of multiple reaction pathways. While molybdenum presents an especially challenging case for experimentalists, it is not difficult to find examples where EXFOR entries do not treat multi-reaction measurements with this level of rigour.

For the integral data, an experimentalist measures some quantity such as heat or activity and identifies a nuclide so that

$$M = \sum_i \lambda_i N_i \sigma_i q_i \phi = M \left(\sum_i f_i \right) \quad (4)$$

where M is the measured quantity, λ_i are decay constants N_i are nuclei fractions, σ_i are effective cross-sections, q_i are measured units per decay of that nuclide and ϕ is

⁶Although the EXFOR entry lists is as “Reaction : (n,np)”.

the scalar flux. Even when it is possible to isolate one nuclide, multiple paths with various σ_i are often present. If it is possible to calculate a ratio of M_C/M_E for one nuclide and only one path leads to the product, the effective cross-section ratio is simply $\sigma_C/\sigma_E = M_C/M_E$. Otherwise to obtain useful data an attempt to deconvolve the mix of errors from multiple pathways is required, where modification of cross-sections changes the path percentages. Often little or no experimental data exists for alternative paths, which could be the cause of discrepancies where the data might be in perfect agreement – or alternatively errors/omissions in other paths can hide bad data in a seemingly well-validated pathway. The need for higher-energy nuclear data drew several pioneers to build a library which would consider those necessary activation reactions whose experimental measurements are unfortunately contaminated by other competing reactions.

The nature of these experiments prevents them from providing an ideal validation, but the integral values can direct nuclear data analysts and experimentalists toward areas of poor understanding. Consider the three nuclide measurements made at FNG whose reaction pathways are summarised in Table 1.

Table 1: Some FNG nuclide measurements which have multiple pathways for production.

Product	Pathway(s)	%
Ta182	W182(n,p)Ta182	49.4
	W182(n,p)Ta182m(IT)Ta182	41.3
	W182(n,p)Ta182n(IT)Ta182m(IT)Ta182	3.7
	W183(n,d)Ta182	1.8
Sc47	Ti47(n,p)Sc47	41.2
	Ti48(n,np)Sc47	25.9
	Ti48(n,d)Sc47	18.1
	V50(n,a)Sc47	9.7
	V51(n,na)Sc47	5.4
In117	Sn117(n,p)In117	87.9
	Sn117(n,p)In117m(IT)In117	1.5
	Sn118(n,np)In117	6.9
	Sn118(n,d)In117	3.1
	Sn120(n,a)Cd117m(b-)In117	0.9

The FISPACT-II simulation of a tungsten foil irradiation shows that ^{182}Ta was produced almost exclusively through the (n,p) on ^{182}W . There is reasonable confidence that whatever uncertainty exists in the (n,d), its contribution will be less than the TENDL-2017 uncertainty for the dominant reaction and this measurement can be used to validate it. The break-down of isomer production, though impressive, is not as certain. Different branching ratios could lead to the same overall result and the

$^{182}\text{W}(\text{n},\text{p})^{182g}\text{Ta}$, say, could not be validated by this measurement.

Useful information from the the ^{47}Sc measurement of a vanadium alloy irradiation is much more difficult to obtain. Four different target nuclides have reaction which produce ^{47}Sc and two reactions have little or no differential data in EXFOR. Since several reactions contribute relatively large fractions to the total ^{47}Sc production, whatever errors they may possess can substantially alter the overall C/E. This integral value cannot be reasonably associated with one reaction without making assumptions about several reaction rates which are more profound than any single-reaction integral data. In scenarios such as this one, no detailed integral validation information can be obtained.

The ^{117}In example is more subtle and need not be dismissed as readily as the ^{47}Sc . The total (n,p) reaction comprises nearly 90% of the nuclide production while the ($\text{n},\text{np+d}$) and (n,a) reactions⁷ both possess EXFOR entries which broadly match the TENDL-2017 cross sections. This agreement with (at least) some experimental data for secondary pathways provides confidence that errors in those reactions are small enough to allow the main reaction to be considered dominant. This report includes the integral cross section for the $^{117}\text{Sn}(\text{n},\text{p})^{117}\text{In}$ from this experiment.

Instead of modifying reactions with competing pathways to the same nuclide, this report takes the most natural estimator for the cross-section ratio:

$$\sigma_i^E = \frac{M_E}{M_C} \sigma_i^C \quad \forall i. \quad (5)$$

This does not account for all of the deviation in nuclide production for mixed-pathway cases in the one reaction considered, but it is the most physically justifiable assumption. Put another way, associating the over(under)-estimation of secondary paths with the primary path and further increasing(decreasing) the primary cross-section may appear more ‘honest’ regarding the total C/E value, but it does not correctly indicate how cross-sections should be modified to better represent the true physical values. If hand-modification of a legacy library was the objective, the previous assumption could be appropriate and mis-allocation of some contribution from a secondary reaction to a primary reaction can still result in more accurate calculations⁸. Isolation of a pathway to ‘improve’ performance at the cost of faithfulness to the underlying physics is an anathema of the TENDL methodology.

As indicated by the examples provided, only strongly dominant reaction pathways are considered. Whenever an individual secondary reaction produces more than 10% of the product nuclide, the differential data has been checked to determine if uncertainty the (supposedly) minor contribution prevents trustworthy use of the dominant reaction

⁷Note that the modern EXFOR source [20] identifies the $^{118}\text{Sn}(\text{n},\text{X})^{117}\text{In}$, which the TENDL-2017 sum of np+d agrees with.

⁸Of course this will always be limited to some specific regime(s), whereas correct modification of physical parameters improves the library *globally*.

for a validation. Very few reactions with less than 90% are included and exclusively where agreement between TENDL and the differential experiments of minor pathways provides the necessary assurance that the uncertainties in those paths are much less than the uncertainty in the dominant.

3 Integral data experiments

Each of the following subsections contain cursory descriptions of all the experimental measurements used in this validation report, divided into the working groups which produced the data. The JAEA FNS data has been completely re-analysed using FISPACT-II with TENDL-2017 and the corresponding section describes the methods employed. The ENEA FNG total heat measurements have also been re-analysed with TENDL-2017 using the same technique, but with separate comparisons for gamma and beta measurements. For the remaining experimental groups, experimental cross-sections are taken from the previous EASY/EAF reports and only an experimental description is provided. The ^{252}Cf and Jülich cross-sections are taken directly from publications. Since experimentalists cannot measure cross-sections directly but rely upon codes and nuclear data libraries to calculate the cross-sections from their results, these data are not as reliable as those produced by the complete analysis done for FNS. Whenever a modification was made to the flux or data in any experiment, comments on it are provided in the corresponding section. Pathway analysis for all but the spontaneous fission of ^{252}Cf and Jülich data are provided in Appendix A.

3.1 Japan Atomic Energy Agency data

A series of experiments were performed by the Japan Atomic Energy Agency (JAEA) using the Fusion Neutron Source (FNS) facility [21, 22, 23, 24, 25], where materials samples were irradiated in a simulated D-T field. The resulting decay power was measured for cooling times of up to thirteen months using the highly sensitive Whole Energy Absorption Spectrometer (WEAS) method, which measures both β and γ emission decay energies. These measurements were made at selected cooling times including, quite impressively, a few tens of seconds after irradiation.

A 2mA deuteron beam was fired on a tritiated titanium target. The resulting neutrons produced a flux of approximately $1\text{E}10 \text{ n cm}^{-2} \text{ s}^{-1}$ at the sample location. The irradiation periods at the FNS were 5 minutes and 7 hours with different sample locations for each irradiation duration. The neutron spectrum for the 5 minute irradiations (fns_5min) is shown in Figure 7(c) and the spectrum for the 7 hour irradiation (fns_7hour) in Figure 7(d).

The flux from position 7 in the 7 hour irradiation possessed a zero flux value between 0.1-1 eV with a non-zero value in the <0.1 eV group. This unphysical result indicates

that the low energy flux is not accurately characterised and for this report the flux was cut at 1 eV.

The full and more detailed analysis of these experiments has been published in another report using the FISPACT-II system with TENDL [7]. In that report, the total measured heat and calculated heat were compared over the period of decay heat measurements. By comparing the two at a time-period where the heat from a specific product is dominant, a C/E value can be obtained for the reaction(s) which produce that nuclide. The data for a 5 minute irradiation of Inconel-600 is shown in Figure 1, where TENDL-2017, ENDF/B-VIII.0, JENDL-4.0u+DDF15, JEFF-3.3 and JEFF-3.3 are each compared. The dominant nuclides are shown with their relative contribution in the TENDL-2017 result. From this analysis, where the heat is almost entirely from one radionuclide we consider it a test of the cross section for its production.

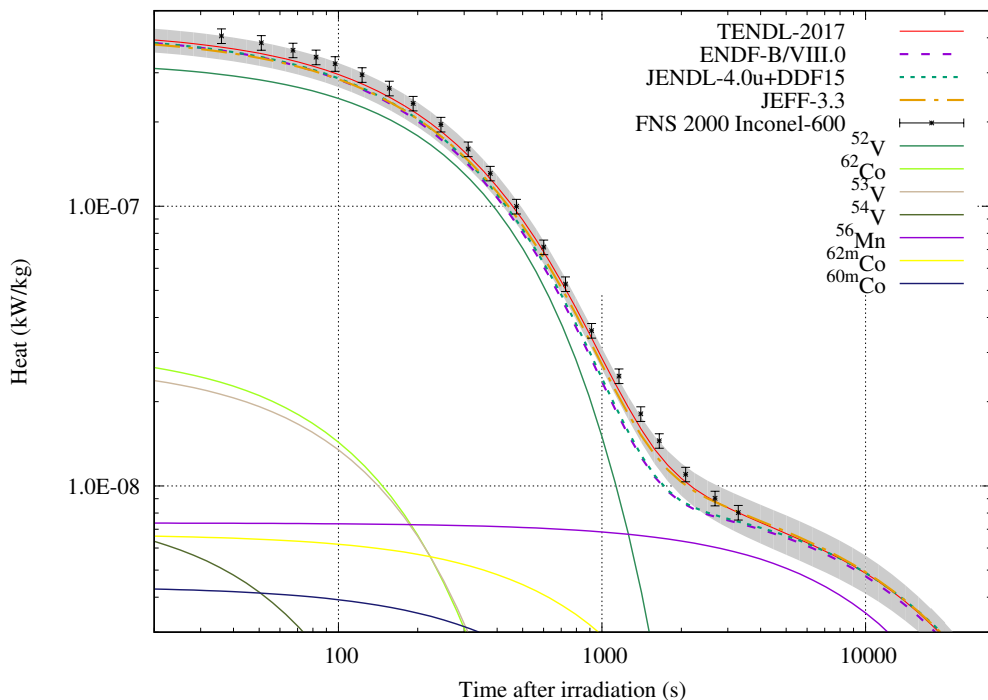


Figure 1: Total decay simulation for an FNS 5 minute irradiation of Inconel-600, with experimental results compared against calculated solutions using FISPACT-II with different nuclear data libraries. The grey band represents uncertainty from TENDL-2017. Individual radionuclide contributions are shown for those that are dominant in the time-periods that were measured.

The ^{52}V and ^{56}Mn nuclides can be isolated from the measurements of this experiment⁹ since they are the dominant nuclides for heat production at particular measurements.

⁹The nuclide contribution graphs with all isotopes in the full report [7] make these distinctions clear.

In this Inconel example, the ^{52}V C/E is taken from comparison with the measurement closest to its half-life, where it contributes over 90% of the total heat output. The C/E is determined by comparing the measured and calculated heat at the data point nearest to the half-life of the nuclide in question. A summary of the products, their half-lives, the pathways for production and uncertainty from the experiment have been drawn directly from the decay heat validation, while the pathway breakdowns for these reactions are summarised in Tables 54 and 55 of the appendix.

3.2 Technische Universität Dresden data

Experiments were carried out by the Technische Universität Dresden (TUD) group in collaboration with RRC KI Moscow and CCA Sergiev Posad using the high-intensity neutron generator SNEG-13 [26]. Neutrons were generated by 280 keV deuteron bombardment on a rotating tritiated titanium target. Neutrons emitted at angles of 4° and 73° were used to irradiate samples. Note that the ‘peak fusion spectra’ made available for calculations does not include the energy regions below 10 MeV, as seen in the flux spectra of figures 7(f) and 8(a). Although measurements were recorded for products made with non-negligible thermal/intermediate reaction pathways, reliable calculations cannot be performed without accurate lower-energy flux data. The measurements from the irradiation of vanadium alloy samples V3Ti1Si, V4Ti4Cr and V5Ti2Cr are available in [27, 28].

Steel samples of SS-316, Eurofer-97 and F82H were irradiated with the same SNEG-13 setup. The original data can be found in [27, 29]. Ceramic samples of LiSO₄ and SiC were also irradiated using SNEG-13. The original data can be found in [30, 31]. Tungsten samples were irradiated using SNEG-13 with limited measurements made in the 77° position. The original data is available in [32]. Note that the SNEG-13 flux was not determined outside the 14 MeV D-T peak and there has been no modification in this report.

Following the collaboration with SNEG-13, a new D-T neutron generator was built in the early 2000s which operated with 10 mA 300 keV deuterium bombardment of tritiated targets. The target could be fixed or rotated and the generator could be operated in sustained or pulsed modes. A full neutron spectrum for each separate irradiation was provided based on neutronics simulations and standard foil calibrations. A copper alloy CuCrZr was irradiated with a neutron spectrum (tud_cucrzr) given in Figure 8(b) and the original data can be found in [33]. This neutron spectrum was already cut at 10 eV and no modification was made in this report.

Later experiments at TUD irradiated yttrium, tantalum and lead. Each of these has a unique neutron spectrum (tud_Y, tud_Ta and tud_Pb), shown in figures 8(f), 8(e) and 8(d), respectively. The original data can be found in [34, 35, 36]. Erbium and lanthanum measurements were subsequently carried out [37, 38, 39] with one spectrum (tud_Er), shown in Figure 8(c), used for all calculations. All of these spectra were produced without knowledge of the thermal neutron flux, as indicated by the sharp

drop in the last energy group. They have therefore been cut at 1E-1 eV.

3.3 Forschungszentrum Karlsruhe data

Experiments carried out by the group at Forschungszentrum Karlsruhe (FZK) used a 19 MeV deuteron beam of the Karlsruhe isochronous cyclotron for a deuteron-beryllium neutron source. This produced a neutron flux of up to $3\text{E}11 \text{ cm}^{-2}\text{s}^{-1}$ over a 1 cm^2 target sample. The spectra produced in these experiments do not show any strong peak and extends to energies beyond 20 MeV, leading to the name ‘white fast-neutron spectrum’. The neutron spectra were calculated using neutronics simulations and foil activation calibrations, but required nuclear data above 20 MeV, introducing complexities for the analysis based on FENDL2.0/A [40]. In total, two separate spectra (fzk_1 and fzk_2) were determined for different experimental campaigns which irradiated numerous samples, as shown in figures 4(a) and 4(b). Steel and vanadium alloy irradiations of V3Ti1Si, V5Ti2Cr and Eurofer-97 were done in [41].

A collection of elemental samples were irradiated including copper and nickel. Two separate tungsten experiments were performed with different measurement diagnostics [41]. A lithium orthosilicate sample was irradiated in the same d-Be setup. The original data is available in [41].

A separate experimental facility at FZK using a d-Li neutron source [42, 43, 44] – similar to that proposed for IFMIF, but with much lower intensity – was used for activation of steels and vanadium alloys. The spectrum (fzk_ss316) is shown in Figure 4(c). The source consists of a 40 MeV beam of deuterons incident on a thick lithium target (22 mm thickness enclosed in a stainless steel case). Although a $3 \mu\text{A}$ beam of 52 MeV deuterons was used, the approximate energy of the deuterons on entering the lithium was 40 MeV. The neutron flux was about $4.3\text{E}-9 \text{ cm}^{-2}\text{s}^{-1}$.

All of these experiments aimed to probe high-energy reactions, ostensibly in preparation for proposed material irradiation facilities. The fluxes of both d-Be and d-Li experiments were not well-characterised in the <10 eV range, where the peak populations were some 10^{-6} of the peak. The flux was cut at 10 eV with $<1\%$ change on all reactions, including the $^{186}\text{W}(\text{n},\gamma)$.

3.4 Frascati Neutron Generator data

Experiments carried out at the Ente Nazionale per l’Energia Atomica (ENEA)¹⁰ Frascati Neutron Generator (FNG) group used a neutron reflector to form an irradiation cavity where the neutron spectrum mimics that of a first wall in a typical fusion reactor. Samples could be irradiated at several distances from the approximately 14 MeV

¹⁰This is the original name given in 1982 for the agency now known as the *Agenzia nazionale per le nuove tecnologie, l’energia e lo sviluppo economico sostenibile*.

neutron source, enclosed within the cavity. The perspex/polyethylene neutron reflector was attached to a mock-up of the ITER inboard shielding. The neutron spectrum was determined through neutronics calculations with multi-foil activation and unfolding.

Vanadium alloy measurements of V4Cr4Ti were carried out in [45] using the spectrum (fng_vanad) shown in Figure 6(c). Steel results for F82H and Eurofer-97 are available in [46, 47, 48]. The spectra for these (fng_f82h and fng_eurofer) are shown in figures 5(c) and 5(b).

Measurements from silicon carbide irradiations were presented in [49, 50]. The spectrum for these irradiations (fng_SiC) is shown in Figure 7(a).

A collection of elemental foils including tungsten, chromium, hafnium, niobium, copper and iron were irradiated in [51, 52, 53, 49]. The various spectra are generally listed by sample (fng_tung, fng_Cr, fng_hafnium), which are shown in figures 6(d), 4(e) and 5(d). Note that the Nb, Cu and Fe data appear in the SiC reference, using the same fng_SiC spectrum.

Measurements of the activation products of a CuCrZr alloy are available in [54]. The spectrum (fng_cucrzs) is shown in Figure 4(f).

A new detector at FNG [55] with capabilities to distinguish between gamma and beta heat contributions was used to collect data for a collection of materials. A set of foils including Al, Cd, Cu, Hf, Mg, Mo, Nb, Ni, Pb, Re, Sn, Ti, W and Zr were irradiated with the fng_heat spectrum shown in Figure 6(f). Since total heat, rather than identifiable spectroscopic peaks, was measured in these experiments the analysis is particularly sensitive to modifications in nuclear data. All of these measurements have been re-analysed using FISPACT-II with TENDL-2017. For any nuclide that was responsible for the majority of the heat (in simulation) for any of the measurement times, the point which is strongest is compared with the experimental result to give a C/E value. An example of one experiment is given in Figure 2, which shows the decay heat from irradiation of a nickel sample.

The simulation includes many nuclides which contribute to the total decay power, but at any given time one nuclide may contribute the vast majority. For example, ^{62}Co is strongly dominant before 200 s and the first measurement is dominated by this nuclide. The break-down of emitted particles responsible for decay heat allows for identification of dominant nuclides in the subsequent measurements, where the stronger ^{62m}Co γ -decay and ^{60m}Co β -decay can be distinguished from each other. Focusing on the measurements taken, as in Figure 3, the determination of C/E from this experiment is based on the measurements which most isolate each nuclide and respect the known decay half-lives of the nuclides.

Since the ^{62}Co is both a dominant gamma and beta emitter, the total decay heat from the first measurement is used for comparison. The ^{62m}Co comparison is derived from the the point where it most dominates gamma heat, in this case the fourth measurement. The ^{60m}Co most strongly dominants beta heat in the third measurement, which

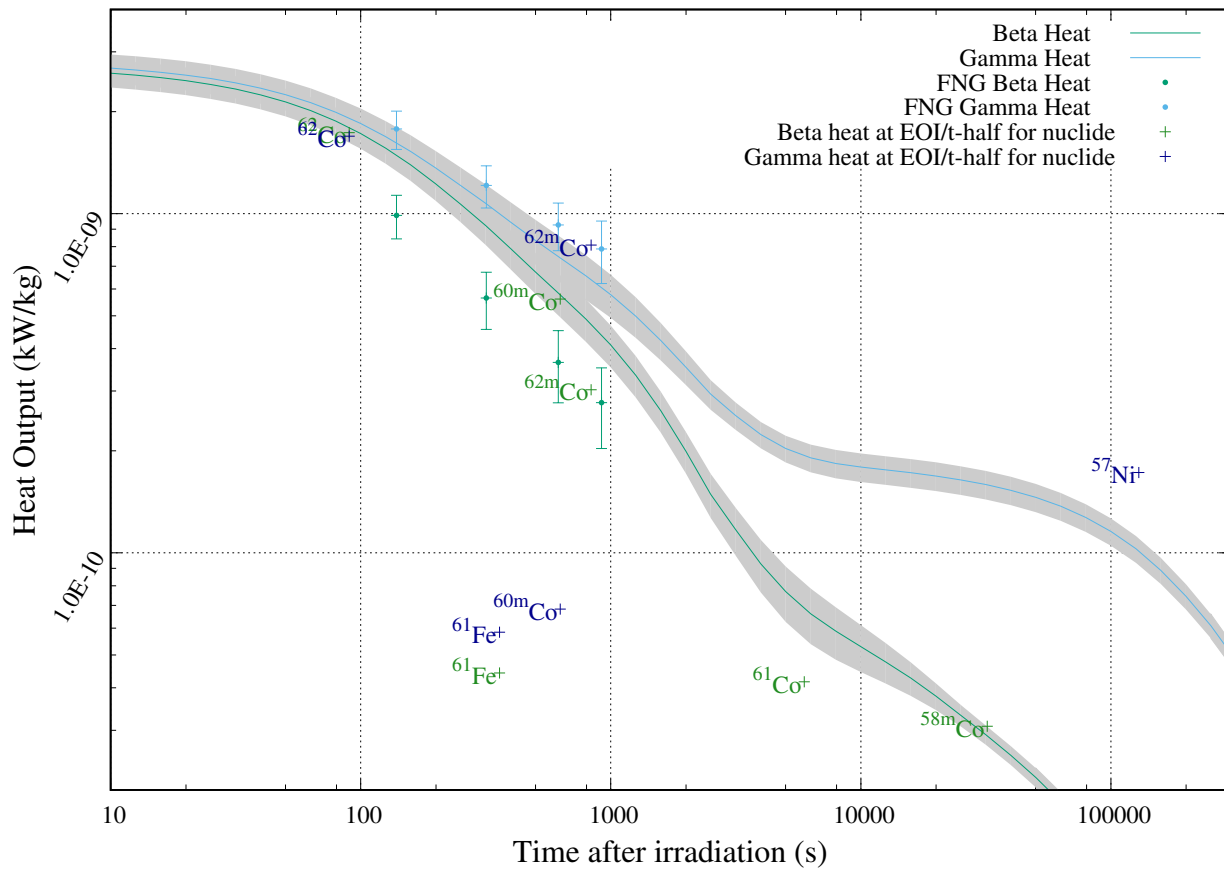


Figure 2: Total beta and gamma heat from irradiation of a nickel sample at FNG against FISPACT-II simulation with TENDL-2017. The grey band represents uncertainty from TENDL-2017. Nuclides are listed at (x,y) positions which are their initial heat at EOI and half-life.

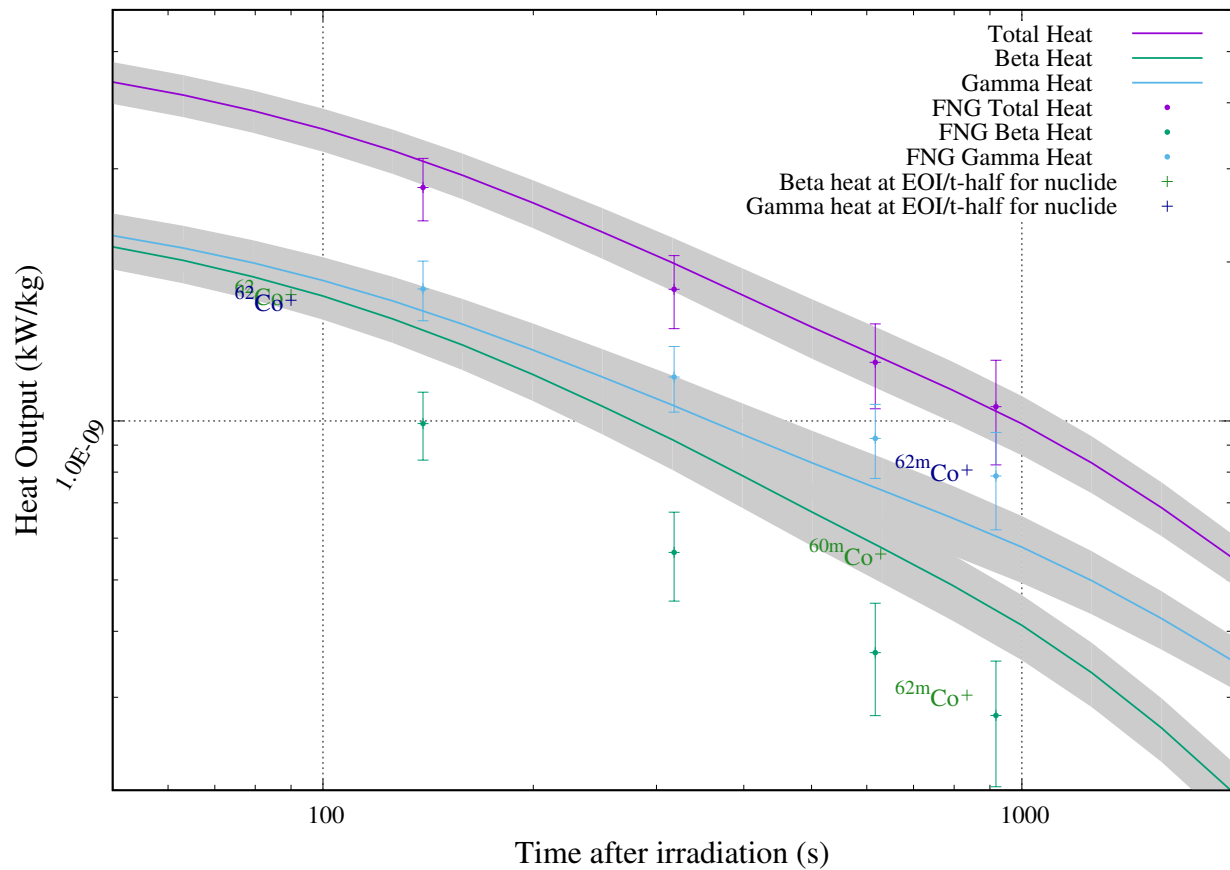


Figure 3: Total heat and beta/gamma contributions from irradiation of a nickel sample at FNG against FISPACT-II simulation with TENDL-2017.

is used as the C/E.

New analysis has been performed with all of the heat measurements at FNG using the original experimental data kindly given by the primary experimentalist, M. Pillon. Several new product nuclides have been unearthed in the reanalysis and a few spurious allocations have been eliminated¹¹. A complete summary of the C/E values and the resulting experimental effective cross sections, as well as the spectroscopic heat measurement types, is included in Table 2.

Table 2: FNG heat measurements extracted from analysis using TENDL-2014 [12] in order to determine effective cross sections that are used in the current TENDL-2017 analysis.

Reaction	$\sigma_{exp}(b)$	$\Delta\sigma_{exp}(b)$	Spec.
Mg-24(n,p)Na-24	1.98E-01	1.01E-02	total
Mg-25(n,p)Na-25	7.17E-02	2.01E-03	beta
Al-27(n,p)Mg-27	7.24E-02	1.16E-03	total
Al-27(n,a)Na-24	1.00E-01	2.10E-03	gamma
Ti-48(n,p)Sc-48	1.06E-01	6.15E-03	gamma
Ti-49(n,p)Sc-49	3.97E-02	2.22E-03	beta
Ti-50(n,p)Sc-50	1.86E-02	5.88E-04	total
Ni-60(n,p)Co-60	4.38E-02	2.36E-03	beta
Ni-62(n,p)Co-62	2.15E-02	6.53E-04	total
Ni-62(n,p)Co-62m	2.33E-02	8.39E-04	gamma
Cu-63(n,2n)Cu-62	5.60E-01	5.72E-02	total
Zr-90(n,2n)Zr-89m	1.48E-01	8.61E-02	gamma
Zr-94(n,p)Y-94	8.06E-03	1.20E-03	beta
Mo-92(n,2n)Mo-91	2.76E-01	7.16E-03	total
Nb-93(n,a)Y-90	1.35E-02	3.28E-03	beta
Nb-93(n,2n)Nb-92m	2.53E-03	3.18E-04	gamma
Ag-107(n,2n)Ag-106	9.67E-01	2.51E-02	total
Ag-109(n,2n)Ag-108	9.61E-01	2.50E-02	beta
Cd-112(n,2n)Cd-111m	7.03E-01	2.64E-02	total
Sn-124(n,2n)Sn-123m	5.84E-01	2.51E-02	beta
Hf-180(n,n)Hf-180m	4.41E-02	2.42E-03	gamma
Hf-180(n,p)Lu-180	3.79E-03	3.00E-04	gamma
Re-185(n,2n)Re-184	2.58E+00	2.17E-01	gamma
W-186(n,2n)W-185	5.64E-01	9.35E-02	total
W-186(n,p)Re-186	2.86E-03	1.48E-04	total
Re-187(n,2n)Re-186	9.54E-01	5.25E-02	beta
Pb-204(n,n)Pb-204m	8.15E-02	3.83E-03	gamma

¹¹Every supposedly dominant nuclide from previous analysis has been identified in this work, but the more trustworthy reaction set given by TENDL-2017 provides better allocation of heat output from a complete set of product nuclides.

Separate elemental foils of scandium, samarium and dysprosium were irradiated with a different spectrum (fng_Dy) shown in Figure 5(a). The original data can be found in [56, 57, 58].

Measurements from the irradiation of yttrium, molybdenum, tantalum, rhenium and tin were made in [59, 60, 61, 62, 63, 64]. Each of these use an individual neutron spectrum labelled by fng_X where X is the element. The various spectra are shown in figures 6(e), 5(e), 6(b), 5(f) and 6(a), respectively. No FNG fluxes were modified.

3.5 Jülich Nuclear Physics Group data

The importance of integral data in spectra extending above 20 MeV led the authors of previous reports to perform literature search for historical measurements that could be used for validation. A series of papers from the group in Jülich led by Qaim [65, 66, 67, 68, 69, 70, 71, 72, 73, 74, 75, 76] has been used. A d-Be neutron spectrum was derived based on the work of Schweimer [77] and Meuldres et al. [78]. The data were fitted to the analytic function

$$\phi(E) = C(BE_d)^{-1/2}(1+y^2)^{-3/2} \quad (6)$$

$$y = \frac{E - E_d}{\sqrt{BE_d}(2 + E_s)} \quad (7)$$

where E is the incident neutron energy, E_d is the deuteron energy, B is the binding energy and C is a normalisation constant. This was then converted into the 211-group VITAMIN-J+ structure. A spectrum derived from Equation (6) was used for calculations, as shown in Figure 4(d). Three campaigns with separate flux magnitudes are referenced throughout as d-Be, d-Be2a and d-Be3.

3.6 National Physics Institute Řež data

Experiments at the National Physics Institute (NPI) Řež used a 37 MeV proton beam driven by the NPI cyclotron to strike a flowing D₂O target [79]. The resulting p-D₂O spectrum was calculated using the Los Alamos high energy proton data library LA-150h with MCNPX and compared with scintillation detector measurements and standard aluminium foil measurements. Considerable effort was taken to characterise the spectrum in detail. Note that this spectrum extends in energy above 20 MeV and is therefore very important in the validation of libraries such as TENDL. The initial version of the Řež spectrum¹² was recognised as incorrect as it was measured at a large distance from the sample and so was not really representative of the spectrum in the sample. Following considerable efforts a new spectrum (rez_DF) was produced [80]

¹²Found as Figure 12 of [11] and referred to as rez_NE.

and this is shown in Figure 7(e). In the initial attempts to characterise the spectrum several elemental foils were placed at a variety of positions 37-67 mm from the source and γ measurements with high-purity Ge detectors were made [81]. Note that the $^{27}\text{Al}(\text{n}, \alpha)^{24}\text{Na}$, $^{209}\text{Bi}(\text{n}, 4\text{n})^{206}\text{Bi}$ and $^{209}\text{Bi}(\text{n}, 3\text{n})^{207}\text{Bi}$ reactions are based on averages of several measurements.

Results from irradiation of Eurofer-97 measurements were made in [82]. Three separate tungsten samples were irradiated in [83] and averaged data is used for the analysis in this report. A tantalum sample was irradiated in [84]. Two separate irradiation periods of 11.3 and 89.2 minutes were used with chromium samples in [85, 86].

Note that the rez_DF neutron spectrum presented in previous reports still contained unphysical variation of several orders of magnitude below 1 keV, as well as alternating bins with zero and non-zero neutron populations. This flux was cut below 1 keV, where the large statistical variations appear.

3.7 Californium-252 spontaneous fission data

Measurements using the spontaneous fission of ^{252}Cf as a neutron source have been extracted from EXFOR and analysed with the spectrum evaluated by Mannhart [87], as shown in Figure 9(a). Note that this neutron spectrum is cut at 14.454 keV.

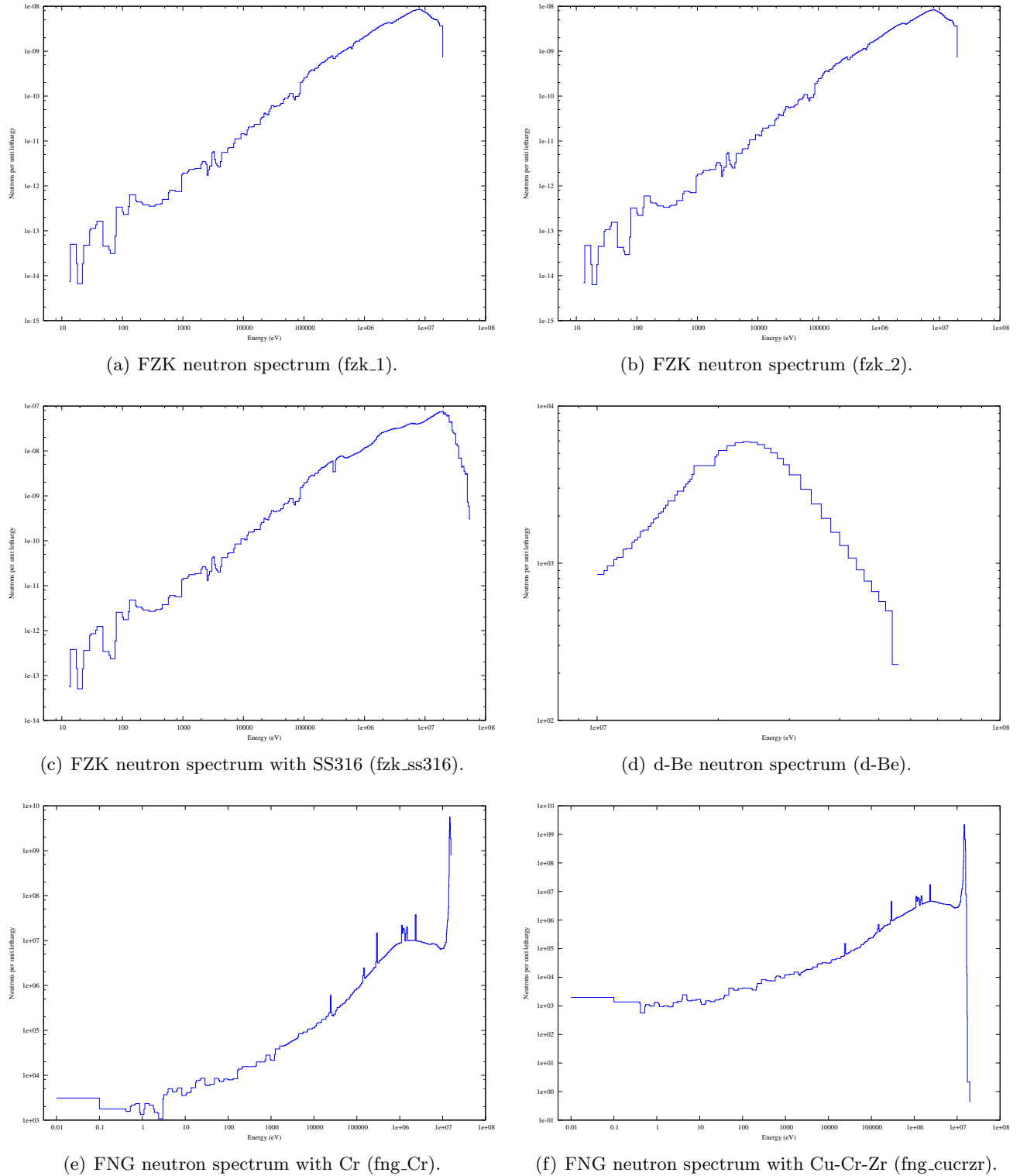


Figure 4: Experimental neutron spectra.

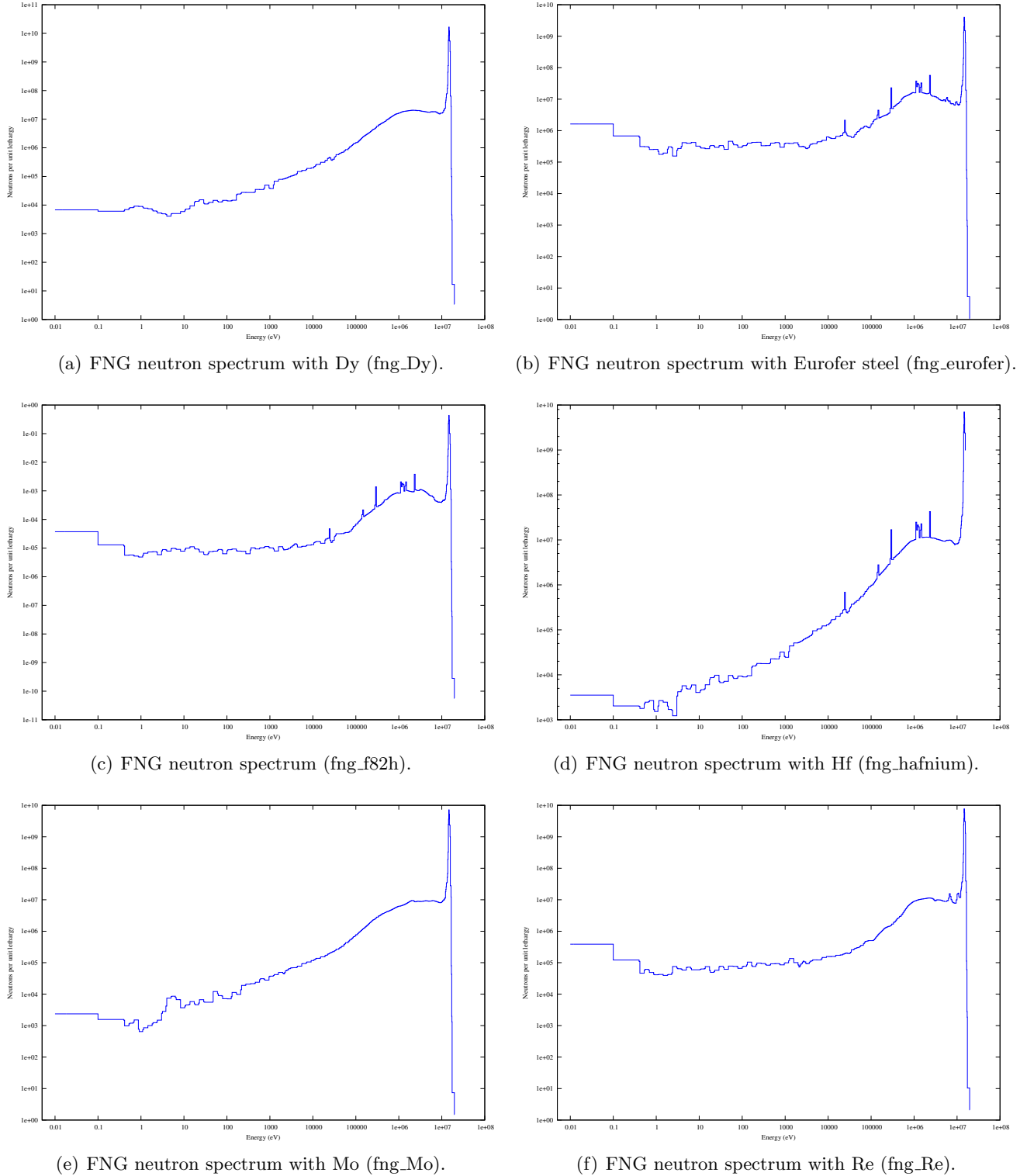


Figure 5: Experimental neutron spectra.

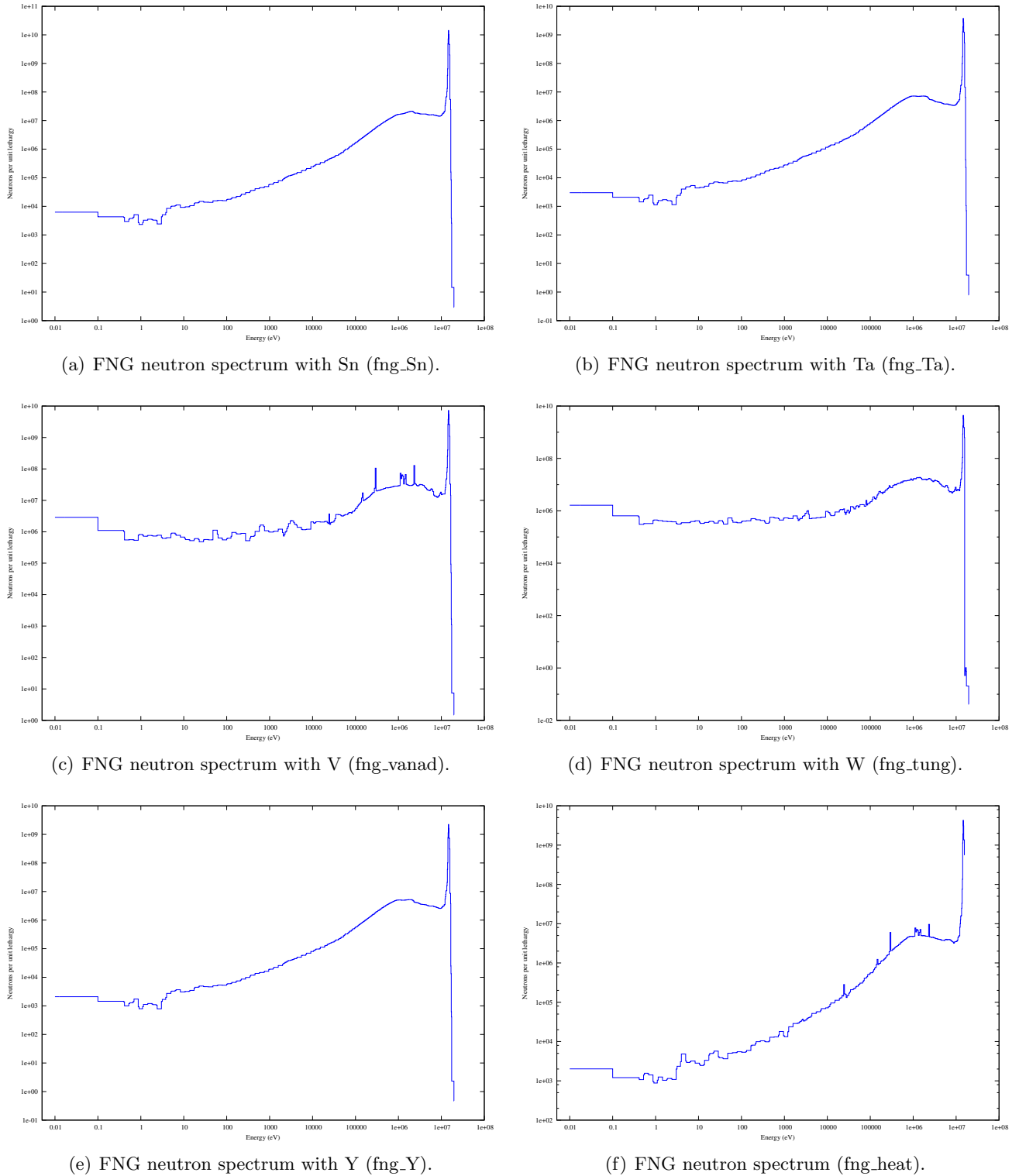


Figure 6: Experimental neutron spectra.

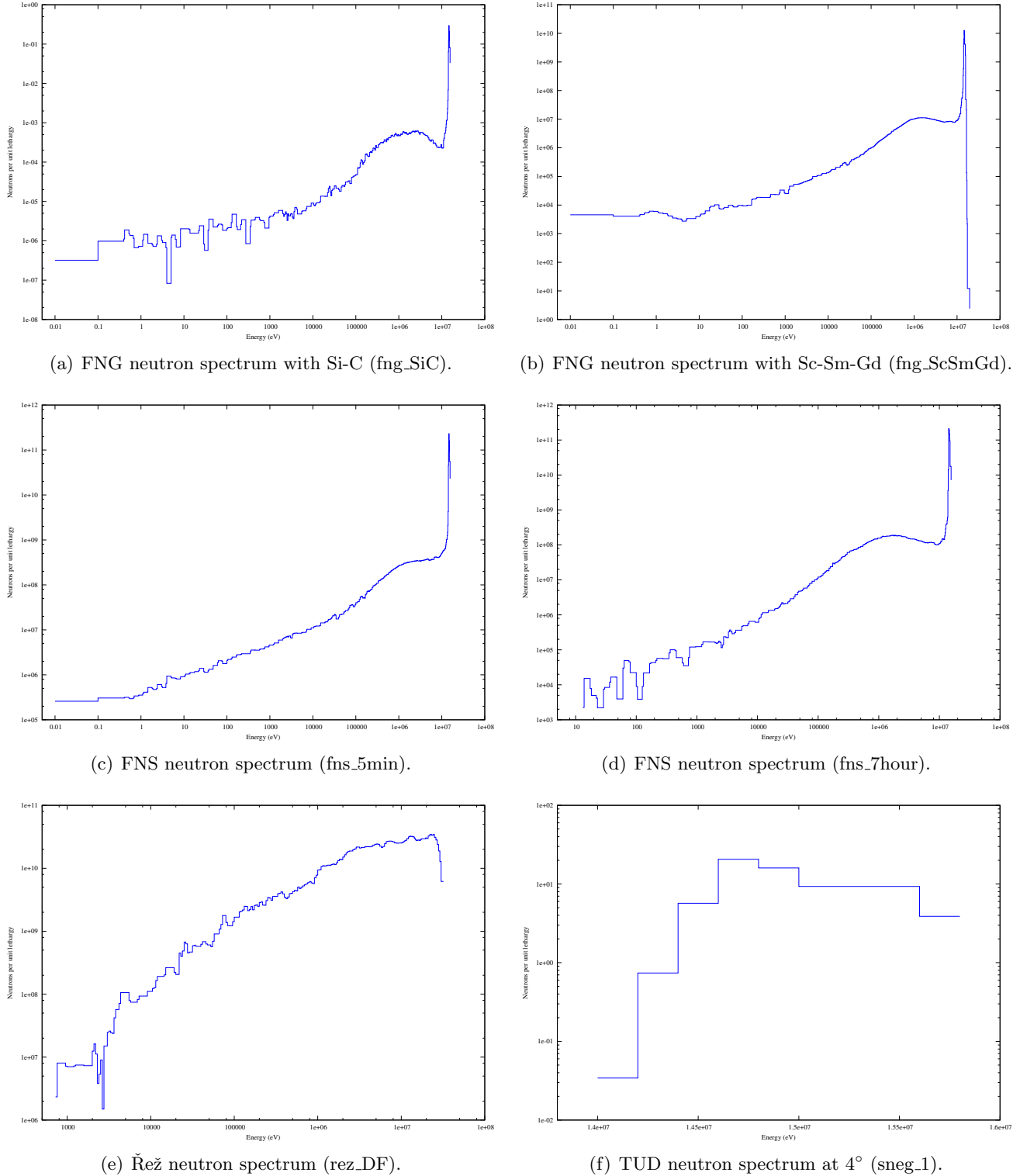


Figure 7: Experimental neutron spectra.

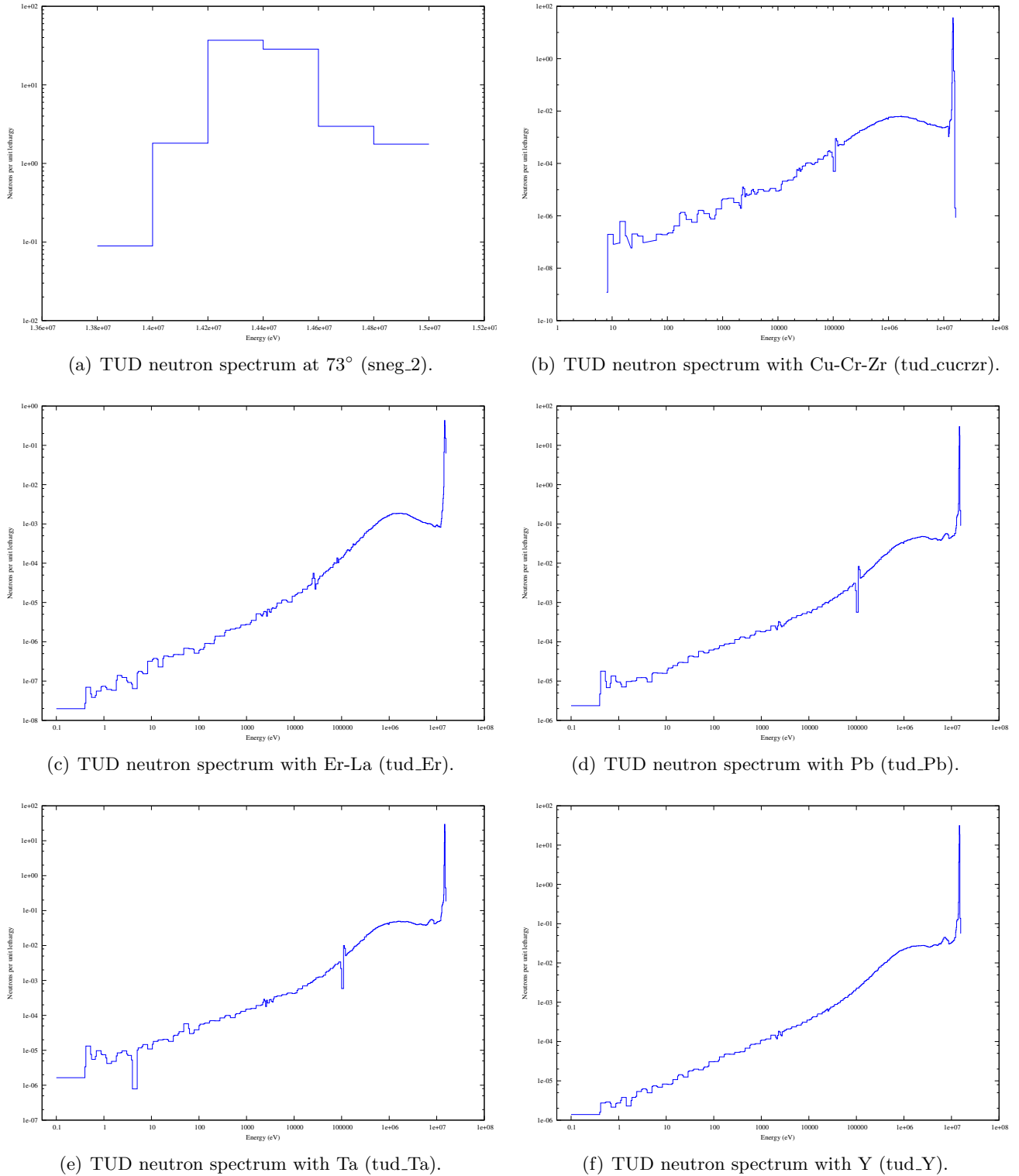


Figure 8: Experimental neutron spectra.

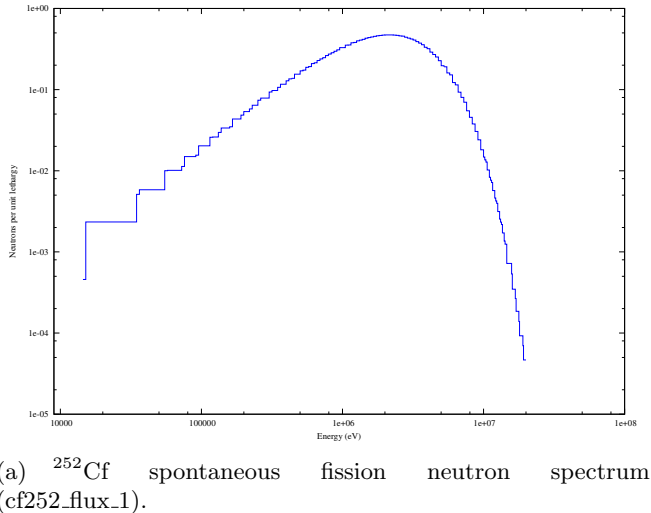


Figure 9: Experimental neutron spectra.

4 Code and libraries

FISPACT-II [4, 5], has been used to perform this validation exercise, using the most up-to-date TENDL-2017 library [2]. The data library processing was performed using CALENDF, NJOY and PREPRO. The cross sections, or excitation curves, are shown in pointwise data plots against the relevant EXFOR data in the next section. The library was processed into the CCFE 709 neutron energy multigroup and was collapsed with the experimental fluxes of the previous section using FISPACT-II.

All of the cross-sections in TENDL-2017 for low-Z nuclides, including $^{1,2,3}\text{H}$, $^{3,4}\text{He}$, $^{6,7}\text{Li}$, ^9Be , $^{10,11}\text{B}$, $^{12,13}\text{C}$, $^{14,15}\text{N}$, ^{16}O and ^{19}F , are imported directly from ENDF/B-VIII.0 without modification. As a result, the data for these nuclides end at 20 MeV and contain problematic gaps, such as the absence of (n,t) and uncertainty data.

The strength of the TALYS/TENDL methodology for nuclear data lies in the consistent production of an entire library. By building upon the most sophisticated nuclear models available and producing data that can be validated against data in the regions where experiments have been performed, TENDL can make the most robust predictions for reaction properties where experimentalists have not yet ventured – and indeed where they may not venture in the indefinite future, due to physical or budgetary challenges. This methodology is absolutely required for simulations of systems where the missing or improperly simplified nuclear data of major libraries may result in erroneous calculations¹³, including fission/fusion reactors, a variety of proposed fast fission reactors and higher-energy physics.

¹³Unfortunately without analysts even being aware of the discrepancies.

Since TENDL transitions from defined pathway data (in the form of specified MT numbers) to a combined residual production MT=5, some high-energy reactions cannot be specified when the reaction occurs above 30 MeV. For many of these reactions, the pathways cannot be accurately isolated and the reactions have been removed in this report. Reactions which have one unique pathway, such as (n,multi-n), are simple sums of the appropriate <30 and >30 MeV values, however reactions with outgoing particles such as ^3H and ^3He are taken from total production cross-sections. These are values produced by the NJOY GASPR module which sums over all of the appropriate pathways:

mt	mt203	mt204	mt205	mt206	mt207
11	0.0	1.0	0.0	0.0	0.0
22	0.0	0.0	0.0	0.0	1.0
24	0.0	0.0	0.0	0.0	1.0
28	1.0	0.0	0.0	0.0	0.0
29	0.0	0.0	0.0	0.0	2.0
32	0.0	1.0	0.0	0.0	0.0
33	0.0	0.0	1.0	0.0	0.0
34	0.0	0.0	0.0	1.0	0.0
41	1.0	0.0	0.0	0.0	0.0
44	2.0	0.0	0.0	0.0	0.0
45	1.0	0.0	0.0	0.0	1.0
103	1.0	0.0	0.0	0.0	0.0
104	0.0	1.0	0.0	0.0	0.0
105	0.0	0.0	1.0	0.0	0.0
106	0.0	0.0	0.0	1.0	0.0
107	0.0	0.0	0.0	0.0	1.0
108	0.0	0.0	0.0	0.0	2.0
111	2.0	0.0	0.0	0.0	0.0
112	1.0	0.0	0.0	0.0	1.0
115	1.0	1.0	0.0	0.0	0.0
116	1.0	0.0	1.0	0.0	0.0
117	0.0	1.0	0.0	0.0	1.0

Since the helion and tritium production reactions often have large cross-sections above 30 MeV, this will be essential for experiments with neutron spectra in that region, such as the d-Be and d-Li experiments. This is made clear with the notation (n,Xt) and (n,Xh) which are calculated from a FISPACT-II collapse using the MT=205 and MT=206 cross-sections. In some cases the experiments cited directly measured this product¹⁴, and the total tritium production is certainly the correct cross-section to compare with. The total values may be overestimated when multi-particle reactions make a substantial contribution to the reaction rate.

¹⁴For example, $^{27}\text{Al}(n,t)^{25}\text{Mg}$, which has a stable residual.

5 Comparison of results

A summary of the reactions covered in the 920 integral data and C/E values is provided in the following Table 3. The remainder of this section is comprised of individual pages for each reaction for which integral data was available. The first figure on each page includes C/E points and error bands for each experimental integral value, plotted against a horizontal gray region which indicates the uncertainty of the effective cross-section calculation based upon TENDL uncertainty data. Note that the low-Z nuclide results (excepting $^{19}\text{F}(\text{n},\text{p})$ and $^{19}\text{F}(\text{n},2\text{n})$) which are based on ENDF/B-VIII.0 data have no uncertainty due to omissions in those libraries. Experimental results which overlap with the calculated band generally support the validation of the data library and FISPACT-II calculations while discrepancies indicate that either the methods, data or experiments contain some flaws. The second graph shows the TENDL differential cross-section plotted against all of the EXFOR data [18] available for the reaction. Note that for readability of the graphs, only the labels of the first 30 EXFOR entries have been kept, although all data-points are shown. In several of these cases the surfeit of data demands more detailed analysis, for example with primary fission or common detector reactions.

Although uncommon, a few rather exotic¹⁵ EXFOR entries are not shown in the differential plots that follow. This exclusively occurs when there are several sets of experimental evidence (>10) that show broad agreement between themselves and with the TENDL data, and when the outlying data falls so far away from all other data that it would require axes that do not show the structure of the TENDL cross-section.

All reactions with target nuclides up to bismuth are included in this section, while plots for actinides can be found in Appendix B.

¹⁵These entries may indeed be members of the ‘suspicious’ EXFOR data [88] which could be subject to modification in the future.

Table 3: Summary of reactions with integral data measurements

Reaction	Spectrum	$\sigma_{exp}(b)$	$\Delta\sigma_{exp}(b)$	C/E
B-10(n,t)Be-8	cf252_flux_1	5.00E-02	2.50E-02	2.06
N-14(n,2n)N-13	fns_5min	7.10E-03	1.14E-03	0.98
N-14(n,g)N-15	cf252_flux_1	4.80E-06	2.40E-06	7.58
O-16(n,p)N-16	fns_5min	3.16E-02	2.21E-03	1.06
F-19(n,2n)F-18	fns_5min	4.80E-02	2.40E-03	1.00
	cf252_flux_1	1.08E-05	1.60E-06	1.81
	cf252_flux_1	1.63E-05	5.00E-07	1.20
F-19(n,p)O-19	fns_5min	1.44E-02	7.21E-04	1.14
Ne-20(n,t)F-18	d-Be	6.82E-03	1.50E-03	2.02
	d-Be	7.50E-03	1.50E-03	1.84
Na-23(n,2n)Na-22	fns_7hour	3.80E-02	2.28E-03	0.85
	fzk_1	4.60E-03	2.76E-03	1.30
Na-23(n,g)Na-24	cf252_flux_1	3.35E-04	1.50E-05	0.89
	fns_7hour	2.51E-04	3.26E-05	0.91
	fns_5min	2.88E-04	1.18E-04	1.15
Na-23(n,p)Ne-23	fns_5min	2.26E-02	1.81E-03	1.42
Na-23(n,t)Ne-21	d-Be	1.45E-02	2.50E-03	0.92
Mg-24(n,p)Na-24	fns_5min	1.56E-01	1.87E-02	0.99
	cf252_flux_1	1.94E-03	9.29E-05	1.10
	cf252_flux_1	2.01E-03	6.00E-05	1.06
	fng_heat	1.98E-01	1.01E-02	0.80
Mg-24(n,t)Na-22	d-Be	4.38E-03	8.11E-04	0.91
	d-Be	6.90E-03	1.00E-03	0.58
Mg-25(n,p)Na-25	fns_5min	6.14E-02	6.75E-03	0.87
	fng_heat	7.17E-02	2.01E-03	0.76
Mg-26(n,a)Ne-23	fns_5min	5.83E-02	6.42E-03	0.86
Al-27(n,p)Mg-27	fns_5min	5.75E-02	3.45E-03	1.06
	fng_heat	7.24E-02	1.16E-03	0.85
	cf252_flux_1	4.89E-03	1.79E-04	0.97
	cf252_flux_1	4.80E-03	9.00E-05	0.99
Al-27(n,t)Mg-25	d-Be3	1.40E-03	4.20E-04	1.14
	d-Be3	1.51E-03	3.00E-04	1.06
	d-Be	7.80E-03	1.20E-03	0.94
Al-27(n,h)Na-25	d-Be2a	3.18E-03	5.80E-04	1.50
	d-Be2a	2.80E-03	5.60E-04	1.70
Al-27(n,a)Na-24	fzk_1	3.40E-02	6.80E-03	0.87
	fng_vanad	9.46E-02	8.92E-03	0.86
	sneg_1	1.25E-01	2.25E-02	0.86
	sneg_2	1.35E-01	2.29E-02	0.86
	fng_f82h	6.66E-02	6.86E-03	1.46
	cf252_flux_1	1.01E-03	2.20E-05	1.02

Reaction	Spectrum	$\sigma_{exp}(b)$	$\Delta\sigma_{exp}(b)$	C/E
Si-28(n,p)Al-28	cf252_flux_1	8.60E-04	5.00E-05	1.20
	rez_DF	2.47E-02	2.90E-04	1.31
	d-Be2a	4.45E-02	6.45E-03	0.84
	d-Be3	4.50E-02	8.00E-03	1.20
	rez_DF	1.15E-01	2.65E-03	0.28
	fns_7hour	1.19E-01	1.42E-02	0.92
	fng_heat	1.00E-01	2.10E-03	1.02
Si-28(n,t)Al-26	fns_5min	1.94E-01	1.94E-02	1.11
	fng_SiC	2.10E-01	6.29E-03	1.00
	fzk_1	6.30E-02	1.57E-02	1.58
	sneg_1	2.79E-01	1.24E-02	0.82
	cf252_flux_1	7.12E-03	2.35E-04	1.09
	cf252_flux_1	9.66E-03	5.50E-04	0.80
Si-29(n,p)Al-29	d-Be	3.75E-03	8.23E-04	1.39
Si-29(n,2p)Mg-28	fns_5min	1.16E-01	1.05E-02	1.04
	fng_SiC	1.16E-01	5.79E-03	1.03
	fzk_1	3.20E-02	4.80E-03	1.29
	sneg_1	1.32E-01	4.11E-03	1.01
	cf252_flux_1	1.79E-03	7.90E-04	1.79
Si-30(n,p)Al-30	fzk_1	8.60E-06	1.03E-06	0.19
Si-30(n,a)Mg-27	sneg_1	7.35E-02	3.27E-03	0.53
P-31(n,p)Si-31	fns_5min	5.41E-02	4.87E-03	1.29
	fng_SiC	5.47E-02	2.19E-03	1.26
	sneg_1	7.36E-02	4.42E-03	1.07
P-31(n,t)Si-29	cf252_flux_1	3.35E-02	2.00E-03	1.13
P-31(n,h)Al-29	d-Be	7.80E-03	1.20E-03	1.92
P-31(n,a)Al-28	d-Be2a	2.88E-03	5.80E-04	2.64
S-32(n,p)P-32	fns_5min	1.12E-01	1.79E-02	0.99
	d-Be2a	3.74E-02	6.45E-03	1.08
S-32(n,t)P-30	fns_7hour	2.29E-01	1.61E-02	0.94
	cf252_flux_1	6.46E-02	3.80E-03	1.14
	cf252_flux_1	7.25E-02	2.95E-03	1.02
	cf252_flux_1	6.84E-02	3.42E-04	1.08
S-34(n,p)P-34	d-Be	4.13E-03	7.86E-04	2.43
S-34(n,a)Si-31	fns_5min	1.91E-02	9.96E-03	3.82
Cl-35(n,2n)Cl-34m	fns_5min	6.64E-03	3.32E-04	1.33
Cl-35(n,t)S-33	d-Be	7.61E-03	1.52E-03	1.63
Cl-37(n,p)S-37	fns_5min	1.68E-02	1.01E-03	1.04
Cl-37(n,a)P-34	fns_5min	3.01E-02	1.80E-03	0.93
Ar-40(n,t)Cl-38	d-Be	5.20E-03	1.20E-03	3.10
	d-Be	1.90E-02	5.00E-03	0.85
K-39(n,2n)K-38g	fns_5min	4.92E-03	2.95E-04	1.05

Reaction	Spectrum	$\sigma_{exp}(b)$	$\Delta\sigma_{exp}(b)$	C/E
K-39(n,pa)S-35	fns_7hour	1.15E-03	7.16E-04	1.67
K-41(n,g)K-42	fns_7hour	7.92E-04	9.51E-05	2.86
K-41(n,h)Cl-39	d-Be2a	1.44E-03	4.30E-04	3.38
K-41(n,a)Cl-38	fns_5min	2.67E-02	1.60E-03	1.18
Ca-40(n,t)K-38	d-Be	4.94E-03	8.24E-04	3.05
	d-Be	9.50E-03	1.50E-03	1.59
Ca-40(n,h)Ar-38	d-Be2a	6.02E-03	1.20E-03	1.38
Ca-42(n,p)K-42	fns_7hour	2.09E-01	1.67E-02	0.89
Ca-44(n,p)K-44	fns_5min	3.70E-02	2.96E-03	1.03
Ca-44(n,t)K-42	d-Be	2.10E-02	4.00E-03	0.69
Ca-48(n,2n)Ca-47	fns_7hour	9.80E-01	9.80E-02	0.93
Sc-45(n,2n)Sc-44g	fns_5min	1.69E-01	1.01E-02	0.95
	fng_ScSmGd	1.19E-01	3.81E-04	1.44
Sc-45(n,2n)Sc-44m	fng_ScSmGd	1.09E-01	5.11E-03	1.07
Sc-45(n,h)K-43	d-Be2a	1.87E-03	4.30E-04	2.34
	d-Be2a	3.18E-03	6.35E-04	1.37
Sc-45(n,a)K-42	fng_ScSmGd	4.74E-02	4.13E-03	1.09
	d-Be2a	1.38E-02	2.37E-03	1.30
Ti-46(n,2n)Ti-45	sneg_1	5.82E-02	7.57E-03	1.02
	cf252_flux_1	9.30E-05	3.10E-05	0.13
Ti-46(n,p)Sc-46	fzk_2	1.21E-01	1.32E-02	0.94
	cf252_flux_1	1.38E-02	3.00E-04	1.00
	cf252_flux_1	1.36E-02	1.21E-03	1.02
	cf252_flux_1	1.24E-02	1.20E-03	1.12
	cf252_flux_1	1.39E-02	1.21E-03	1.00
	rez_DF	7.82E-02	1.82E-03	1.31
	sneg_1	2.38E-01	3.58E-02	0.93
	fng_vanad	1.03E-01	6.29E-03	1.67
	fzk_1	8.10E-02	1.10E-02	1.40
	d-Be3	1.26E-01	2.40E-02	1.16
Ti-47(n,p)Sc-47	fns_7hour	2.37E-01	1.42E-02	0.96
	cf252_flux_1	2.03E-02	1.10E-03	0.96
	cf252_flux_1	1.89E-02	4.00E-04	1.03
	cf252_flux_1	1.94E-02	9.70E-05	1.01
	cf252_flux_1	2.20E-02	9.00E-04	0.89
Ti-48(n,p)Sc-48	cf252_flux_1	2.16E-02	1.18E-03	0.91
	fns_7hour	6.44E-02	3.87E-03	0.91
	fns_5min	5.55E-02	2.78E-03	0.98
	fng_heat	1.06E-01	6.15E-03	0.53
	cf252_flux_1	4.20E-04	1.00E-05	1.03
	cf252_flux_1	4.17E-04	1.59E-05	1.03
	cf252_flux_1	3.80E-04	2.00E-05	1.13
	fzk_ss316	9.52E-03	6.32E-04	2.11

Reaction	Spectrum	$\sigma_{exp}(b)$	$\Delta\sigma_{exp}(b)$	C/E
	fzk_1	4.61E-03	4.61E-04	2.89
Ti-48(n,t)Sc-46	d-Be	9.61E-04	2.29E-04	4.36
	d-Be3	7.03E-05	2.05E-05	3.63
Ti-49(n,p)Sc-49	fng_heat	3.97E-02	2.22E-03	0.92
Ti-50(n,p)Sc-50	fns_5min	1.28E-02	7.71E-04	1.07
	fng_heat	1.86E-02	5.88E-04	0.77
Ti-50(n,a)Ca-47	fng_vanad	9.19E-03	2.05E-03	0.53
V-51(n,na)Sc-47	fzk_ss316	5.33E-03	1.27E-04	1.48
	d-Be2a	9.03E-03	2.15E-03	2.82
	d-Be3	3.50E-03	8.00E-04	1.37
	rez_DF	4.58E-03	6.01E-05	1.66
V-51(n,g)V-52	fng_vanad	6.53E-02	3.98E-03	1.07
	cf252_flux_1	2.80E-03	3.00E-04	0.97
V-51(n,p)Ti-51	fns_5min	2.37E-02	1.18E-03	1.11
	fng_vanad	2.01E-02	1.11E-03	1.07
	sneg_1	2.75E-02	1.92E-03	1.05
	cf252_flux_1	7.10E-04	1.10E-04	0.76
	cf252_flux_1	9.30E-04	1.00E-04	0.58
	cf252_flux_1	7.13E-04	5.88E-05	0.75
V-51(n,t)Ti-49	d-Be3	5.00E-04	1.50E-04	0.99
	d-Be	4.40E-03	1.00E-03	1.15
V-51(n,h)Sc-49	d-Be2a	1.59E-03	4.30E-04	1.66
	d-Be2a	1.34E-03	2.69E-04	1.97
	d-Be3	2.50E-04	8.00E-05	0.27
V-51(n,a)Sc-48	fns_7hour	1.59E-02	9.55E-04	0.98
	fng_f82h	1.67E-02	4.00E-03	0.87
	sneg_1	1.70E-02	6.38E-04	1.02
	sneg_2	1.59E-02	7.39E-04	1.01
	cf252_flux_1	3.88E-05	1.20E-06	1.00
	fzk_ss316	6.30E-03	2.78E-04	0.89
	fzk_ss316	5.89E-03	1.54E-04	0.96
	fzk_ss316	5.80E-03	1.36E-04	0.97
	fng_vanad	1.34E-02	6.97E-04	0.93
	d-Be2a	1.05E-02	1.72E-03	0.80
Cr-50(n,2n)Cr-49	rez_DF	5.12E-03	9.40E-05	0.91
	fng_vanad	2.29E-02	4.29E-03	0.88
	fng_Cr	3.01E-02	5.82E-03	0.82
	fzk_ss316	3.50E-02	1.23E-02	0.65
	fzk_ss316	6.79E-02	1.90E-02	0.34
	fzk_ss316	3.61E-02	1.34E-02	0.63
	rez_DF	2.27E-02	4.54E-04	0.86
	rez_DF	2.79E-02	1.68E-03	0.70
Cr-52(n,2n)Cr-51	fns_5min	4.78E-02	2.87E-03	0.51
	fns_7hour	3.37E-01	2.02E-02	1.00

Reaction	Spectrum	$\sigma_{exp}(b)$	$\Delta\sigma_{exp}(b)$	C/E
	fzk_2	3.90E-02	5.85E-03	1.21
	fng_Cr	3.38E-01	3.05E-02	1.03
	fng_cucrzs	4.62E-01	3.69E-02	0.75
	tud_cucrzs	3.27E-01	3.53E-02	1.14
	fng_vanad	2.76E-01	2.27E-02	1.03
	fng_f82h	3.25E-01	4.12E-02	1.01
	fng_eurofer	3.18E-01	2.26E-02	0.96
	sneg_1	5.18E-01	1.26E-02	0.80
	fzk_ss316	1.79E-01	4.00E-03	0.88
	fzk_ss316	1.77E-01	3.76E-03	0.89
	fzk_ss316	1.98E-01	6.02E-03	0.80
	rez_DF	1.31E-01	9.71E-04	1.00
	rez_DF	1.22E-01	2.44E-03	1.07
	rez_DF	1.40E-01	2.81E-03	0.94
Cr-52(n,p)V-52	fns_5min	6.60E-02	4.62E-03	1.15
	sneg_1	8.11E-02	4.49E-03	1.01
	fng_Cr	7.12E-02	9.92E-03	1.07
	cf252_flux_1	1.07E-03	7.00E-05	1.15
	rez_DF	1.80E-02	8.30E-04	1.34
Cr-52(n,t)V-50	d-Be3	2.03E-04	6.09E-05	0.98
	d-Be3	1.65E-04	3.35E-05	1.21
	d-Be	3.05E-02	3.50E-03	0.11
Cr-53(n,3n)Cr-51	d-Be3	1.06E-02	1.60E-03	0.74
Cr-53(n,p)V-53	sneg_1	5.95E-02	5.89E-03	0.90
	cf252_flux_1	3.06E-04	2.70E-05	1.81
	rez_DF	3.84E-03	1.85E-03	3.66
Cr-53(n,h)Ti-51	d-Be3	2.60E-04	8.00E-05	0.32
Cr-54(n,a)Ti-51	rez_DF	2.05E-03	1.54E-05	1.58
Mn-55(n,2n)Mn-54	fns_7hour	7.32E-01	3.66E-02	0.97
	cf252_flux_1	5.80E-04	1.40E-04	0.73
	cf252_flux_1	4.08E-04	9.00E-06	1.04
Mn-55(n,g)Mn-56	fns_7hour	7.20E-04	5.04E-05	1.12
	fns_5min	4.00E-03	2.80E-04	1.12
Mn-55(n,p)Cr-55	fns_5min	2.45E-02	1.47E-03	1.11
Mn-55(n,t)Cr-53	d-Be	4.90E-03	1.20E-03	1.77
	d-Be3	6.40E-04	2.00E-04	2.12
	d-Be3	1.40E-03	2.80E-04	0.97
Mn-55(n,h)V-53	d-Be2a	1.38E-03	6.88E-04	1.88
	d-Be2a	1.79E-03	3.59E-04	1.45
Mn-55(n,a)V-52	fns_5min	2.06E-02	1.23E-03	1.16
	d-Be2a	7.31E-03	1.51E-03	1.32
Fe-54(n,2n)Fe-53	sneg_1	9.23E-03	2.58E-03	1.44
Fe-54(n,3n)Fe-52g	fzk_ss316	1.08E-04	5.38E-05	1.01
	fzk_ss316	1.17E-04	1.63E-05	0.94

Reaction	Spectrum	$\sigma_{exp}(b)$	$\Delta\sigma_{exp}(b)$	C/E
	rez_DF	3.76E-05	1.09E-06	0.90
Fe-54(n,p)Mn-54	fns_7hour	3.34E-01	3.68E-02	0.88
	sneg_1	3.09E-01	1.54E-02	0.89
	sneg_2	3.43E-01	1.71E-02	0.92
	fzk_2	2.87E-01	4.30E-02	0.96
	fng_f82h	2.69E-01	1.90E-02	0.99
	cf252_flux_1	8.46E-02	2.00E-03	1.02
	cf252_flux_1	9.25E-02	5.00E-03	0.94
	cf252_flux_1	8.78E-02	8.78E-04	0.99
	cf252_flux_1	8.76E-02	4.35E-03	0.99
	cf252_flux_1	7.90E-02	3.00E-03	1.10
	fzk_1	2.82E-01	2.82E-02	0.97
	fzk_ss316	2.19E-01	4.56E-03	1.02
	fzk_ss316	2.11E-01	4.58E-03	1.05
	rez_DF	1.96E-01	1.43E-03	1.15
	fng_eurofer	2.46E-01	1.70E-02	0.98
	fng_vanad	2.44E-01	7.42E-02	0.94
Fe-54(n,a)Cr-51	fng_SiC	8.22E-02	4.11E-03	0.97
Fe-56(n,p)Mn-56	fns_5min	8.69E-02	4.34E-03	1.09
	fns_7hour	1.21E-01	6.03E-03	0.85
	fng_f82h	9.31E-02	6.58E-03	0.99
	fng_SiC	9.58E-02	4.79E-03	0.97
	fng_vanad	9.16E-02	1.45E-02	0.84
	sneg_1	1.07E-01	3.27E-03	0.96
	sneg_2	1.10E-01	4.59E-03	1.00
	cf252_flux_1	1.15E-03	8.00E-05	1.28
	cf252_flux_1	1.45E-03	6.00E-05	1.02
	cf252_flux_1	1.45E-03	3.50E-05	1.02
	cf252_flux_1	1.18E-03	8.00E-05	1.25
	cf252_flux_1	1.40E-03	1.68E-05	1.05
	fzk_ss316	3.43E-02	9.91E-04	1.07
	fzk_ss316	3.36E-02	9.90E-04	1.10
	rez_DF	2.32E-02	4.13E-04	1.44
Fe-56(n,t)Mn-54	d-Be3	3.90E-04	1.17E-04	1.20
	d-Be3	3.99E-04	7.99E-05	1.17
	d-Be	4.10E-02	6.00E-03	0.14
Fe-56(n,h)Cr-54	d-Be2a	5.41E-03	5.31E-04	0.66
Fe-57(n,p)Mn-57	sneg_1	7.12E-02	9.26E-03	0.89
Fe-58(n,g)Fe-59	fng_SiC	1.26E-03	6.30E-05	1.16
	fng_eurofer	2.48E-02	4.27E-03	0.85
	fng_f82h	5.98E-03	5.14E-04	1.00
	rez_DF	1.78E-03	6.18E-05	0.74
Co-59(n,2n)Co-58m	fns_7hour	3.13E-01	1.56E-02	1.39
	rez_DF	1.31E-01	2.62E-02	1.02

Reaction	Spectrum	$\sigma_{exp}(b)$	$\Delta\sigma_{exp}(b)$	C/E
Co-59(n,2n)Co-58	fns_7hour	7.54E-01	3.77E-02	0.93
	cf252_flux_1	5.70E-04	3.00E-05	0.72
	rez_DF	1.19E-01	2.38E-02	1.80
Co-59(n,3n)Co-57	rez_DF	2.47E-02	9.89E-04	0.74
	d-Be3	1.12E-02	1.80E-03	0.75
Co-59(n,g)Co-60	cf252_flux_1	6.97E-03	3.40E-04	0.69
	fng_eurofer	7.25E-01	1.22E-01	0.85
Co-59(n,p)Fe-59	cf252_flux_1	1.96E-03	1.00E-05	0.88
	rez_DF	1.53E-02	6.13E-04	1.25
Co-59(n,t)Fe-57	d-Be3	6.40E-04	2.00E-04	1.05
	d-Be3	4.90E-04	9.80E-05	1.37
	d-Be	3.10E-03	7.00E-04	1.70
Co-59(n,h)Mn-57	d-Be2a	1.44E-03	5.80E-04	1.78
	d-Be2a	1.47E-03	2.44E-04	1.75
Co-59(n,a)Mn-56	fns_5min	2.52E-02	1.26E-03	1.10
	cf252_flux_1	2.00E-04	1.00E-05	1.12
	cf252_flux_1	2.17E-04	1.40E-05	1.03
	cf252_flux_1	2.22E-04	4.00E-06	1.00
	cf252_flux_1	2.00E-04	1.00E-05	1.12
	rez_DF	6.74E-03	2.70E-04	1.16
	d-Be2a	8.39E-03	1.72E-03	1.21
Co-59(n,2a)V-52	d-Be2a	1.08E-04	6.45E-05	0.17
Ni-58(n,2n)Ni-57	fns_7hour	3.12E-02	1.56E-03	1.00
	fng_f82h	3.65E-02	1.01E-02	0.85
	fzk_2	5.42E-03	5.42E-04	0.87
	sneg_1	4.37E-02	3.06E-03	0.92
	sneg_2	3.27E-02	2.29E-03	0.91
	cf252_flux_1	8.95E-06	2.80E-07	0.97
	fzk_ss316	1.94E-02	1.93E-03	0.99
	fzk_ss316	2.57E-02	6.16E-03	0.75
	rez_DF	1.54E-02	6.45E-04	1.05
Ni-58(n,3n)Ni-56	fzk_ss316	4.48E-04	2.50E-05	0.28
	d-Be3	2.00E-05	1.00E-05	1.22
Ni-58(n,np)Co-57	fns_7hour	6.54E-01	3.27E-02	0.99
	fng_vanad	5.29E-01	1.07E-01	0.97
	fzk_2	1.07E-01	1.07E-02	0.93
	sneg_1	7.20E-01	5.04E-02	0.99
	sneg_2	6.43E-01	3.86E-02	1.05
	fng_f82h	5.08E-01	4.79E-02	1.18
	fng_eurofer	4.76E-01	1.38E-01	1.15
	fzk_ss316	2.44E-01	5.63E-03	1.05
	fzk_ss316	3.34E-01	3.39E-02	0.77
	rez_DF	2.13E-01	4.02E-03	1.01
Ni-58(n,p)Co-58	fns_7hour	2.91E-01	1.46E-02	1.03

Reaction	Spectrum	$\sigma_{exp}(b)$	$\Delta\sigma_{exp}(b)$	C/E
	fzk_2	4.37E-01	4.37E-02	0.77
	fng_vanad	2.72E-01	4.09E-02	0.87
	sneg_1	2.98E-01	2.09E-02	0.91
	cf252_flux_1	9.50E-02	4.50E-03	1.24
	cf252_flux_1	1.05E-01	5.00E-03	1.12
	cf252_flux_1	1.13E-01	4.80E-03	1.04
	cf252_flux_1	1.19E-01	6.00E-03	0.99
	cf252_flux_1	1.21E-01	2.00E-03	0.97
	fzk_ss316	2.43E-01	5.39E-03	1.07
	fzk_ss316	2.22E-01	1.33E-02	1.17
	rez_DF	2.19E-01	2.68E-03	1.22
Ni-60(n,p)Co-60m	fns_5min	6.23E-02	3.12E-03	1.09
	fng_heat	4.38E-02	2.36E-03	1.57
Ni-60(n,p)Co-60	fzk_2	5.52E-02	5.52E-03	0.77
	sneg_1	1.51E-01	1.20E-02	0.84
	sneg_2	1.62E-01	1.29E-02	0.87
	fzk_ss316	5.56E-02	2.25E-03	0.82
	d-Be3	8.20E-02	1.60E-02	0.81
Ni-60(n,t)Co-58	d-Be	6.10E-02	8.00E-03	0.11
Ni-60(n,2p)Fe-59	fzk_ss316	8.62E-04	1.55E-04	1.06
Ni-61(n,p)Co-61	fzk_2	1.88E-02	2.82E-03	1.15
Ni-62(n,p)Co-62g	fns_5min	1.90E-02	1.14E-03	1.11
	fng_heat	2.15E-02	6.53E-04	1.02
Ni-62(n,p)Co-62m	fns_5min	1.54E-02	1.08E-03	1.51
	fng_heat	1.85E-02	2.50E-03	0.91
Ni-62(n,a)Fe-59	fzk_2	4.60E-03	4.60E-04	0.86
	sneg_1	3.09E-02	4.11E-03	0.82
Cu-63(n,2n)Cu-62	fns_5min	4.61E-01	2.30E-02	1.05
	tud_cucrzs	4.91E-01	5.55E-02	1.08
	cf252_flux_1	3.00E-04	2.70E-05	0.67
	cf252_flux_1	1.83E-04	7.00E-06	1.10
	fng_heat	5.60E-01	5.72E-02	0.90
Cu-63(n,3n)Cu-61	d-Be3	4.26E-03	1.21E-03	0.70
Cu-63(n,g)Cu-64	cf252_flux_1	1.76E-02	1.40E-03	0.50
Cu-63(n,t)Ni-61	d-Be3	8.20E-04	2.63E-04	2.23
	d-Be	5.31E-03	1.43E-03	2.40
Cu-63(n,h)Co-61	d-Be2a	3.91E-03	7.82E-04	1.36
Cu-63(n,a)Co-60	fns_7hour	5.01E-02	5.01E-03	0.81
	fng_SiC	1.99E-02	9.94E-04	1.83
	fzk_2	1.50E-02	1.50E-03	0.80
	fng_cucrzs	3.51E-02	3.16E-03	1.06
	tud_cucrzs	3.44E-02	3.34E-03	1.20
	cf252_flux_1	6.71E-04	1.80E-05	1.04
	cf252_flux_1	7.09E-04	1.70E-05	0.99

Reaction	Spectrum	$\sigma_{exp}(b)$	$\Delta\sigma_{exp}(b)$	C/E
Cu-65(n,2n)Cu-64	fng_vanad	2.24E-02	8.93E-03	1.36
	fns_7hour	8.57E-01	6.00E-02	1.04
	fng_SiC	9.40E-01	1.88E-02	0.90
	fzk_2	1.57E-01	1.57E-02	0.84
	fng_cucrzs	9.79E-01	6.86E-02	0.88
	tud_cucrzs	8.16E-01	2.84E-01	1.15
Cu-65(n,g)Cu-66	cf252_flux_1	8.00E-03	1.20E-03	0.62
	Cu-65(n,a)Co-62m	cf252_flux_1	8.00E-03	1.20E-03
Cu-65(n,na)Co-61	fng_cucrzs	5.80E-03	8.71E-04	0.85
	tud_cucrzs	4.83E-03	5.50E-04	1.13
	fzk_2	1.21E-03	1.94E-04	0.69
Cu-65(n,p)Ni-65	fng_SiC	1.25E-03	1.25E-04	1.51
	fzk_2	7.10E-04	1.42E-04	1.08
	fng_cucrzs	2.27E-03	2.27E-04	0.82
	tud_cucrzs	1.50E-03	1.36E-04	1.15
	d-Be3	5.10E-03	1.20E-03	1.00
	fns_5min	1.51E-01	7.56E-03	0.85
Zn-64(n,2n)Zn-63	cf252_flux_1	4.11E-02	1.30E-03	1.04
	cf252_flux_1	3.82E-02	1.50E-03	1.12
	cf252_flux_1	4.64E-02	2.30E-03	0.92
	cf252_flux_1	3.94E-02	1.00E-03	1.09
	cf252_flux_1	4.18E-02	1.75E-03	1.02
	cf252_flux_1	4.13E-02	2.82E-03	1.04
Zn-64(n,t)Cu-62	d-Be	6.70E-02	8.00E-03	0.12
Zn-64(n,h)Ni-62	d-Be2a	1.94E-02	3.88E-03	0.43
Zn-67(n,h)Ni-65	d-Be2a	9.89E-04	2.80E-04	2.94
Zn-68(n,g)Zn-69m	cf252_flux_1	1.85E-03	1.20E-04	0.86
Zn-68(n,h)Ni-66	d-Be2a	1.05E-03	3.66E-04	3.67
Zn-68(n,a)Ni-65	d-Be2a	4.08E-03	8.60E-04	1.12
Ga-69(n,2n)Ga-68	fns_5min	7.70E-01	4.62E-02	1.04
Ga-69(n,t)Zn-67	d-Be	4.27E-03	8.13E-04	2.27
Ga-71(n,2n)Ga-70	fns_5min	9.34E-01	5.60E-02	1.00
Ge-74(n,p)Ga-74	fns_5min	1.31E-02	7.86E-04	1.05
Ge-74(n,t)Ga-72	d-Be	6.20E-02	1.30E-02	0.07
Ge-76(n,2n)Ge-75m	fns_5min	5.34E-01	3.74E-02	1.42
Ge-76(n,2n)Ge-75	fns_5min	1.06E+00	7.39E-02	1.00
As-75(n,p)Ge-75m	fns_5min	1.00E-02	8.04E-04	1.20
As-75(n,p)Ge-75	fns_5min	1.72E-02	1.03E-03	1.11

Reaction	Spectrum	$\sigma_{exp}(b)$	$\Delta\sigma_{exp}(b)$	C/E
As-75(n,t)Ge-73	d-Be	3.80E-03	8.00E-04	2.40
As-75(n,h)Ga-73	d-Be2a	1.03E-03	4.30E-04	5.17
	d-Be2a	1.49E-03	2.99E-04	3.57
As-75(n,a)Ga-72	d-Be2a	4.73E-03	1.08E-03	1.07
Se-78(n,2n)Se-77m	fns_5min	6.90E-01	8.97E-02	0.87
Se-80(n,t)As-78	d-Be	5.50E-02	1.20E-02	0.06
Se-82(n,2n)Se-81	fns_5min	9.50E-01	6.65E-02	1.13
Br-79(n,2n)Br-78	fns_5min	8.28E-01	9.11E-02	0.99
Br-81(n,2n)Br-80g	fns_5min	3.33E-01	3.66E-02	1.11
Rb-85(n,2n)Rb-84	fns_5min	9.97E-01	5.98E-02	0.96
Rb-87(n,2n)Rb-86m	fns_5min	4.10E-01	2.46E-02	1.02
Sr-84(n,2n)Sr-83	fns_7hour	6.71E-01	4.03E-02	0.87
Sr-84(n,g)Sr-85m	cf252_flux_1	2.42E-01	2.70E-02	0.19
	cf252_flux_1	3.54E-02	2.34E-03	1.26
Sr-86(n,2n)Sr-85	fns_7hour	9.17E-01	7.33E-02	0.95
Sr-86(n,g)Sr-87m	cf252_flux_1	1.82E-01	2.20E-02	0.07
Sr-88(n,2n)Sr-87m	fns_7hour	2.68E-01	1.61E-02	0.89
Sr-88(n,p)Rb-88	fns_5min	1.42E-02	7.09E-04	1.14
Y-89(n,n)Y-89m	fns_5min	3.76E-01	2.63E-02	1.11
	fng_Y	3.31E-01	1.99E-02	1.21
Y-89(n,2n)Y-88	fns_7hour	1.08E+00	7.58E-02	0.84
	fns_5min	8.42E-01	1.68E-01	1.05
	fng_Y	8.91E-01	8.91E-03	0.99
	tud_Y	8.00E-01	9.00E-02	1.10
	rez_DF	1.94E-01	5.82E-03	1.49
Y-89(n,3n)Y-87	rez_DF	4.61E-02	1.38E-03	0.70
Y-89(n,g)Y-90m	tud_Y	3.82E-04	1.96E-04	1.18
	fng_Y	3.57E-04	1.07E-05	1.27
Y-89(n,t)Sr-87	d-Be	6.50E-03	2.00E-03	2.30
Y-89(n,a)Rb-86m	fns_5min	1.64E-03	9.83E-05	1.48
	fng_Y	2.03E-03	2.64E-04	1.18
Y-89(n,a)Rb-86	fng_Y	1.42E-02	1.84E-03	0.54
Zr-90(n,2n)Zr-89m	fns_5min	1.17E-01	5.84E-03	1.10
	fng_heat	1.48E-01	8.61E-02	0.91
Zr-90(n,2n)Zr-89	fns_7hour	7.11E-01	4.26E-02	0.99
	fng_cucrzr	9.24E-01	6.47E-02	0.76
	tud_cucrzr	6.71E-01	6.91E-02	1.14
	cf252_flux_1	2.67E-04	1.50E-05	0.82
	cf252_flux_1	2.21E-04	6.00E-06	0.99
	rez_DF	1.86E-01	5.57E-03	1.40
	fng_Y	6.07E-01	7.28E-02	1.15
Zr-90(n,p)Y-90m	cf252_flux_1	4.50E-05	6.00E-06	1.08
Zr-90(n,t)Y-88	d-Be	5.10E-02	1.10E-02	0.07

Reaction	Spectrum	$\sigma_{exp}(b)$	$\Delta\sigma_{exp}(b)$	C/E
Zr-94(n,g)Zr-95	cf252_flux_1	8.75E-03	6.50E-04	0.66
Zr-94(n,p)Y-94	fns_5min	7.92E-03	3.96E-04	1.19
	fng_heat	8.06E-03	1.20E-03	1.22
Zr-96(n,2n)Zr-95	fns_7hour	1.48E+00	7.42E-02	0.99
	fzk_1	4.73E-01	8.21E-02	0.71
Zr-96(n,g)Zr-97	cf252_flux_1	4.17E-03	2.10E-04	1.56
Nb-93(n,2n)Nb-92m	fns_7hour	4.68E-01	2.34E-02	0.96
	fng_heat	5.18E-01	6.52E-02	0.84
	fng_SiC	3.93E-01	1.18E-02	1.06
	fzk_2	2.76E-01	4.14E-02	0.29
	fzk_ss316	1.58E-01	1.58E-02	0.91
	fzk_ss316	1.07E-01	2.90E-02	1.35
	rez_DF	1.23E-01	3.68E-03	0.99
	fng_vanad	4.81E-01	6.59E-02	0.72
	fzk_1	7.06E-02	7.80E-02	1.13
	d-Be3	1.78E-01	2.40E-02	1.19
	d-Be3	2.02E-01	2.40E-02	1.05
Nb-93(n,3n)Nb-91m	rez_DF	1.84E-02	1.66E-03	0.79
Nb-93(n,4n)Nb-90	rez_DF	1.93E-05	2.51E-06	2.19
Nb-93(n,na)Y-89m	fns_5min	3.45E-03	2.42E-04	0.65
Nb-93(n,g)Nb-94m	fns_5min	5.11E-03	3.58E-04	0.86
Nb-93(n,t)Zr-91	d-Be3	6.10E-04	2.00E-04	0.54
	d-Be3	4.90E-04	9.80E-05	0.67
	d-Be	4.10E-03	8.00E-04	0.55
Nb-93(n,h)Y-91m	d-Be2a	2.15E-04	6.45E-05	3.62
Nb-93(n,h)Y-91	d-Be2a	1.61E-03	2.80E-04	4.11
	d-Be2a	1.54E-03	3.08E-04	4.30
Nb-93(n,a)Y-90g	fng_heat	1.35E-02	3.28E-03	0.45
Nb-93(n,a)Y-90m	fns_5min	4.97E-03	2.98E-04	1.05
	fng_SiC	4.76E-03	2.86E-04	1.08
	d-Be2a	1.93E-03	4.30E-04	1.51
	d-Be3	2.80E-03	3.00E-04	0.96
Nb-93(n,a)Y-90	d-Be2a	4.09E-03	4.30E-04	1.39
	d-Be3	3.80E-03	5.00E-04	1.50
Mo-92(n,2n)Mo-91	fns_5min	2.15E-01	1.08E-02	0.99
	fng_heat	2.76E-01	7.16E-03	0.81
	fng_Mo	2.35E-01	2.83E-03	0.95
Mo-92(n,3n)Mo-90	fzk_ss316	2.92E-03	1.61E-03	1.70
Mo-92(n,np)Nb-91m	fns_7hour	1.85E-01	1.66E-02	1.26
Mo-92(n,na)Zr-88	fzk_ss316	3.99E-03	2.39E-03	1.84
Mo-92(n,p)Nb-92m	fns_7hour	6.15E-02	3.08E-03	1.05
	fzk_ss316	3.29E-02	1.61E-03	1.21
	fng_Mo	5.49E-02	2.09E-03	1.10

Reaction	Spectrum	$\sigma_{exp}(b)$	$\Delta\sigma_{exp}(b)$	C/E
Mo-92(n,p)Nb-92	cf252_flux_1	1.68E-02	7.00E-04	0.49
Mo-92(n,a)Zr-89	sneg_1	2.27E-02	2.04E-03	1.48
	cf252_flux_1	4.20E-04	2.00E-05	0.31
	fzk_ss316	8.69E-03	3.84E-04	1.25
	fng_Mo	2.68E-02	2.33E-03	1.14
Mo-92(n,pa)Y-88	fzk_ss316	1.51E-03	5.13E-04	0.21
Mo-95(n,3n)Mo-93m	fzk_ss316	8.38E-03	1.39E-03	0.83
Mo-95(n,p)Nb-95g	fns_7hour	3.44E-02	2.07E-03	0.96
	fng_vanad	4.25E-02	1.54E-02	0.60
	sneg_1	3.73E-02	3.32E-03	0.94
	fng_Mo	3.18E-02	2.78E-03	1.02
Mo-95(n,p)Nb-95m	cf252_flux_1	1.44E-04	1.44E-04	0.32
	fng_Mo	7.30E-03	6.58E-04	0.85
	fzk_ss316	5.41E-03	7.03E-04	0.46
Mo-95(n,p)Nb-95	cf252_flux_1	2.20E-02	2.00E-03	0.01
Mo-96(n,np)Nb-95	fzk_ss316	9.30E-03	4.15E-04	1.44
Mo-96(n,p)Nb-96	sneg_1	2.08E-02	2.08E-03	1.06
	fng_Mo	2.03E-02	1.14E-03	0.99
Mo-98(n,g)Mo-99	cf252_flux_1	2.63E-02	1.30E-03	0.77
Mo-98(n,t)Nb-96	d-Be3	5.04E-04	1.63E-04	0.92
Mo-98(n,a)Zr-95	fns_7hour	7.47E-03	1.42E-03	0.86
Mo-100(n,2n)Mo-99	fns_7hour	1.50E+00	7.52E-02	0.96
	sneg_1	1.53E+00	1.22E-01	0.99
	sneg_2	1.51E+00	1.21E-01	1.00
	fng_vanad	1.12E+00	3.63E-01	0.99
	fzk_ss316	4.13E-01	9.55E-03	1.09
	fzk_ss316	3.28E-01	1.31E-01	1.38
	fng_Mo	1.29E+00	4.04E-02	1.09
Mo-100(n,g)Mo-101	cf252_flux_1	1.48E-02	1.11E-03	1.21
Mo-100(n,a)Zr-97	fzk_ss316	8.16E-02	1.71E-02	0.02
Ru-96(n,2n)Ru-95	fns_5min	5.50E-01	2.75E-02	0.96
Ru-100(n,p)Tc-100	fns_5min	2.94E-02	3.23E-03	1.02
Ru-102(n,p)Tc-102m	fns_5min	6.60E-03	3.30E-04	1.09
Rh-103(n,n)Rh-103m	fns_5min	1.41E-01	3.65E-02	2.40
Rh-103(n,2n)Rh-102g	rez_DF	7.05E-01	3.52E-02	0.21
Rh-103(n,3n)Rh-101m	rez_DF	5.51E-02	2.20E-03	1.40
Rh-103(n,g)Rh-104	fns_5min	2.66E-02	2.12E-03	2.45
Rh-103(n,p)Ru-103	rez_DF	4.75E-03	1.90E-04	1.99
Pd-106(n,t)Rh-104	d-Be	3.60E-02	6.00E-03	0.19
Pd-108(n,2n)Pd-107m	fns_5min	3.60E-01	1.80E-02	1.20
Pd-110(n,2n)Pd-109m	fns_5min	3.24E-01	1.94E-02	1.32
Pd-110(n,2n)Pd-109	fns_5min	1.45E+00	8.71E-02	0.98
Ag-107(n,2n)Ag-106g	fns_5min	6.96E-01	3.48E-02	0.99

Reaction	Spectrum	$\sigma_{exp}(b)$	$\Delta\sigma_{exp}(b)$	C/E
	fng_heat	9.67E-01	2.51E-02	0.74
Ag-107(n,t)Pd-105	d-Be3	4.99E-04	1.59E-04	2.62
	d-Be	4.54E-03	8.26E-04	2.37
Ag-107(n,h)Rh-105	d-Be2a	3.30E-03	6.61E-04	0.93
	d-Be2a	2.24E-03	3.57E-04	1.37
Ag-109(n,2n)Ag-108g	fns_5min	5.91E-01	4.14E-02	0.97
	fng_heat	9.61E-01	2.50E-02	0.62
Cd-110(n,g)Cd-111	cf252_flux_1	2.04E-01	7.00E-03	0.30
Cd-112(n,2n)Cd-111m	fns_5min	4.64E-01	2.32E-02	1.20
	fng_heat	6.83E-01	2.64E-02	0.85
Cd-116(n,g)Cd-117	cf252_flux_1	3.80E-02	1.40E-02	0.46
In-113(n,2n)In-112m	cf252_flux_1	3.75E-03	1.85E-03	0.33
In-113(n,2n)In-112	cf252_flux_1	9.50E-03	4.75E-03	0.16
In-115(n,2n)In-114g	fns_5min	1.99E-01	5.29E-03	1.22
In-115(n,na)Ag-111	d-Be2a	3.66E-03	6.45E-04	6.33
In-115(n,g)In-116m	cf252_flux_1	1.24E-01	3.60E-03	0.37
	cf252_flux_1	1.39E-01	6.00E-02	0.33
In-115(n,g)In-116	fns_5min	7.06E-02	2.83E-03	2.44
In-115(n,t)Cd-113	d-Be	3.90E-03	7.99E-04	2.16
In-115(n,h)Ag-113g	d-Be2a	2.15E-04	6.45E-05	4.39
In-115(n,h)Ag-113	d-Be2a	1.04E-03	2.14E-04	0.91
In-115(n,a)Ag-112	d-Be2a	2.58E-03	6.45E-04	2.09
Sn-112(n,2n)Sn-111	fng_Sn	1.17E+00	1.05E-01	0.96
Sn-114(n,2n)Sn-113	fng_Sn	1.94E+00	9.37E-02	0.58
Sn-114(n,np)In-113m	fng_Sn	4.23E-03	9.91E-04	0.37
Sn-116(n,p)In-116	fng_Sn	2.47E-02	7.41E-04	1.28
Sn-116(n,np)In-115m	fng_Sn	1.10E-03	1.05E-04	0.40
Sn-117(n,p)In-117m	fng_Sn	4.09E-03	6.39E-04	0.79
Sn-117(n,p)In-117	fng_Sn	1.81E-02	6.55E-04	0.75
Sn-118(n,2n)Sn-117m	fns_7hour	9.50E-01	1.14E-01	0.80
	fng_Sn	1.32E+00	3.27E-02	0.57
Sn-118(n,p)In-118m	fns_5min	4.93E-03	3.45E-04	1.36
Sn-118(n,a)Cd-115g	fng_Sn	1.23E-03	2.37E-04	0.47
Sn-120(n,2n)Sn-119m	fns_7hour	4.80E-01	1.01E-01	1.22
Sn-120(n,p)In-120m	fns_5min	8.33E-03	1.00E-03	0.06
Sn-120(n,a)Cd-117g	fng_Sn	3.84E-04	5.32E-05	0.56
Sn-120(n,a)Cd-117m	fng_Sn	3.90E-04	6.11E-05	1.06
Sn-124(n,2n)Sn-123g	fns_7hour	1.04E+00	1.46E-01	1.09
	fng_Sn	2.21E+00	8.96E-01	0.50
Sn-124(n,2n)Sn-123m	fns_5min	4.01E-01	2.41E-02	1.19
	fng_heat	5.84E-01	2.51E-02	0.85
	fng_Sn	5.60E-01	1.71E-02	0.88
Sb-121(n,2n)Sb-120g	fns_5min	7.77E-01	4.66E-02	1.24

Reaction	Spectrum	$\sigma_{exp}(b)$	$\Delta\sigma_{exp}(b)$	C/E
Sb-121(n,t)Sn-119	d-Be	4.50E-03	1.36E-03	2.00
Te-128(n,t)Sb-126	d-Be	2.50E-02	6.00E-03	0.12
Te-130(n,2n)Te-129g	fns_5min	5.63E-01	4.51E-02	0.95
I-127(n,2n)I-126	cf252_flux_1	2.07E-03	7.00E-05	1.03
I-127(n,g)I-128	fns_5min	1.93E-02	1.16E-03	1.73
I-127(n,h)Sb-125	d-Be2a	5.59E-04	1.08E-04	4.02
I-127(n,a)Sb-124	d-Be2a	1.93E-03	3.23E-04	2.99
Cs-133(n,2n)Cs-132	fns_5min	1.12E+00	8.98E-02	1.10
Cs-133(n,h)I-131	d-Be2a	4.78E-04	9.02E-05	1.15
Ba-134(n,2n)Ba-133m	fns_7hour	7.25E-01	1.01E-01	1.09
Ba-134(n,g)Ba-135	cf252_flux_1	2.55E-01	2.80E-02	0.22
Ba-134(n,t)Cs-132	d-Be	1.50E-02	2.00E-03	0.29
Ba-136(n,2n)Ba-135m	fns_7hour	9.45E-01	1.42E-01	1.06
Ba-136(n,g)Ba-137	cf252_flux_1	2.93E-01	2.90E-02	0.08
Ba-136(n,p)Cs-136	fns_7hour	5.03E-03	2.61E-03	1.08
Ba-138(n,2n)Ba-137m	fns_5min	6.65E-01	5.32E-02	1.36
Ba-138(n,g)Ba-139	cf252_flux_1	3.80E-03	4.00E-04	0.66
	cf252_flux_1	1.30E-03	2.60E-04	1.92
Ba-138(n,p)Cs-138	fns_5min	2.54E-03	2.54E-04	1.08
La-139(n,g)La-140	tud_Er	2.48E-03	1.56E-04	1.00
La-139(n,p)Ba-139	fns_5min	3.66E-03	1.58E-03	1.01
	tud_Er	4.00E-03	9.53E-04	0.85
La-139(n,t)Ba-137	d-Be	7.00E-03	1.50E-03	0.93
La-139(n,h)Cs-137	d-Be2a	4.52E-04	8.60E-05	1.62
	d-Be2a	4.65E-04	6.15E-05	1.58
La-139(n,a)Cs-136	d-Be2a	2.04E-03	3.23E-04	1.13
	tud_Er	2.05E-03	2.05E-03	1.03
Ce-140(n,2n)Ce-139m	fns_5min	6.98E-01	4.89E-02	1.18
Ce-140(n,a)Ba-137m	fns_5min	2.62E-03	1.83E-04	1.11
Ce-142(n,p)La-142	fns_5min	4.05E-03	1.66E-03	1.21
Pr-141(n,2n)Pr-140	fns_5min	1.01E+00	8.09E-02	1.49
Pr-141(n,t)Ce-139	d-Be	9.40E-03	2.00E-03	1.43
	d-Be	2.30E-02	6.00E-03	0.58
Nd-142(n,2n)Nd-141m	fns_5min	4.11E-01	5.34E-02	1.35
Nd-146(n,h)Ce-144	d-Be2a	2.58E-04	8.60E-05	2.73
Nd-146(n,a)Ce-143	d-Be2a	2.15E-03	3.23E-04	1.75
Nd-150(n,2n)Nd-149	fns_5min	8.29E-01	1.24E-01	1.78
Sm-144(n,2n)Sm-143m	fns_5min	4.87E-01	5.85E-02	0.98
Sm-144(n,2n)Sm-143	fns_5min	1.04E+00	1.14E-01	1.01
Sm-150(n,p)Pm-150	fng_ScSmGd	6.05E-03	7.26E-04	1.02
Sm-152(n,a)Nd-149	fng_ScSmGd	2.55E-03	3.06E-04	1.04
Sm-154(n,2n)Sm-153	fng_ScSmGd	1.84E+00	6.42E-02	0.98
Gd-158(n,p)Eu-158	fng_ScSmGd	3.17E-03	1.46E-04	1.01

Reaction	Spectrum	$\sigma_{exp}(b)$	$\Delta\sigma_{exp}(b)$	C/E
Gd-158(n,a)Sm-155	fng_ScSmGd	1.11E-03	6.67E-05	1.06
Gd-160(n,2n)Gd-159	fns_5min	1.26E+00	2.39E-01	1.35
	fng_ScSmGd	1.96E+00	6.08E-02	0.91
Gd-160(n,g)Gd-161	fns_5min	3.78E-03	6.43E-04	1.45
Gd-160(n,p)Eu-160	fns_5min	1.77E-03	4.42E-04	0.96
Tb-159(n,2n)Tb-158m	fns_5min	3.24E-01	5.65E-01	0.74
Tb-159(n,p)Gd-159	fns_5min	2.04E-02	3.93E-02	0.27
Tb-159(n,t)Gd-157	d-Be	7.90E-03	2.00E-03	2.15
Tb-159(n,a)Eu-156	d-Be2a	1.55E-03	2.58E-04	2.23
Dy-156(n,2n)Dy-155	fng_Dy	1.53E+00	8.09E-02	1.07
Dy-158(n,2n)Dy-157	fng_Dy	1.92E+00	7.28E-02	0.97
Dy-162(n,p)Tb-162	fns_5min	2.48E-03	2.97E-04	1.51
	fng_Dy	4.08E-03	1.92E-04	0.96
Dy-162(n,t)Tb-160	d-Be	1.60E-02	3.30E-03	0.32
Dy-163(n,p)Tb-163	fng_Dy	3.33E-03	1.37E-04	1.07
Dy-164(n,g)Dy-165g	fng_Dy	2.97E-02	1.34E-03	0.66
Dy-164(n,g)Dy-165m	fns_5min	1.01E-01	1.51E-02	1.30
Dy-164(n,g)Dy-165	fns_5min	3.56E-02	8.19E-03	5.34
Dy-164(n,p)Tb-164	fns_5min	1.13E-03	1.47E-04	2.09
Ho-165(n,2n)Ho-164m	fns_5min	7.14E-01	1.00E-01	1.19
Ho-165(n,2n)Ho-164	fns_5min	1.44E+00	2.02E-01	1.20
Ho-165(n,t)Dy-163	d-Be	9.80E-03	2.00E-03	2.07
Ho-165(n,h)Tb-163	d-Be2a	1.72E-04	4.30E-05	8.39
Ho-165(n,a)Tb-162	d-Be2a	1.85E-03	3.23E-04	1.30
Er-162(n,2n)Er-161	tud_Er	1.42E+00	1.19E-01	1.03
Er-164(n,2n)Er-163	tud_Er	1.84E+00	1.73E-01	0.93
Er-166(n,2n)Er-165	fns_5min	3.54E-01	1.31E-01	5.02
Er-166(n,p)Ho-166g	tud_Er	3.50E-03	2.20E-04	0.75
Er-167(n,p)Ho-167	tud_Er	2.87E-03	1.61E-04	1.24
Er-168(n,p)Ho-168	fns_5min	2.10E-03	2.10E-04	1.06
	tud_Er	2.39E-03	1.79E-04	0.87
Er-170(n,p)Ho-170g	tud_Er	1.52E-03	2.84E-04	0.57
Er-170(n,d)Ho-169	tud_Er	1.69E-04	3.97E-05	0.66
Tm-169(n,2n)Tm-168	fns_5min	1.98E+00	4.96E-01	0.90
Yb-168(n,2n)Yb-167	fns_5min	1.53E+00	5.65E-01	1.10
Yb-174(n,p)Tm-174	fns_5min	1.82E-03	3.10E-04	1.06
Yb-174(n,h)Er-172	d-Be2a	2.15E-04	5.38E-05	1.06
Yb-174(n,a)Er-171	d-Be2a	1.93E-03	3.23E-04	1.82
Lu-175(n,g)Lu-176m	fns_5min	5.23E-02	1.10E-02	1.33
Lu-175(n,2n)Lu-174g	rez_DF	5.94E-01	1.78E-02	0.45
Lu-175(n,3n)Lu-173	rez_DF	1.68E-01	5.04E-03	1.51
Lu-175(n,4n)Lu-172	rez_DF	1.74E-02	5.23E-04	1.23
Hf-174(n,2n)Hf-173	fng_hafnium	1.86E+00	3.73E-01	1.02

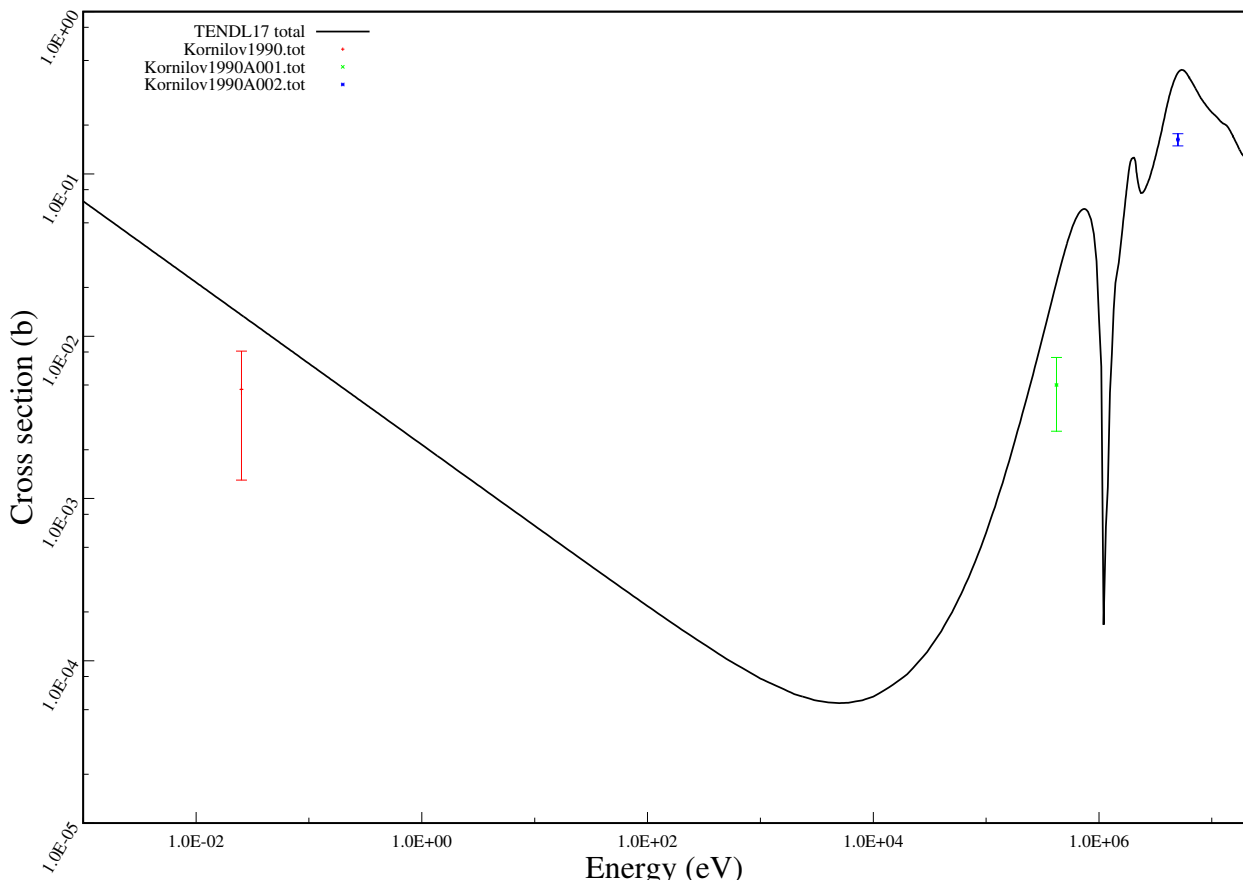
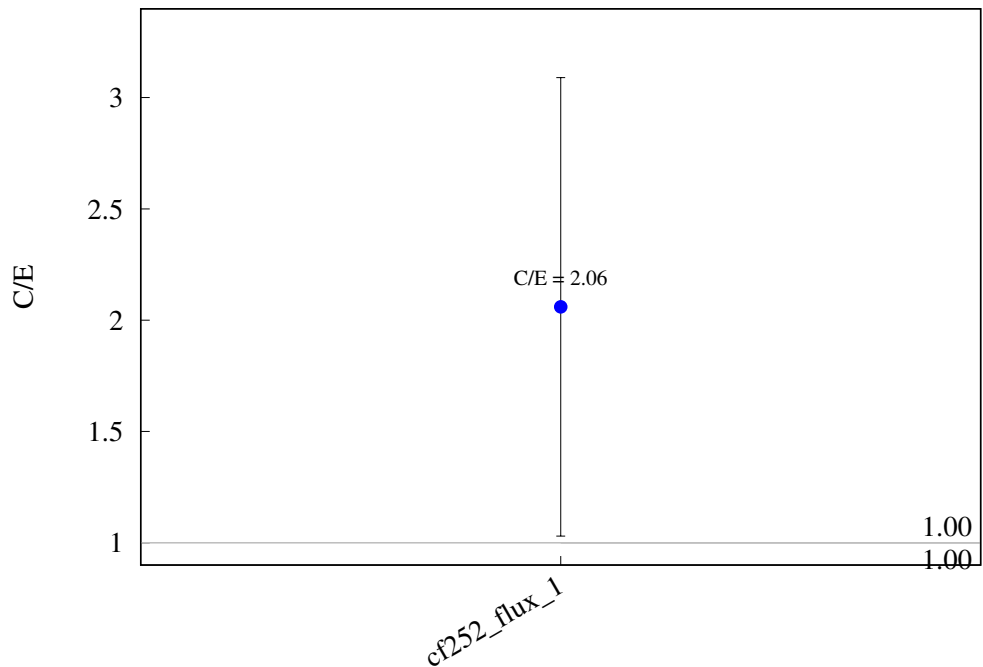
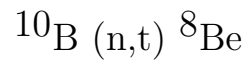
Reaction	Spectrum	$\sigma_{exp}(b)$	$\Delta\sigma_{exp}(b)$	C/E
Hf-176(n,2n)Hf-175	fng_hafnium	1.75E+00	1.96E-01	1.01
Hf-178(n,p)Lu-178m	fng_hafnium	5.94E-04	1.08E-04	1.01
Hf-178(n,p)Lu-178	fng_hafnium	3.67E-03	1.18E-03	0.86
Hf-179(n,p)Lu-179	fng_hafnium	1.08E-02	2.51E-03	0.60
Hf-180(n,n)Hf-180m	fng_heat	4.41E-02	2.42E-03	0.65
	fng_hafnium	1.14E-02	6.65E-04	2.48
	fns_5min	1.80E-02	1.44E-03	1.60
Hf-180(n,2n)Hf-179m	fns_5min	6.05E-02	4.84E-03	3.52
Hf-180(n,g)Hf-181	fng_hafnium	9.28E-03	1.51E-03	0.40
Hf-180(n,p)Lu-180	fns_5min	3.52E-03	2.11E-04	0.68
	fng_hafnium	3.87E-03	9.36E-04	0.62
	fng_heat	3.79E-03	3.00E-04	0.66
Ta-181(n,2n)Ta-180g	fns_7hour	7.57E-01	7.57E-02	1.45
	fns_5min	1.05E+00	1.36E-01	0.96
	fng_Ta	1.01E+00	2.32E-02	1.00
	tud_Ta	8.11E-01	2.08E-01	1.20
	rez_DF	2.92E-01	8.07E-03	1.00
	rez_DF	3.30E-01	3.99E-03	0.88
Ta-181(n,na)Lu-177m	rez_DF	3.00E-05	1.23E-06	6.18
Ta-181(n,na)Lu-177	rez_DF	4.91E-04	6.61E-06	2.53
Ta-181(n,4n)Ta-178m	rez_DF	1.25E-02	2.36E-04	0.16
Ta-181(n,g)Ta-182n	fng_Ta	1.20E-04	4.13E-05	0.30
Ta-181(n,g)Ta-182	fng_eurofer	1.19E+00	1.79E-01	1.00
	cf252_flux_1	1.20E-01	6.50E-03	0.68
	cf252_flux_1	8.92E-02	1.07E-03	0.92
	fng_Ta	4.21E-02	2.90E-03	0.71
	rez_DF	2.00E-01	3.27E-03	0.22
	rez_DF	3.38E-02	2.91E-04	1.29
	fns_7hour	1.09E-02	2.41E-03	0.49
Ta-181(n,p)Hf-181	fns_7hour	7.53E-03	1.43E-03	0.45
	fng_Ta	3.40E-03	4.31E-04	1.04
	tud_Ta	2.94E-03	3.85E-04	1.06
	rez_DF	1.74E-03	1.65E-05	1.46
Ta-181(n,t)Hf-179n	rez_DF	2.83E-06	6.00E-08	0.00
Ta-181(n,t)Hf-179	d-Be3	5.90E-04	2.40E-04	1.08
	d-Be	4.50E-03	1.30E-03	1.44
Ta-181(n,h)Lu-179	d-Be2a	9.20E-05	2.59E-05	3.78
Ta-181(n,a)Lu-178g	fng_Ta	1.01E-03	4.04E-04	0.65
Ta-181(n,a)Lu-178m	fng_Ta	2.31E-04	2.77E-05	1.56
	tud_Ta	2.20E-04	2.30E-05	1.42
W-180(n,2n)W-179m	fzk_2	8.70E-02	2.61E-02	0.99
W-180(n,3n)W-178	fzk_2	1.71E-02	2.56E-03	0.92
W-182(n,2n)W-181	fns_7hour	1.57E+00	2.35E-01	1.27
	fng_tung	1.37E+00	1.75E-01	1.18

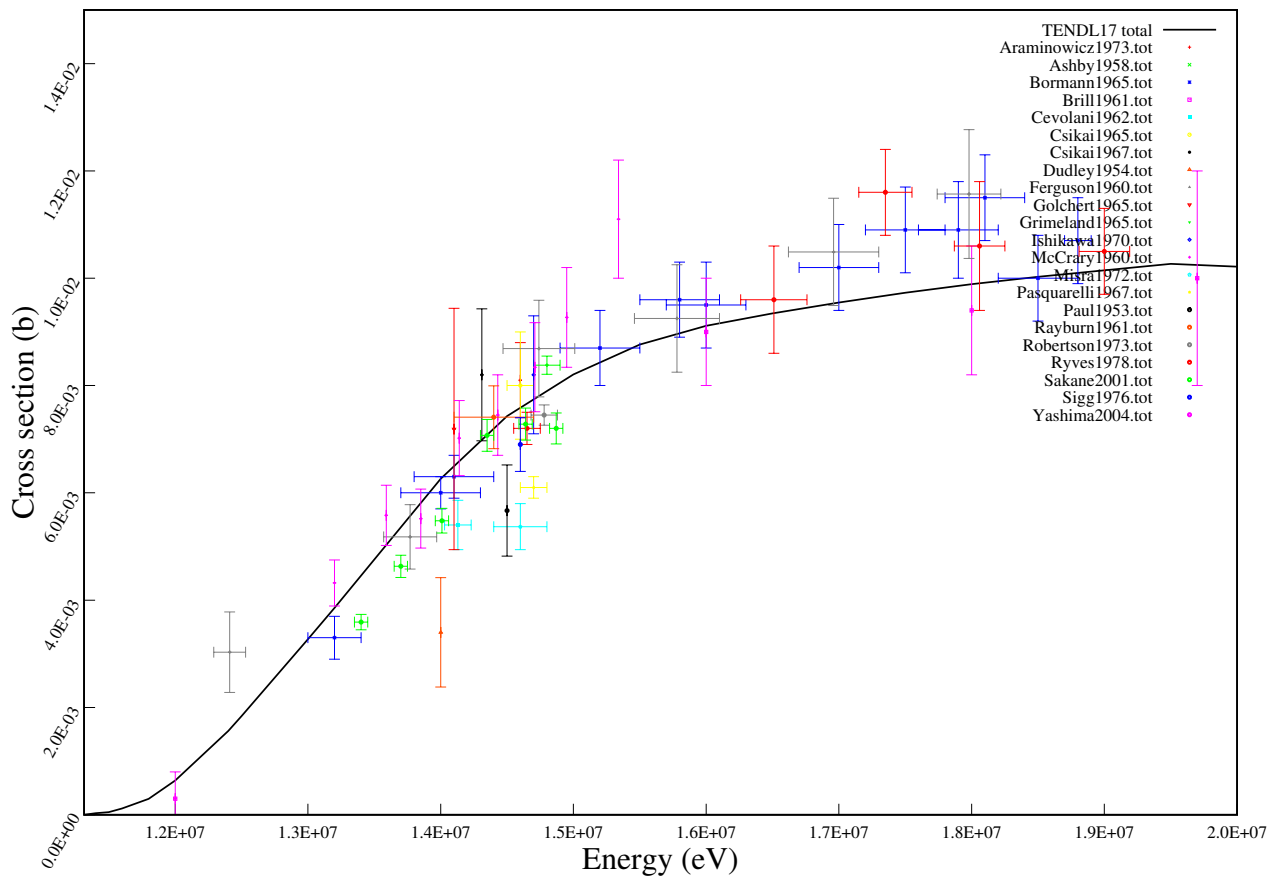
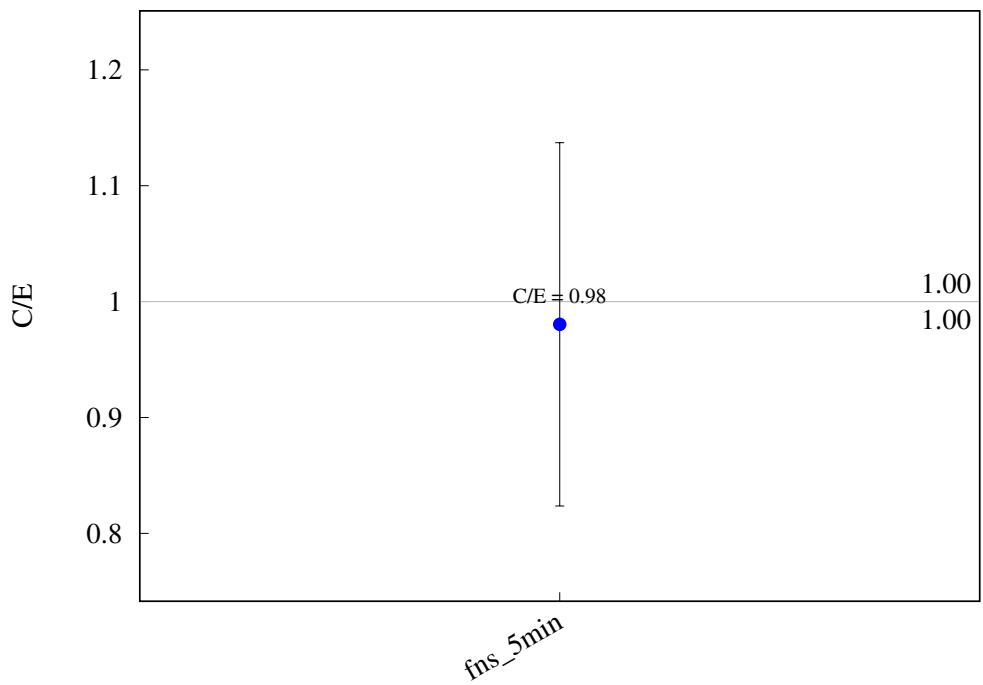
Reaction	Spectrum	$\sigma_{exp}(b)$	$\Delta\sigma_{exp}(b)$	C/E
	fzk_2	5.39E-01	7.24E-02	0.86
	fng_eurofer	1.44E+00	1.66E-01	1.13
W-182(n,p)Ta-182	sneg_1	6.30E-03	2.02E-03	0.88
	fng_tung	3.73E-03	6.19E-04	1.10
	sneg_1	4.44E-03	3.02E-04	1.24
	sneg_2	3.87E-03	8.12E-04	1.13
	fzk_ss316	2.92E-02	3.80E-03	0.16
	fzk_2	7.10E-04	1.06E-04	1.18
	rez_DF	2.92E-03	1.10E-04	1.24
W-182(n,a)Hf-179n	rez_DF	1.85E-05	1.81E-06	12.29
W-183(n,p)Ta-183	sneg_1	5.02E-03	3.45E-04	1.50
	sneg_2	4.88E-03	4.51E-04	1.22
	fng_f82h	4.15E-03	2.71E-04	1.43
W-184(n,p)Ta-184	fns_7hour	2.27E-03	1.59E-04	0.99
	fng_tung	2.63E-03	2.28E-04	0.81
	fng_f82h	1.98E-03	2.94E-04	1.13
	sneg_1	2.78E-03	1.80E-04	1.04
	fzk_ss316	2.13E-03	3.13E-04	1.41
	fzk_2	6.29E-04	9.43E-05	0.81
	rez_DF	1.84E-03	3.78E-05	1.45
W-184(n,t)Ta-182	d-Be	1.20E-02	2.00E-03	0.44
W-184(n,a)Hf-181	fng_tung	6.27E-04	5.39E-05	1.07
	fzk_2	1.66E-04	2.49E-05	1.05
	sneg_1	7.52E-04	5.64E-05	1.22
	sneg_2	5.35E-04	9.64E-05	1.25
	rez_DF	4.14E-04	1.51E-05	2.51
W-186(n,2n)W-185m	fns_5min	3.22E-01	4.18E-02	2.01
	fng_heat	5.64E-01	9.35E-02	1.18
	fng_tung	5.71E-01	9.30E-02	0.97
	sneg_1	7.83E-01	5.64E-02	0.89
W-186(n,2n)W-185	fns_7hour	1.38E+00	2.06E-01	1.28
	fzk_2	4.86E-01	6.84E-02	0.91
	fng_tung	1.34E+00	1.65E-01	1.02
	rez_DF	5.41E-01	1.78E-02	0.88
W-186(n,np)Ta-185	rez_DF	2.73E-03	6.53E-05	1.23
W-186(n,na)Hf-182m	fzk_2	2.00E-06	8.00E-07	0.92
	rez_DF	4.55E-05	6.83E-06	4.05
W-186(n,g)W-187	fng_f82h	3.48E-01	2.46E-02	0.88
	fng_tung	1.29E+00	8.29E-02	0.96
	sneg_1	4.34E-03	3.90E-04	0.27
	fzk_ss316	2.28E-02	1.48E-03	0.57
W-186(n,p)Ta-186	fns_5min	1.26E-03	1.63E-04	1.49
	fng_heat	2.86E-03	1.48E-04	0.69
	fng_tung	1.84E-03	2.75E-04	0.92

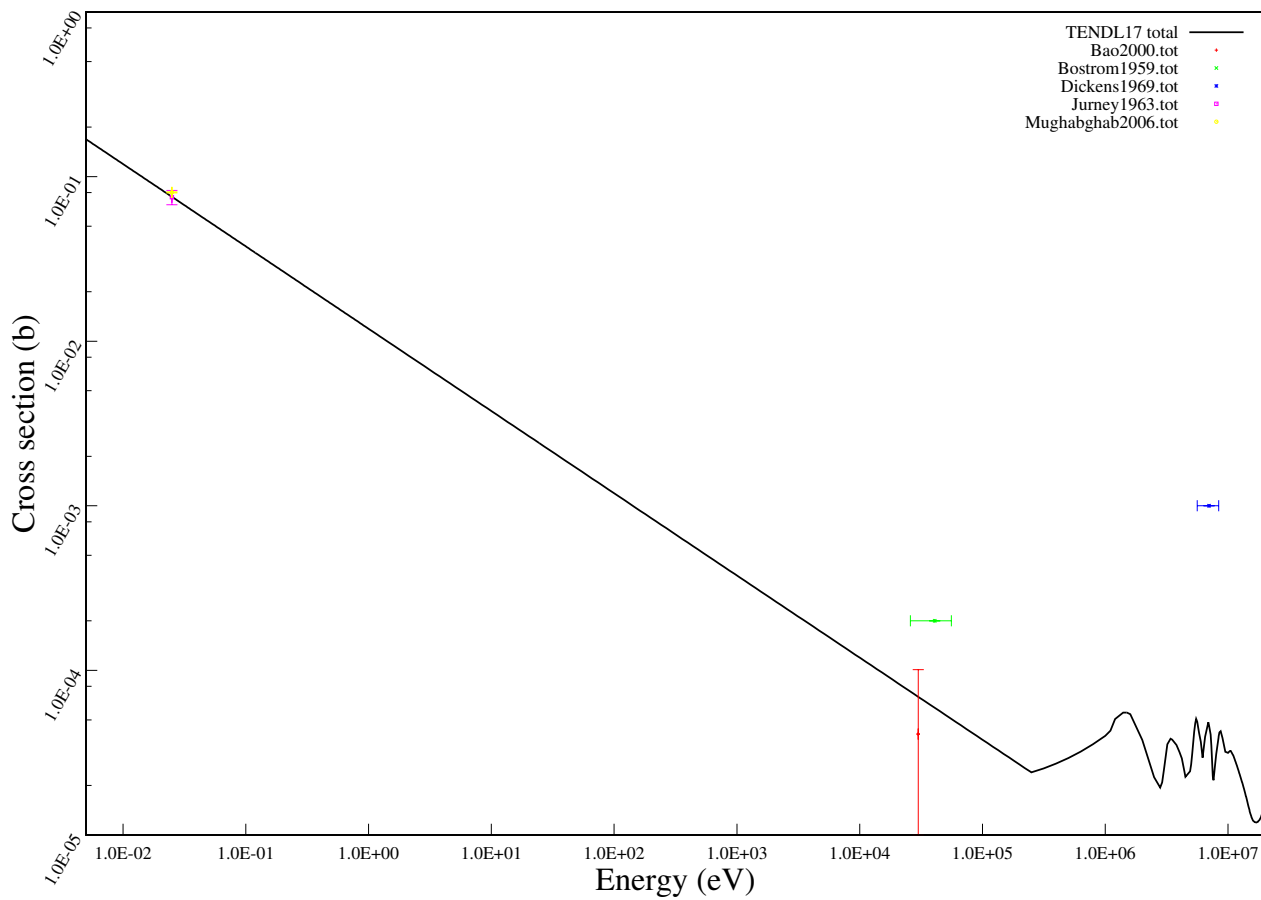
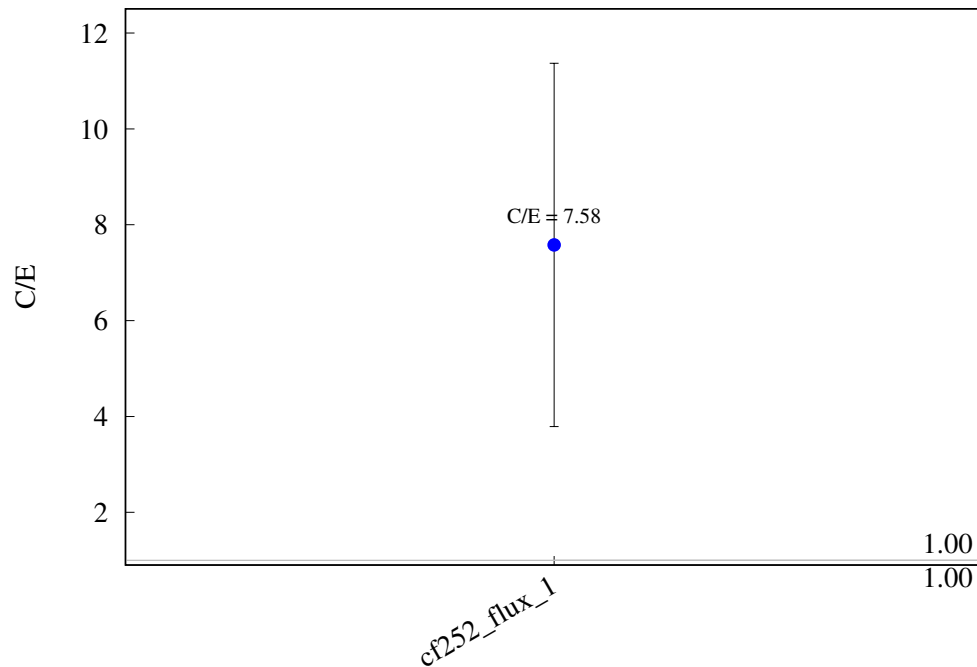
Reaction	Spectrum	$\sigma_{exp}(b)$	$\Delta\sigma_{exp}(b)$	C/E
	fzk_2	5.44E-04	8.16E-05	0.87
	sneg_1	2.29E-03	3.66E-04	1.02
W-186(n,h)Hf-184	d-Be2a	1.18E-04	3.23E-05	2.20
W-186(n,a)Hf-183	fng_tung	5.33E-04	8.43E-05	0.84
	fzk_2	1.27E-04	1.90E-05	1.03
	sneg_1	7.18E-04	1.08E-04	0.85
	d-Be2a	1.40E-03	2.15E-04	2.19
	rez_DF	4.62E-04	2.31E-05	2.26
Re-185(n,2n)Re-184g	fns_7hour	1.66E+00	8.30E-02	1.02
	fng_heat	2.58E+00	2.17E-01	0.63
	fng_Re	1.87E+00	2.82E-01	0.87
Re-185(n,2n)Re-184m	fns_7hour	3.73E-01	2.24E-02	1.01
	fng_Re	2.99E-01	6.46E-02	1.23
Re-185(n,3n)Re-183	fng_Re	4.41E-02	1.37E-02	1.39
Re-185(n,p)W-185m	fns_5min	1.37E-03	1.64E-04	1.13
Re-187(n,2n)Re-186g	fns_7hour	1.60E+00	1.60E-01	1.14
	fns_5min	1.42E+00	1.28E-01	1.17
	fng_heat	9.54E-01	5.25E-02	1.78
	fng_Re	1.86E+00	2.64E-01	0.92
Re-187(n,g)Re-188m	fng_Re	7.02E-03	4.46E-03	1.27
	fns_5min	3.98E-03	3.58E-04	1.19
Re-187(n,g)Re-188	fng_Re	3.19E-01	6.93E-02	0.65
Re-187(n,p)W-187	fng_Re	4.43E-03	6.55E-04	1.04
Re-187(n,t)W-185	d-Be	3.30E-03	5.63E-04	2.26
Re-187(n,a)Ta-184	fng_Re	7.10E-04	1.59E-04	0.99
Os-192(n,2n)Os-191m	fns_5min	2.42E-01	3.14E-02	3.22
Ir-193(n,2n)Ir-192m	fns_5min	1.87E-01	2.81E-02	0.98
Pt-198(n,2n)Pt-197m	fns_5min	8.09E-01	6.47E-02	1.27
Au-197(n,2n)Au-196m	fns_5min	1.03E+00	4.18E-02	1.16
Au-197(n,2n)Au-196n	fns_5min	9.17E-02	5.50E-03	1.30
	rez_DF	3.46E-02	1.73E-03	1.17
Au-197(n,2n)Au-196	cf252_flux_1	4.30E-03	5.00E-04	1.30
	cf252_flux_1	5.27E-03	2.26E-04	1.06
	cf252_flux_1	5.25E-03	3.10E-04	1.06
	cf252_flux_1	5.80E-03	2.90E-04	0.96
	cf252_flux_1	5.50E-03	1.40E-04	1.02
	rez_DF	4.99E-01	2.00E-02	1.01
Au-197(n,3n)Au-195	rez_DF	2.75E-01	1.38E-02	1.00
Au-197(n,4n)Au-194	rez_DF	2.88E-02	8.64E-04	0.87
Au-197(n,g)Au-198	cf252_flux_1	1.10E-01	5.00E-03	0.67
	cf252_flux_1	7.70E-02	7.70E-05	0.96
	cf252_flux_1	7.80E-02	3.00E-03	0.95
Au-197(n,t)Pt-195	d-Be	3.90E-03	9.00E-04	1.39

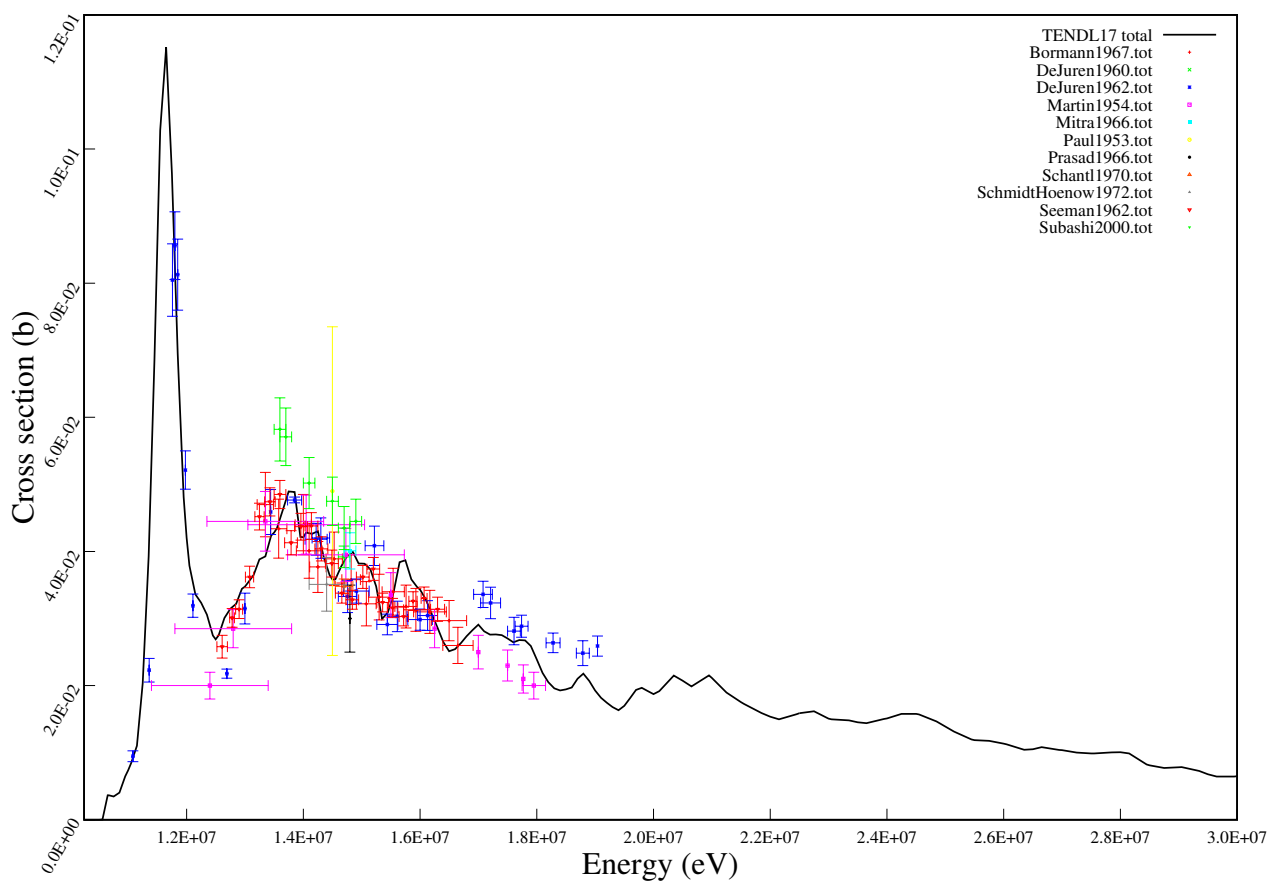
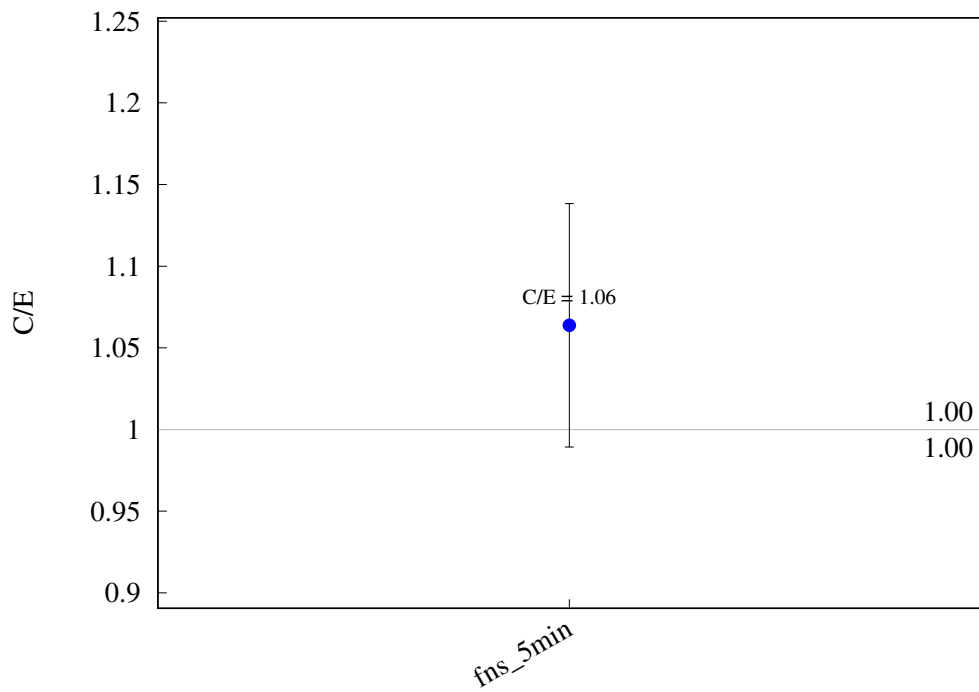
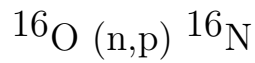
Reaction	Spectrum	$\sigma_{exp}(b)$	$\Delta\sigma_{exp}(b)$	C/E
Au-197(n,h)Ir-195g	d-Be2a	1.07E-04	3.23E-05	2.49
Au-197(n,h)Ir-195	d-Be2a	8.03E-05	1.95E-05	3.32
Au-197(n,a)Ir-194g	d-Be2a	1.44E-03	2.15E-04	1.88
Au-197(n,a)Ir-194m	d-Be2a	1.07E-04	2.15E-05	0.00
Hg-198(n,g)Hg-199	cf252_flux_1	1.68E-01	6.00E-03	0.32
Hg-200(n,2n)Hg-199m	fns_5min	7.87E-01	6.30E-02	1.15
Tl-203(n,2n)Tl-202	fns_5min	1.41E+00	1.97E-01	1.22
Tl-205(n,g)Tl-206	fns_5min	1.85E-03	9.26E-05	1.52
Tl-205(n,p)Hg-205	fns_5min	1.58E-03	9.45E-05	1.26
Tl-205(n,t)Hg-203	d-Be3	6.07E-04	2.80E-04	1.54
	d-Be	4.60E-03	1.35E-03	2.13
	d-Be	2.00E-02	4.00E-03	0.49
Pb-204(n,n)Pb-204m	fns_5min	4.60E-02	1.75E-02	2.01
	fng_heat	8.15E-02	3.83E-03	1.12
	tud_Pb	6.19E-02	5.63E-03	1.50
Pb-204(n,2n)Pb-203m	fns_5min	1.40E+00	8.38E-02	0.72
Pb-204(n,2n)Pb-203	fns_7hour	2.13E+00	1.07E-01	0.94
	tud_Pb	1.94E+00	1.67E-01	0.95
Pb-206(n,a)Hg-203	tud_Pb	5.02E-04	5.42E-05	1.02
	fns_7hour	1.57E-03	1.00E-03	0.34
Pb-208(n,p)Tl-208	fns_5min	9.98E-04	5.99E-05	0.74
	tud_Pb	8.38E-04	8.88E-05	0.73
Pb-208(n,t)Tl-206	d-Be3	5.81E-04	1.76E-04	0.59
	d-Be	1.60E-02	3.00E-03	0.31
Bi-209(n,3n)Bi-207	rez_DF	2.96E-01	2.09E-02	0.89
Bi-209(n,4n)Bi-206	rez_DF	3.01E-02	8.53E-04	0.83
Bi-209(n,p)Pb-209	fns_5min	1.09E-03	3.10E-03	1.96
Bi-209(n,t)Pb-207	d-Be3	7.80E-04	2.50E-04	0.56
	d-Be	3.70E-03	7.00E-04	1.02
Bi-209(n,h)Tl-207	d-Be2a	6.14E-05	2.05E-05	4.69
Bi-209(n,a)Tl-206	fns_5min	3.26E-04	5.21E-05	3.33
Th-232(n,f)	cf252_flux_1	8.94E-02	2.40E-03	0.90
	cf252_flux_1	8.47E-02	4.90E-03	0.95
Pa-231(n,f)	cf252_flux_1	9.70E-01	4.50E-02	0.89
U-233(n,f)	cf252_flux_1	1.95E+00	3.12E-02	0.98
	cf252_flux_1	1.89E+00	4.80E-02	1.01
U-234(n,f)	cf252_flux_1	1.20E+00	1.40E-02	1.00
U-235(n,f)	cf252_flux_1	1.27E+00	1.82E-02	0.96
	cf252_flux_1	1.21E+00	2.20E-02	1.01
	cf252_flux_1	1.22E+00	1.90E-02	1.00
	cf252_flux_1	1.05E+00	3.10E-02	1.17
	cf252_flux_1	1.23E+00	1.70E-02	1.00
U-236(n,f)	cf252_flux_1	6.12E-01	8.00E-03	0.98

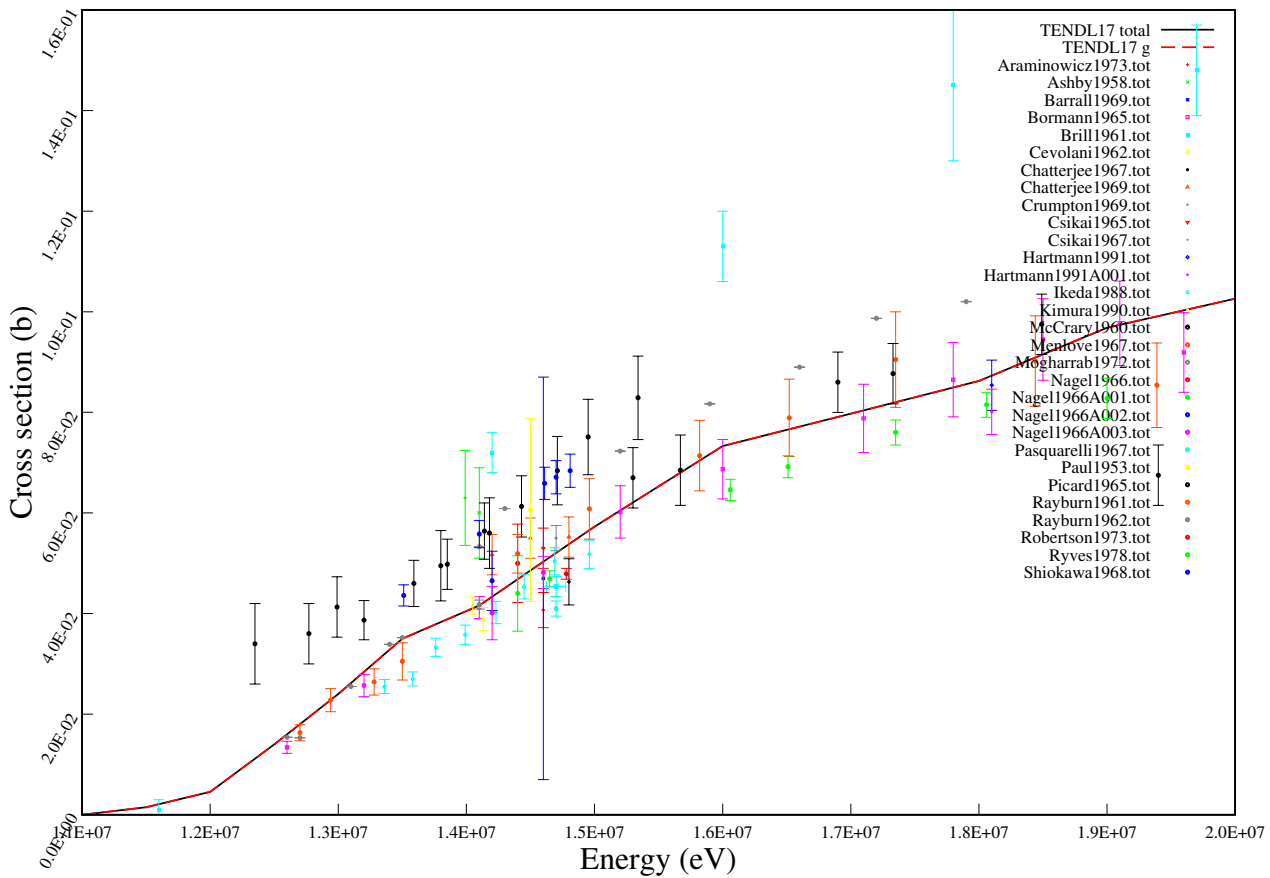
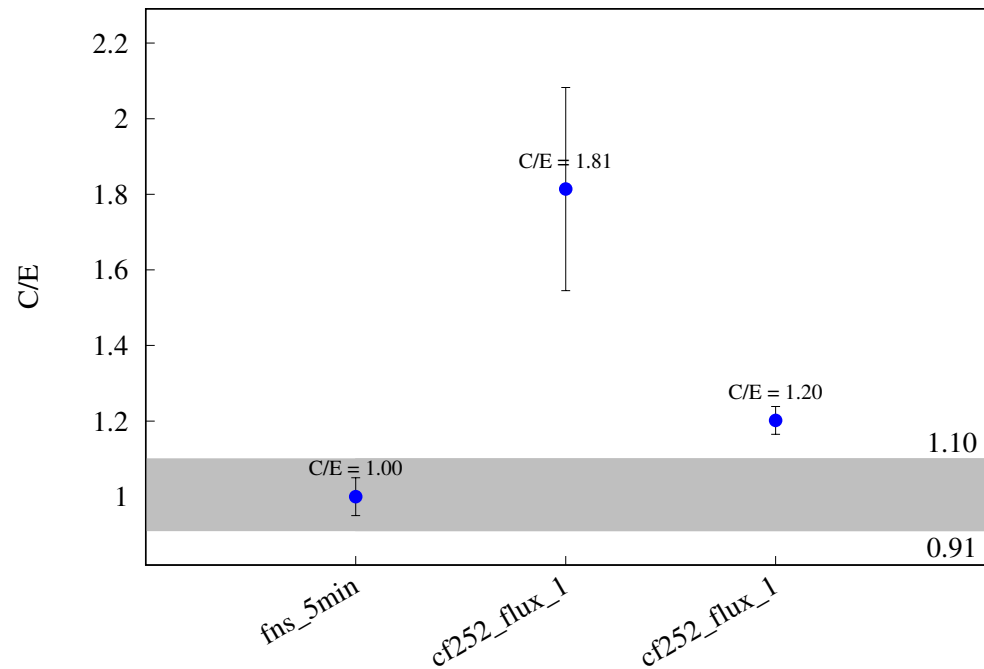
Reaction	Spectrum	$\sigma_{exp}(b)$	$\Delta\sigma_{exp}(b)$	C/E
U-238(n,2n)U-237	cf252_flux_1	1.92E-01	1.90E-03	0.11
	cf252_flux_1	1.22E-02	1.50E-03	1.75
U-238(n,f)	cf252_flux_1	3.29E-01	1.00E-02	0.98
	cf252_flux_1	3.24E-01	1.40E-02	0.99
	cf252_flux_1	2.88E-01	7.00E-03	1.12
	cf252_flux_1	3.08E-01	1.70E-02	1.04
	cf252_flux_1	3.32E-01	5.00E-03	0.97
	cf252_flux_1	3.11E-01	1.40E-02	1.03
Np-237(n,2n)Np-236m	cf252_flux_1	4.66E-03	4.66E-04	0.25
Np-237(n,f)	cf252_flux_1	1.26E+00	6.00E-02	1.07
	cf252_flux_1	1.38E+00	1.00E-01	0.98
	cf252_flux_1	1.37E+00	2.00E-02	0.98
	cf252_flux_1	1.44E+00	2.29E-02	0.94
Pu-239(n,f)	cf252_flux_1	1.80E+00	6.00E-02	1.00
	cf252_flux_1	1.84E+00	2.40E-02	0.98
	cf252_flux_1	1.86E+00	3.01E-02	0.97
	cf252_flux_1	1.79E+00	4.10E-02	1.00
Pu-240(n,f)	cf252_flux_1	1.34E+00	3.20E-02	1.02
	cf252_flux_1	1.31E+00	3.00E-02	1.05
Pu-241(n,f)	cf252_flux_1	1.62E+00	8.00E-02	1.00
	cf252_flux_1	1.74E+00	5.40E-02	0.93
Am-243(n,f)	cf252_flux_1	1.14E+00	2.30E-02	0.96

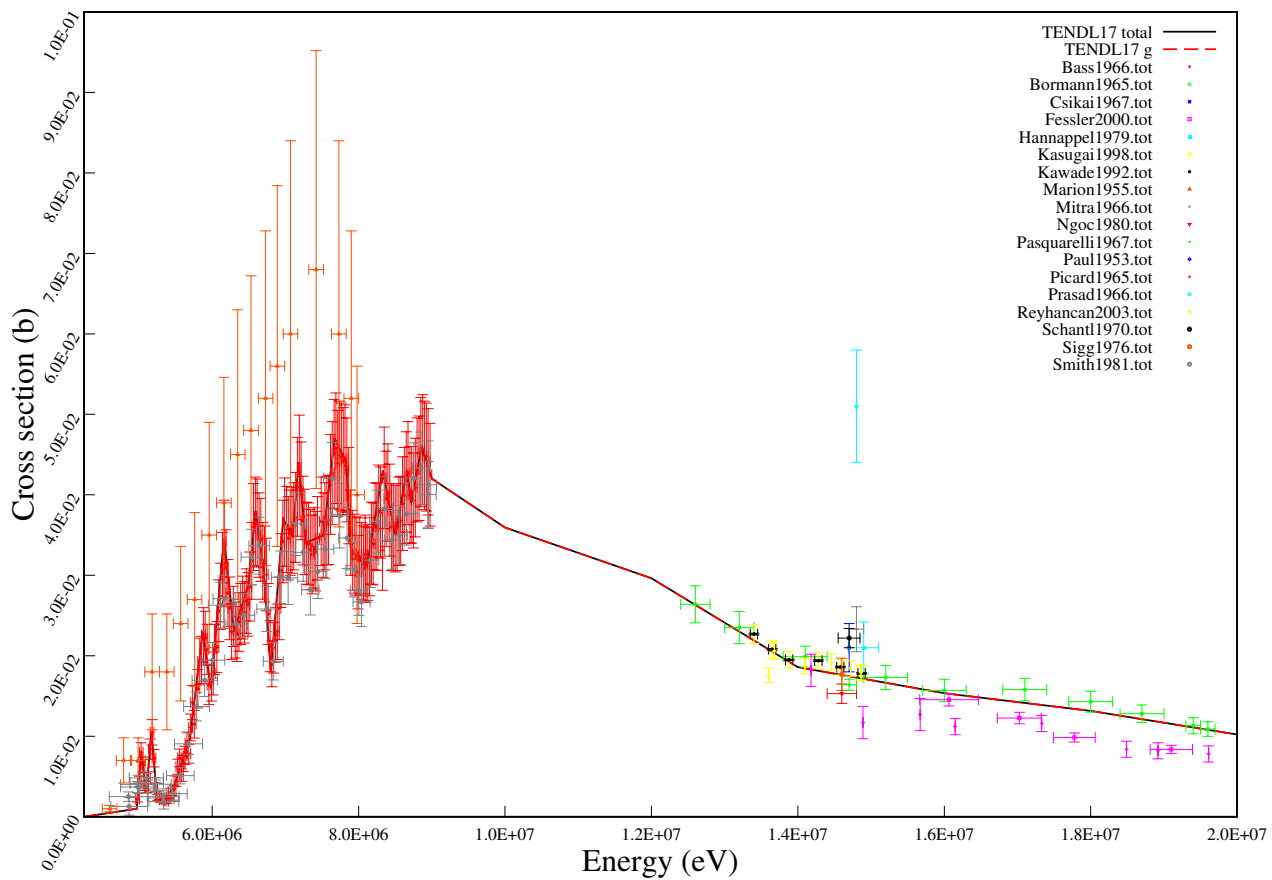
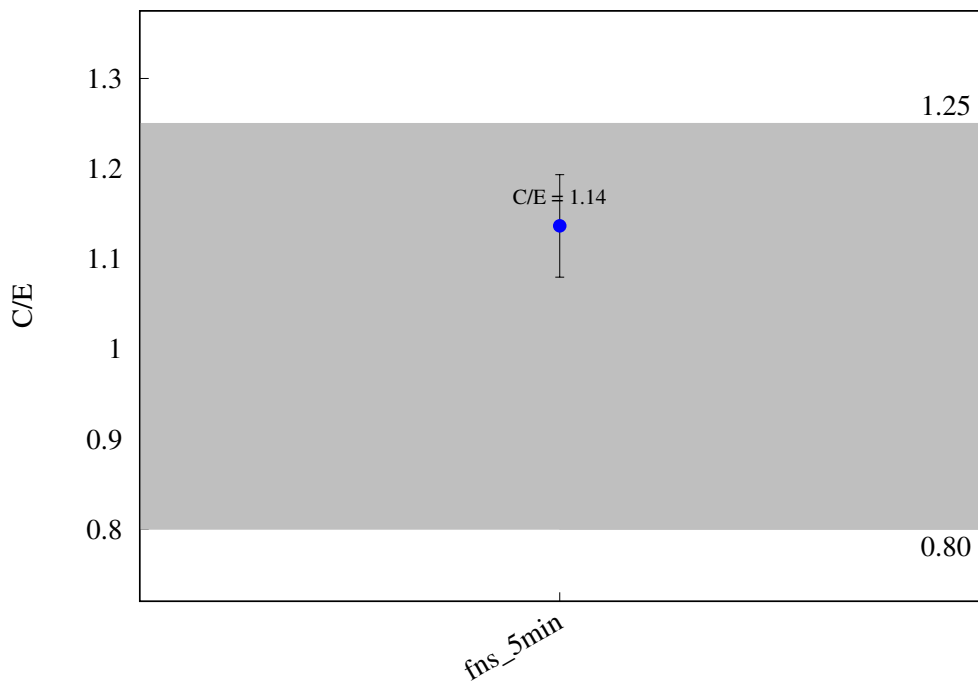
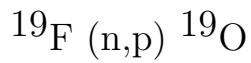


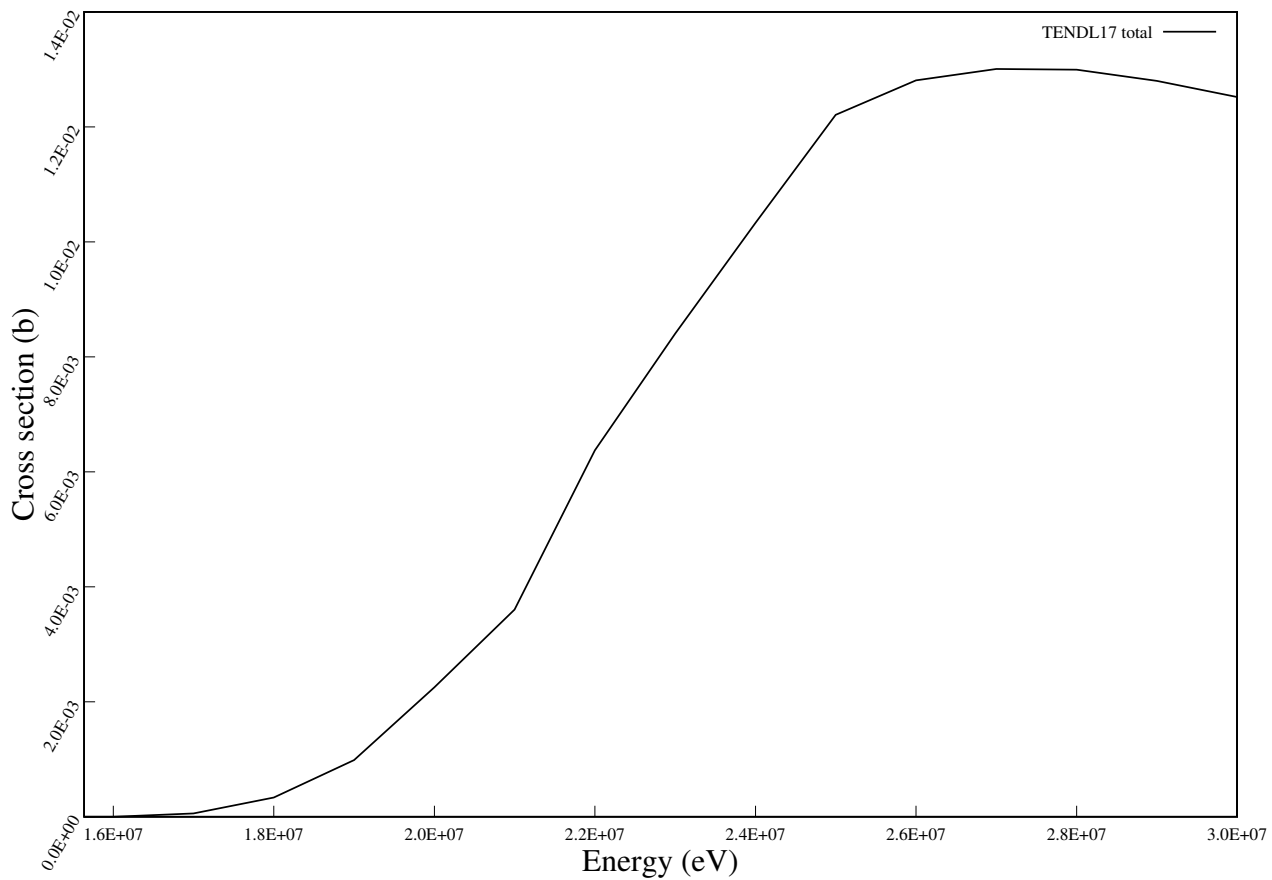
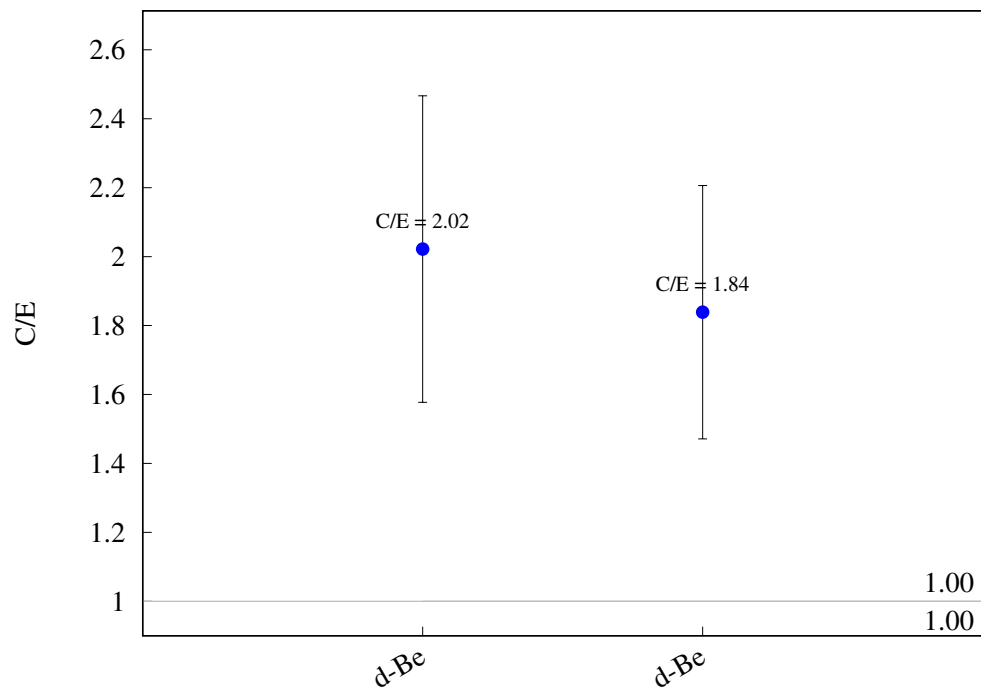
^{14}N (n,2n) ^{13}N 

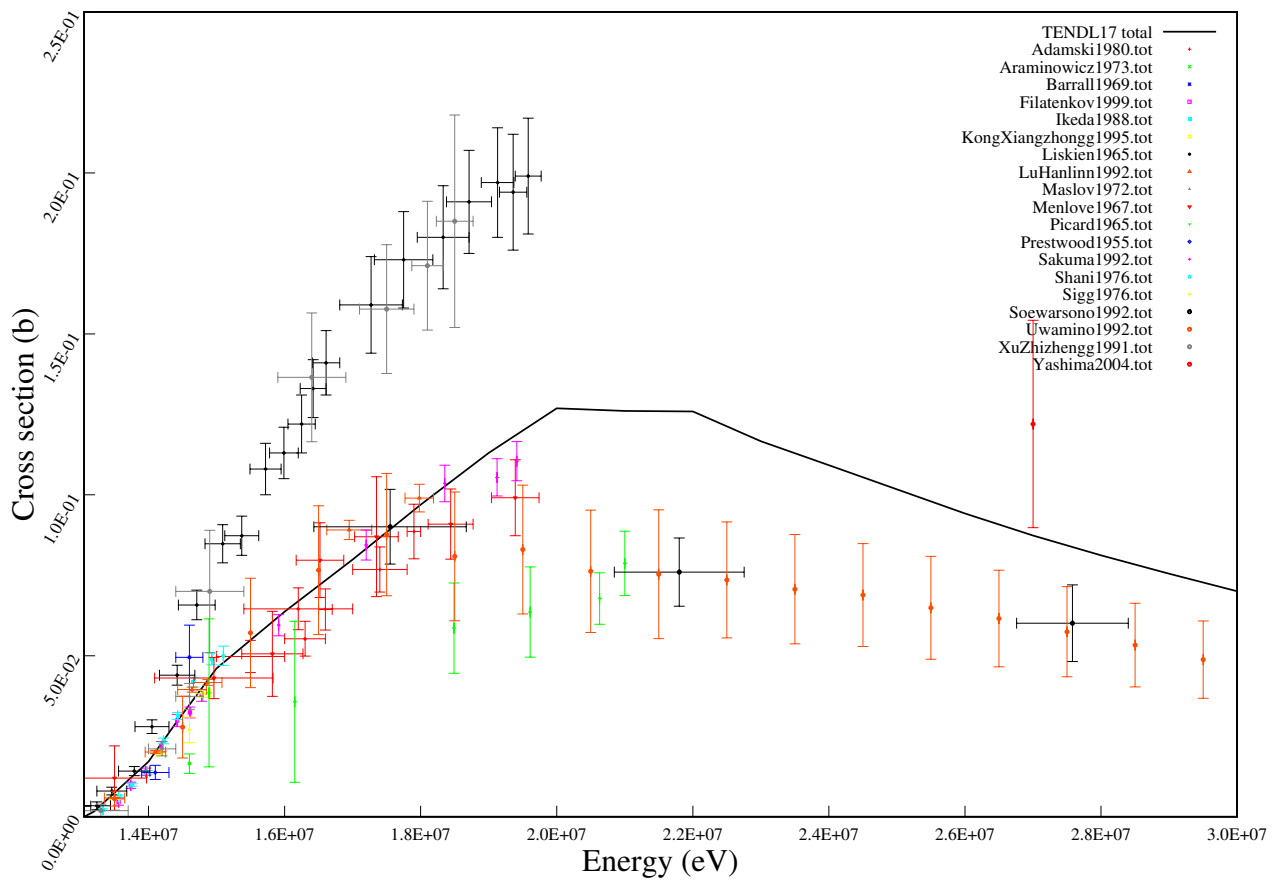
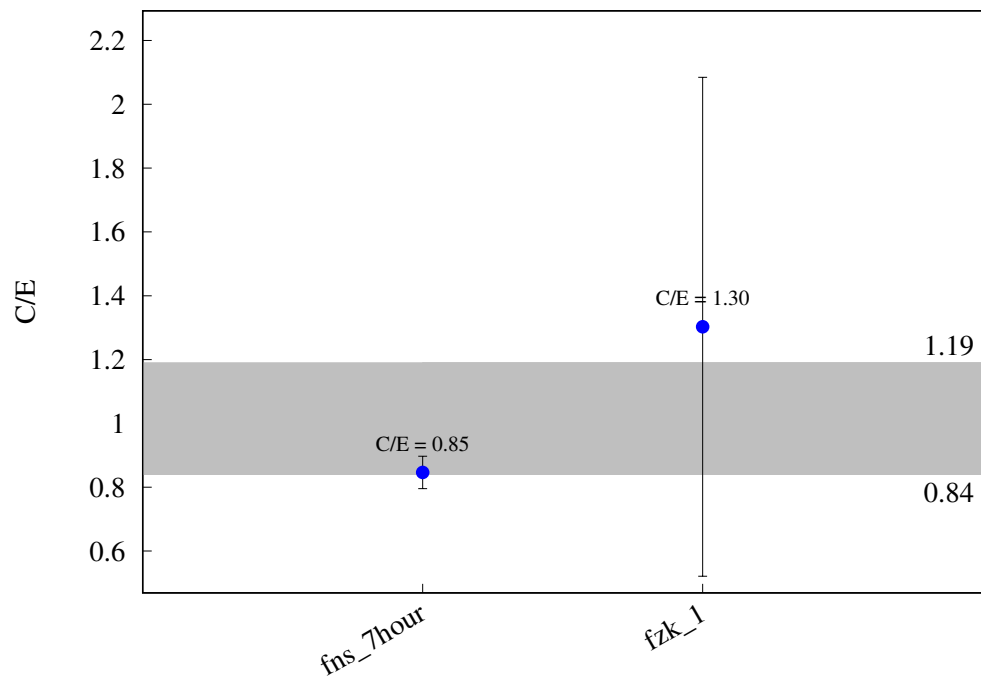
^{14}N (n,g) ^{15}N 

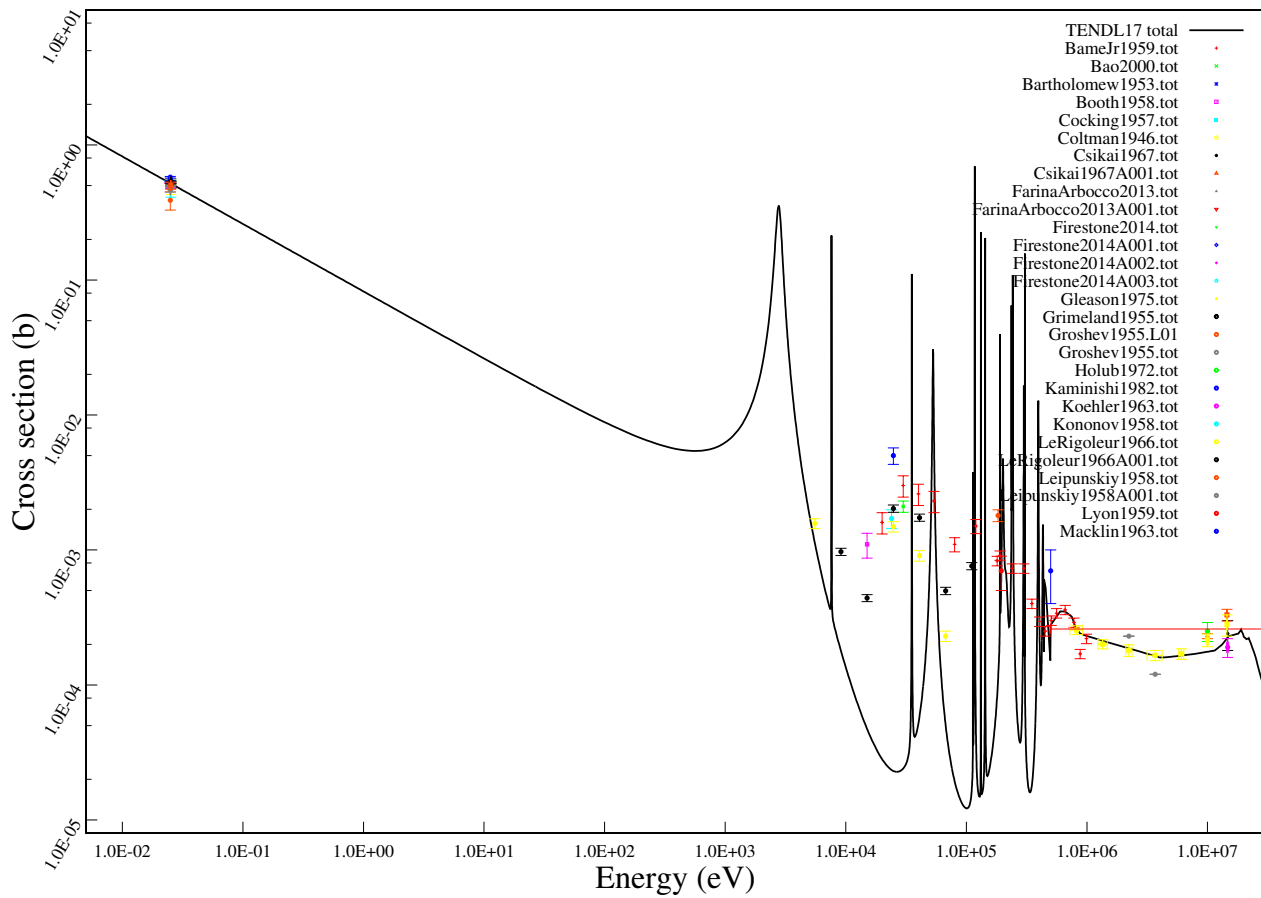
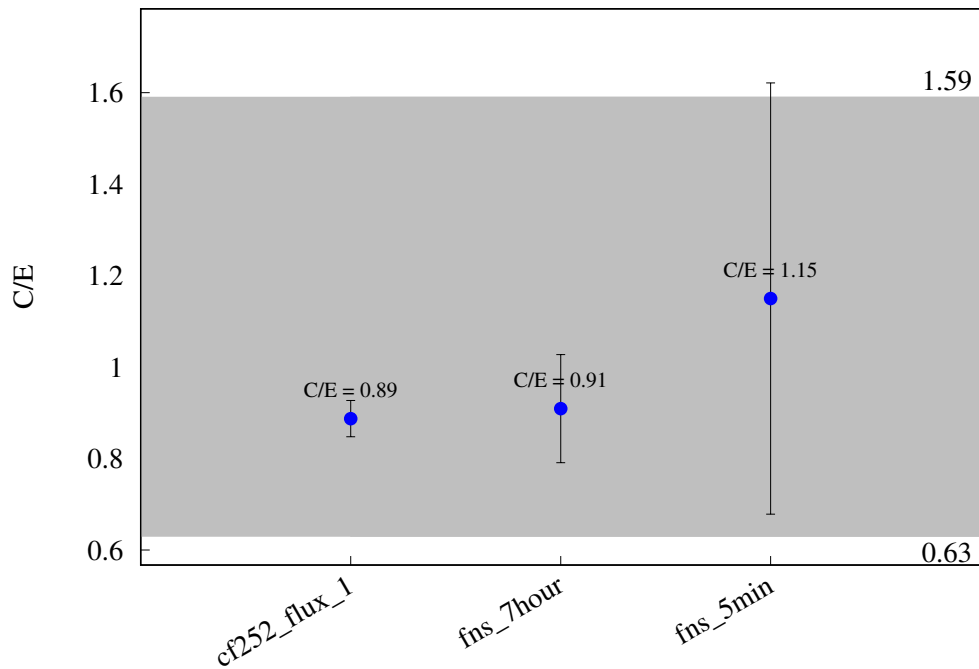


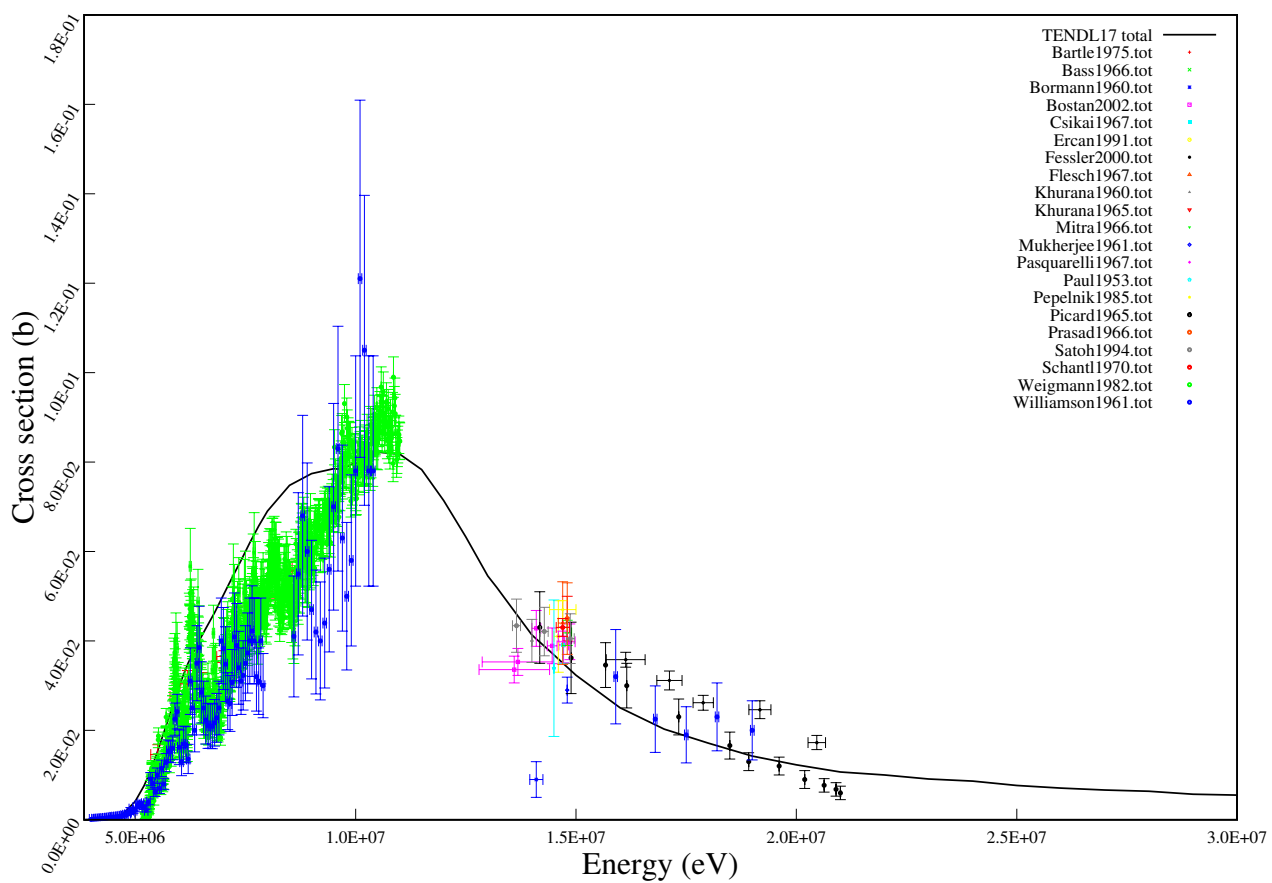
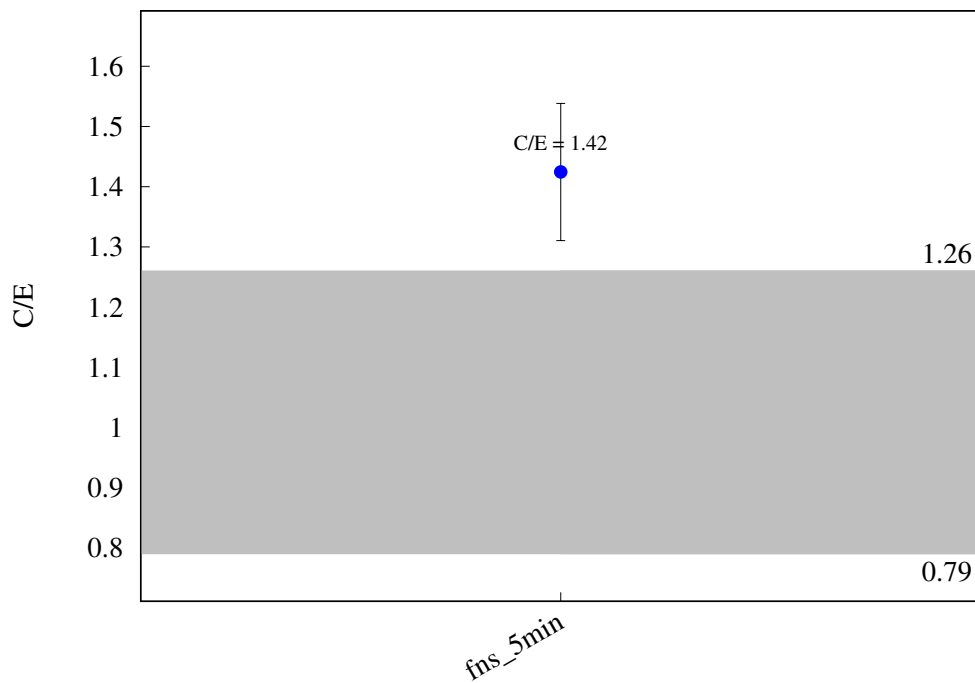
^{19}F (n,2n) ^{18}F 

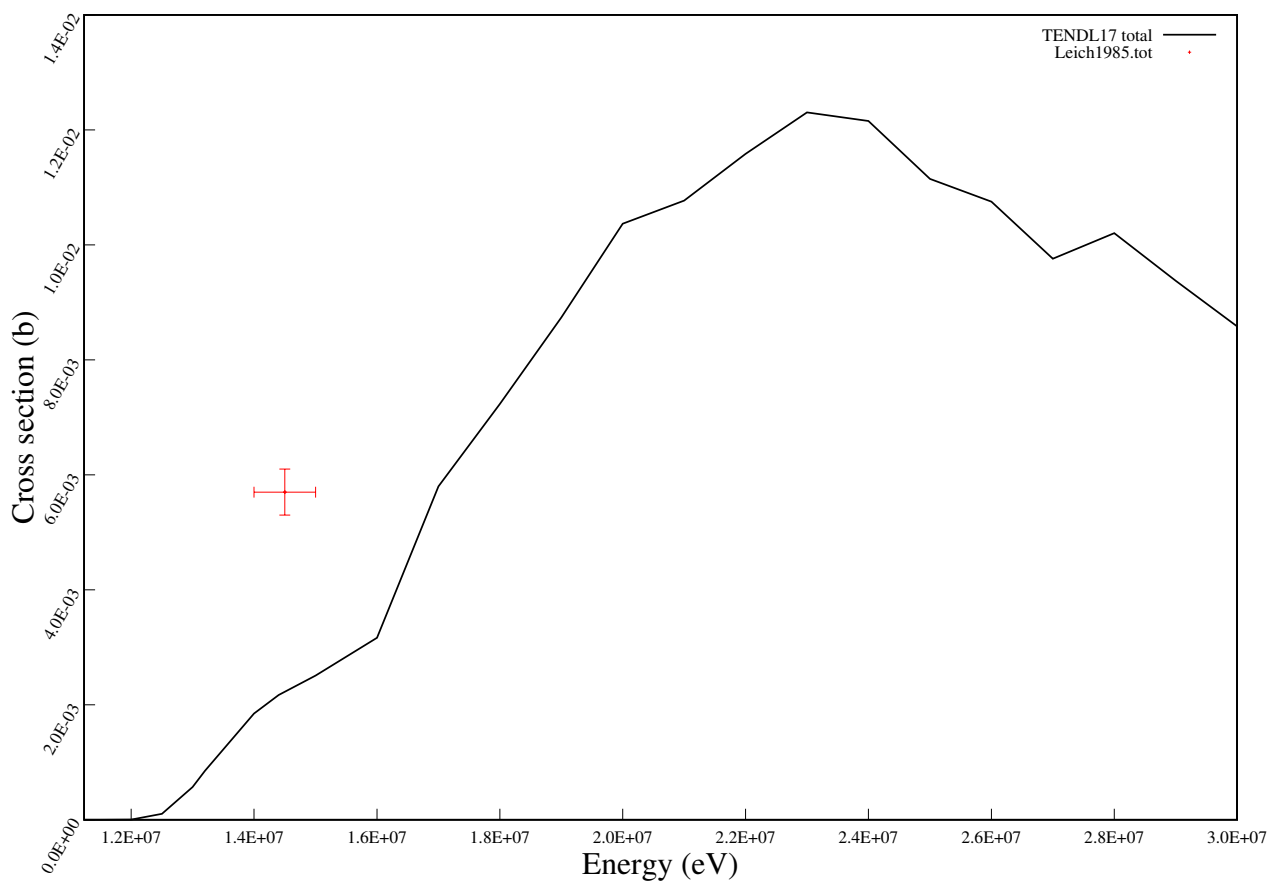
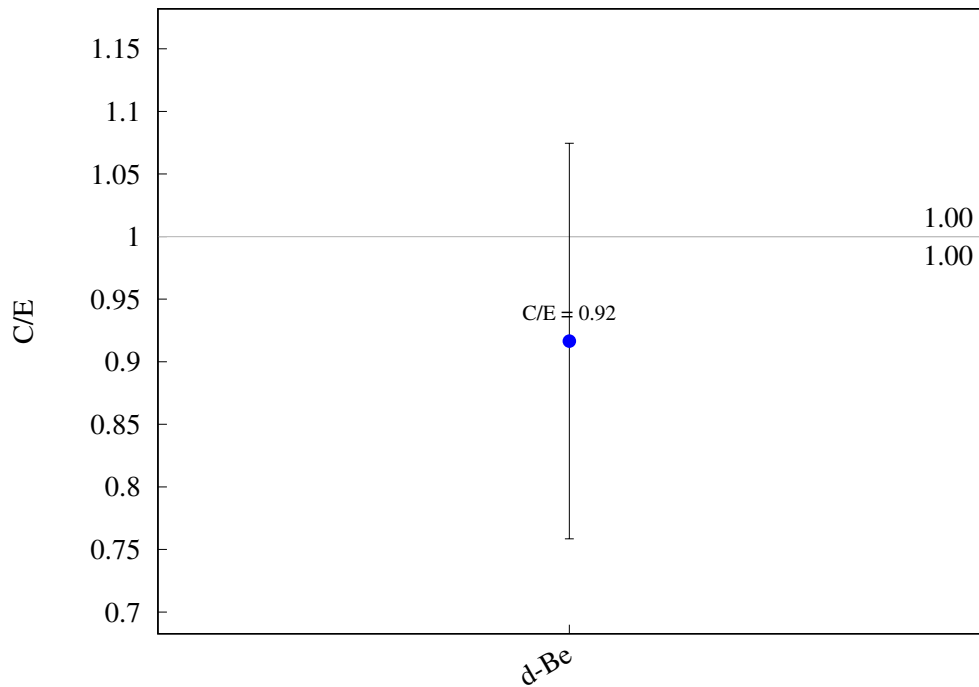


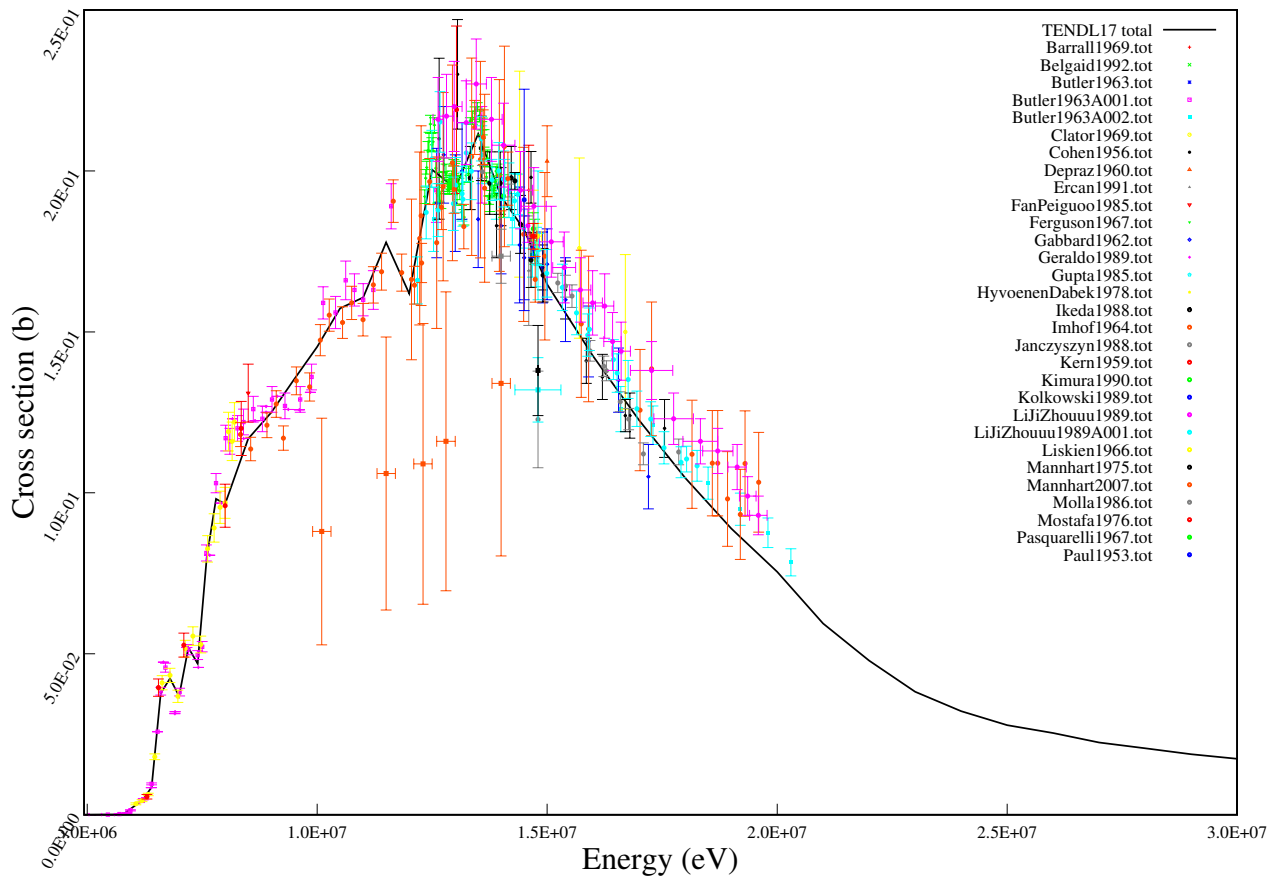
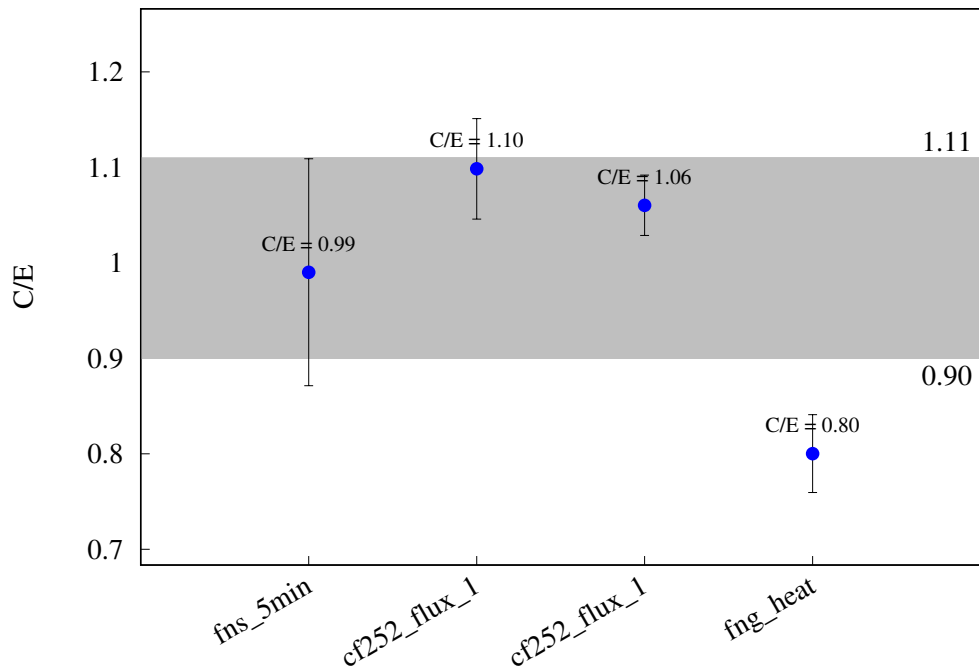
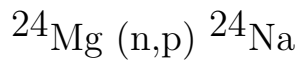
^{20}Ne (n,t) ^{18}F 

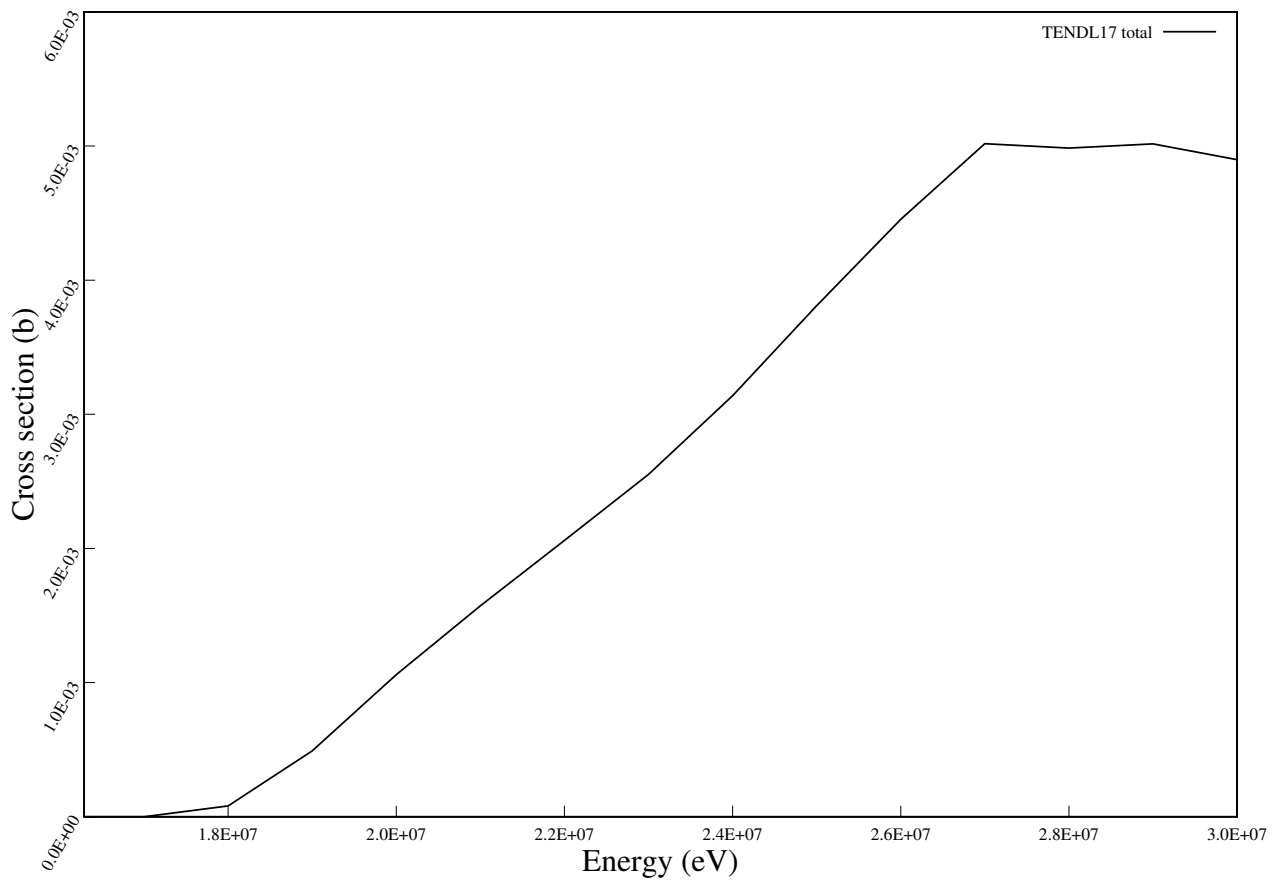
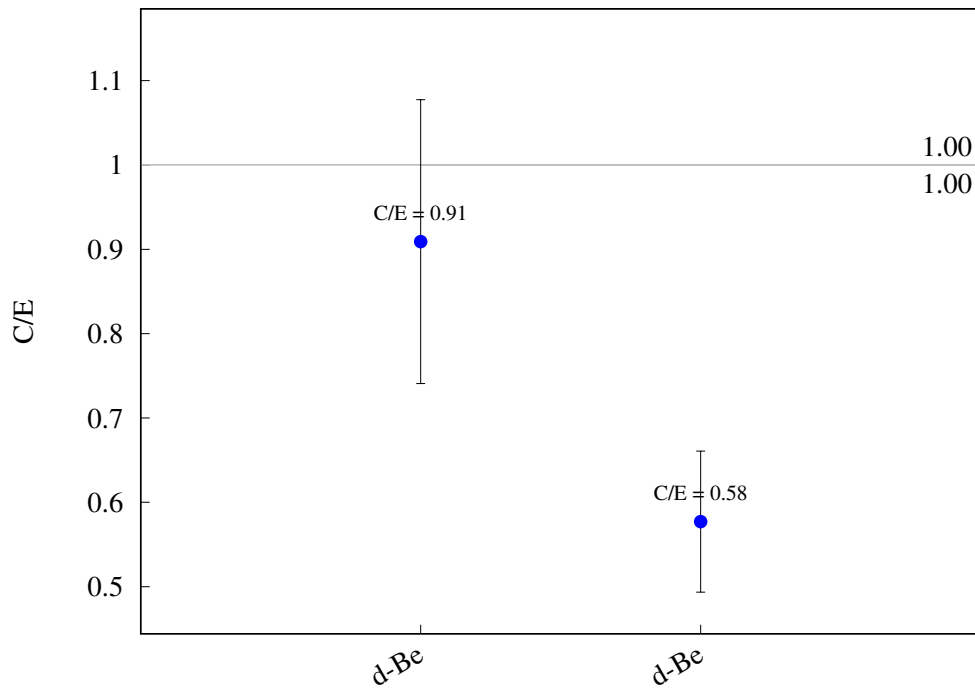
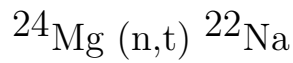
^{23}Na (n,2n) ^{22}Na 

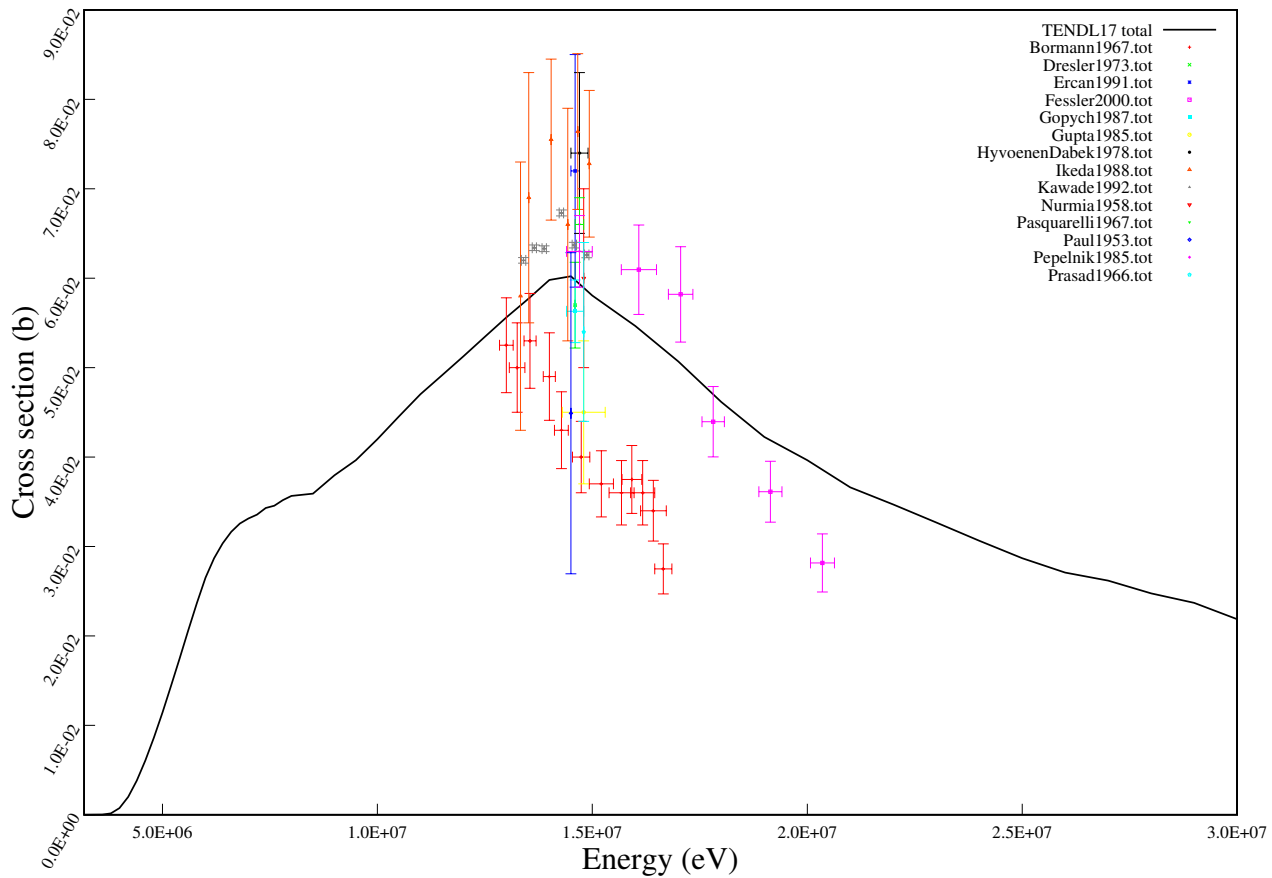
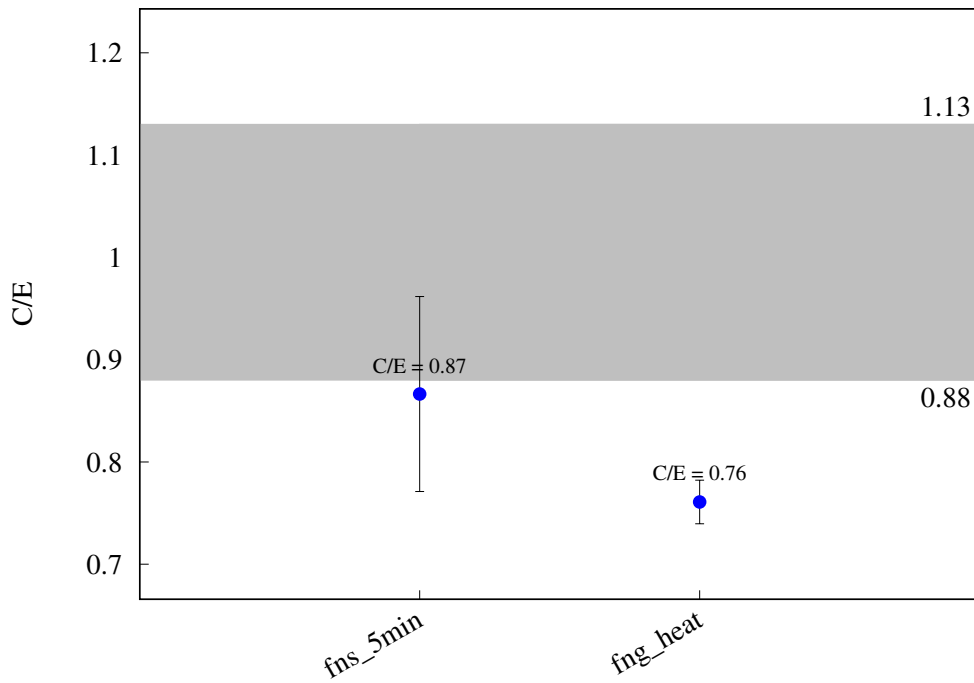
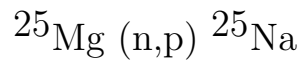
^{23}Na (n,g) ^{24}Na 

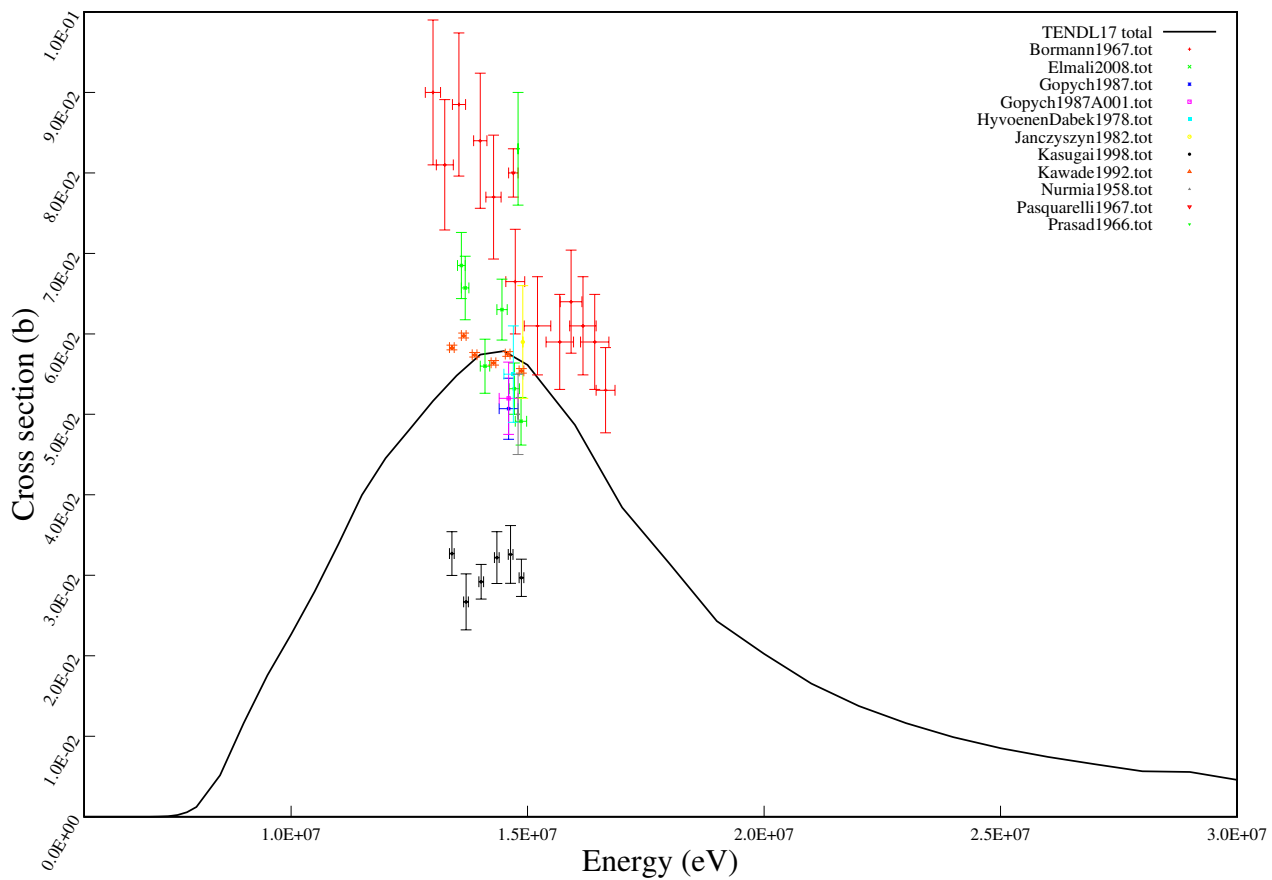
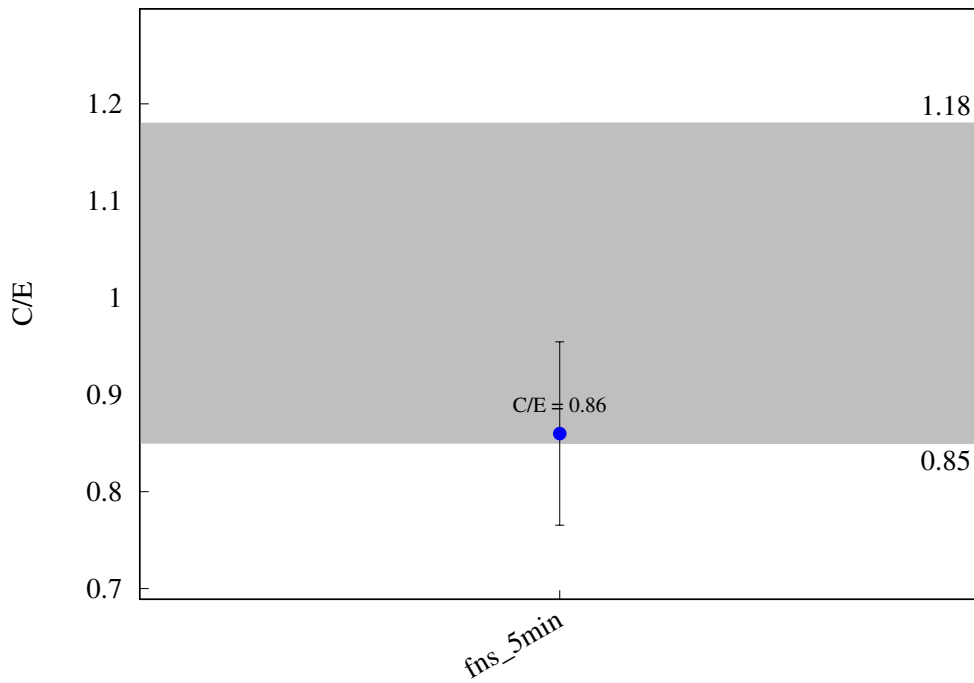
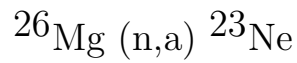
^{23}Na (n,p) ^{23}Ne 

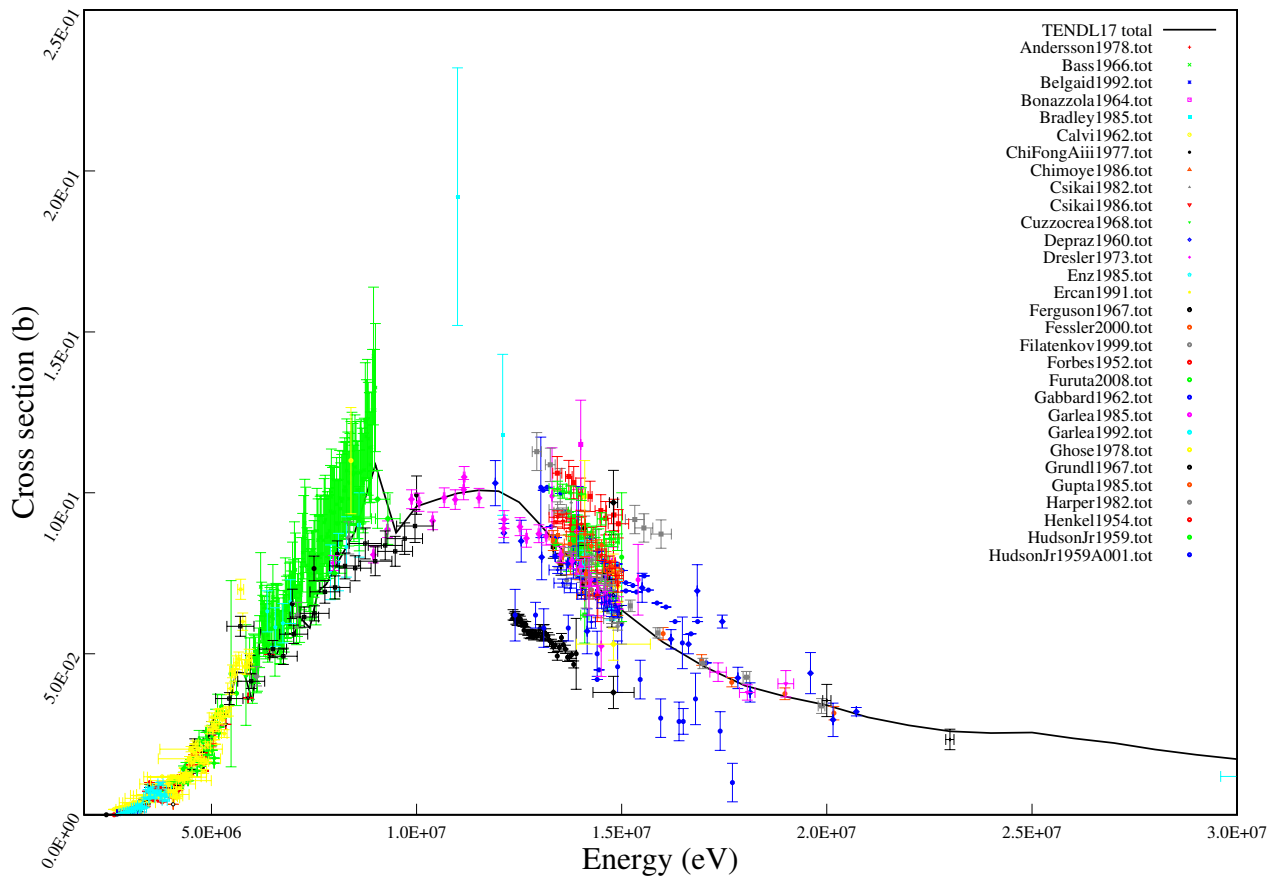
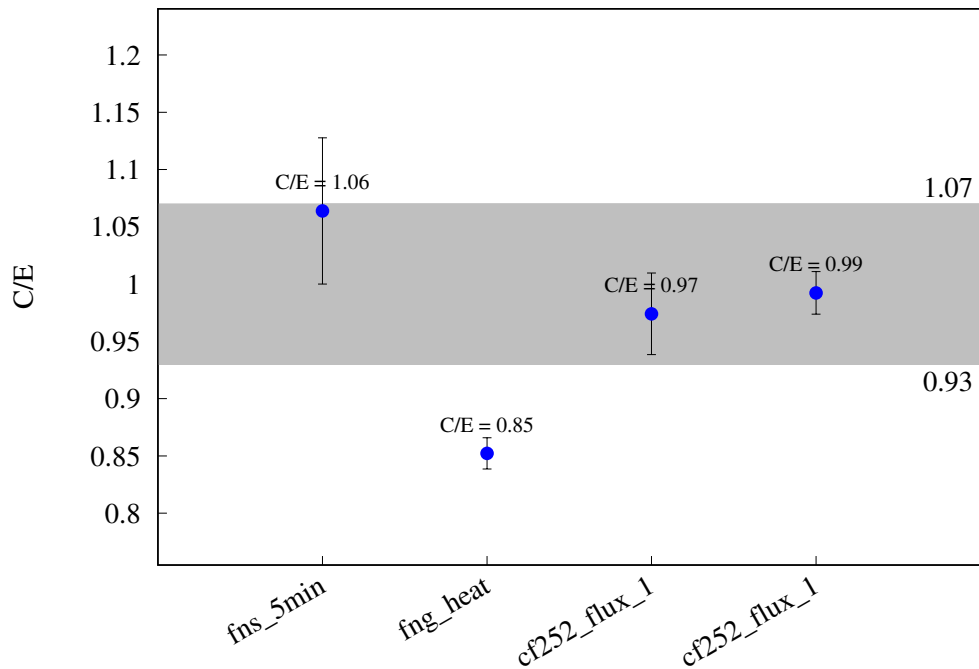
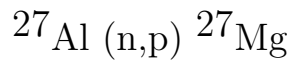
$^{23}\text{Na} (\text{n},\text{t}) ^{21}\text{Ne}$ 

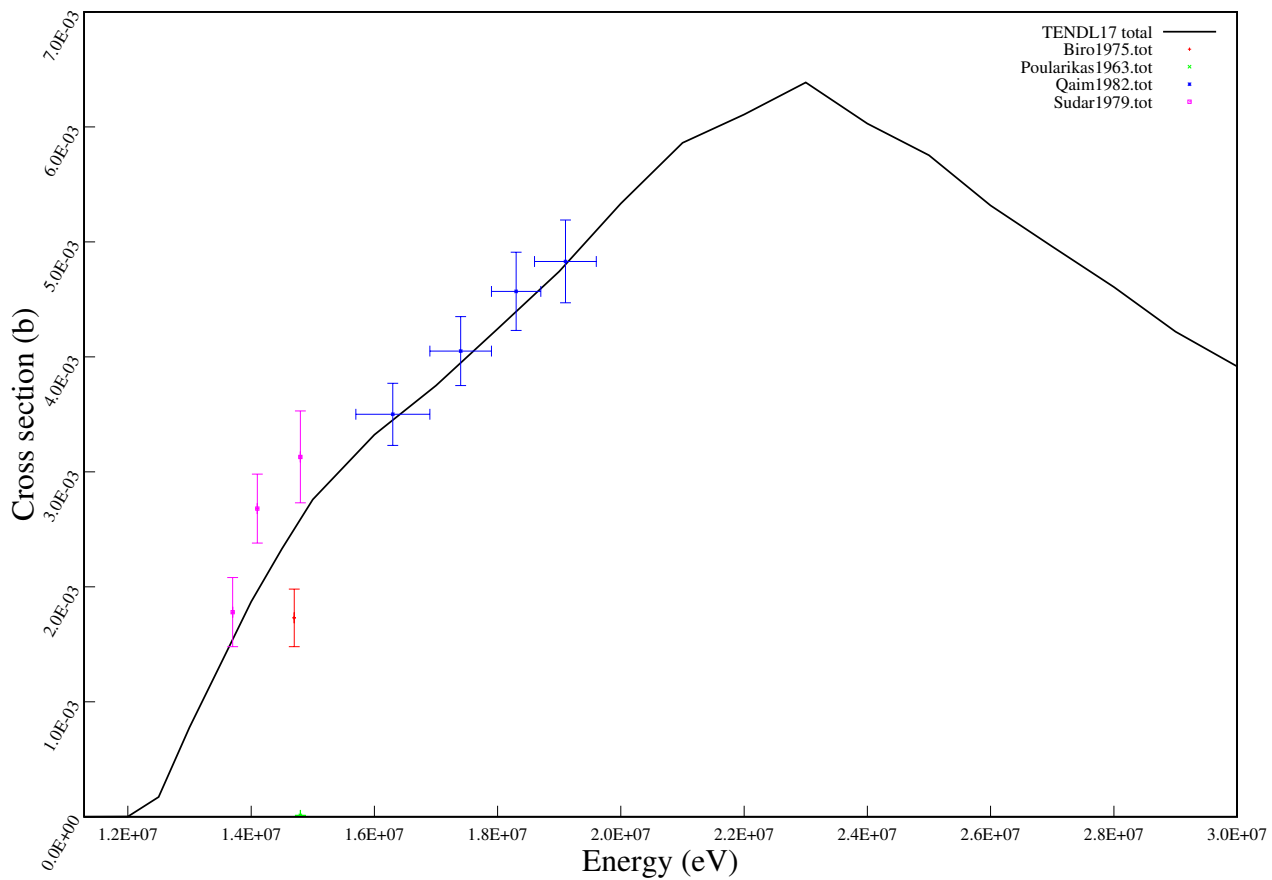
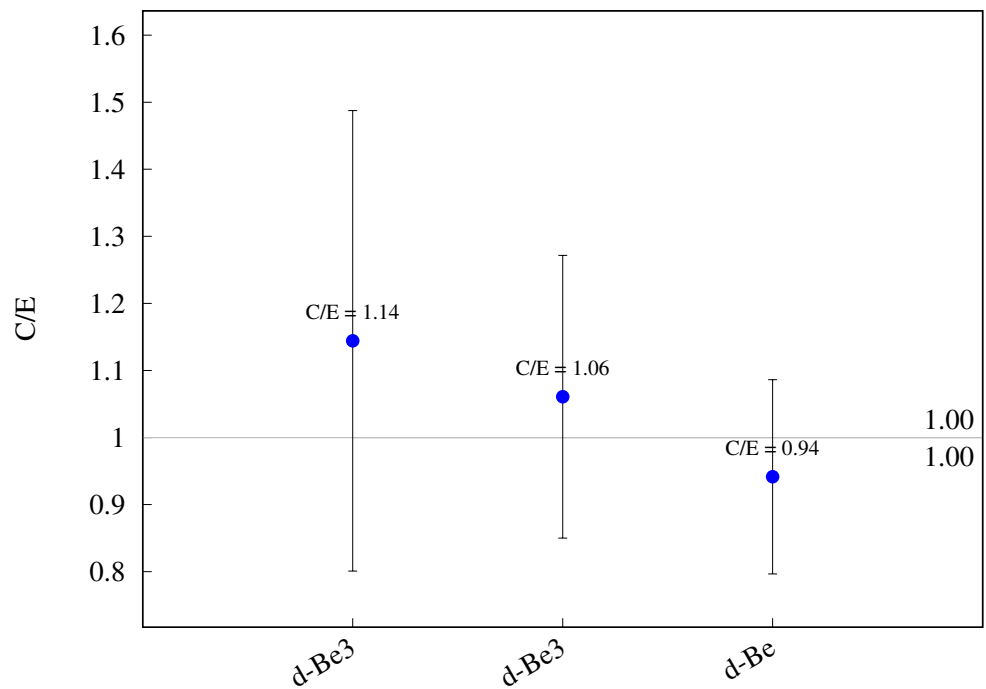


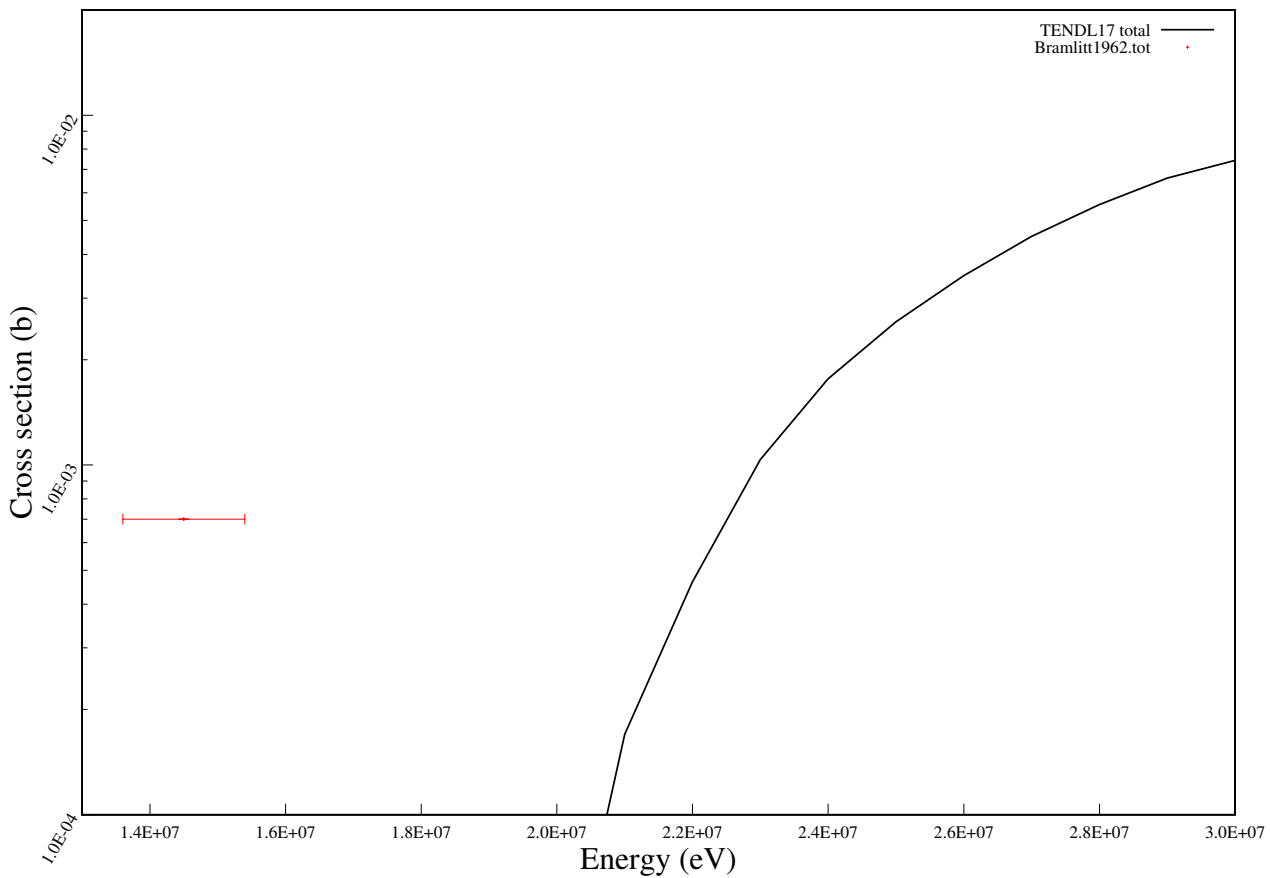
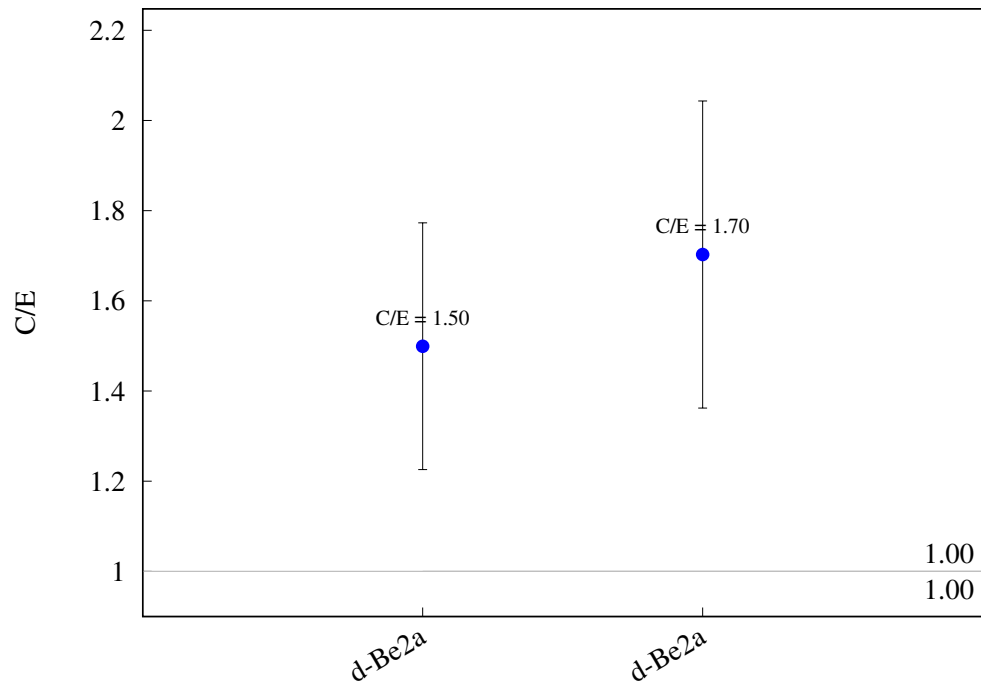
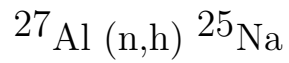


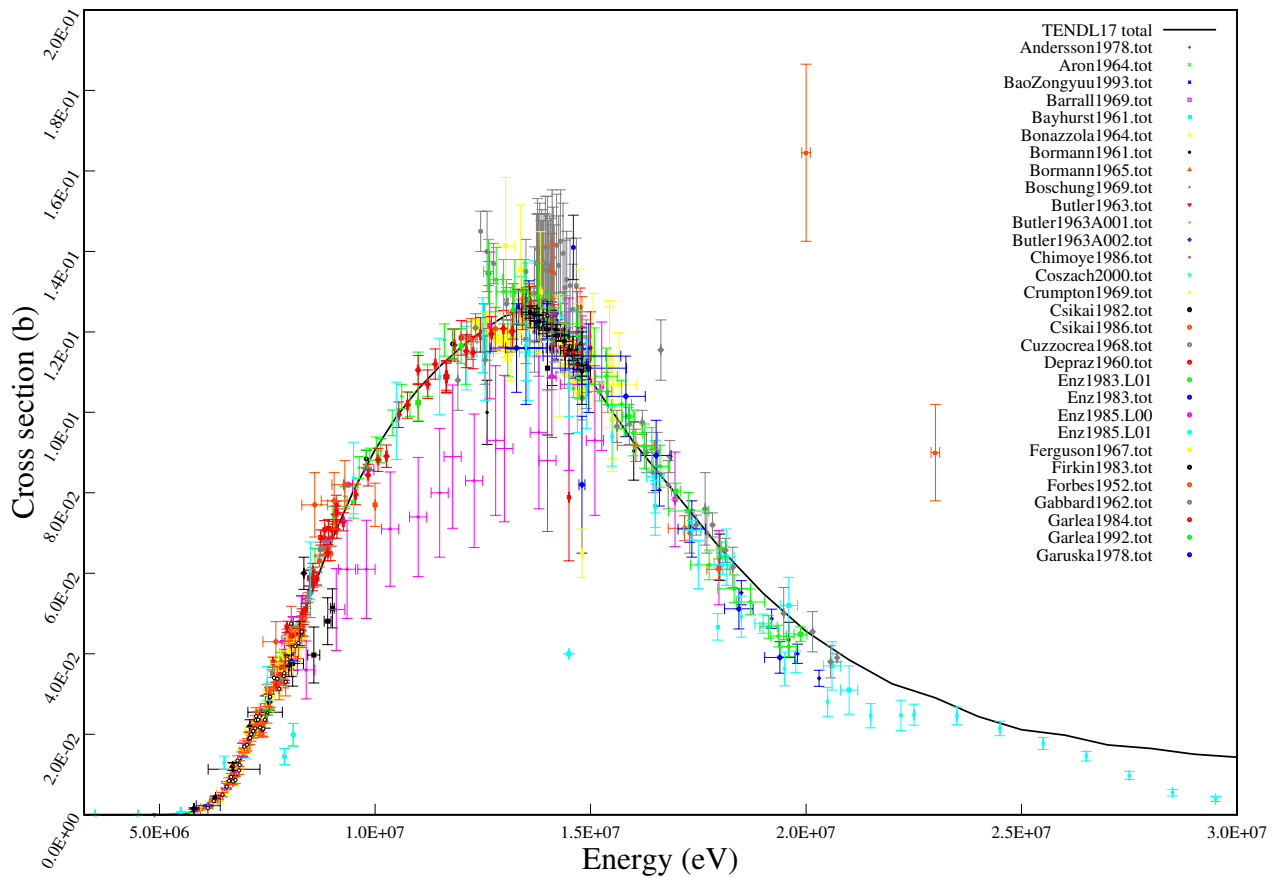
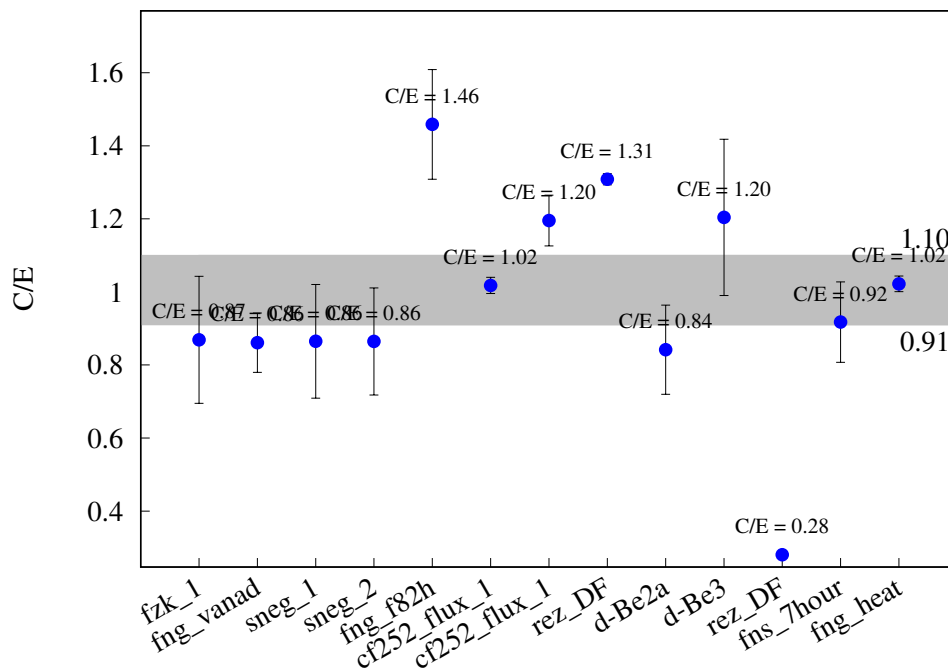


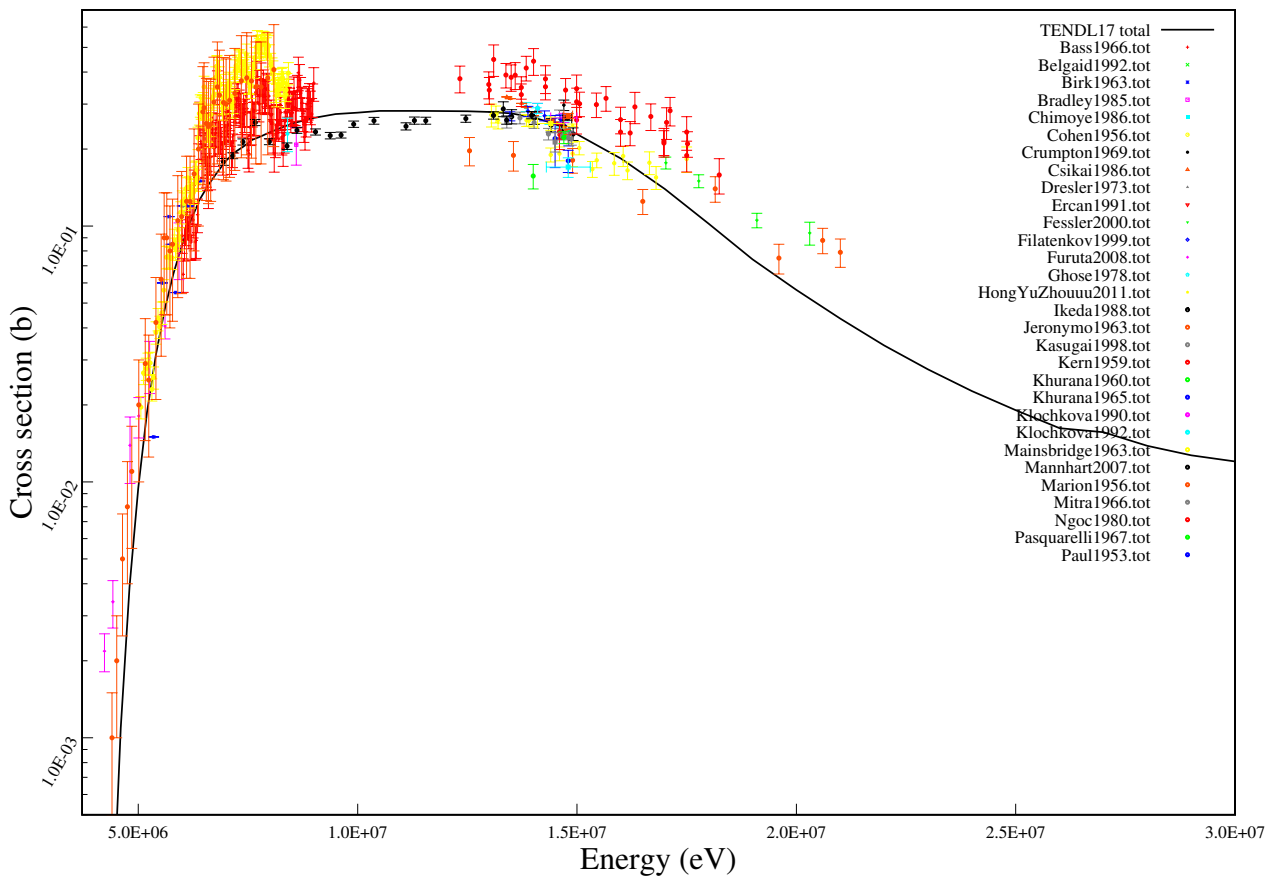
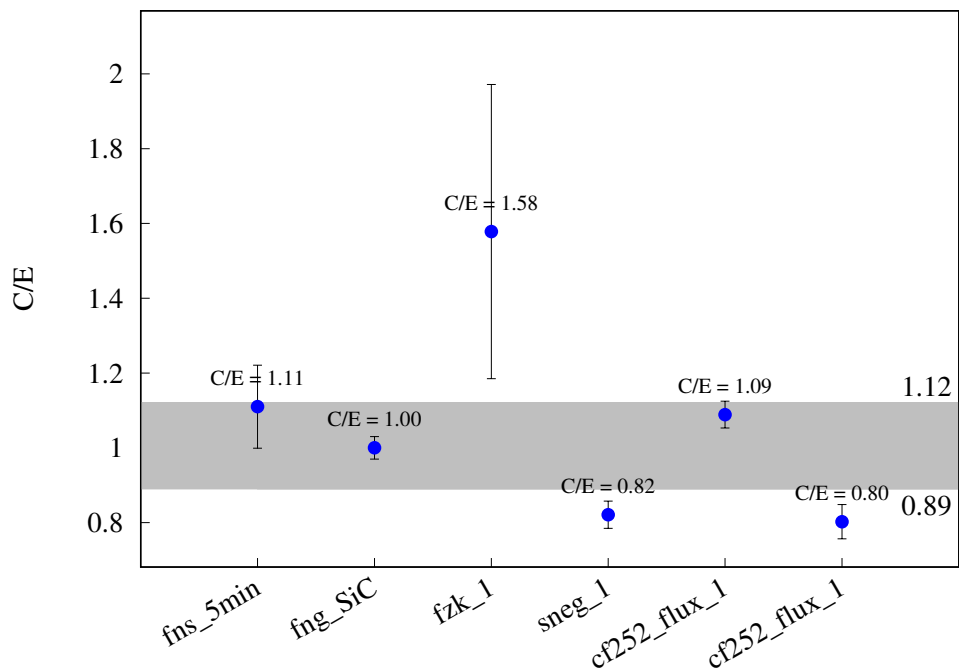


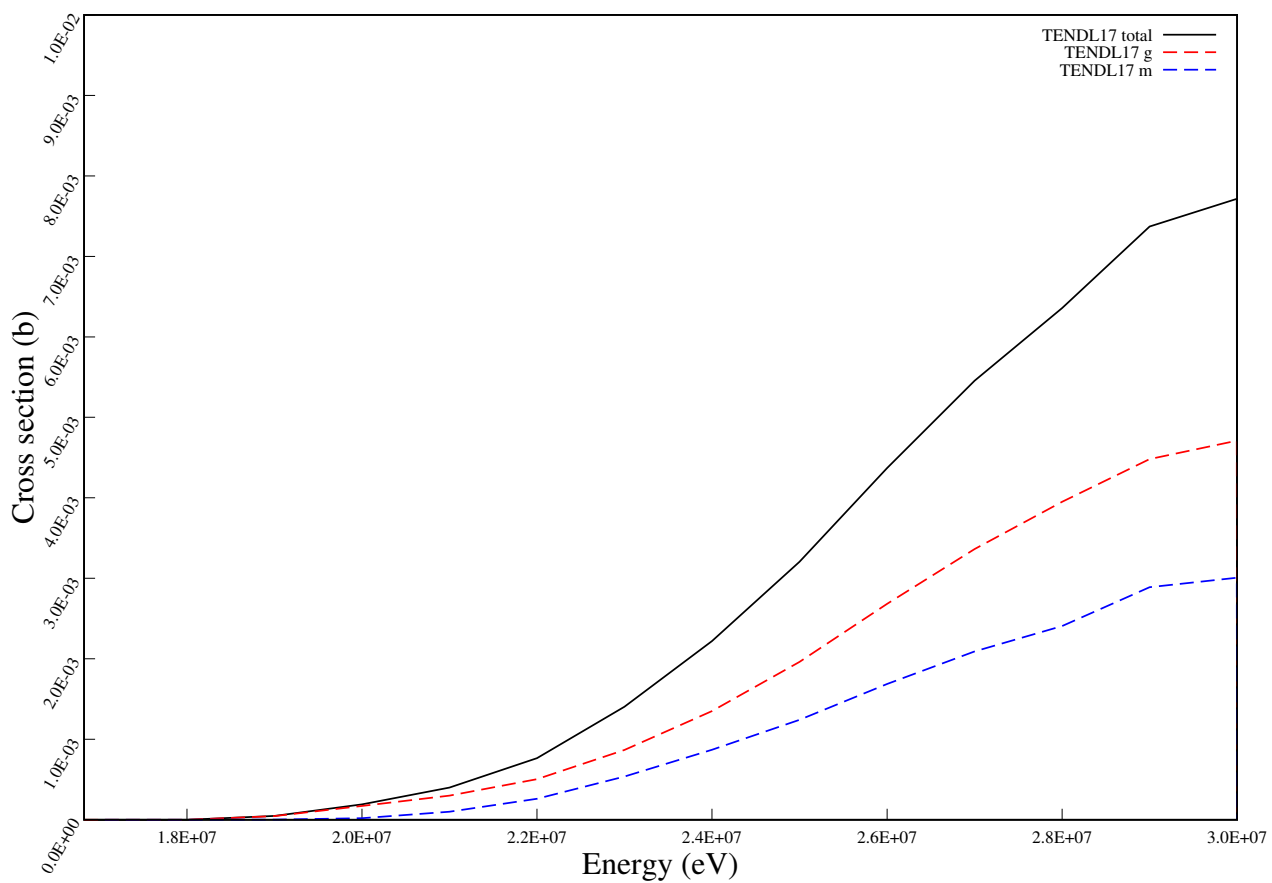
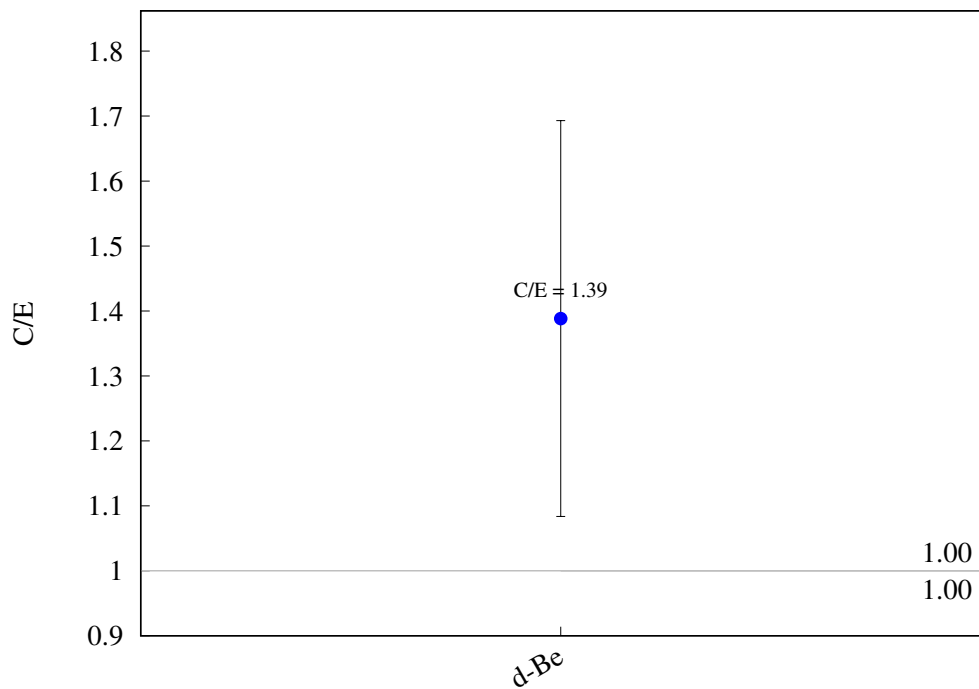


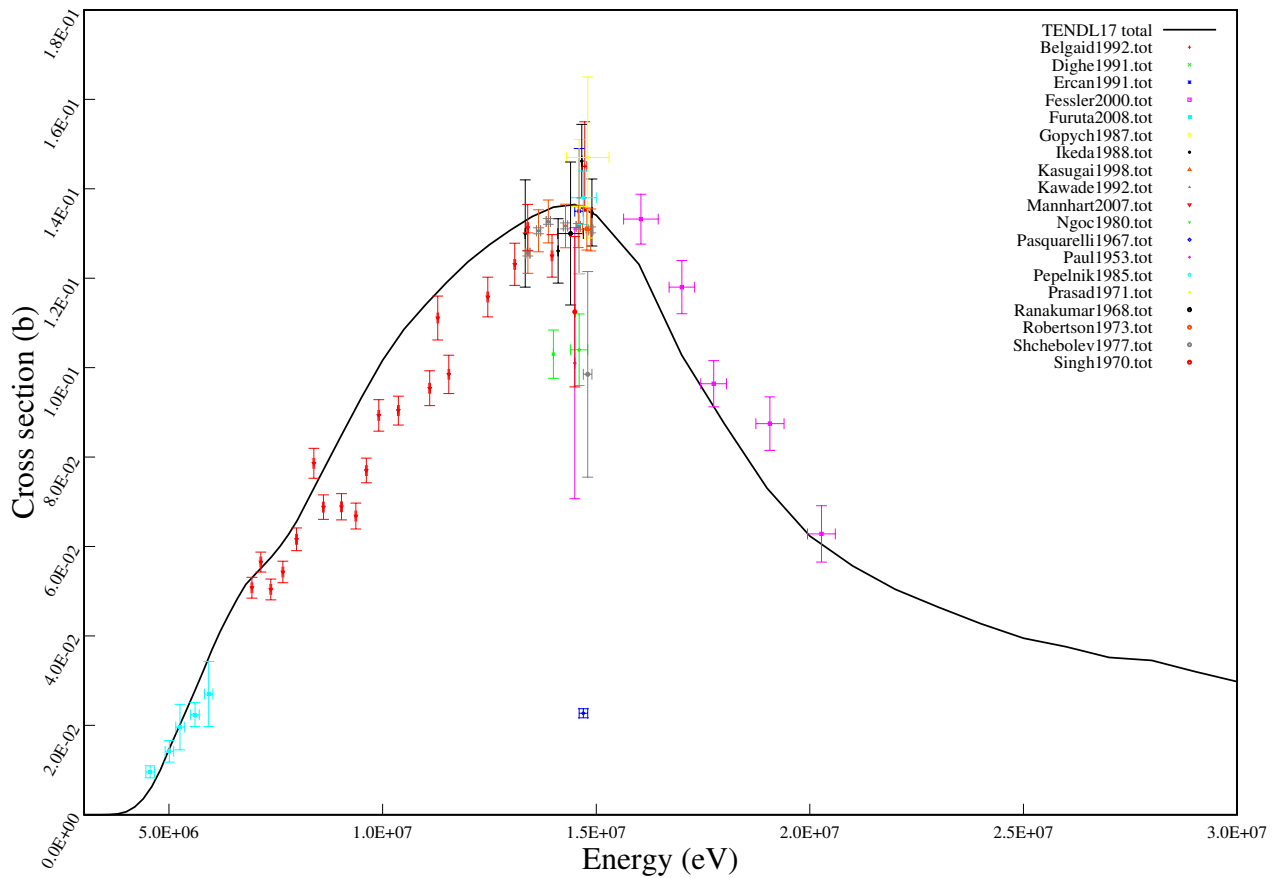
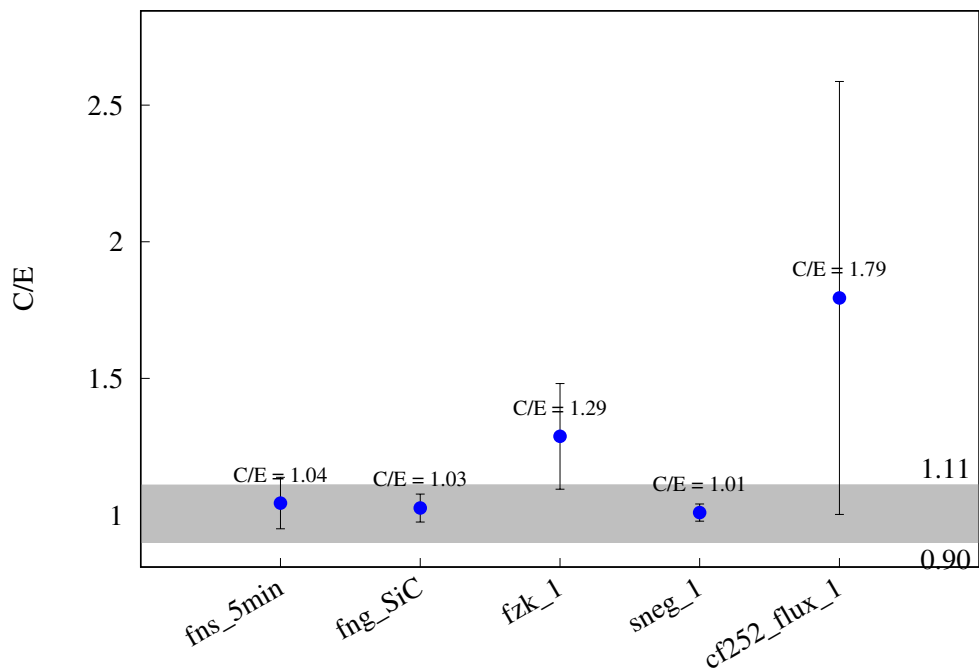
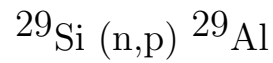
$^{27}\text{Al} (\text{n},\text{t}) ^{25}\text{Mg}$ 

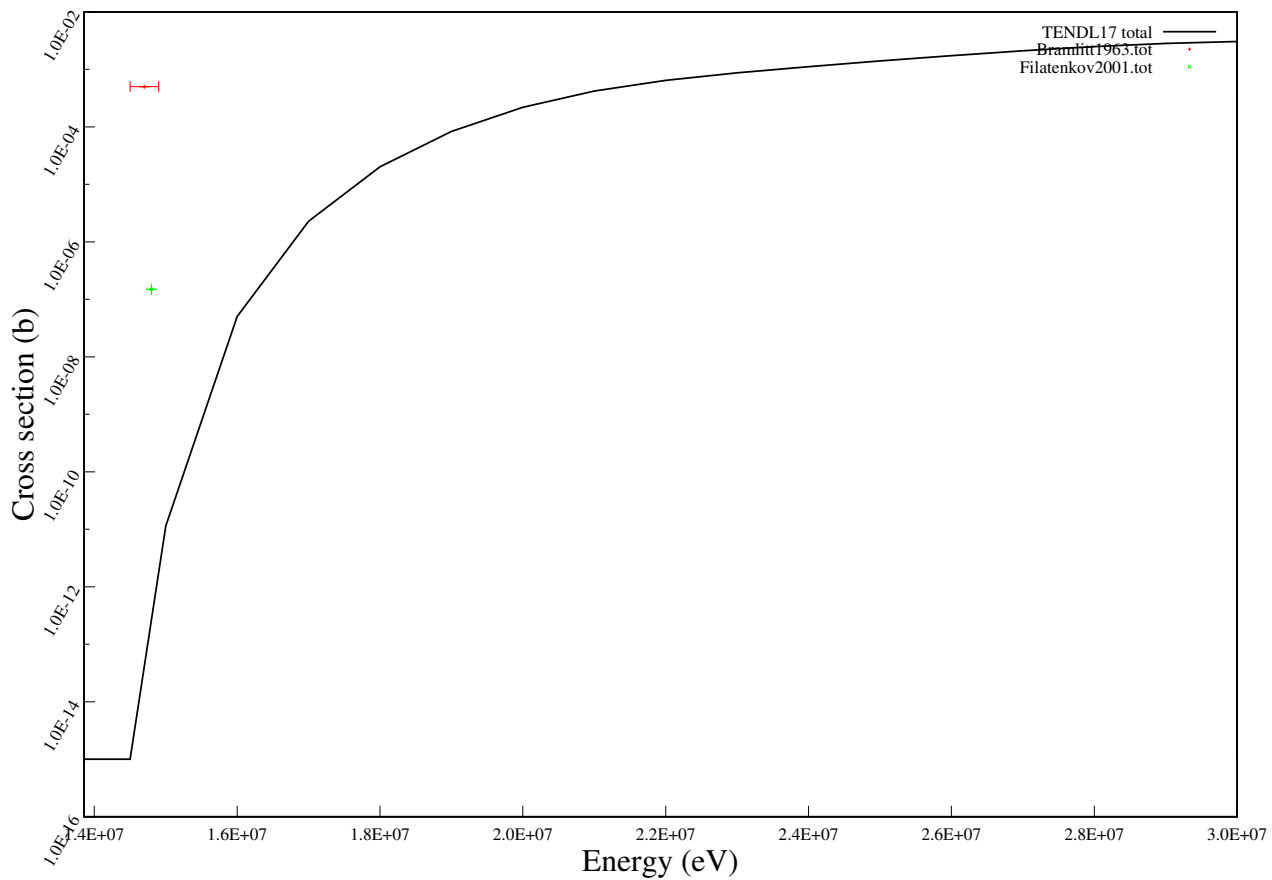
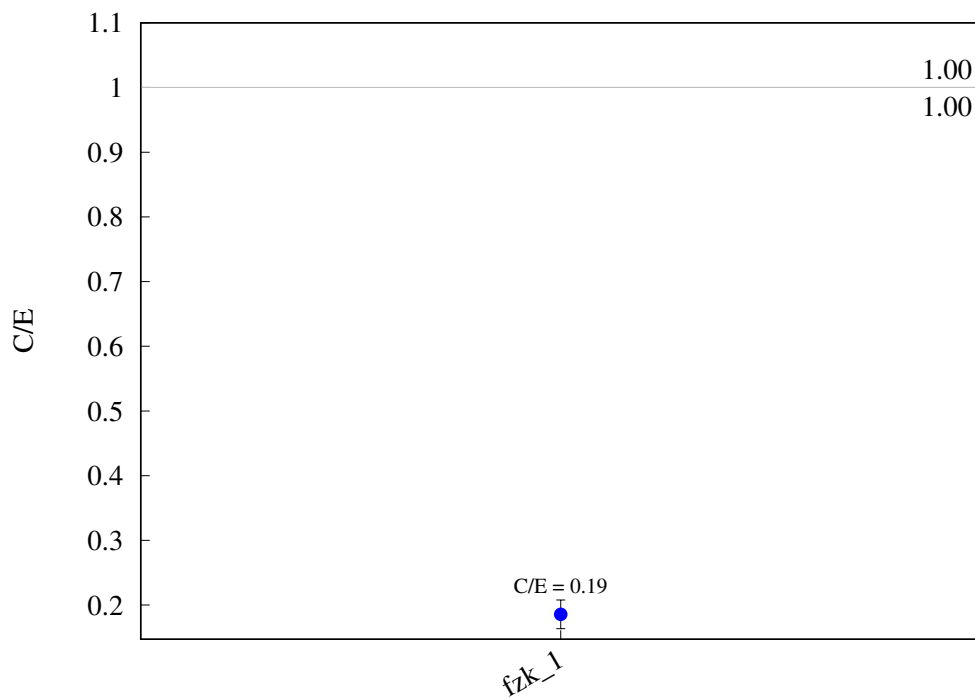
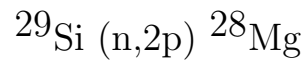


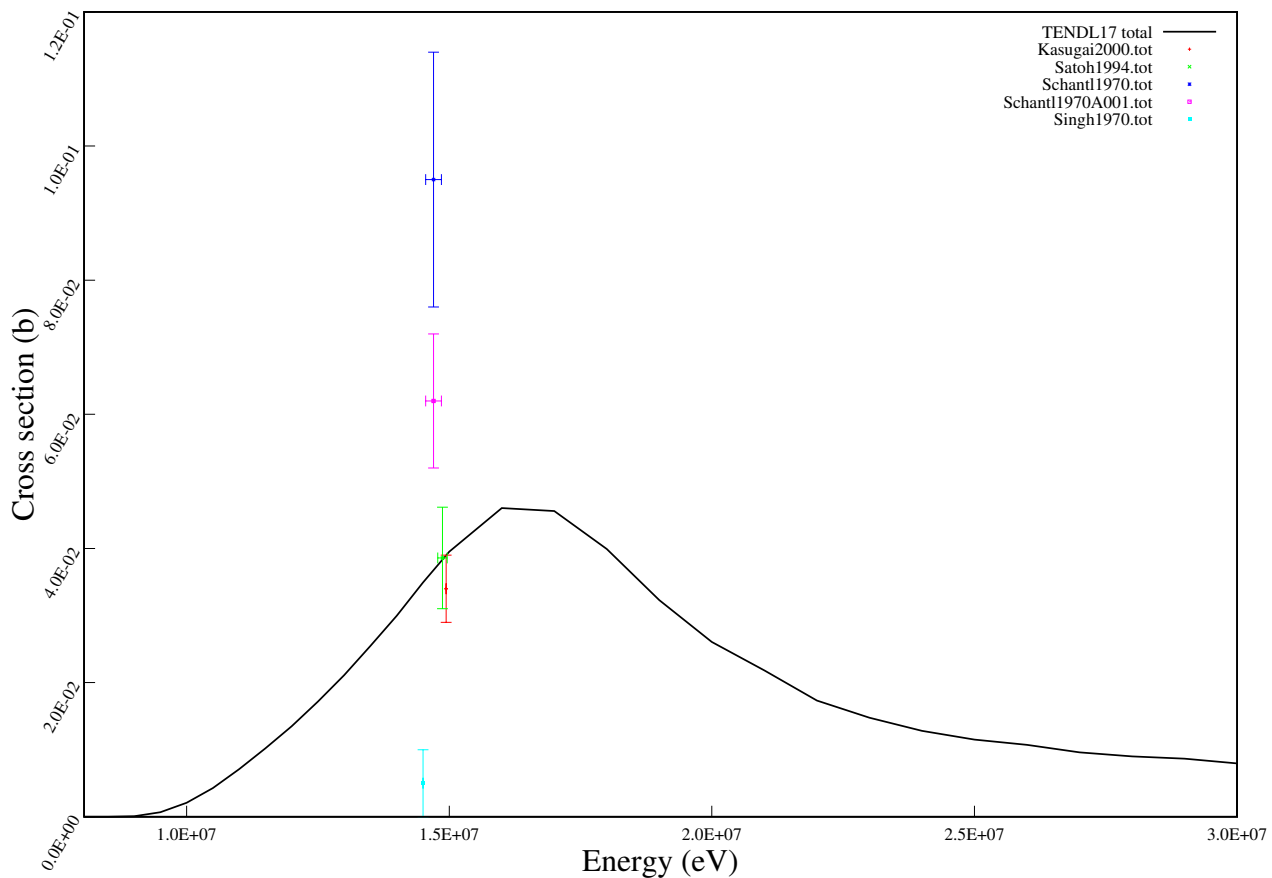
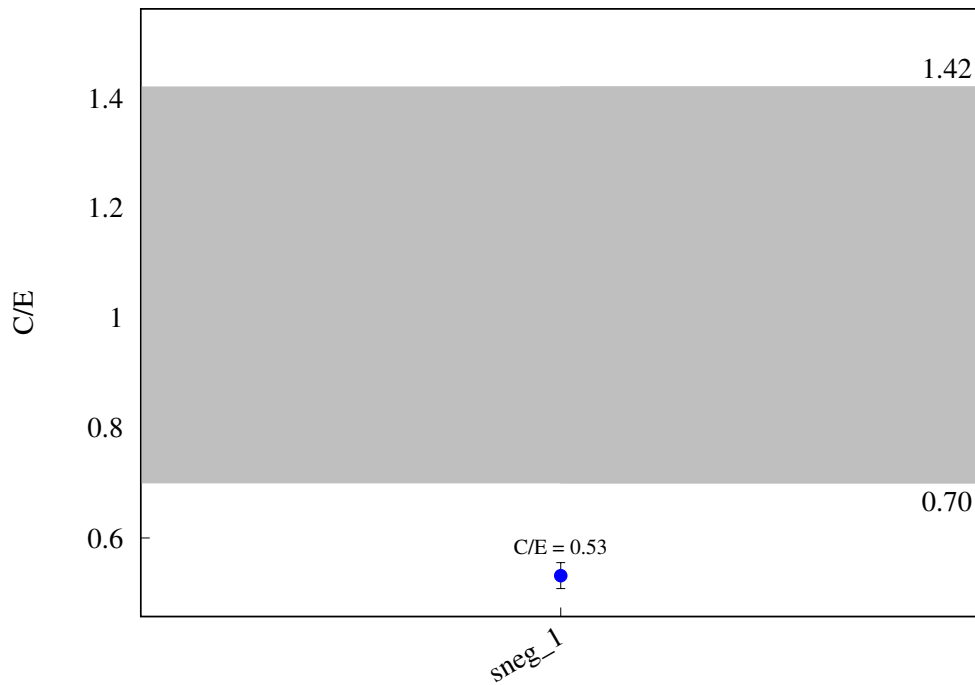
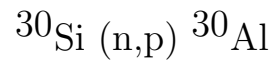
$^{27}\text{Al} (\text{n},\text{a}) ^{24}\text{Na}$ 

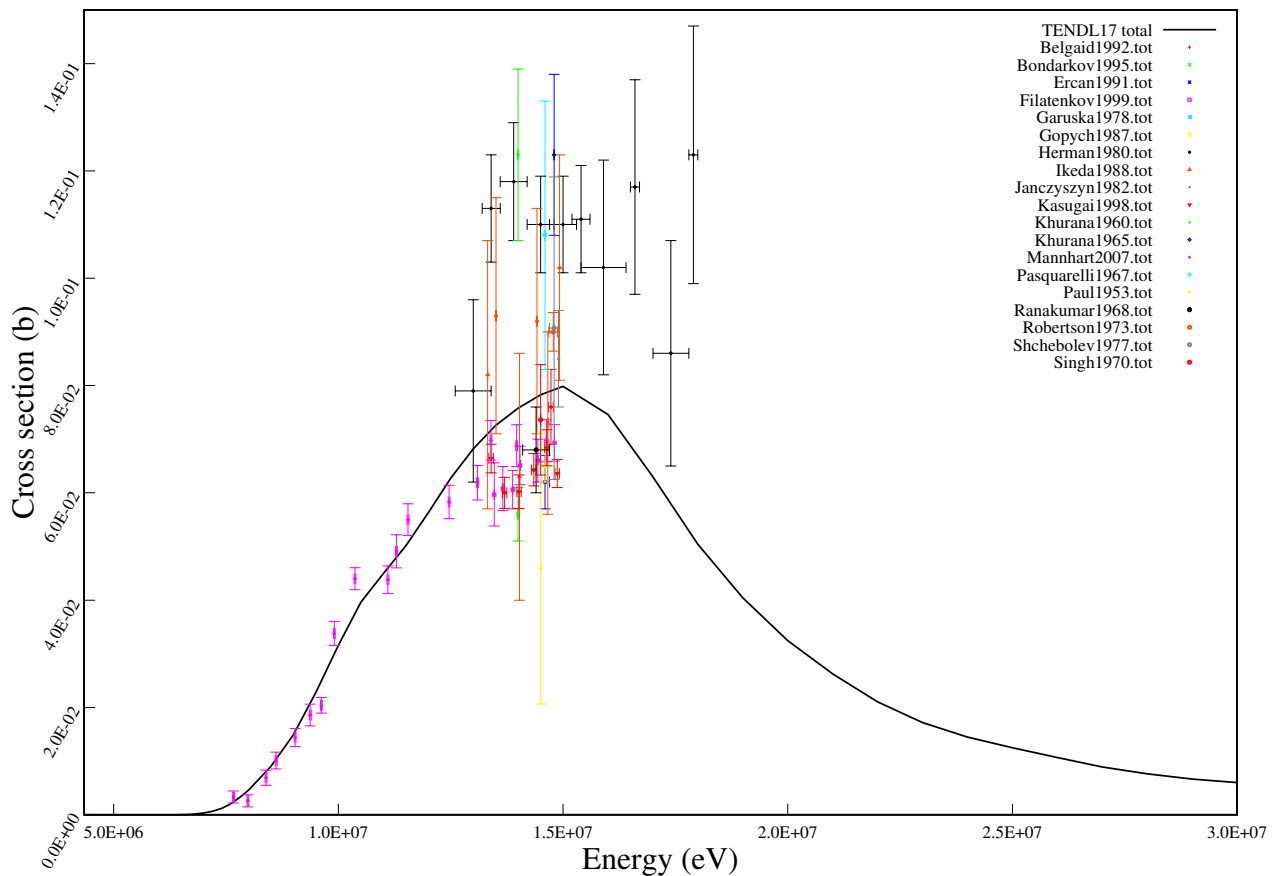
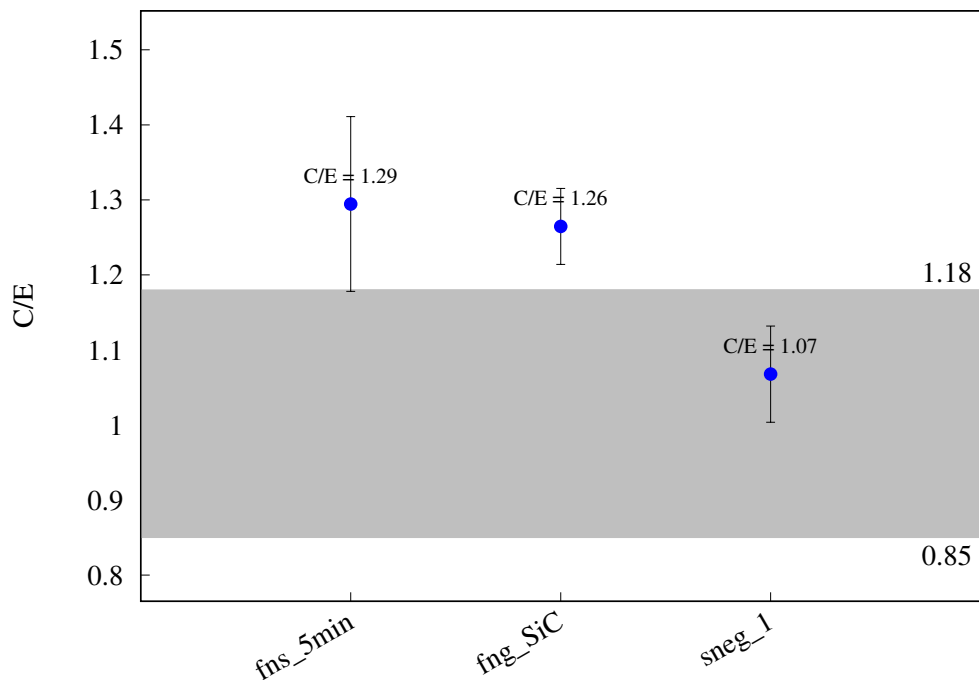
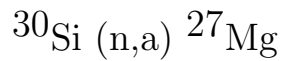
$^{28}\text{Si} (\text{n},\text{p}) ^{28}\text{Al}$ 

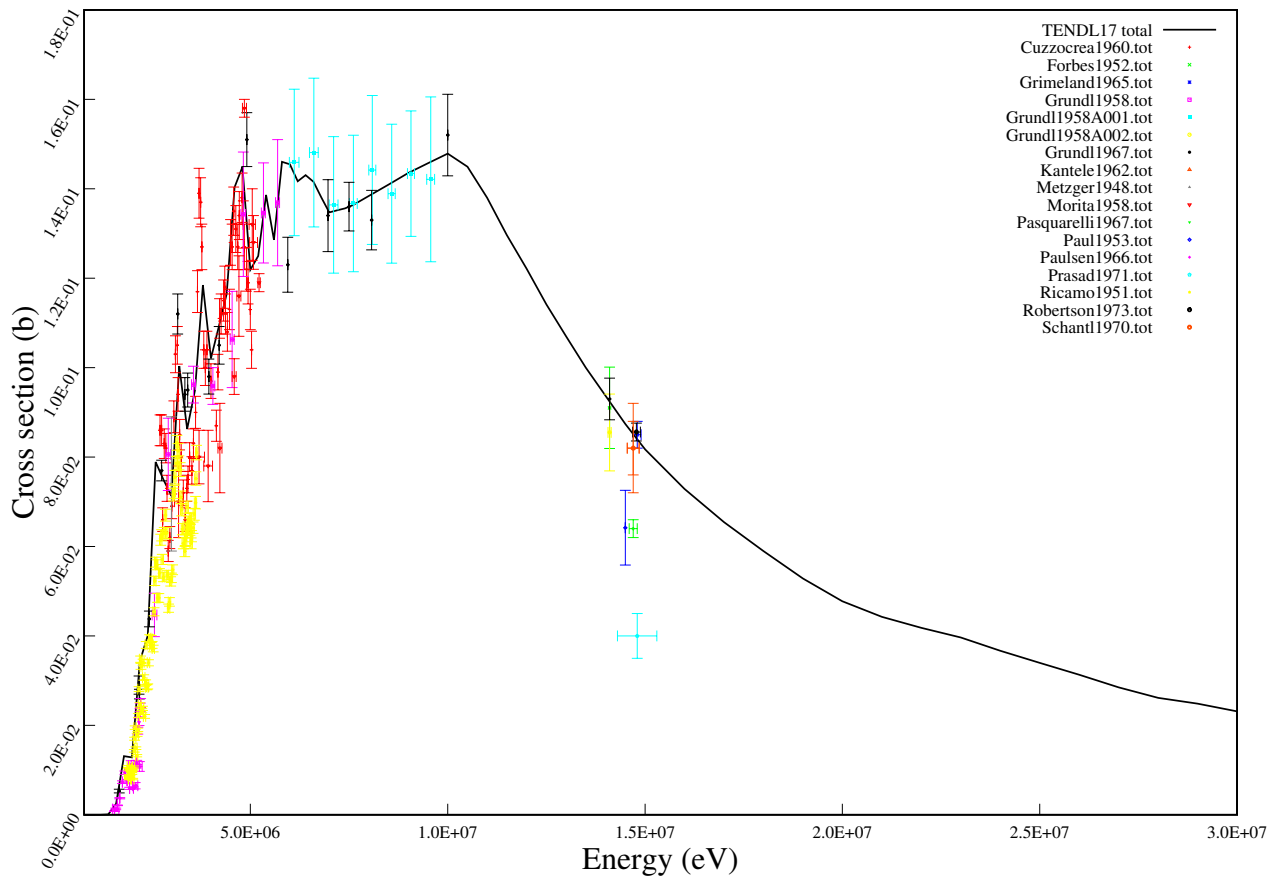
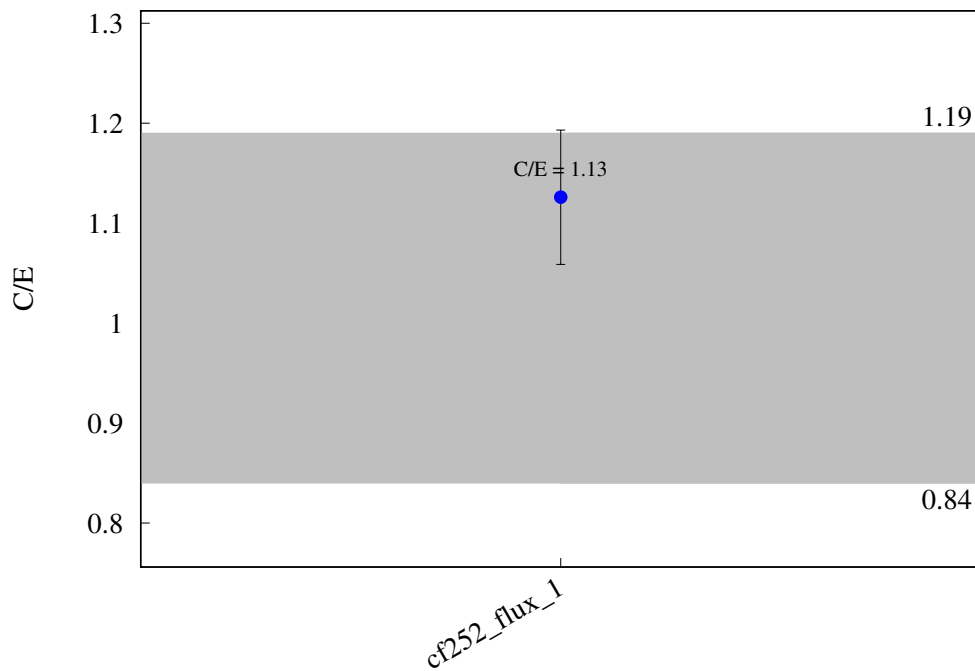
$^{28}\text{Si} (\text{n},\text{t}) ^{26}\text{Al}$ 

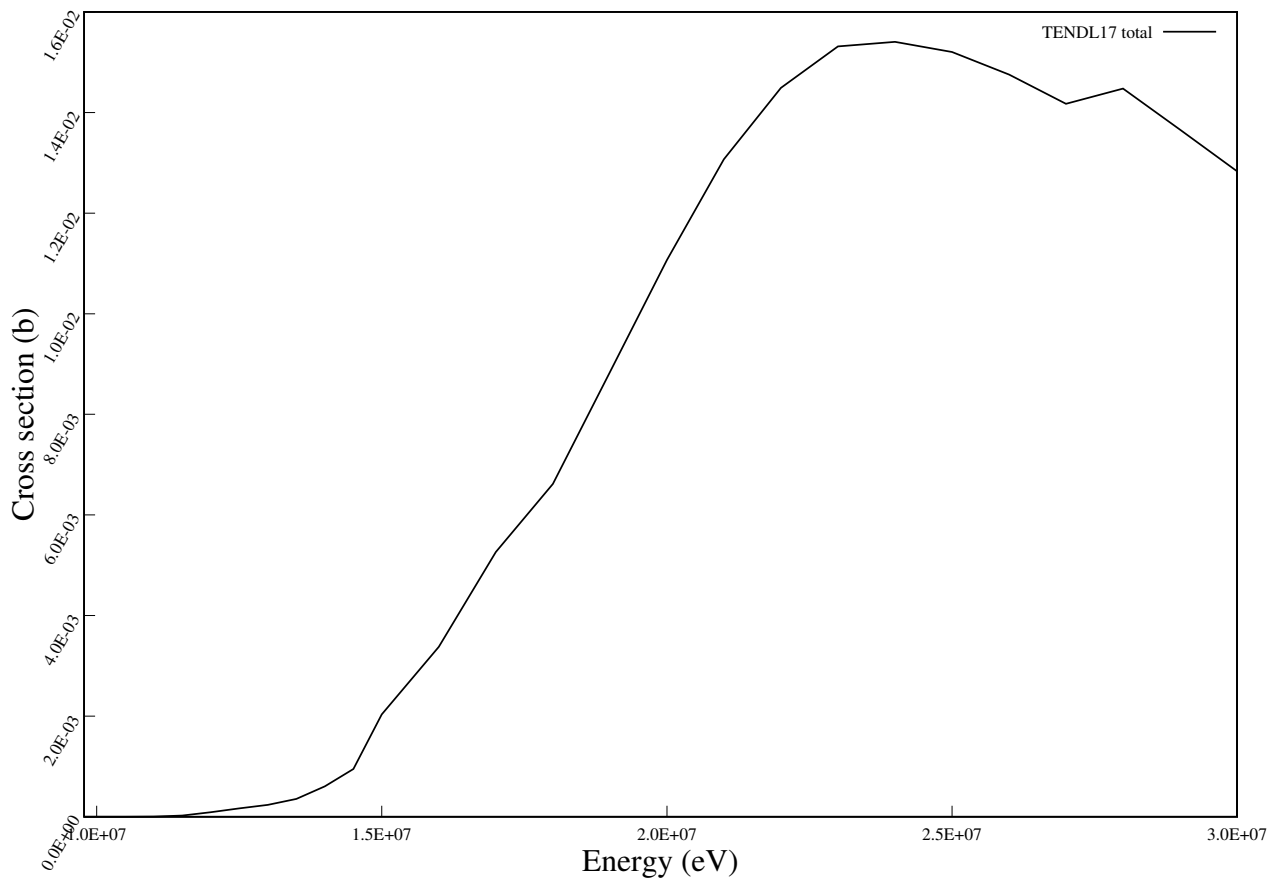
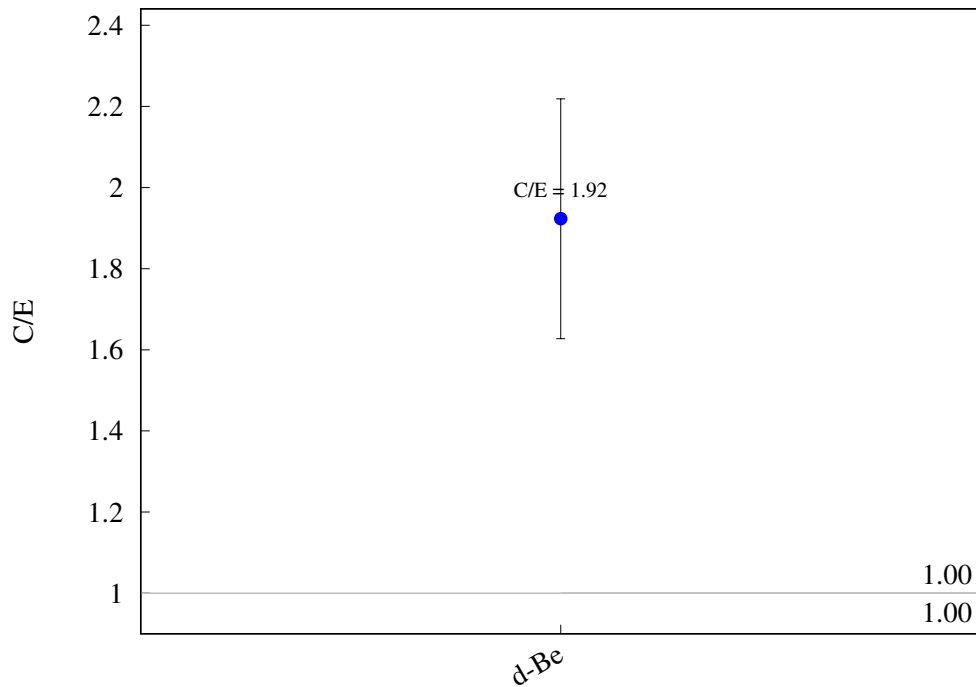


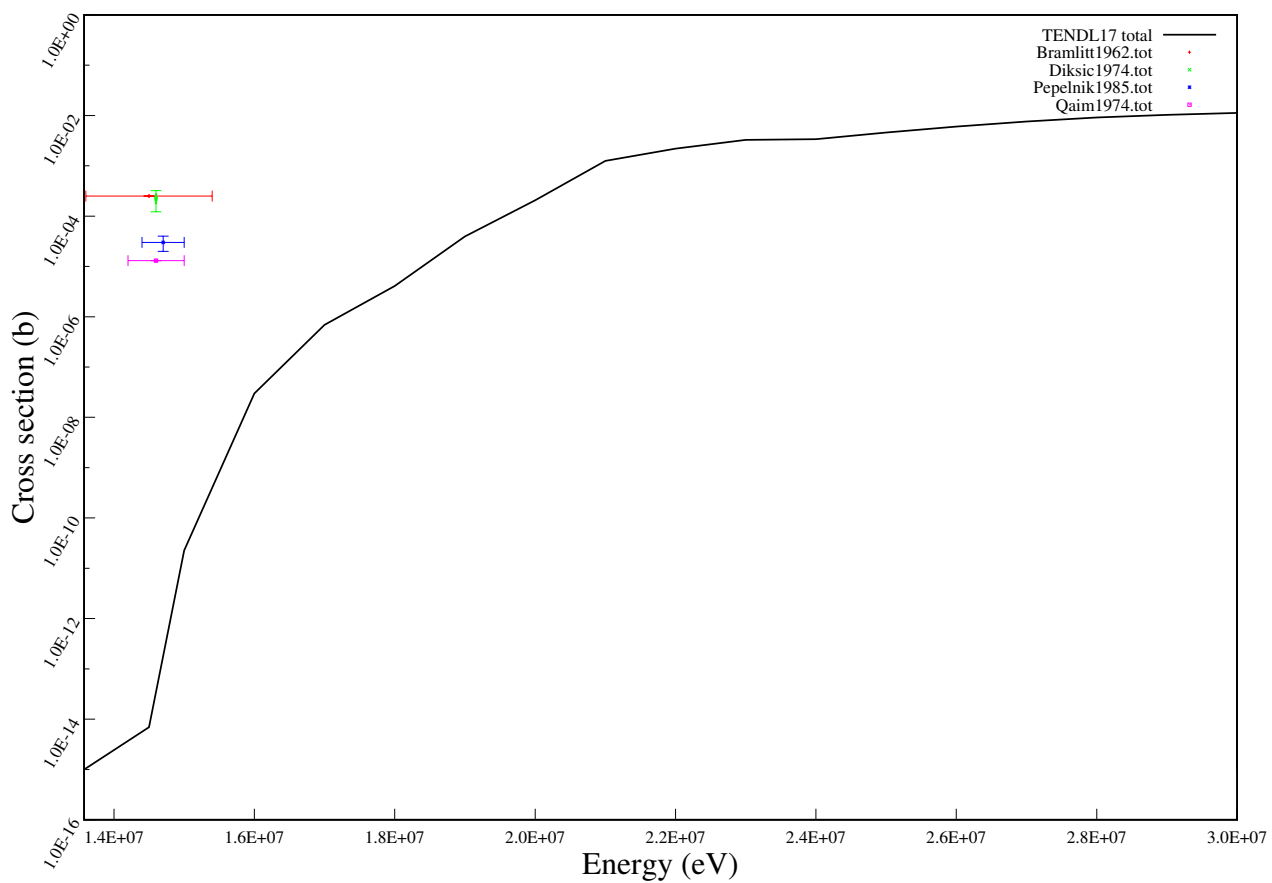
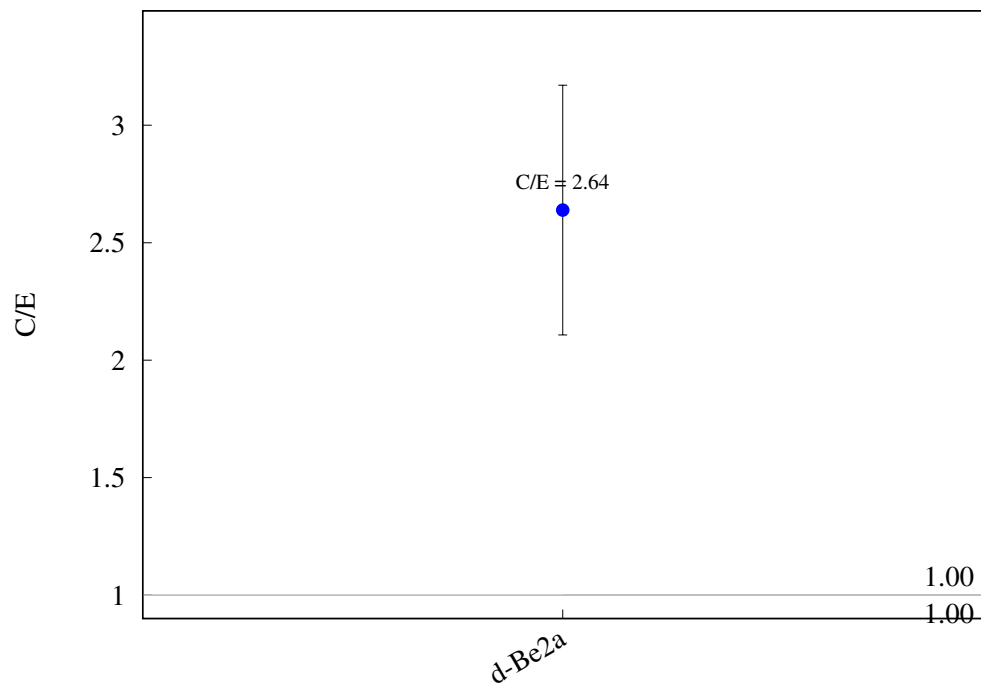


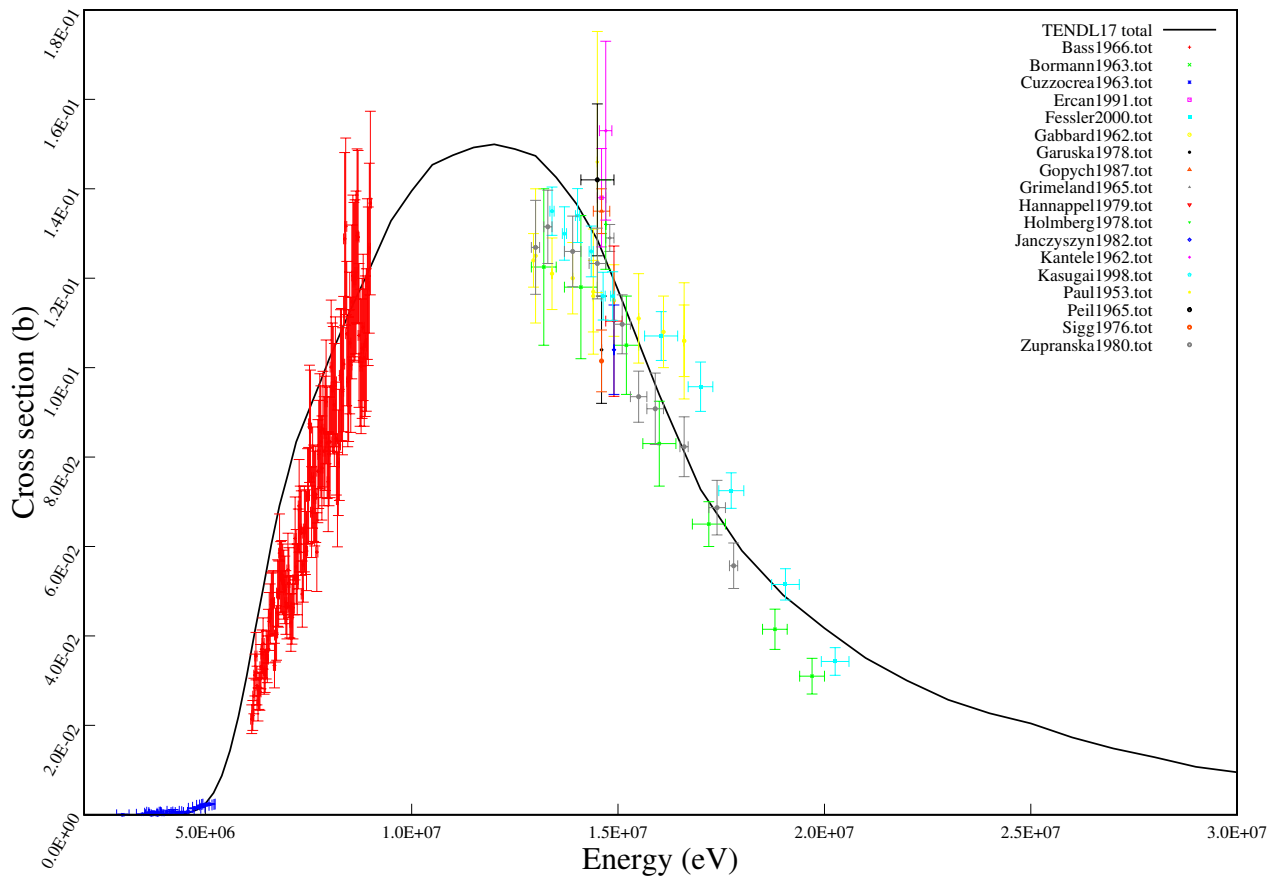
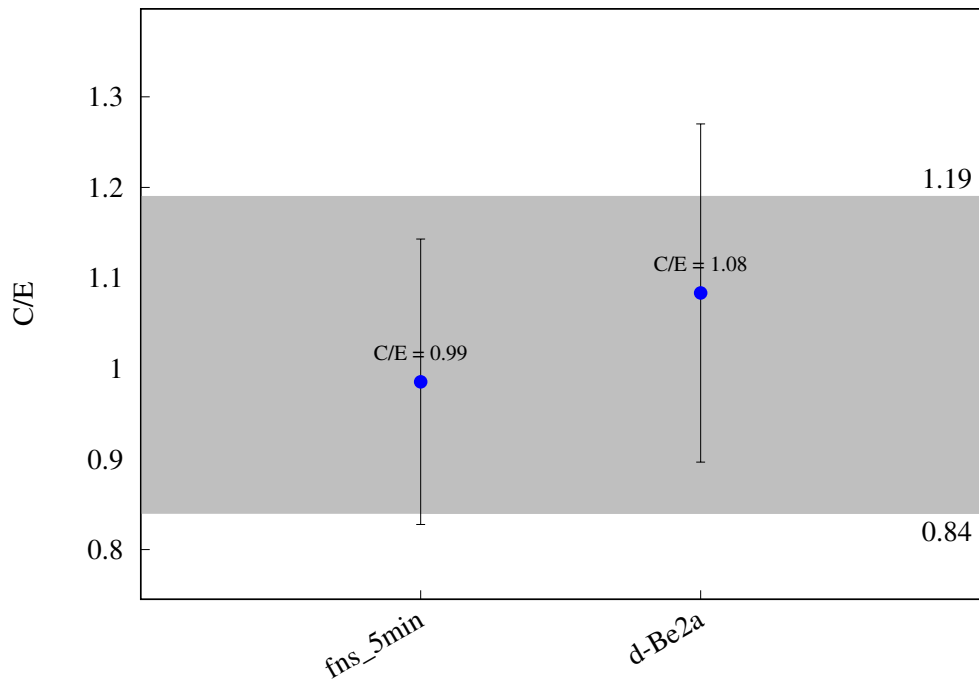


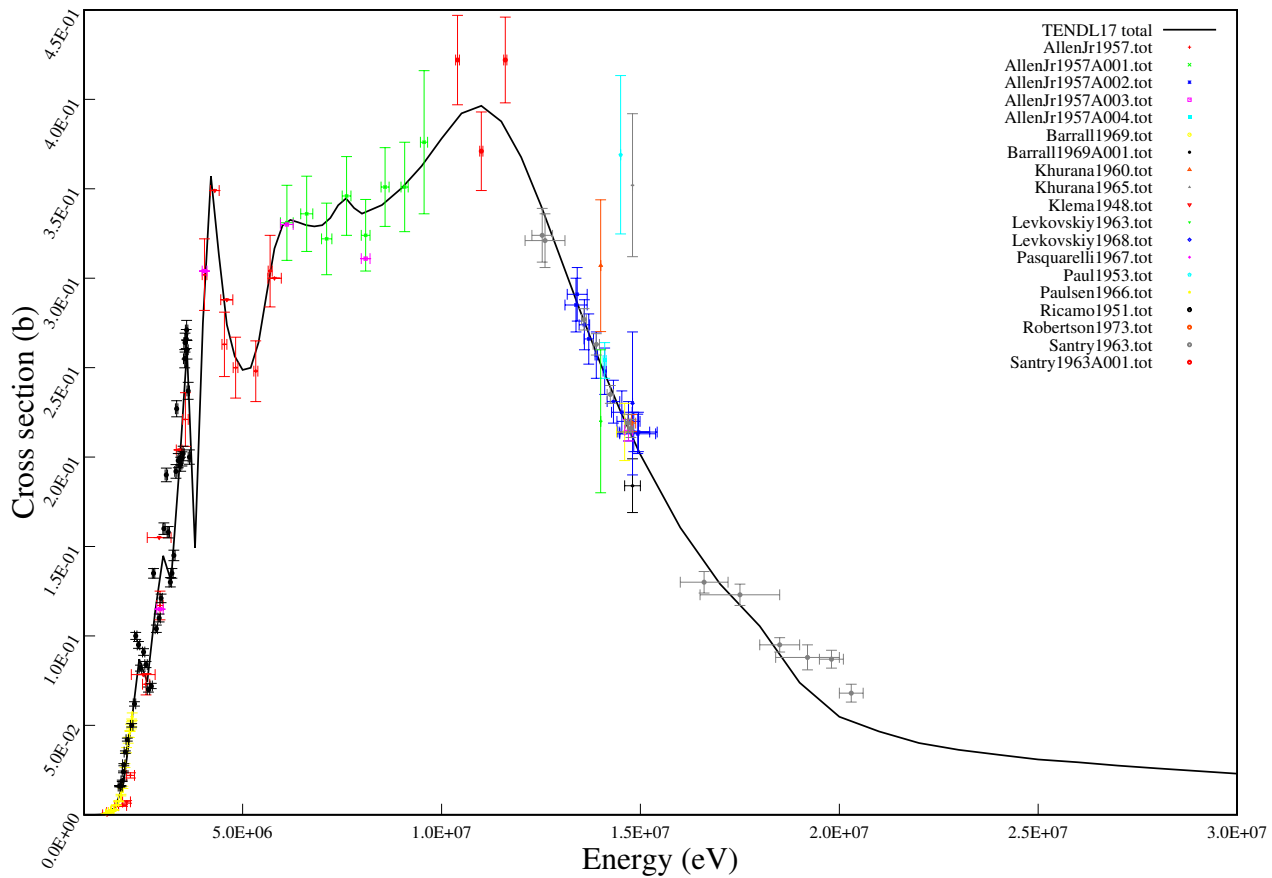
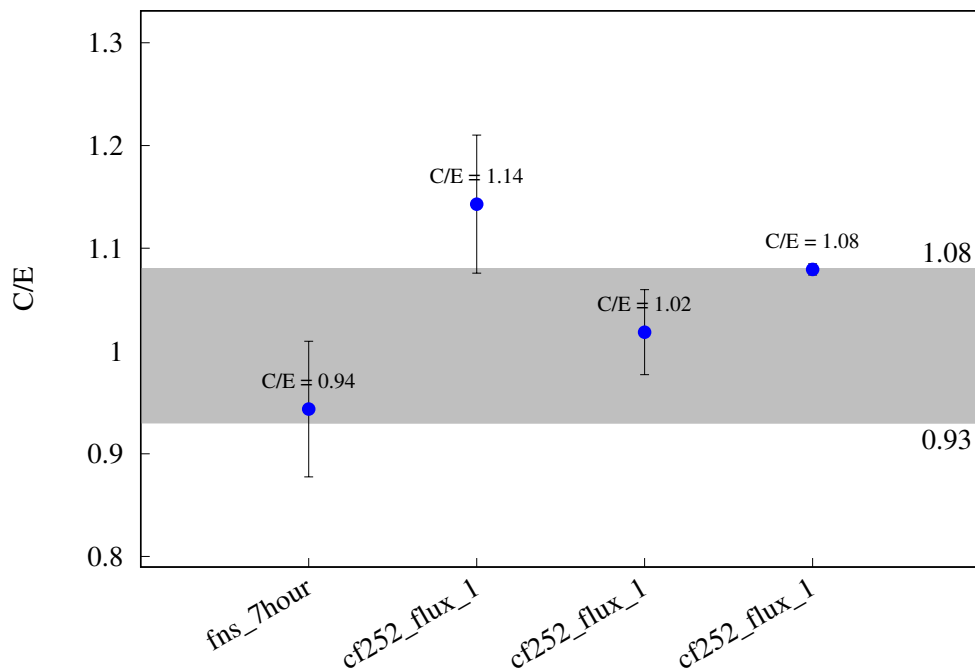


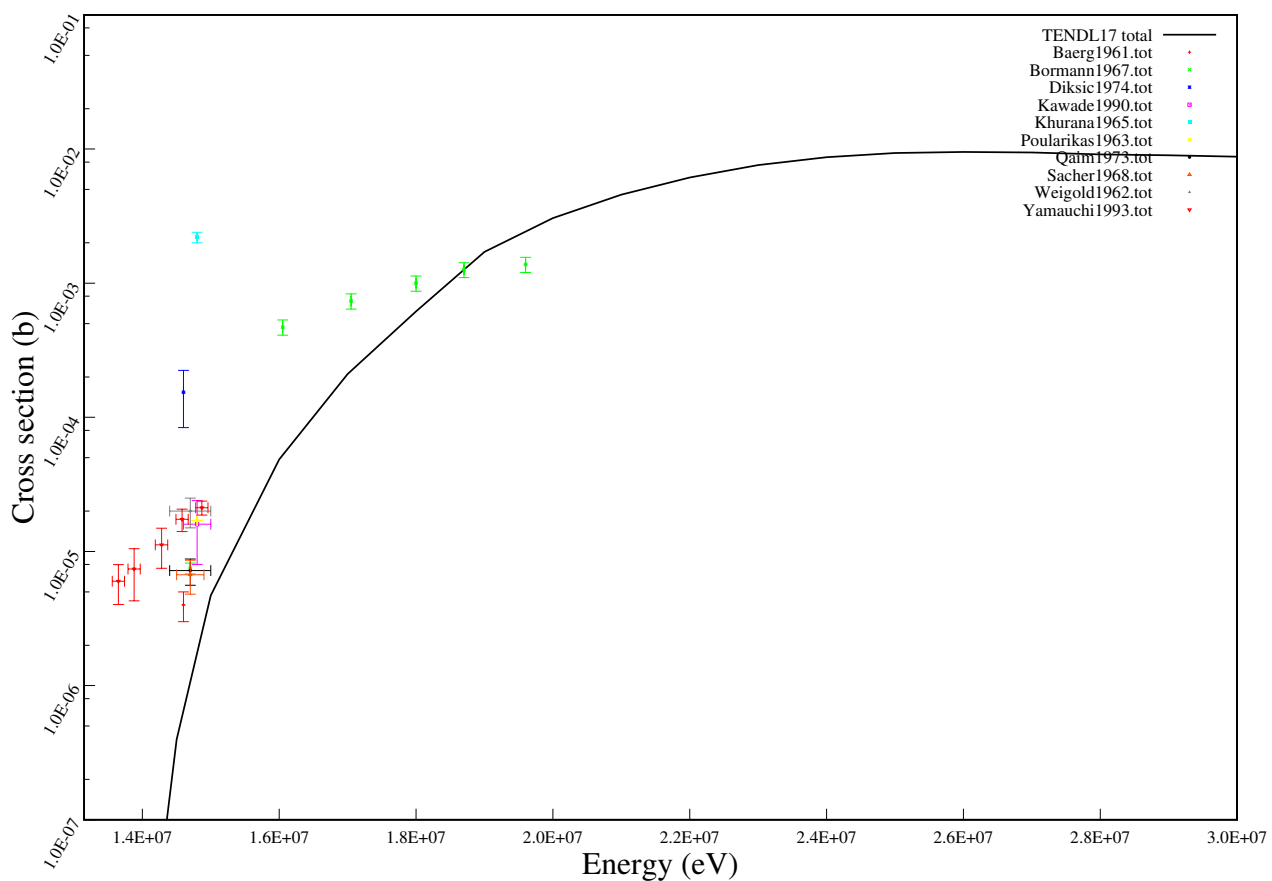
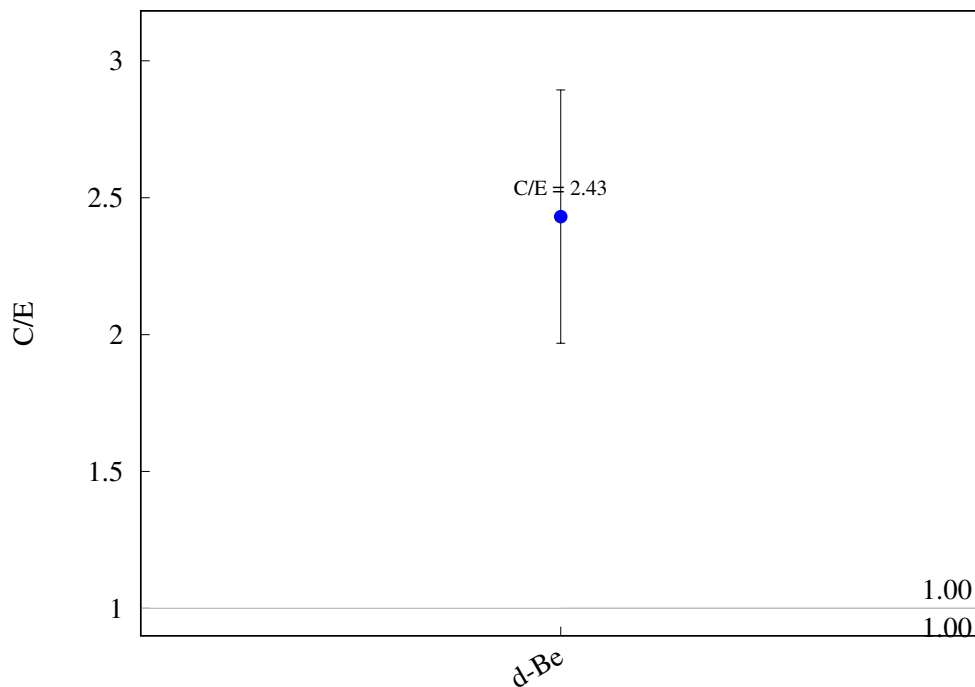
^{31}P (n,p) ^{31}Si 

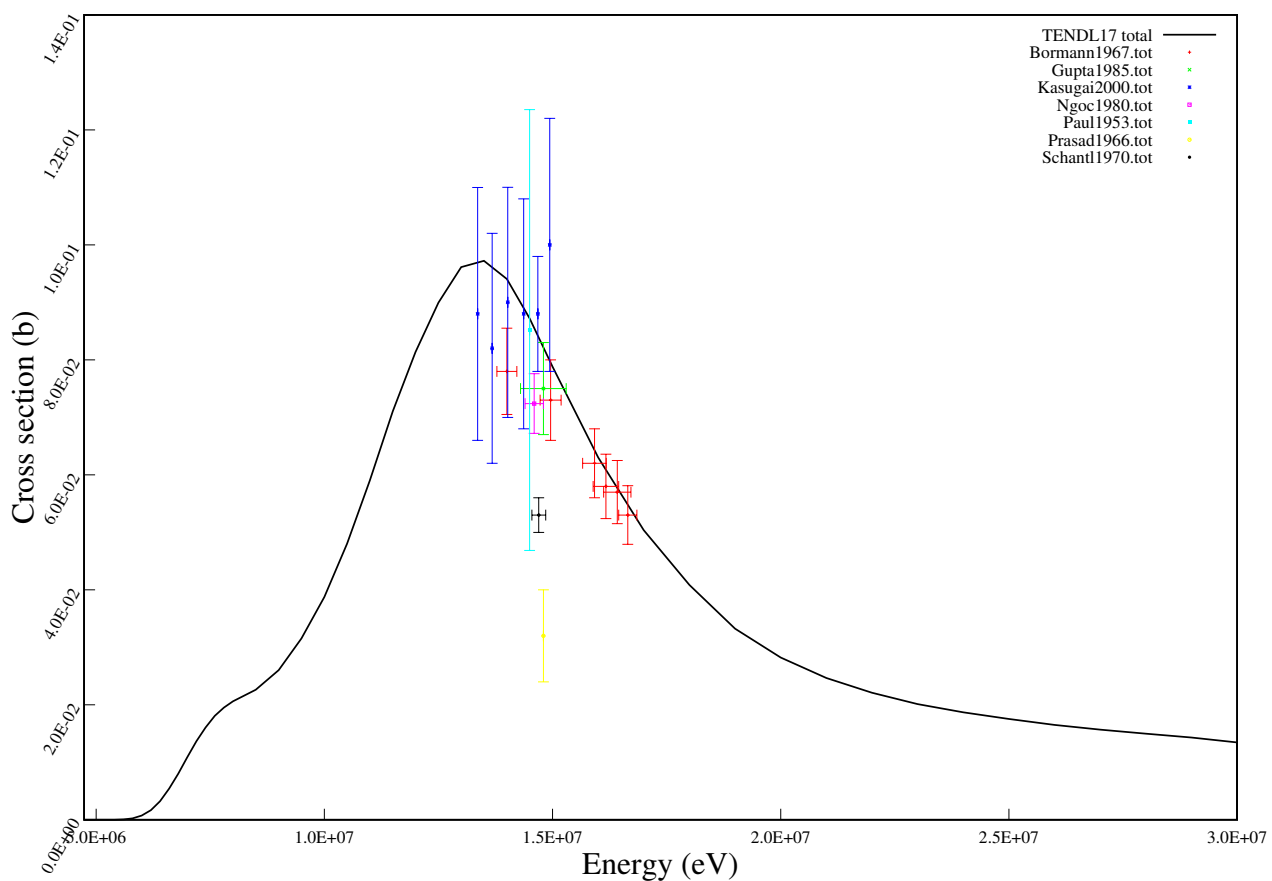
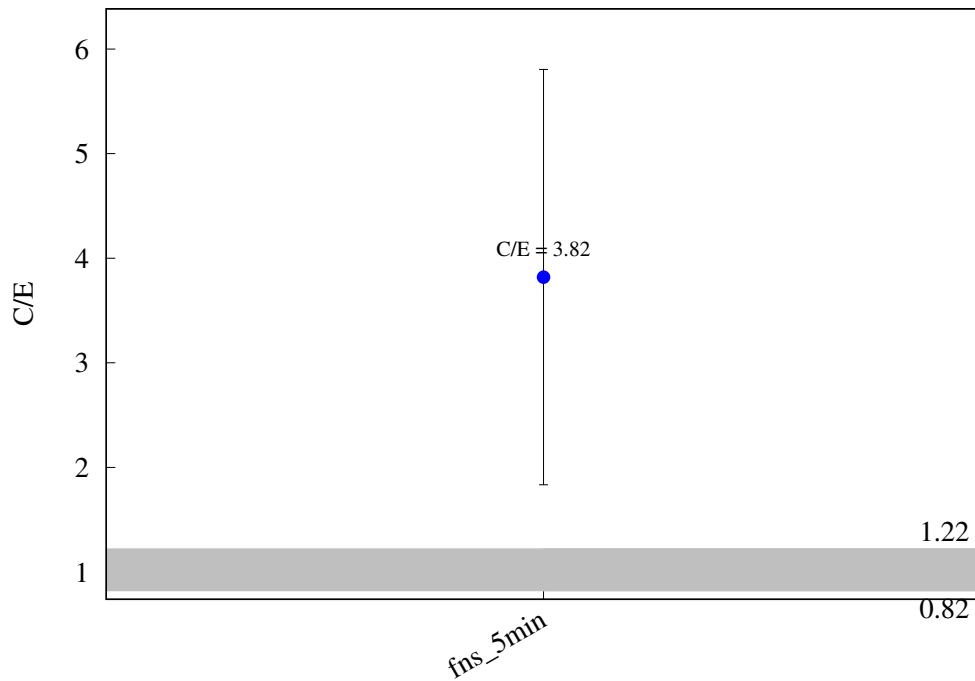
^{31}P (n,t) ^{29}Si 

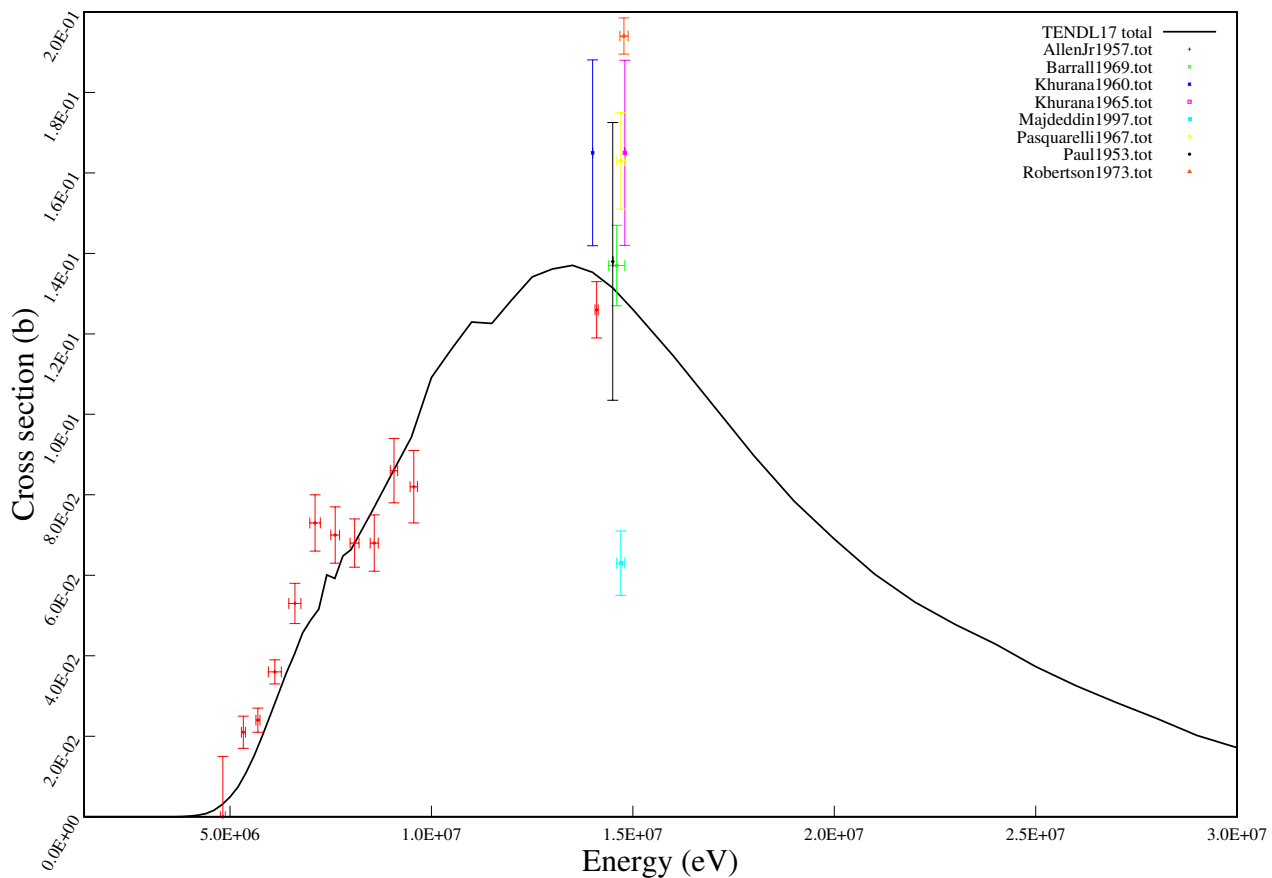
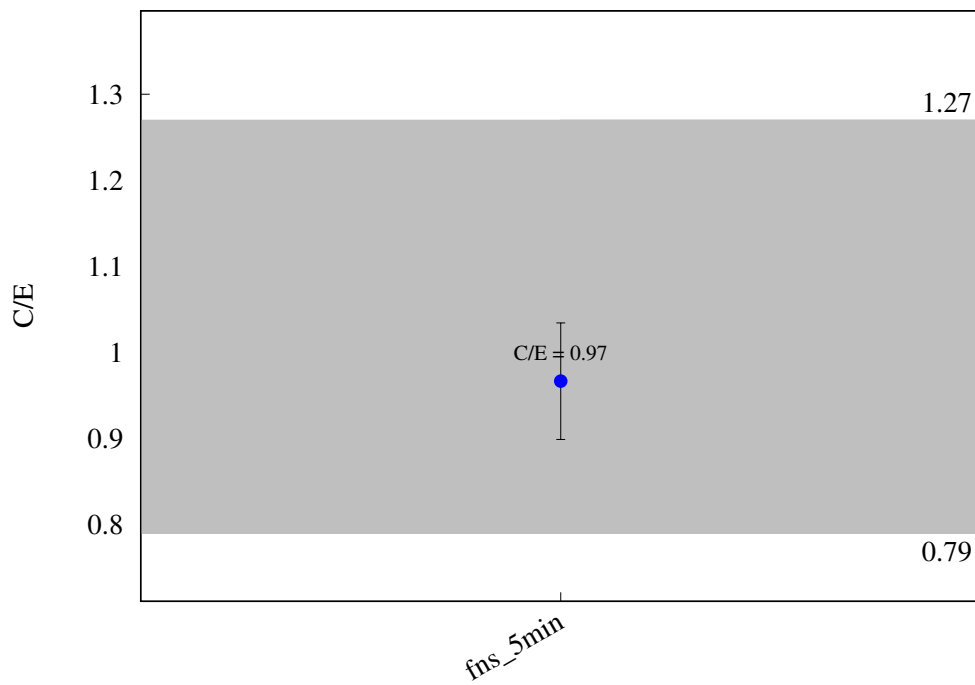
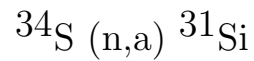
^{31}P (n,h) ^{29}Al 

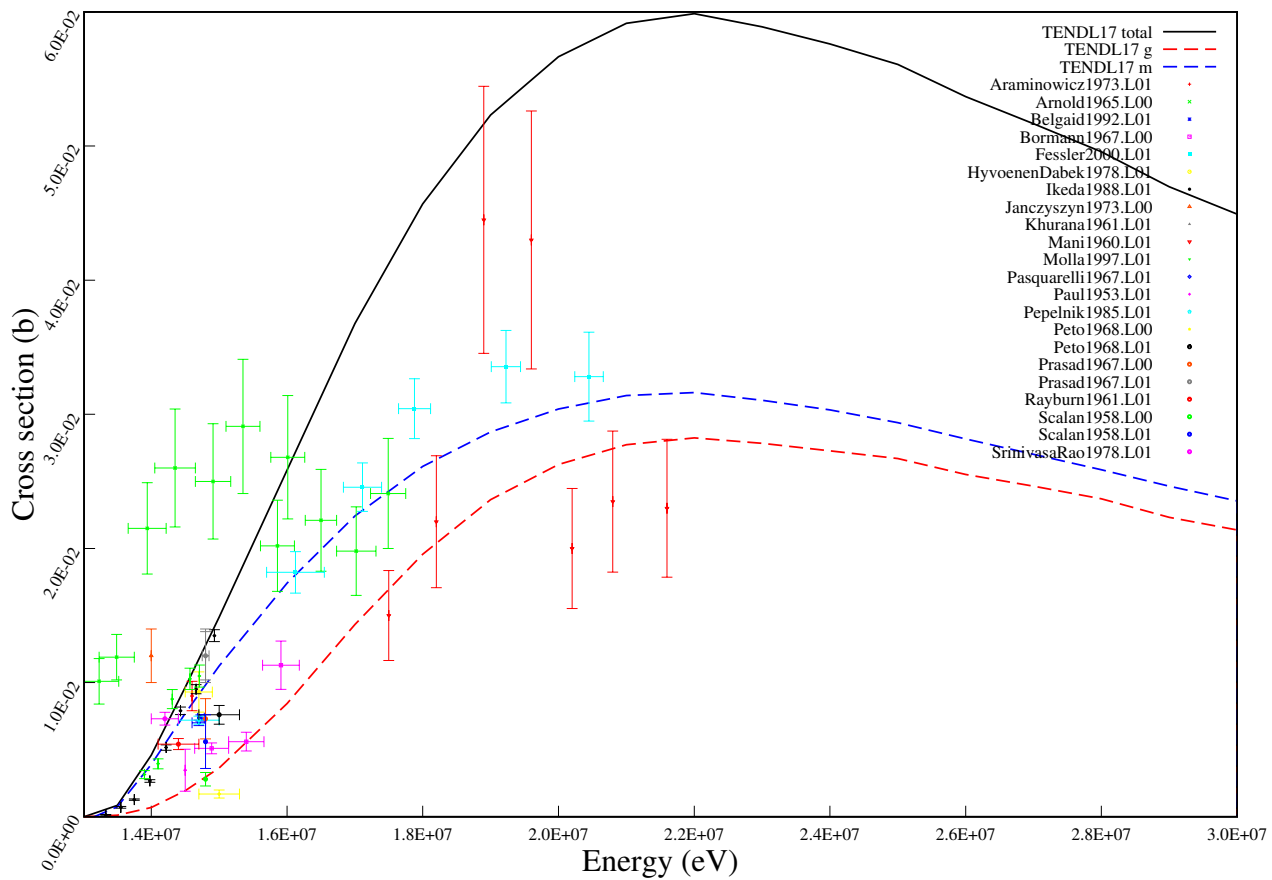
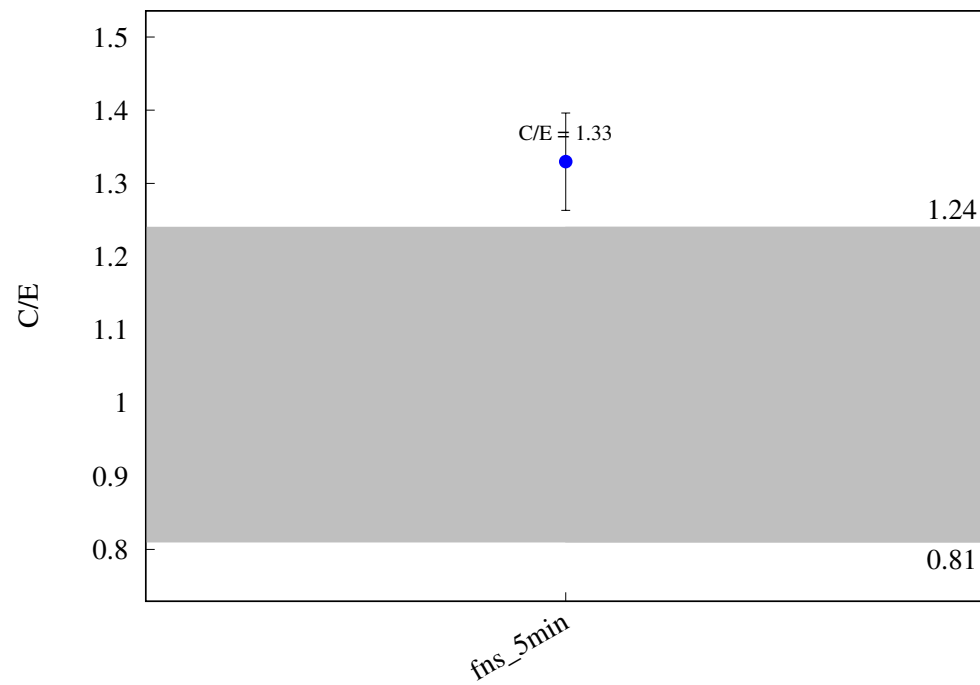
^{31}P (n,a) ^{28}Al 

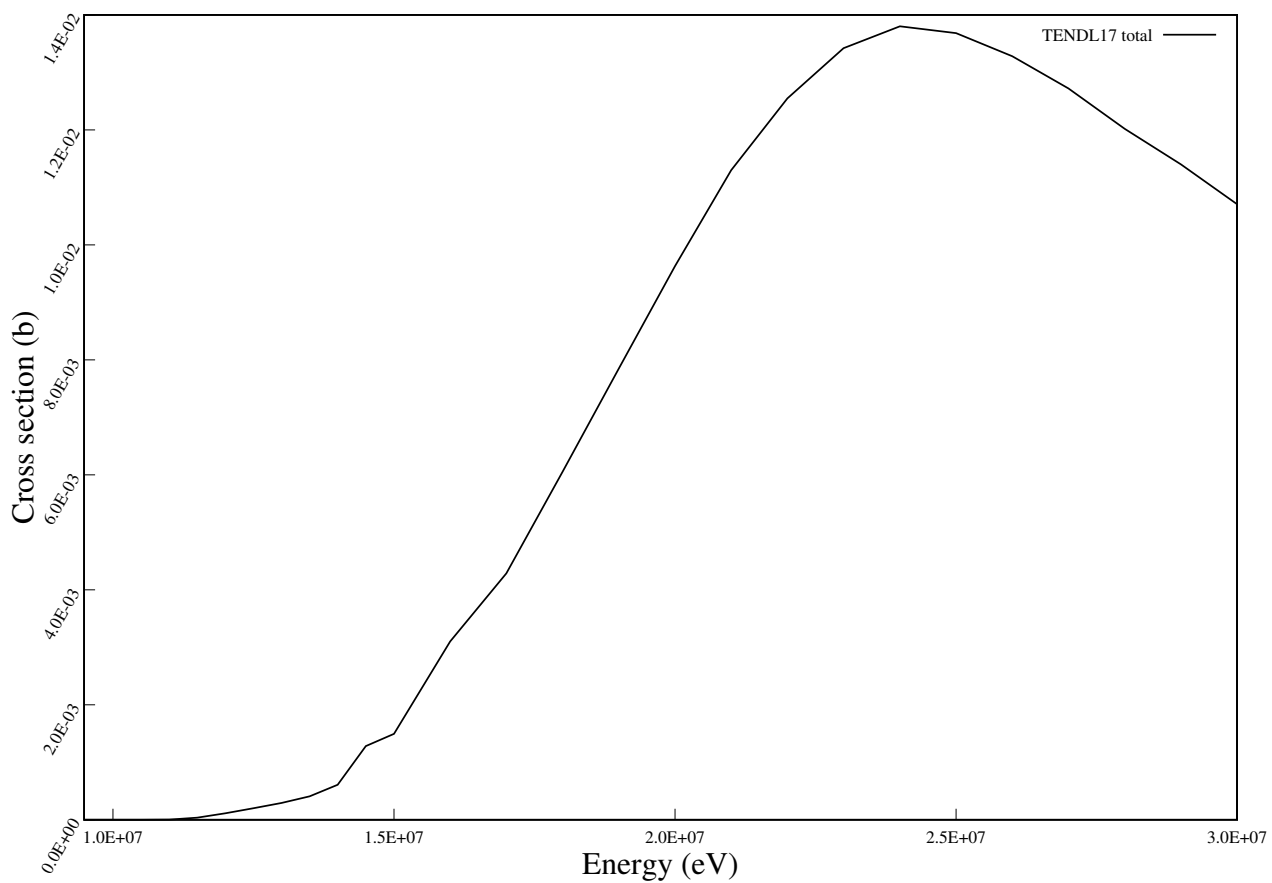
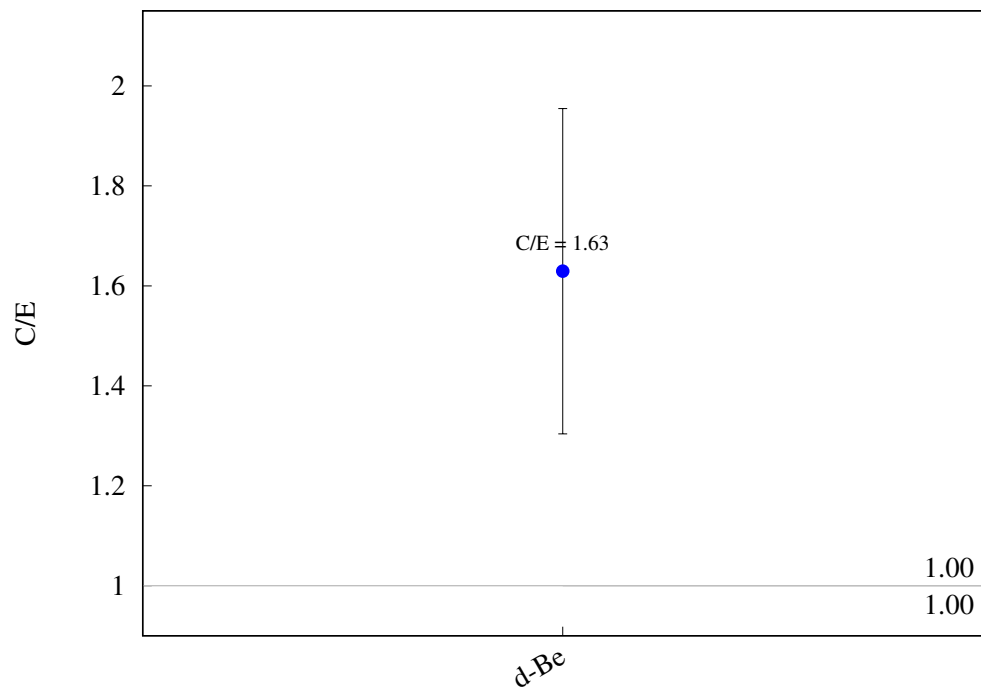
$^{32}\text{S} (\text{n},\text{p}) ^{32}\text{P}$ 

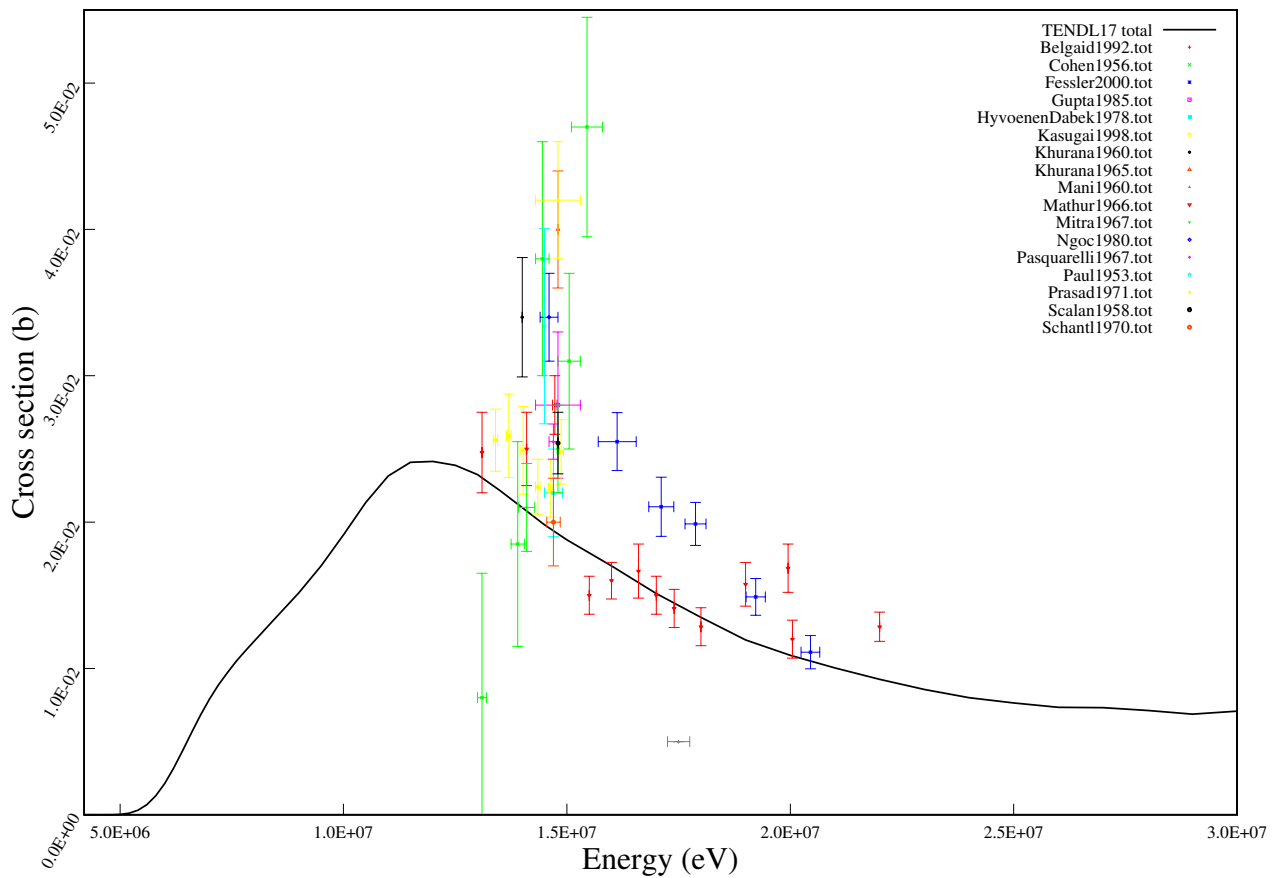
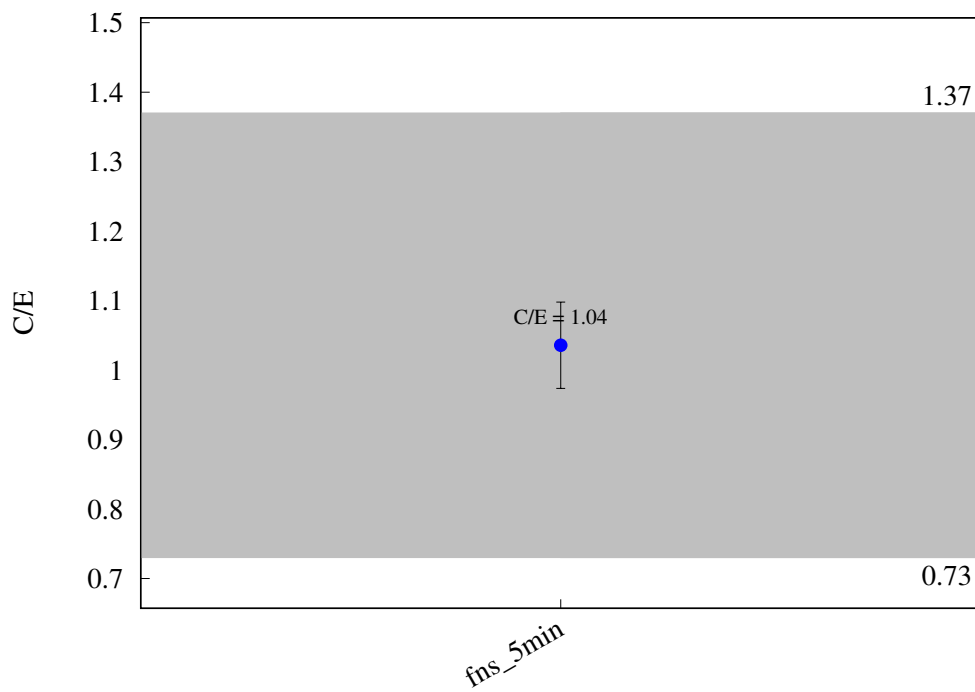
$^{32}\text{S} (\text{n},\text{t}) ^{30}\text{P}$ 

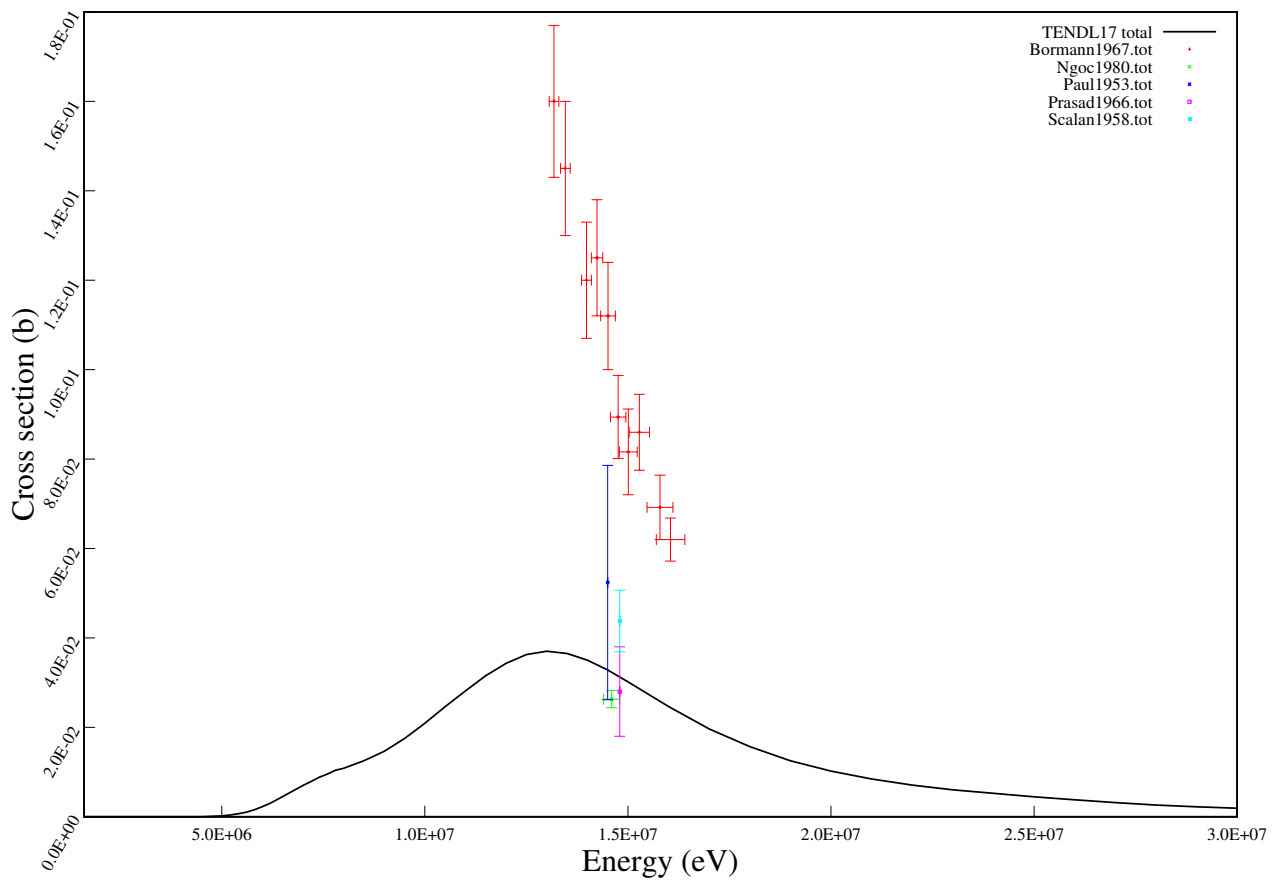
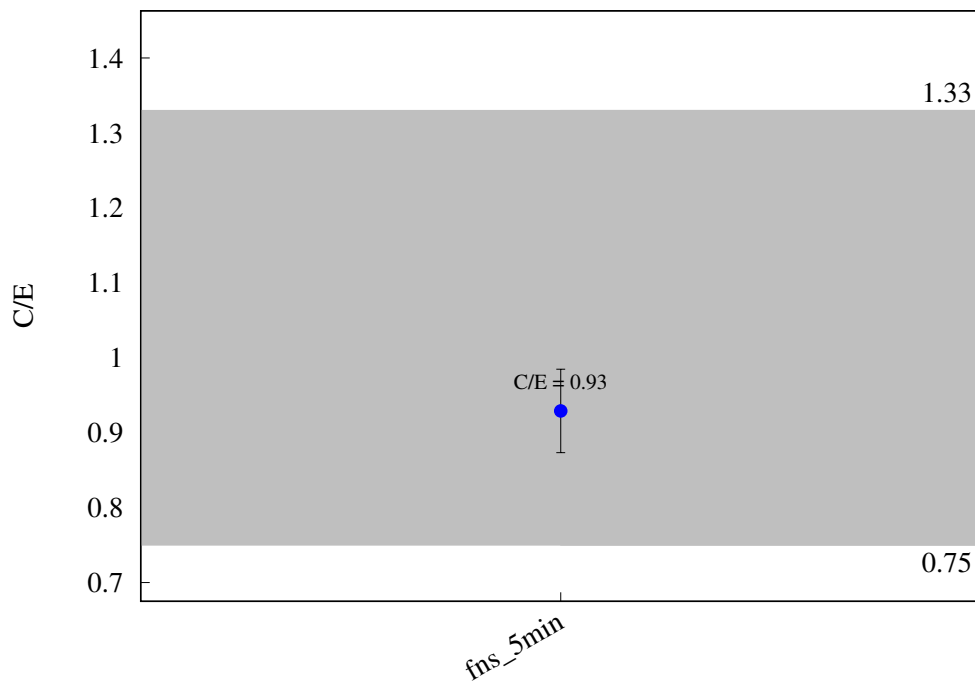
$^{34}\text{S} (\text{n},\text{p}) ^{34}\text{P}$ 

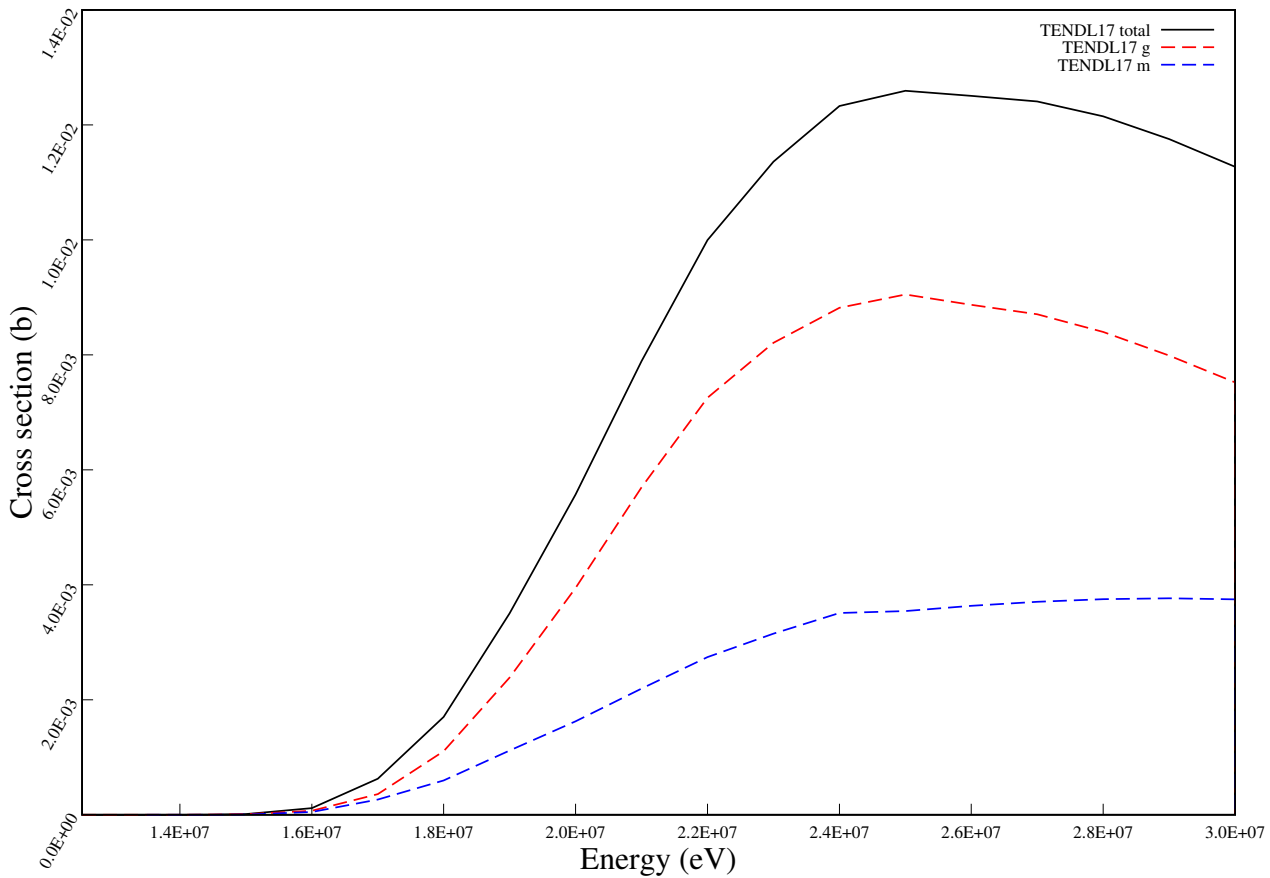
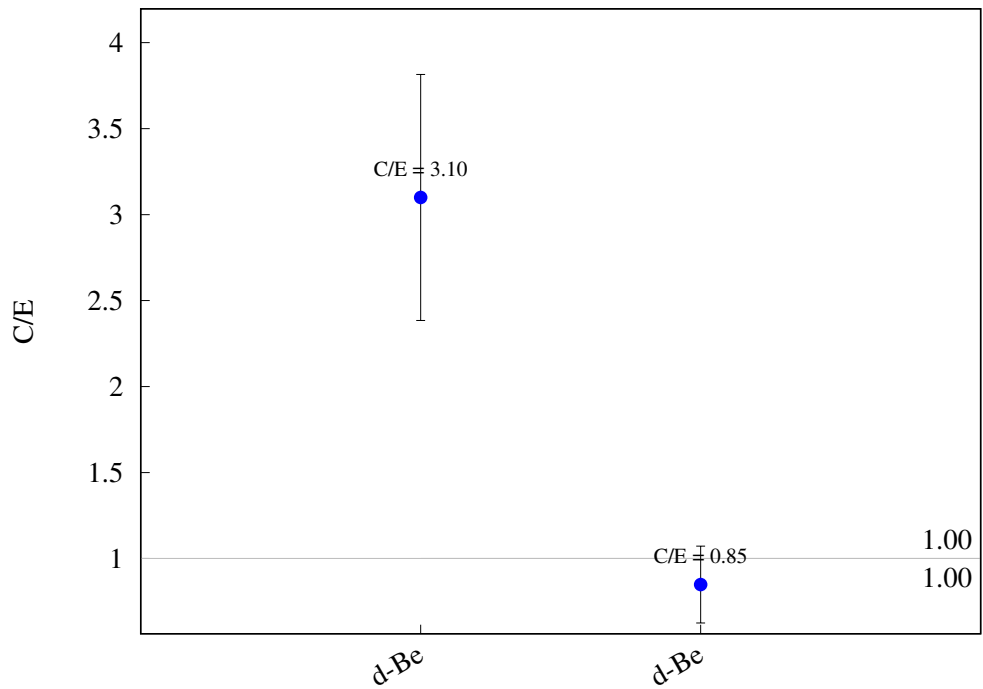


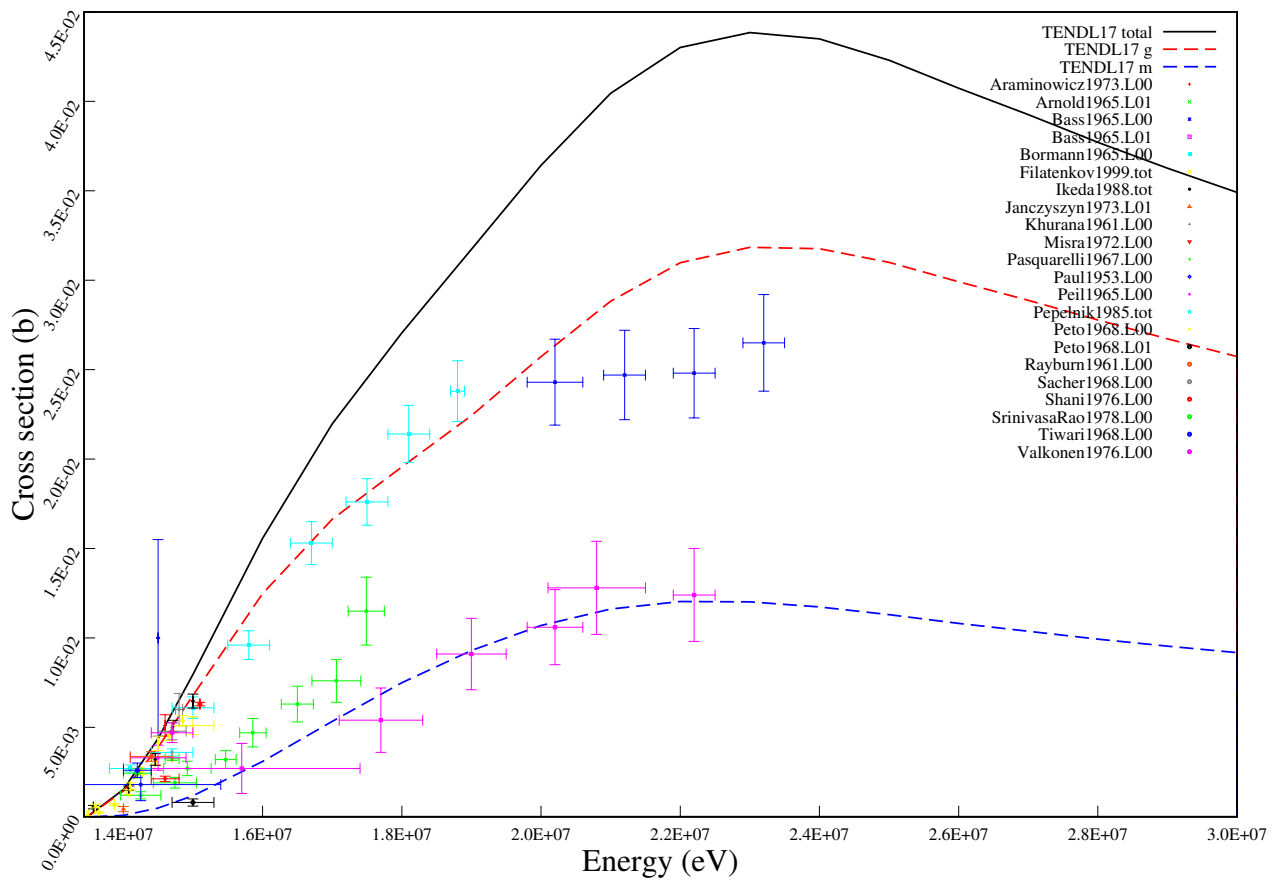
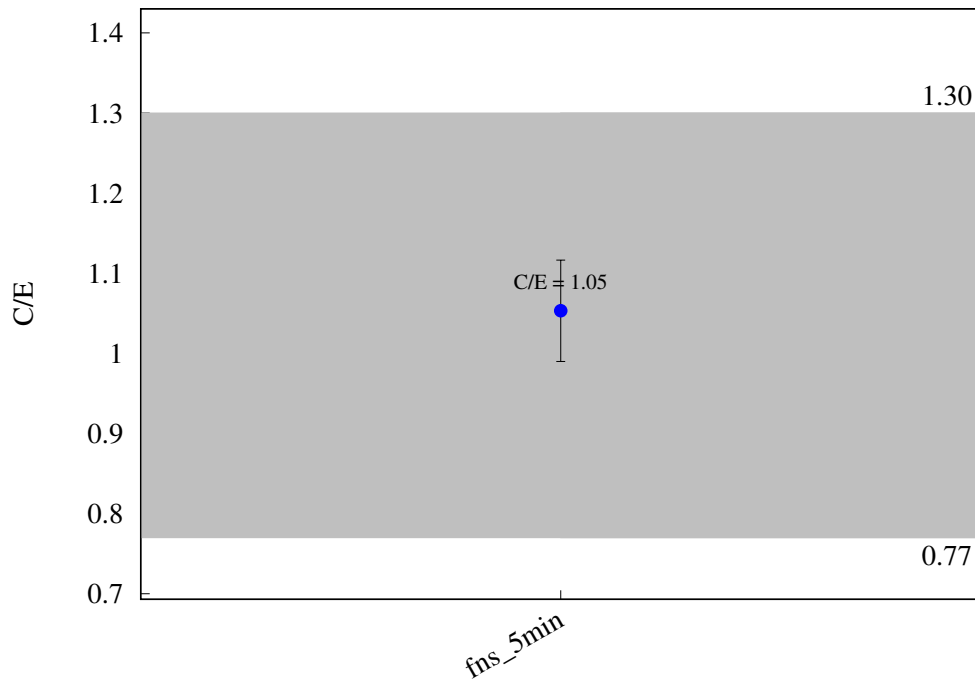
^{35}Cl (n,2n) ^{34m}Cl 

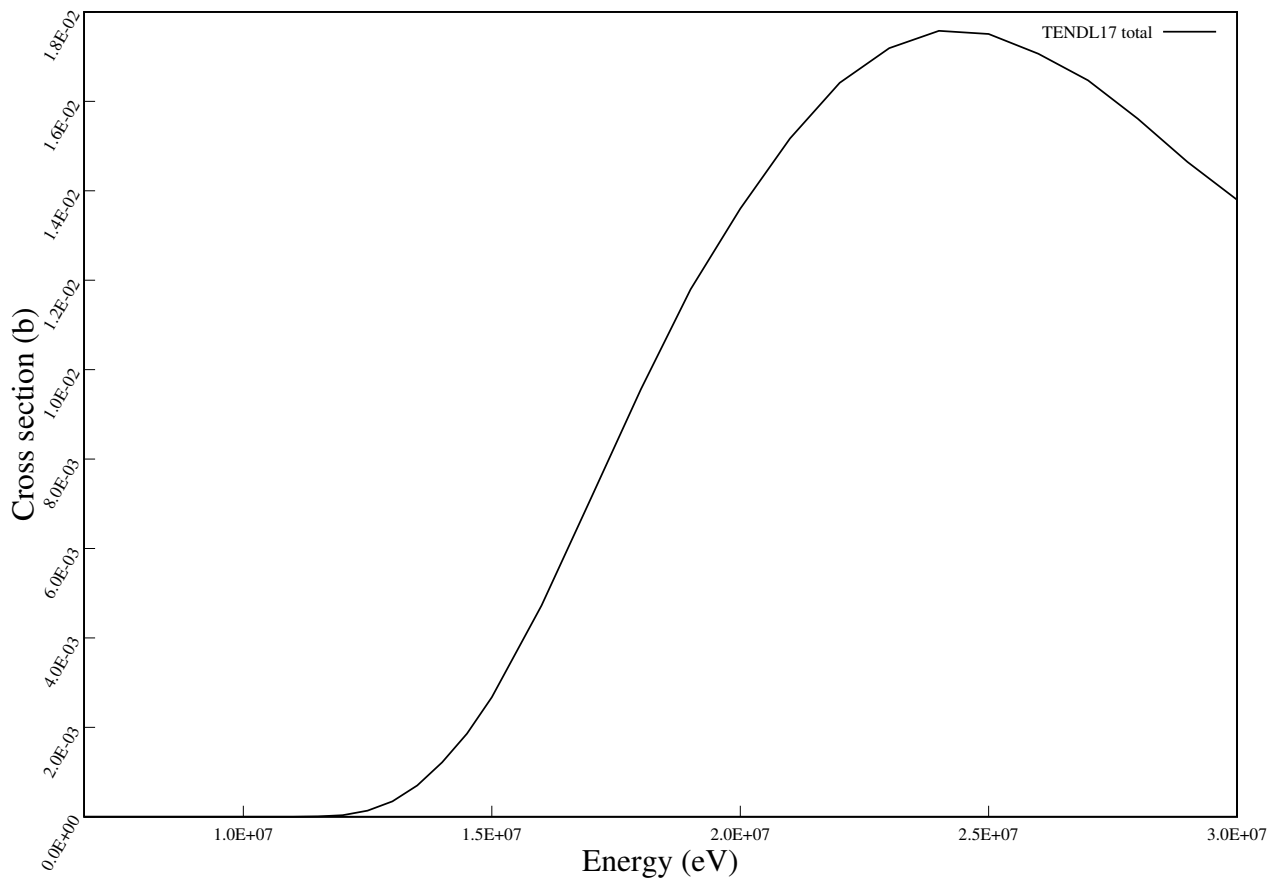
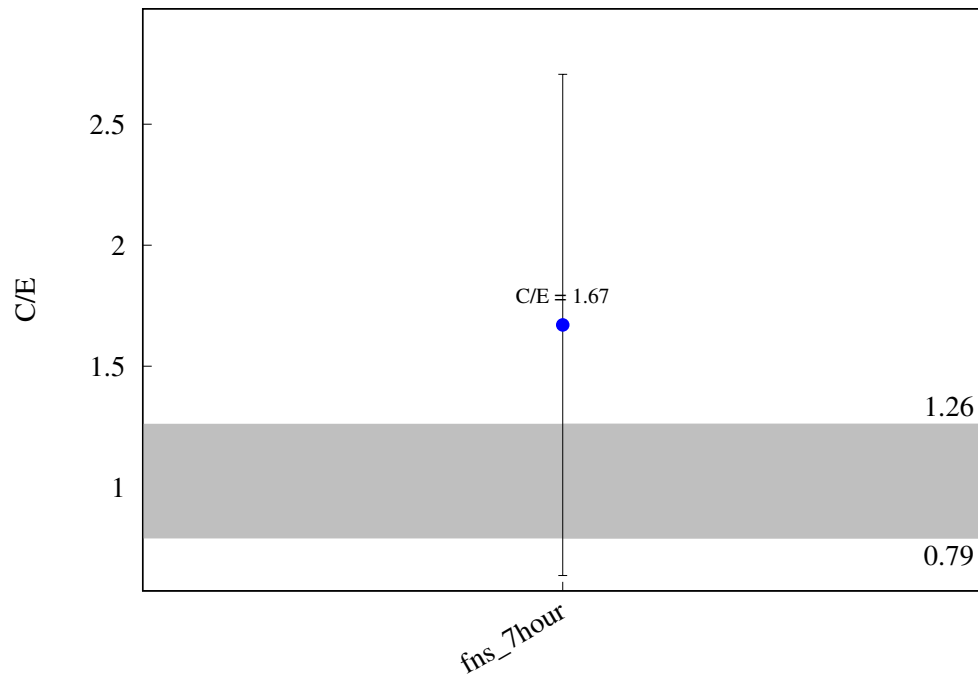
^{35}Cl (n,t) ^{33}S 

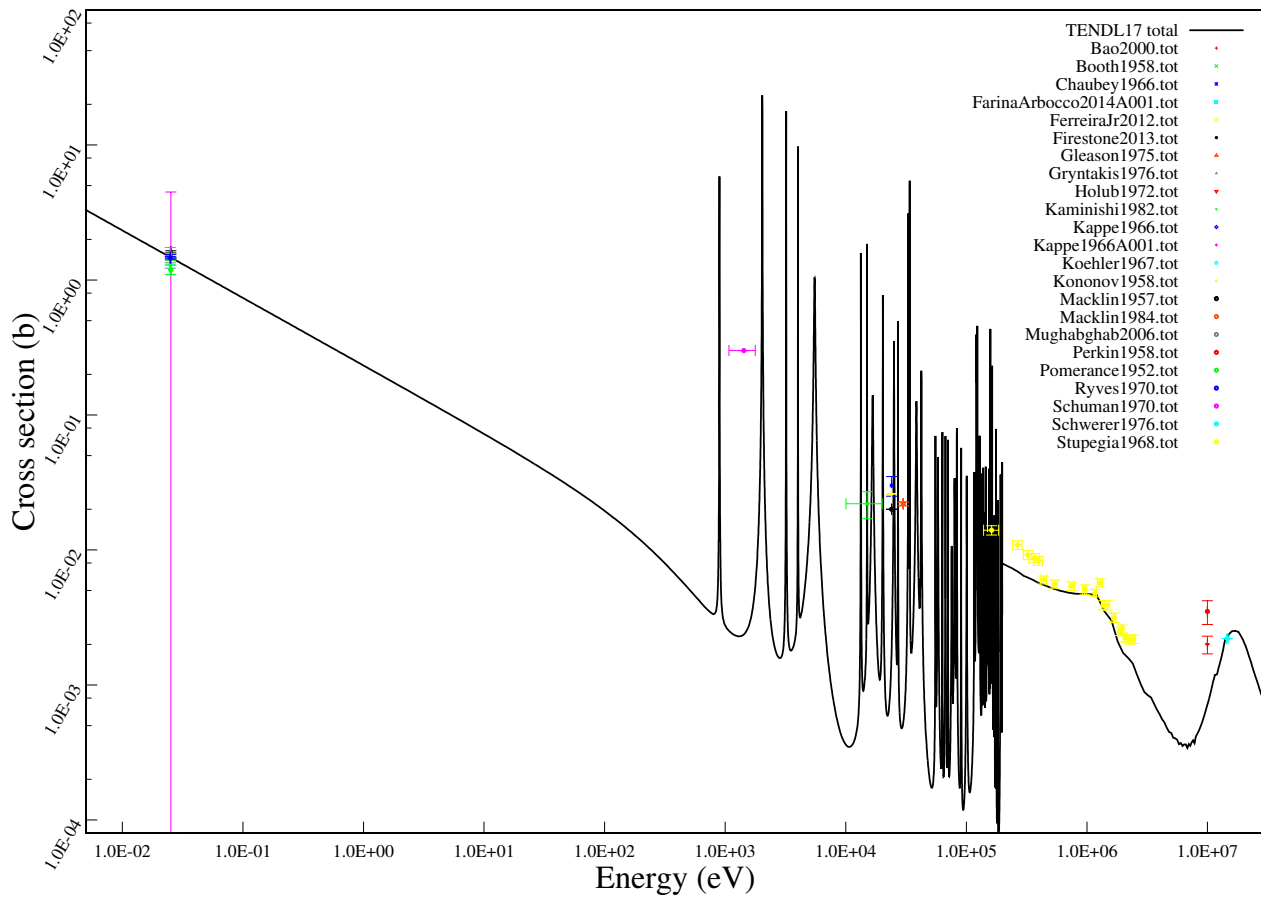
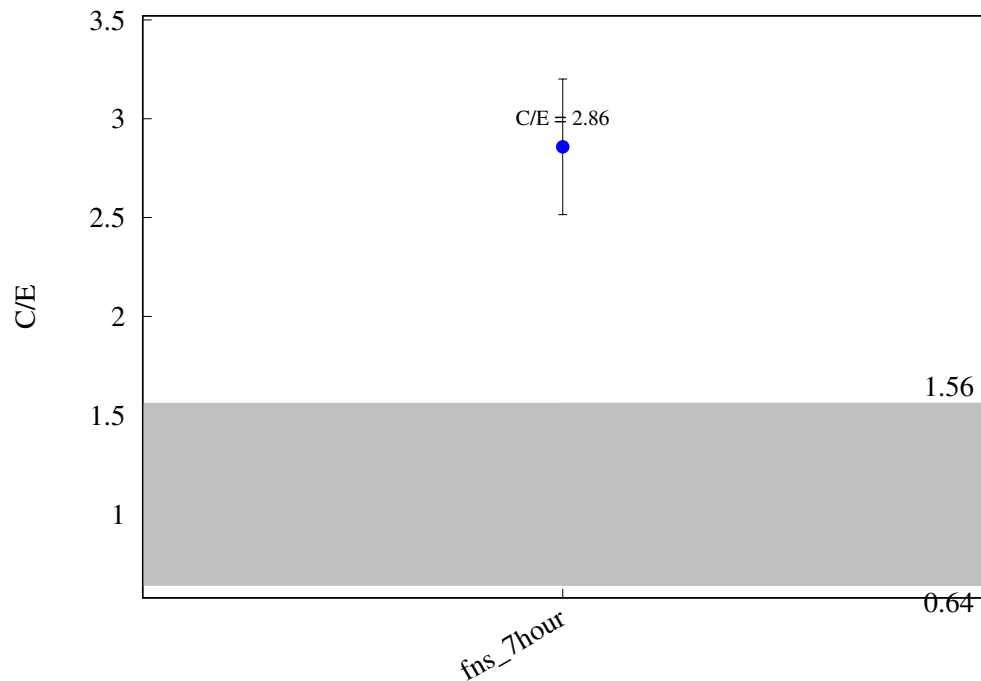
$^{37}\text{Cl} (\text{n},\text{p}) ^{37}\text{S}$ 

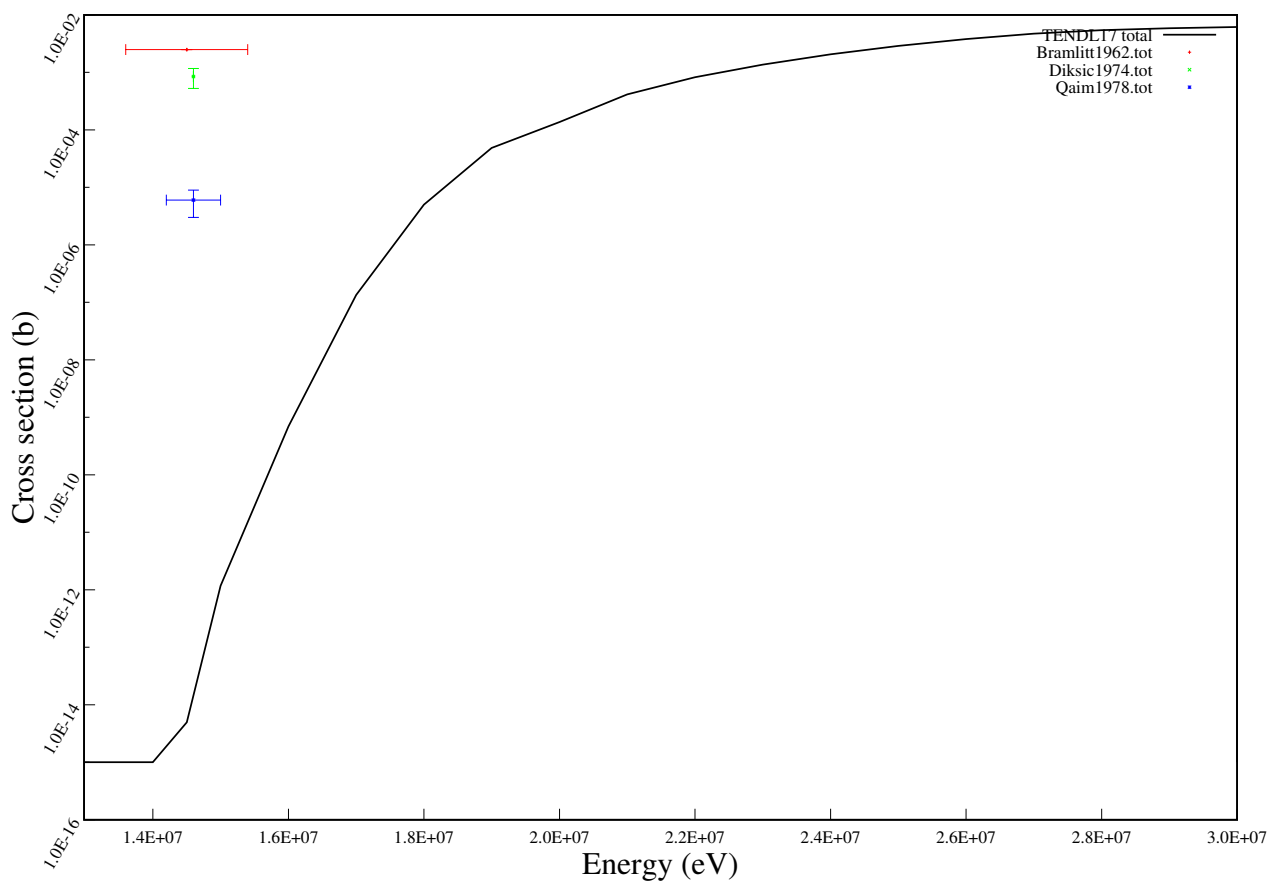
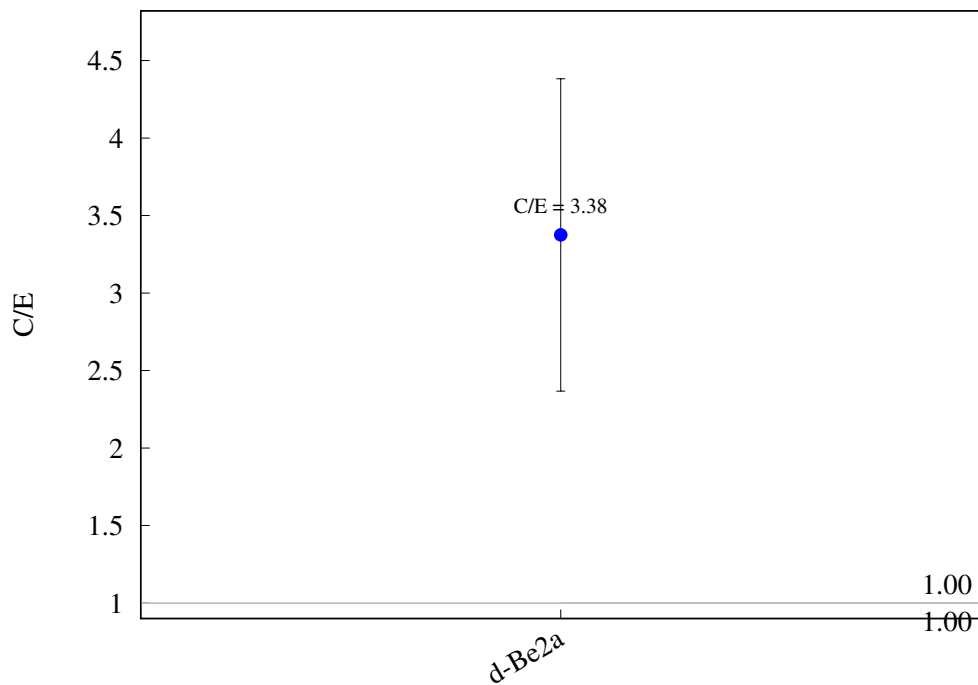
^{37}Cl (n,a) ^{34}P 

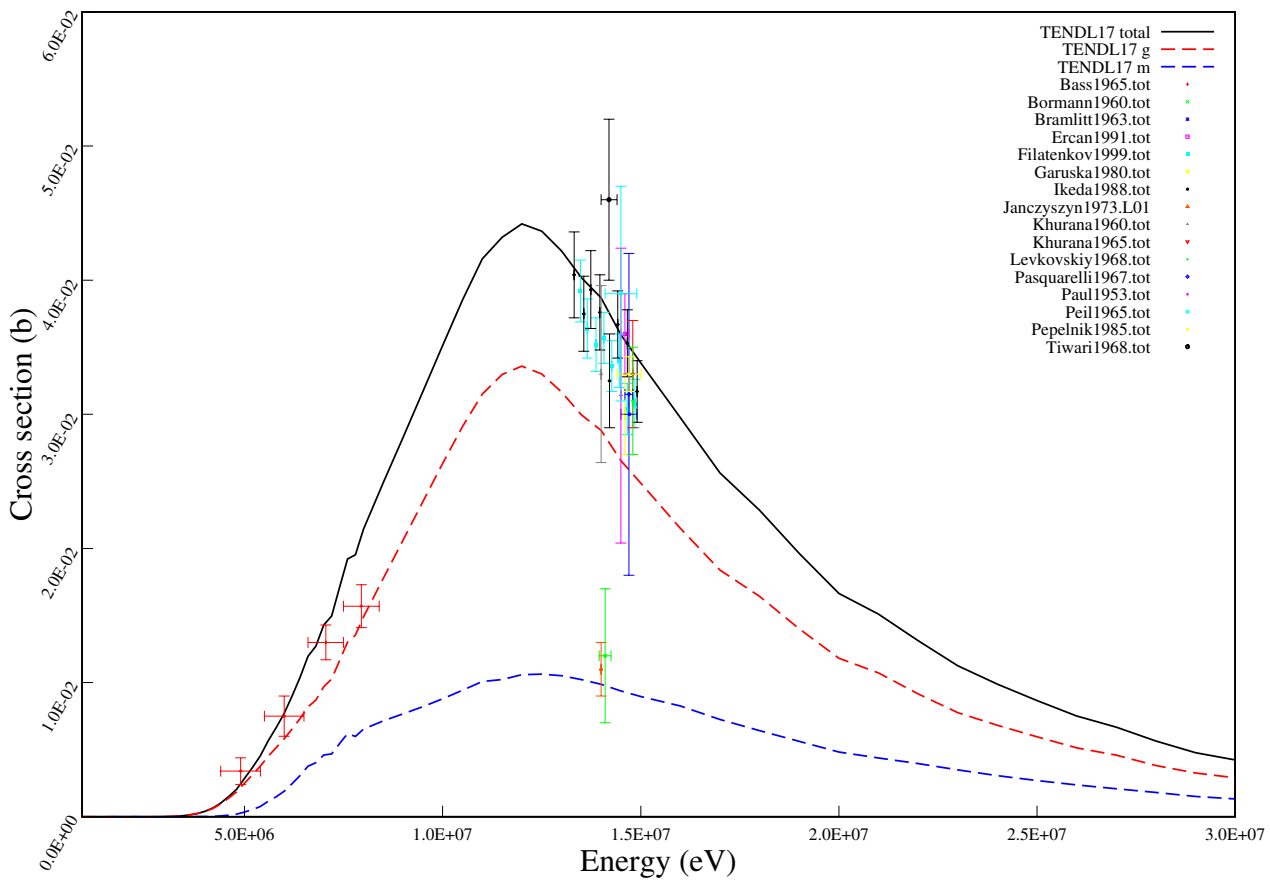
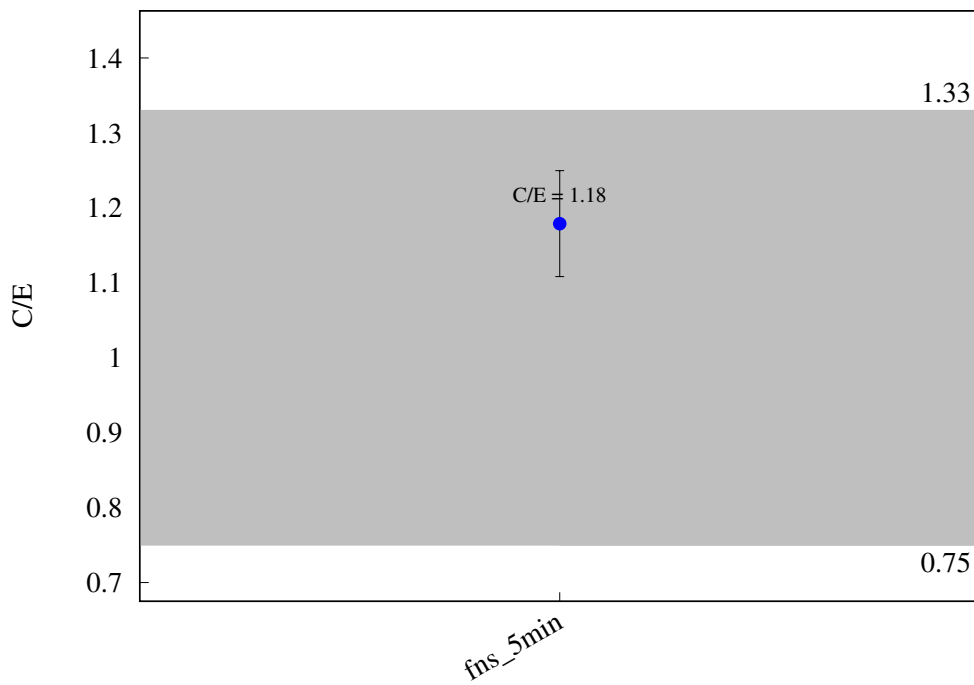
^{40}Ar (n,t) ^{38}Cl 

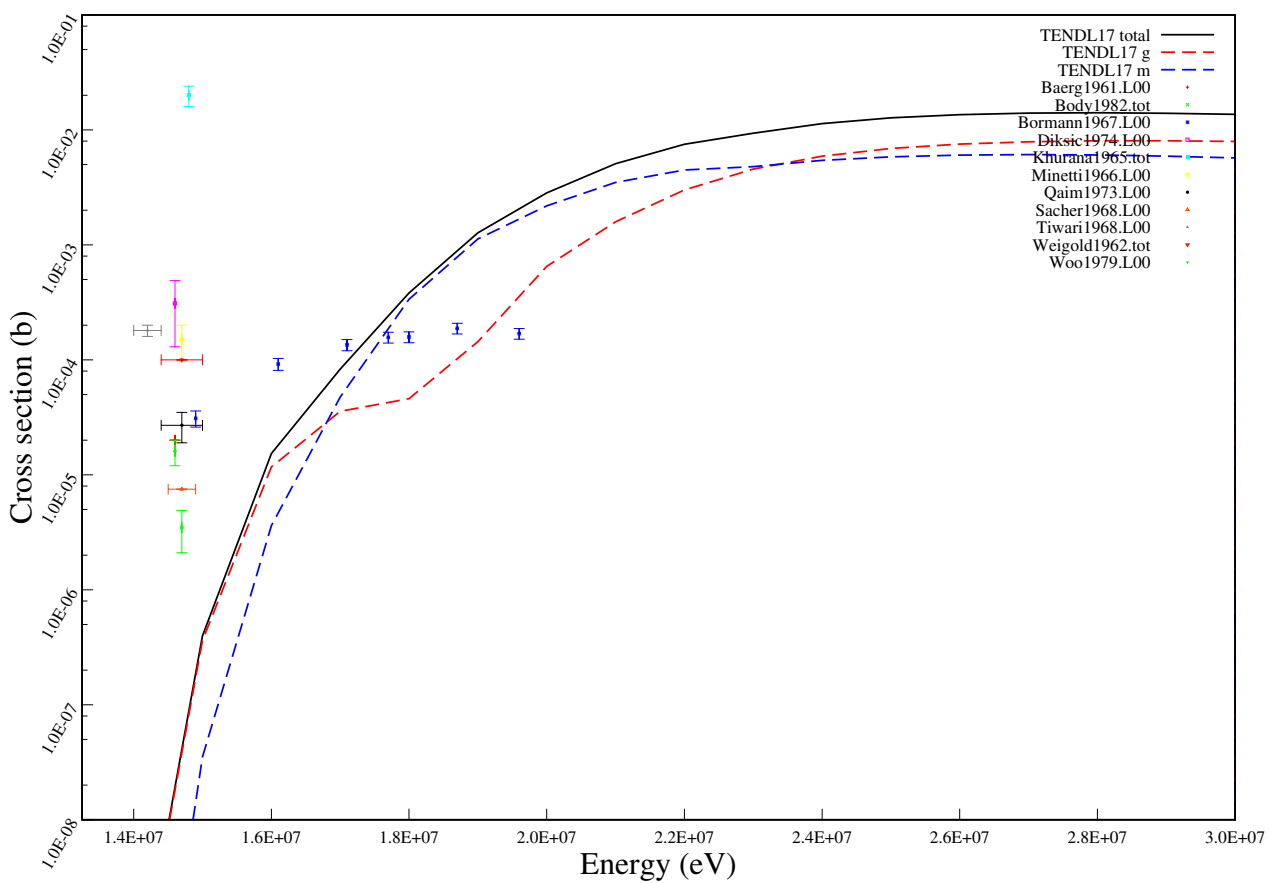
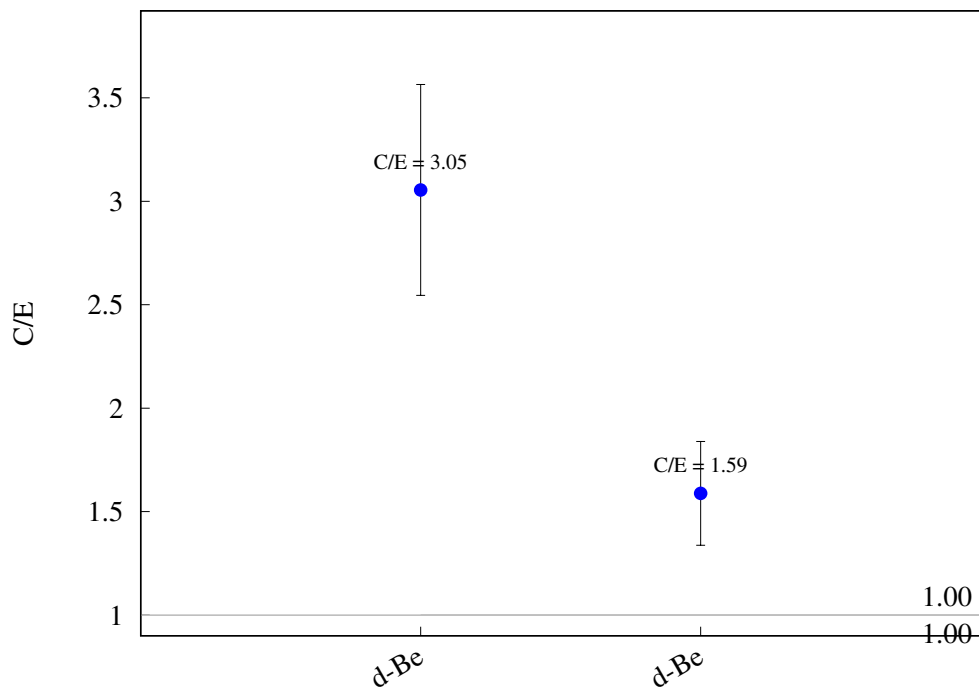
^{39}K (n,2n) ^{38}gK 

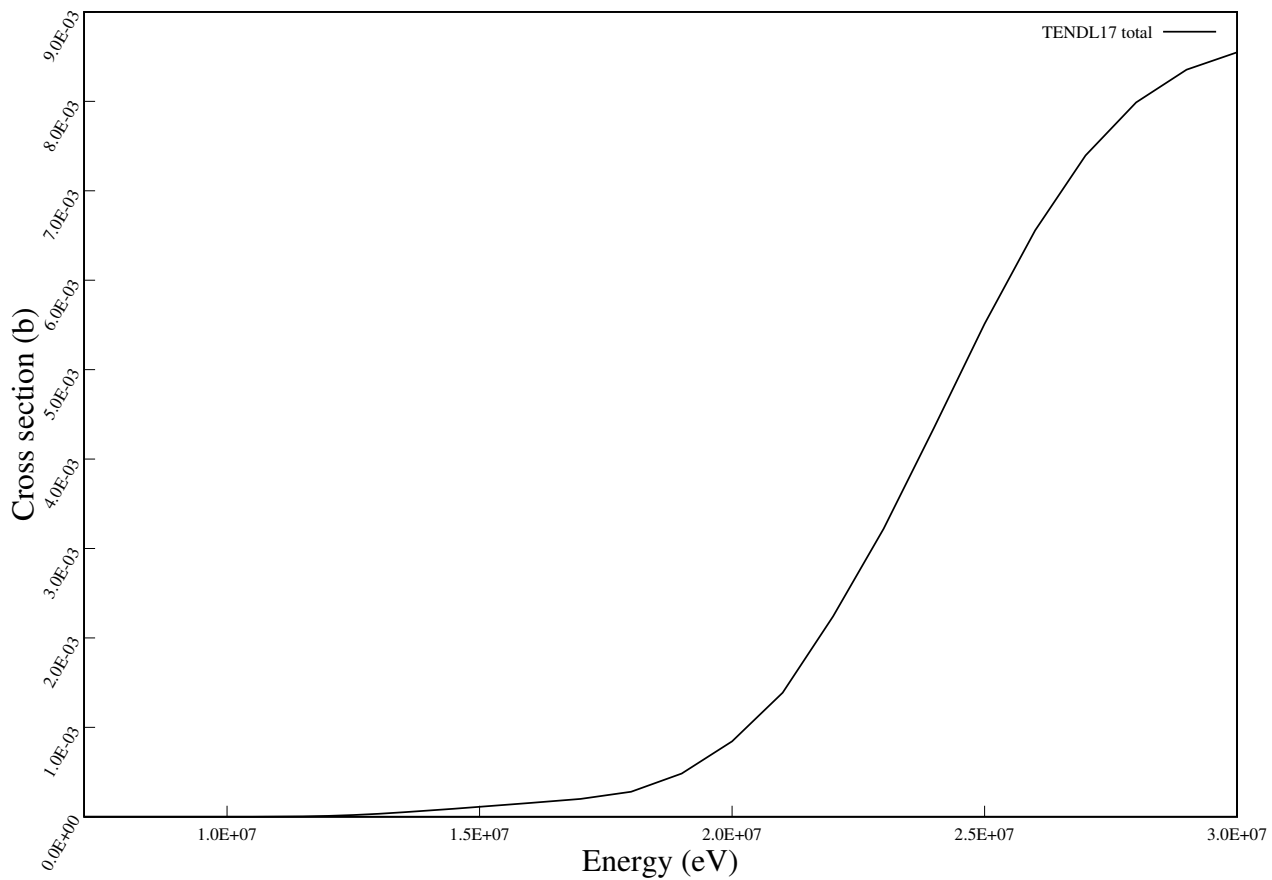
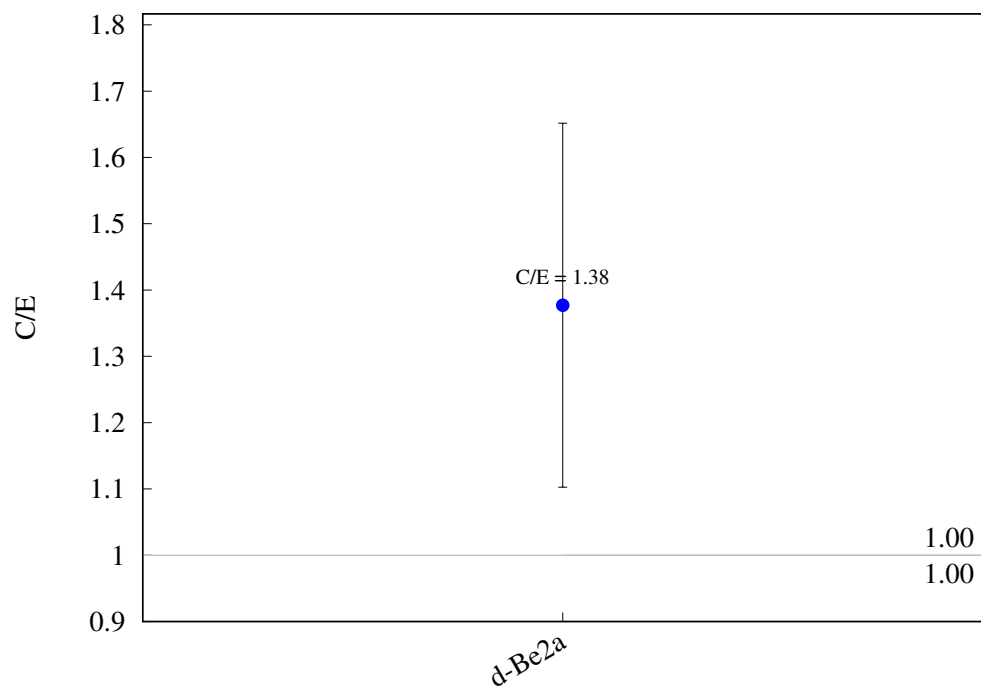
^{39}K (n,pa) ^{35}S 

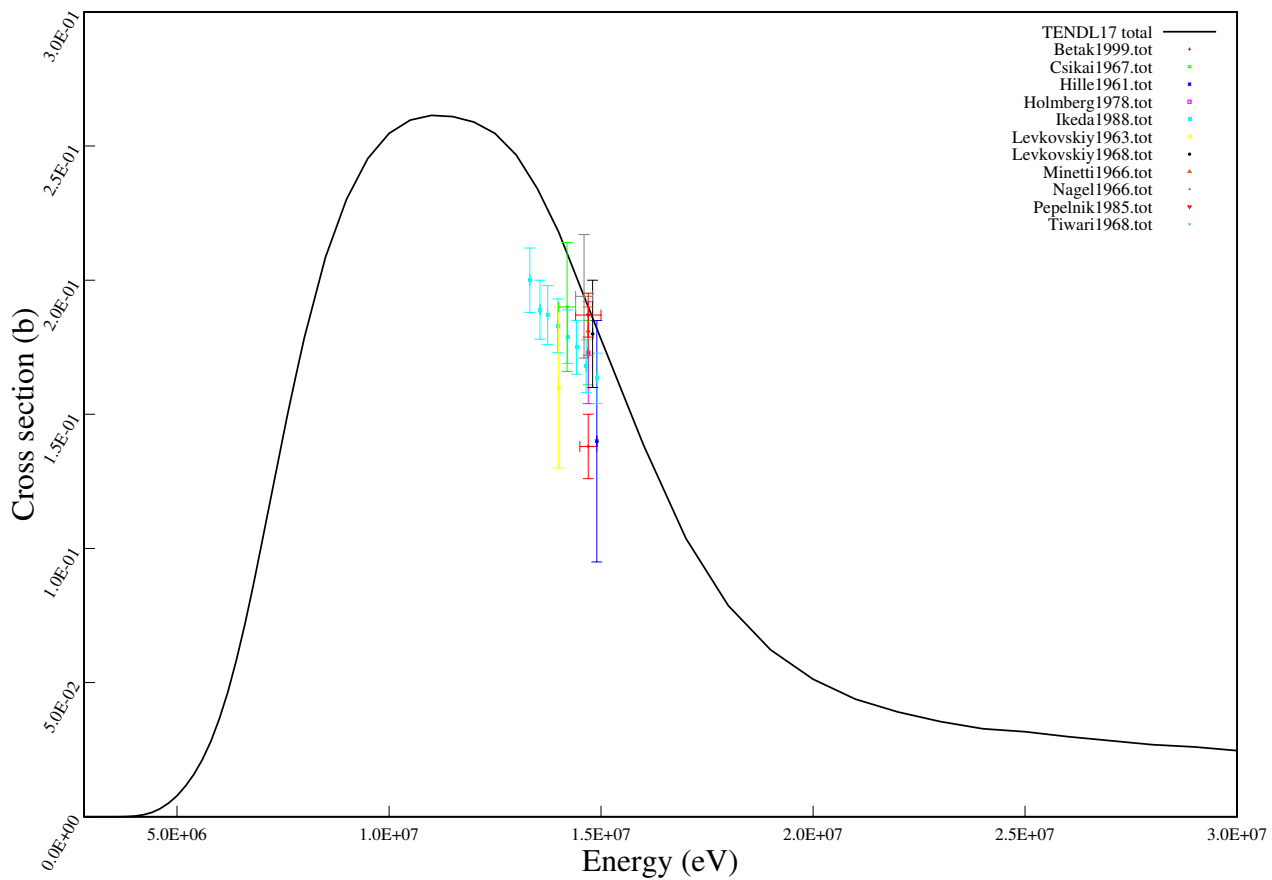
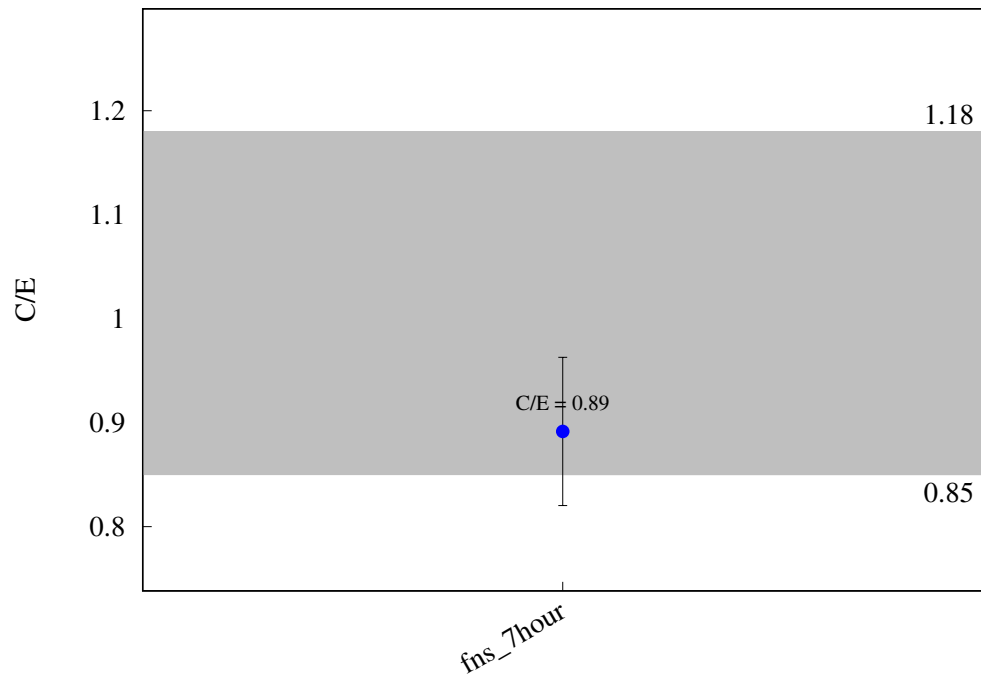
^{41}K (n,g) ^{42}K 

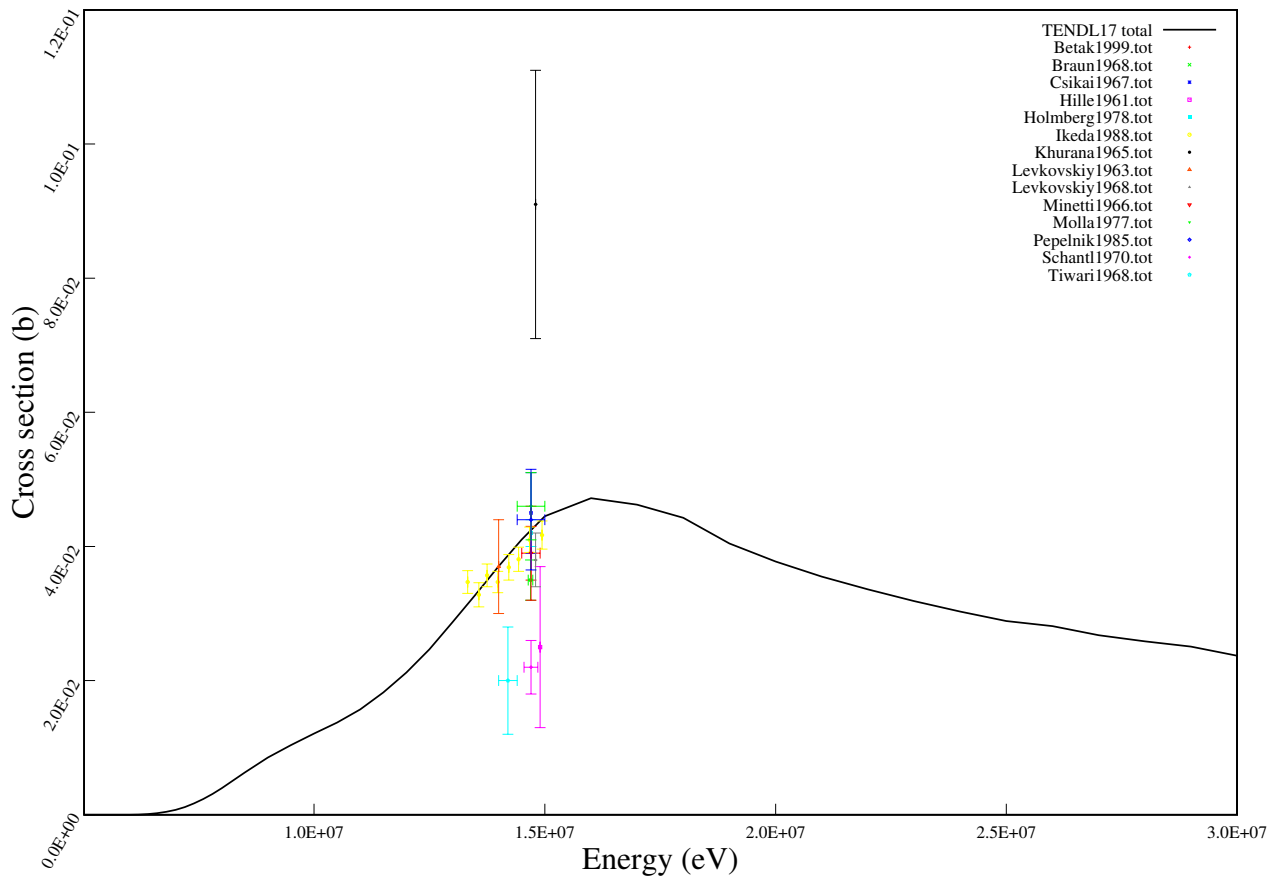
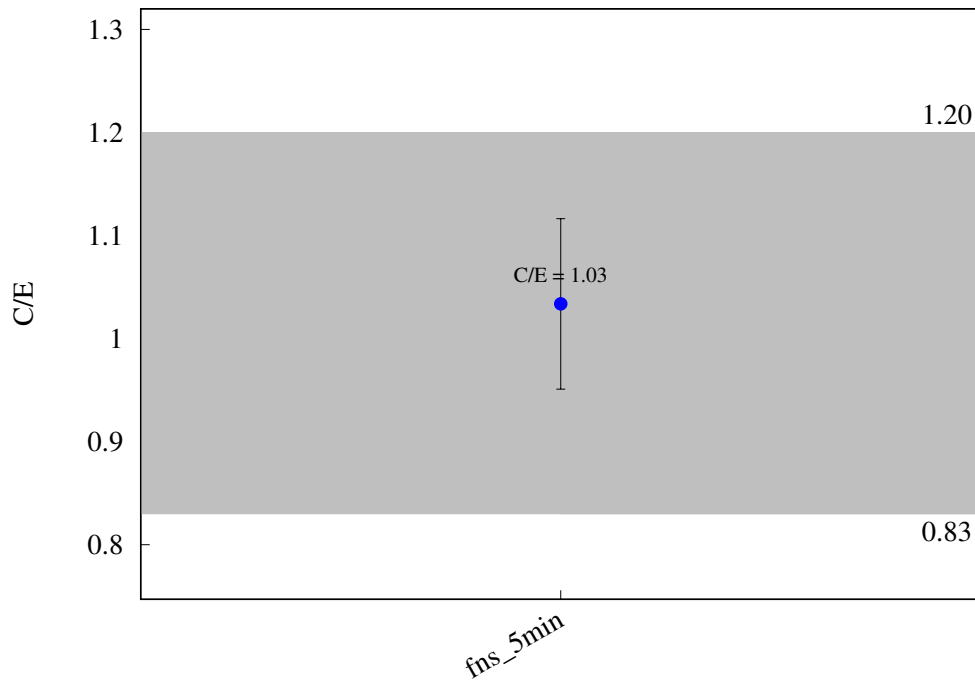
$^{41}\text{K} (\text{n},\text{h}) ^{39}\text{Cl}$ 

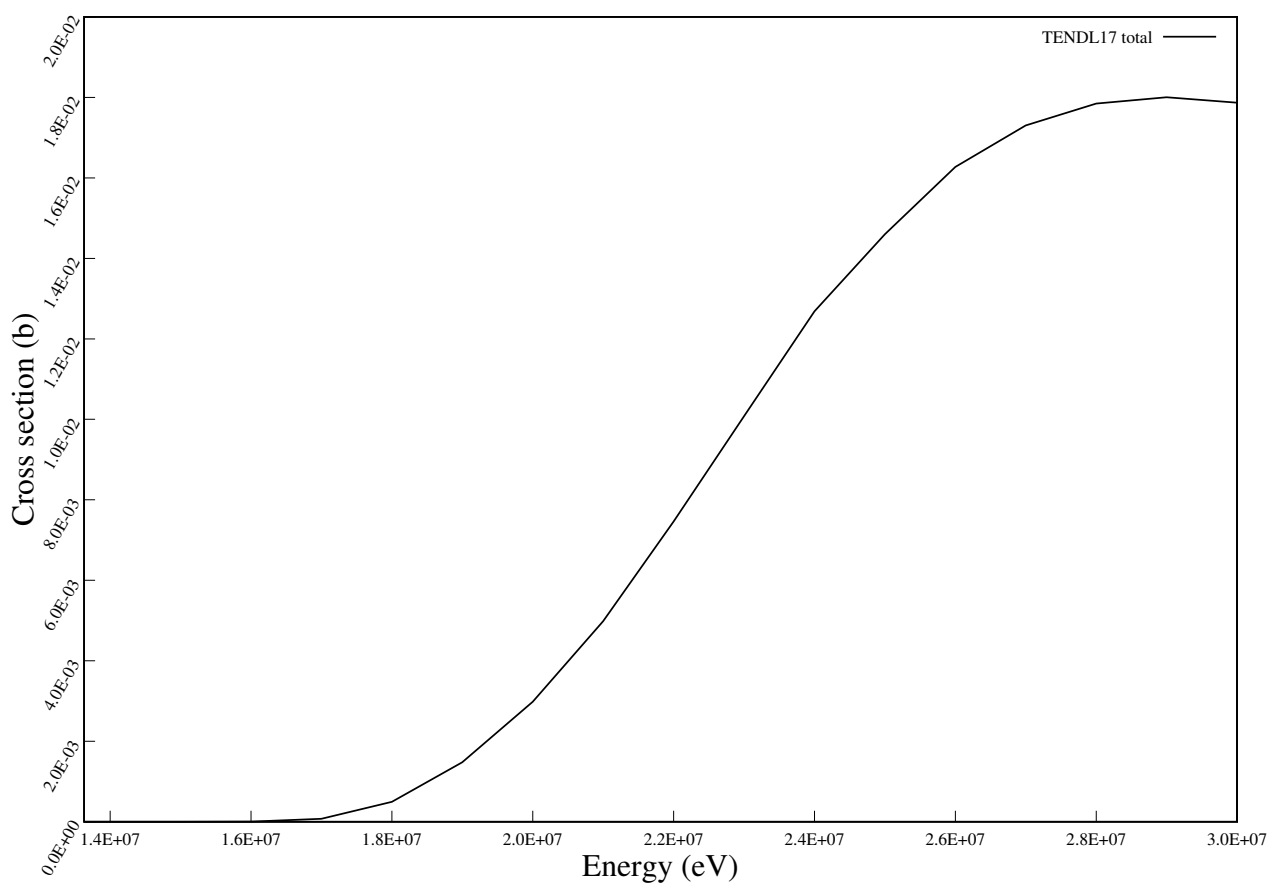
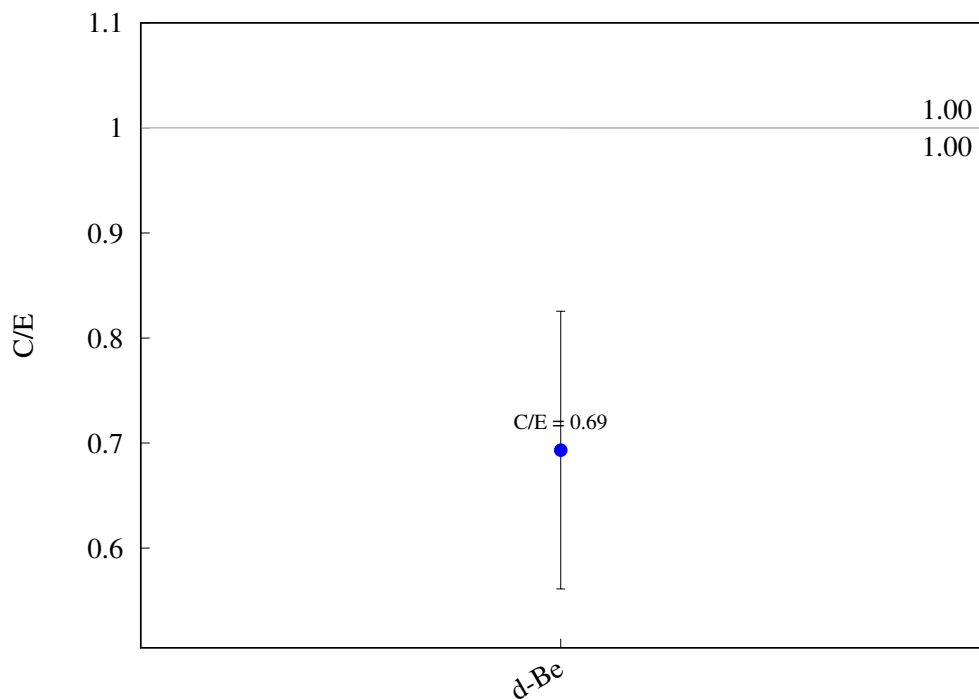
$^{41}\text{K} (\text{n},\text{a}) ^{38}\text{Cl}$ 

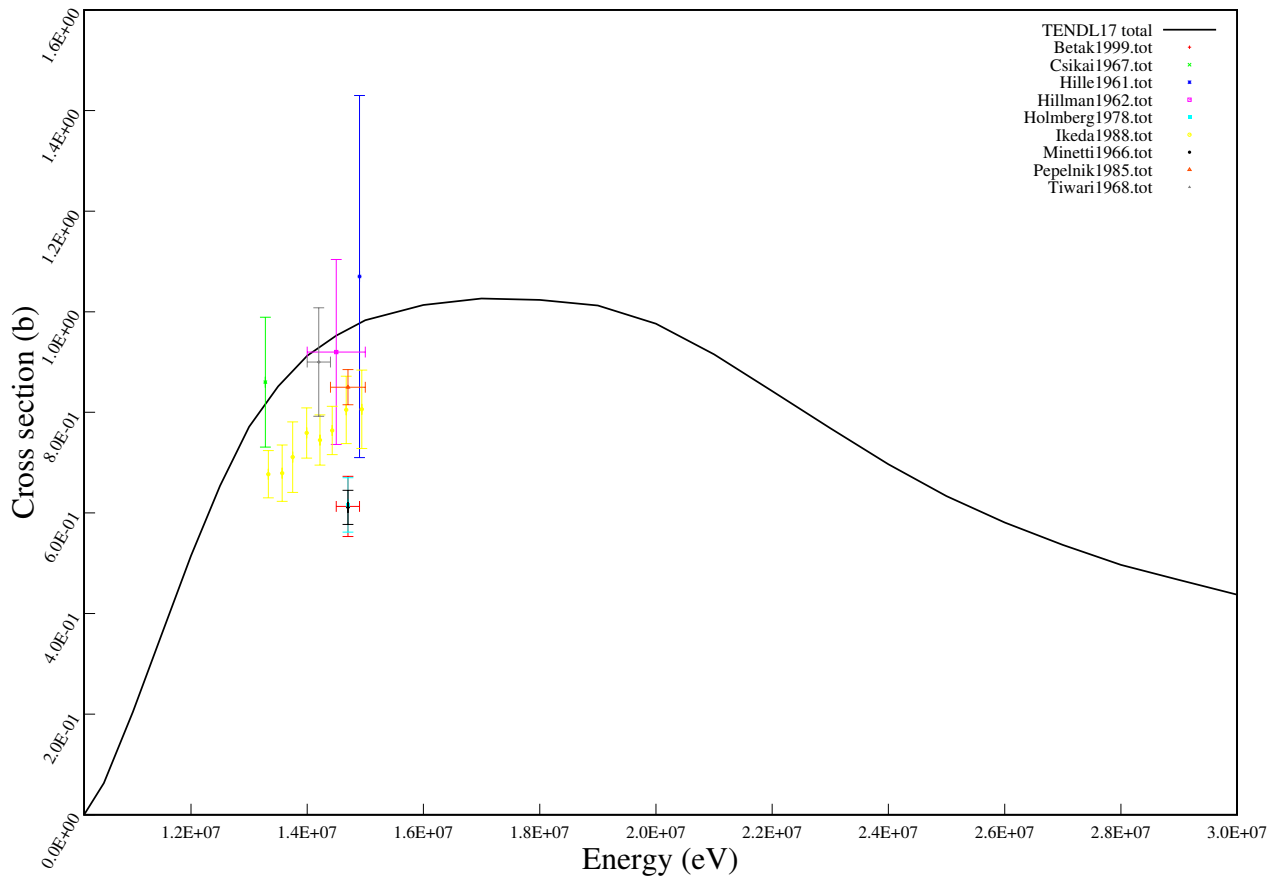
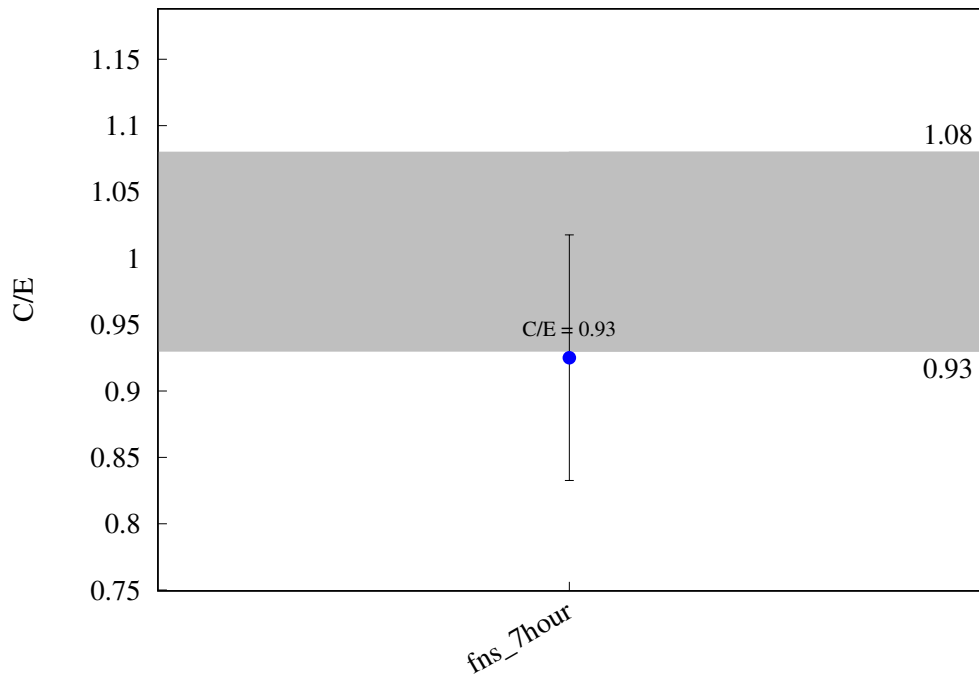
^{40}Ca (n,t) ^{38}K 

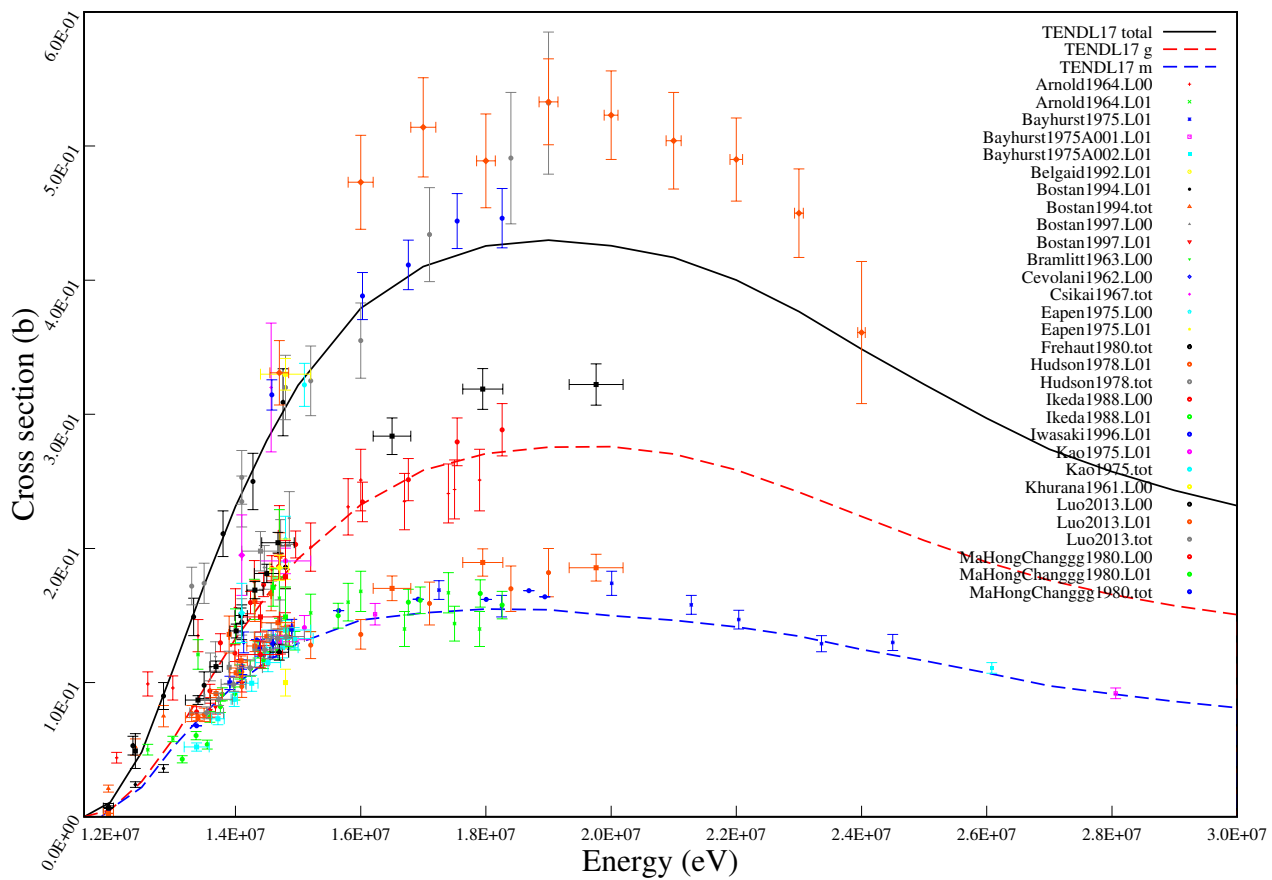
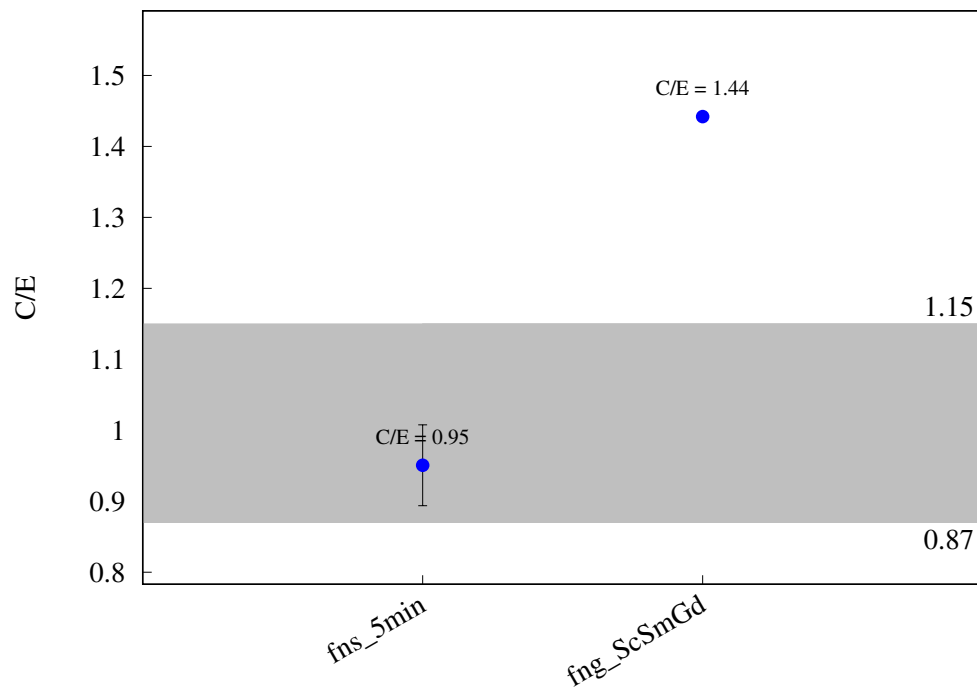
^{40}Ca (n,h) ^{38}Ar 

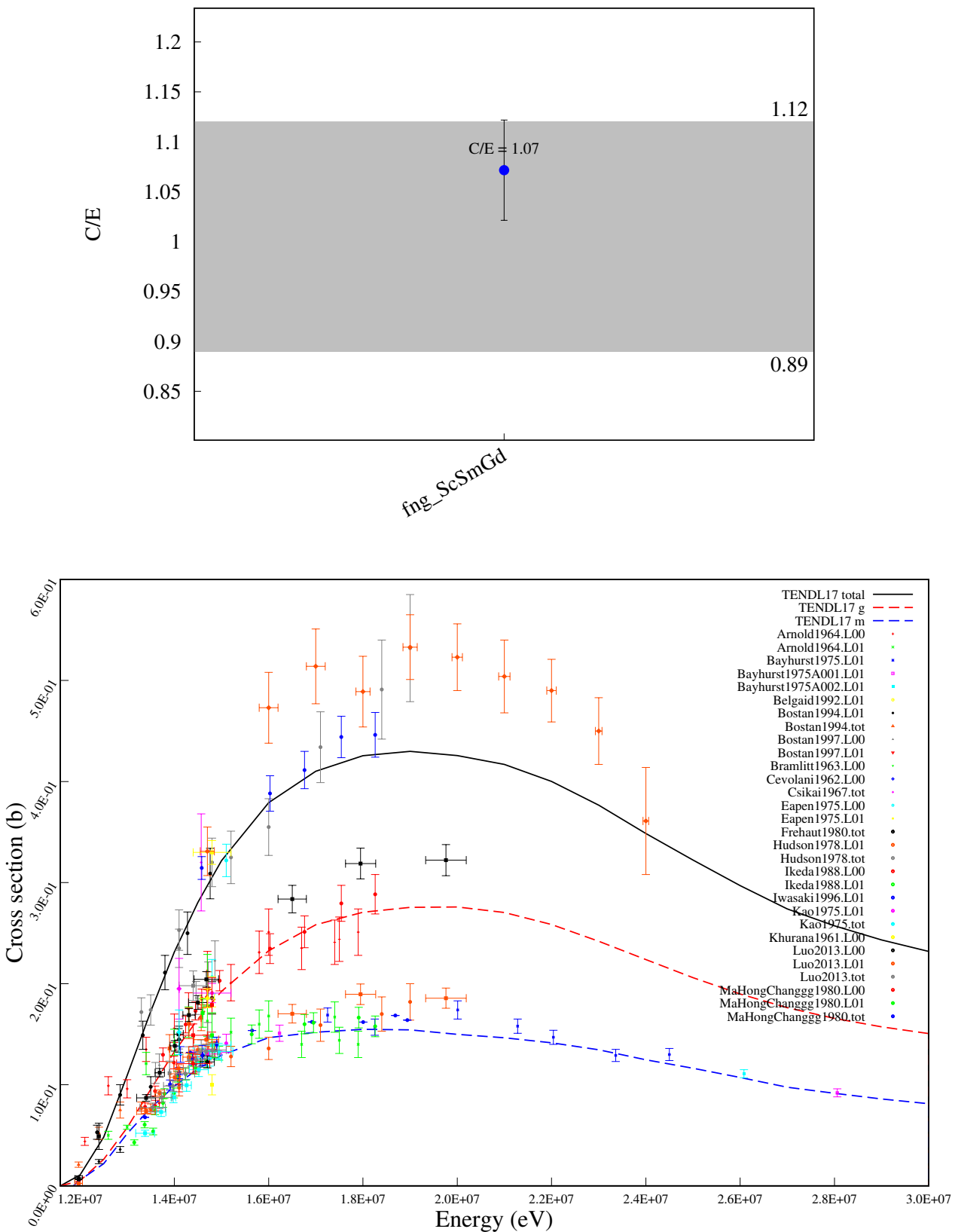
^{42}Ca (n,p) ^{42}K 

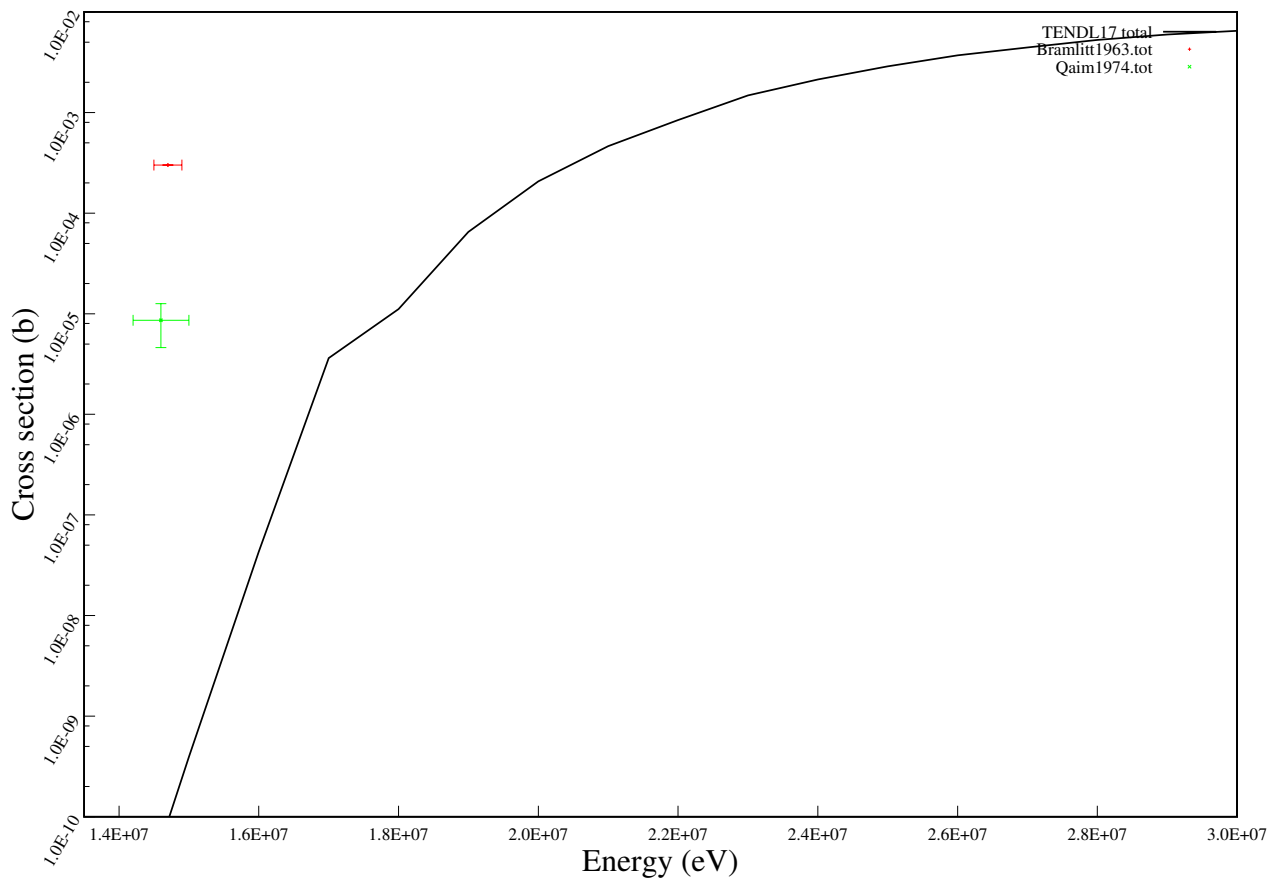
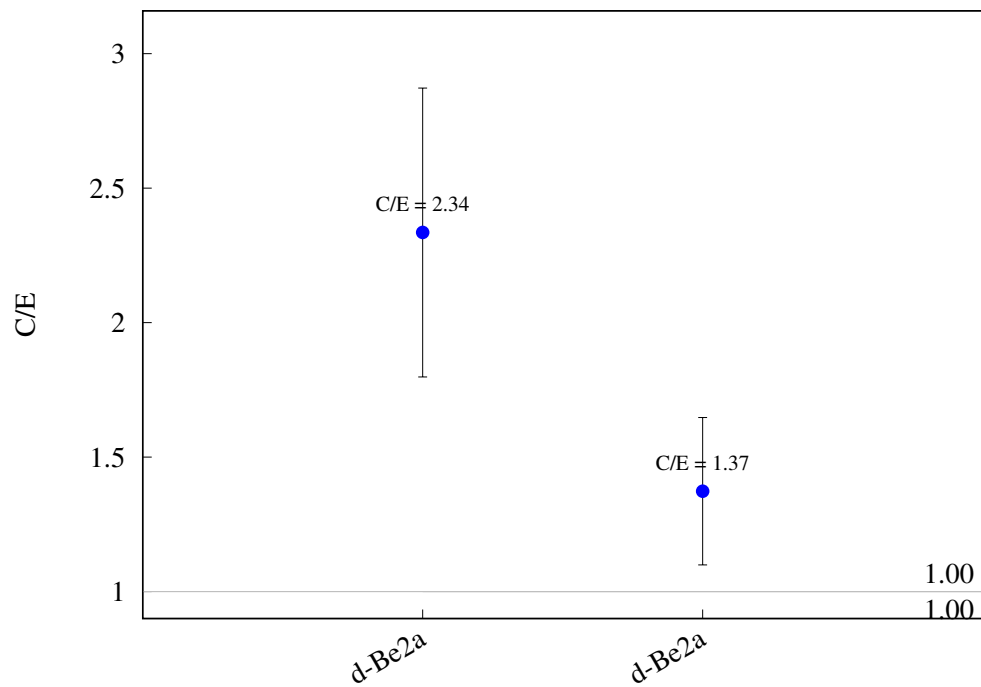
^{44}Ca (n,p) ^{44}K 

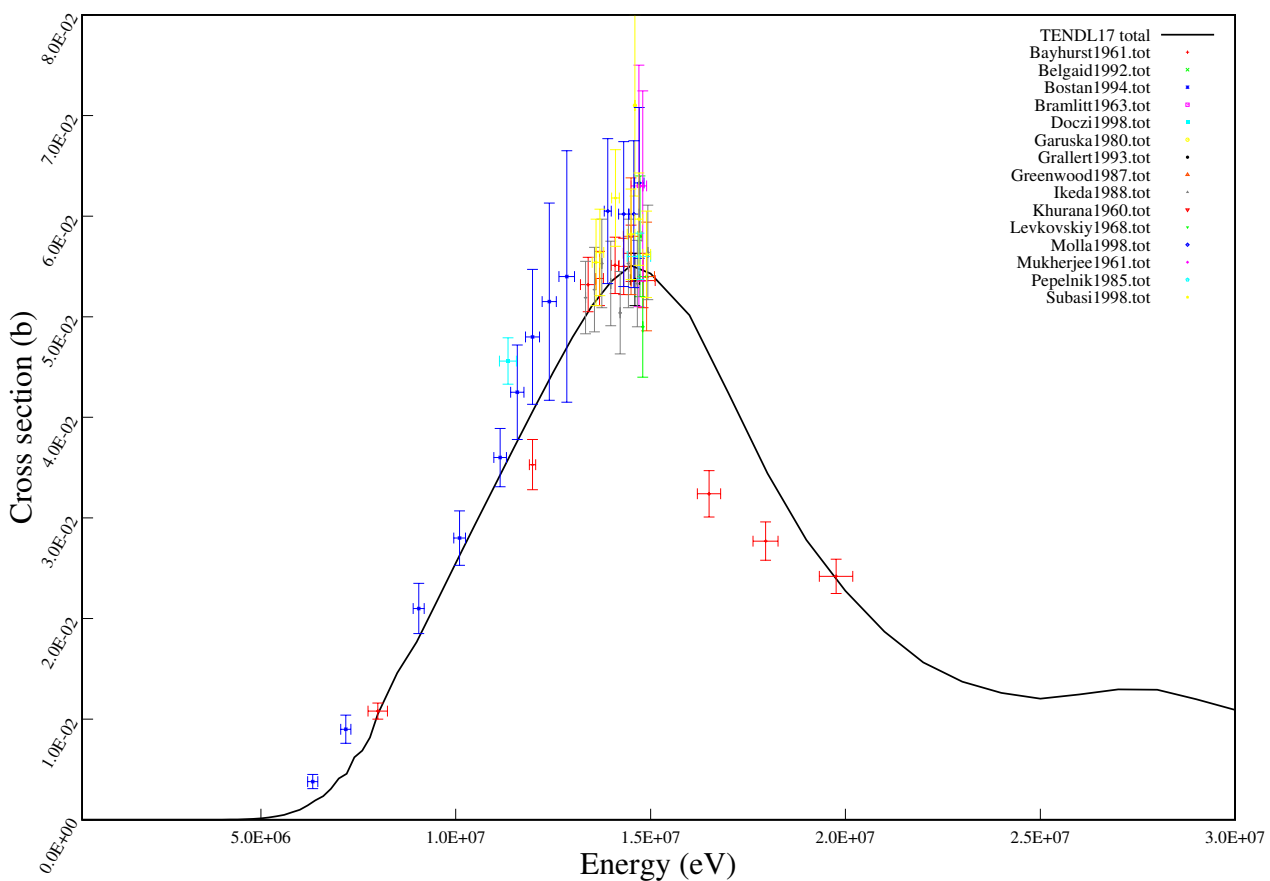
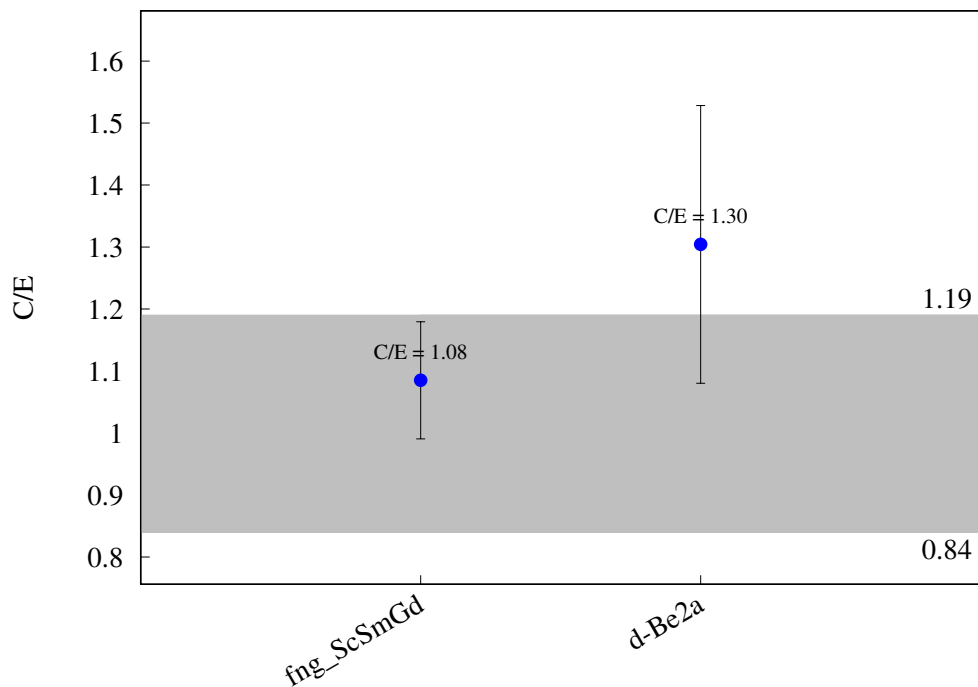
$^{44}\text{Ca} (\text{n},\text{t}) ^{42}\text{K}$ 

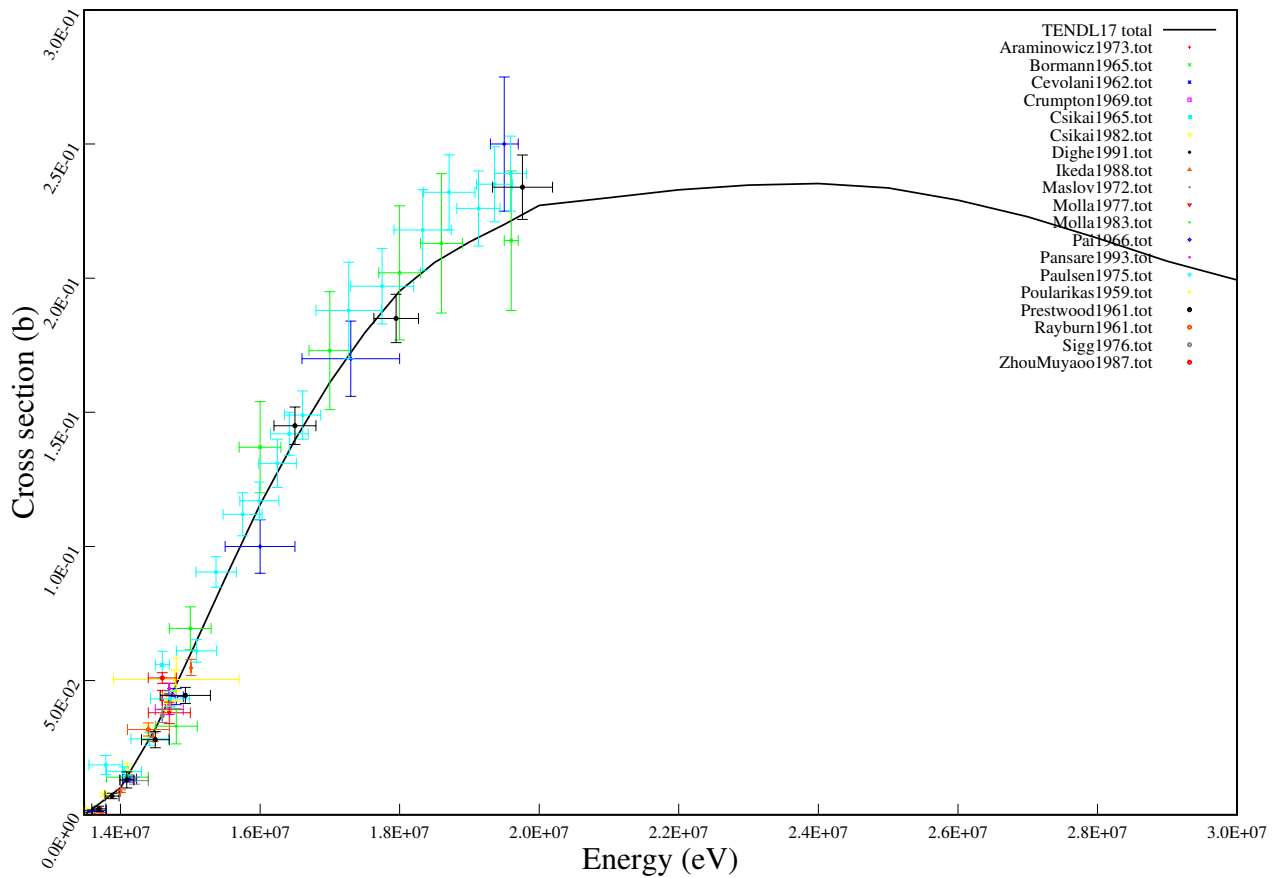
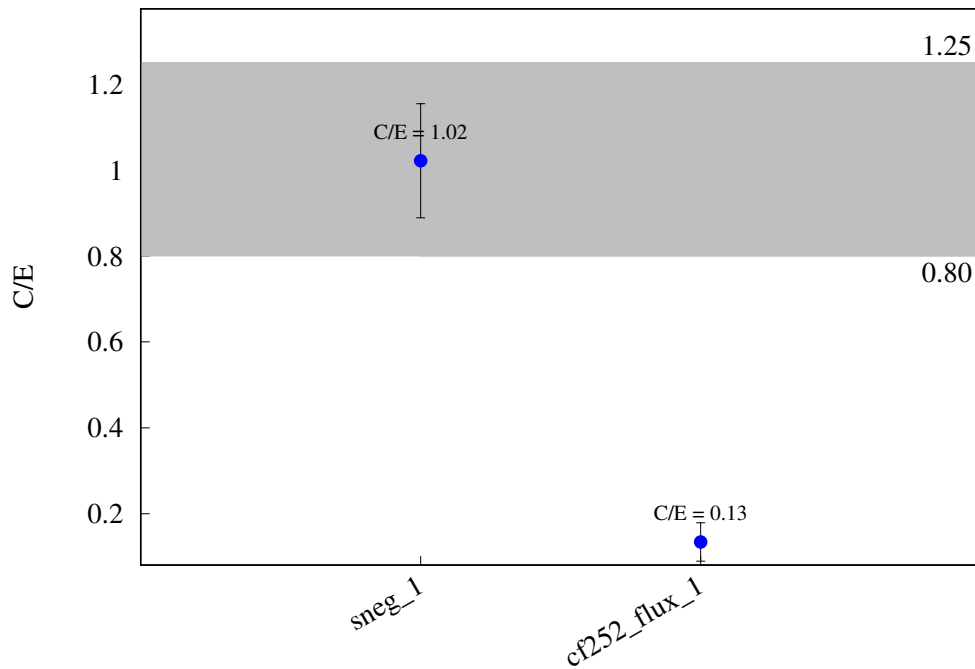
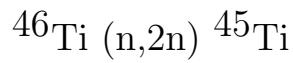
^{48}Ca (n,2n) ^{47}Ca 

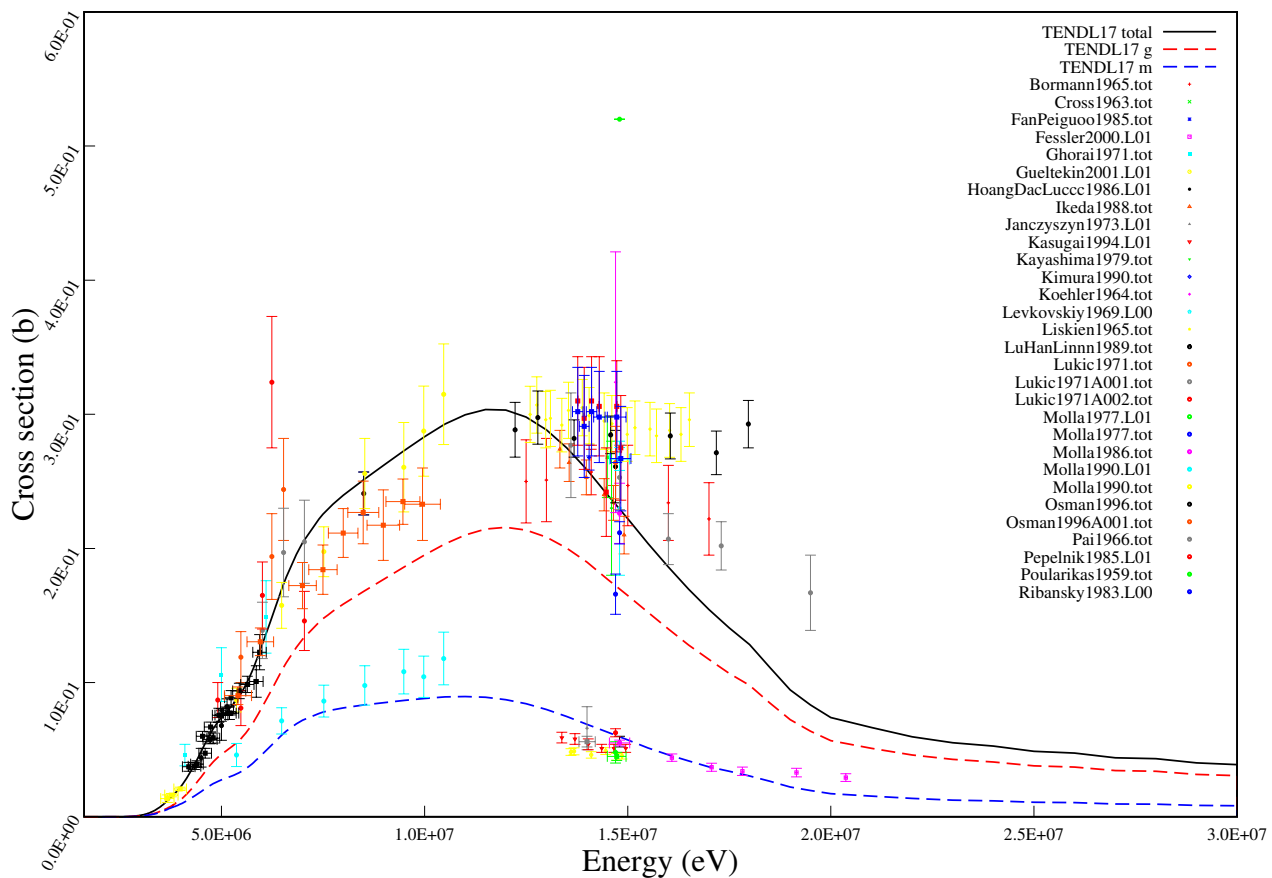
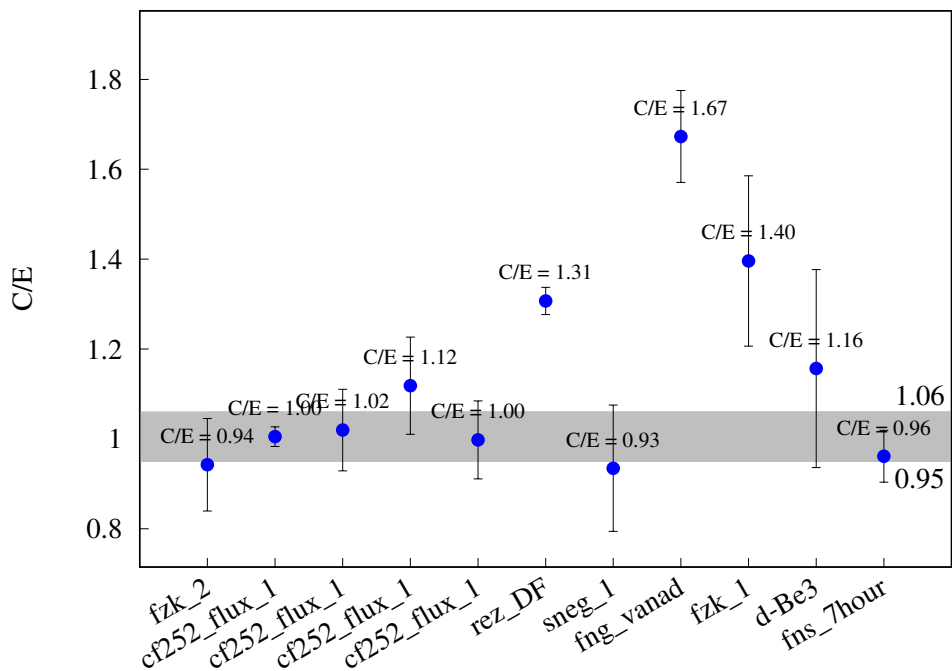
^{45}Sc (n,2n) ^{44}Sc 

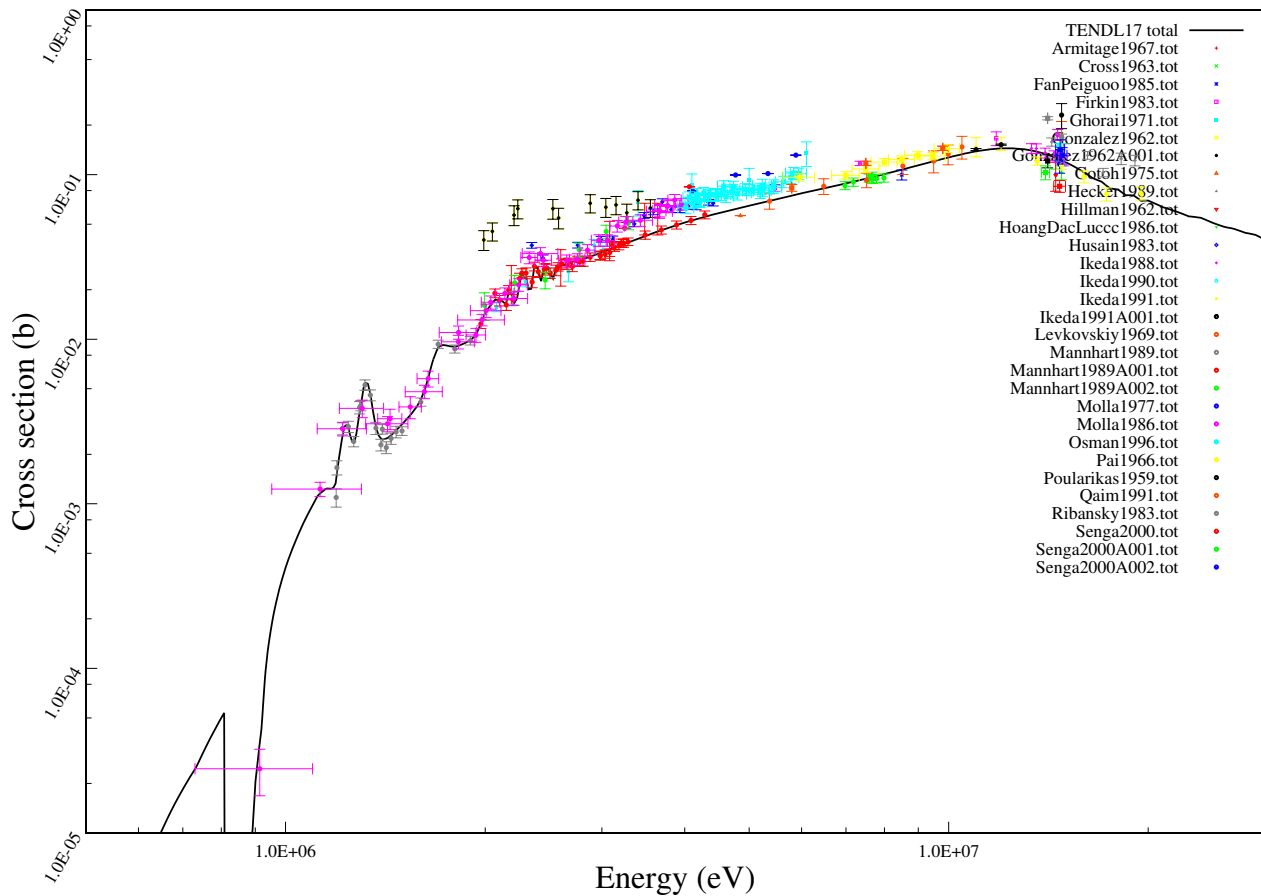
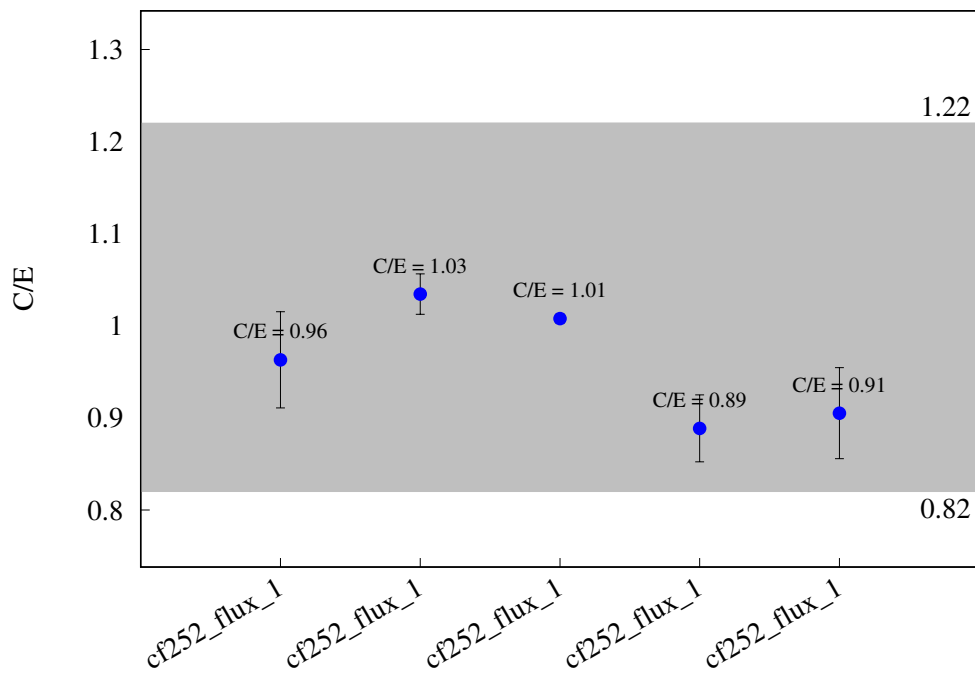
^{45}Sc (n,2n) ^{44m}Sc 

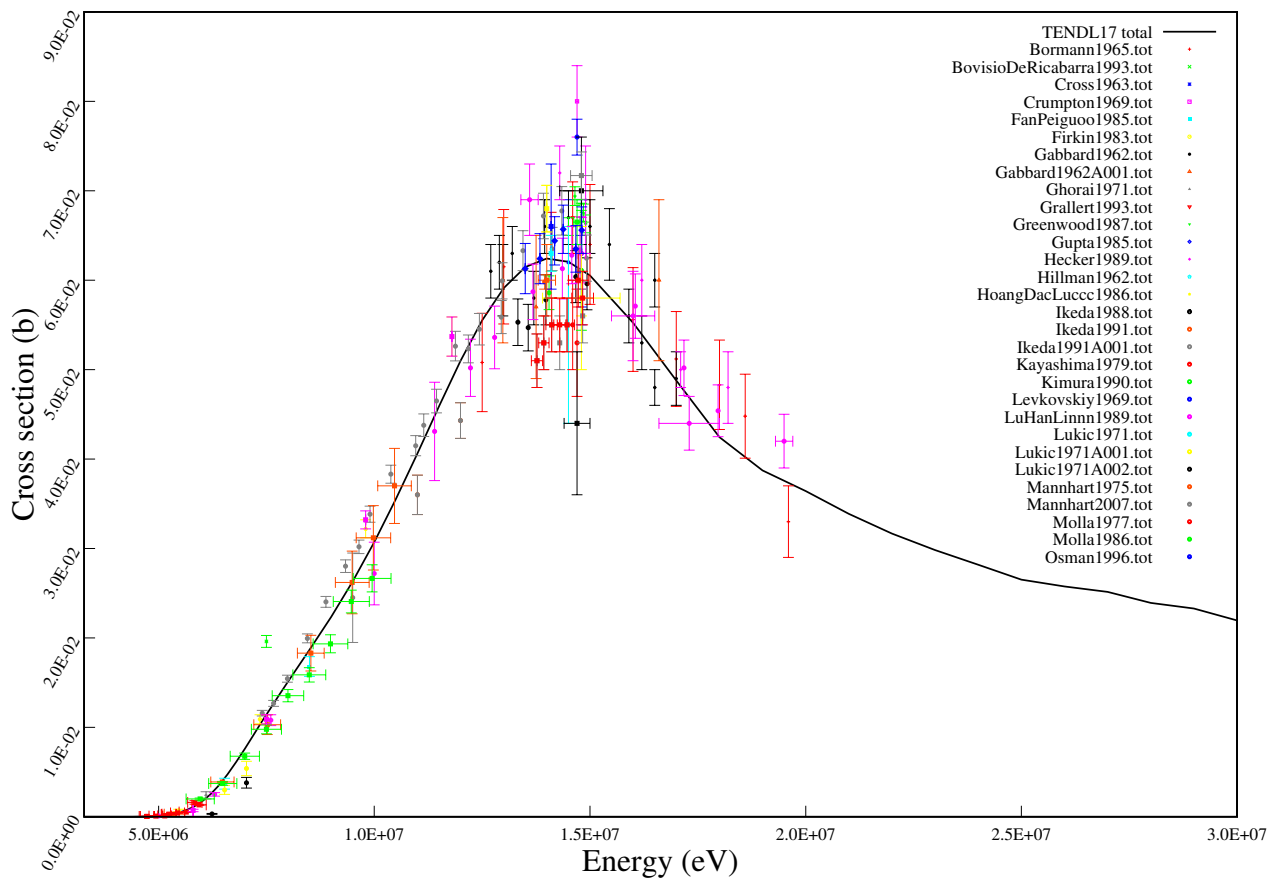
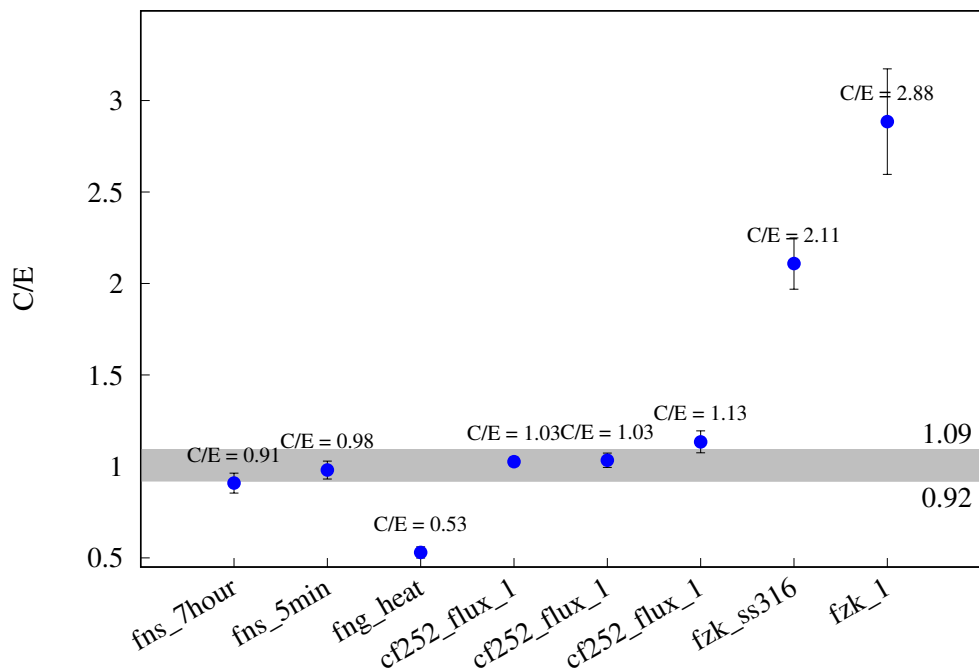
$^{45}\text{Sc} (\text{n},\text{h}) ^{43}\text{K}$ 

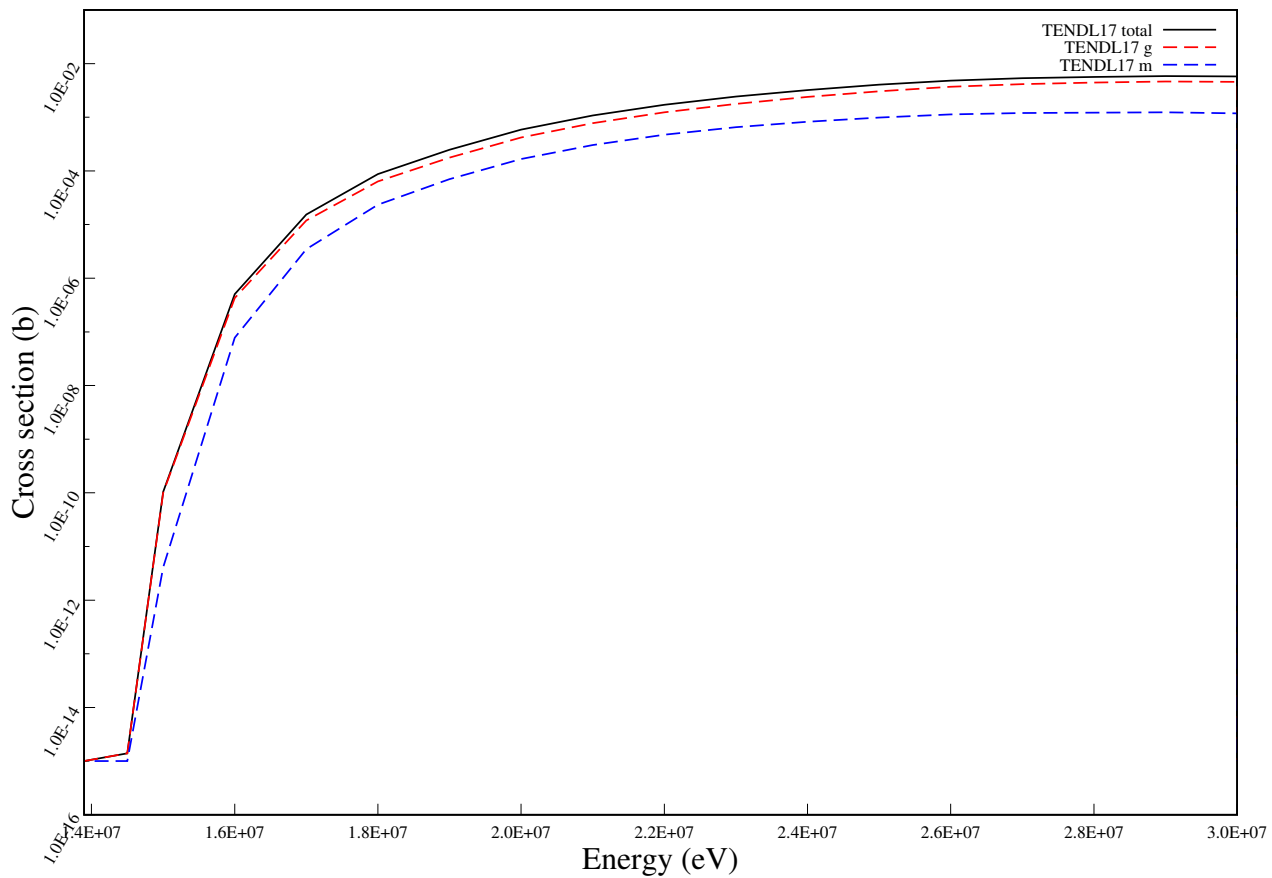
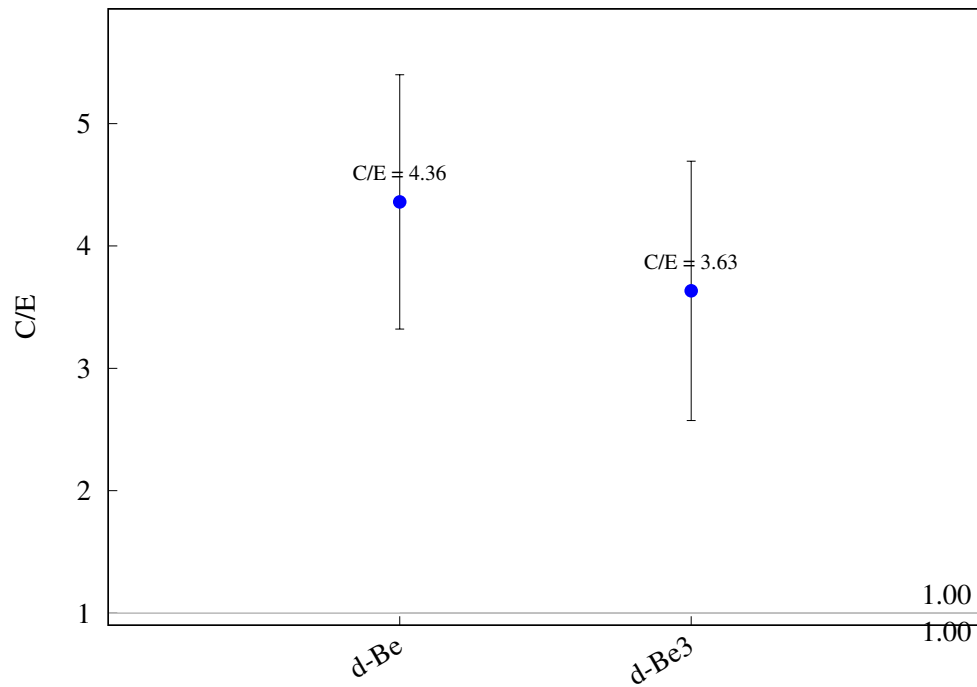
$^{45}\text{Sc} (\text{n},\text{a}) ^{42}\text{K}$ 

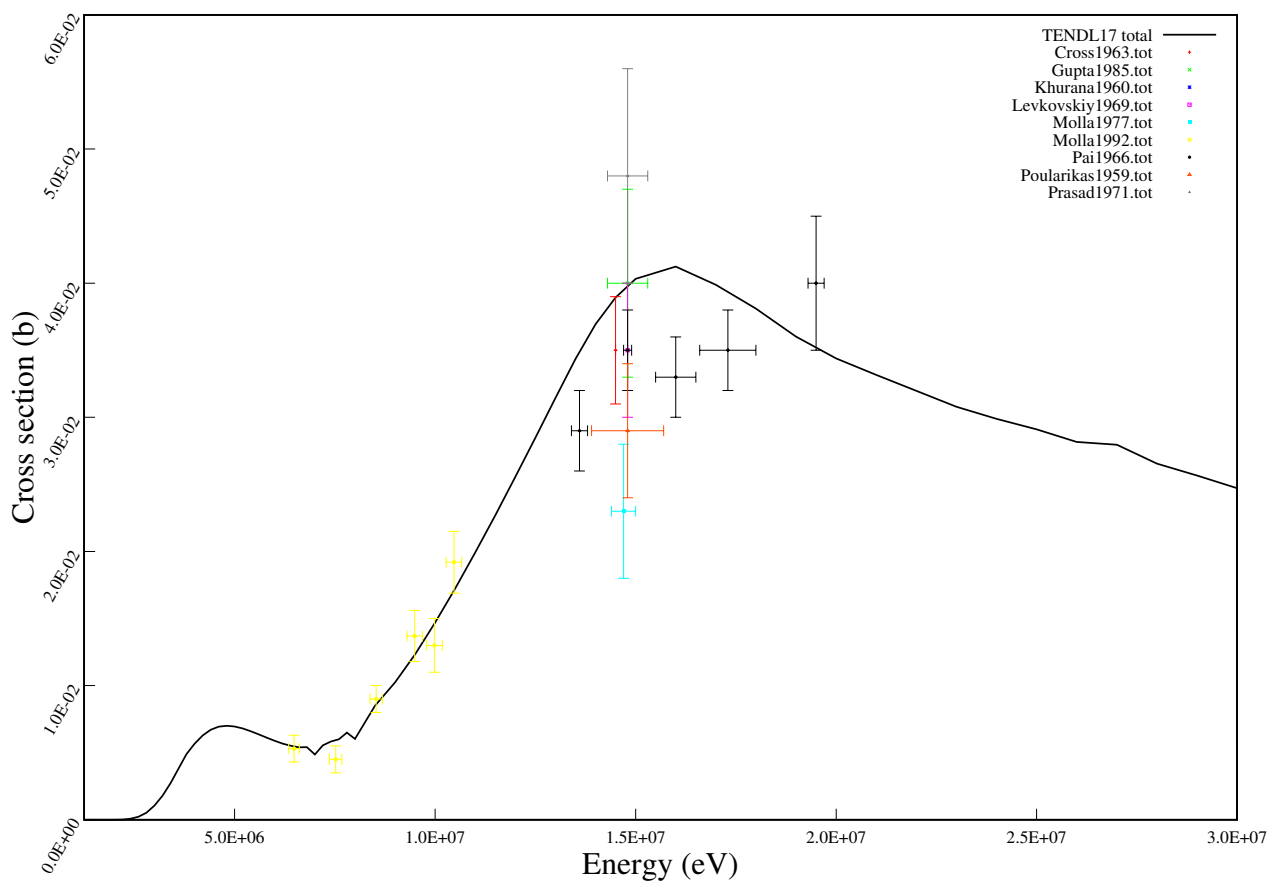
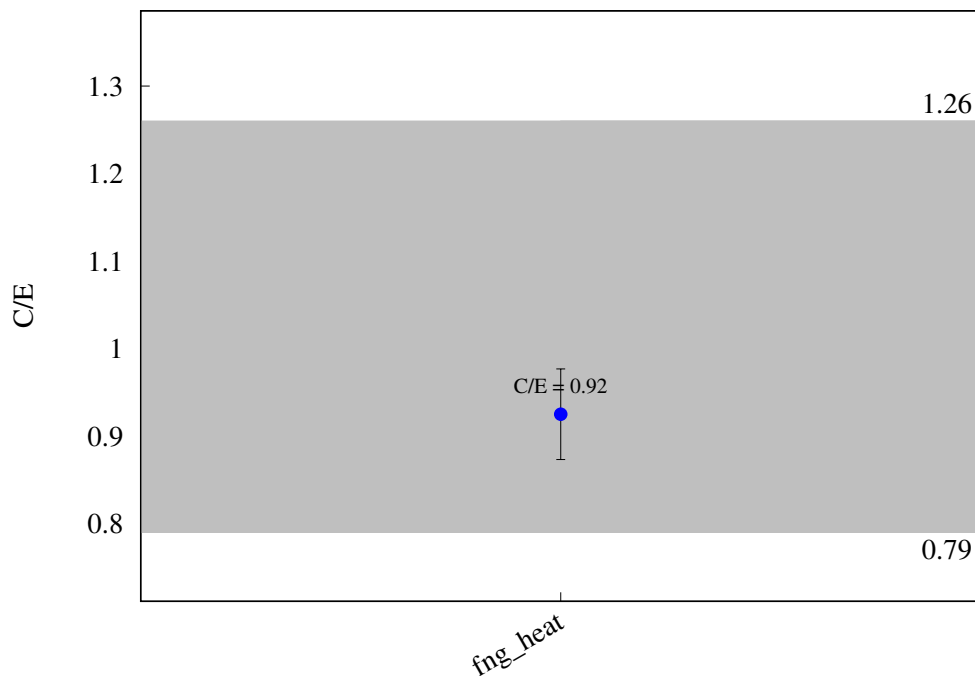


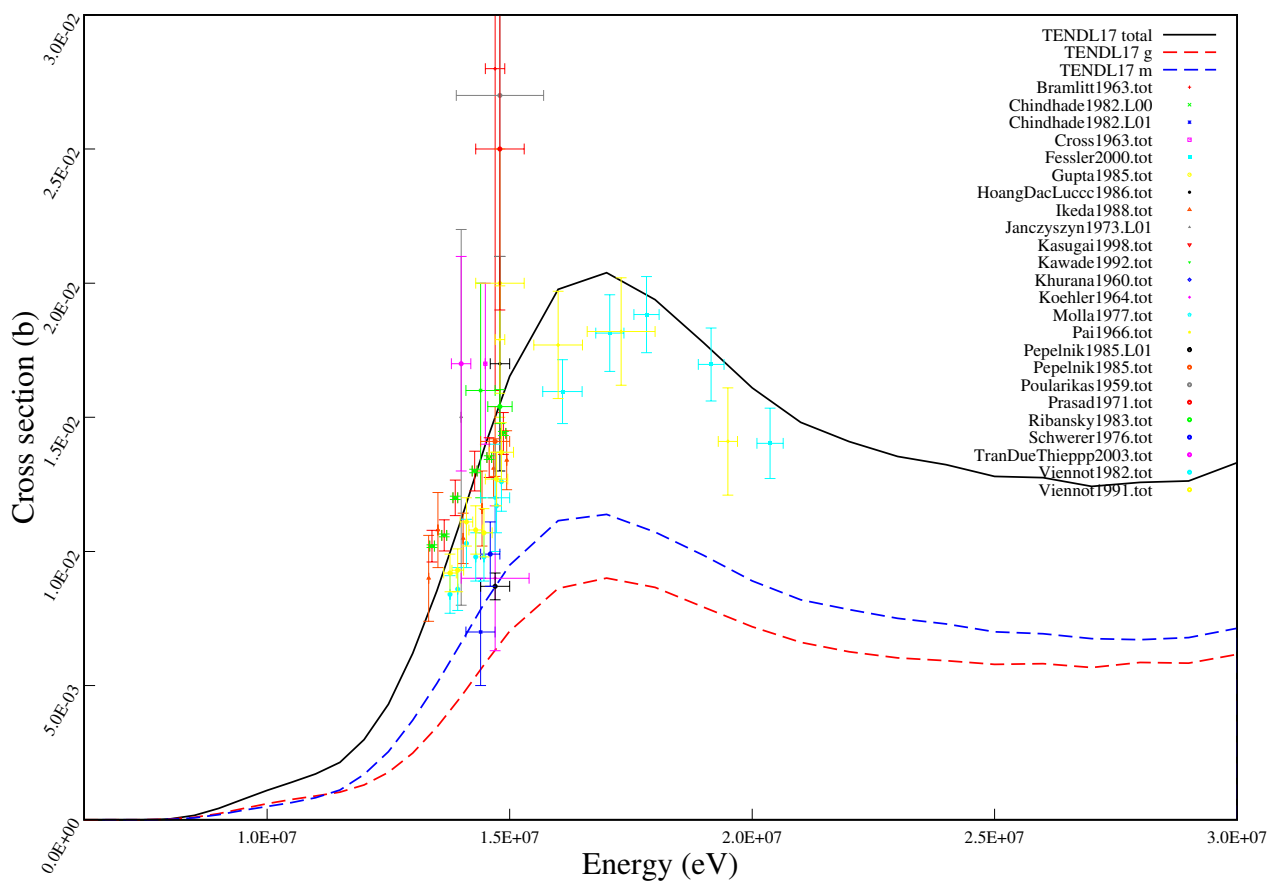
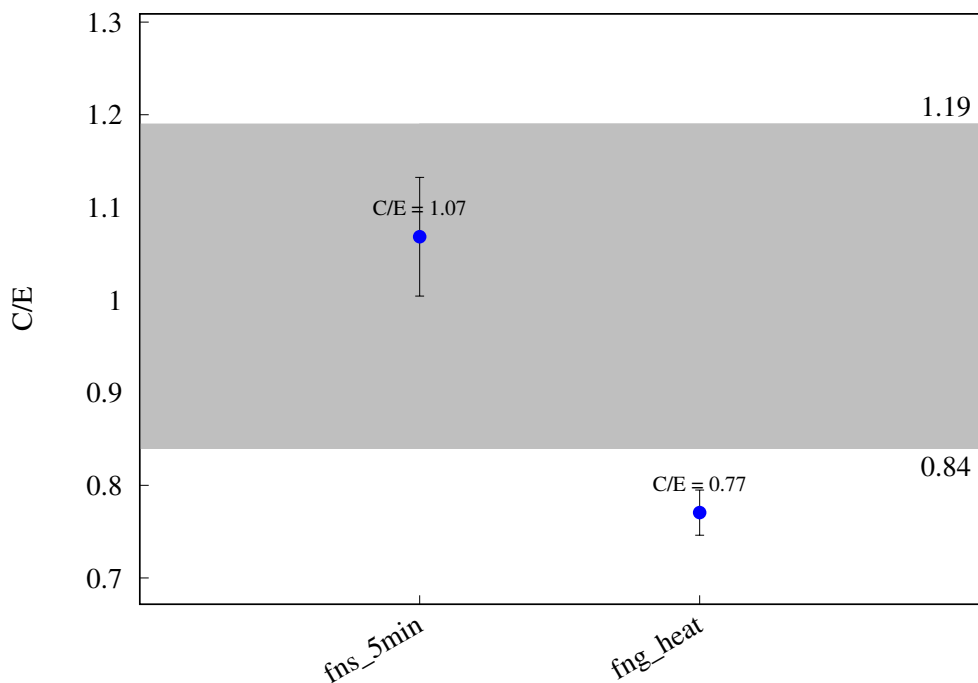
^{46}Ti (n,p) ^{46}Sc 

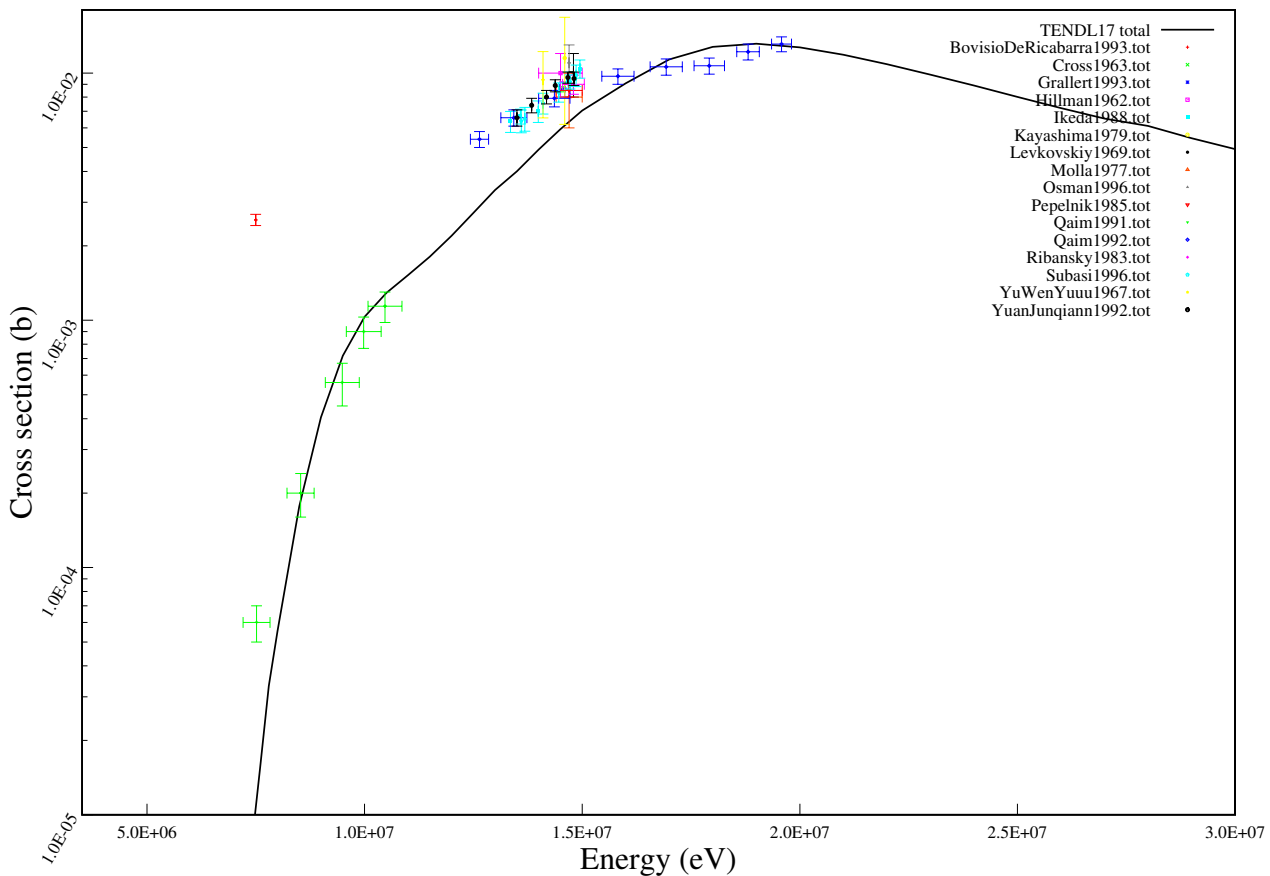
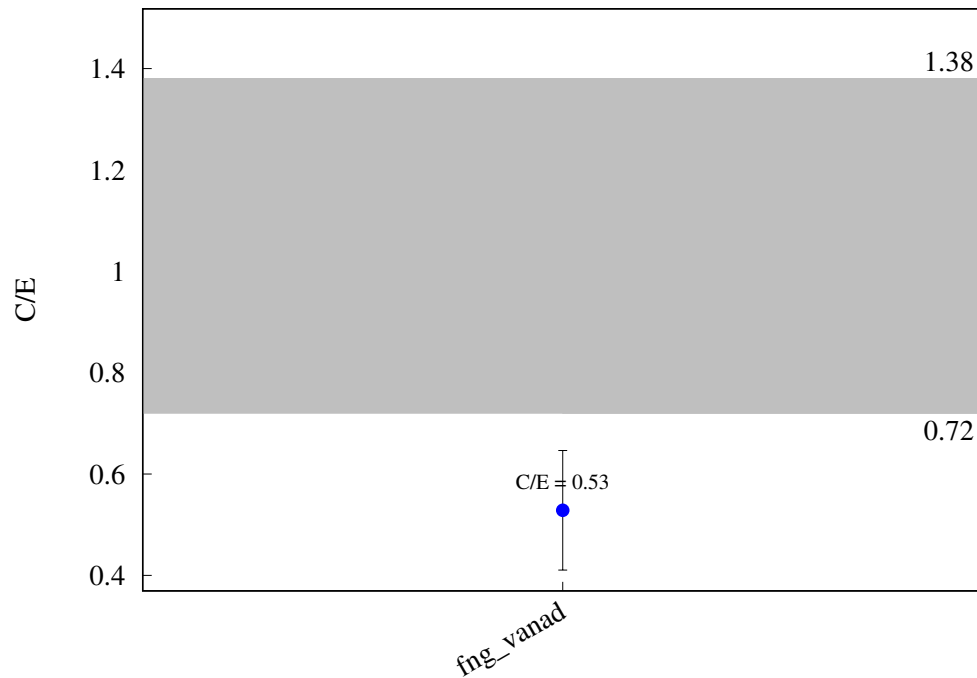
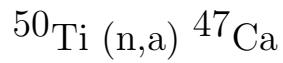
$^{47}\text{Ti} (\text{n},\text{p}) ^{47}\text{Sc}$ 

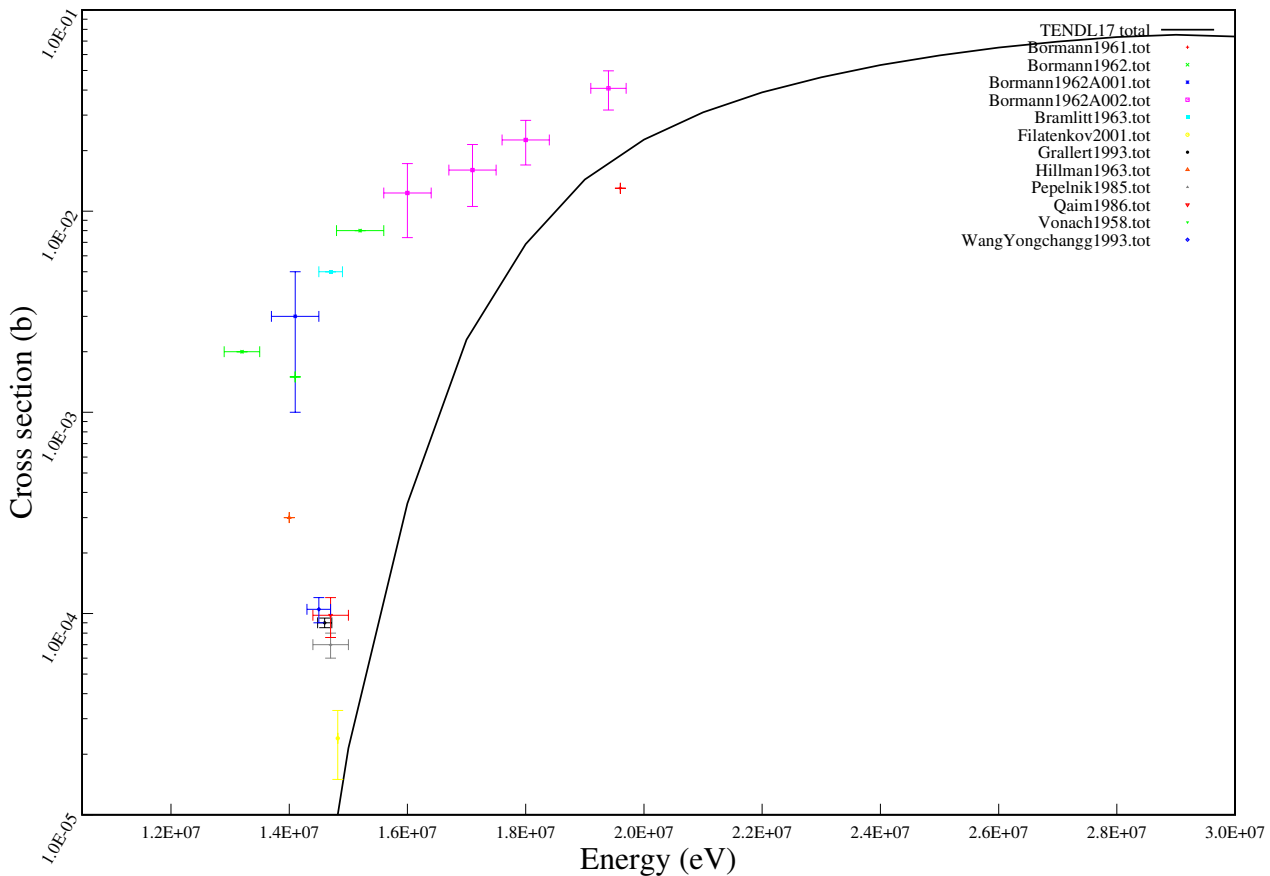
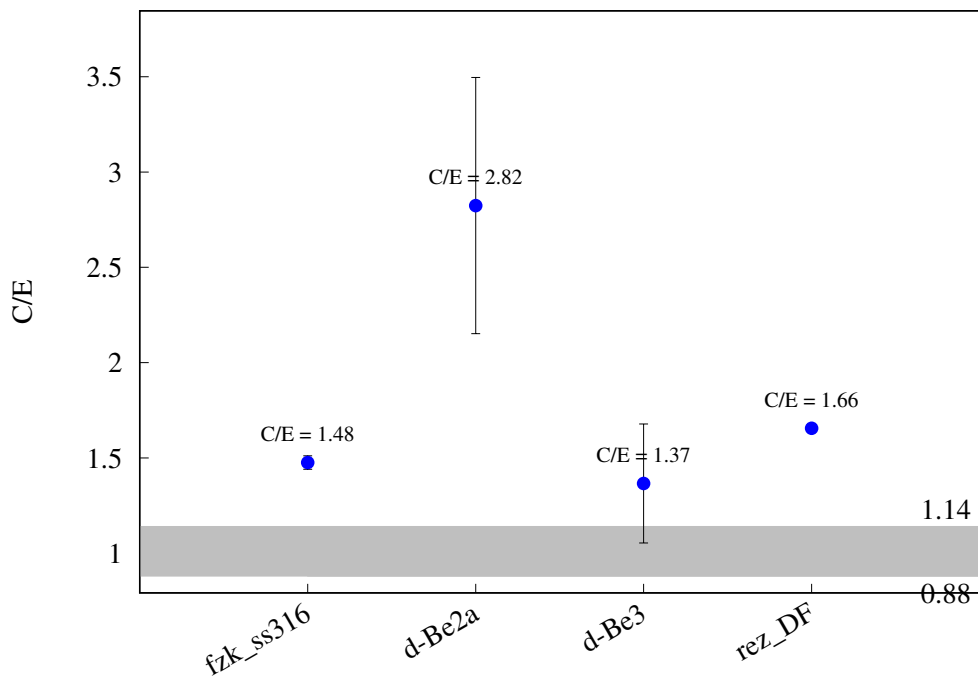
^{48}Ti (n,p) ^{48}Sc 

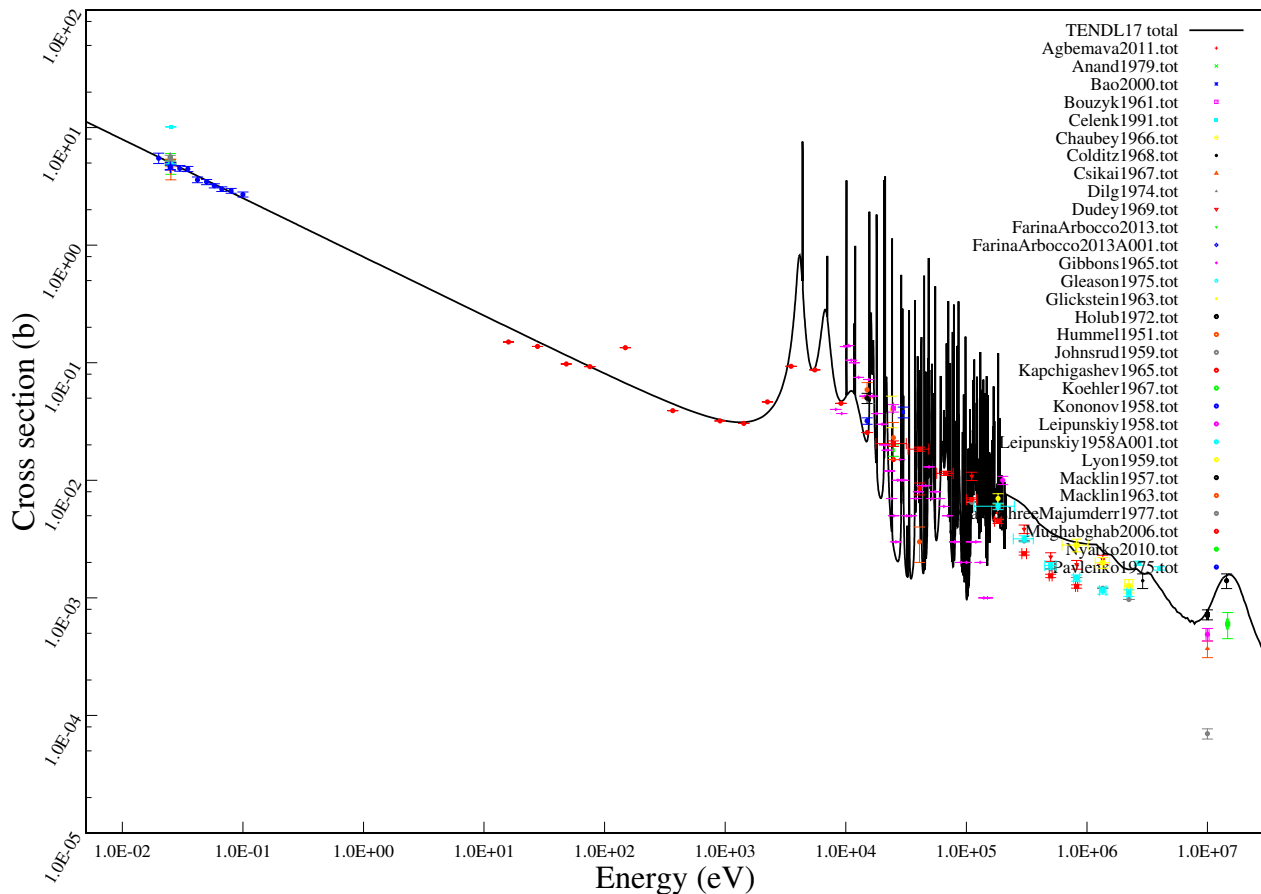
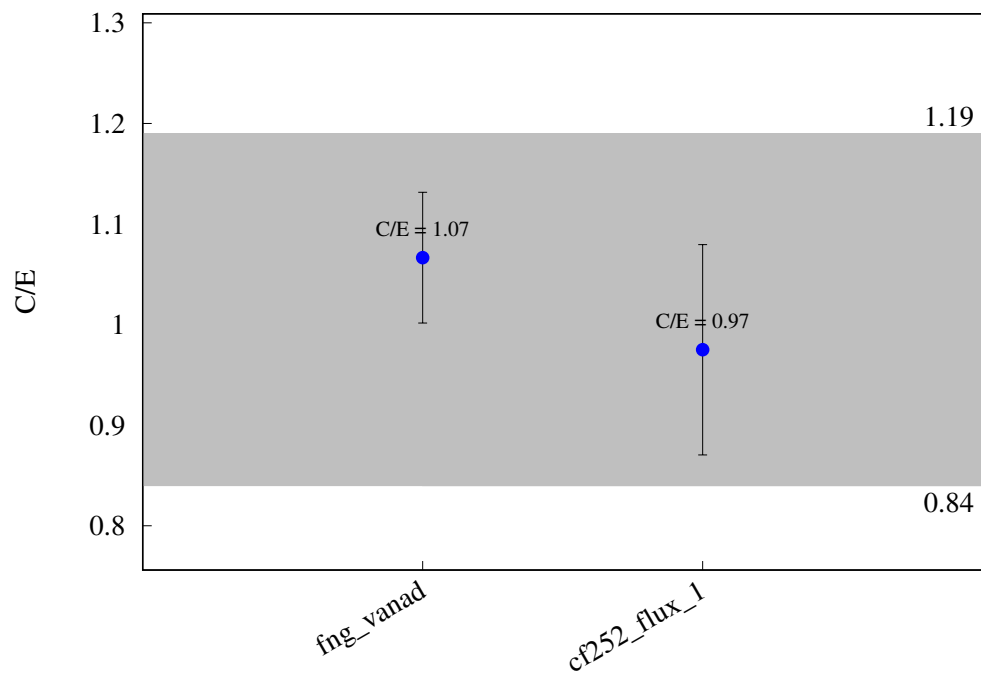
^{48}Ti (n,t) ^{46}Sc 

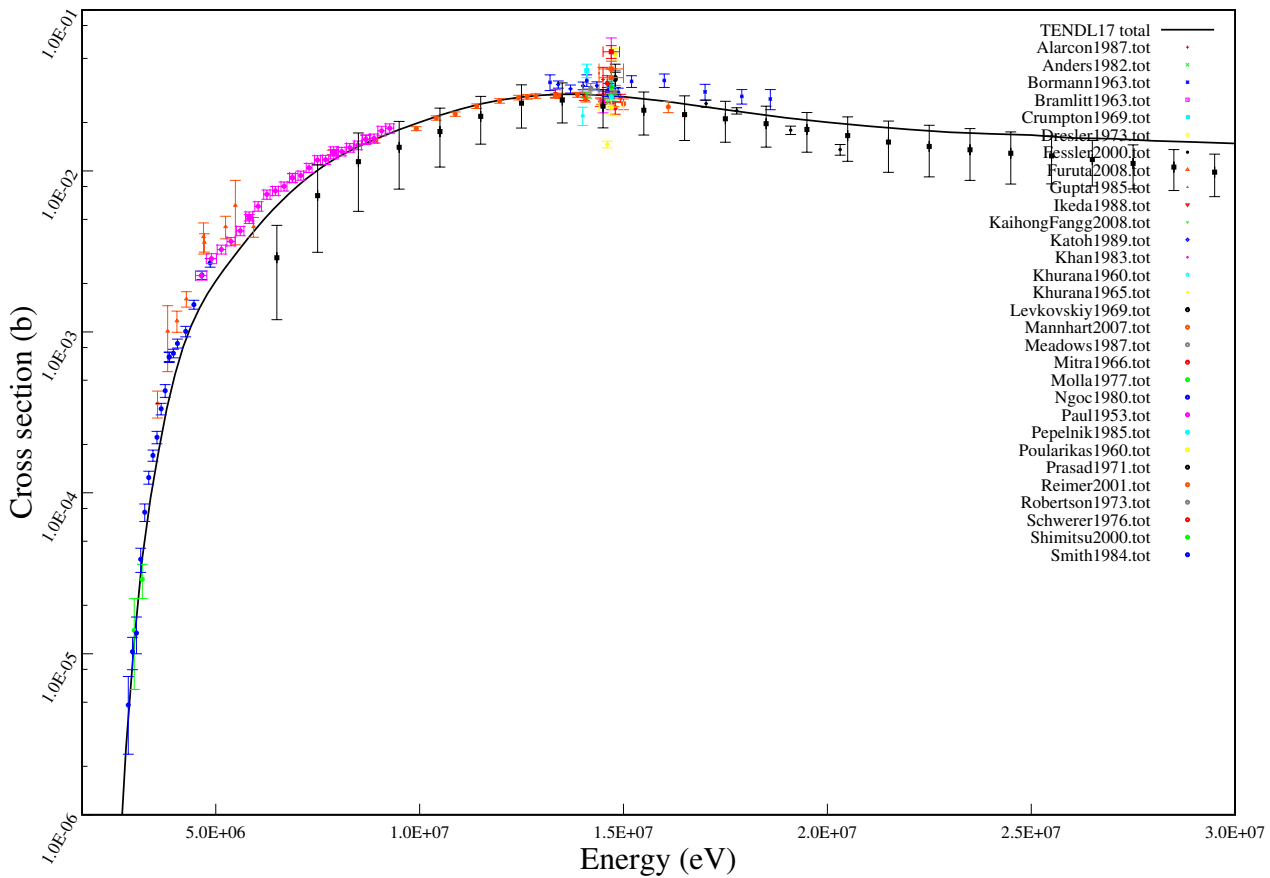
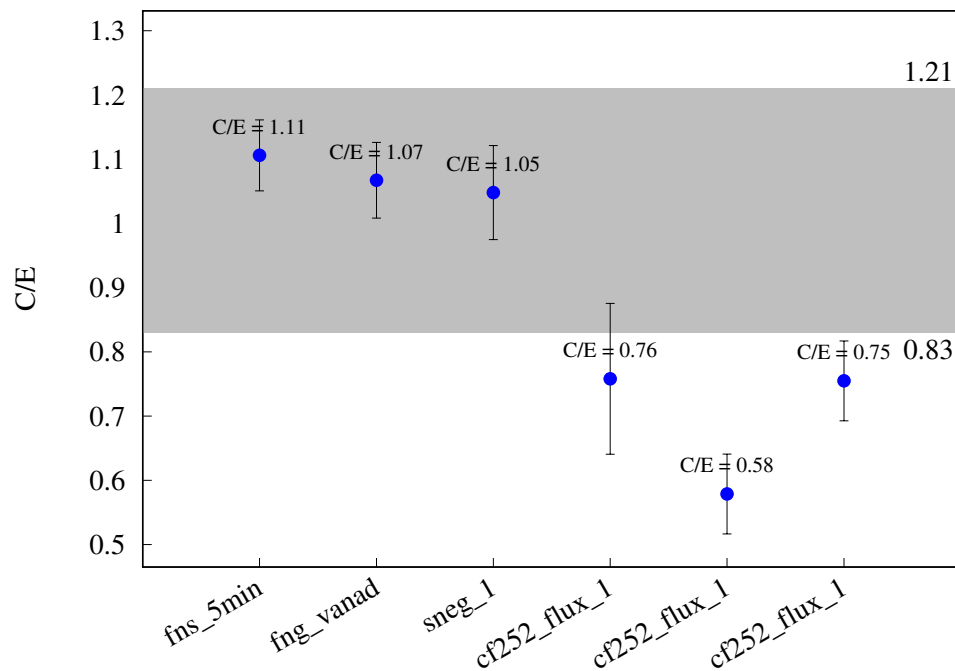
^{49}Ti (n,p) ^{49}Sc 

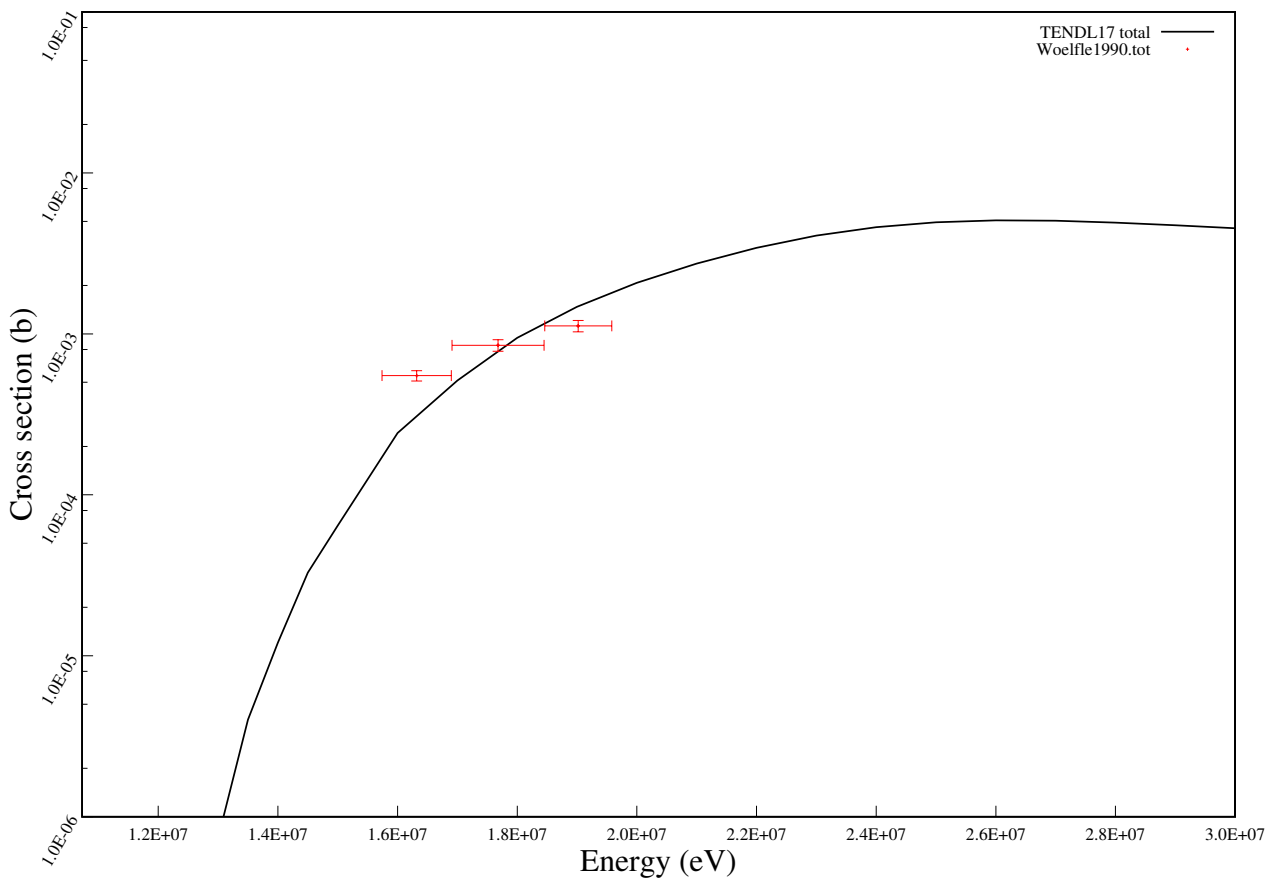
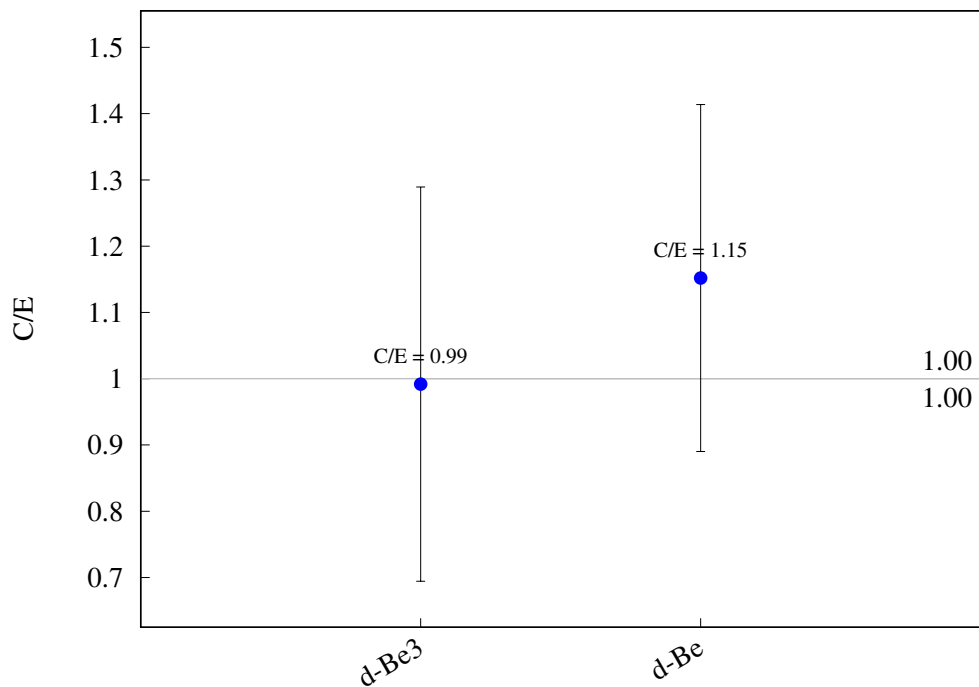
^{50}Ti (n,p) ^{50}Sc 

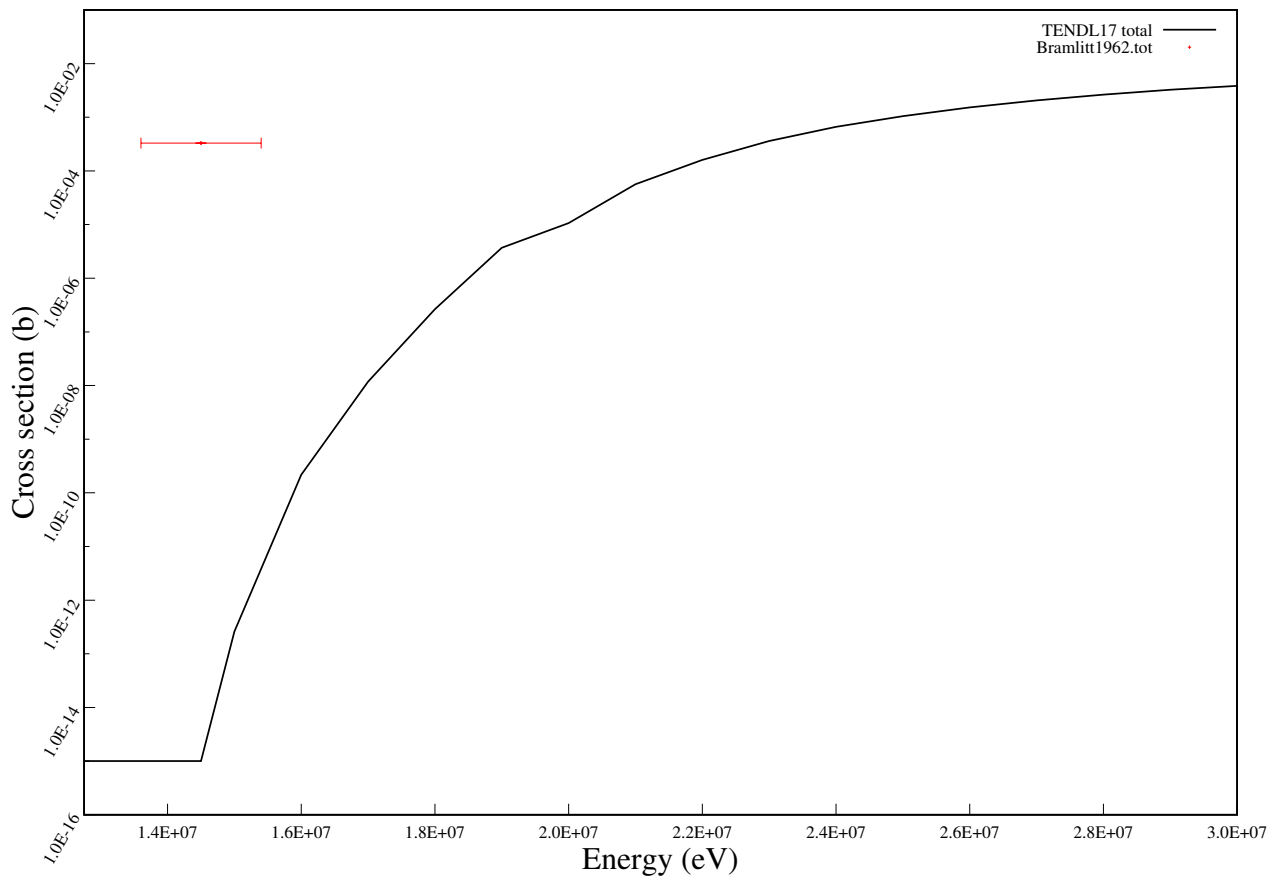
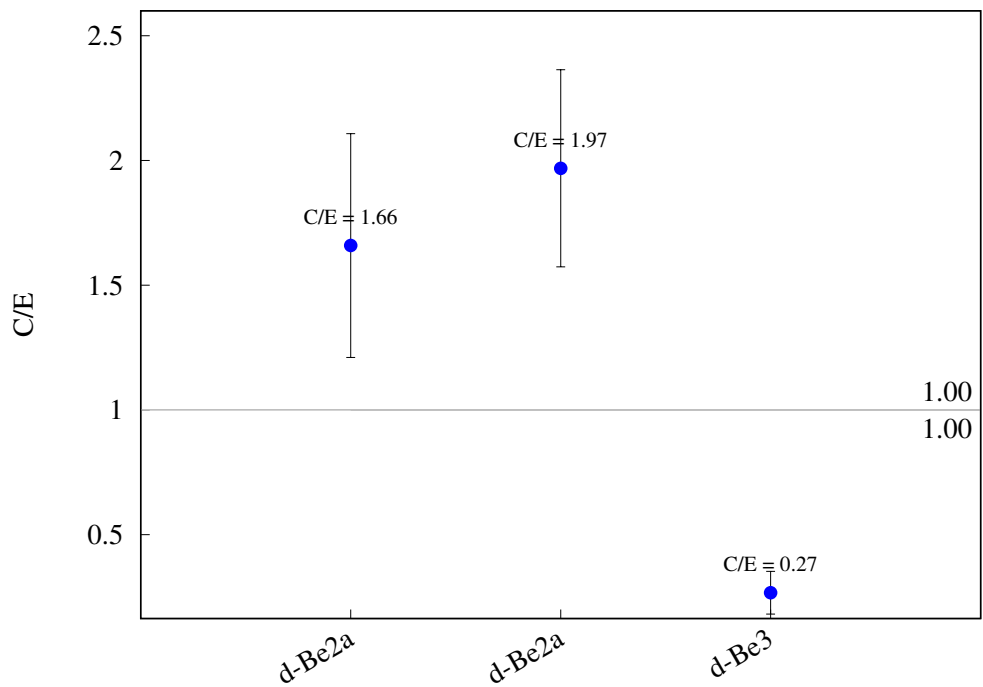


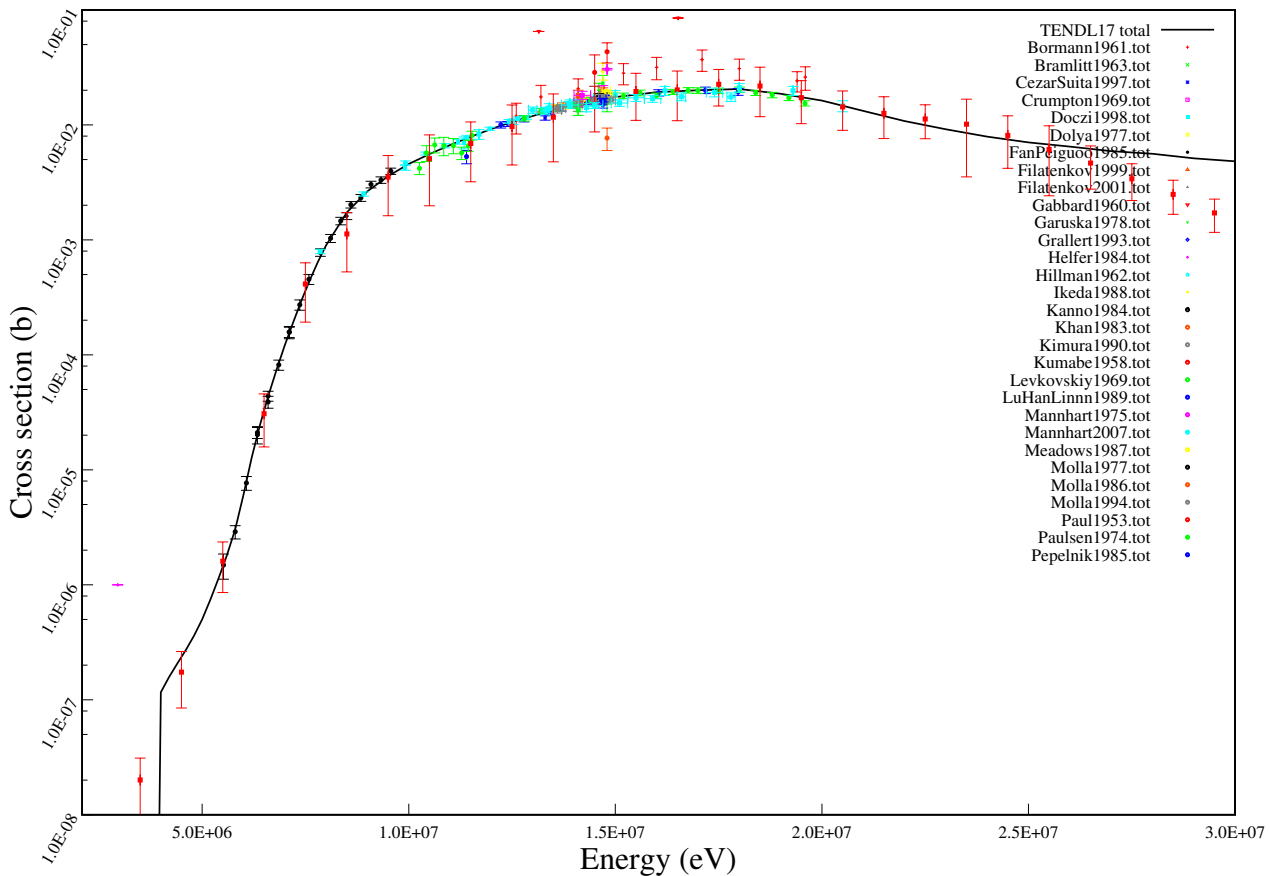
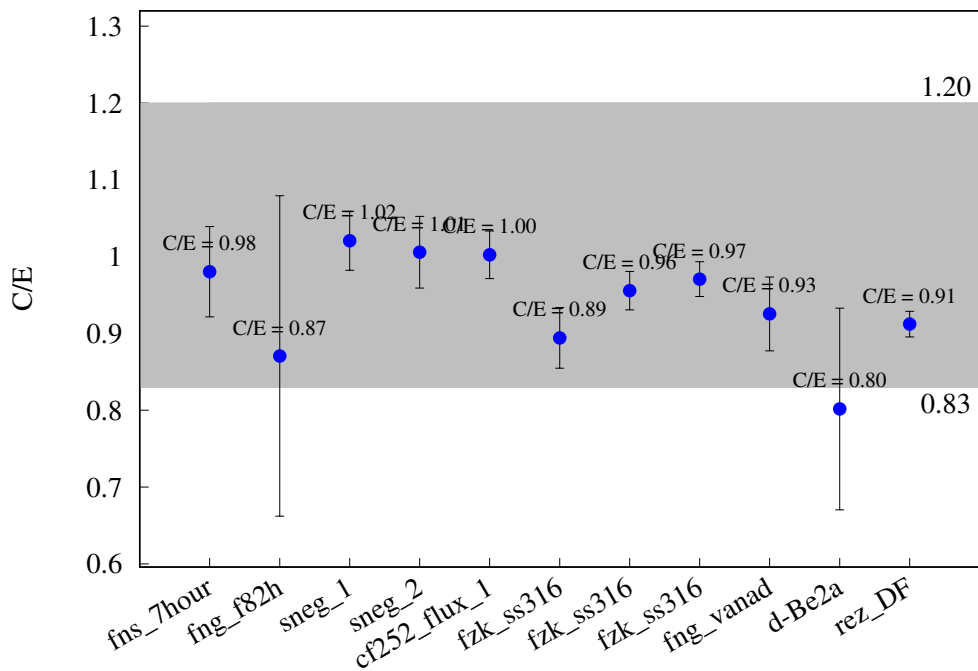
$^{51}\text{V} (\text{n},\text{na}) ^{47}\text{Sc}$ 

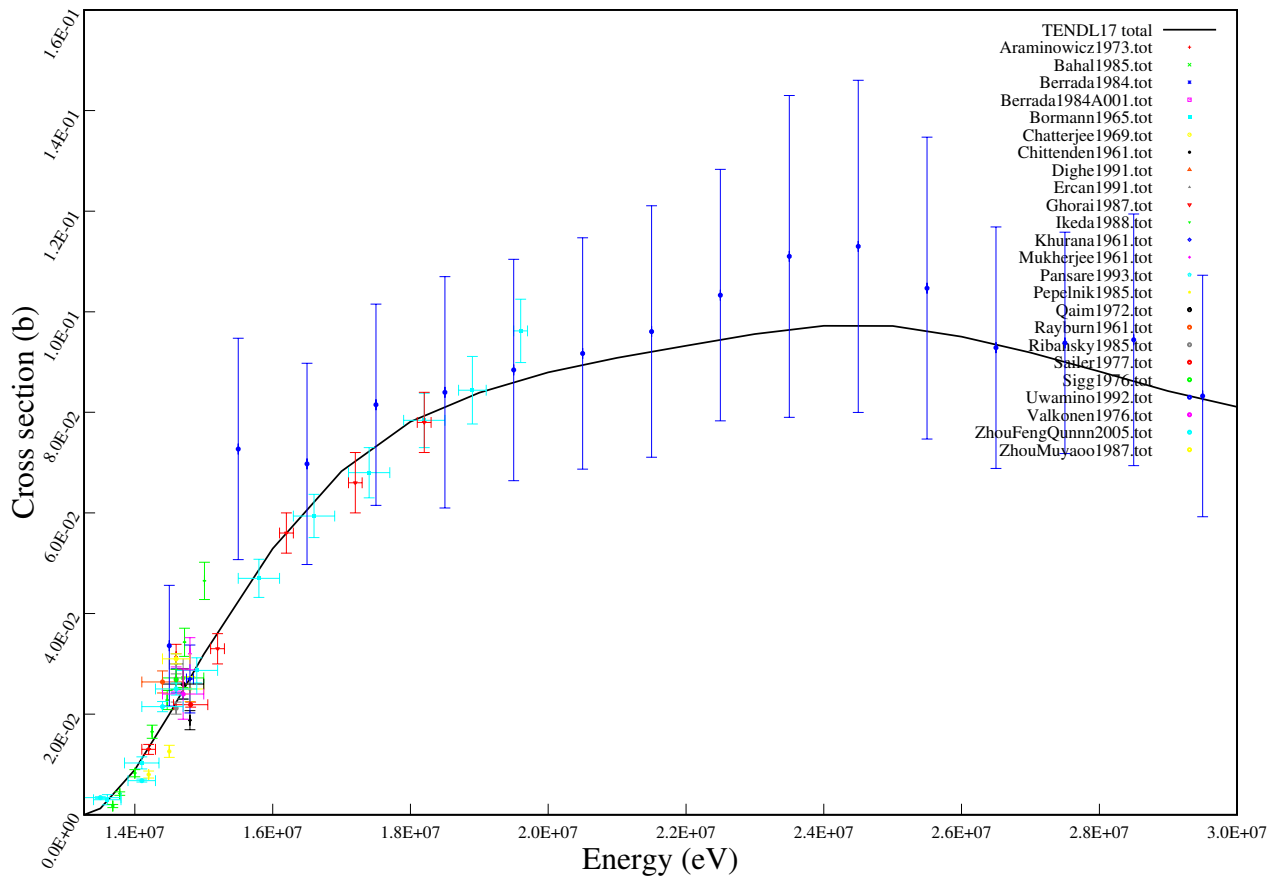
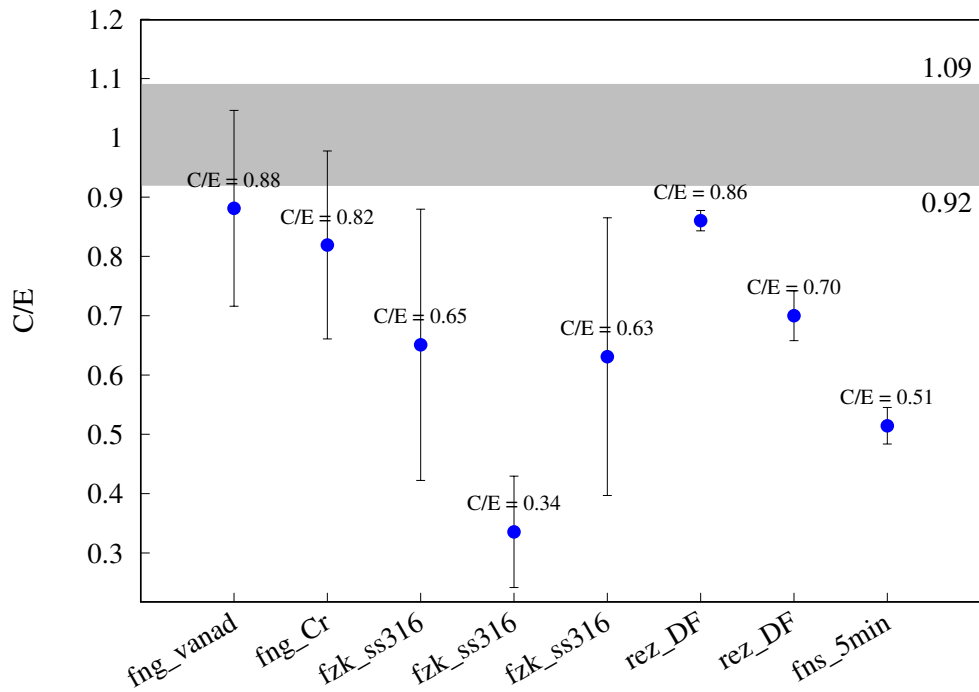
^{51}V (n,g) ^{52}V 

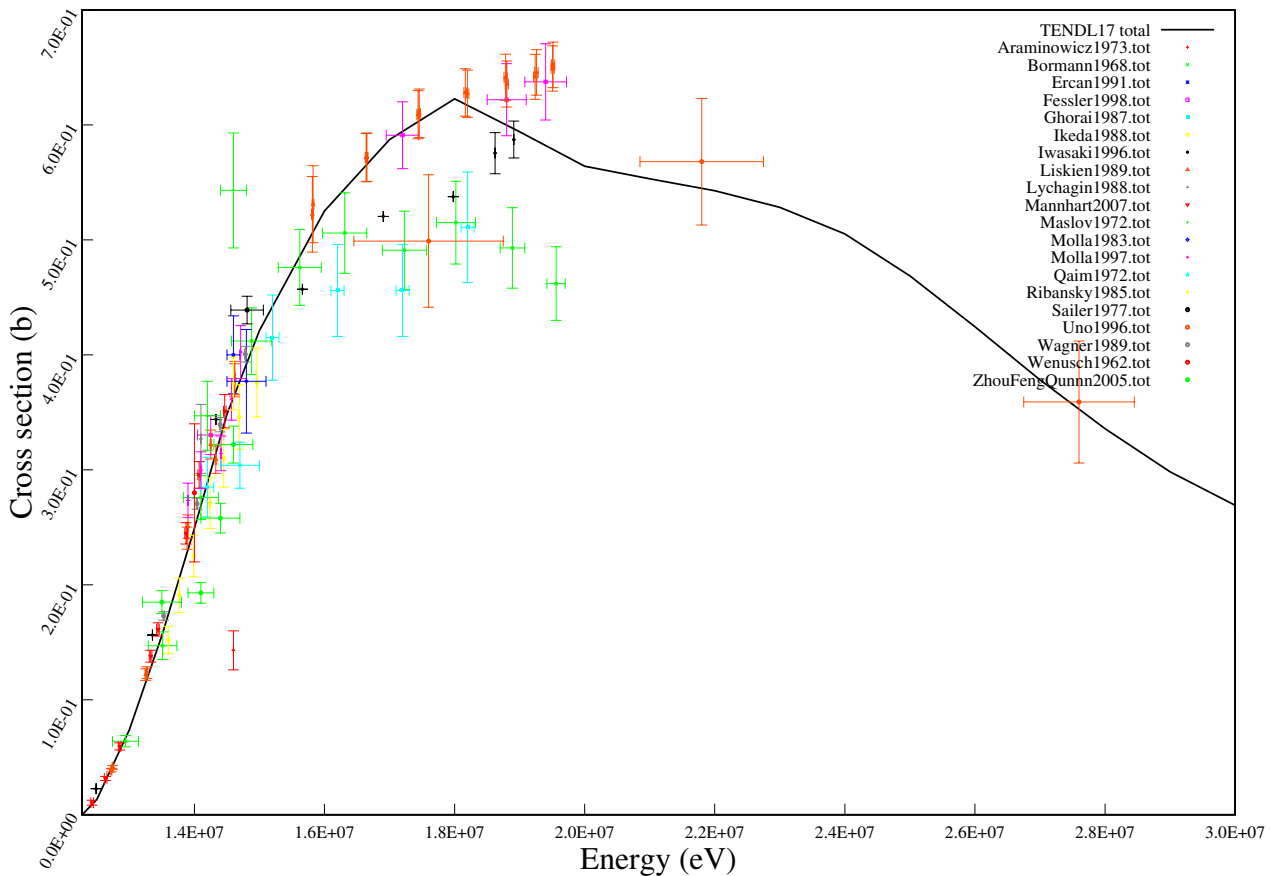
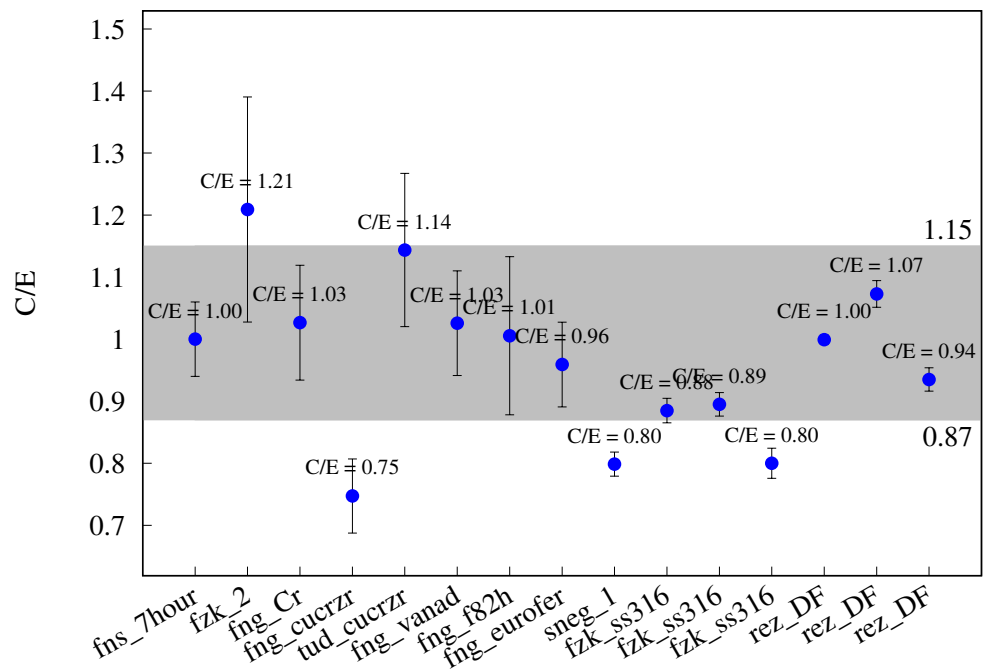
^{51}V (n,p) ^{51}Ti 

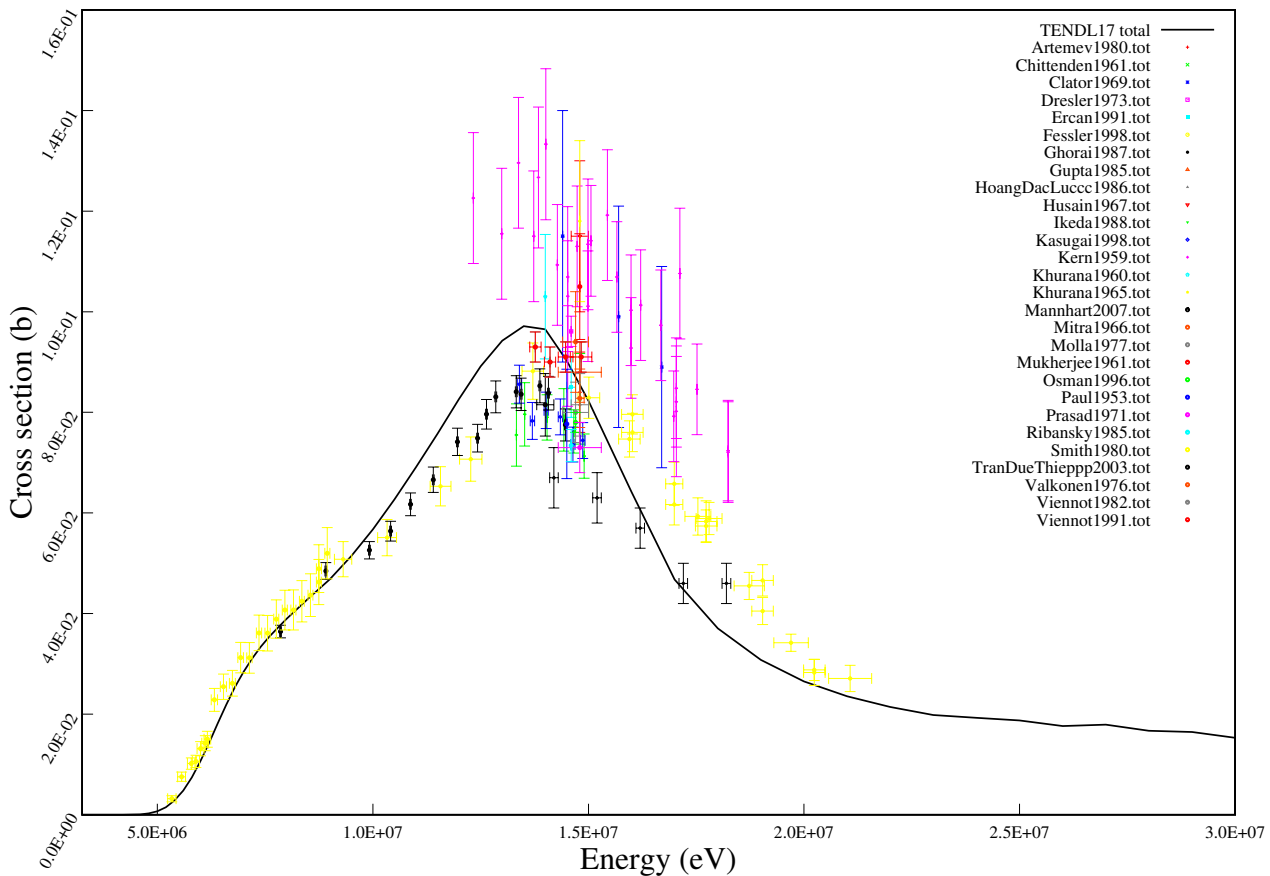
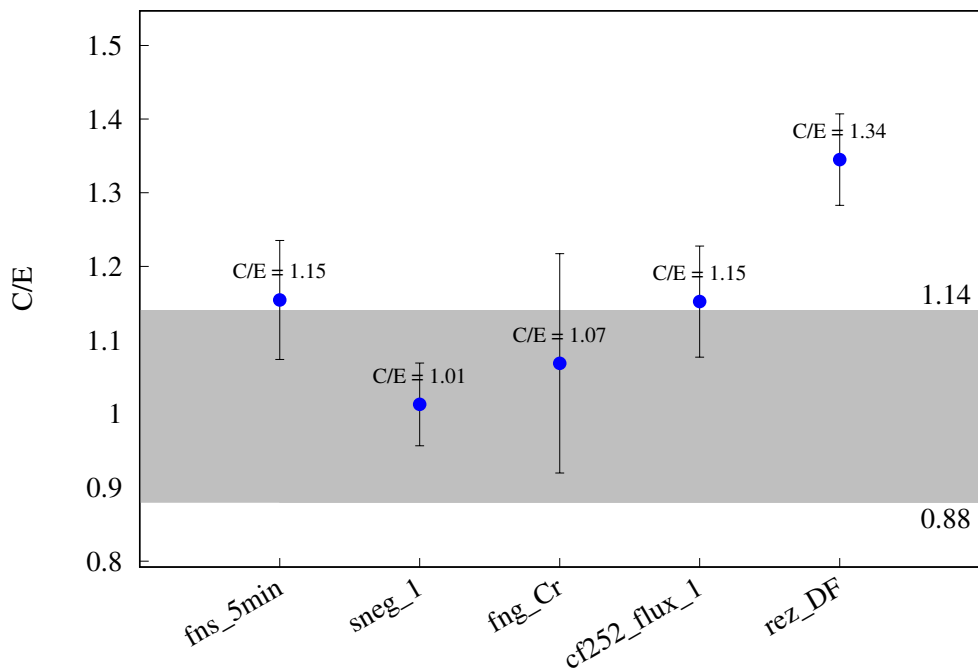
$^{51}\text{V} (\text{n},\text{t}) ^{49}\text{Ti}$ 

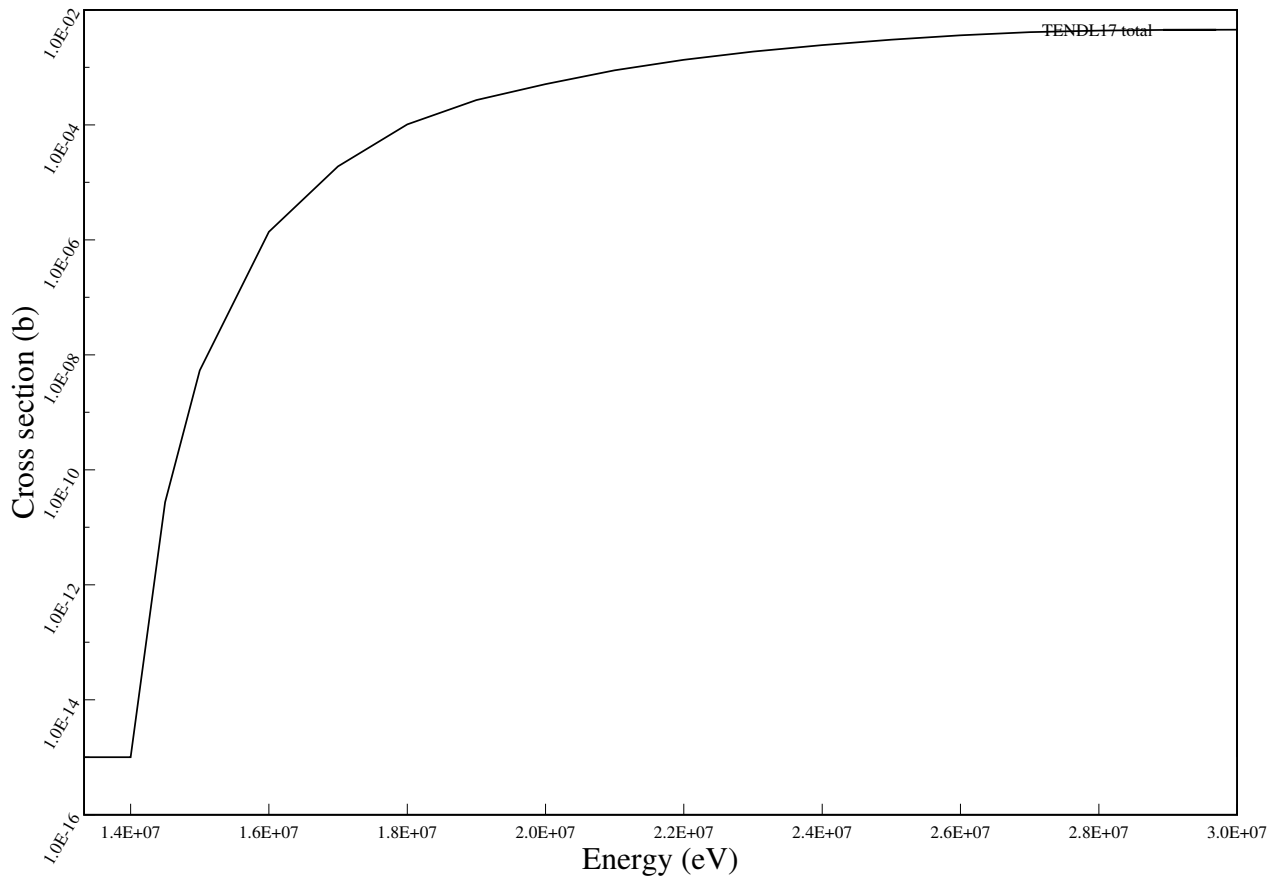
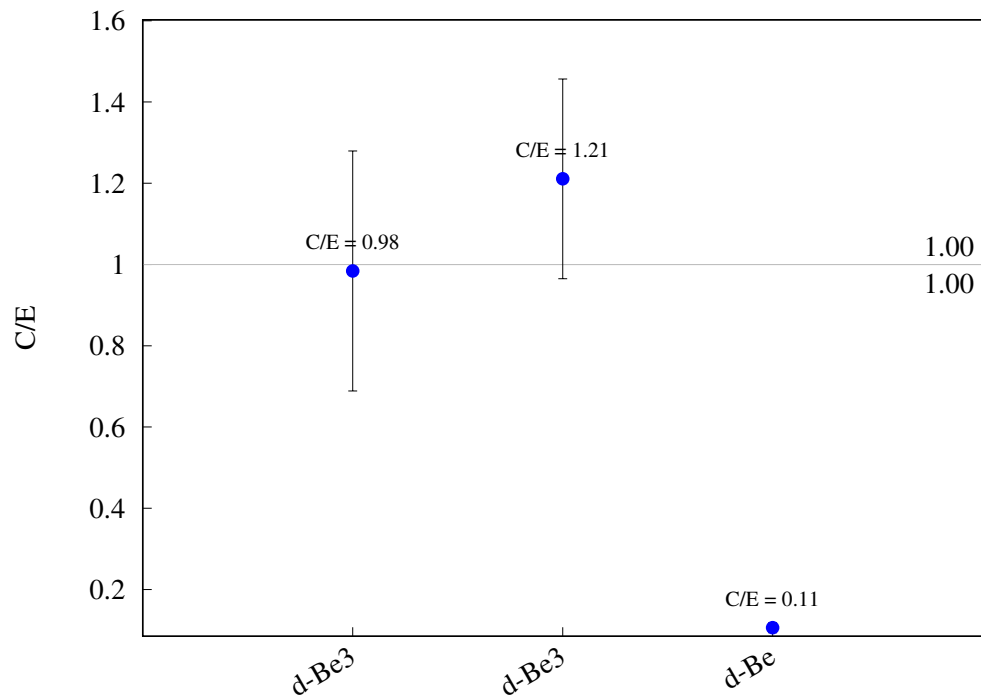
$^{51}\text{V} (\text{n},\text{h}) ^{49}\text{Sc}$ 

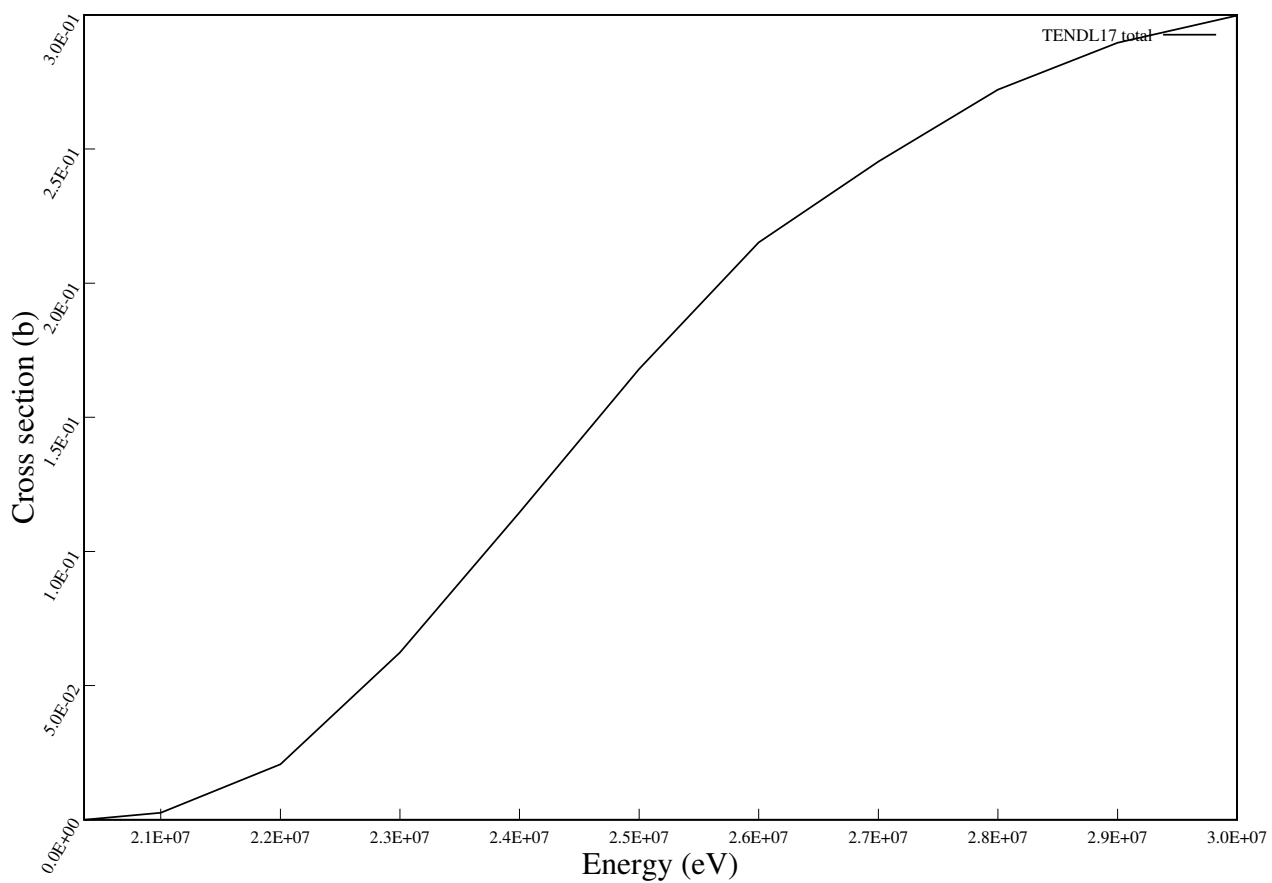
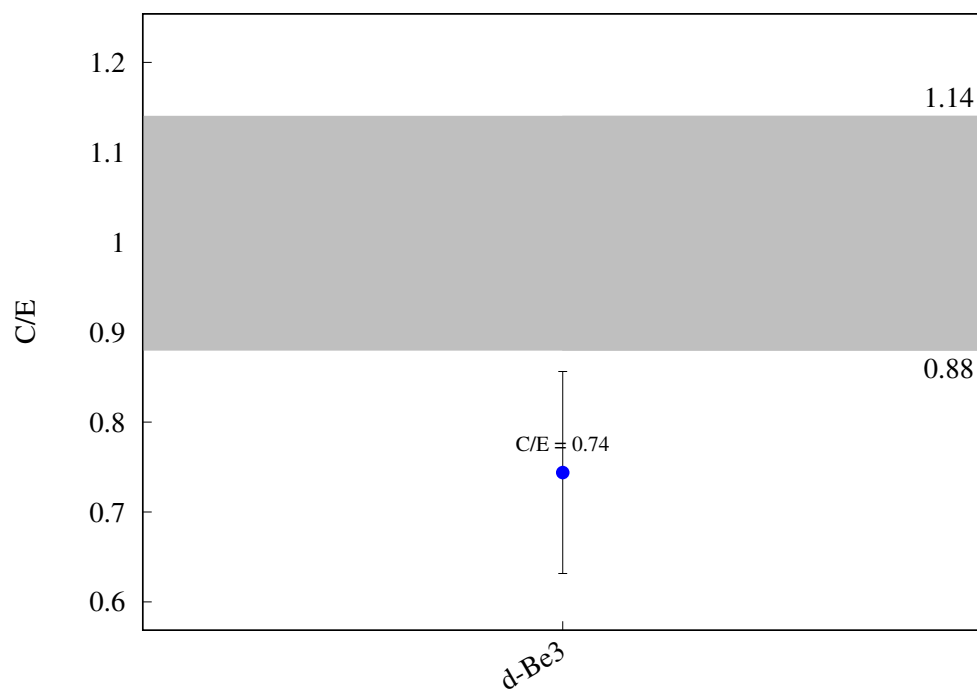
$^{51}\text{V} (\text{n,a}) ^{48}\text{Sc}$ 

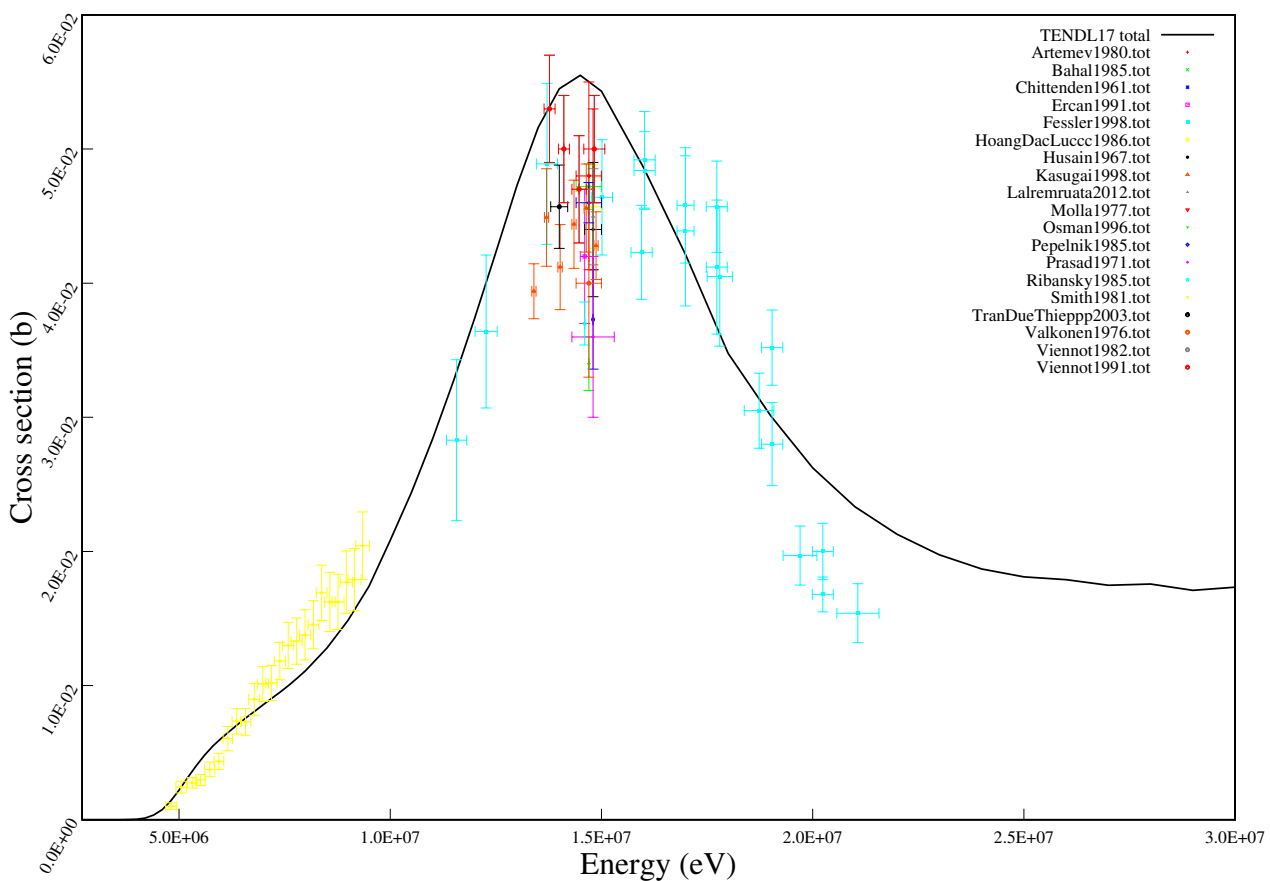
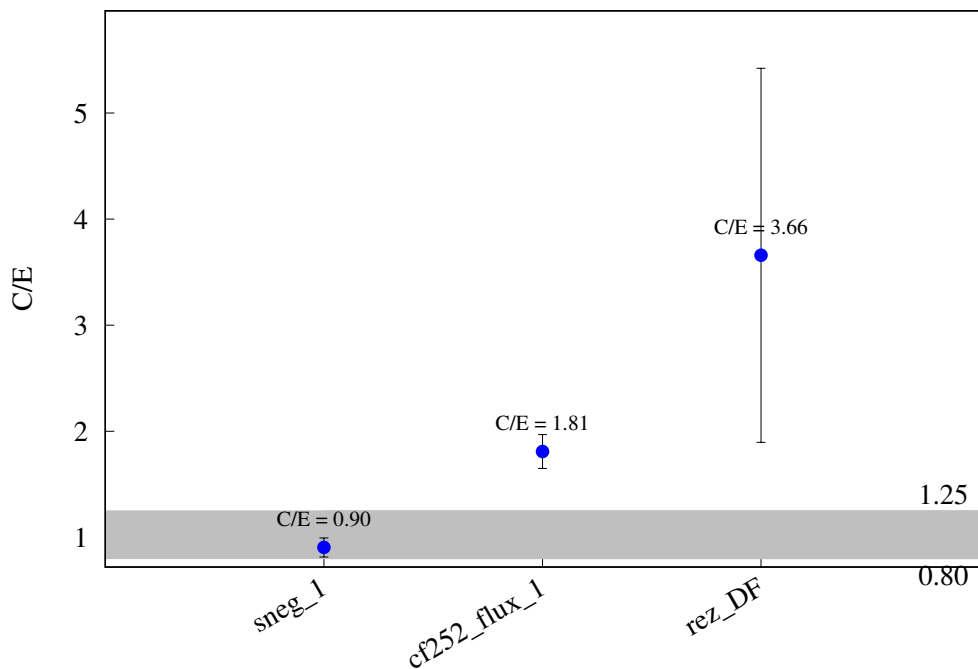
^{50}Cr (n,2n) ^{49}Cr 

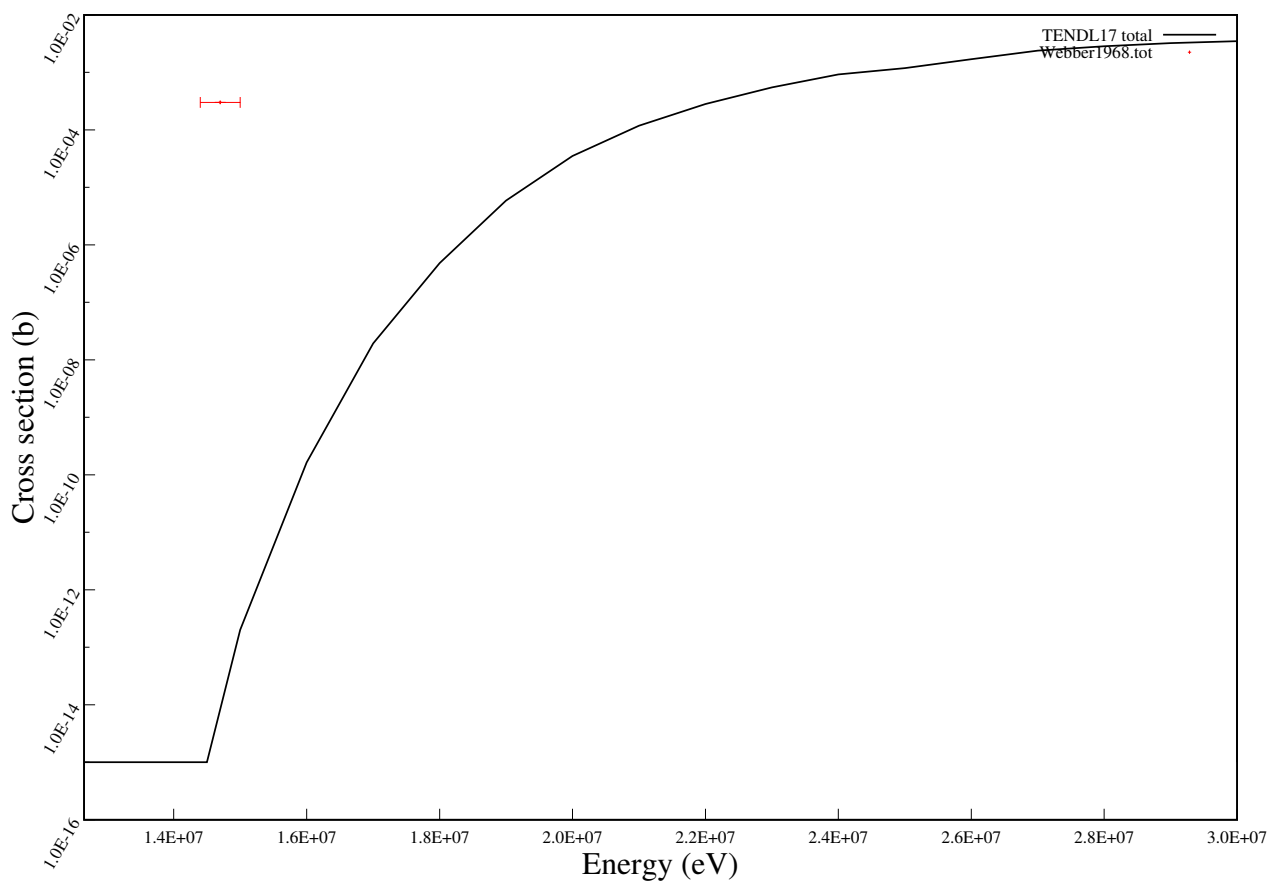
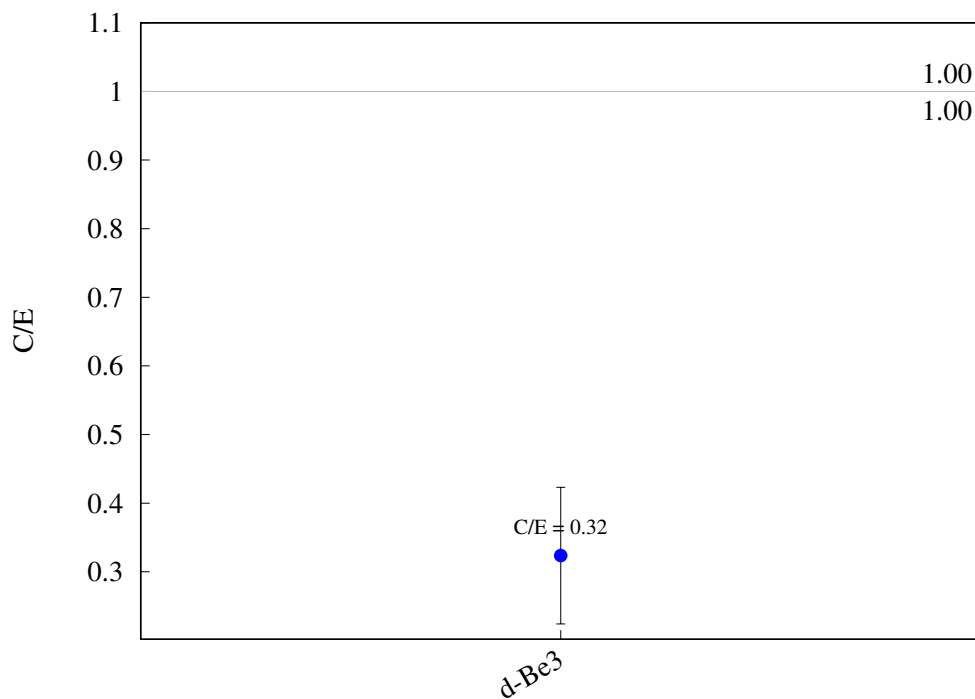
^{52}Cr (n,2n) ^{51}Cr 

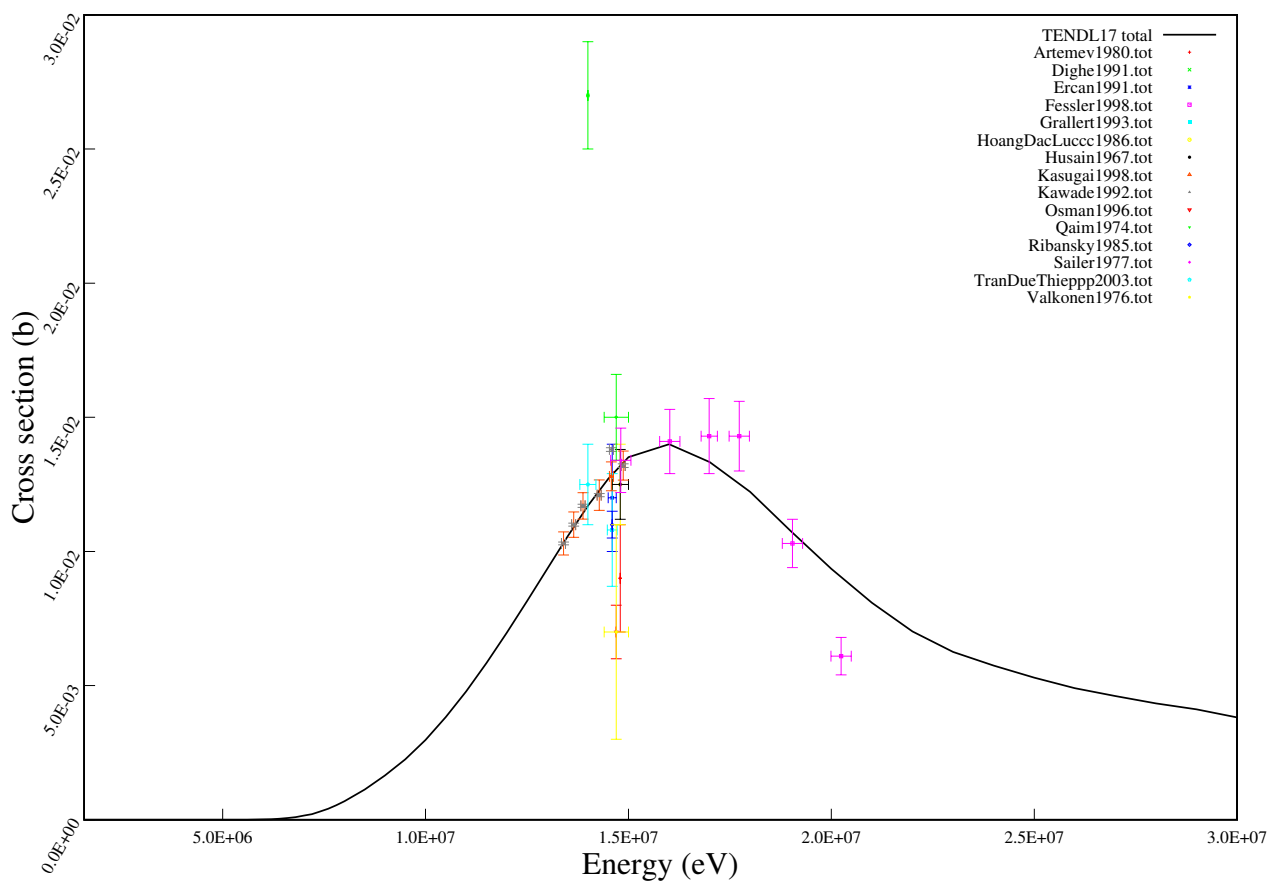
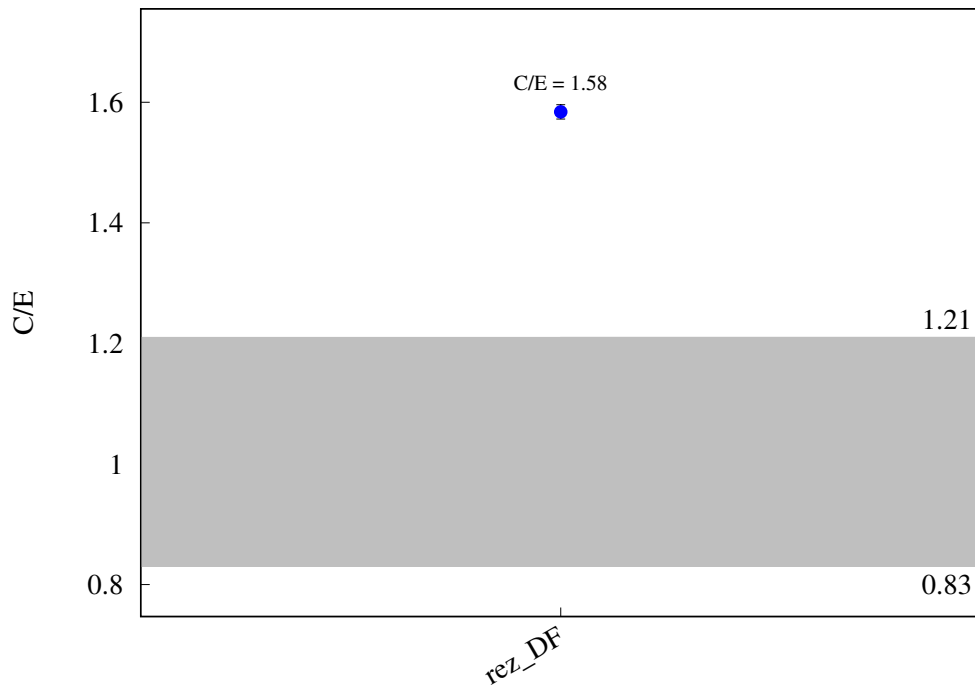
^{52}Cr (n,p) ^{52}V 

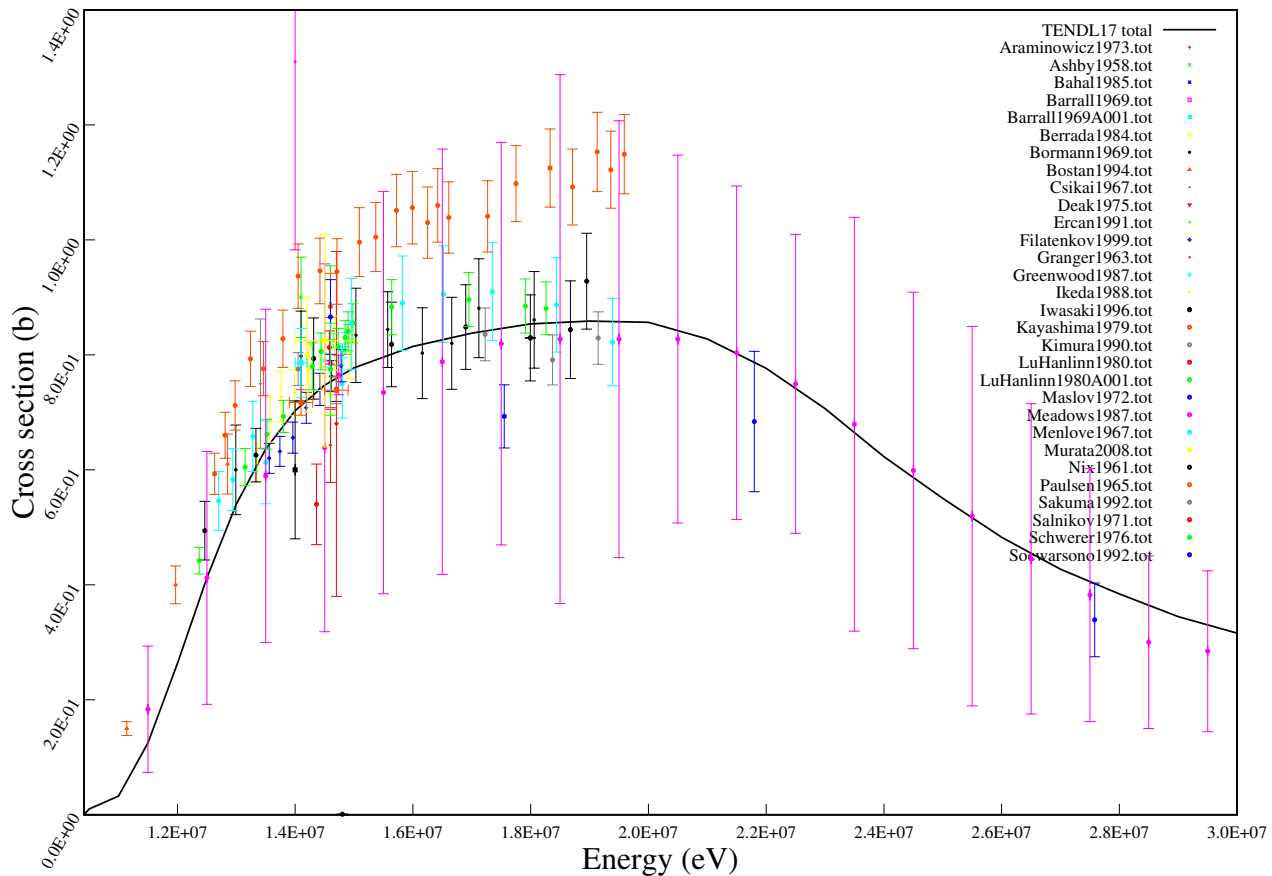
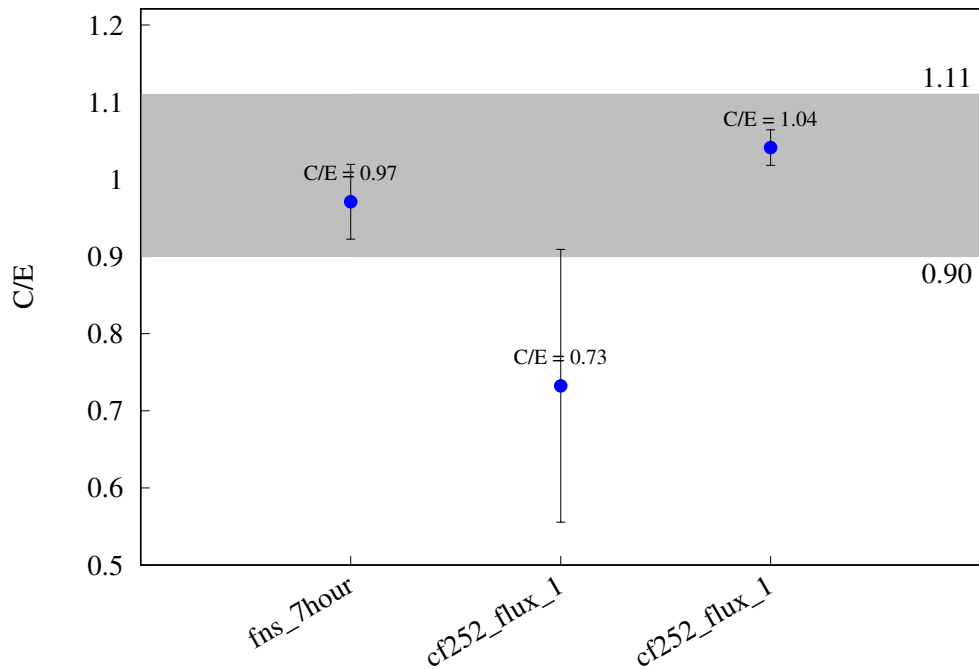
^{52}Cr (n,t) 50V

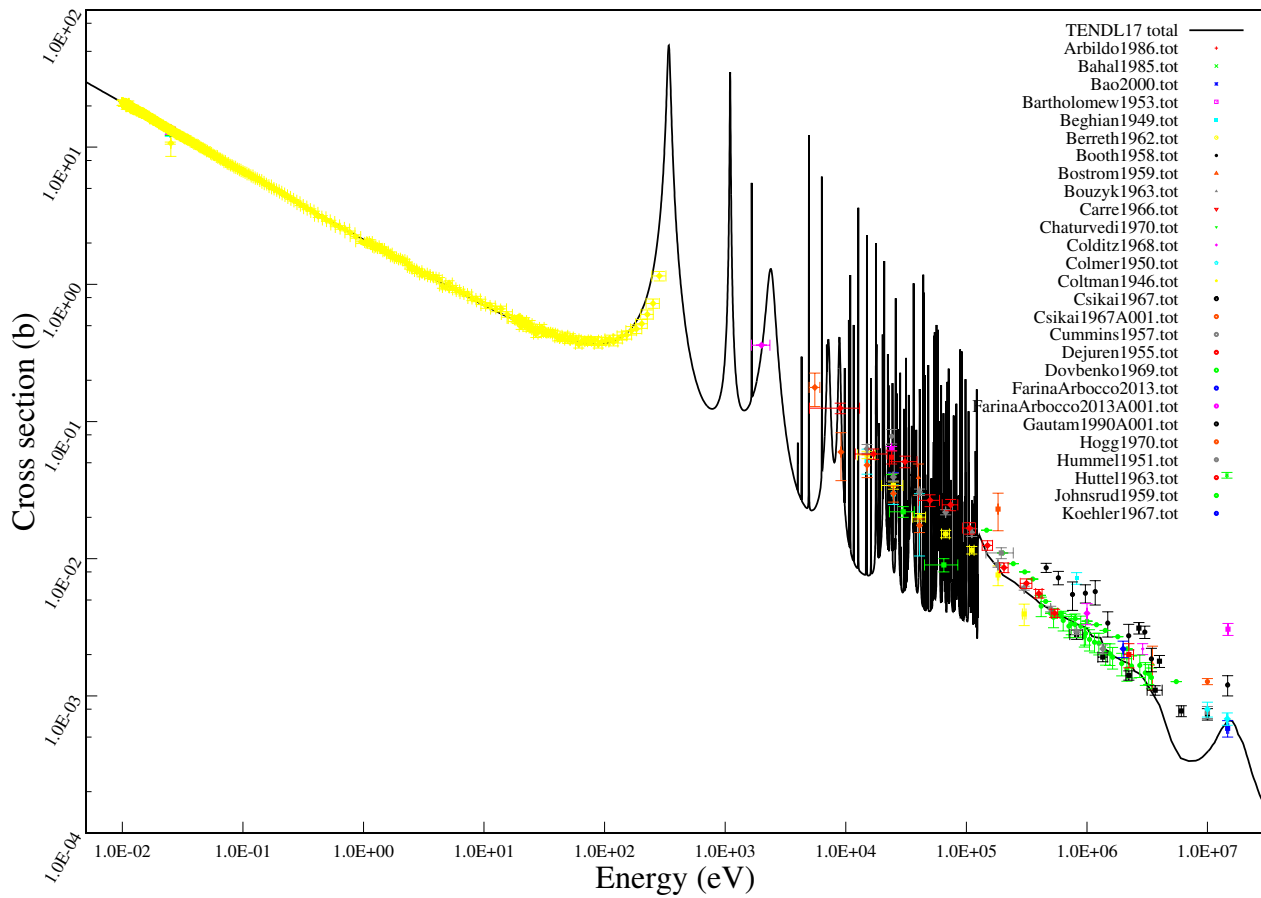
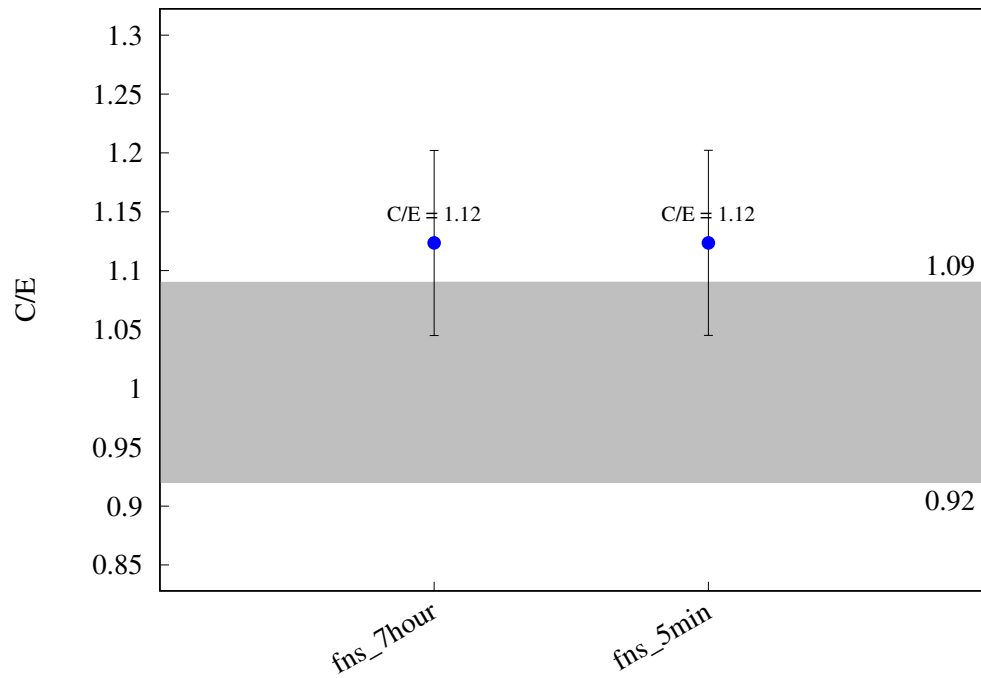
^{53}Cr (n,3n) ^{51}Cr 

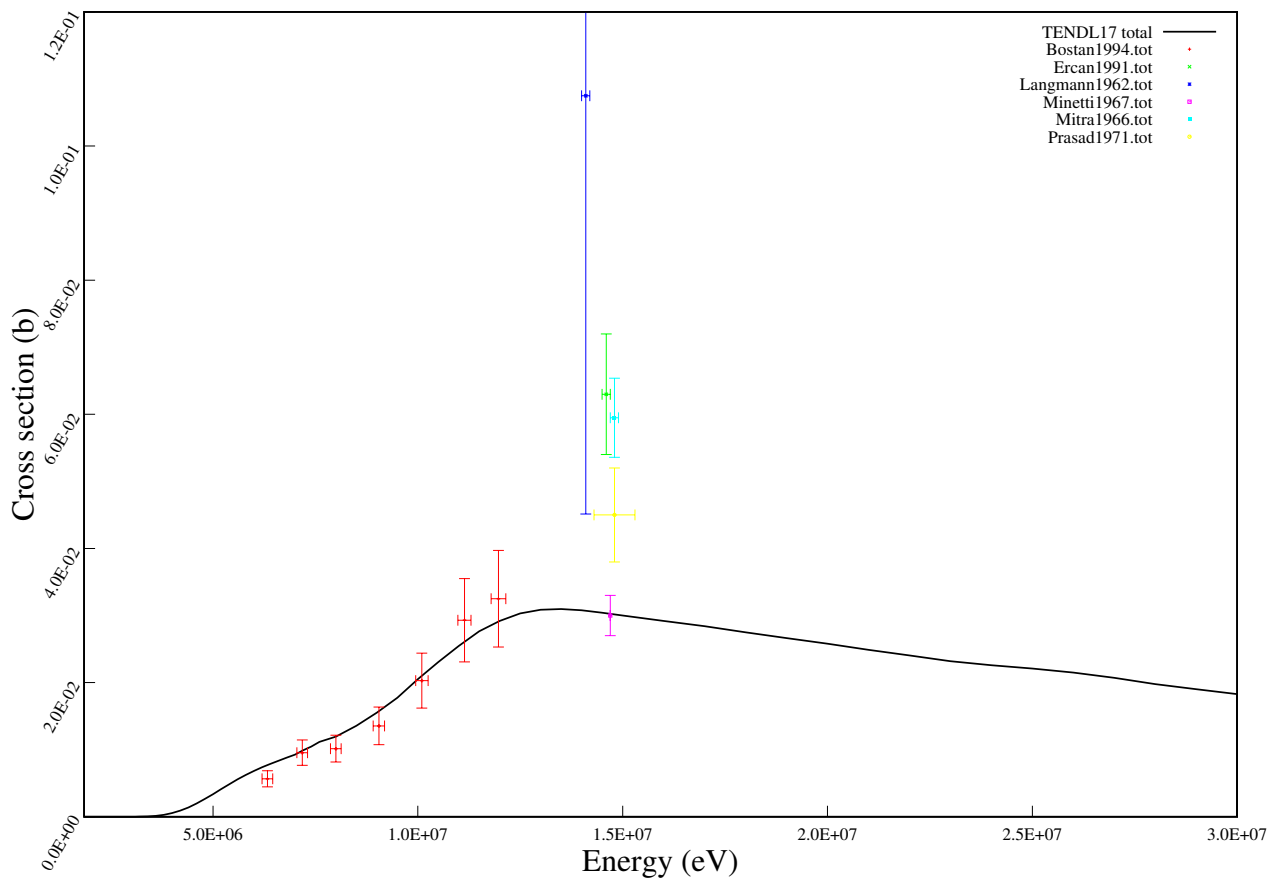
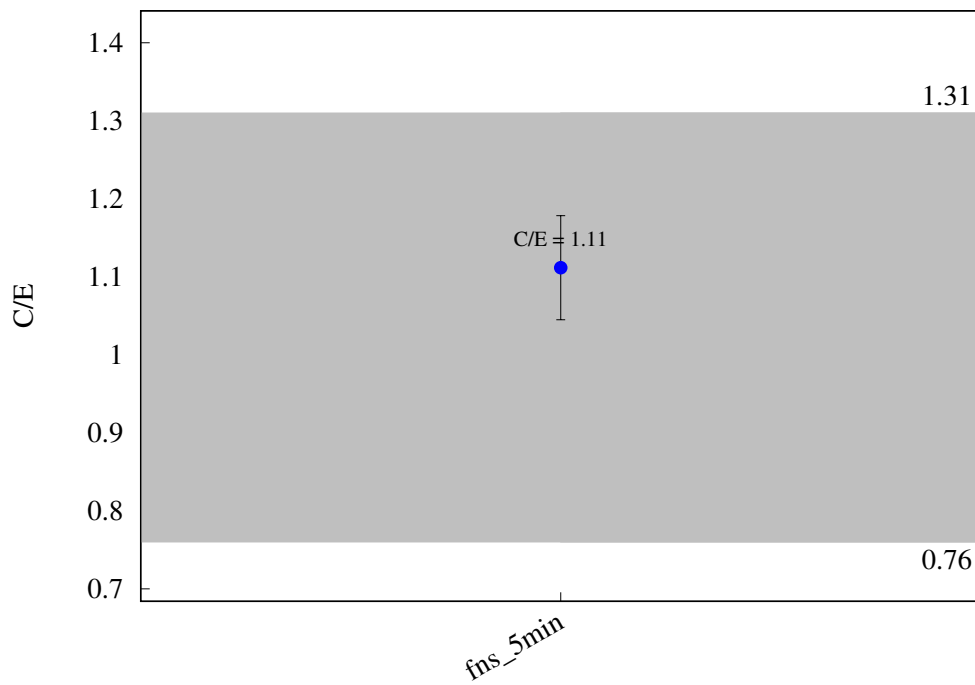
^{53}Cr (n,p) ^{53}V 

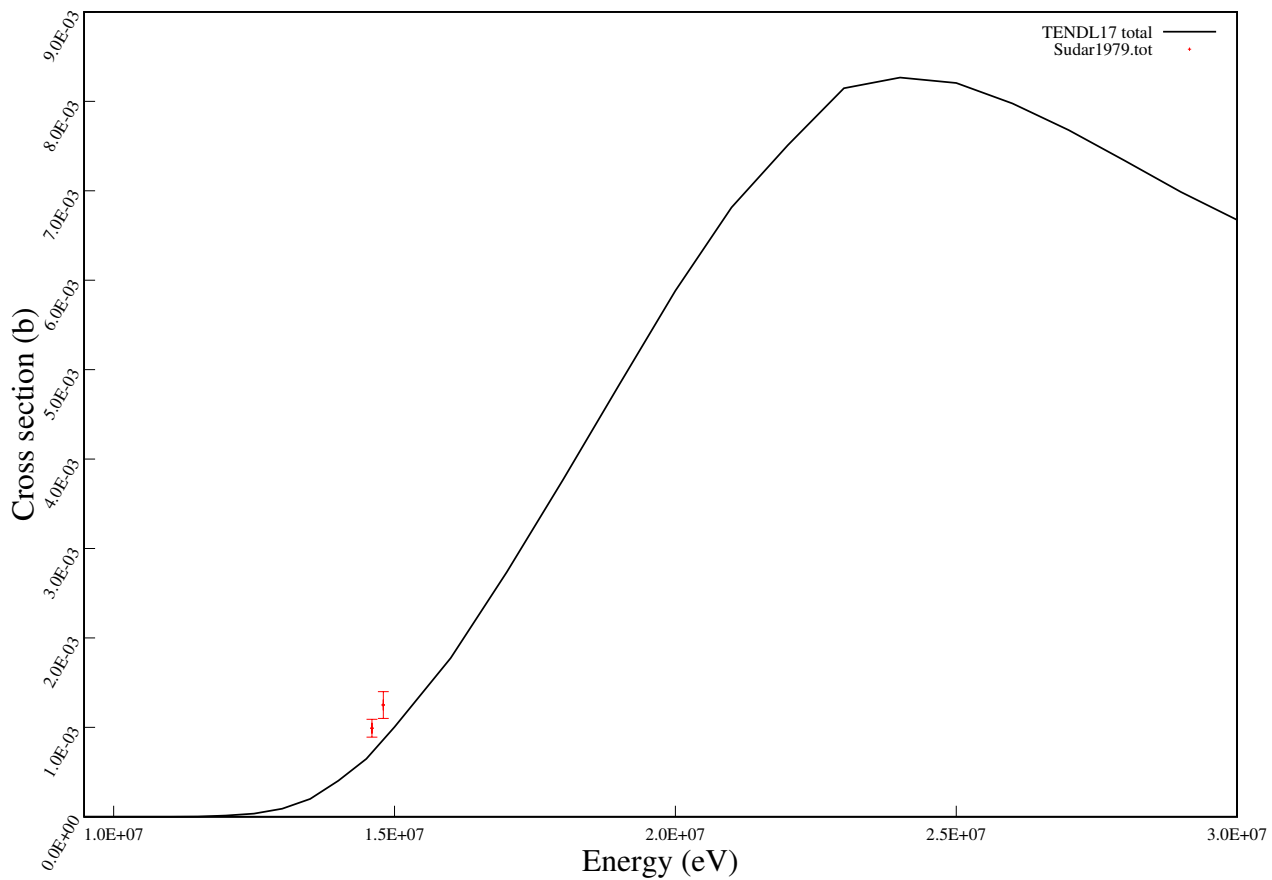
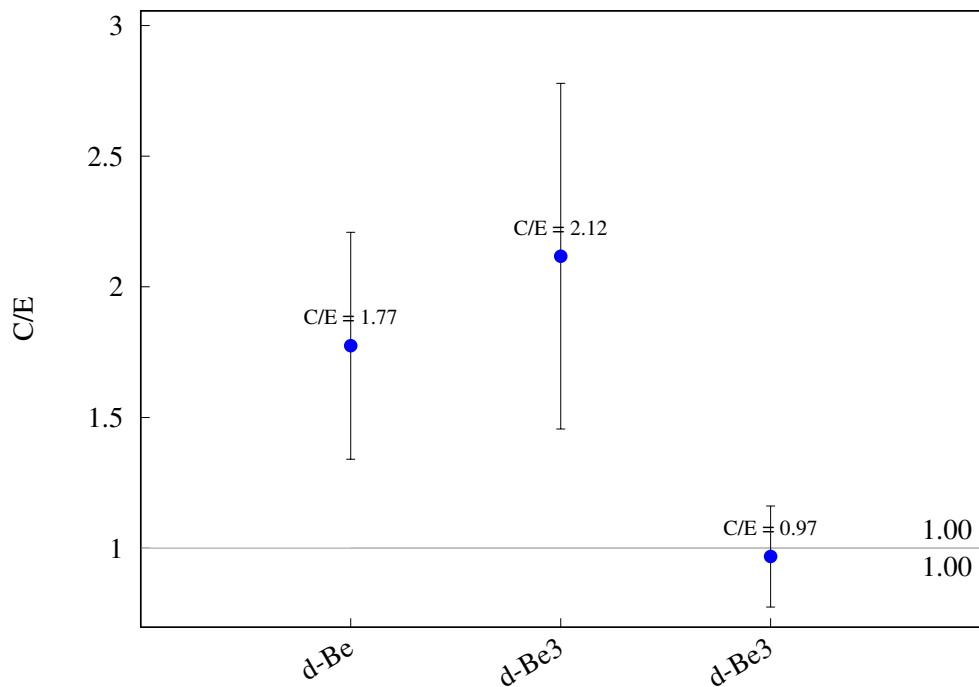
$^{53}\text{Cr} (\text{n},\text{h}) ^{51}\text{Ti}$ 

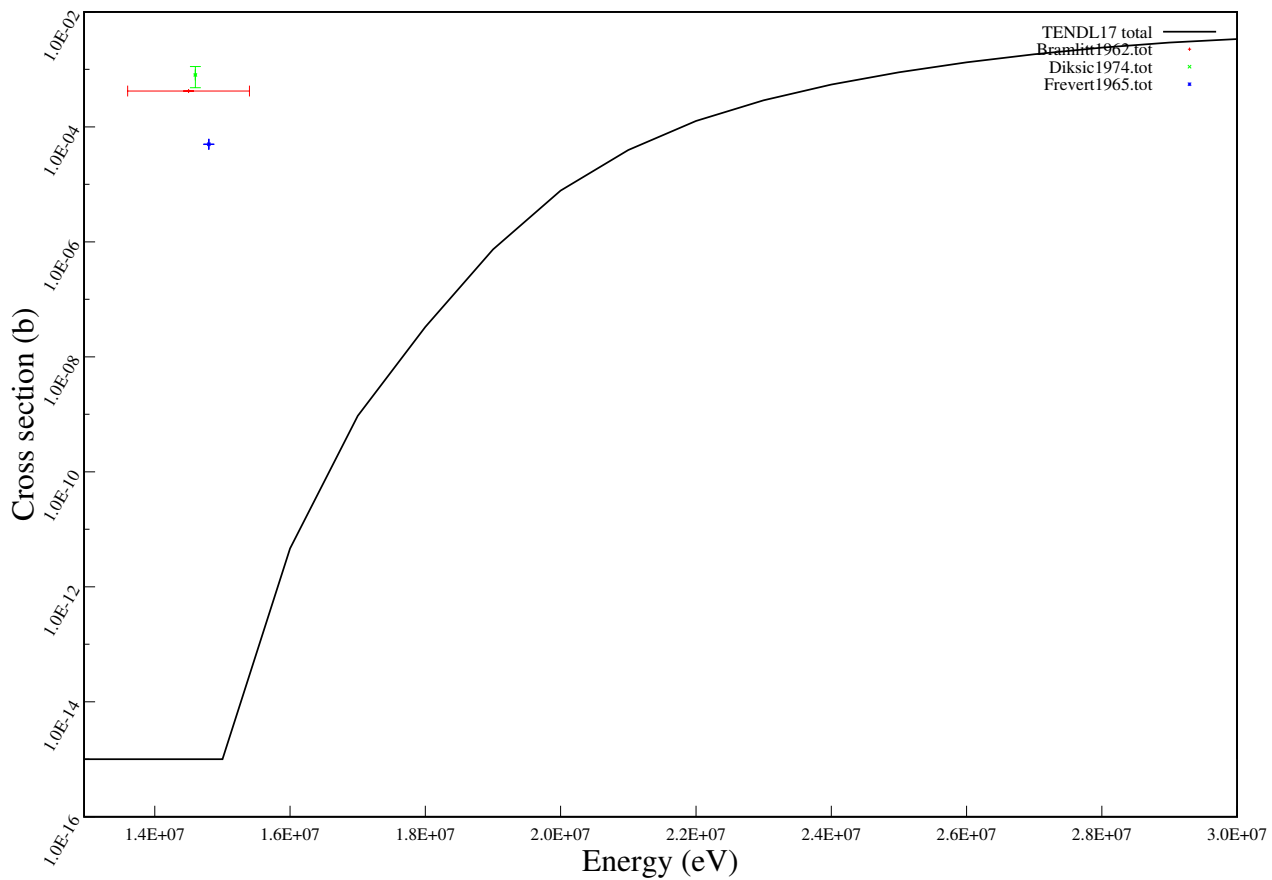
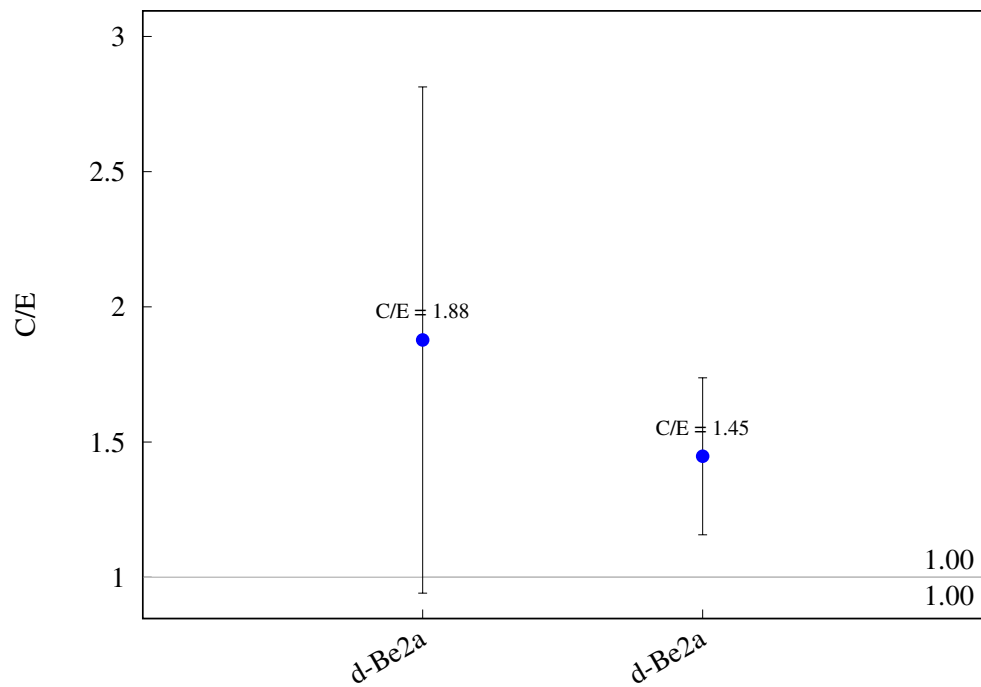
^{54}Cr (n,a) ^{51}Ti 

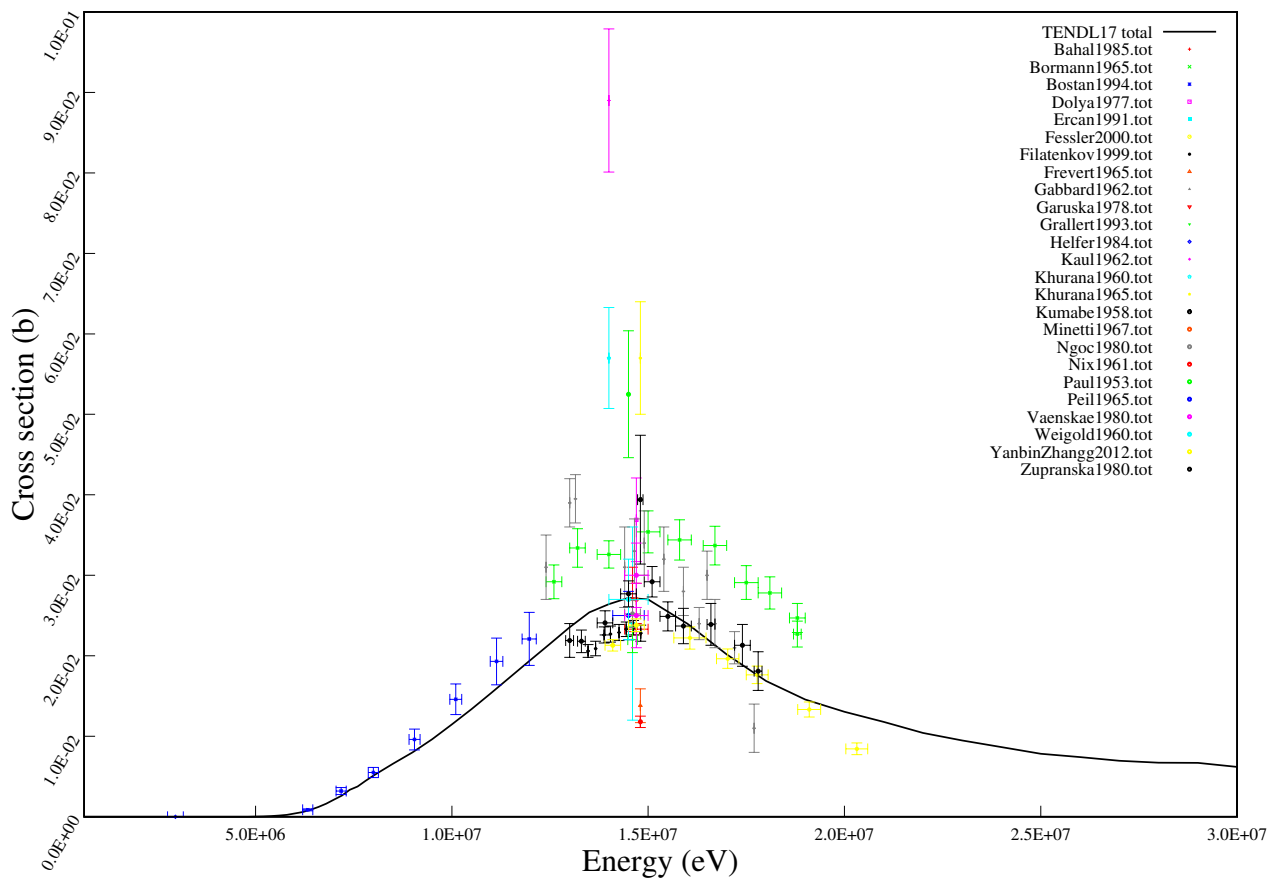
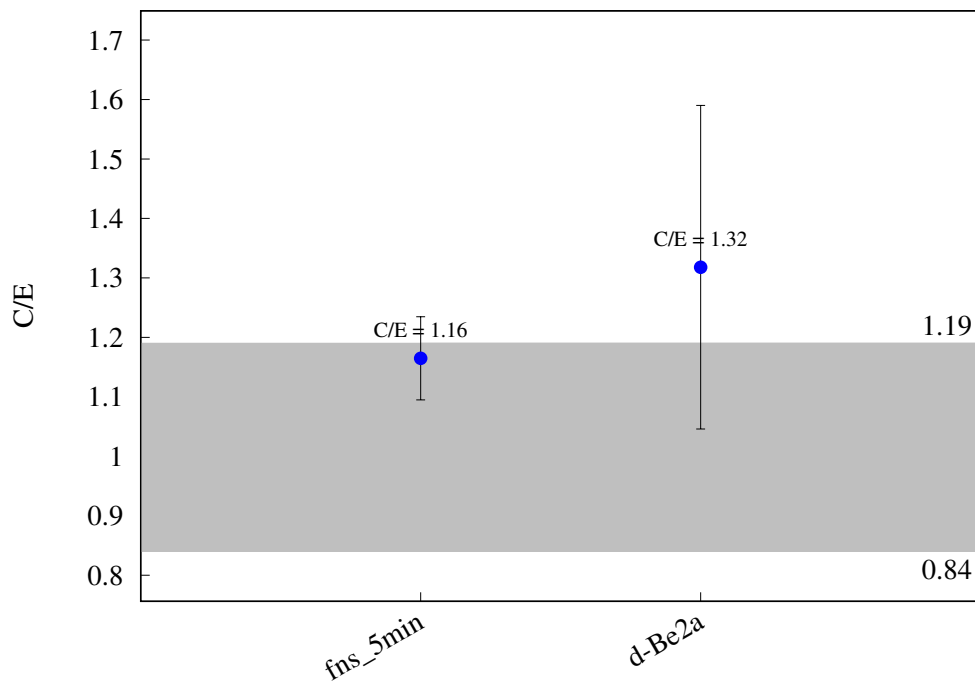


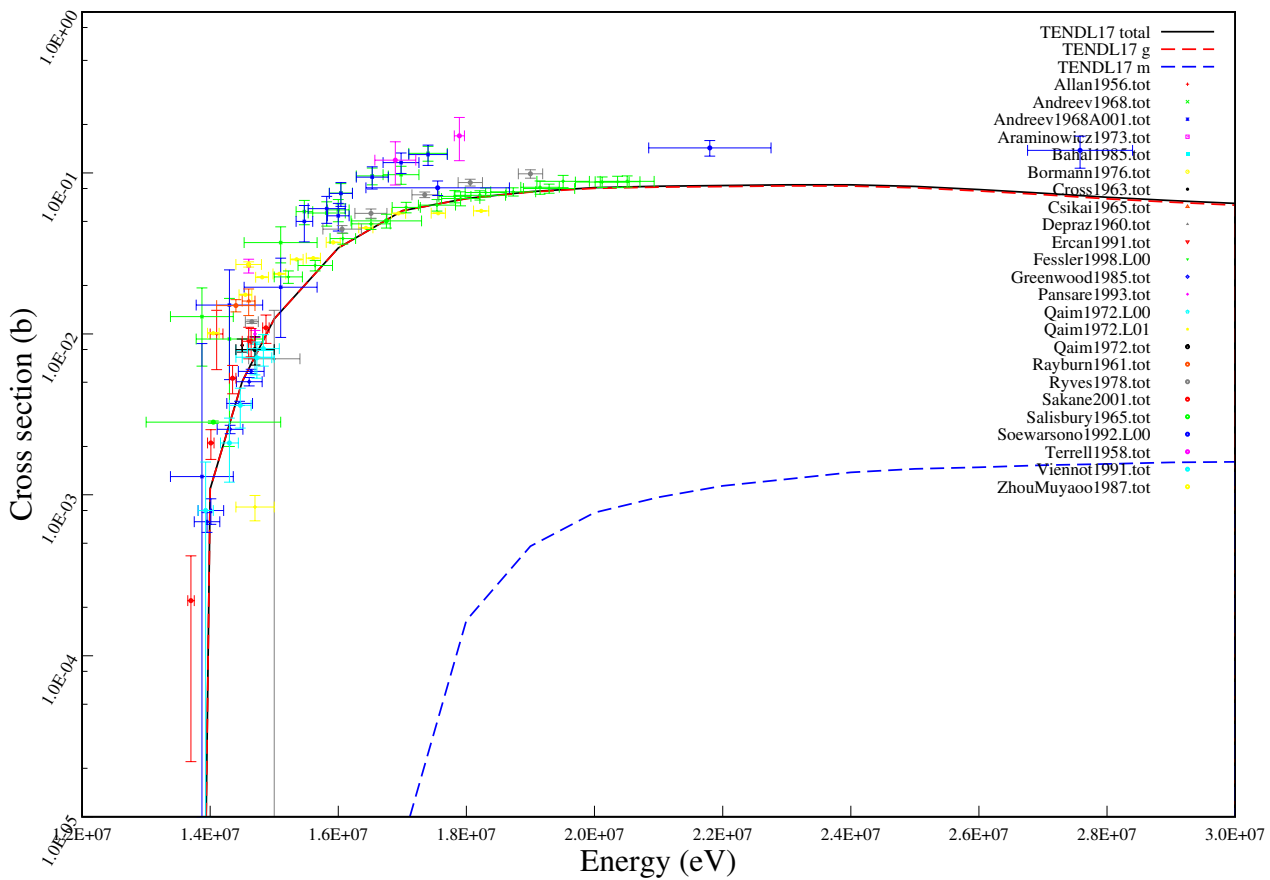
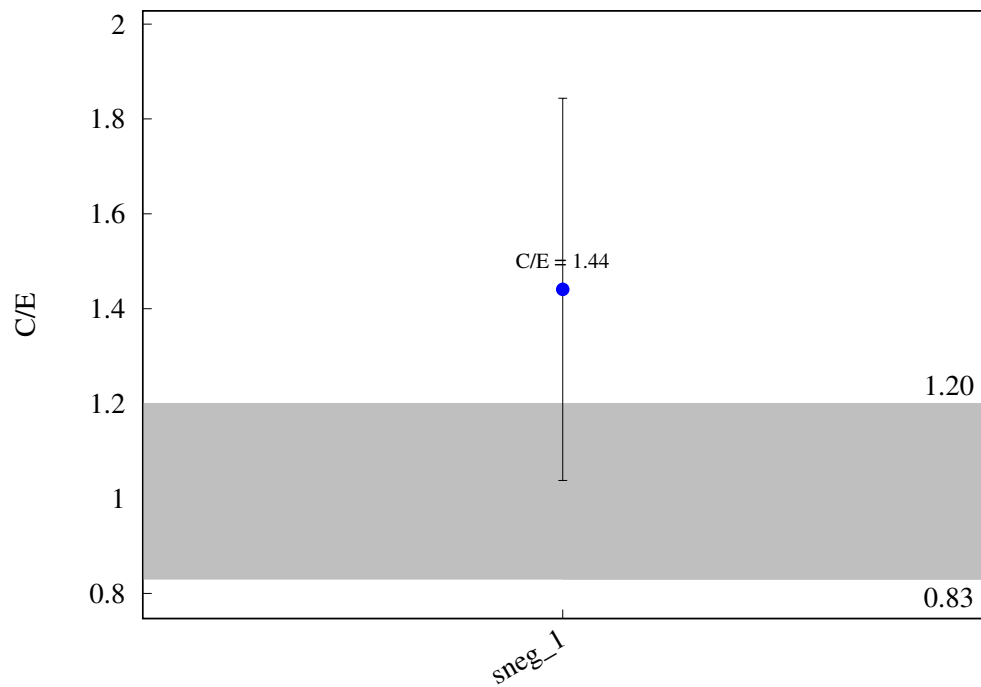
^{55}Mn (n,g) ^{56}Mn 

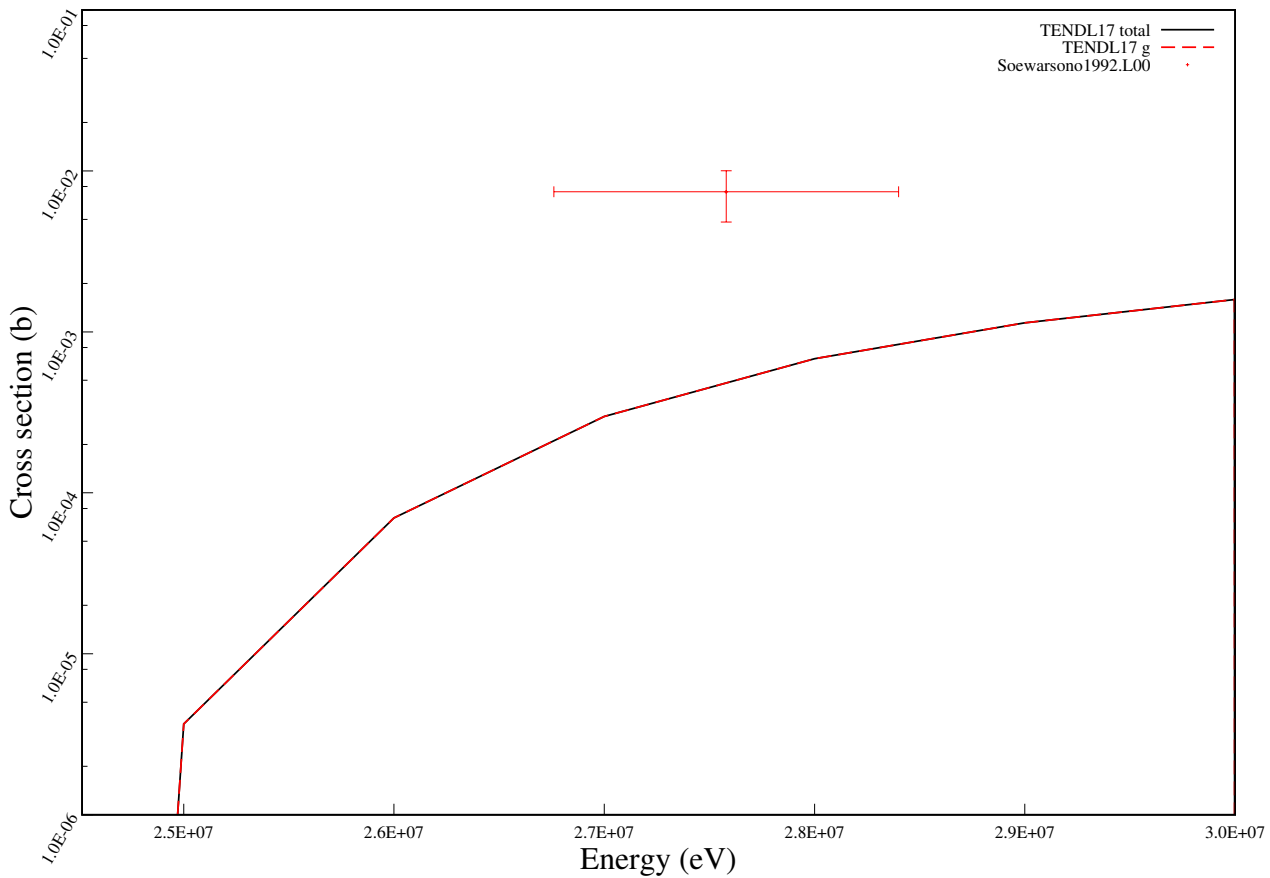
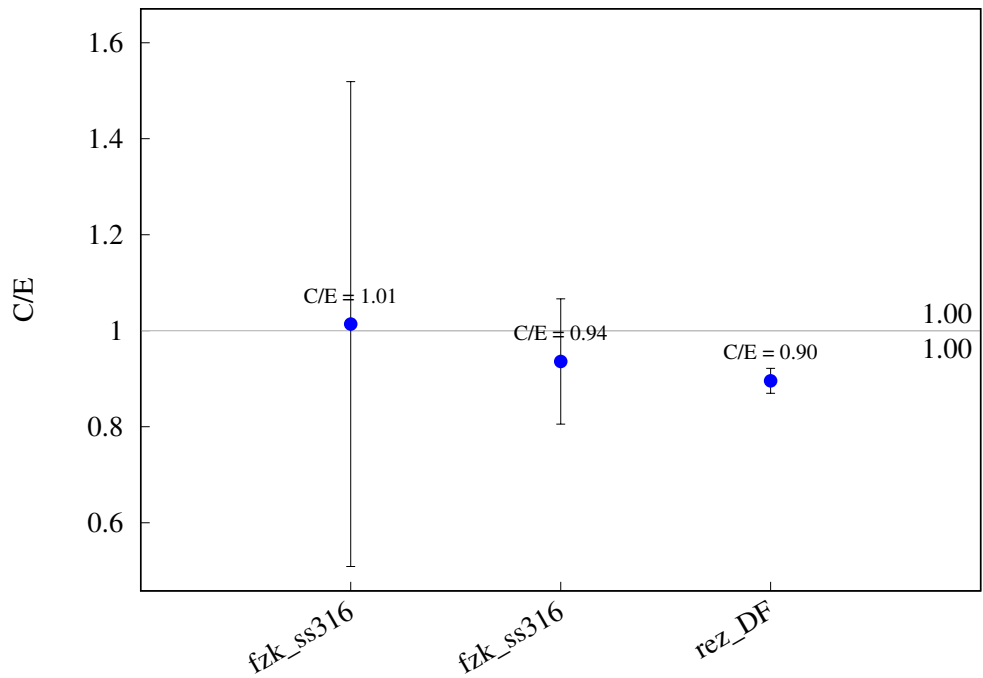
^{55}Mn (n,p) ^{55}Cr 

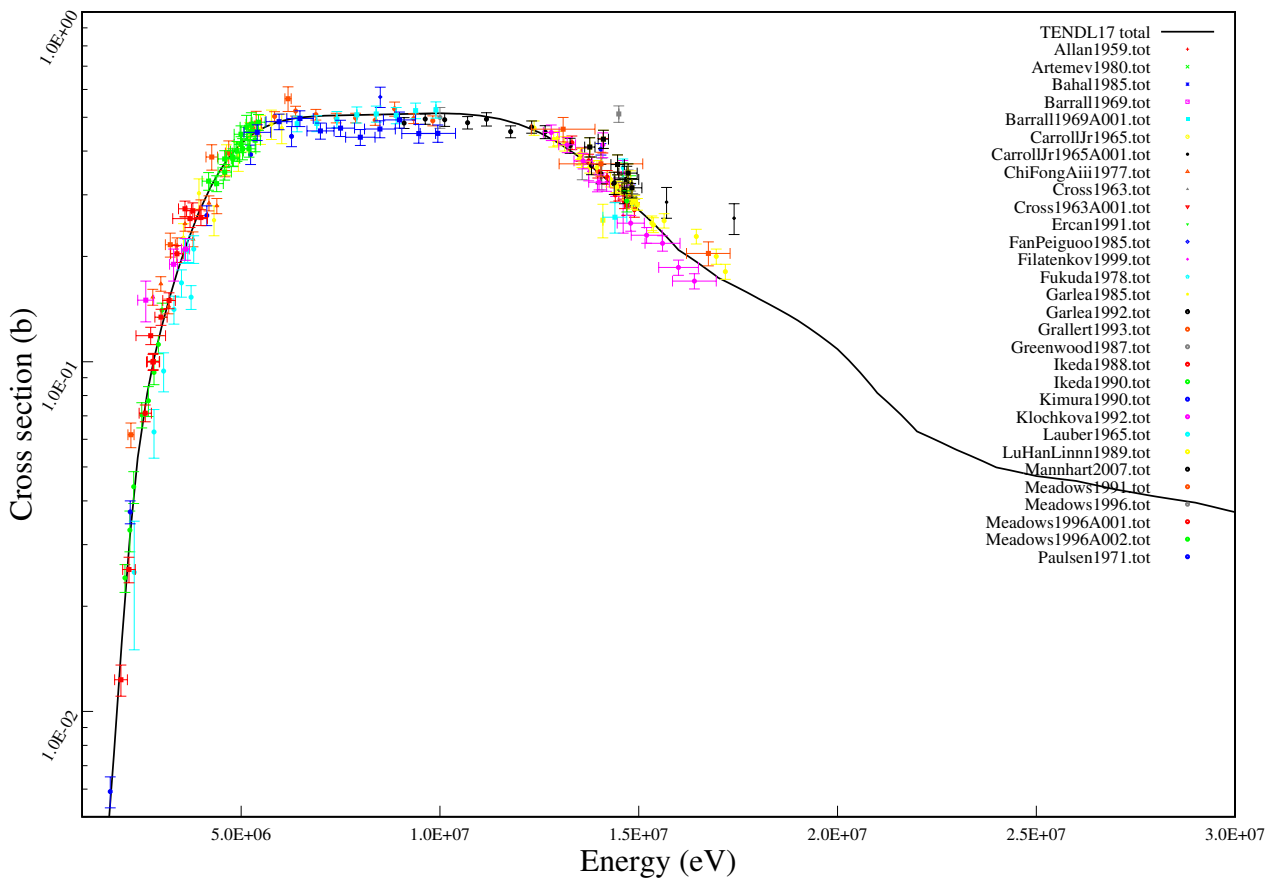
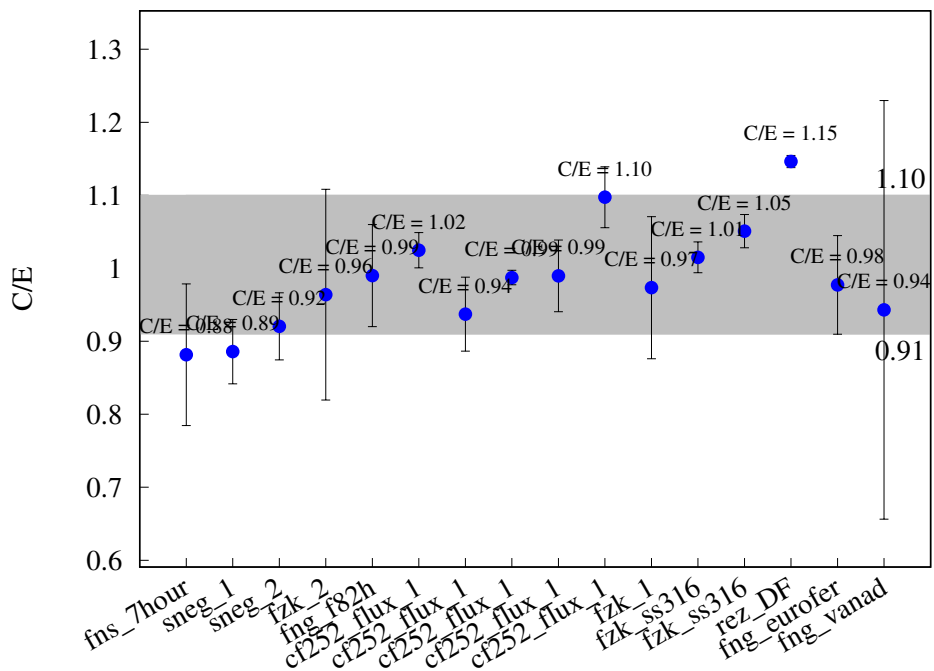
$^{55}\text{Mn} (\text{n},\text{t}) ^{53}\text{Cr}$ 

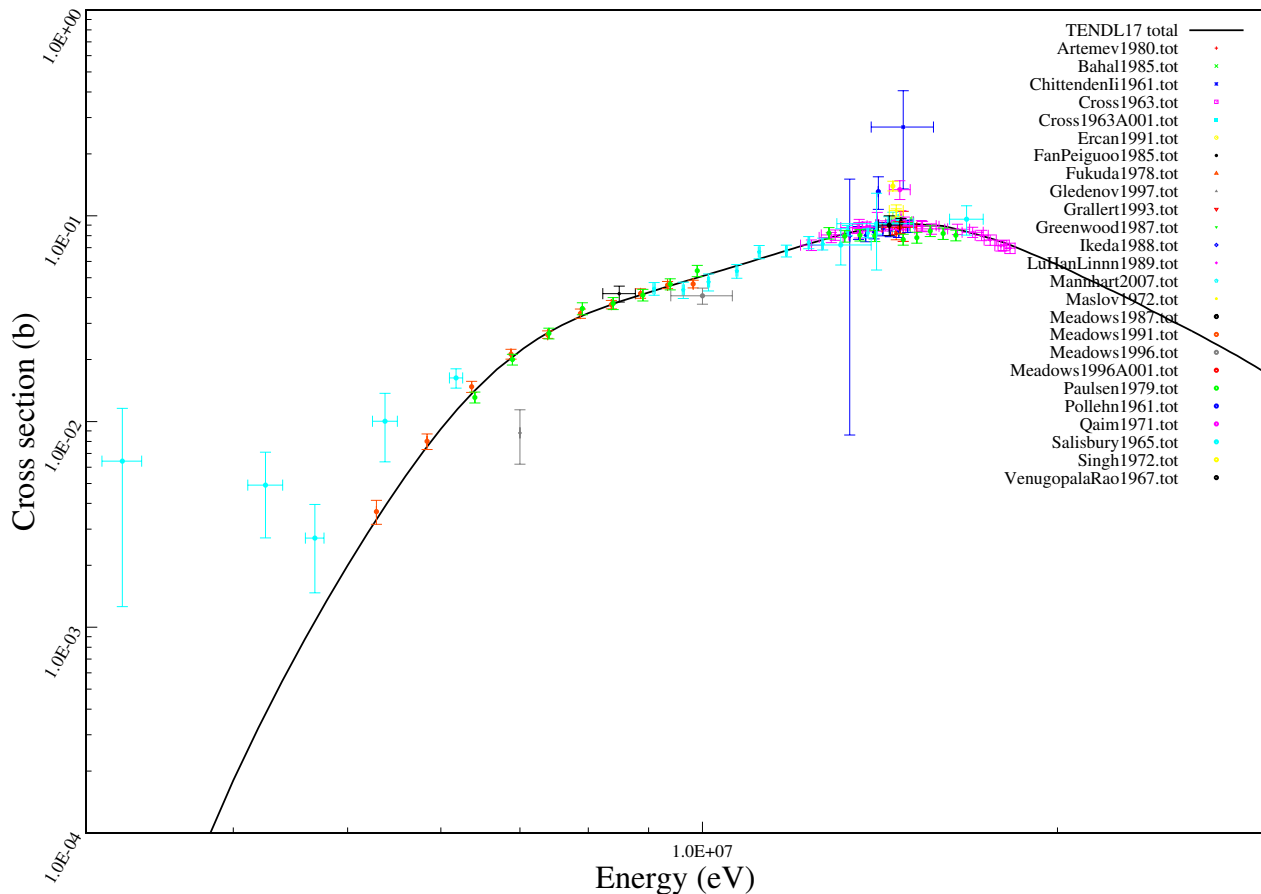
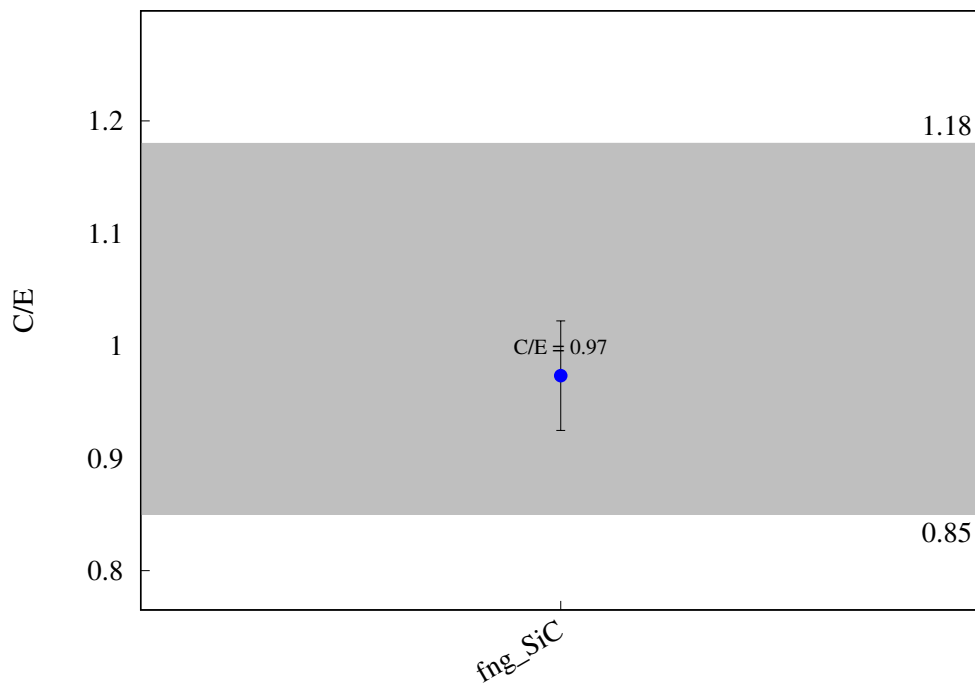
$^{55}\text{Mn} (\text{n},\text{h}) ^{53}\text{V}$ 

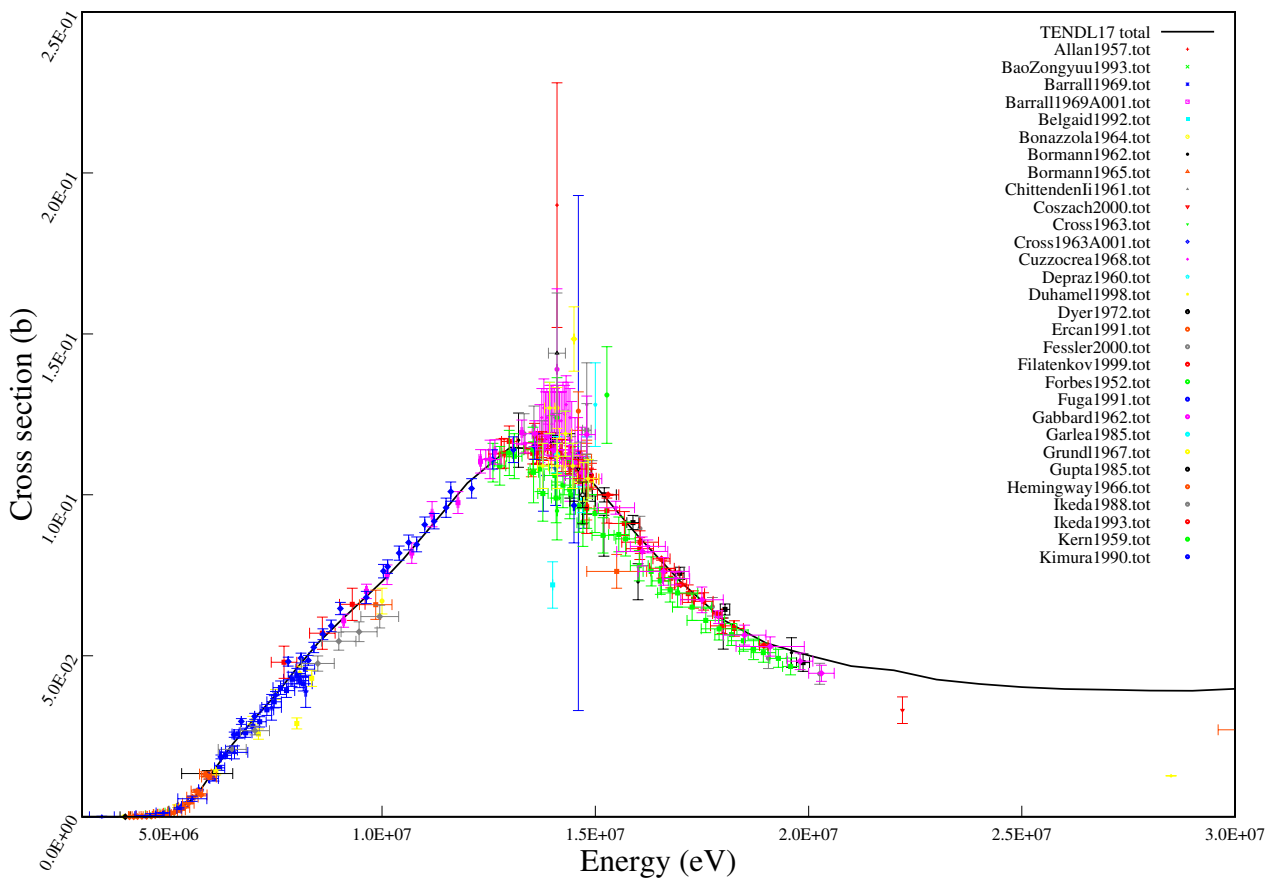
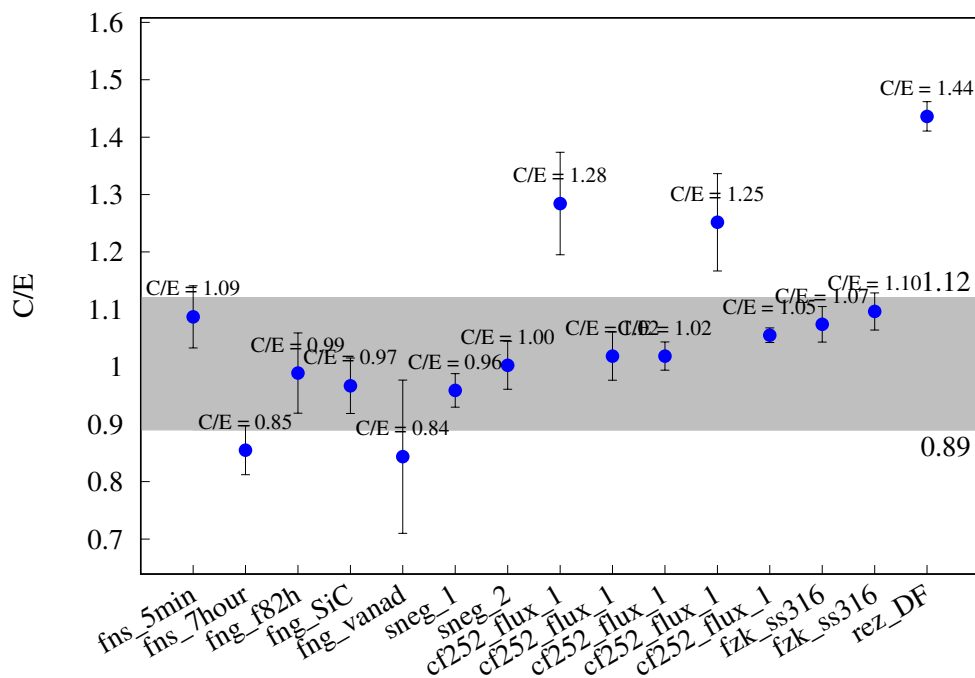
^{55}Mn (n,a) ^{52}V 

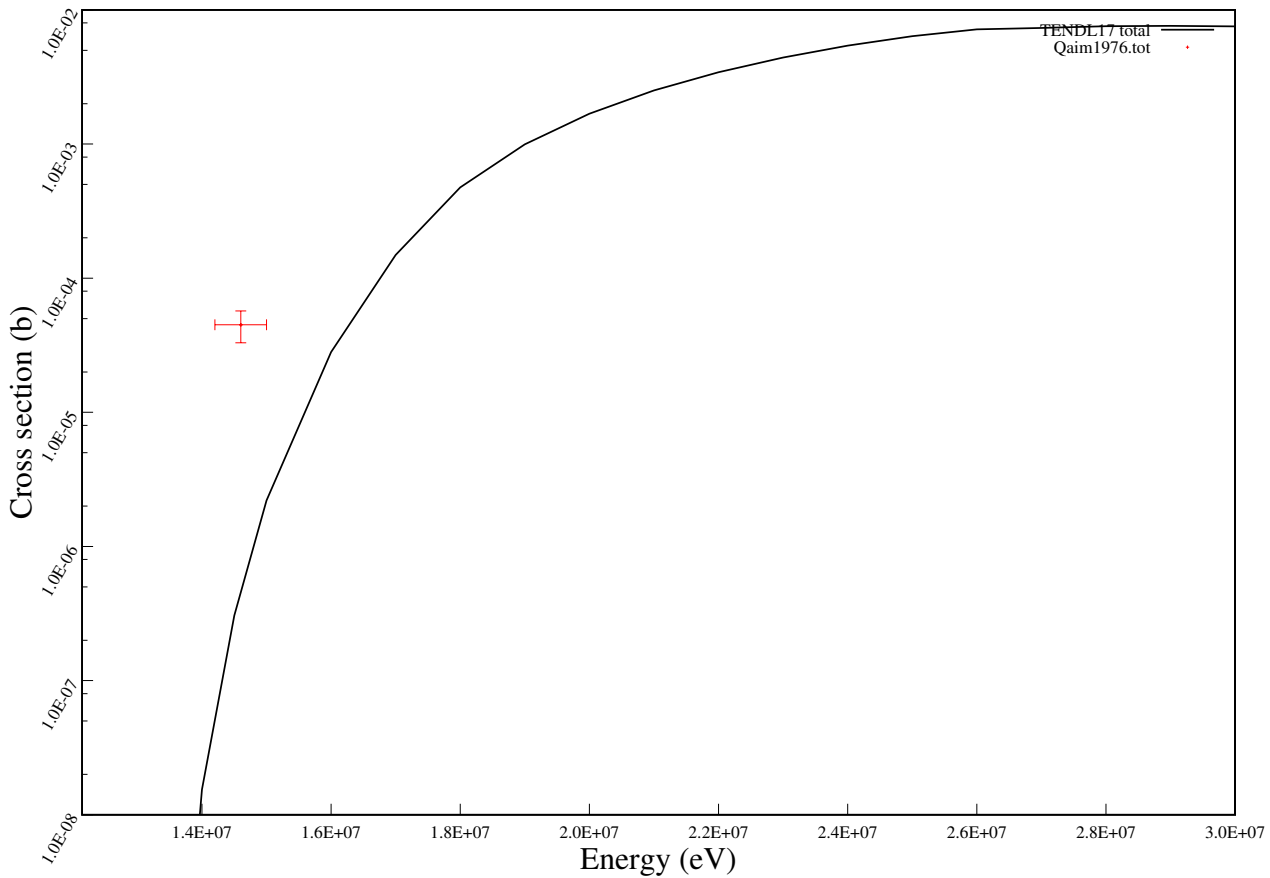
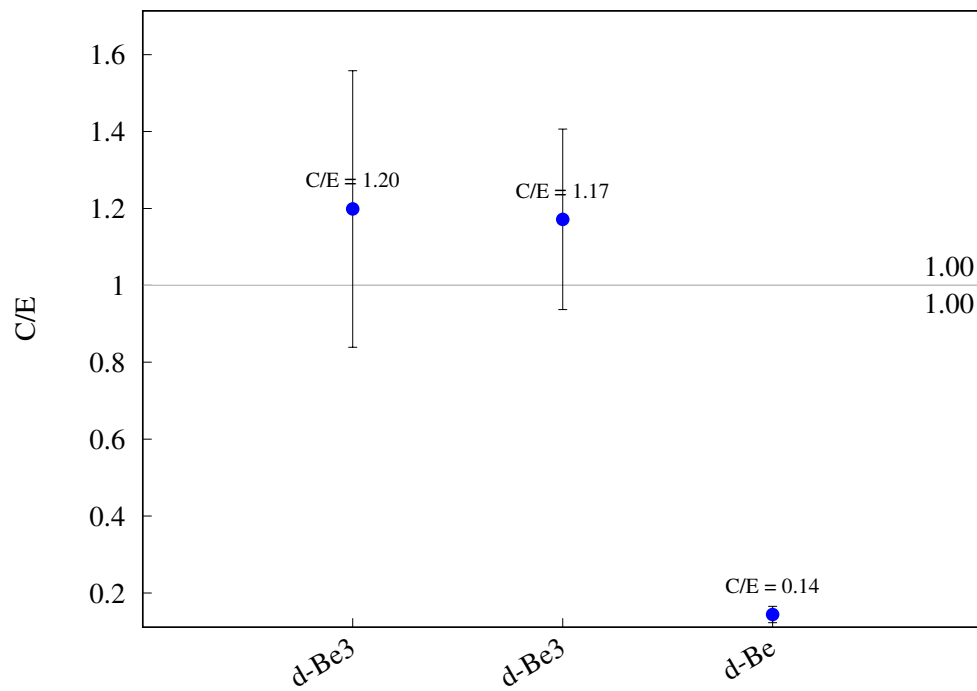
^{54}Fe (n,2n) ^{53}Fe 

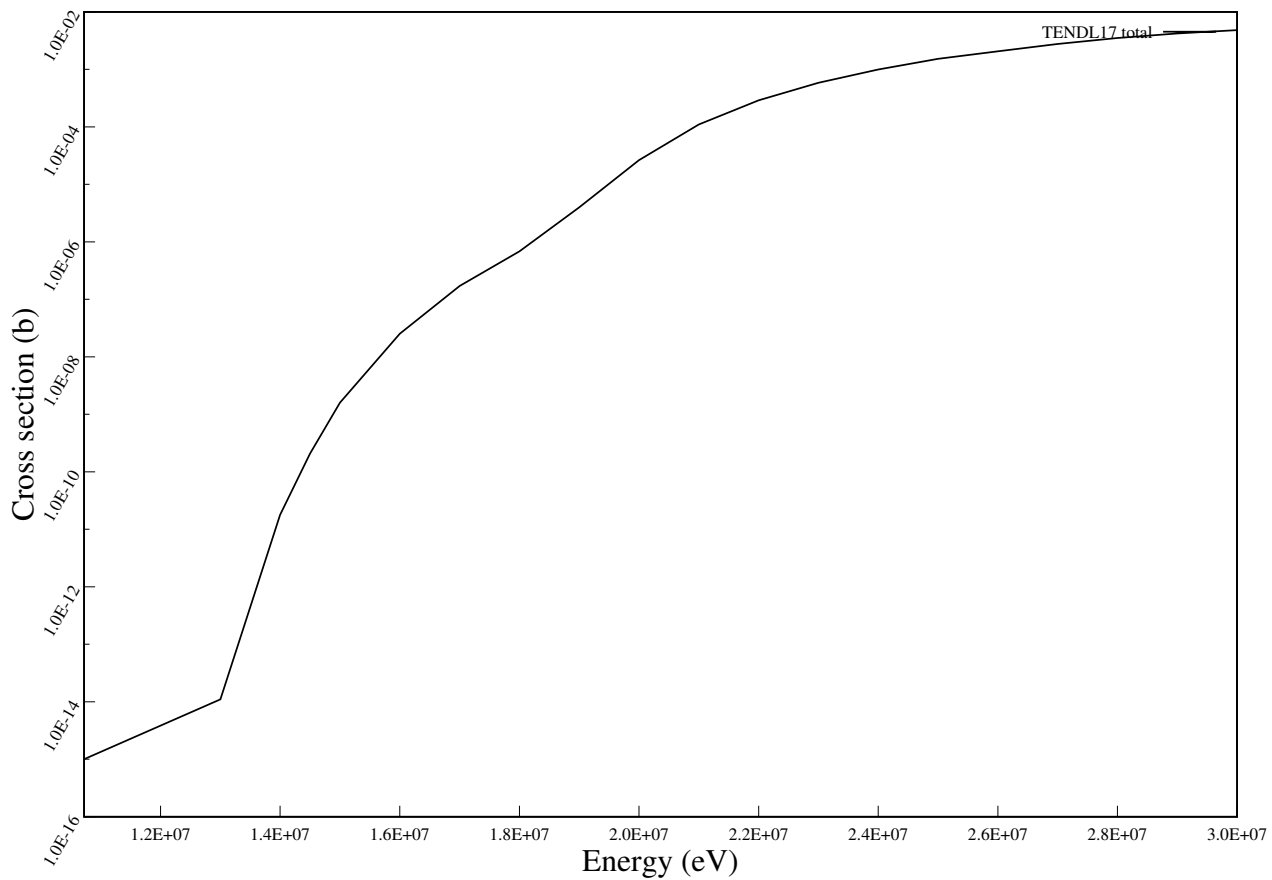
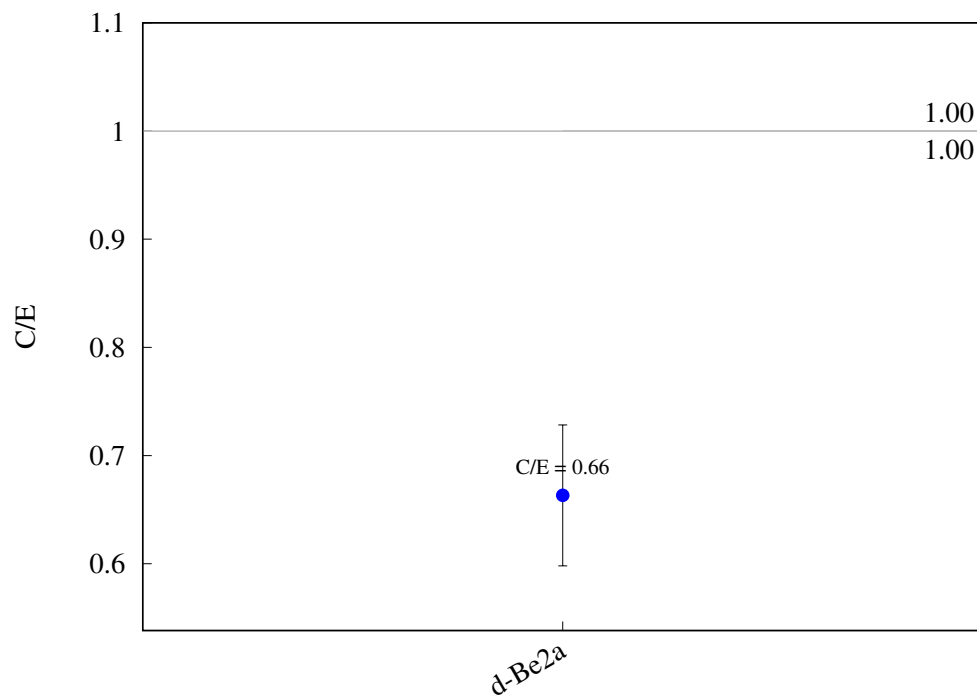
^{54}Fe (n,3n) $^{52}\text{g}\text{Fe}$ 

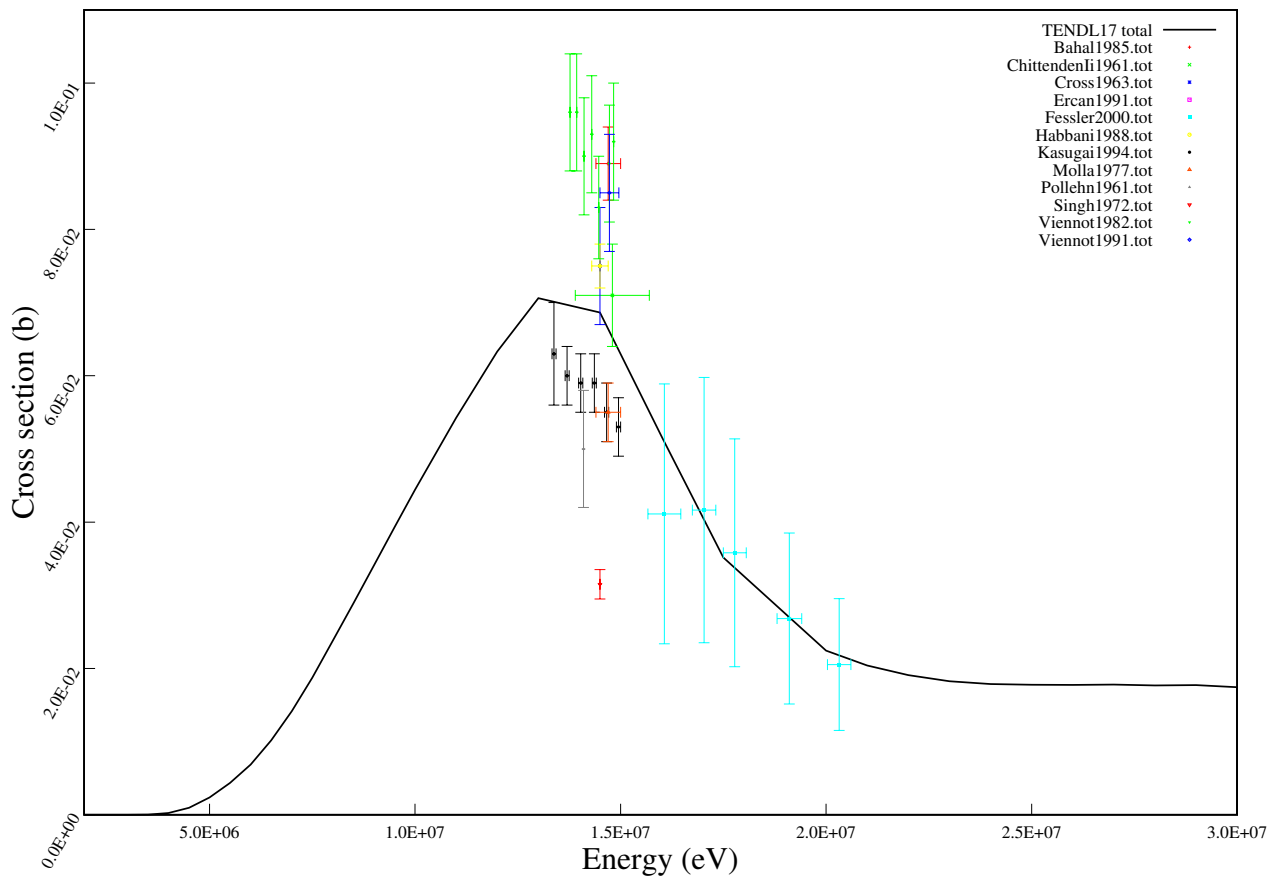
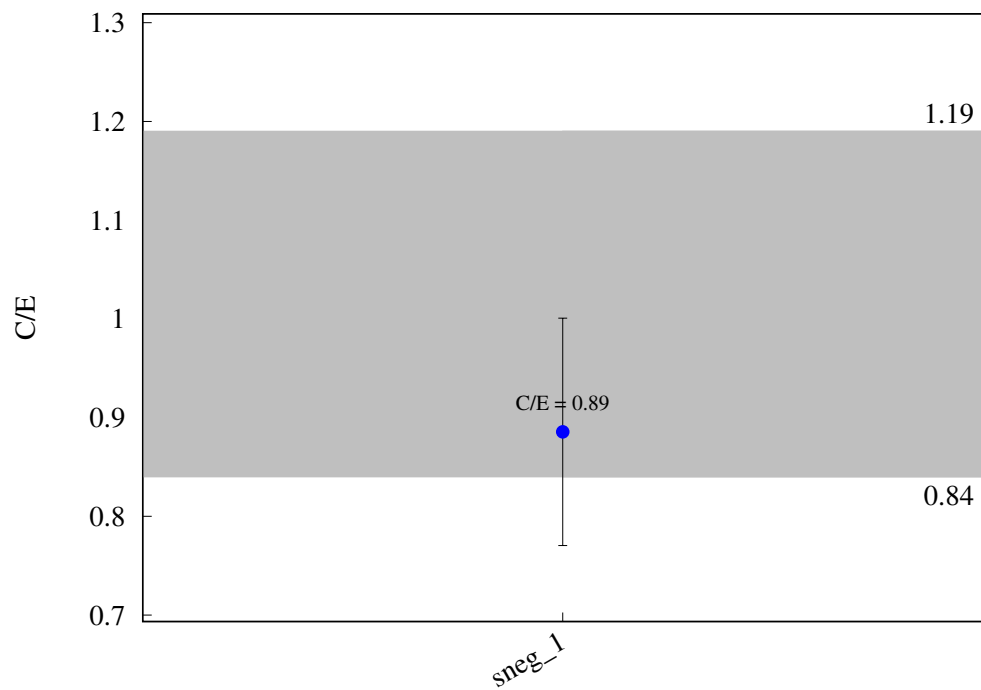
^{54}Fe (n,p) ^{54}Mn 

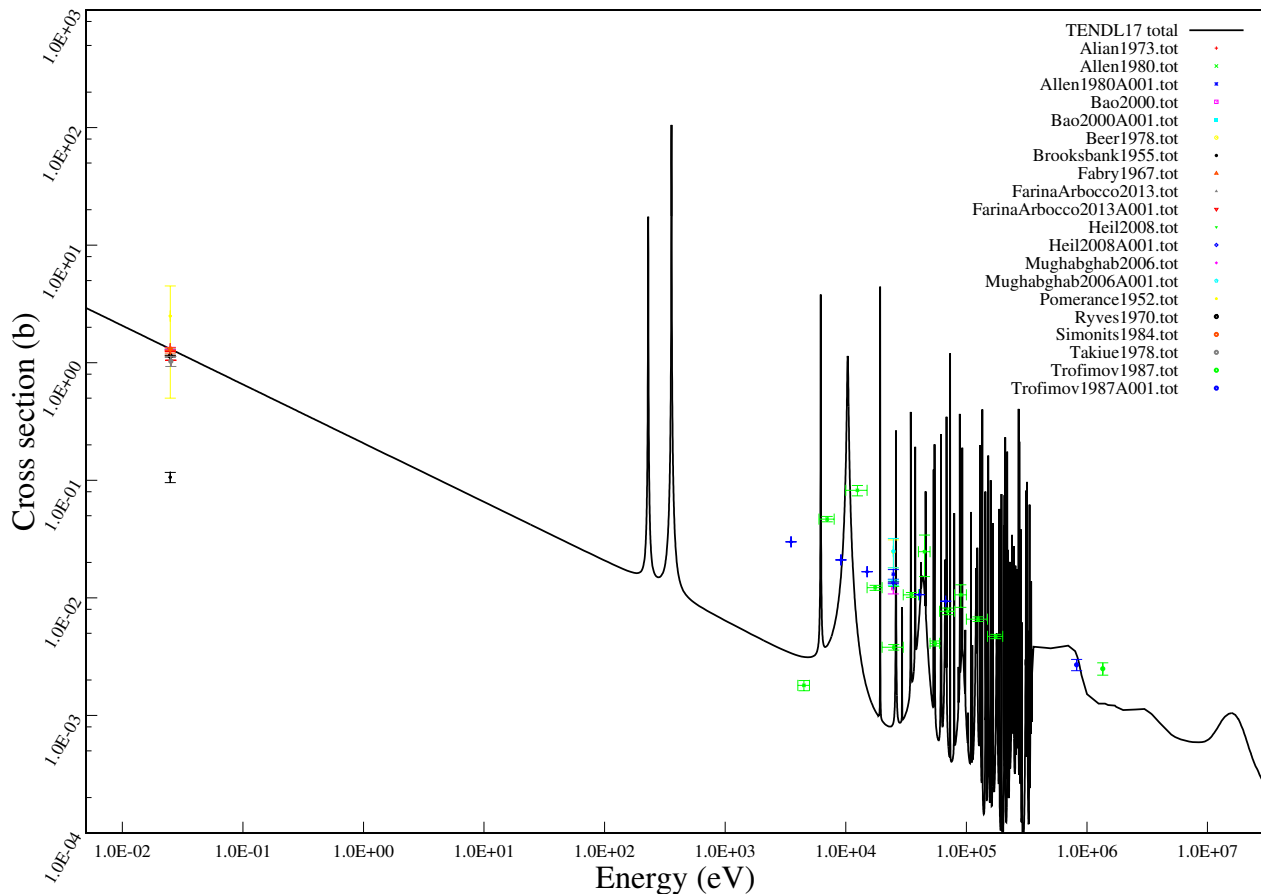
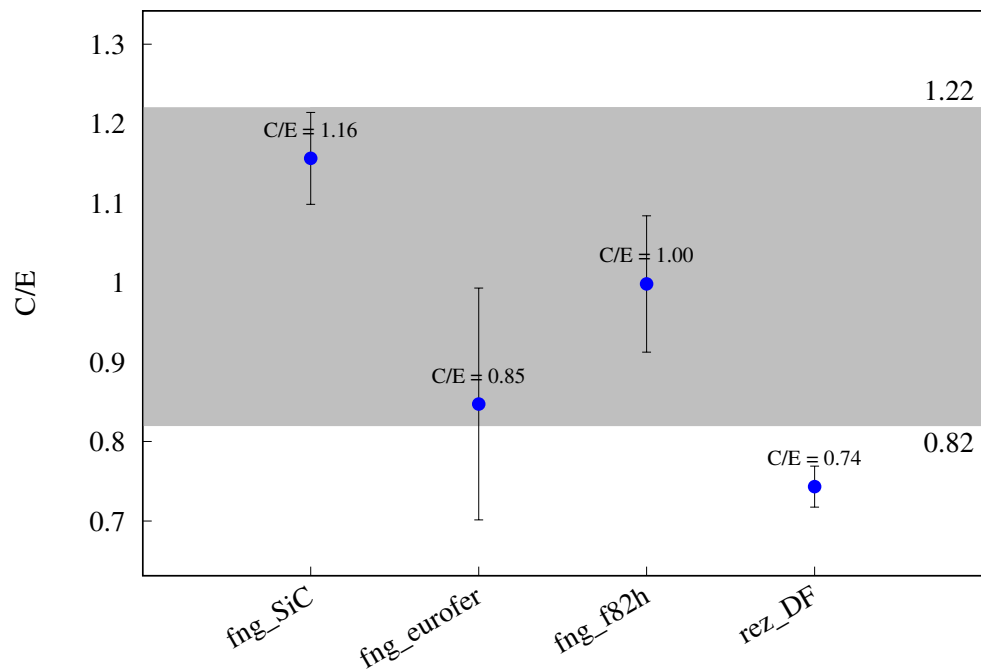
$^{54}\text{Fe} (\text{n,a}) ^{51}\text{Cr}$ 

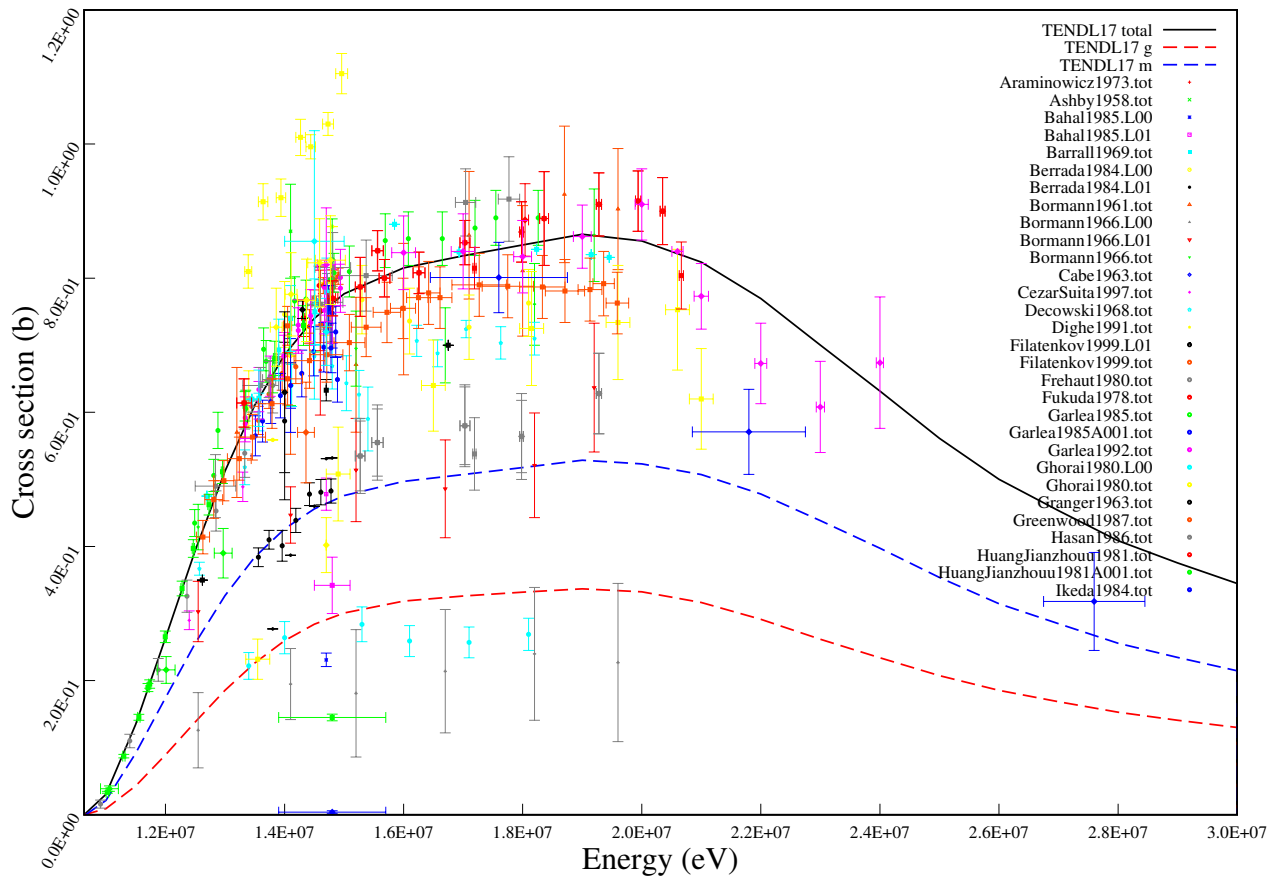
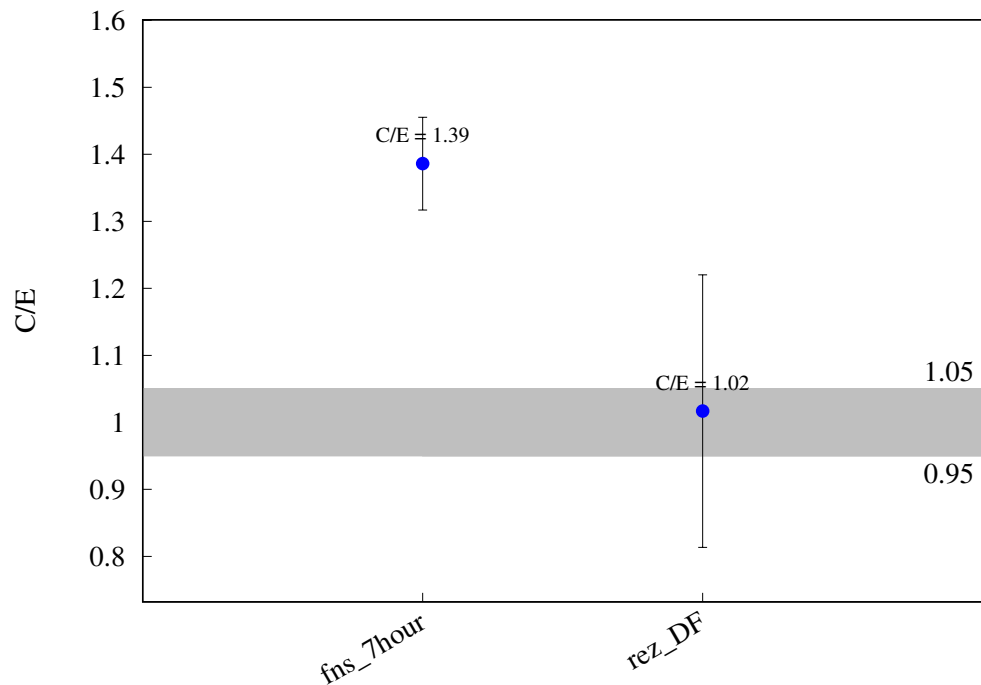
^{56}Fe (n,p) ^{56}Mn 

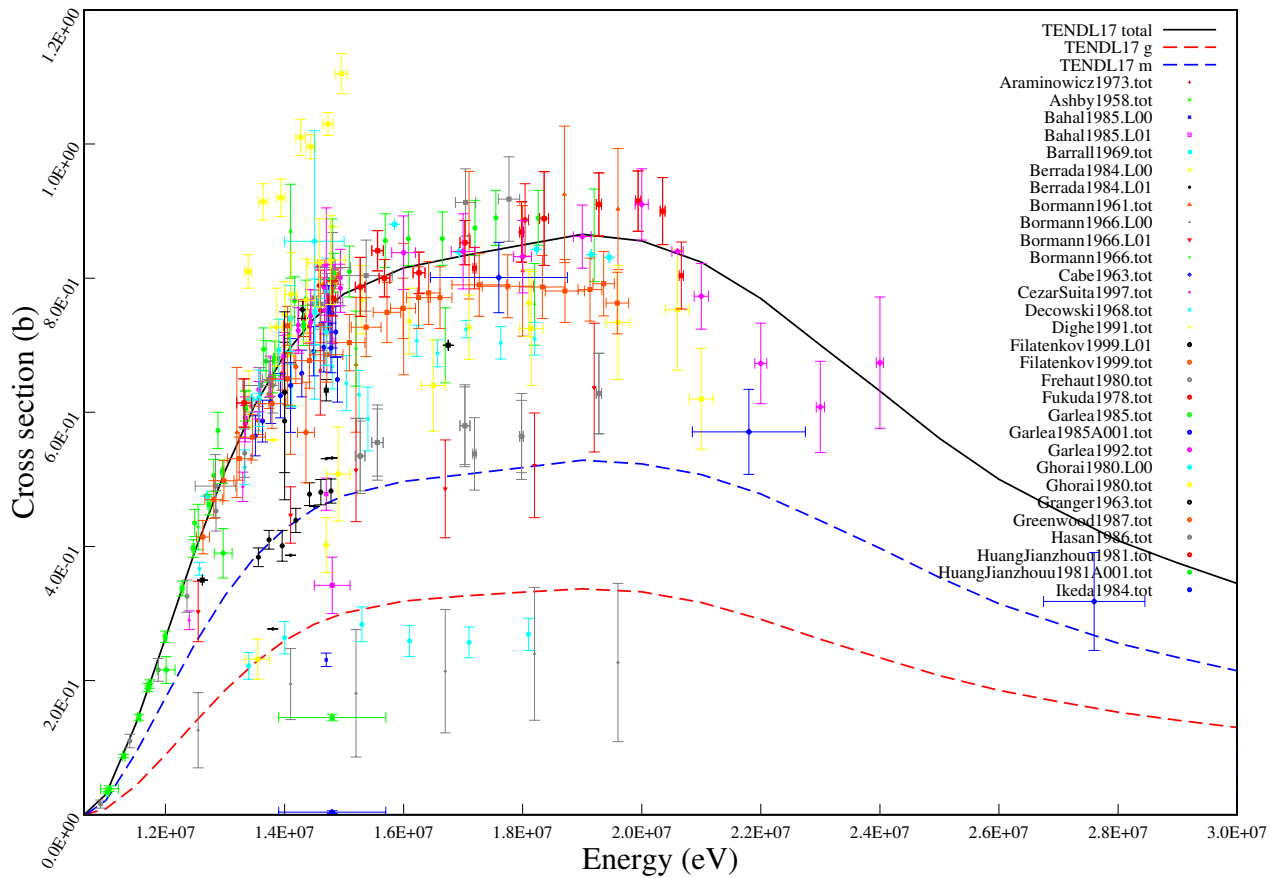
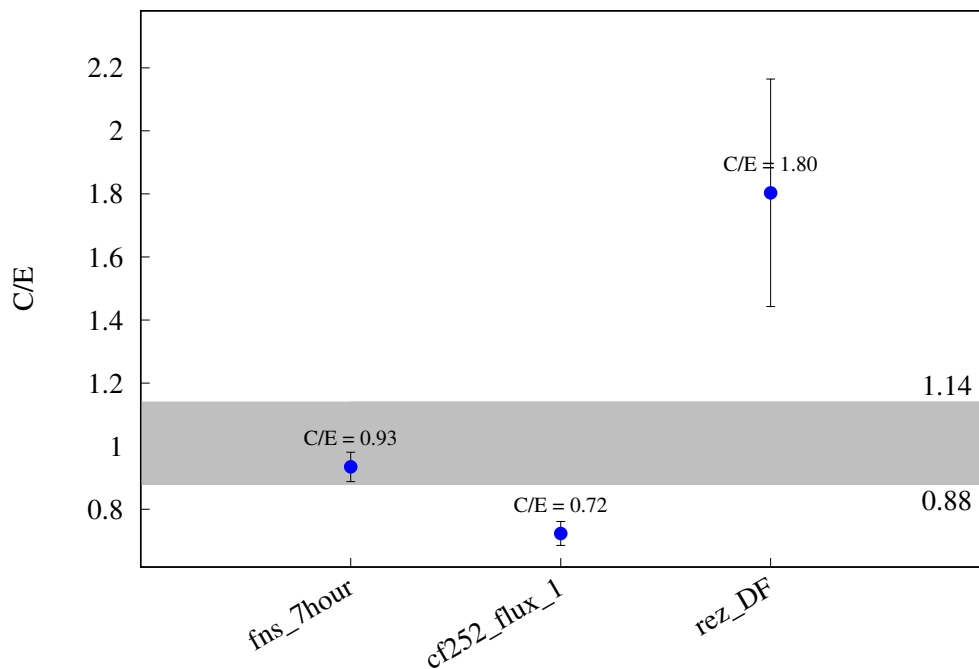
^{56}Fe (n,t) ^{54}Mn 

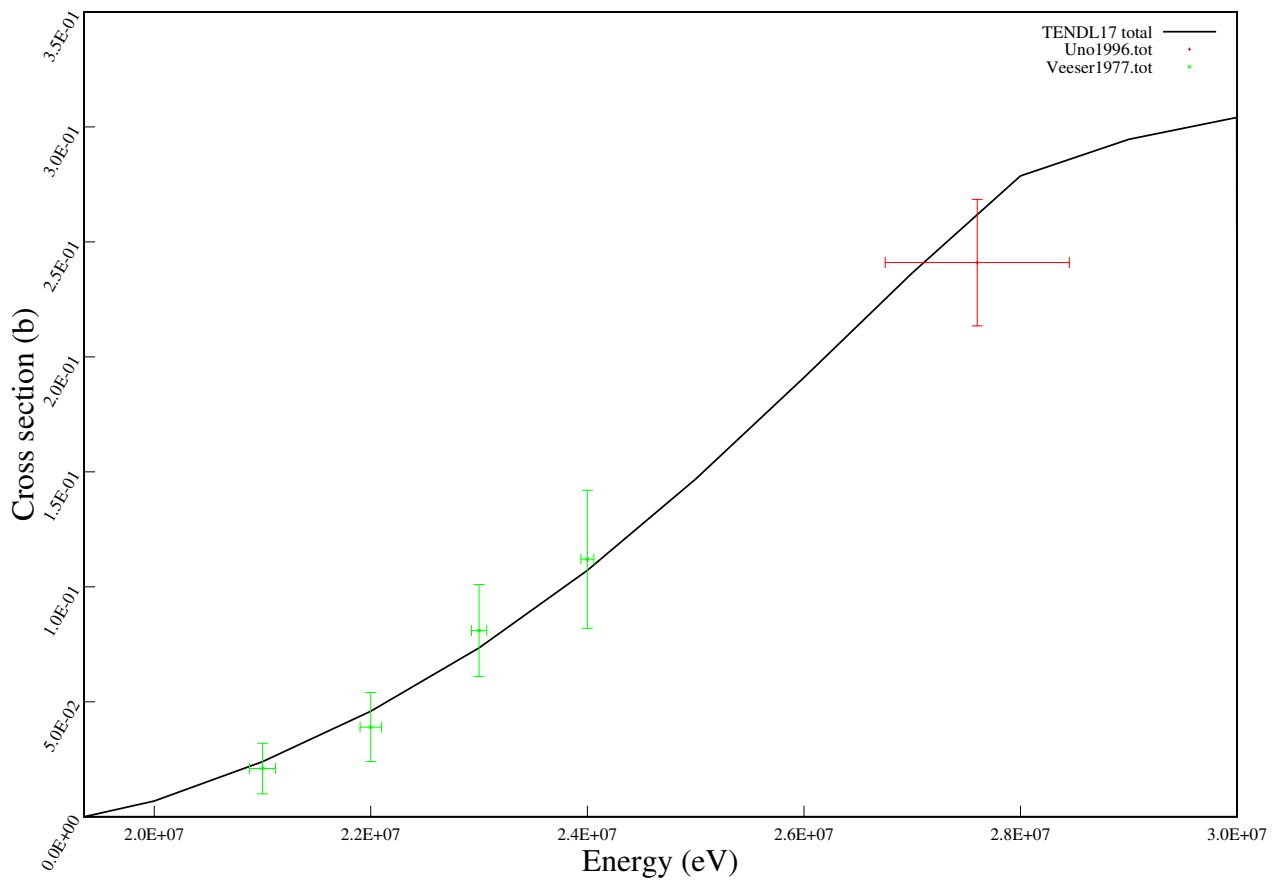
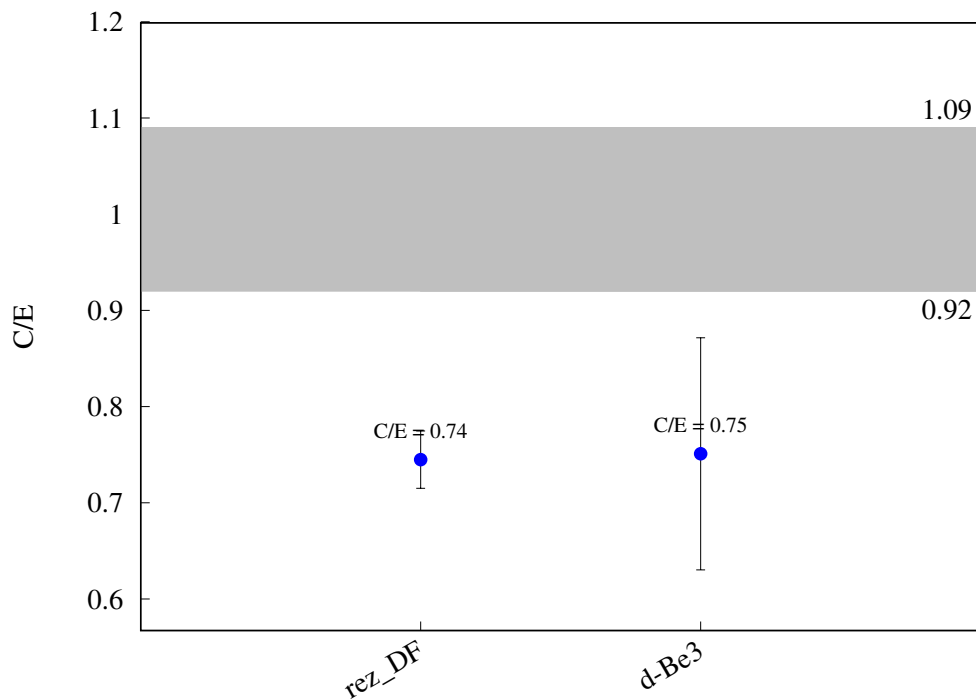
^{56}Fe (n,h) ^{54}Cr 

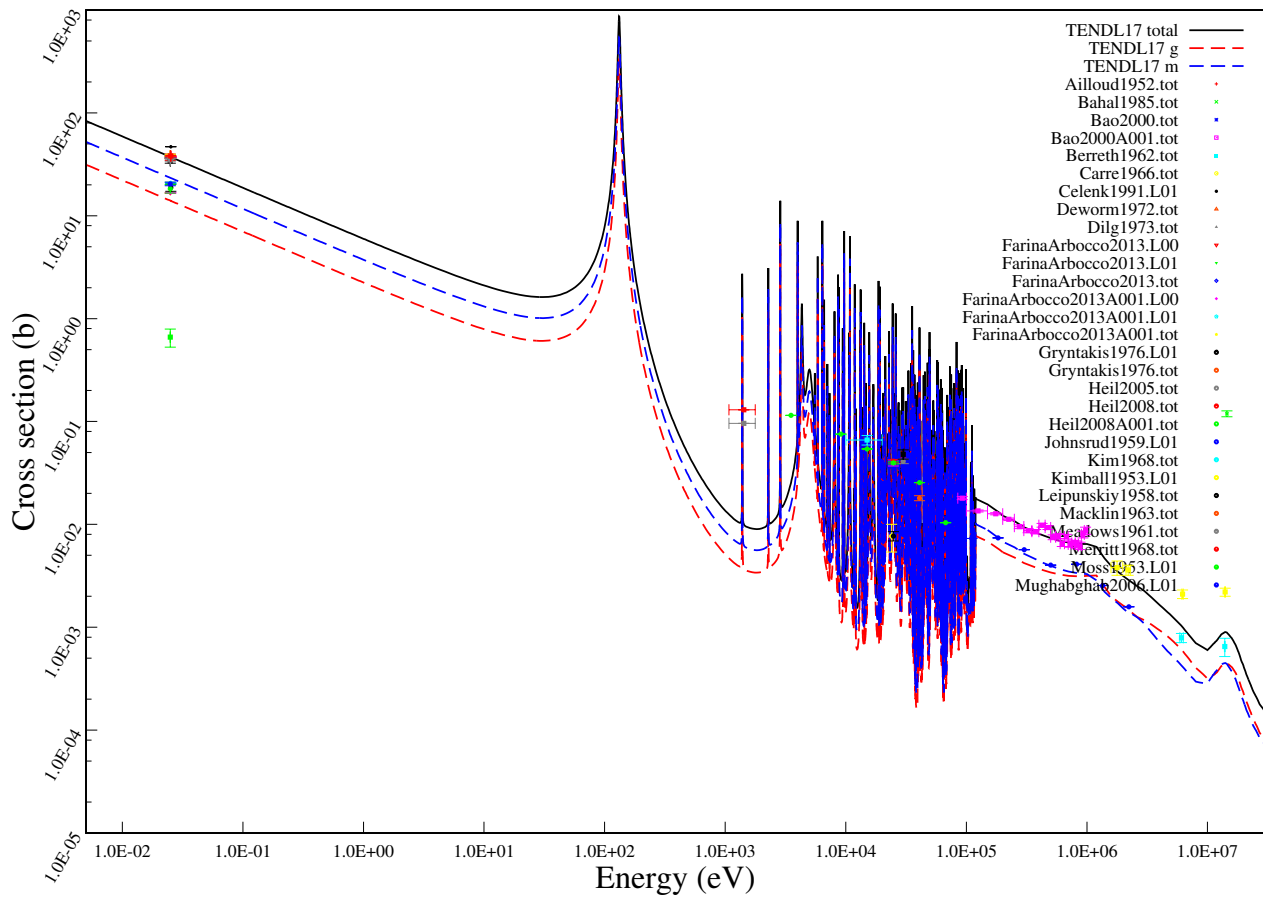
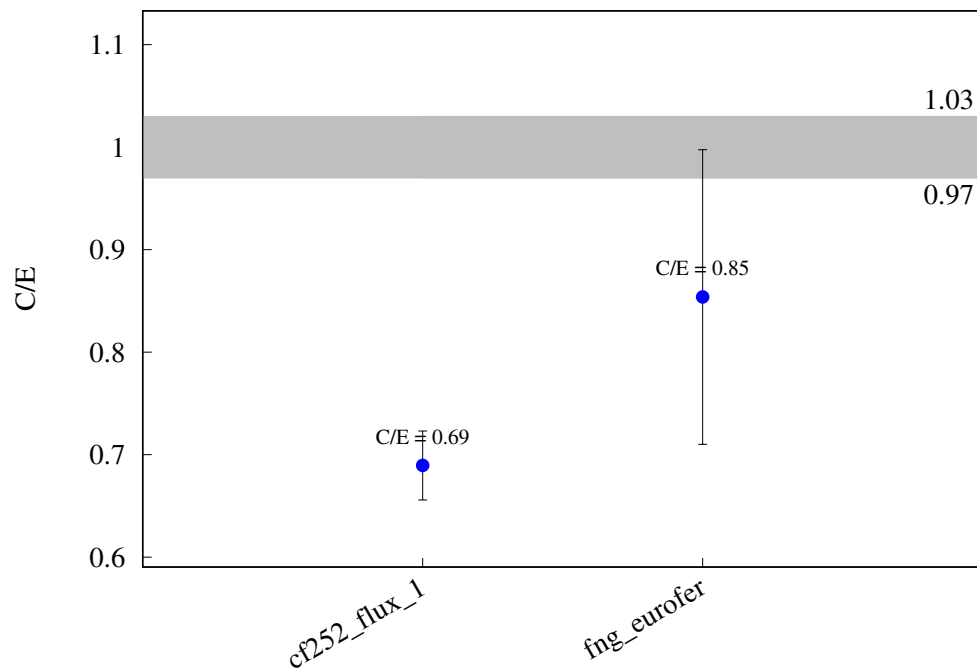
^{57}Fe (n,p) ^{57}Mn 

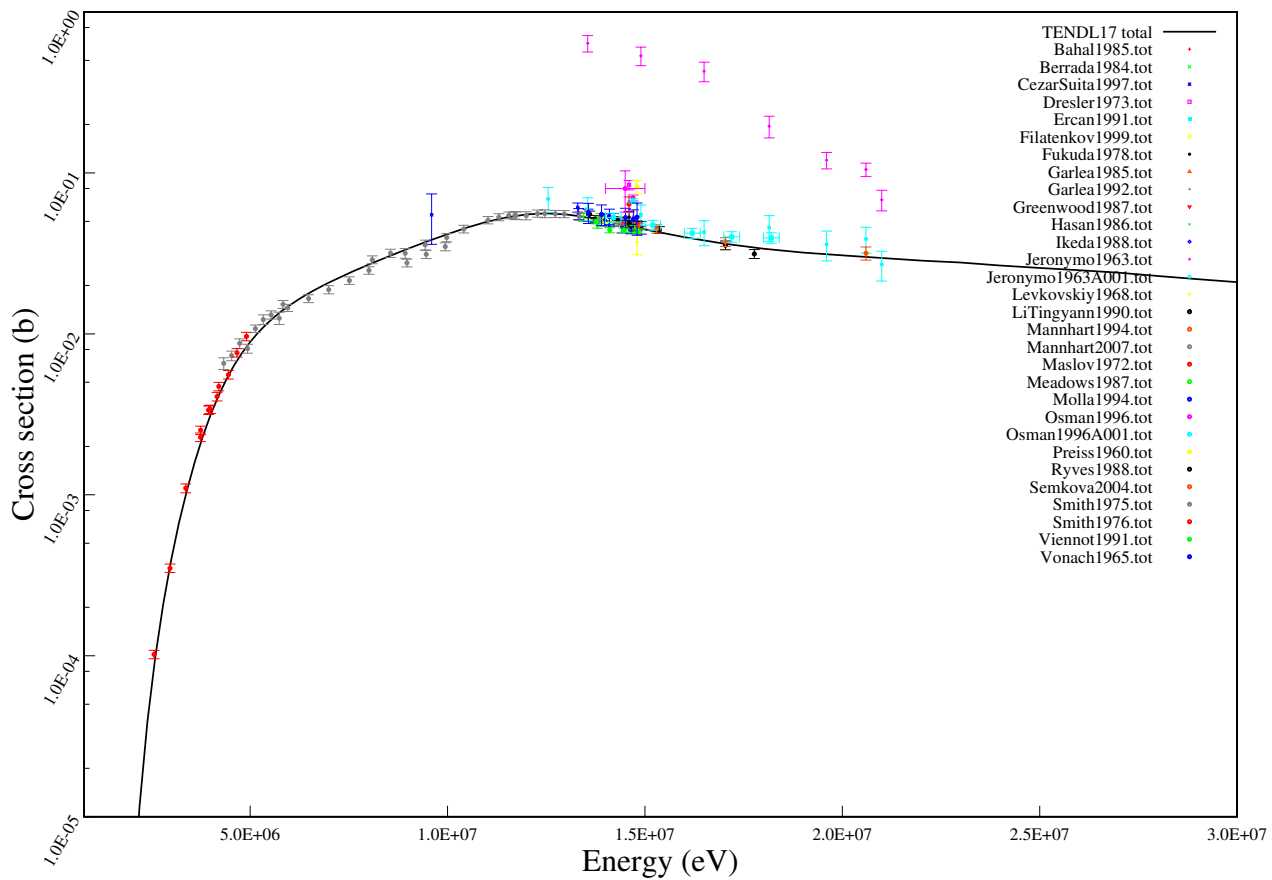
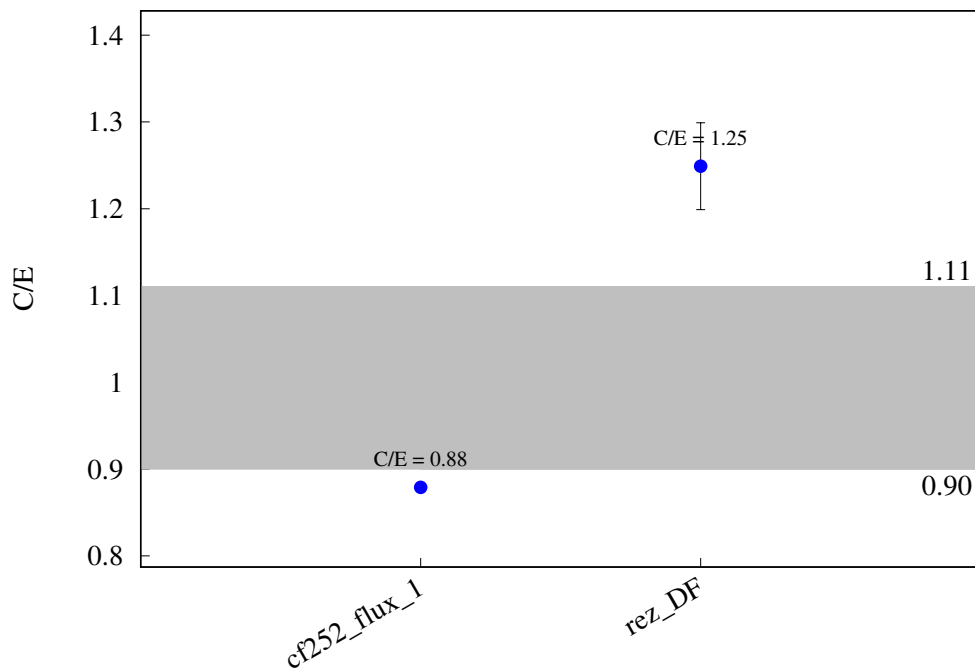
^{58}Fe (n,g) ^{59}Fe 

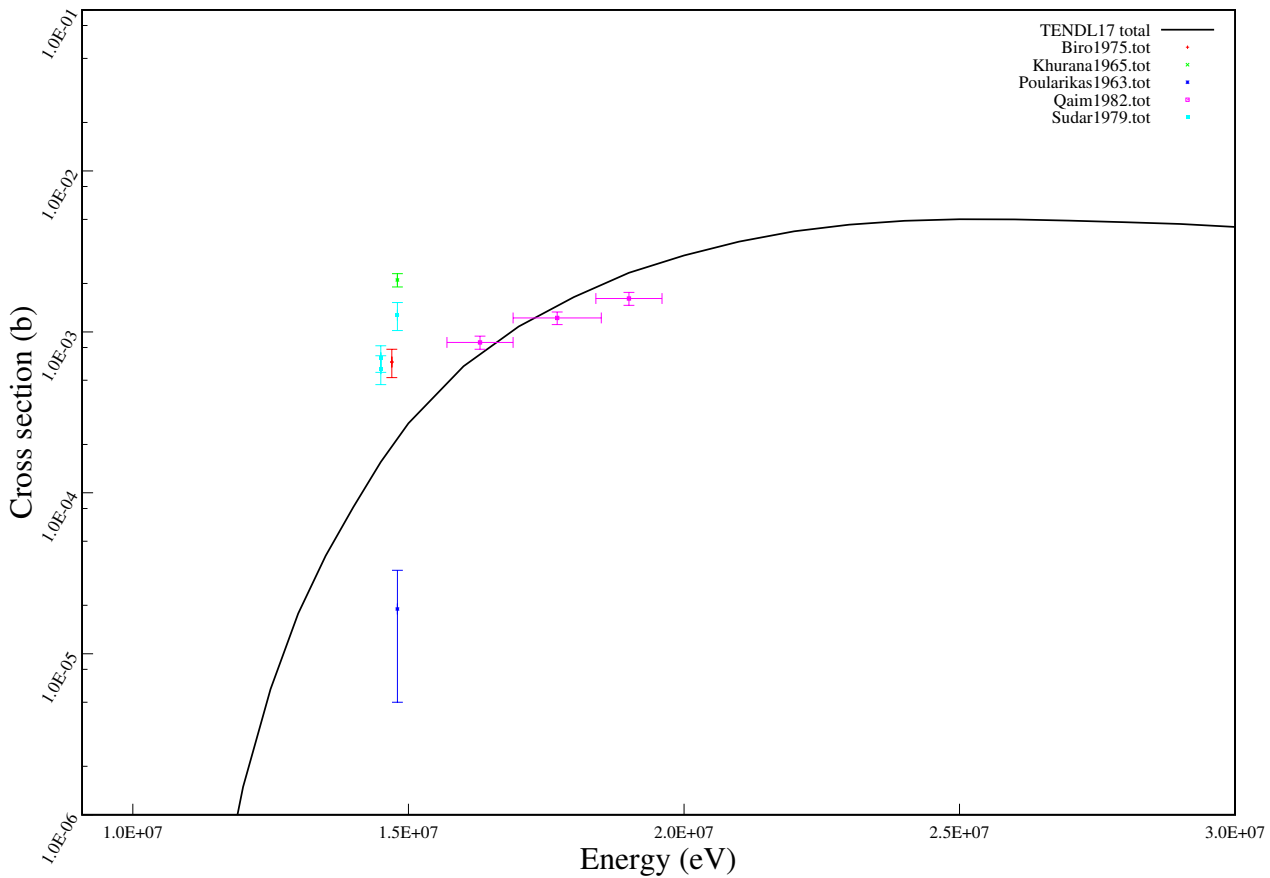
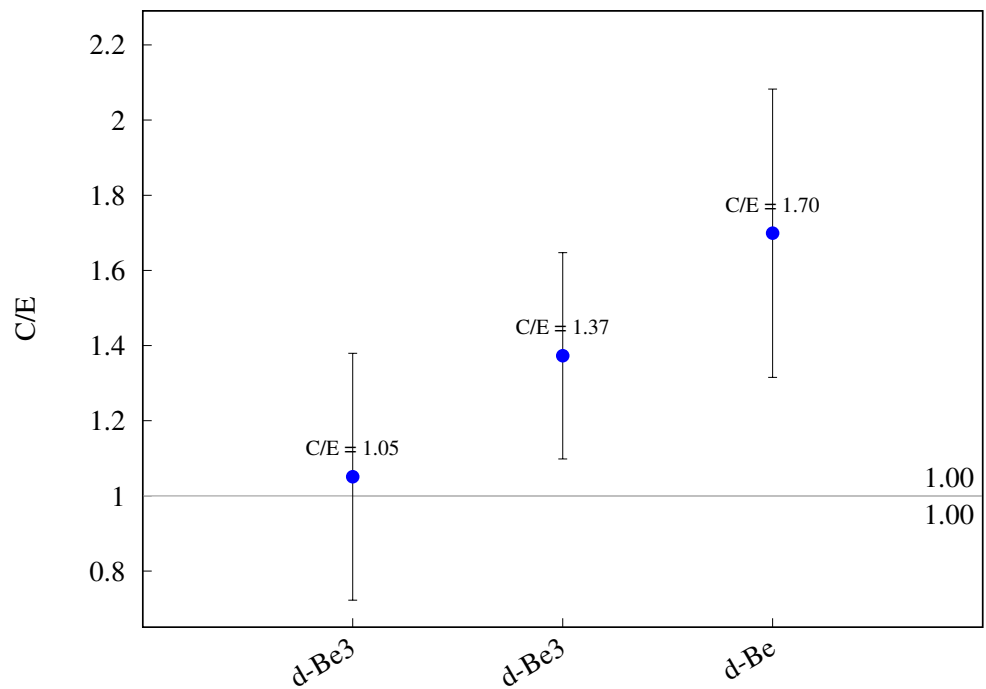
^{59}Co (n,2n) ^{58m}Co 

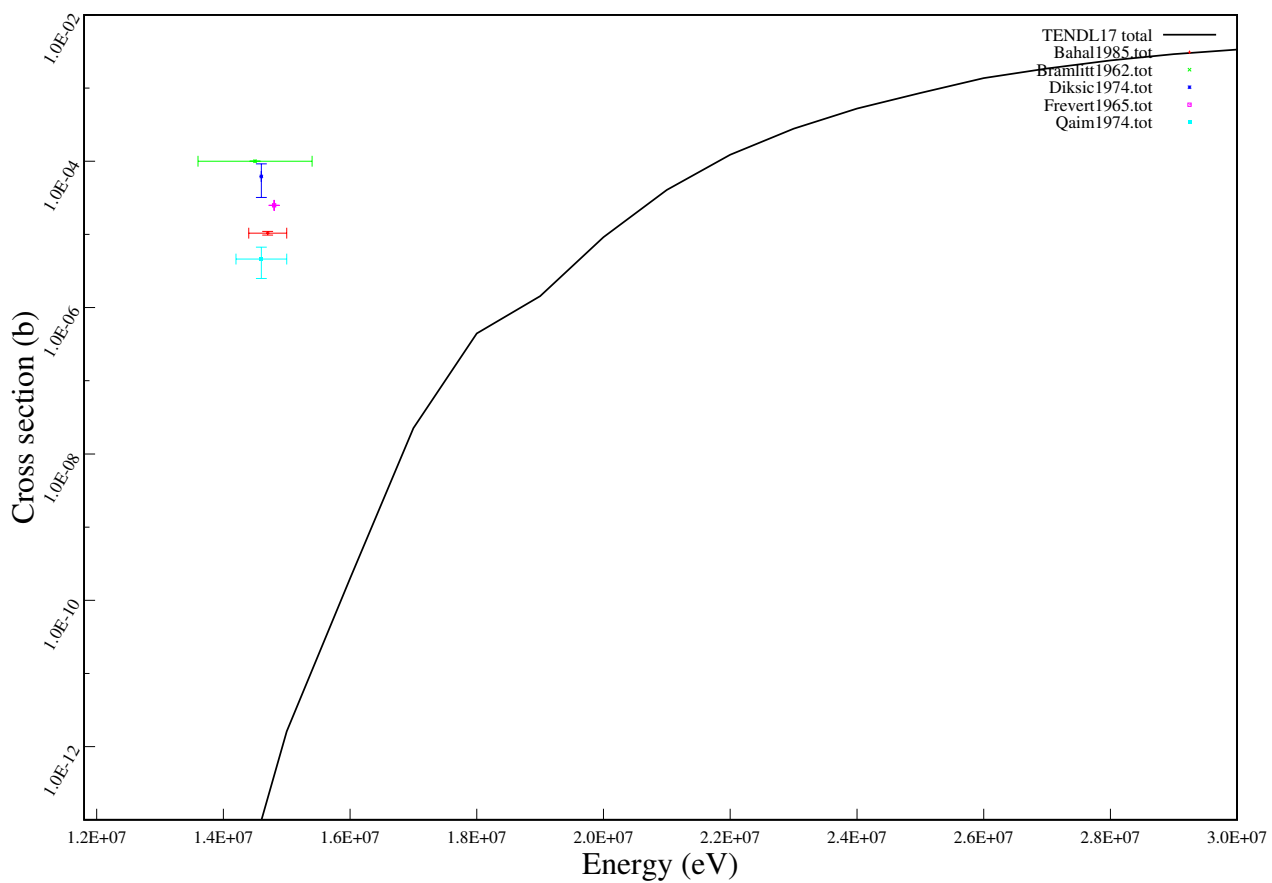
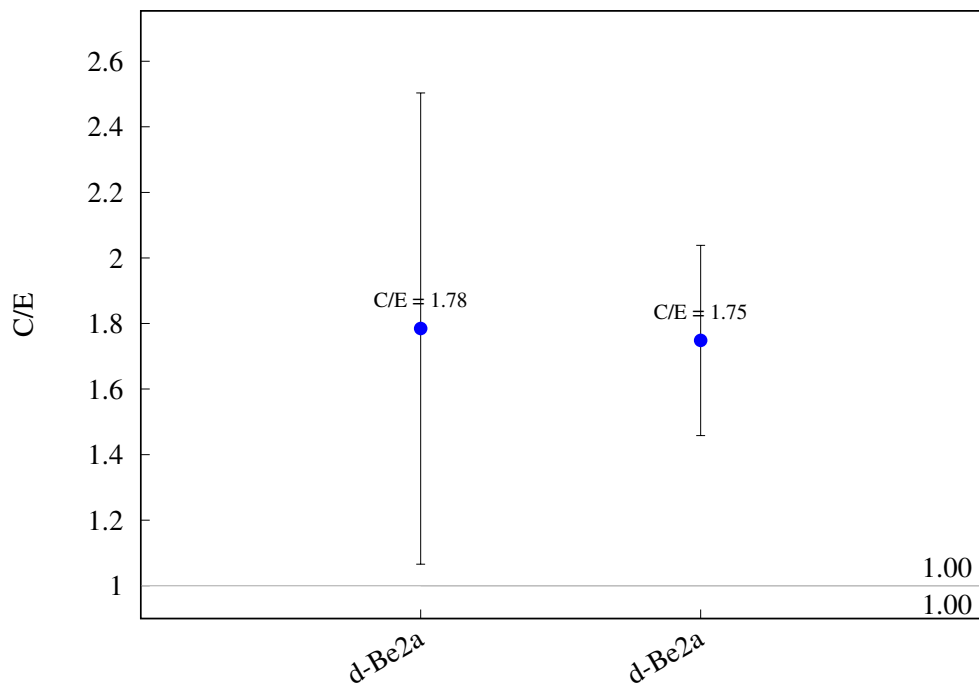
^{59}Co (n,2n) ^{58}Co 

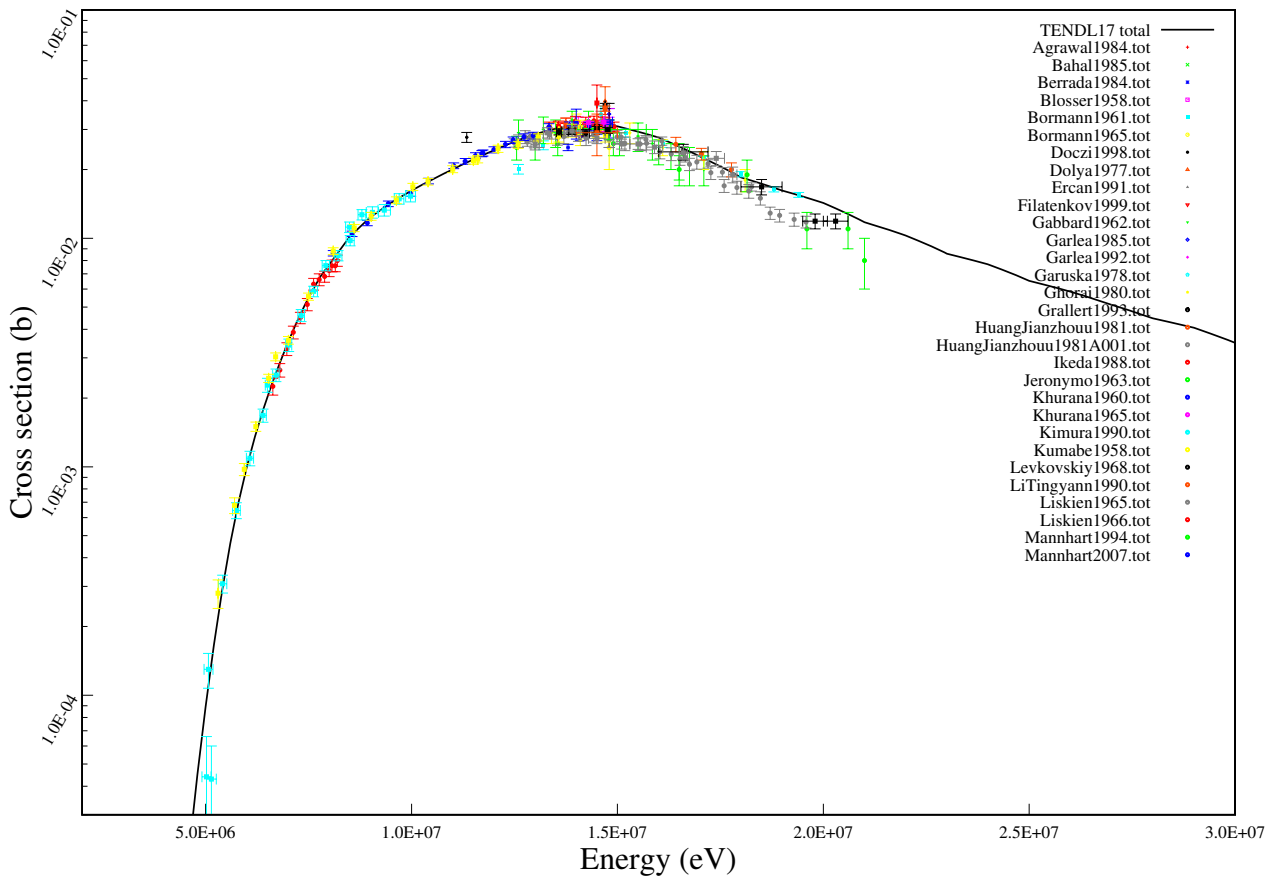
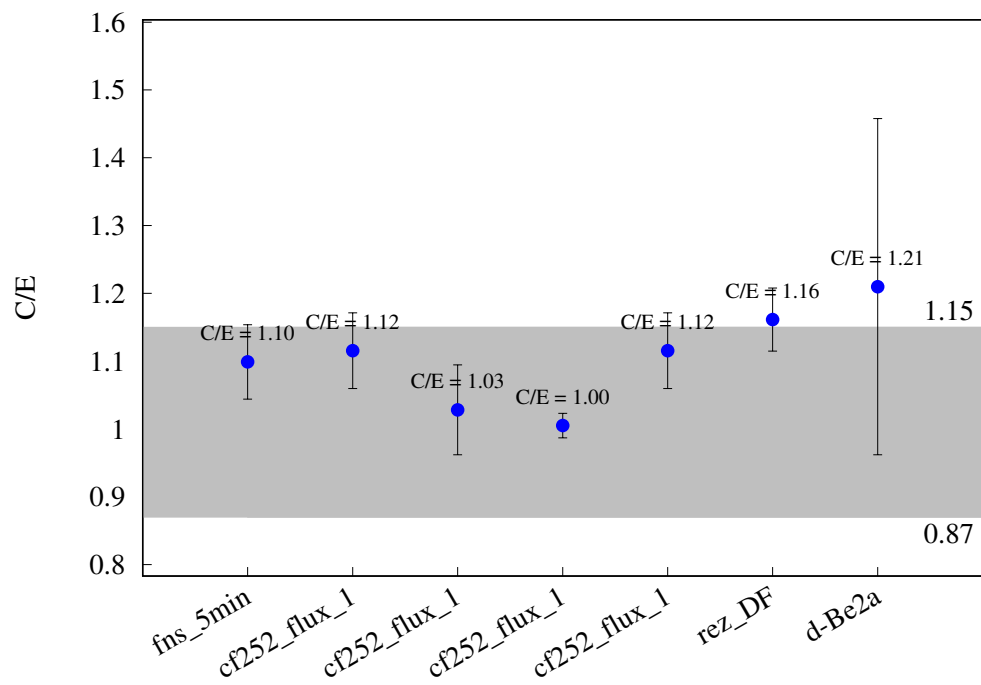
^{59}Co (n,3n) ^{57}Co 

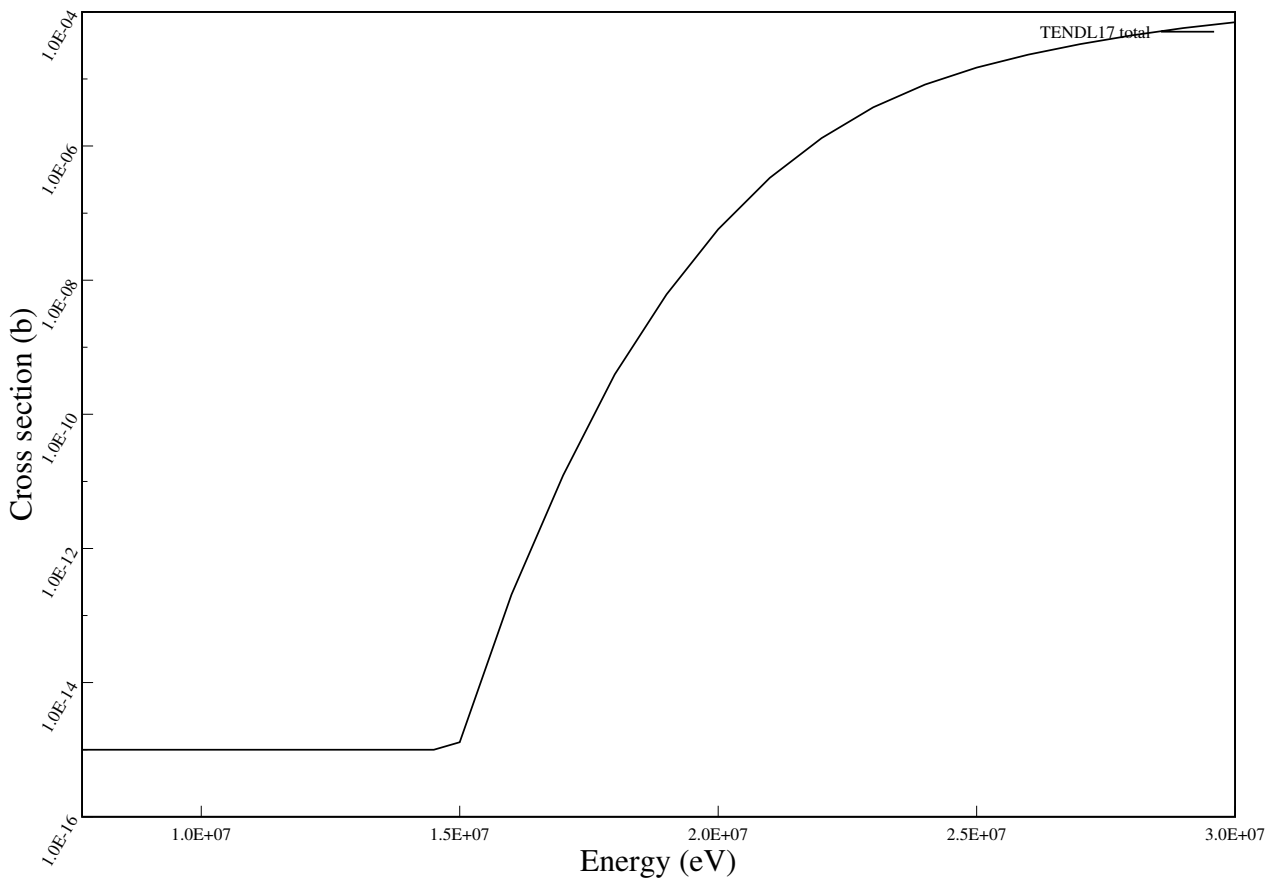
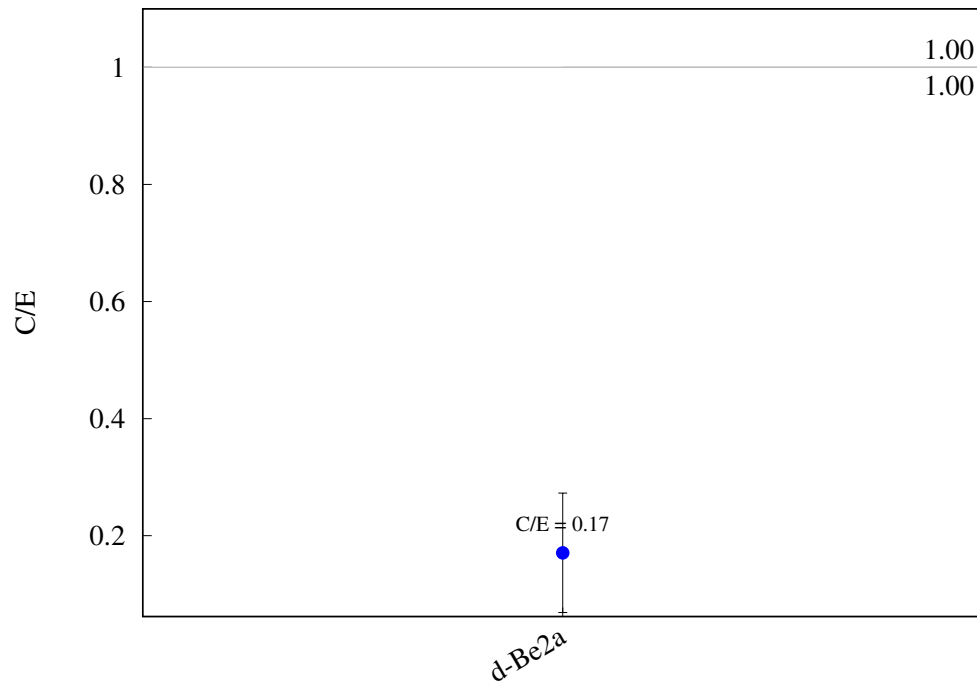
^{59}Co (n,g) ^{60}Co 

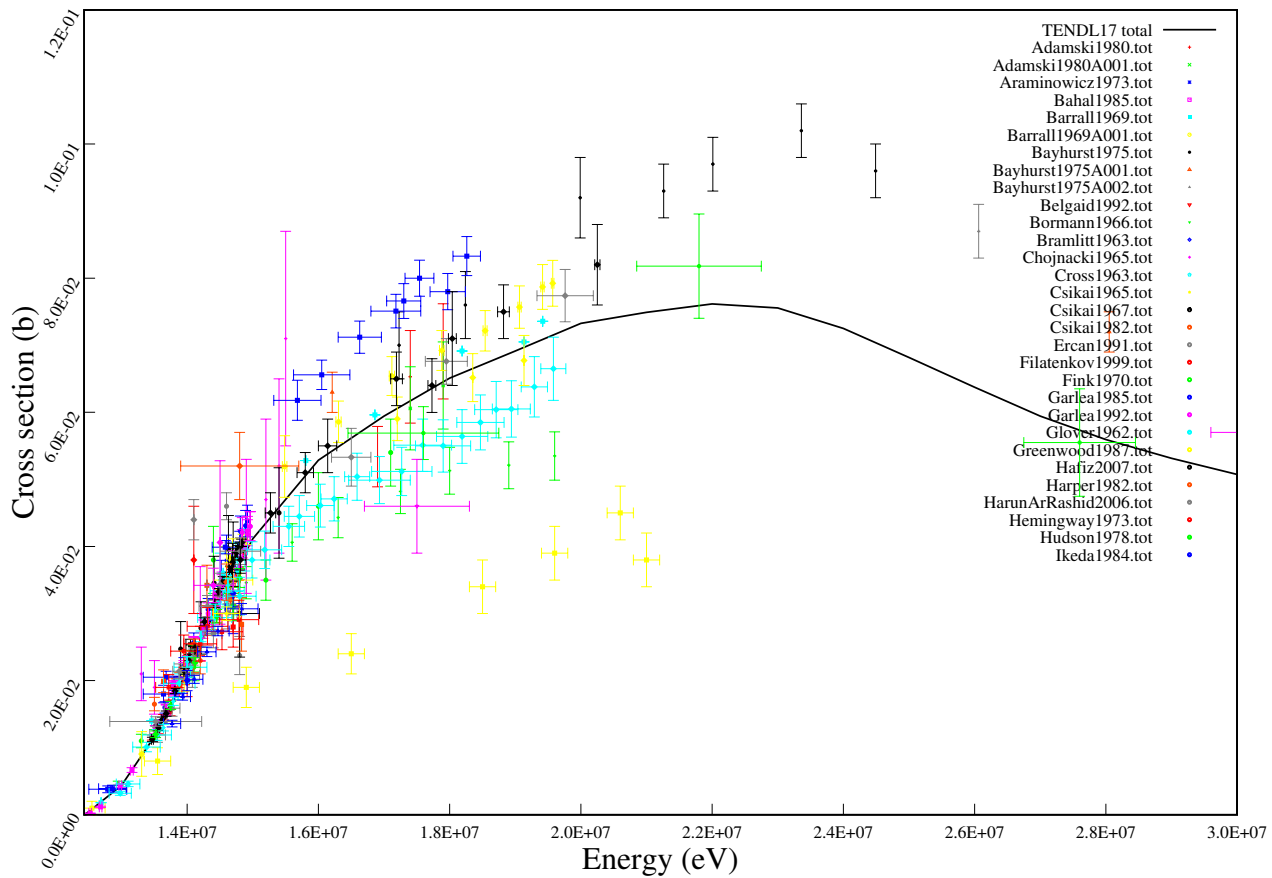
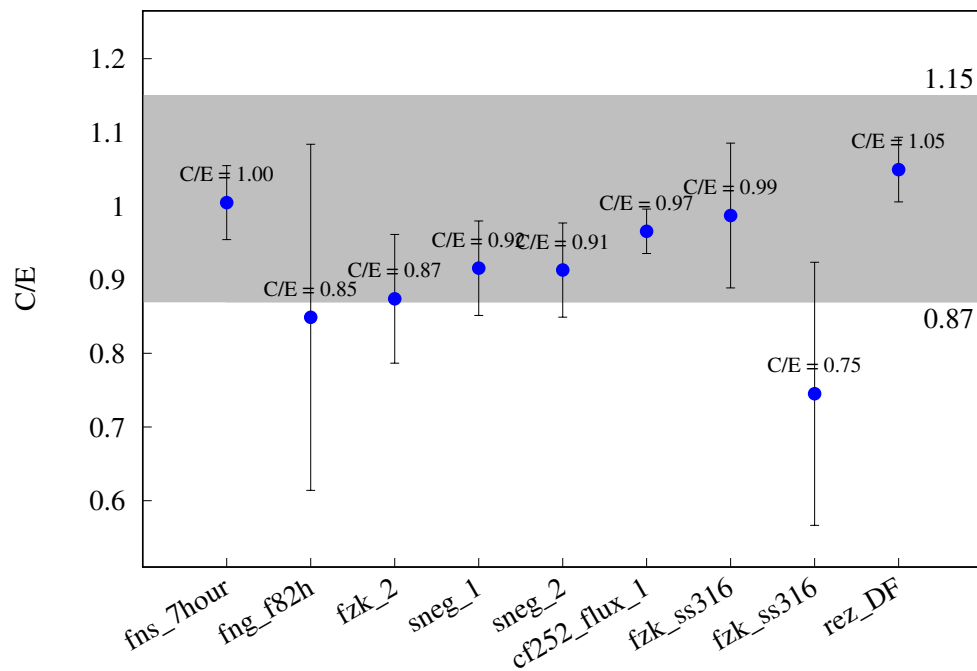
^{59}Co (n,p) ^{59}Fe 

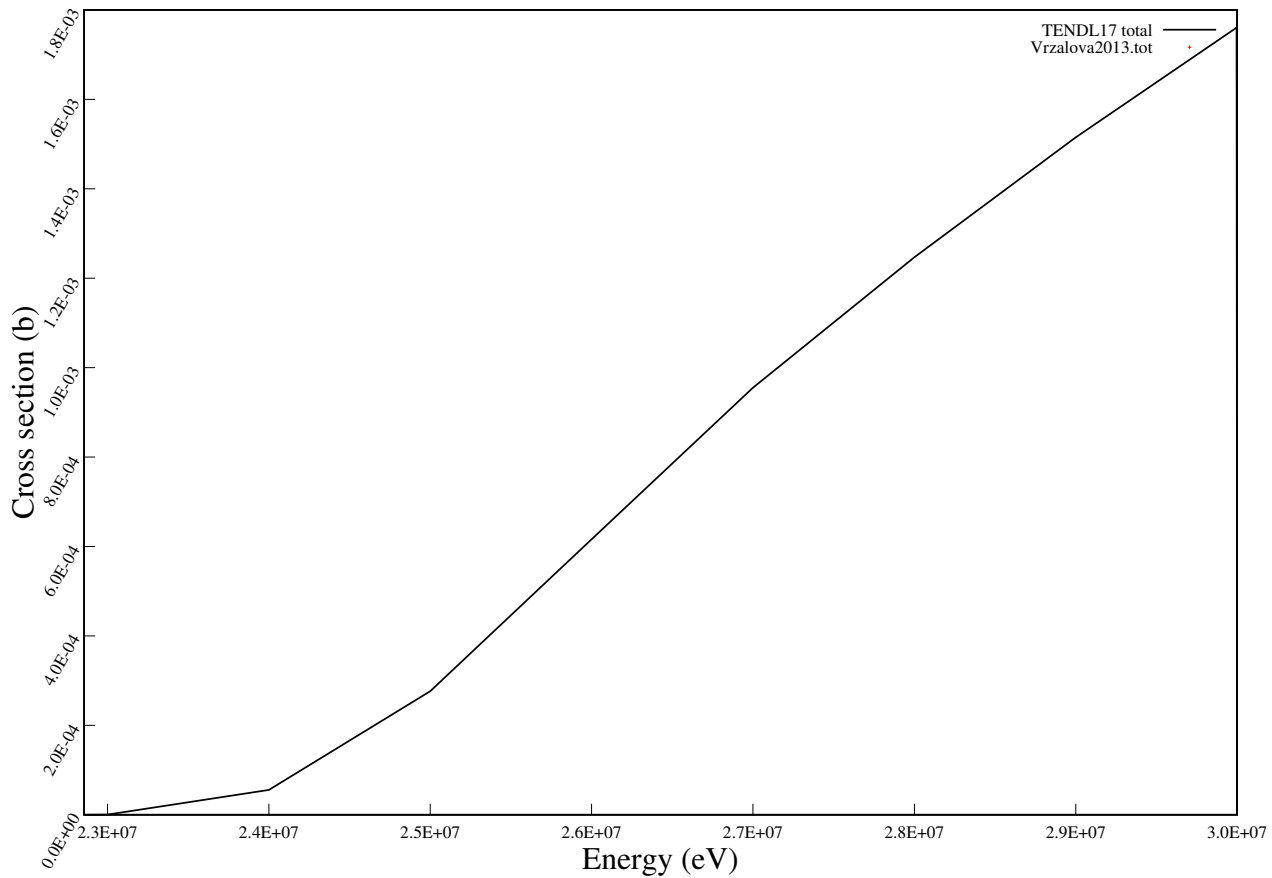
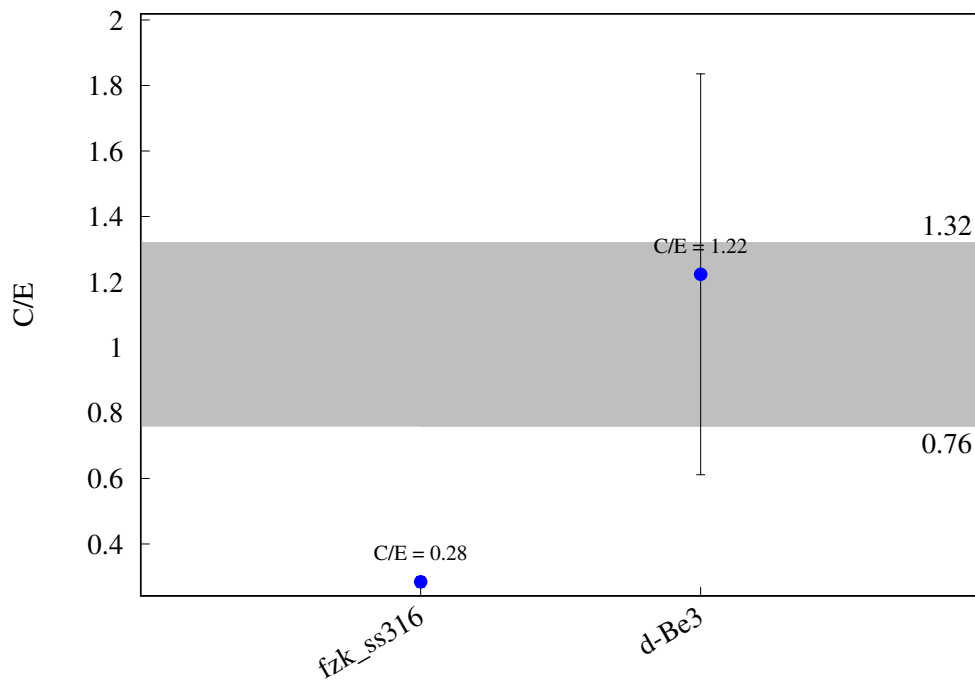
^{59}Co (n,t) ^{57}Fe 

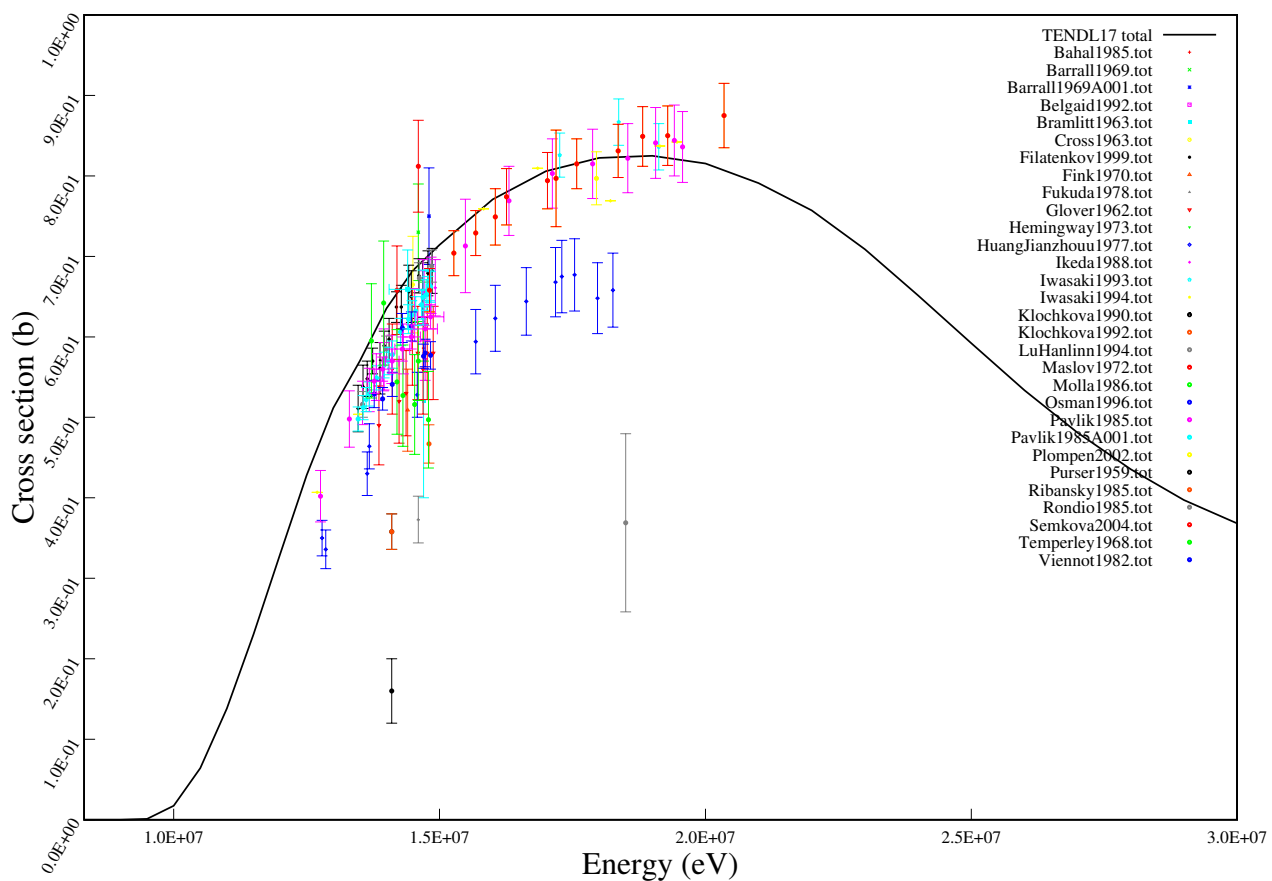
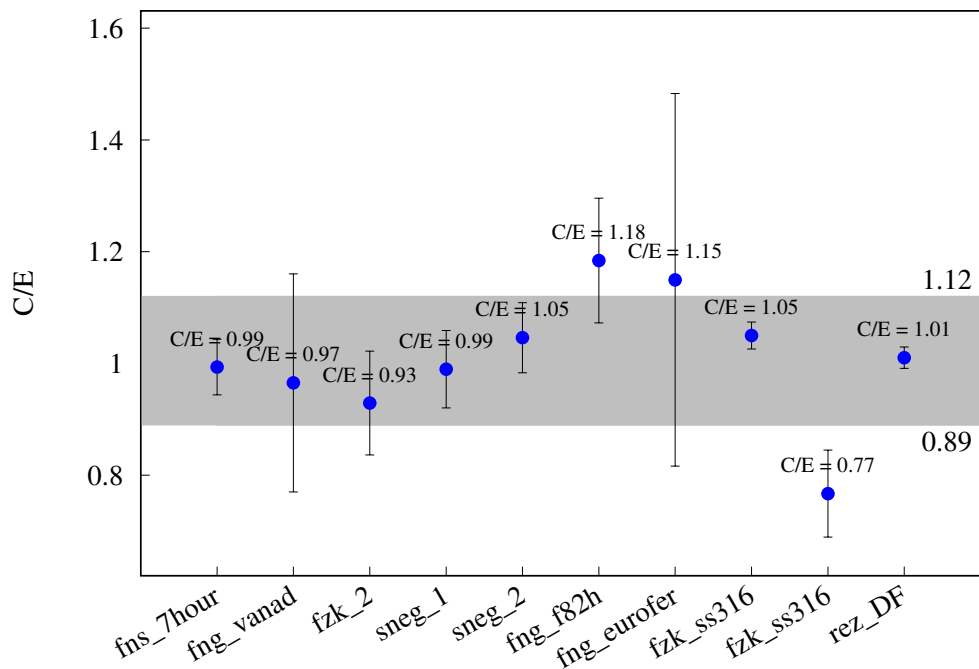
^{59}Co (n,h) ^{57}Mn 

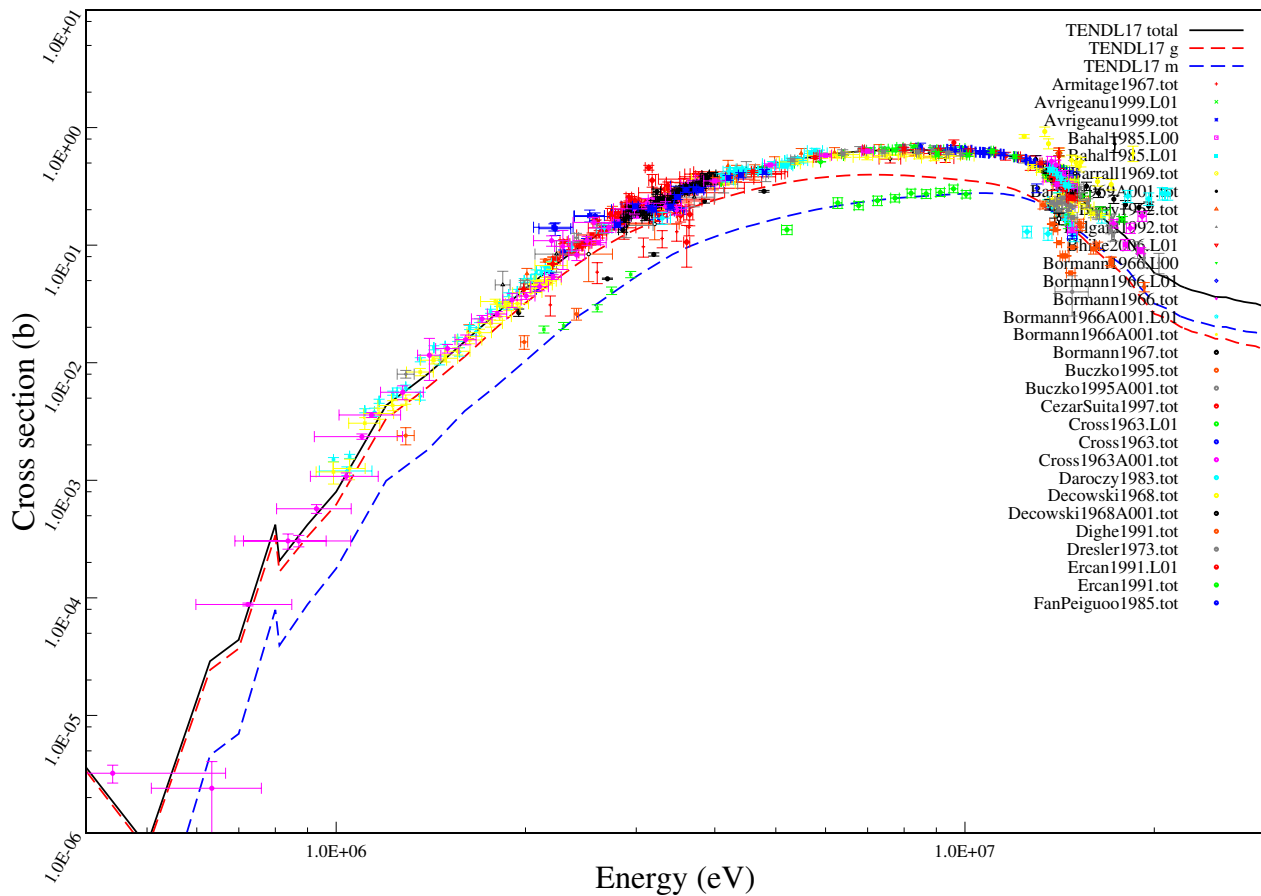
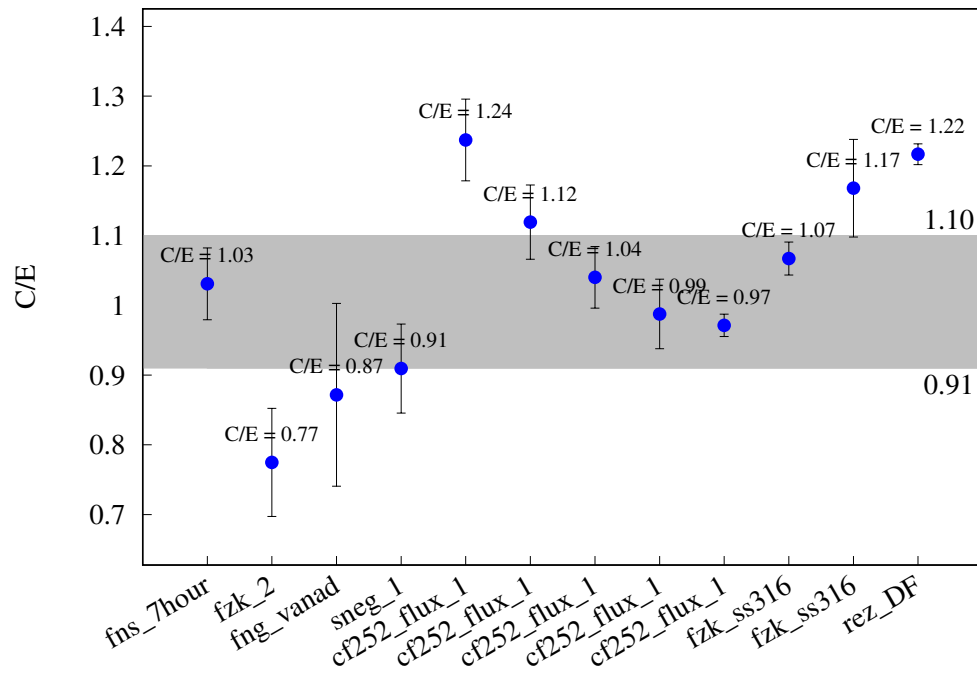
^{59}Co (n,a) ^{56}Mn 

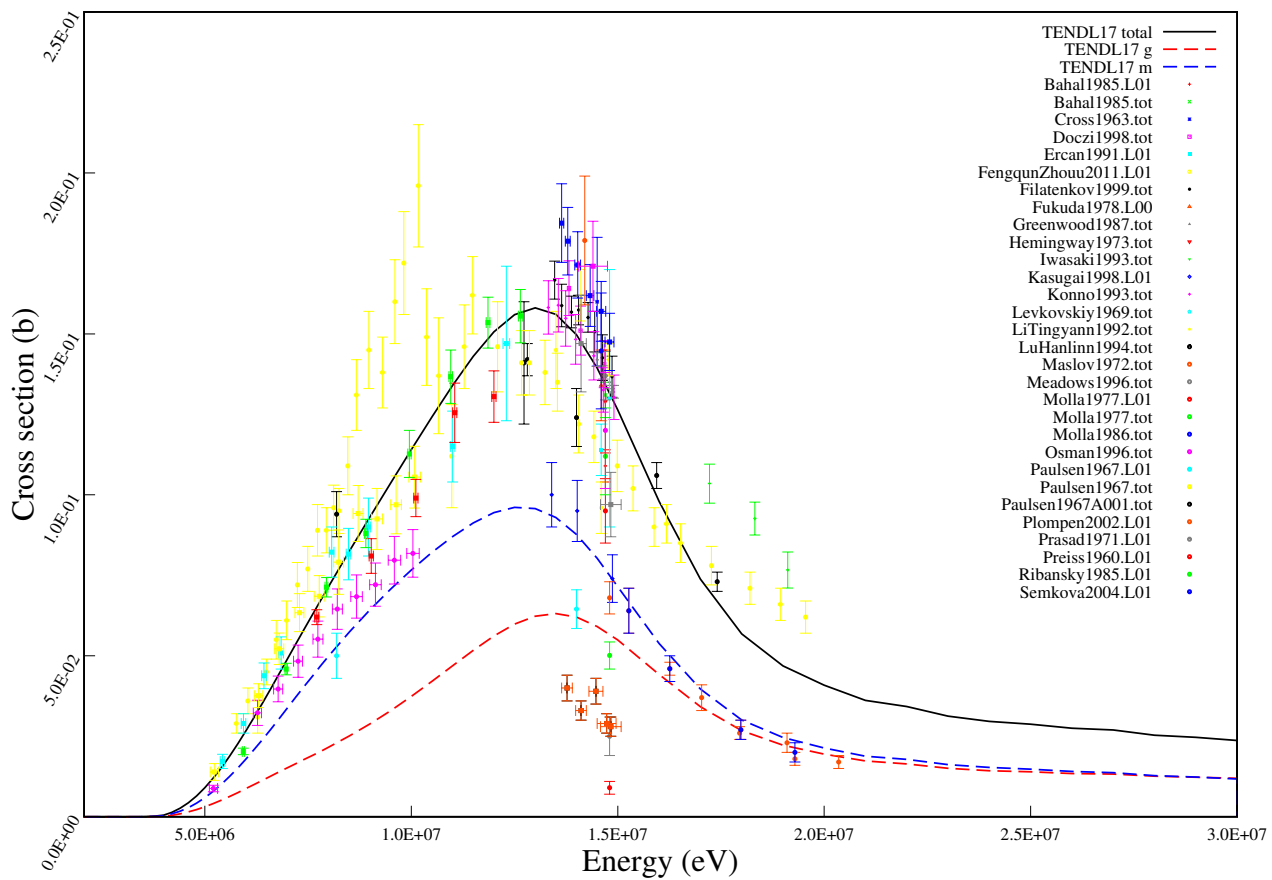
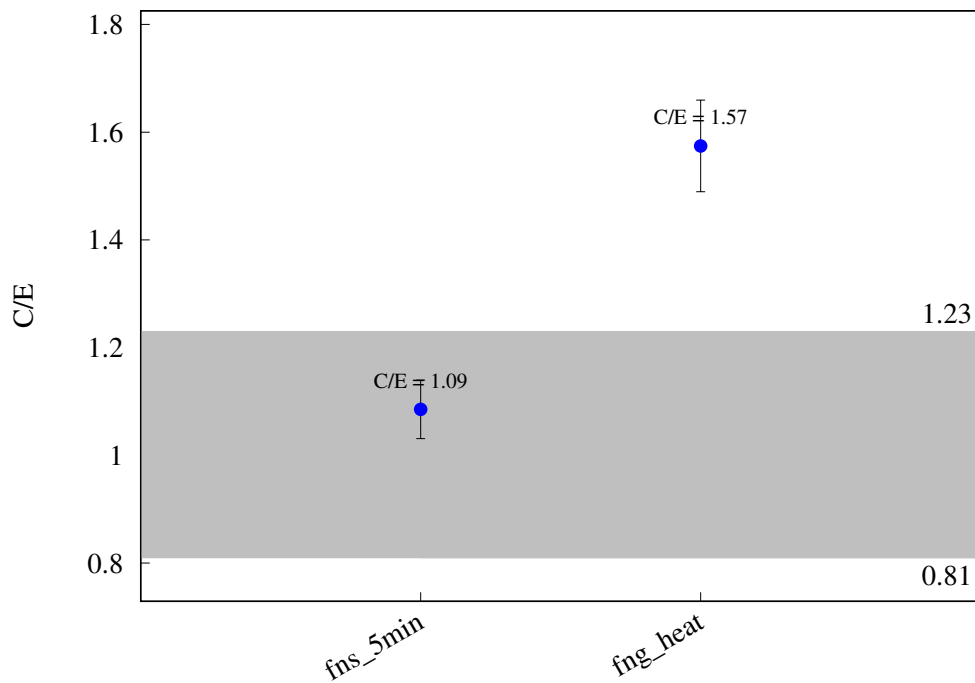
^{59}Co (n,2a) ^{52}V 

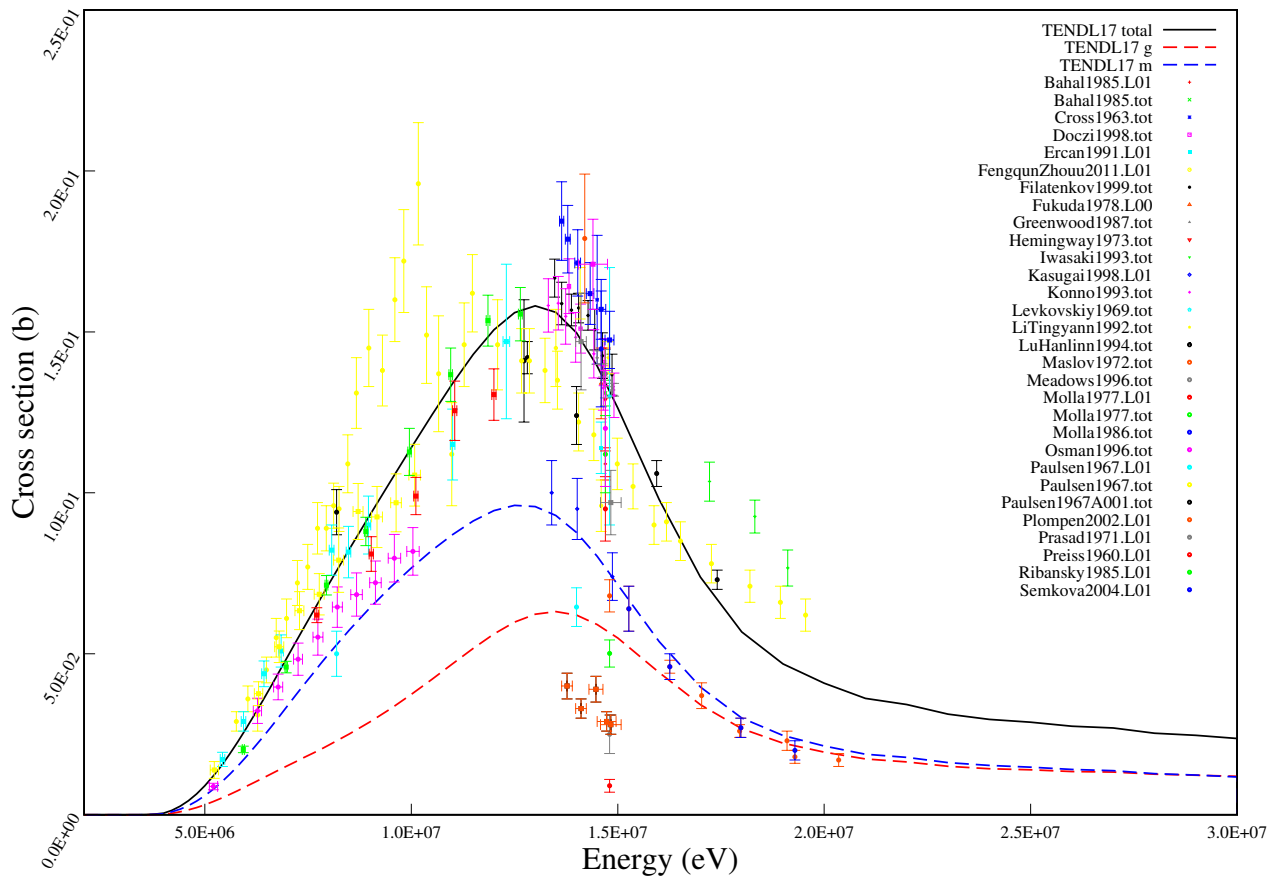
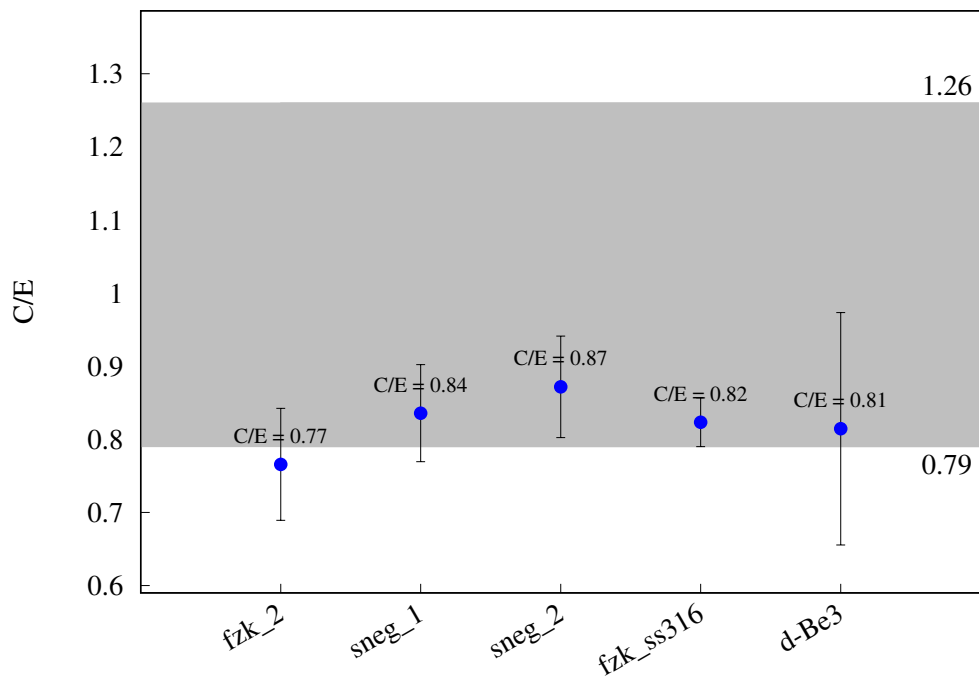
^{58}Ni (n,2n) ^{57}Ni 

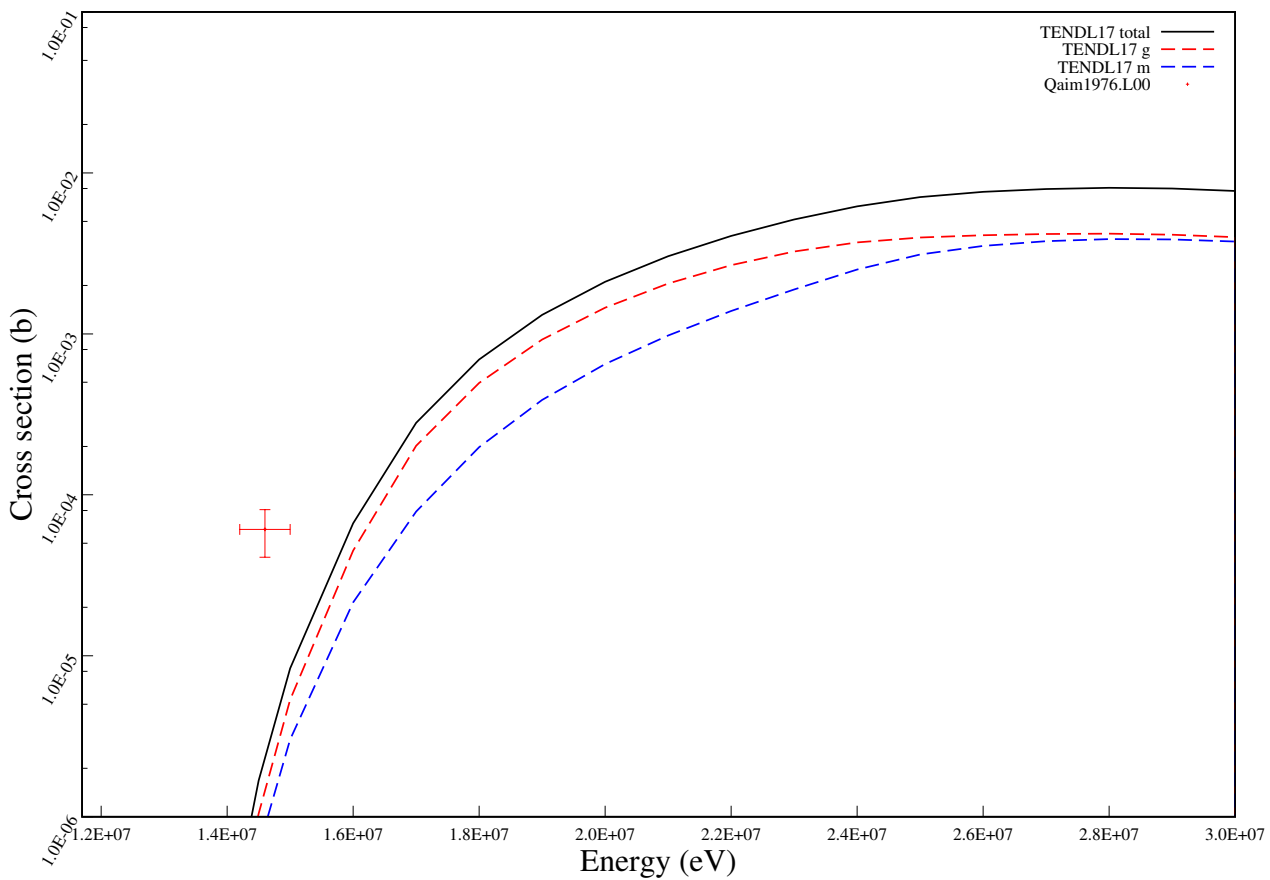
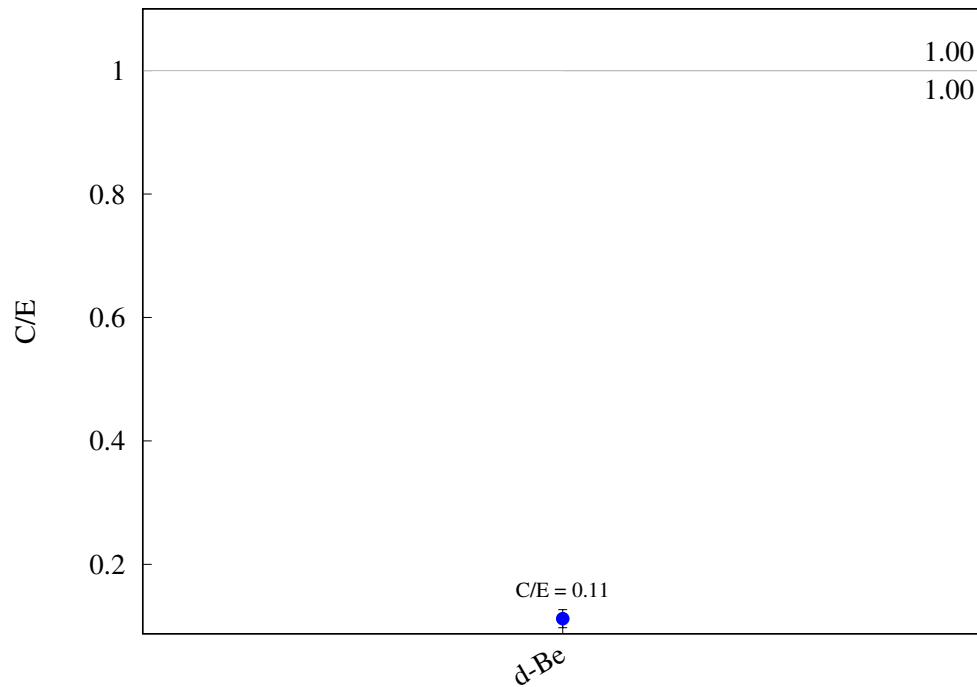
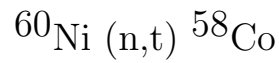
^{58}Ni (n,3n) ^{56}Ni 

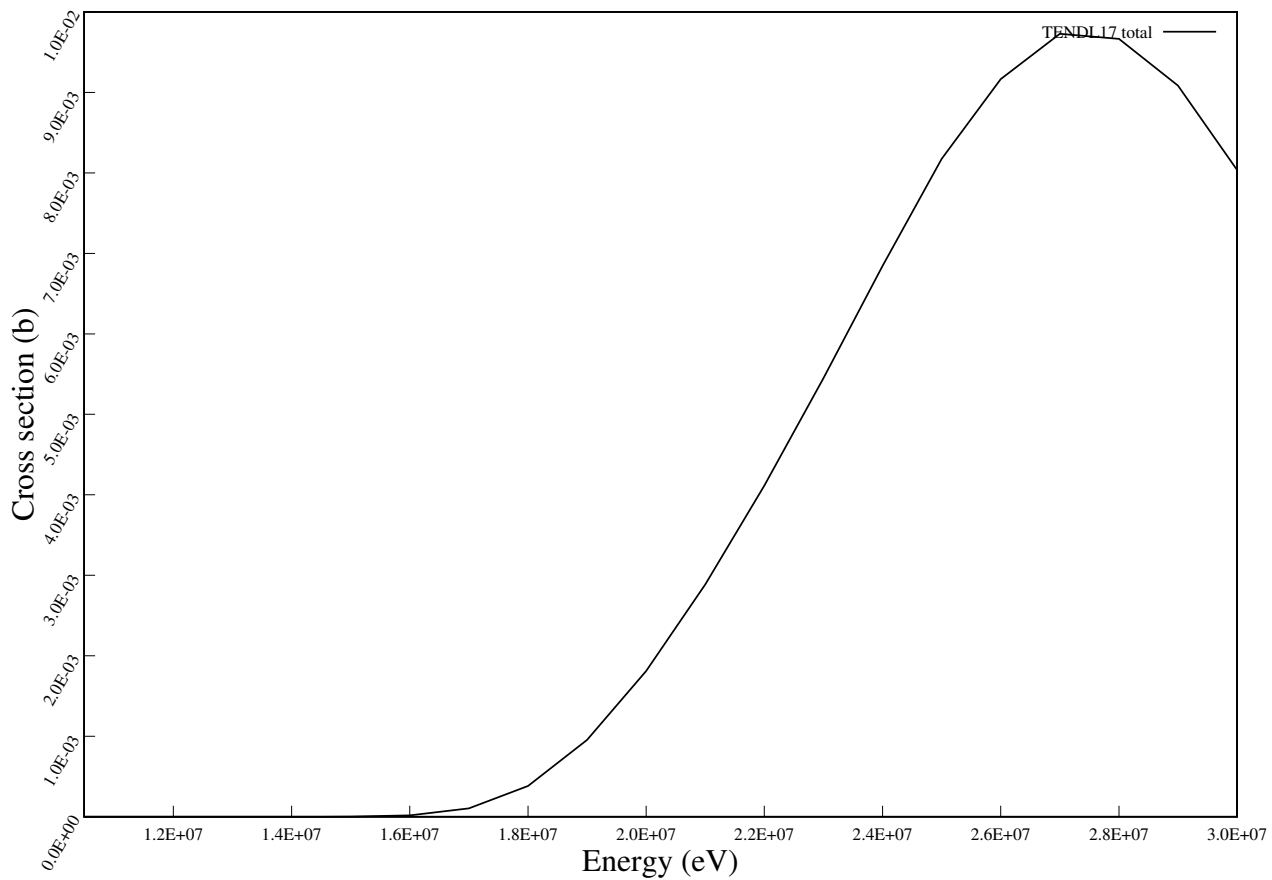
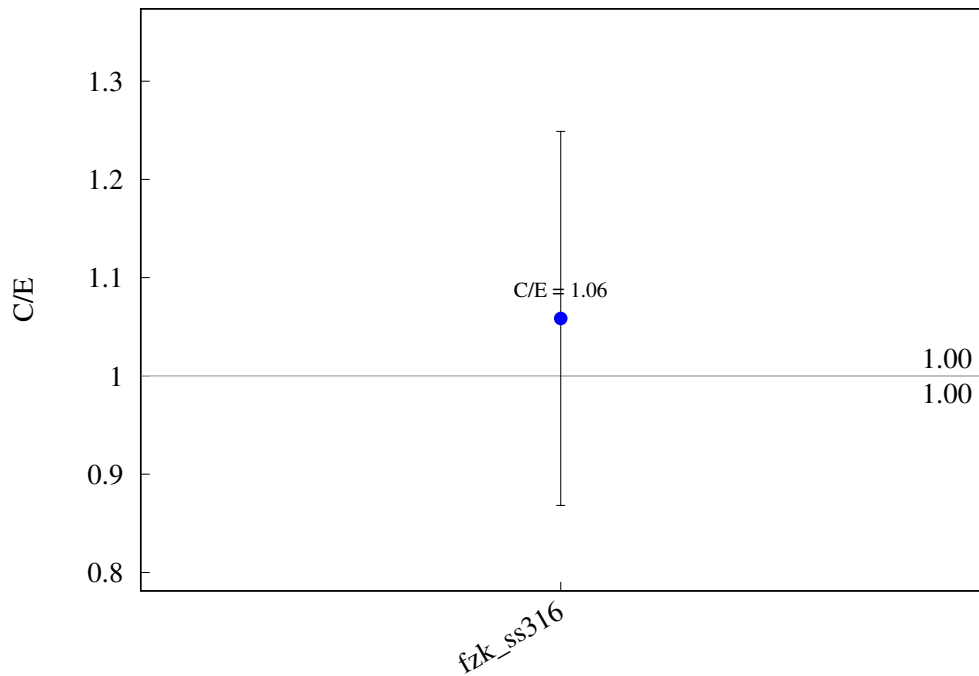
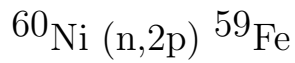
^{58}Ni (n,np) ^{57}Co 

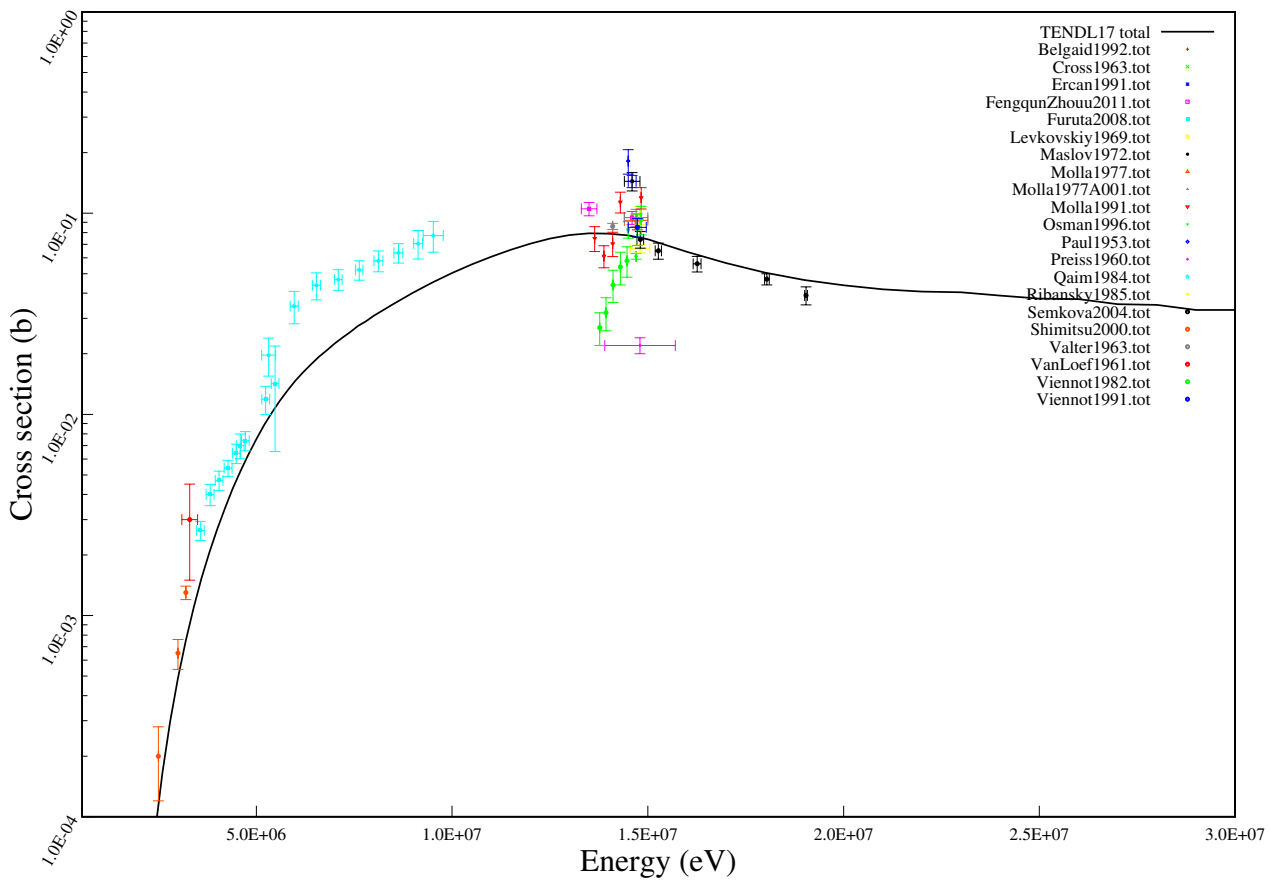
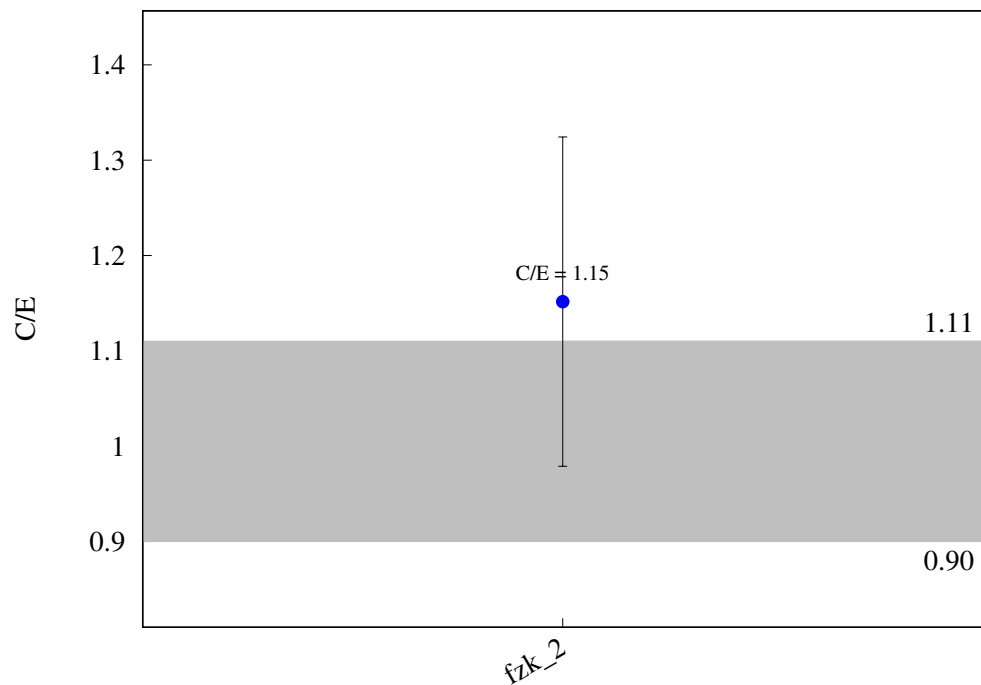
^{58}Ni (n,p) ^{58}Co 

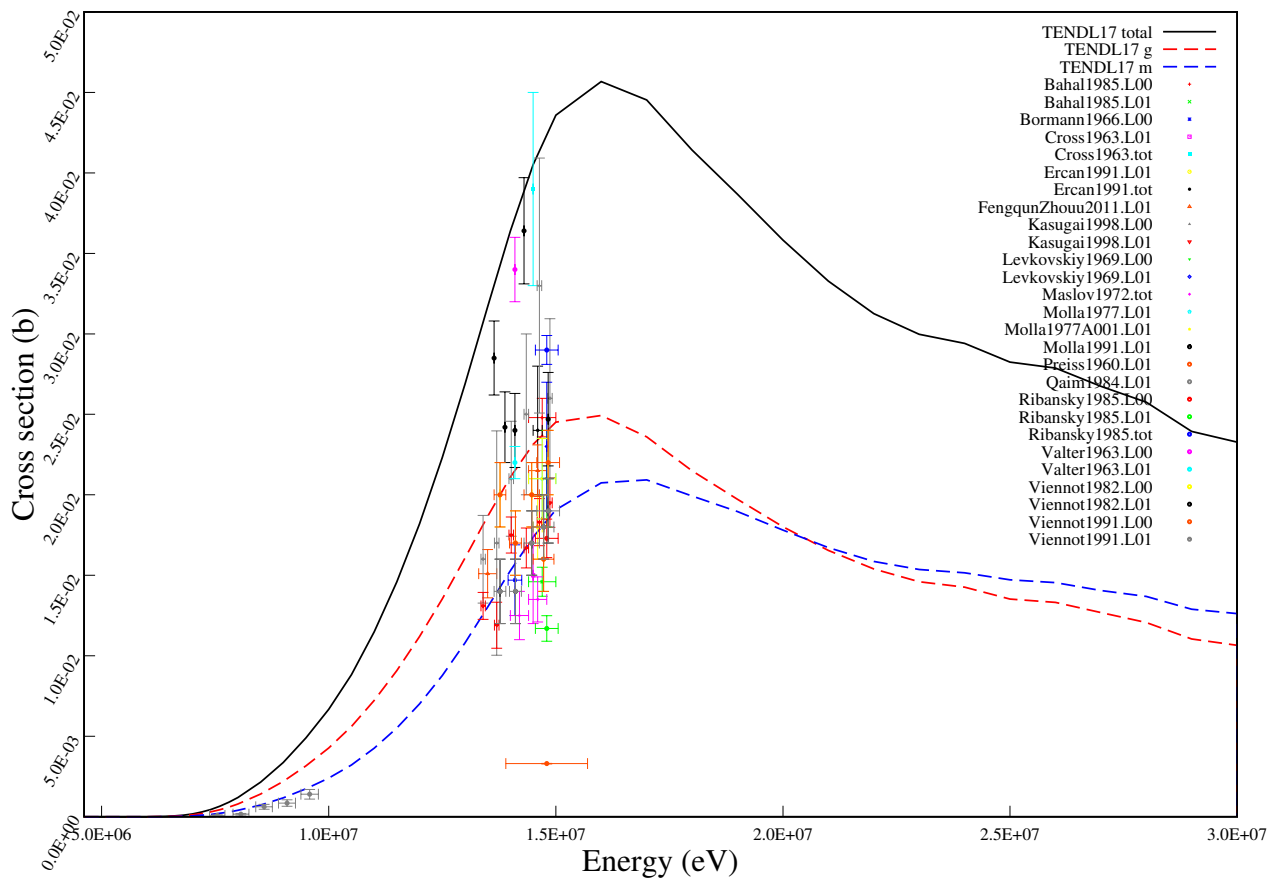
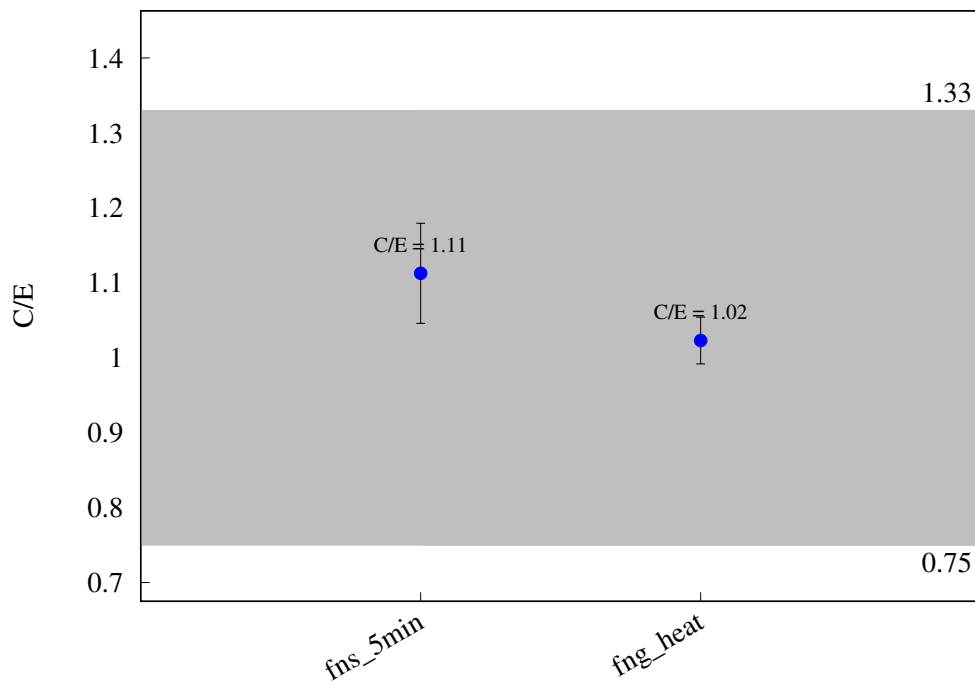
^{60}Ni (n,p) ^{60}mCo 

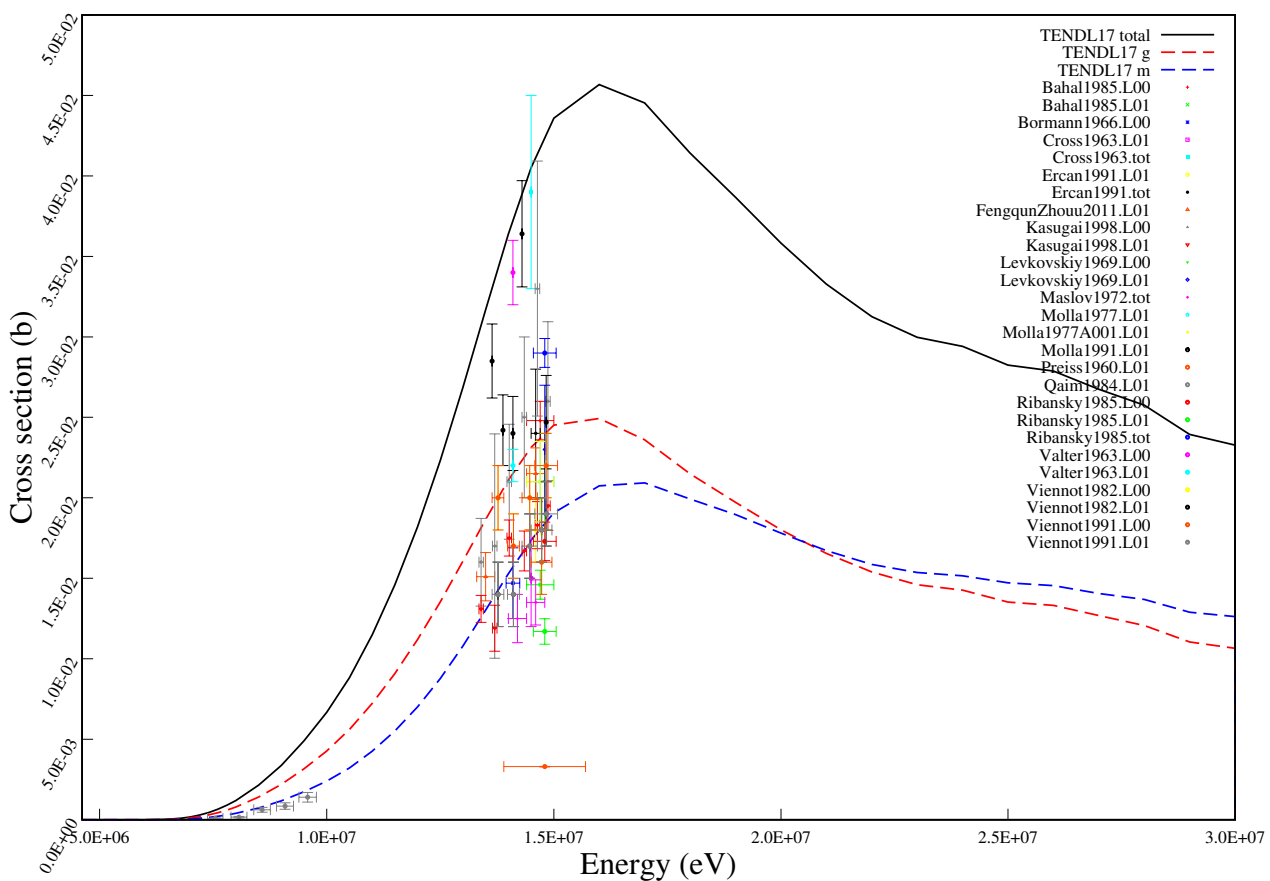
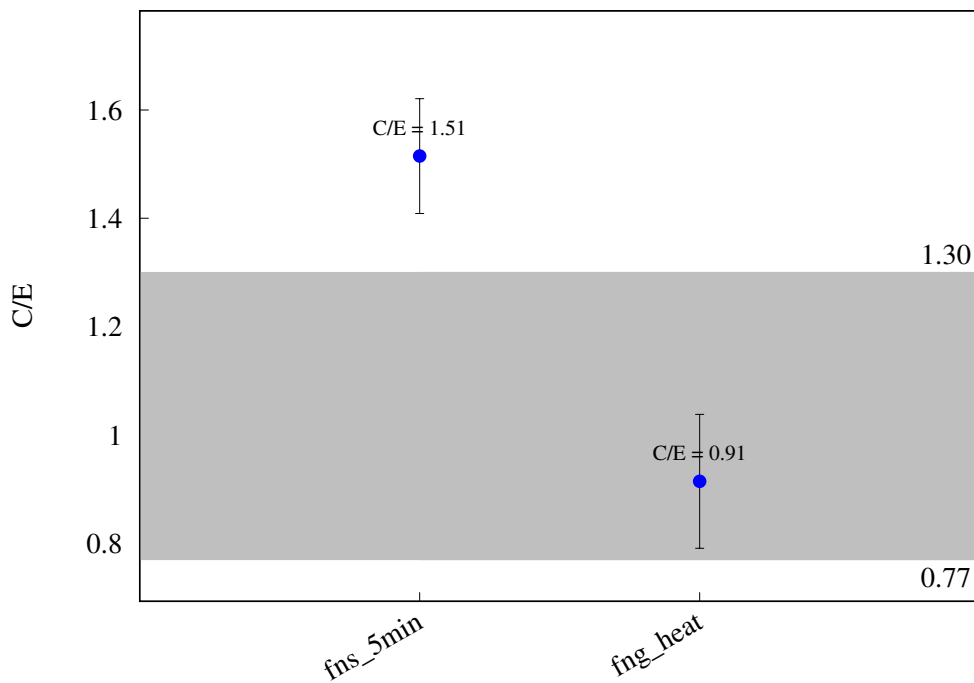
$^{60}\text{Ni} (\text{n},\text{p}) ^{60}\text{Co}$ 

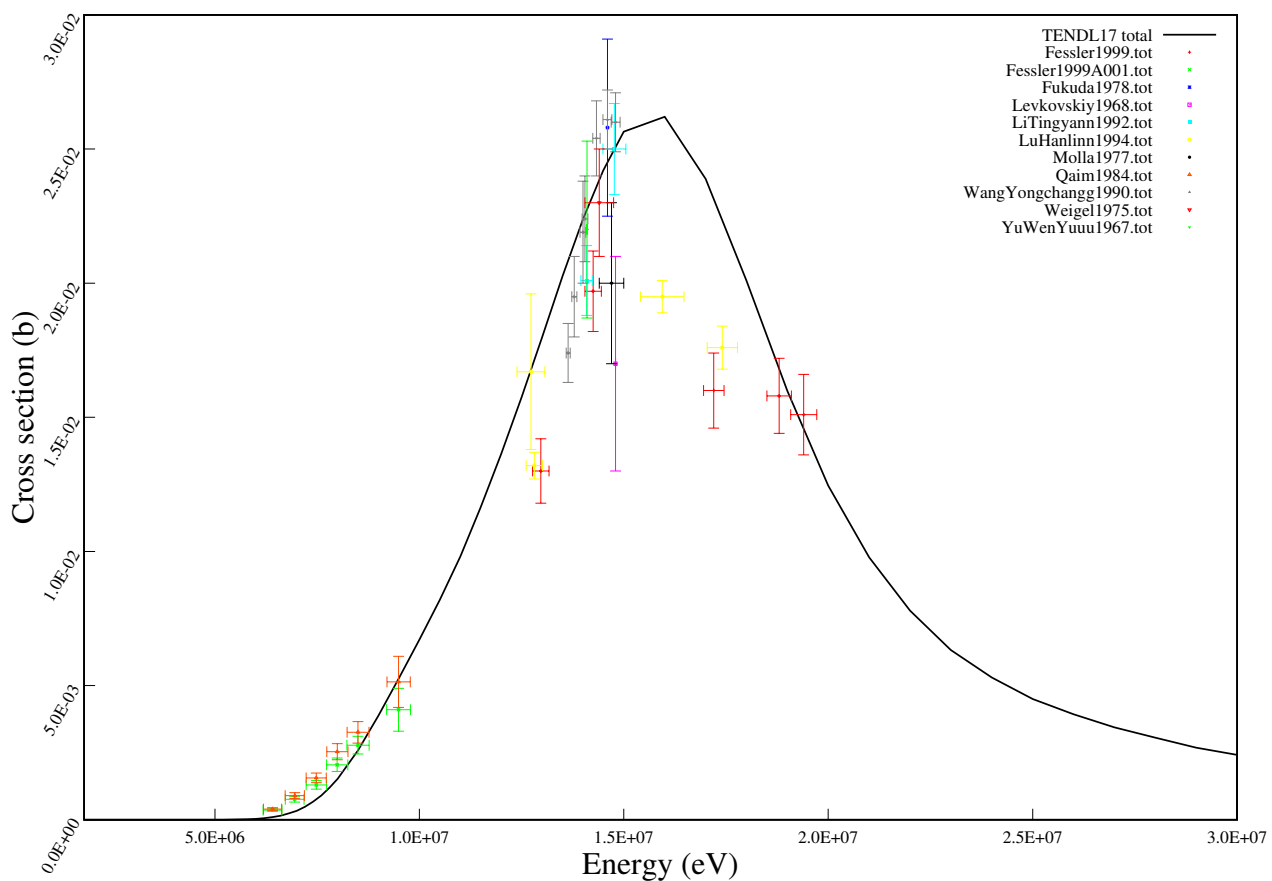
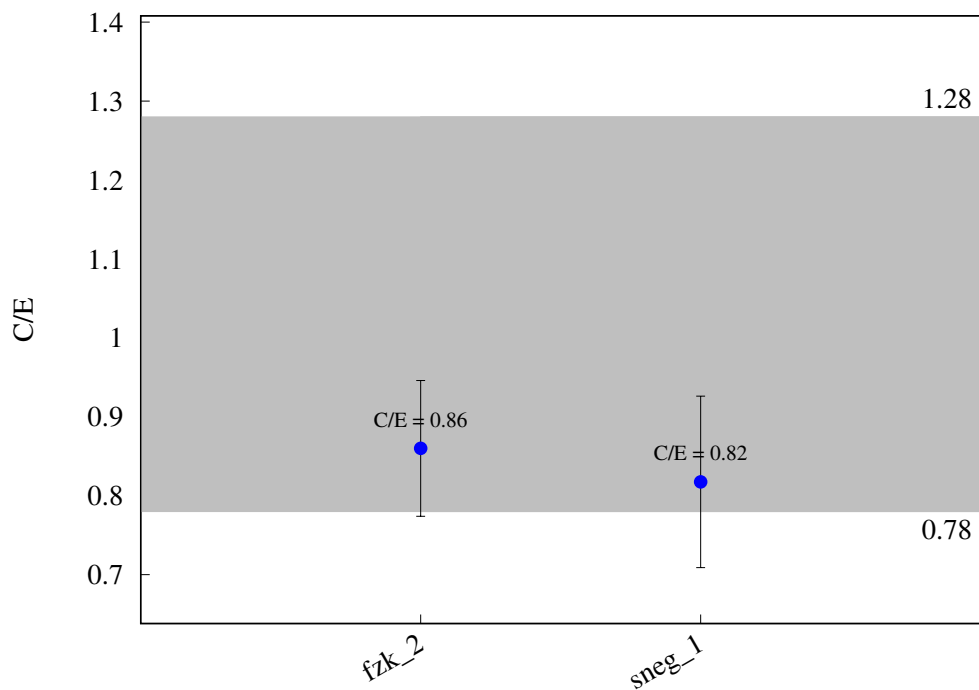


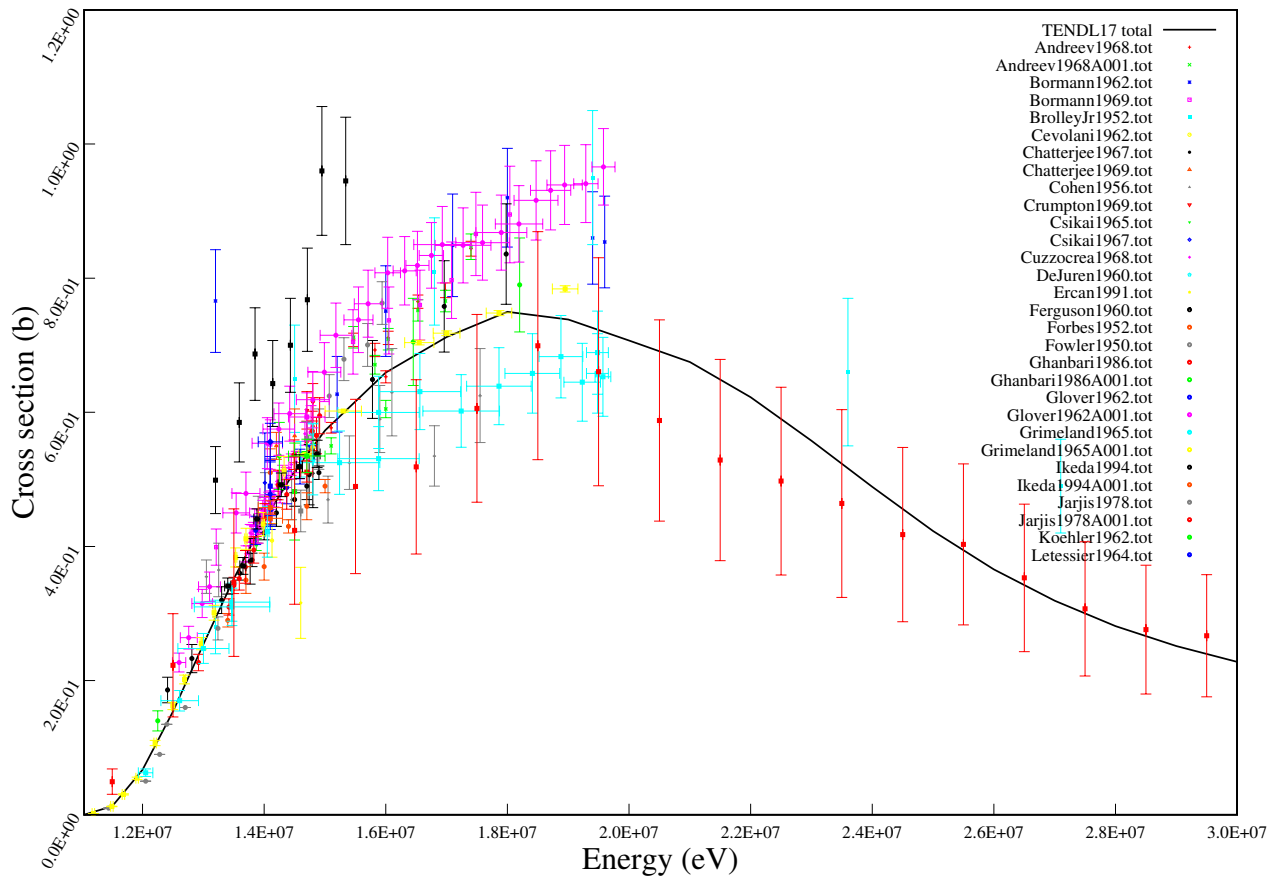
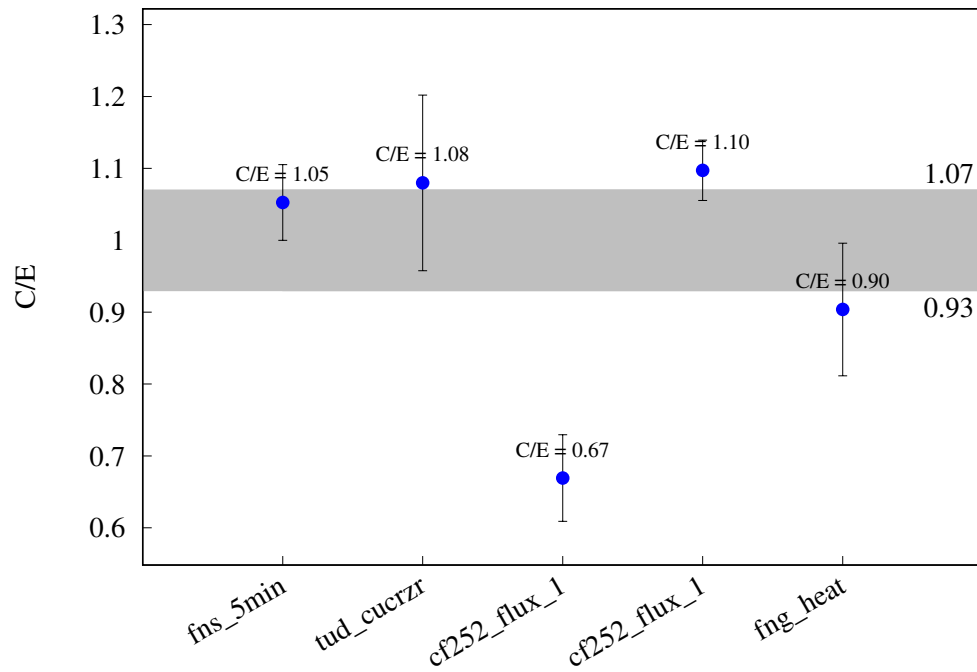


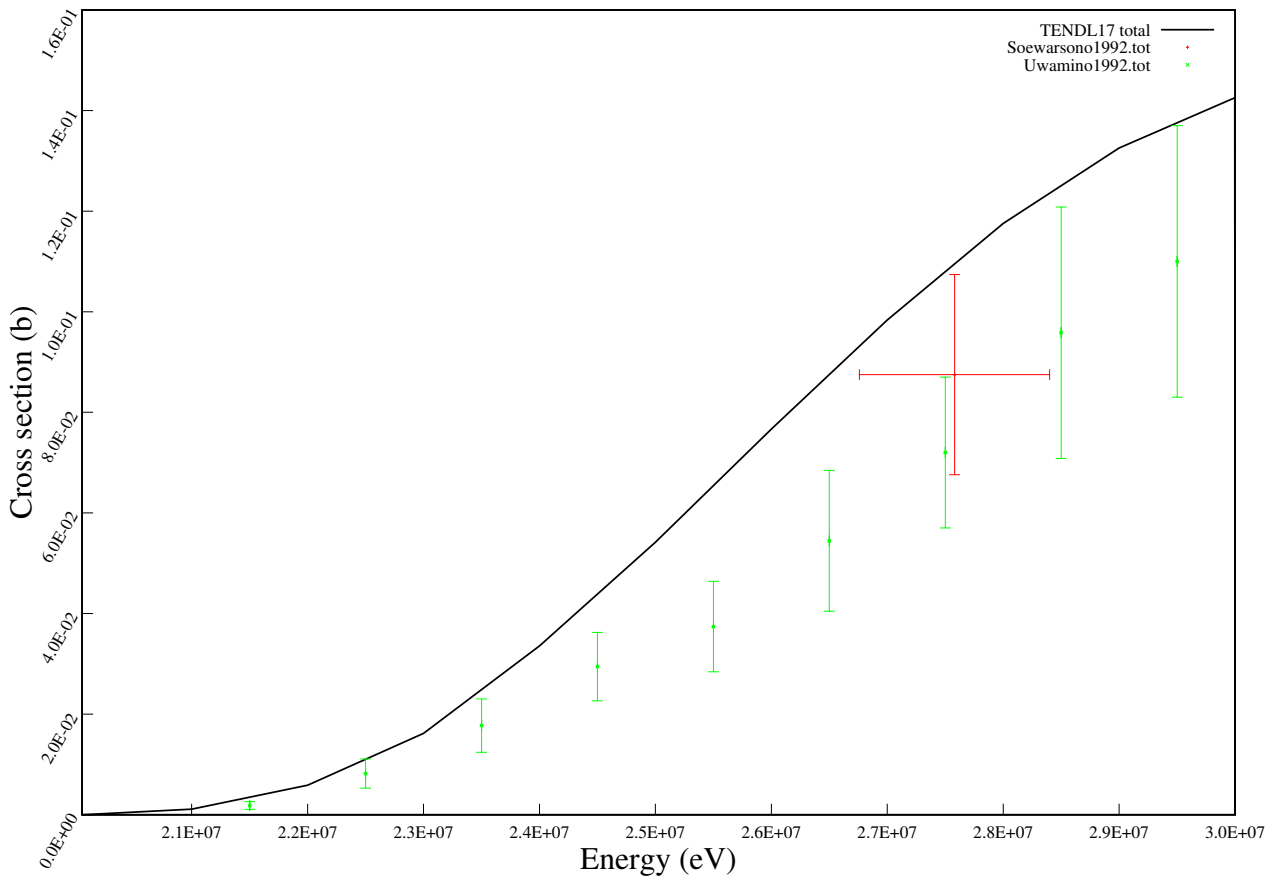
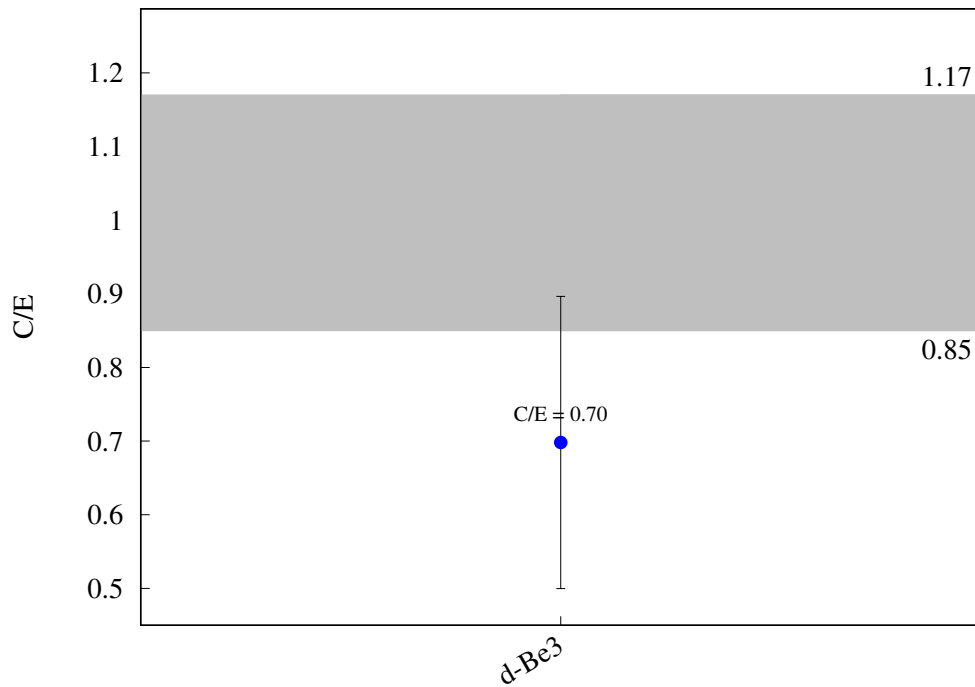
^{61}Ni (n,p) ^{61}Co 

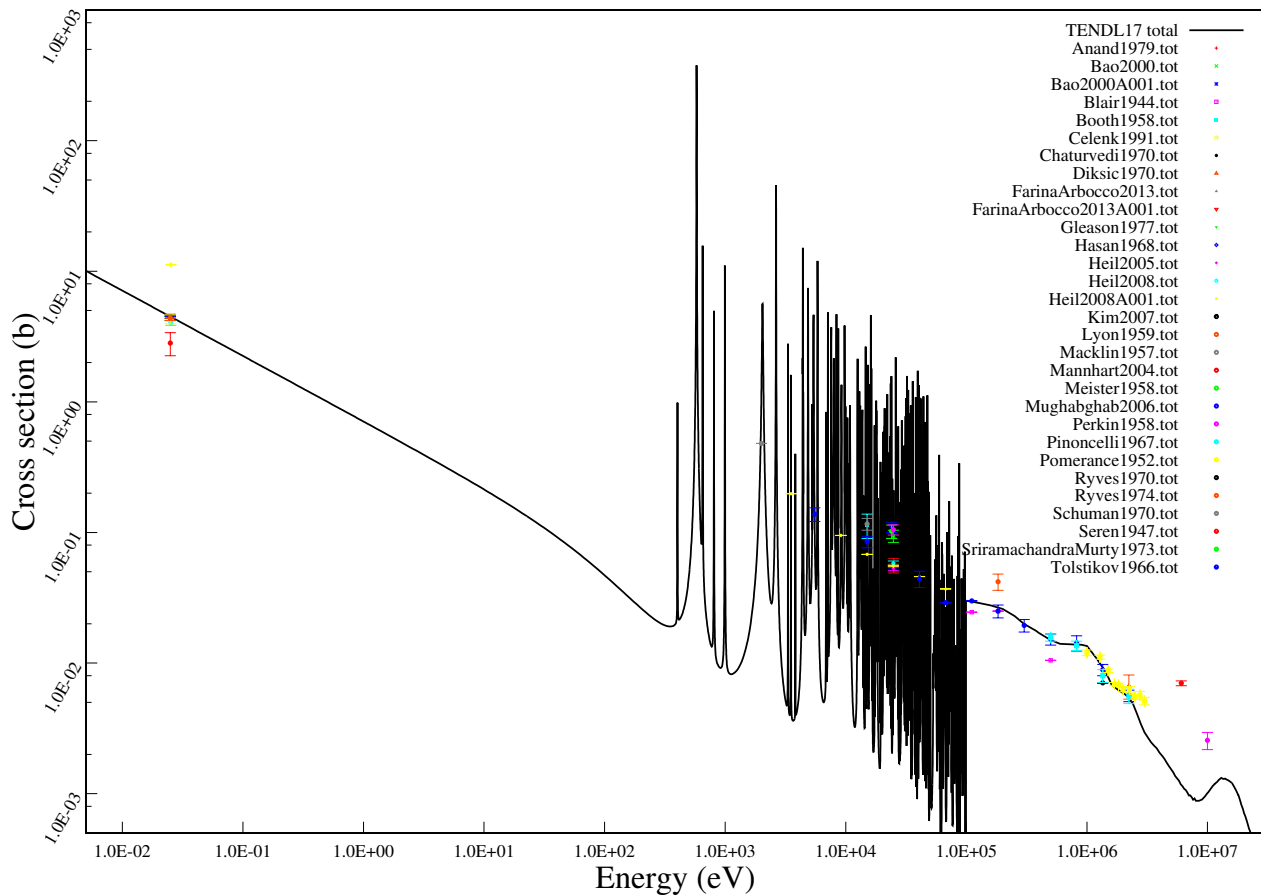
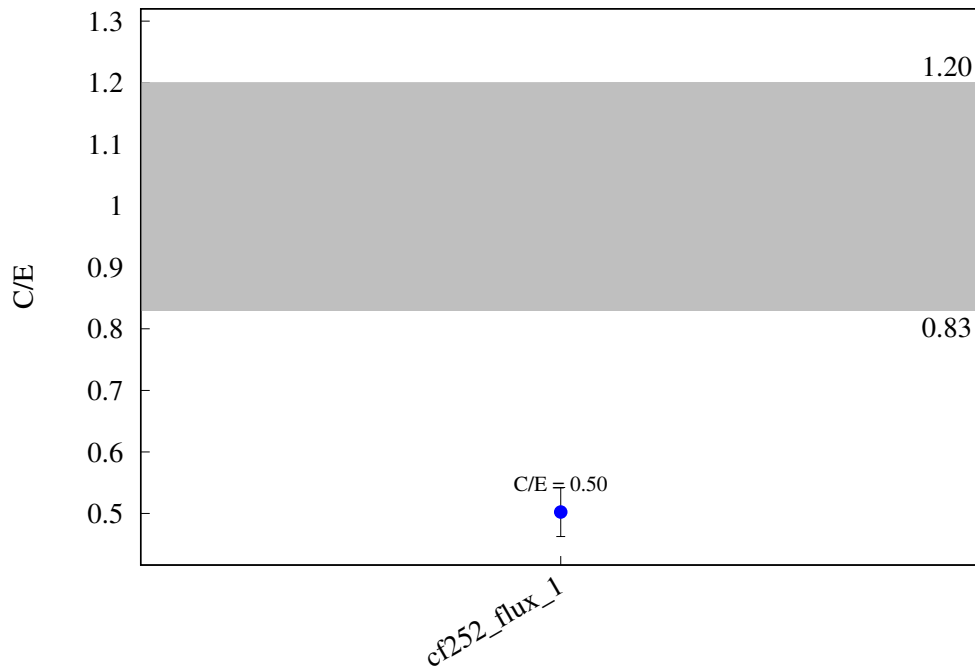
^{62}Ni (n,p) ^{62}gCo 

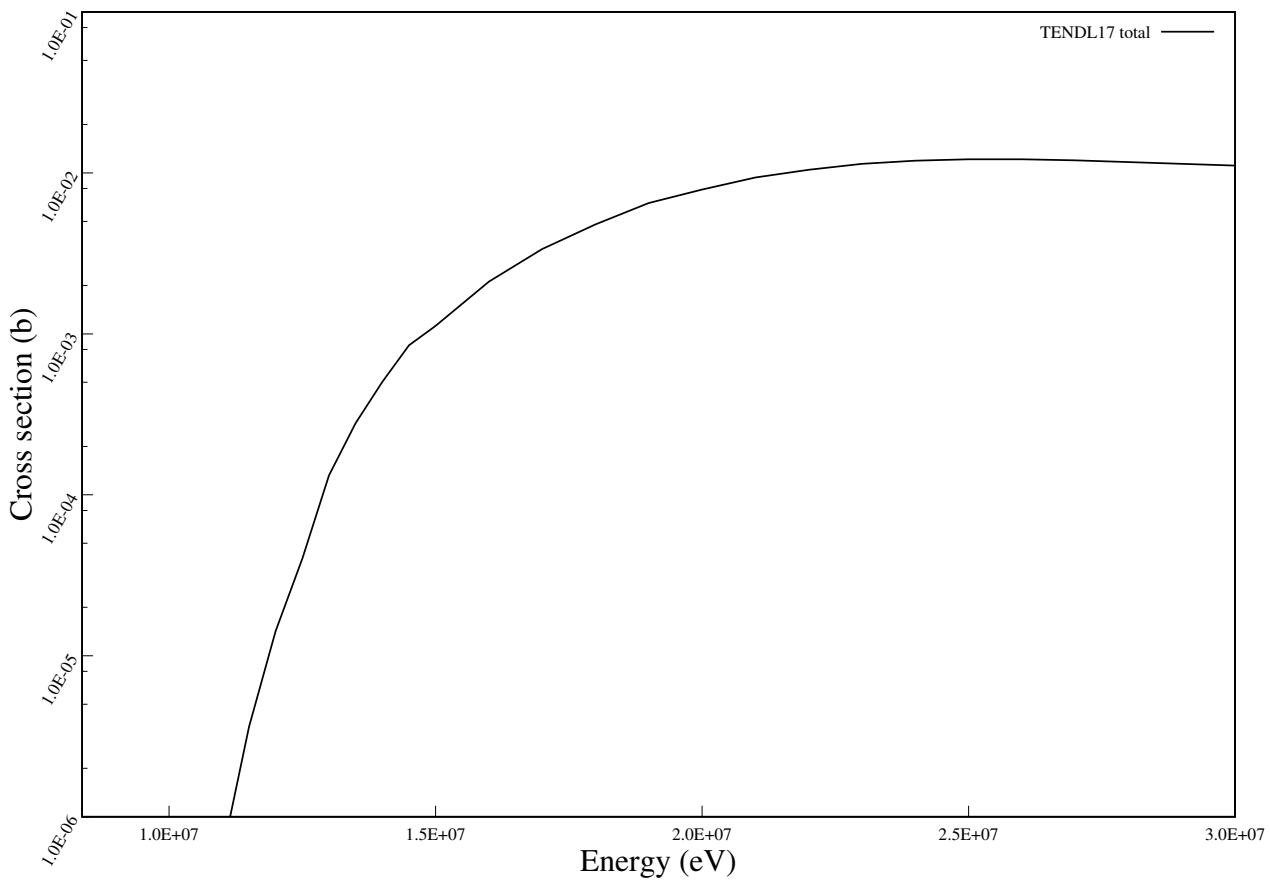
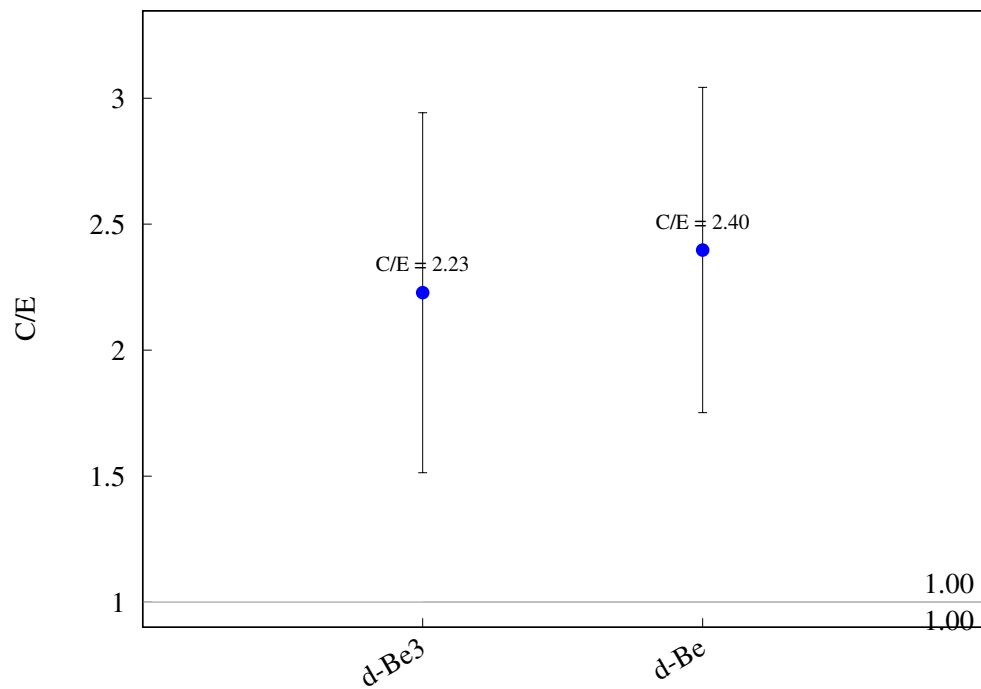
^{62}Ni (n,p) $^{62\text{m}}\text{Co}$ 

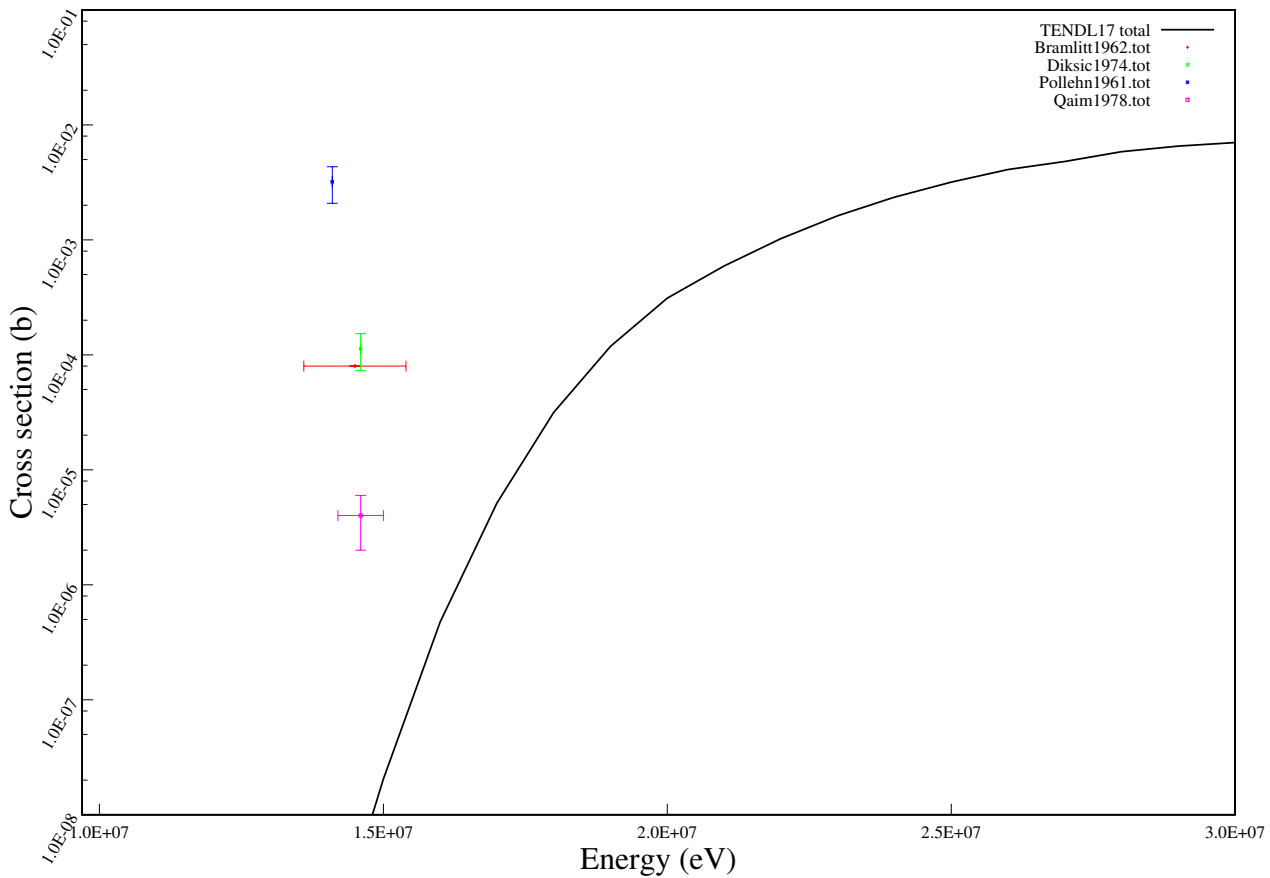
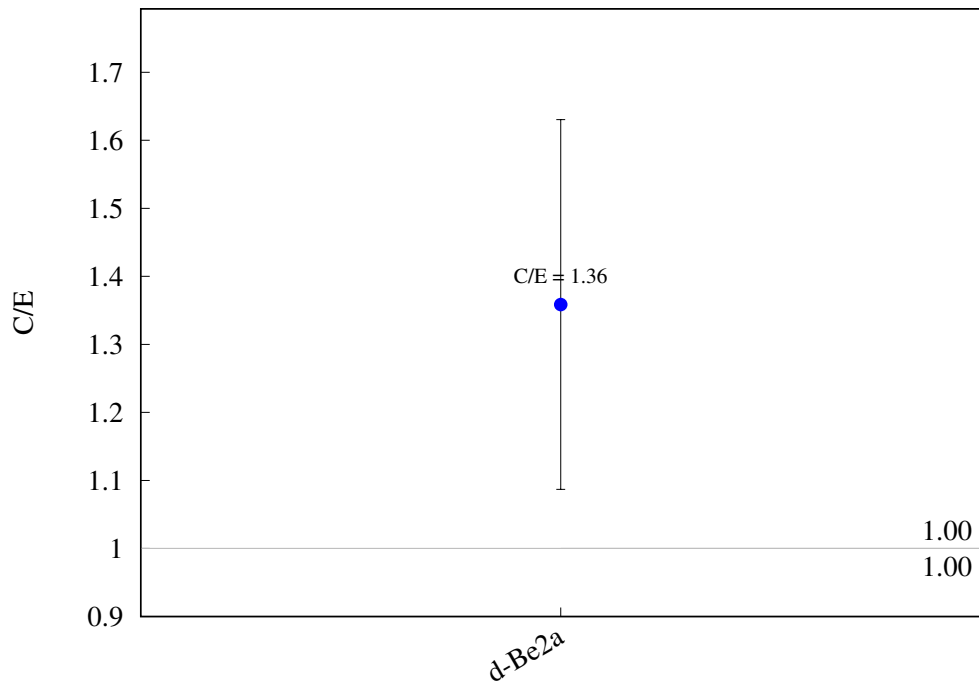
^{62}Ni (n,a) ^{59}Fe 

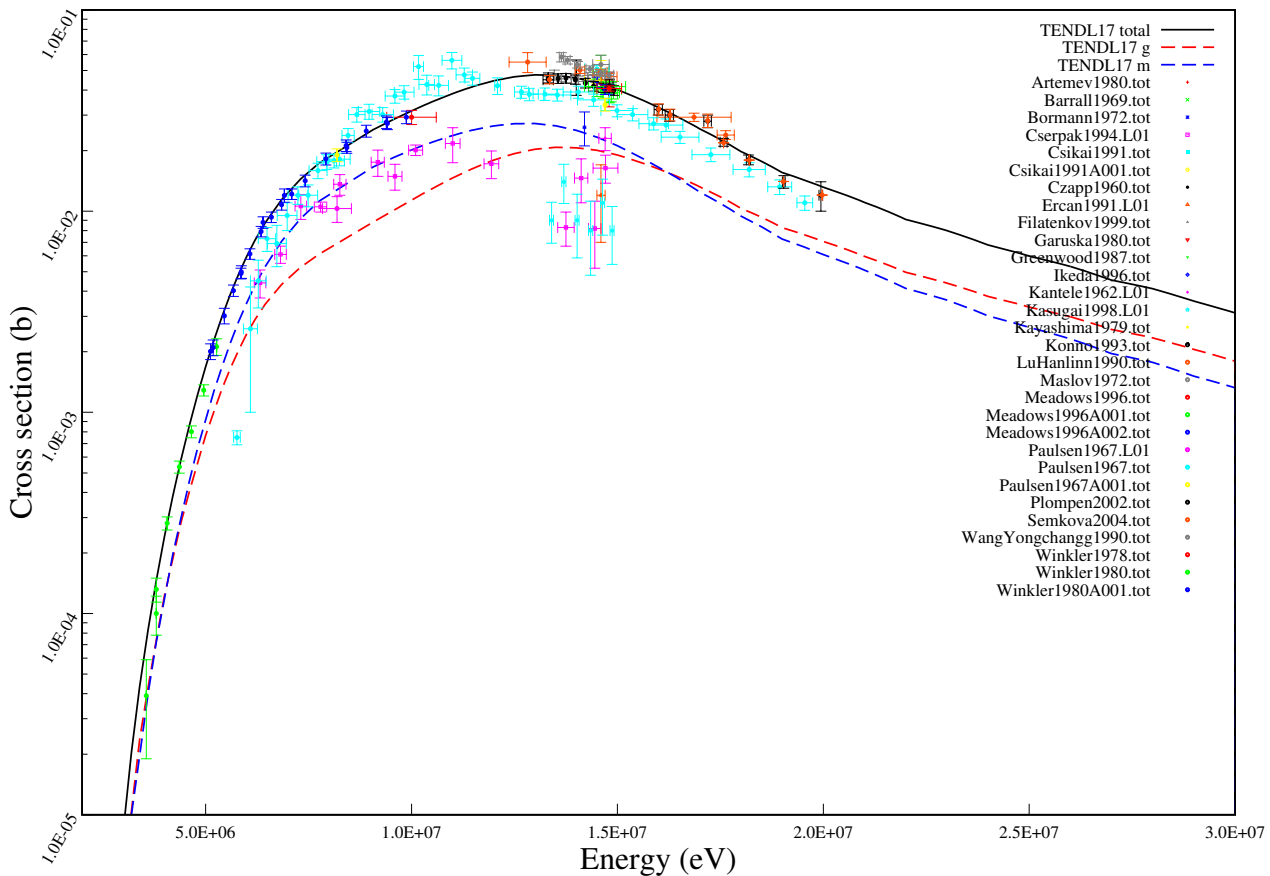
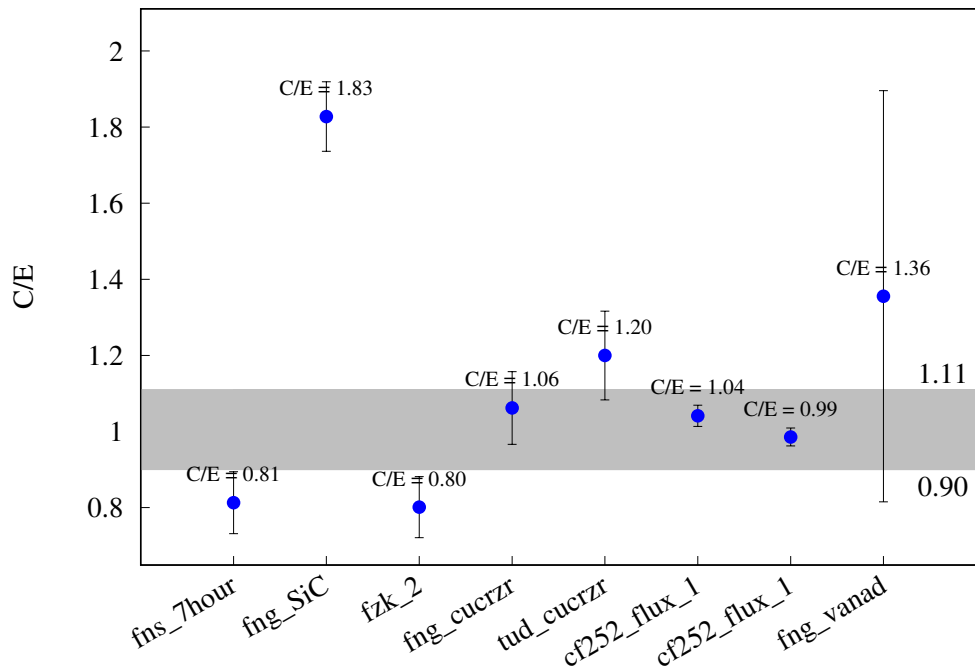
^{63}Cu (n,2n) ^{62}Cu 

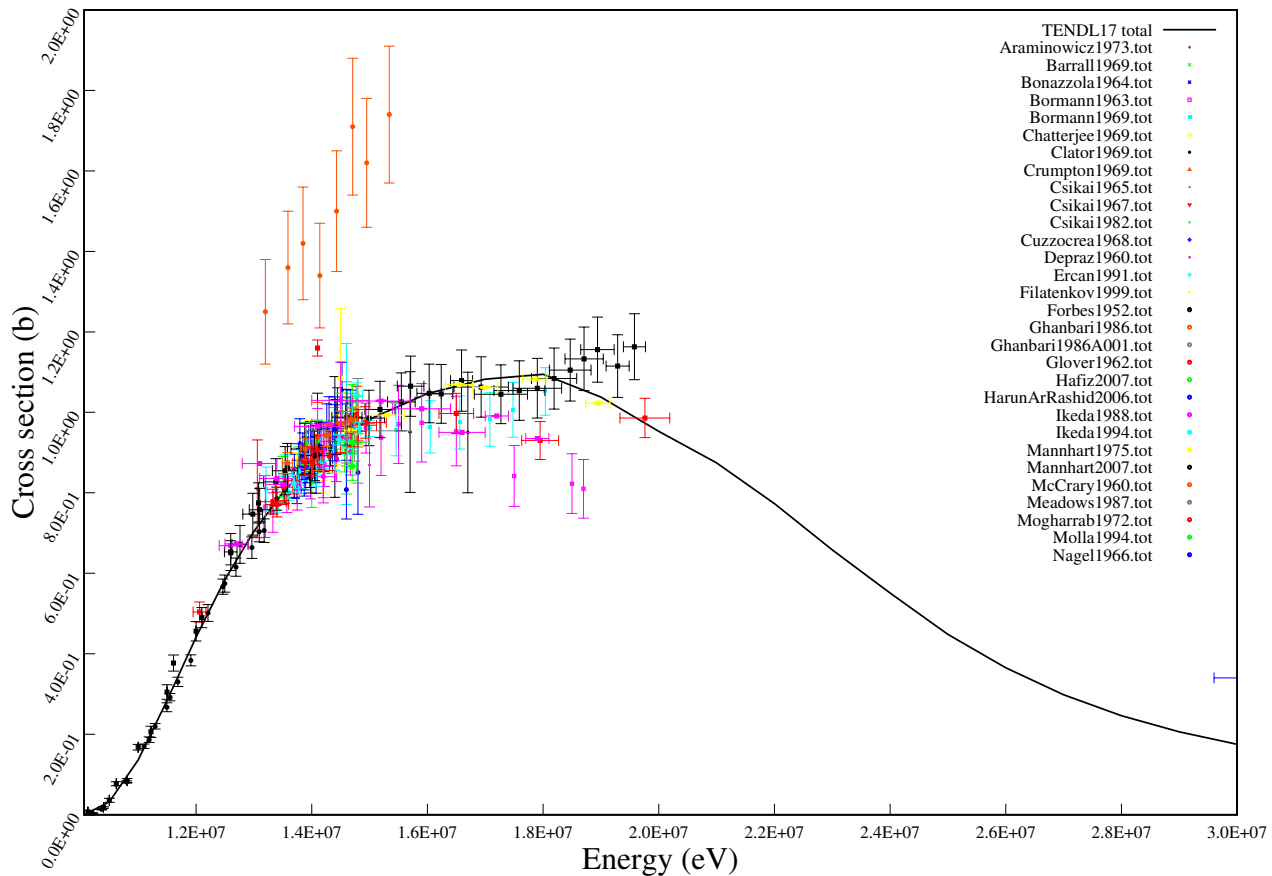
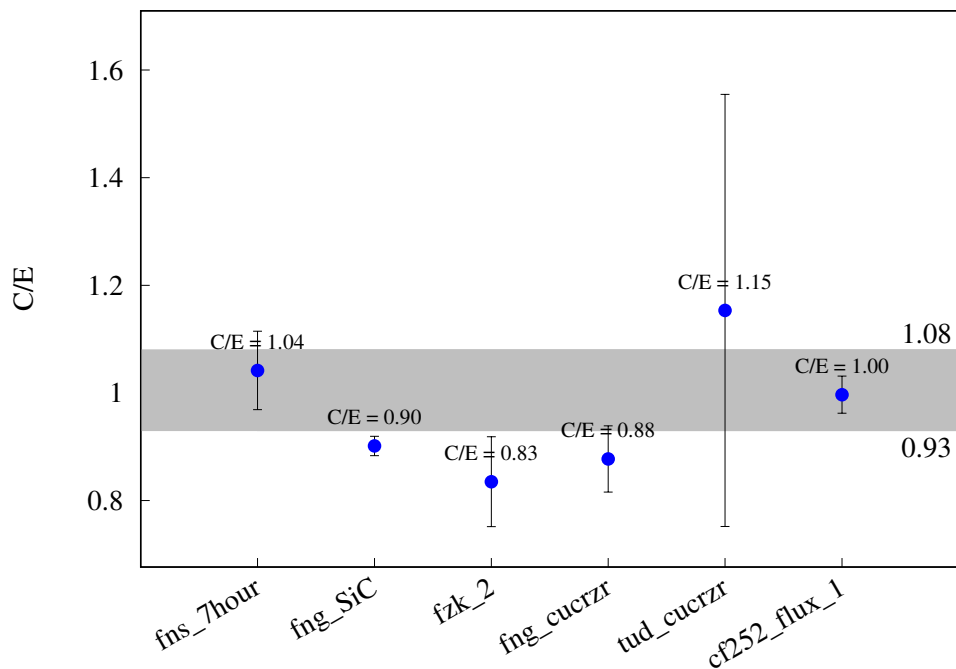
^{63}Cu (n,3n) ^{61}Cu 

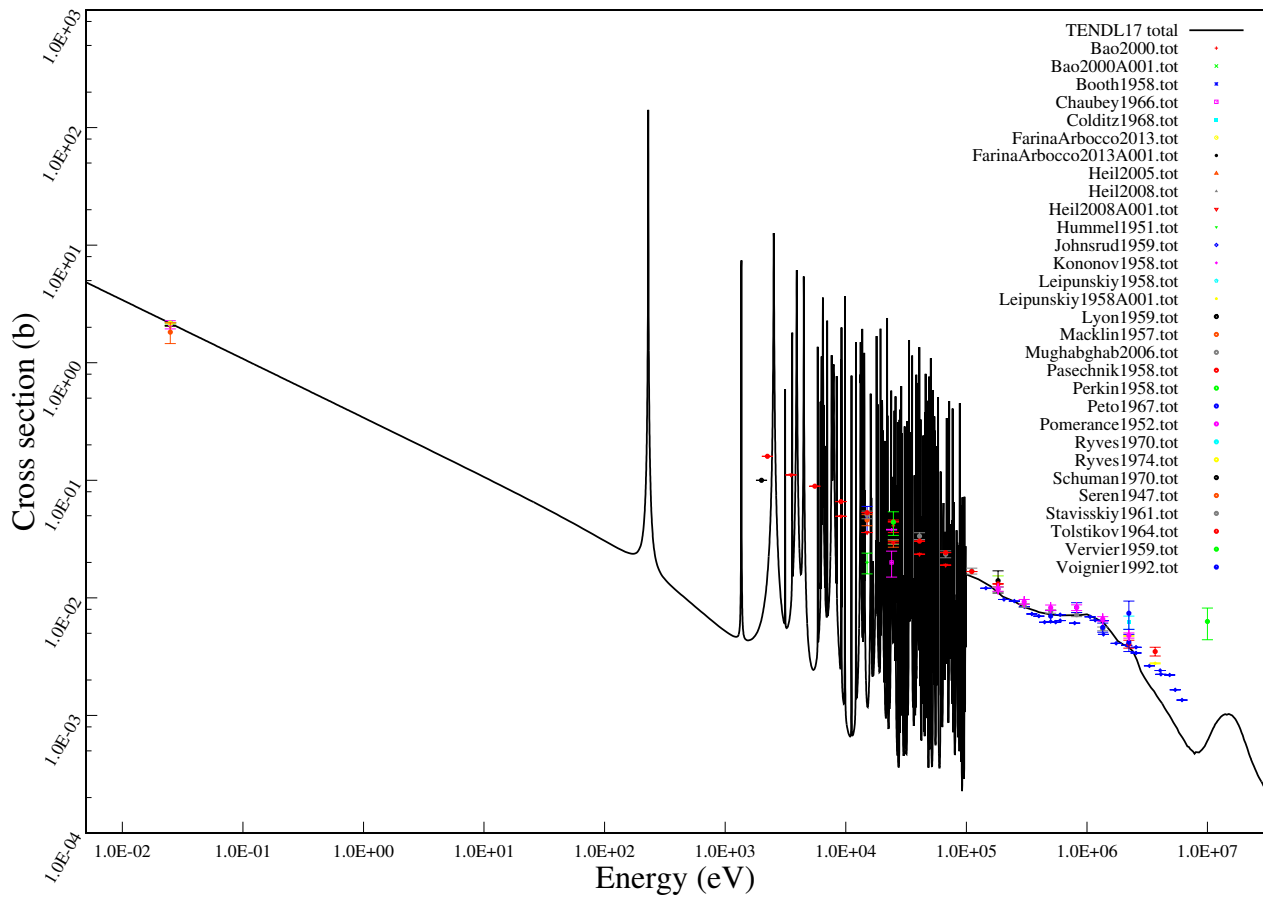
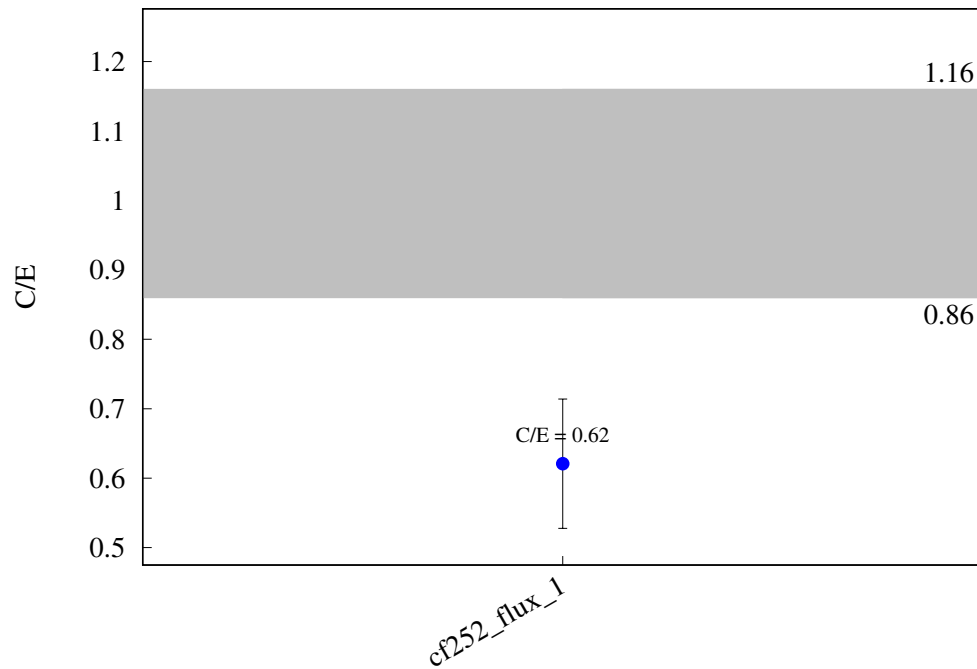
^{63}Cu (n,g) ^{64}Cu 

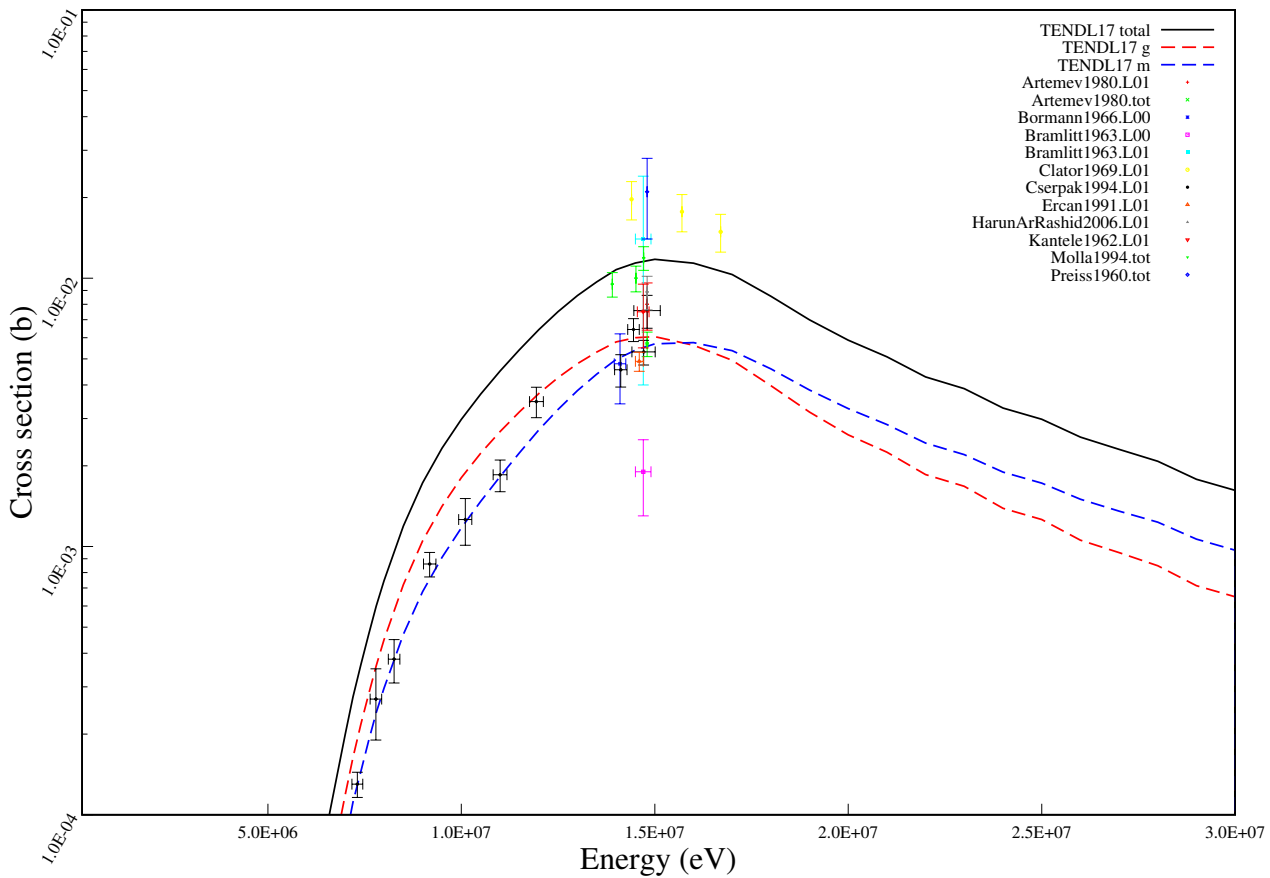
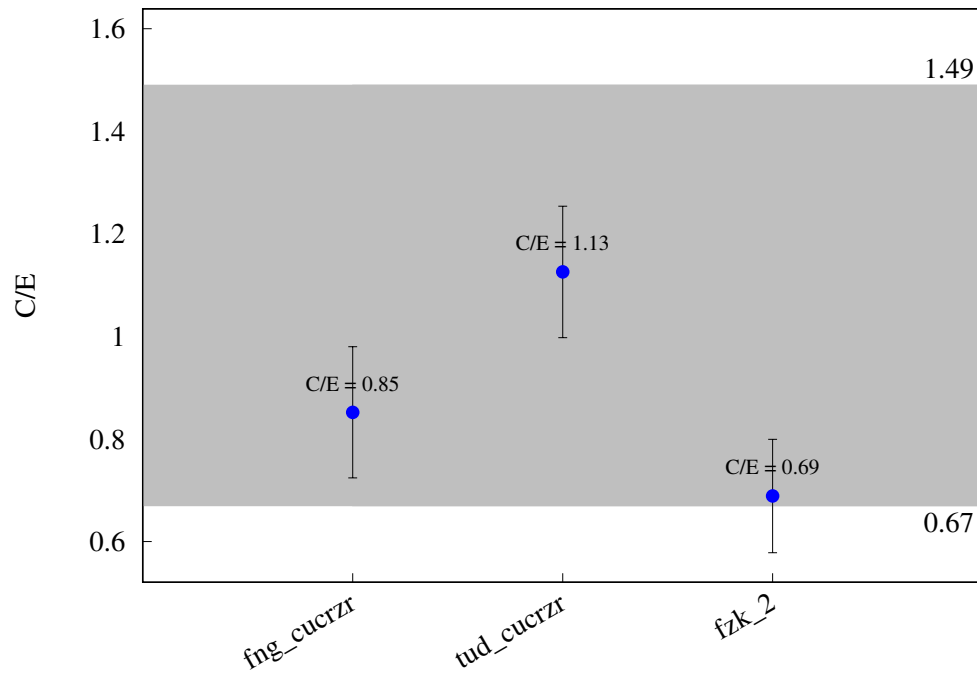
$^{63}\text{Cu} (\text{n},\text{t}) ^{61}\text{Ni}$ 

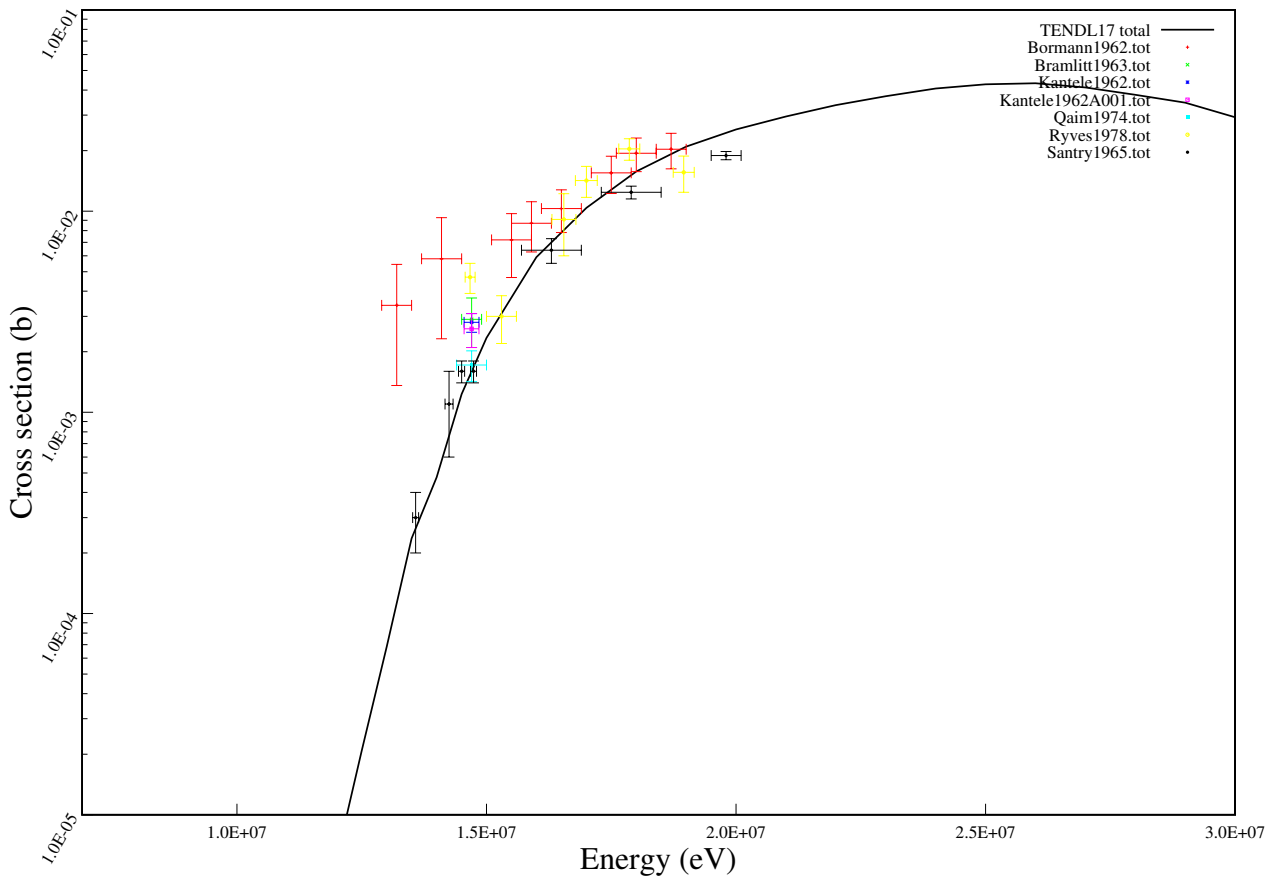
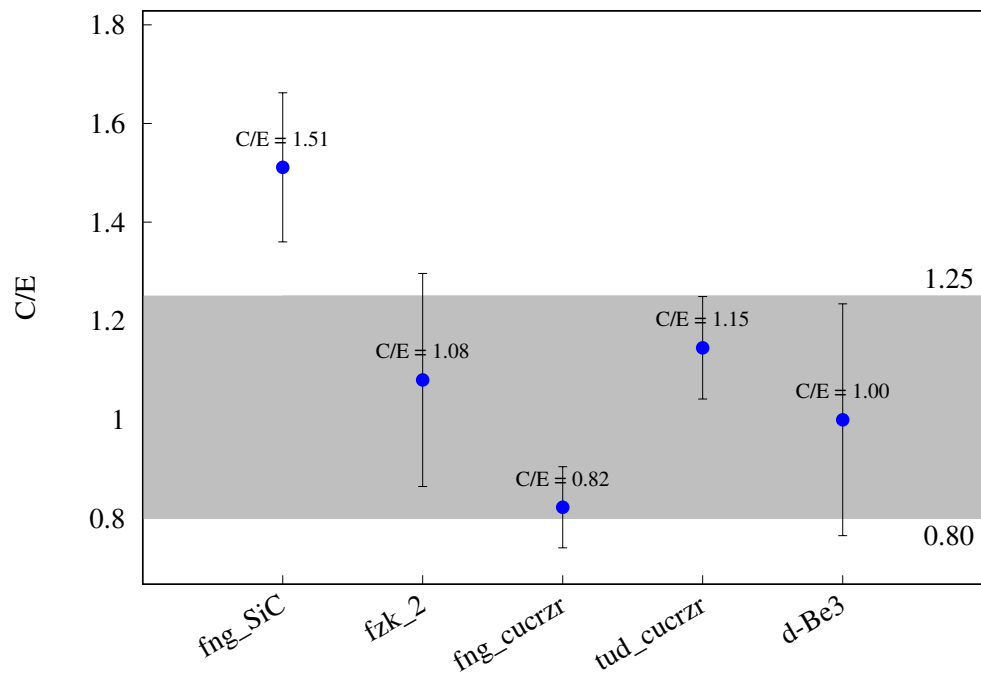
^{63}Cu (n,h) ^{61}Co 

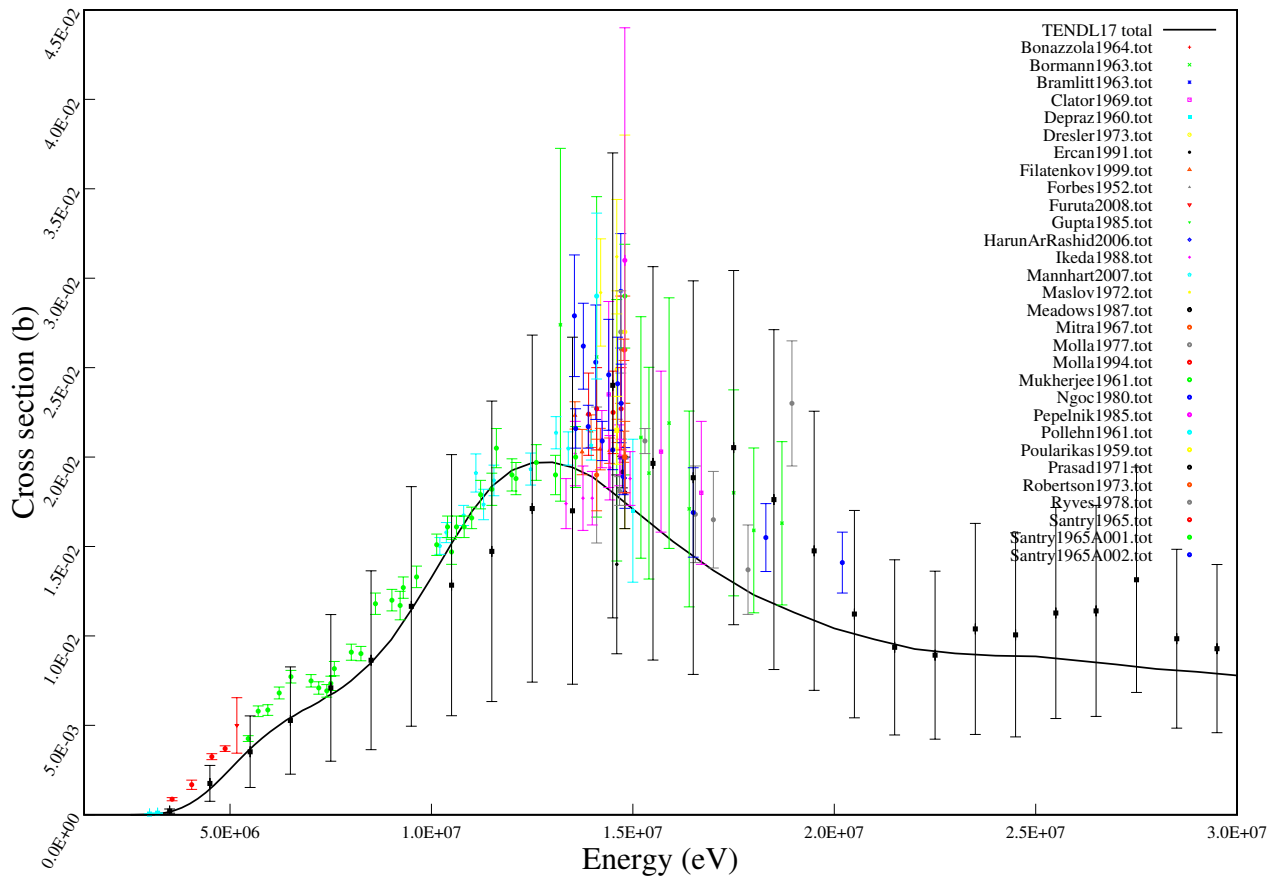
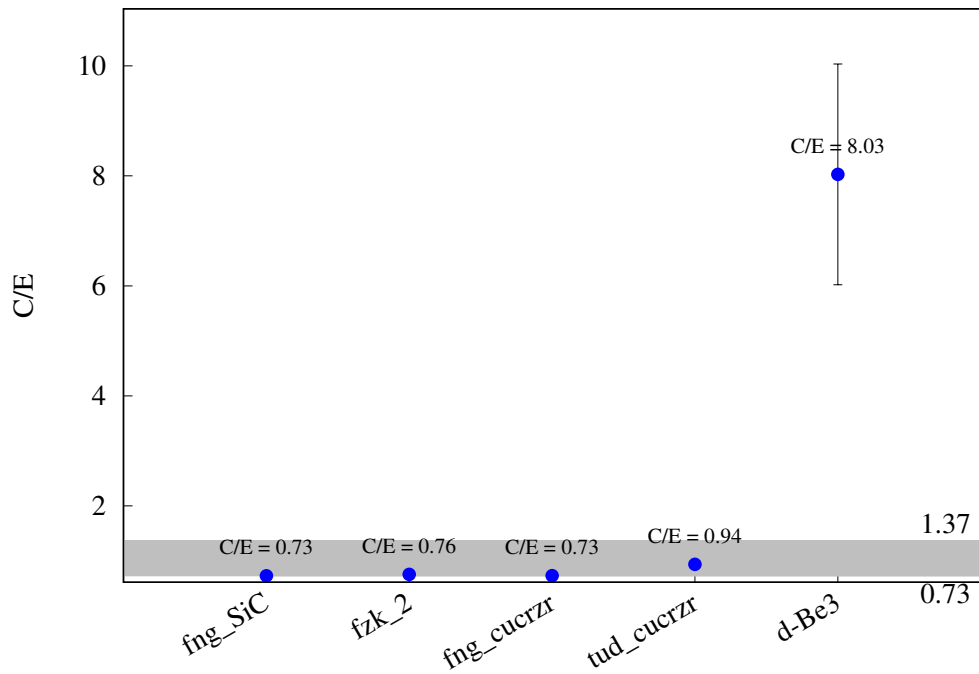
^{63}Cu (n,a) ^{60}Co 

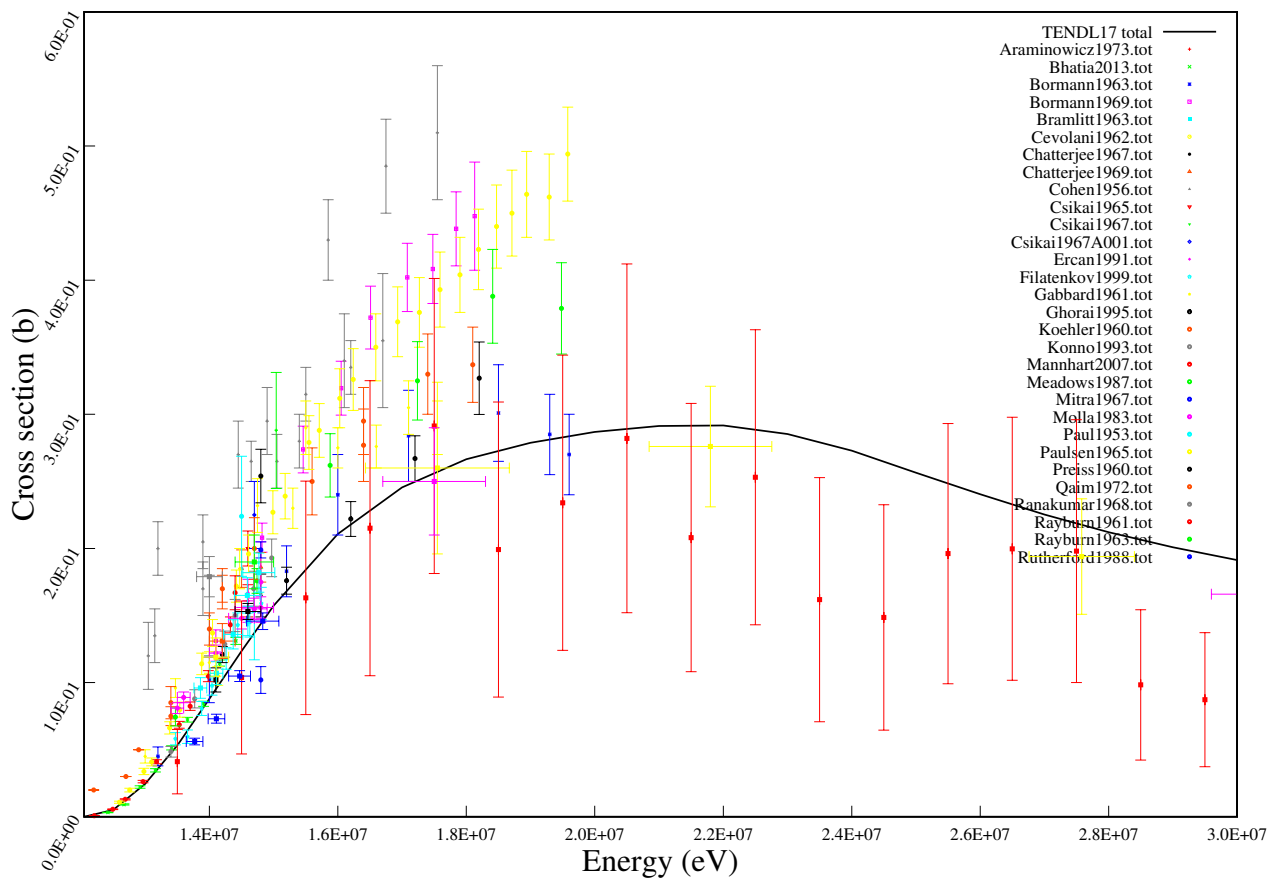
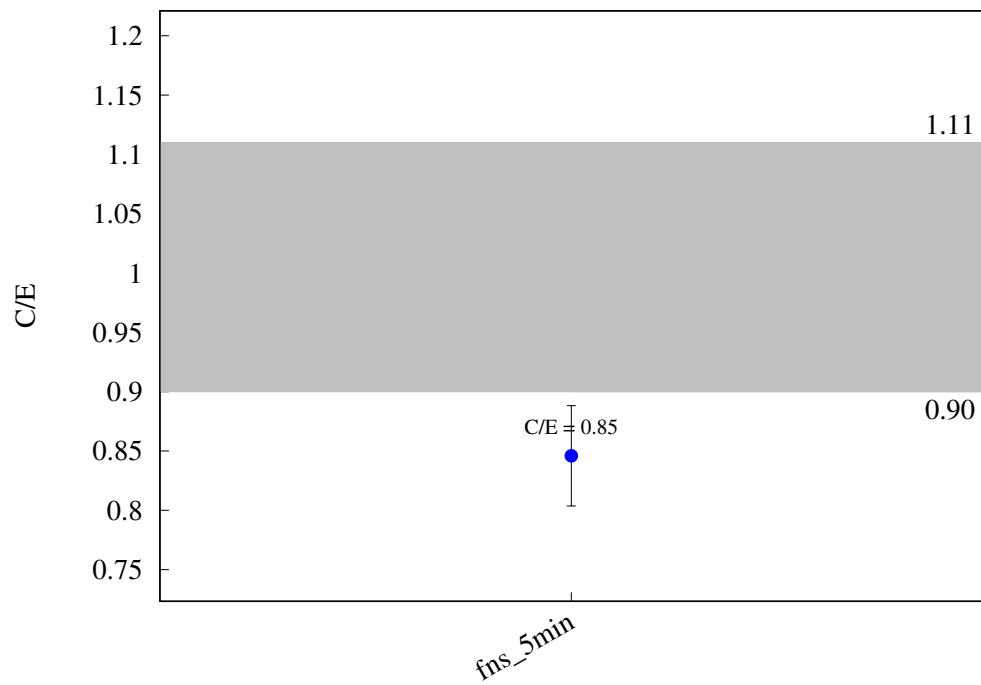
^{65}Cu (n,2n) ^{64}Cu 

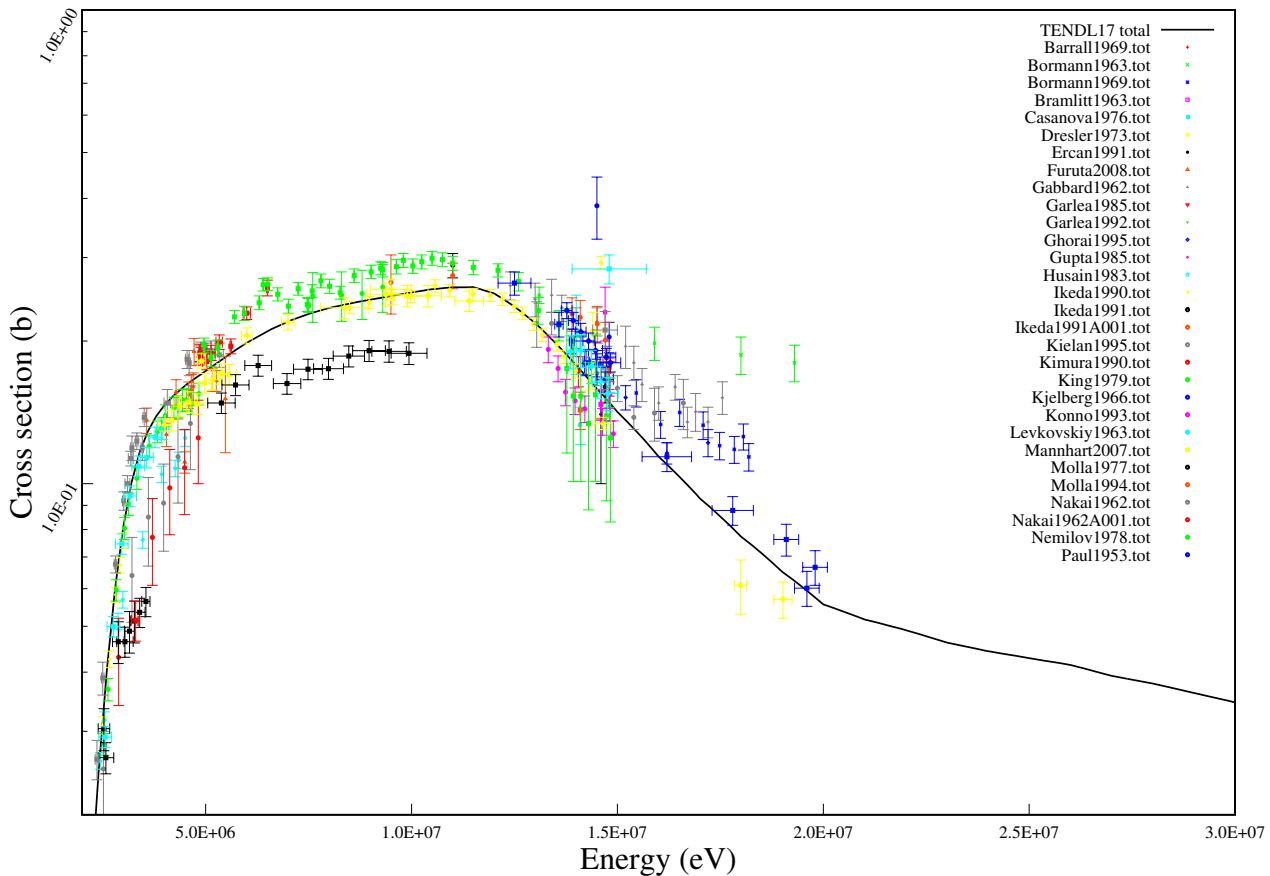
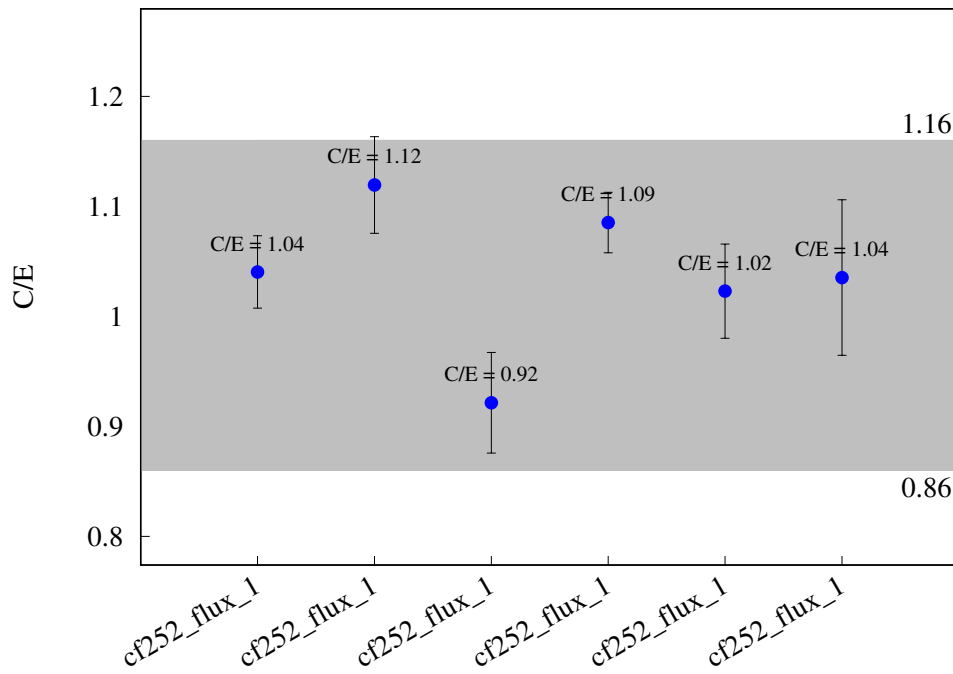
^{65}Cu (n,g) ^{66}Cu 

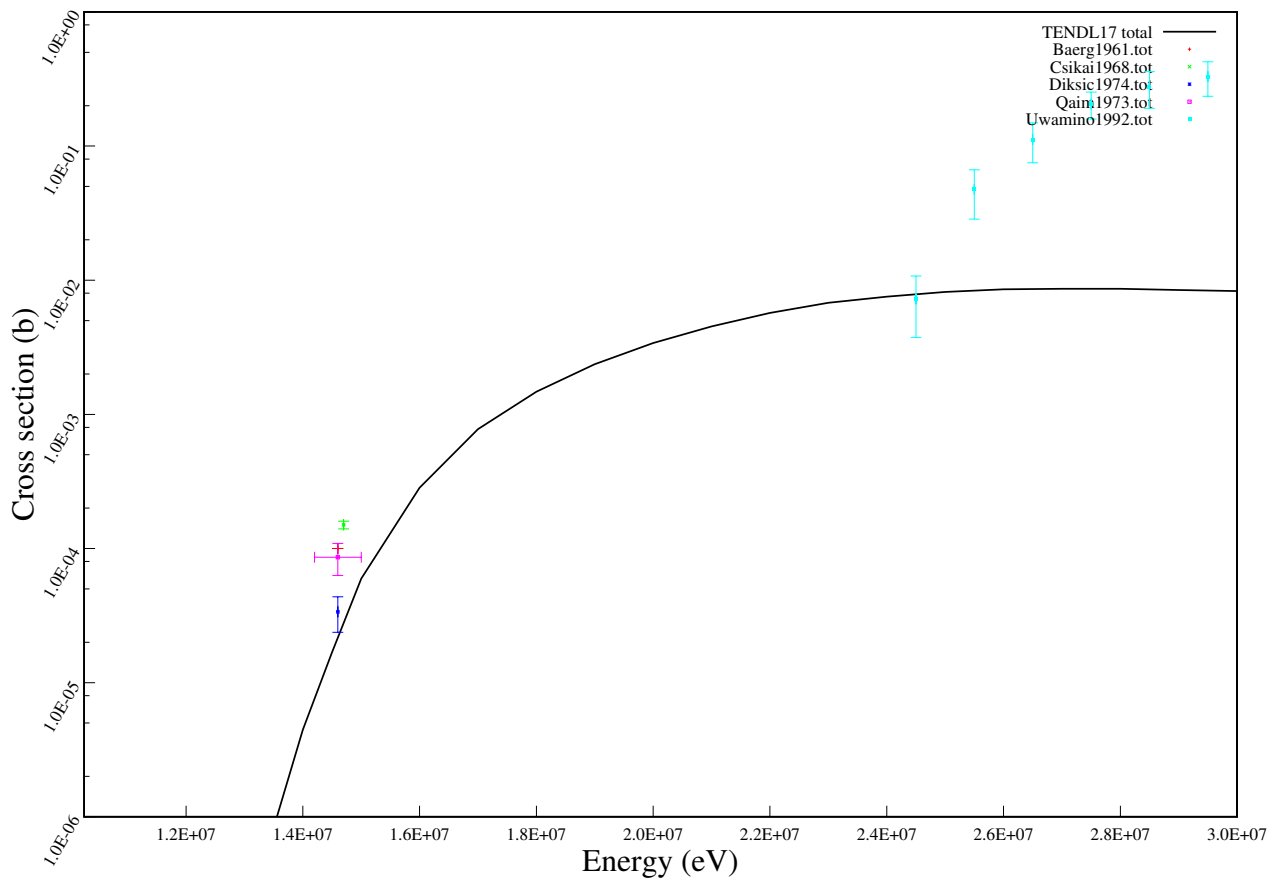
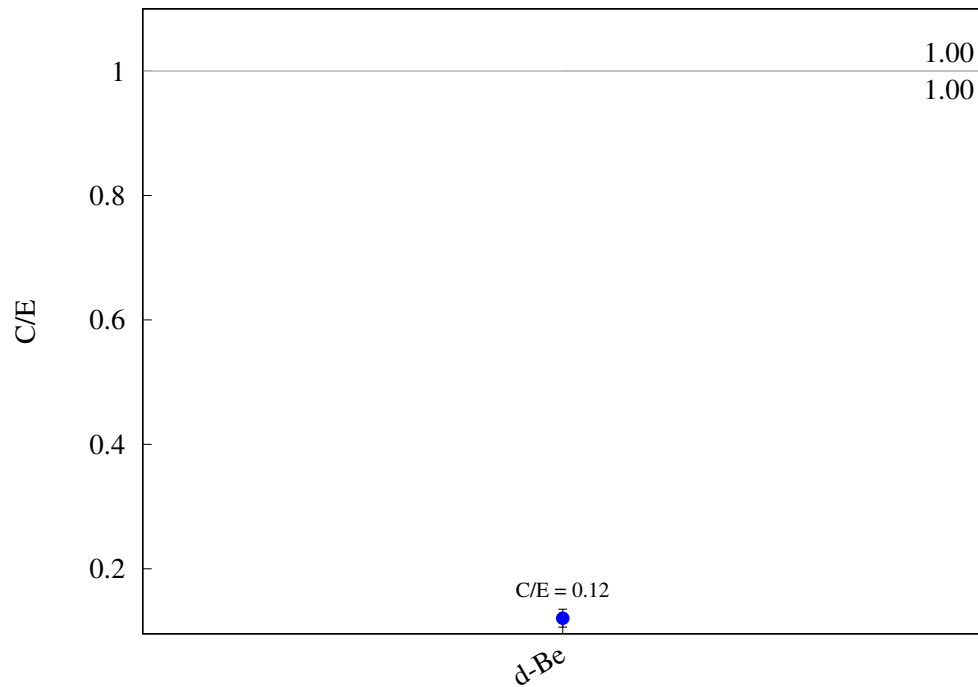
^{65}Cu (n,a) ^{62m}Co 

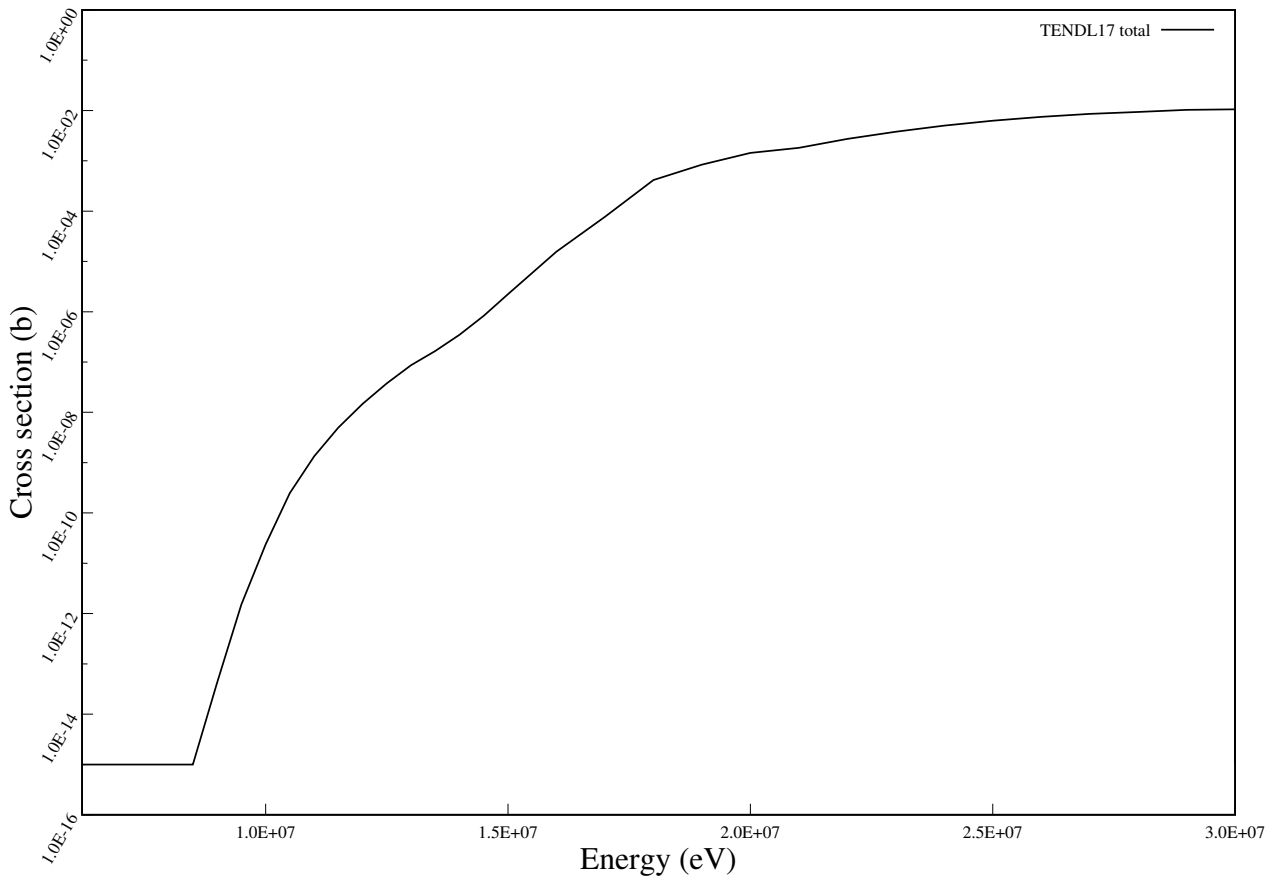
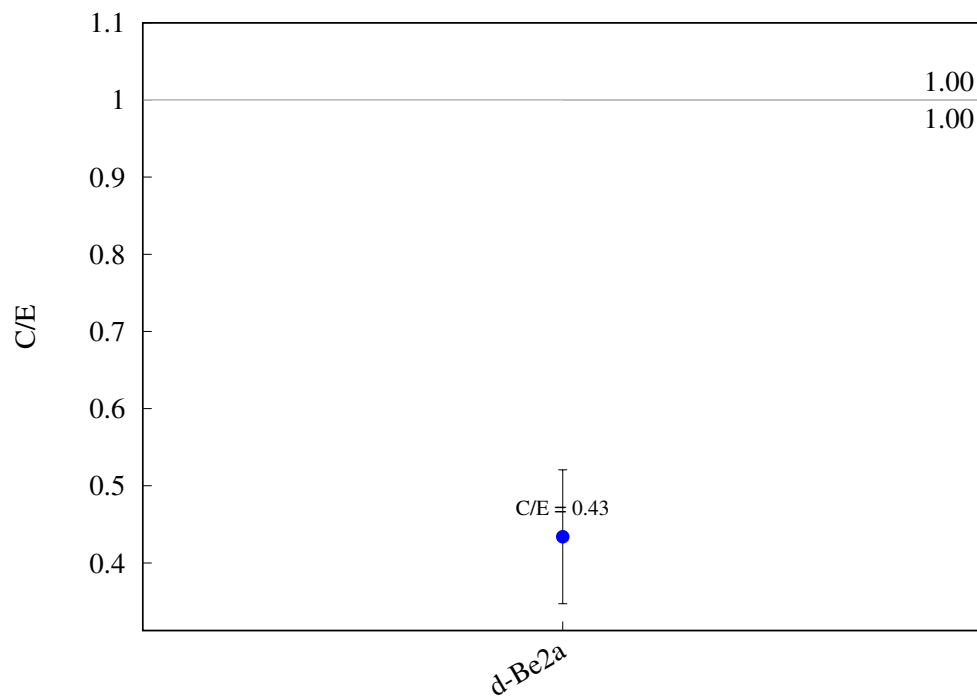
^{65}Cu (n,na) ^{61}Co 

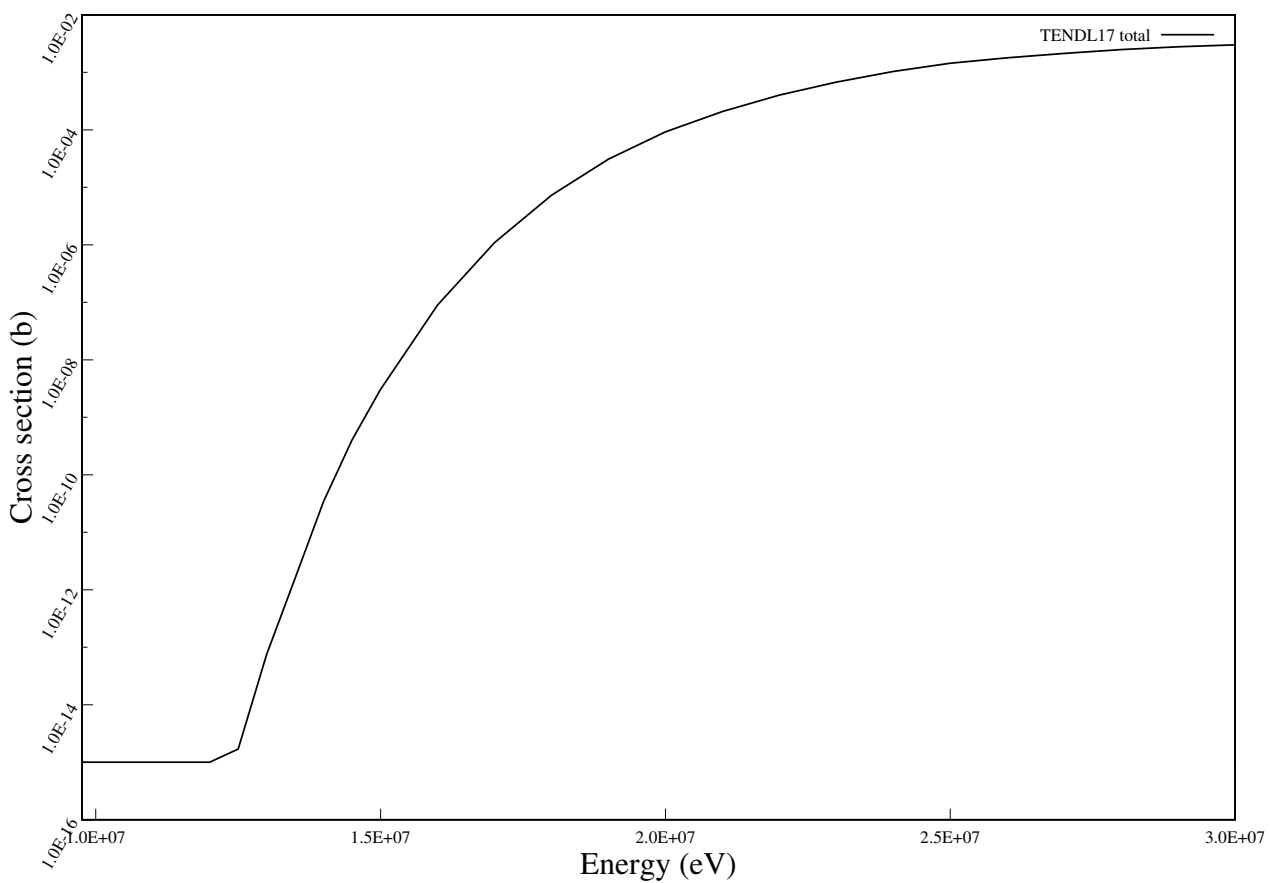
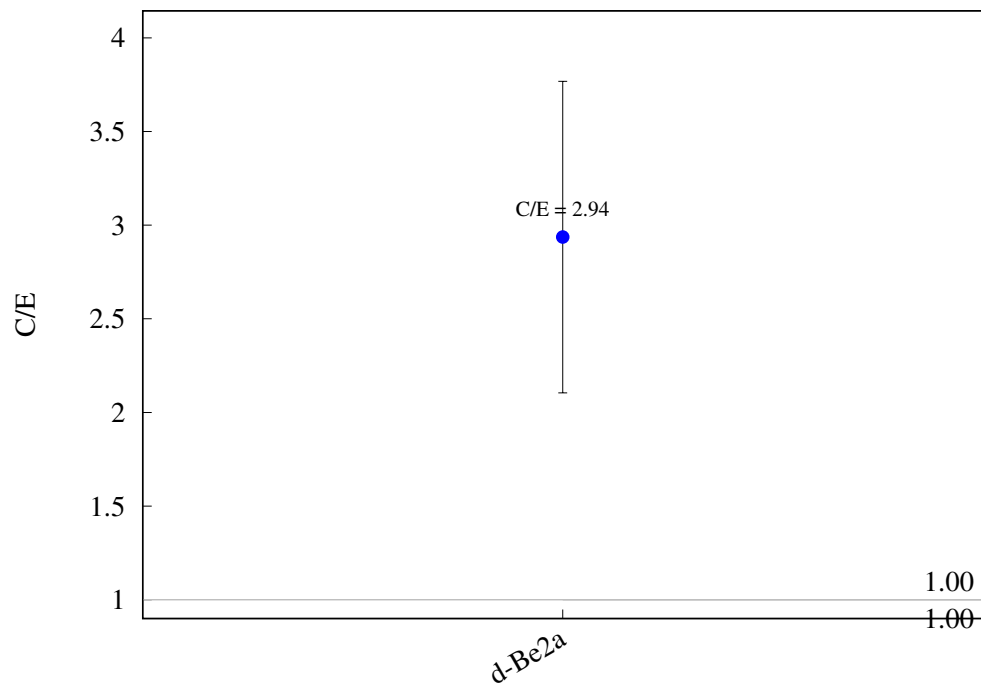
$^{65}\text{Cu} (\text{n},\text{p}) ^{65}\text{Ni}$ 

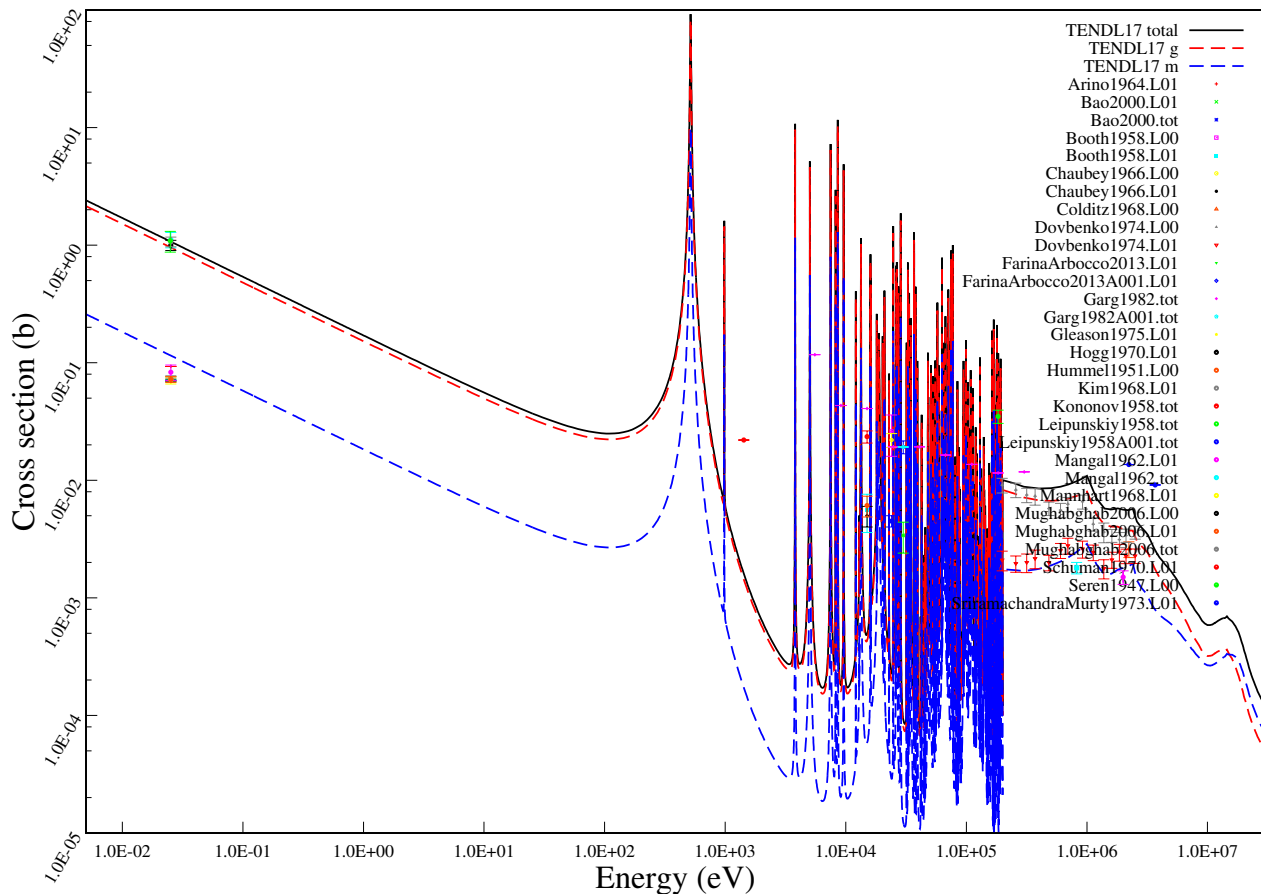
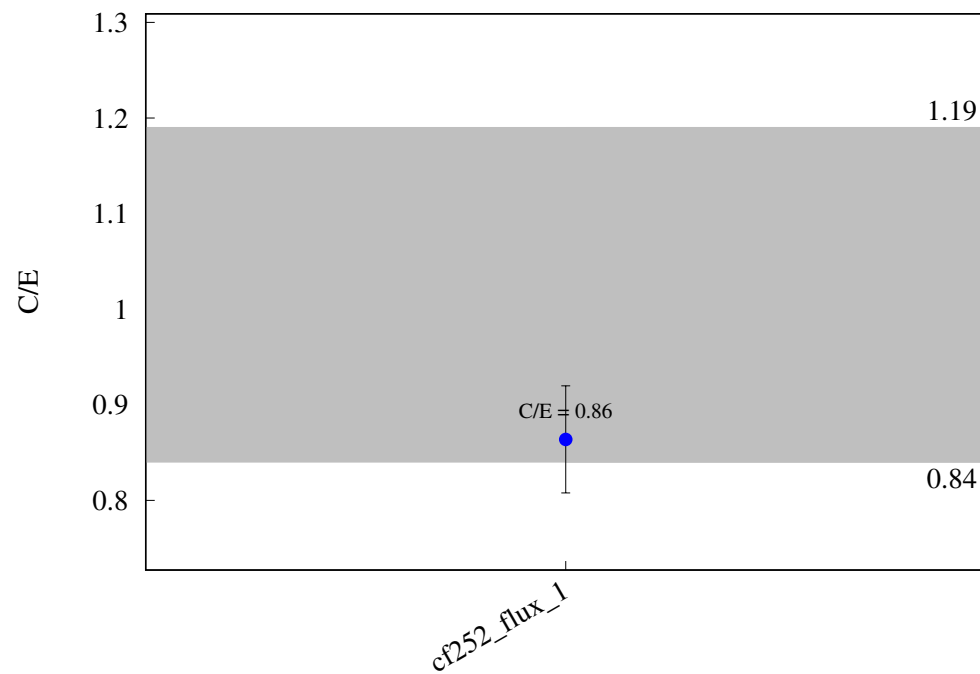
^{64}Zn (n,2n) ^{63}Zn 

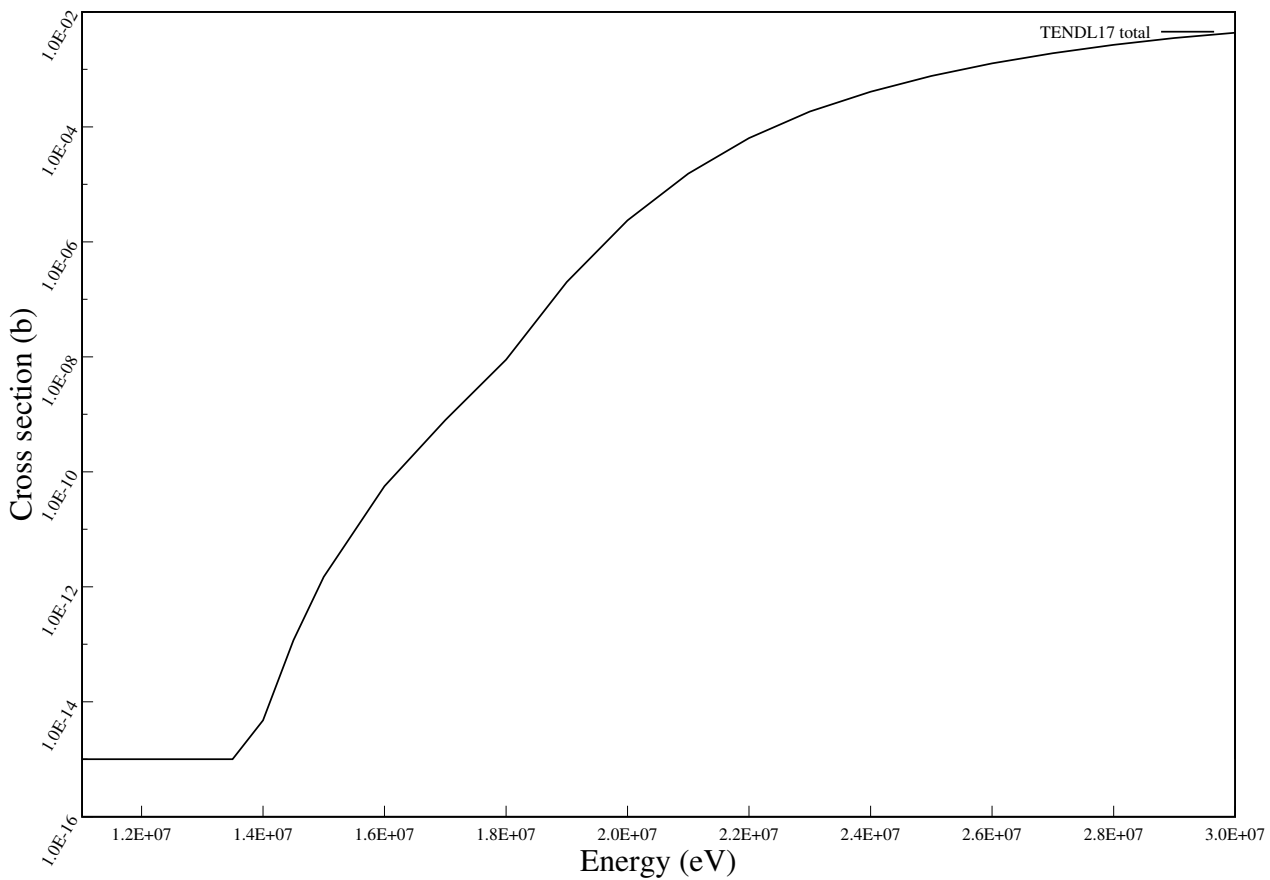
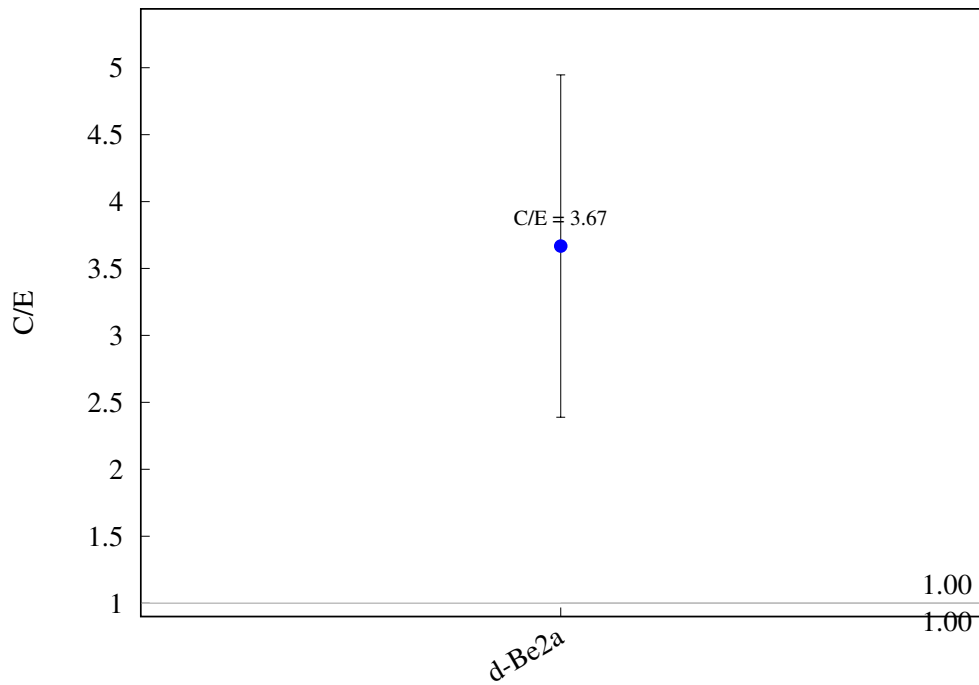
^{64}Zn (n,p) ^{64}Cu 

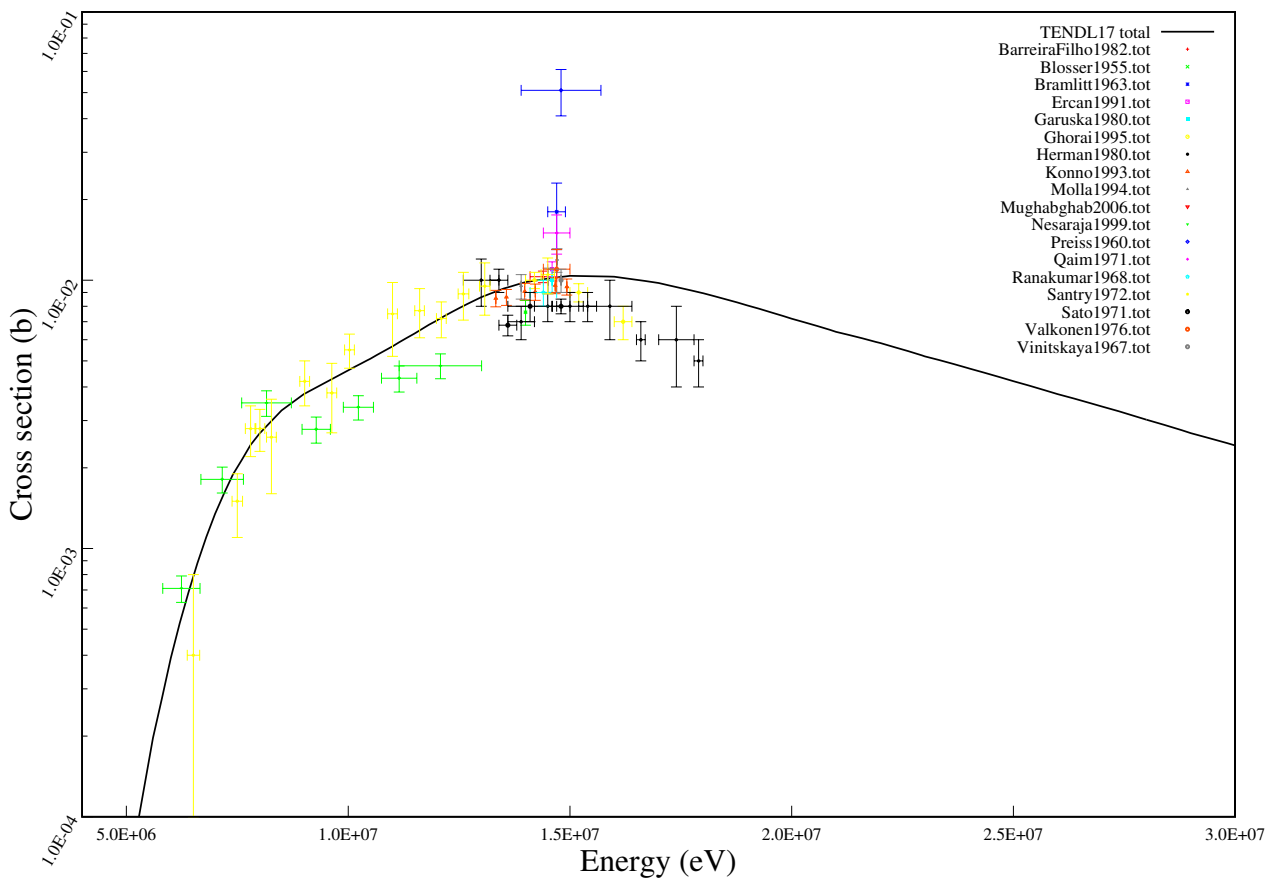
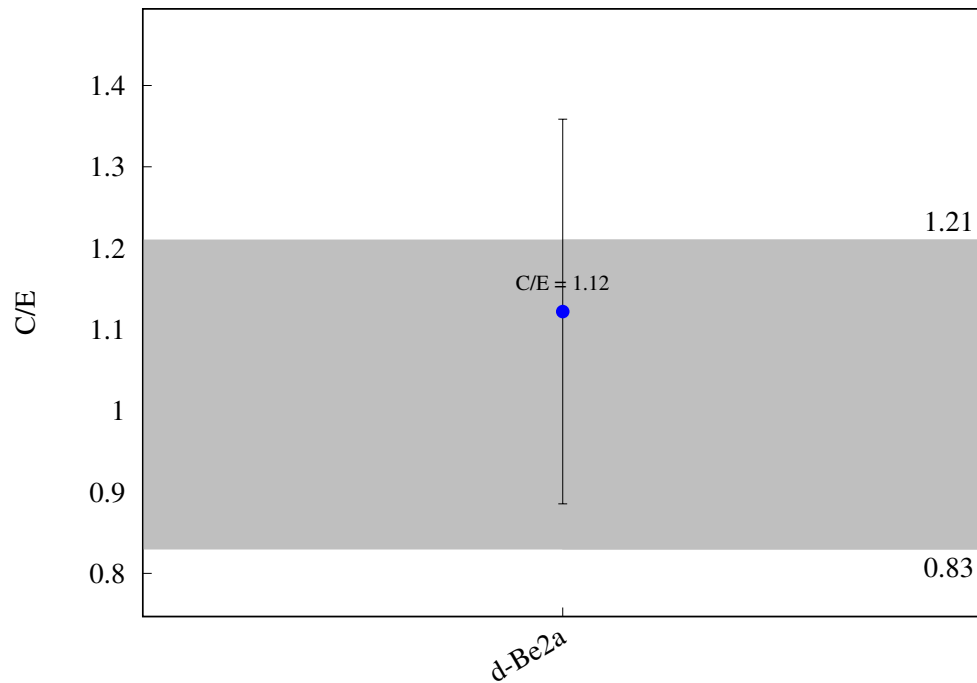
^{64}Zn (n,t) ^{62}Cu 

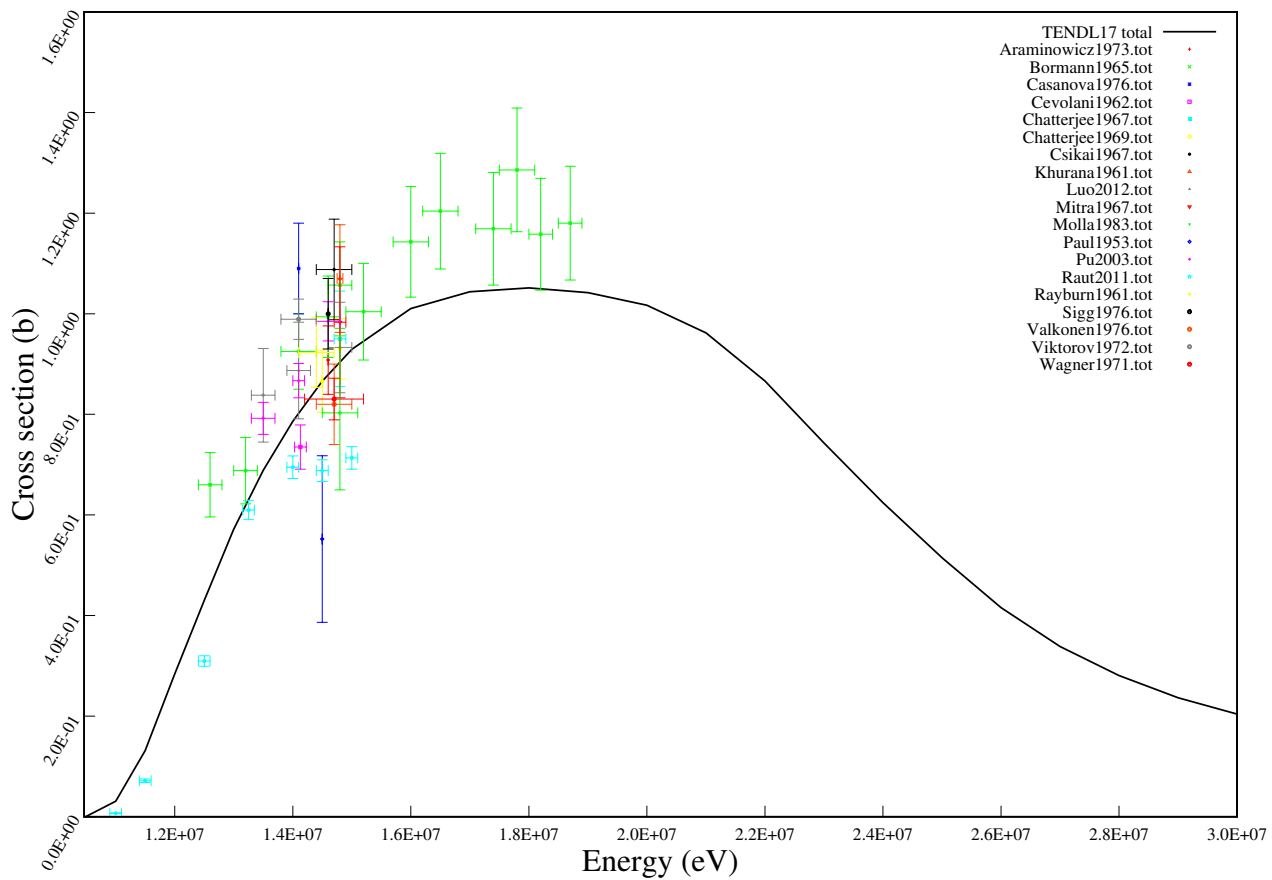
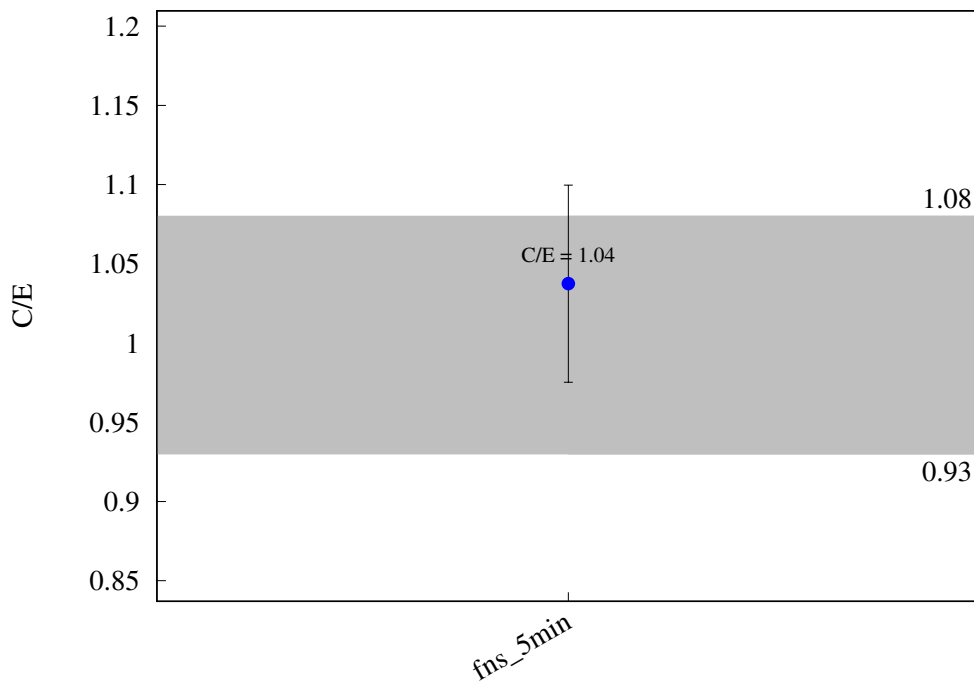
^{64}Zn (n,h) ^{62}Ni 

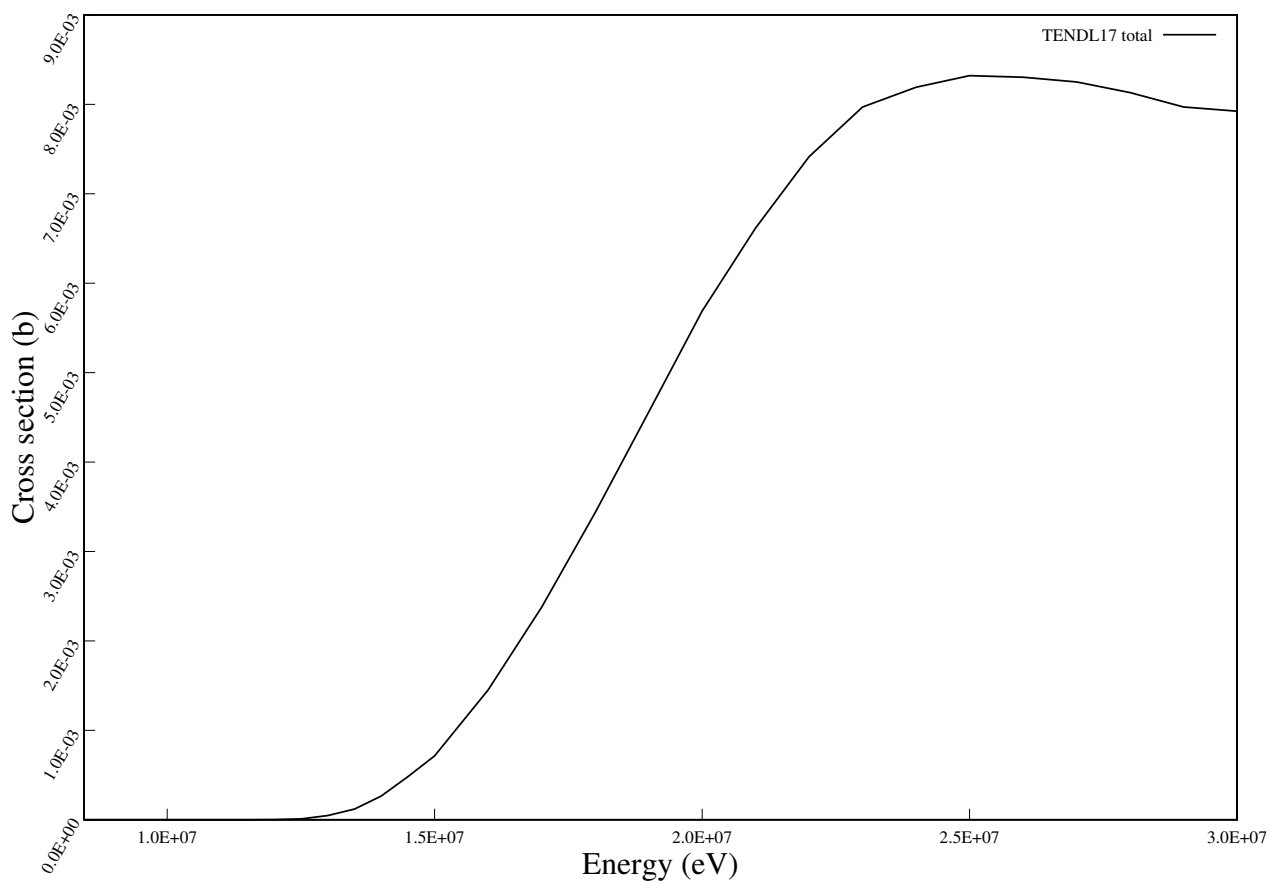
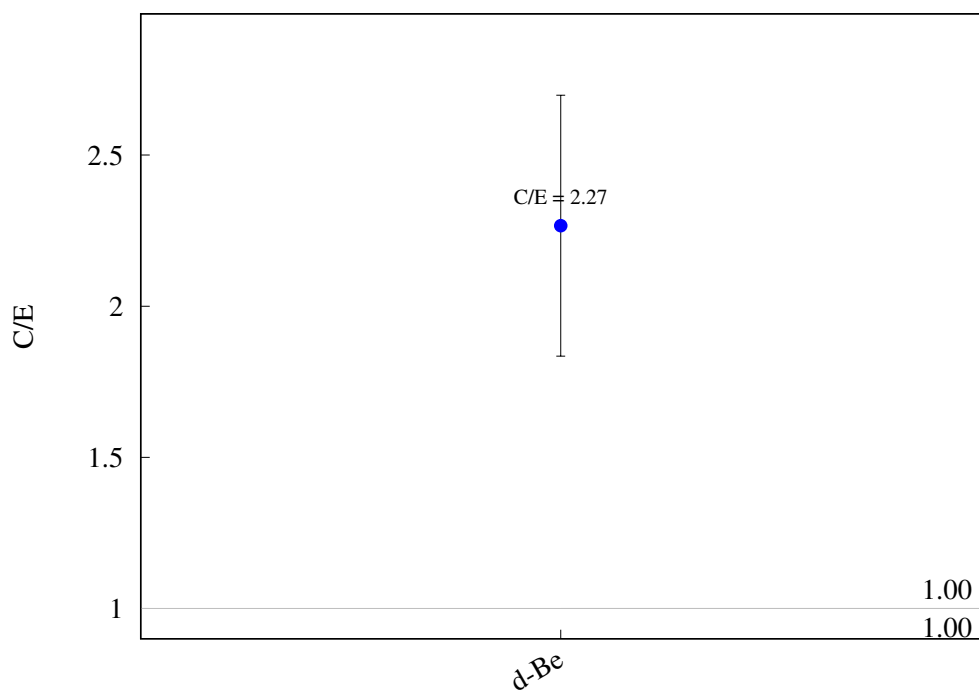
^{67}Zn (n,h) ^{65}Ni 

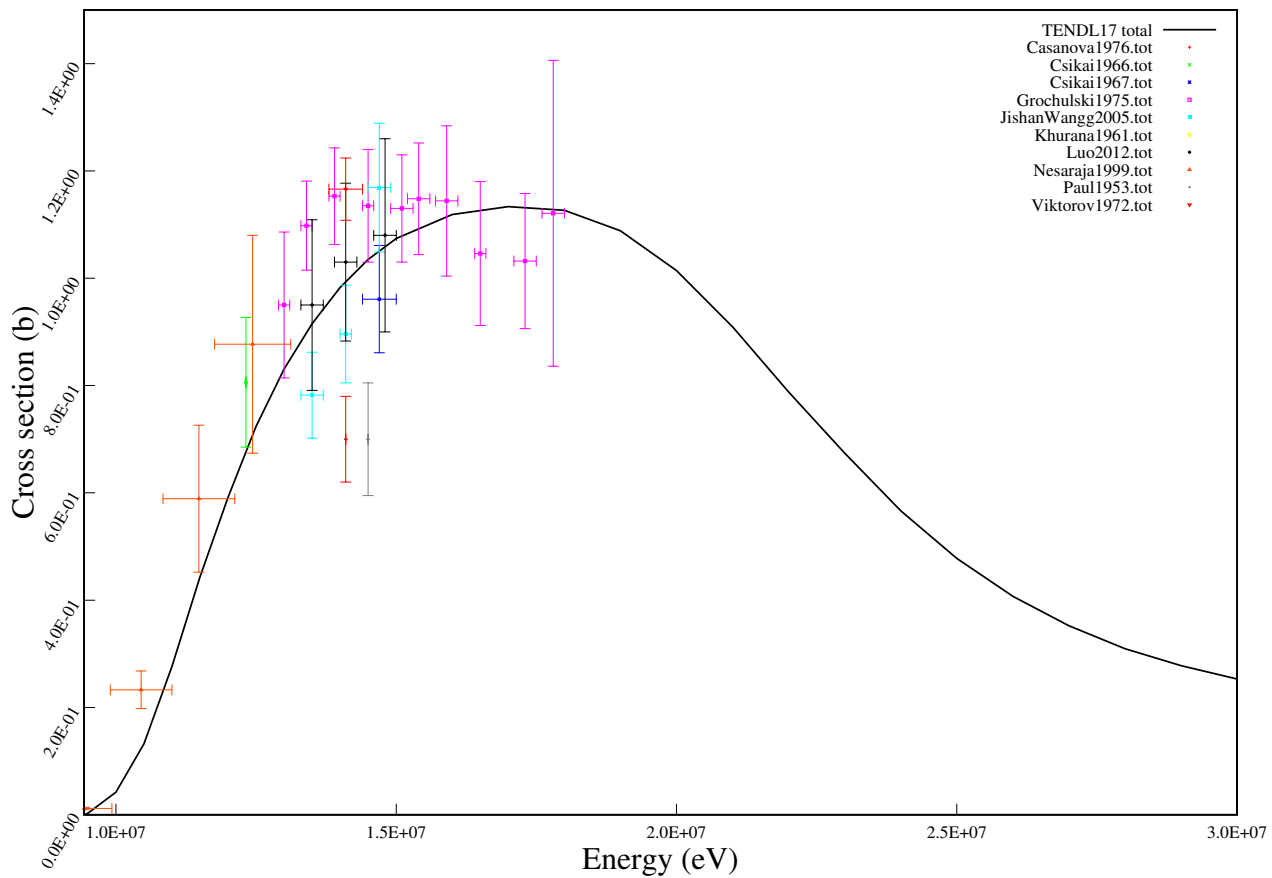
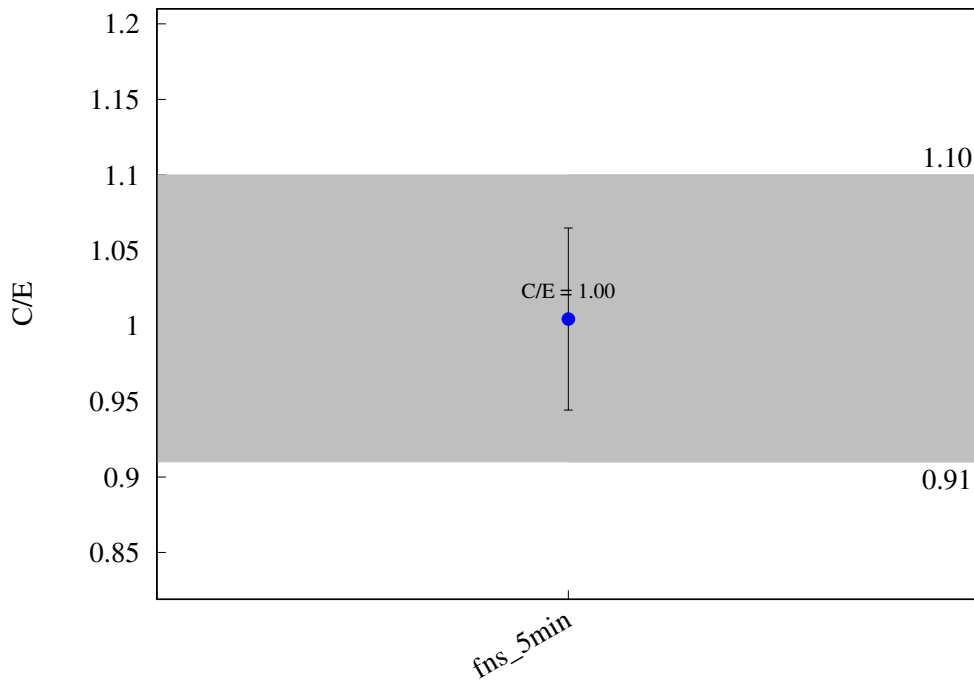
^{68}Zn (n,g) ^{69m}Zn 

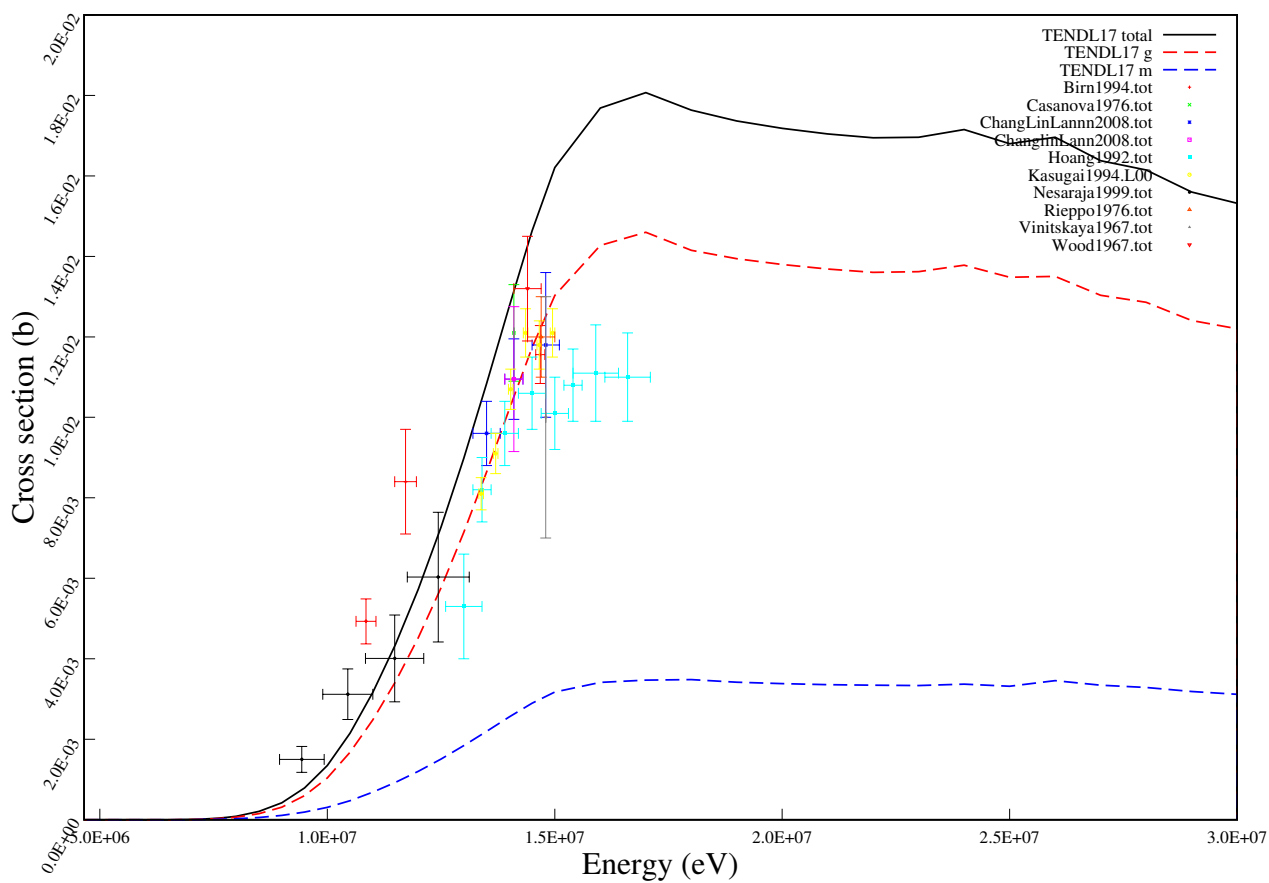
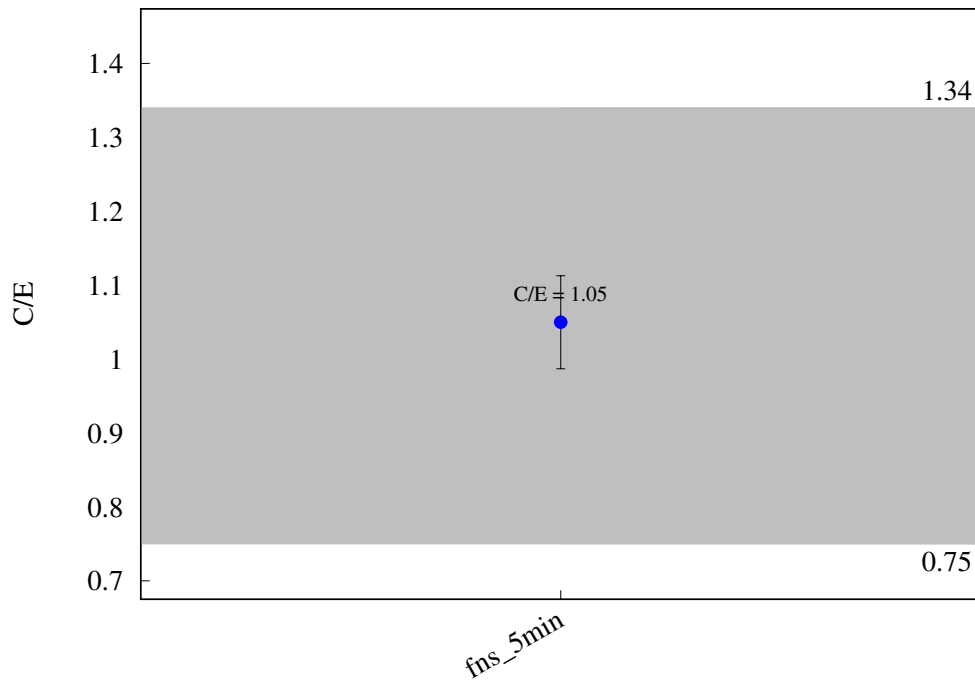
^{68}Zn (n,h) ^{66}Ni 

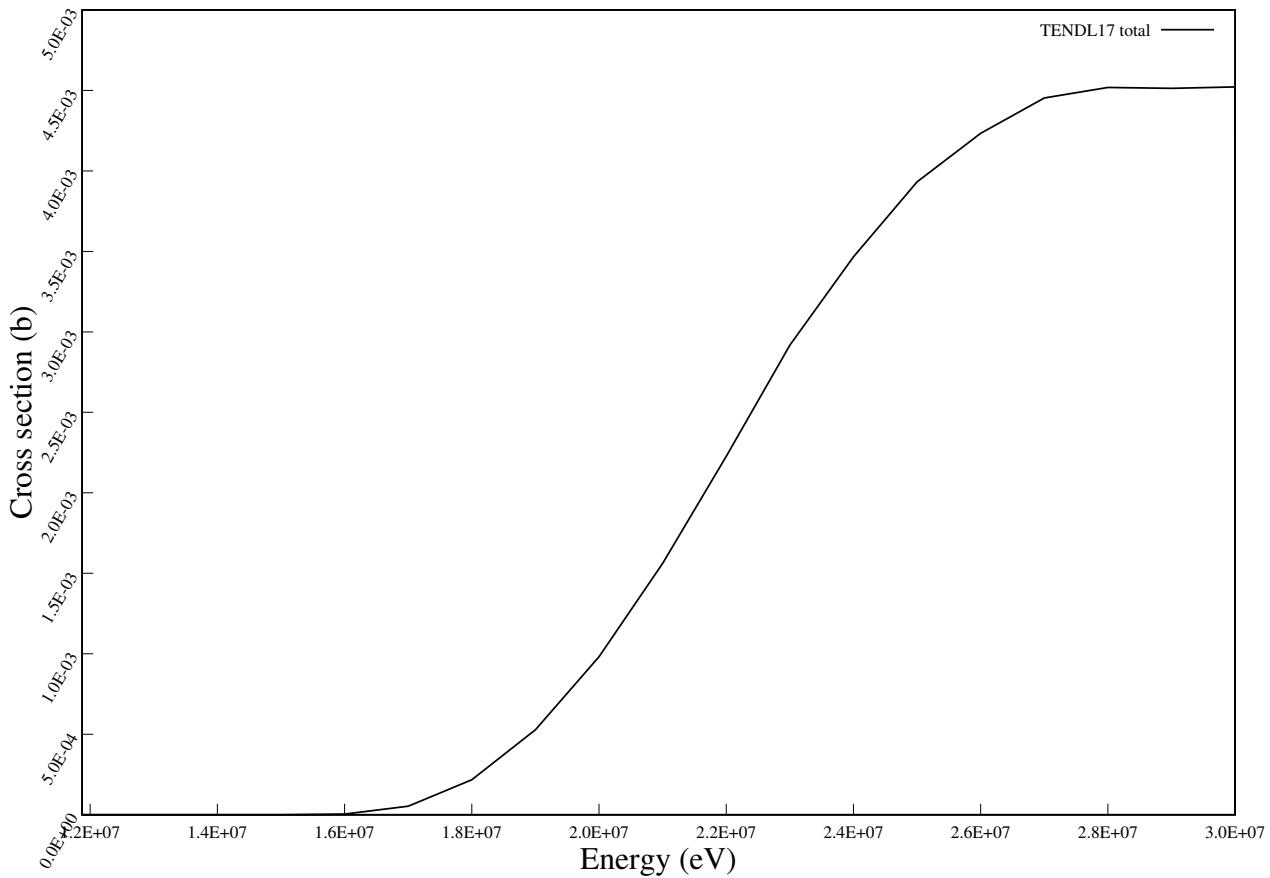
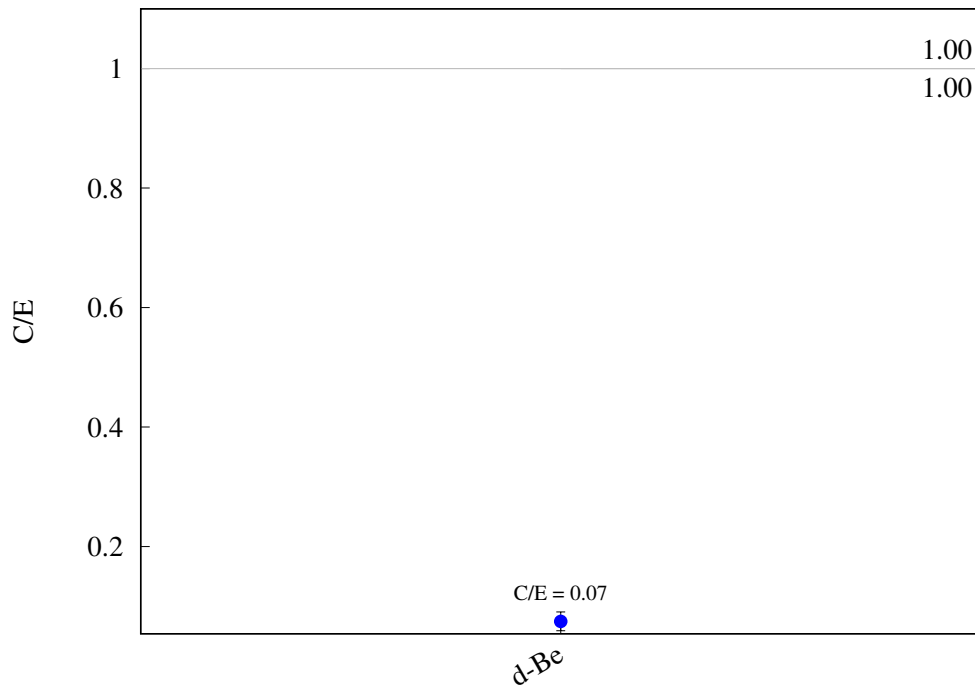
^{68}Zn (n,a) ^{65}Ni 

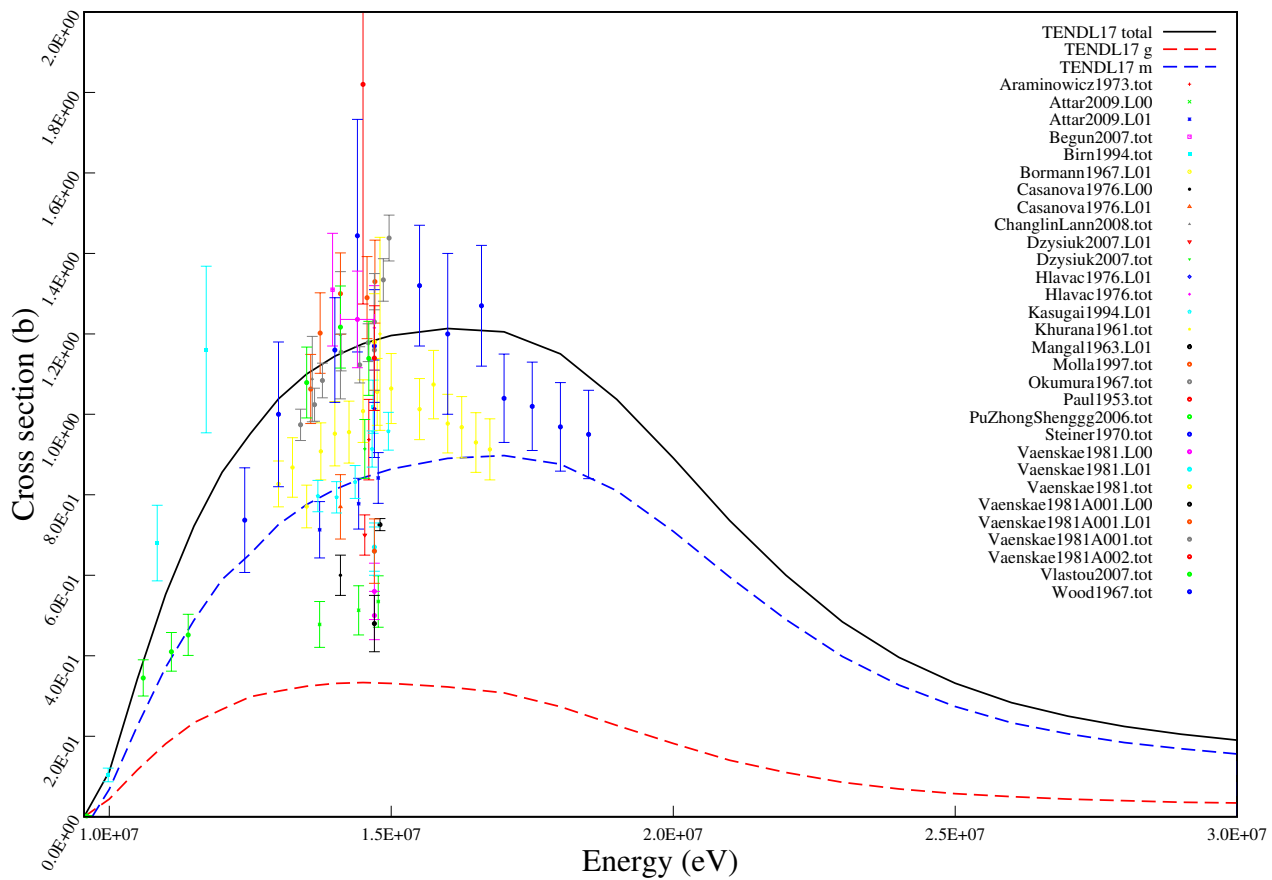
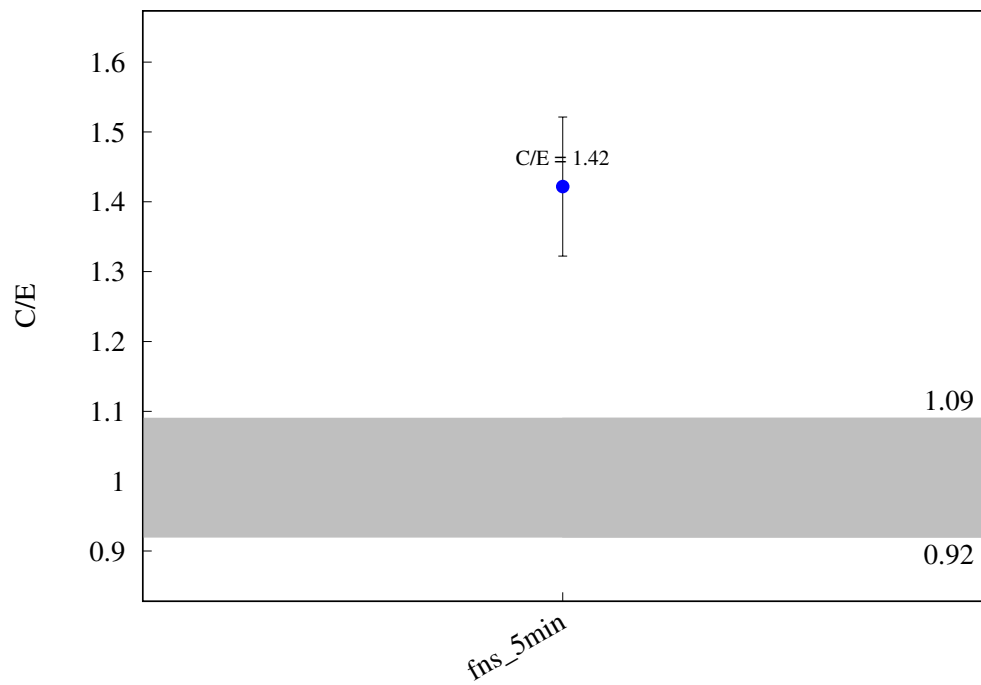
^{69}Ga (n,2n) ^{68}Ga 

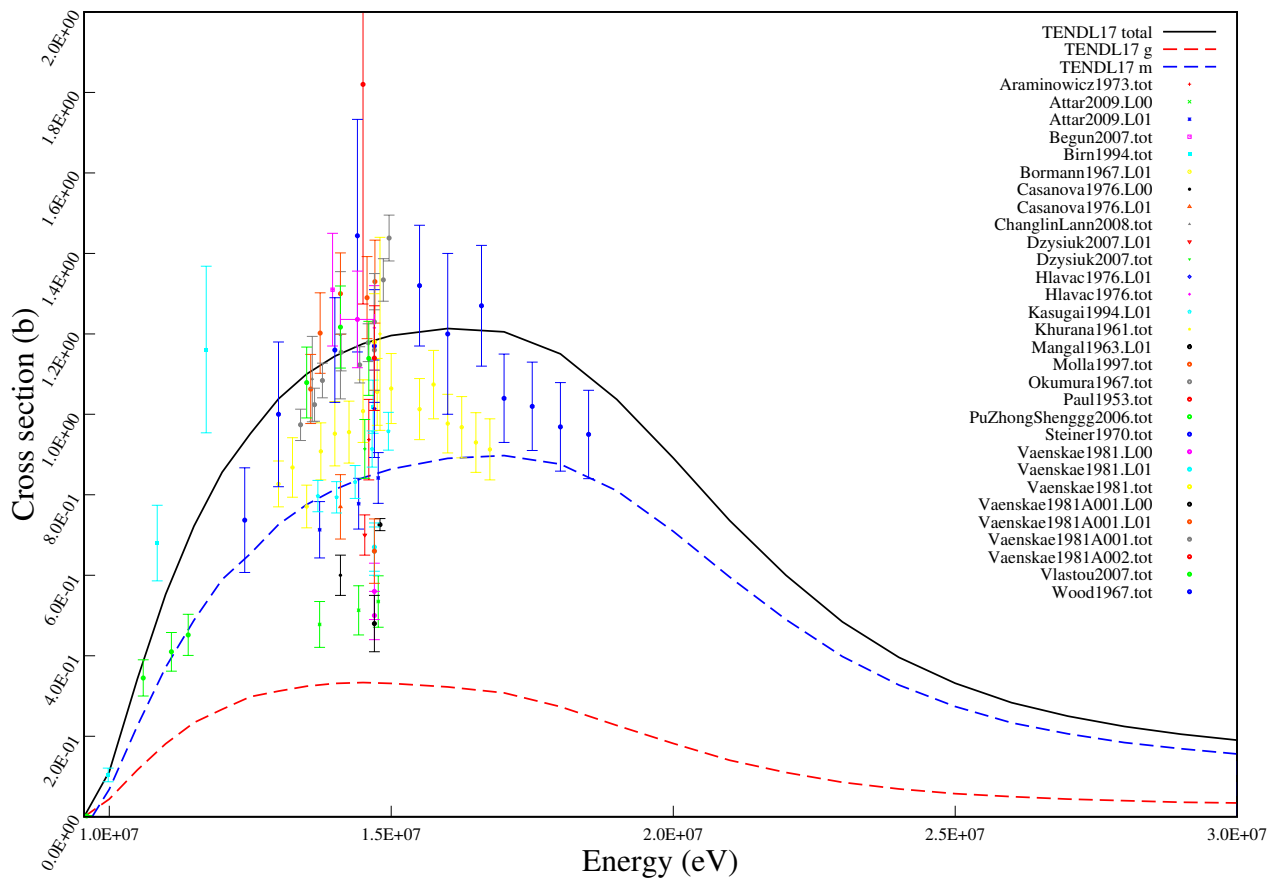
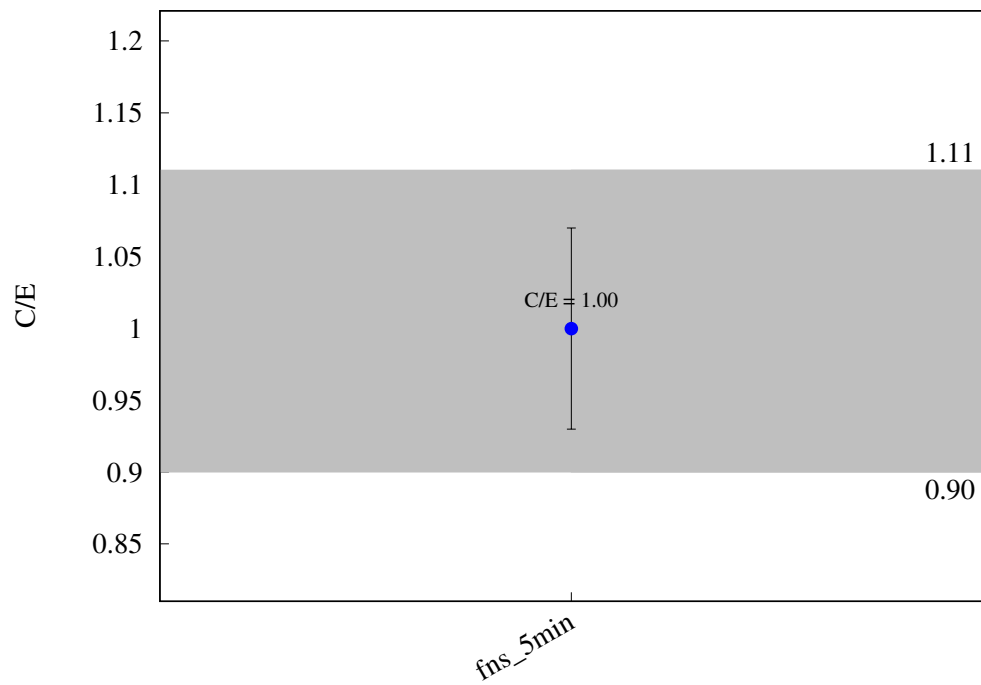
^{69}Ga (n,t) ^{67}Zn 

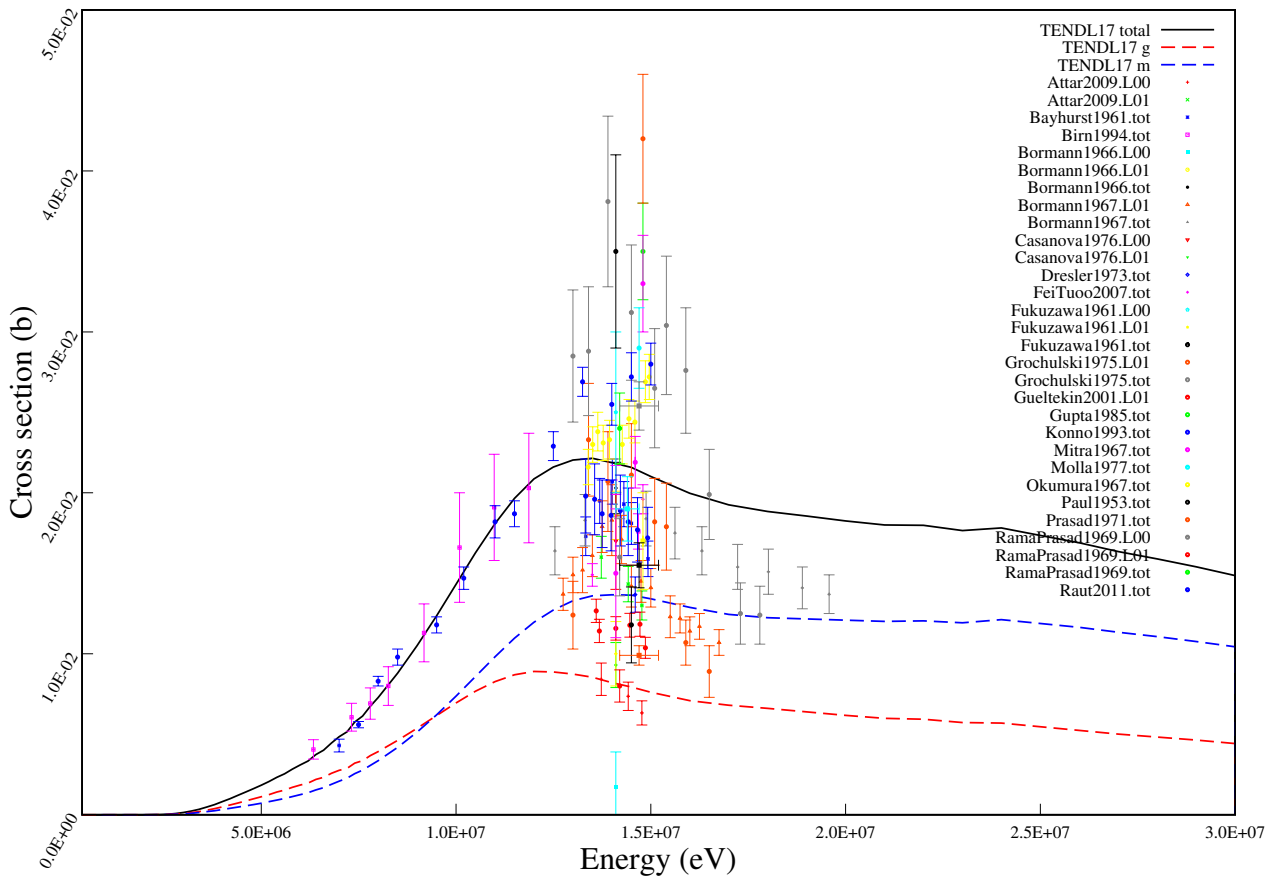
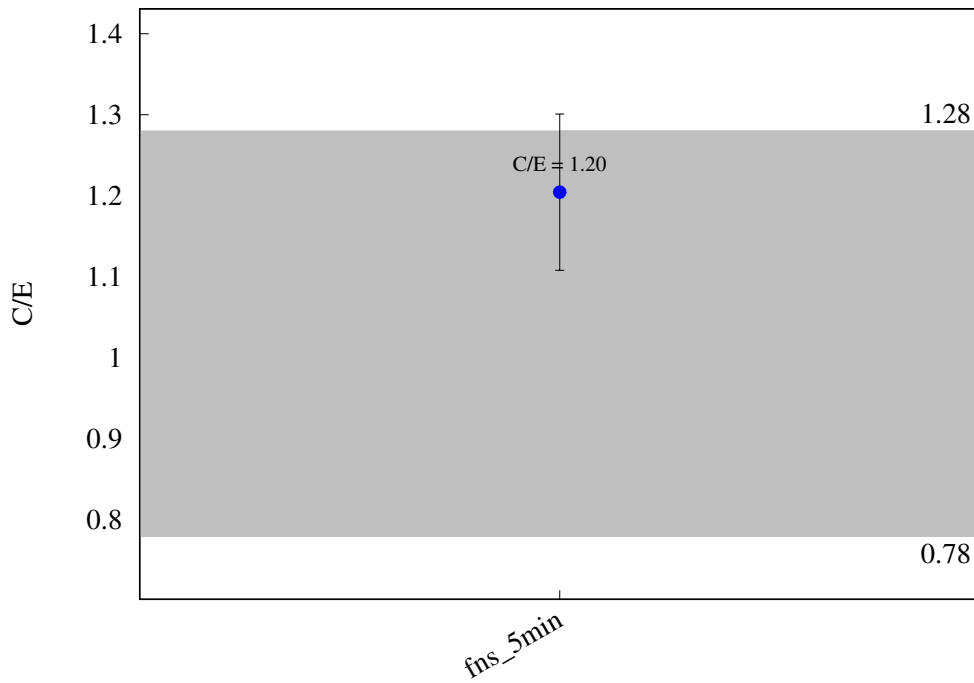
^{71}Ga (n,2n) ^{70}Ga 

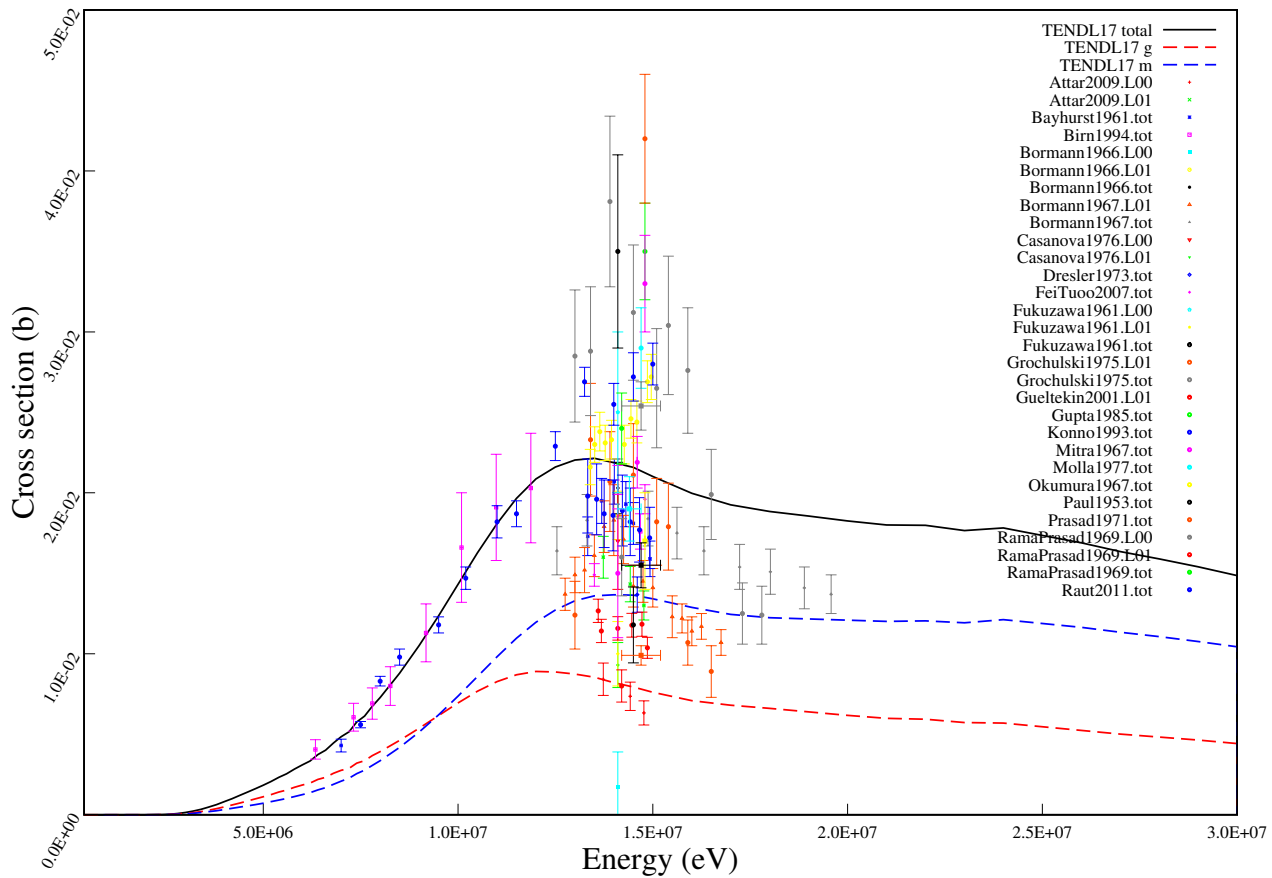
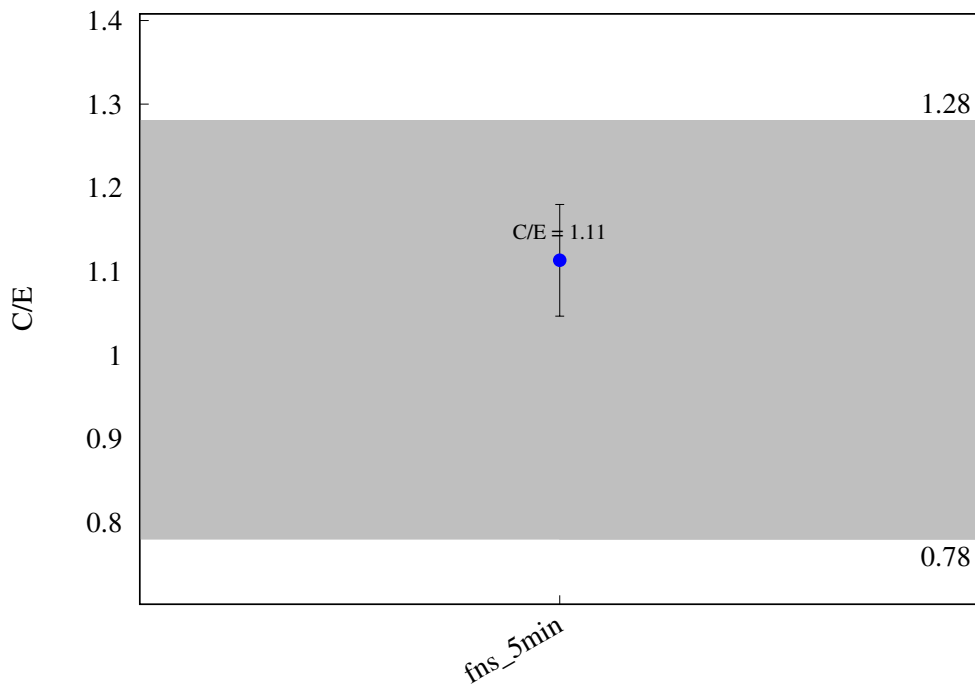
^{74}Ge (n,p) ^{74}Ga 

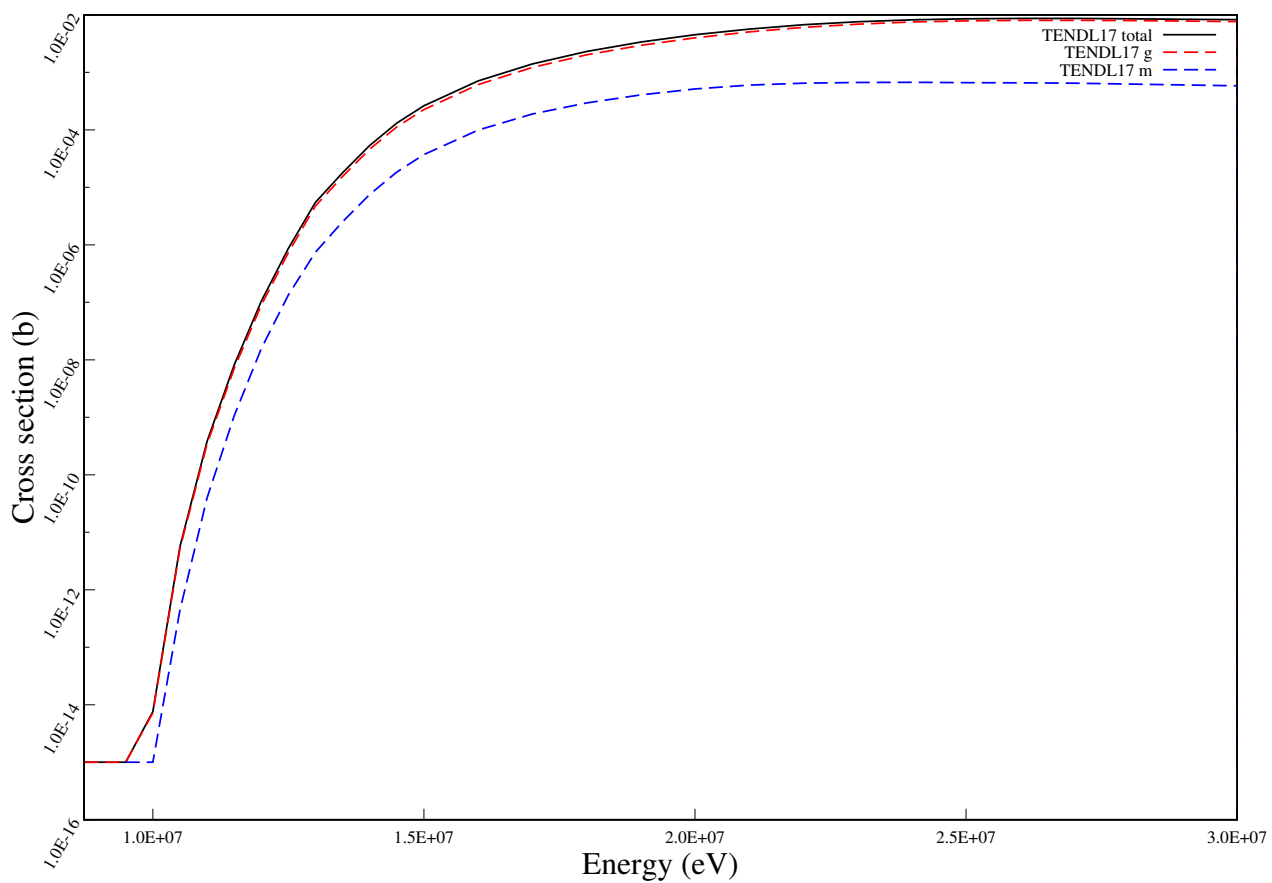
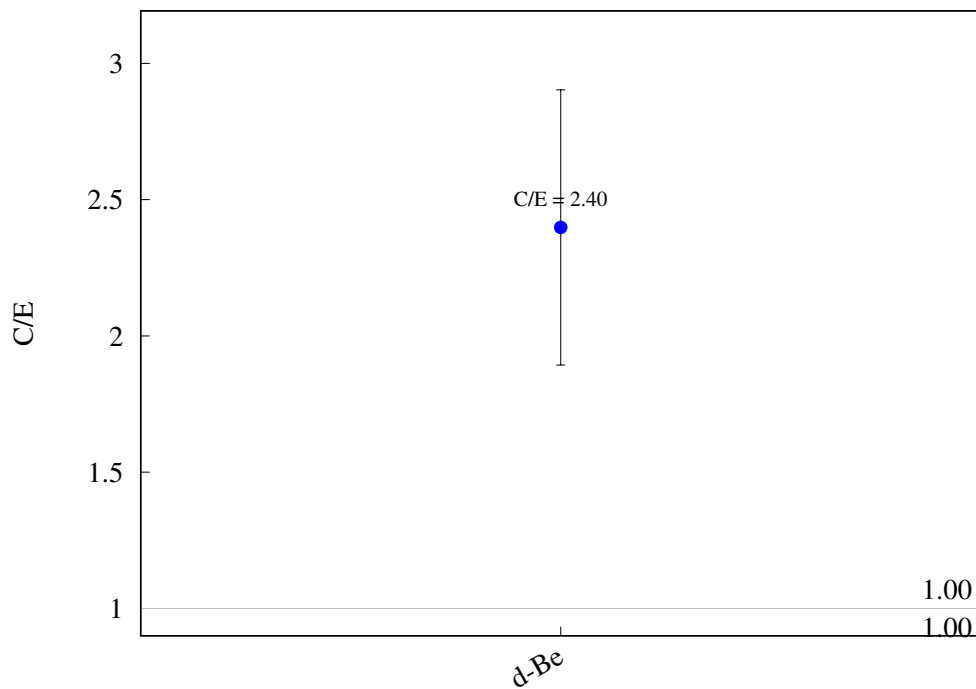
^{74}Ge (n,t) ^{72}Ga 

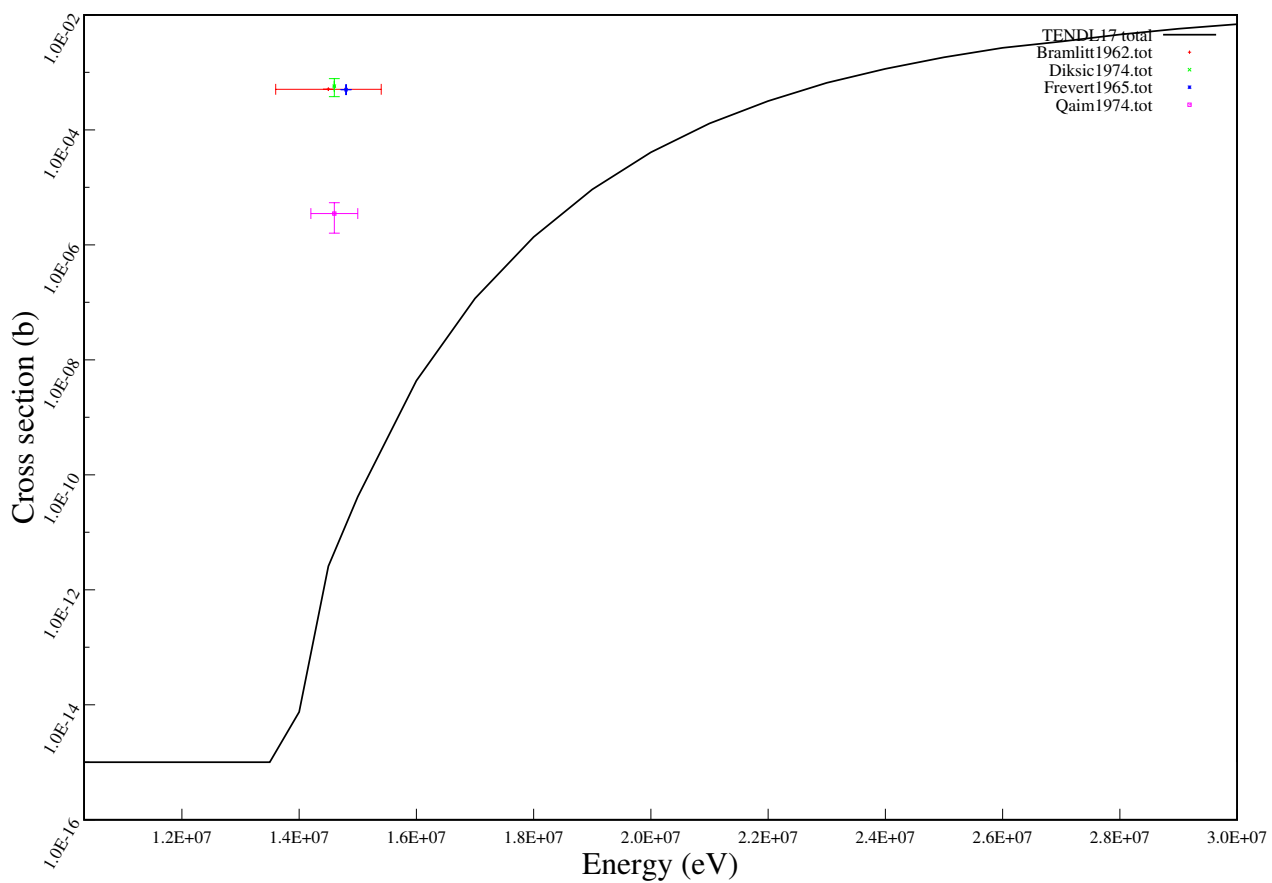
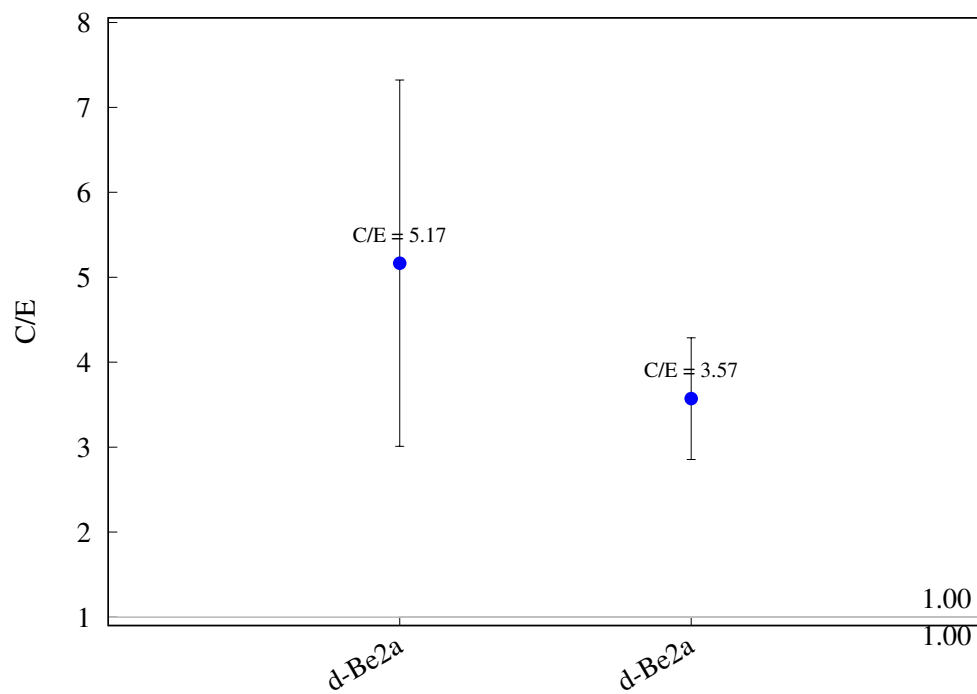
^{76}Ge (n,2n) $^{75\text{m}}\text{Ge}$ 

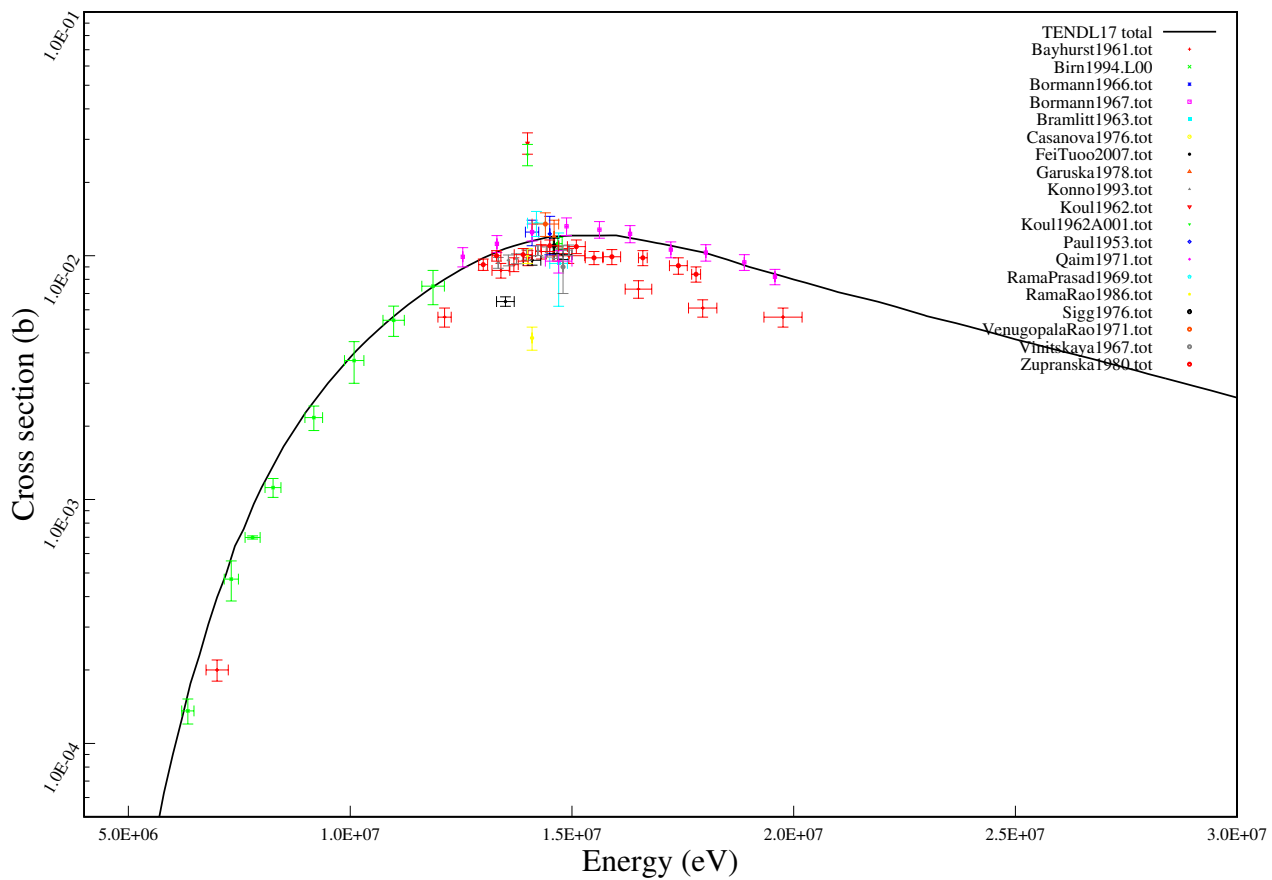
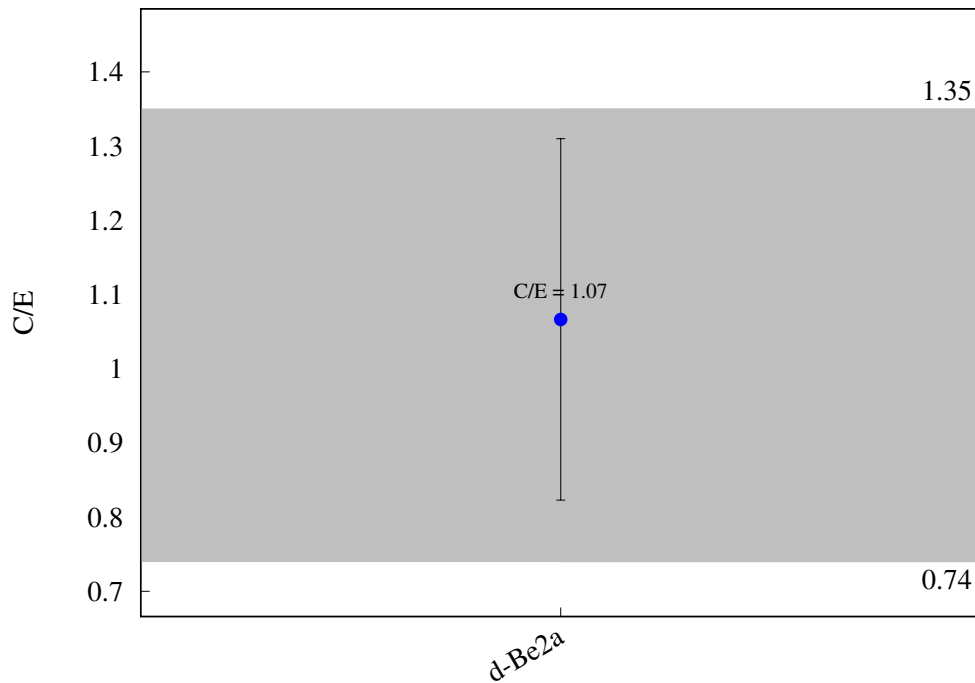
^{76}Ge (n,2n) ^{75}Ge 

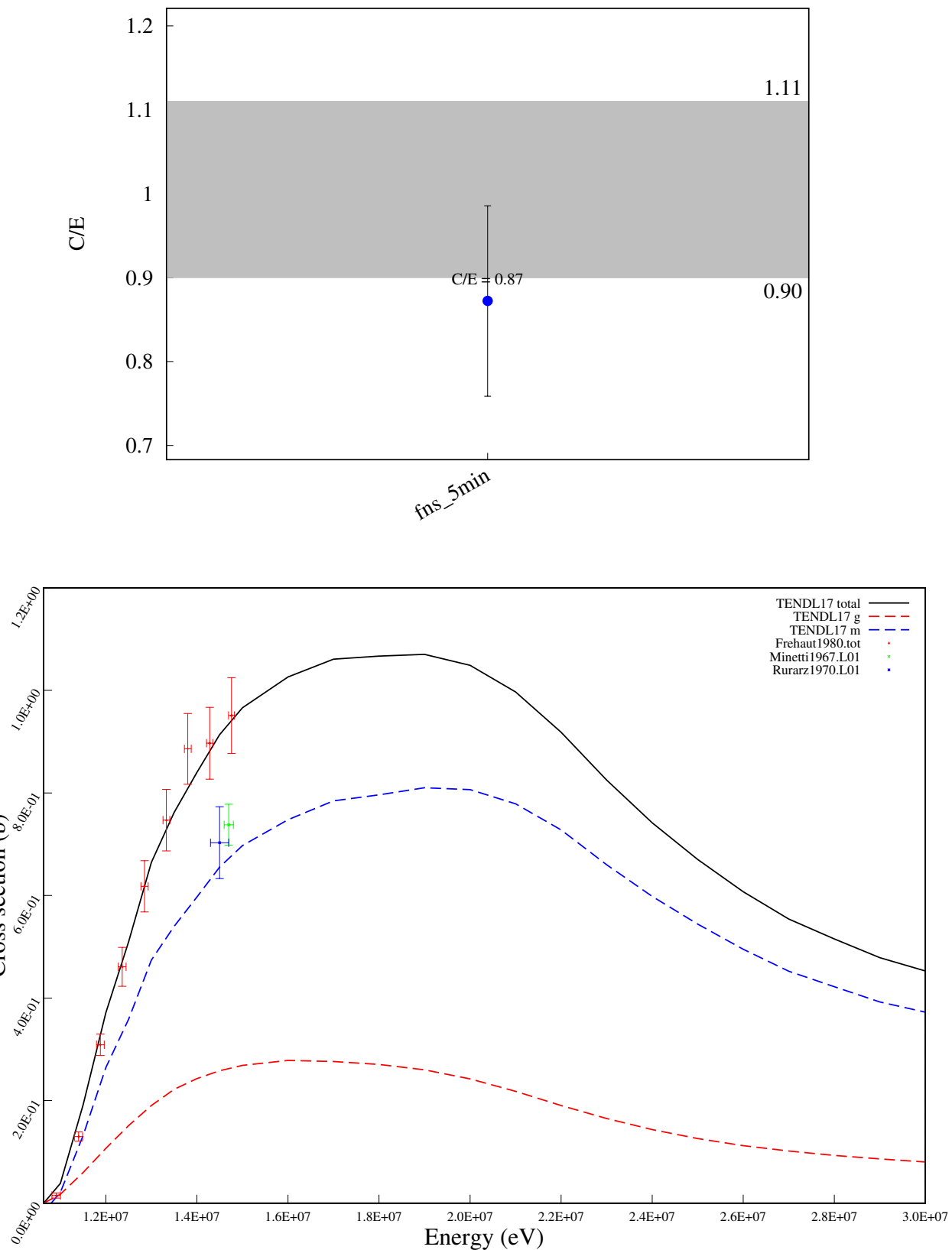
^{75}As (n,p) $^{75\text{m}}\text{Ge}$ 

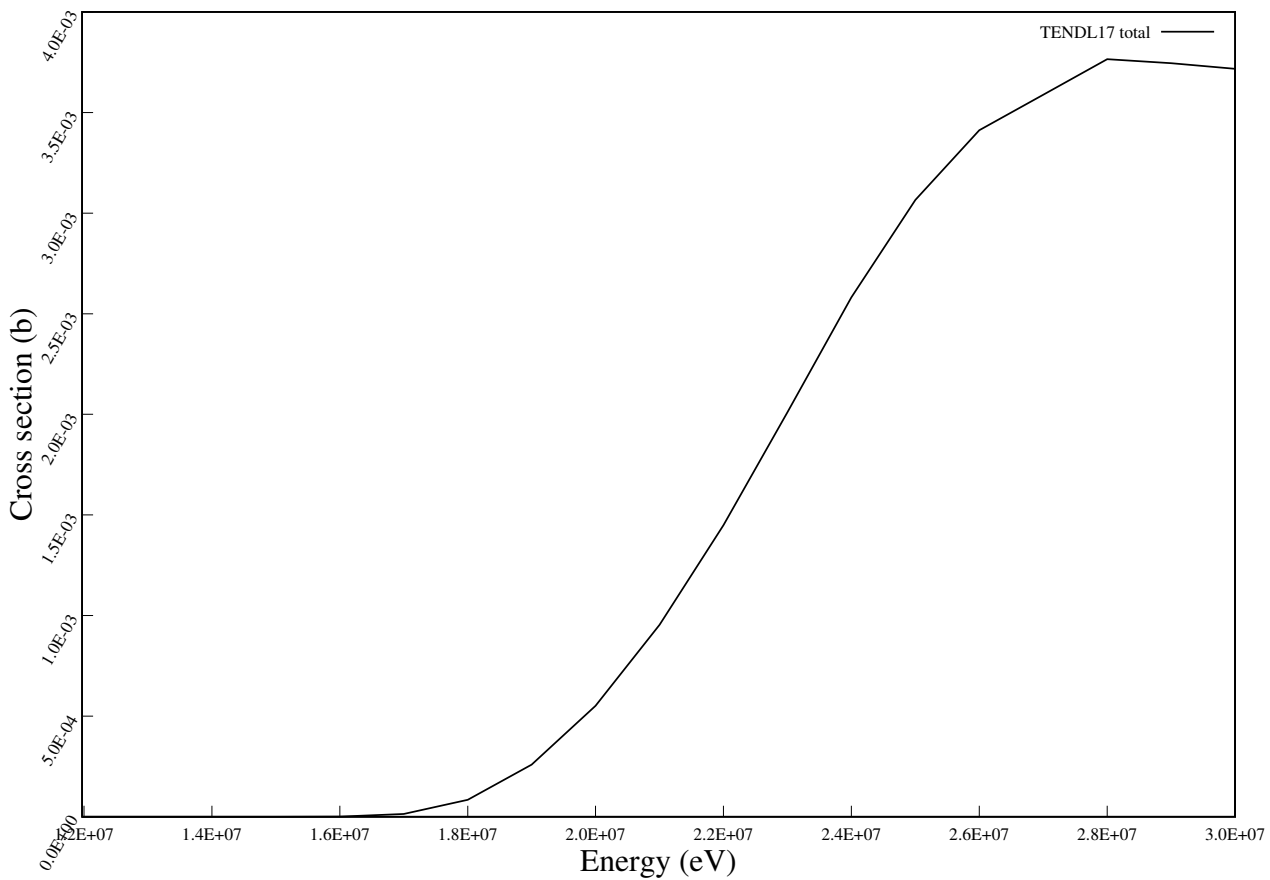
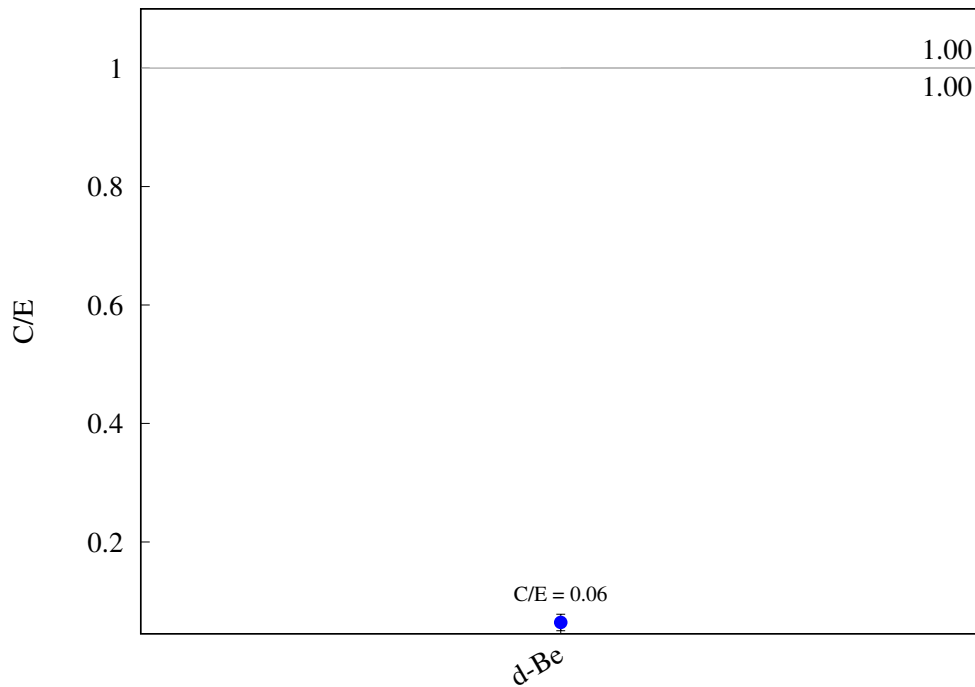
$^{75}\text{As} (\text{n},\text{p}) ^{75}\text{Ge}$ 

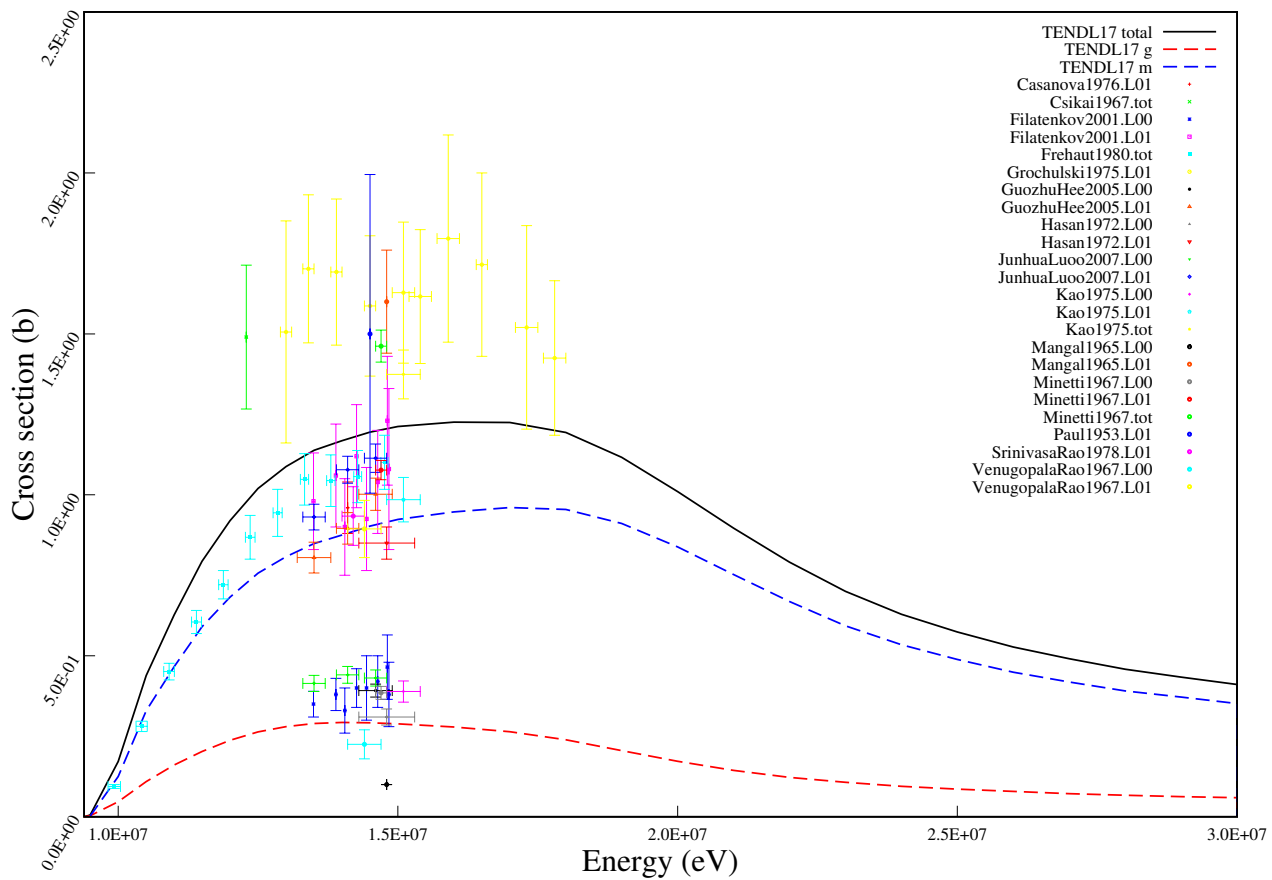
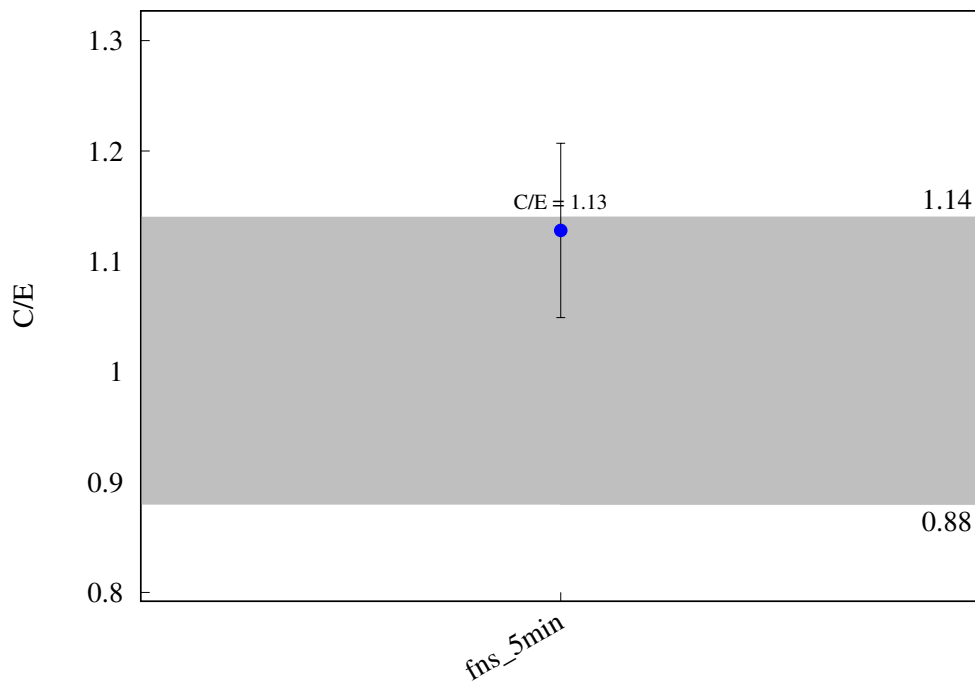
$^{75}\text{As} (\text{n},\text{t}) ^{73}\text{Ge}$ 

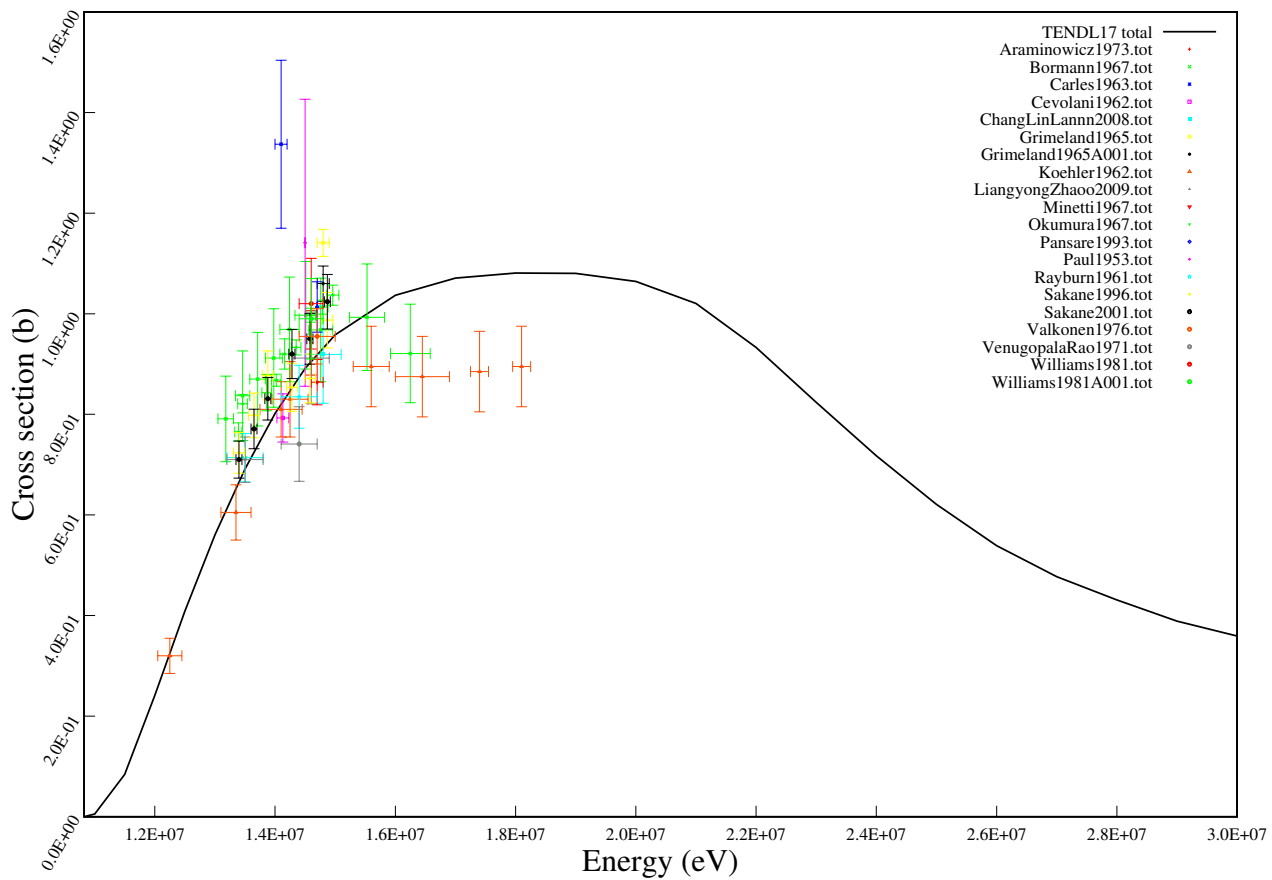
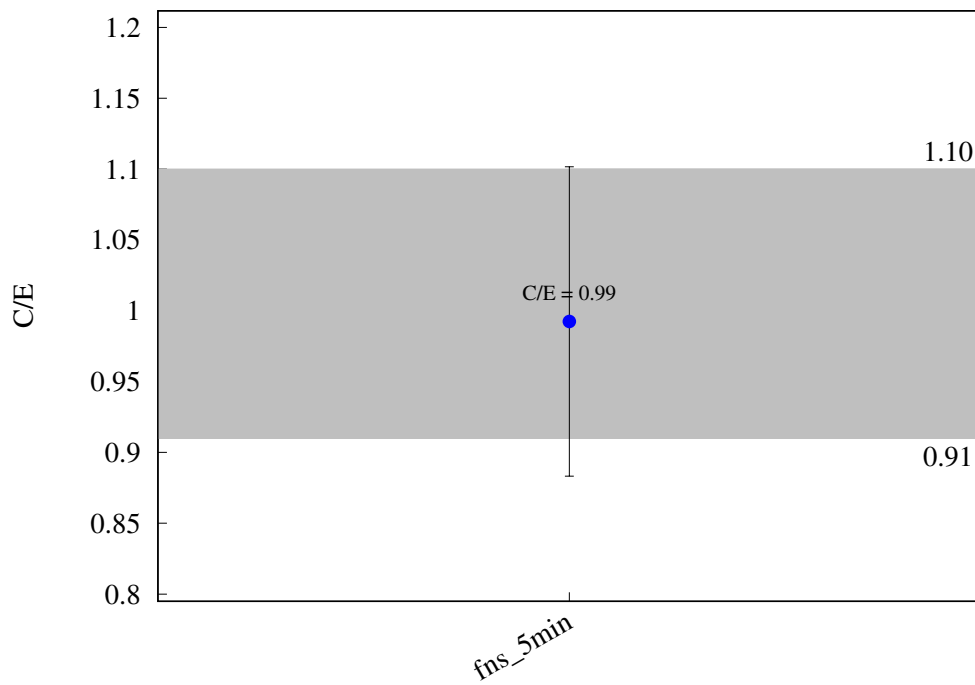
$^{75}\text{As} (\text{n},\text{h}) ^{73}\text{Ga}$ 

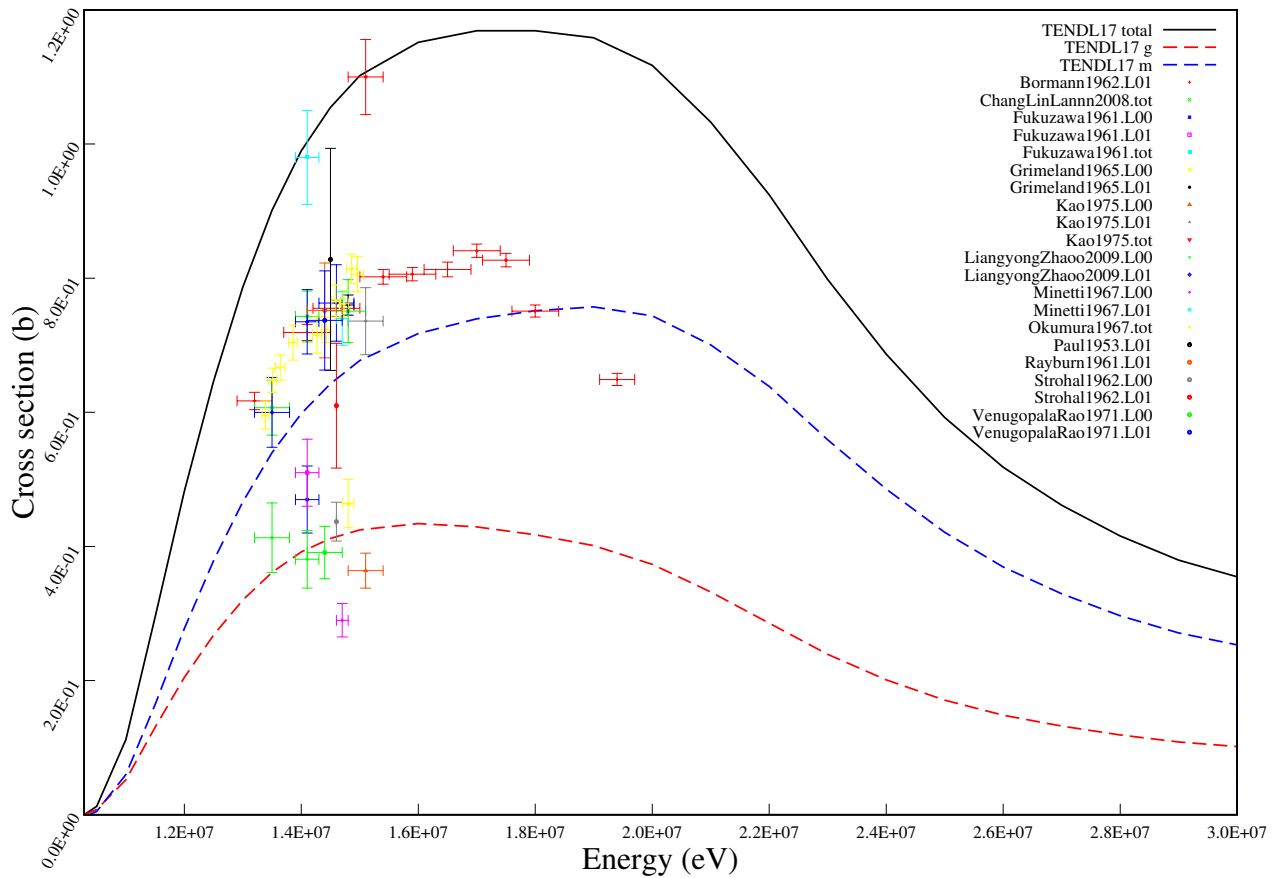
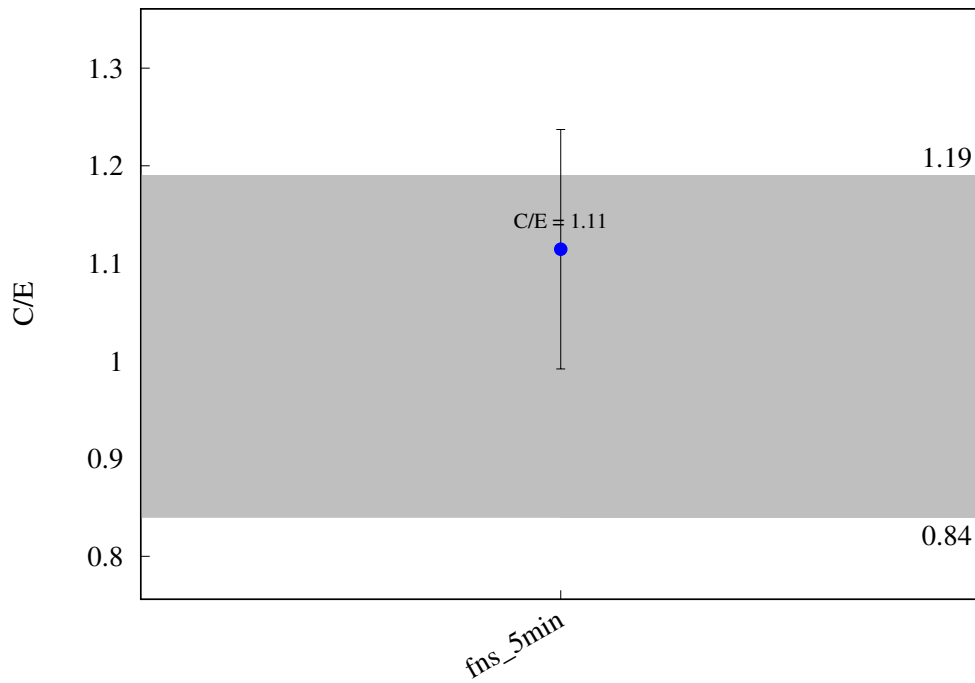
$^{75}\text{As} (\text{n},\text{a}) ^{72}\text{Ga}$ 

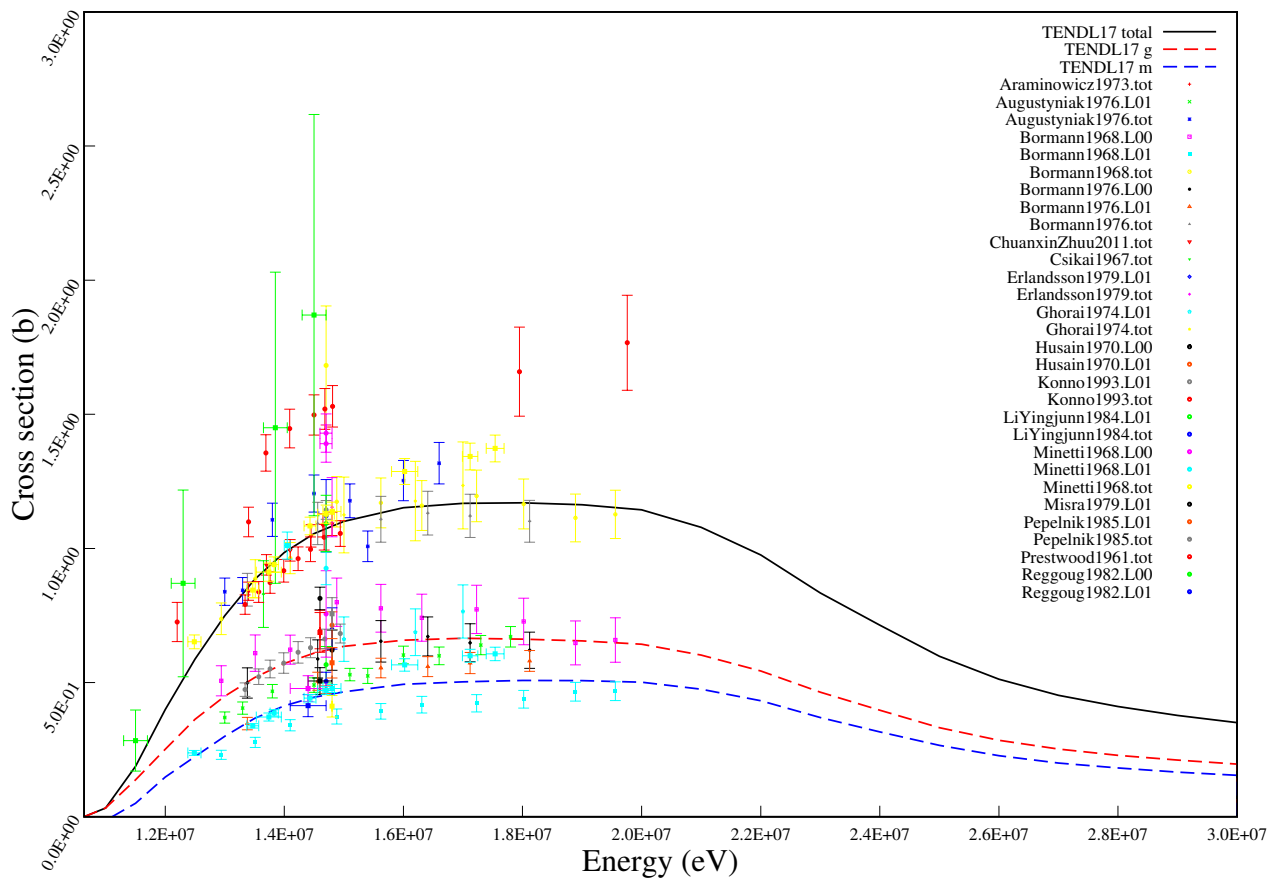
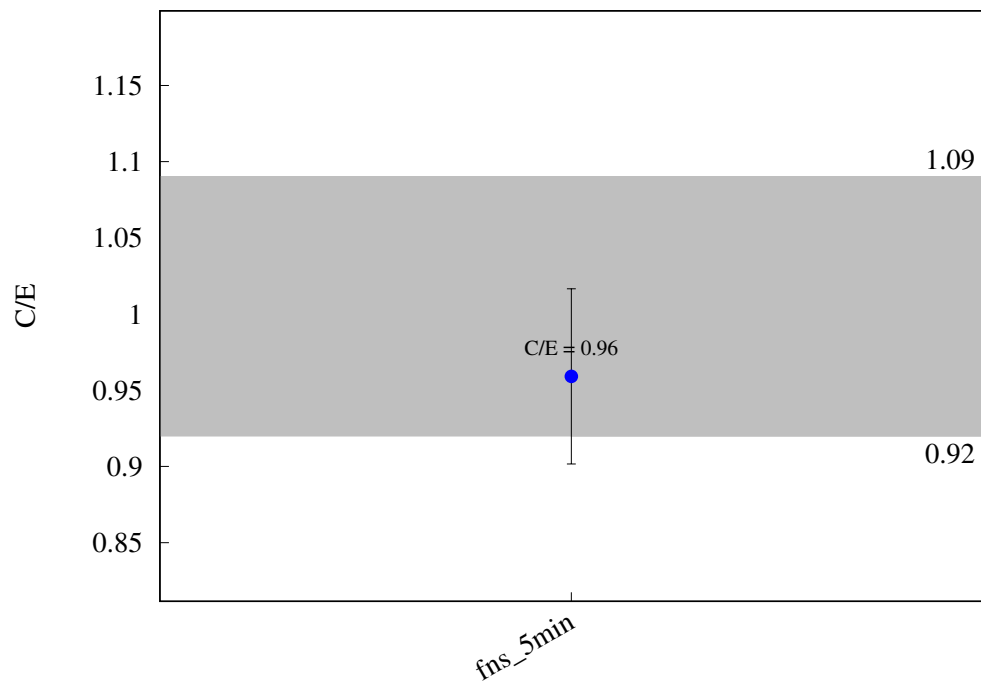
^{78}Se (n,2n) $^{77\text{m}}\text{Se}$ 

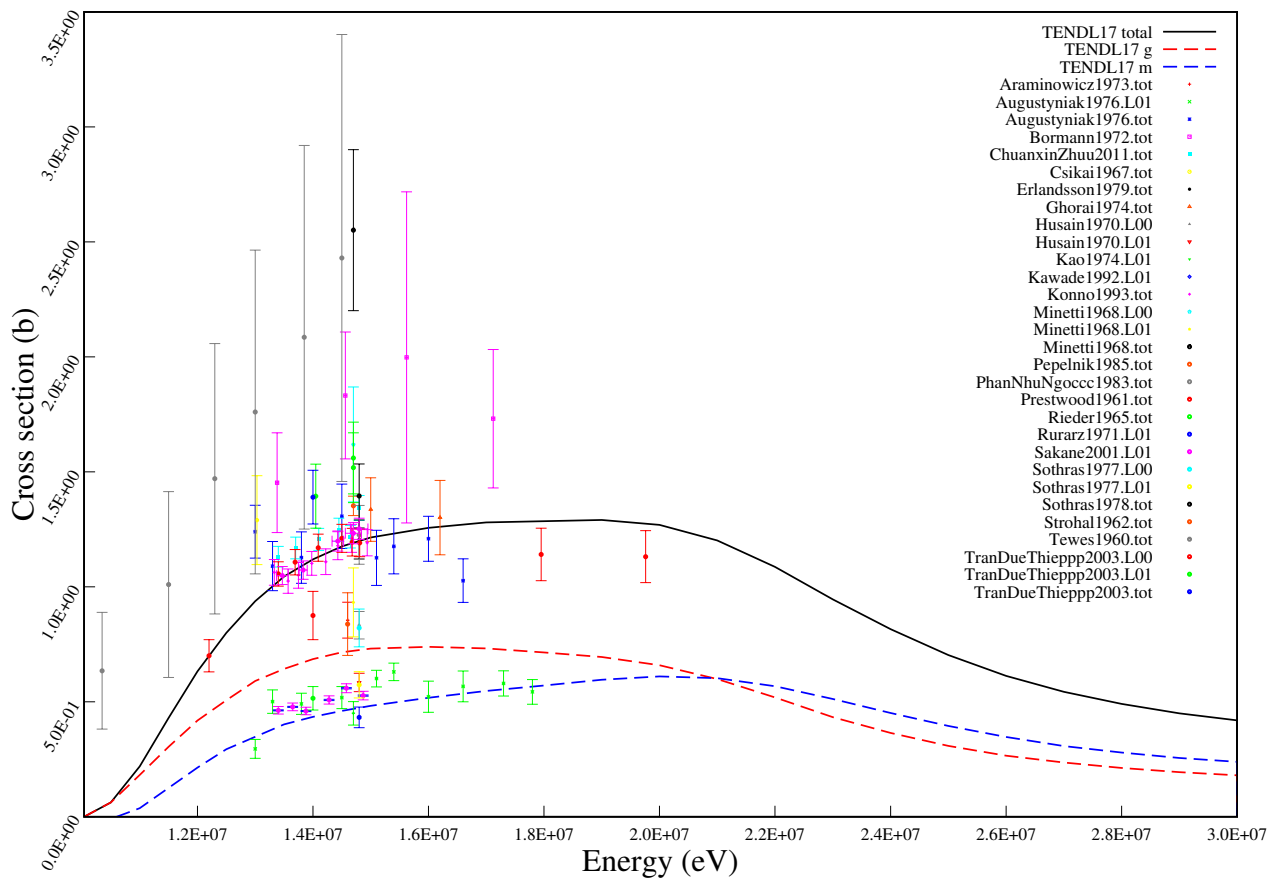
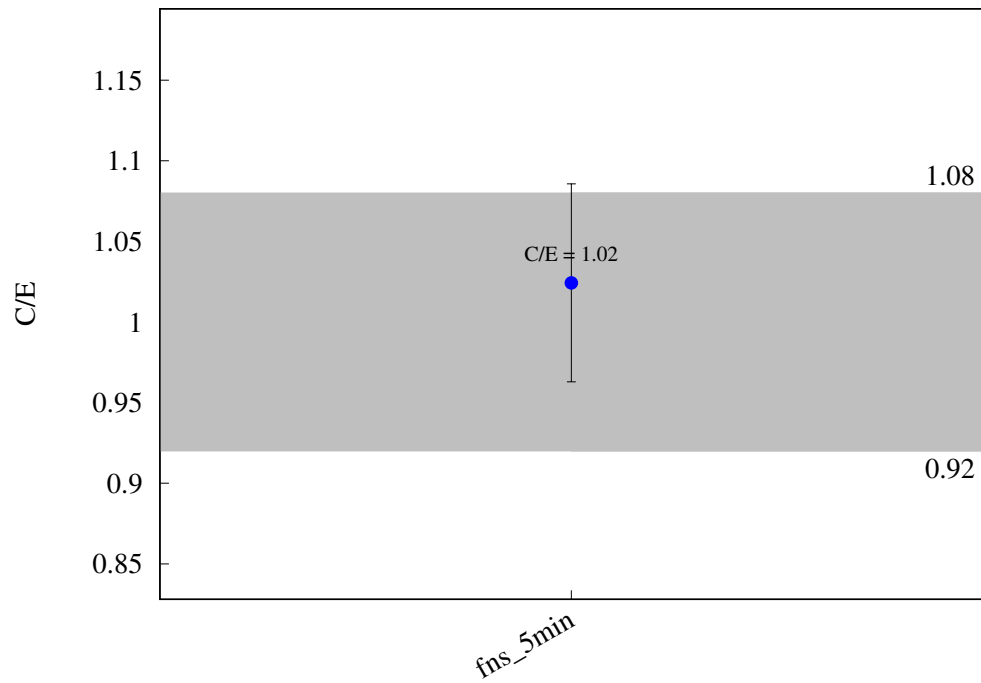
^{80}Se (n,t) ^{78}As 

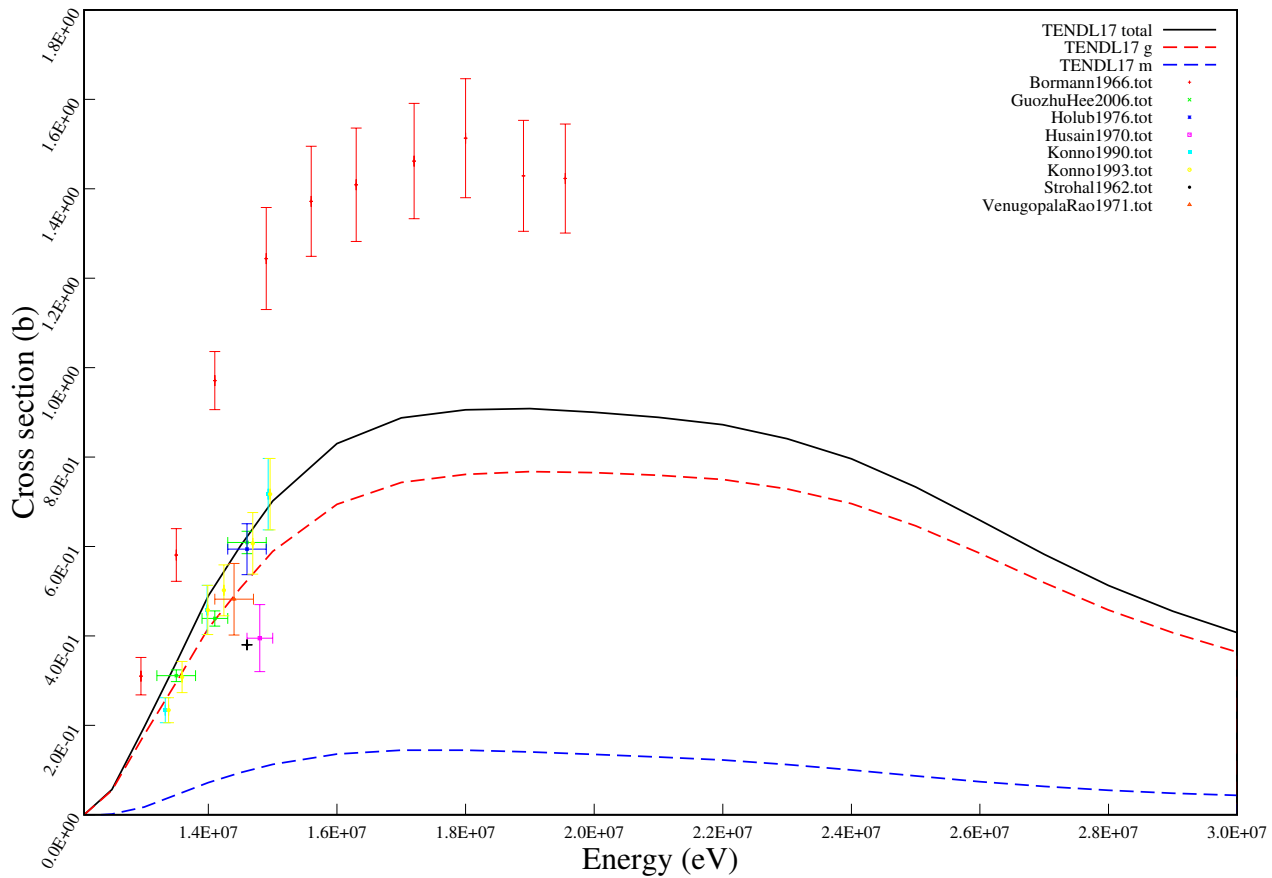
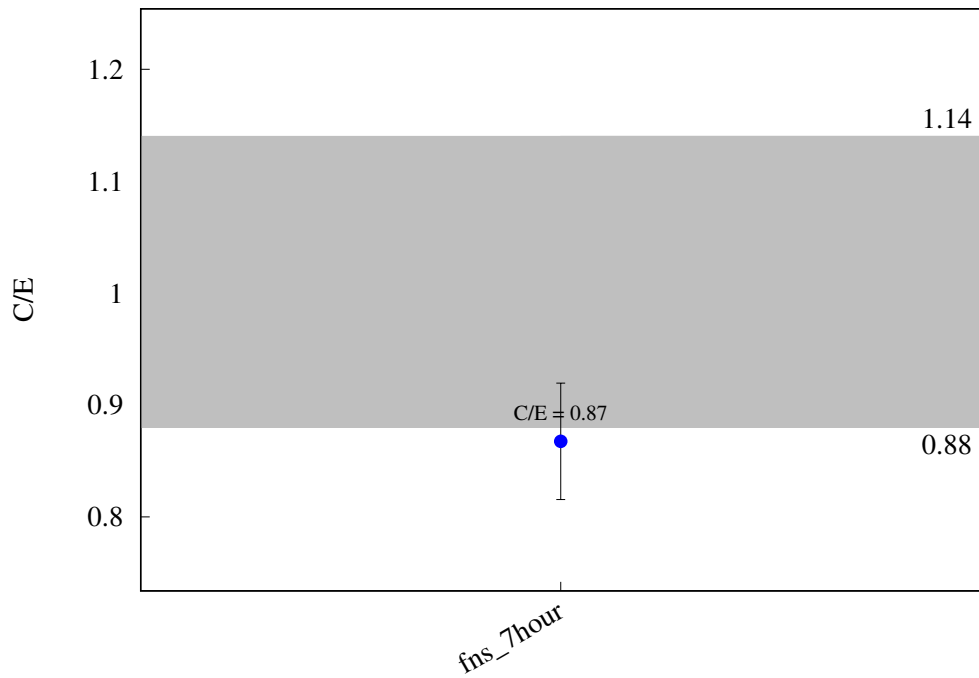
^{82}Se (n,2n) ^{81}Se 

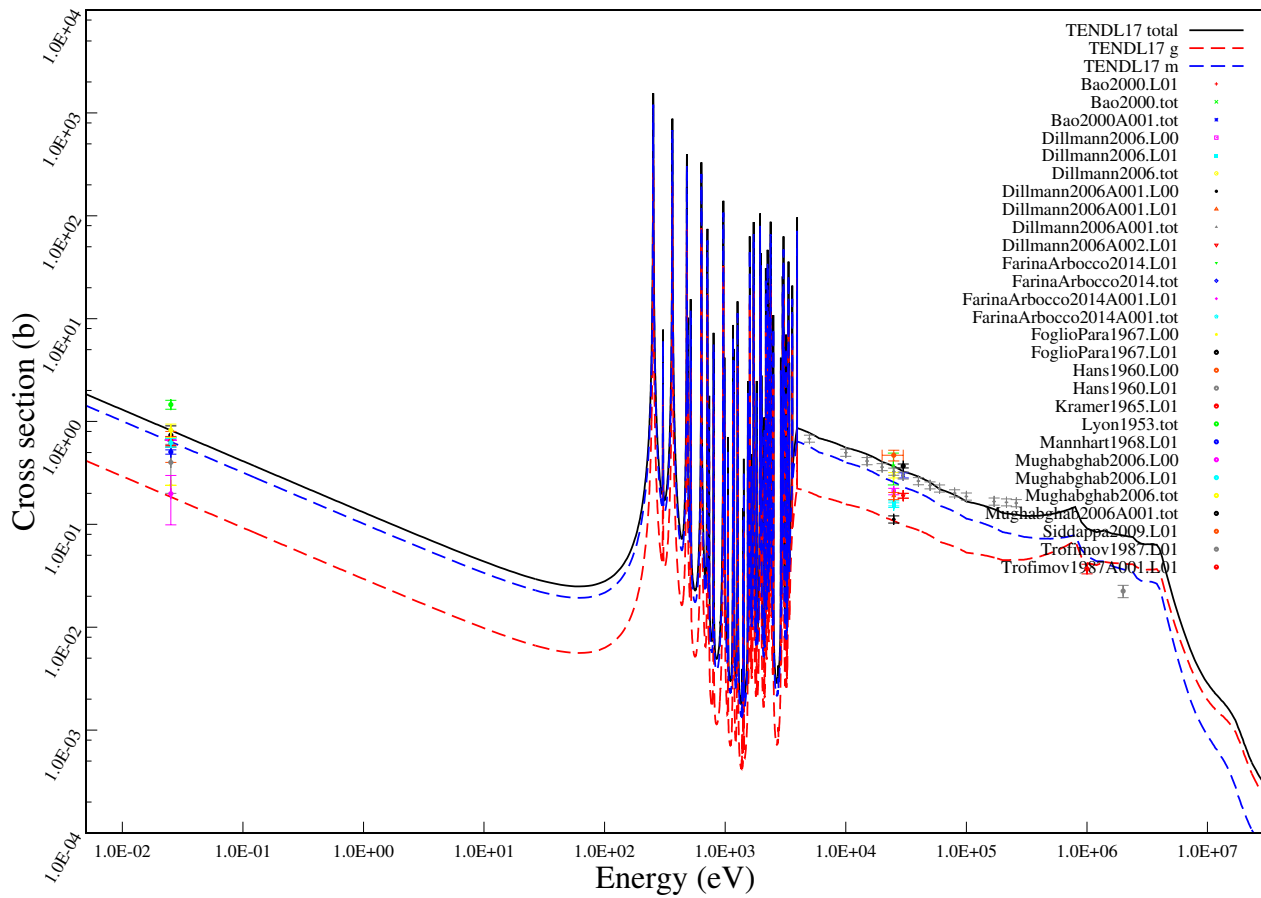
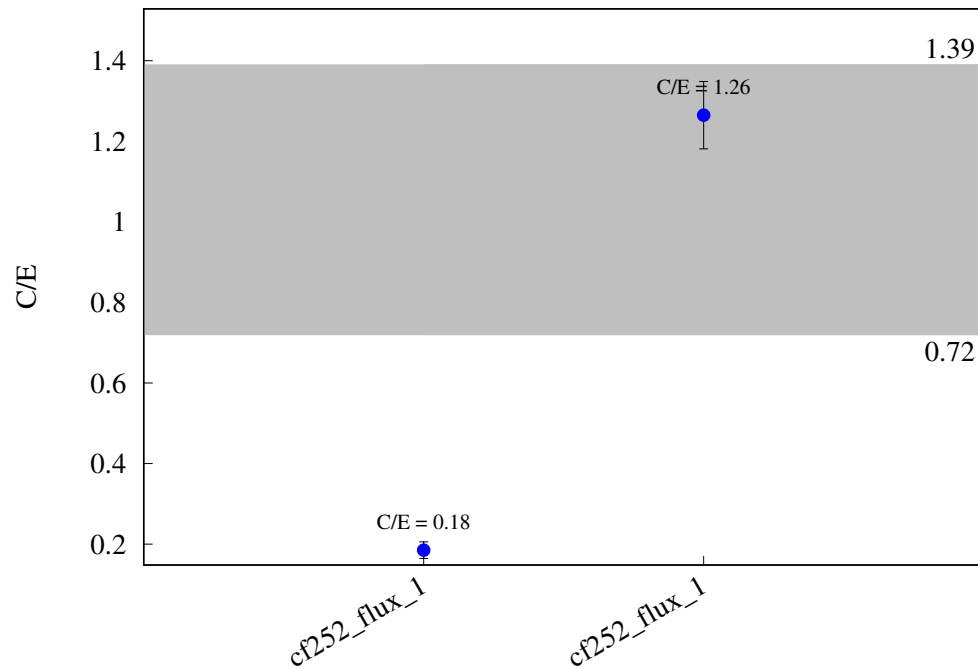
^{79}Br (n,2n) ^{78}Br 

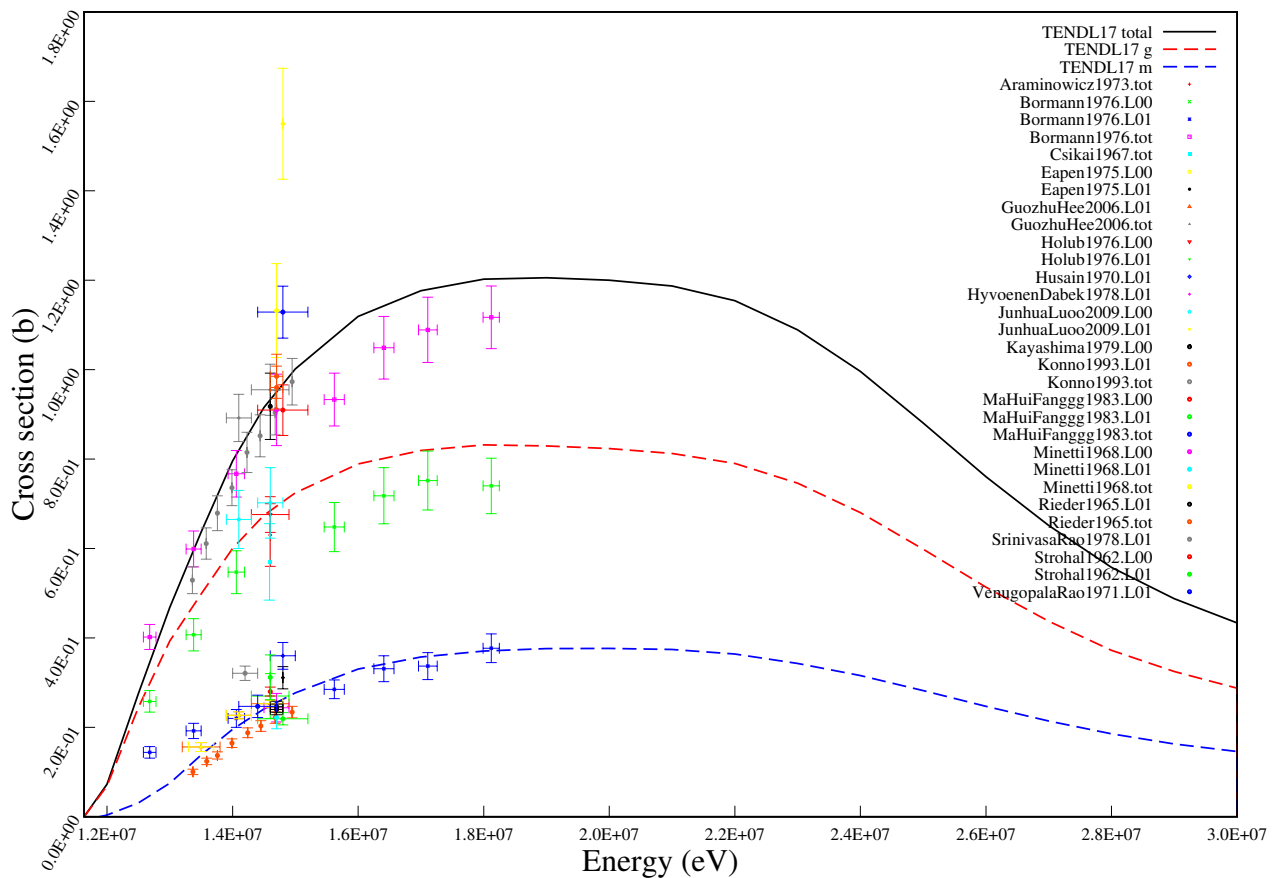
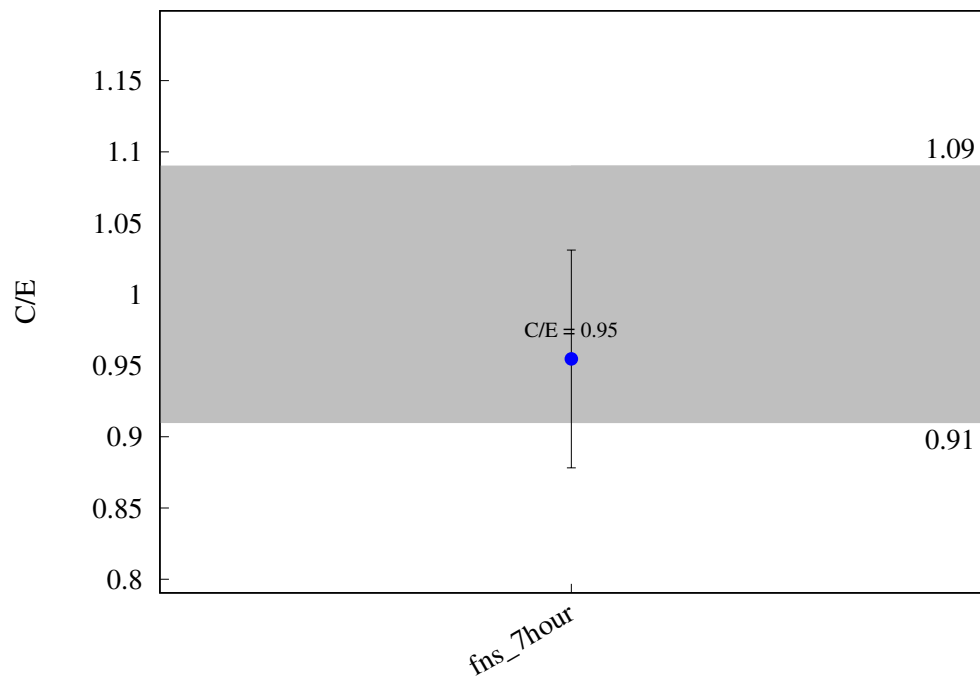
^{81}Br (n,2n) ^{80}gBr 

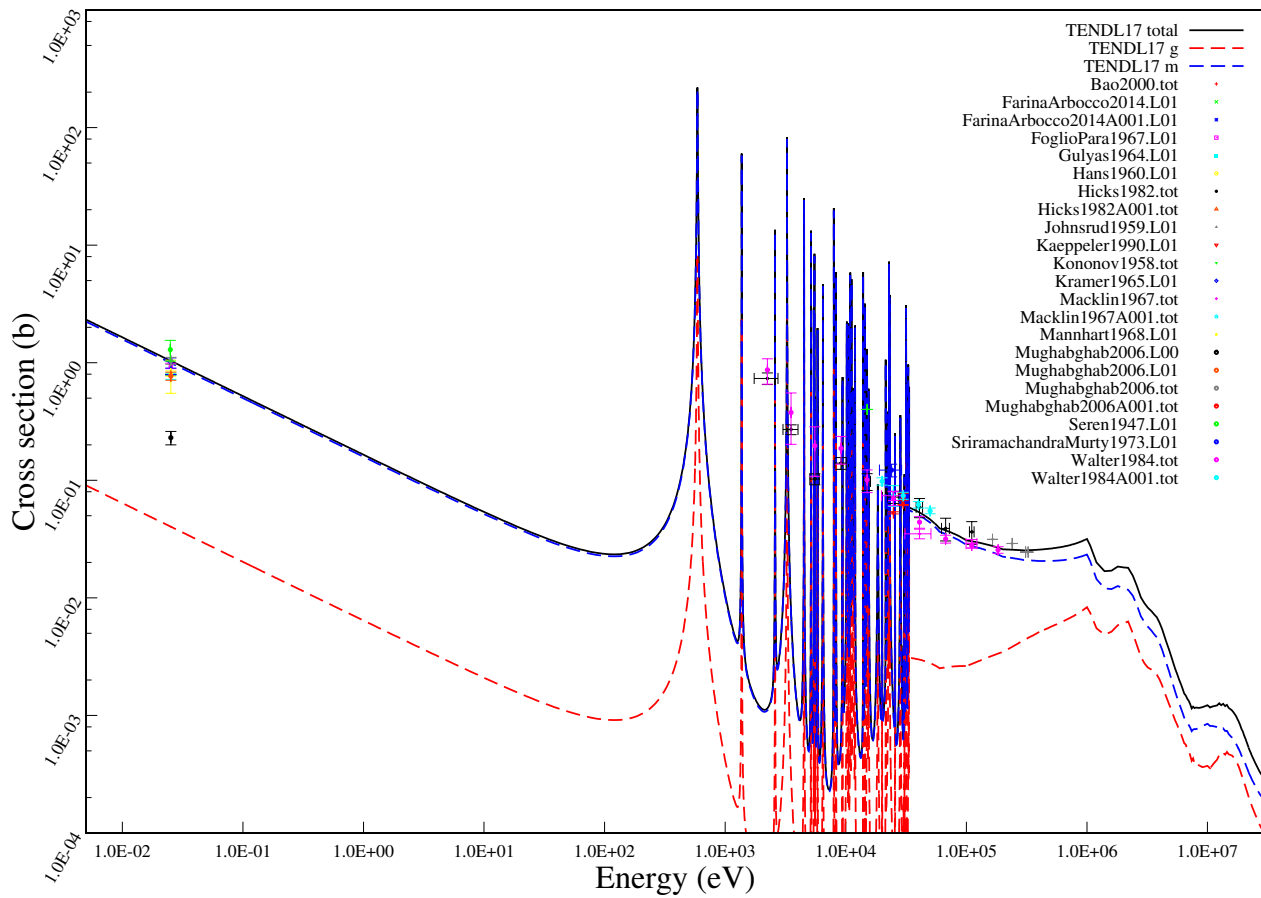
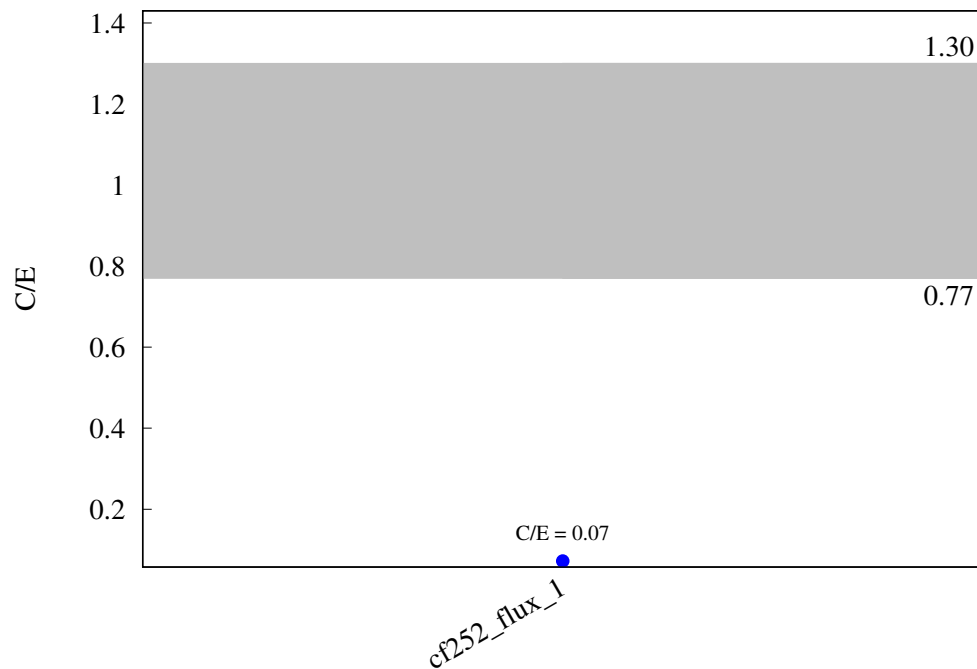
^{85}Rb (n,2n) ^{84}Rb 

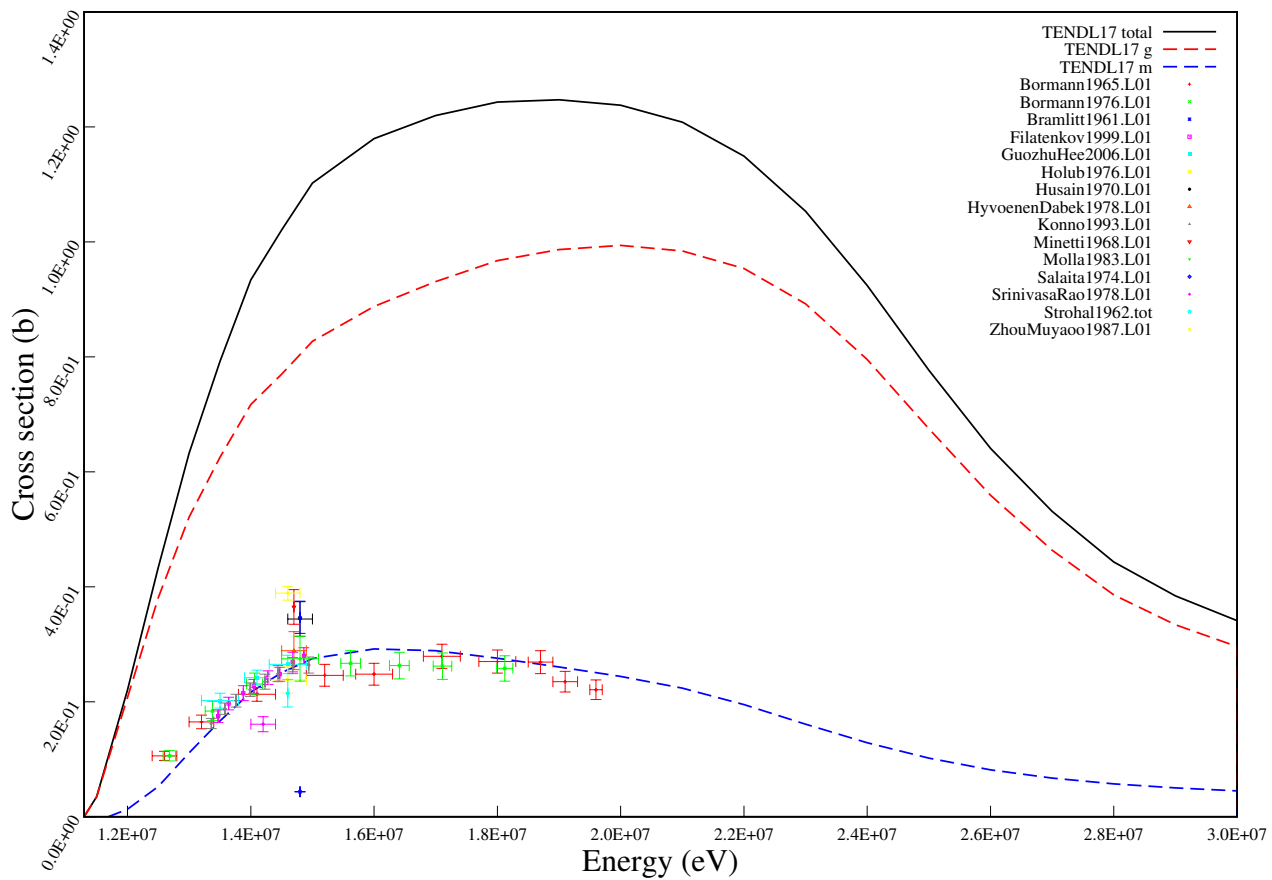
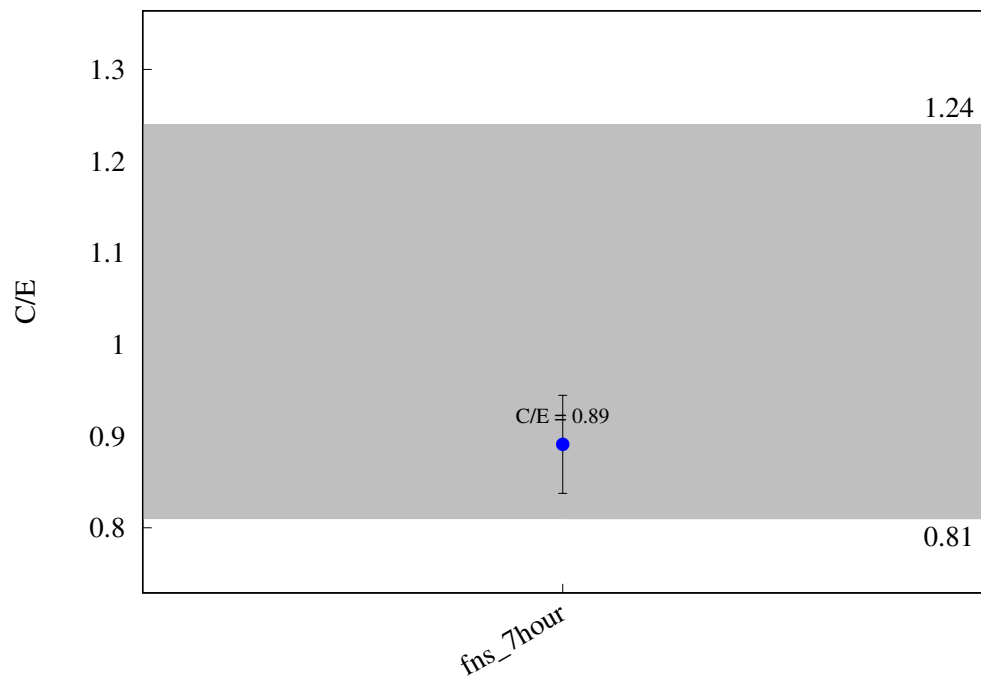
^{87}Rb (n,2n) ^{86m}Rb 

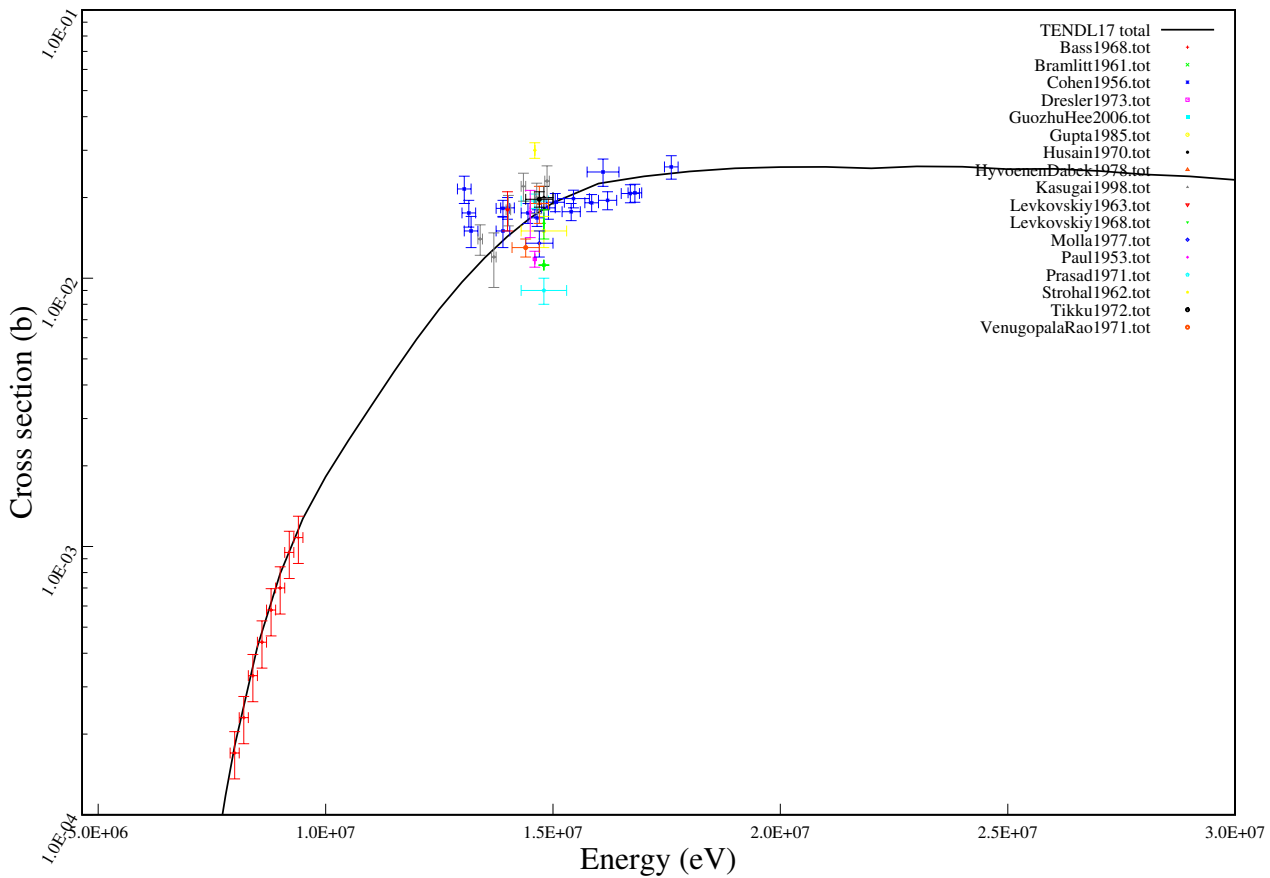
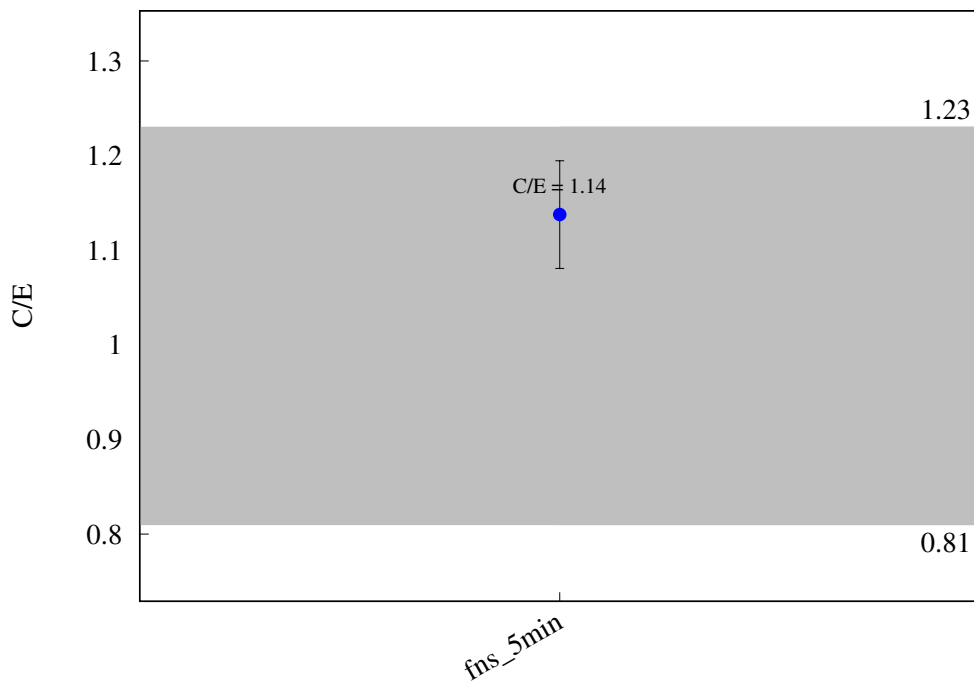
^{84}Sr (n,2n) ^{83}Sr 

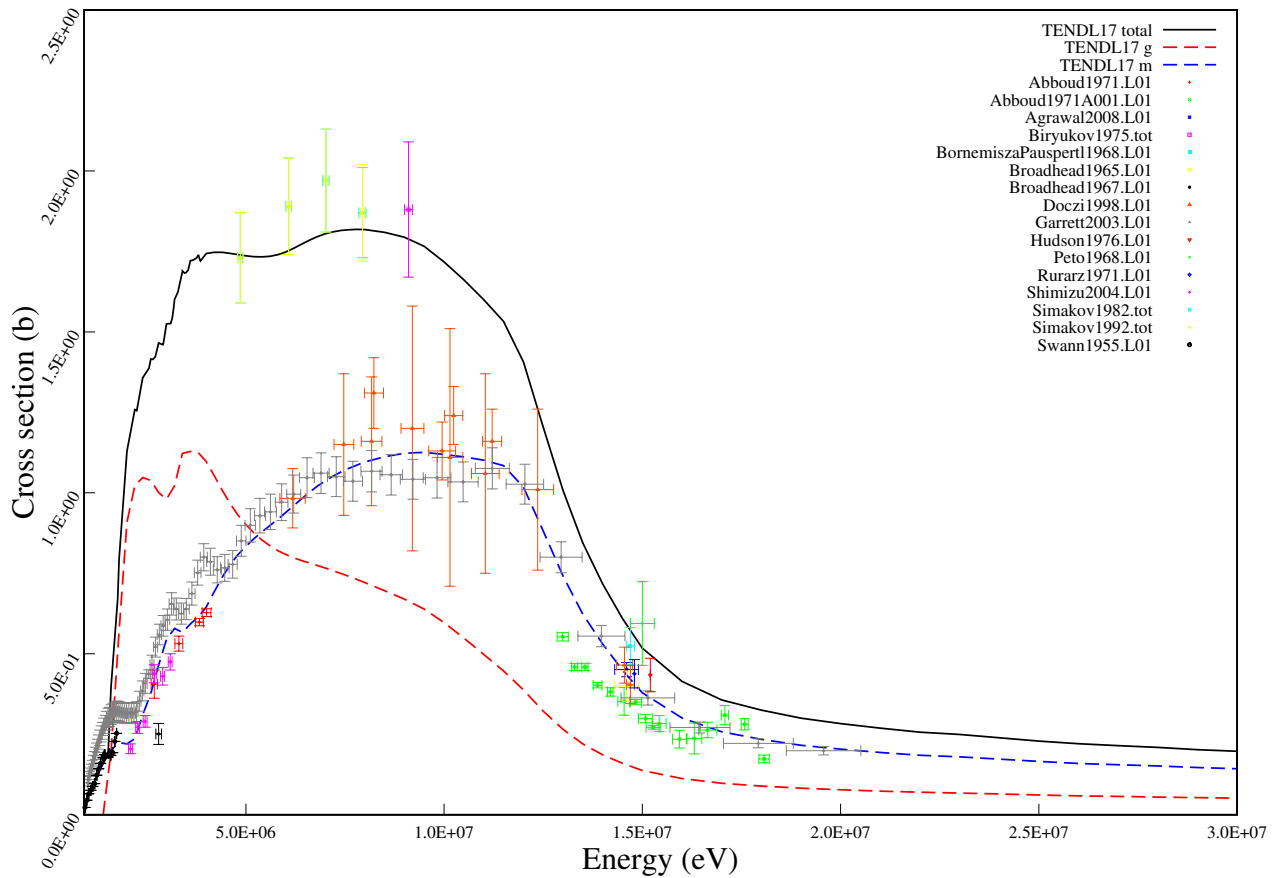
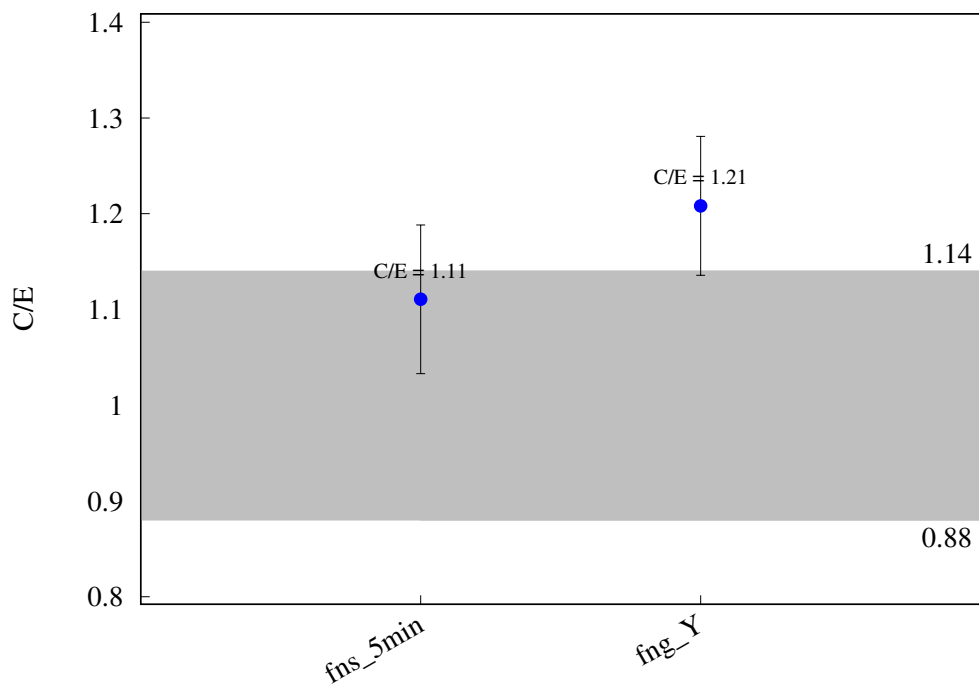
^{84}Sr (n,g) ^{85m}Sr 

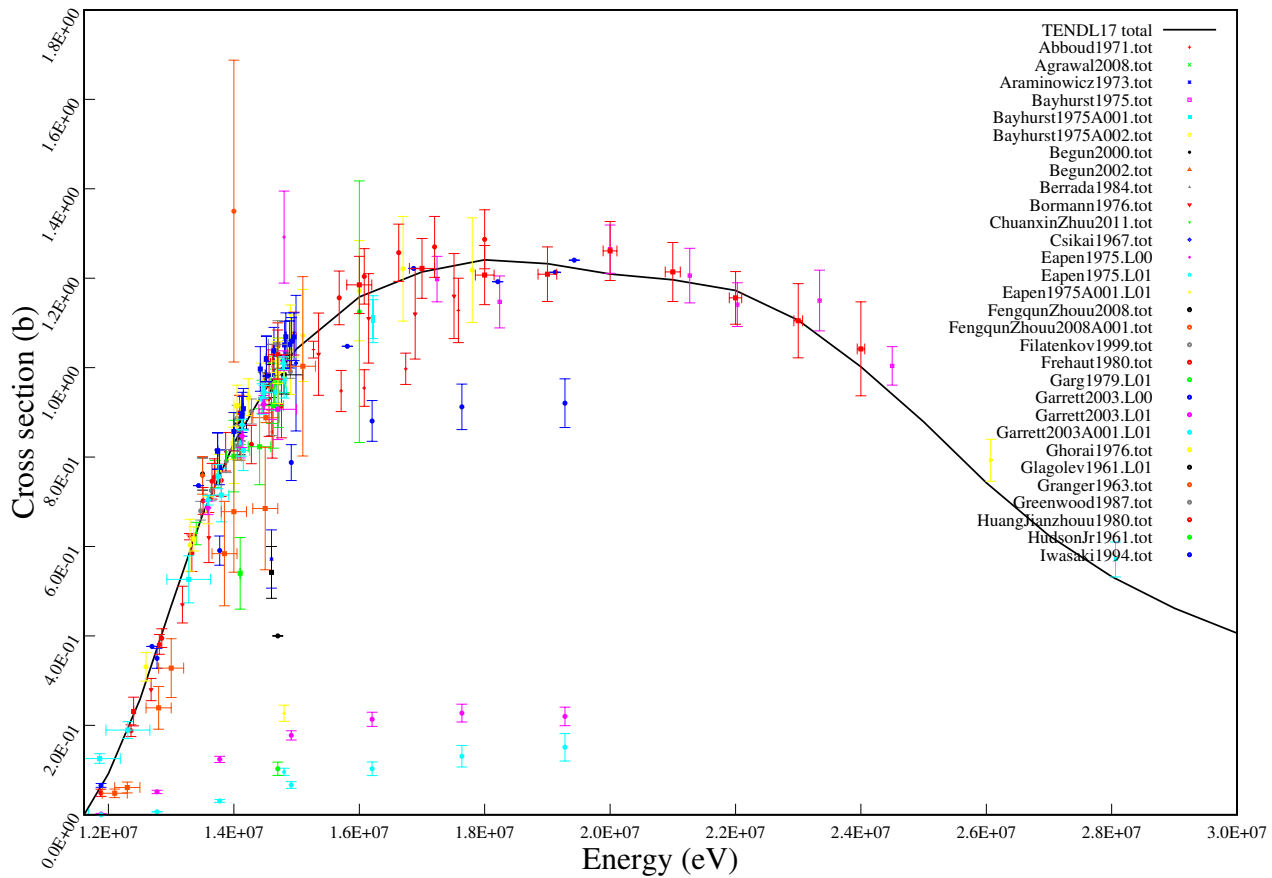
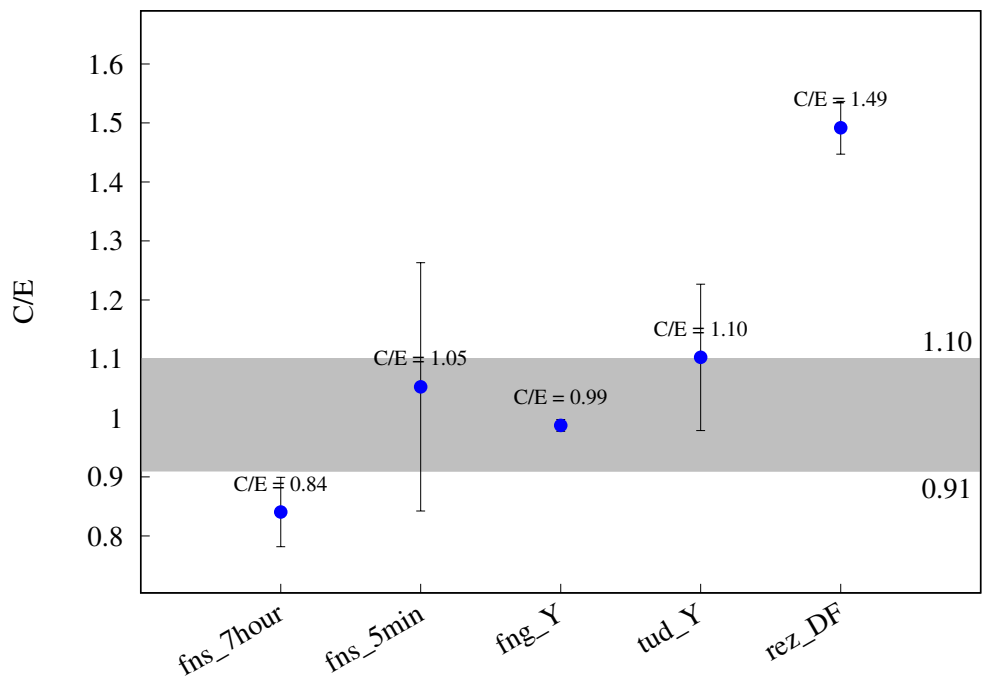
^{86}Sr (n,2n) ^{85}Sr 

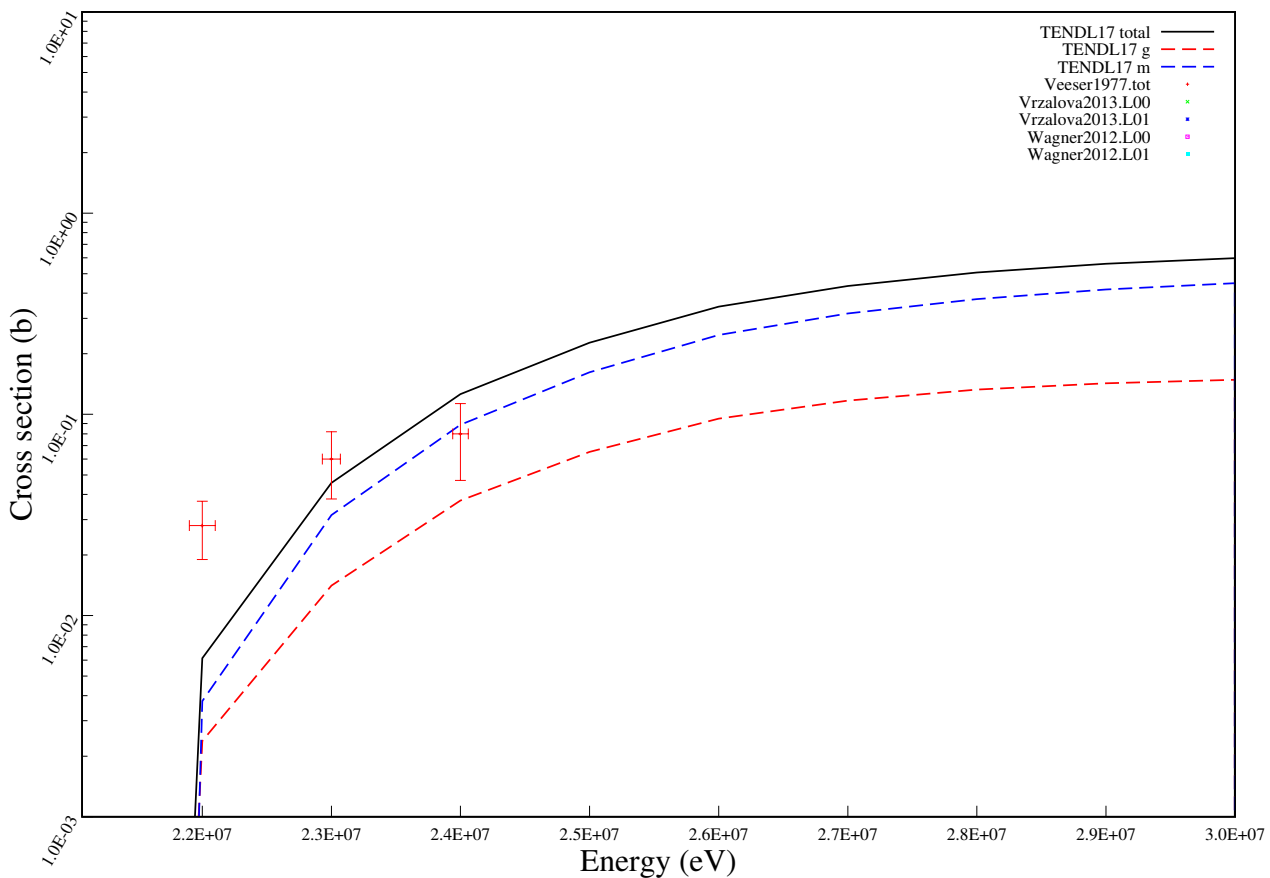
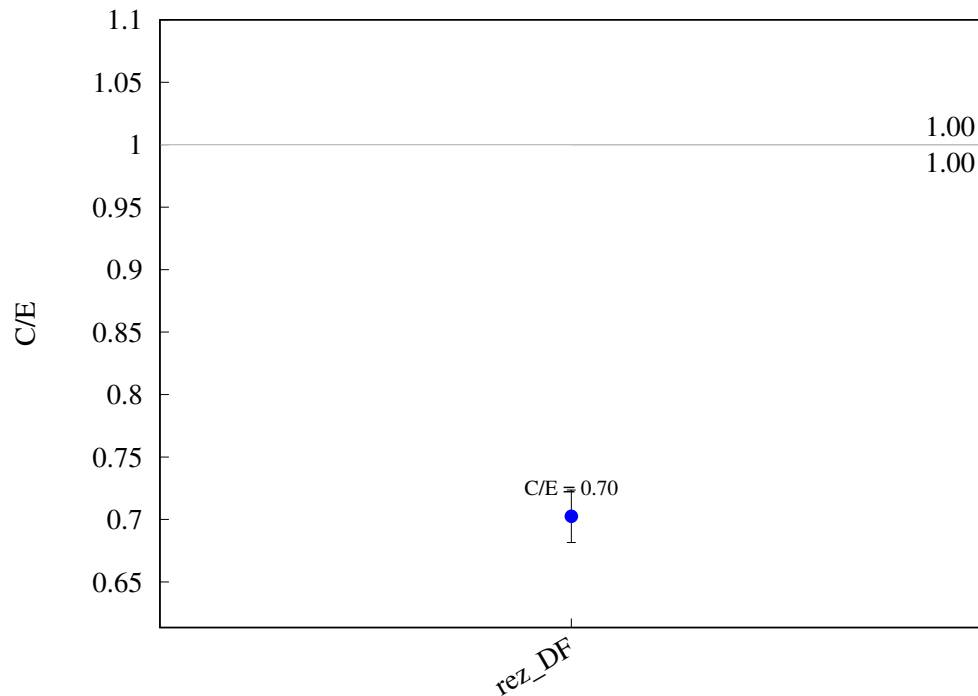
^{86}Sr (n,g) ^{87m}Sr 

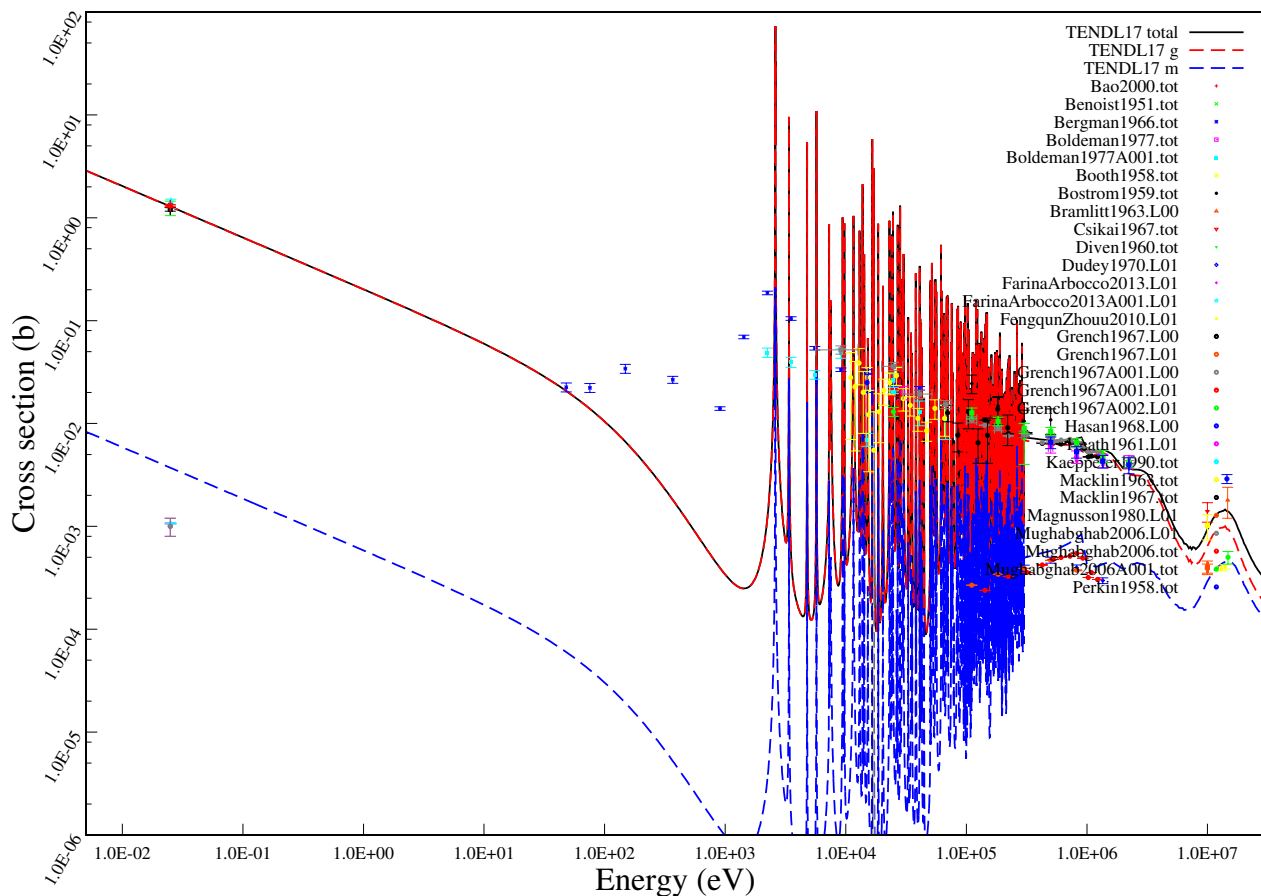
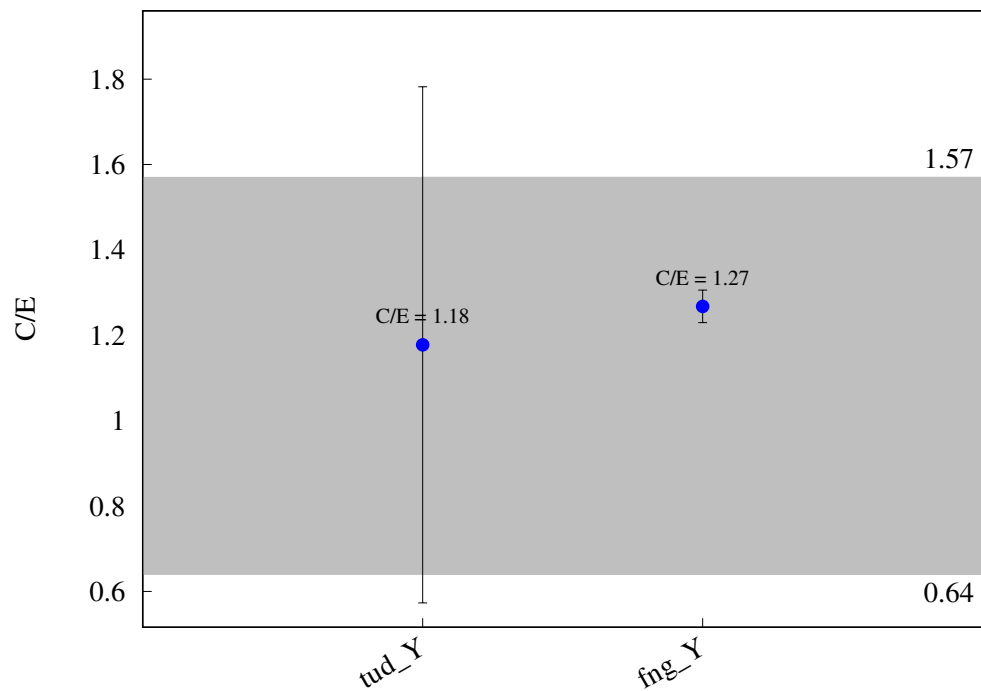
^{88}Sr (n,2n) ^{87m}Sr 

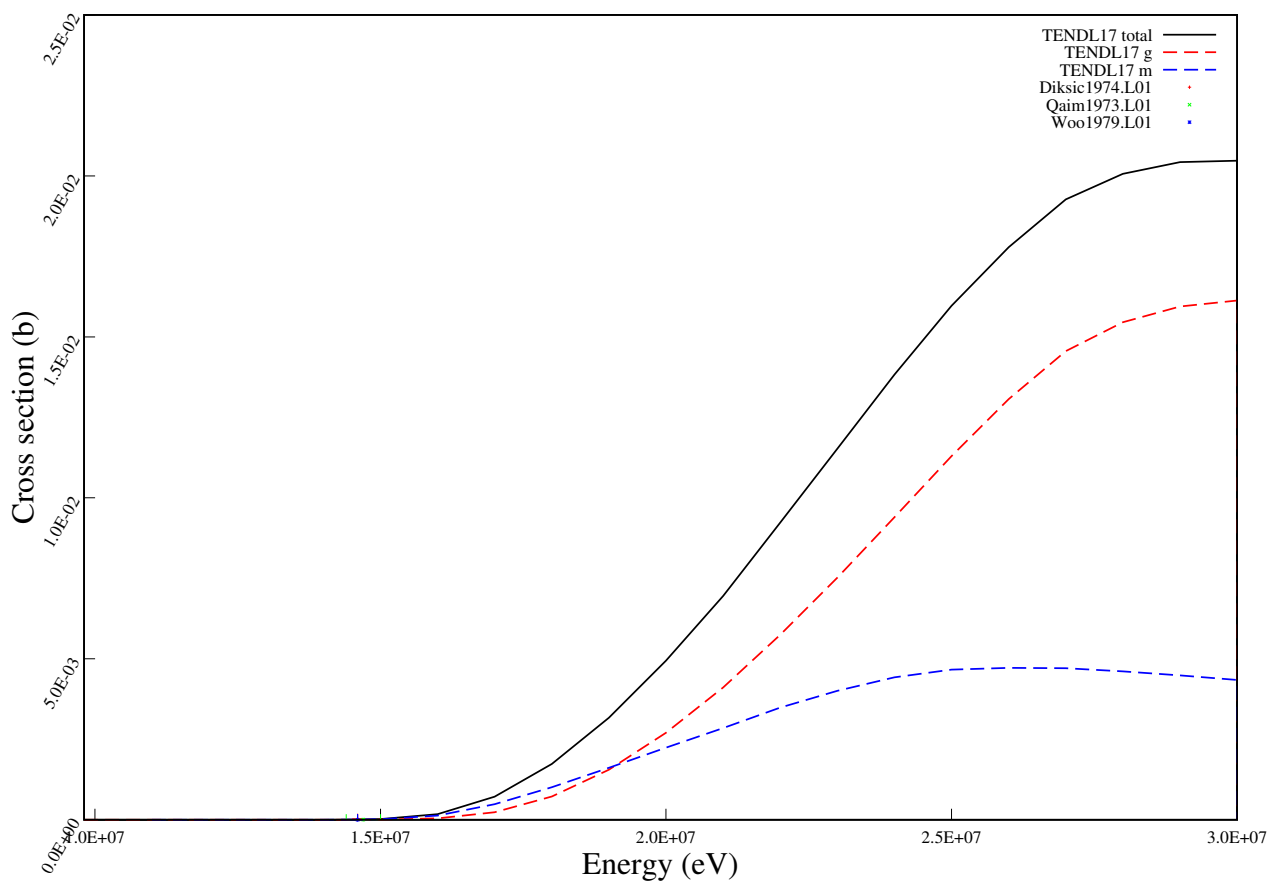
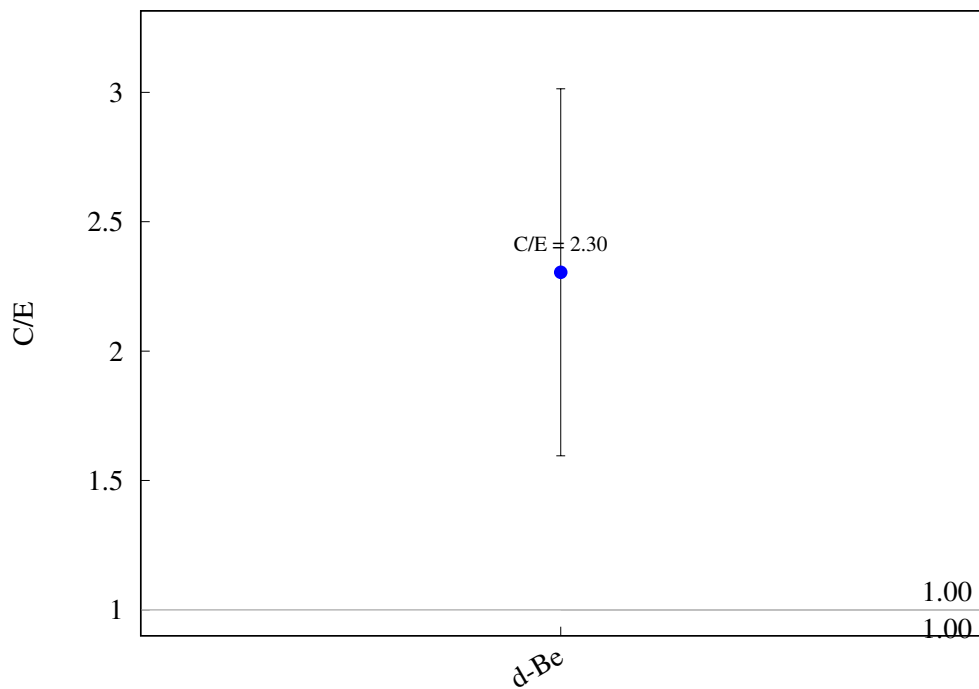
^{88}Sr (n,p) ^{88}Rb 

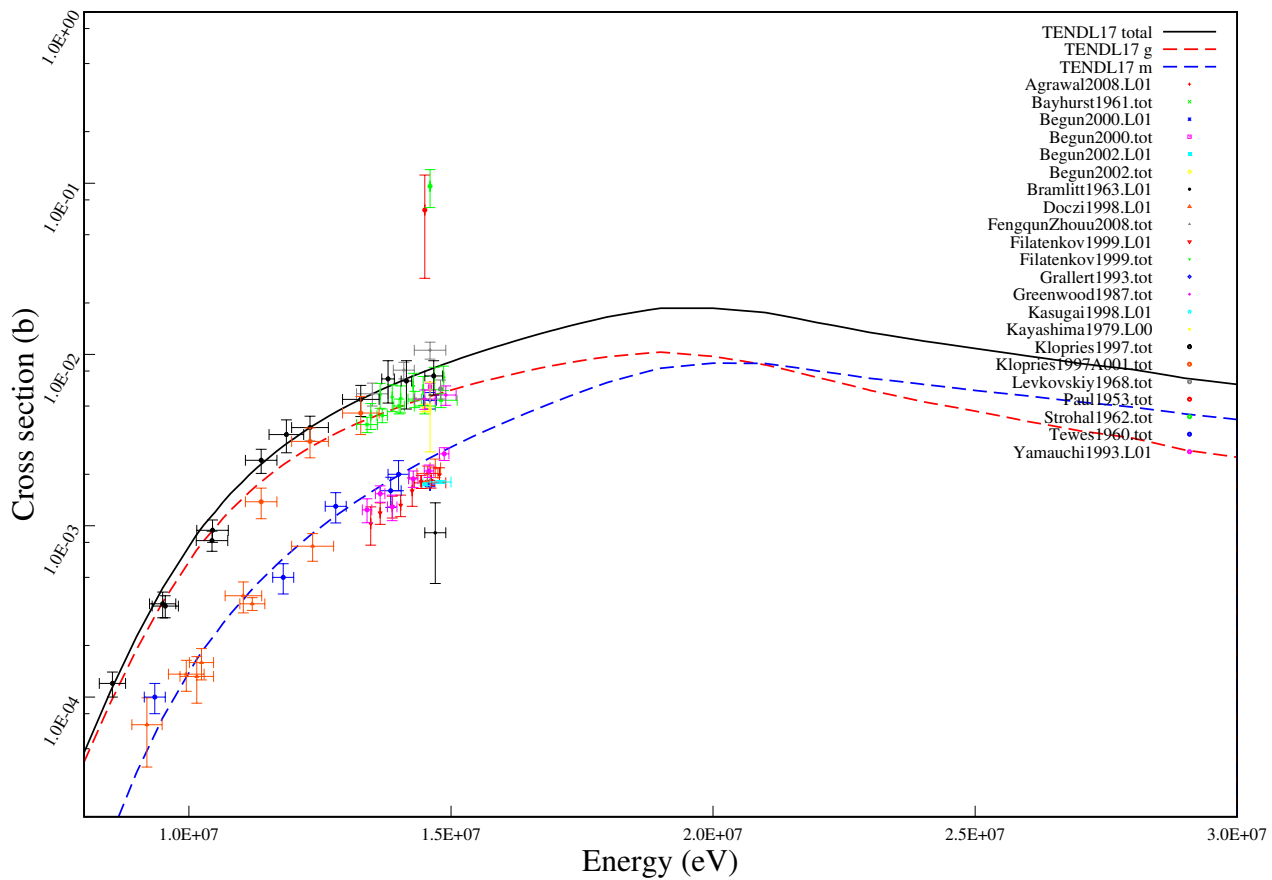
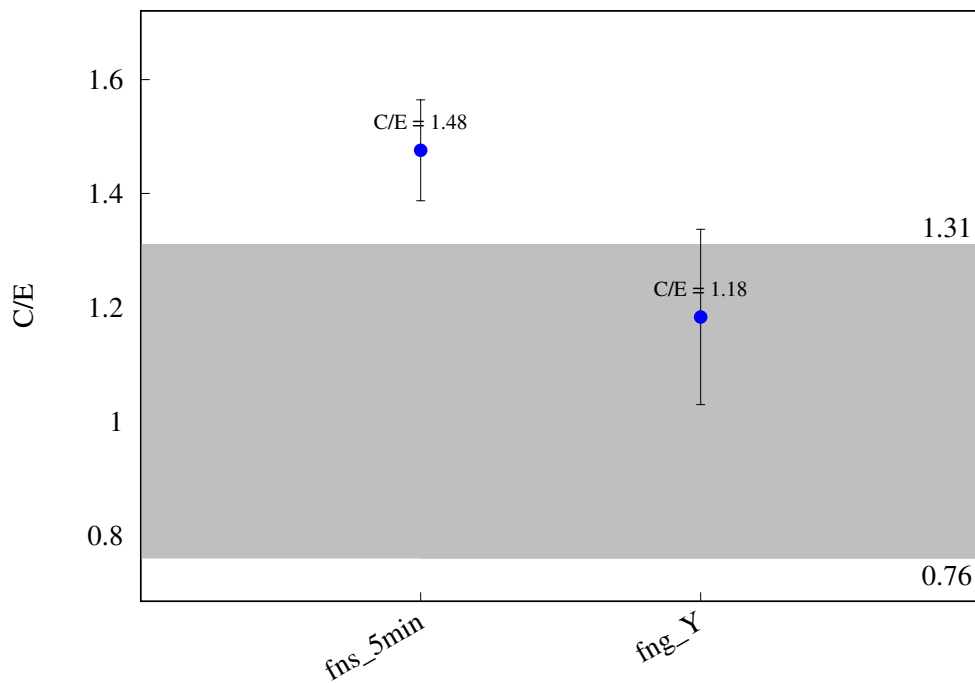
^{89}Y (n,n) $^{89\text{m}}\text{Y}$ 

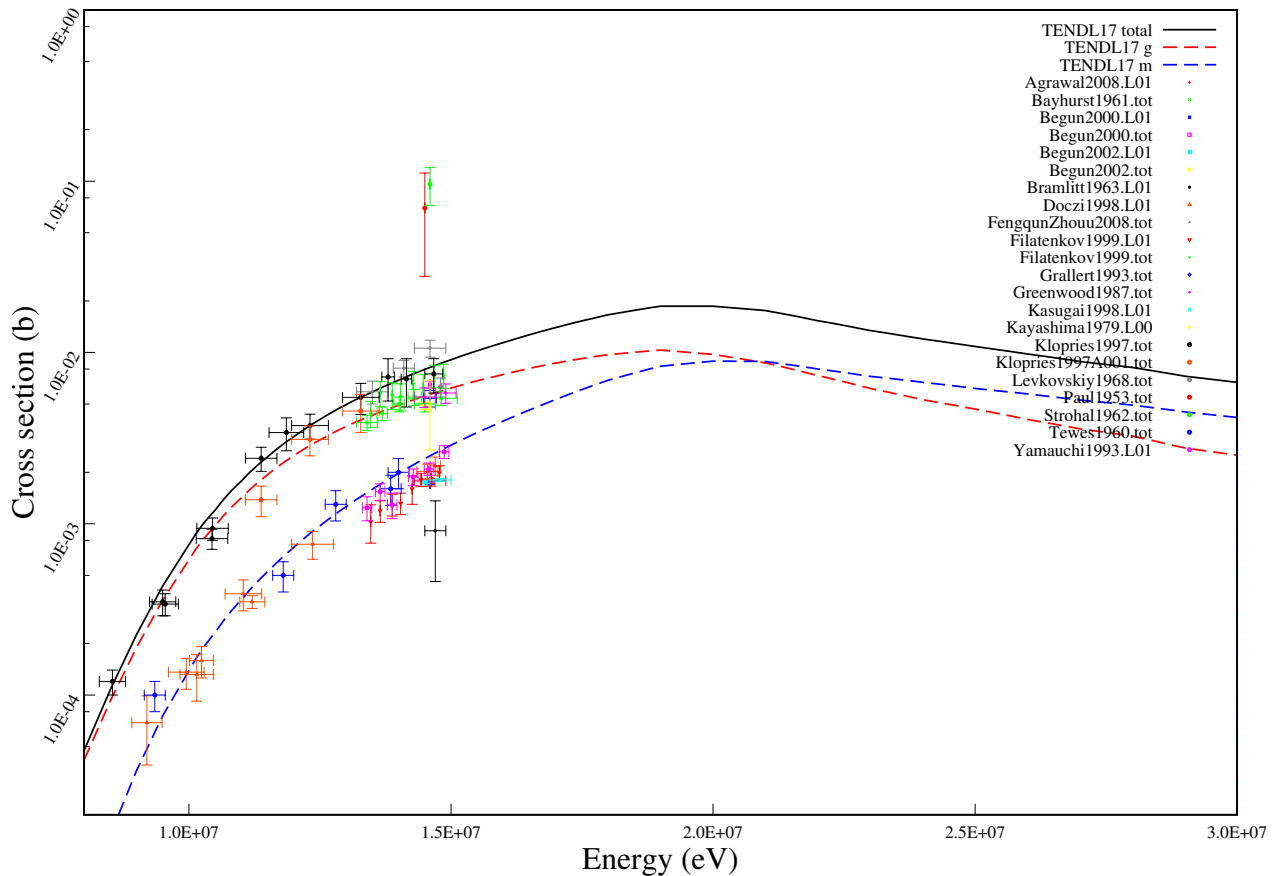
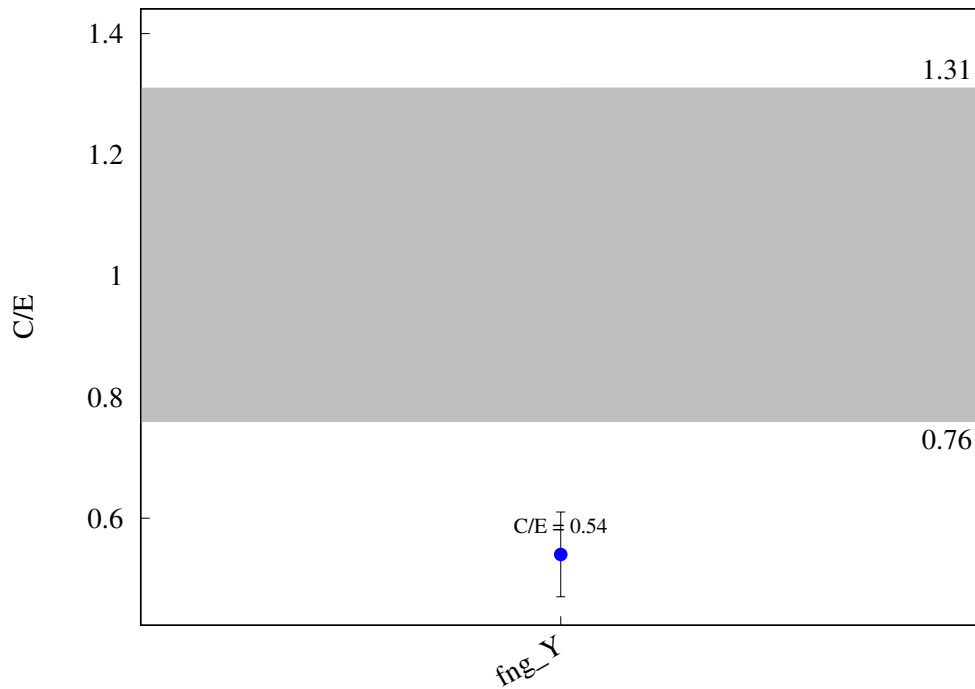
^{89}Y (n,2n) ^{88}Y 

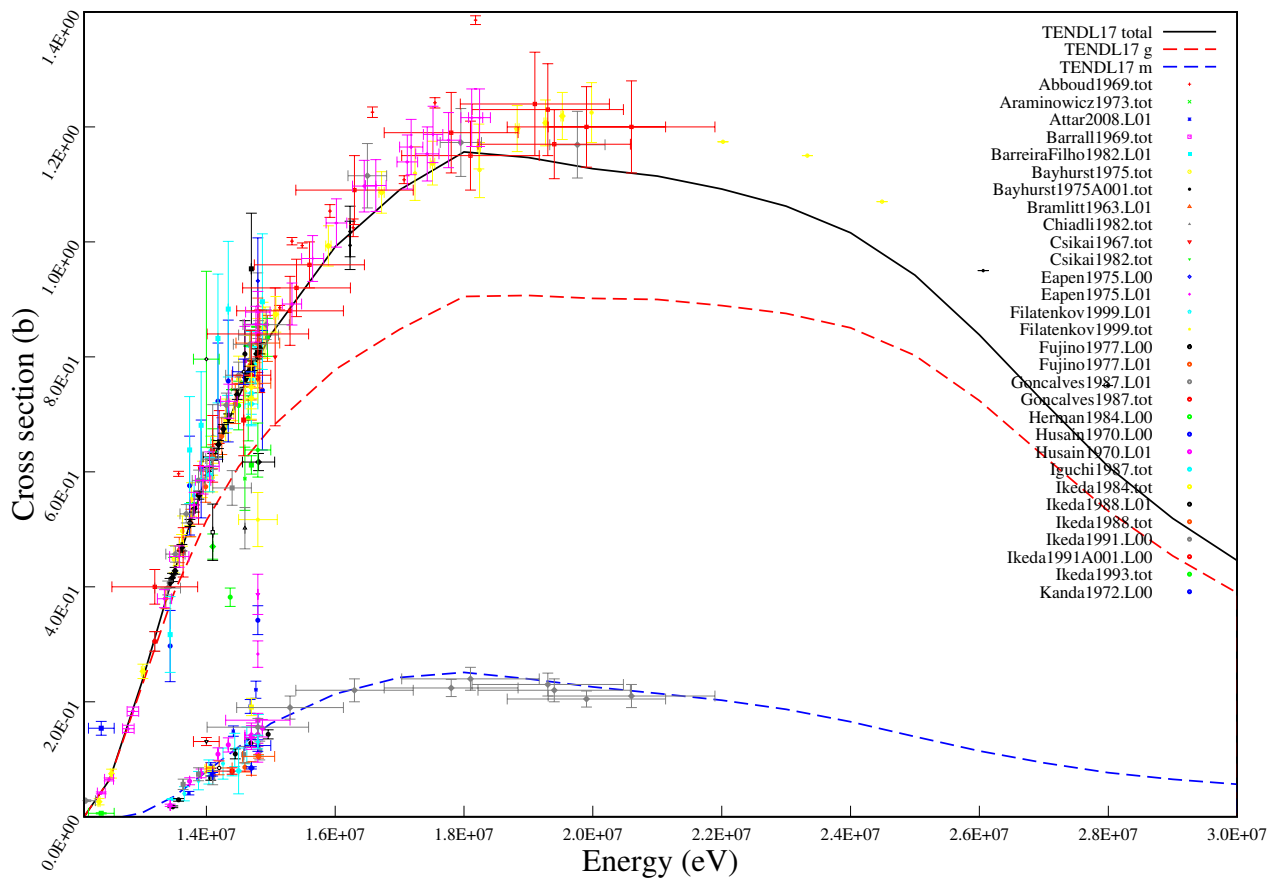
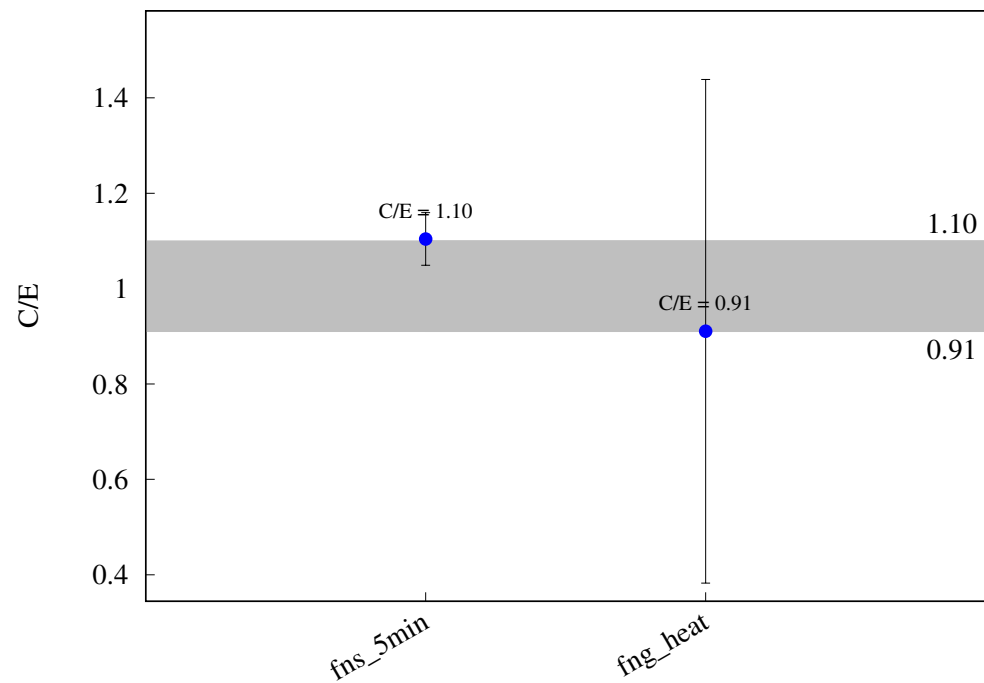
^{89}Y ($n,3n$) ^{87}Y 

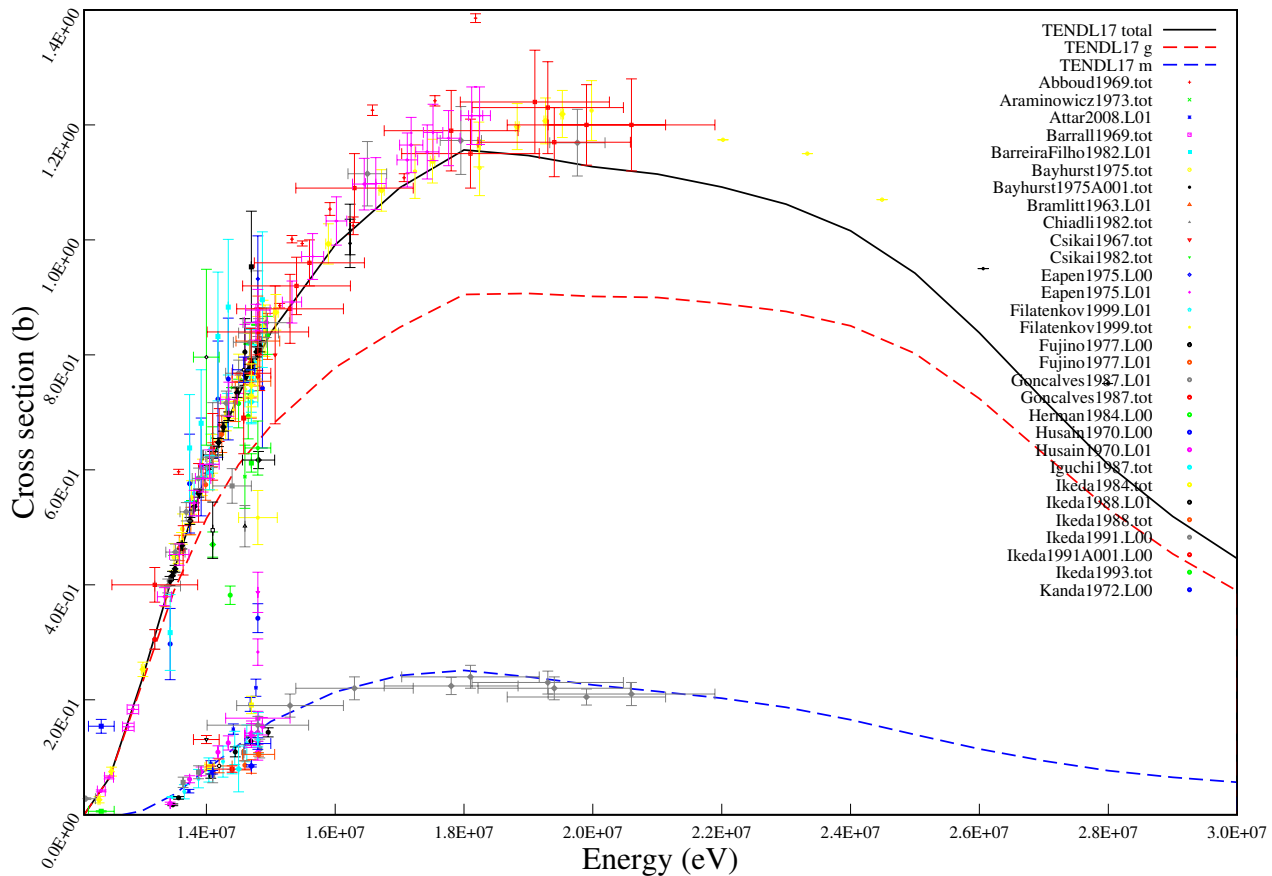
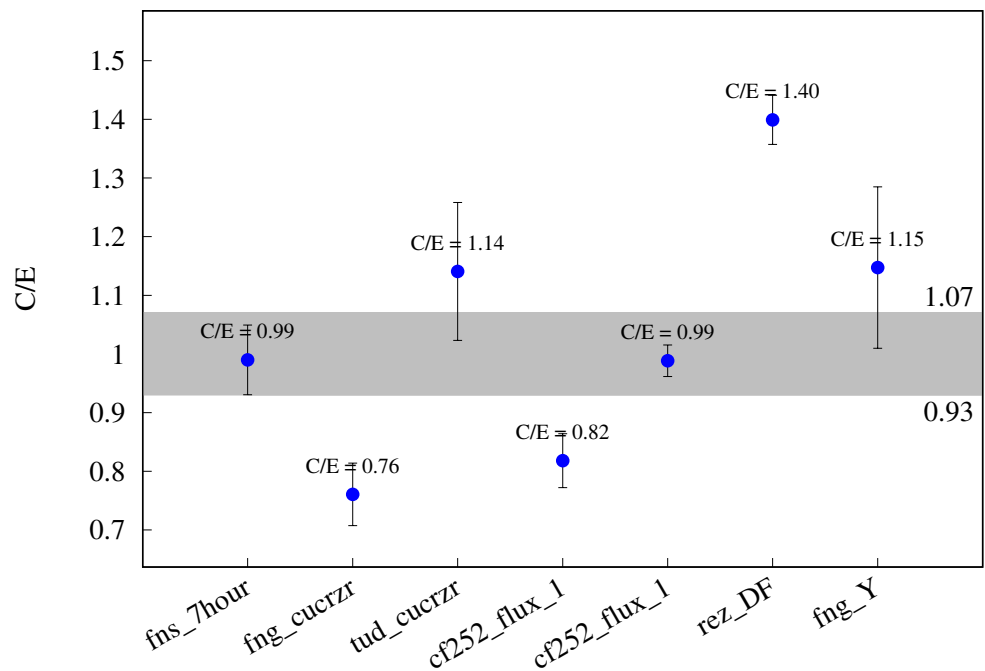
^{89}Y (n,g) ^{90m}Y 

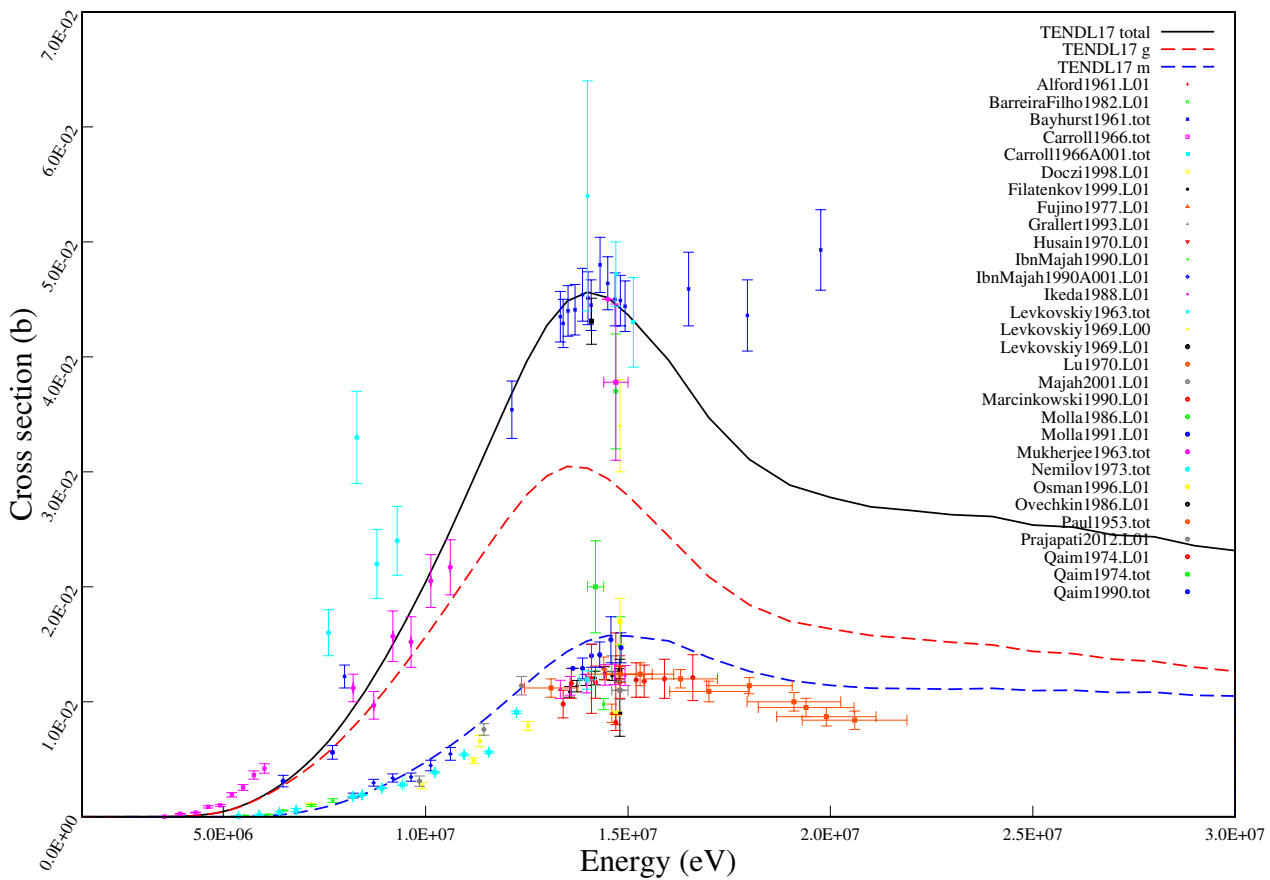
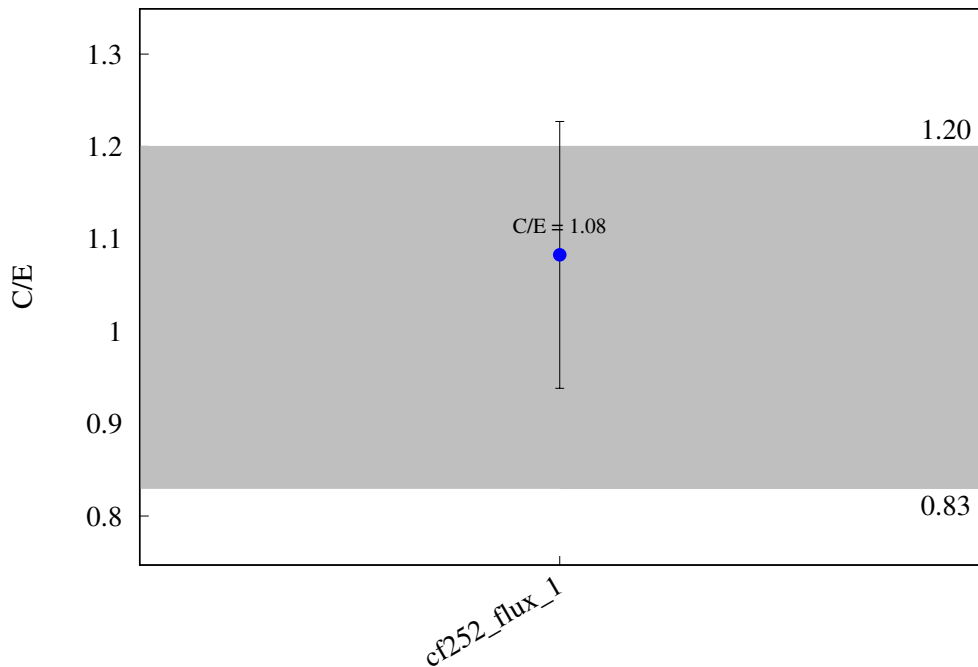
$^{89}\text{Y} (\text{n},\text{t}) ^{87}\text{Sr}$ 

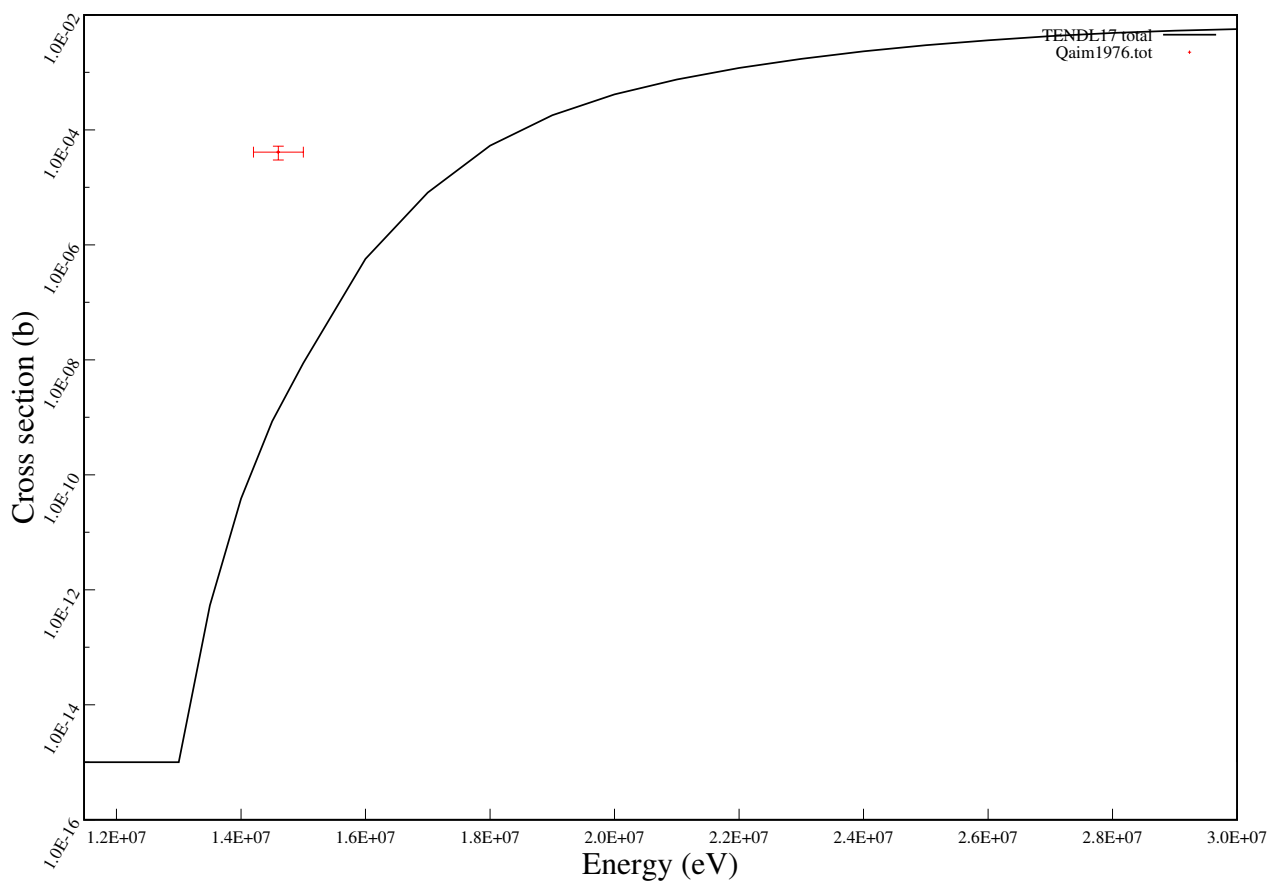
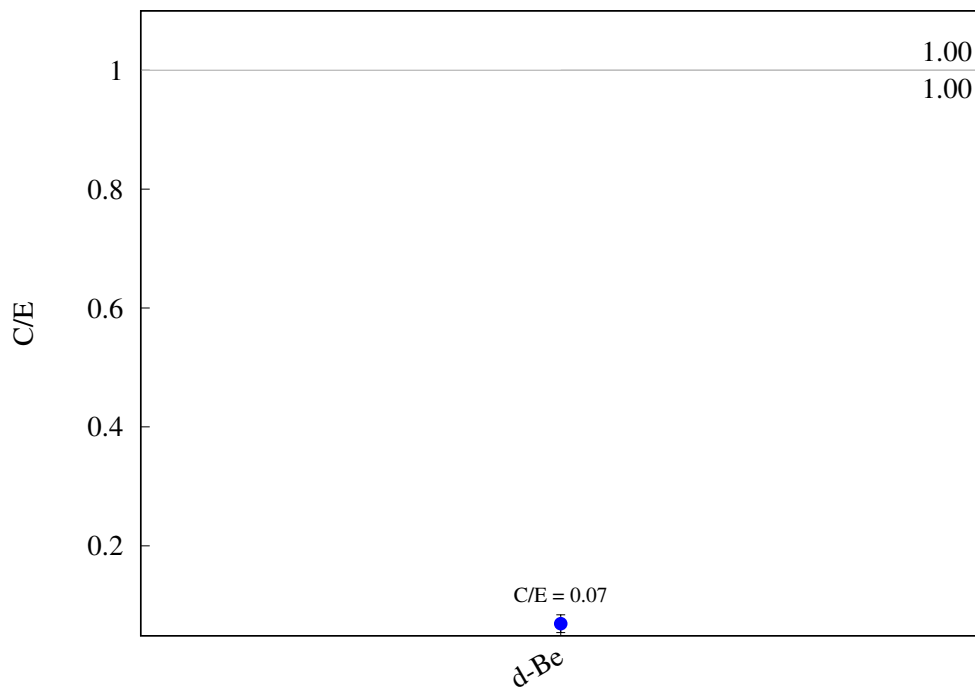
^{89}Y (n,a) ^{86m}Rb 

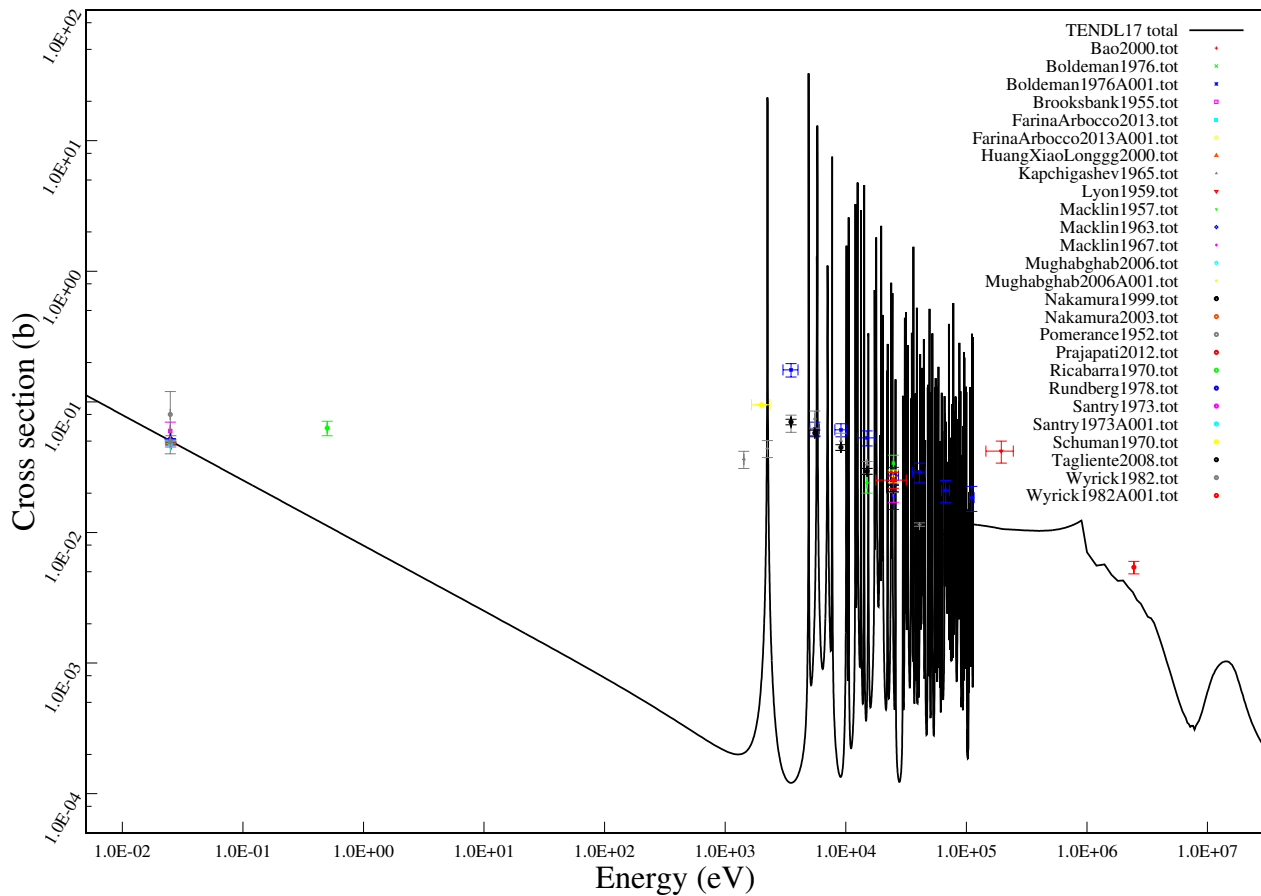
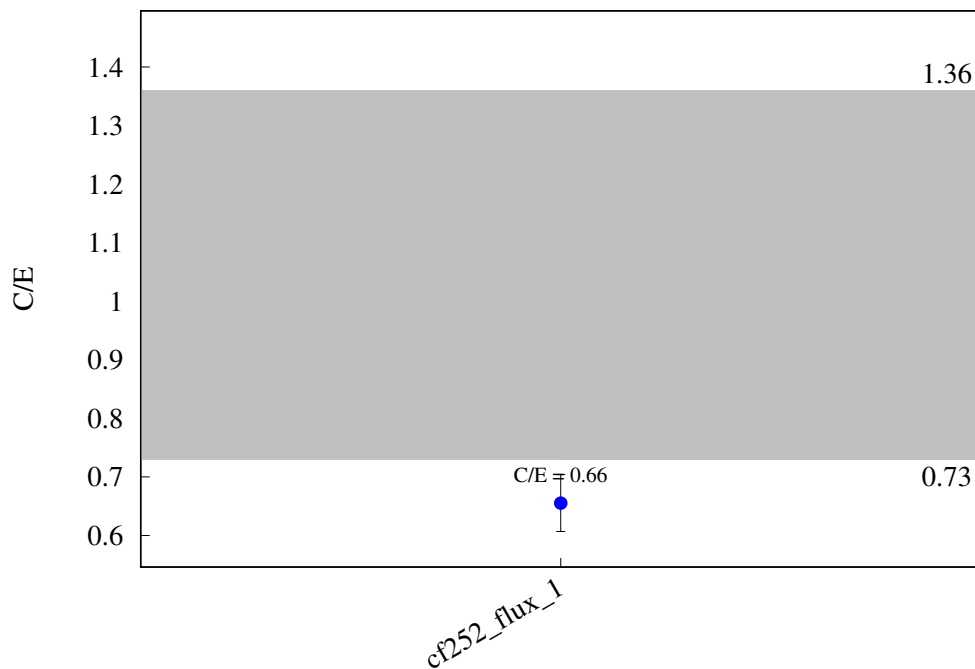
$^{89}\text{Y} (\text{n},\text{a}) ^{86}\text{Rb}$ 

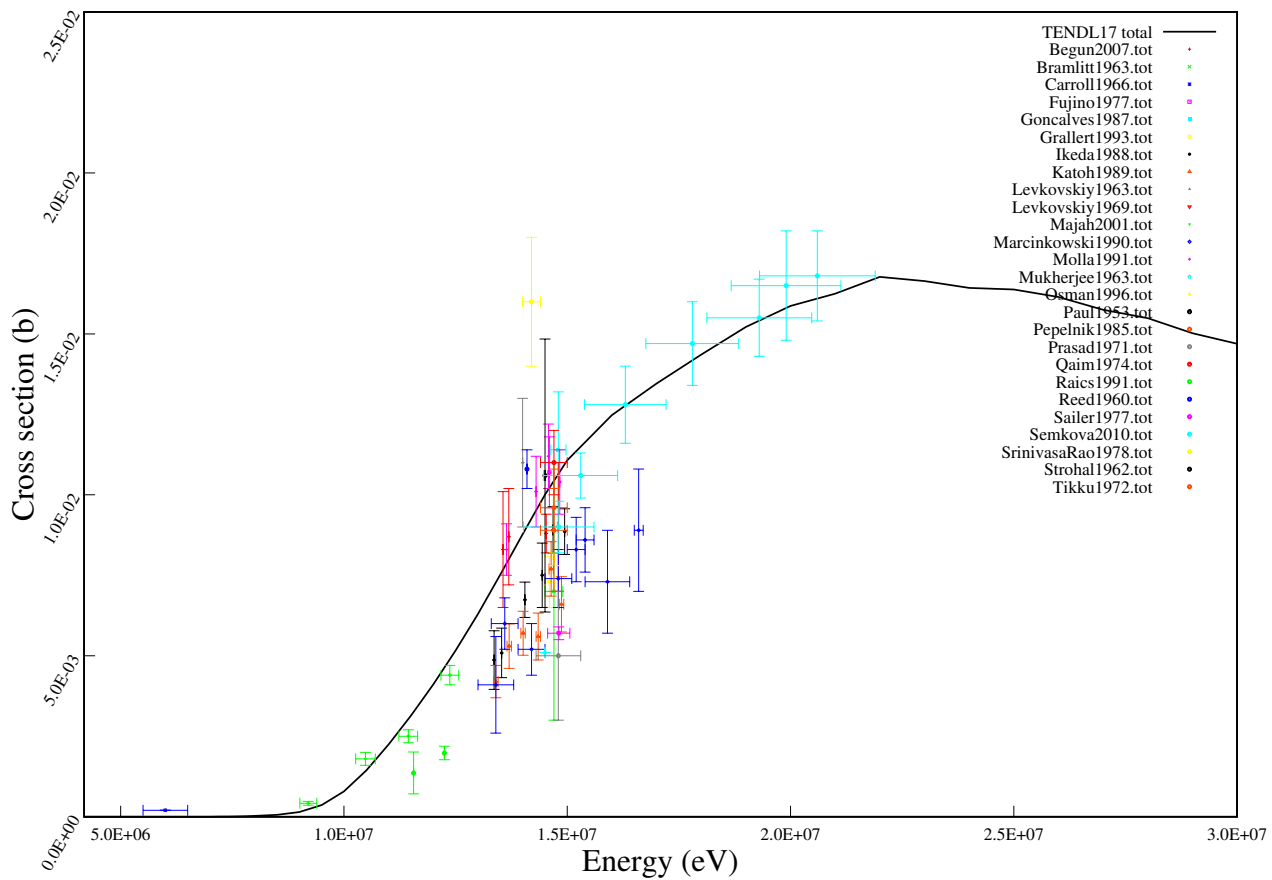
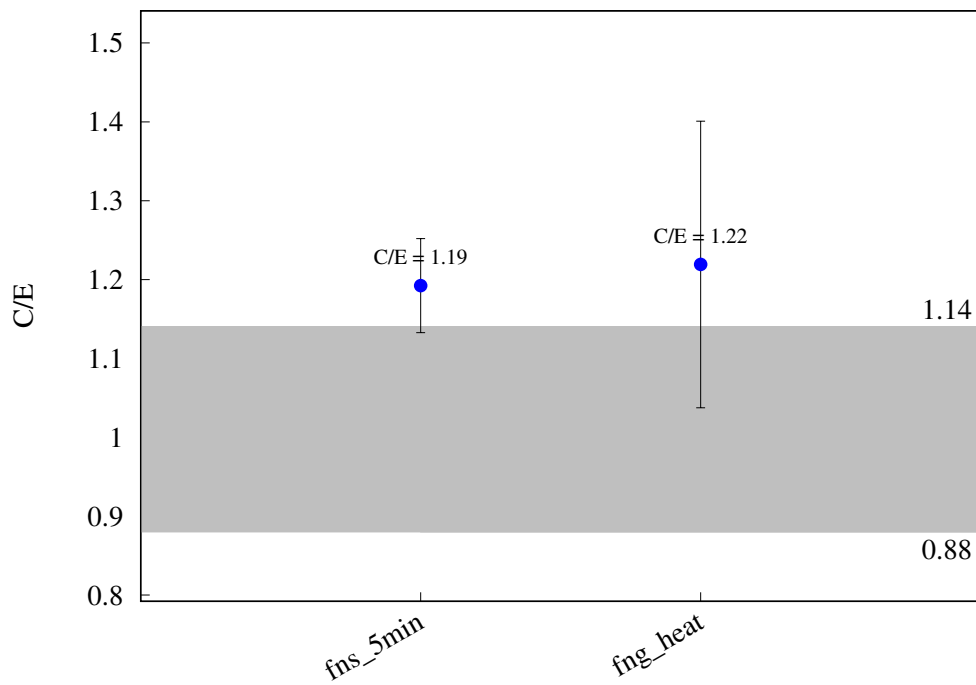
^{90}Zr (n,2n) ^{89m}Zr 

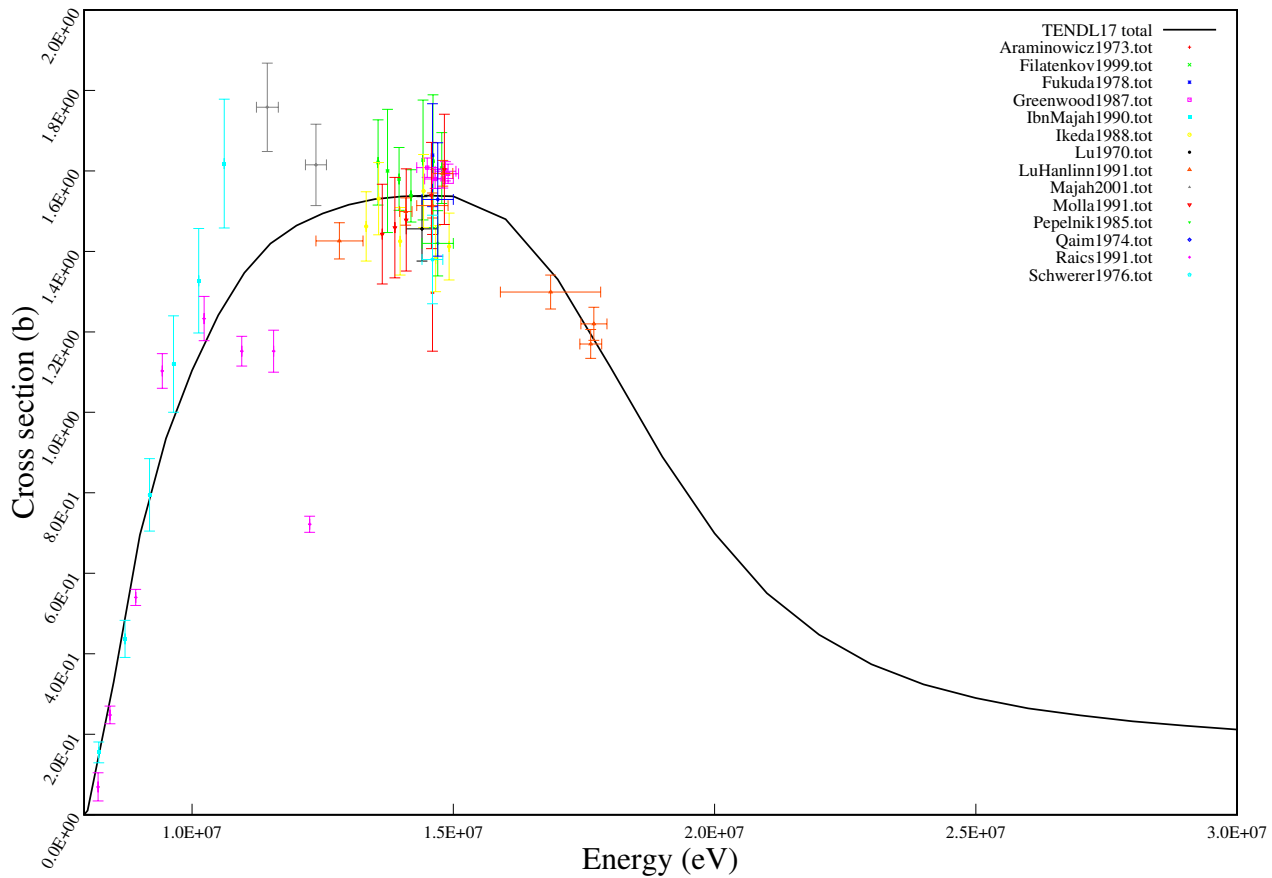
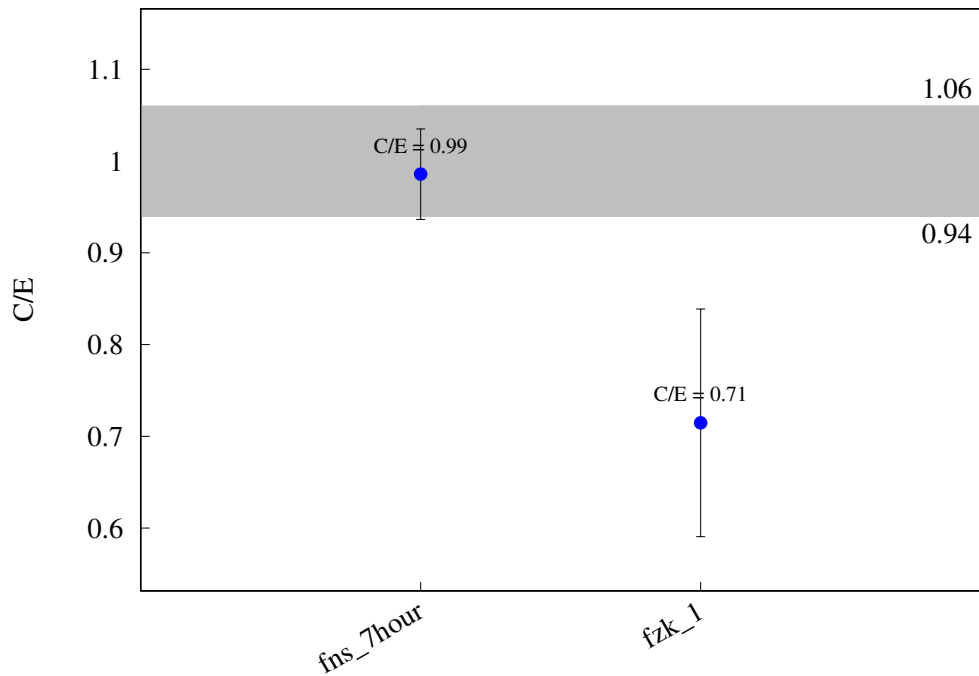
^{90}Zr (n,2n) ^{89}Zr 

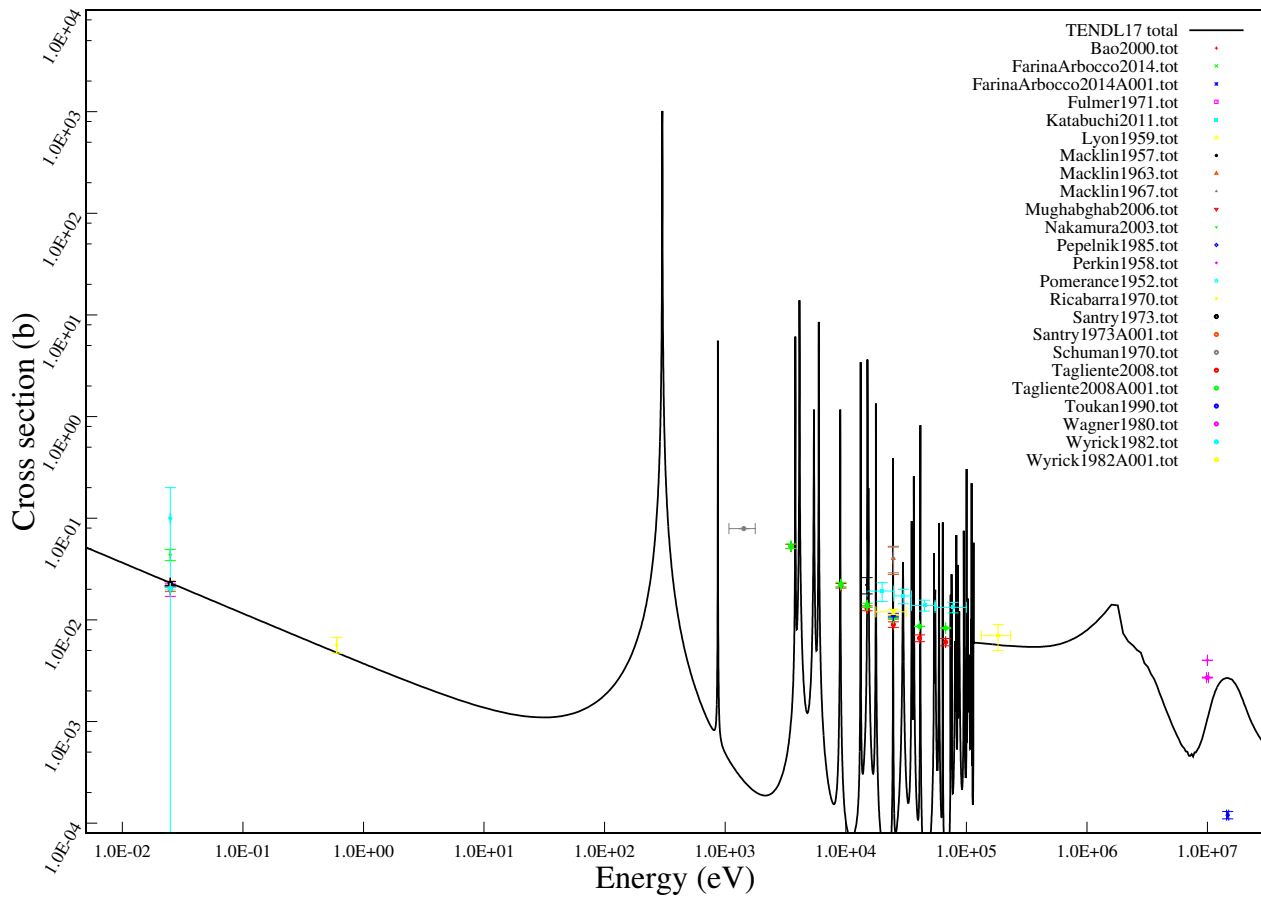
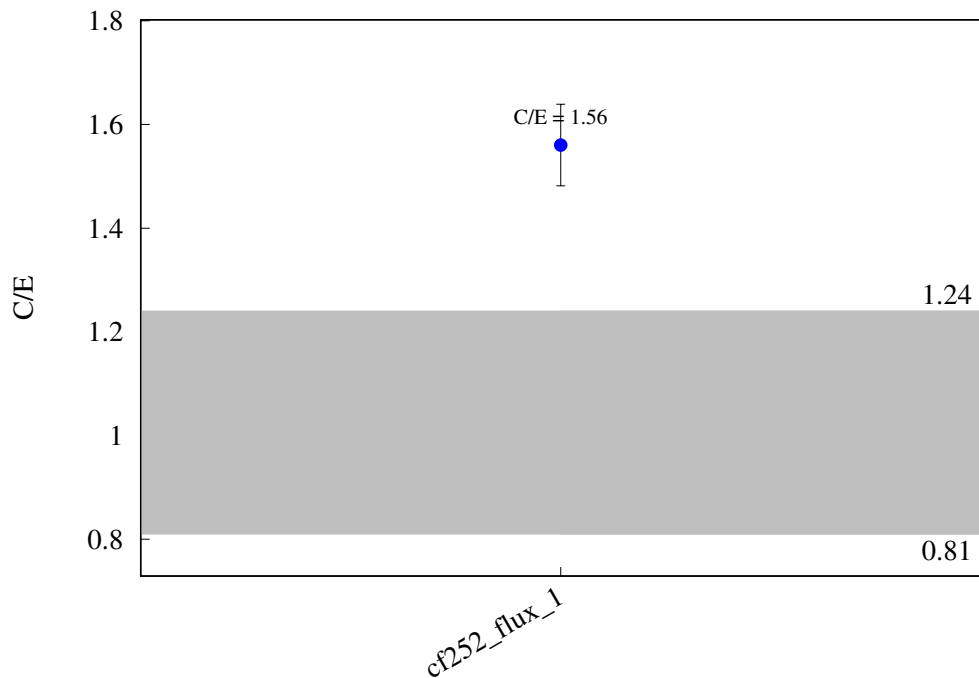
^{90}Zr (n,p) $^{90\text{m}}\text{Y}$ 

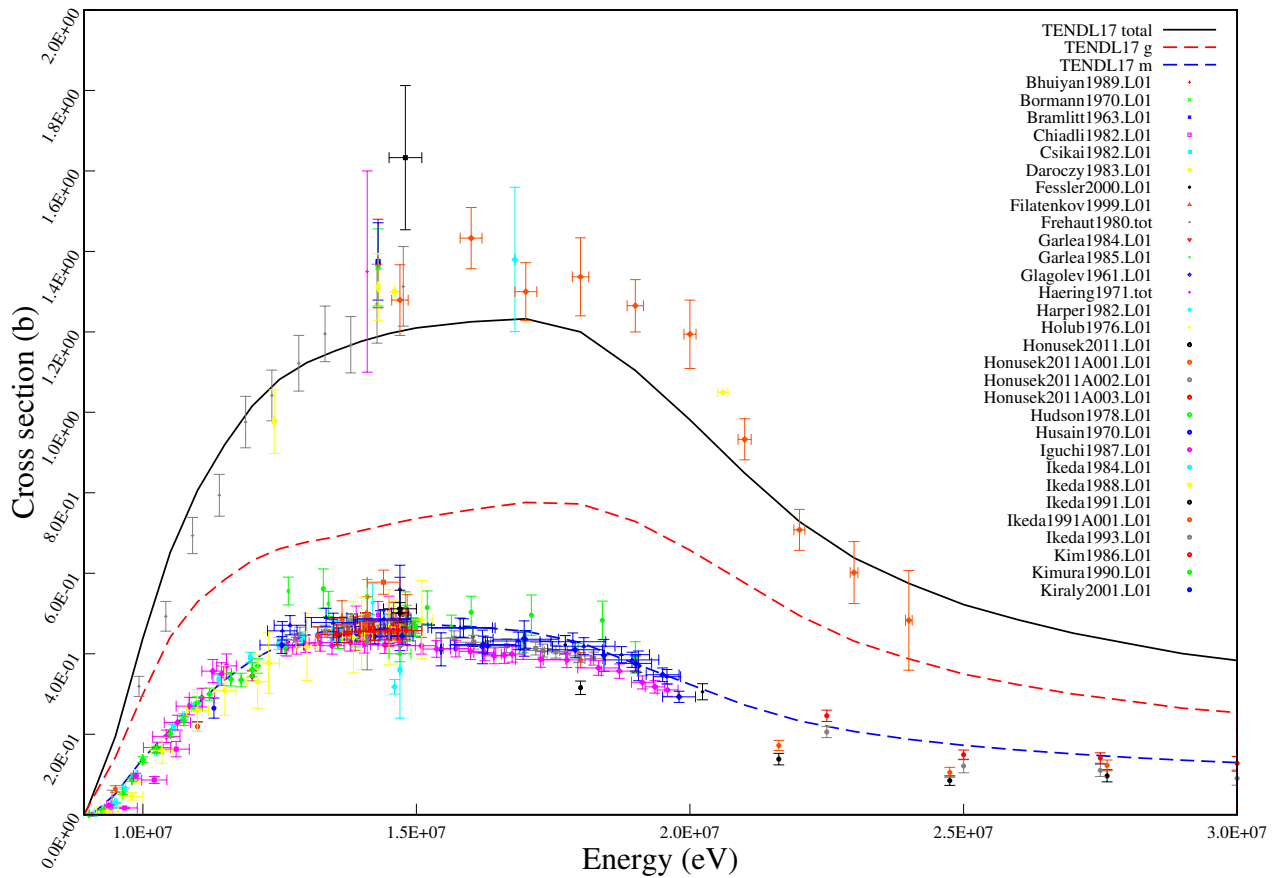
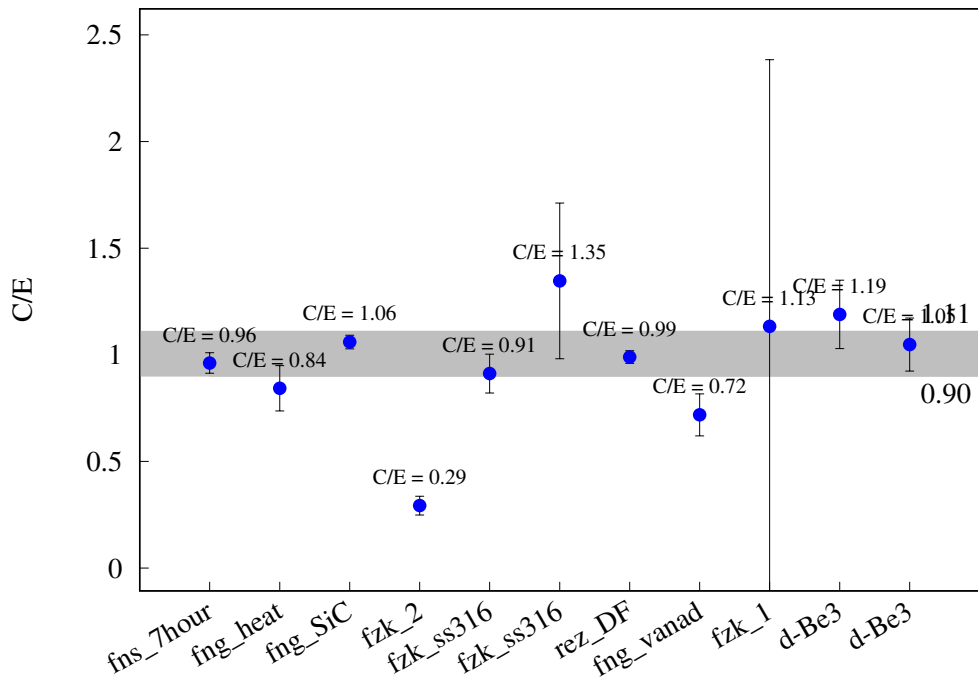
$^{90}\text{Zr} (\text{n},\text{t}) ^{88}\text{Y}$ 

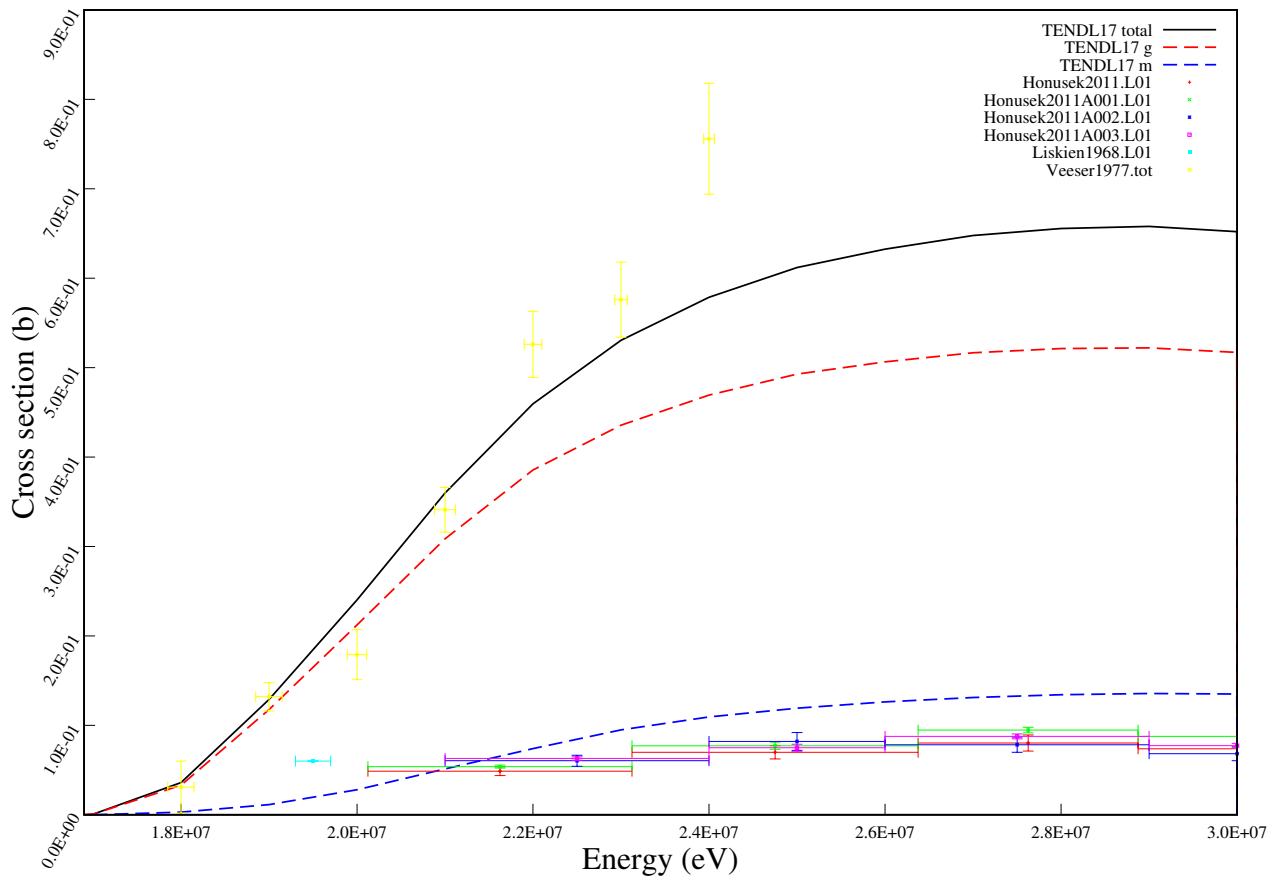
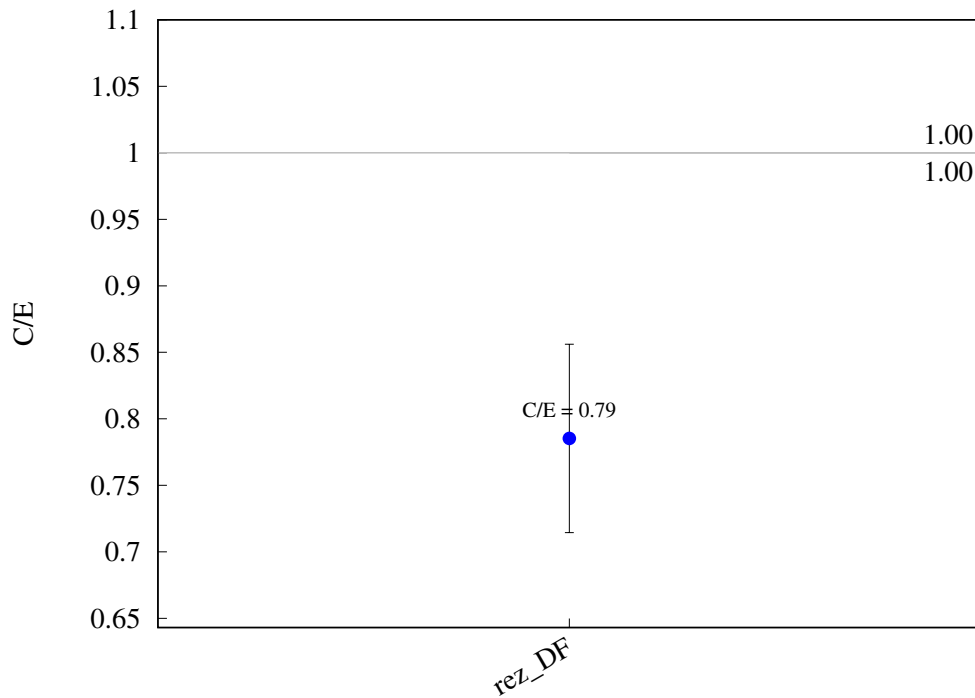
^{94}Zr (n,g) ^{95}Zr 

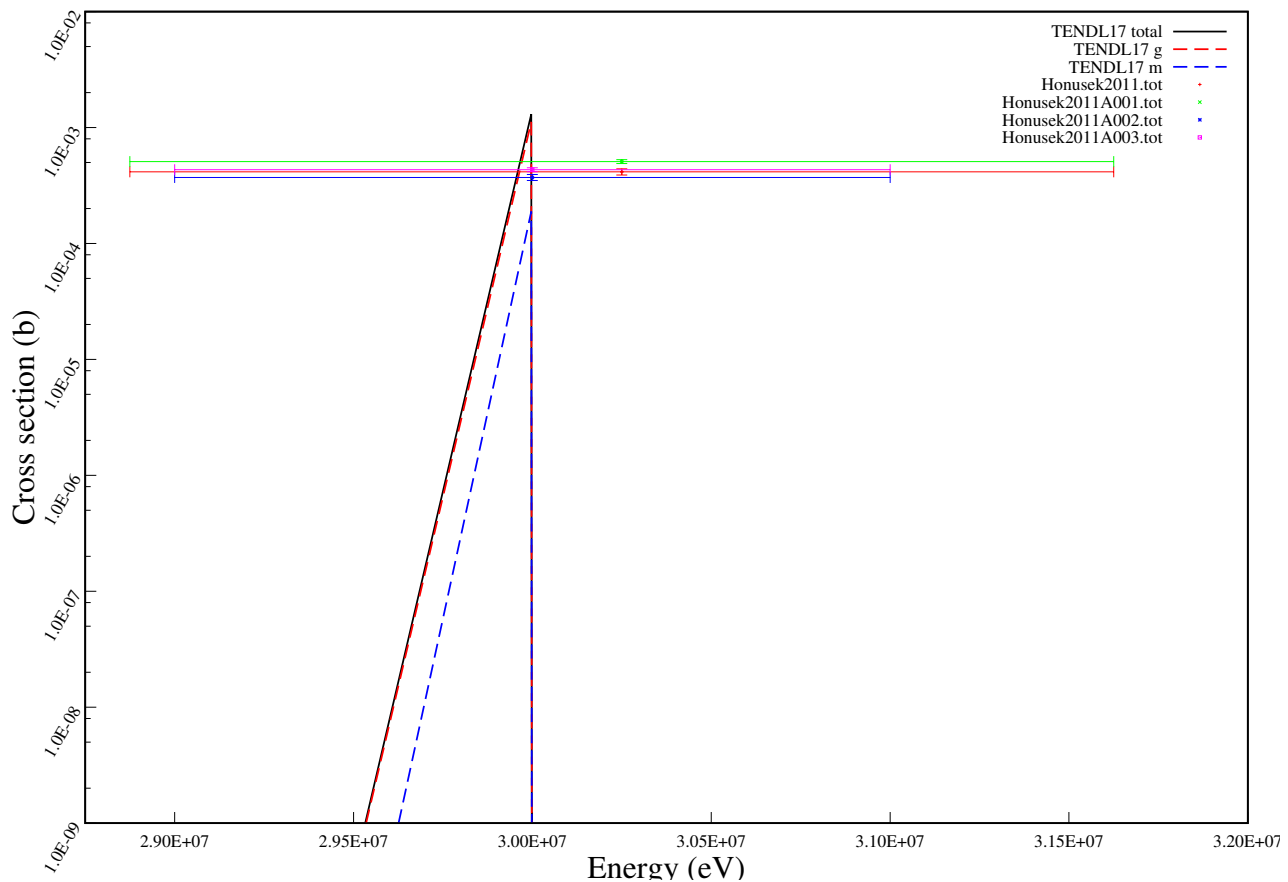
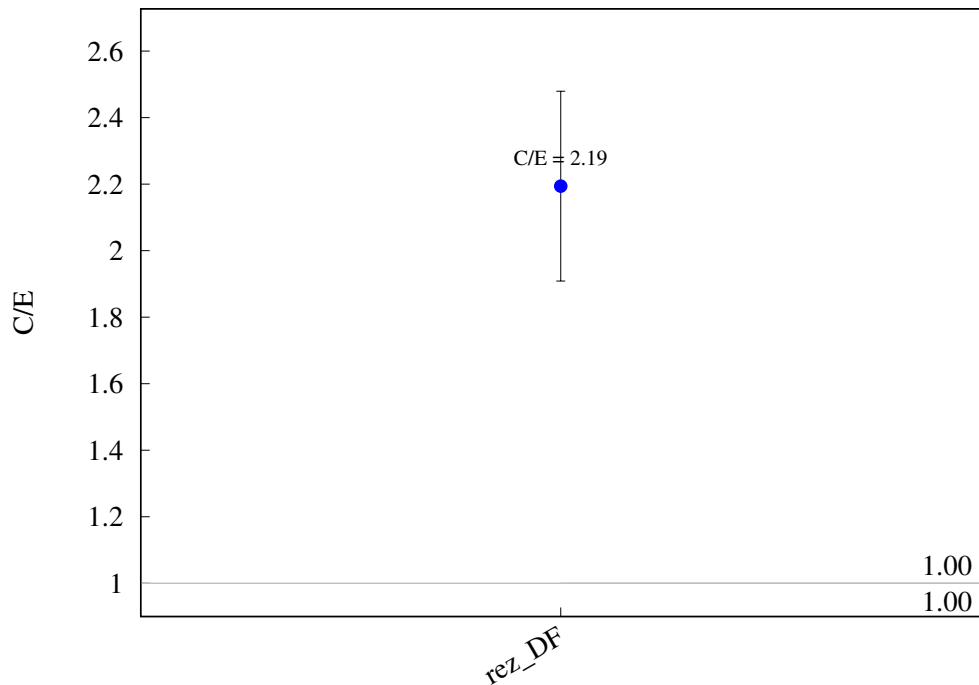
^{94}Zr (n,p) ^{94}Y 

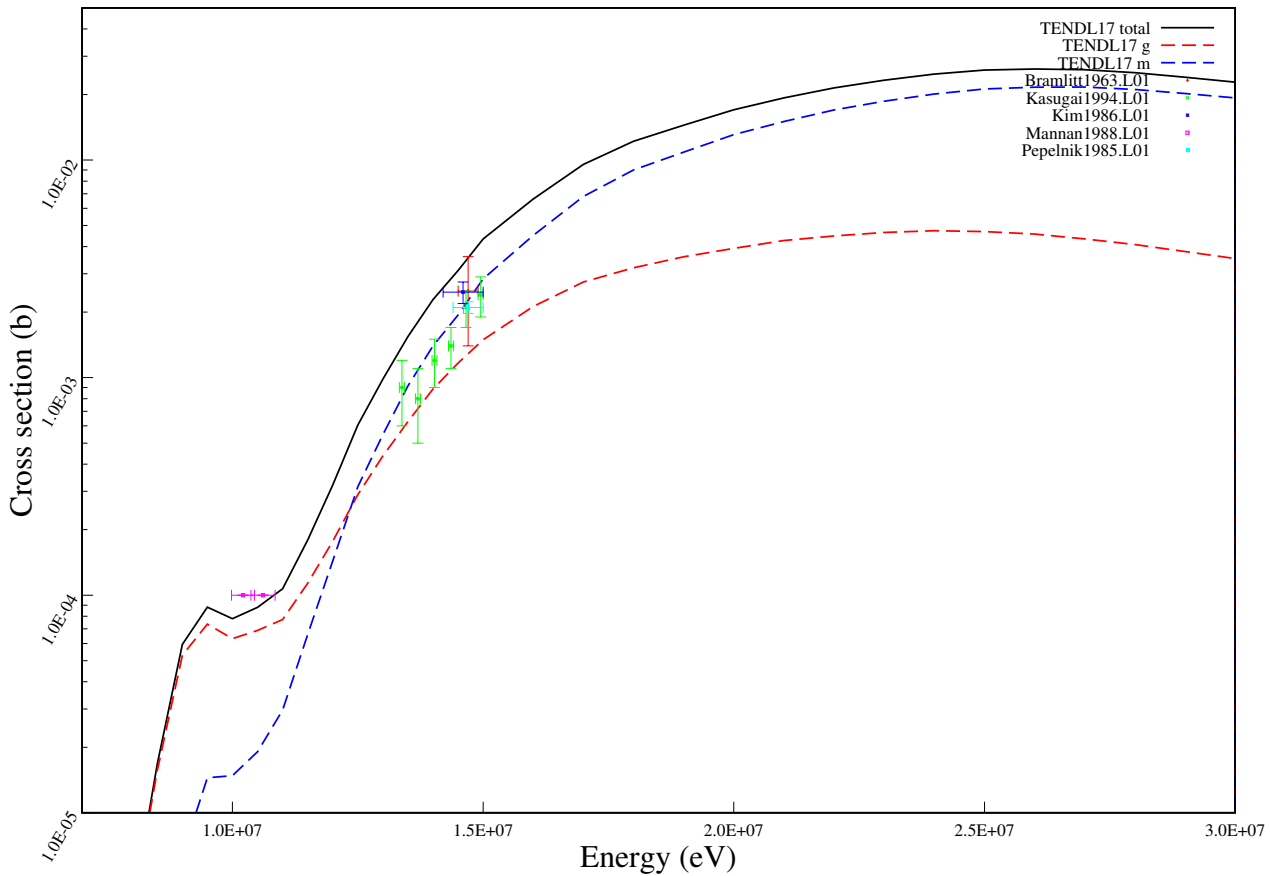
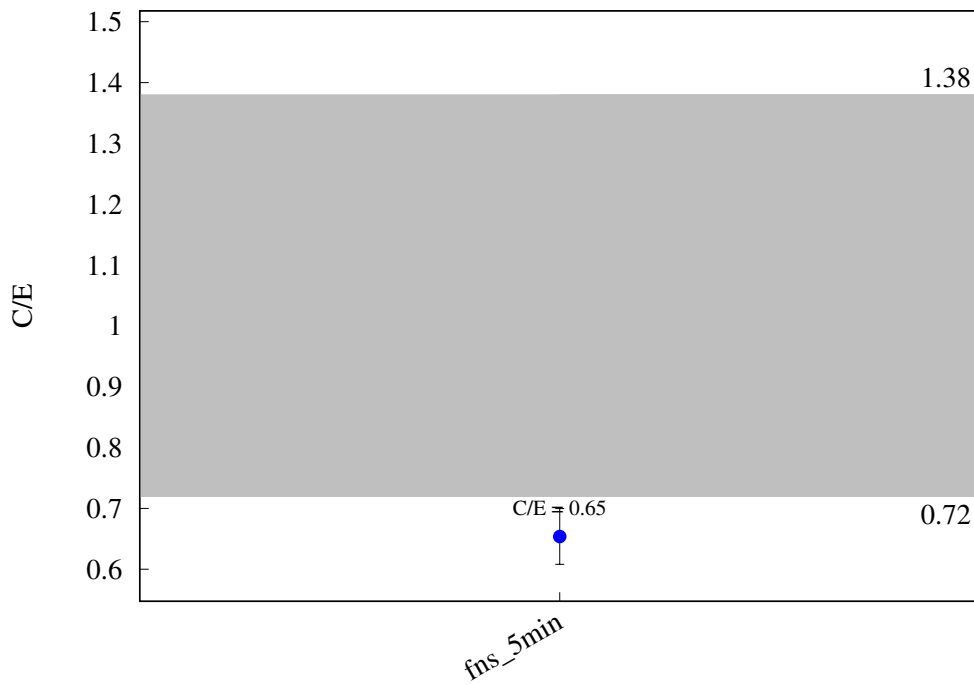
^{96}Zr (n,2n) ^{95}Zr 

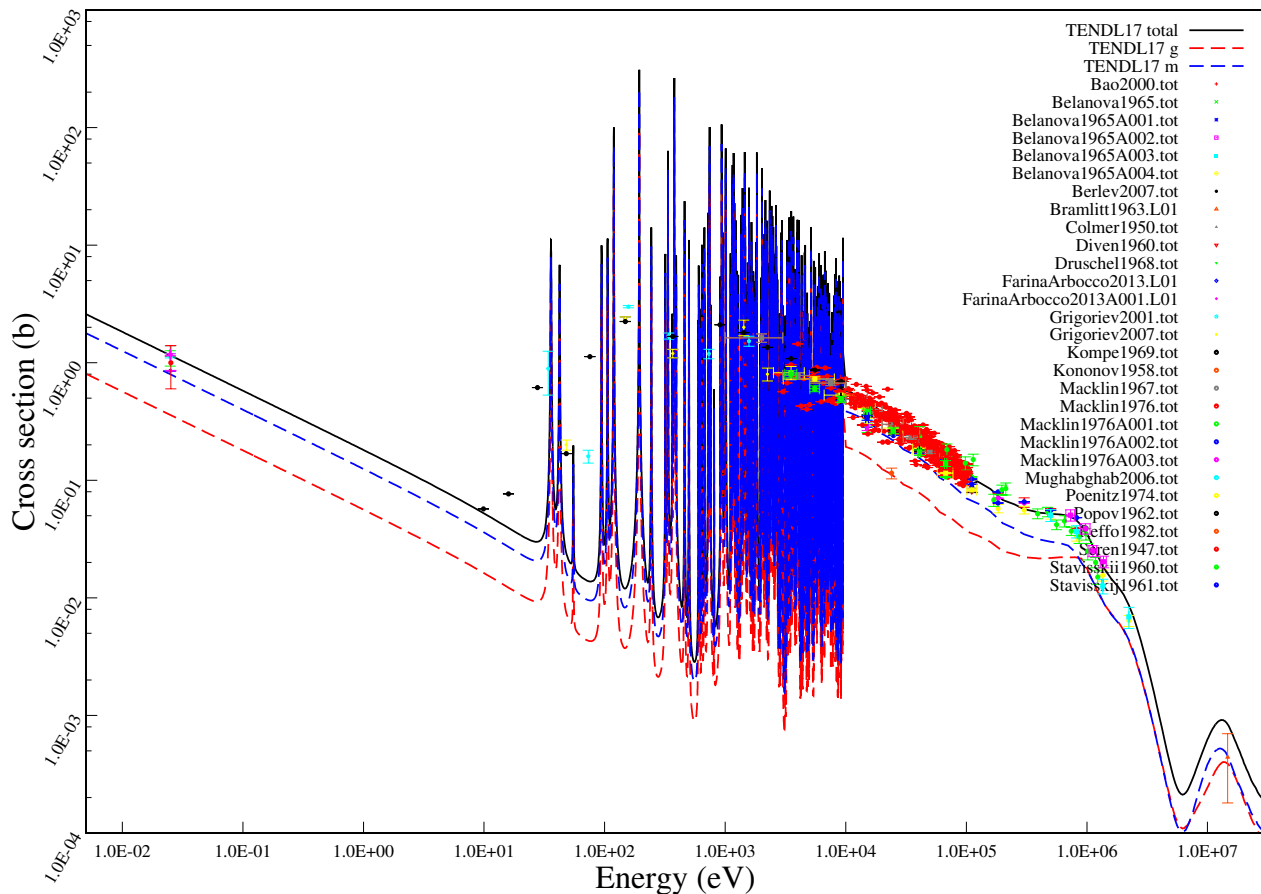
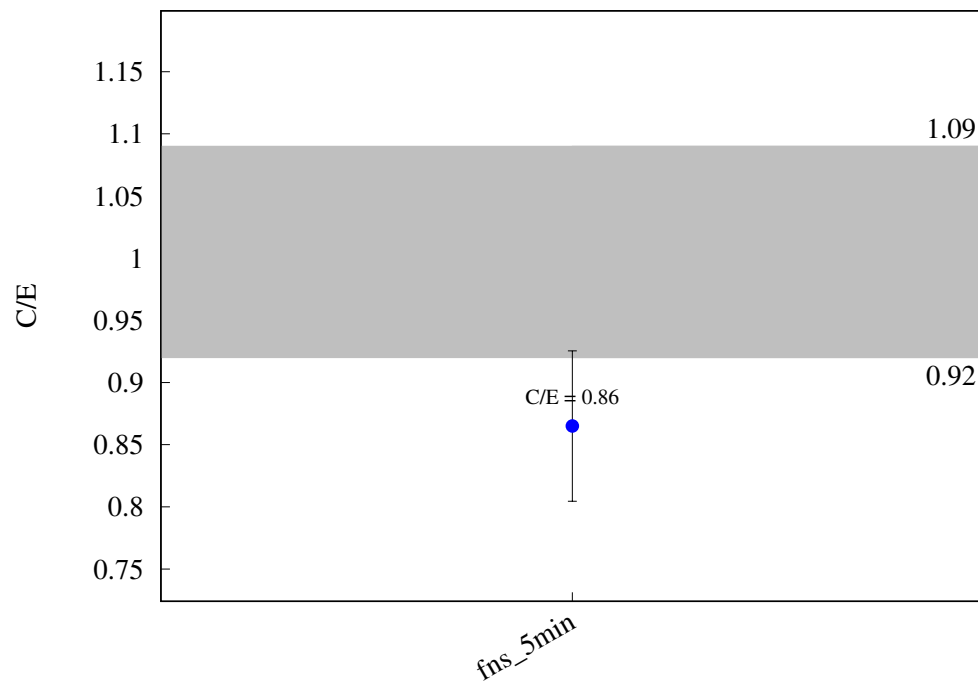
^{96}Zr (n,g) ^{97}Zr 

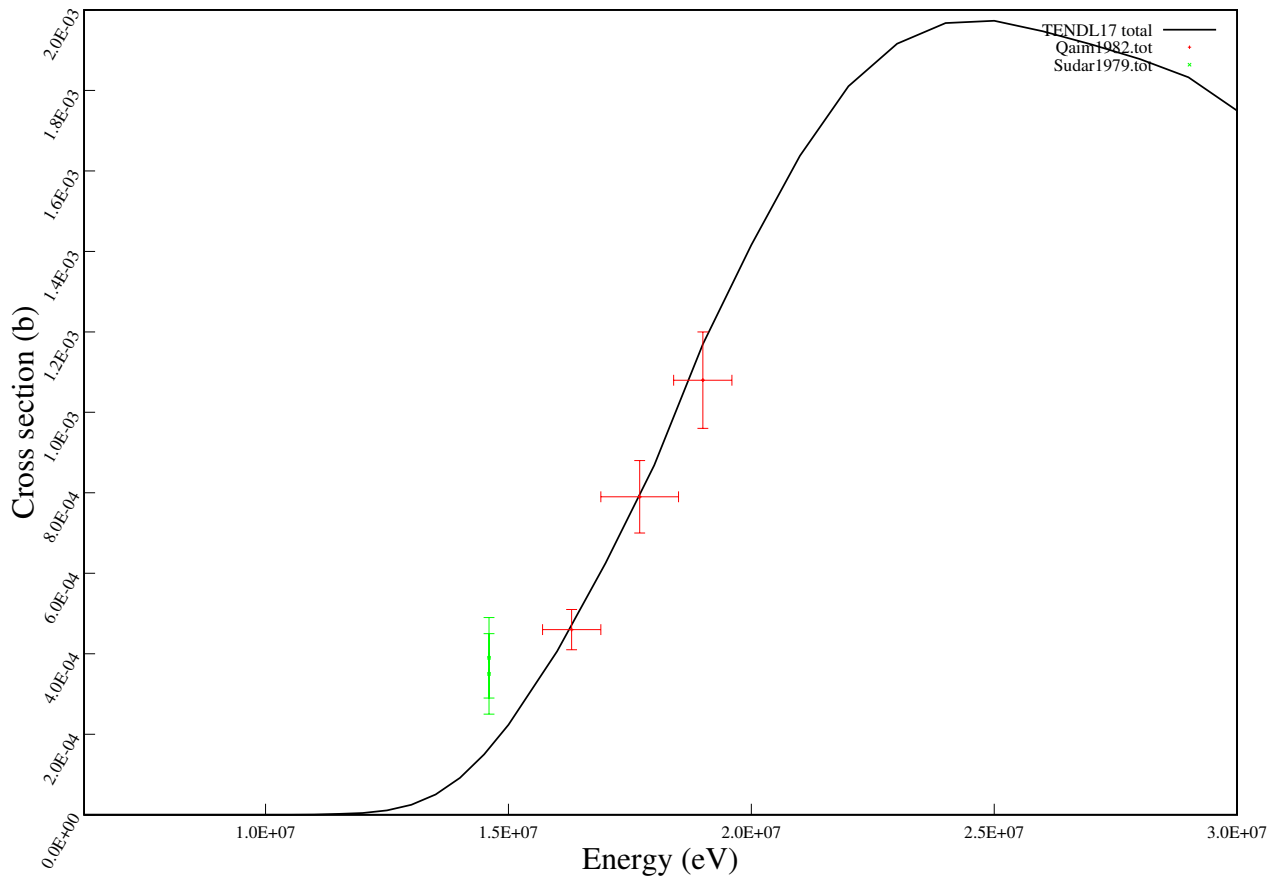
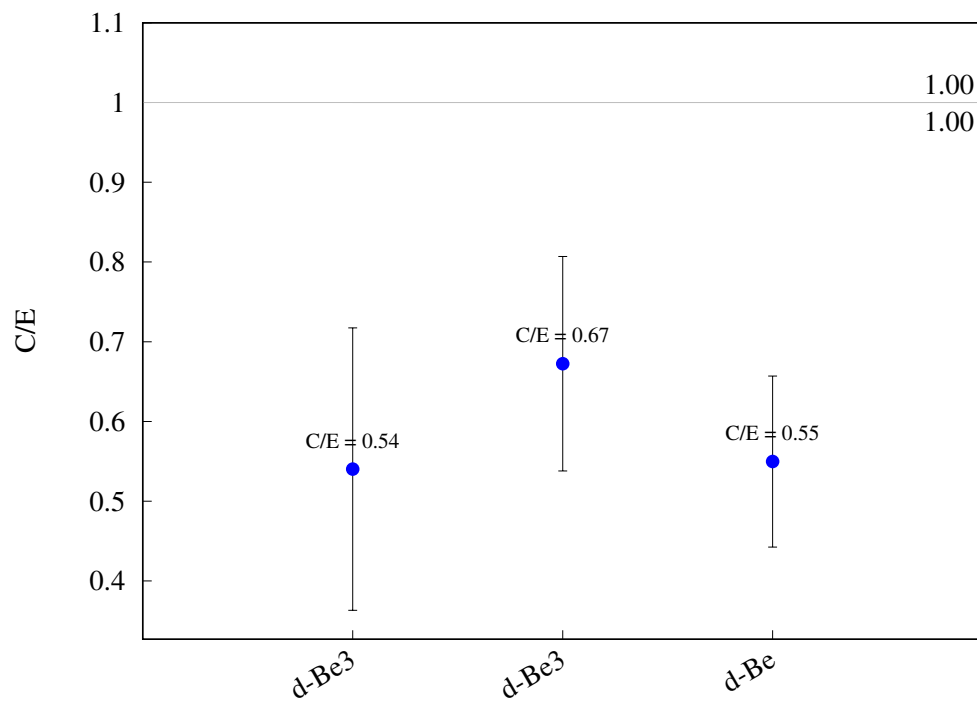
^{93}Nb ($n,2n$) $^{92\text{m}}\text{Nb}$ 

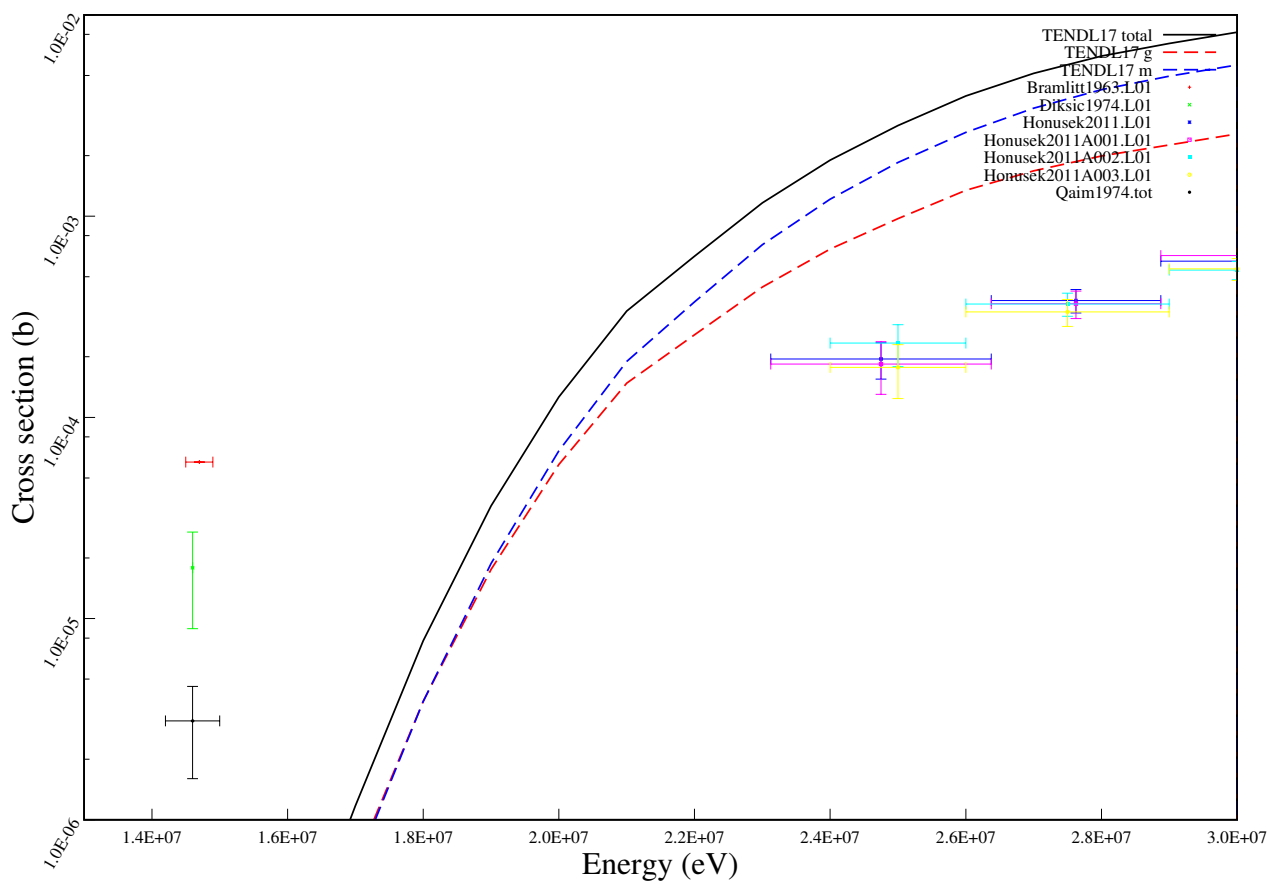
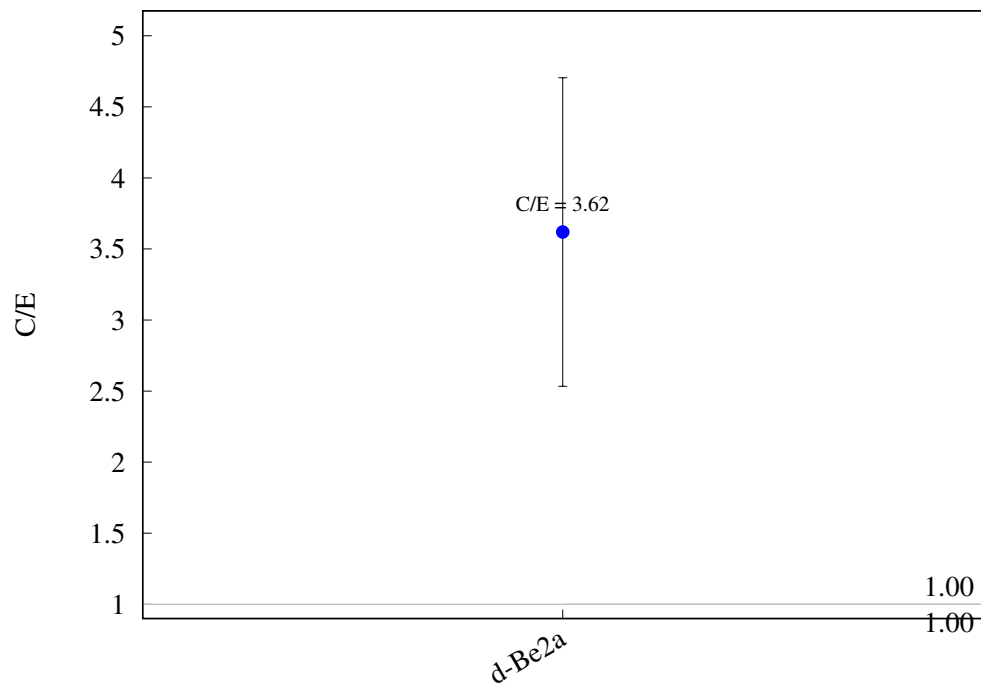
^{93}Nb (n,3n) $^{91\text{m}}\text{Nb}$ 

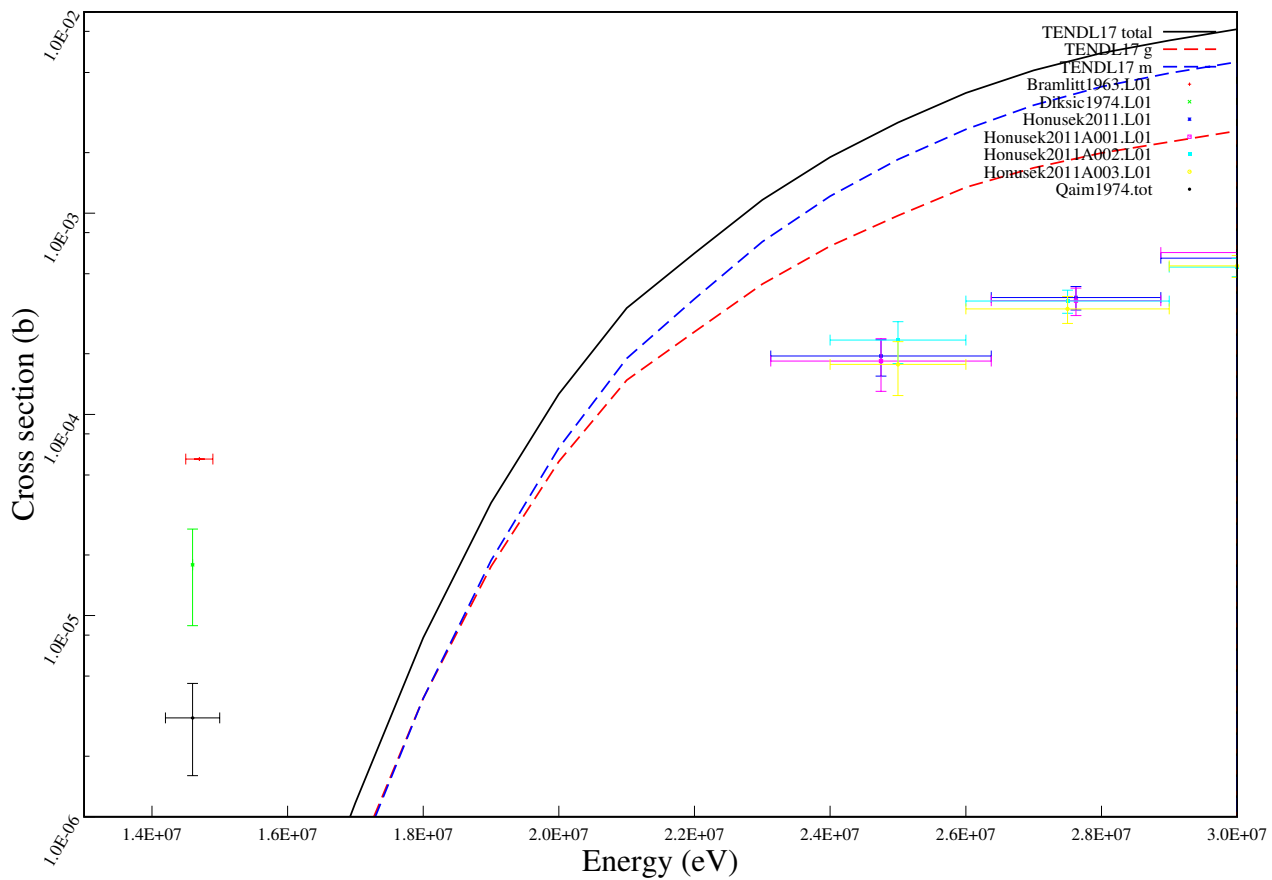
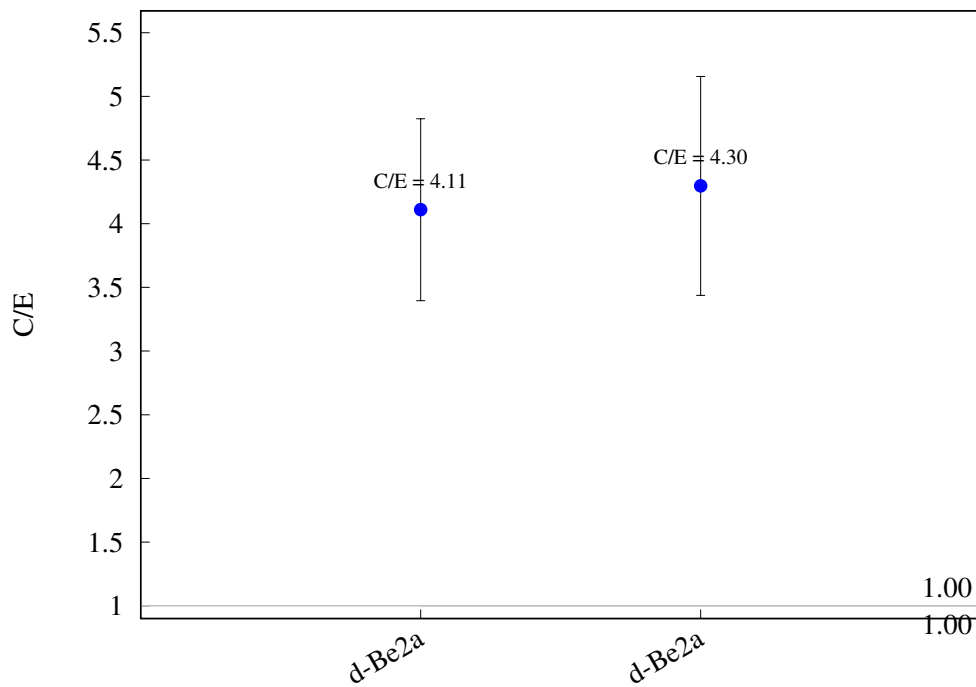
^{93}Nb ($n,4n$) ^{90}Nb 

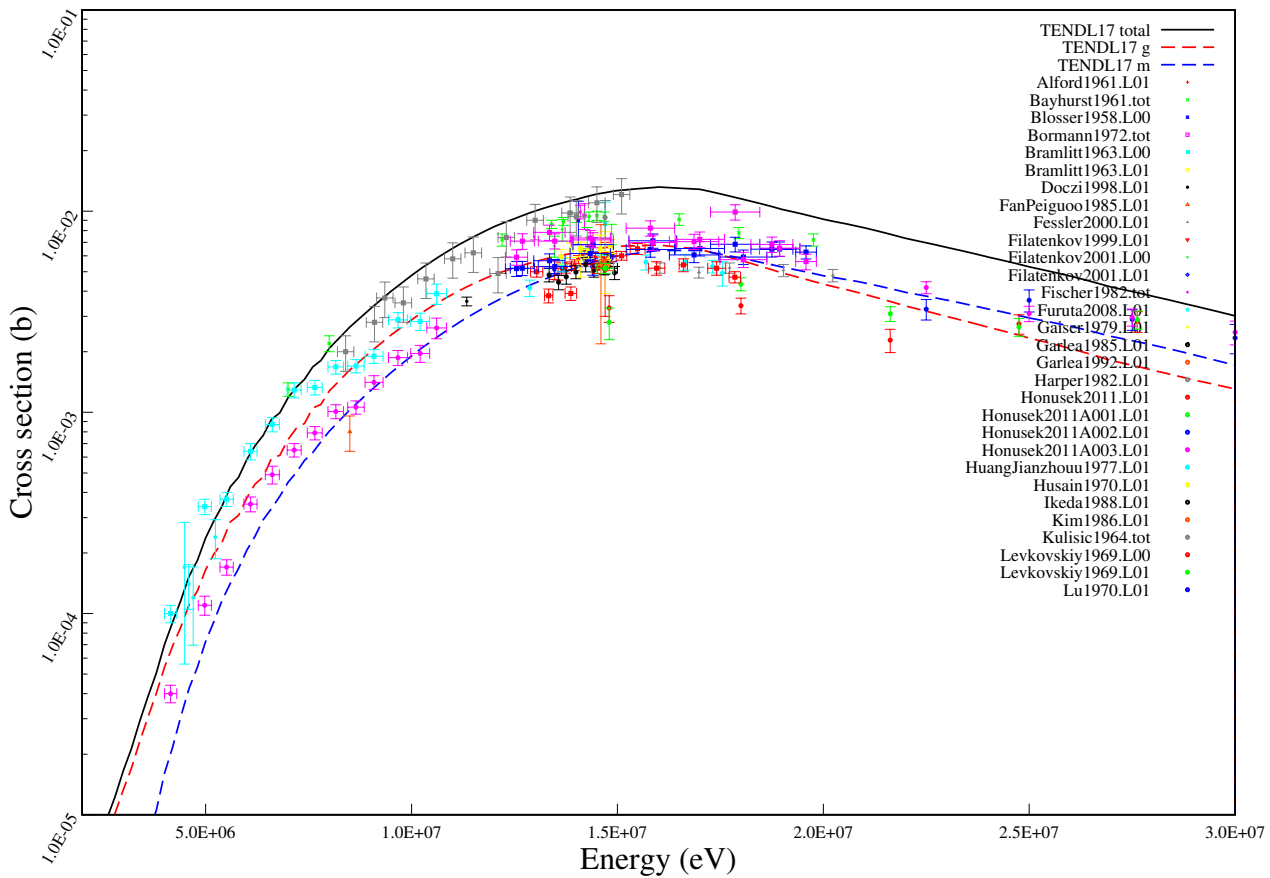
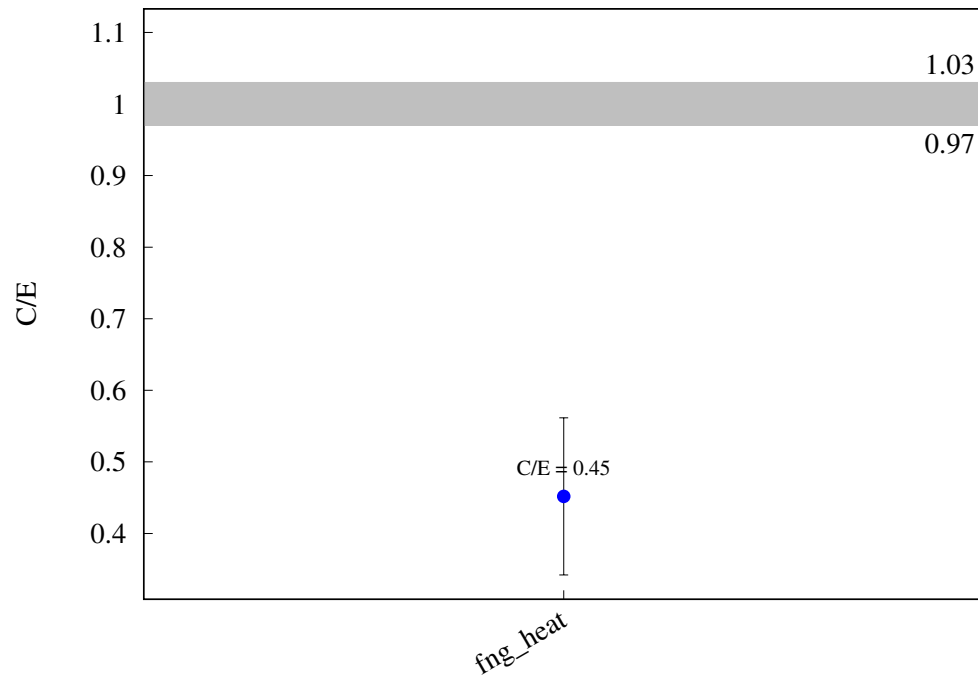
^{93}Nb (n,na) ^{89m}Y 

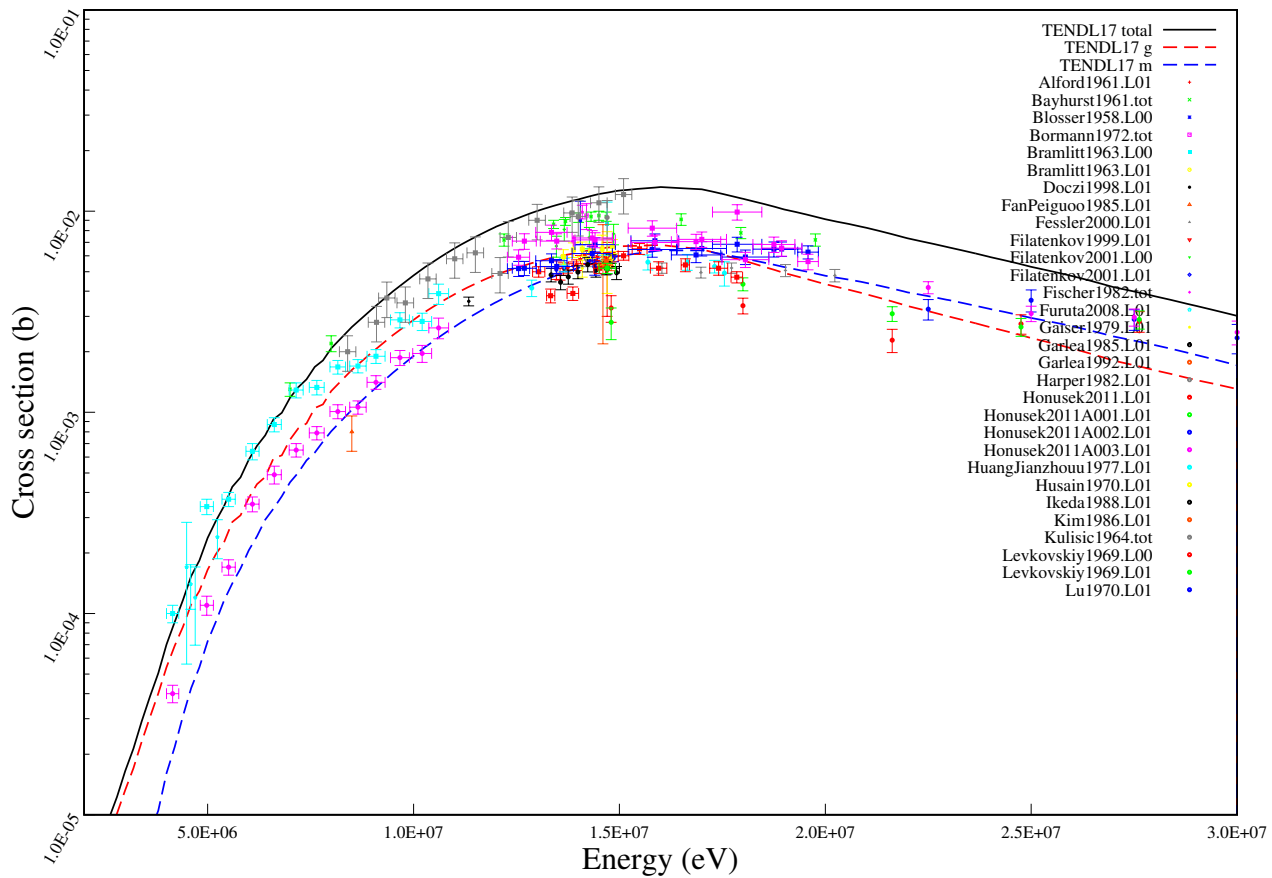
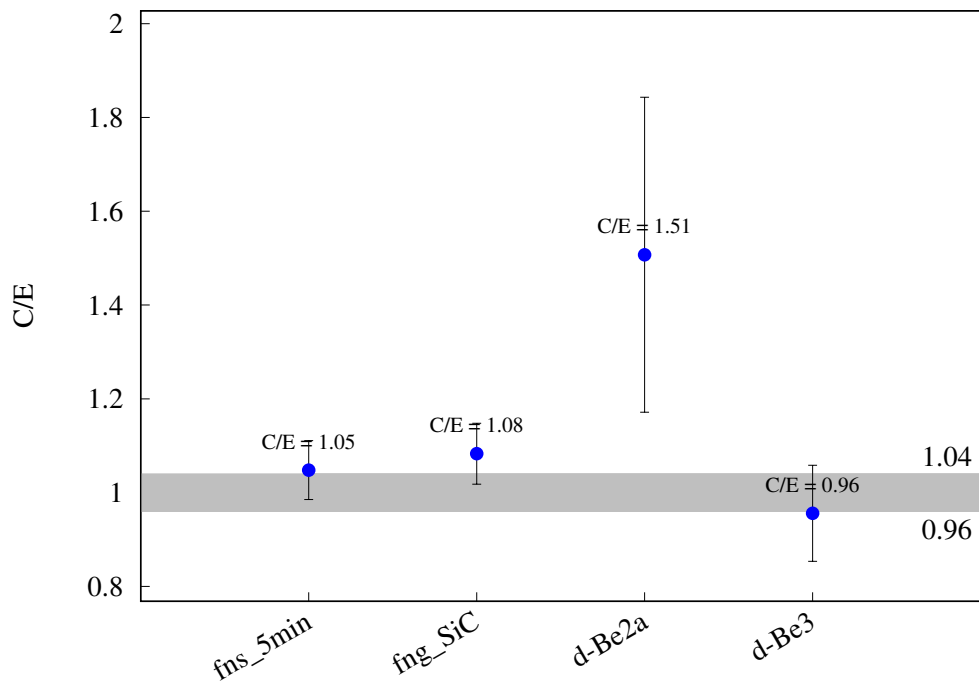
^{93}Nb (n,g) ^{94m}Nb 

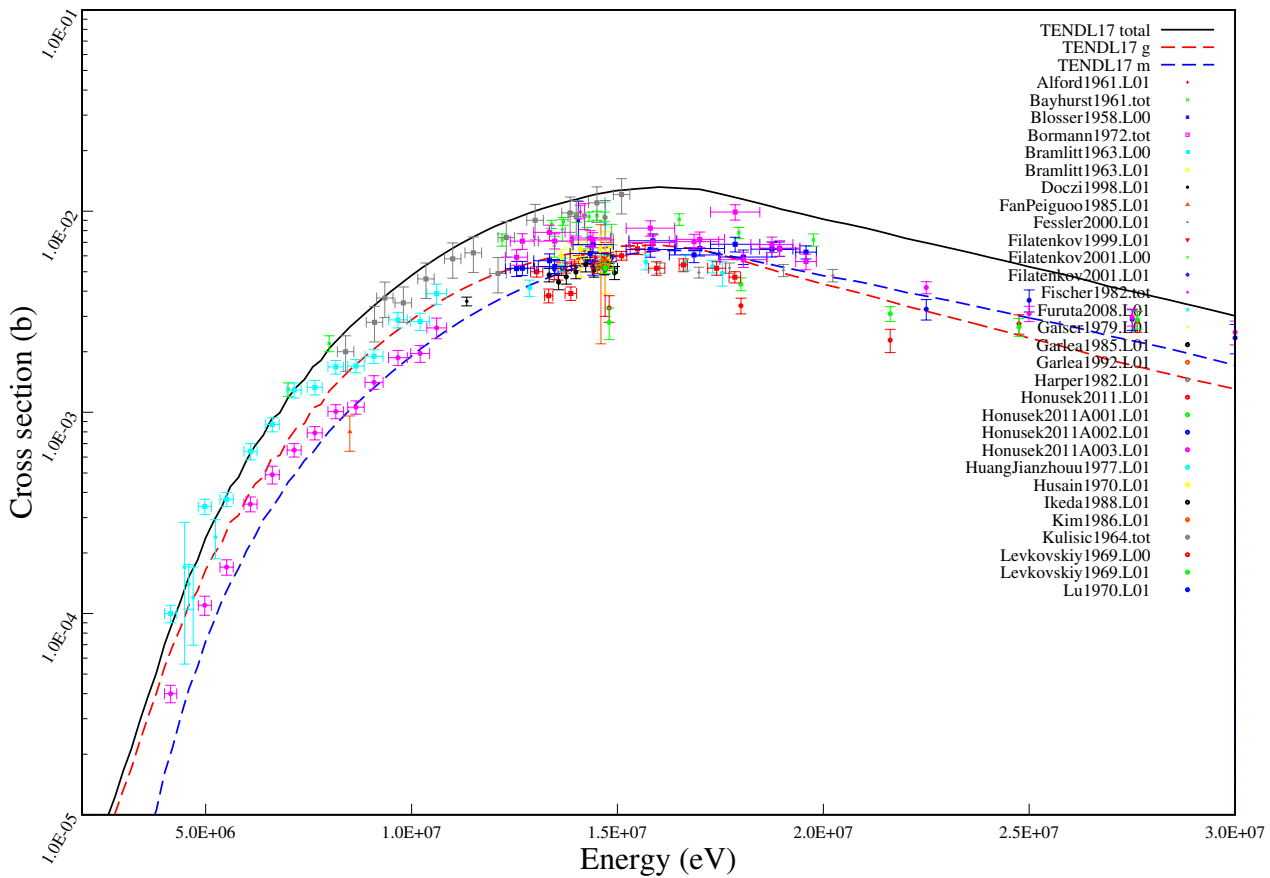
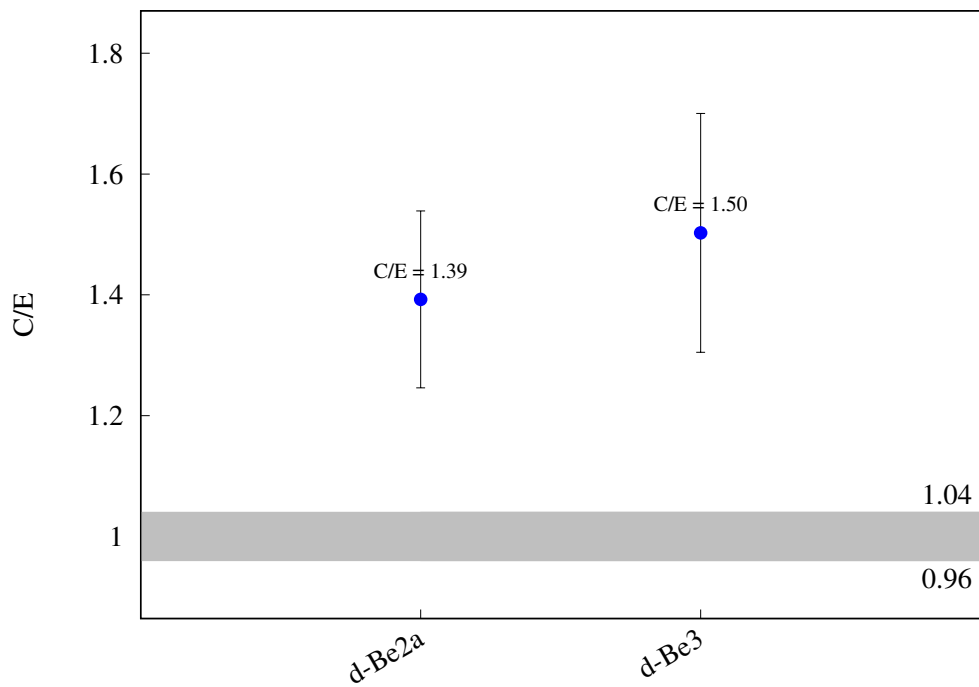
$^{93}\text{Nb} (\text{n},\text{t}) ^{91}\text{Zr}$ 

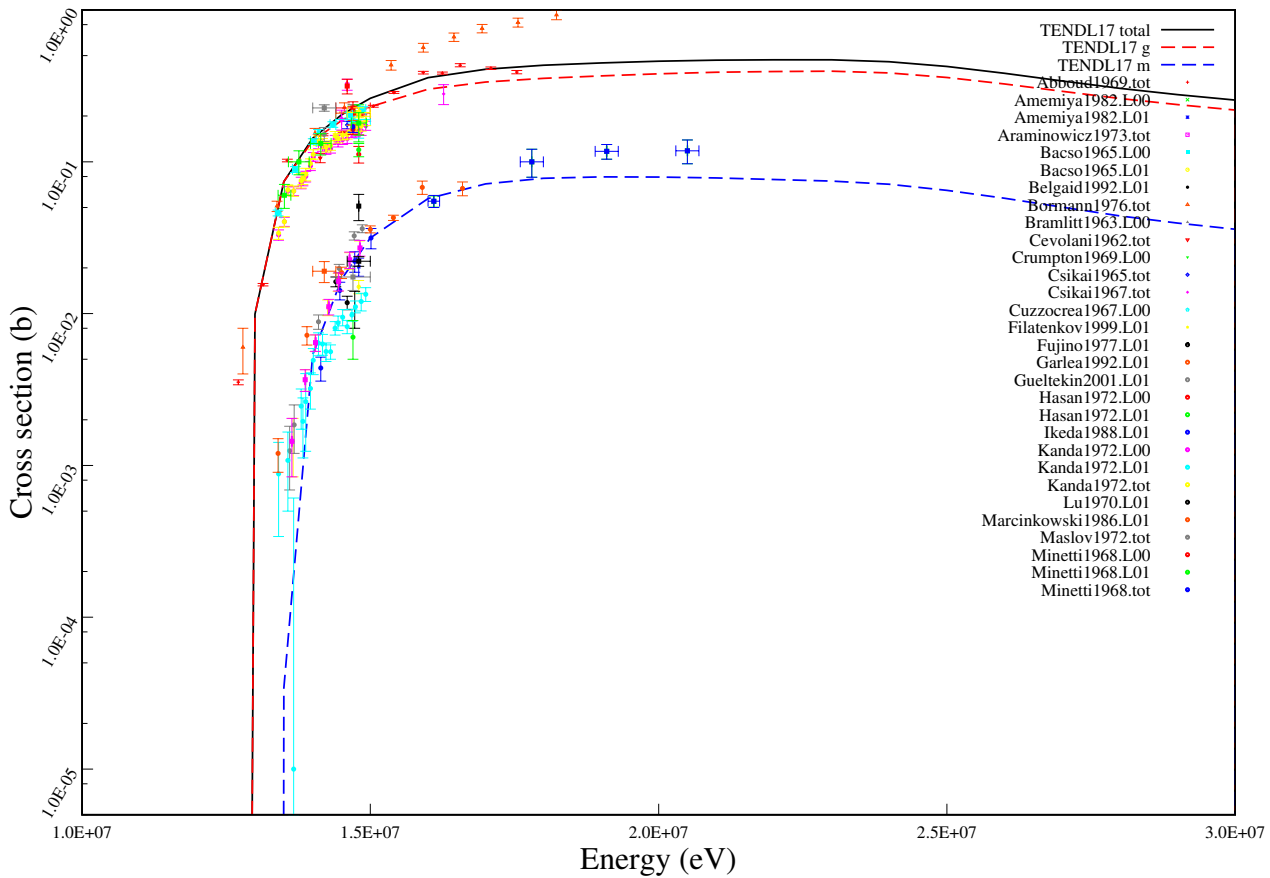
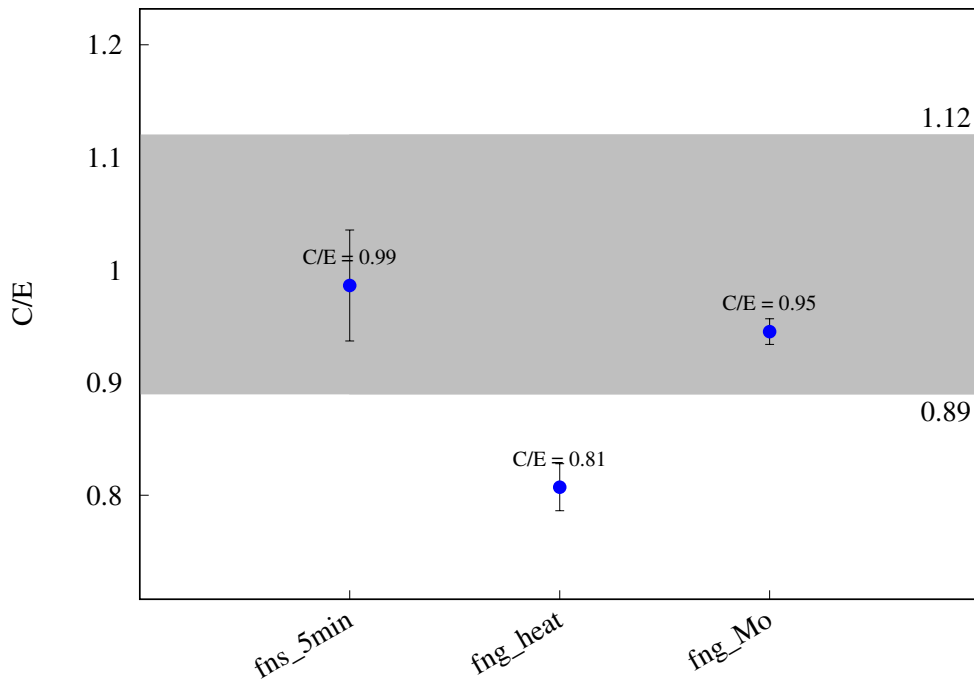
$^{93}\text{Nb} (\text{n},\text{h}) ^{91m}\text{Y}$ 

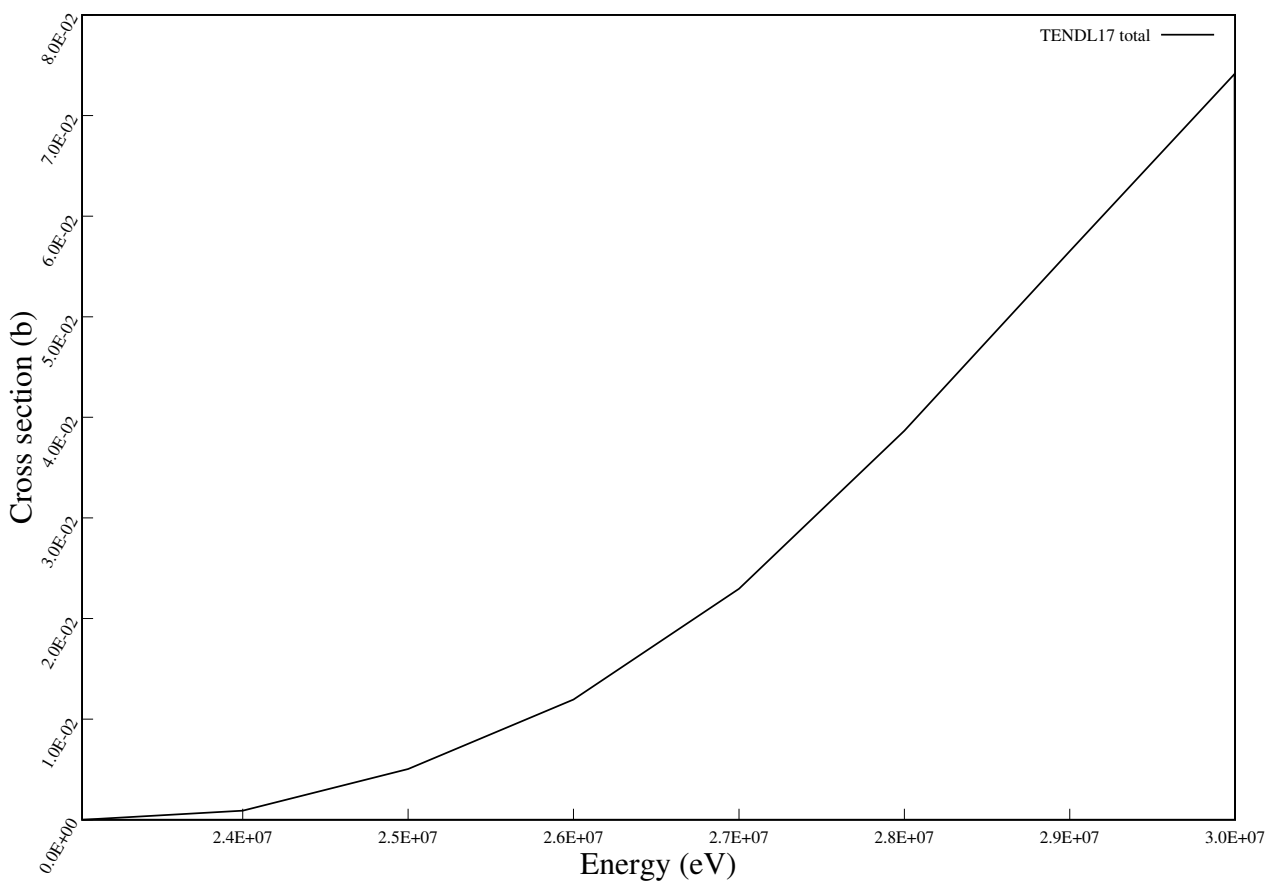
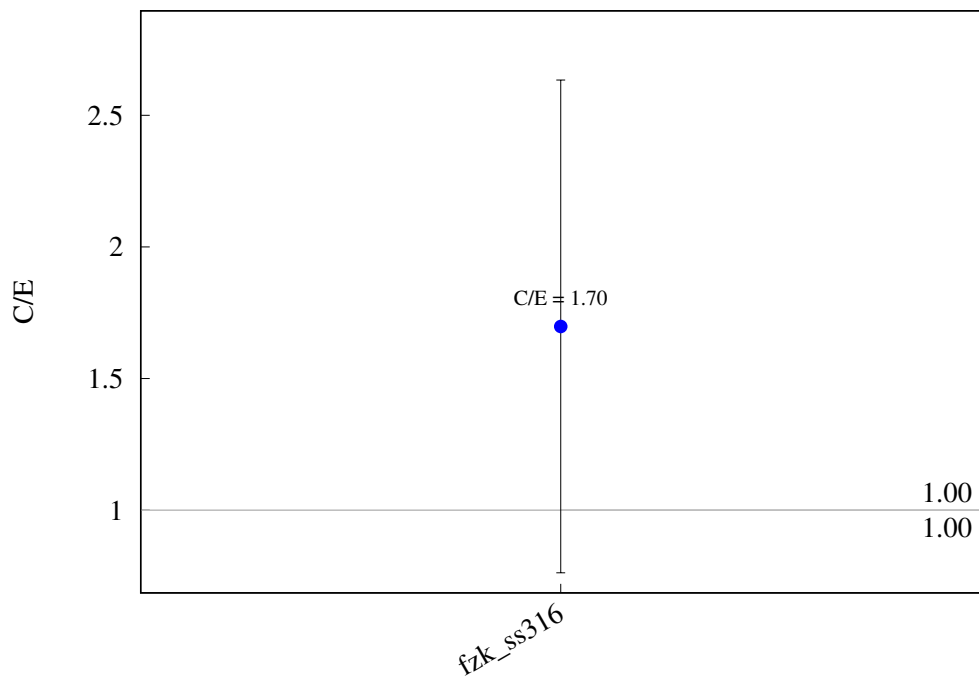
$^{93}\text{Nb} (\text{n},\text{h}) ^{91}\text{Y}$ 

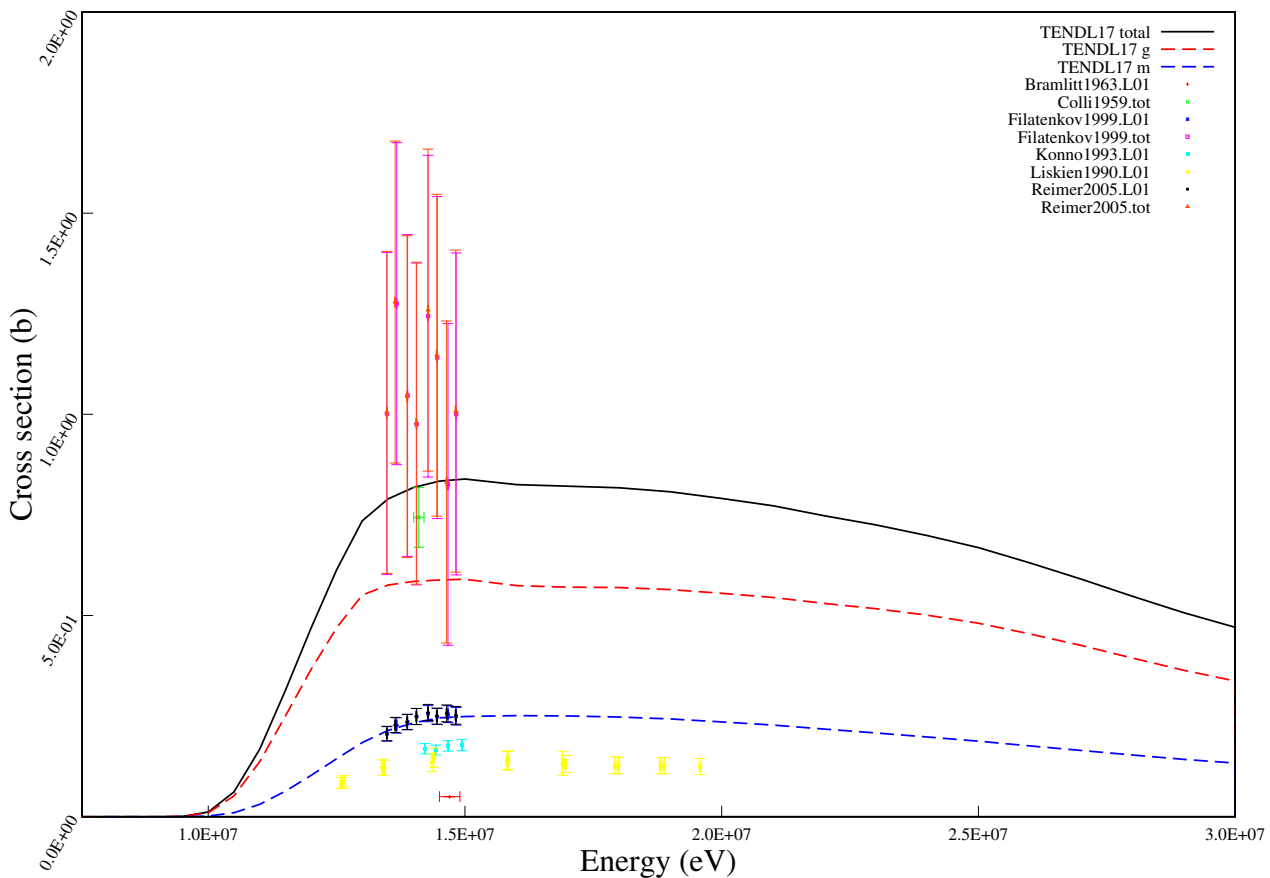
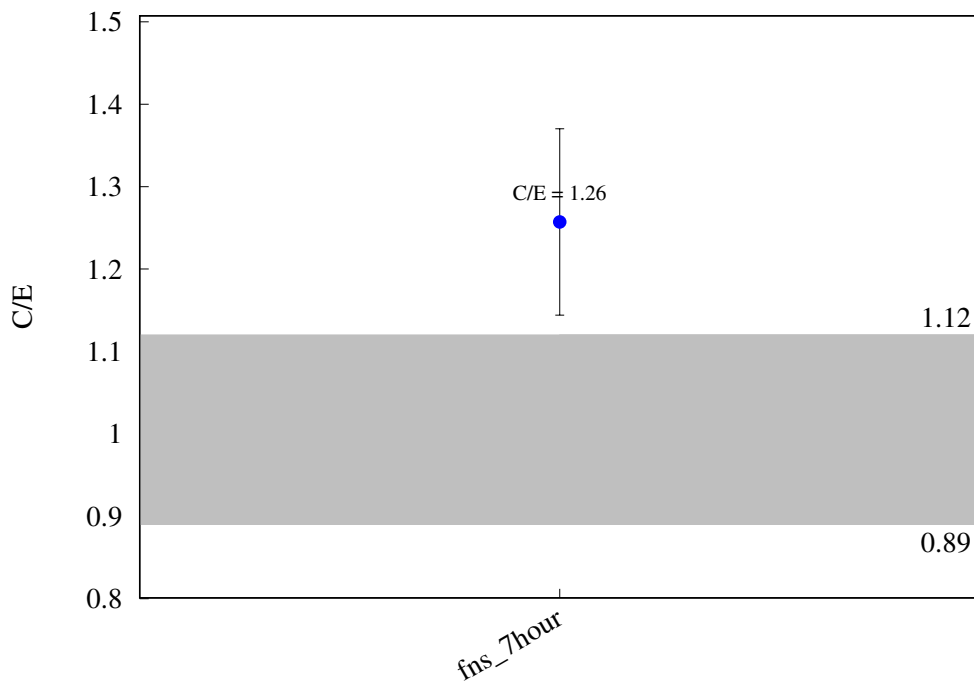
^{93}Nb (n,a) ^{90}gY 

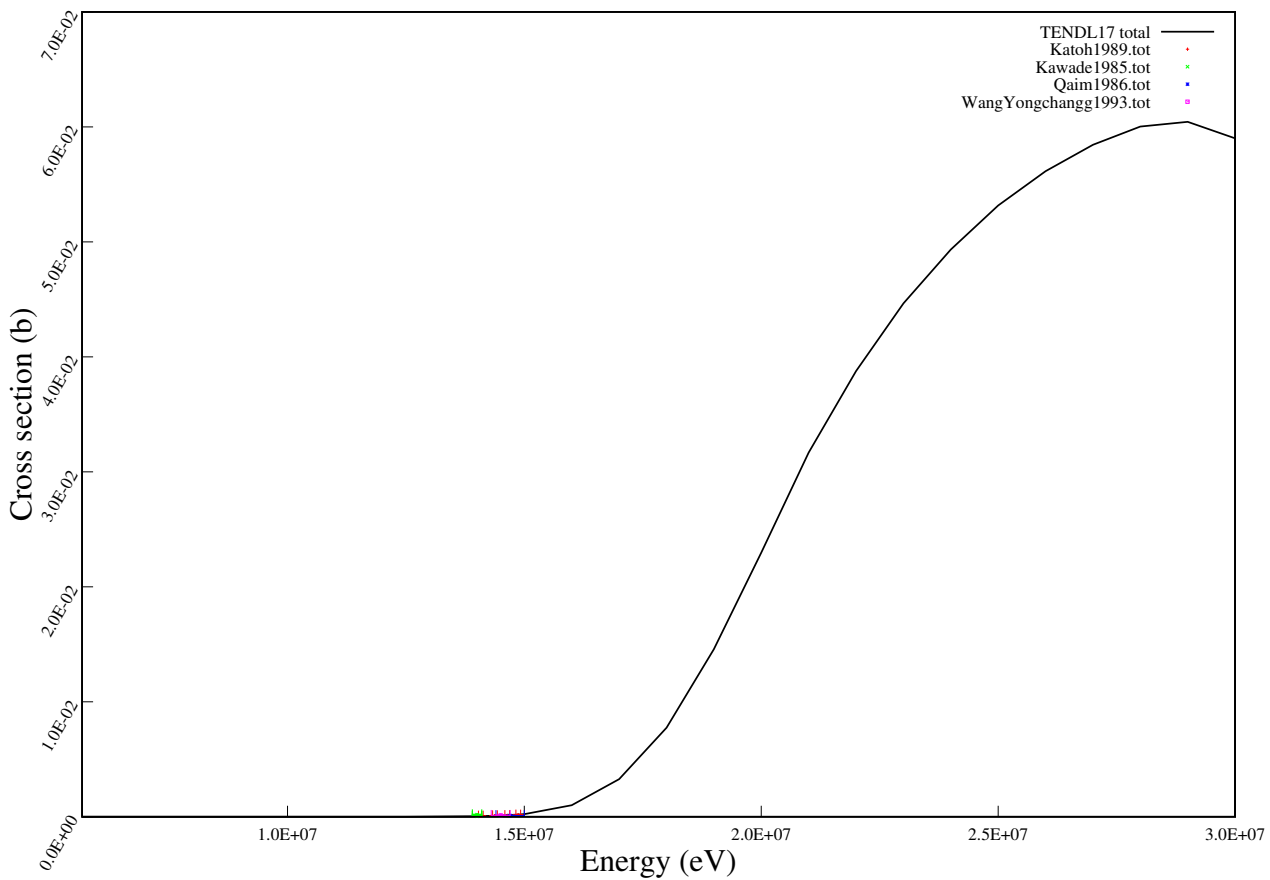
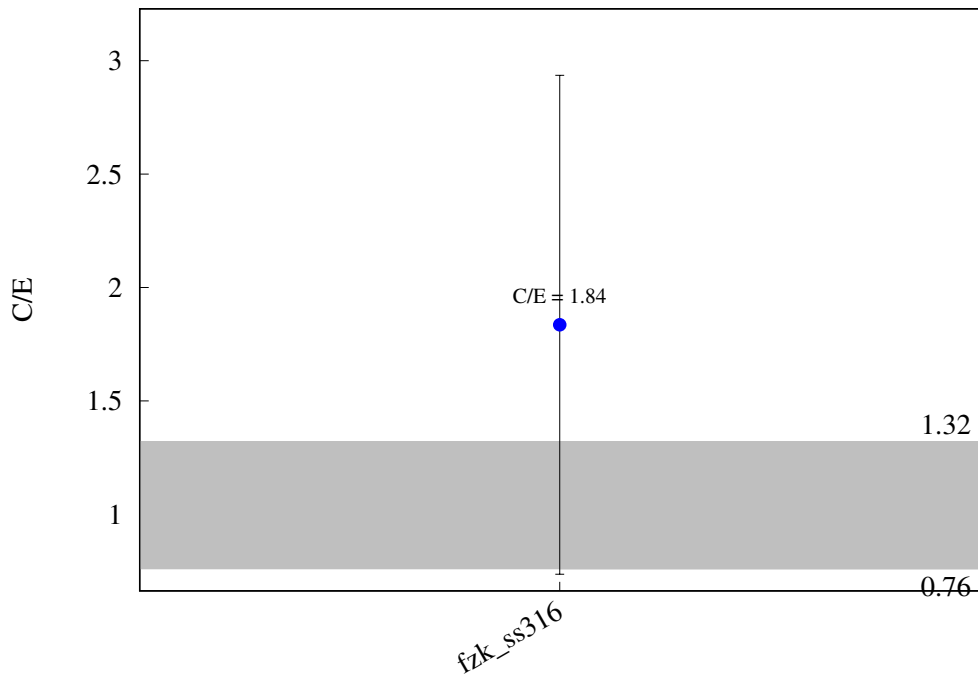
$^{93}\text{Nb} (\text{n,a}) ^{90m}\text{Y}$ 

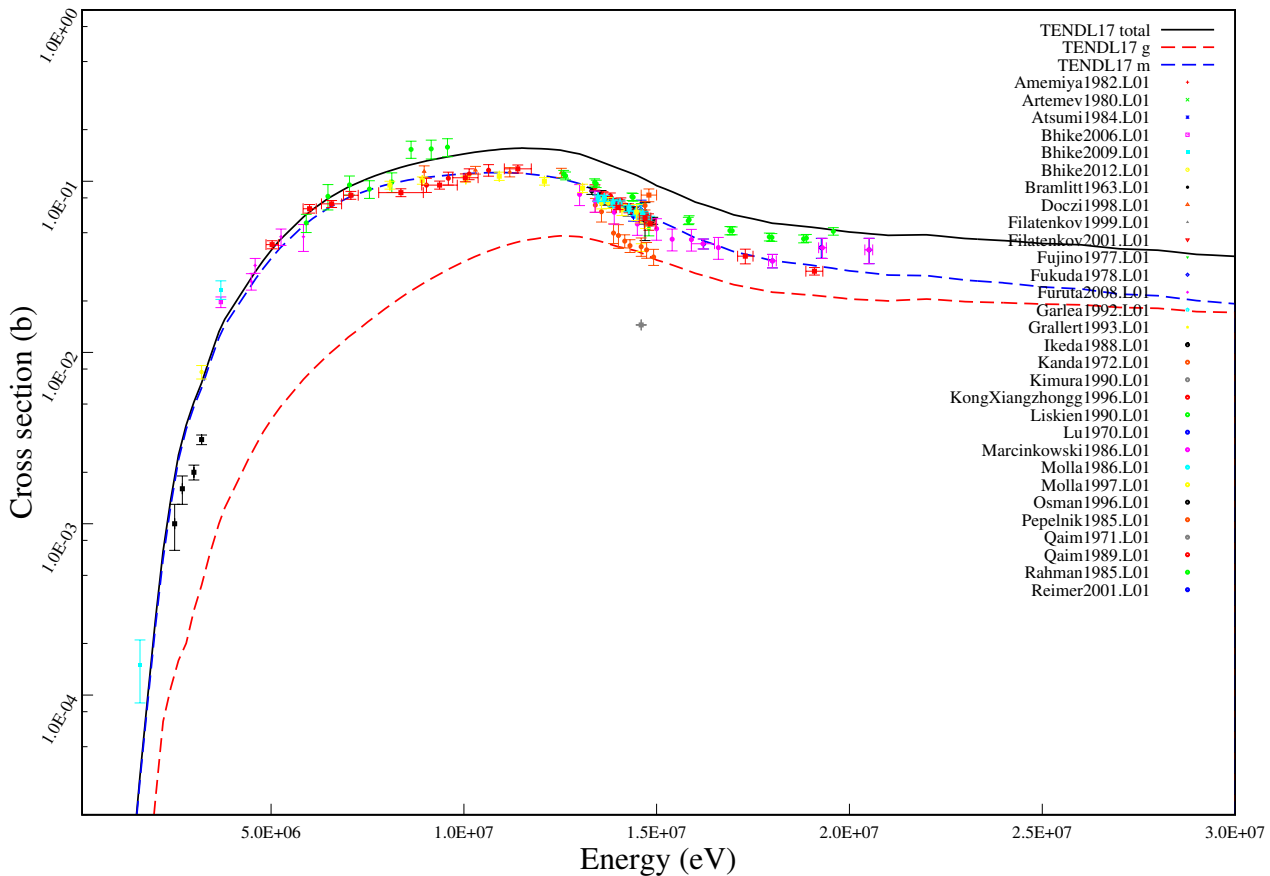
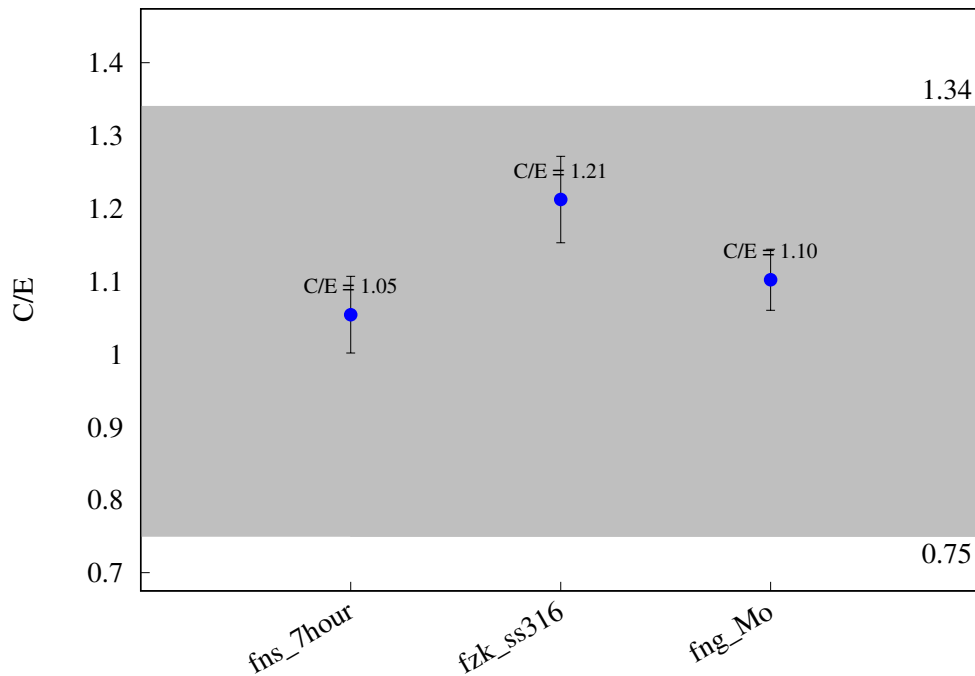
$^{93}\text{Nb} (\text{n,a}) ^{90}\text{Y}$ 

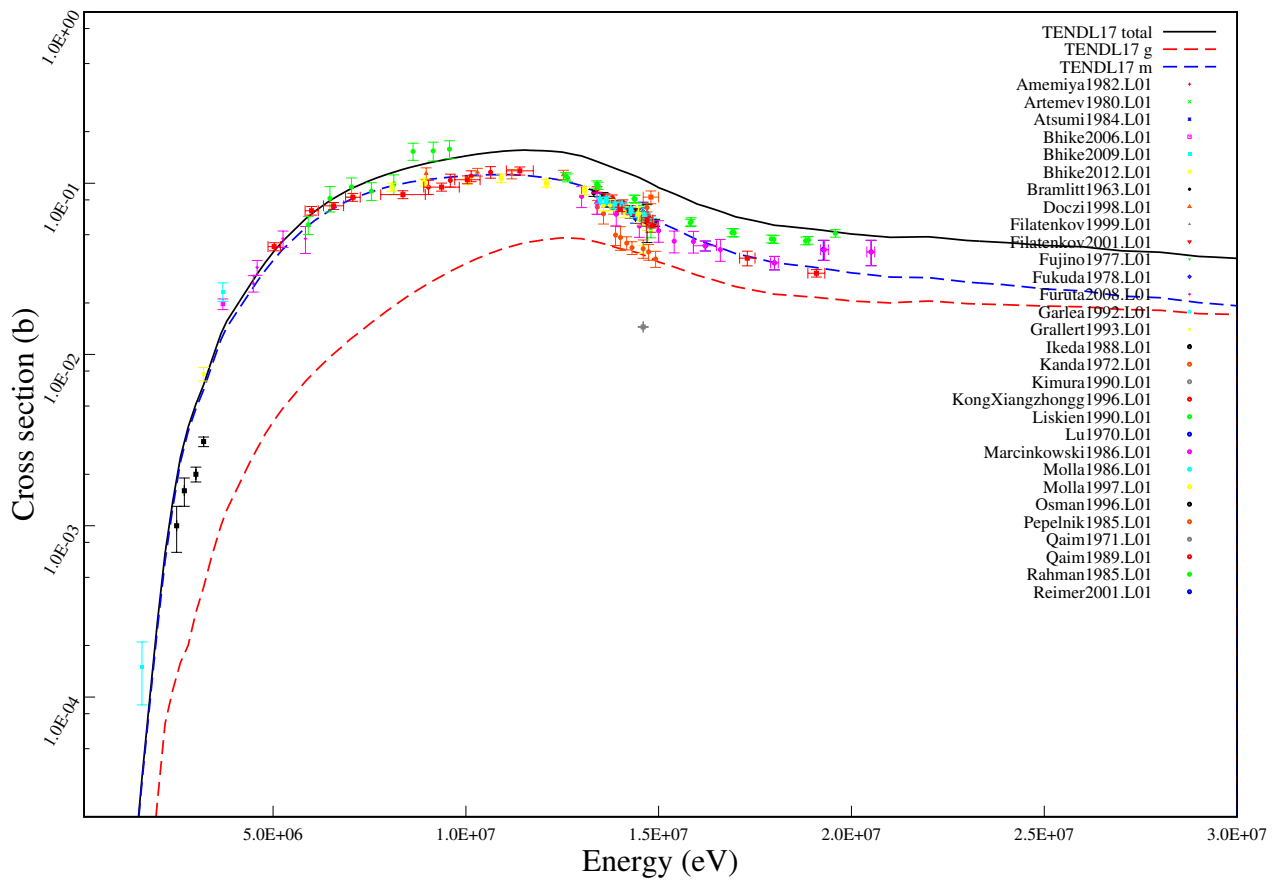
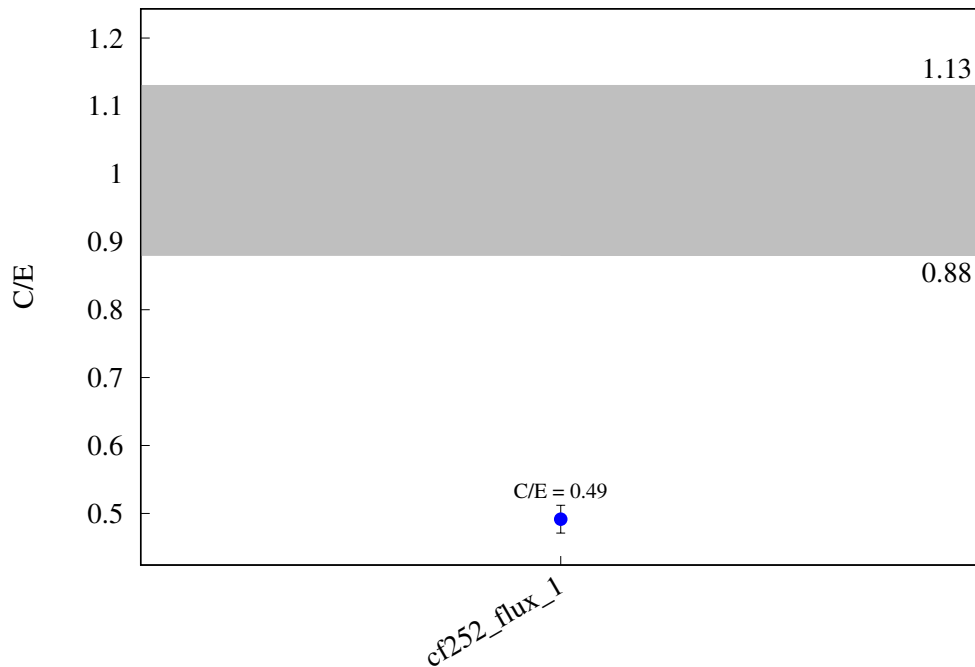
^{92}Mo (n,2n) ^{91}Mo 

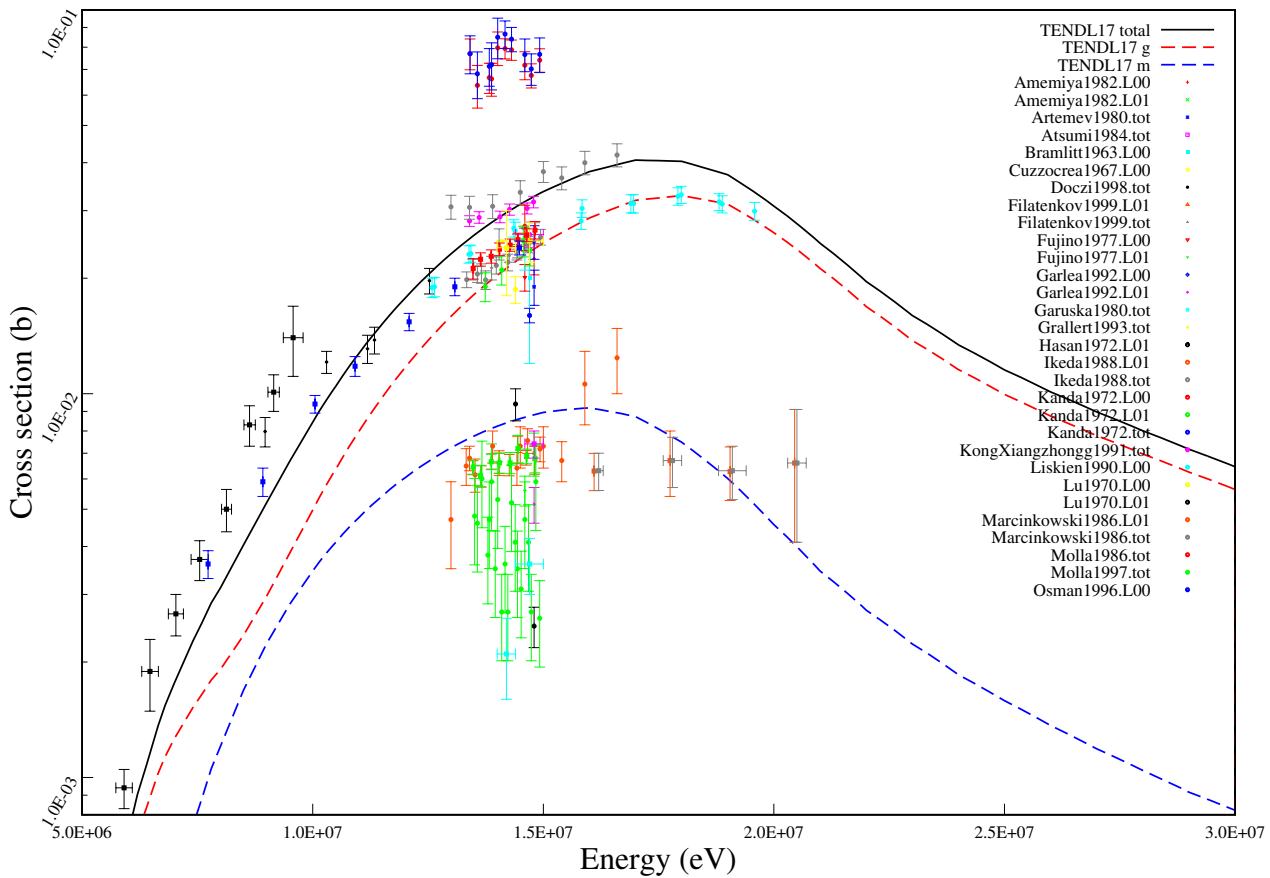
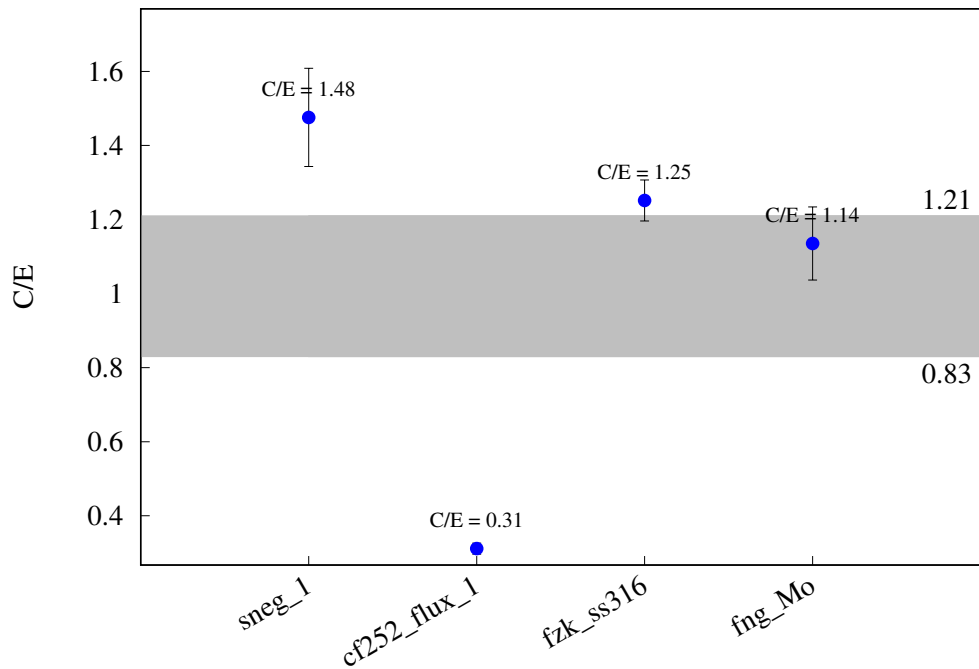
^{92}Mo (n,3n) ^{90}Mo 

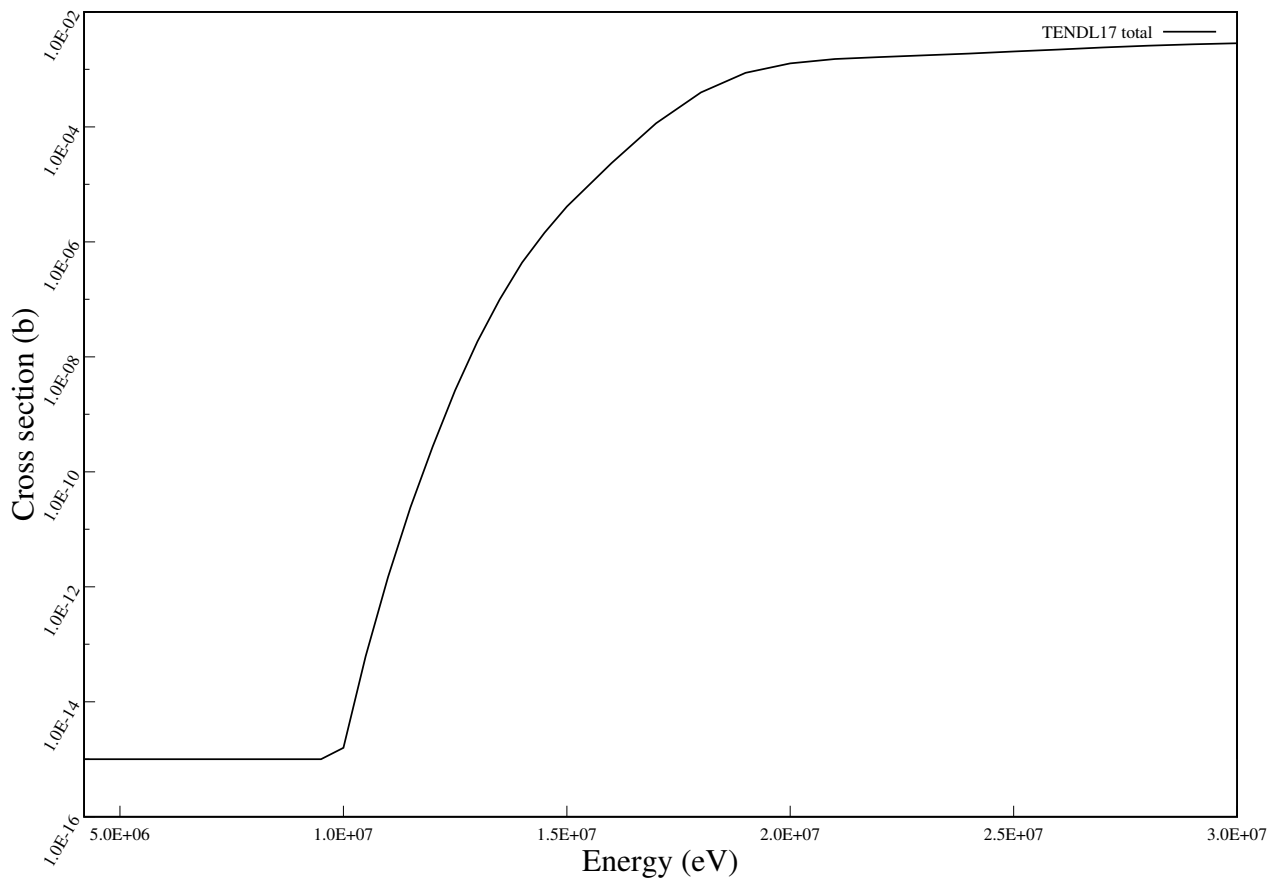
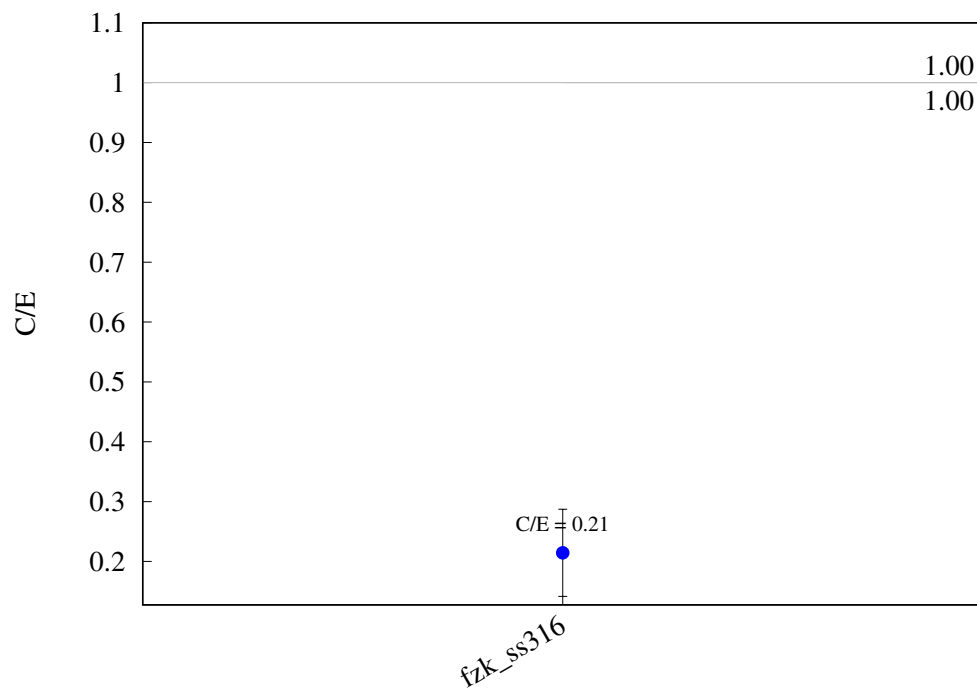
^{92}Mo (n,np) $^{91\text{m}}\text{Nb}$ 

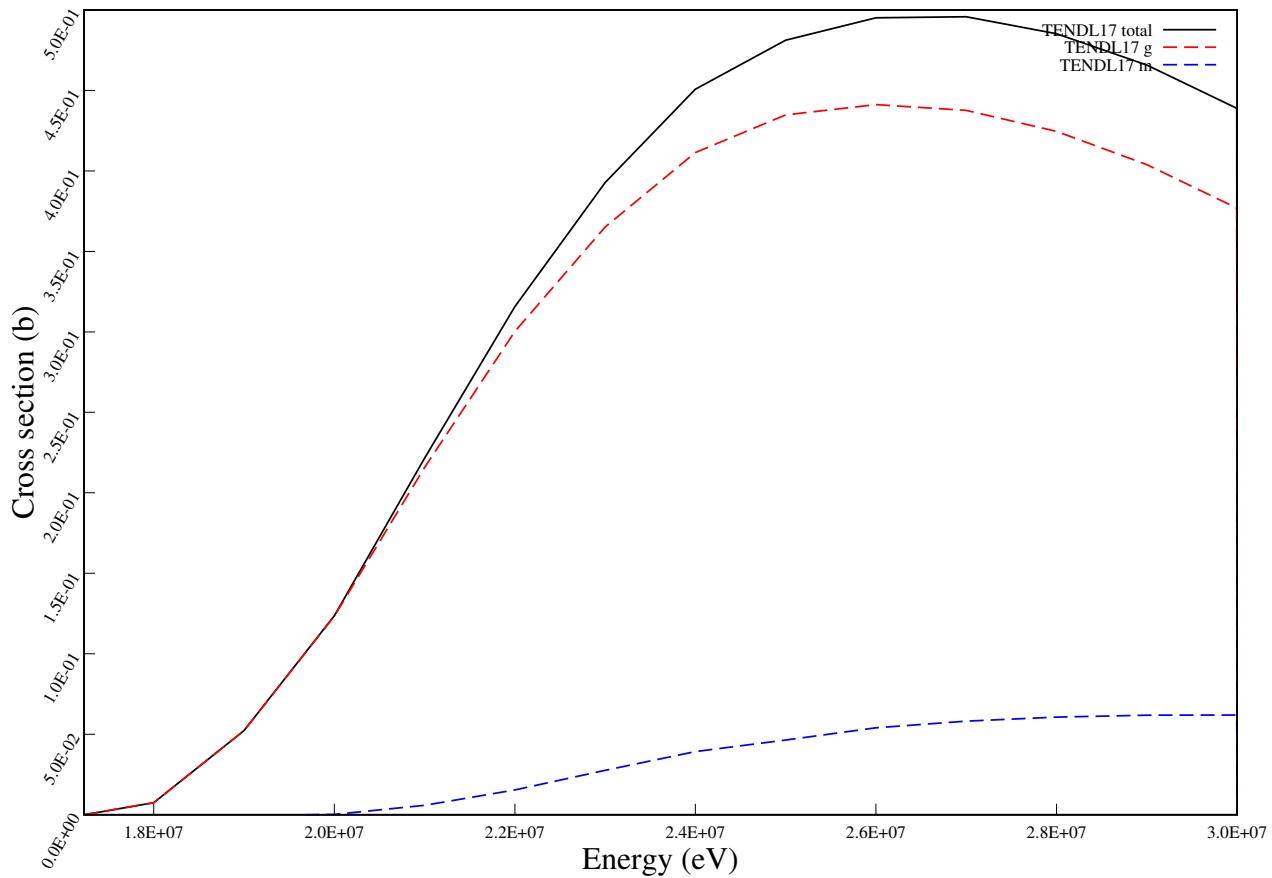
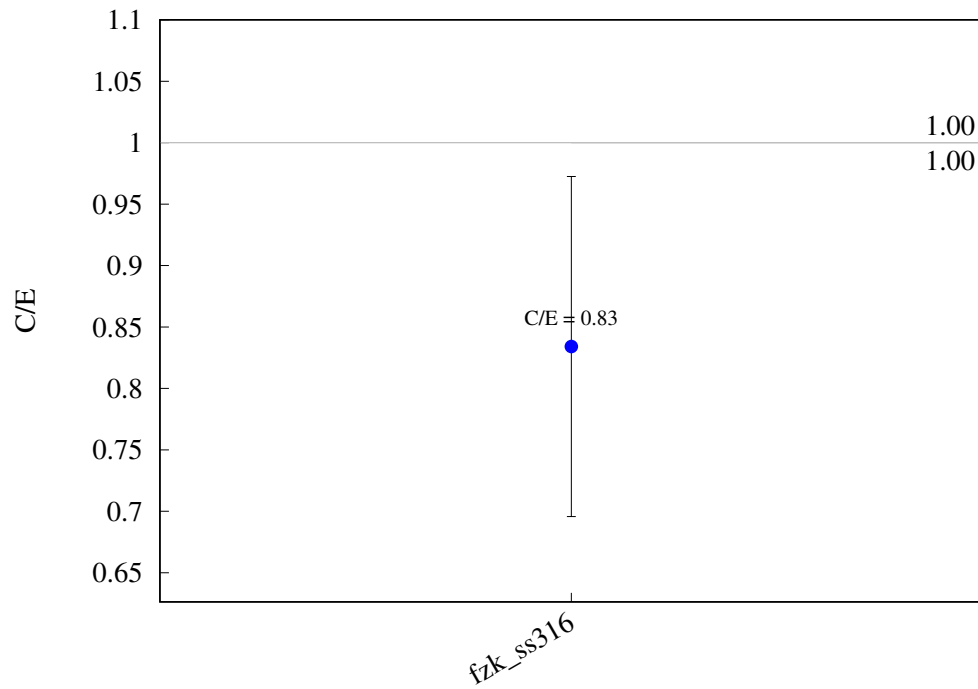
^{92}Mo (n,na) ^{88}Zr 

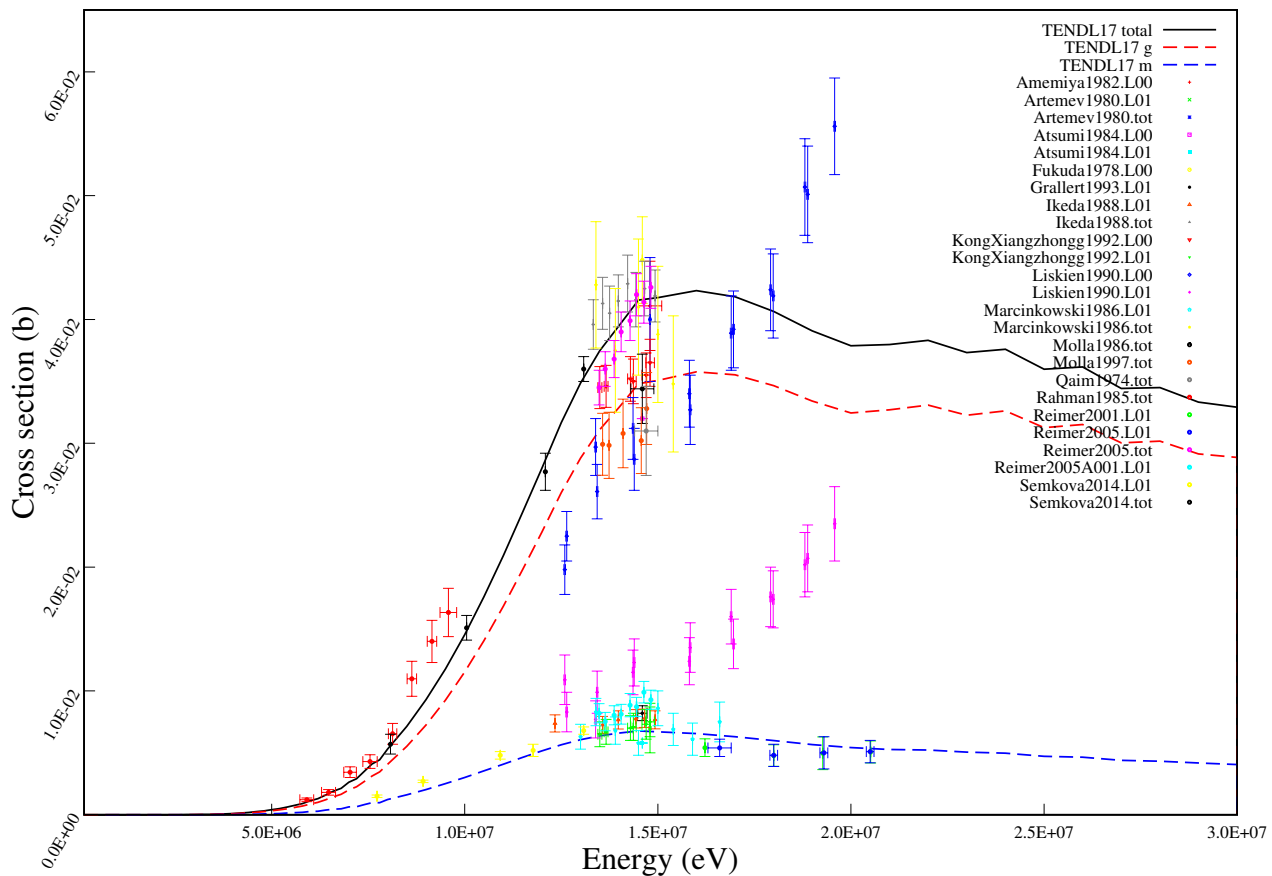
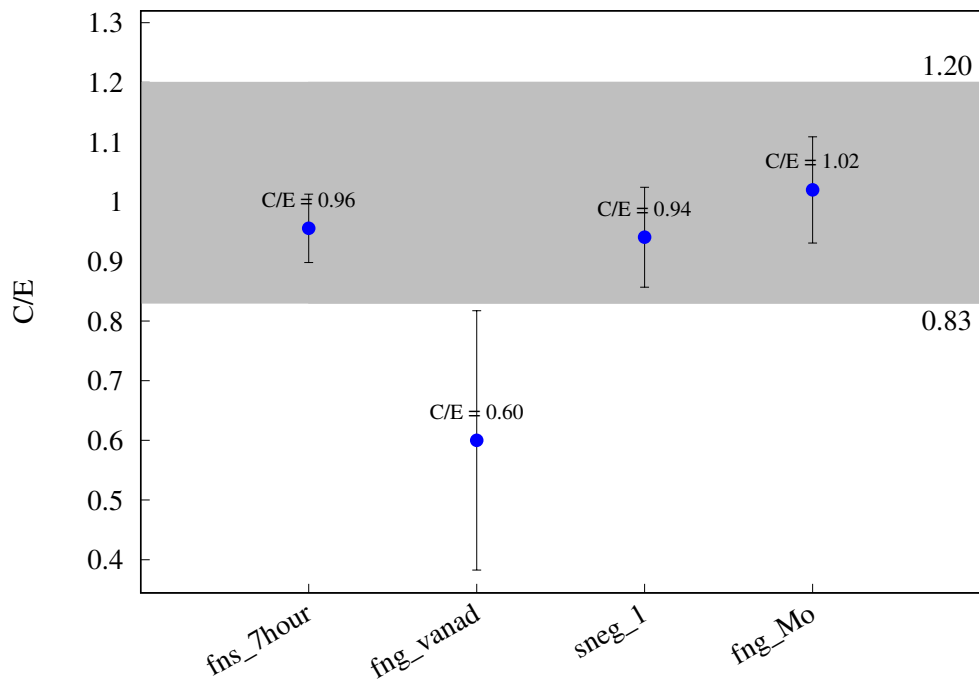
^{92}Mo (n,p) $^{92\text{m}}\text{Nb}$ 

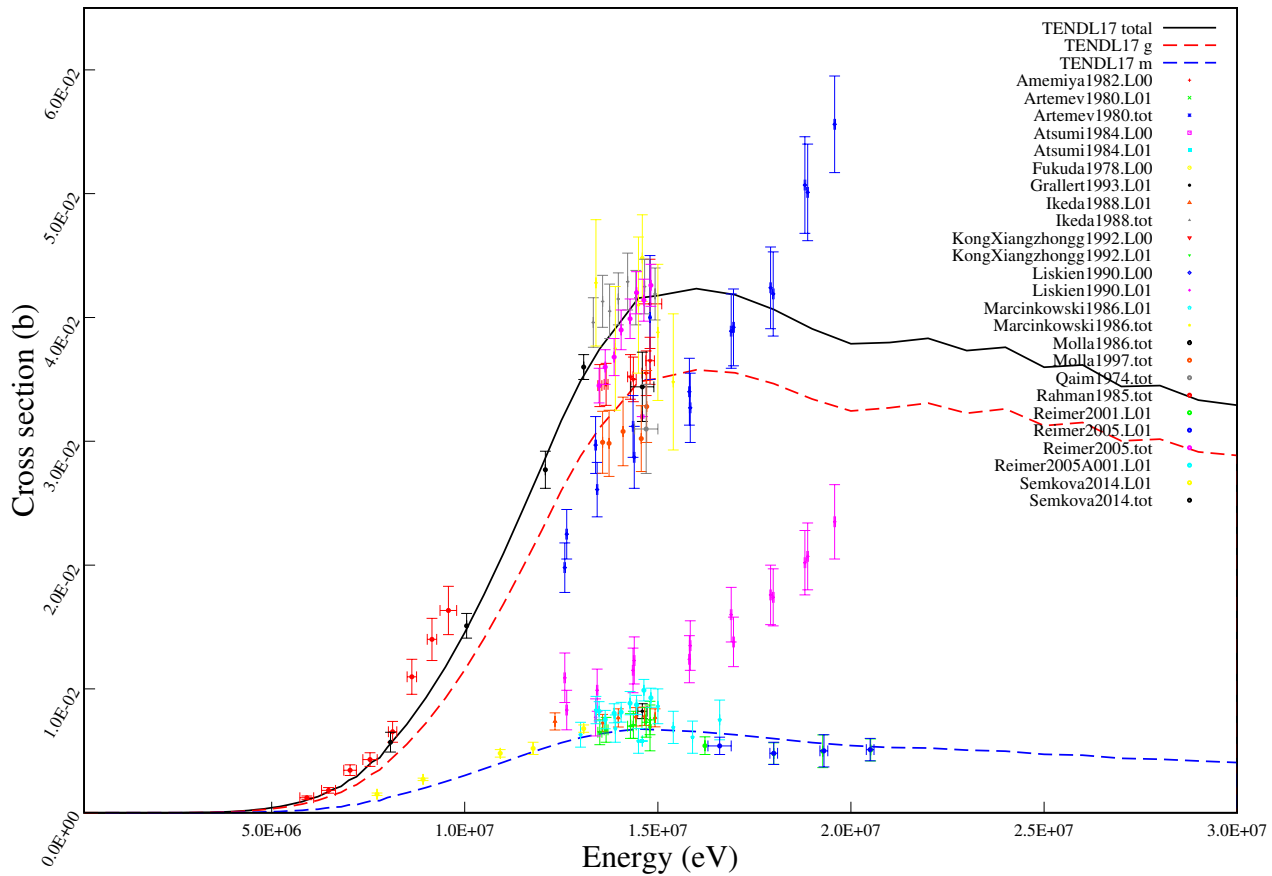
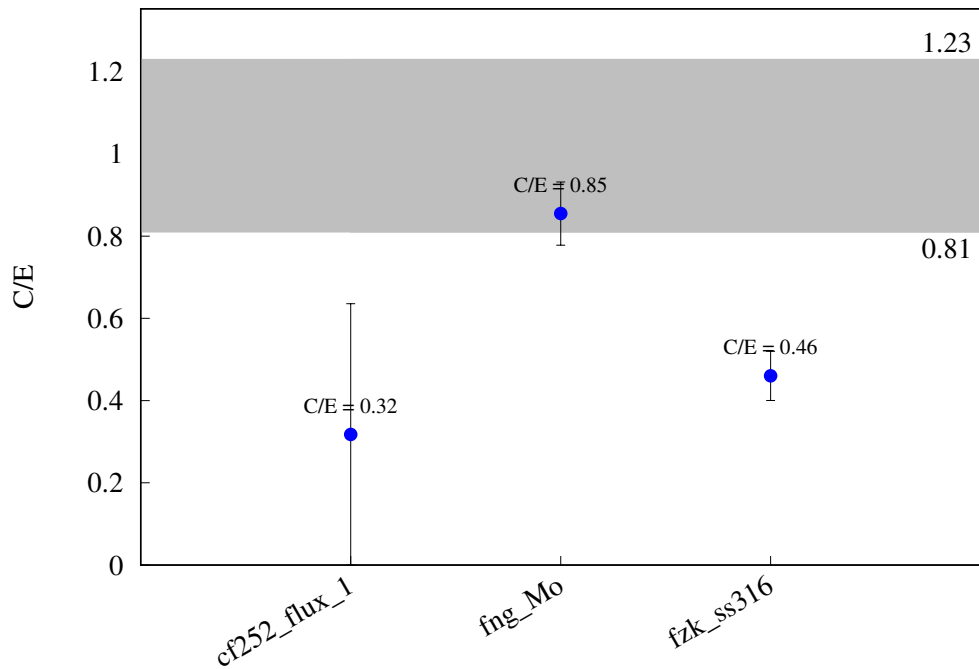
^{92}Mo (n,p) ^{92}Nb 

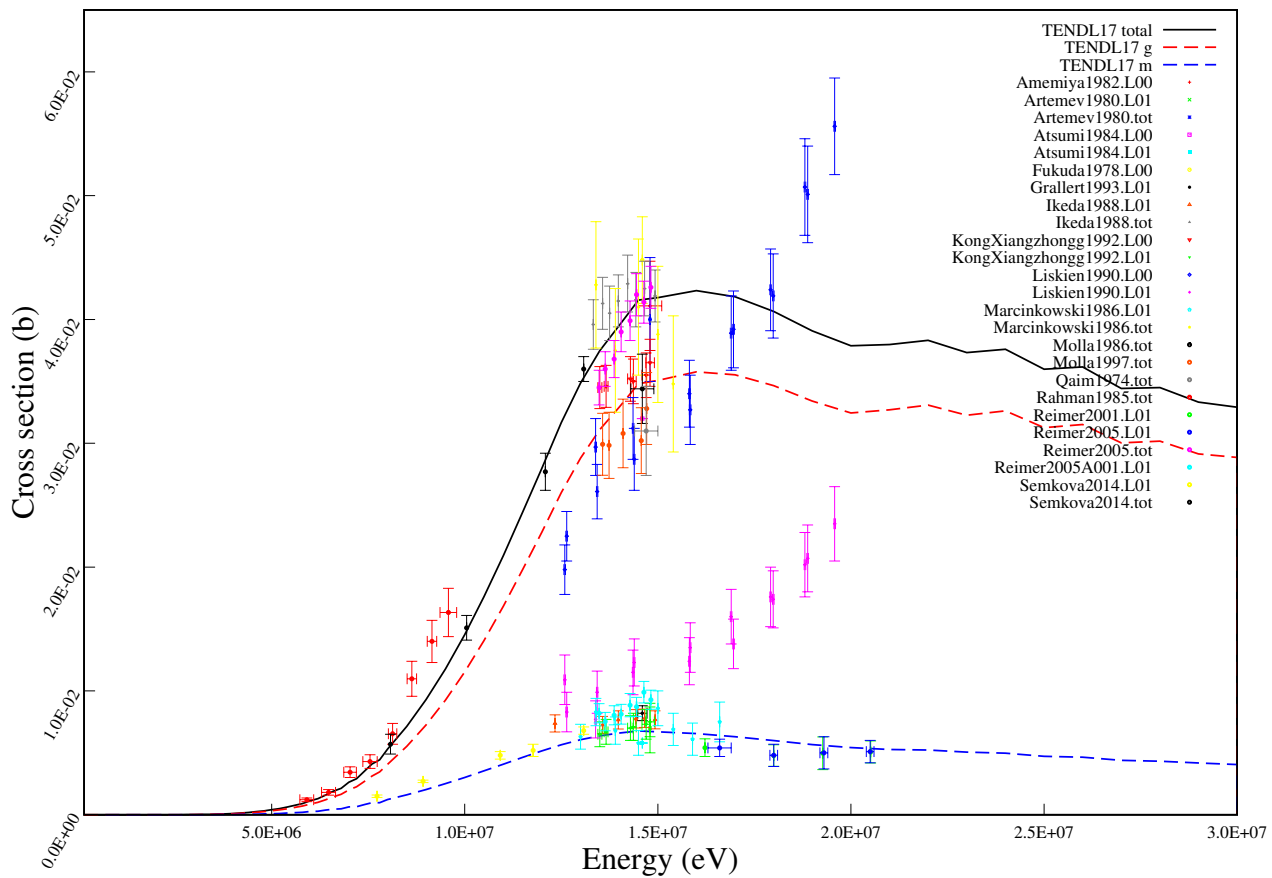
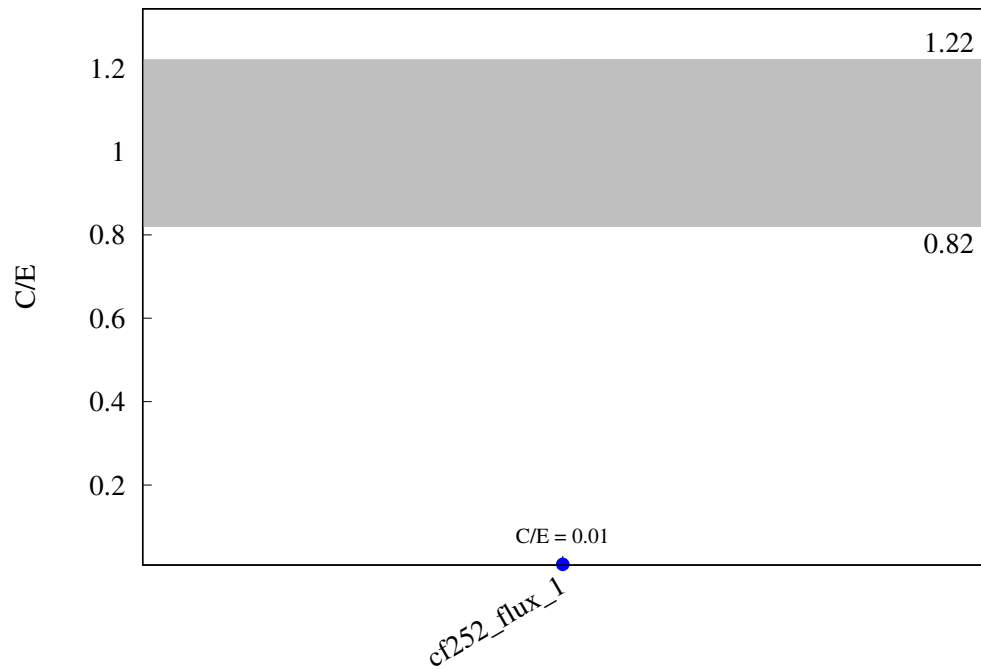
^{92}Mo (n,a) ^{89}Zr 

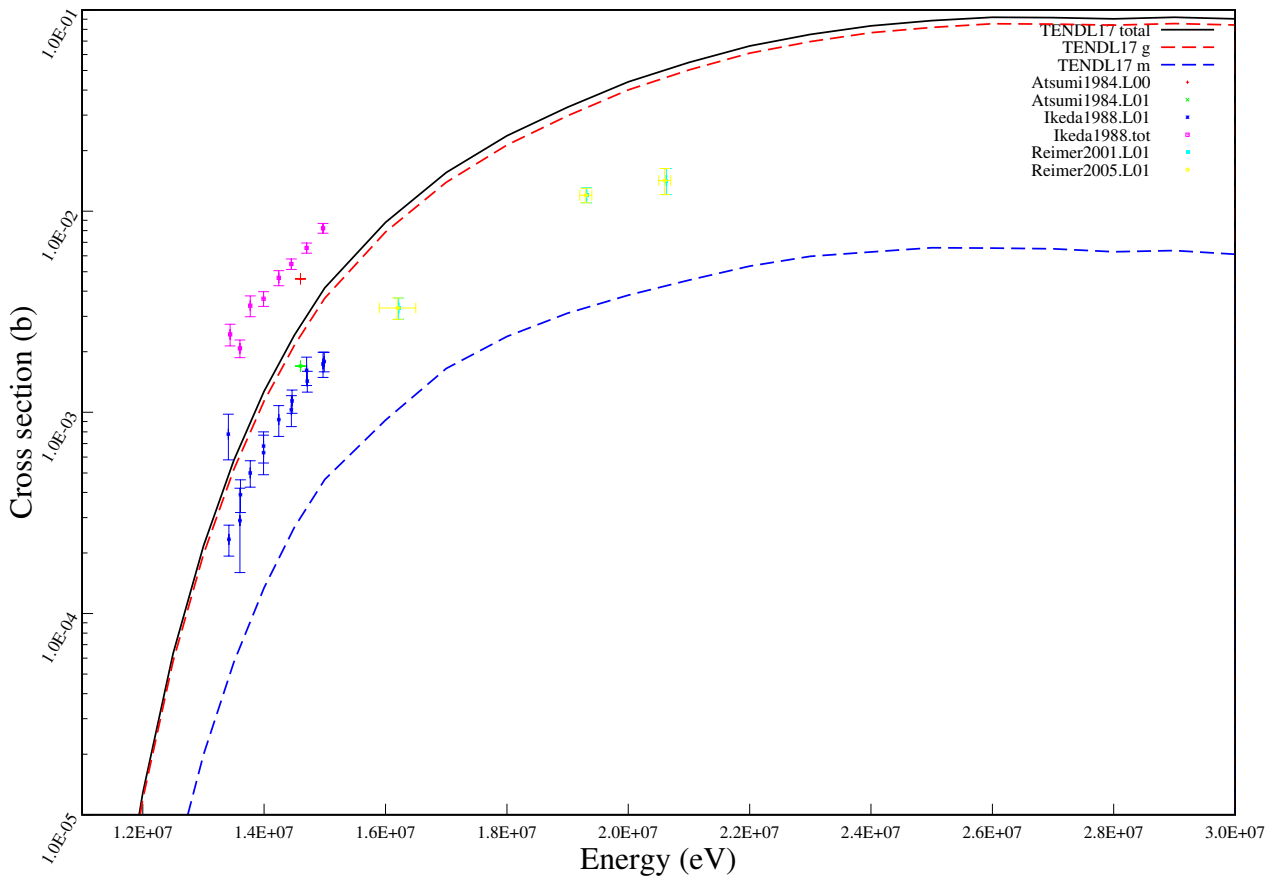
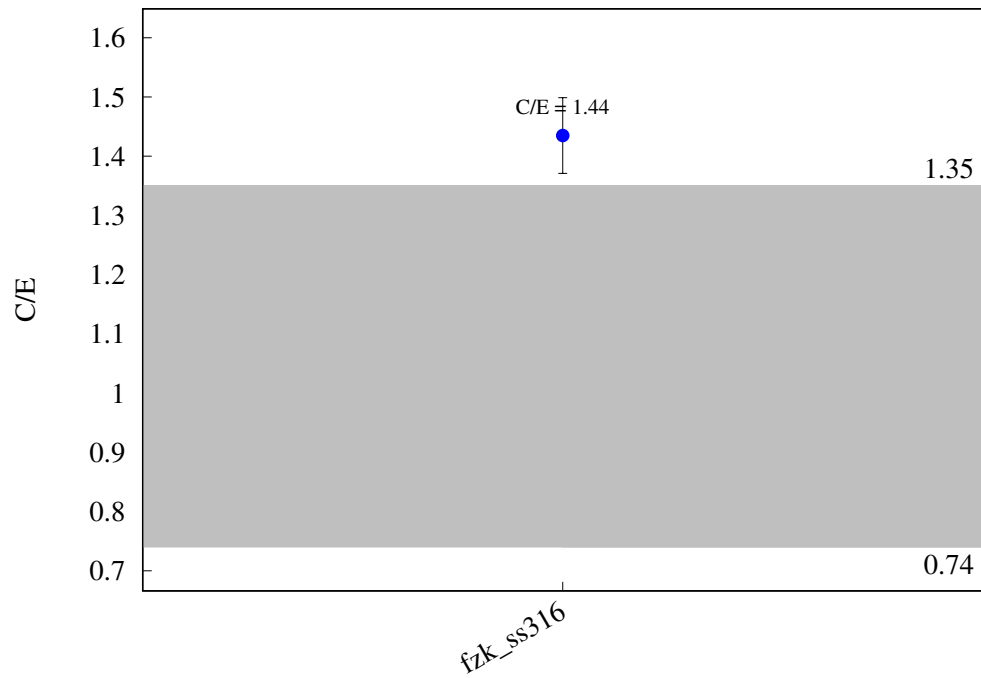
^{92}Mo (n,pa) ^{88}Y 

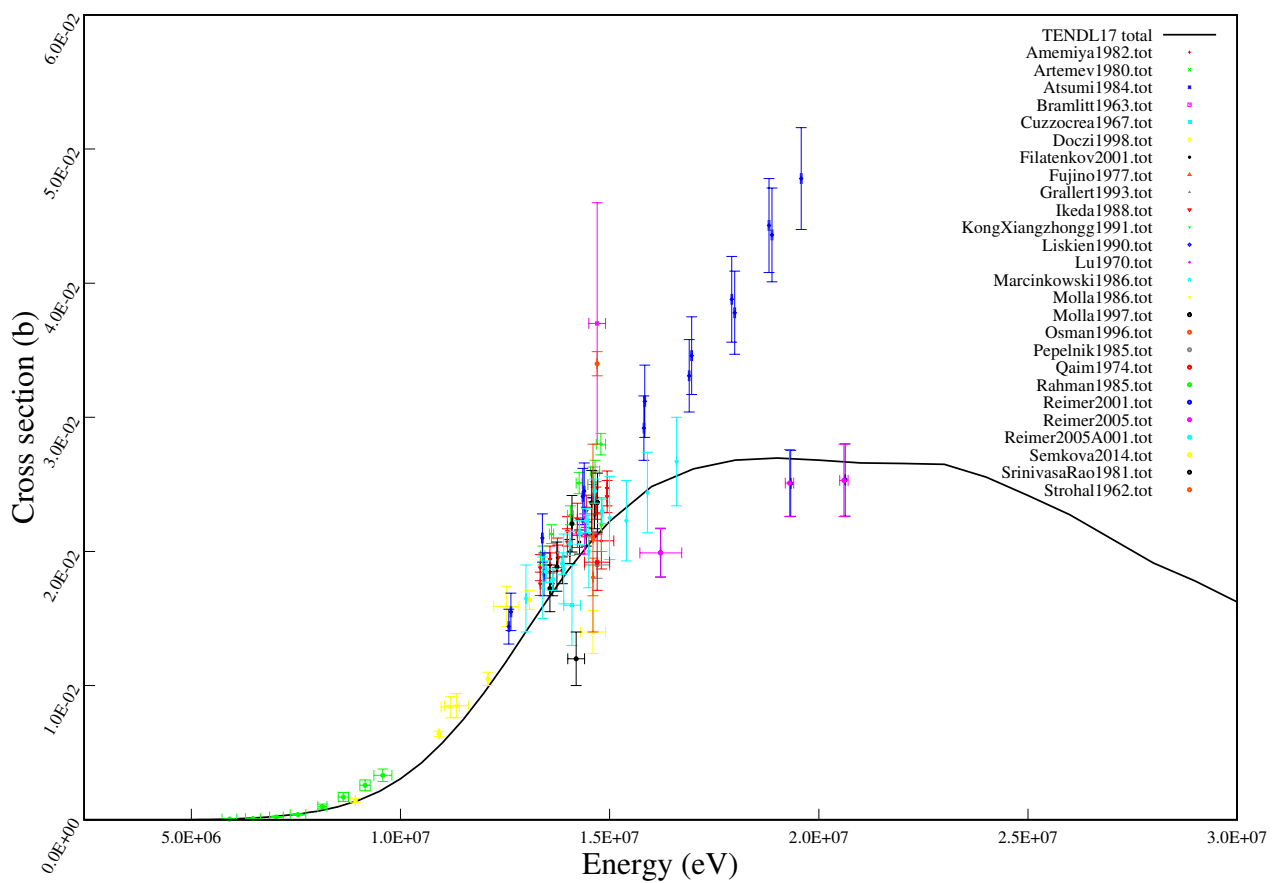
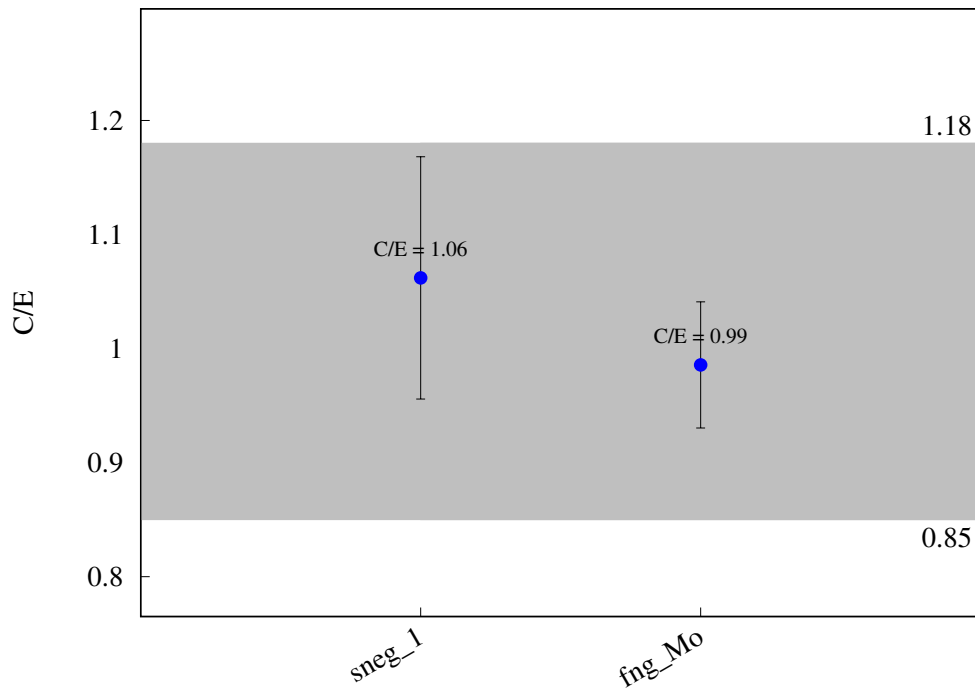
^{95}Mo (n,3n) $^{93\text{m}}\text{Mo}$ 

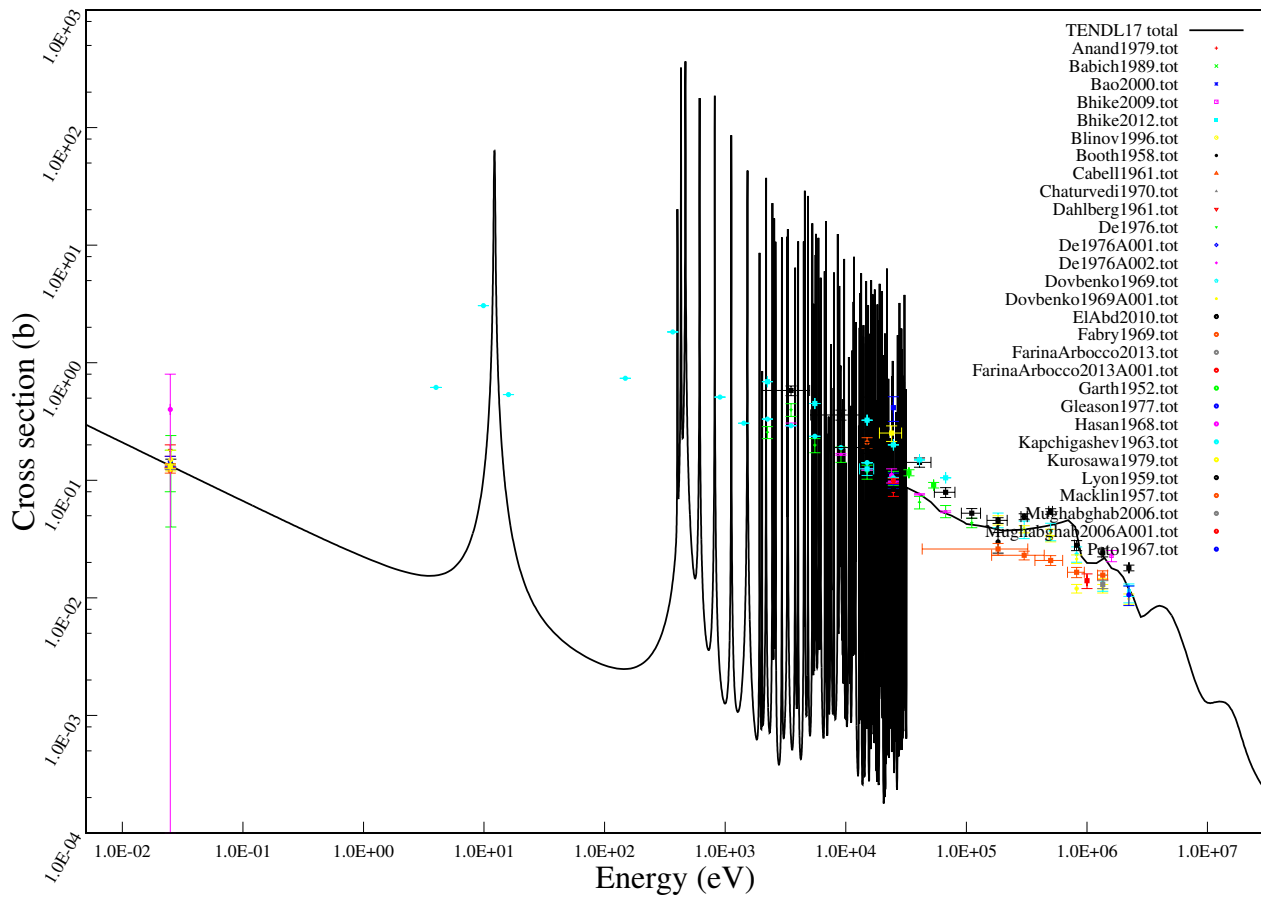
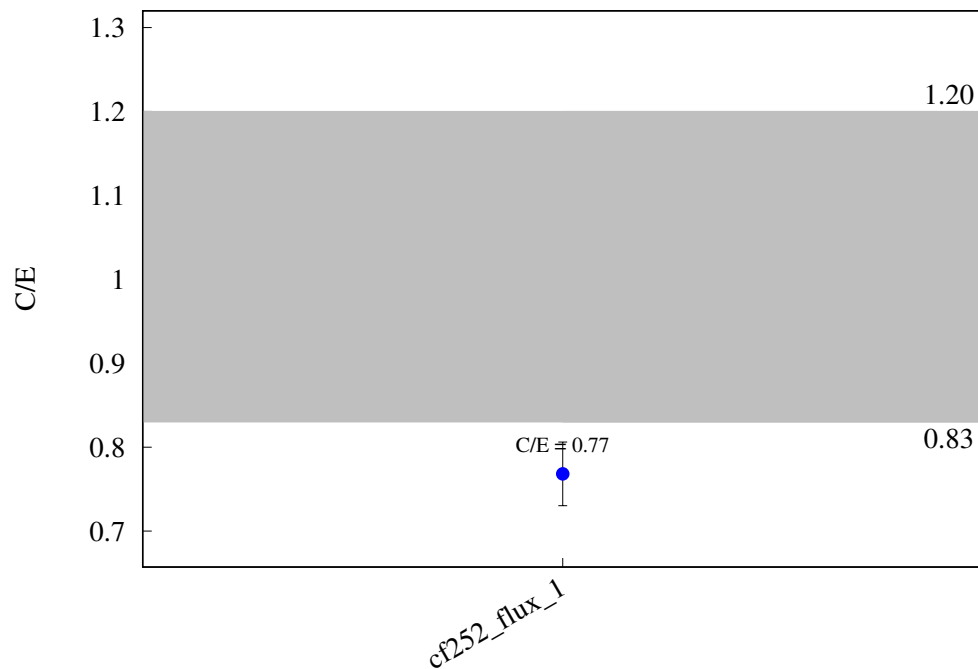
^{95}Mo (n,p) ^{95}Nb 

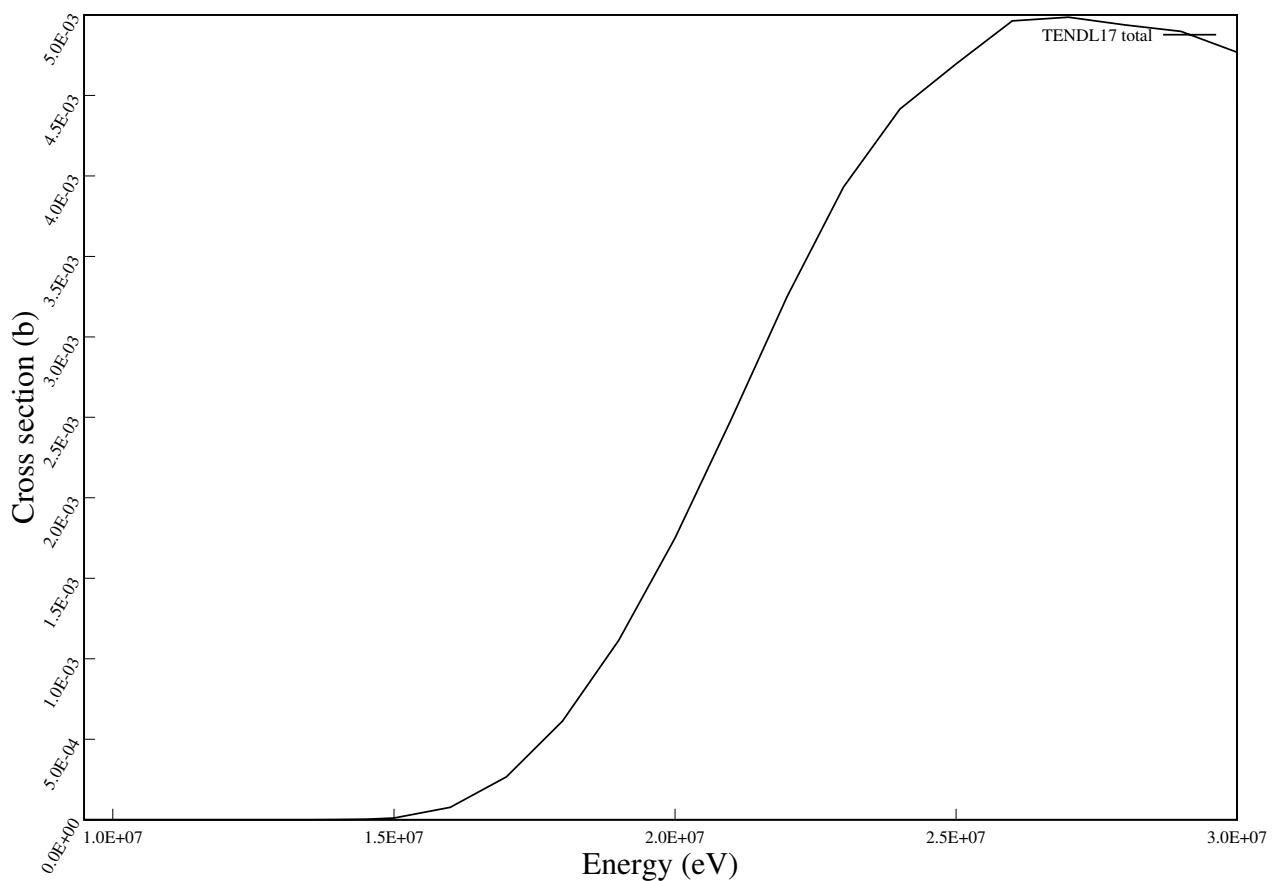
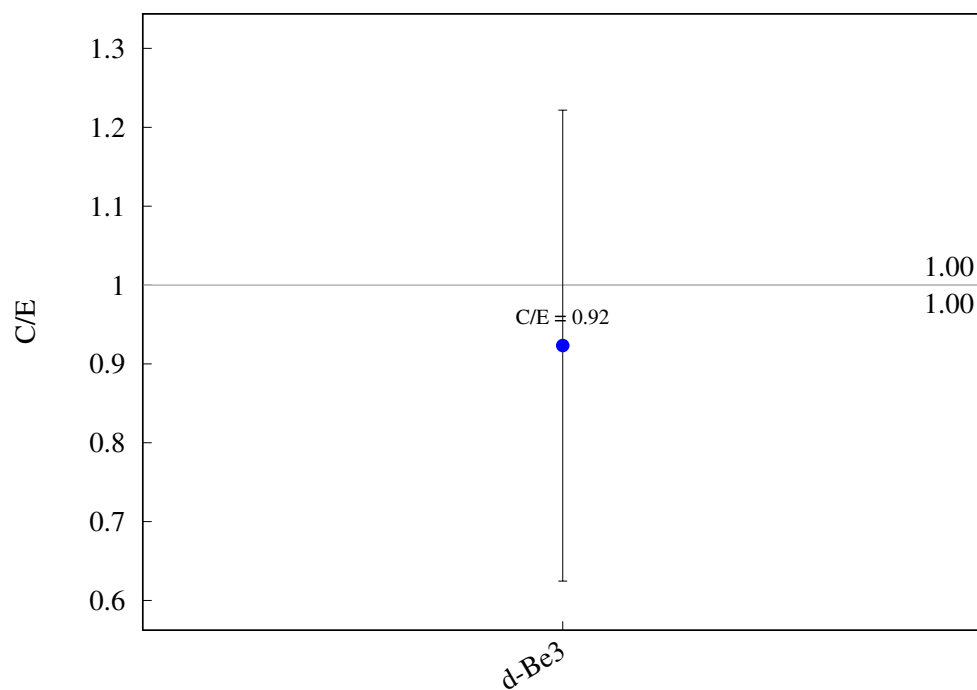
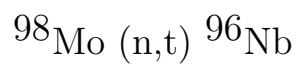
^{95}Mo (n,p) $^{95\text{m}}\text{Nb}$ 

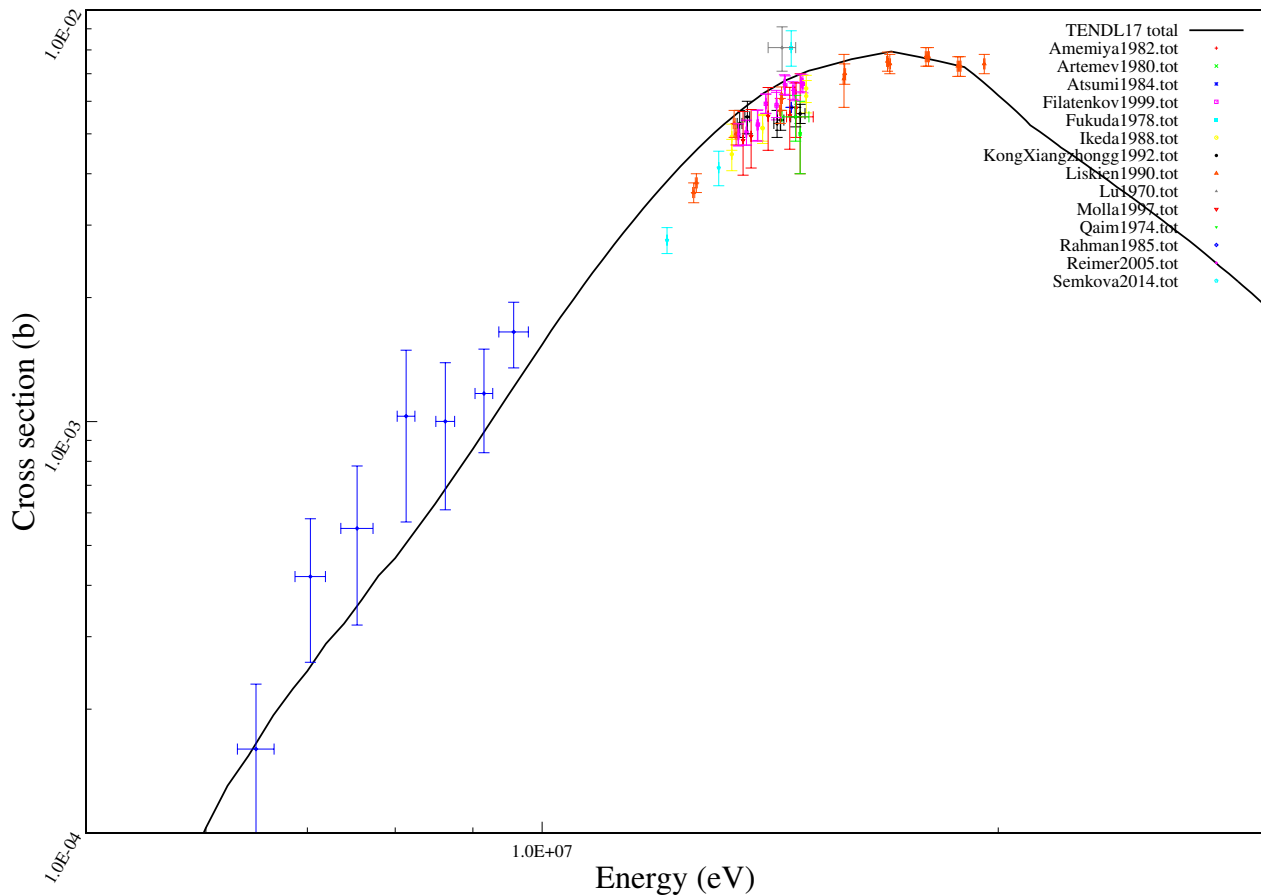
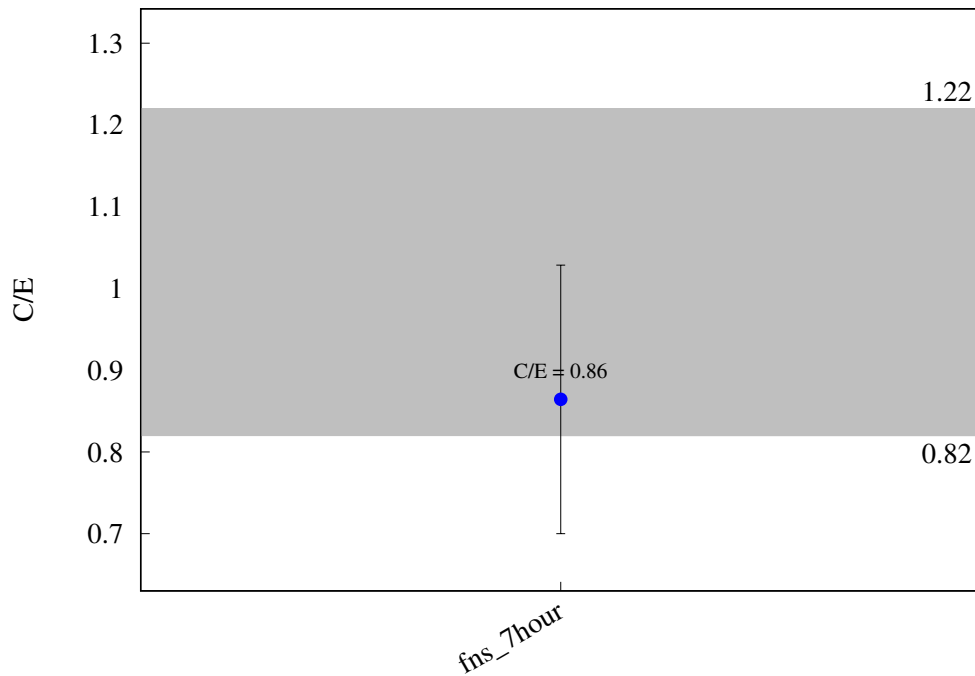
^{95}Mo (n,p) ^{95}Nb 

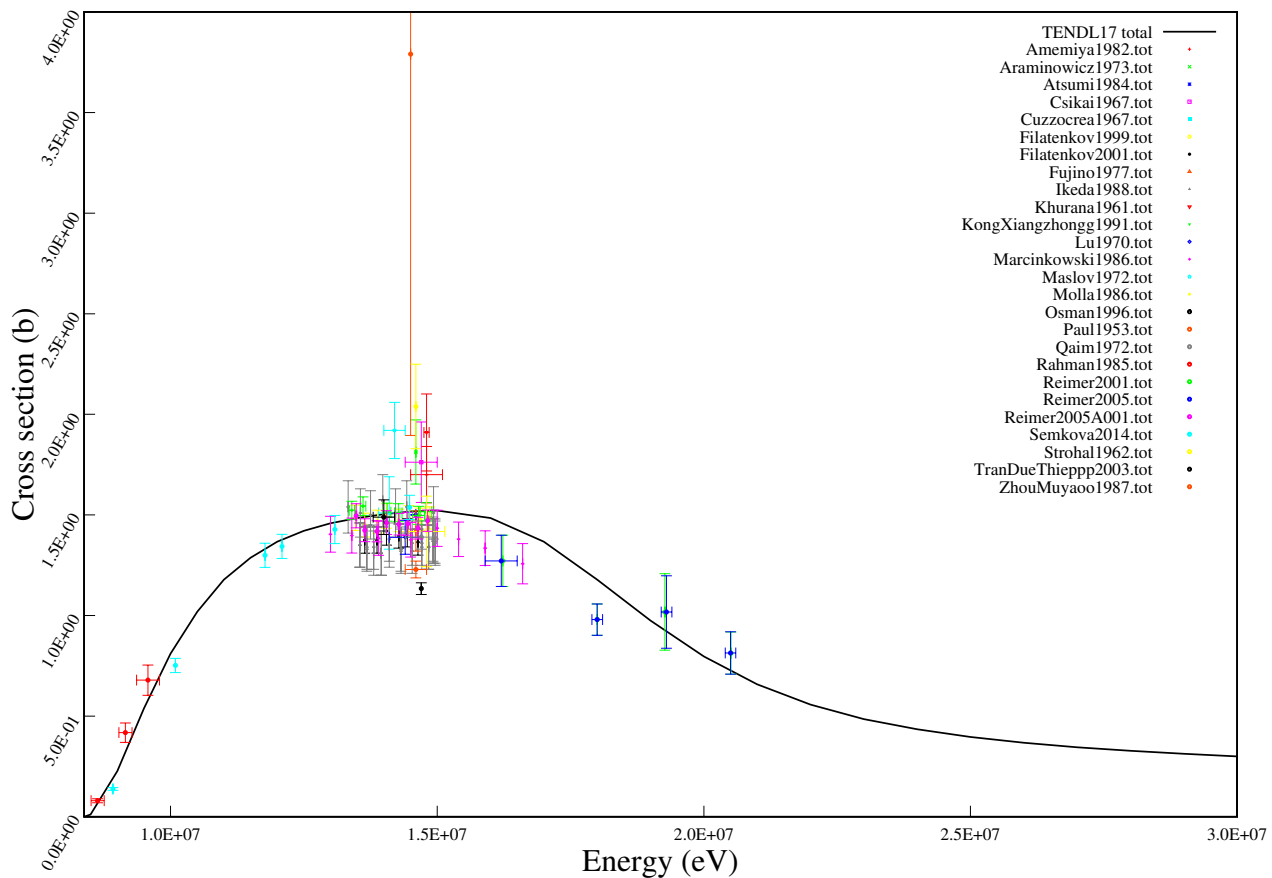
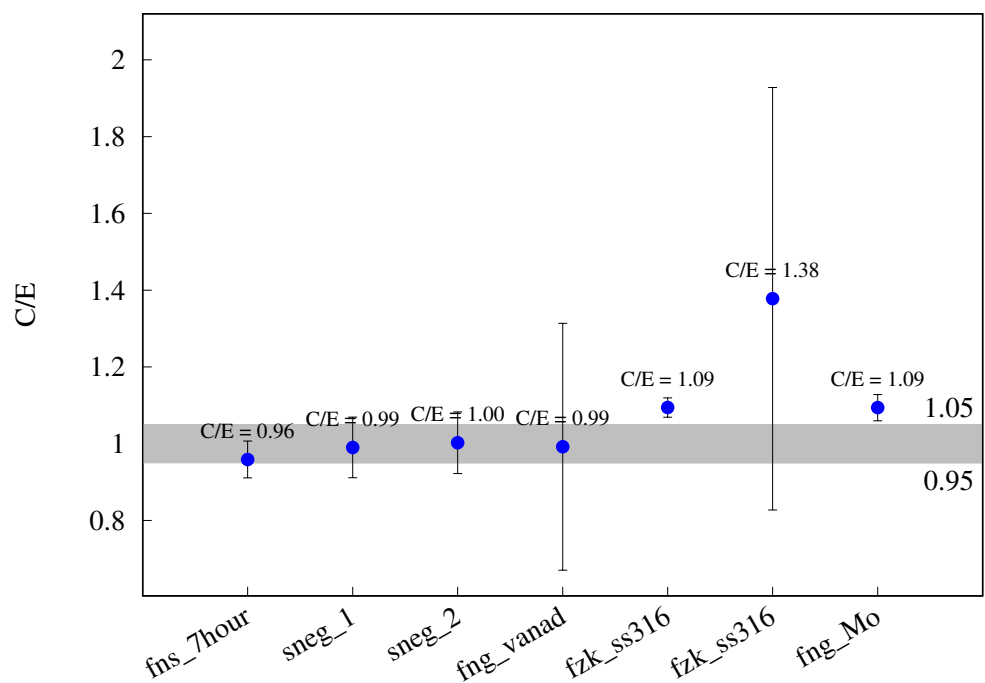
^{96}Mo (n,np) ^{95}Nb 

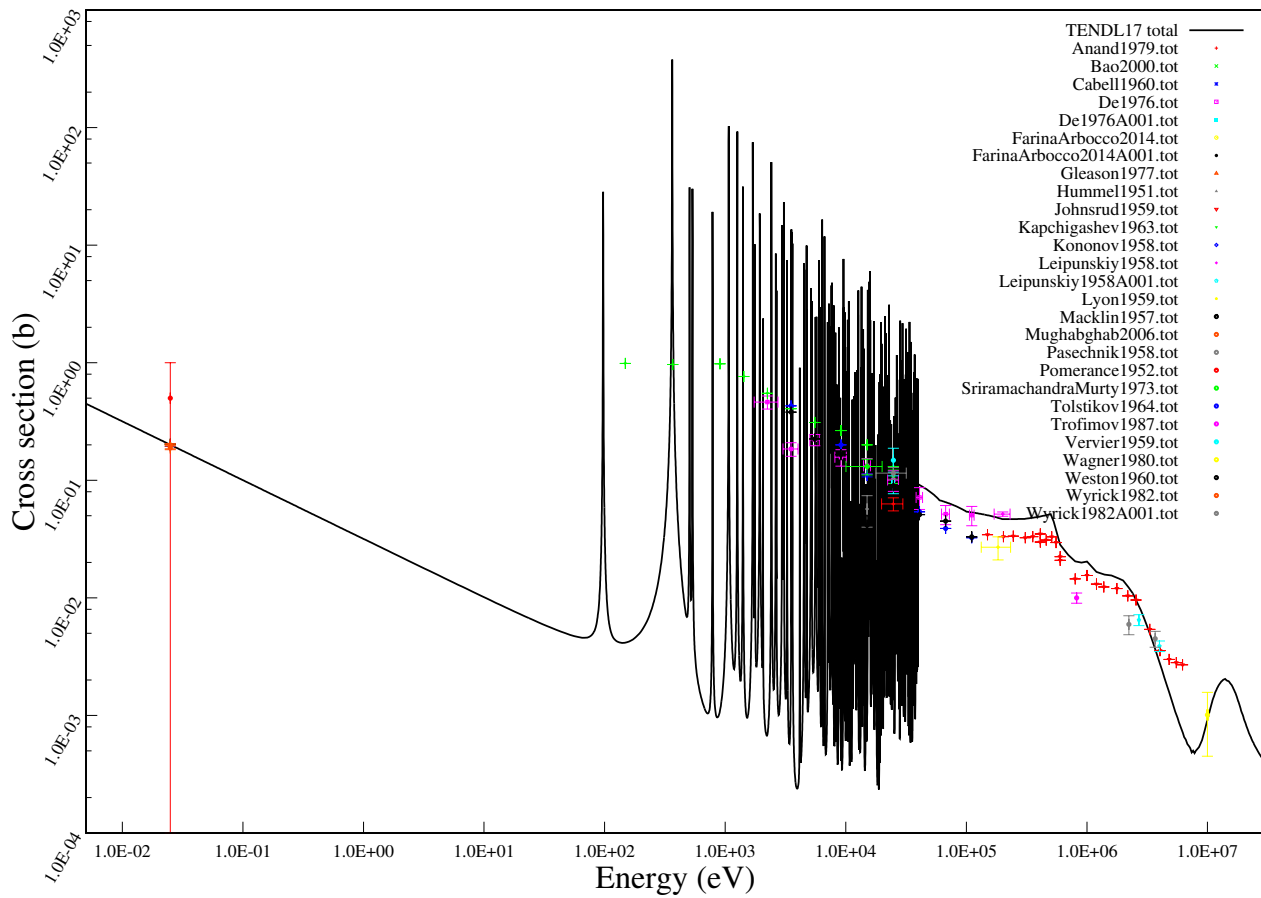
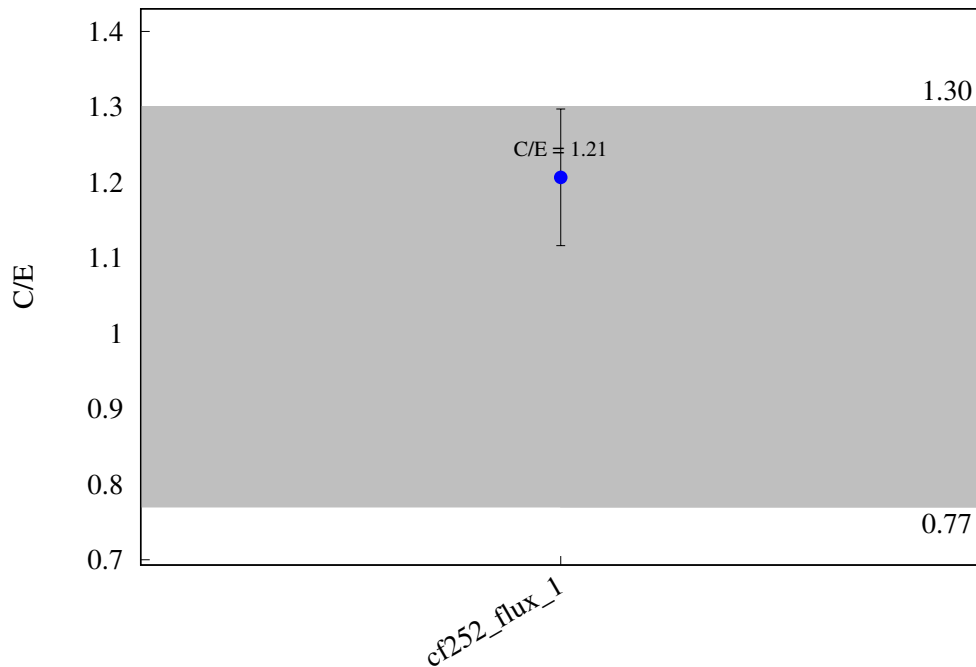
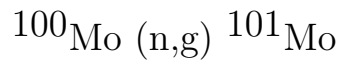
^{96}Mo (n,p) ^{96}Nb 

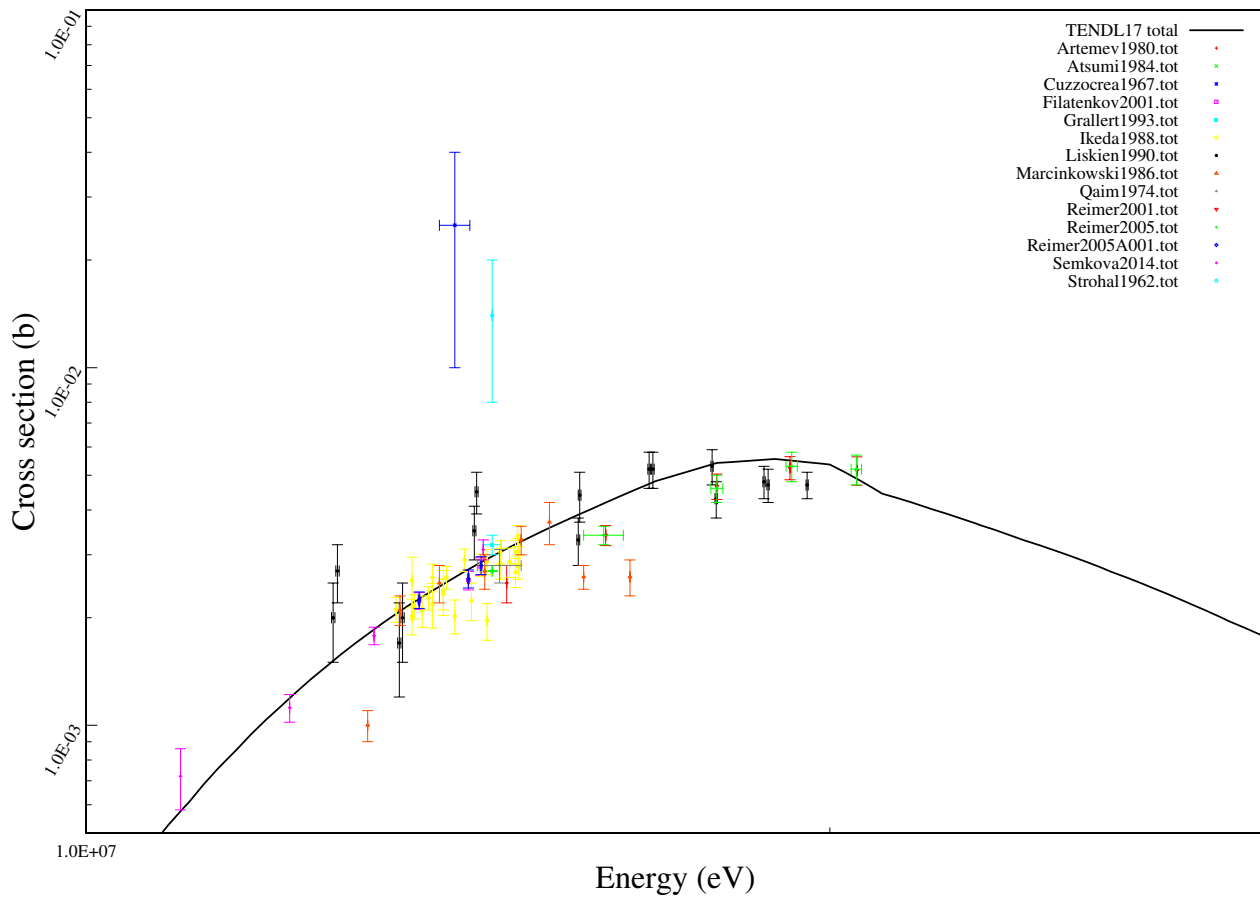
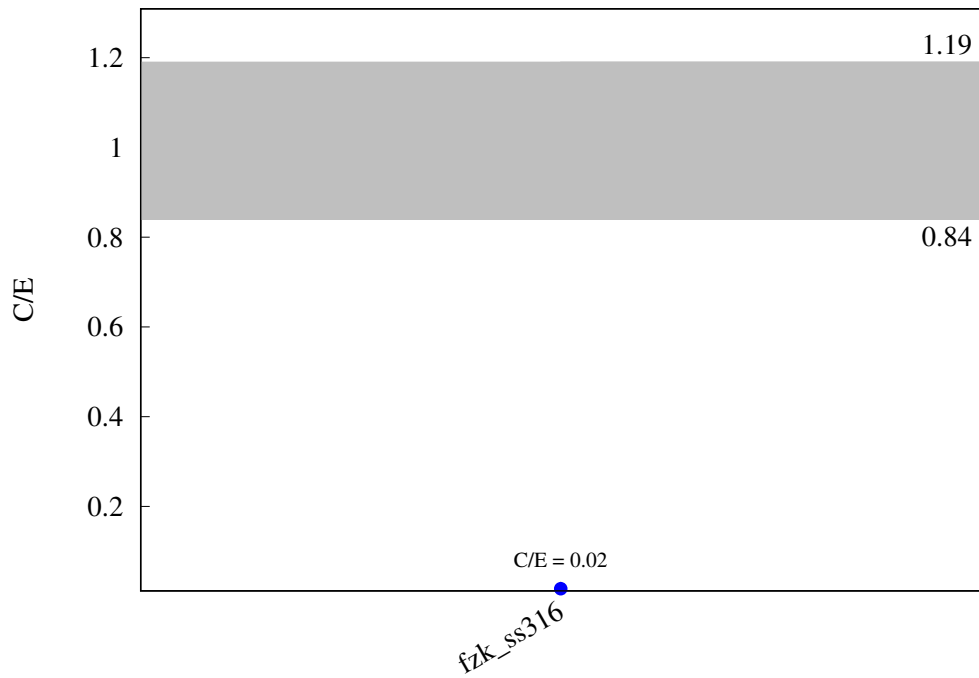
^{98}Mo (n,g) ^{99}Mo 

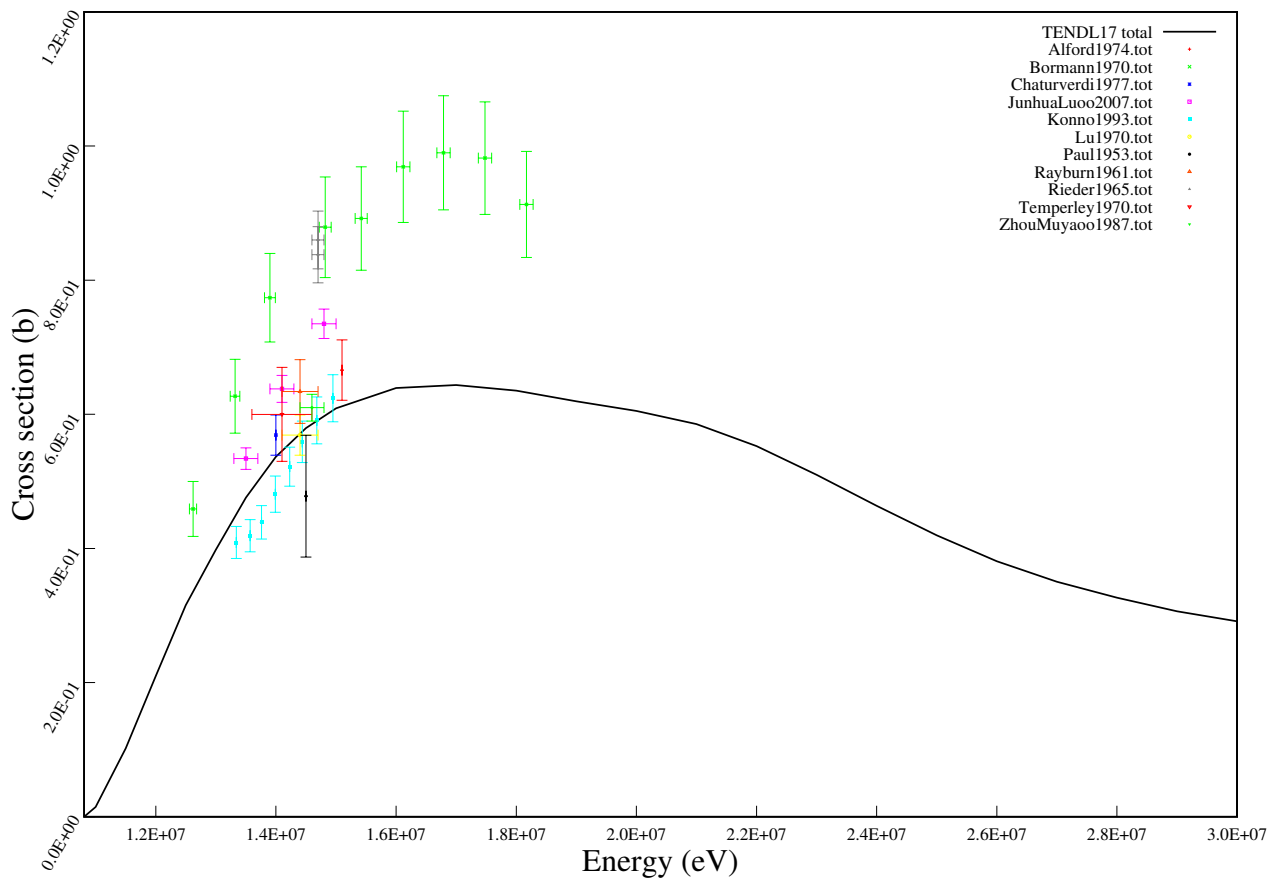
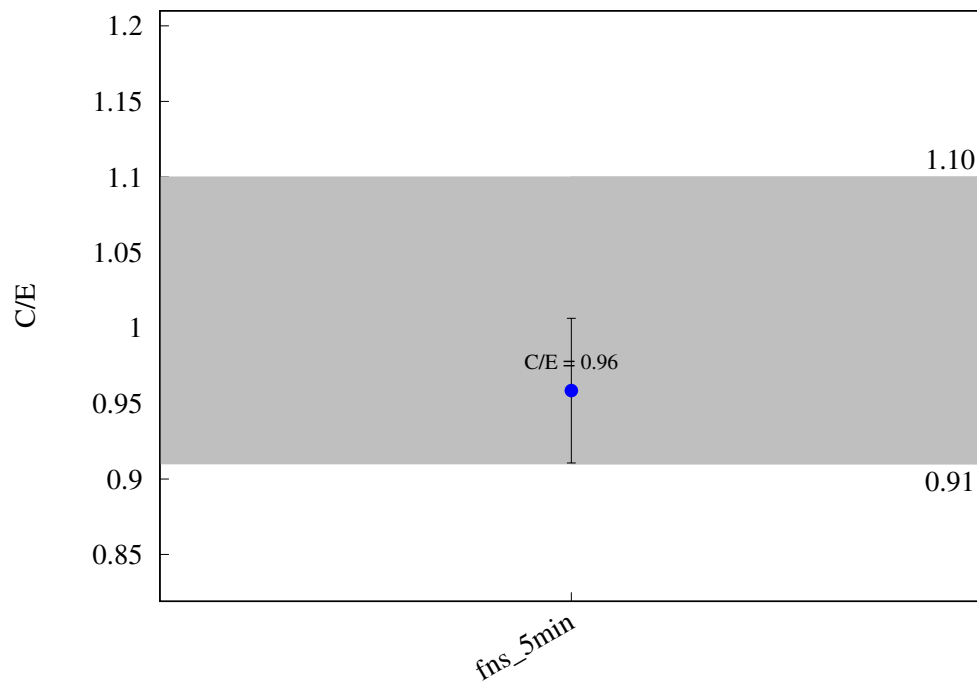


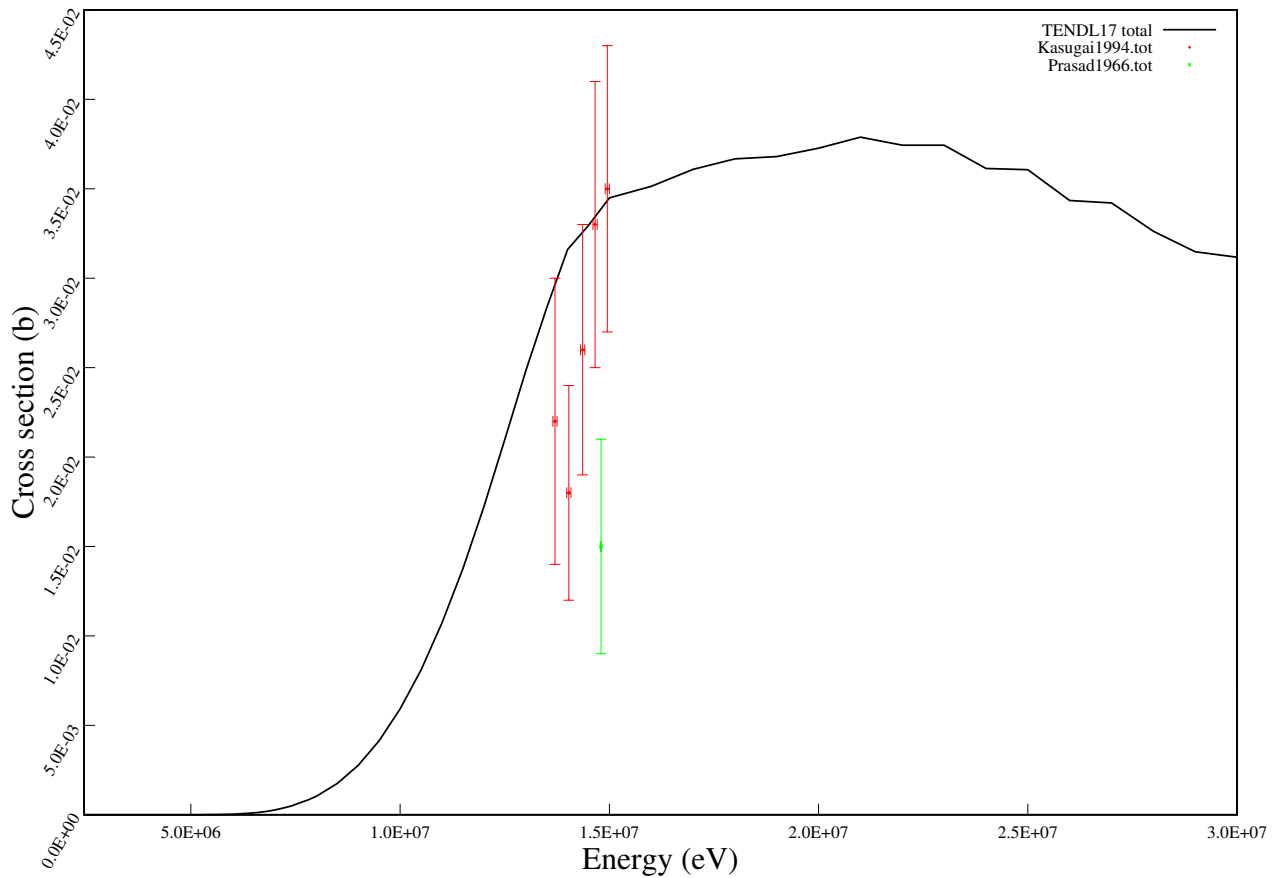
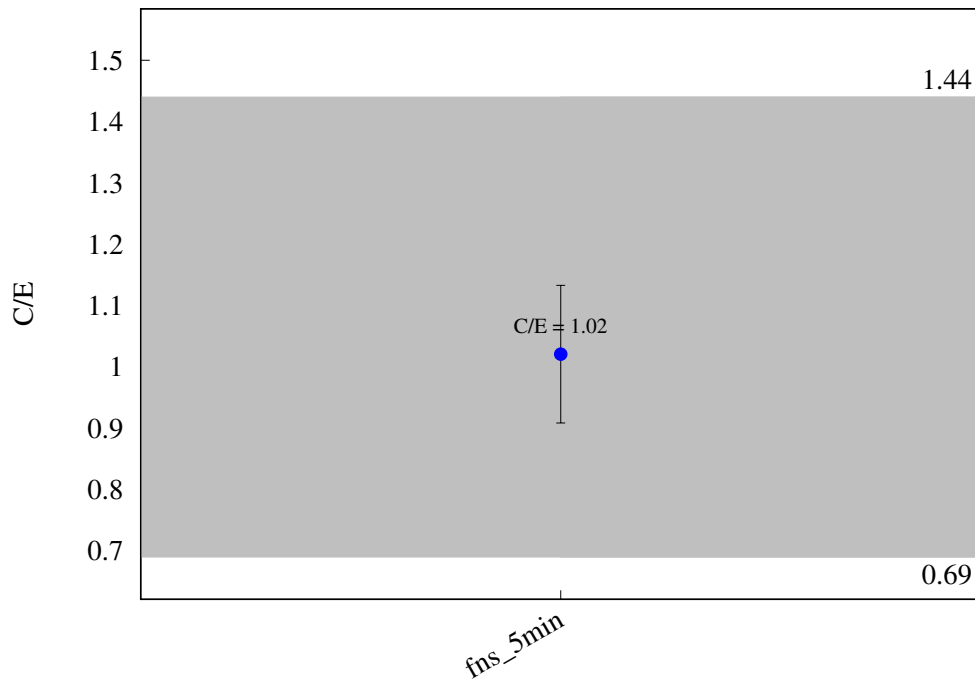
$^{98}\text{Mo} (\text{n},\text{a}) ^{95}\text{Zr}$ 

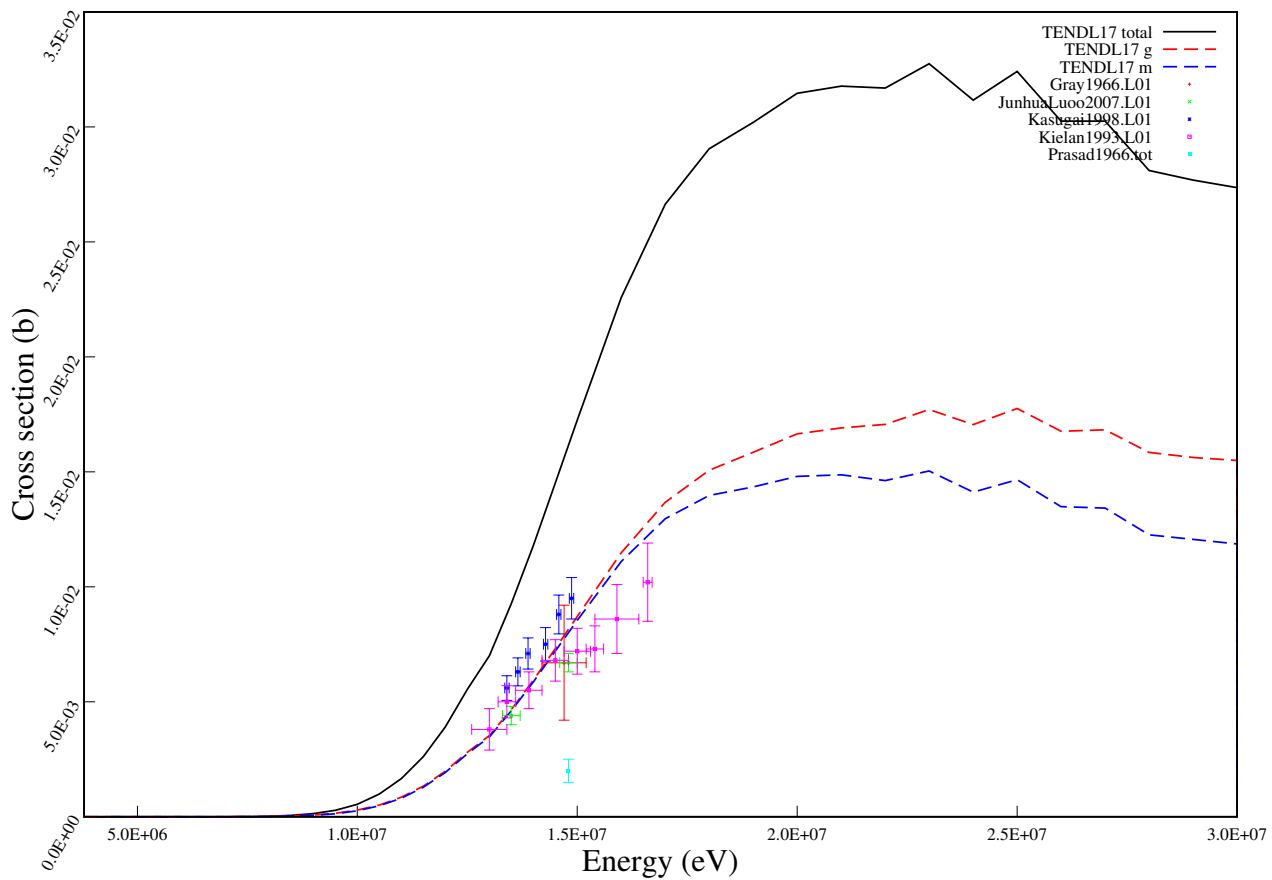
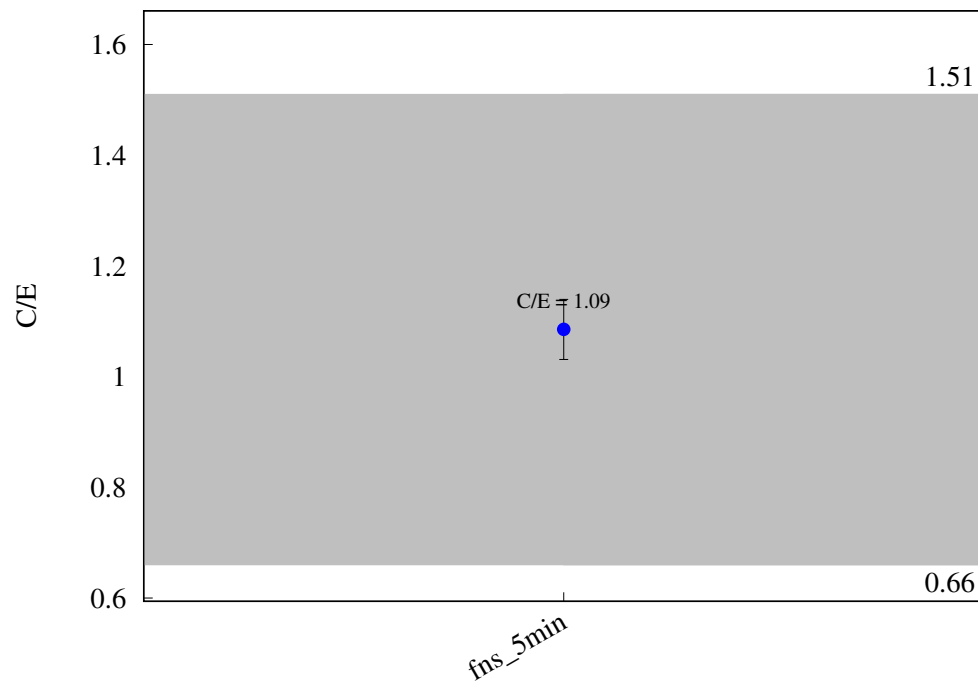
^{100}Mo (n,2n) ^{99}Mo 

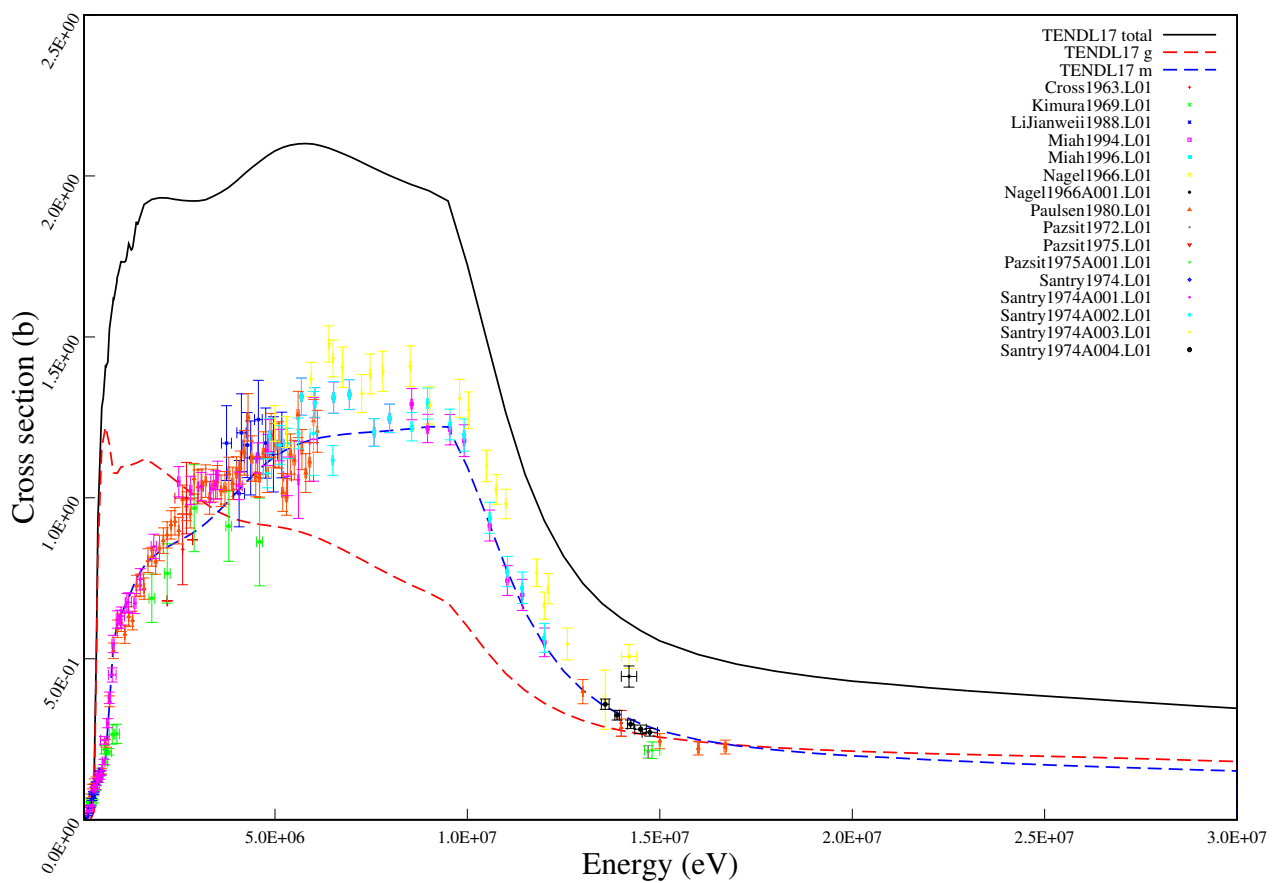
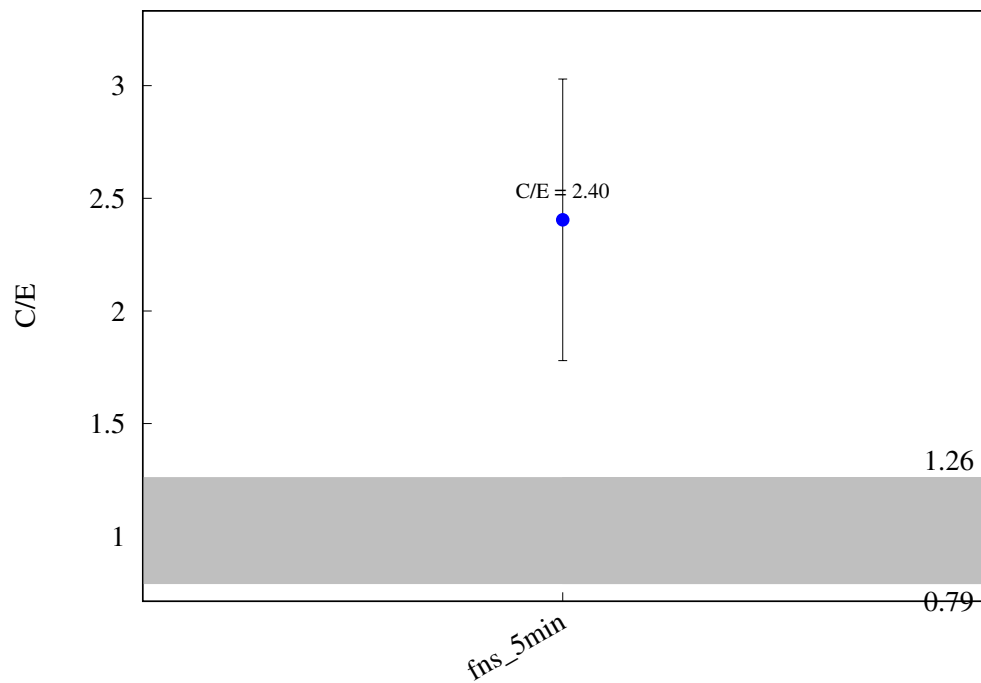


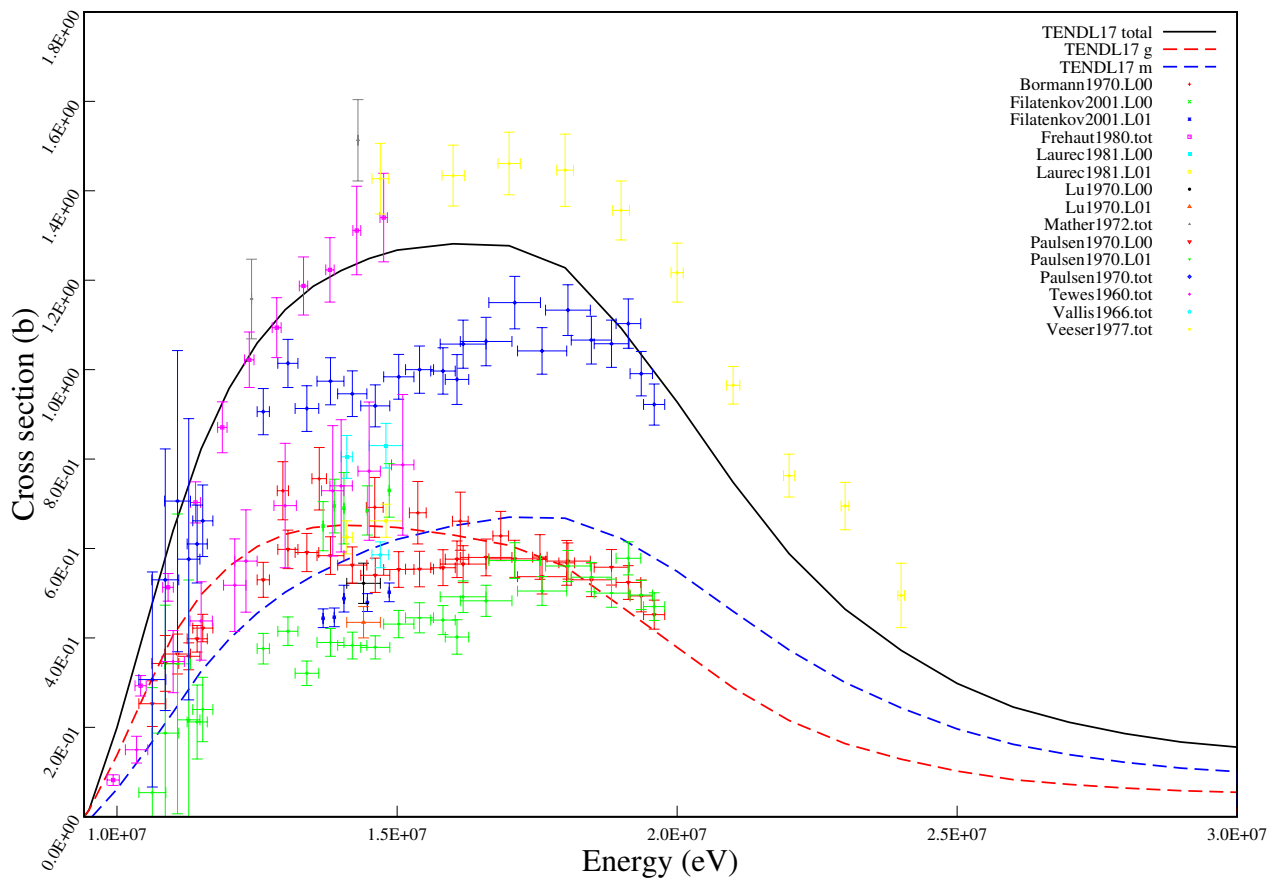
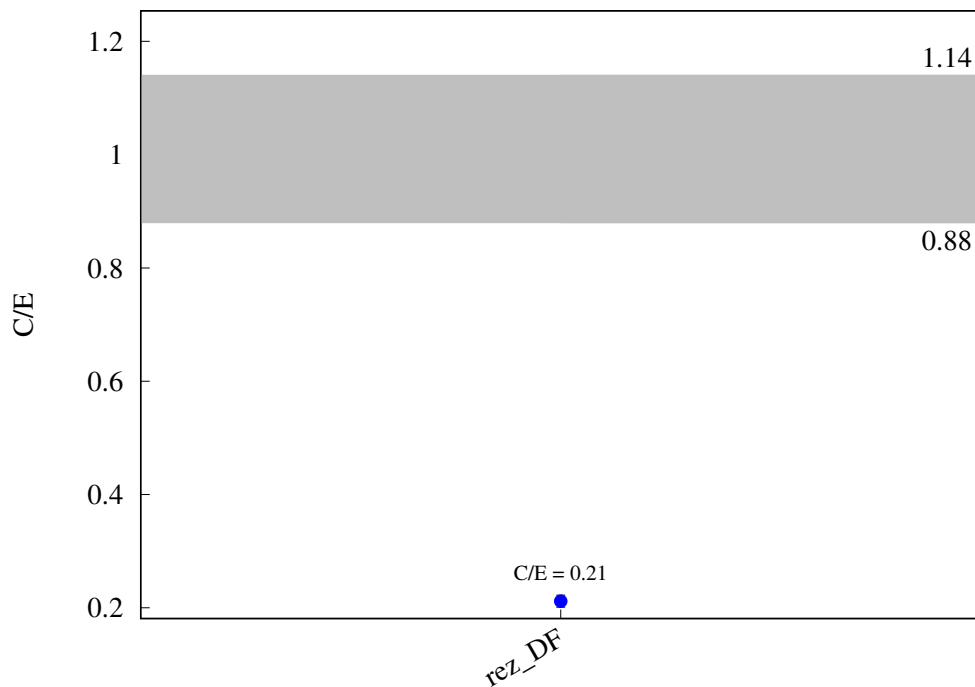
$^{100}\text{Mo} (\text{n},\text{a}) ^{97}\text{Zr}$ 

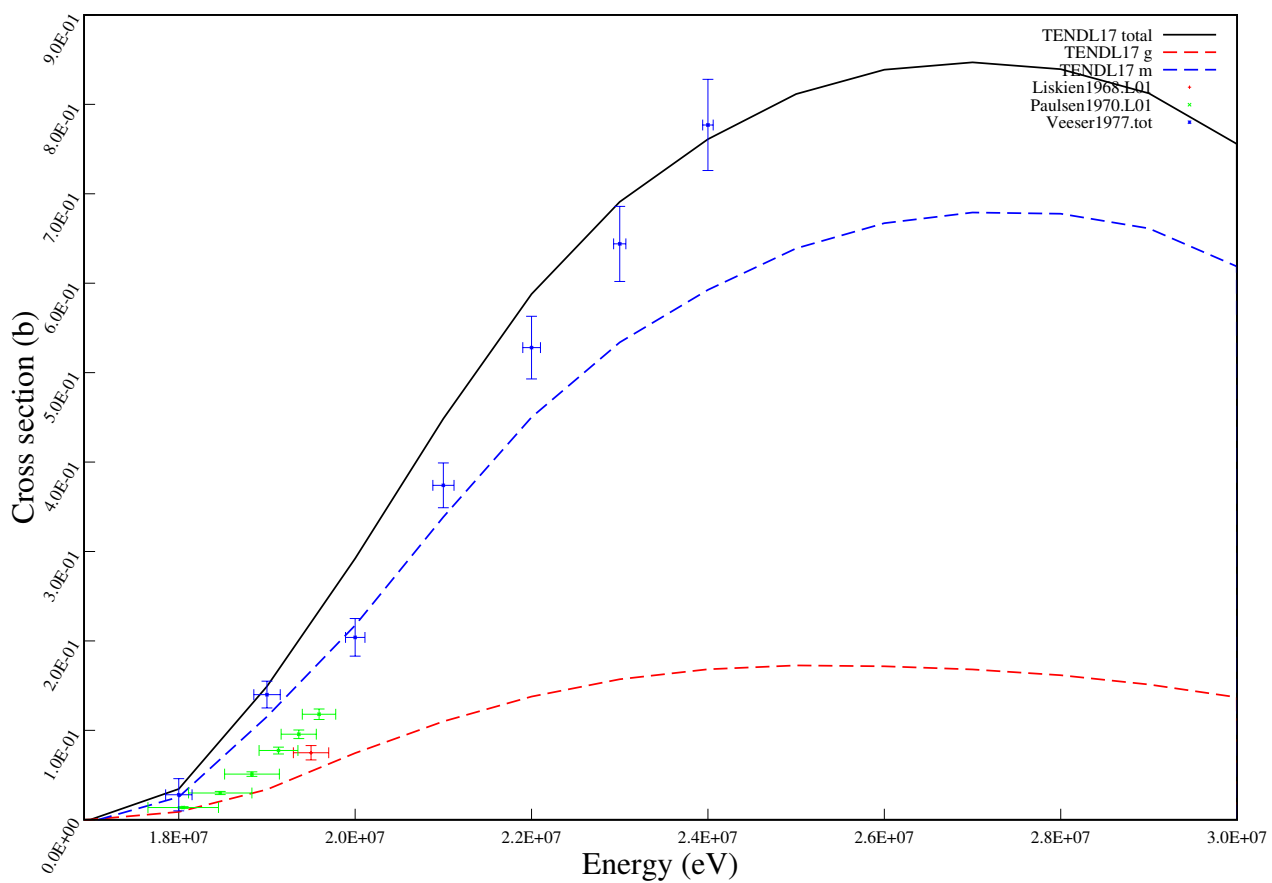
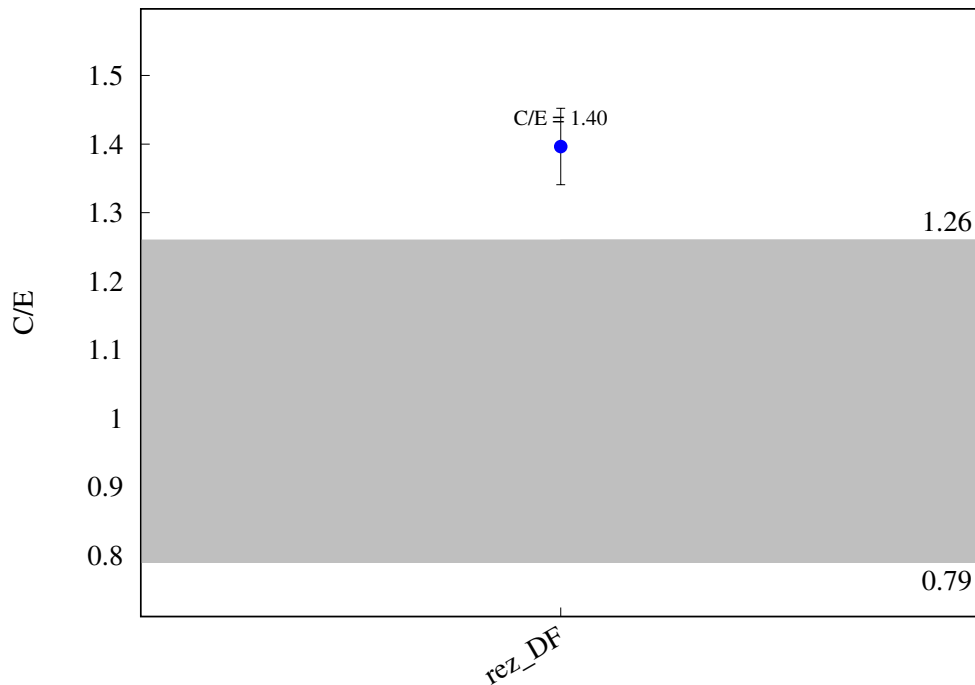
^{96}Ru (n,2n) ^{95}Ru 

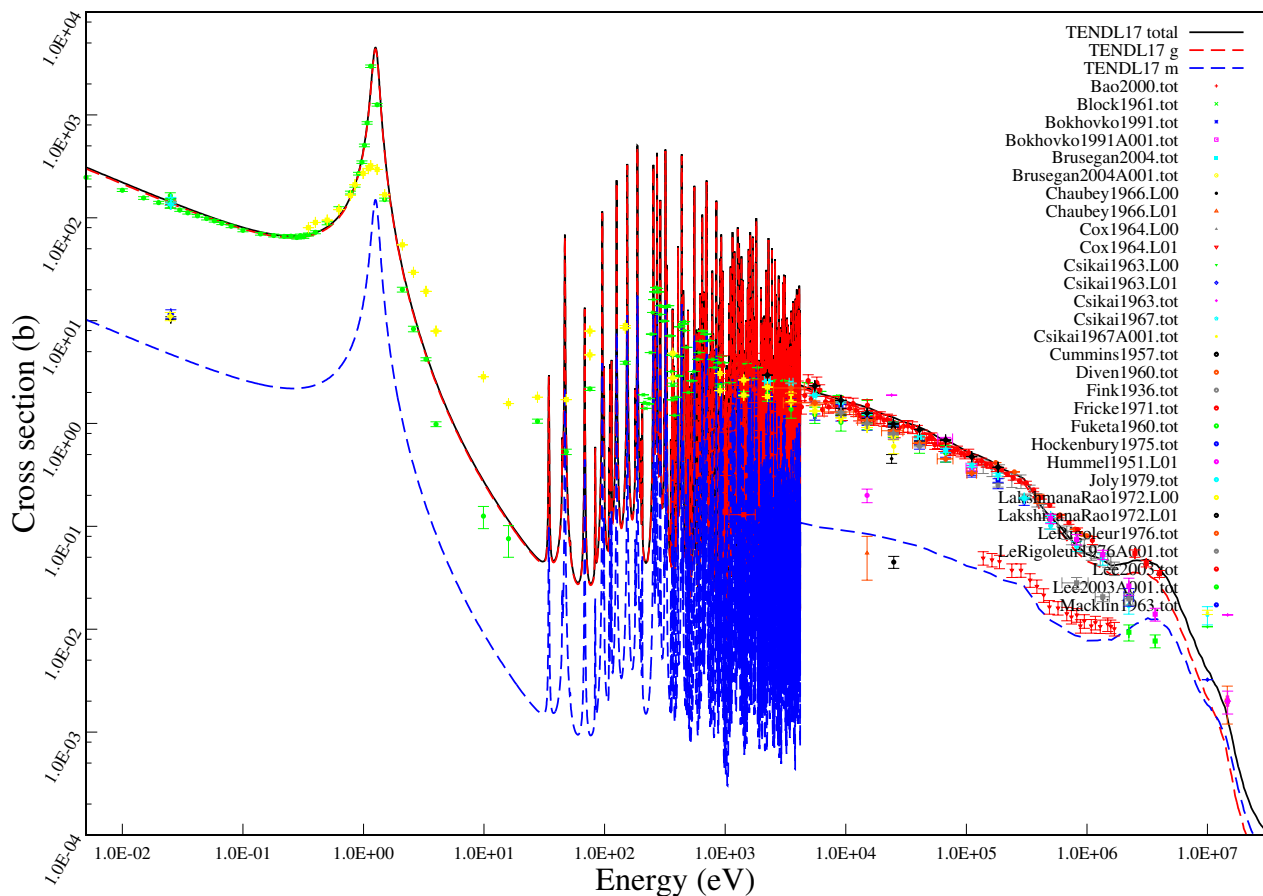
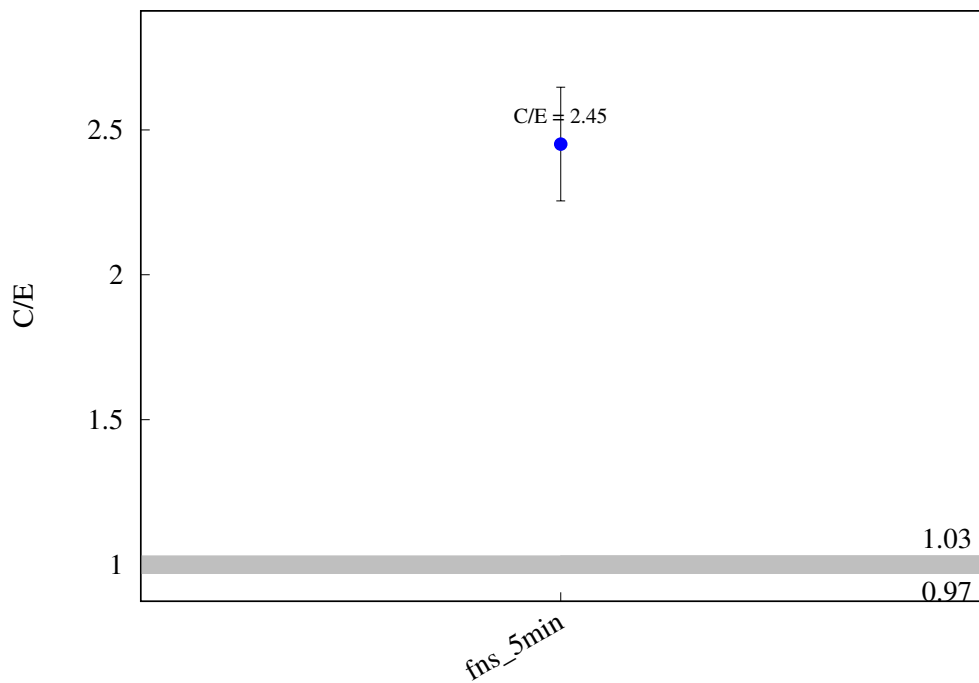
$^{100}\text{Ru} (\text{n},\text{p}) ^{100}\text{Tc}$ 

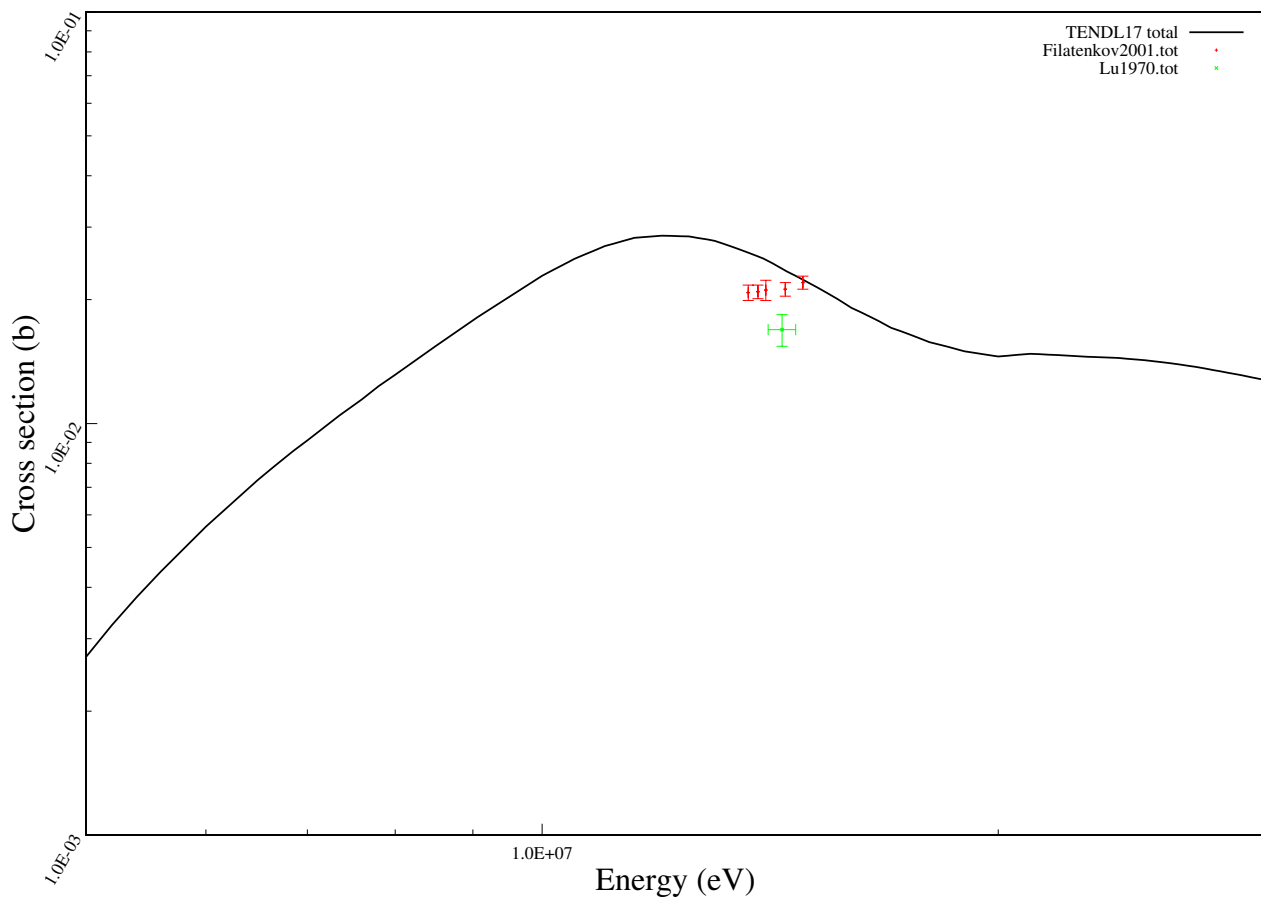
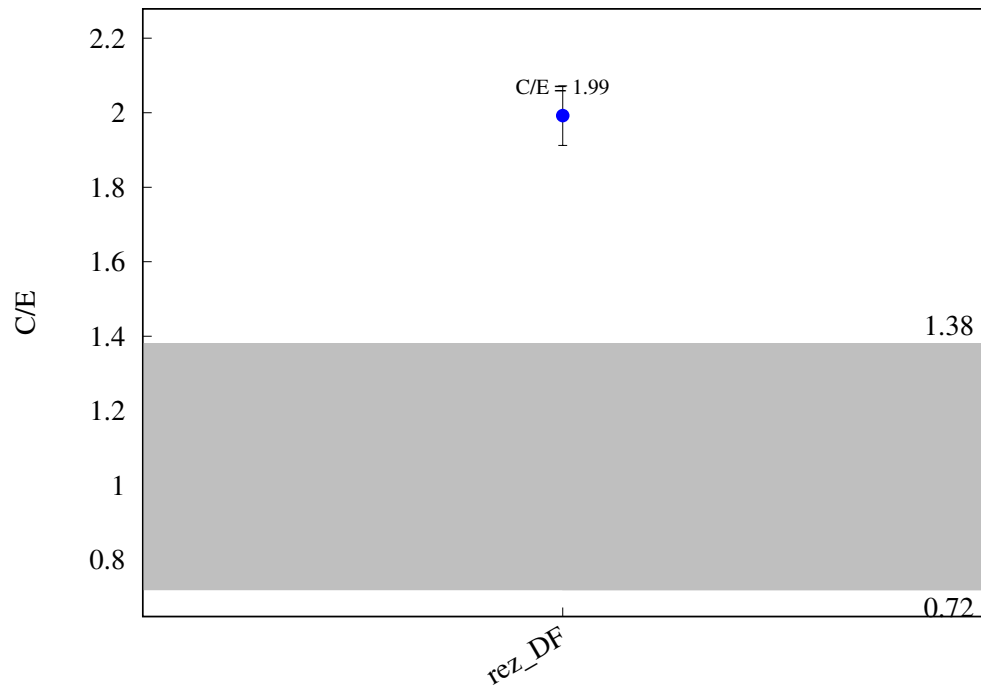
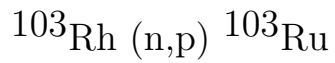
^{102}Ru (n,p) $^{102\text{m}}\text{Tc}$ 

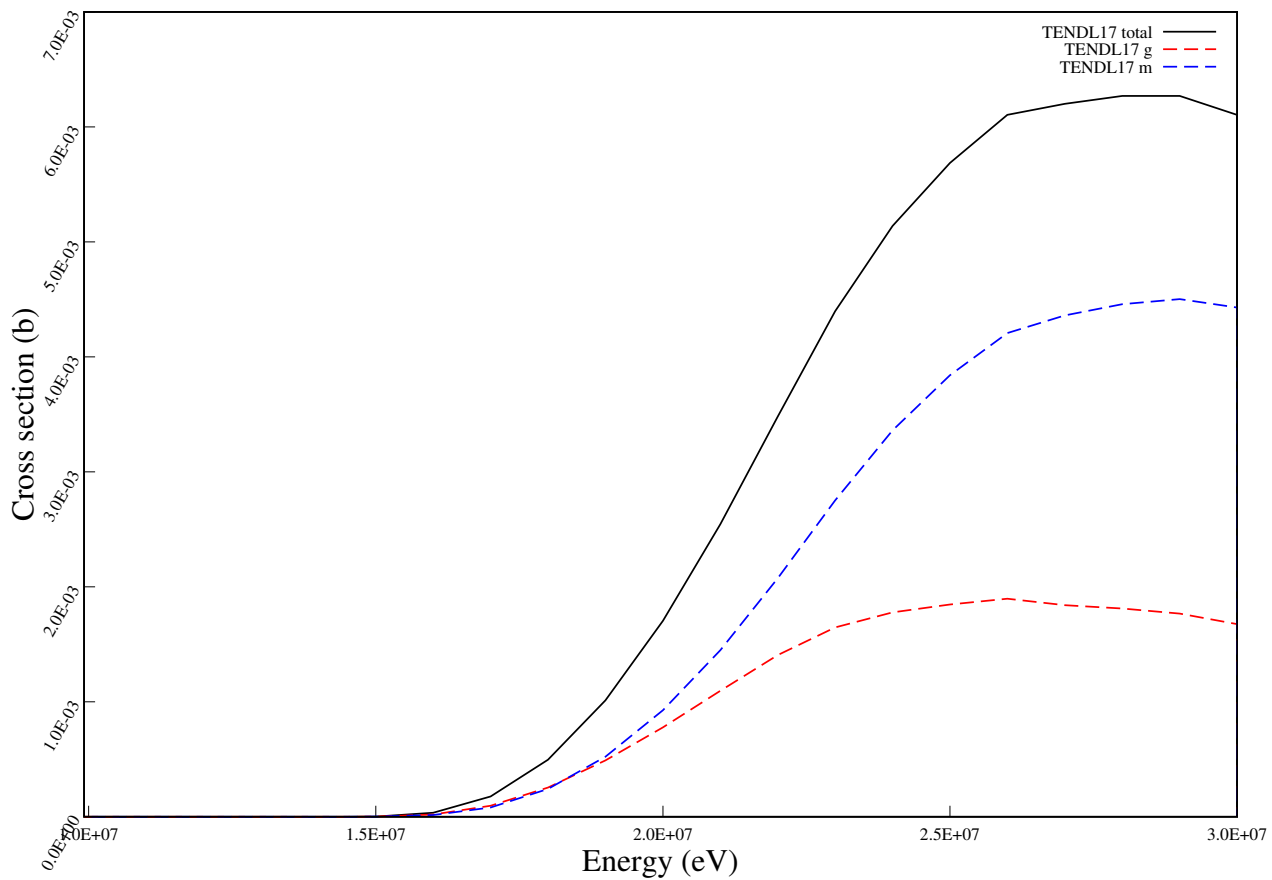
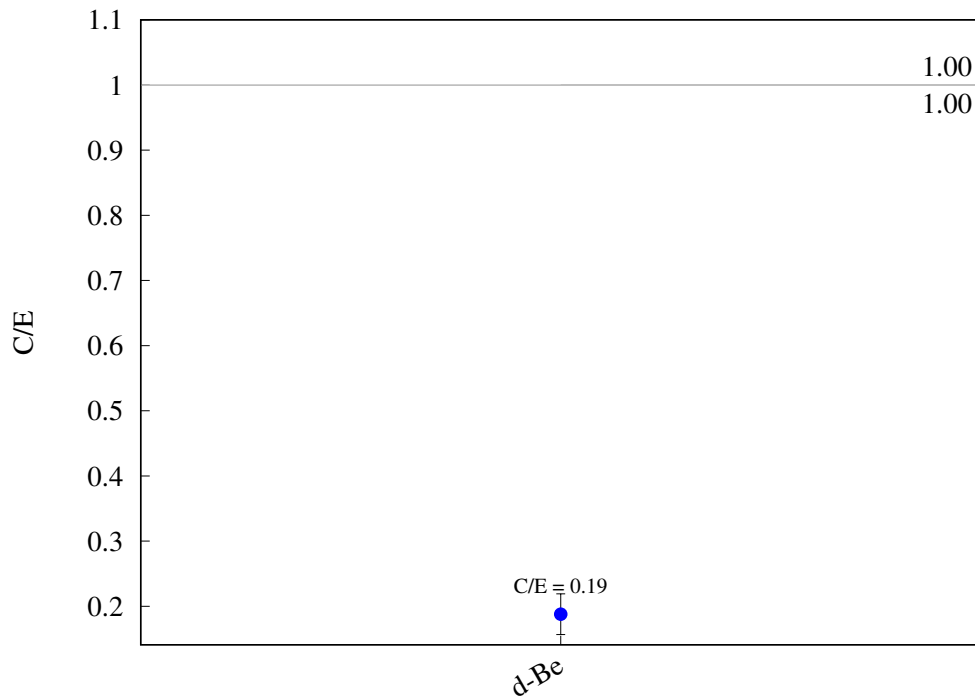
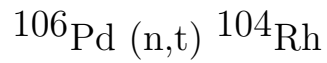
^{103}Rh (n,n) $^{103\text{m}}\text{Rh}$ 

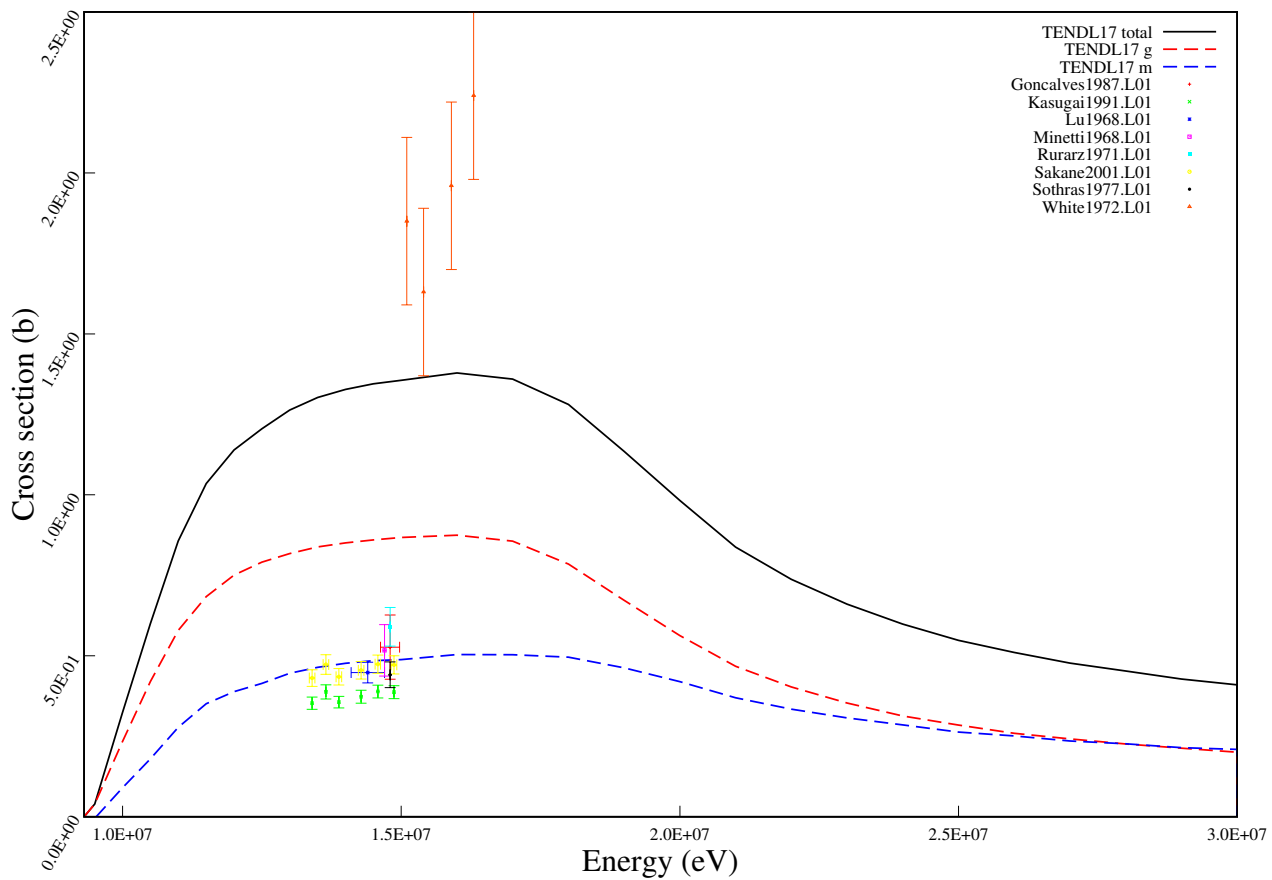
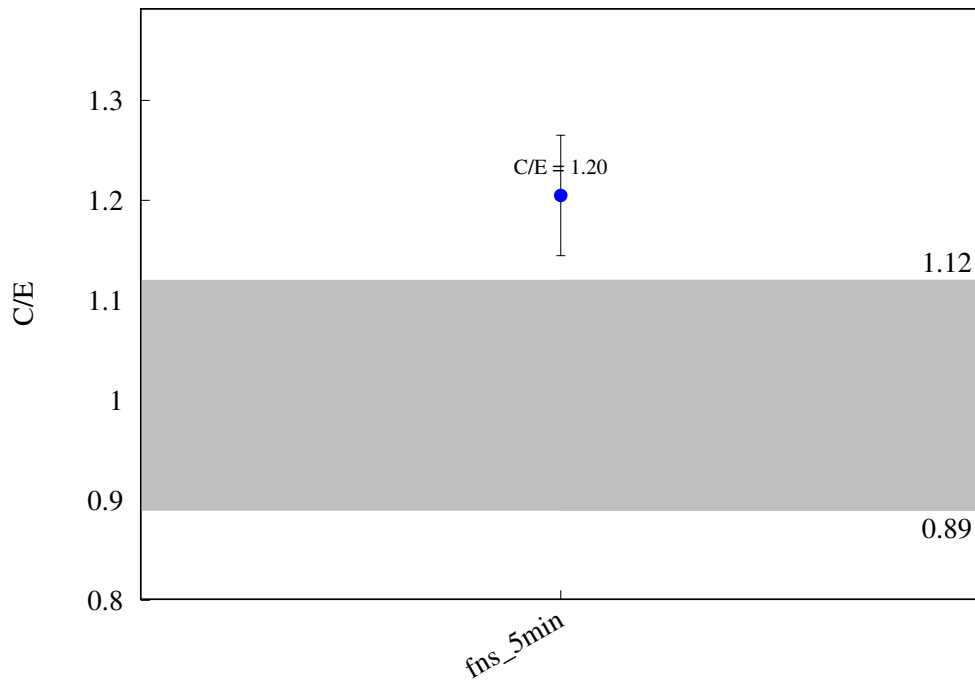
^{103}Rh (n,2n) ^{102}gRh 

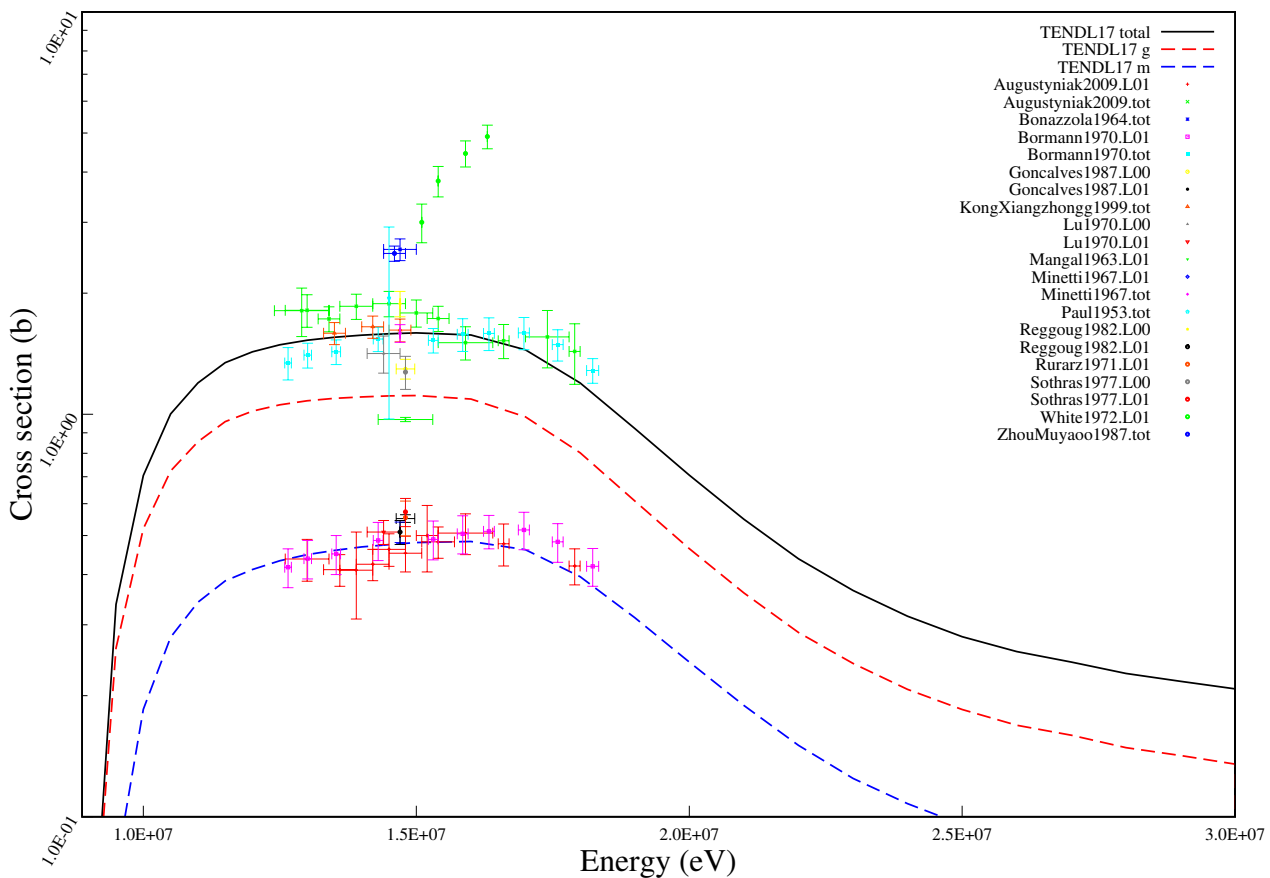
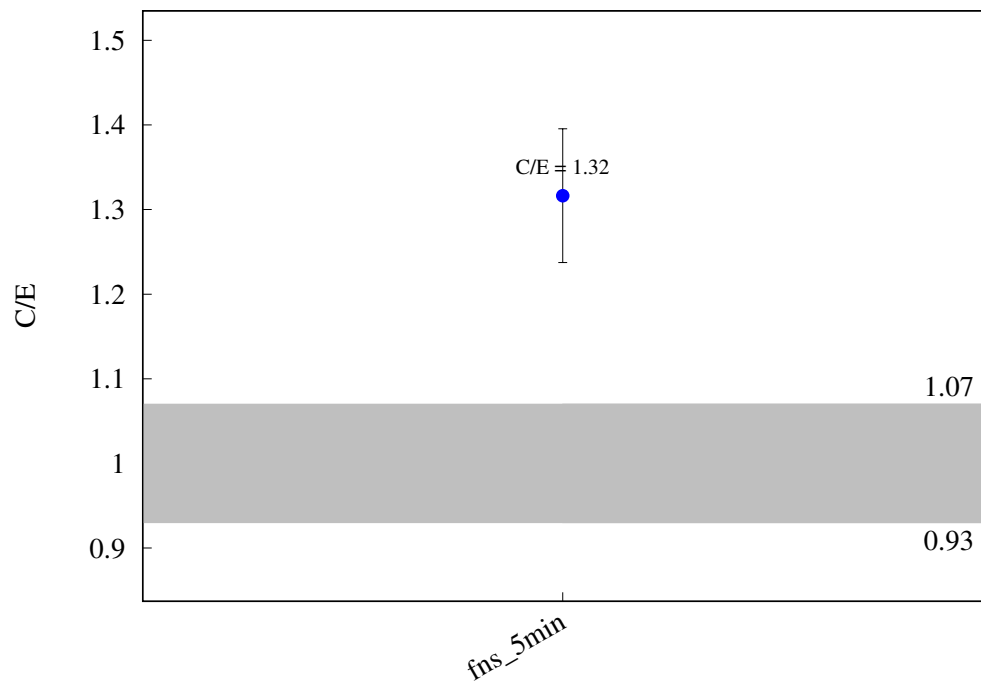
^{103}Rh (n,3n) $^{101\text{m}}\text{Rh}$ 

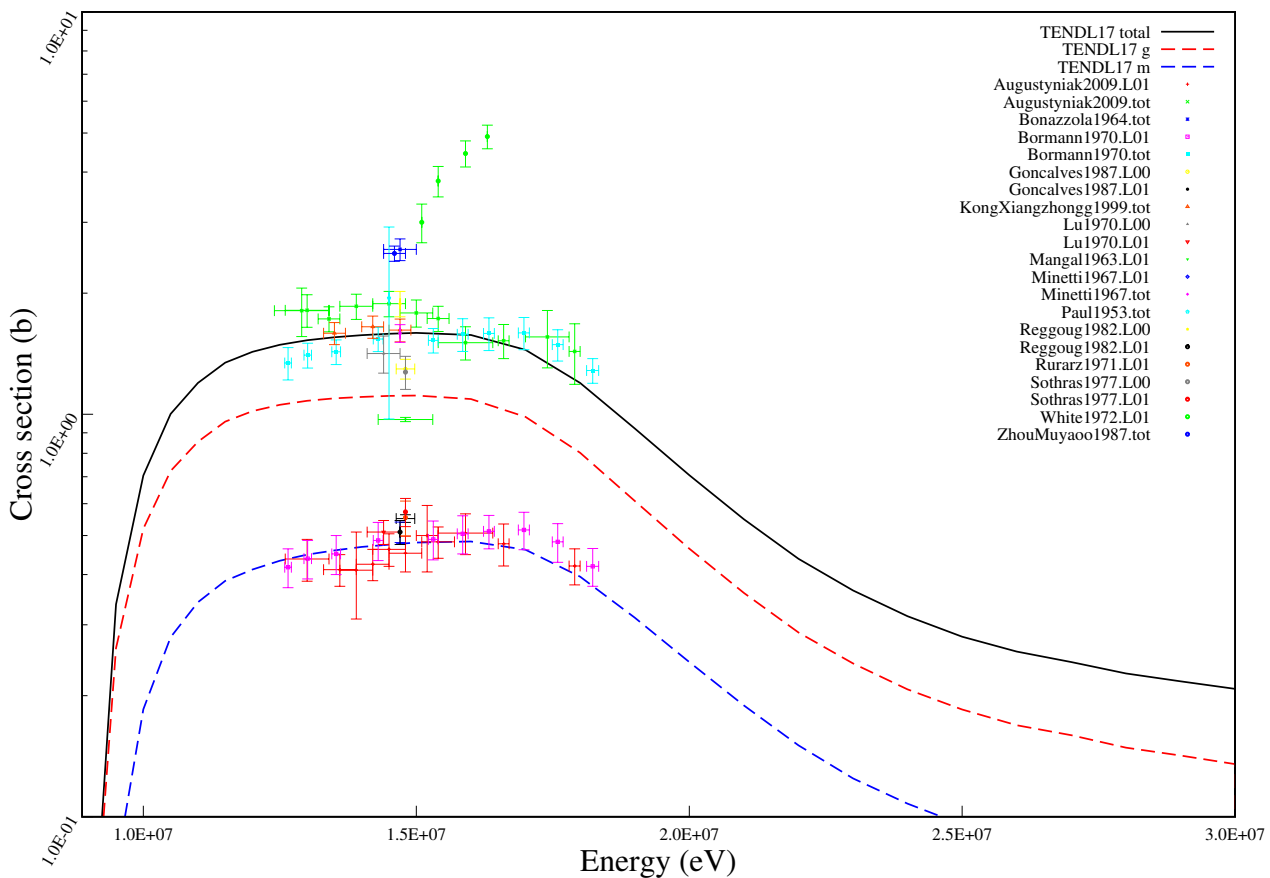
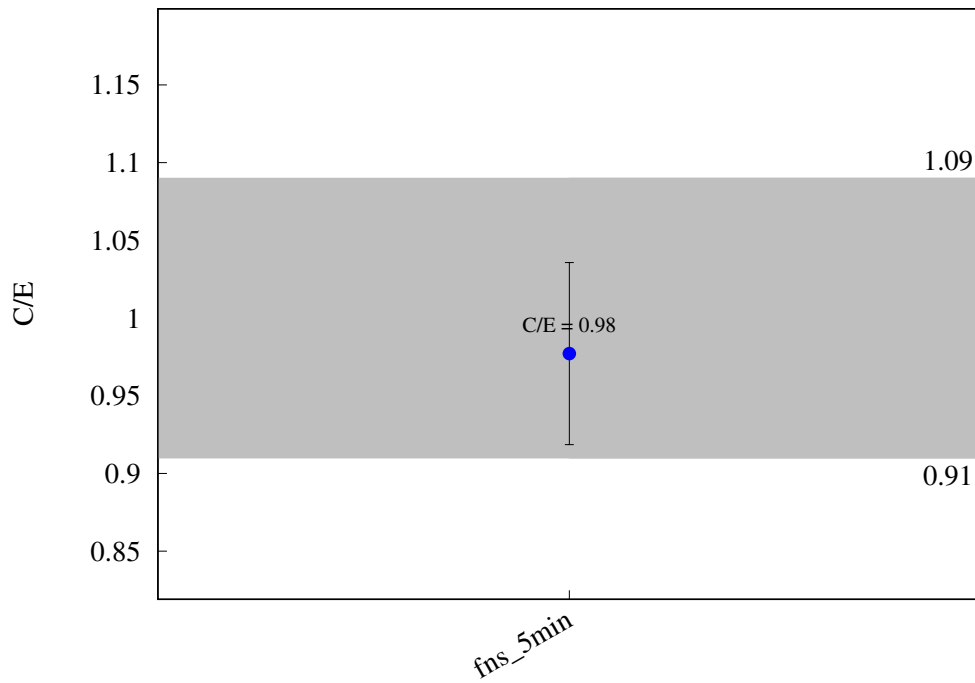
^{103}Rh (n,g) ^{104}Rh 

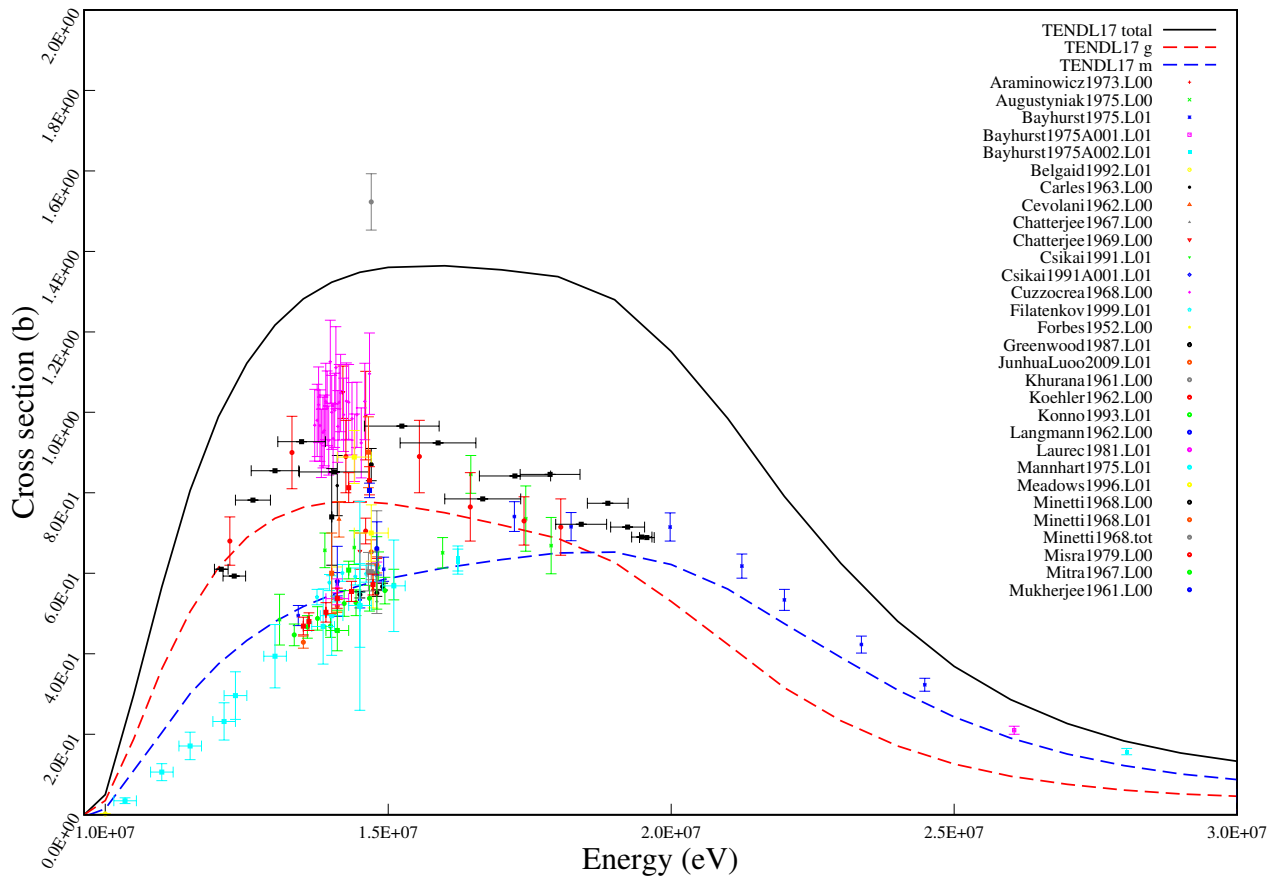
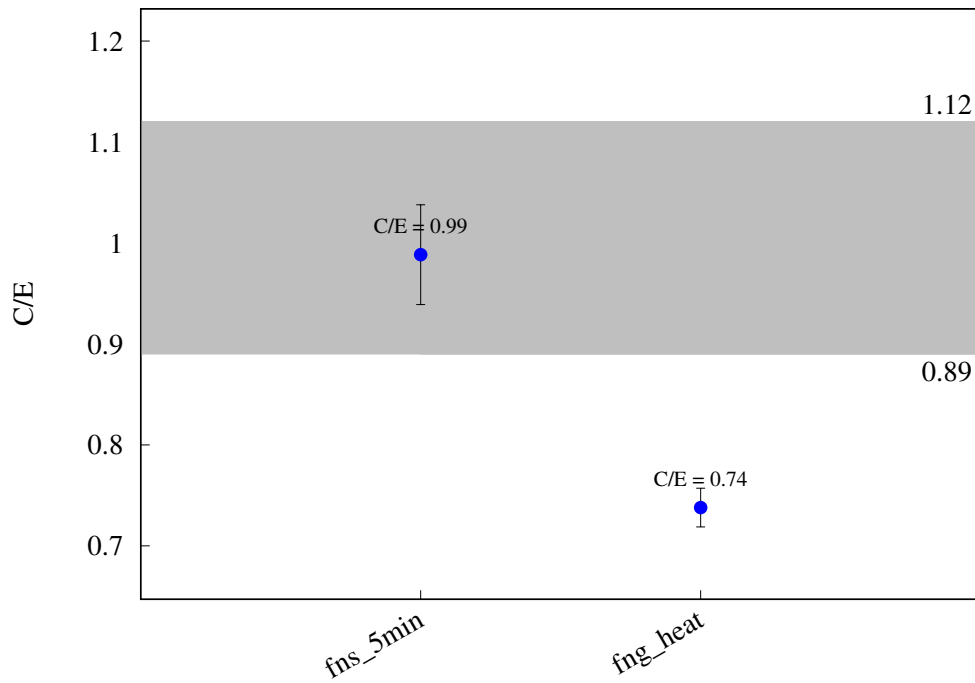


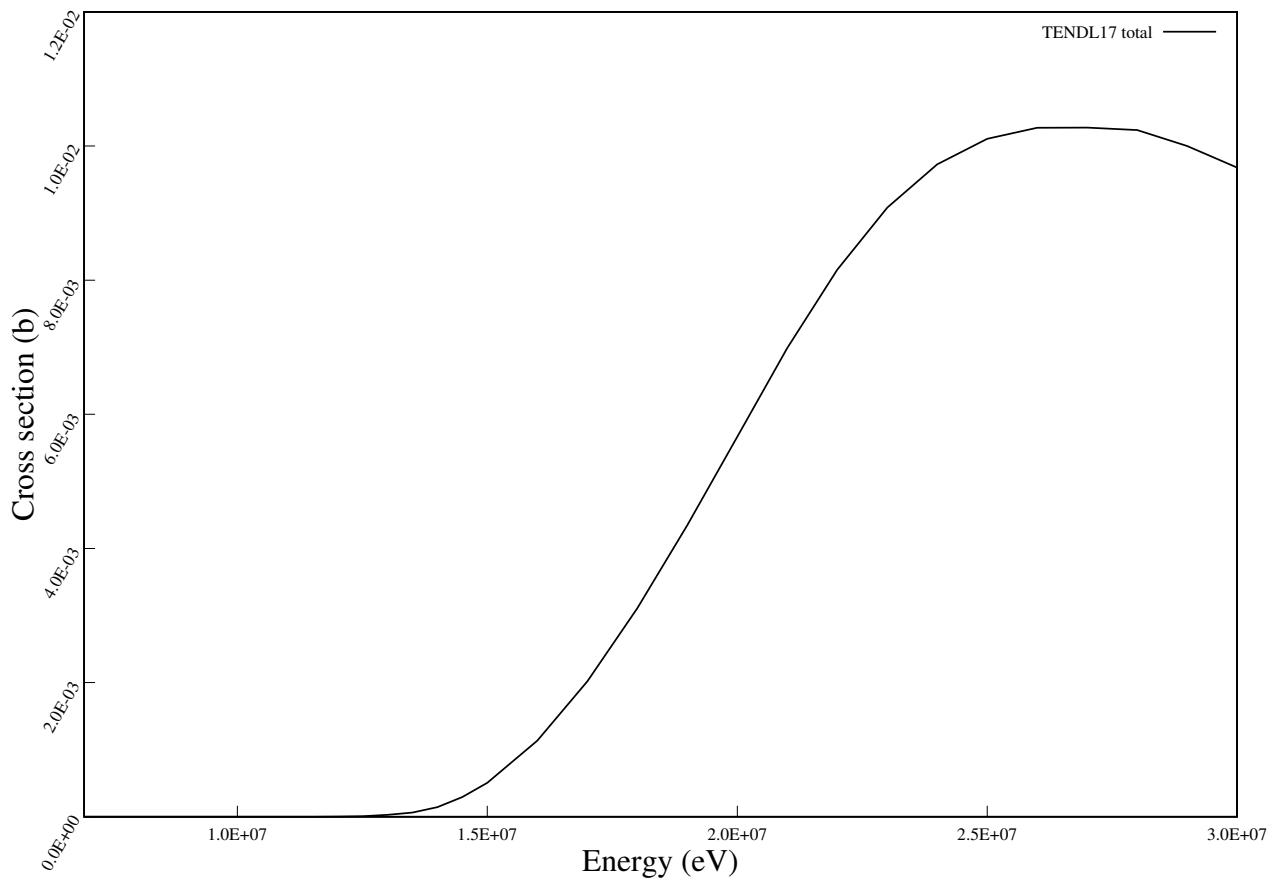
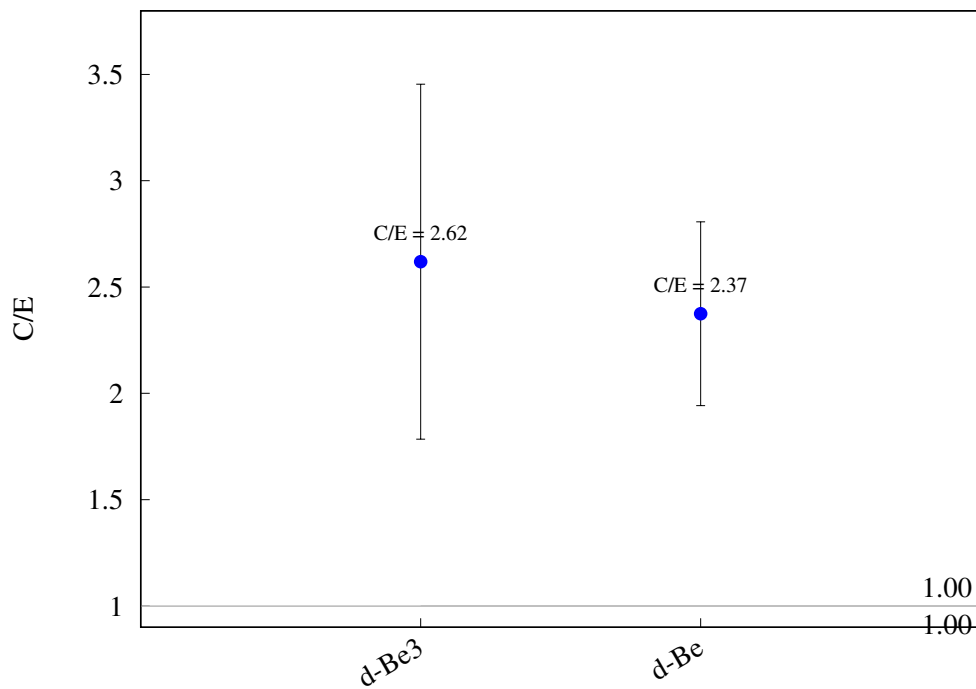


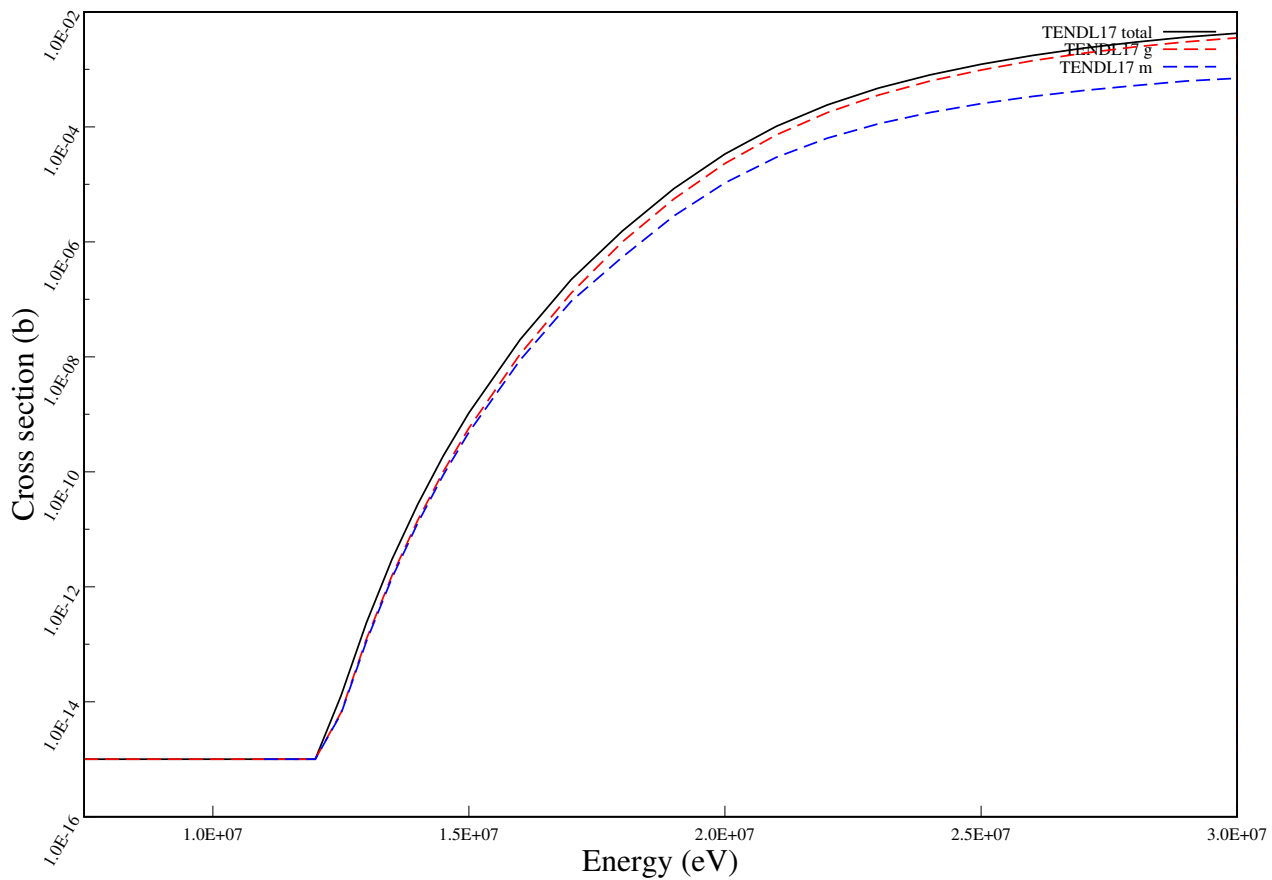
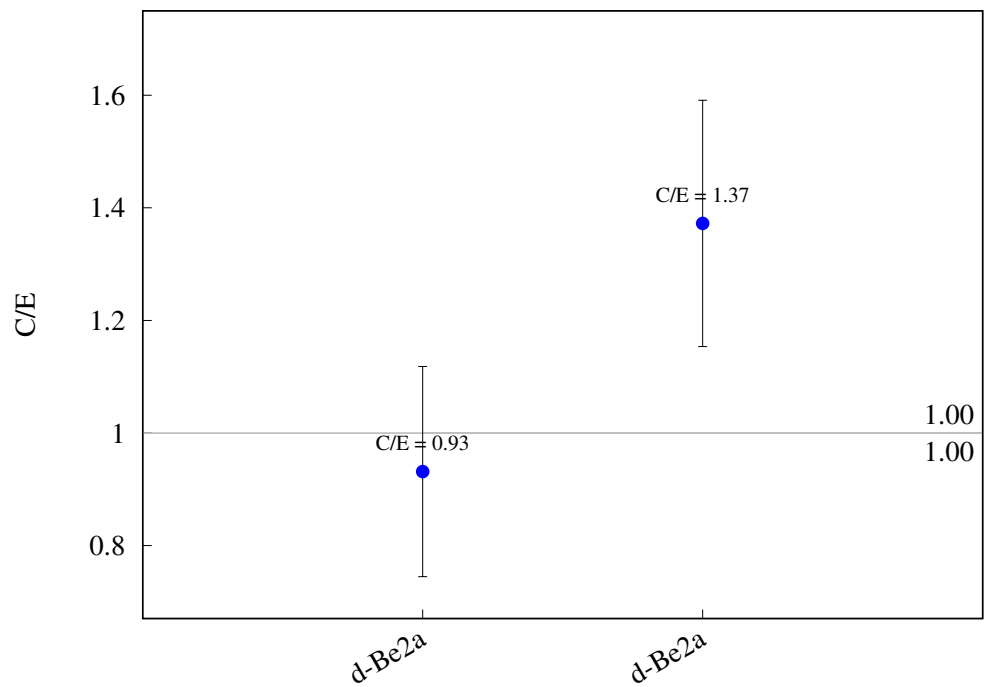
^{108}Pd (n,2n) ^{107m}Pd 

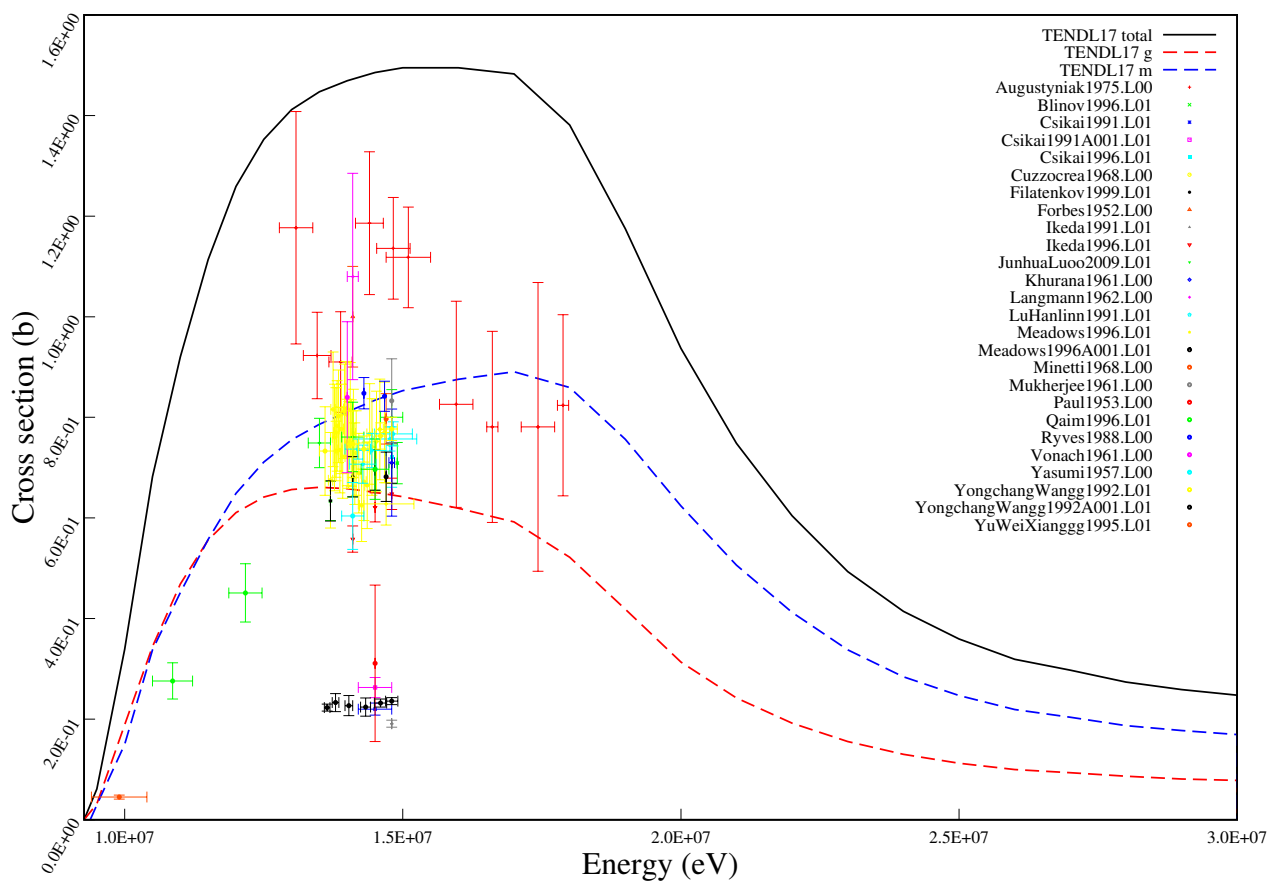
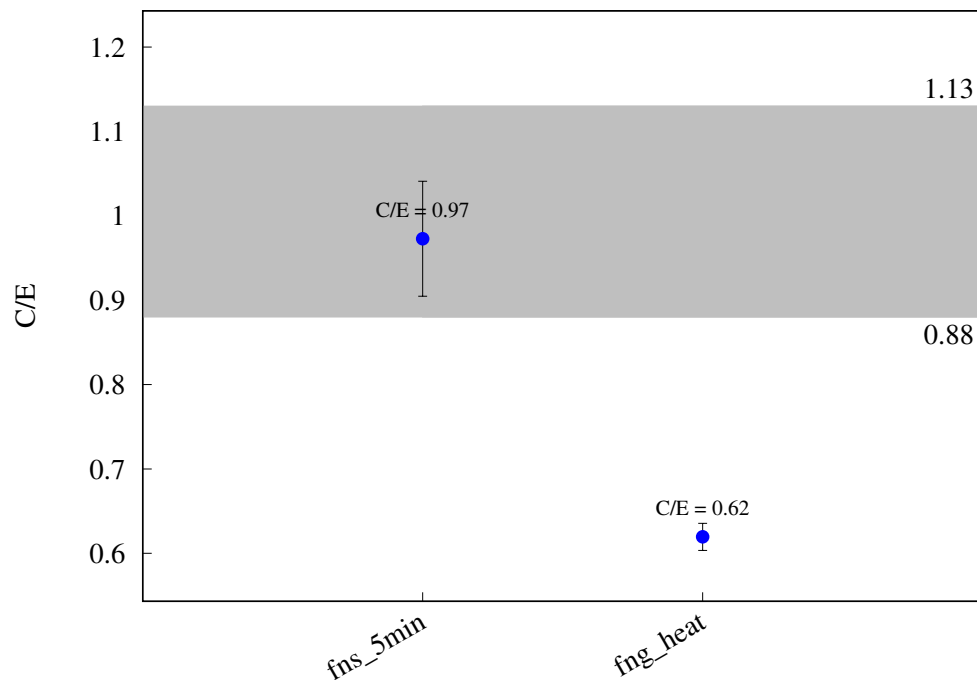
^{110}Pd (n,2n) ^{109m}Pd 

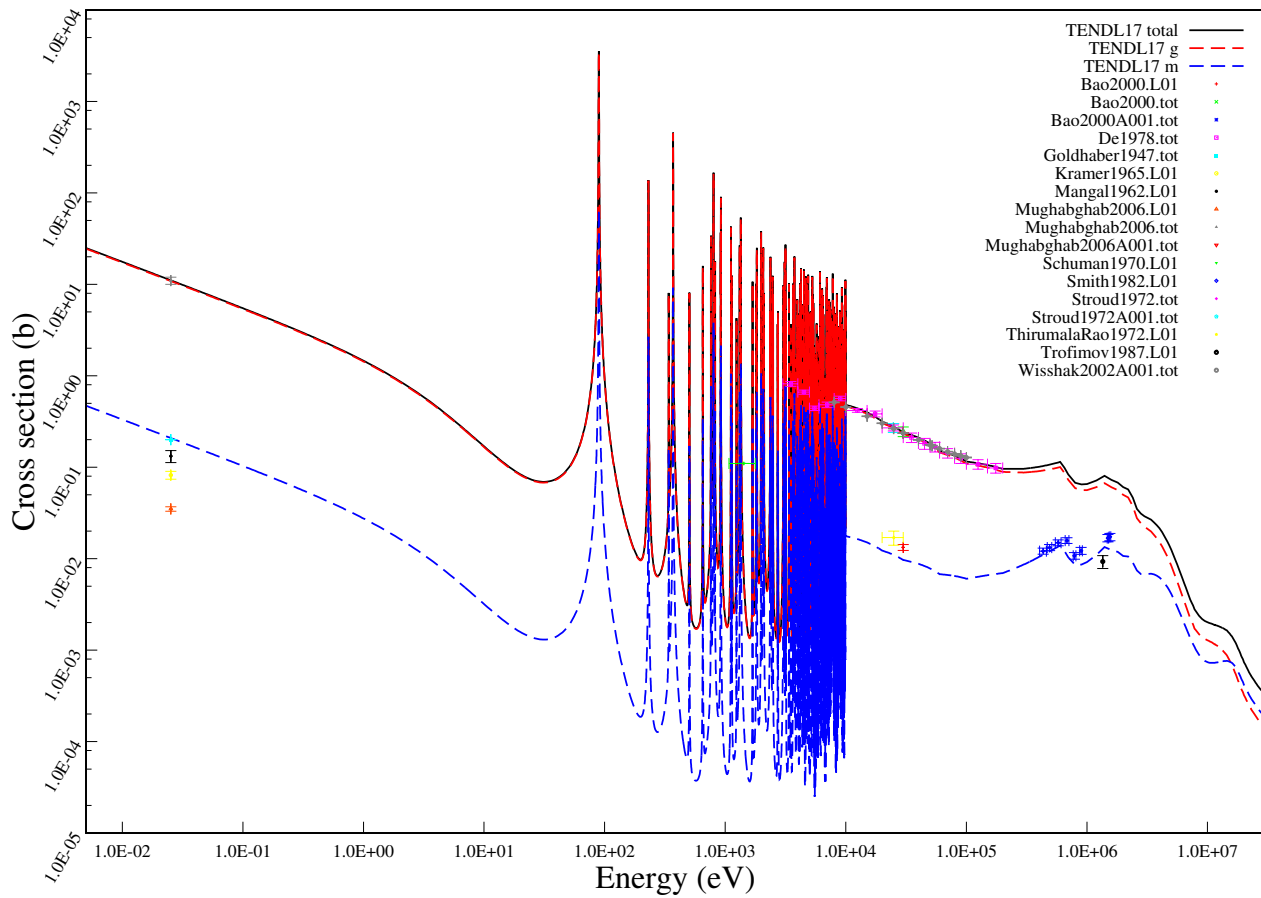
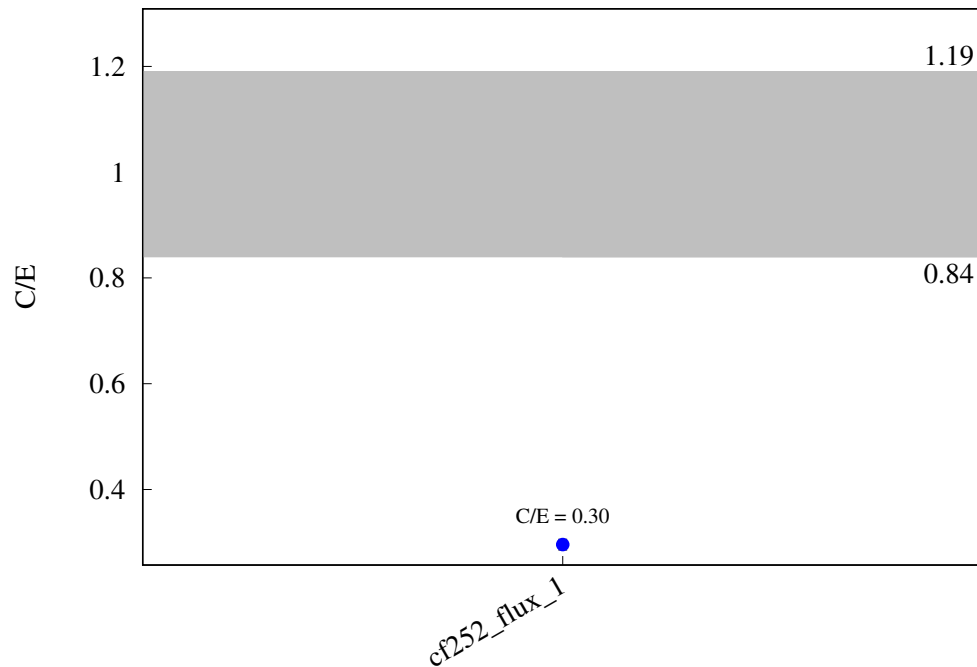
^{110}Pd (n,2n) ^{109}Pd 

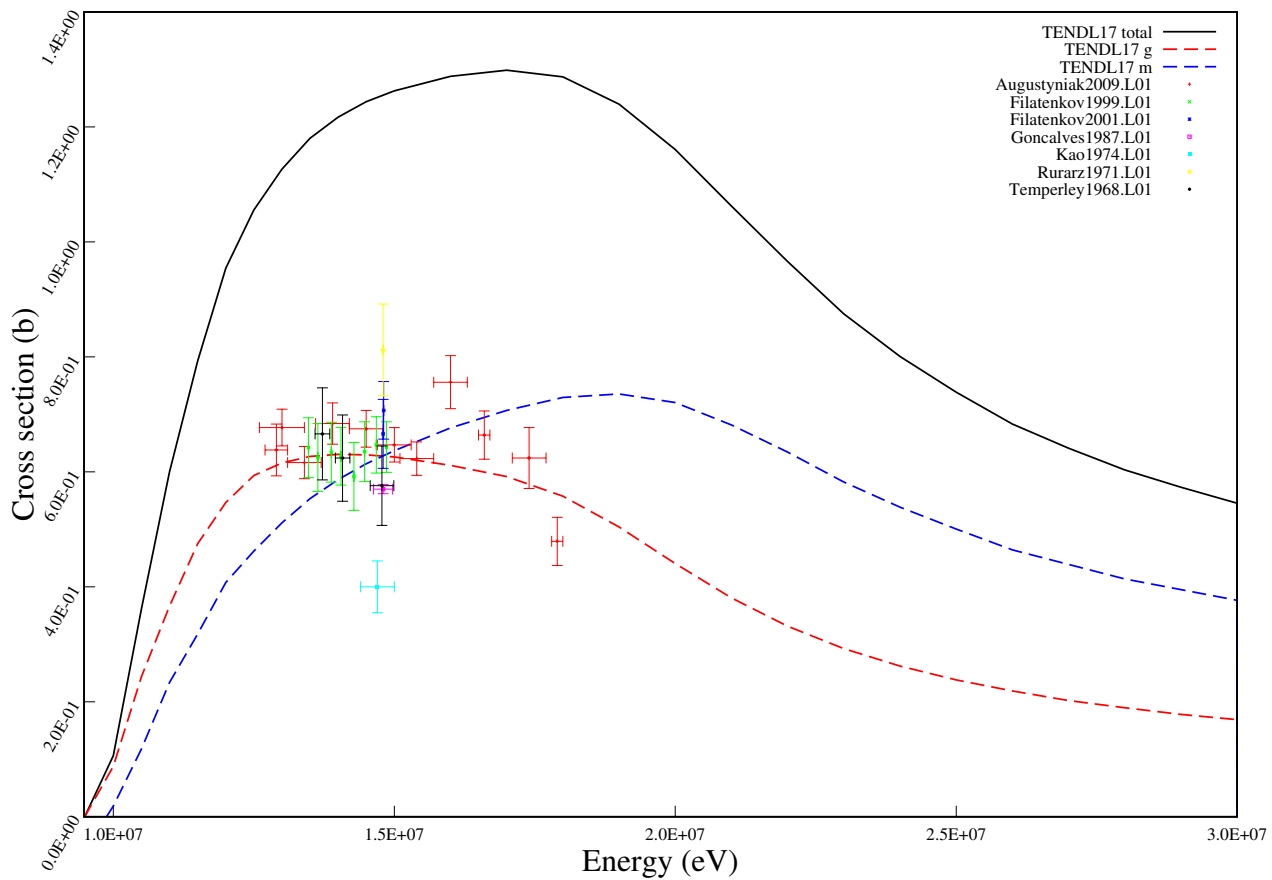
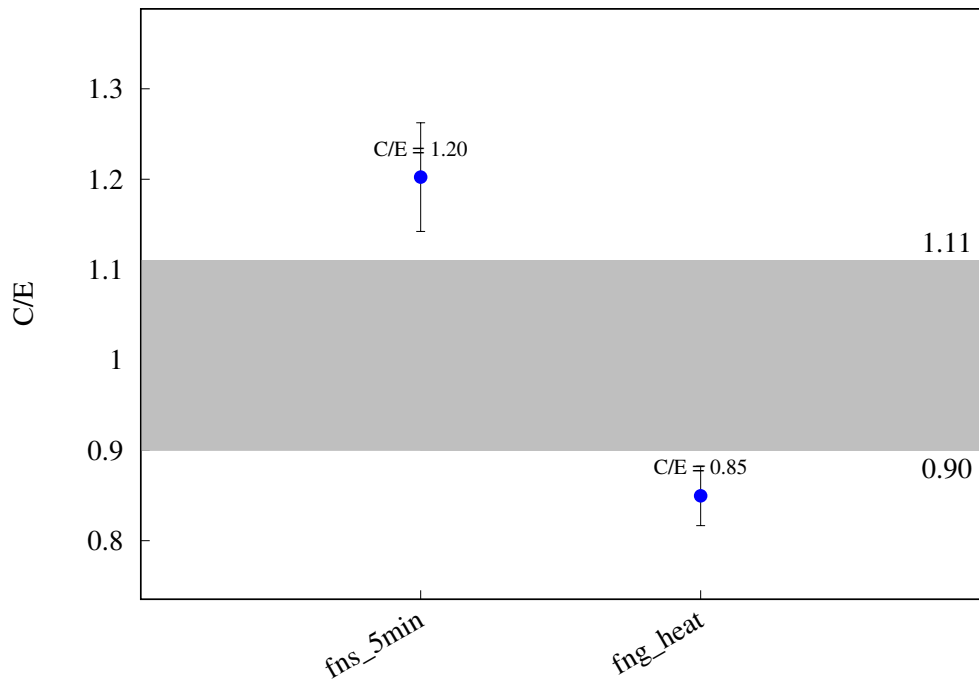
^{107}Ag (n,2n) ^{106}gAg 

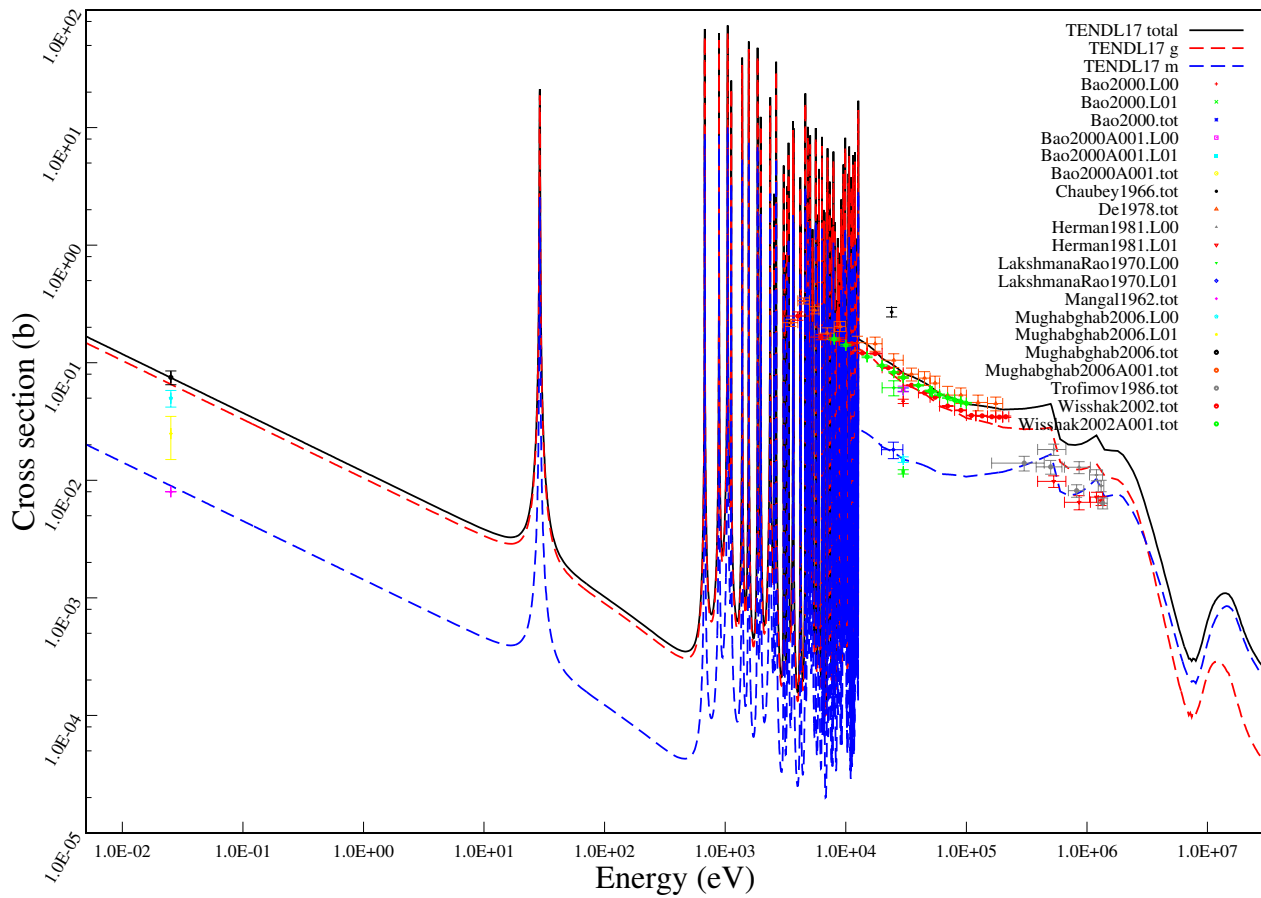
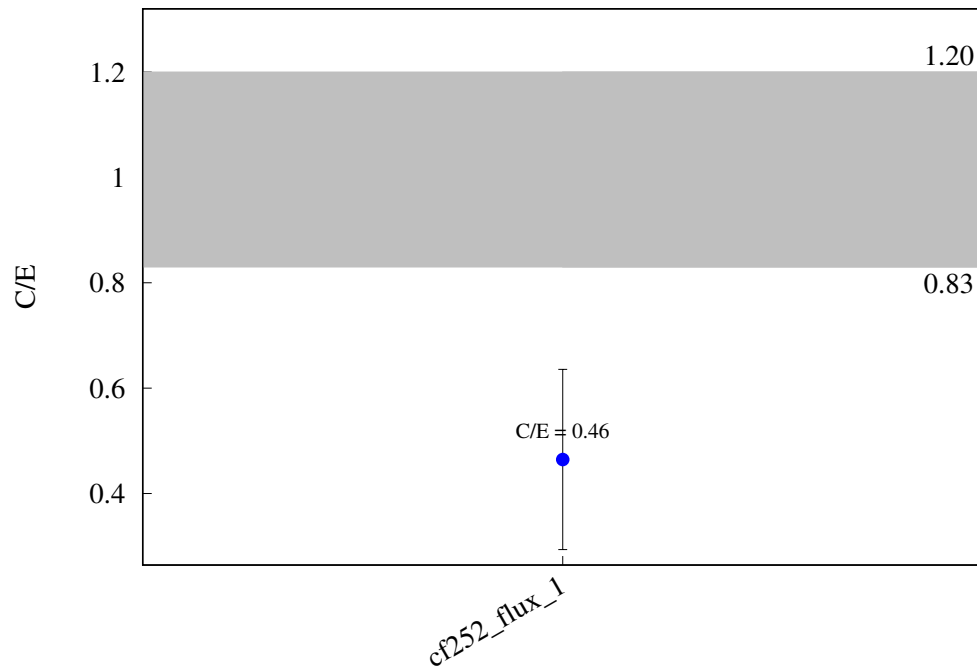
$^{107}\text{Ag} (\text{n},\text{t}) ^{105}\text{Pd}$ 

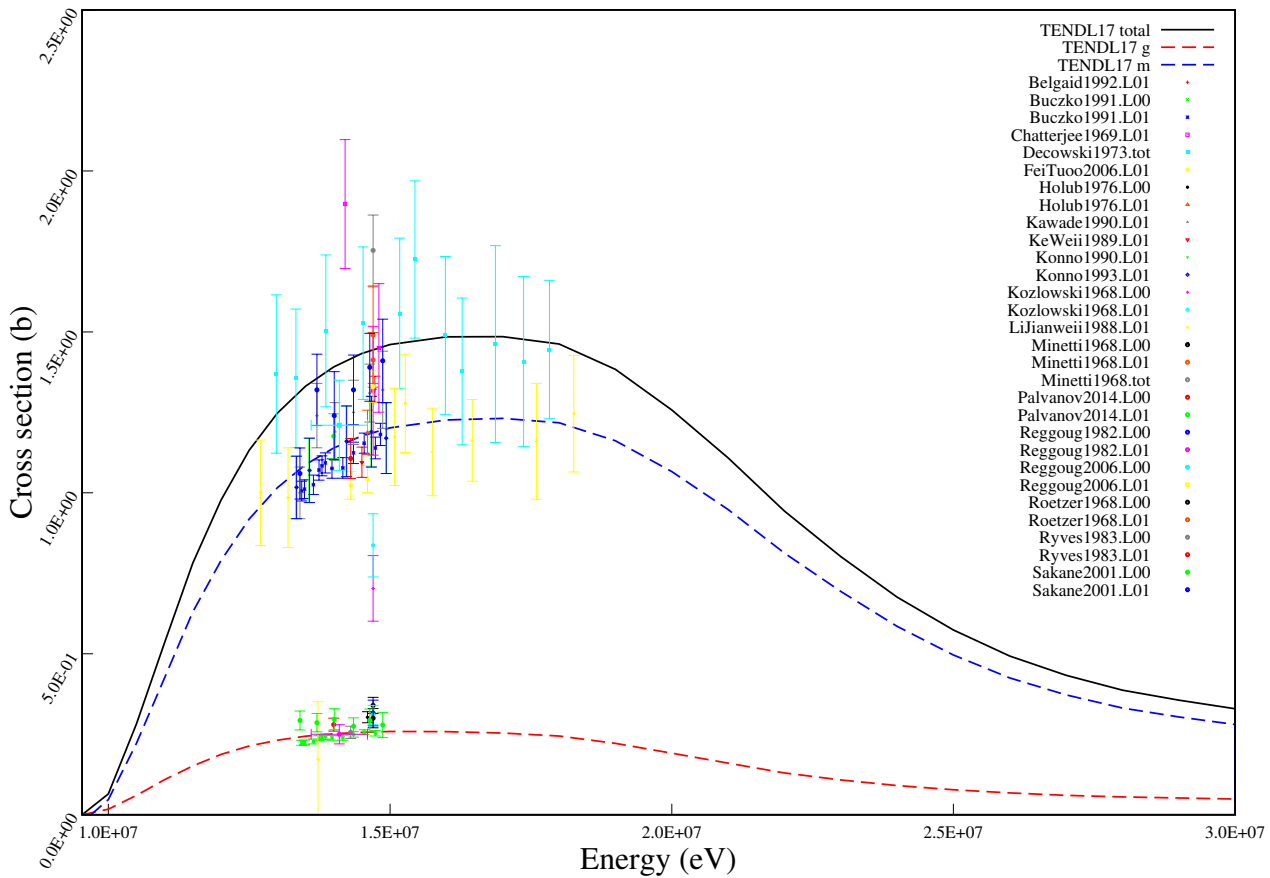
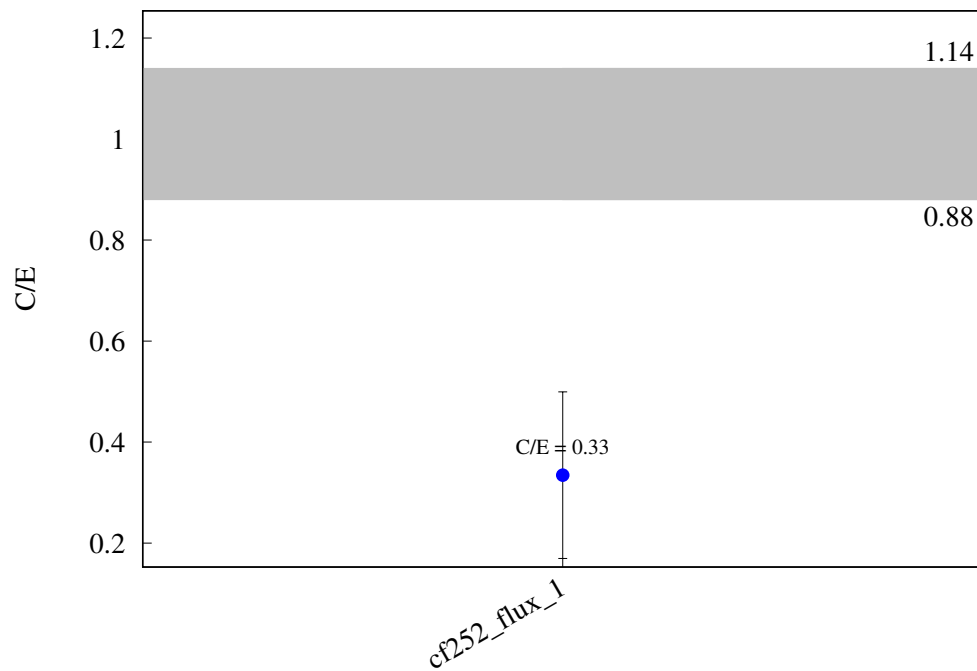
$^{107}\text{Ag} (\text{n},\text{h}) ^{105}\text{Rh}$ 

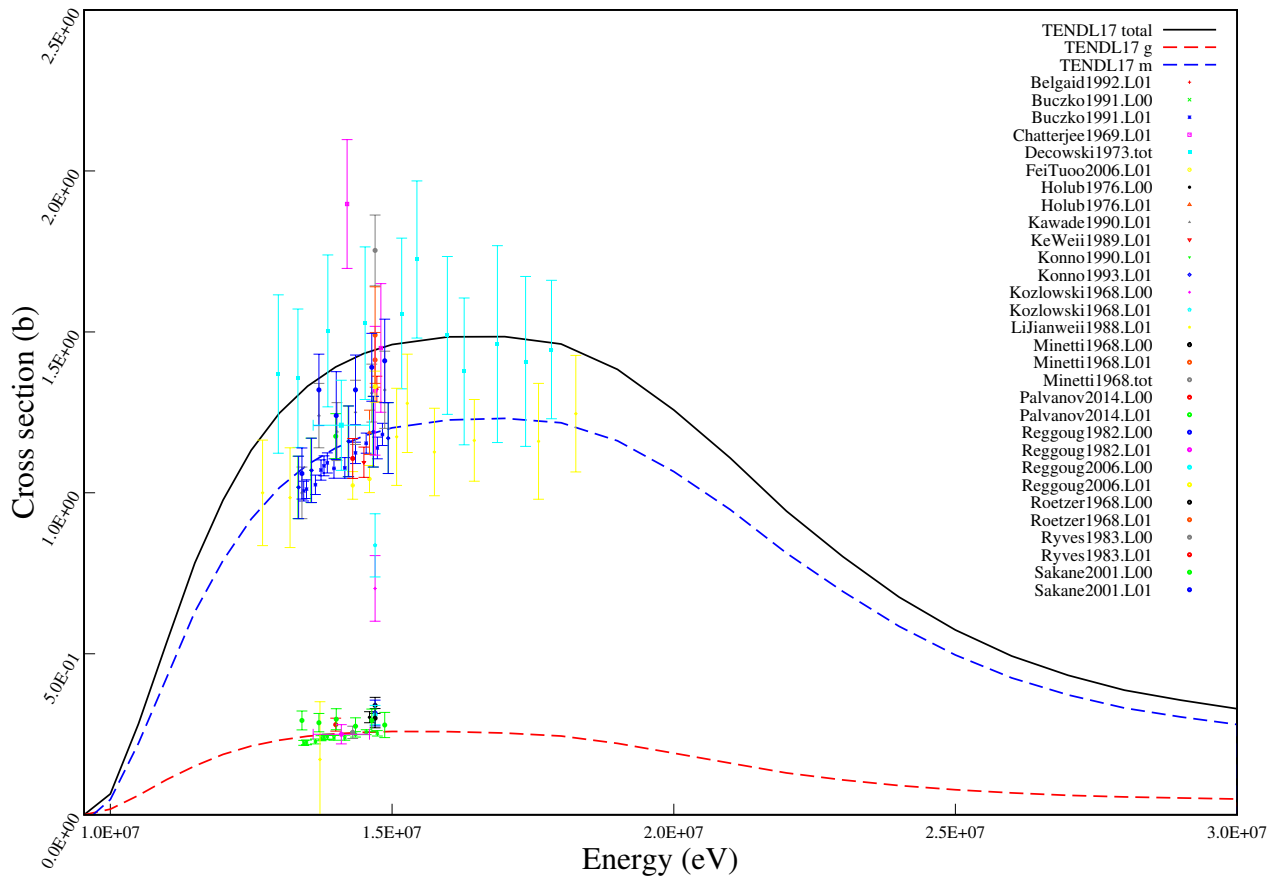
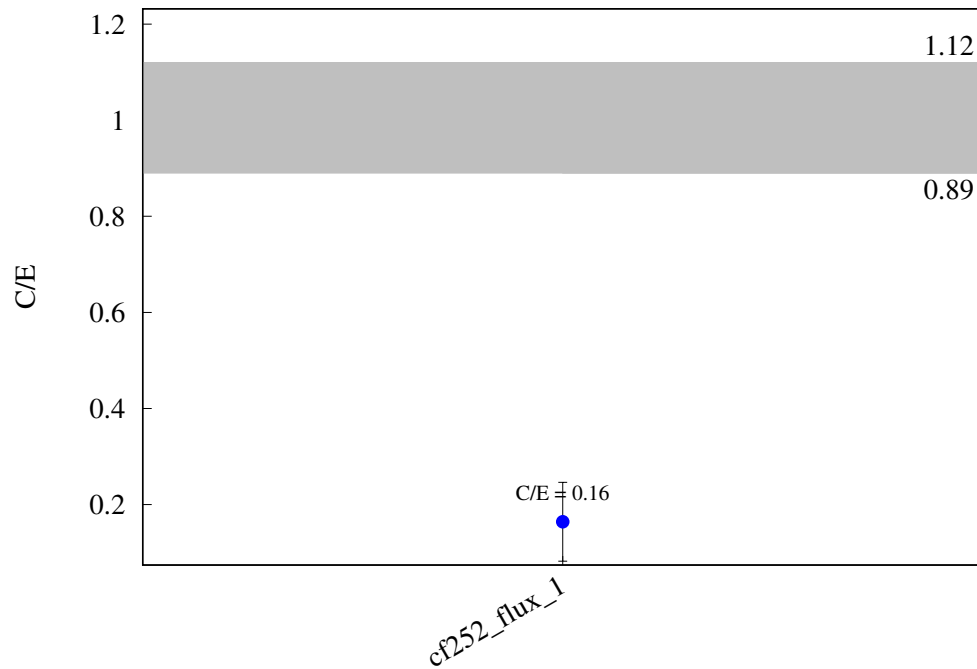
^{109}Ag (n,2n) ^{108}gAg 

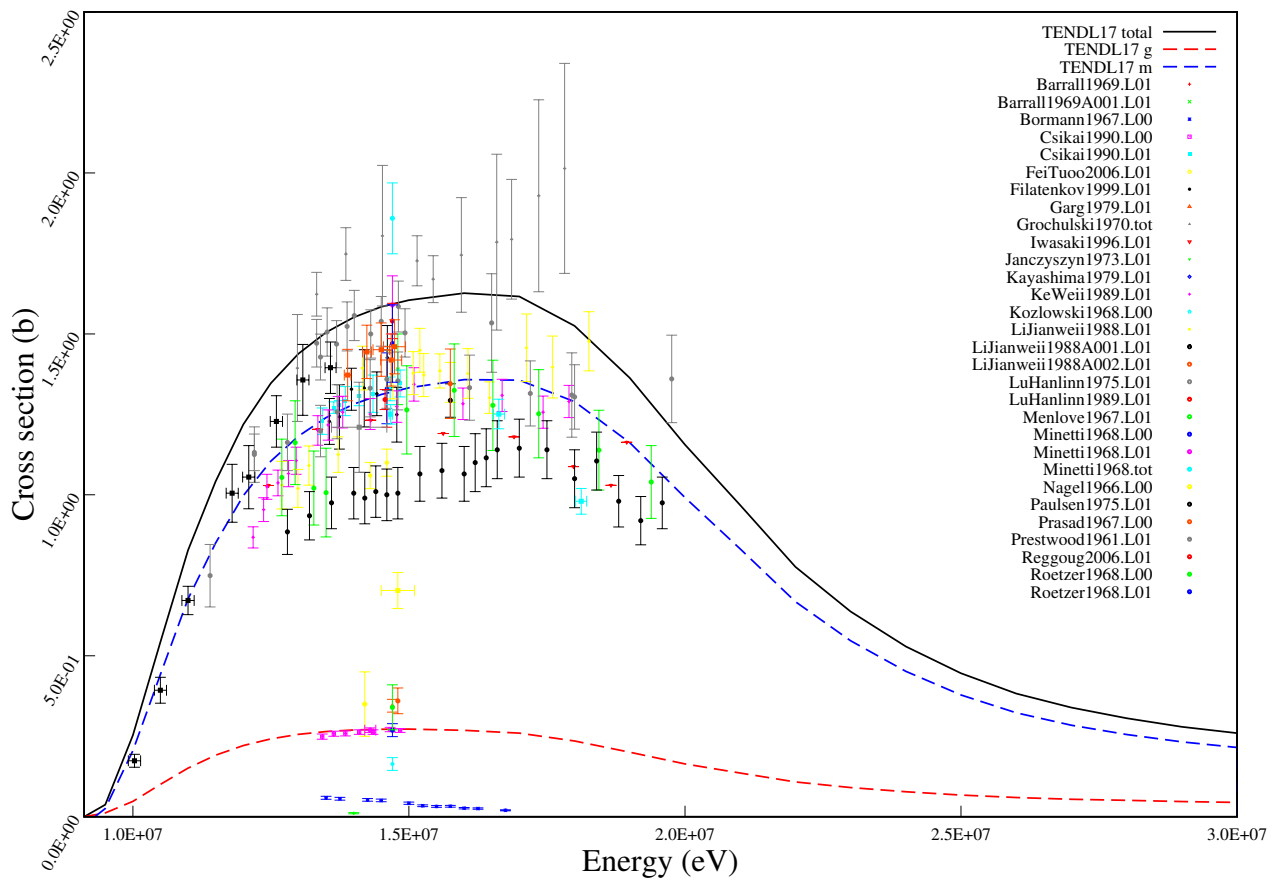
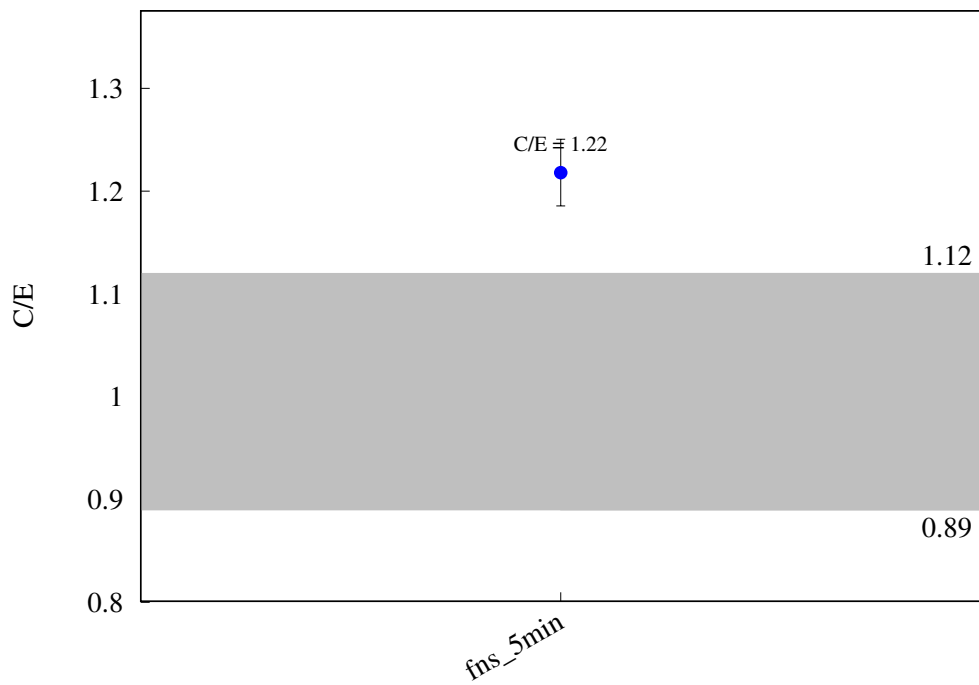
^{110}Cd (n,g) ^{111}Cd 

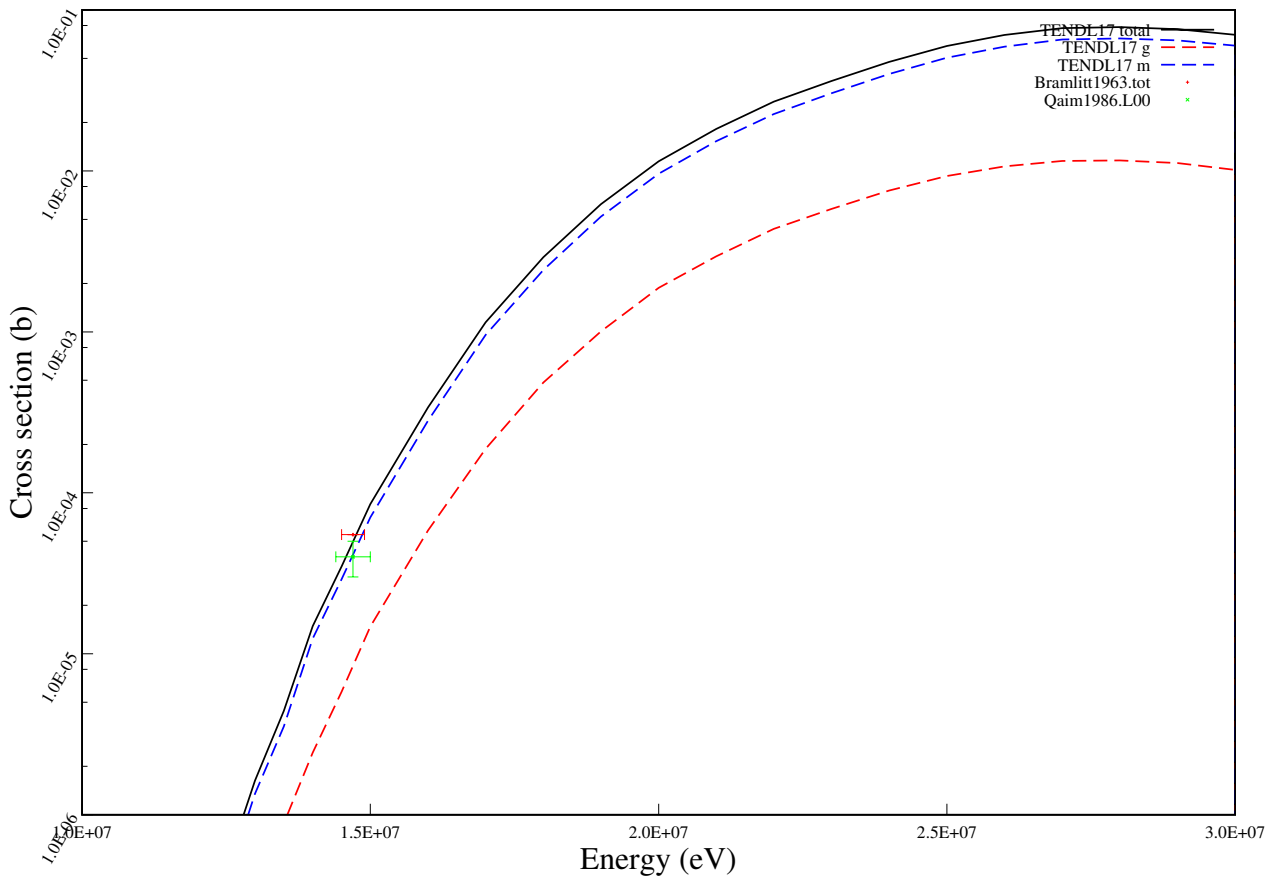
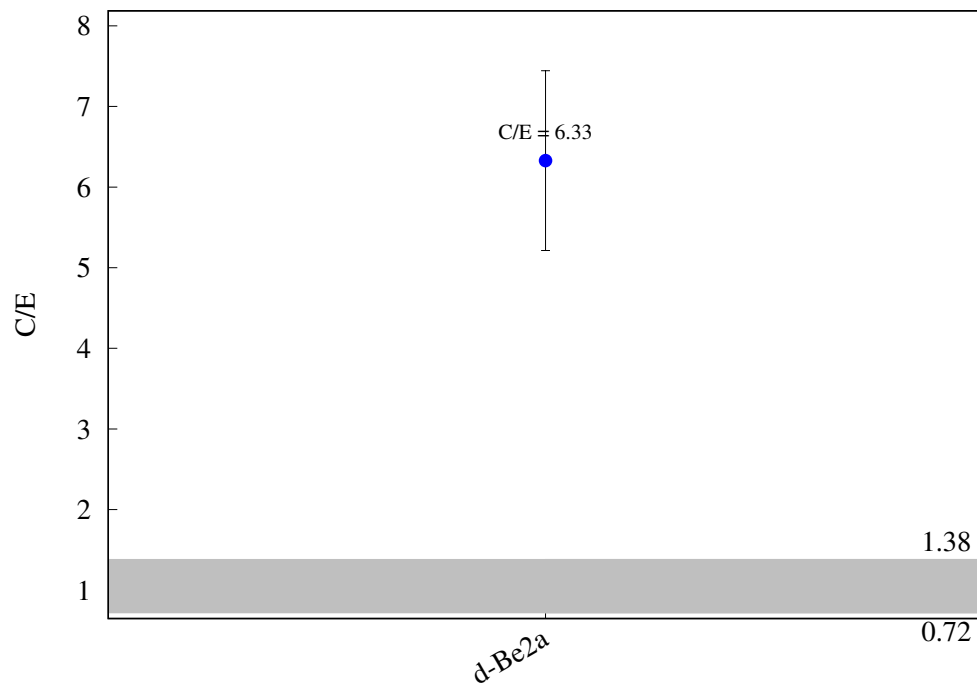
^{112}Cd (n,2n) ^{111m}Cd 

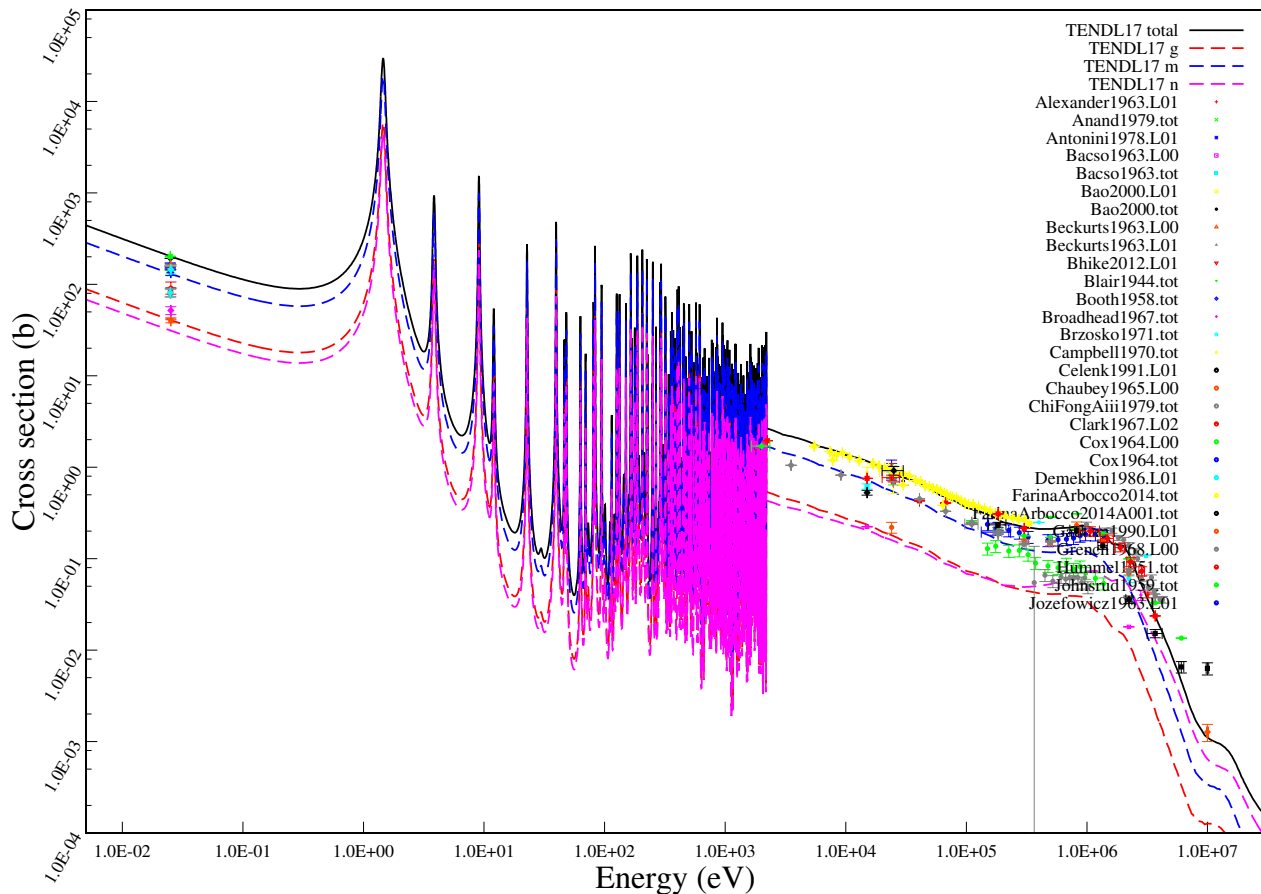
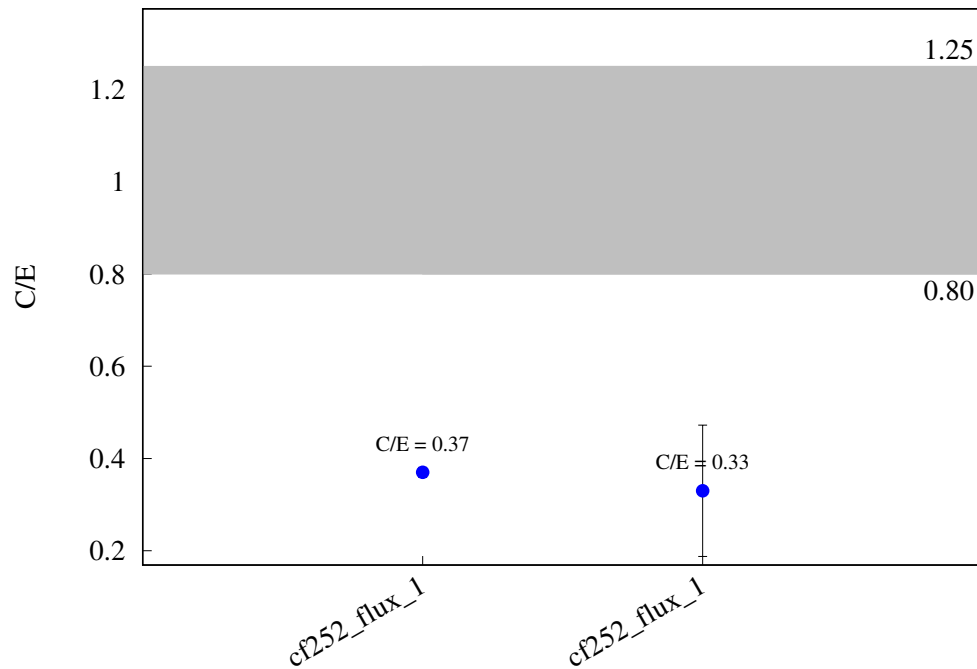
^{116}Cd (n,g) ^{117}Cd 

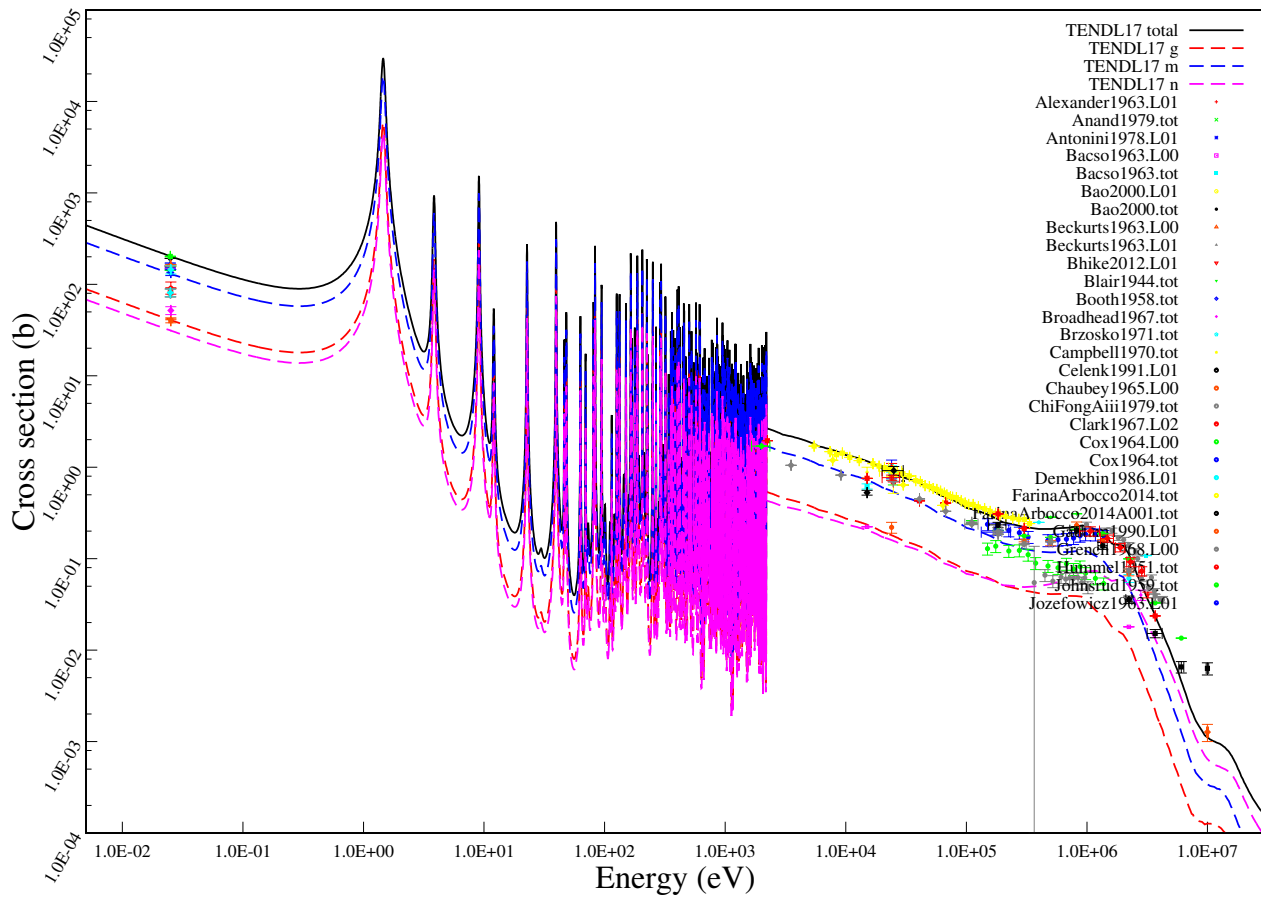
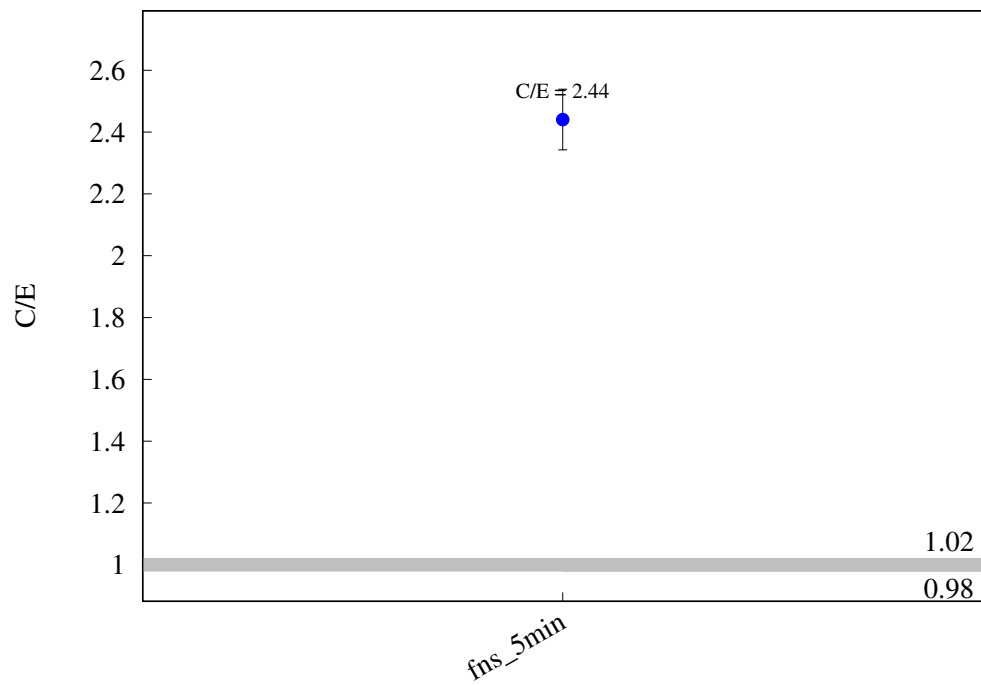
^{113}In ($n,2n$) ^{112m}In 

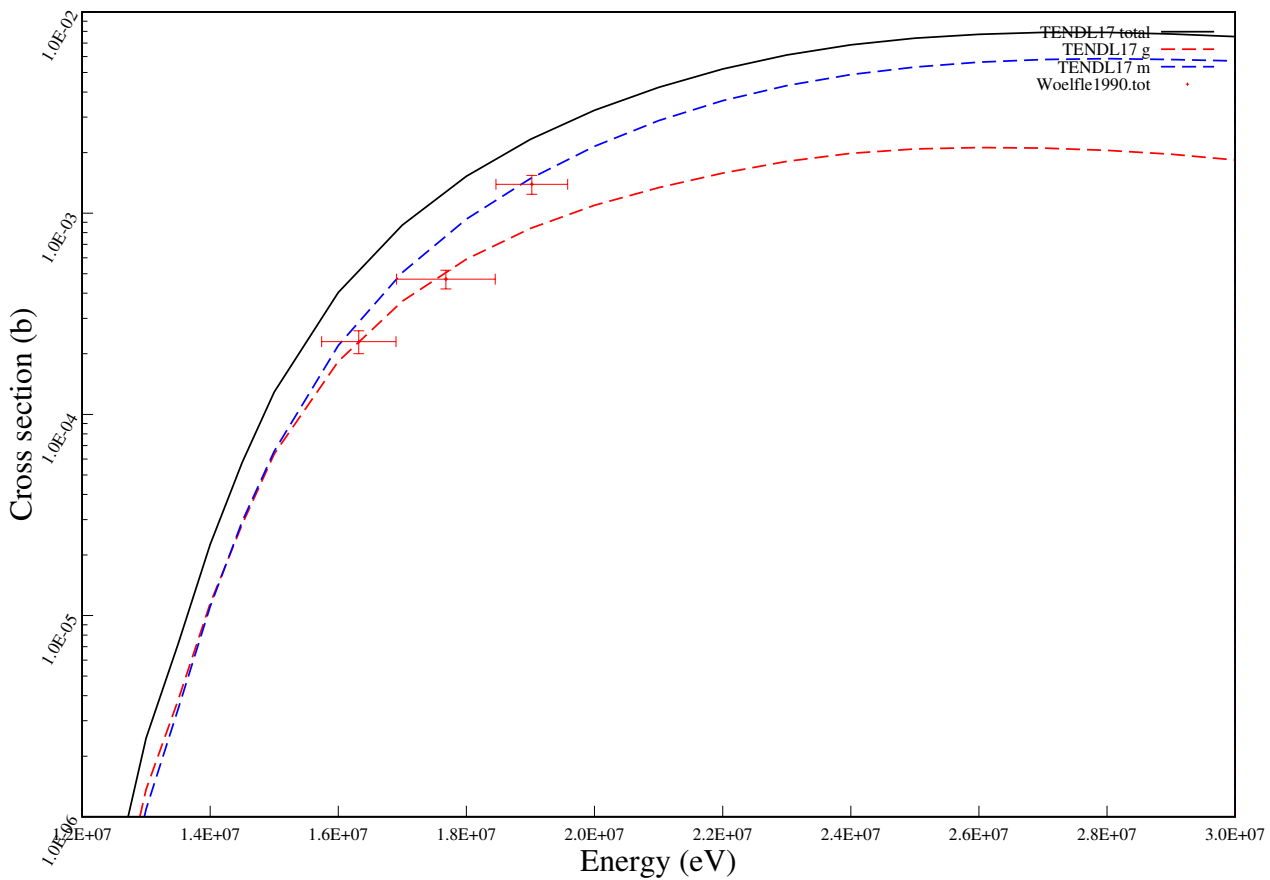
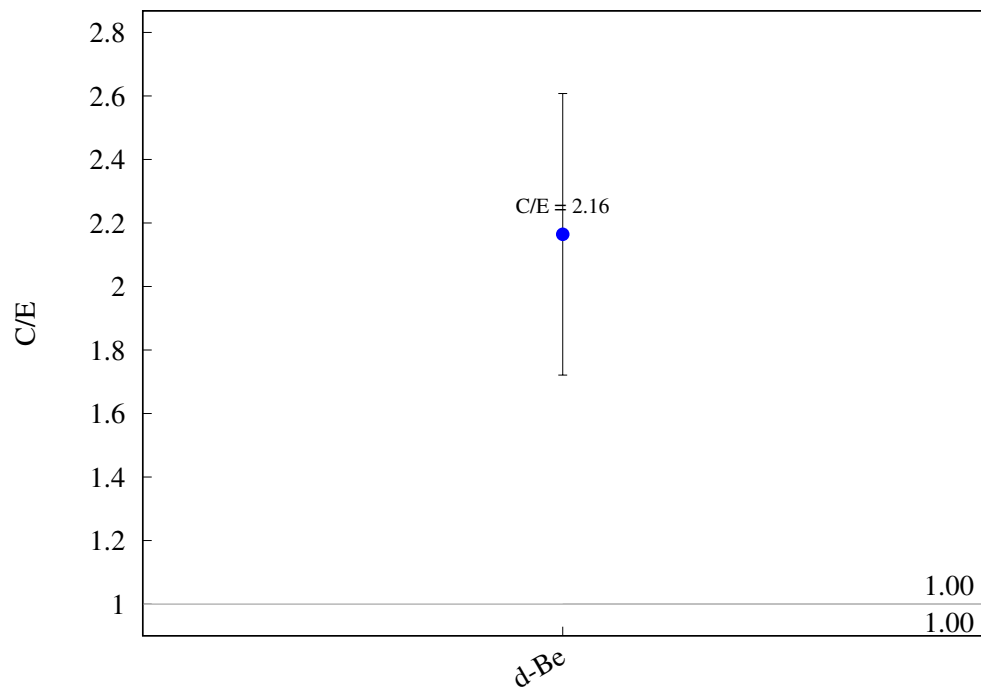
^{113}In (n,2n) ^{112}In 

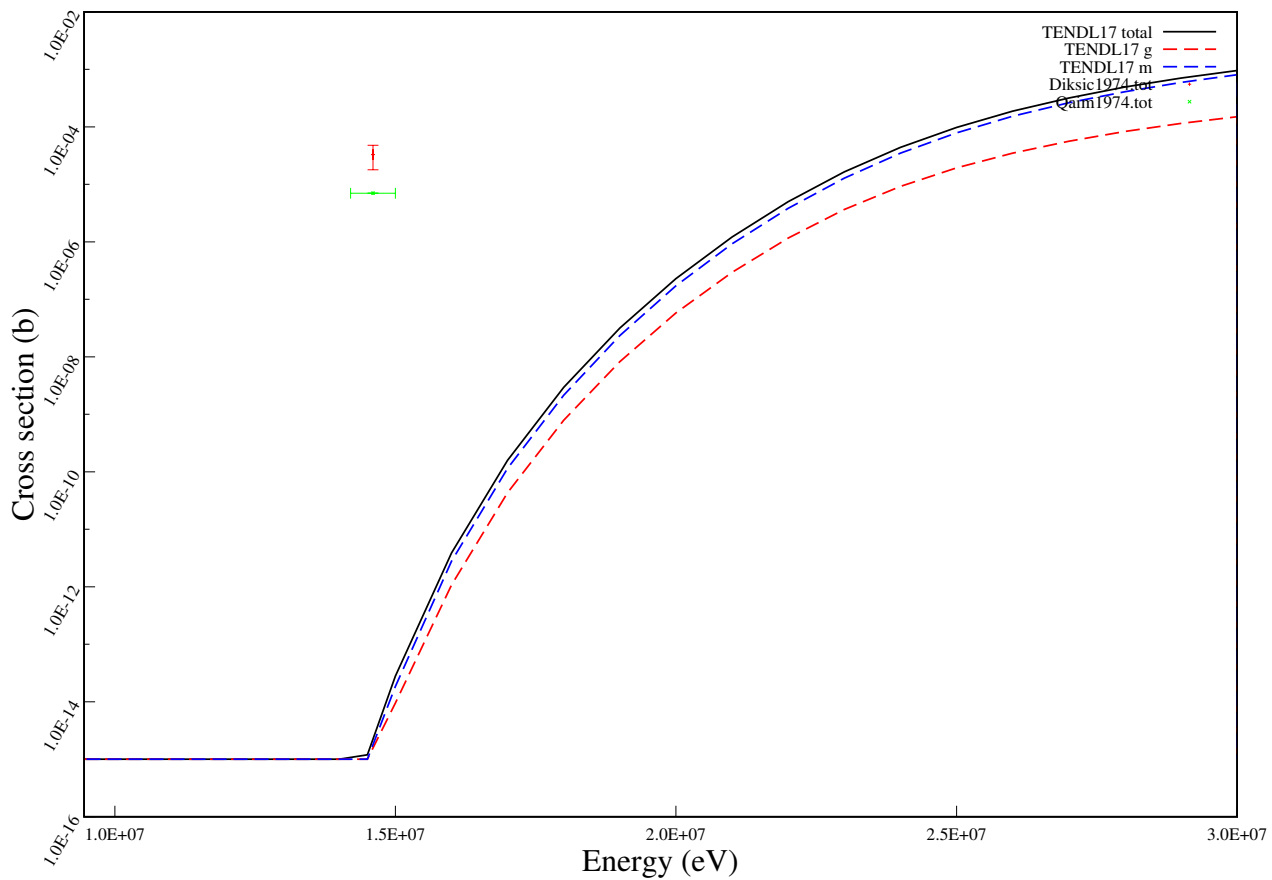
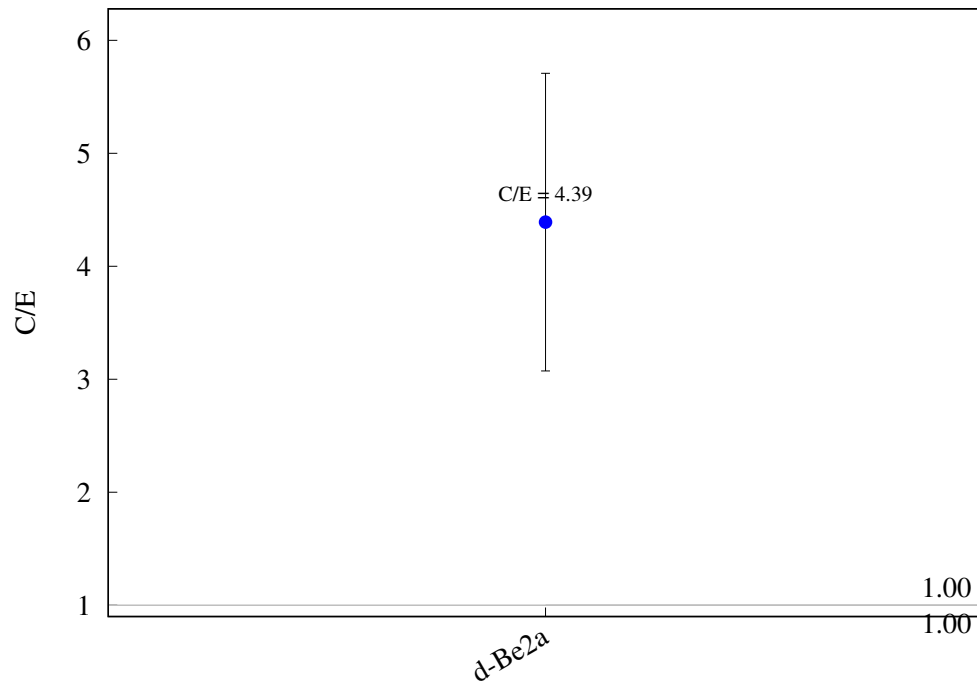
^{115}In (n,2n) ^{114}gIn 

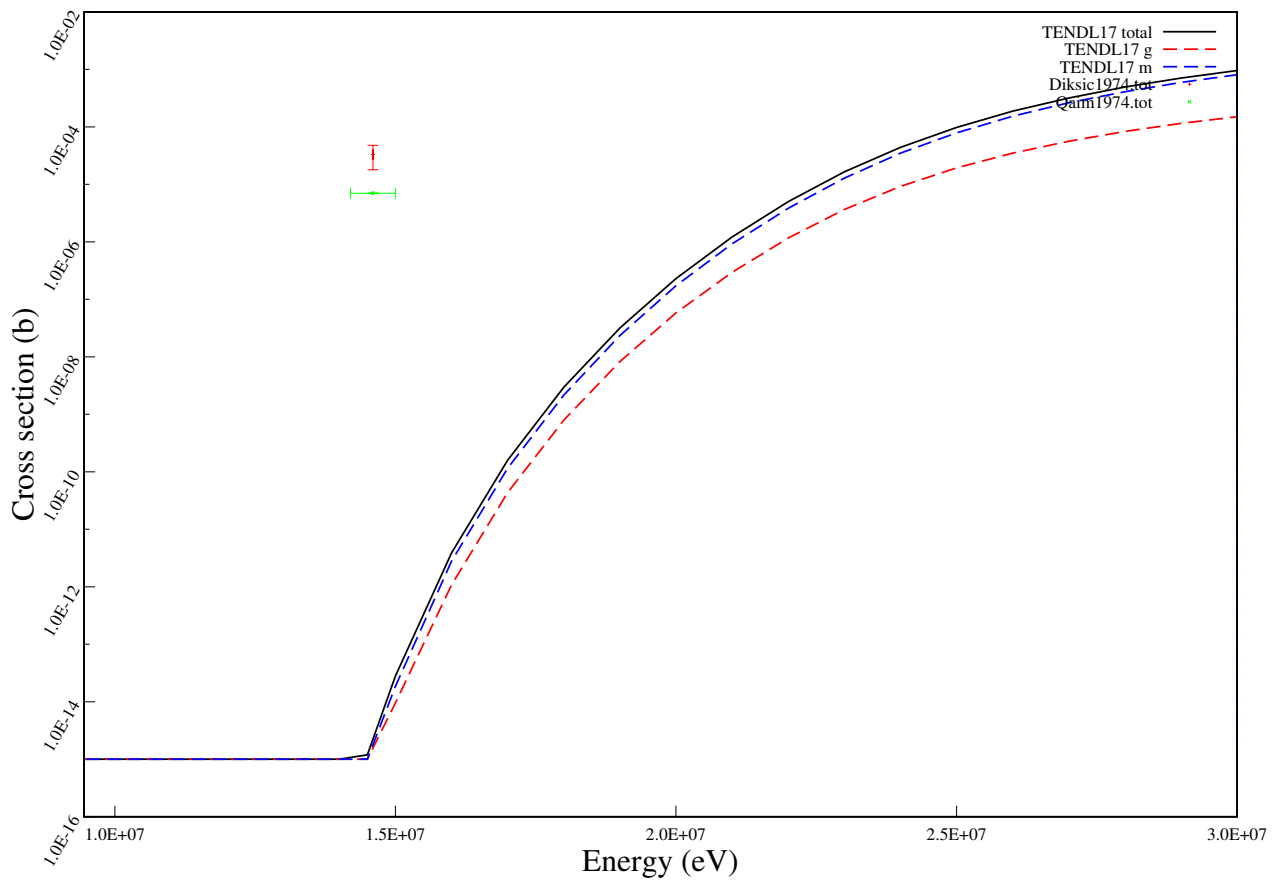
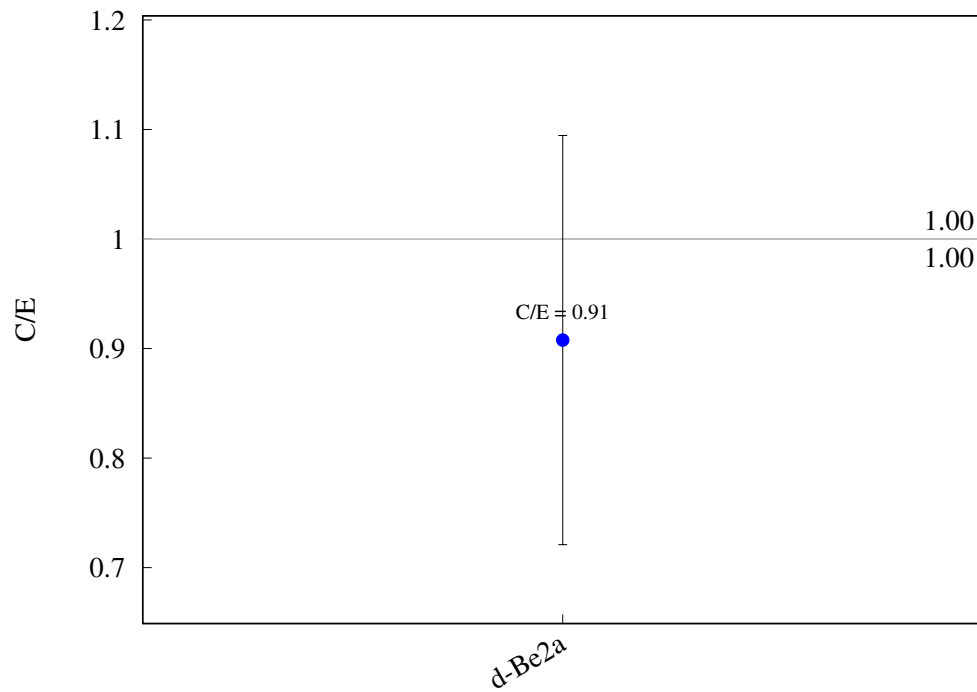
$^{115}\text{In} (\text{n},\text{na}) ^{111}\text{Ag}$ 

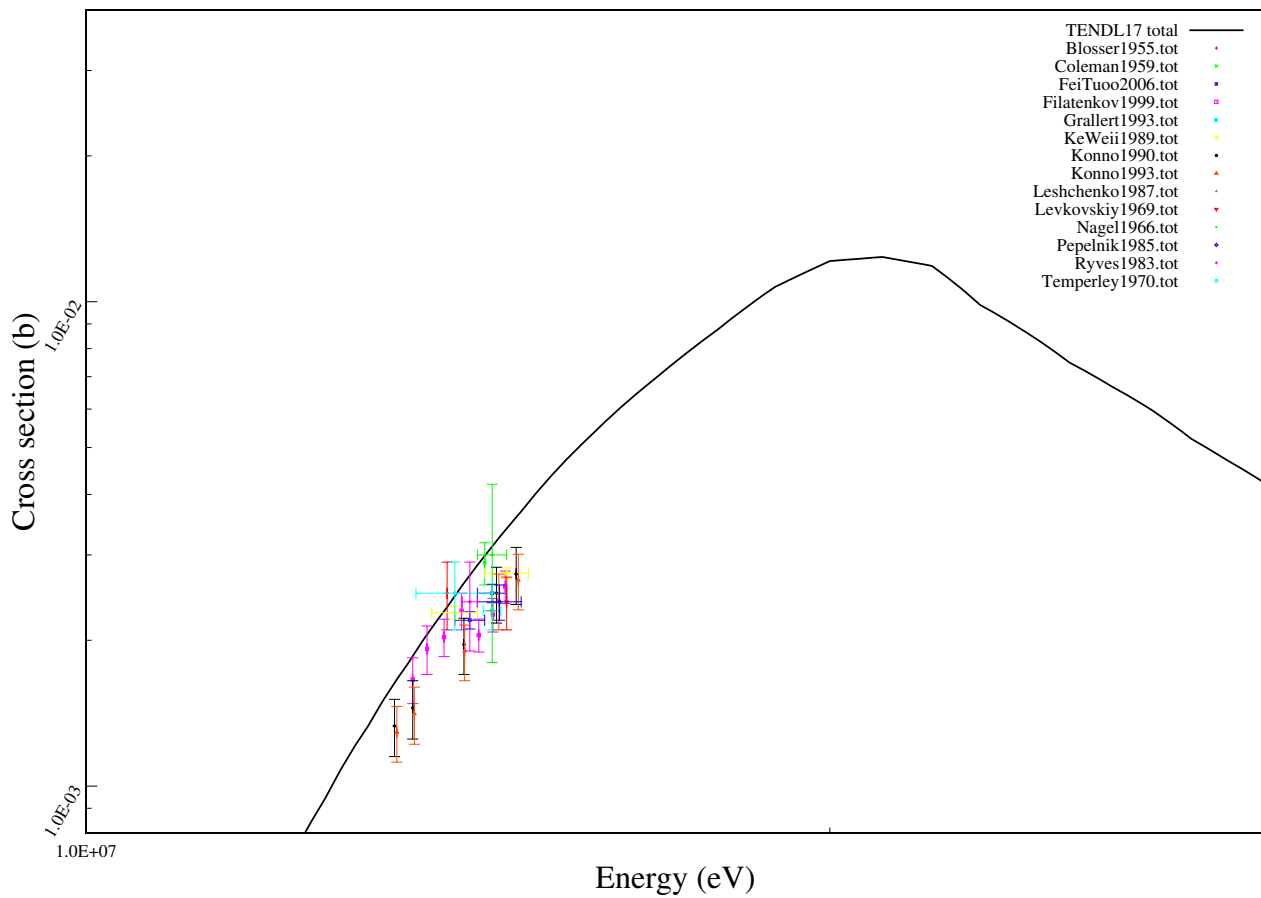
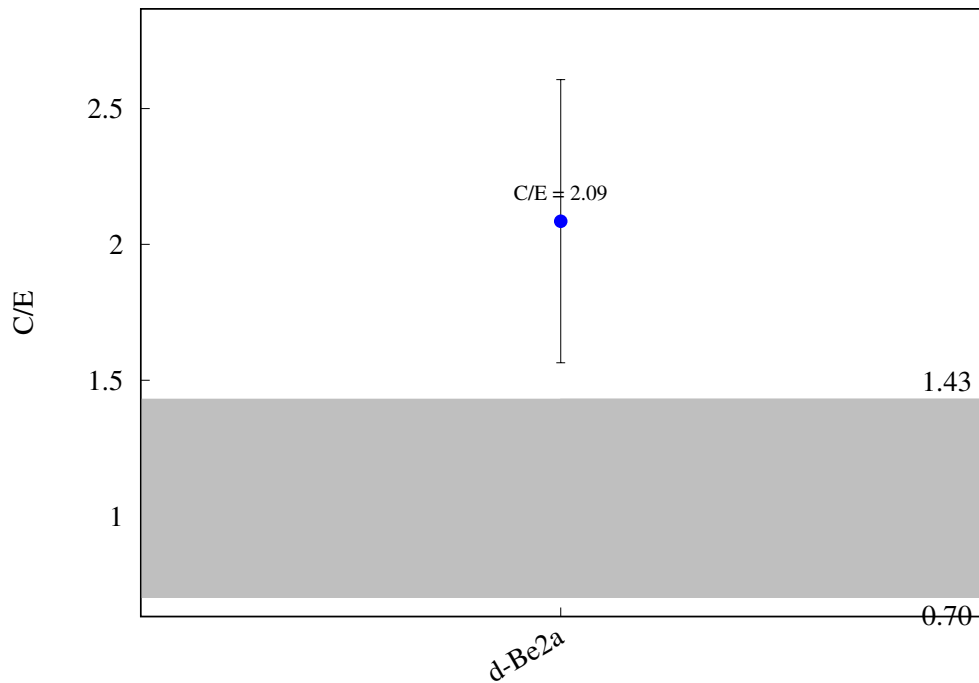
^{115}In (n,g) ^{116m}In 

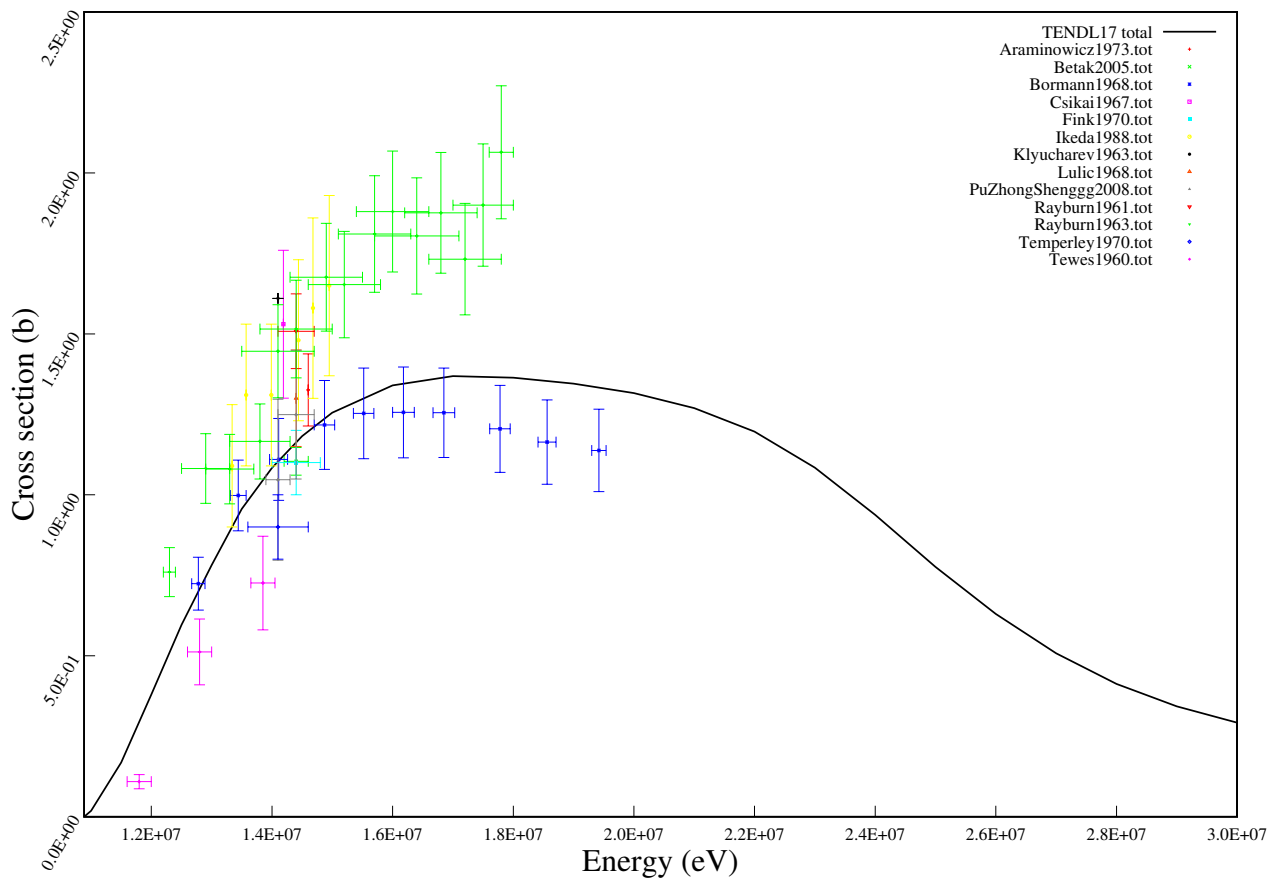
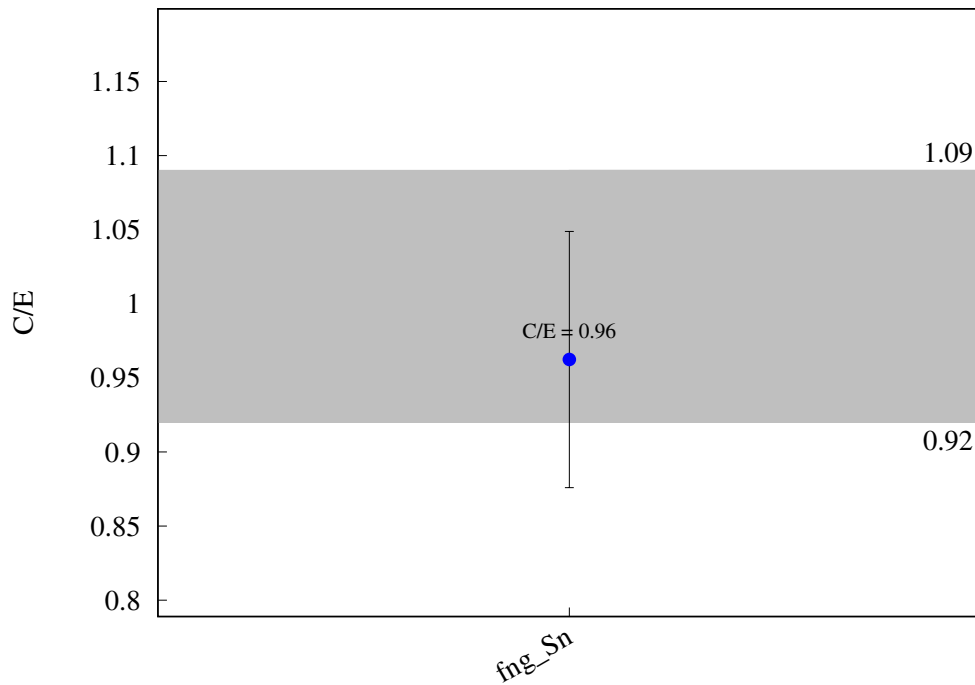
^{115}In (n,g) ^{116}In 

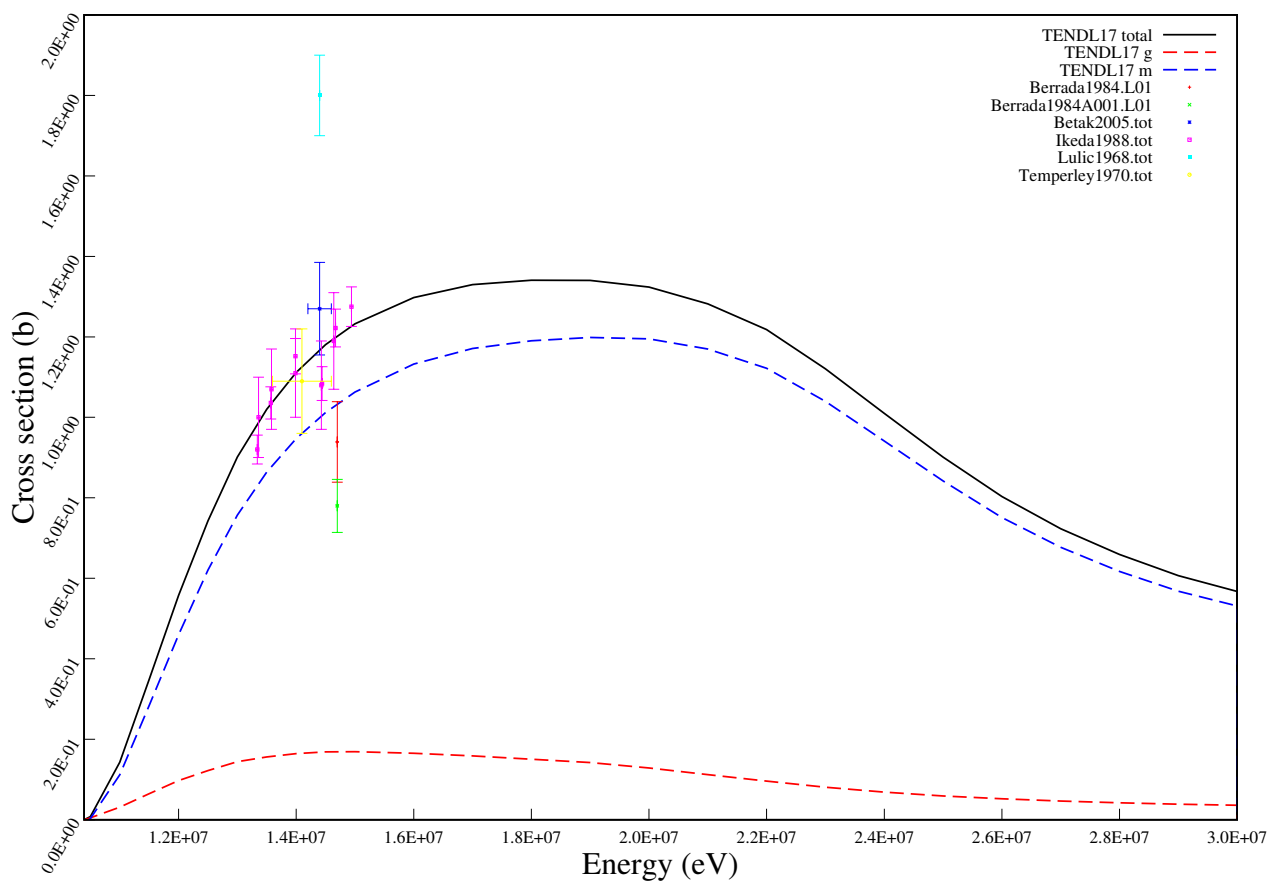
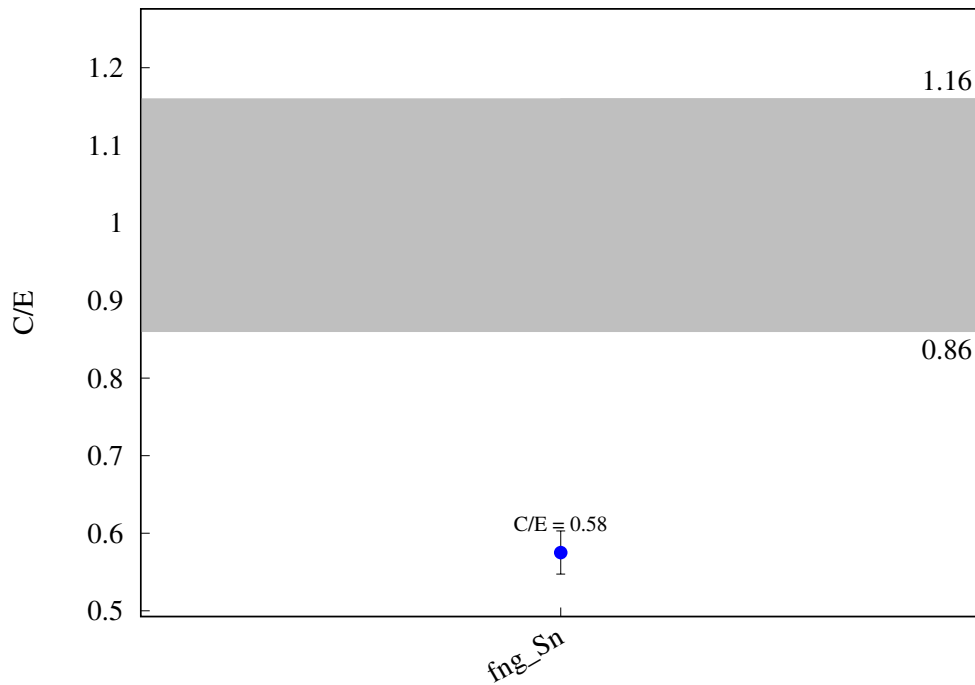
^{115}In (n,t) ^{113}Cd 

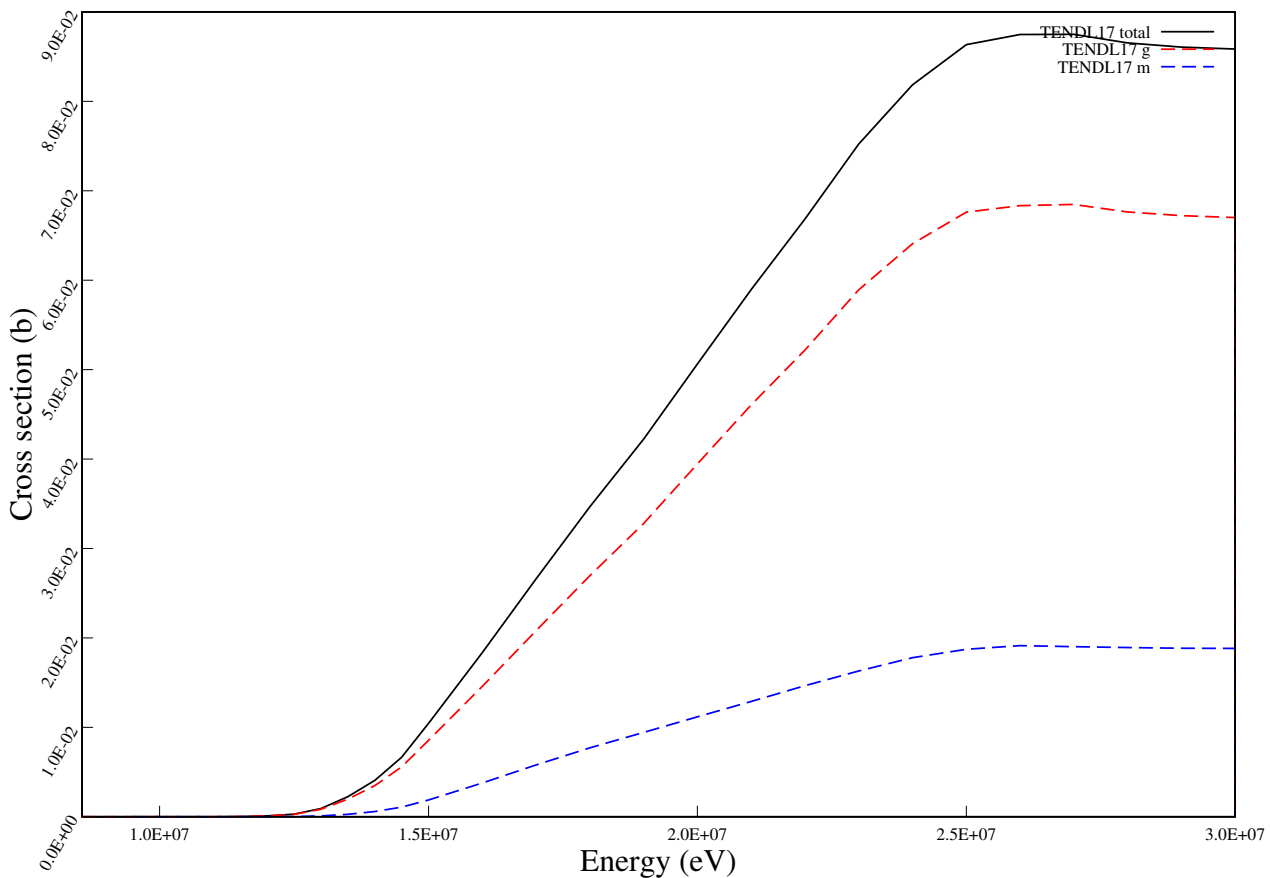
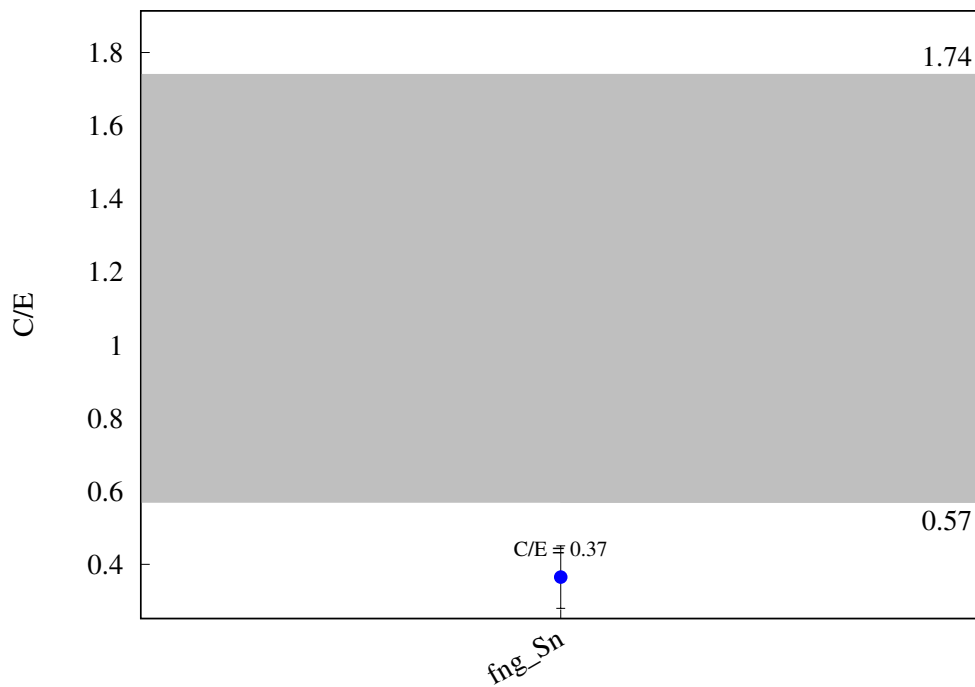
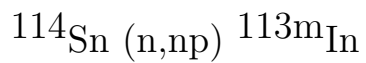
^{115}In (n,h) ^{113}gAg 

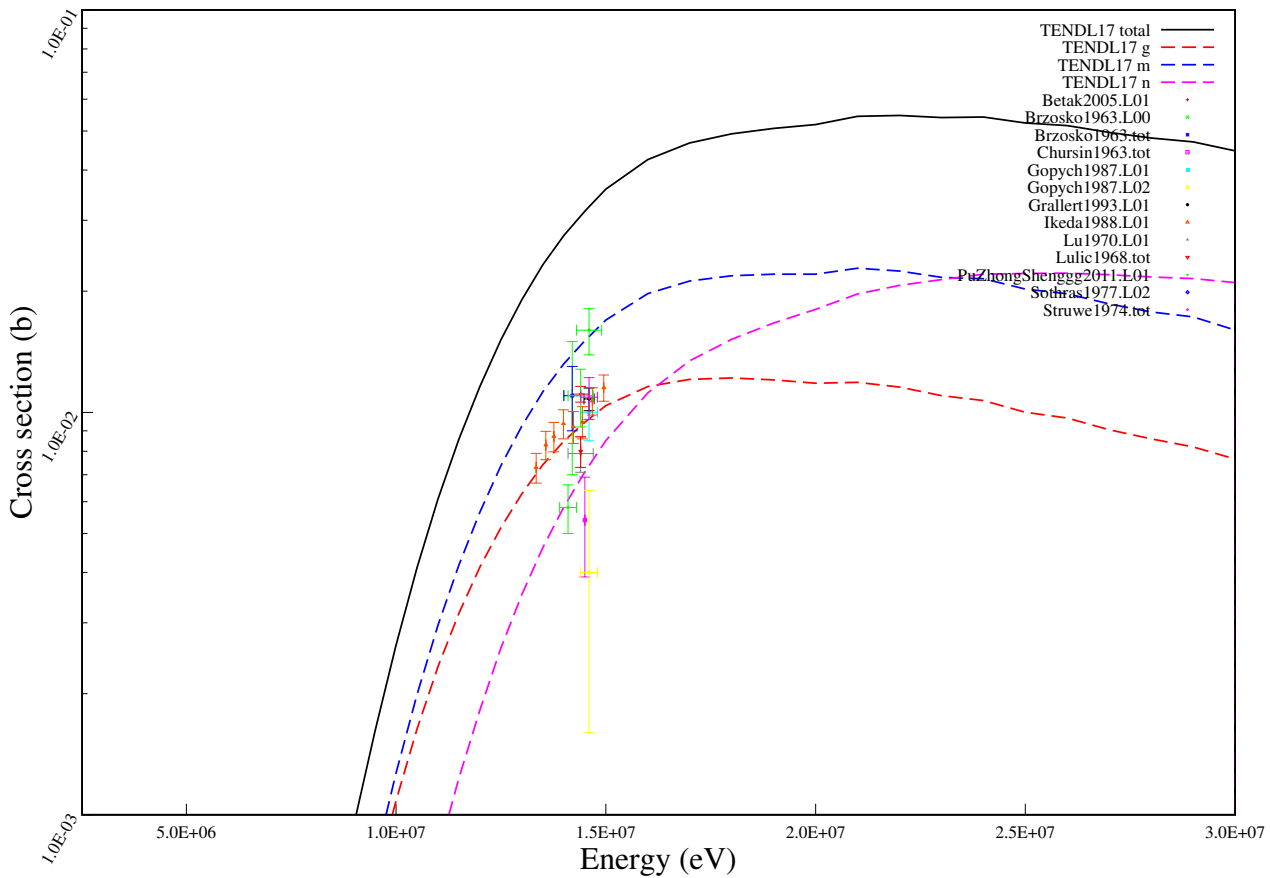
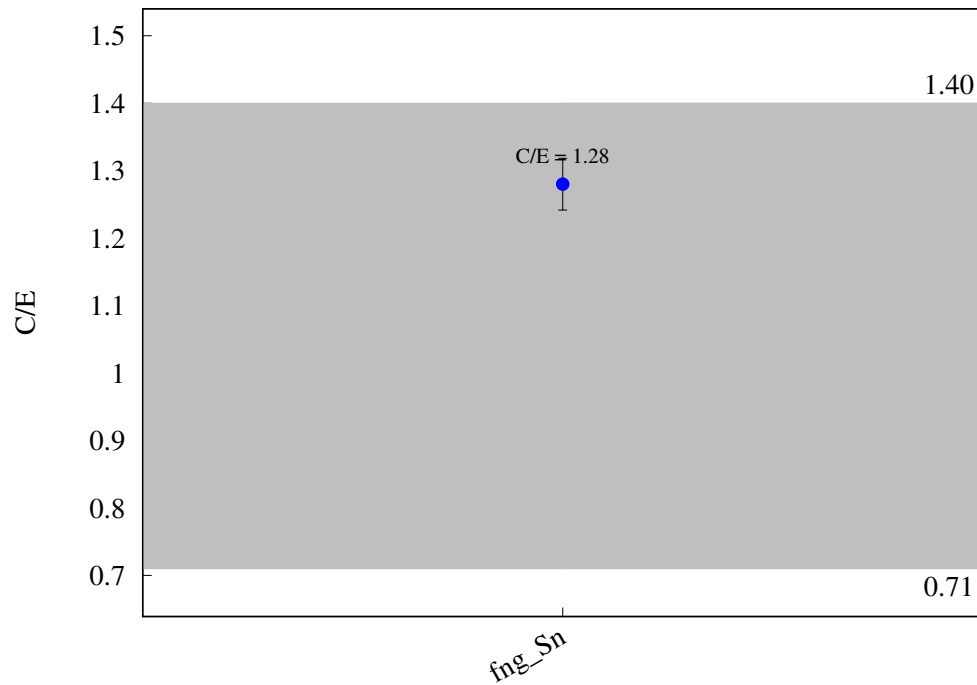
^{115}In (n,h) ^{113}Ag 

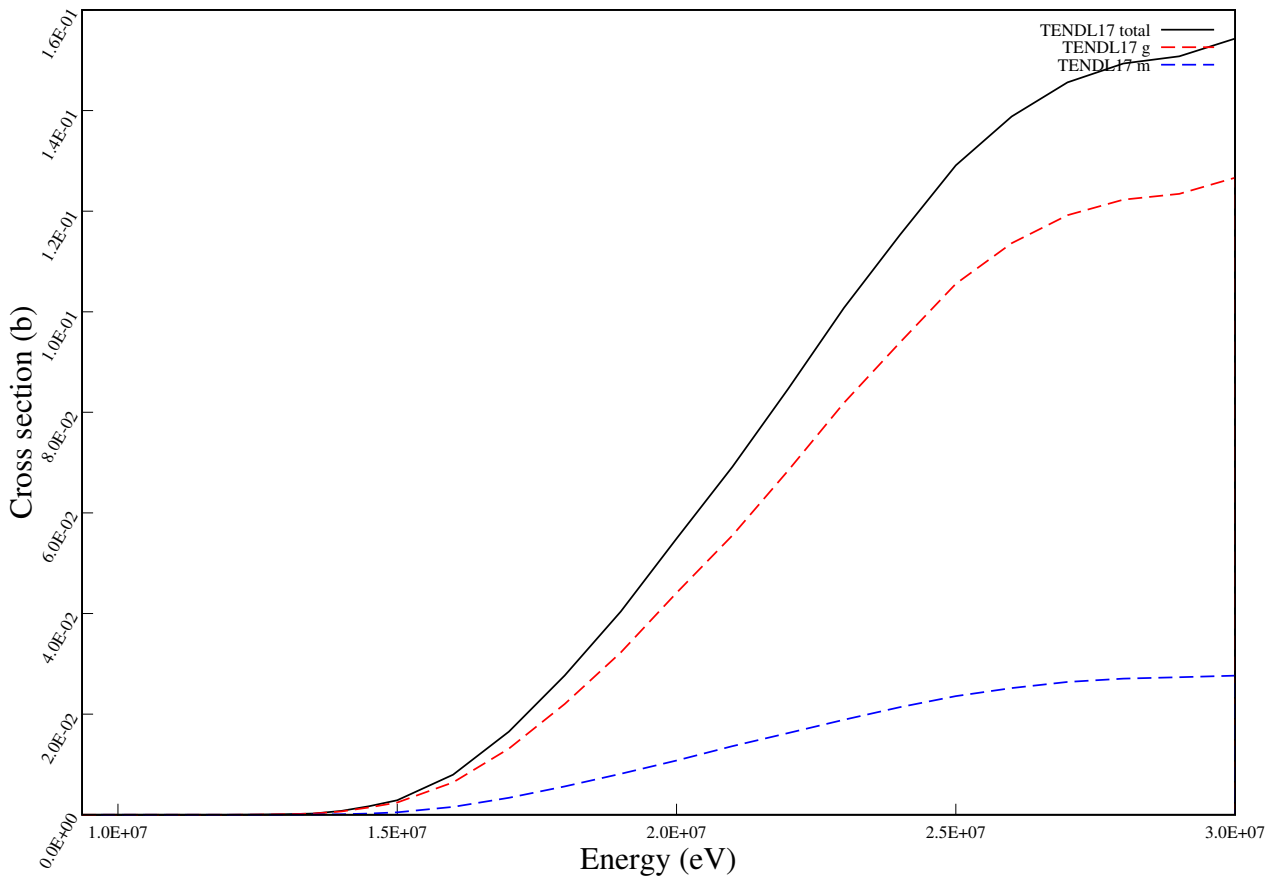
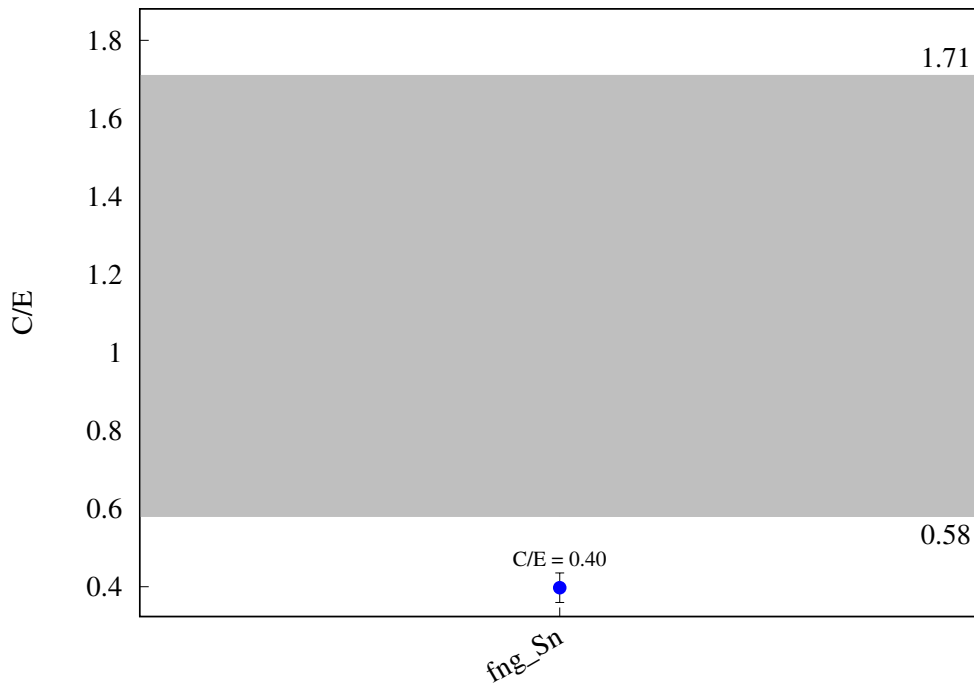
^{115}In (n,a) ^{112}Ag 

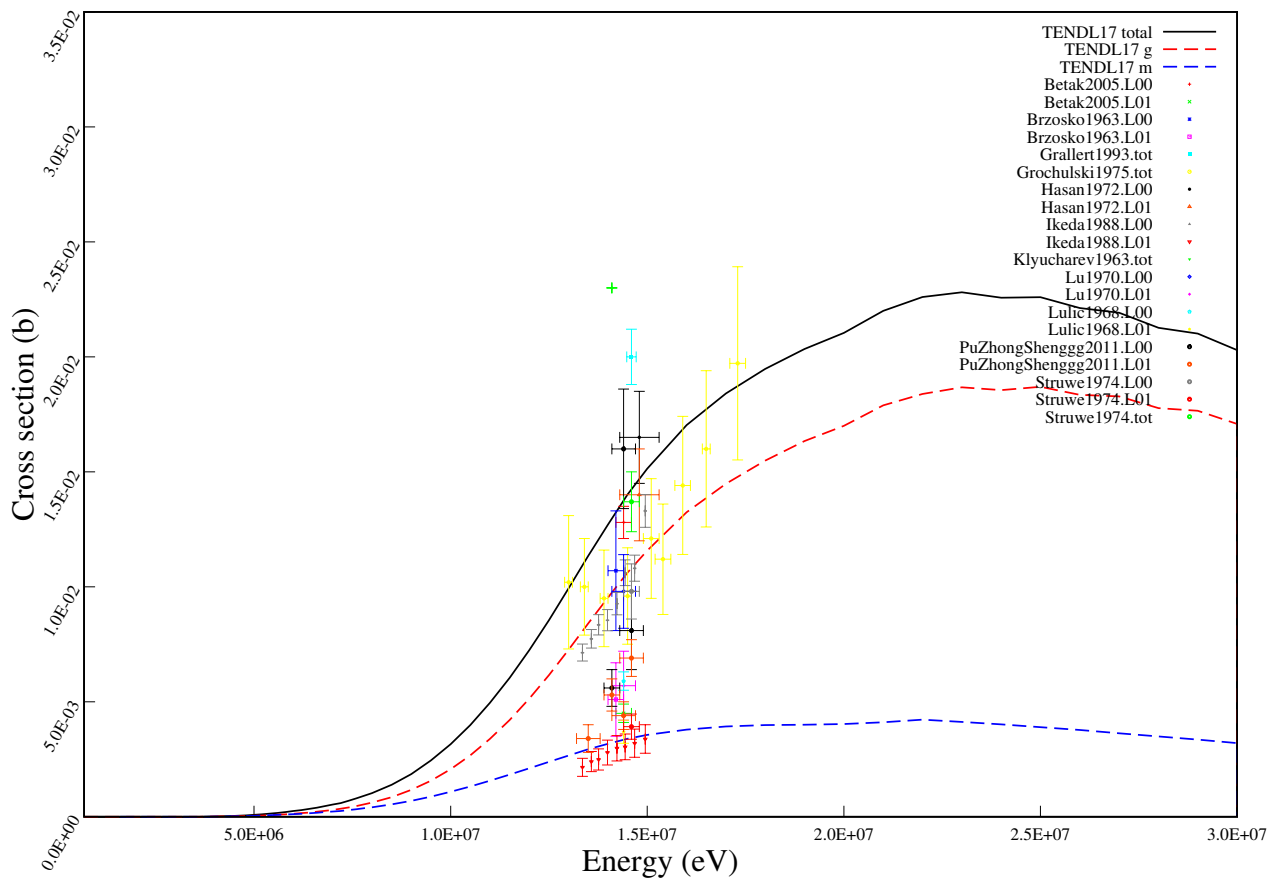
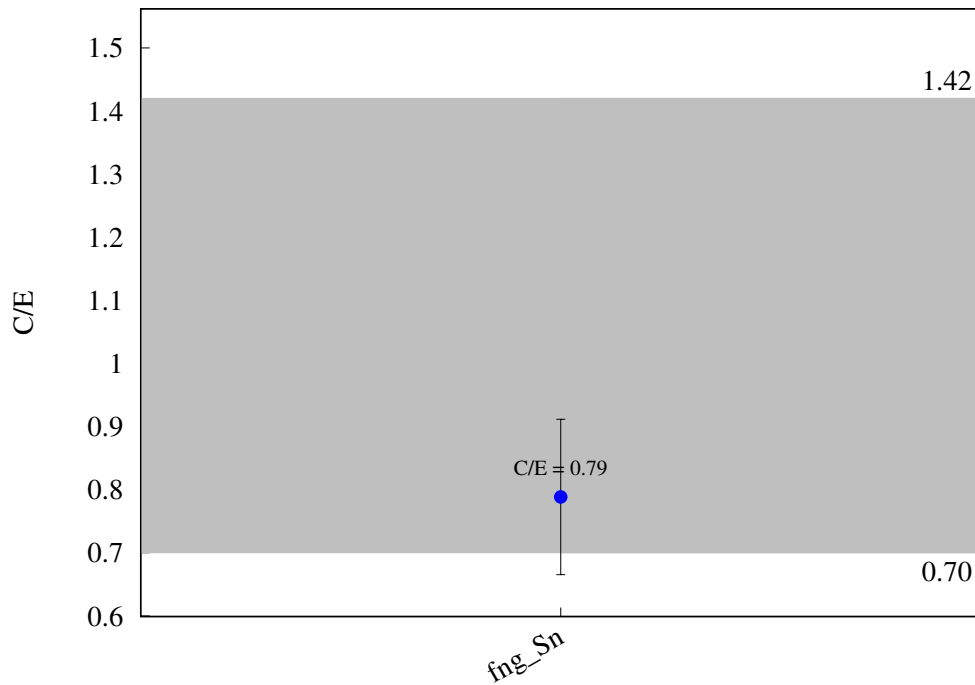


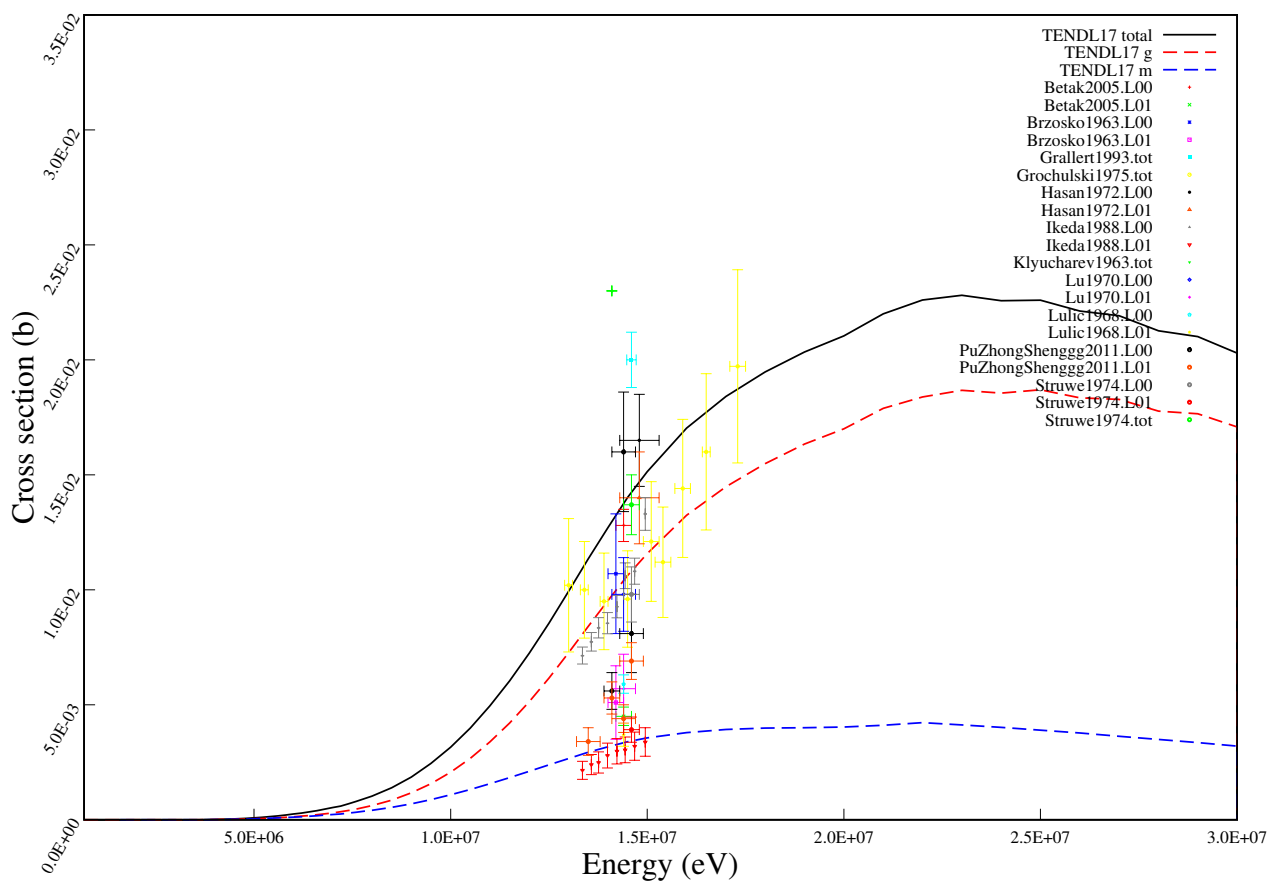
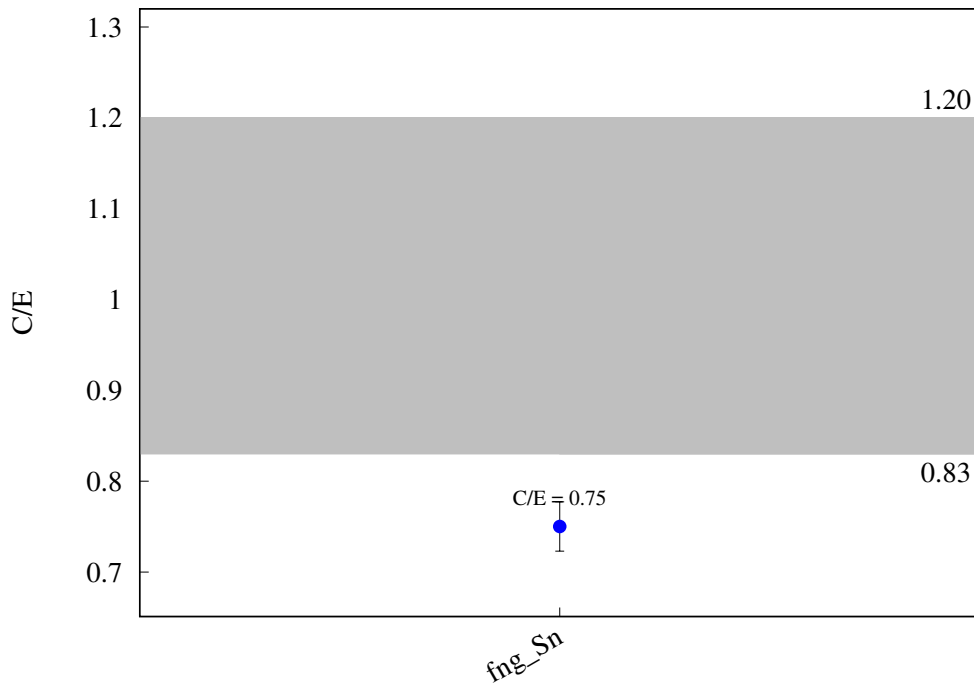


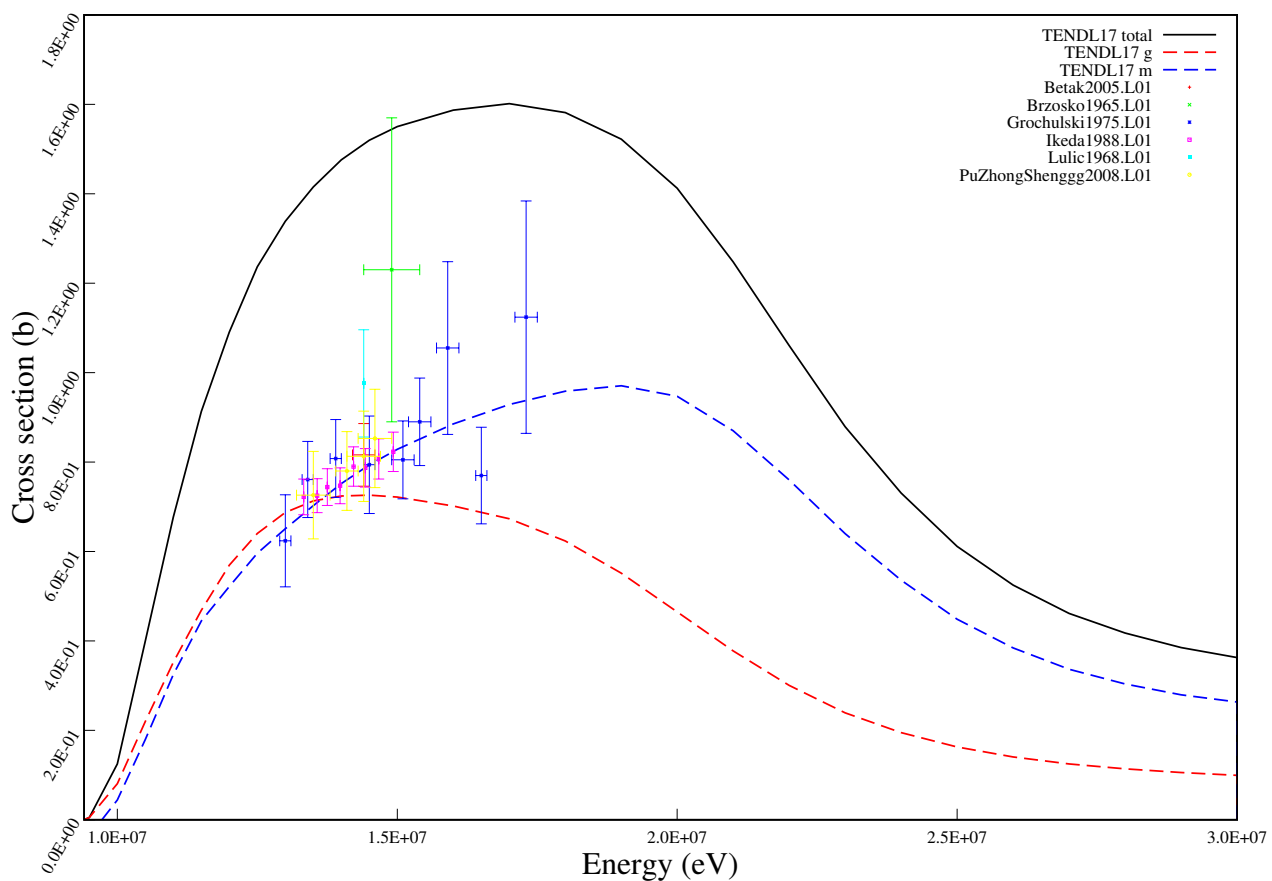
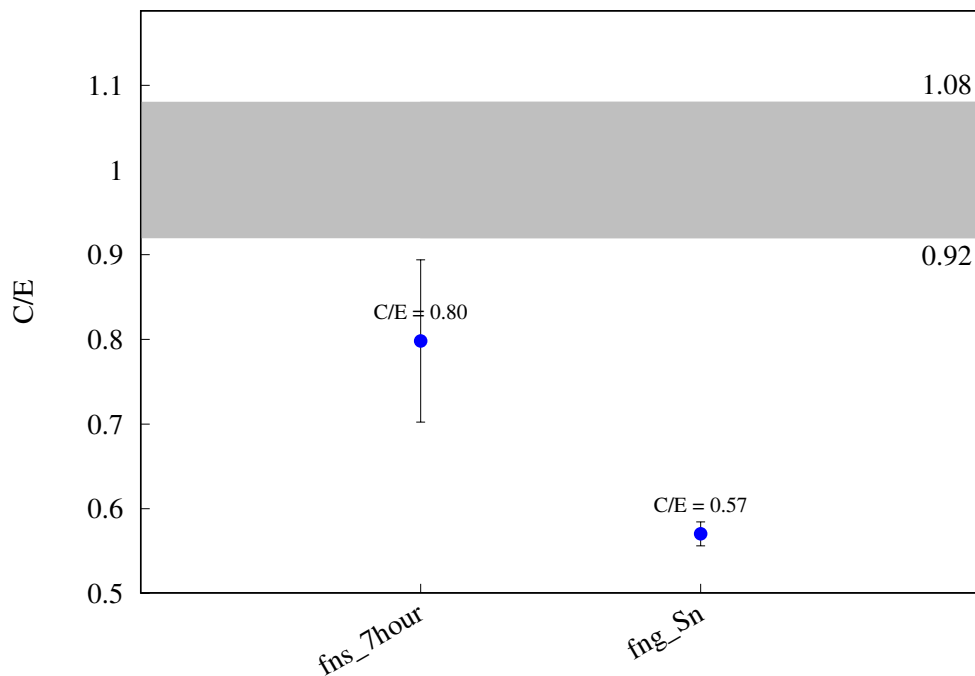


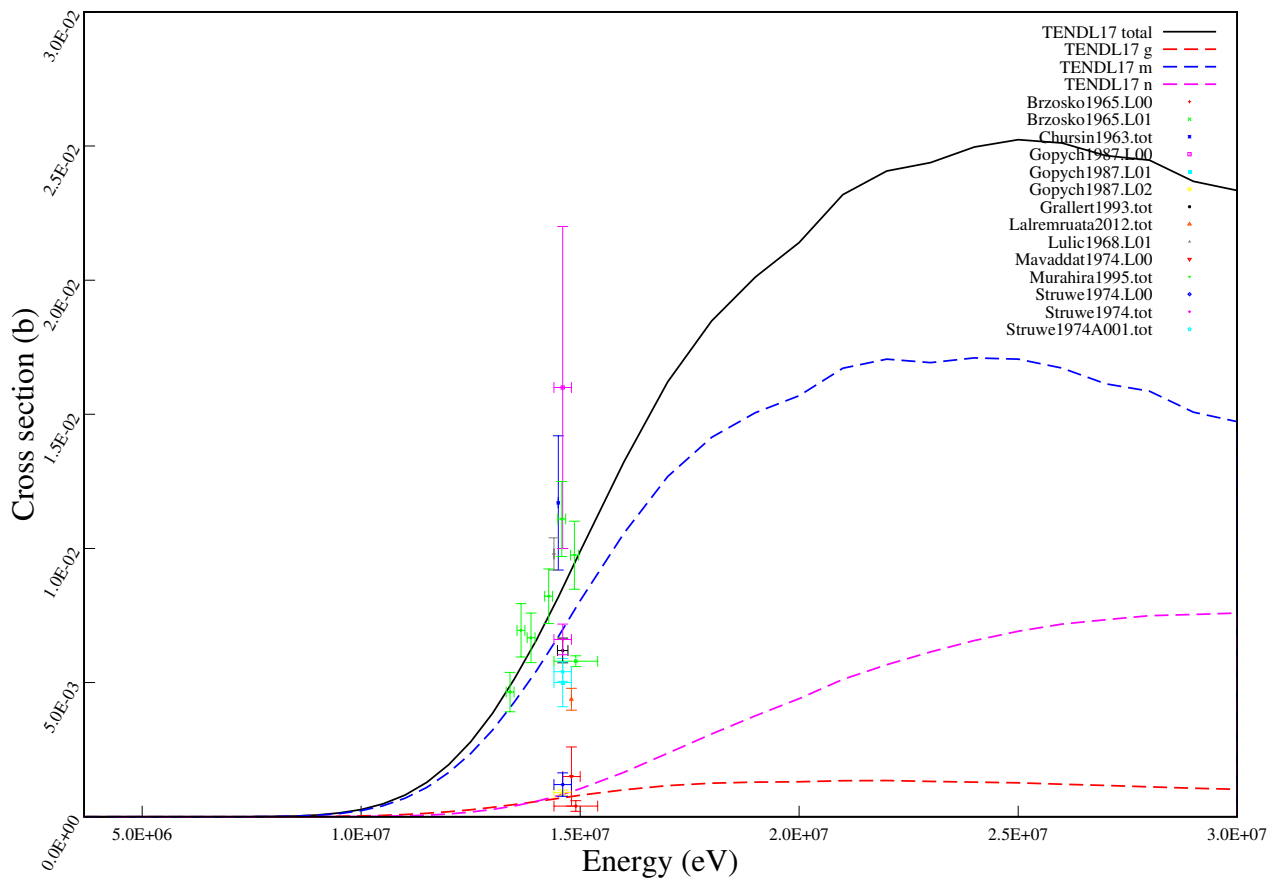
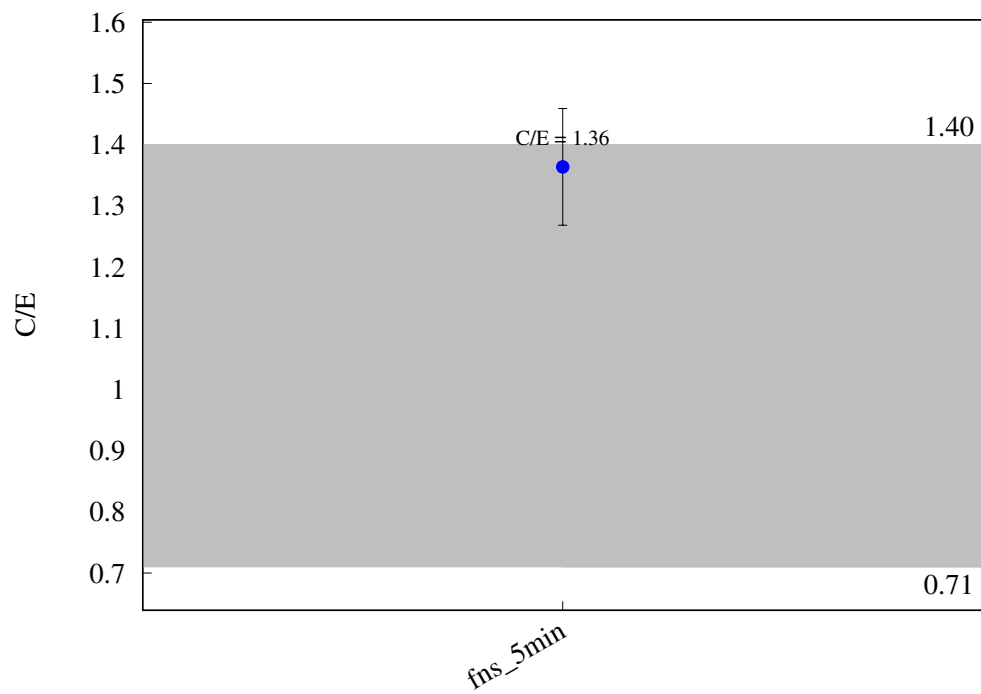
^{116}Sn (n,p) ^{116}In 

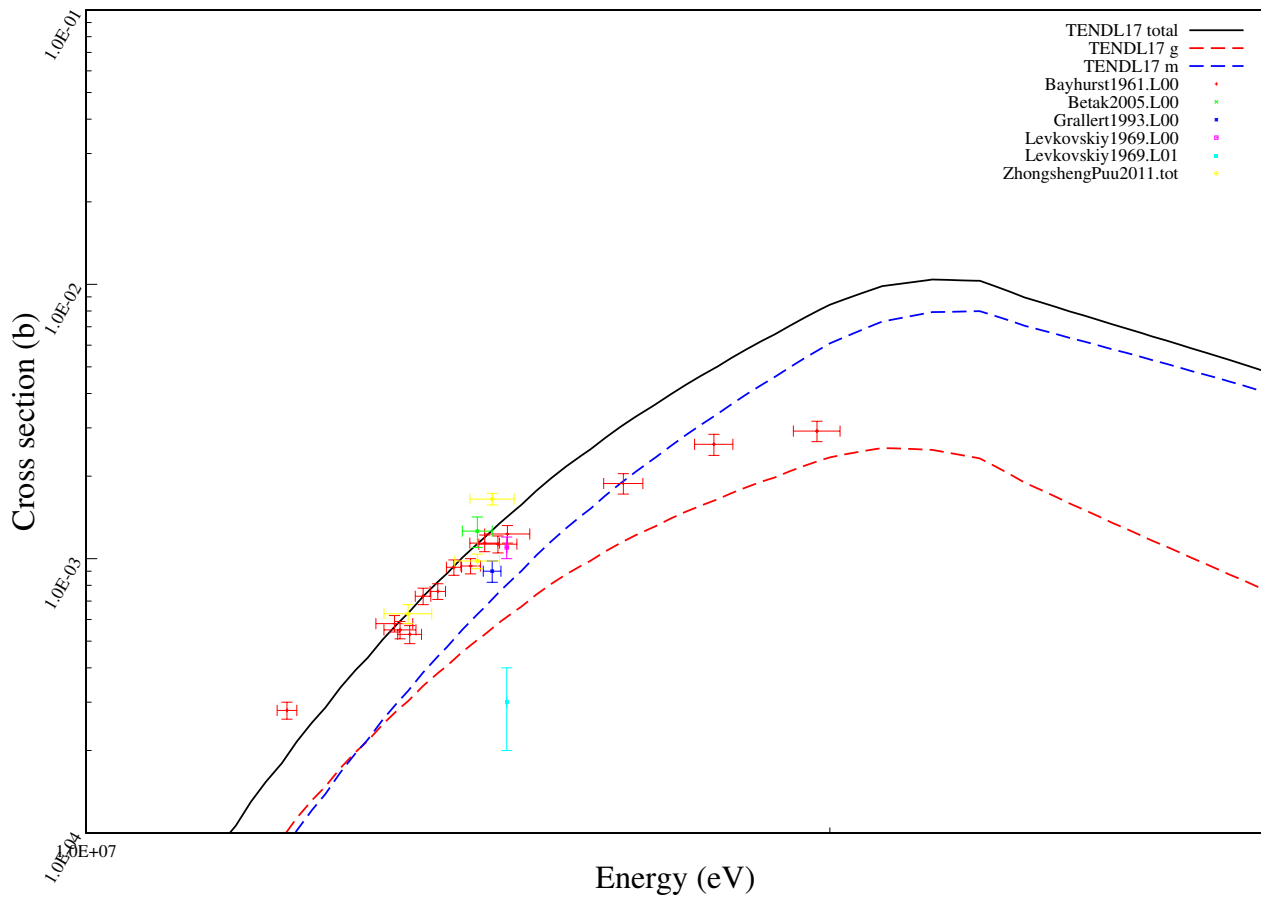
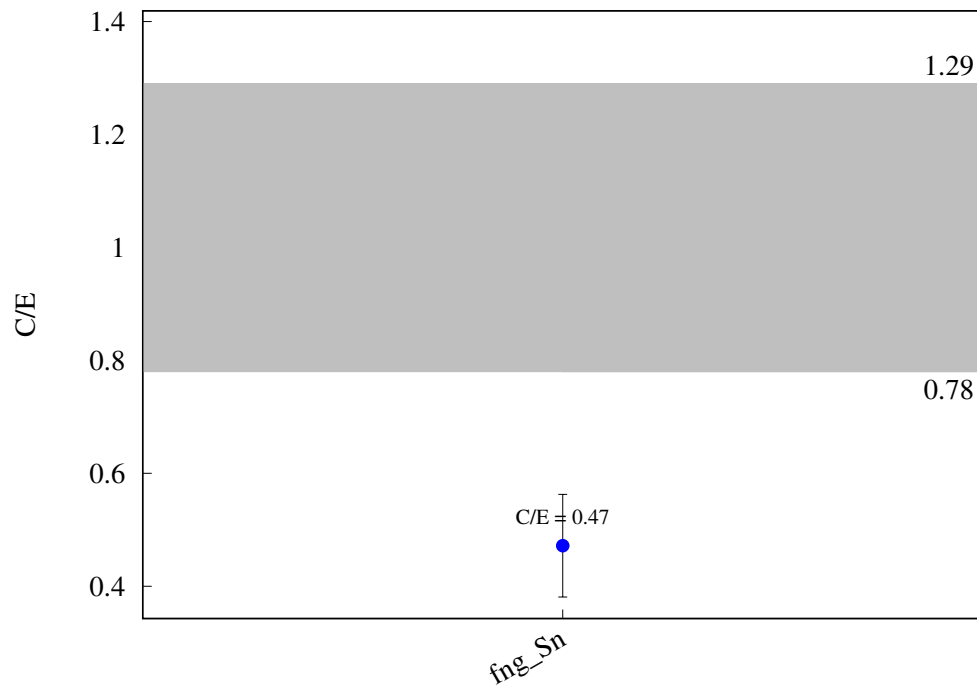
^{116}Sn (n,np) ^{115m}In 

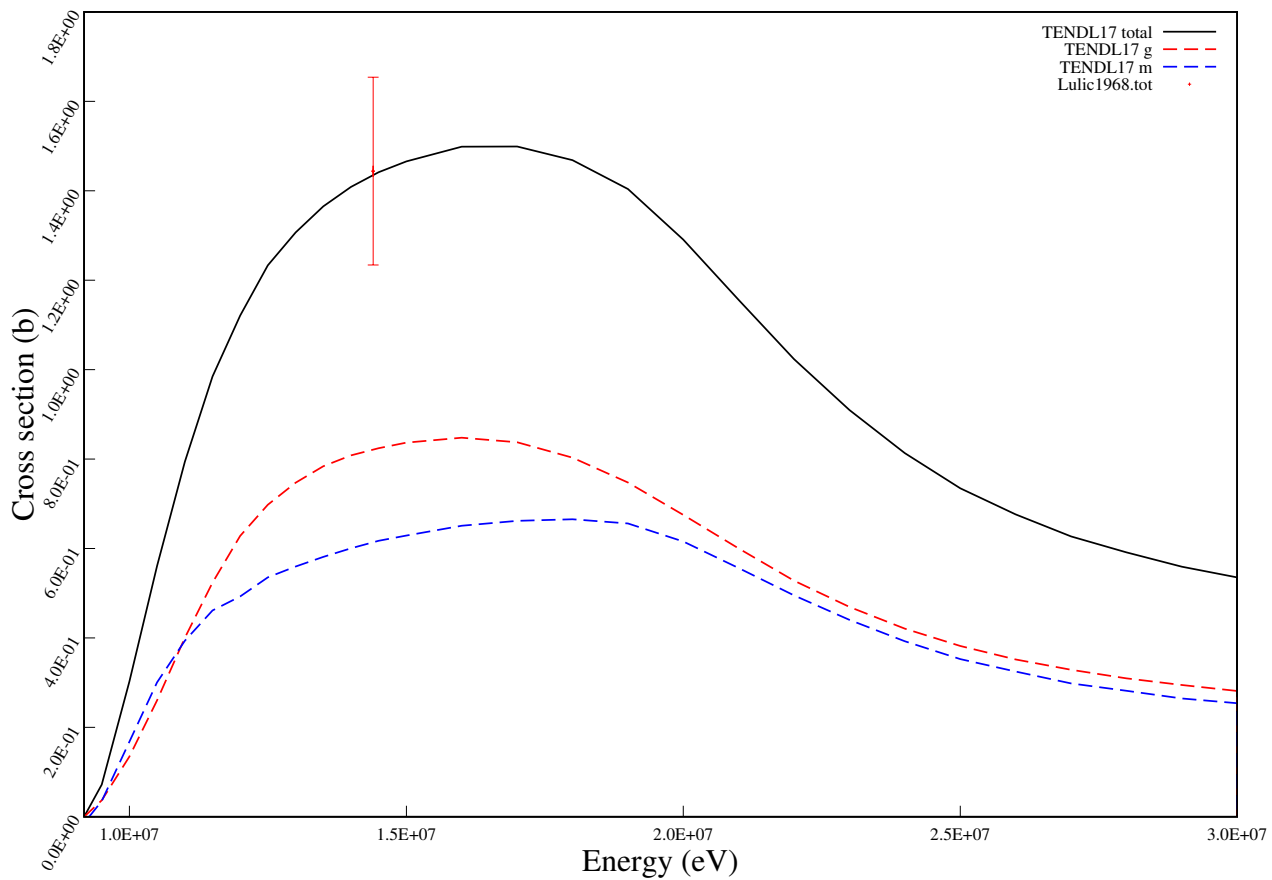
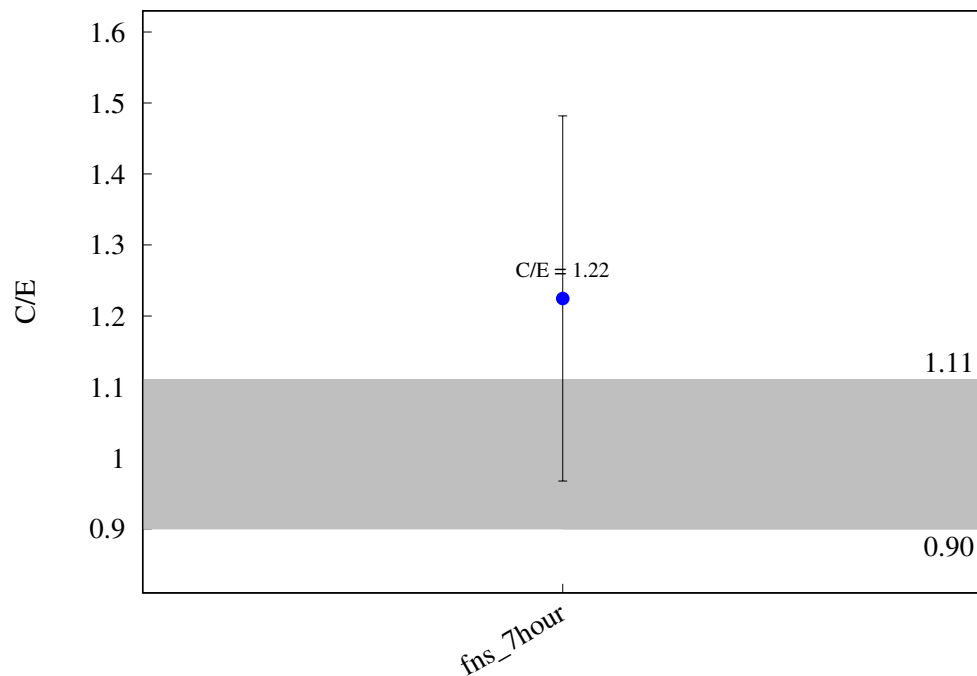
^{117}Sn (n,p) $^{117\text{m}}\text{In}$ 

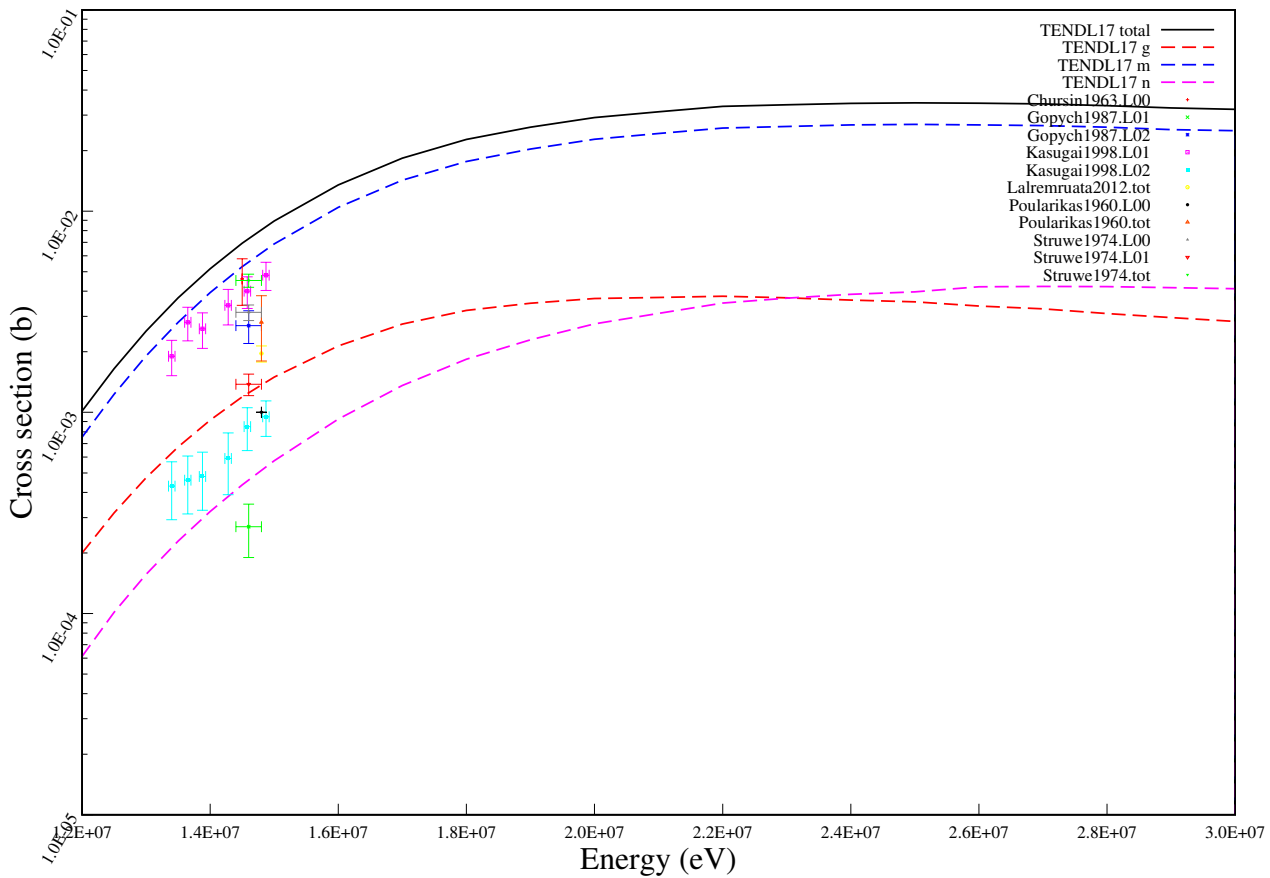
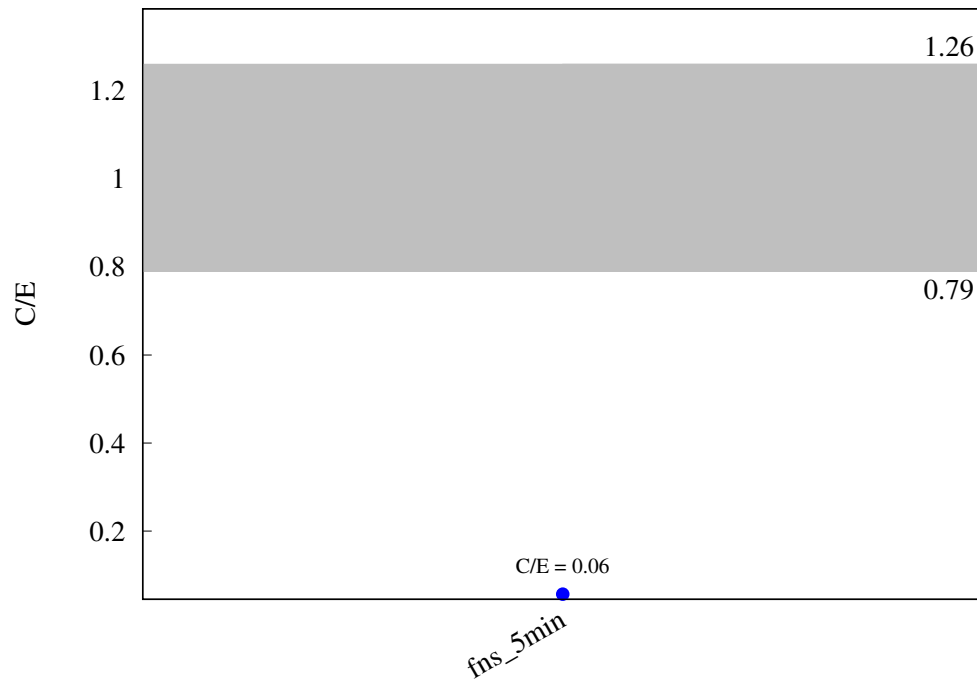
^{117}Sn (n,p) ^{117}In 

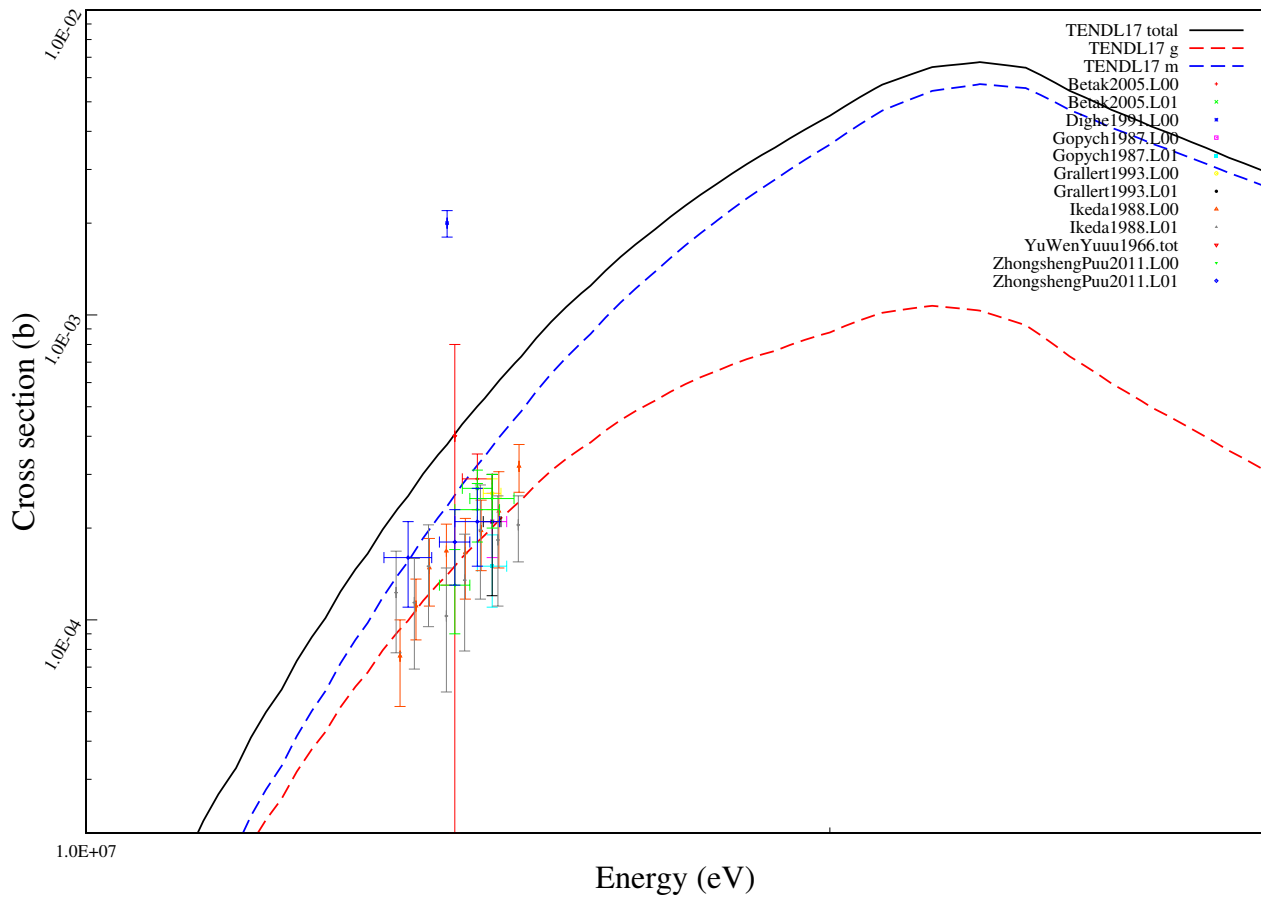
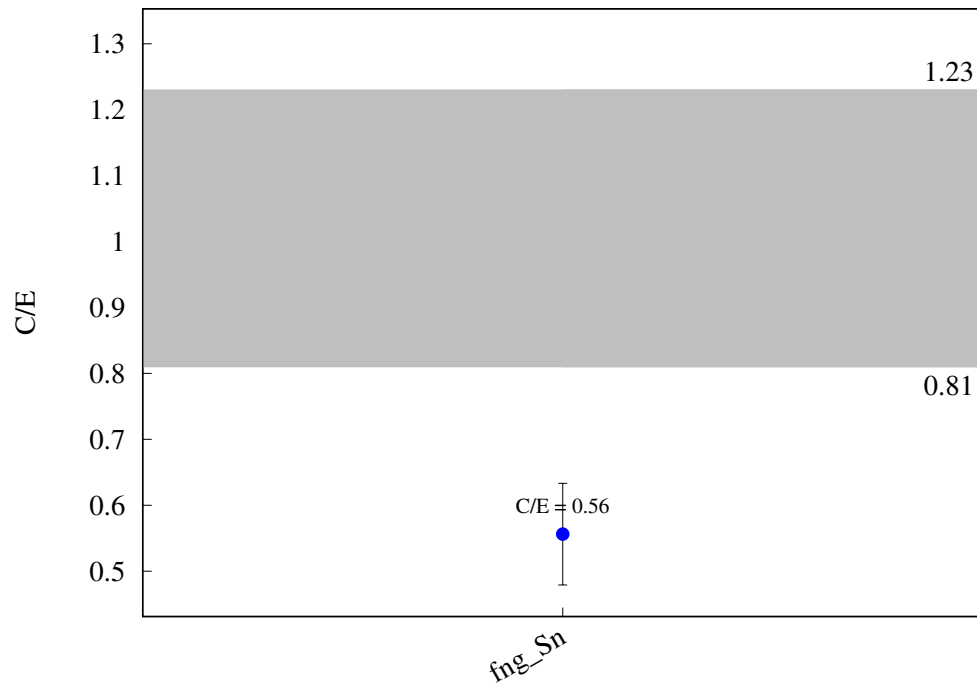
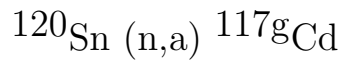
^{118}Sn ($n,2n$) ^{117m}Sn 

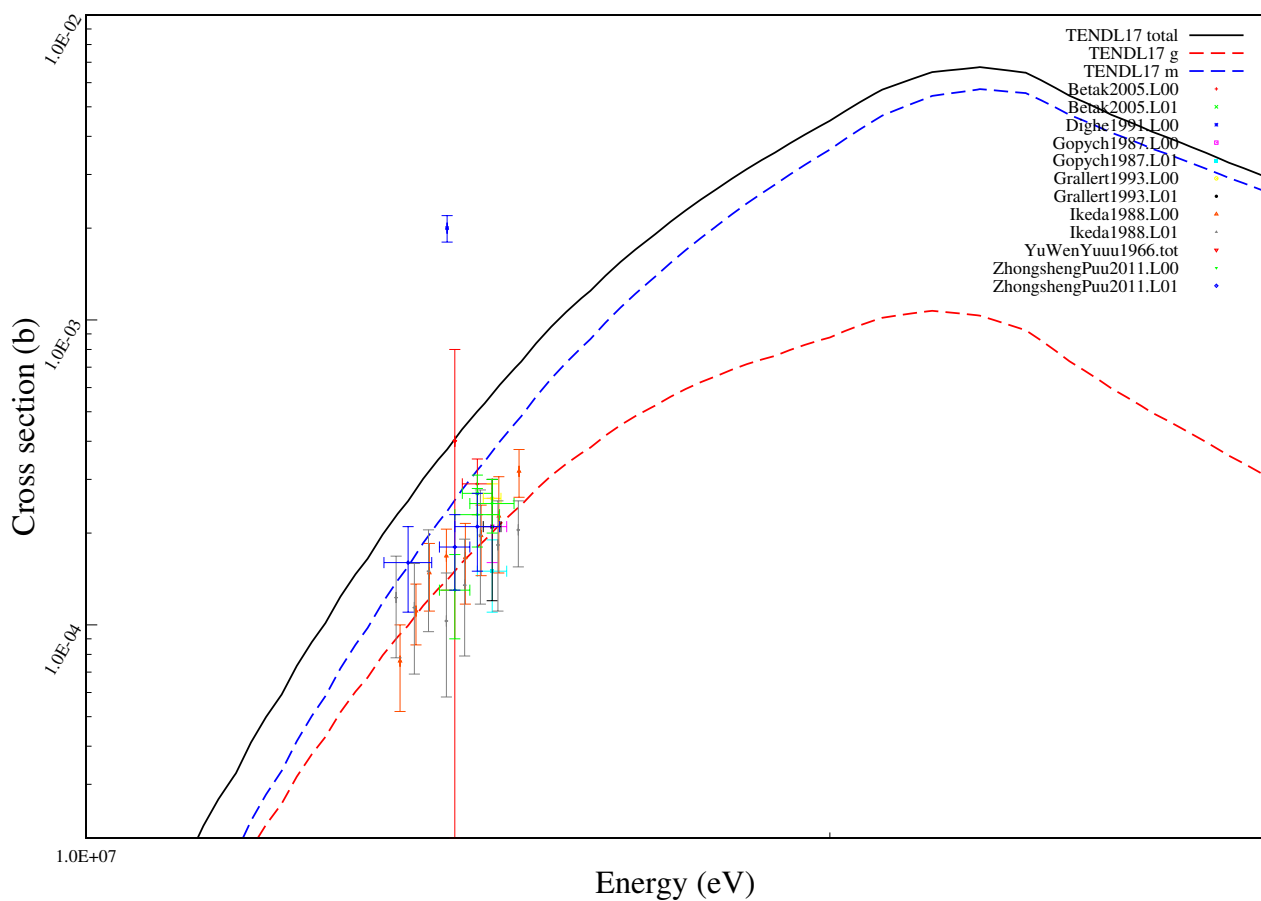
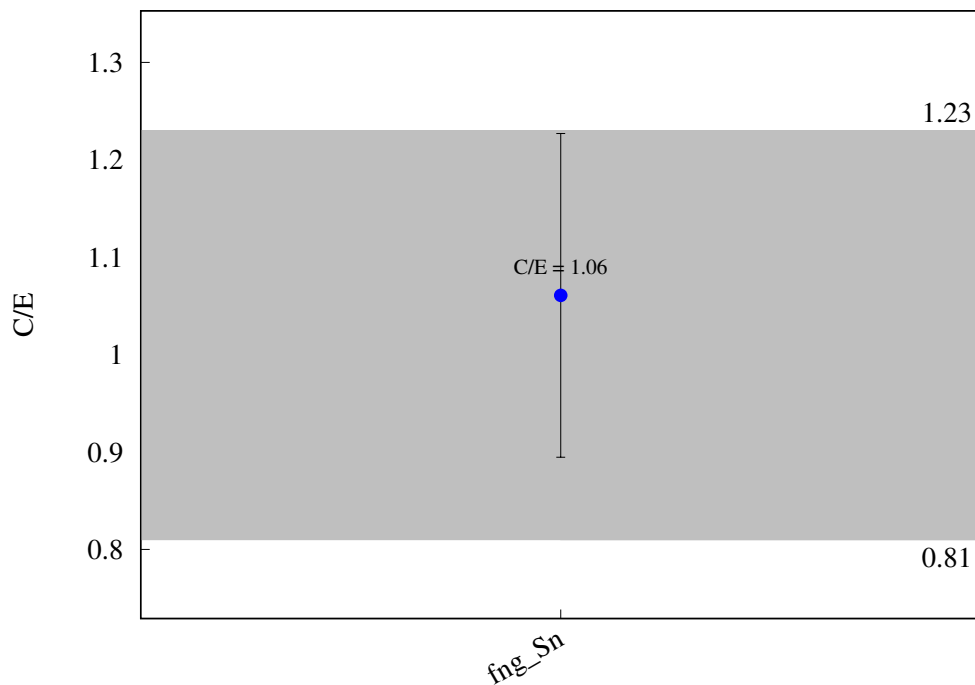
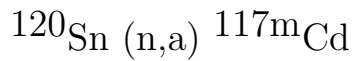
^{118}Sn (n,p) $^{118\text{m}}\text{In}$ 

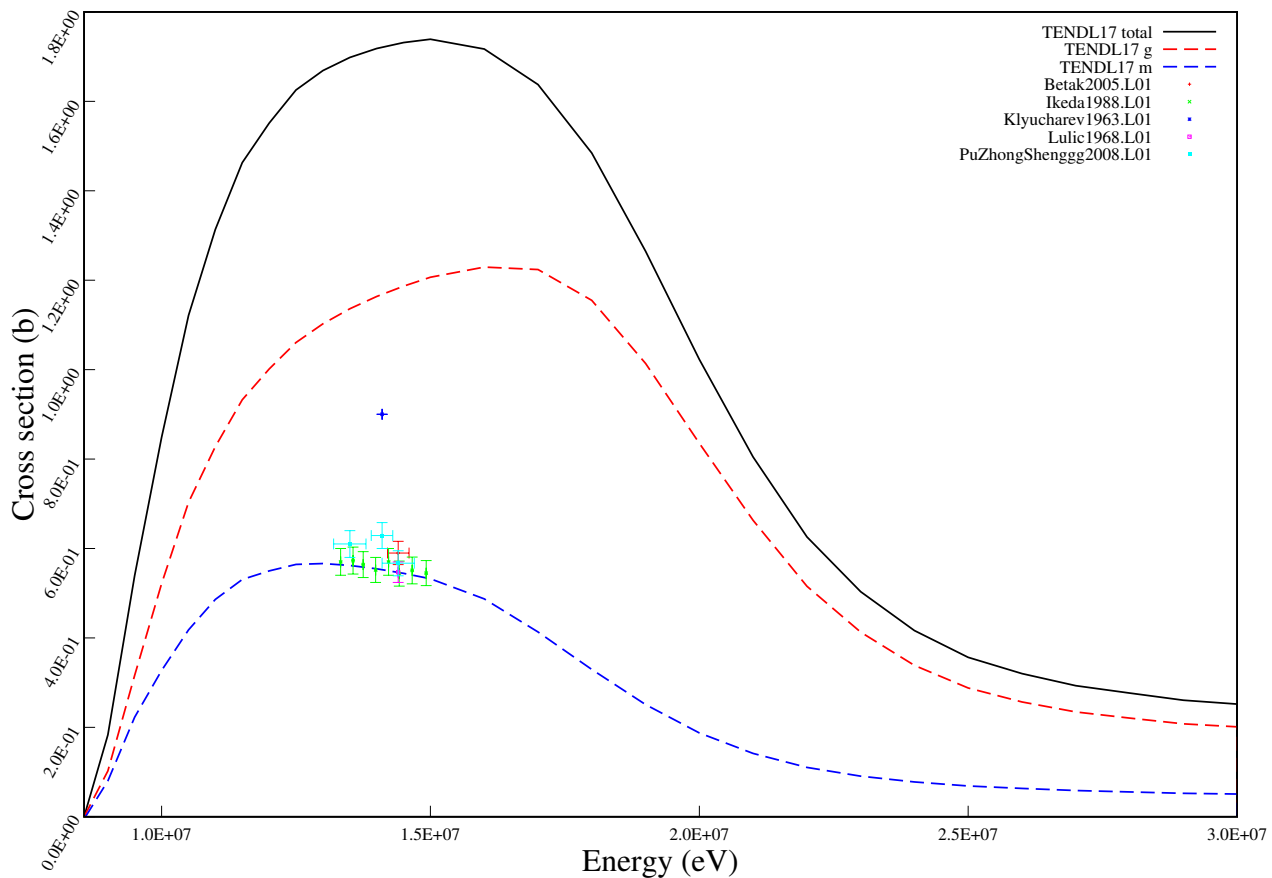
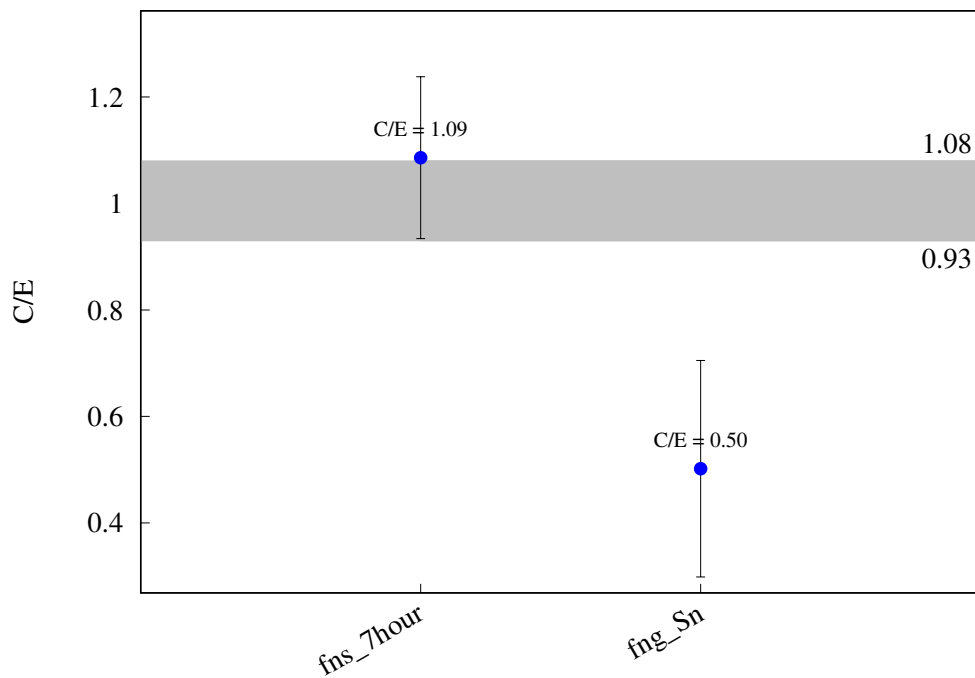
^{118}Sn (n,a) ^{115}gCd 

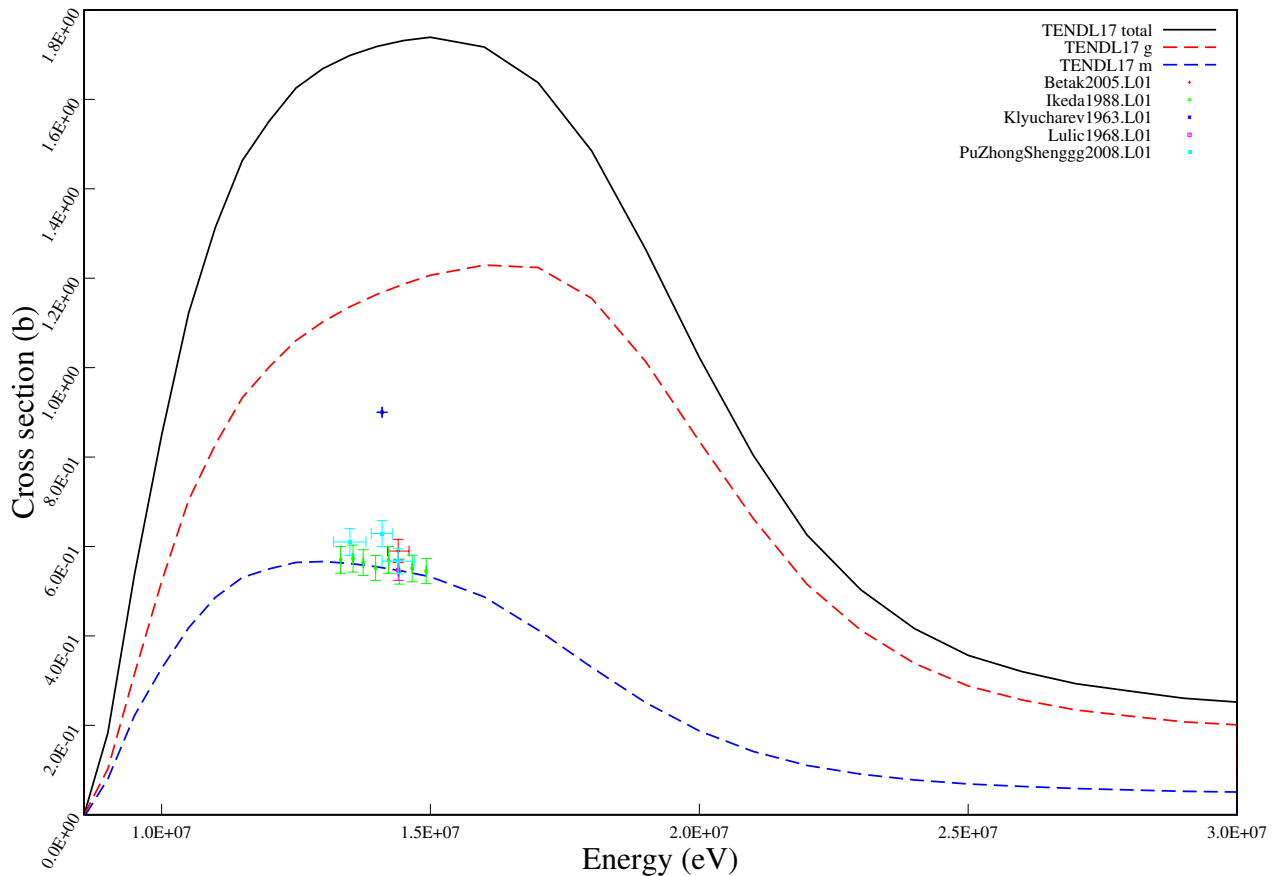
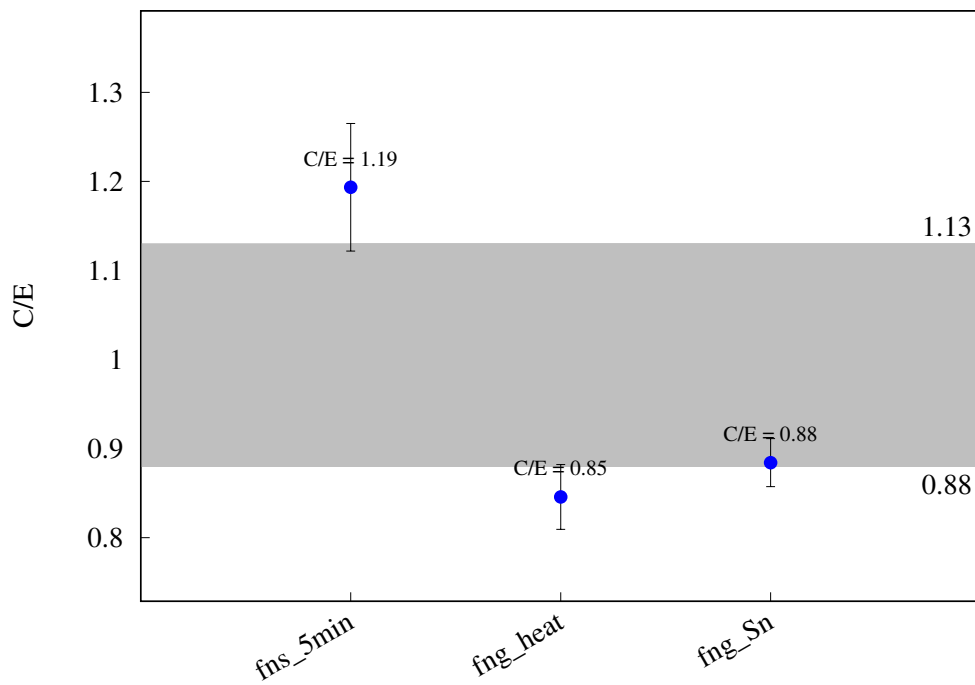
^{120}Sn ($n,2n$) ^{119m}Sn 

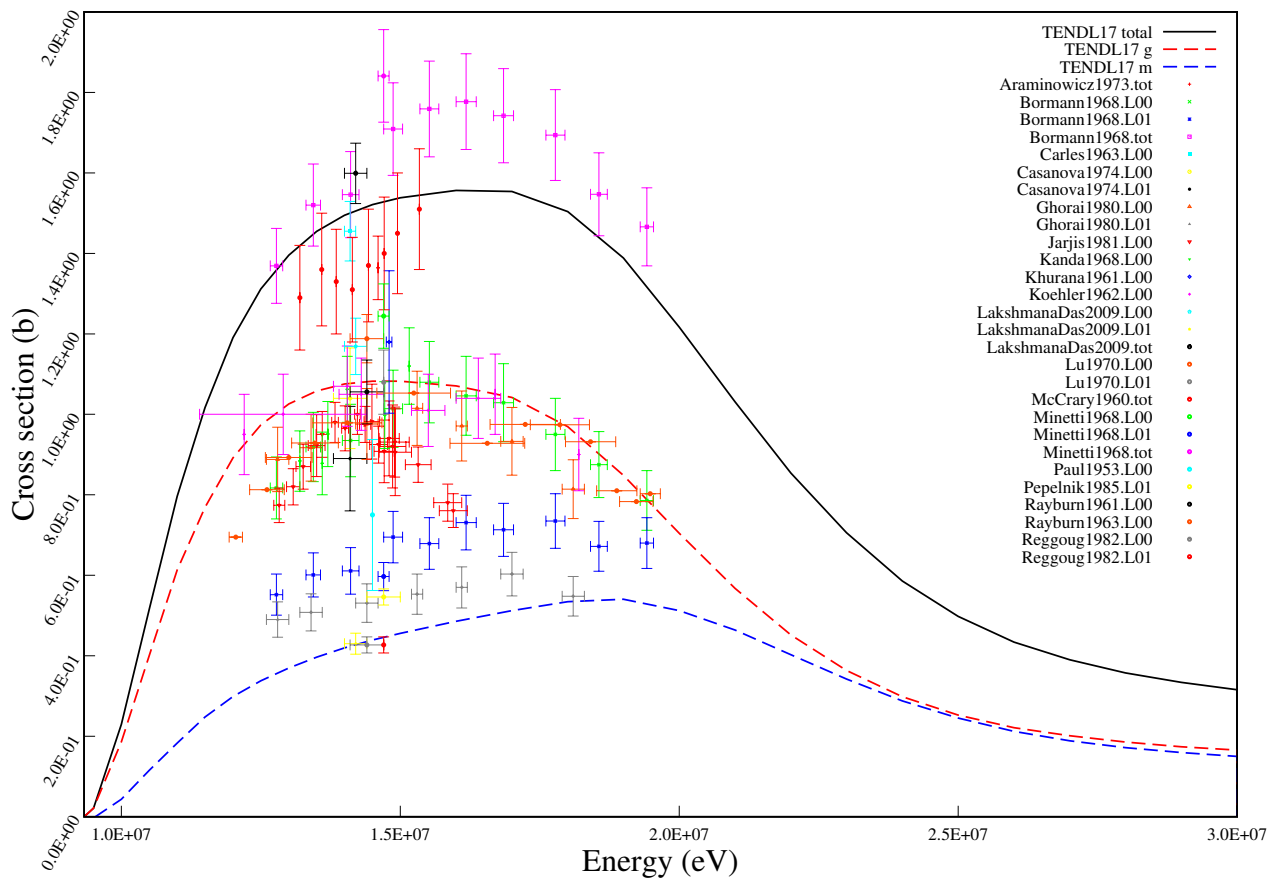
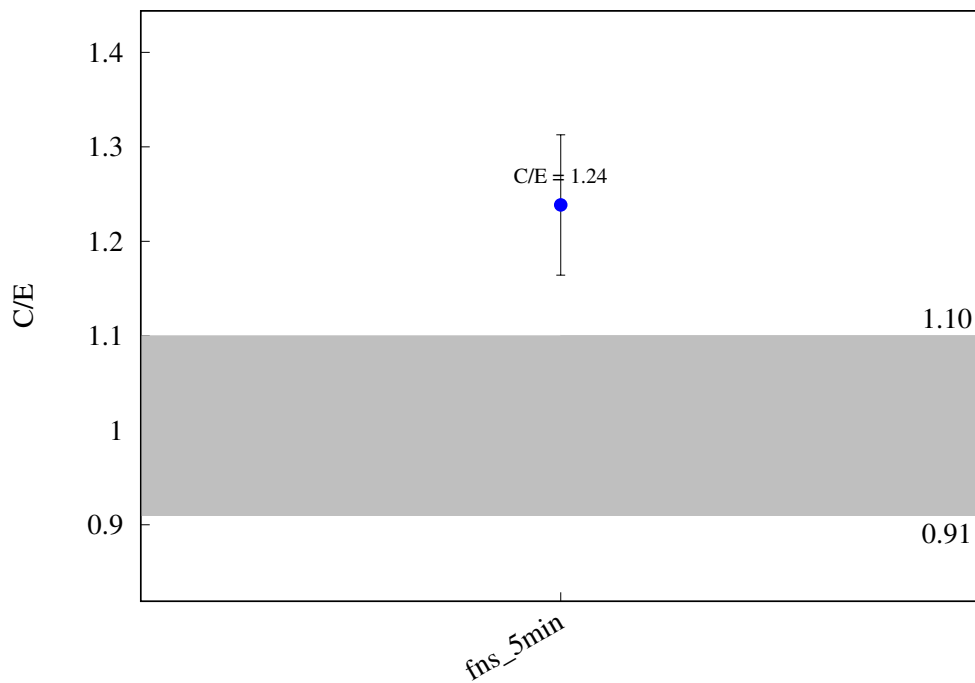
^{120}Sn (n,p) $^{120\text{m}}\text{In}$ 

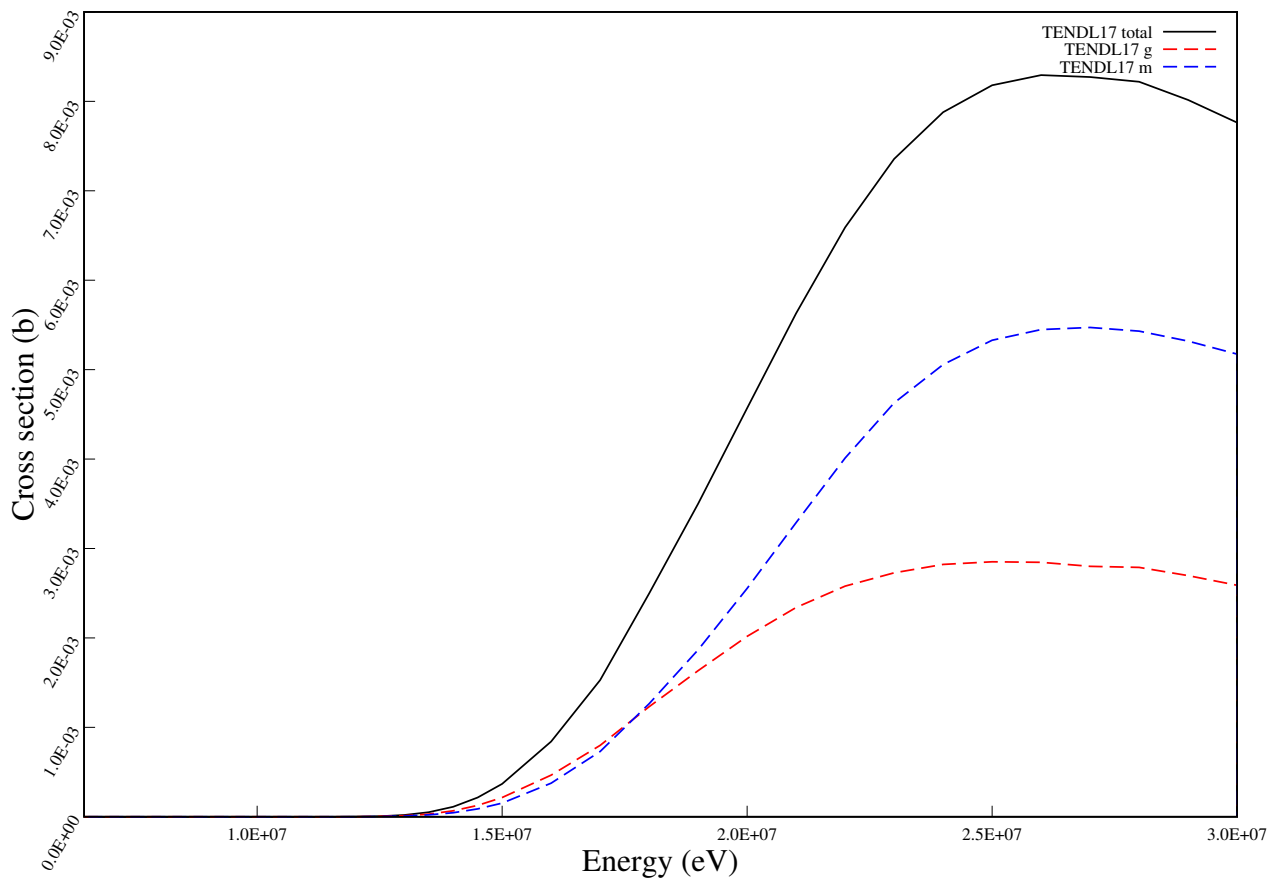
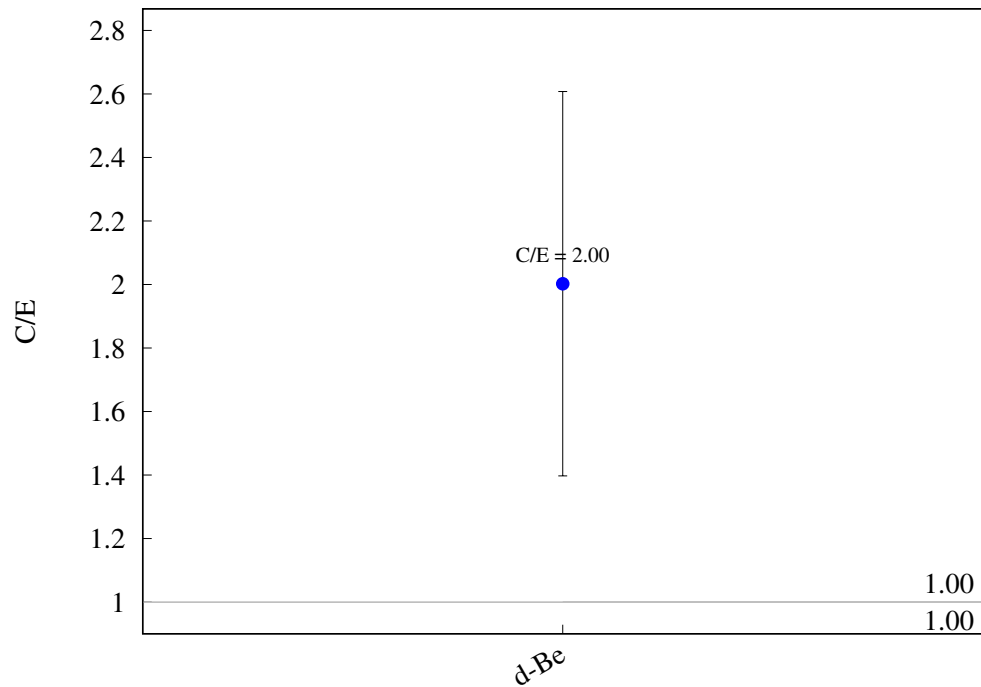
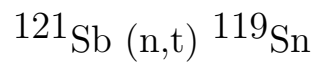


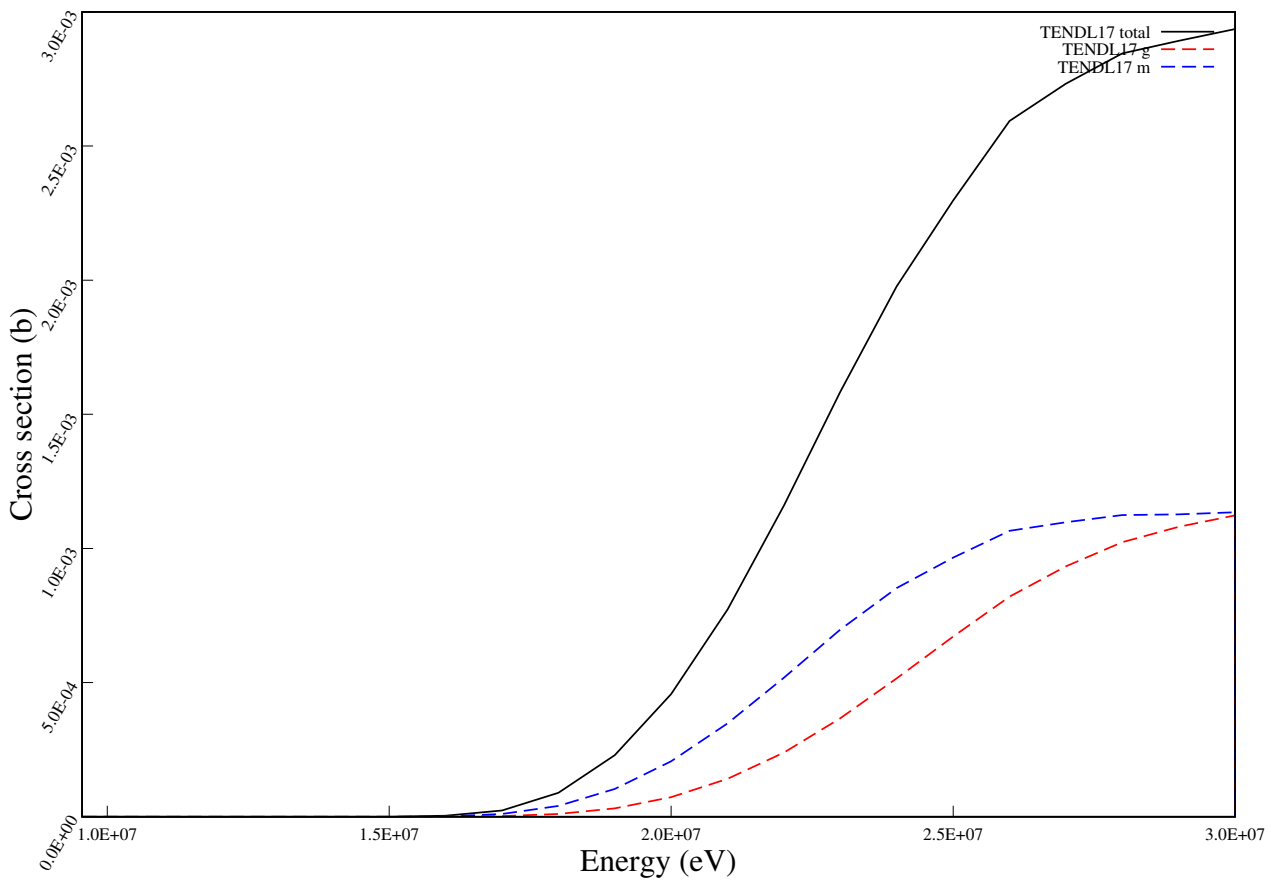
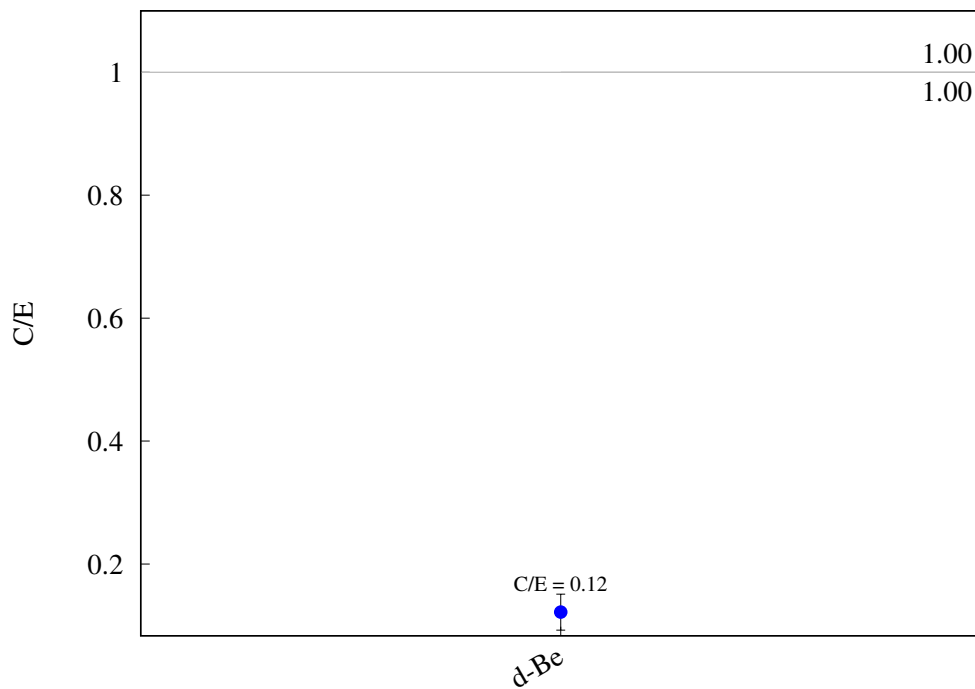


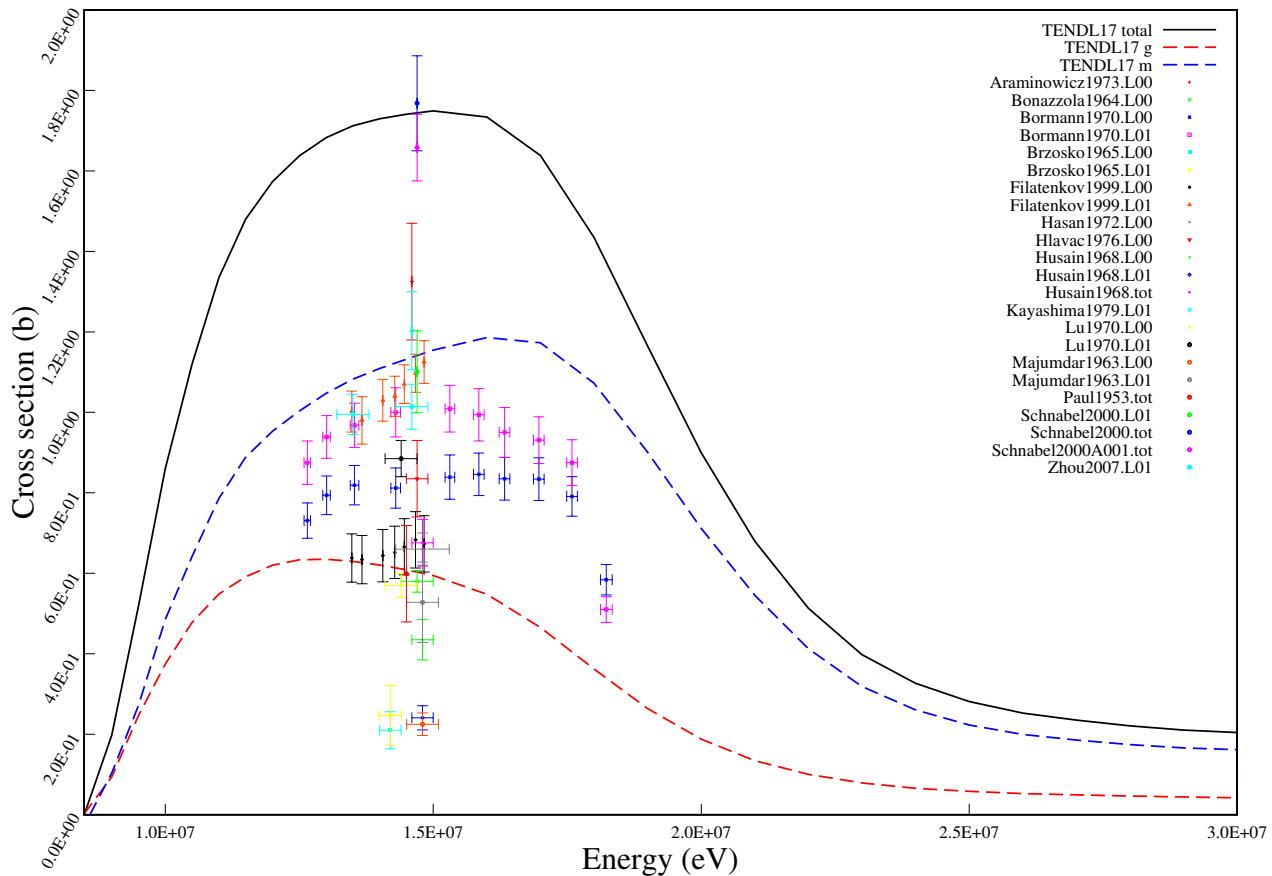
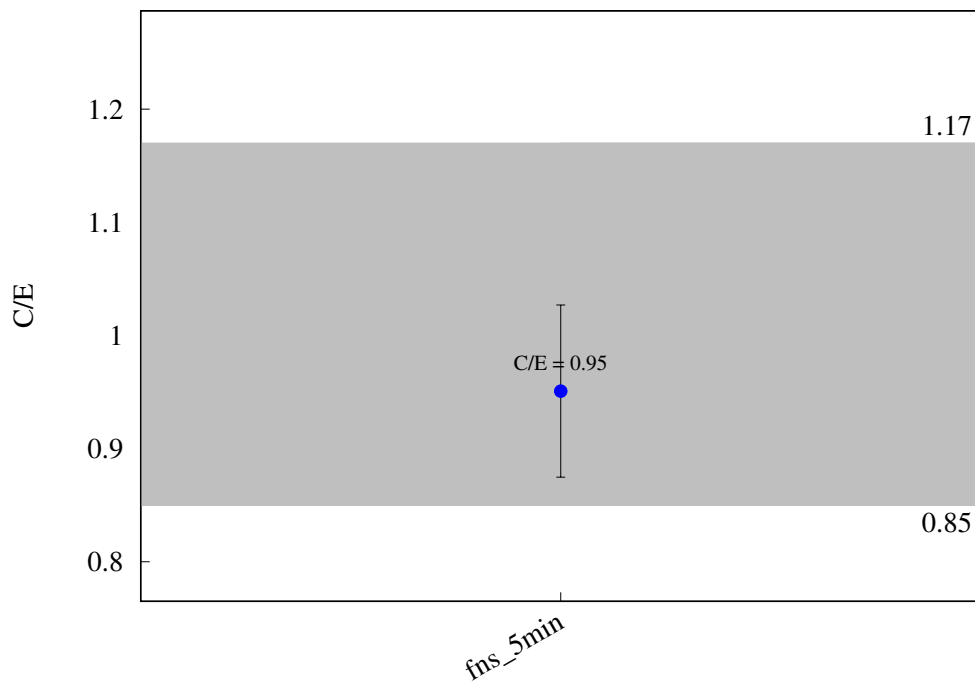
^{124}Sn (n,2n) ^{123}gSn 

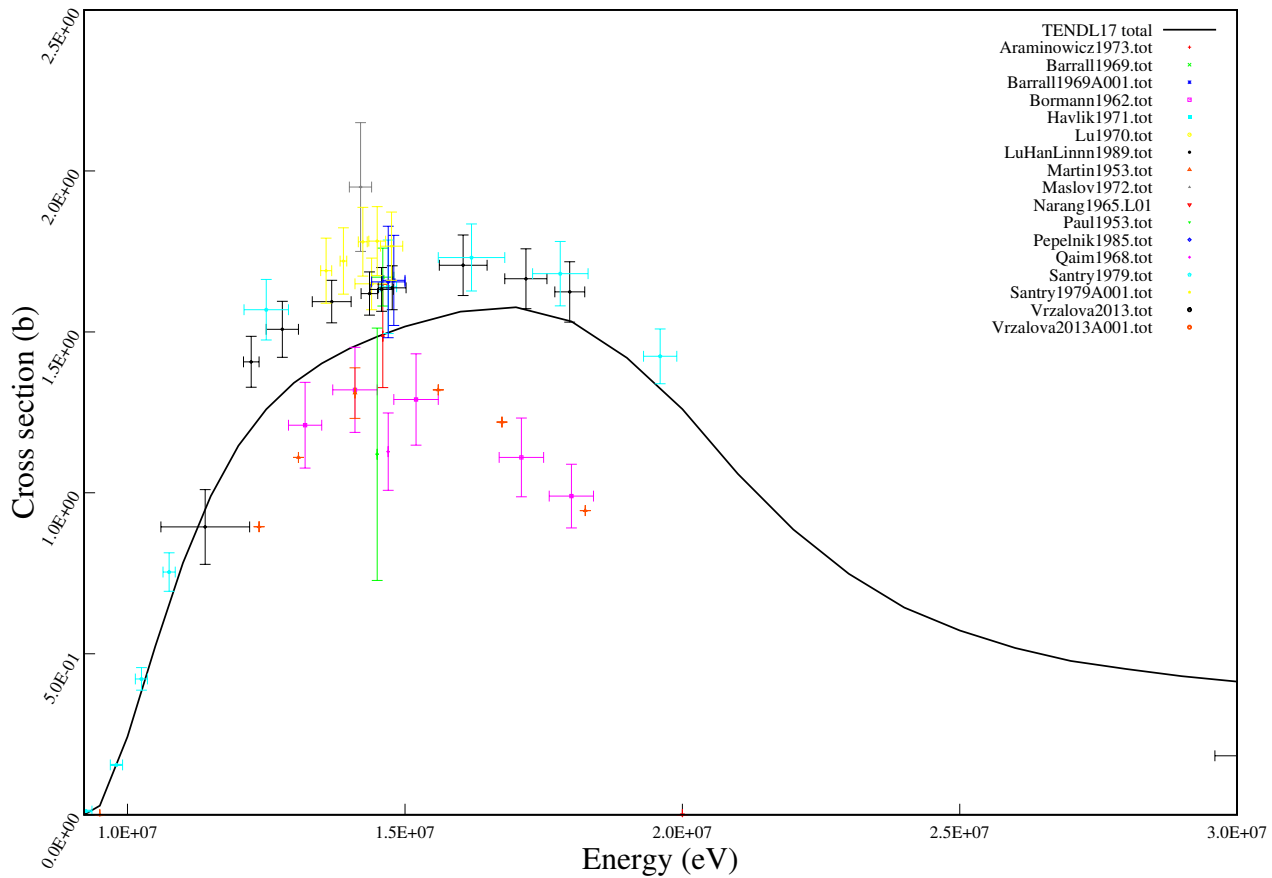
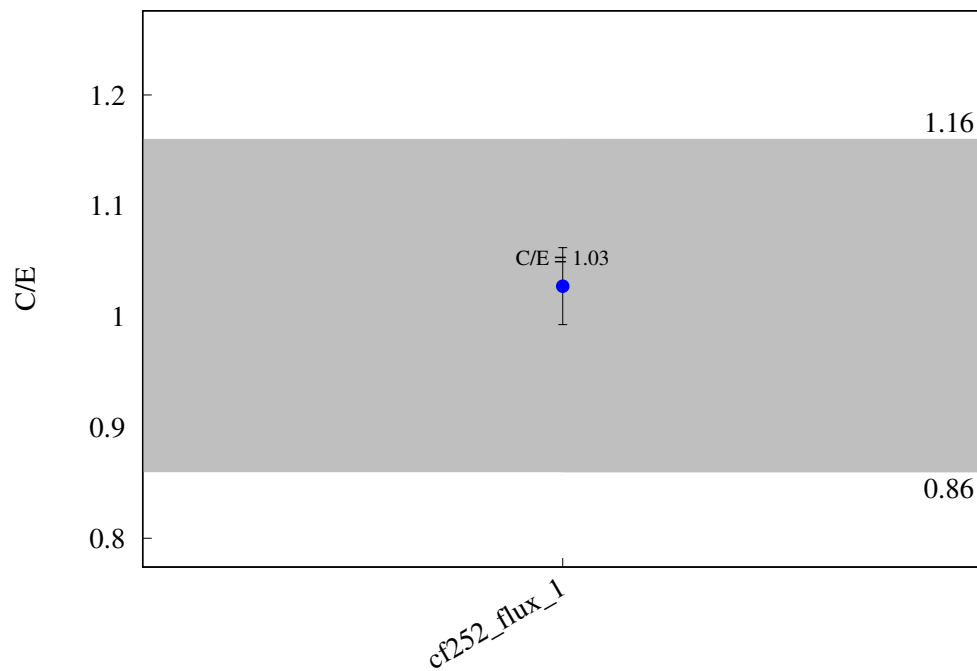
^{124}Sn ($n,2n$) $^{123\text{m}}\text{Sn}$ 

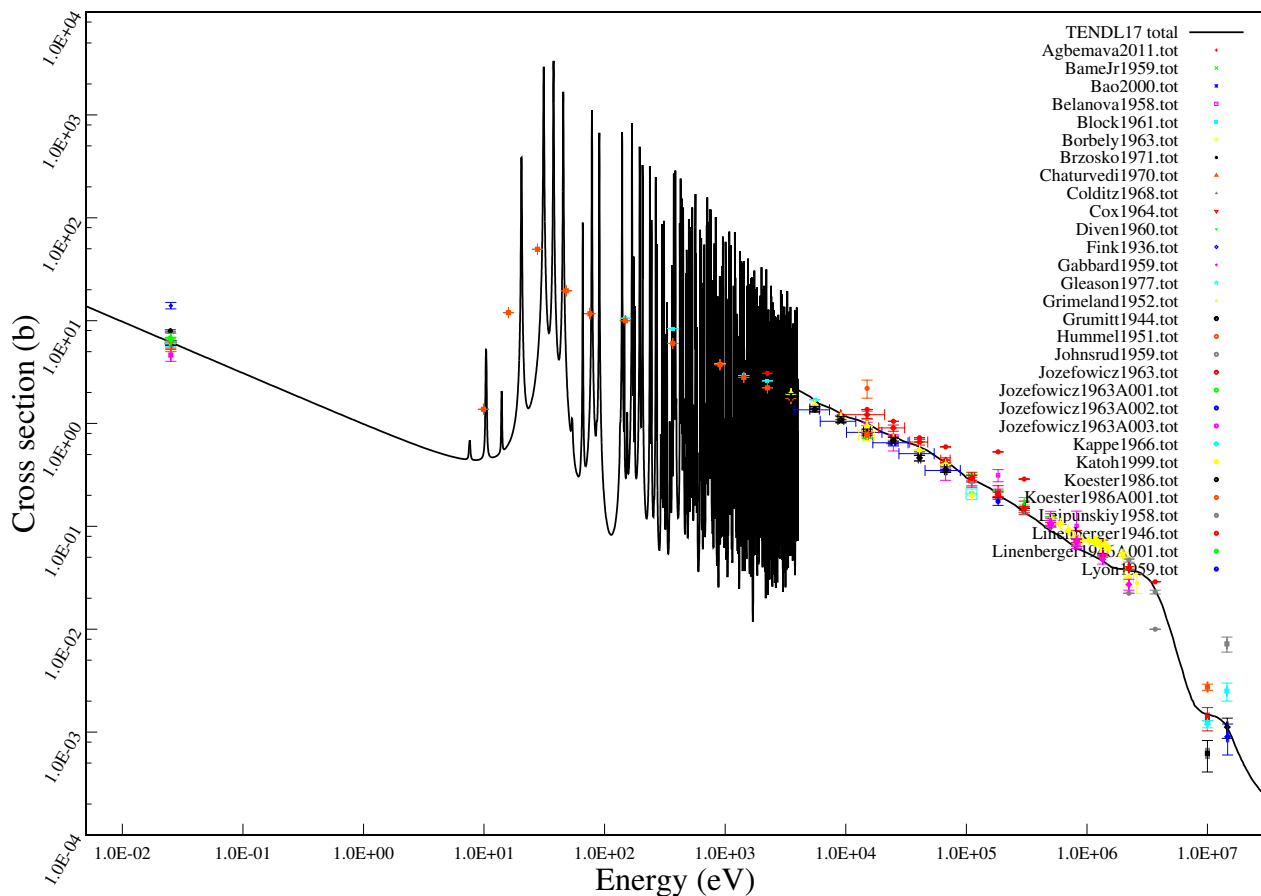
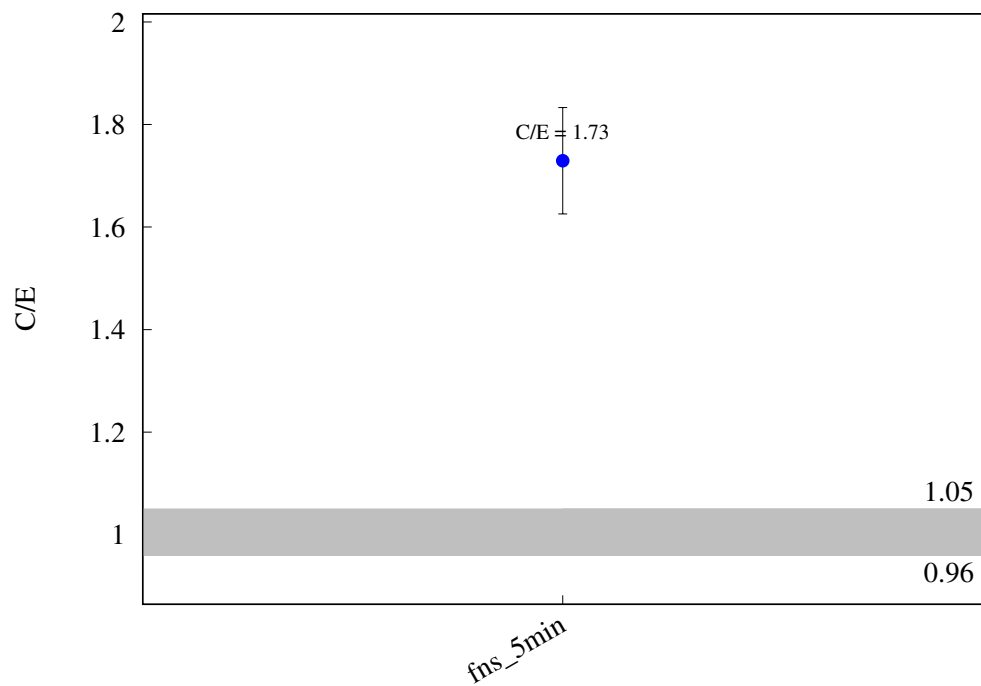
^{121}Sb (n,2n) ^{120}gSb 

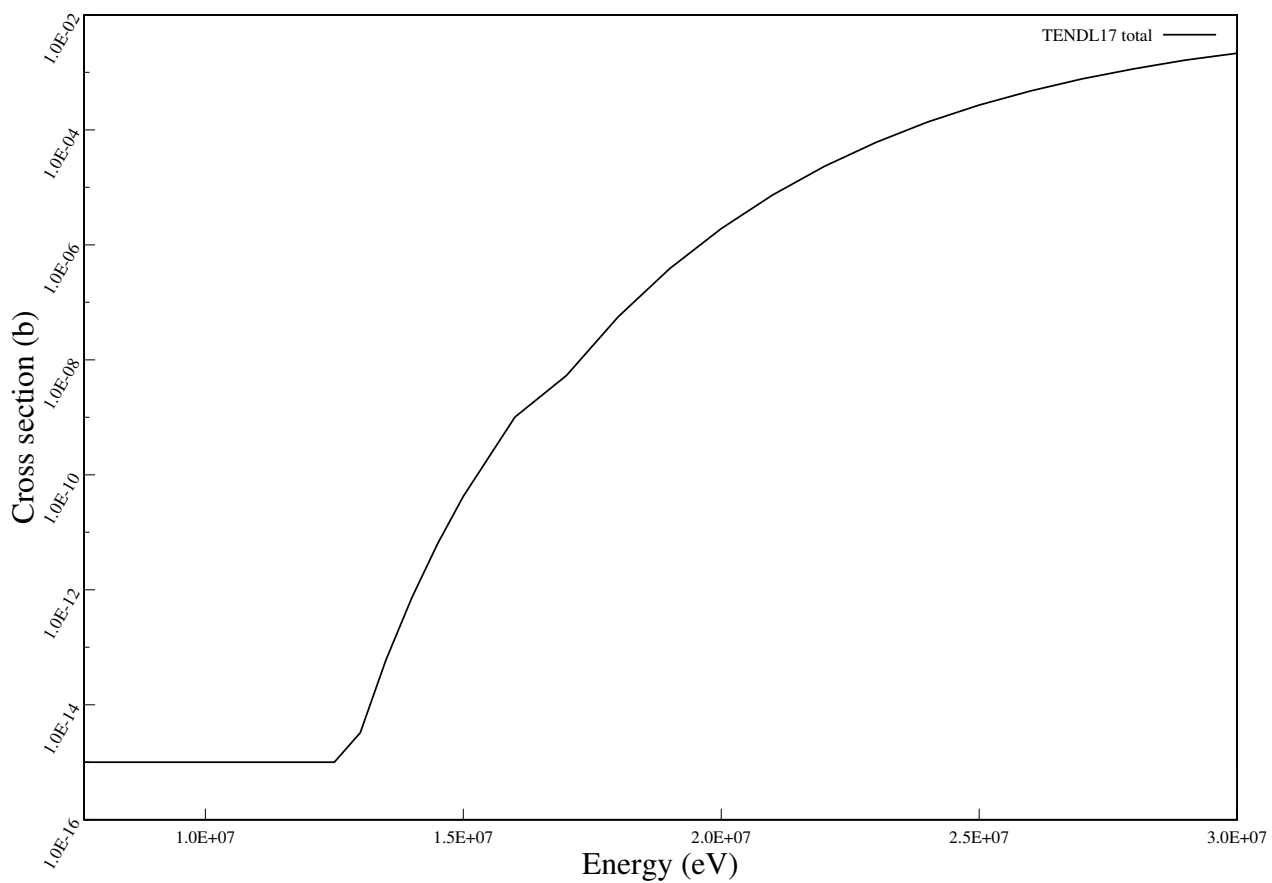
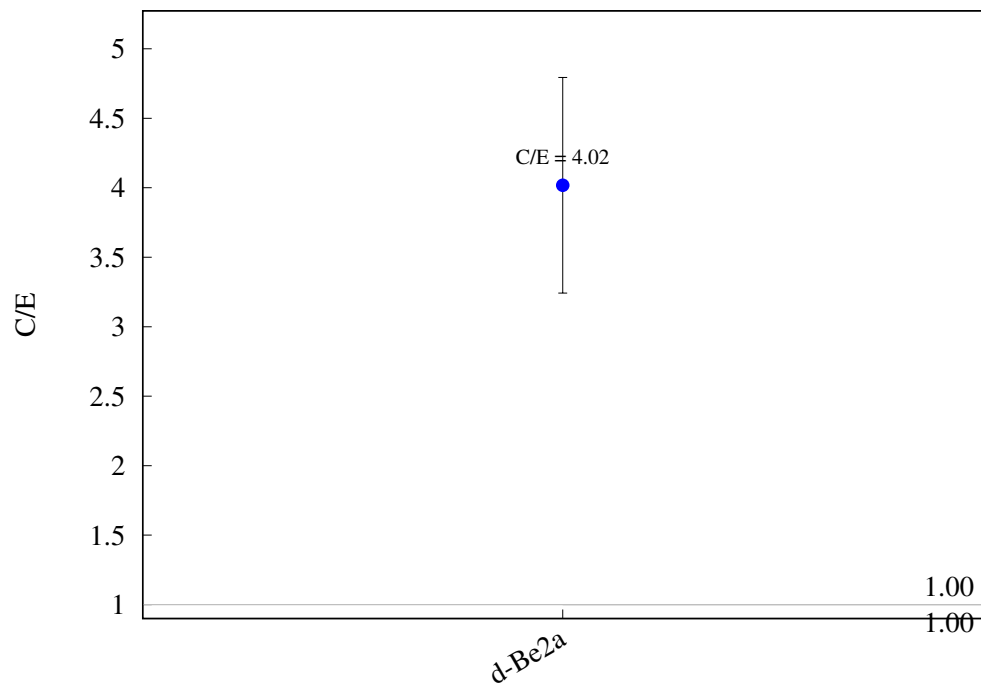


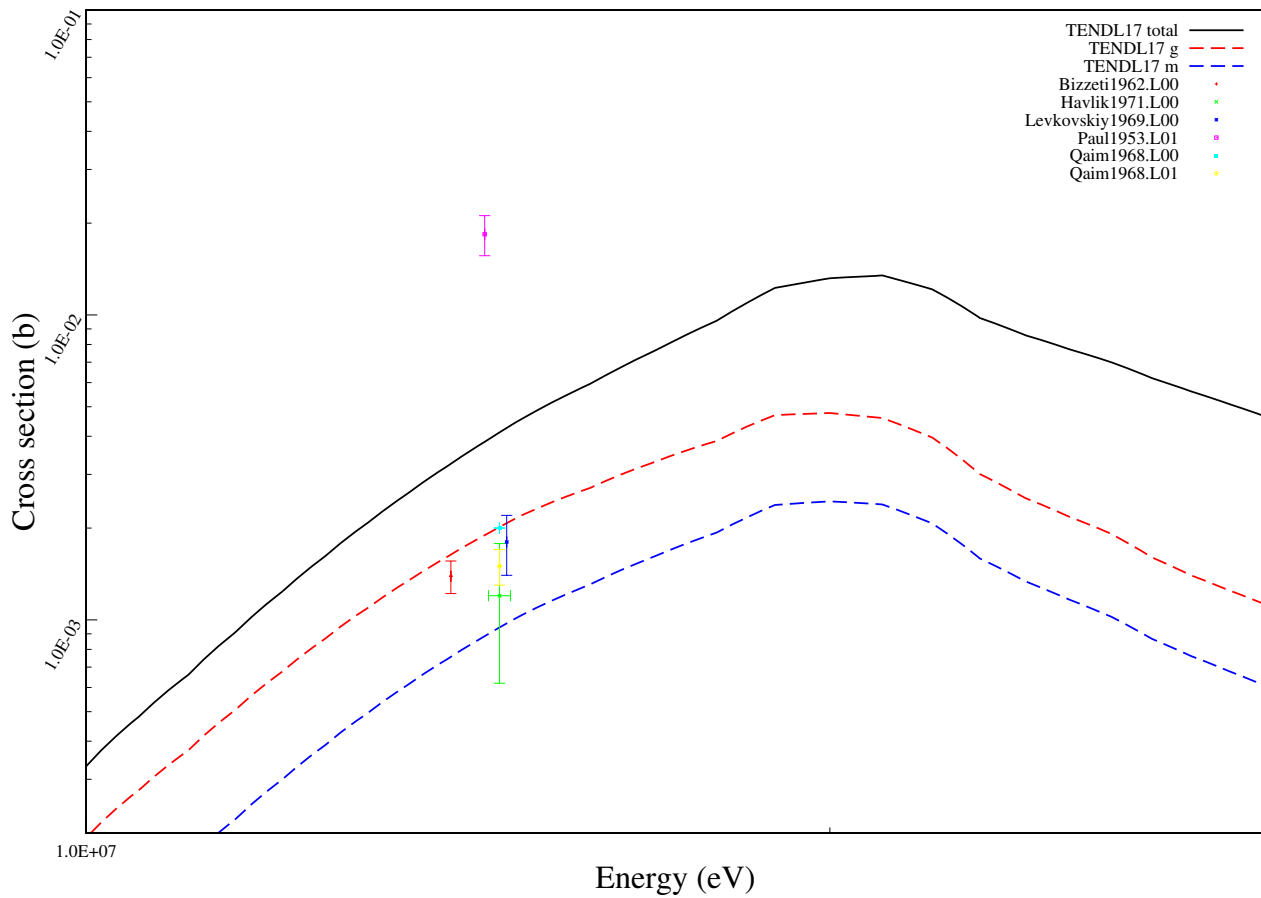
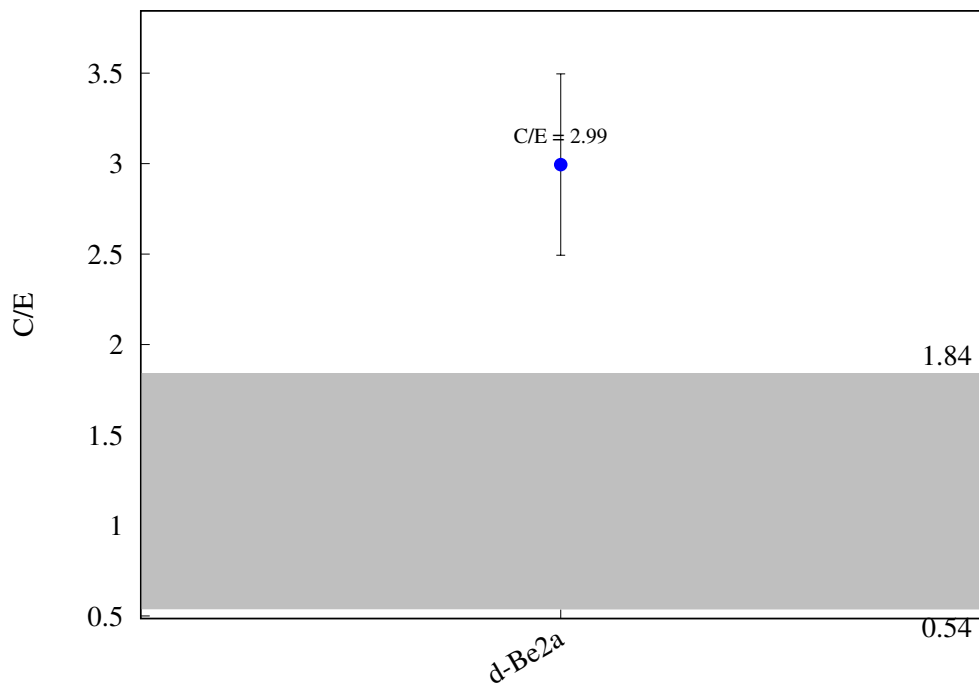
$^{128}\text{Te} (\text{n},\text{t}) ^{126}\text{Sb}$ 

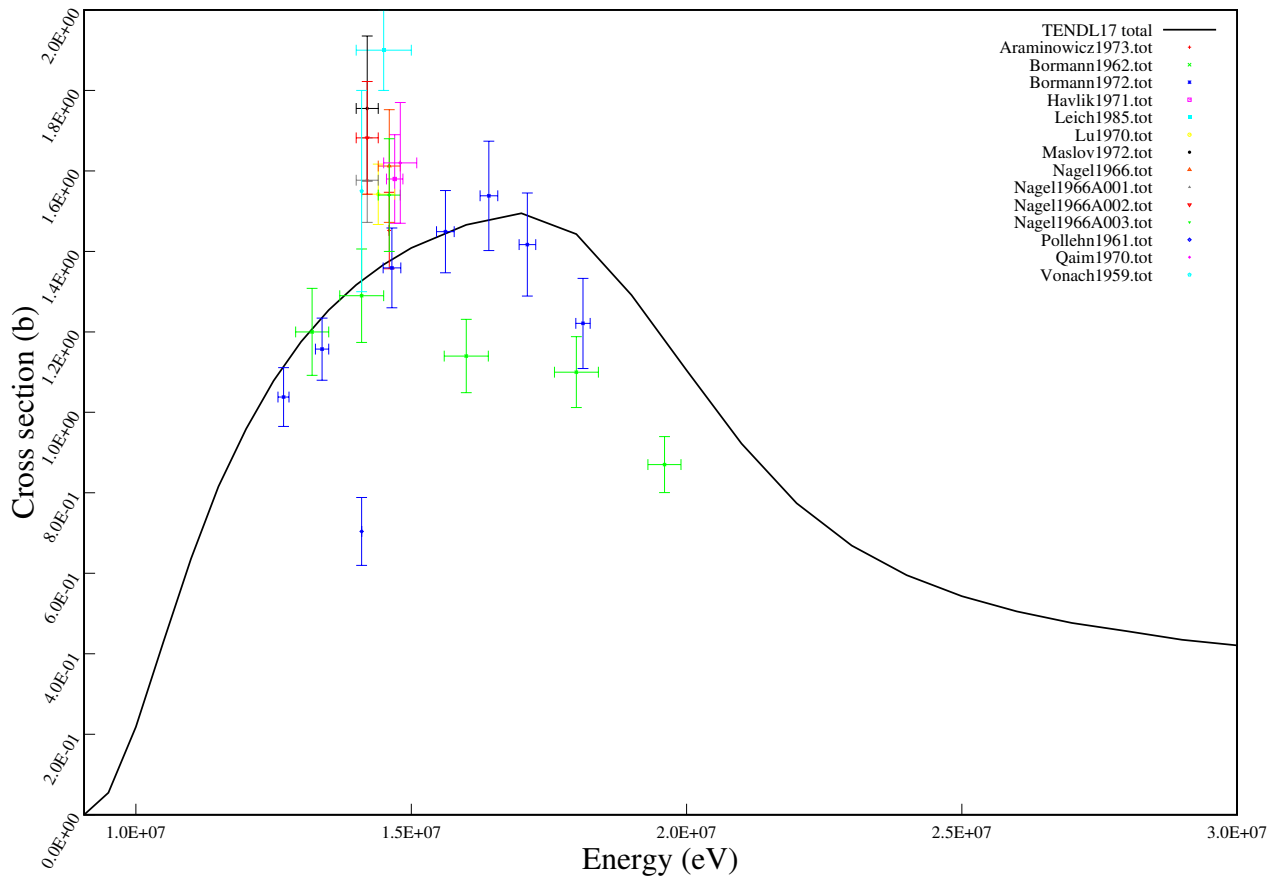
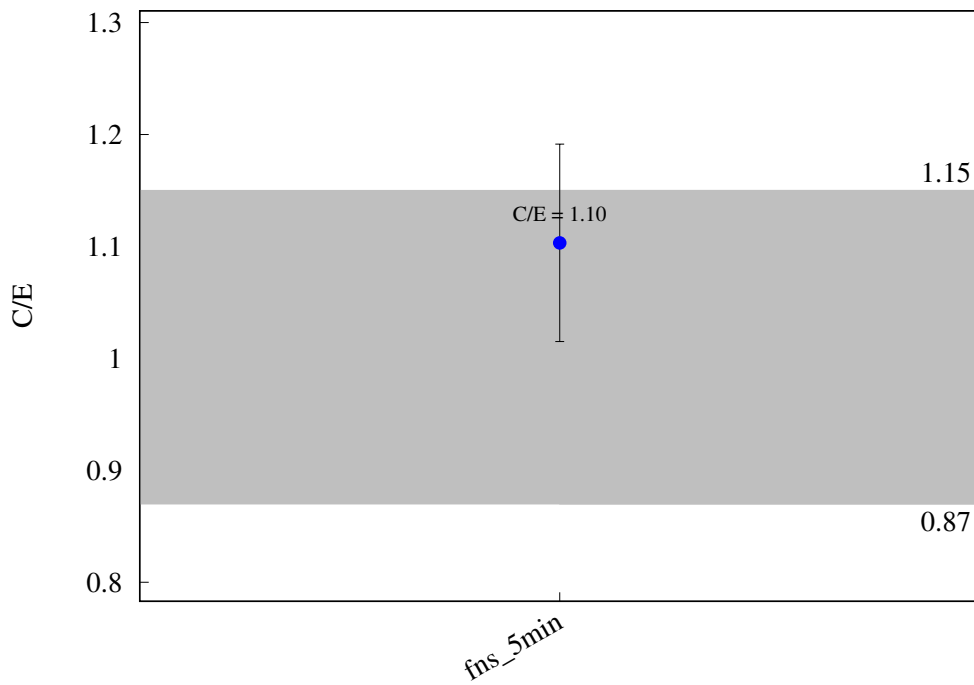
^{130}Te (n,2n) ^{129}gTe 

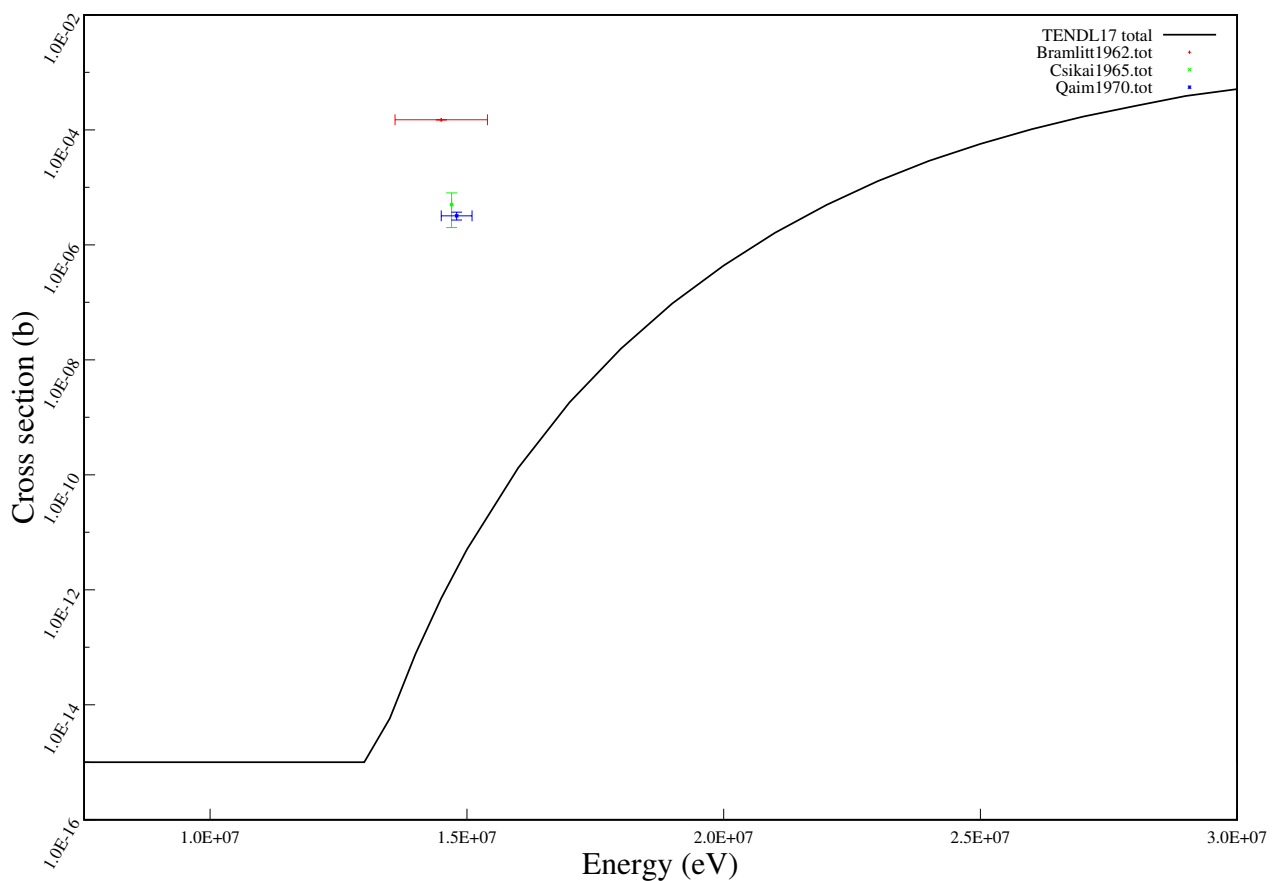
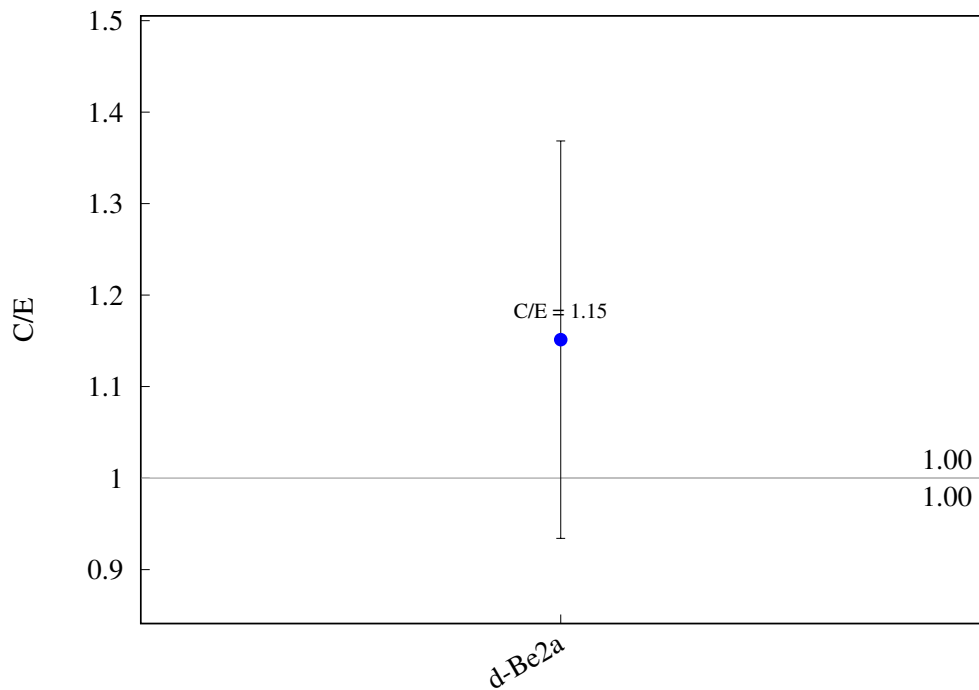
^{127}I (n,2n) ^{126}I 

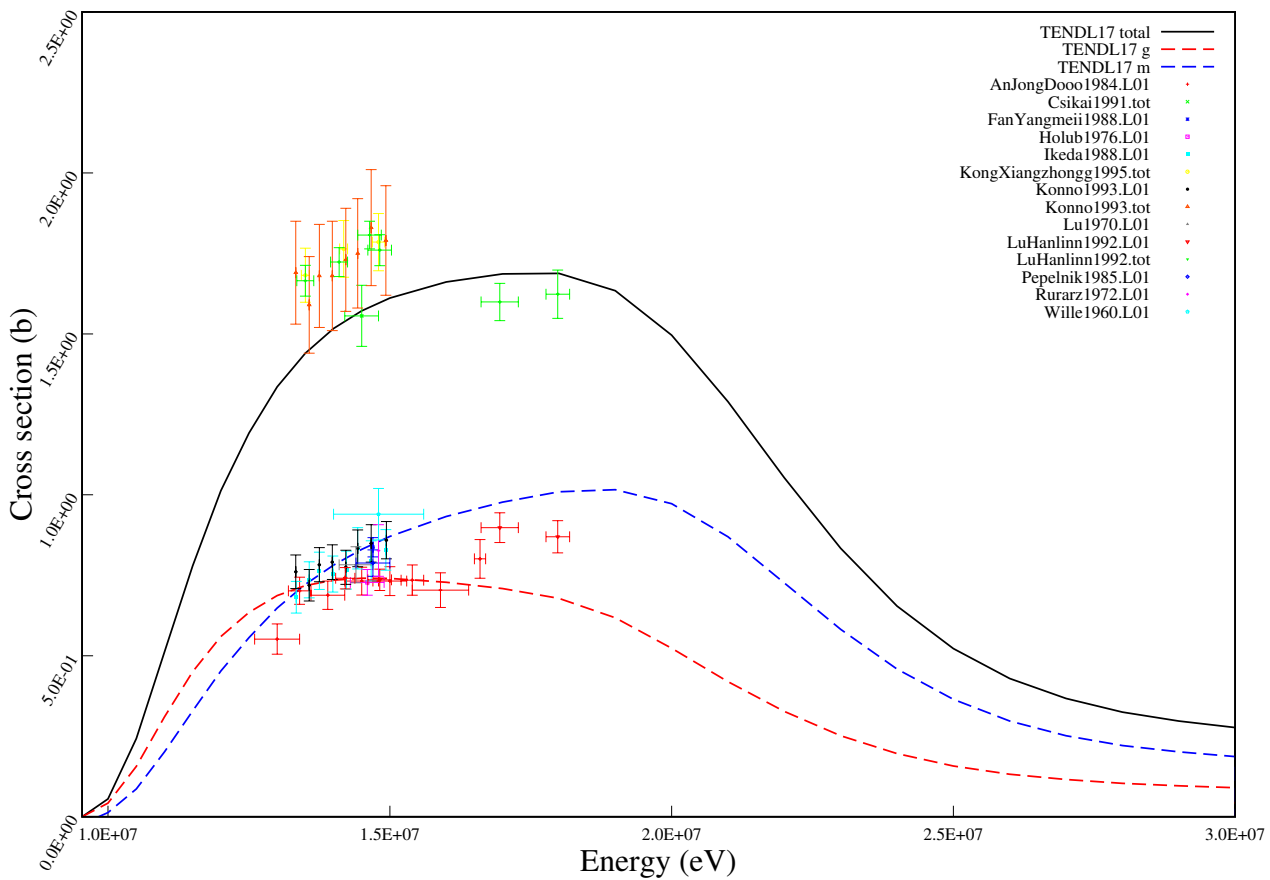
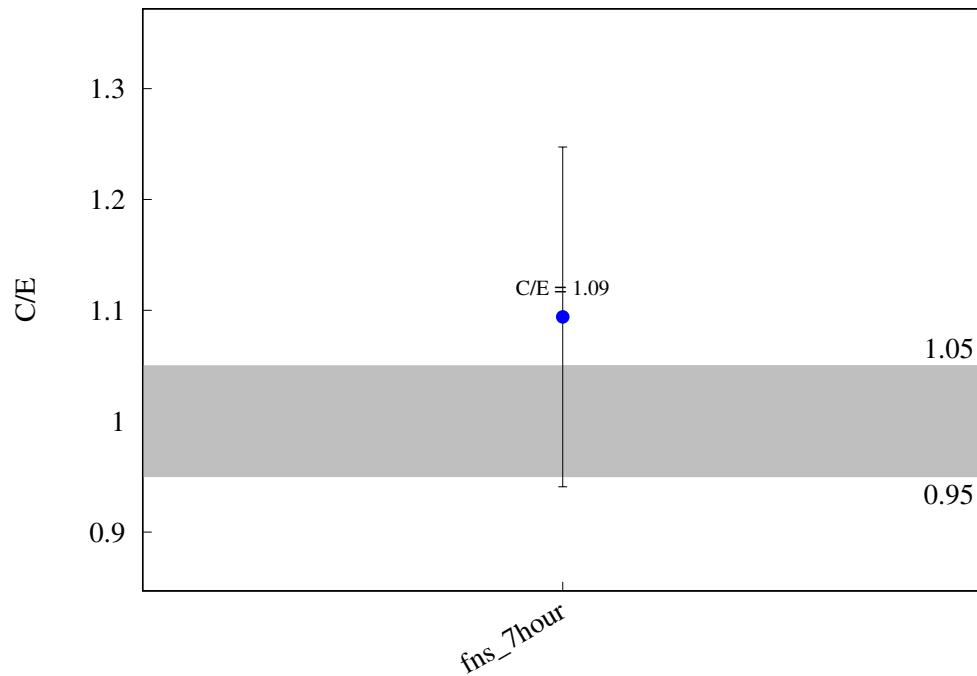
^{127}I (n,g) ^{128}I 

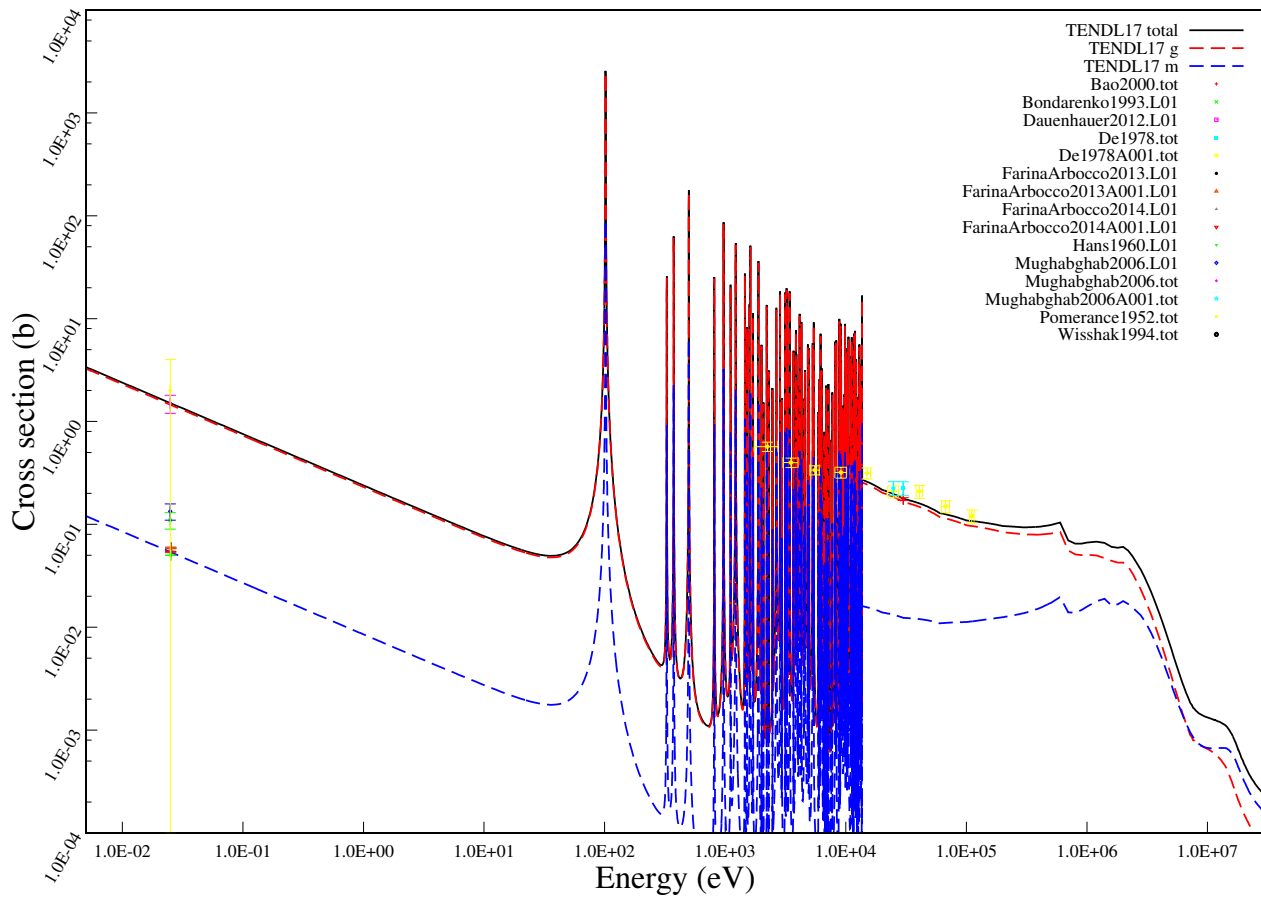
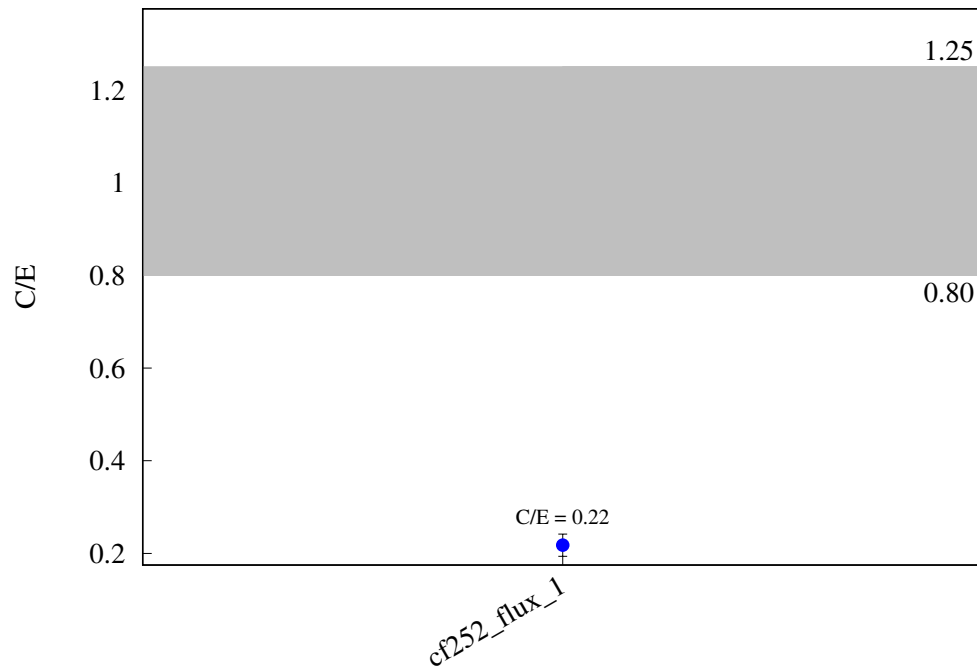
^{127}I (n,h) ^{125}Sb 

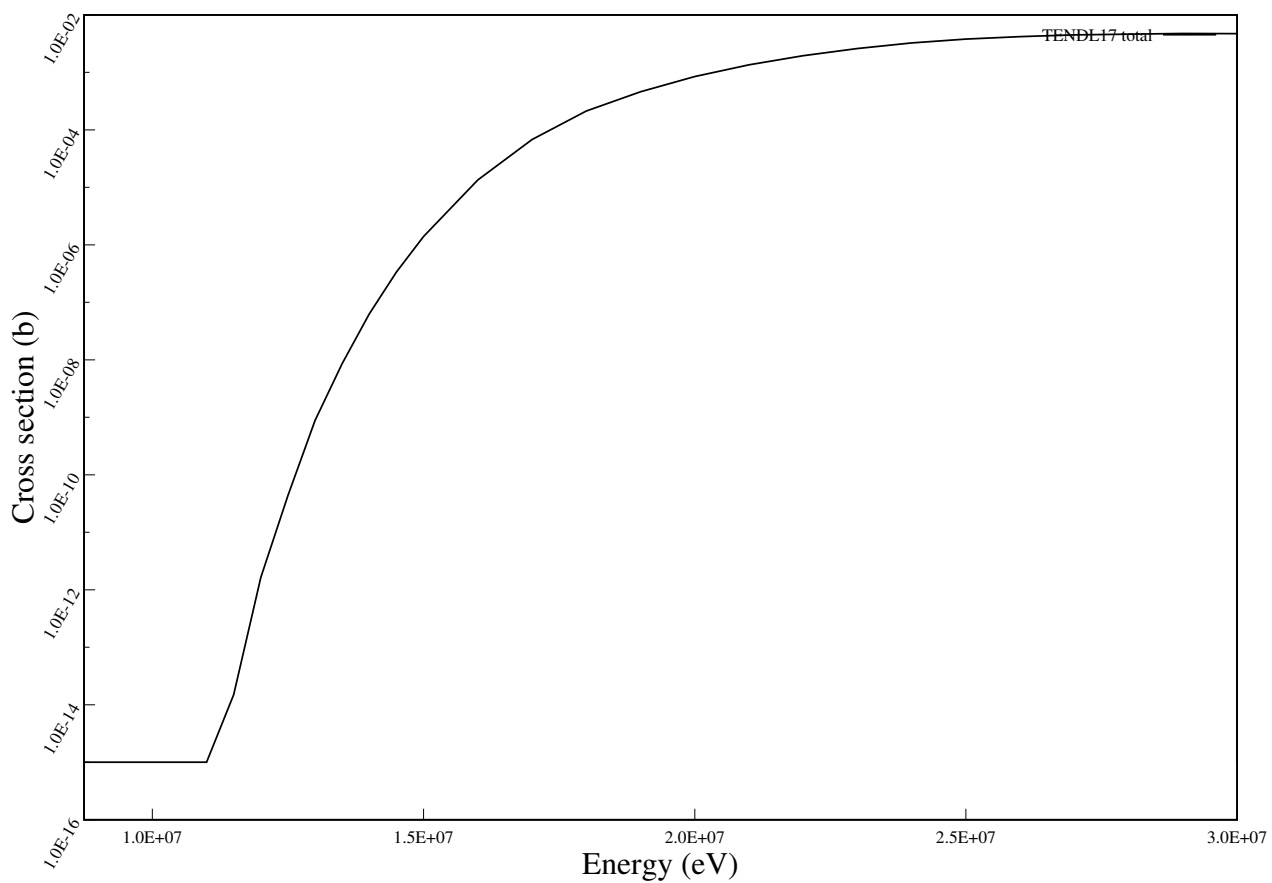
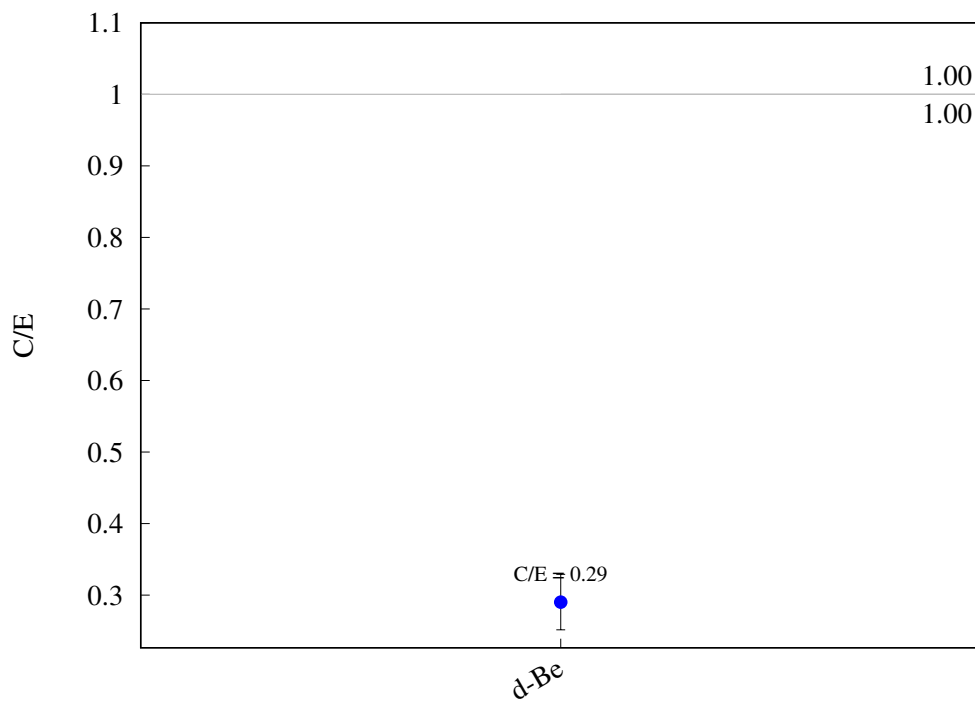
^{127}I (n,a) ^{124}Sb 

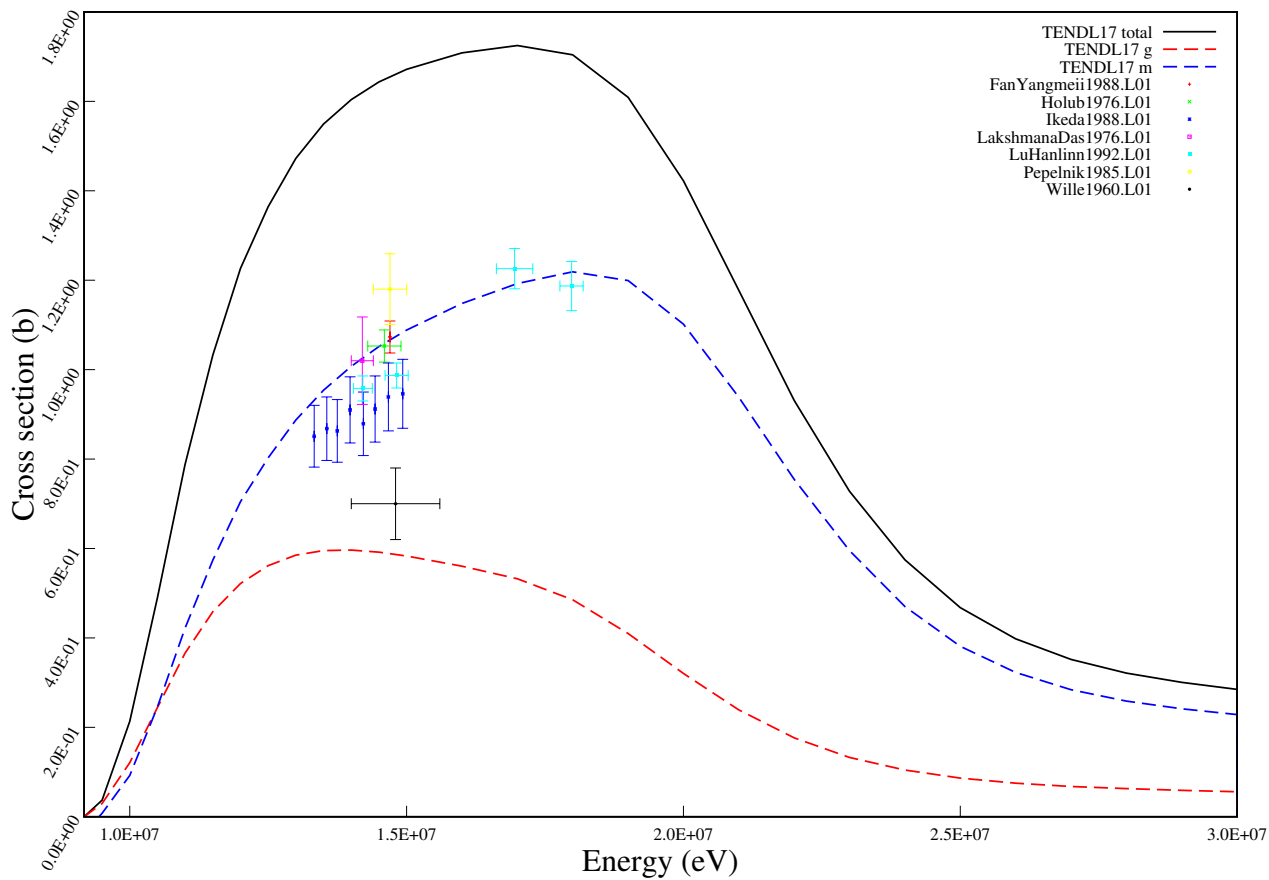
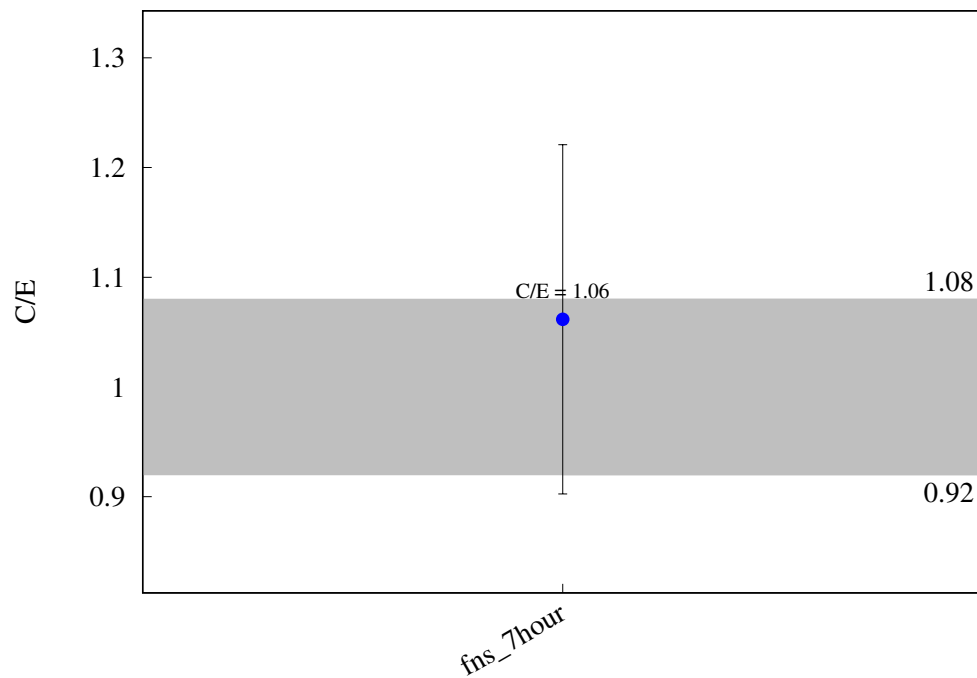
^{133}Cs (n,2n) ^{132}Cs 

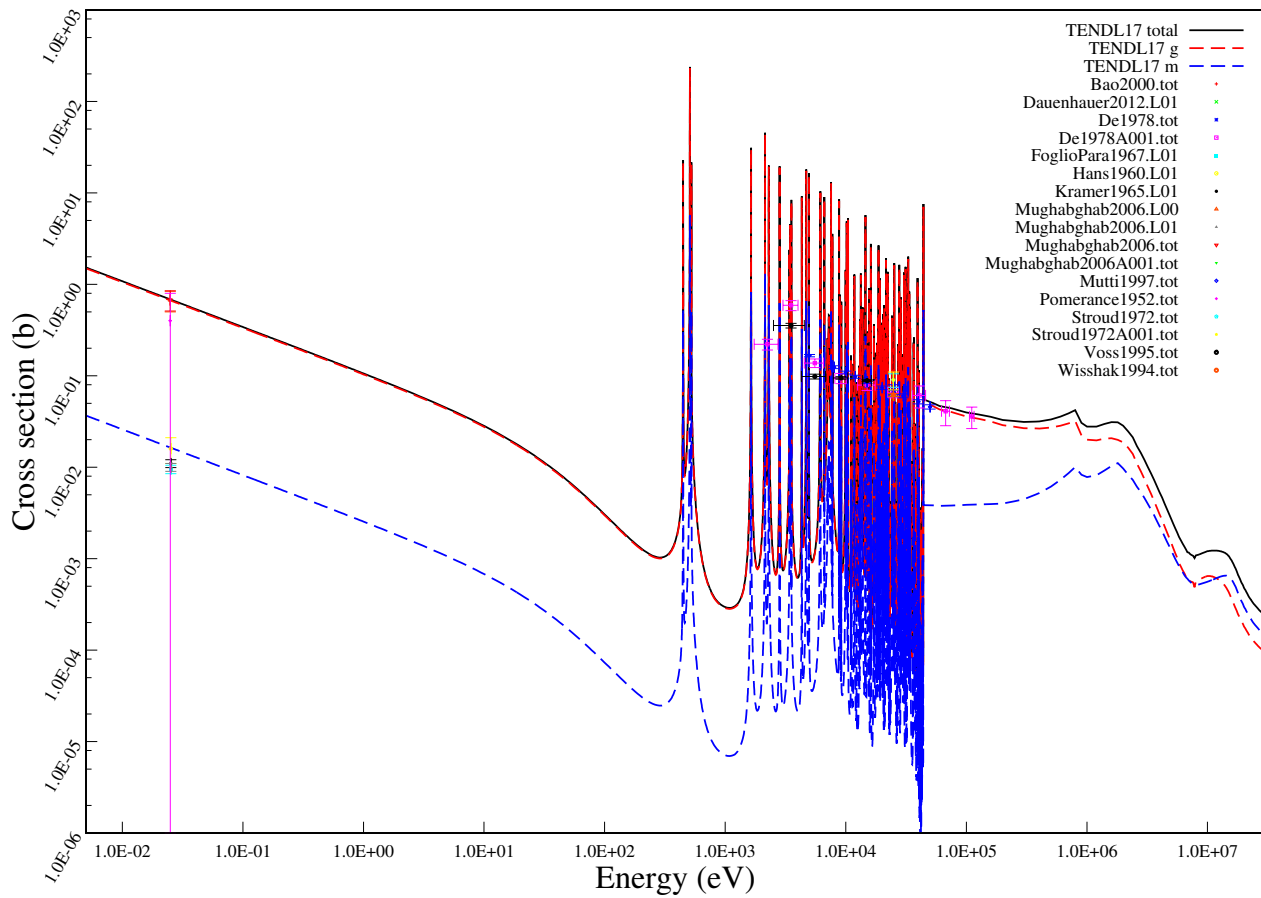
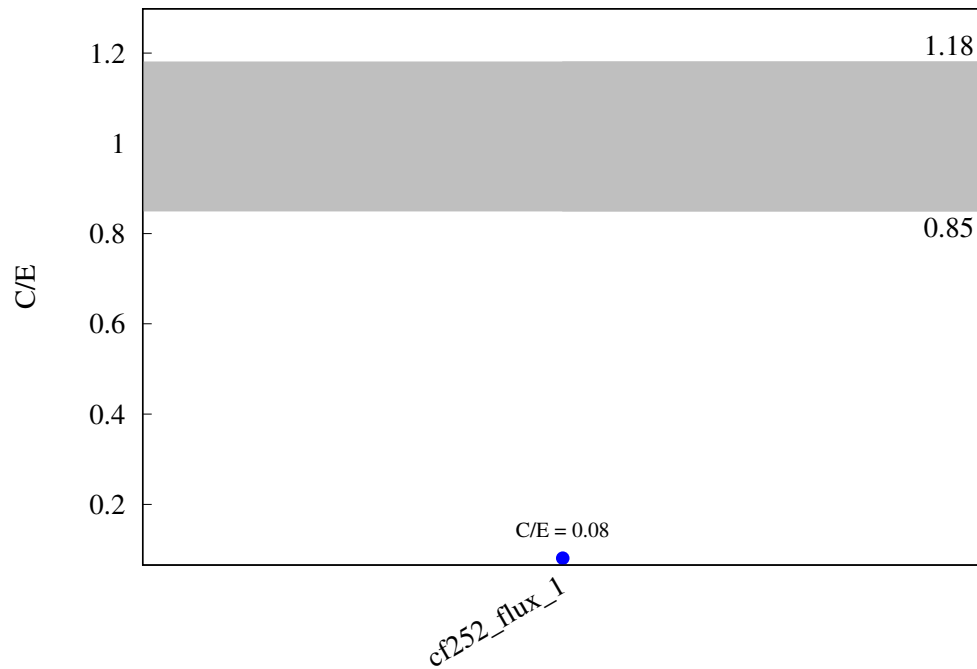
$^{133}\text{Cs} (\text{n},\text{h}) ^{131}\text{I}$ 

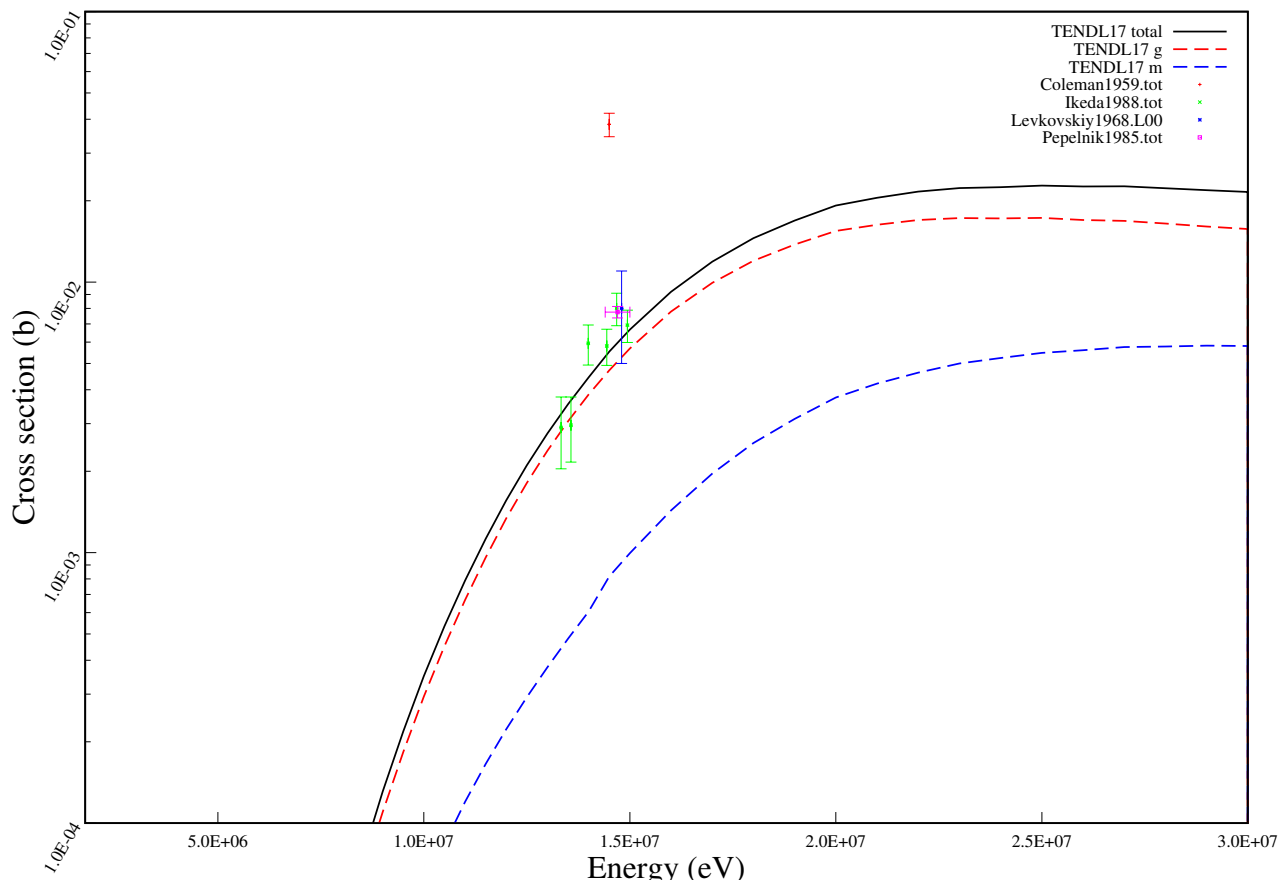
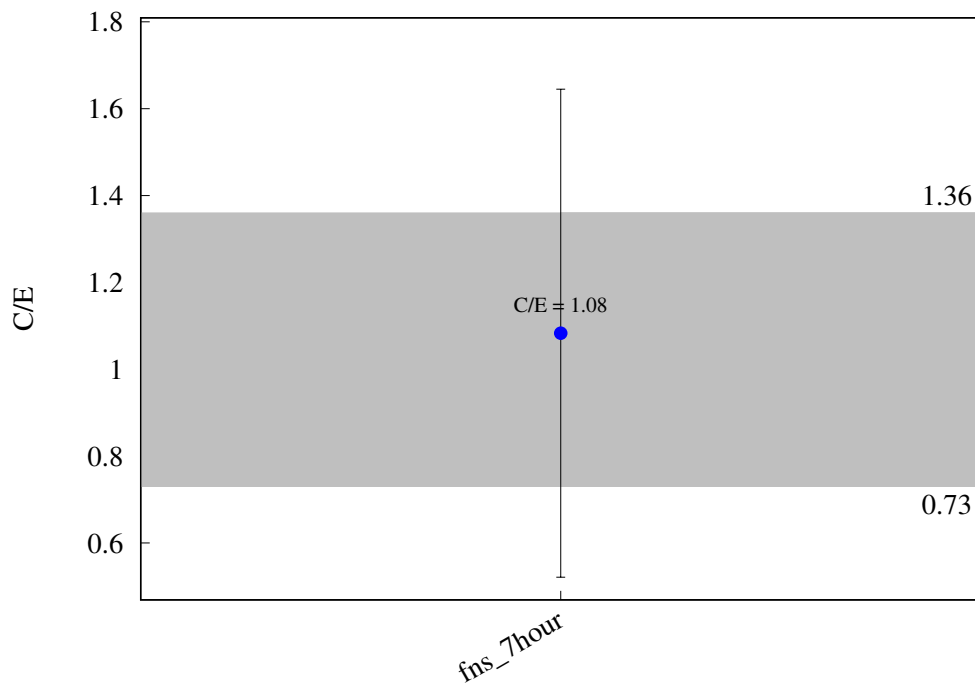
^{134}Ba (n,2n) $^{133\text{m}}\text{Ba}$ 

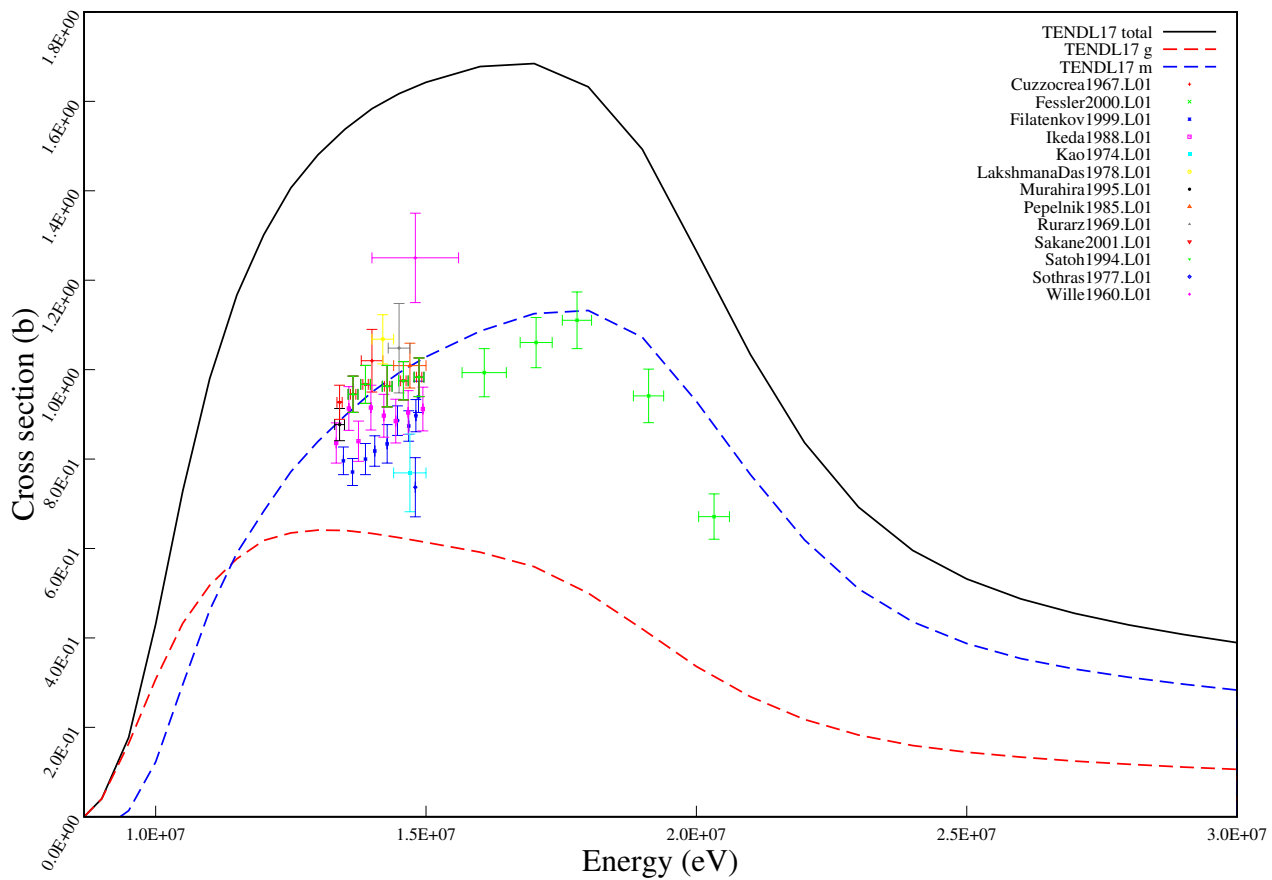
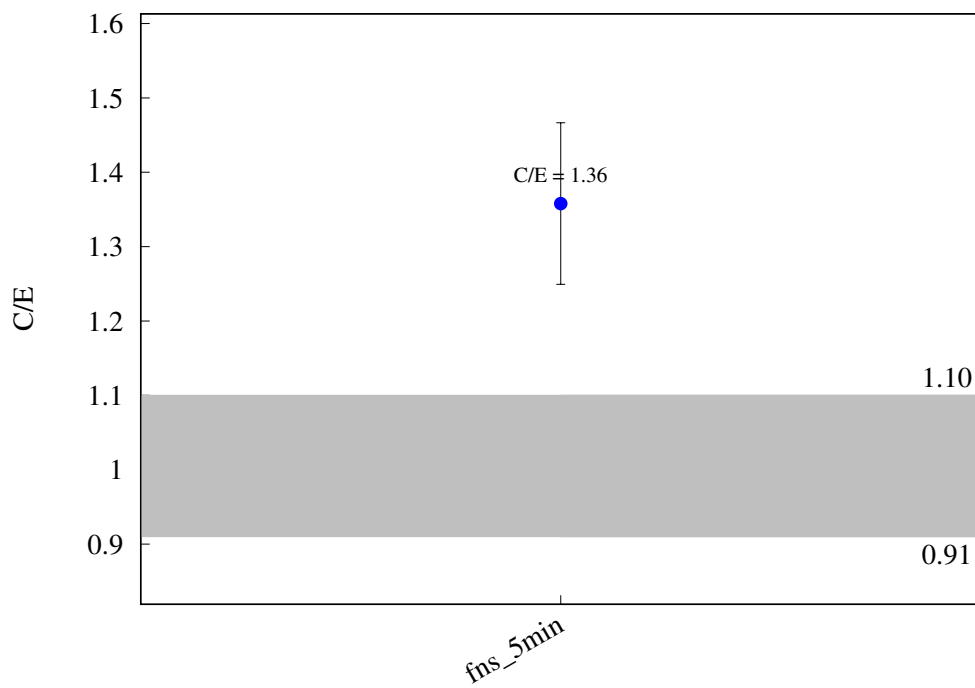
^{134}Ba (n,g) ^{135}Ba 

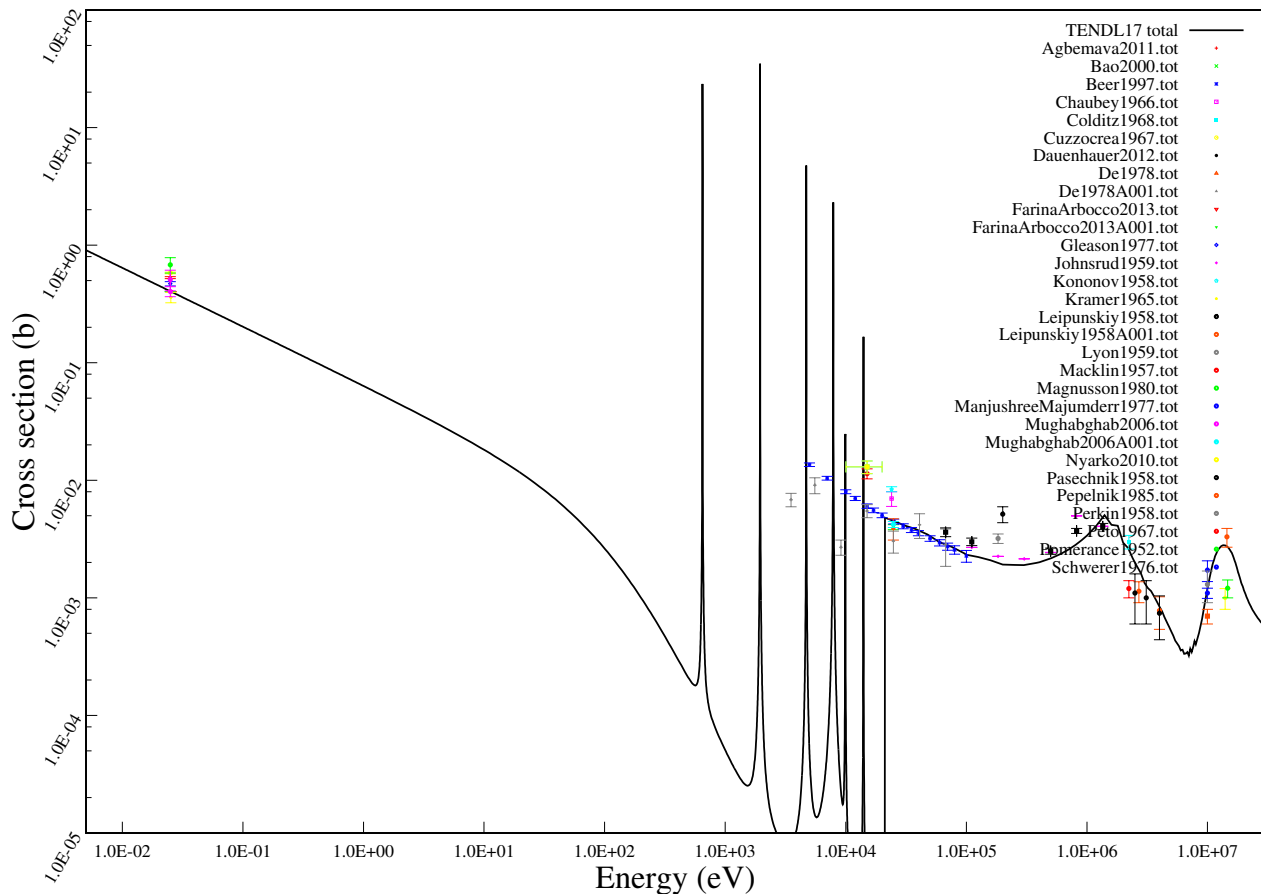
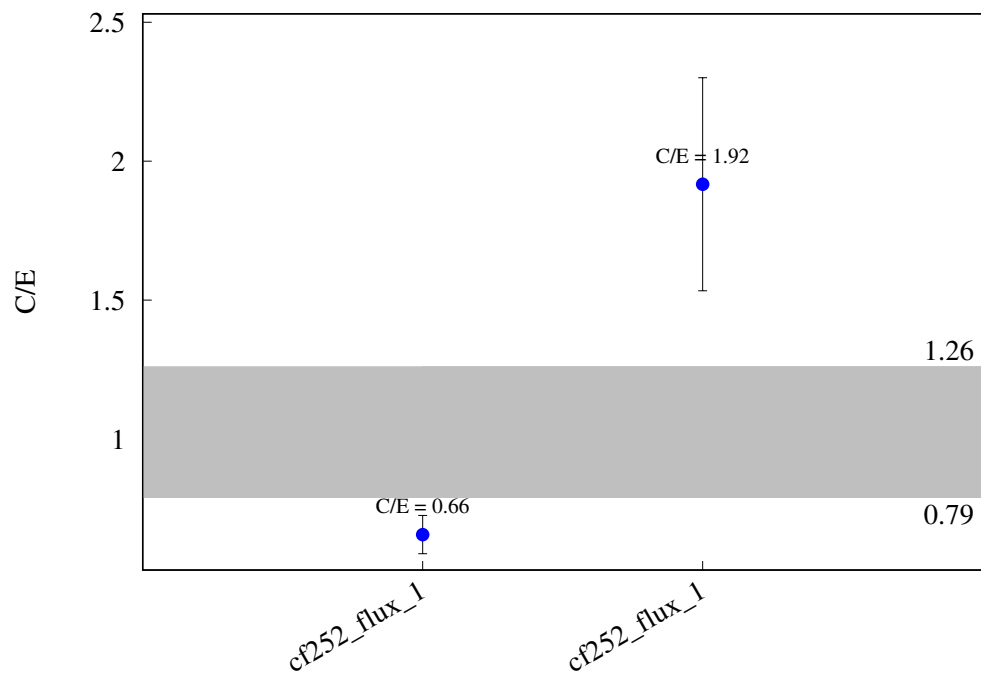
$^{134}\text{Ba} (\text{n},\text{t}) ^{132}\text{Cs}$ 

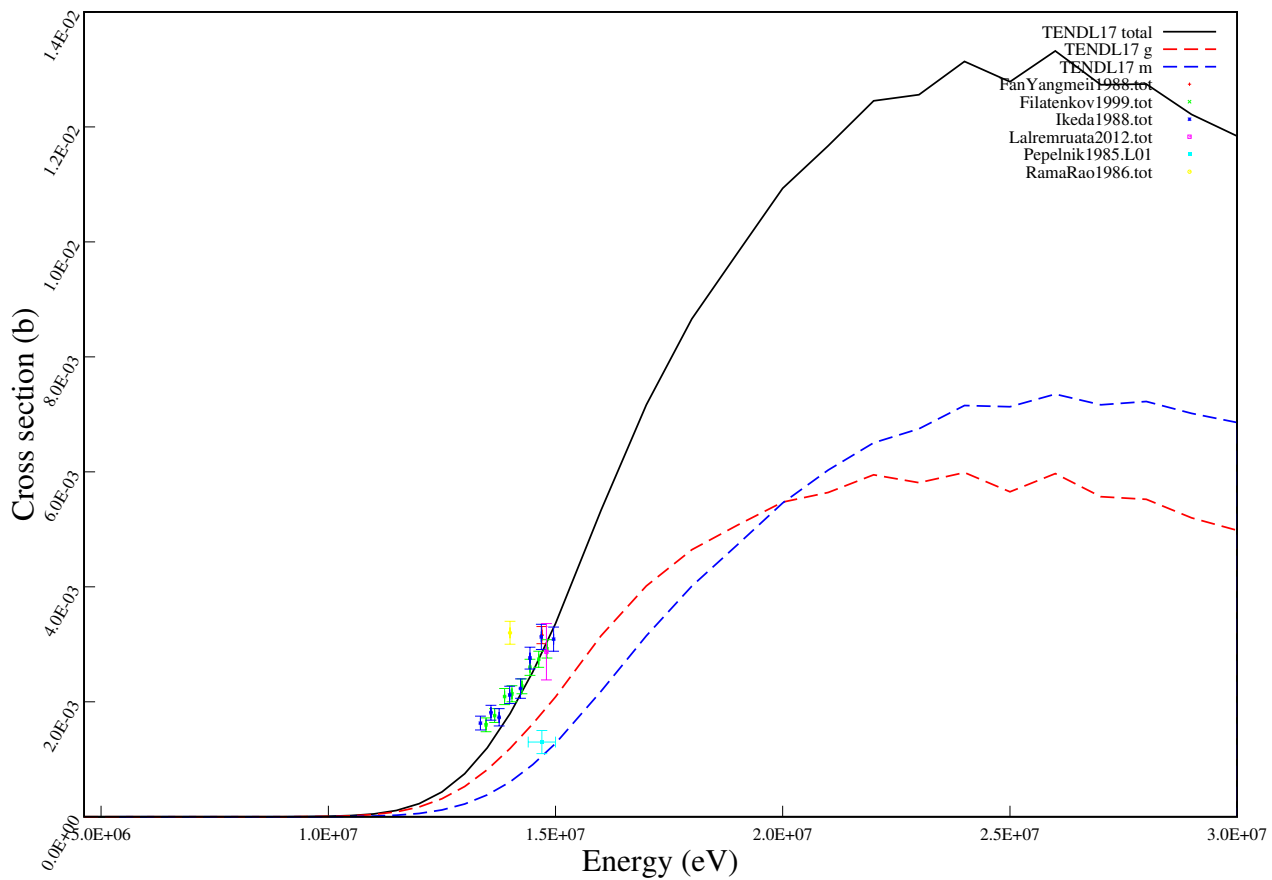
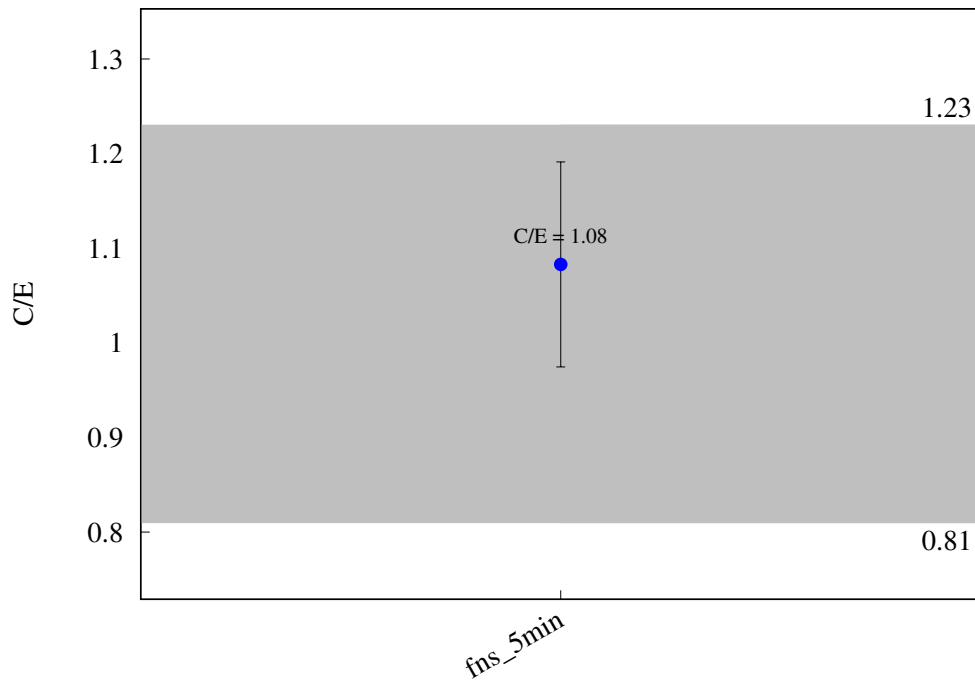
^{136}Ba (n,2n) ^{135m}Ba 

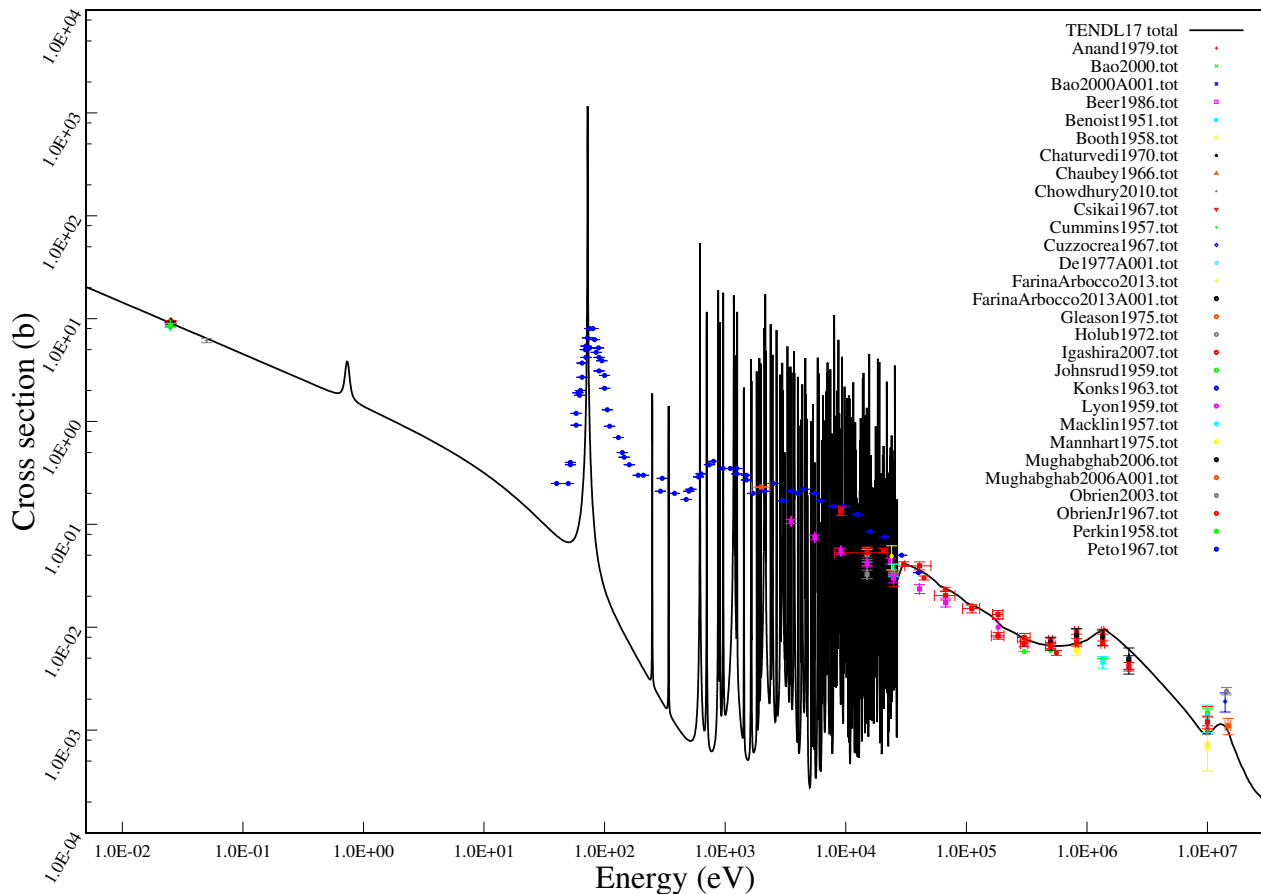
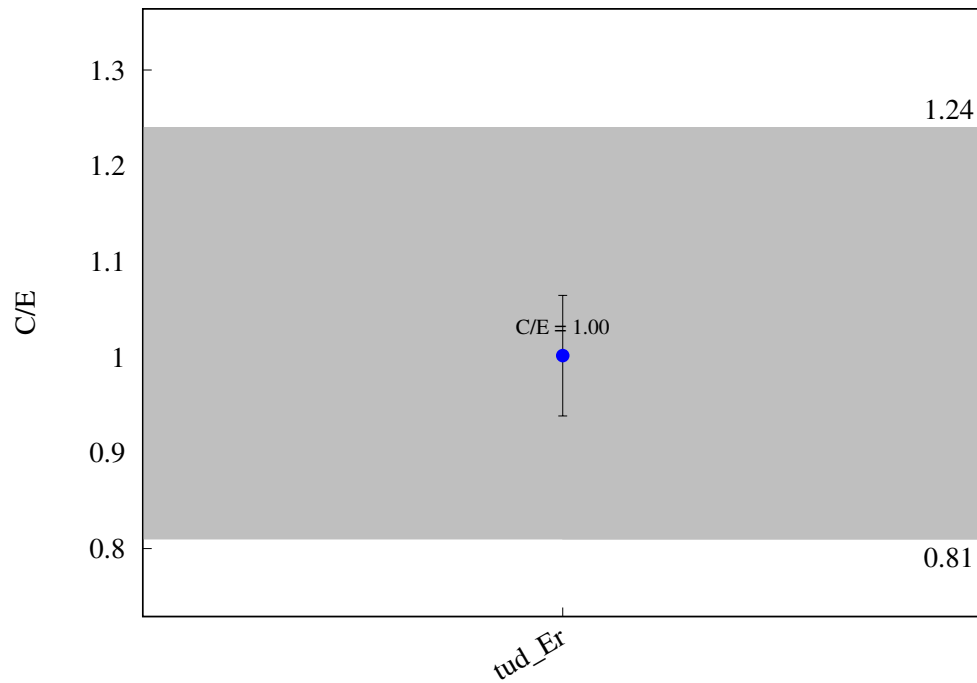
^{136}Ba (n,g) ^{137}Ba 

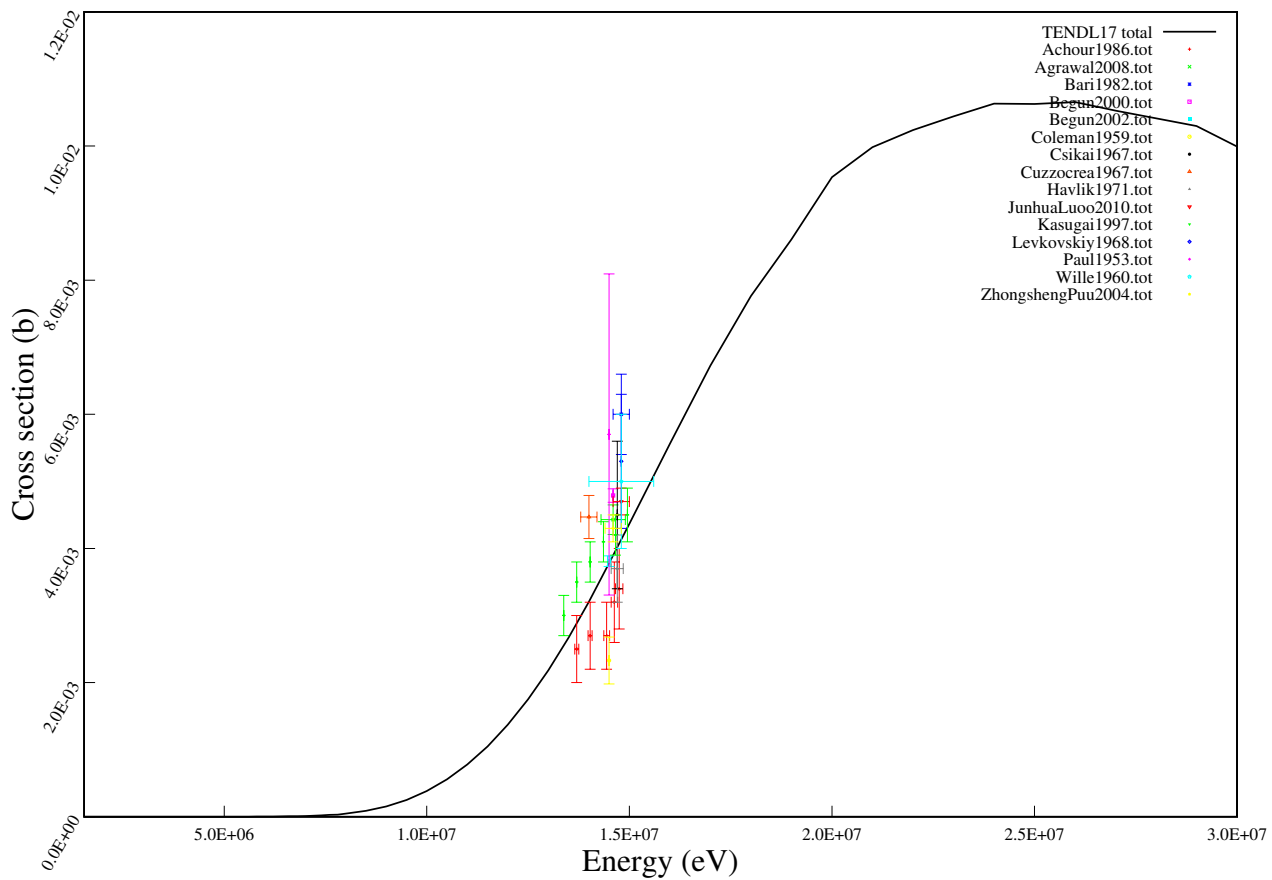
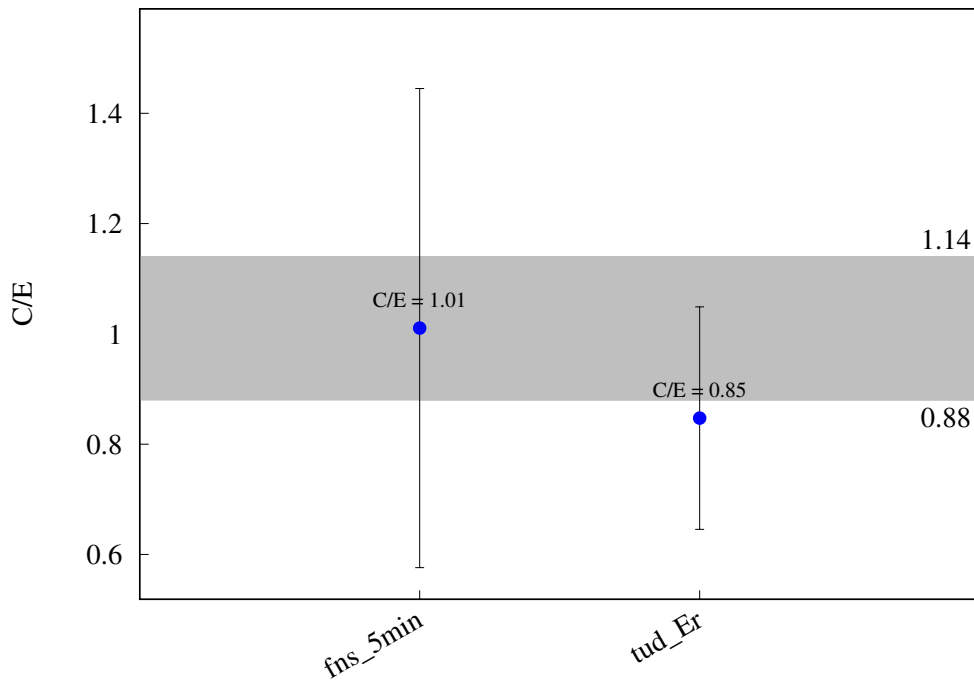
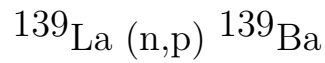
^{136}Ba (n,p) ^{136}Cs 

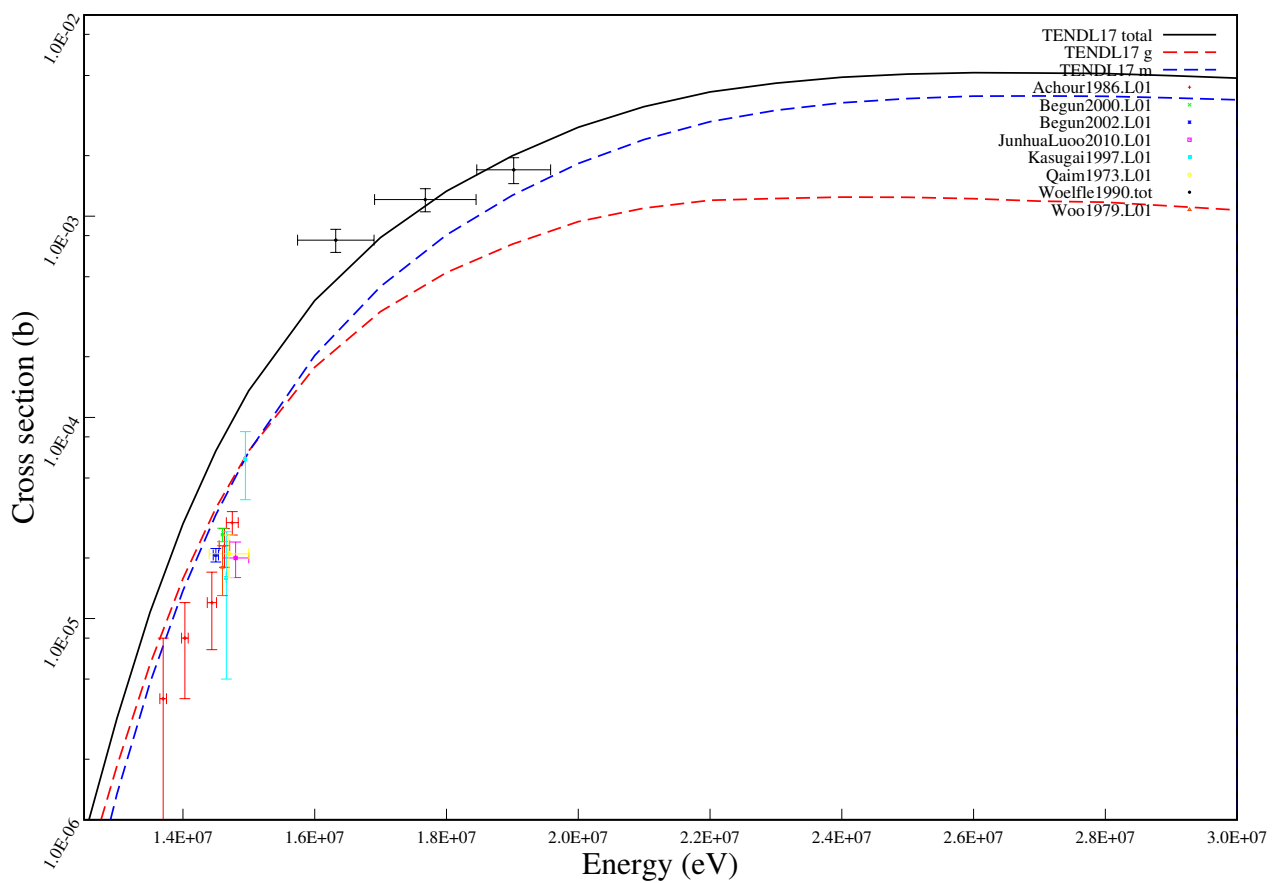
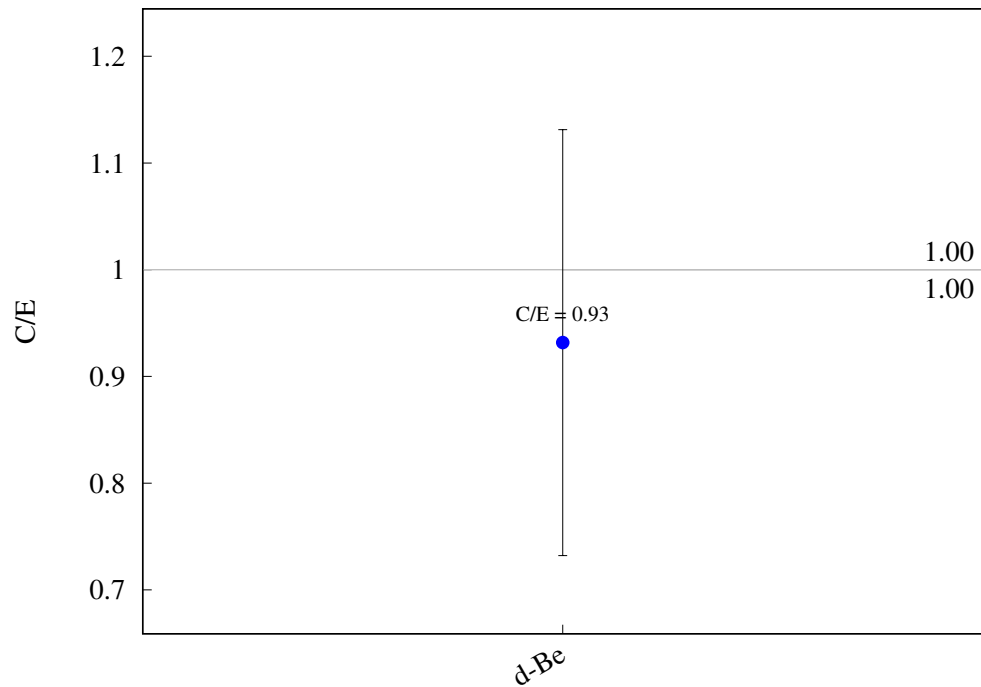
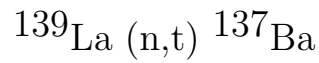
^{138}Ba (n,2n) $^{137\text{m}}\text{Ba}$ 

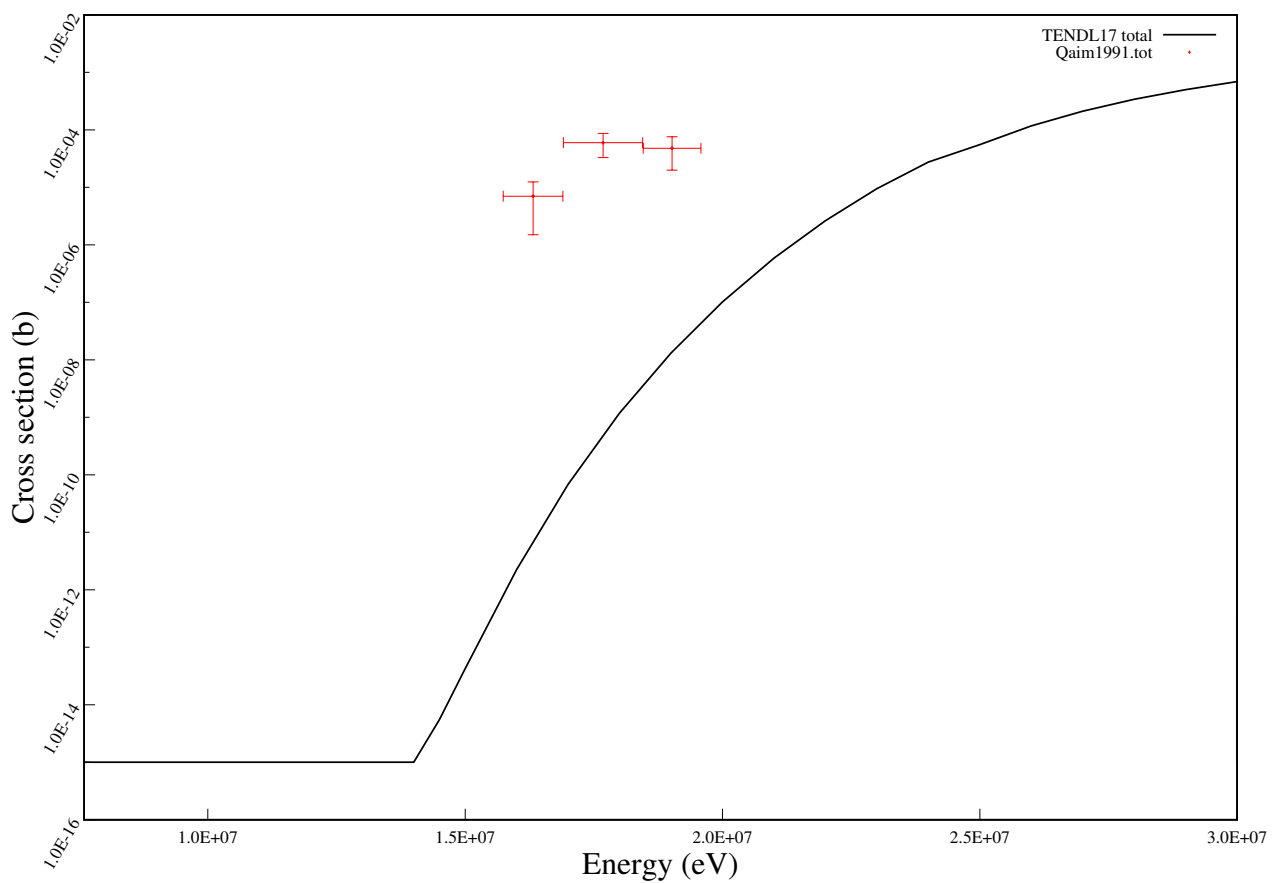
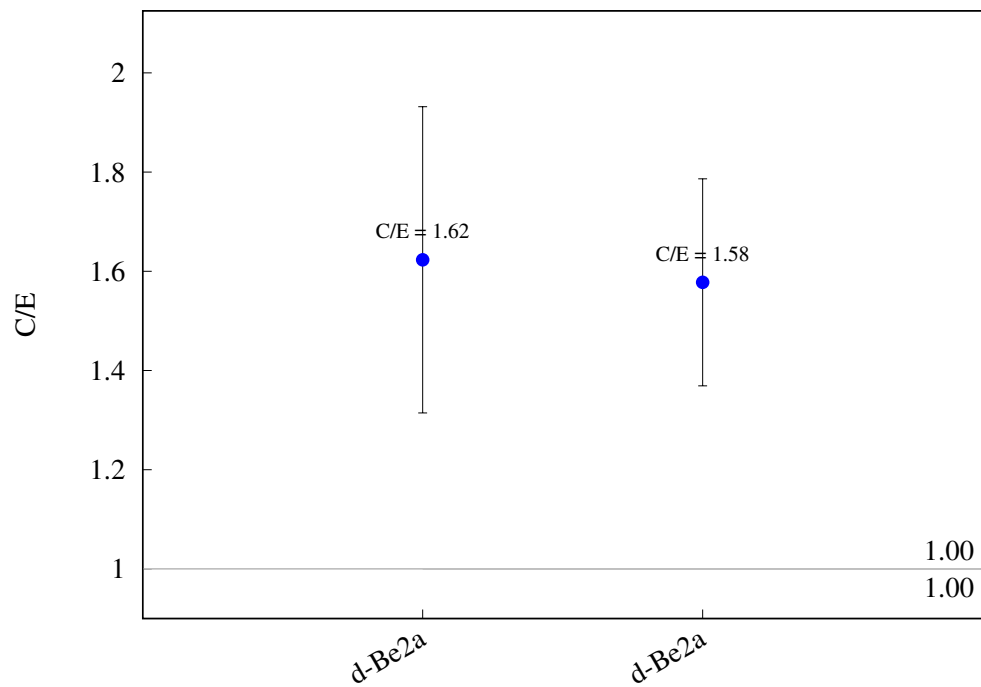
^{138}Ba (n,g) ^{139}Ba 

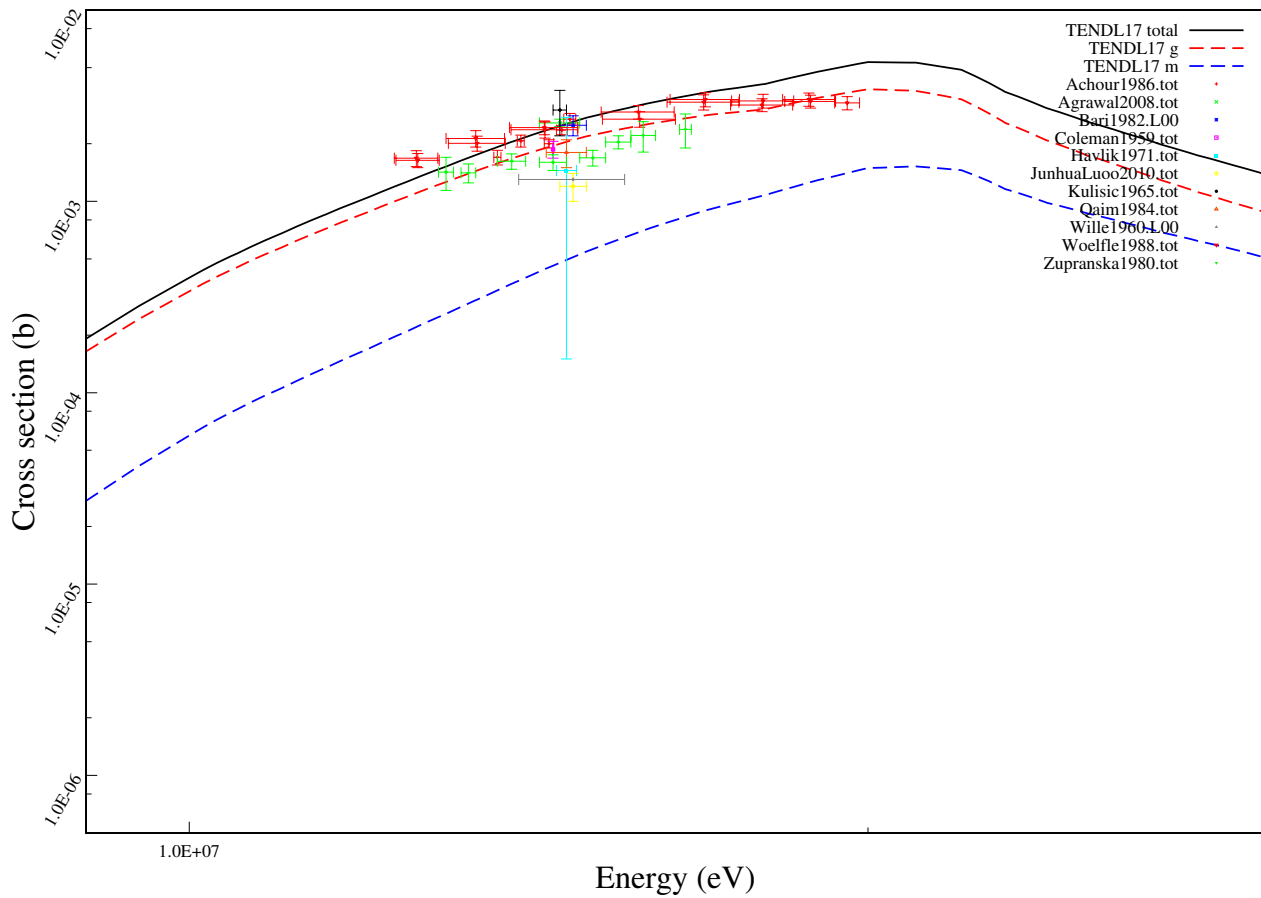
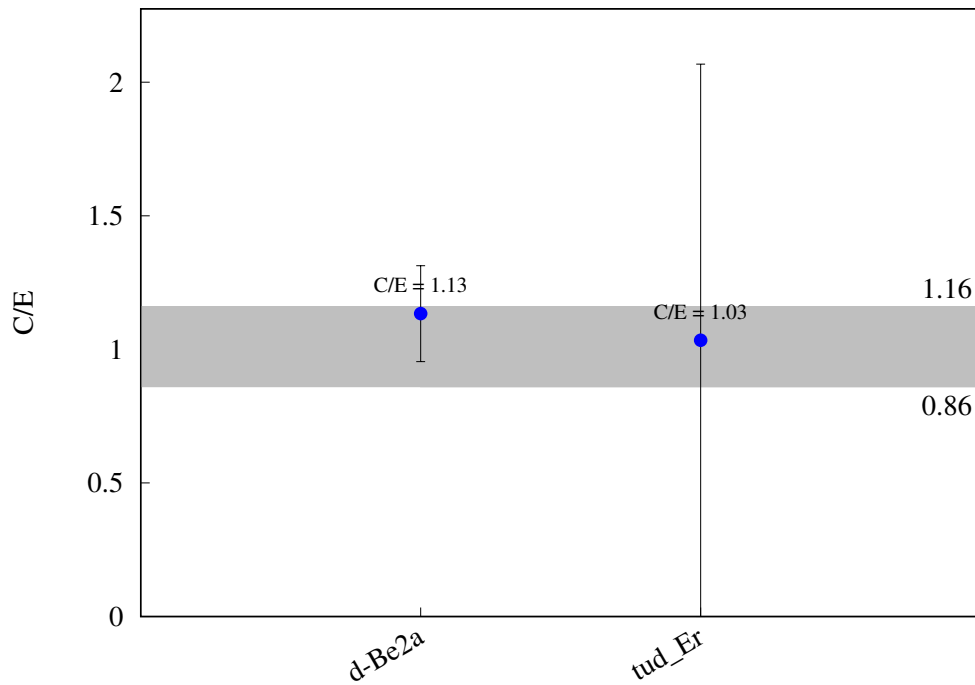
$^{138}\text{Ba} (\text{n},\text{p}) ^{138}\text{Cs}$ 

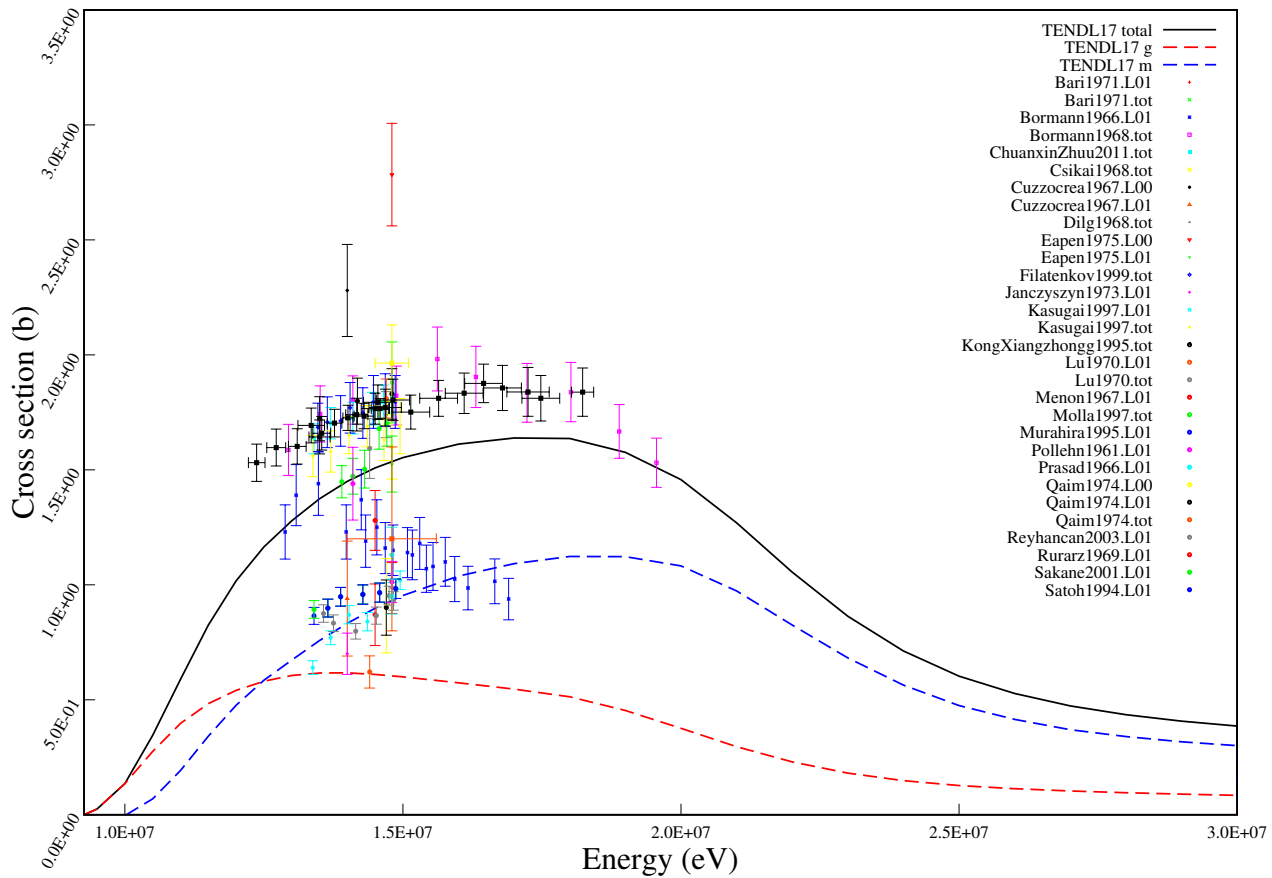
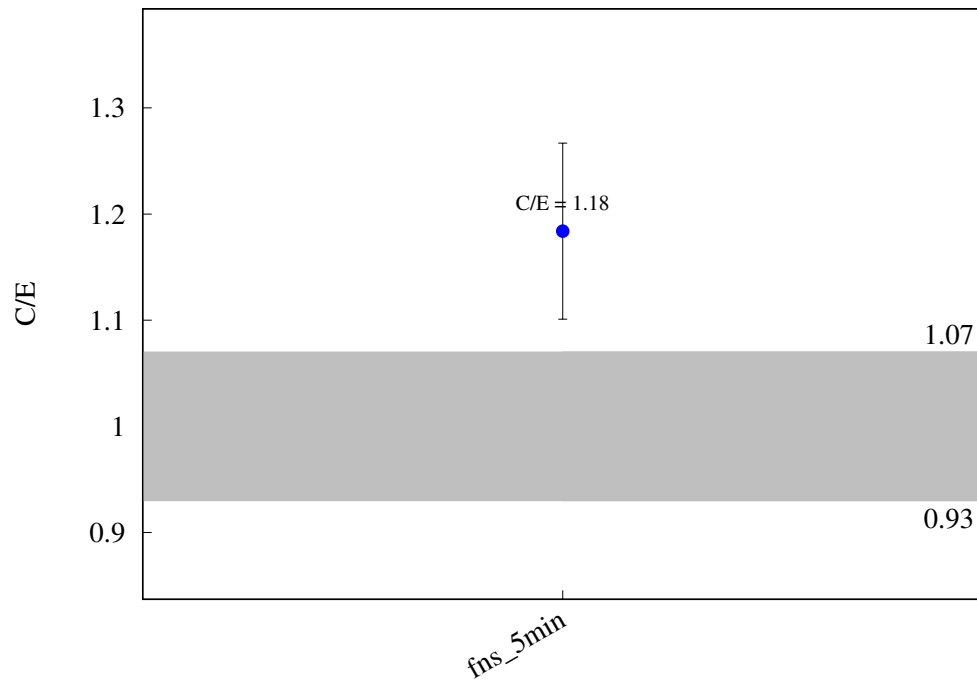
^{139}La (n,g) ^{140}La 

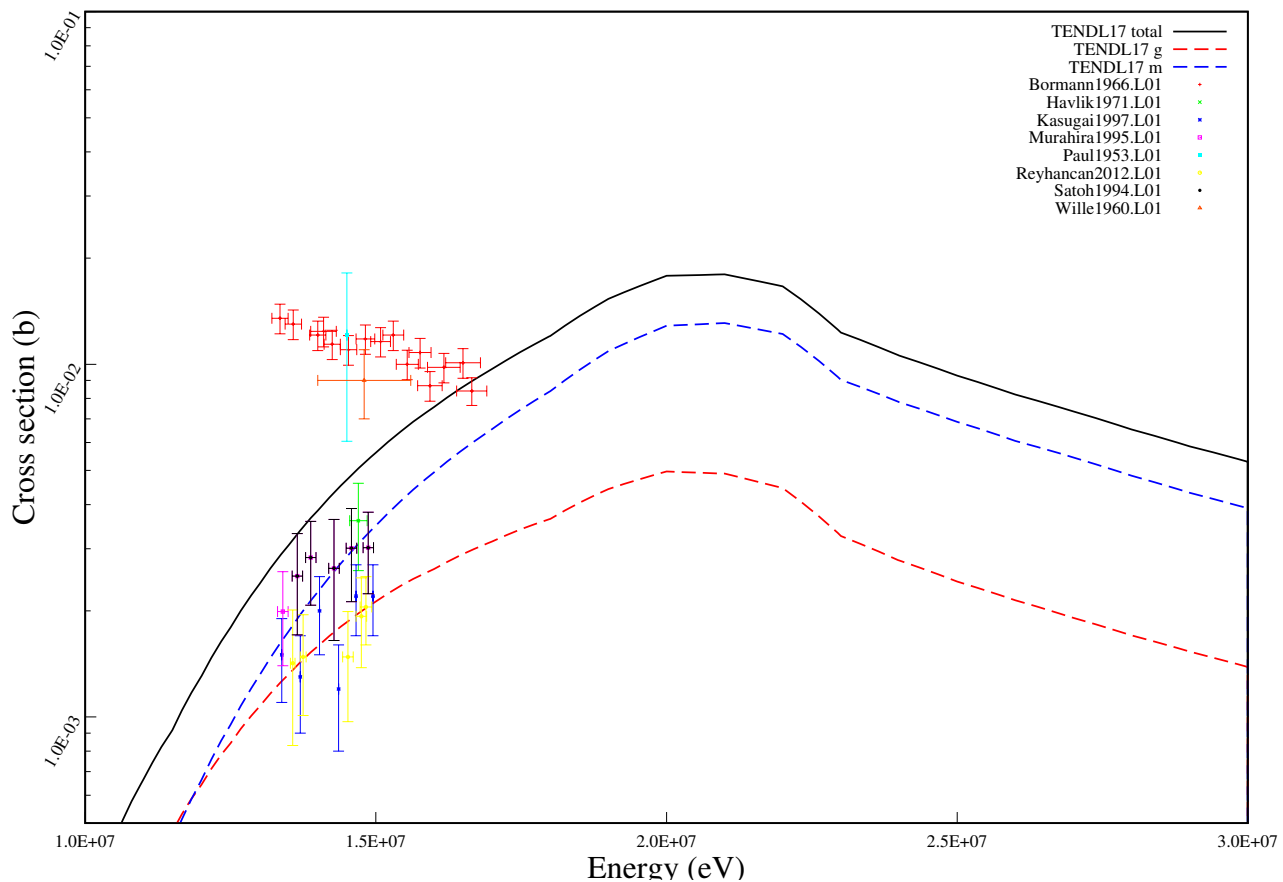
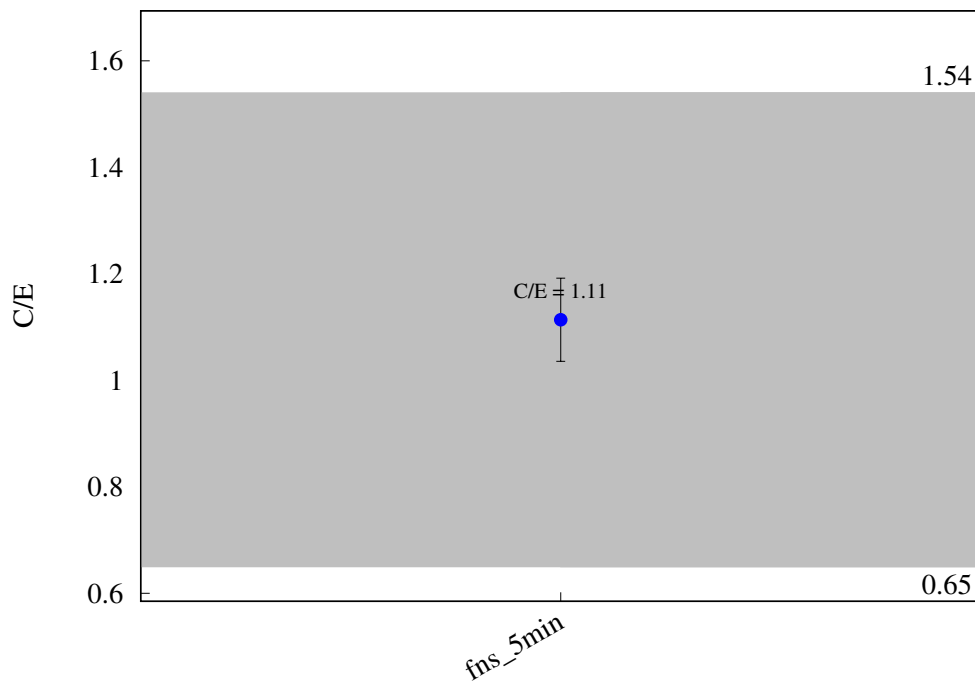


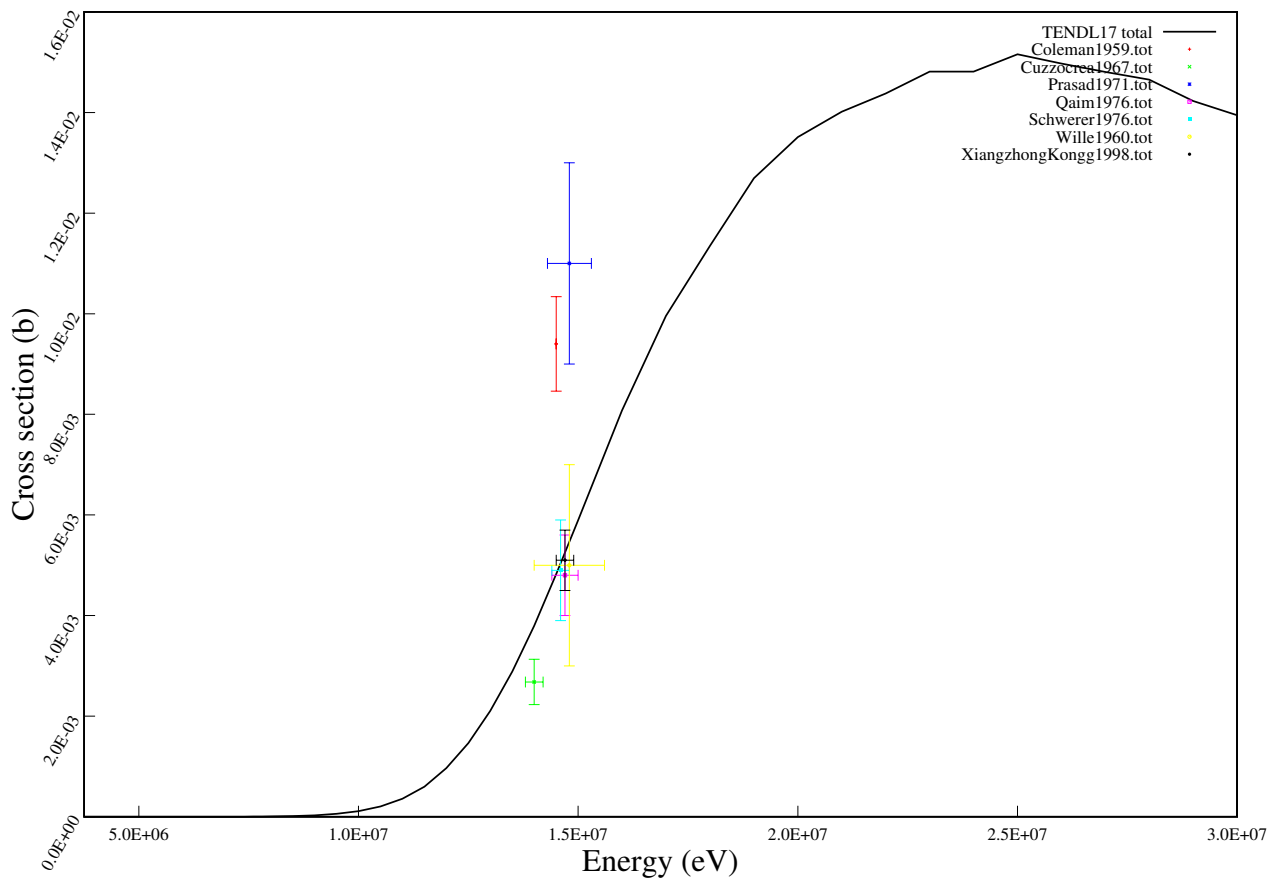
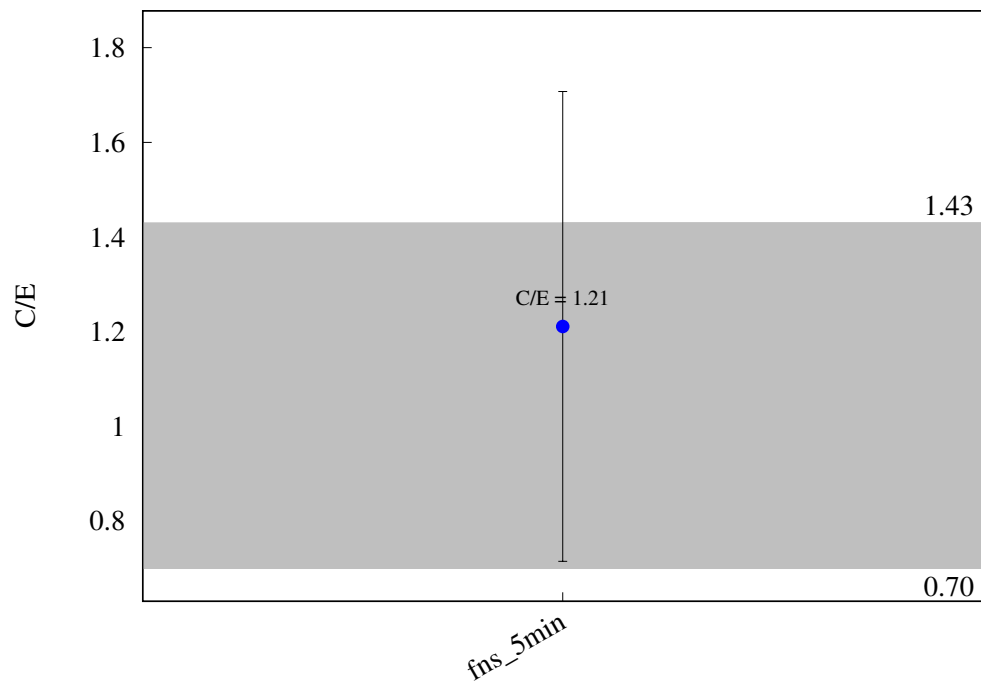


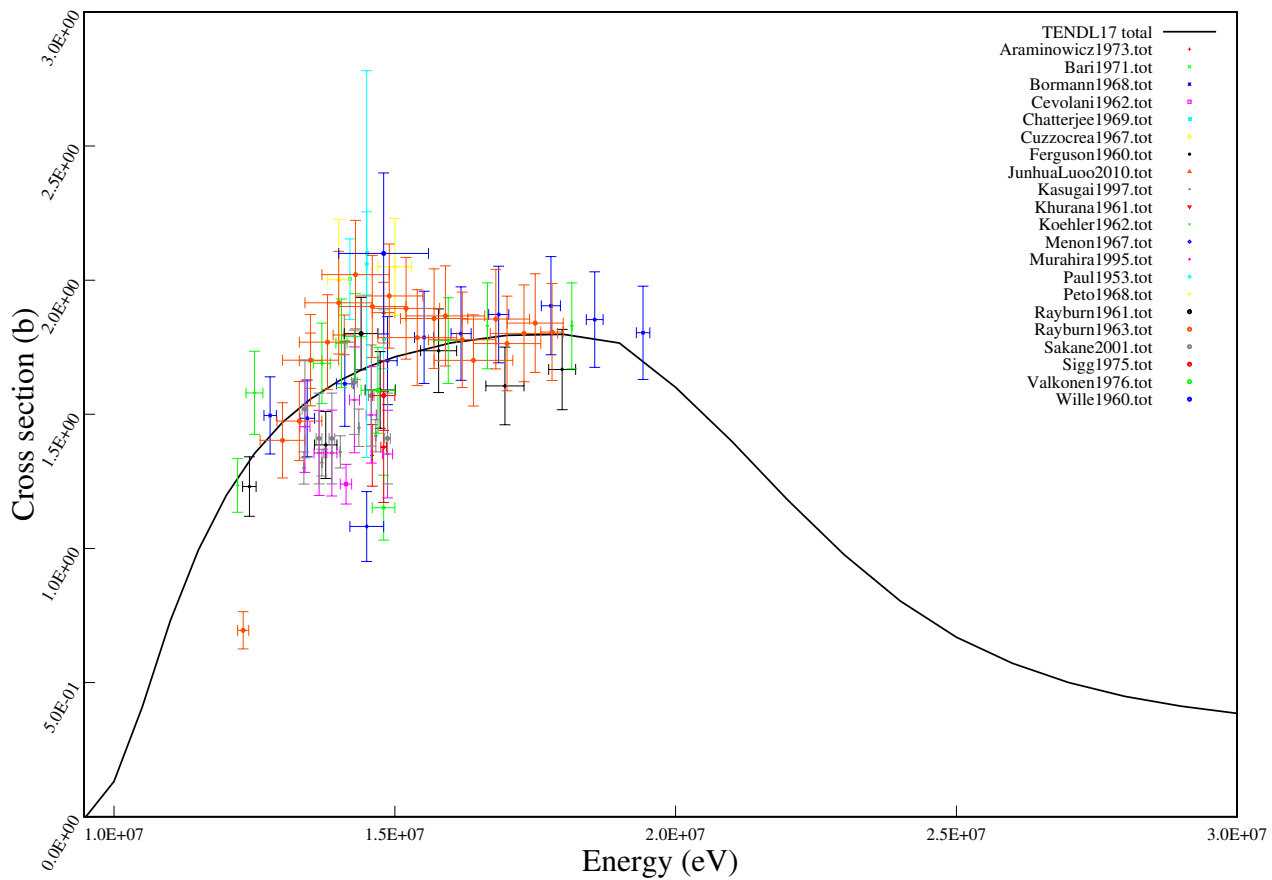
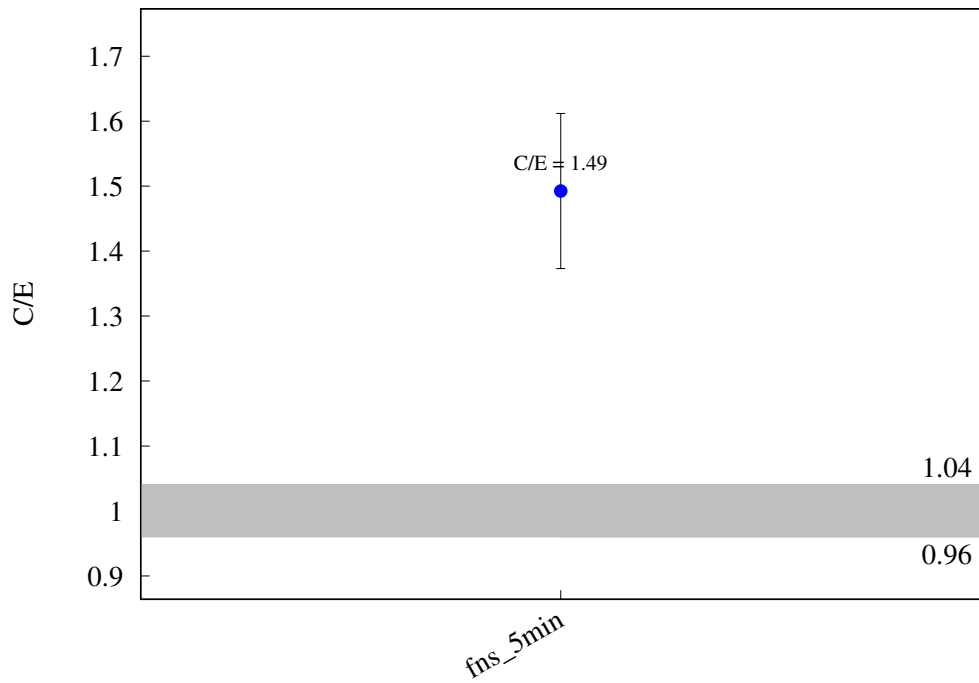
$^{139}\text{La} (\text{n},\text{h}) ^{137}\text{Cs}$ 

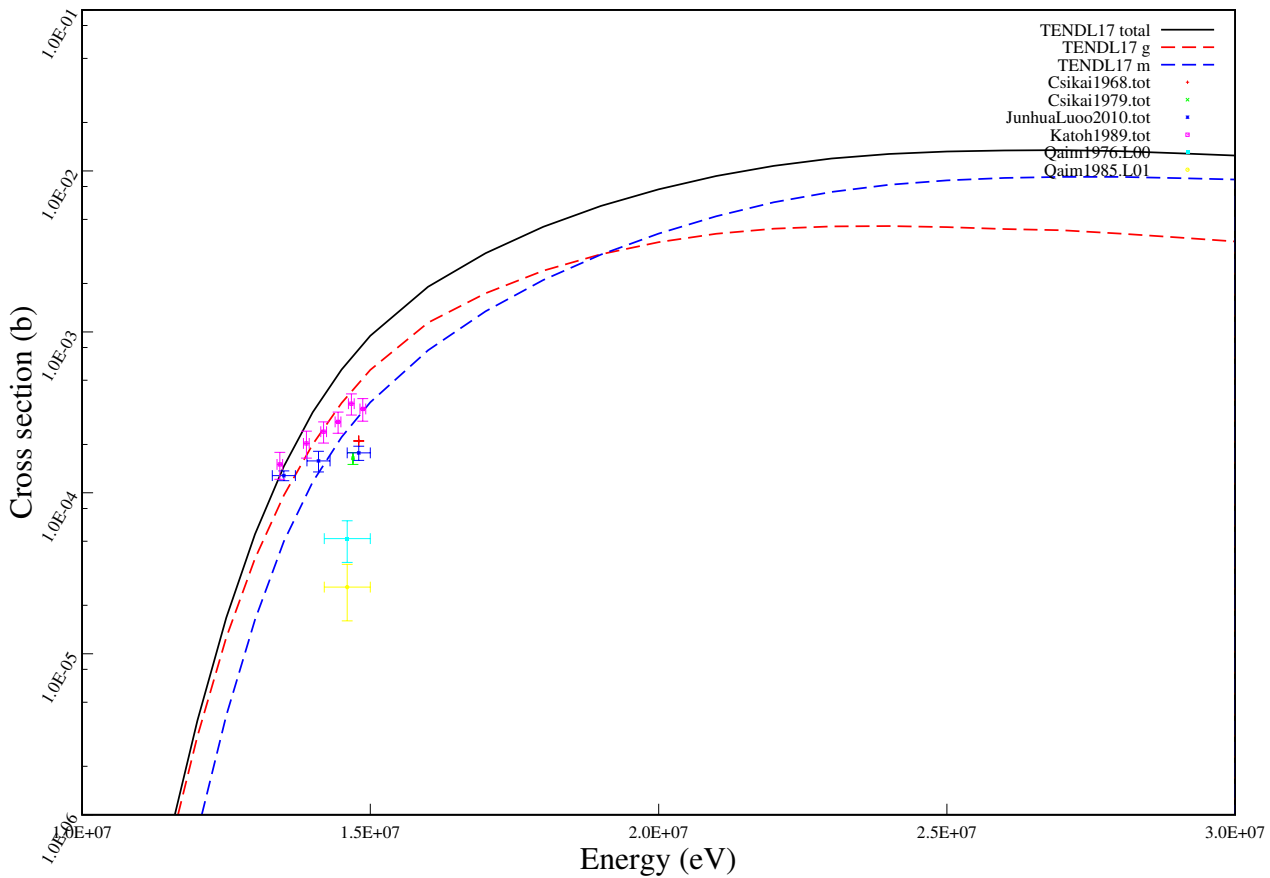
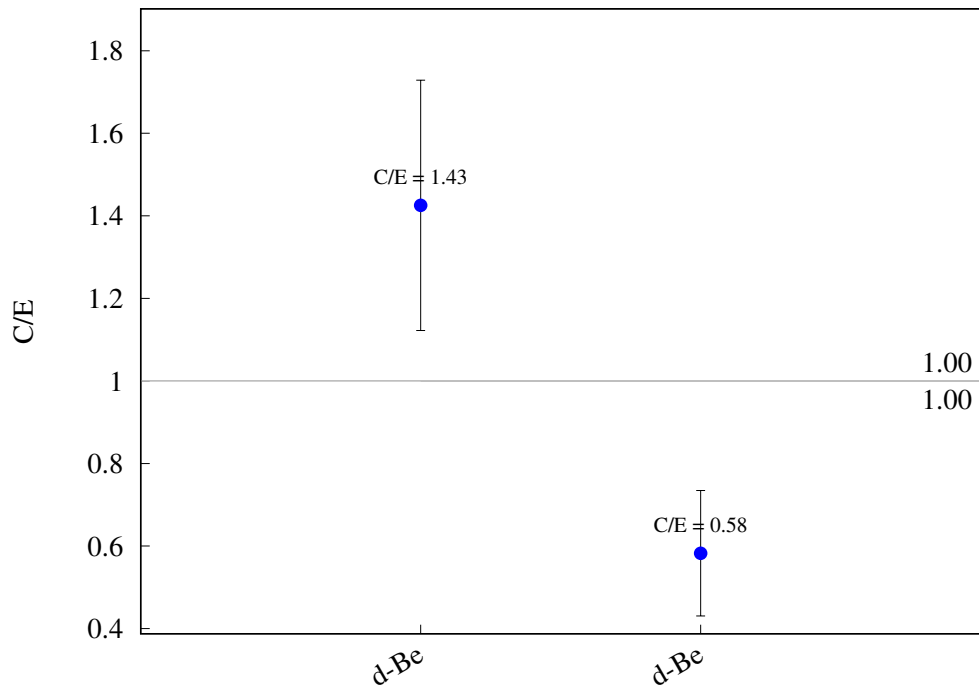
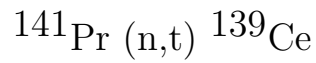
$^{139}\text{La} (\text{n},\text{a}) ^{136}\text{Cs}$ 

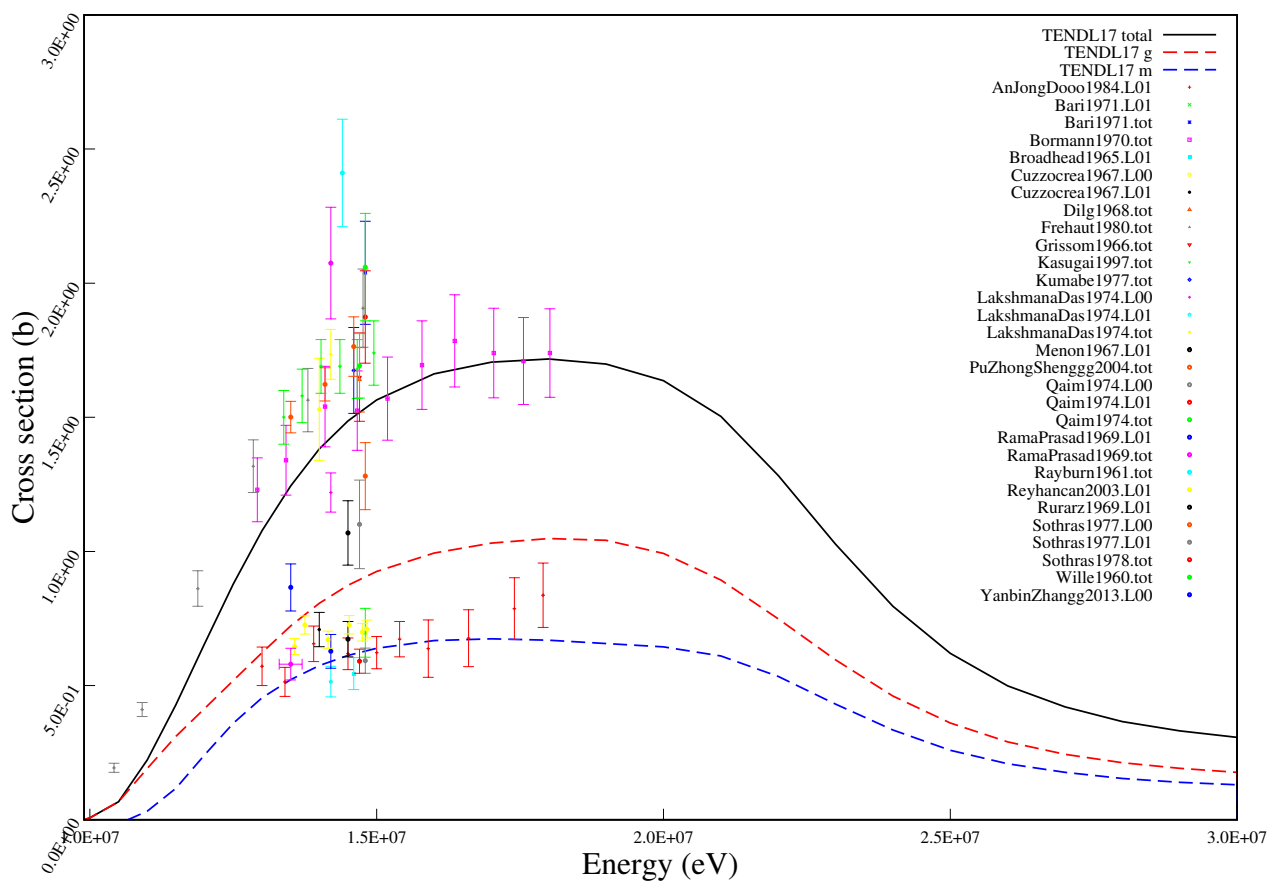
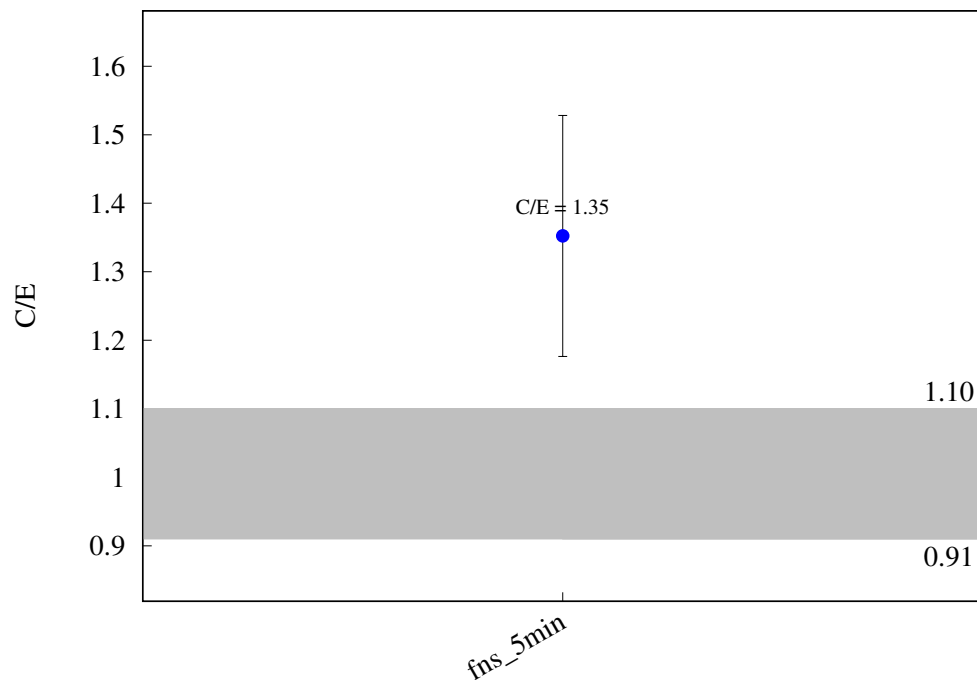
^{140}Ce (n,2n) ^{139m}Ce 

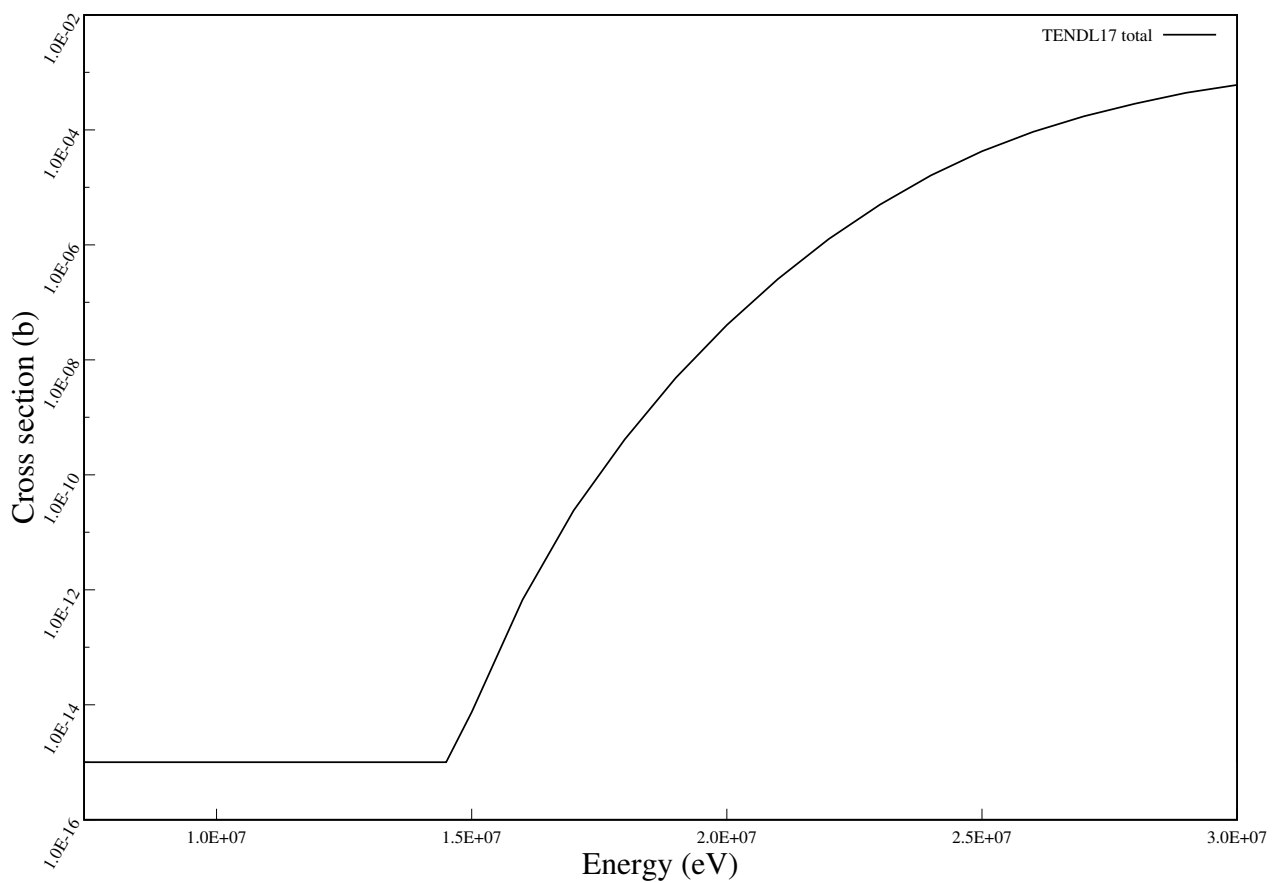
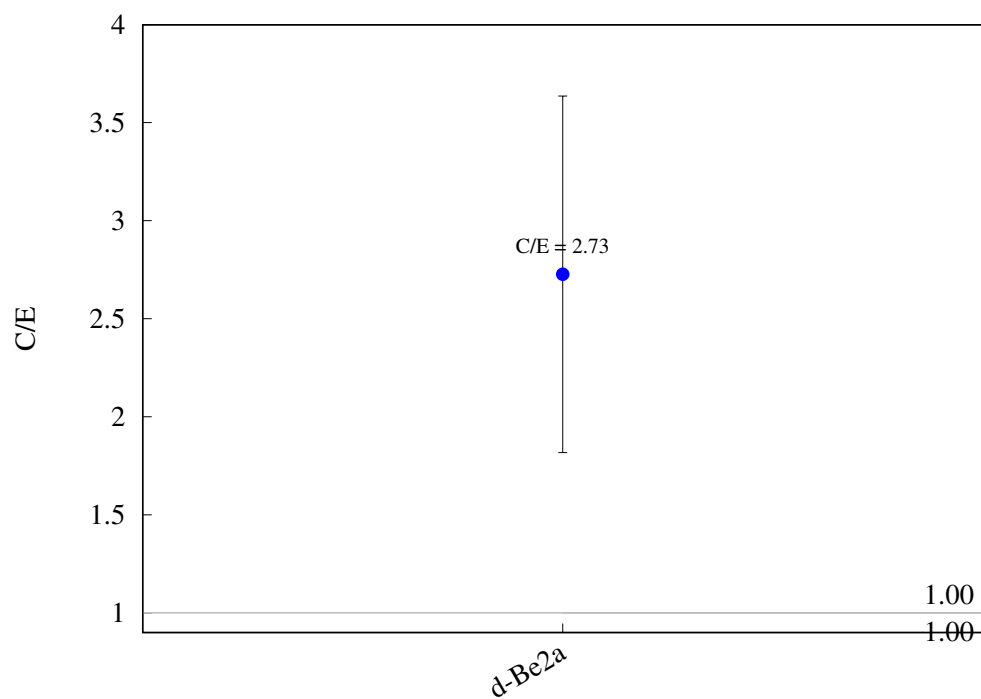
$^{140}\text{Ce} (\text{n},\text{a}) ^{137m}\text{Ba}$ 

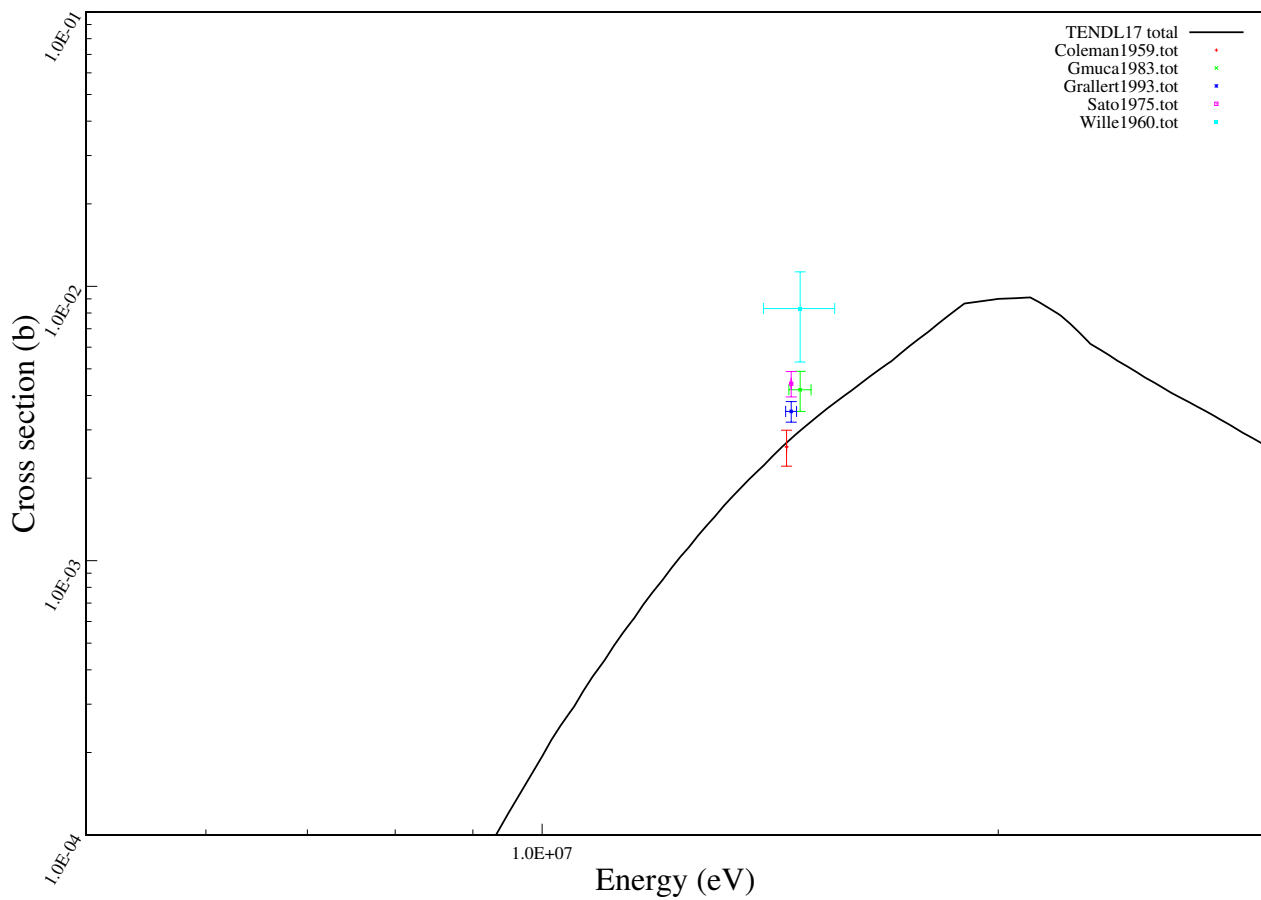
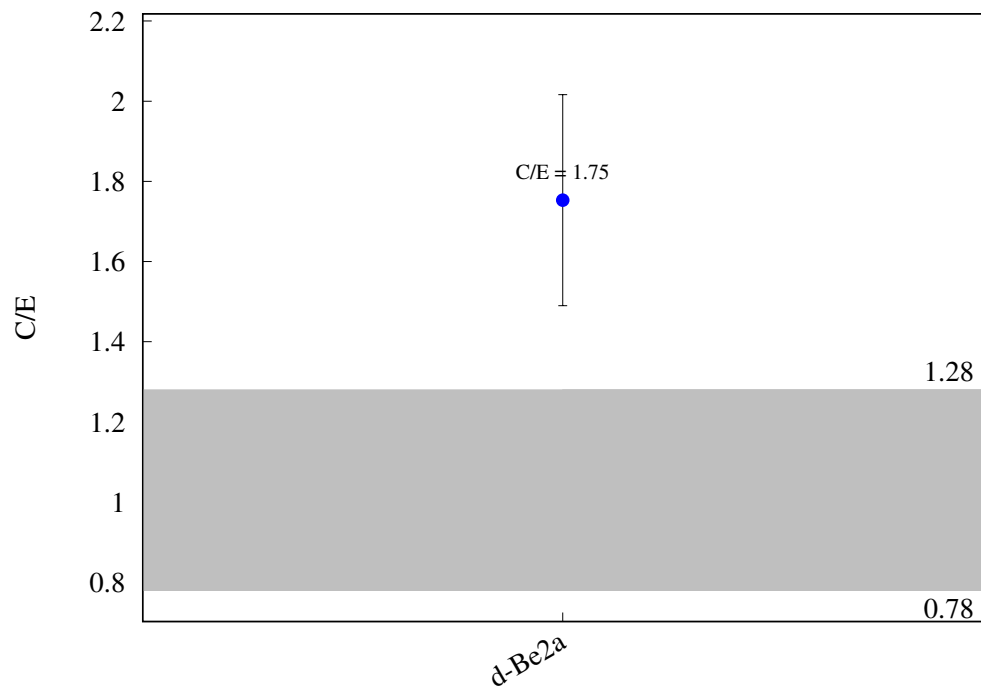
$^{142}\text{Ce} (\text{n},\text{p}) ^{142}\text{La}$ 

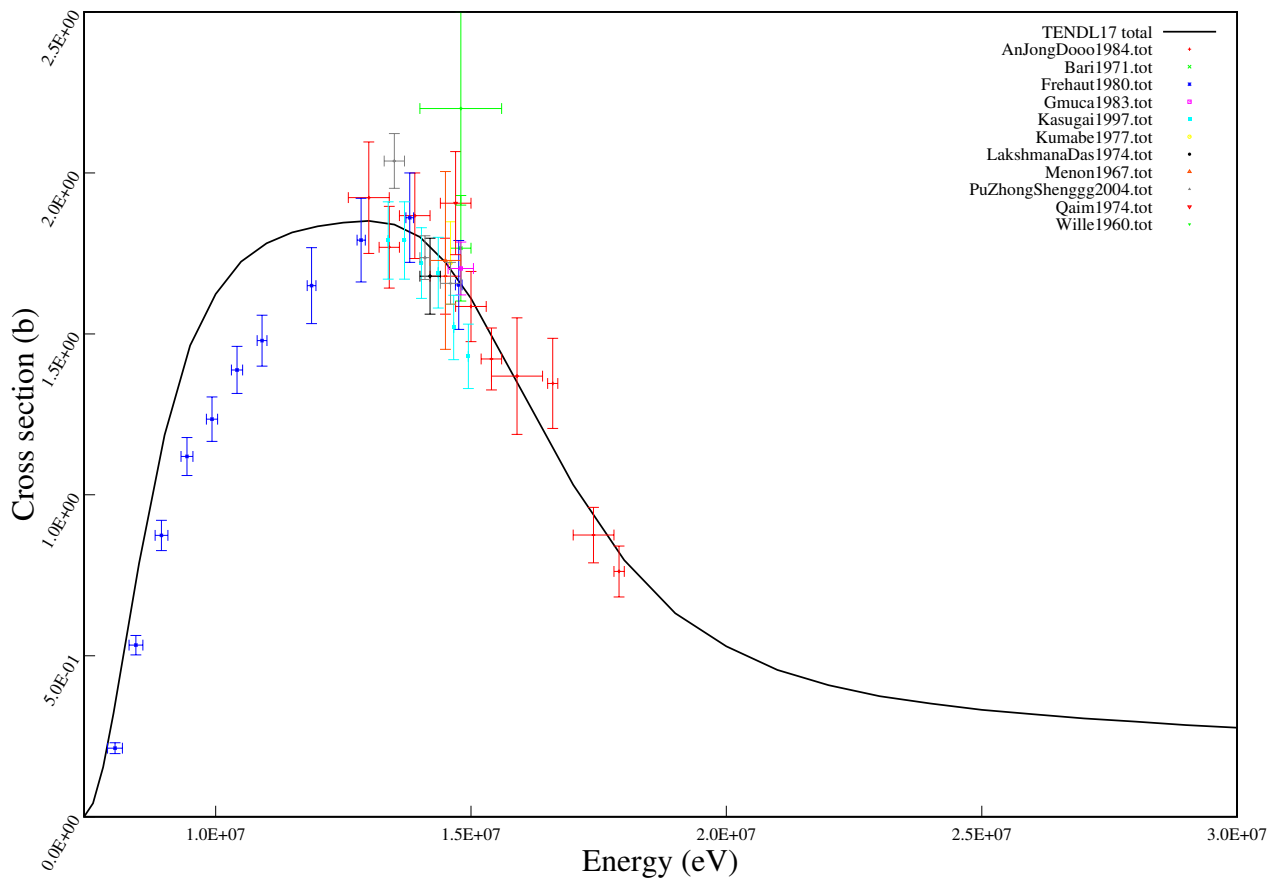
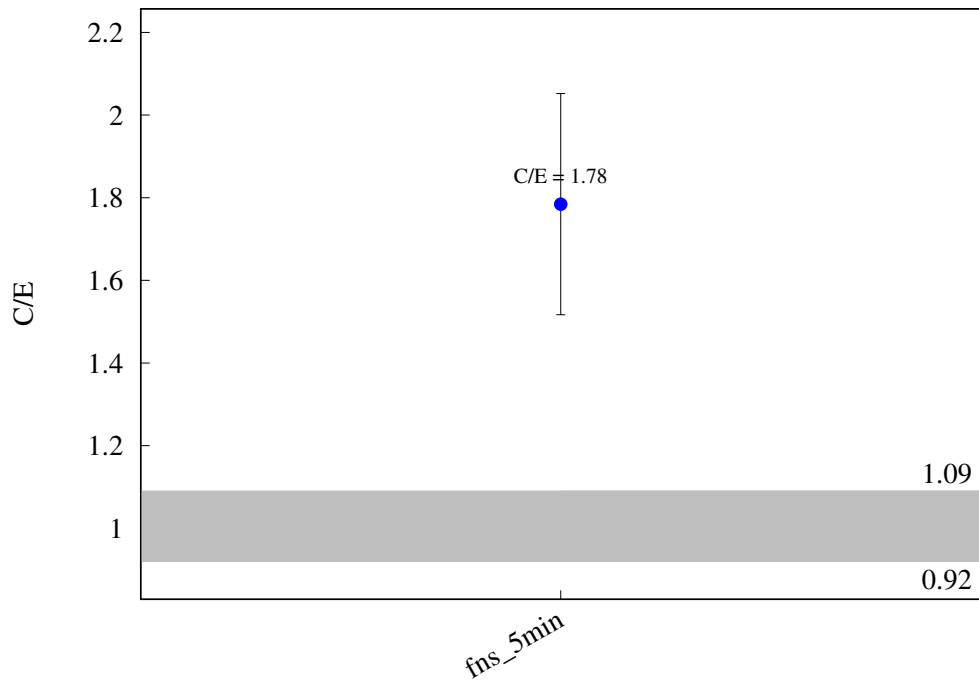
^{141}Pr (n,2n) ^{140}Pr 

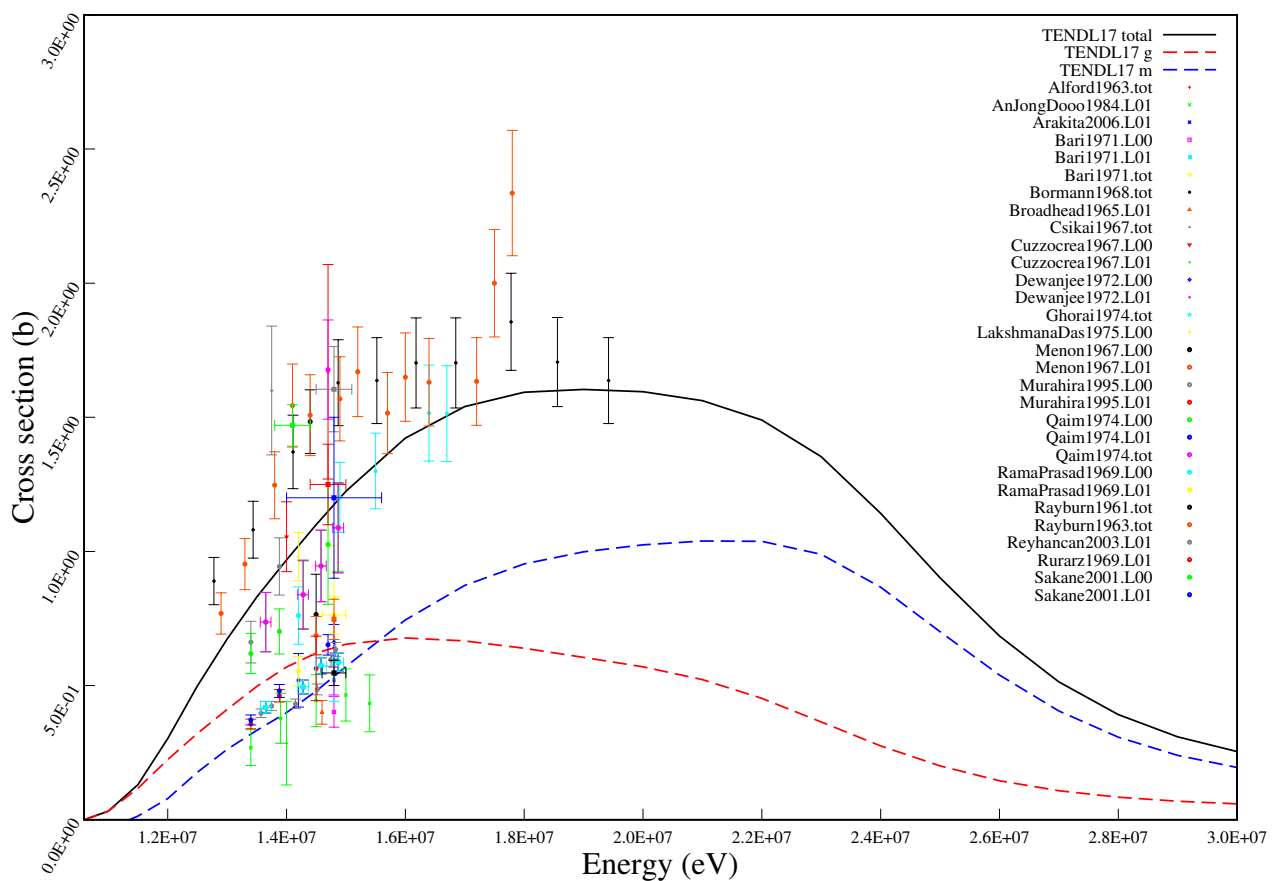
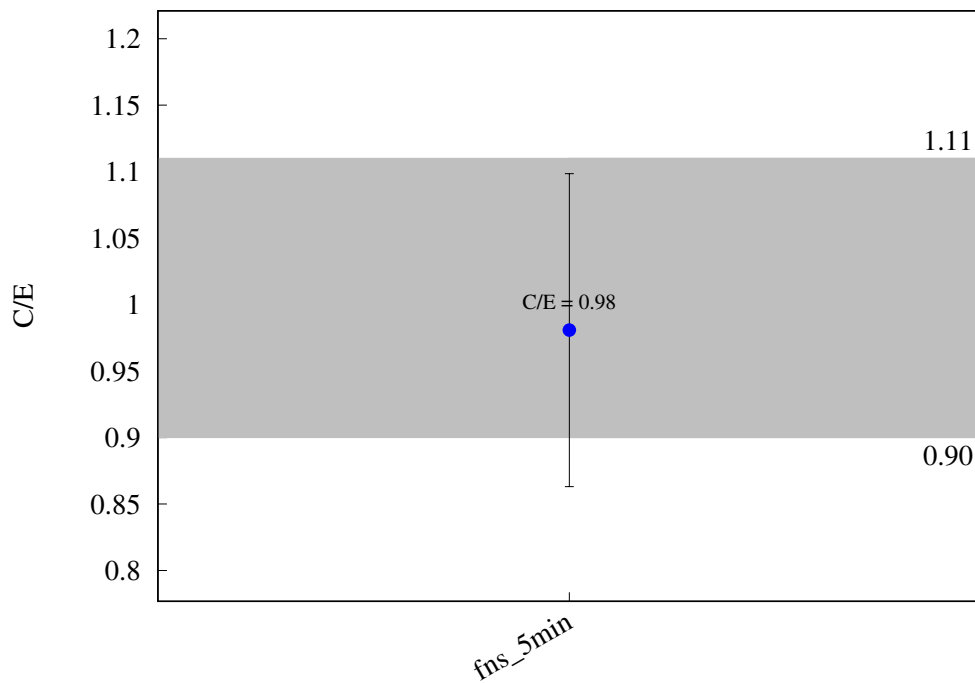


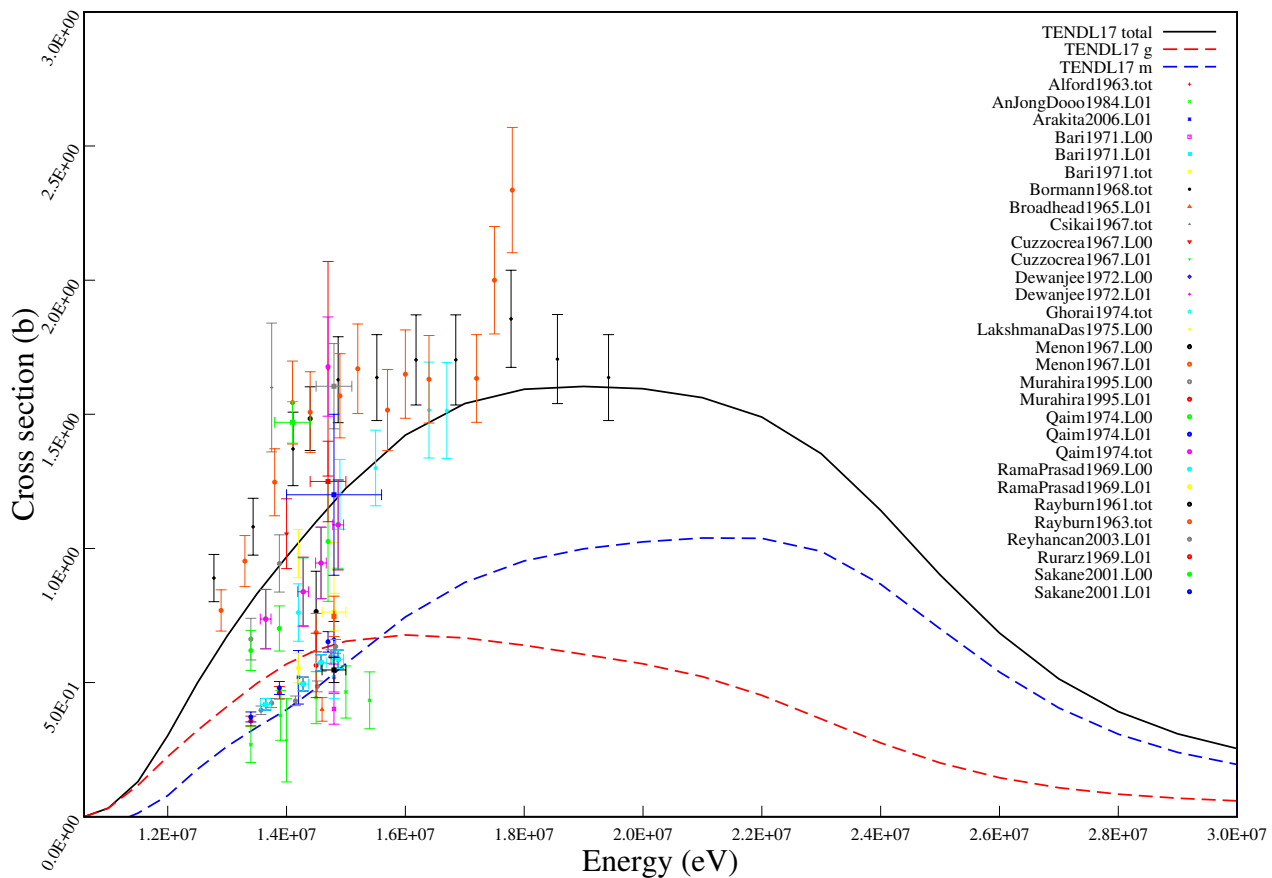
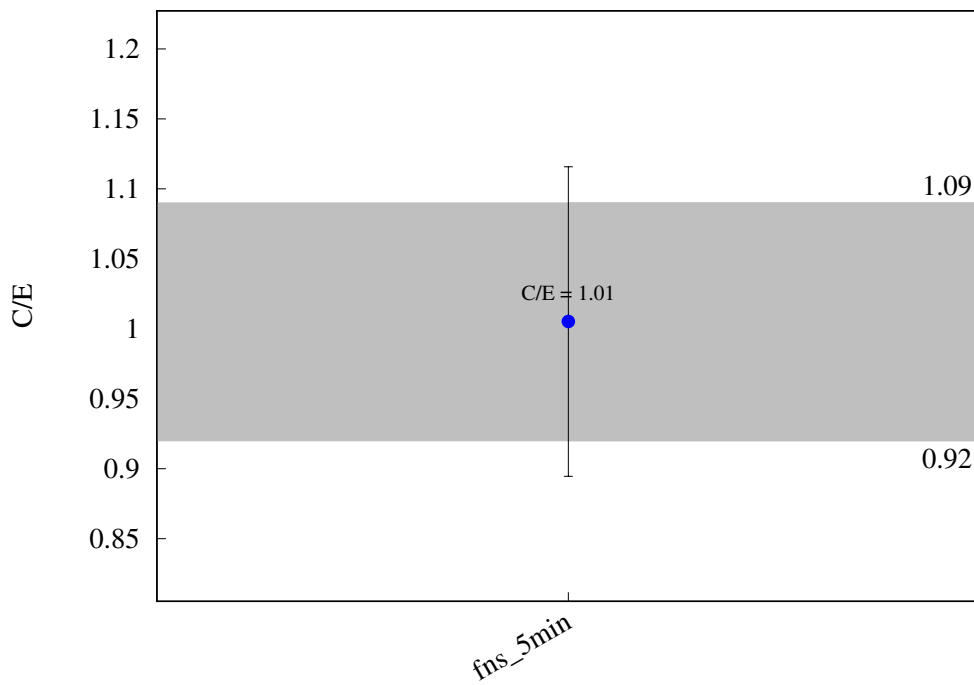
^{142}Nd ($n,2n$) ^{141m}Nd 

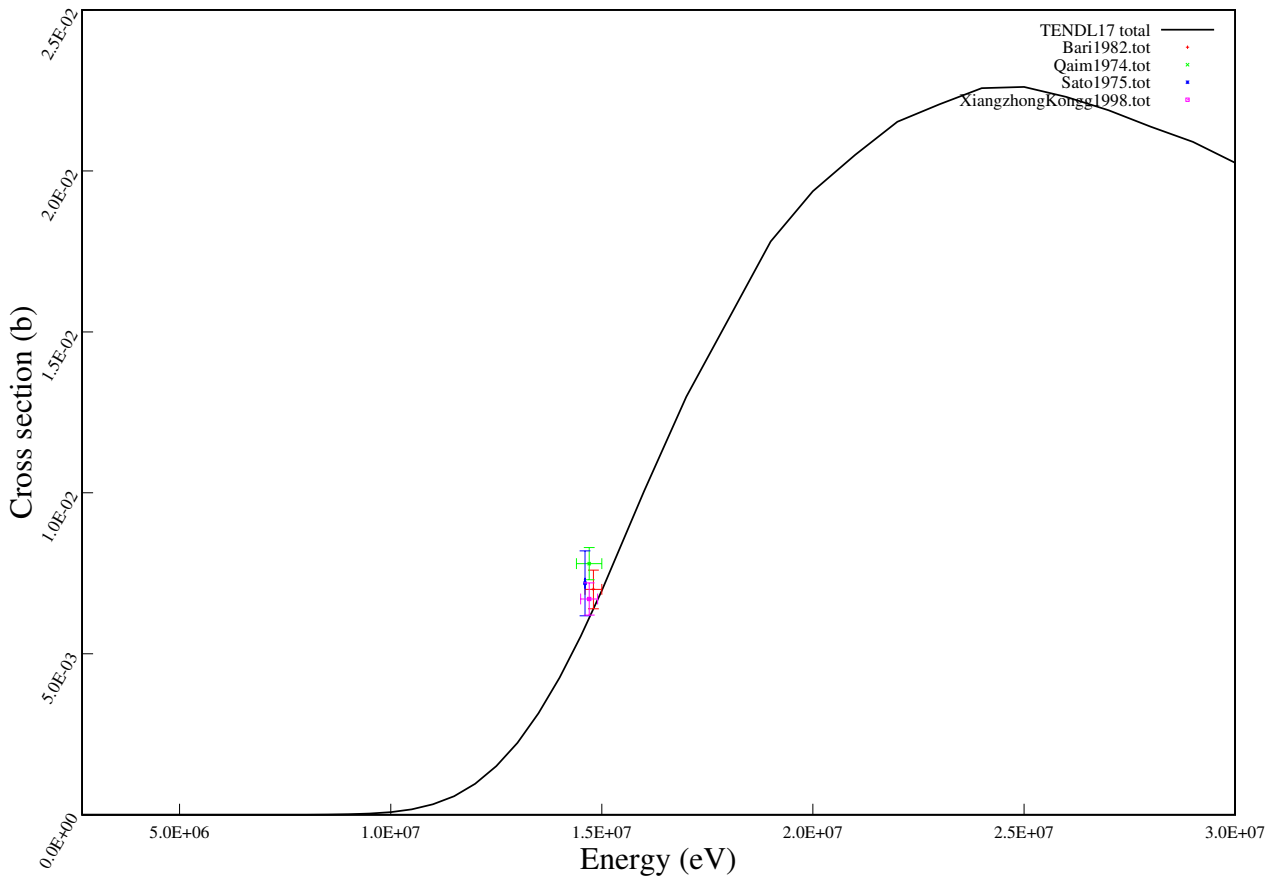
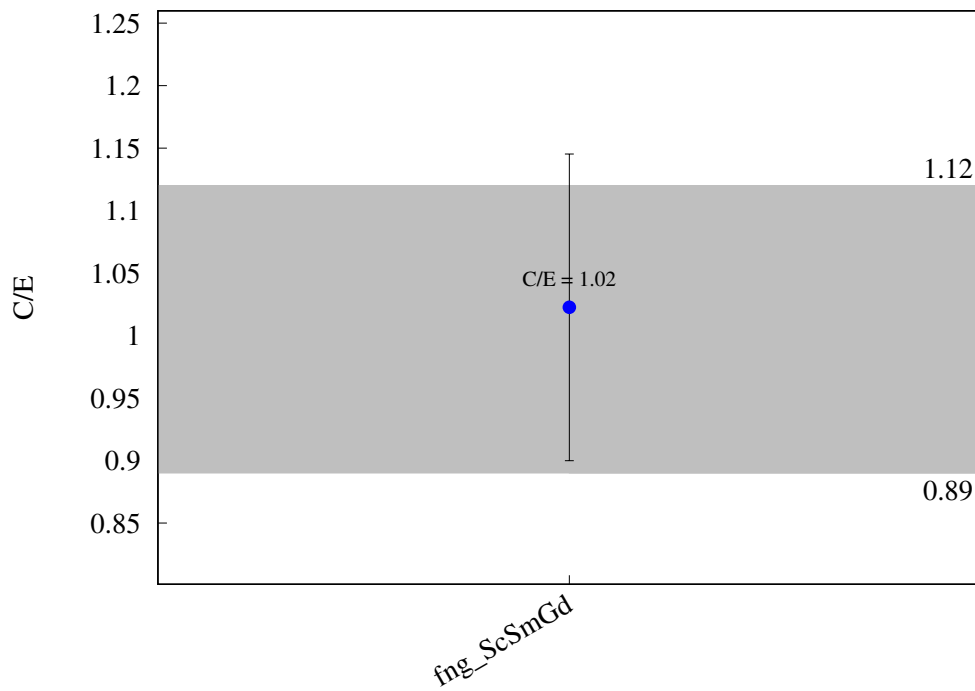
^{146}Nd (n,h) ^{144}Ce 

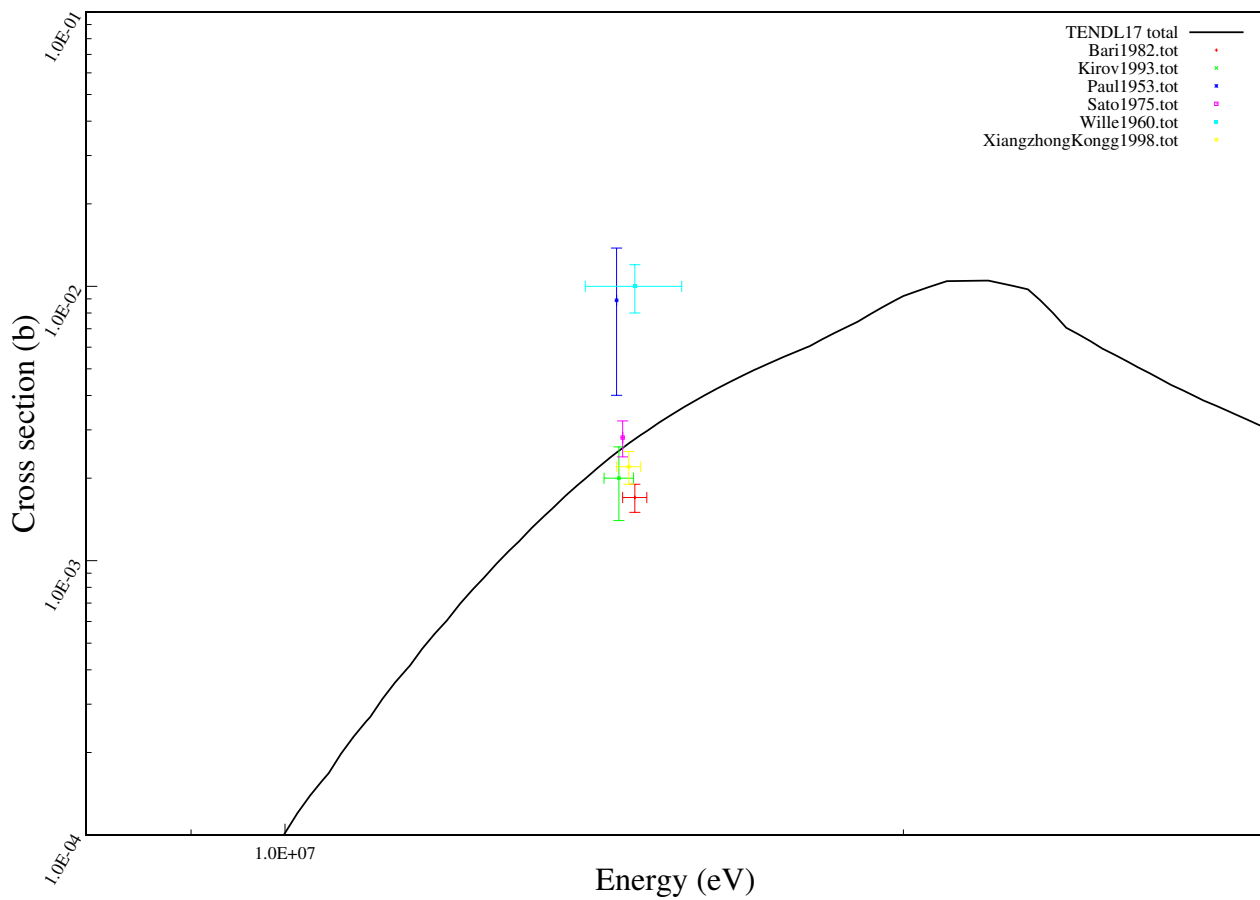
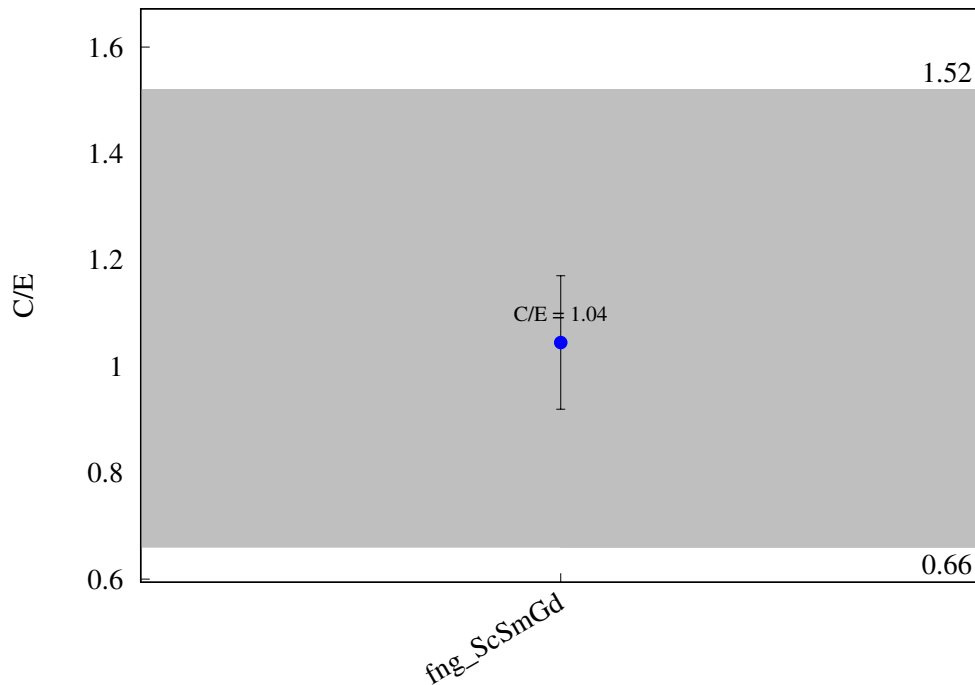
^{146}Nd (n,a) ^{143}Ce 

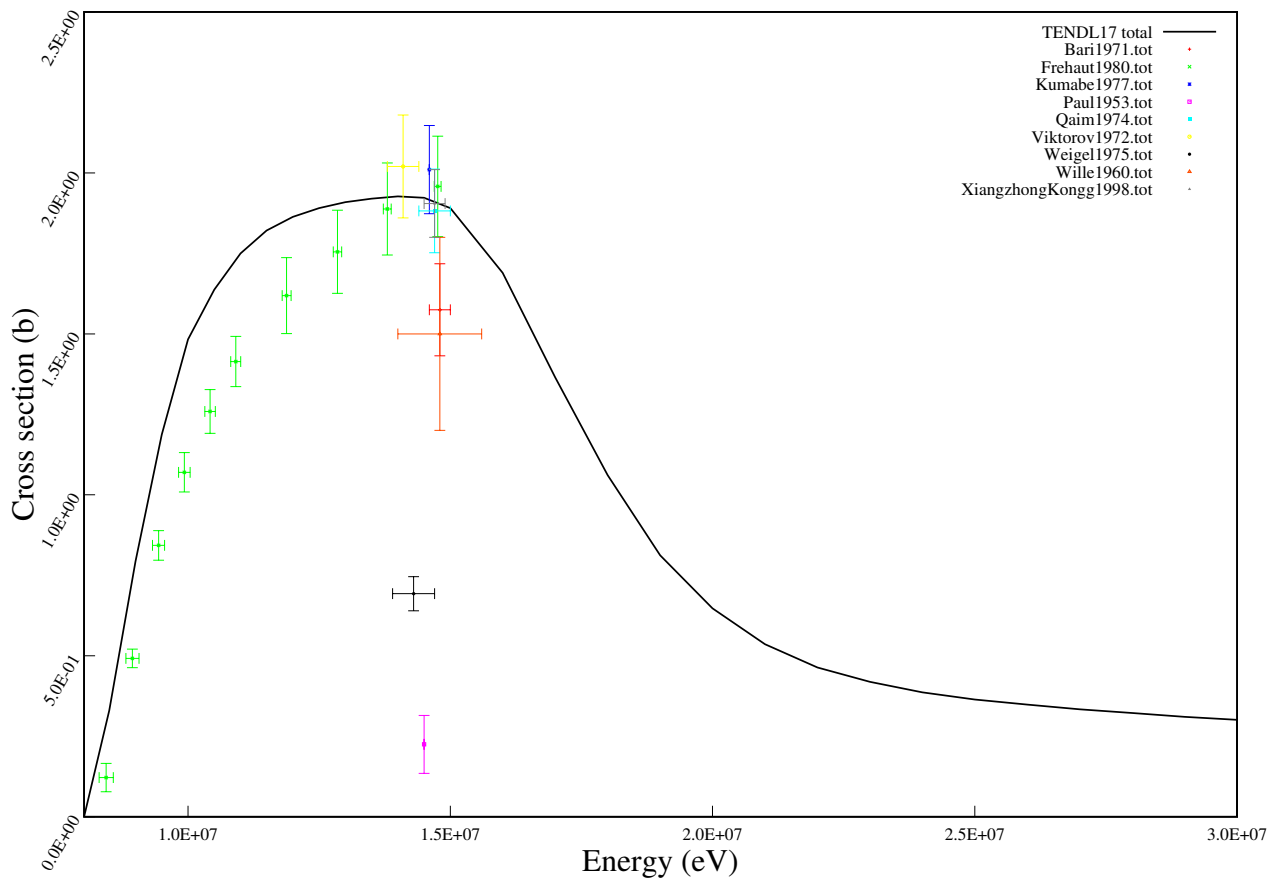
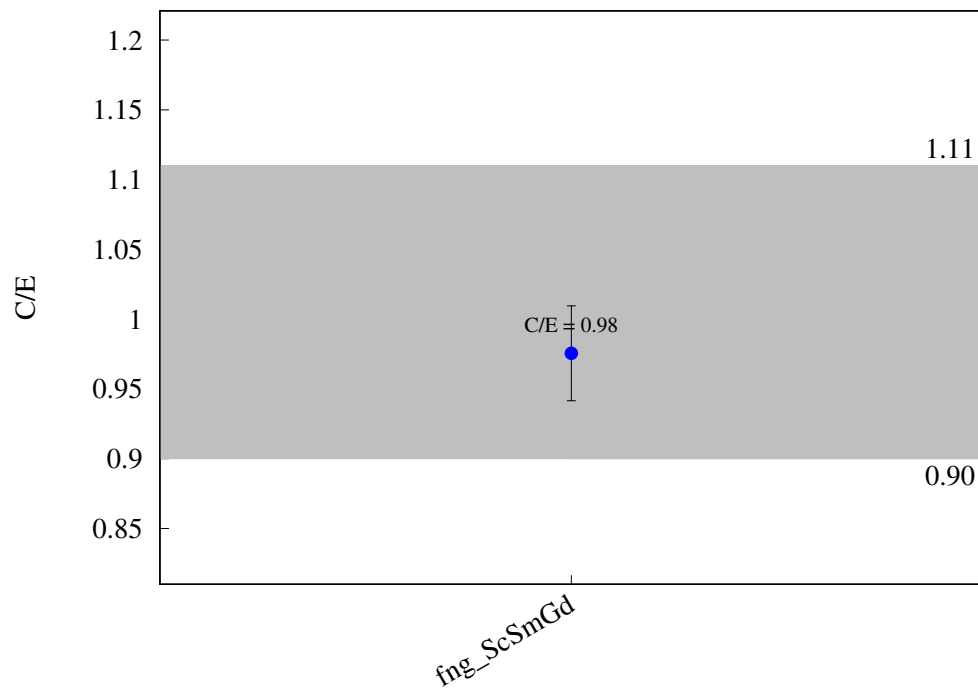


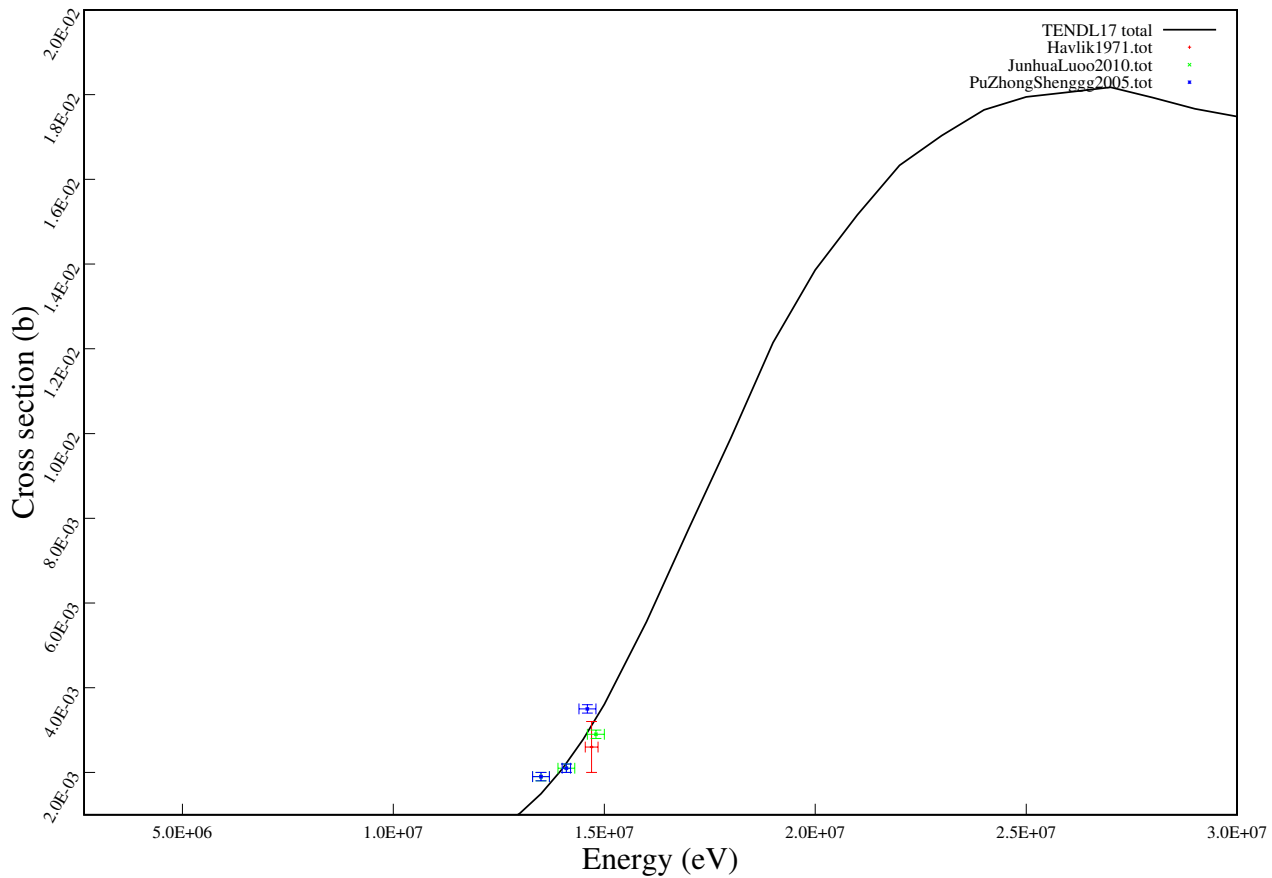
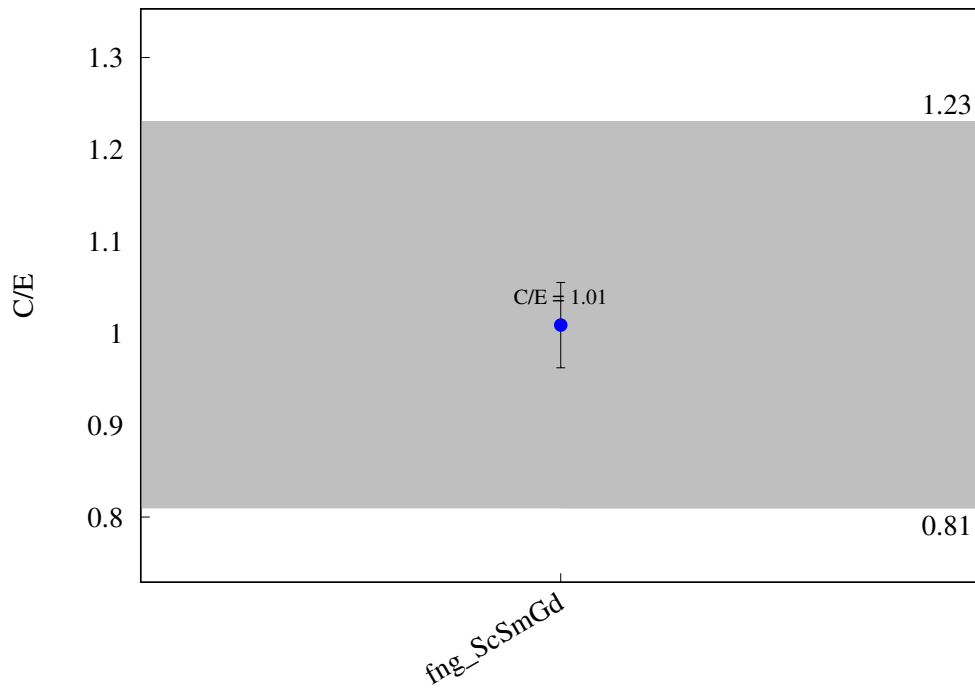
^{144}Sm (n,2n) $^{143\text{m}}\text{Sm}$ 

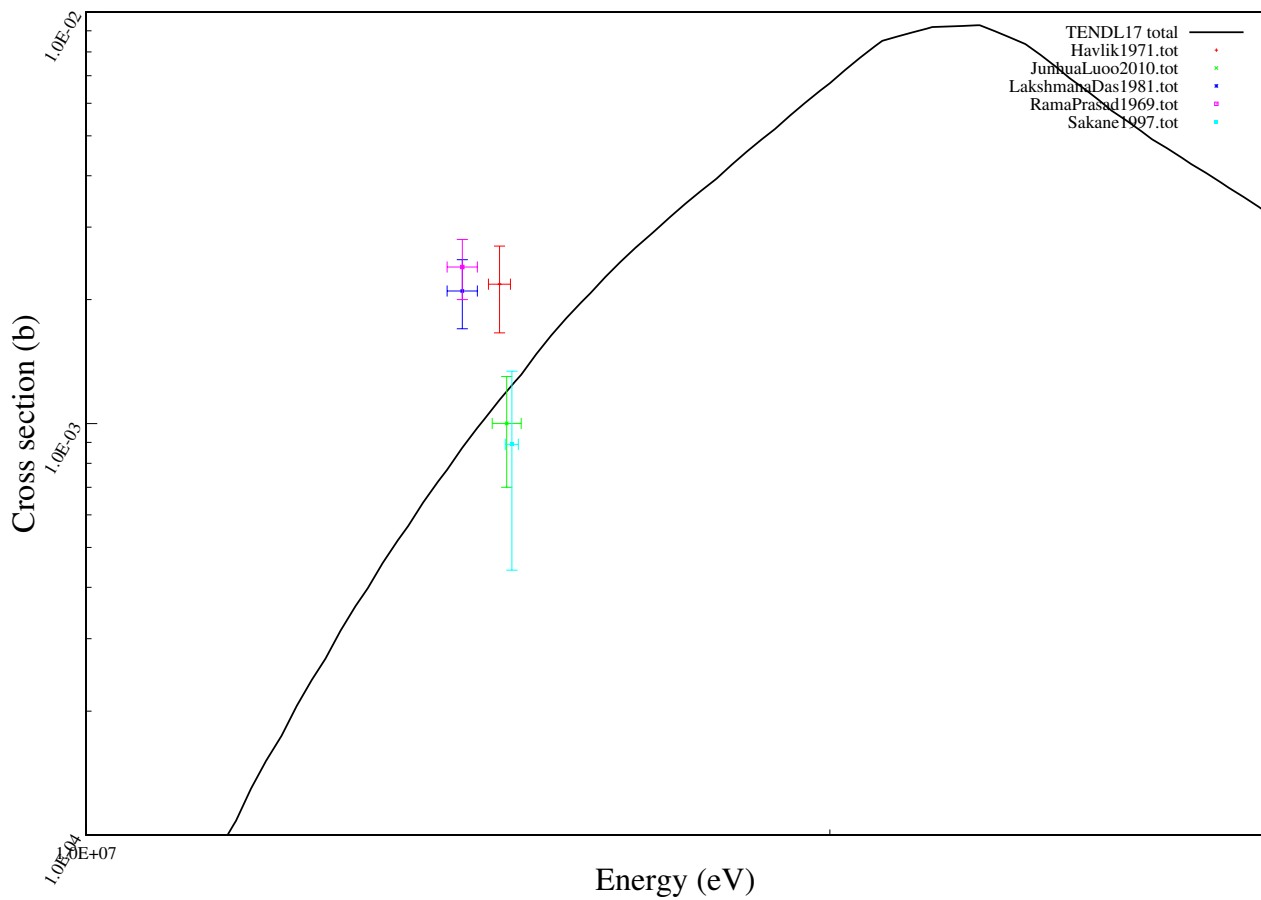
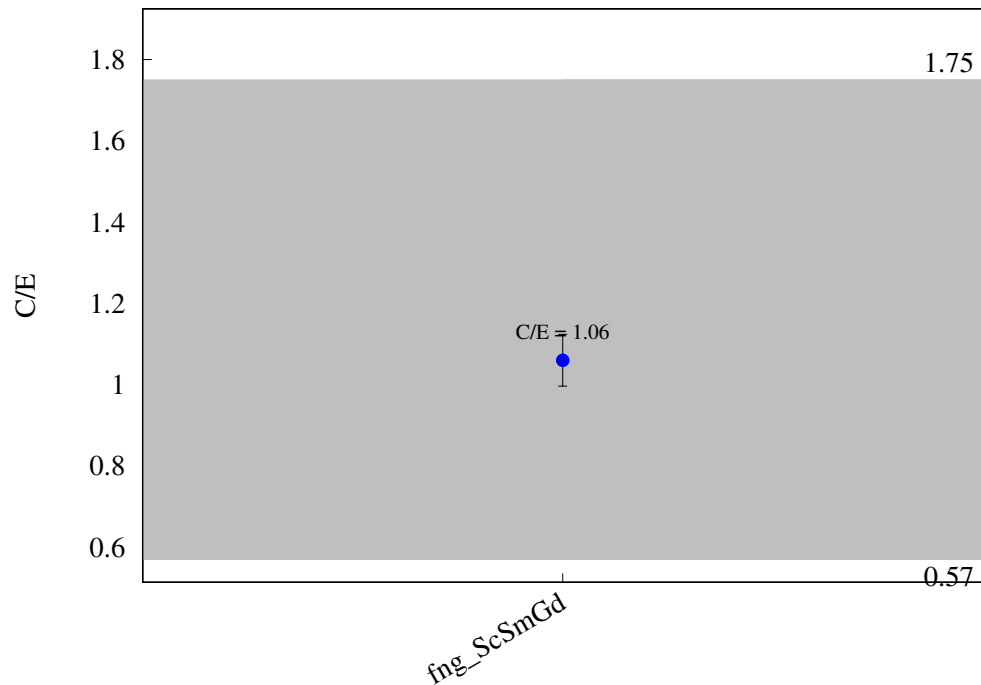


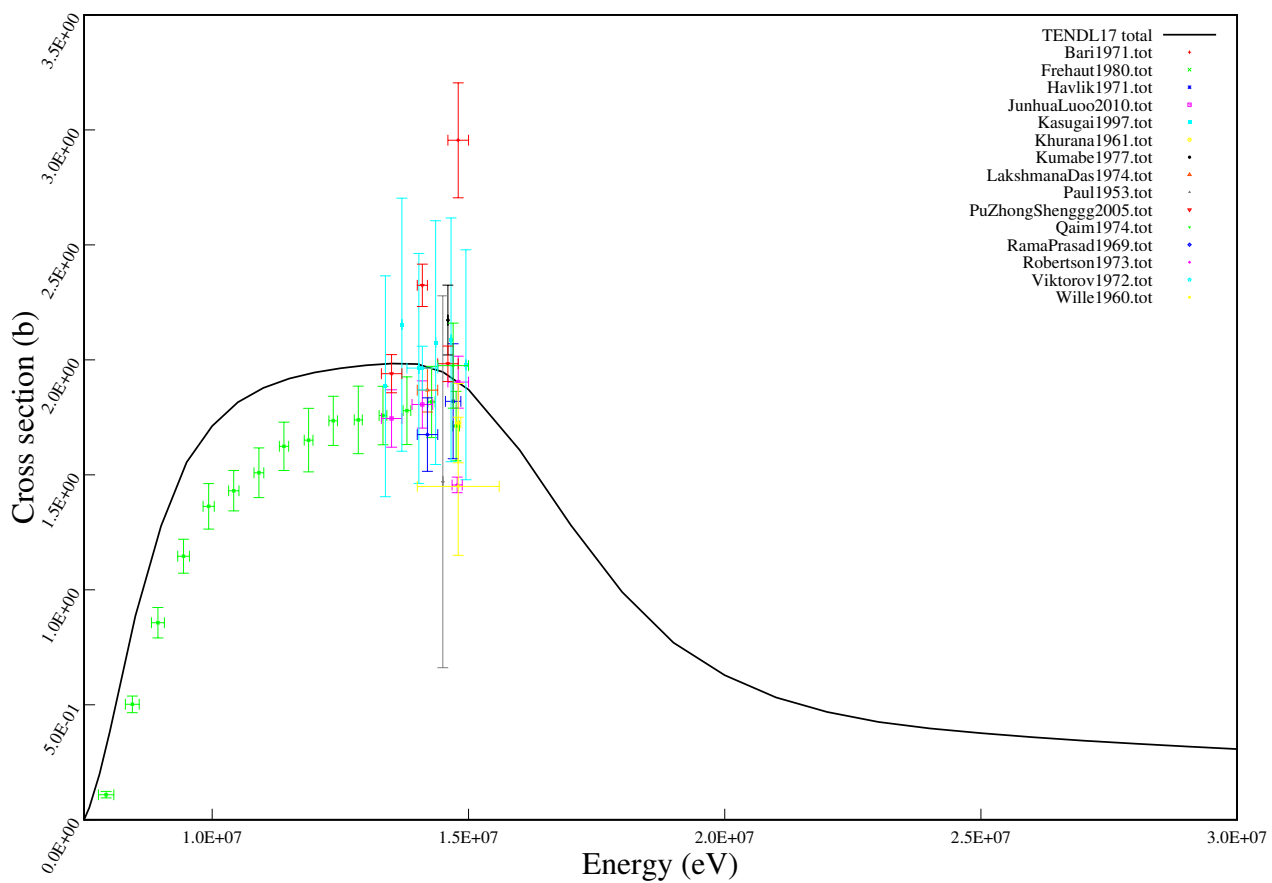
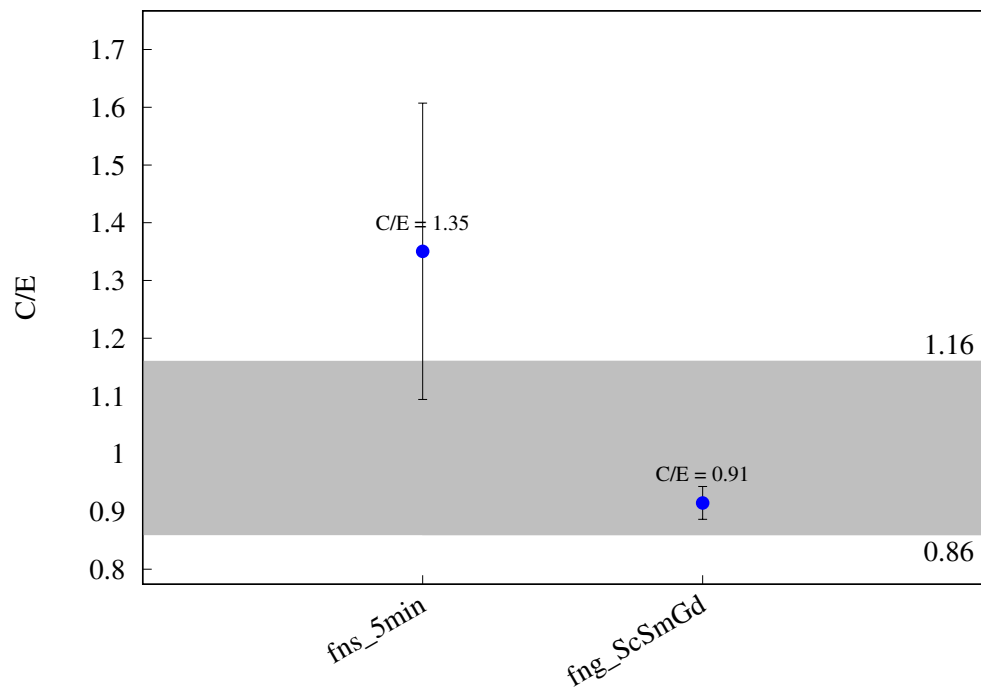
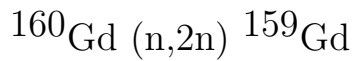
$^{150}\text{Sm} (\text{n},\text{p}) ^{150}\text{Pm}$ 

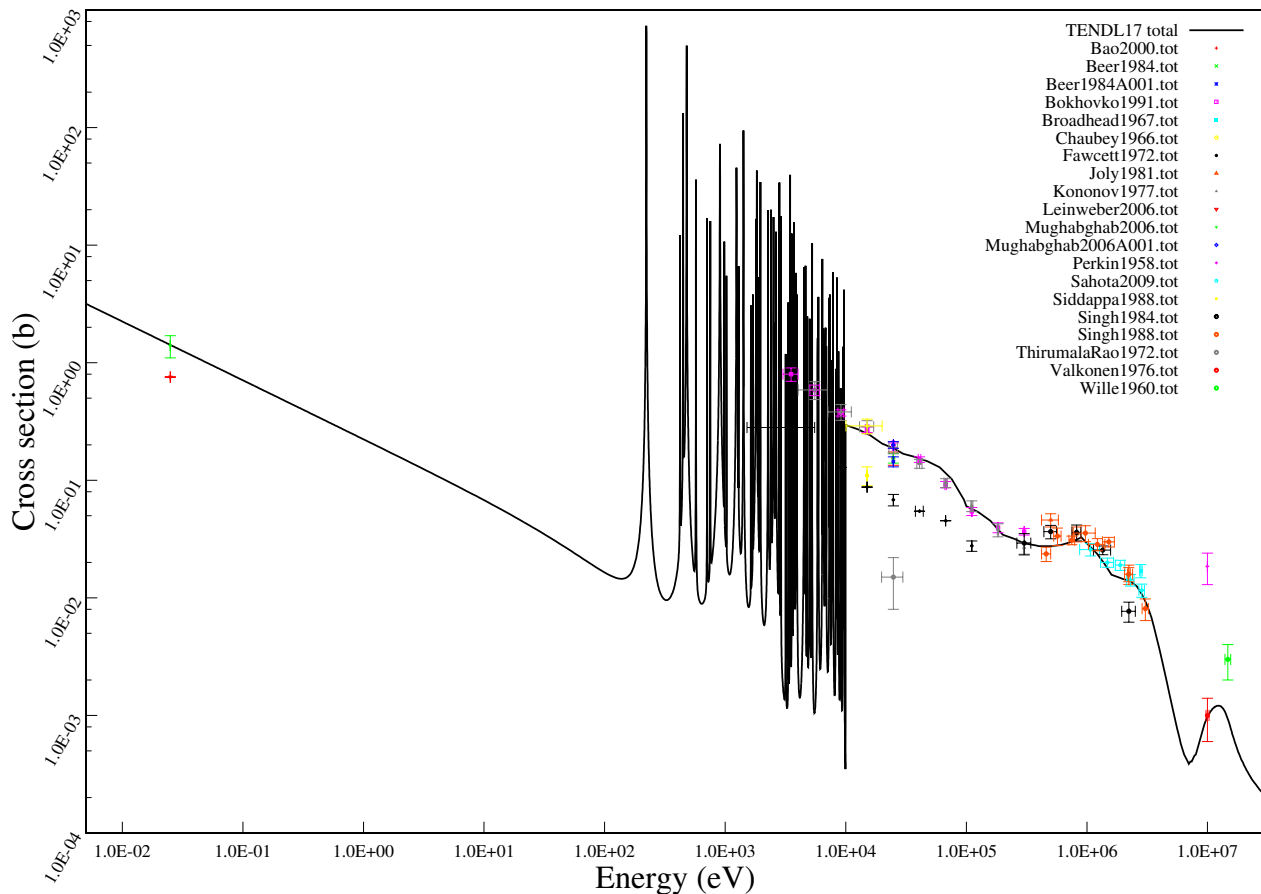
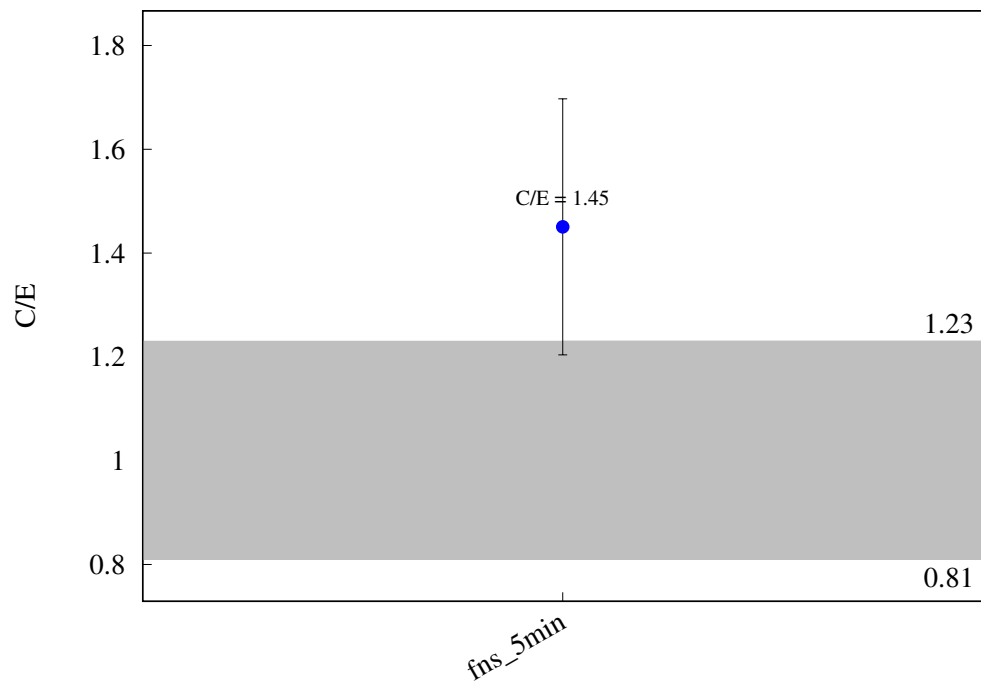
^{152}Sm (n,a) ^{149}Nd 

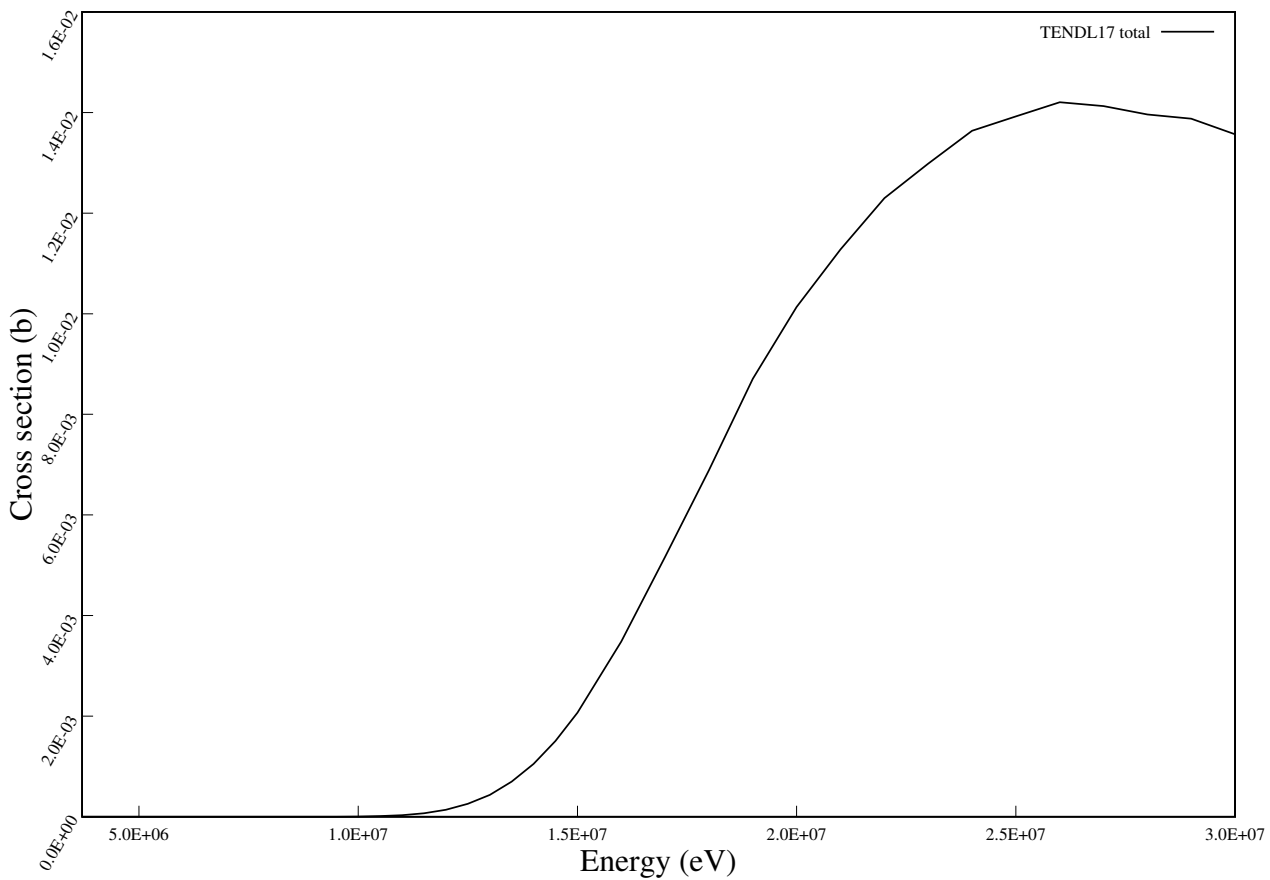
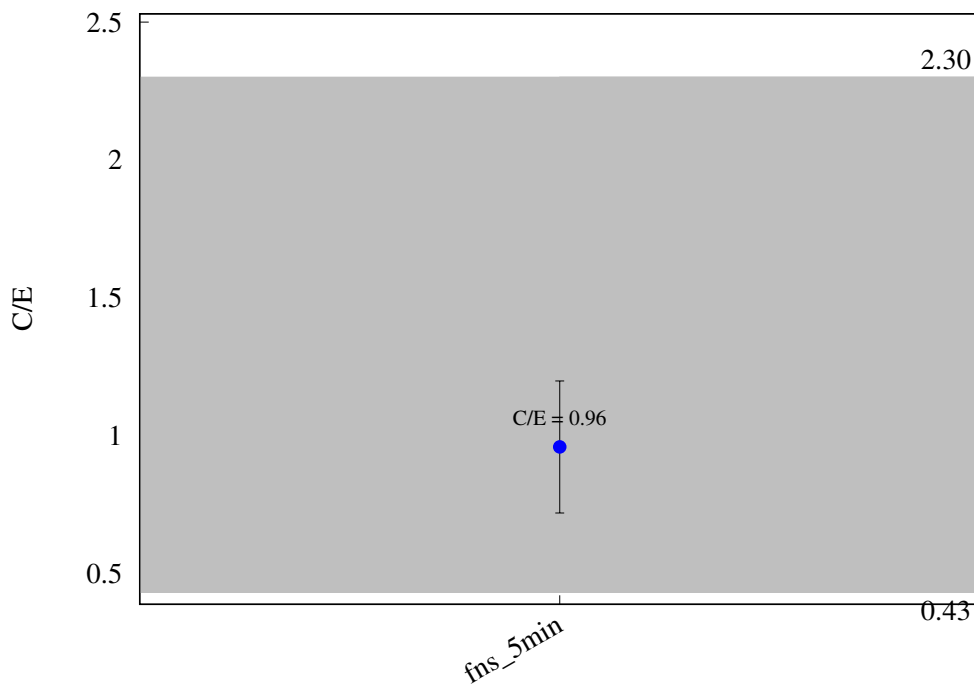
^{154}Sm (n,2n) ^{153}Sm 

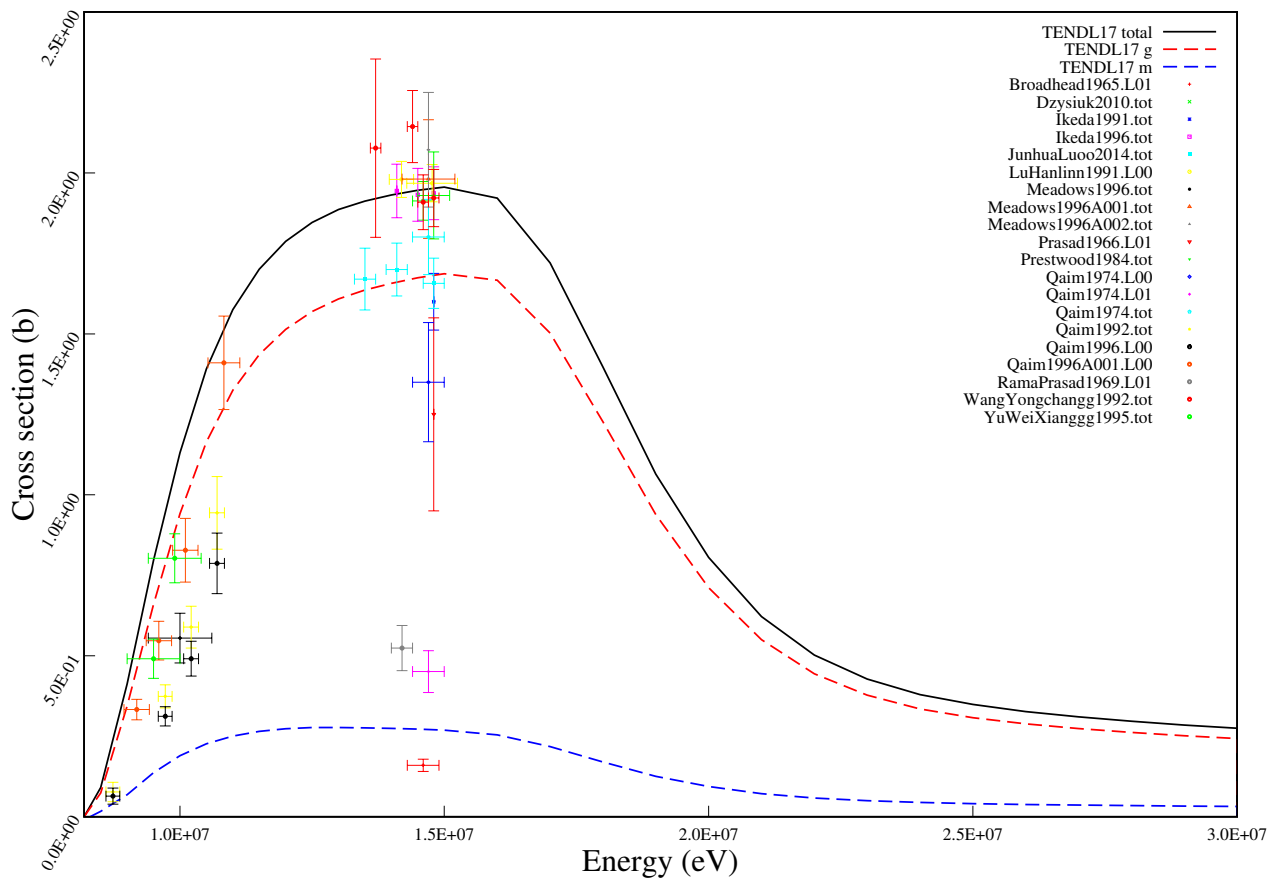
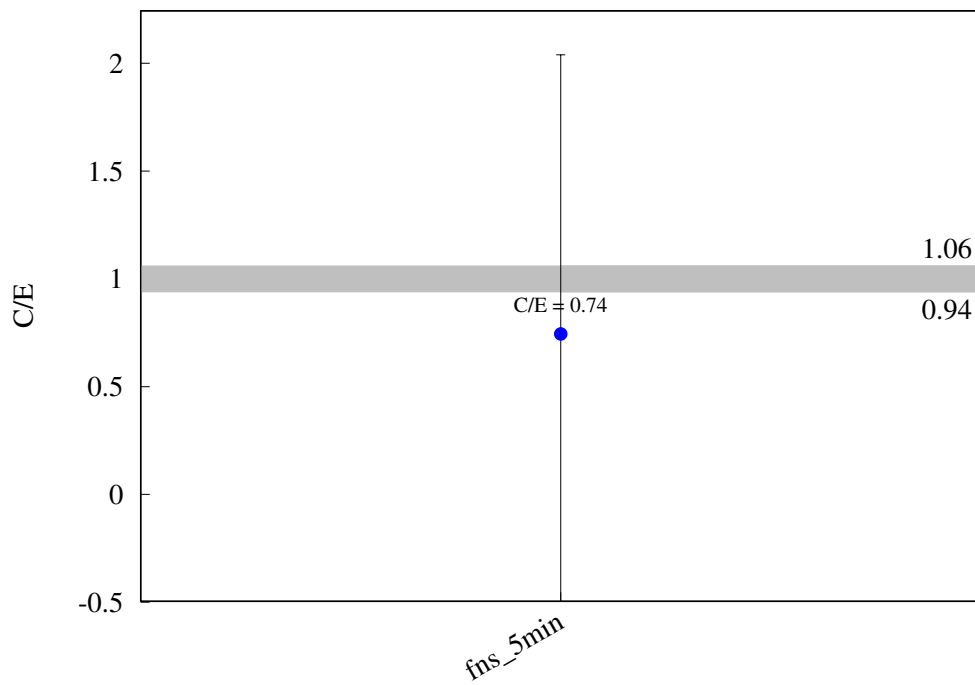
^{158}Gd (n,p) ^{158}Eu 

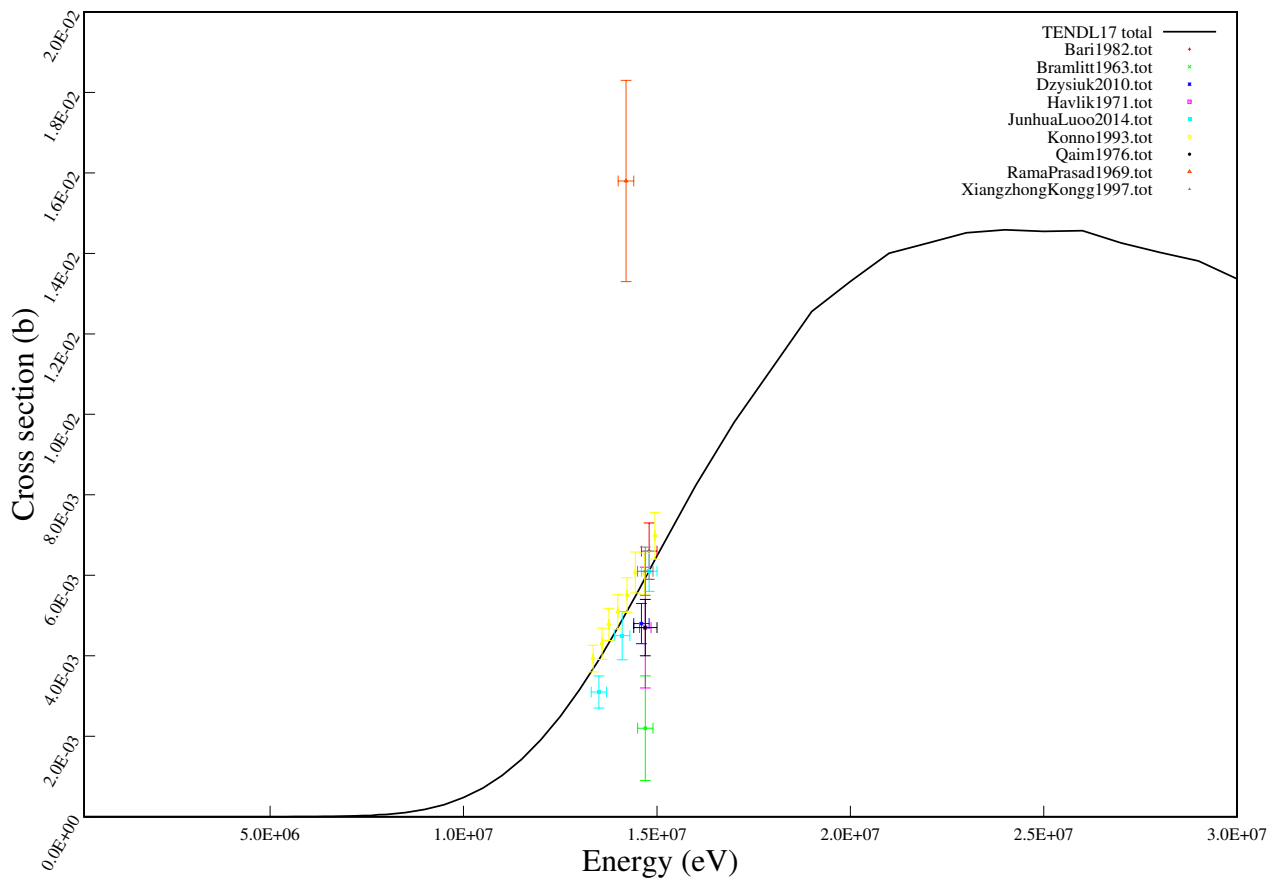
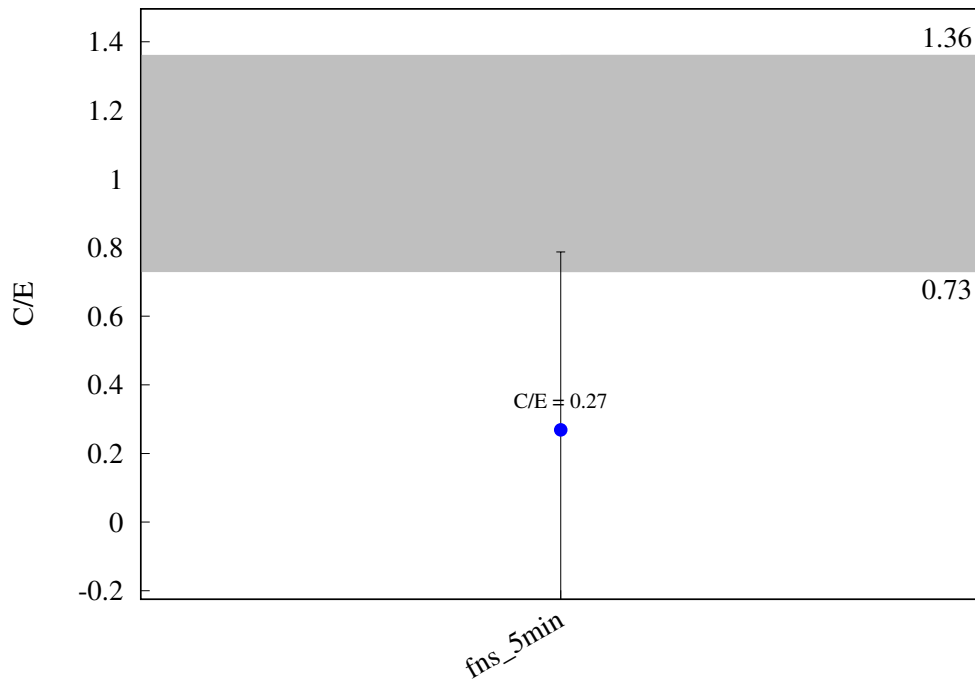
$^{158}\text{Gd} (\text{n,a}) ^{155}\text{Sm}$ 

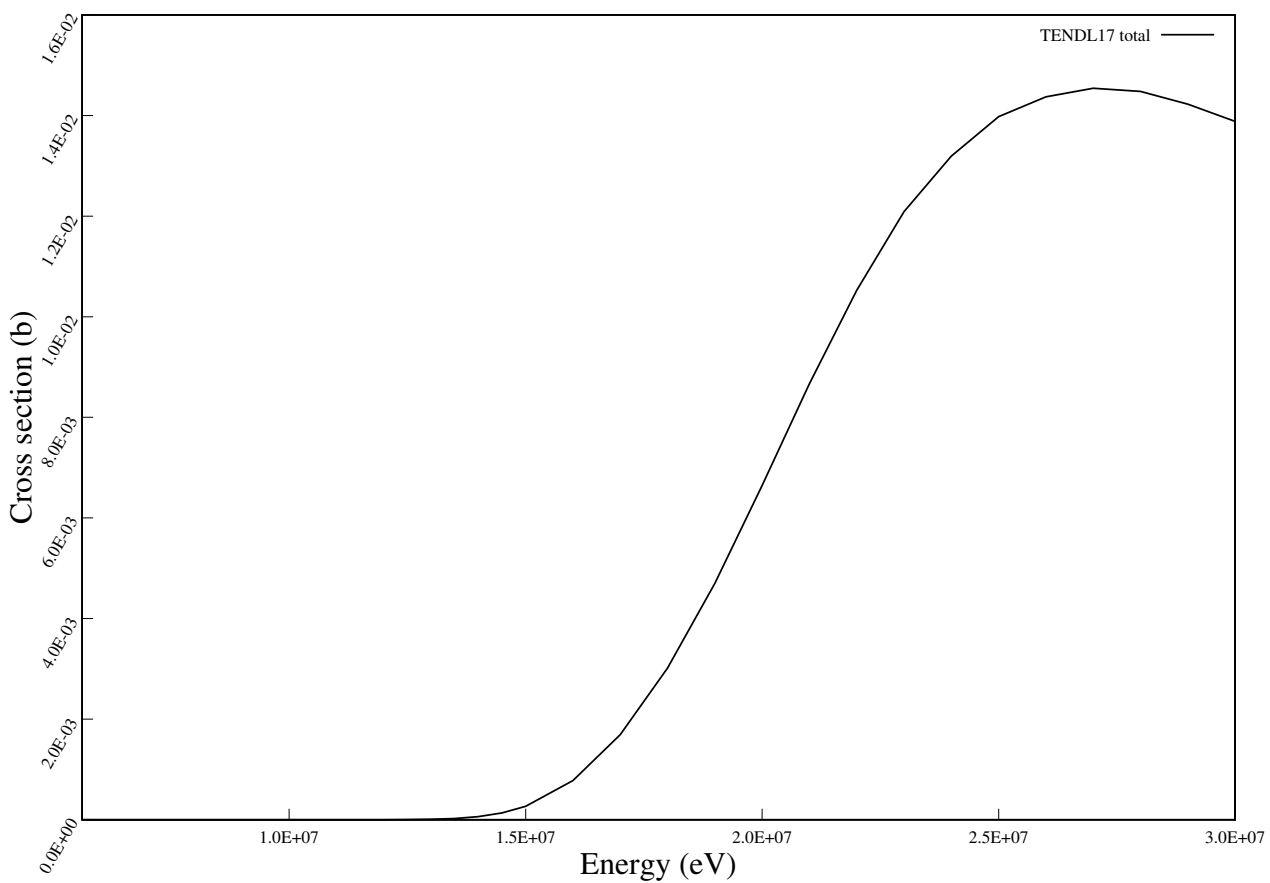
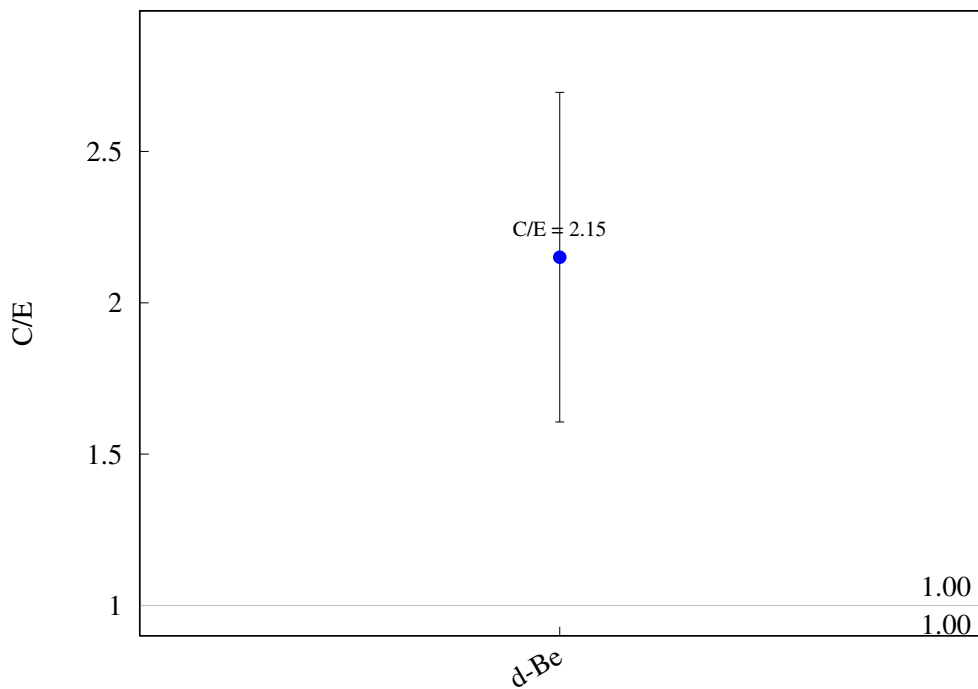


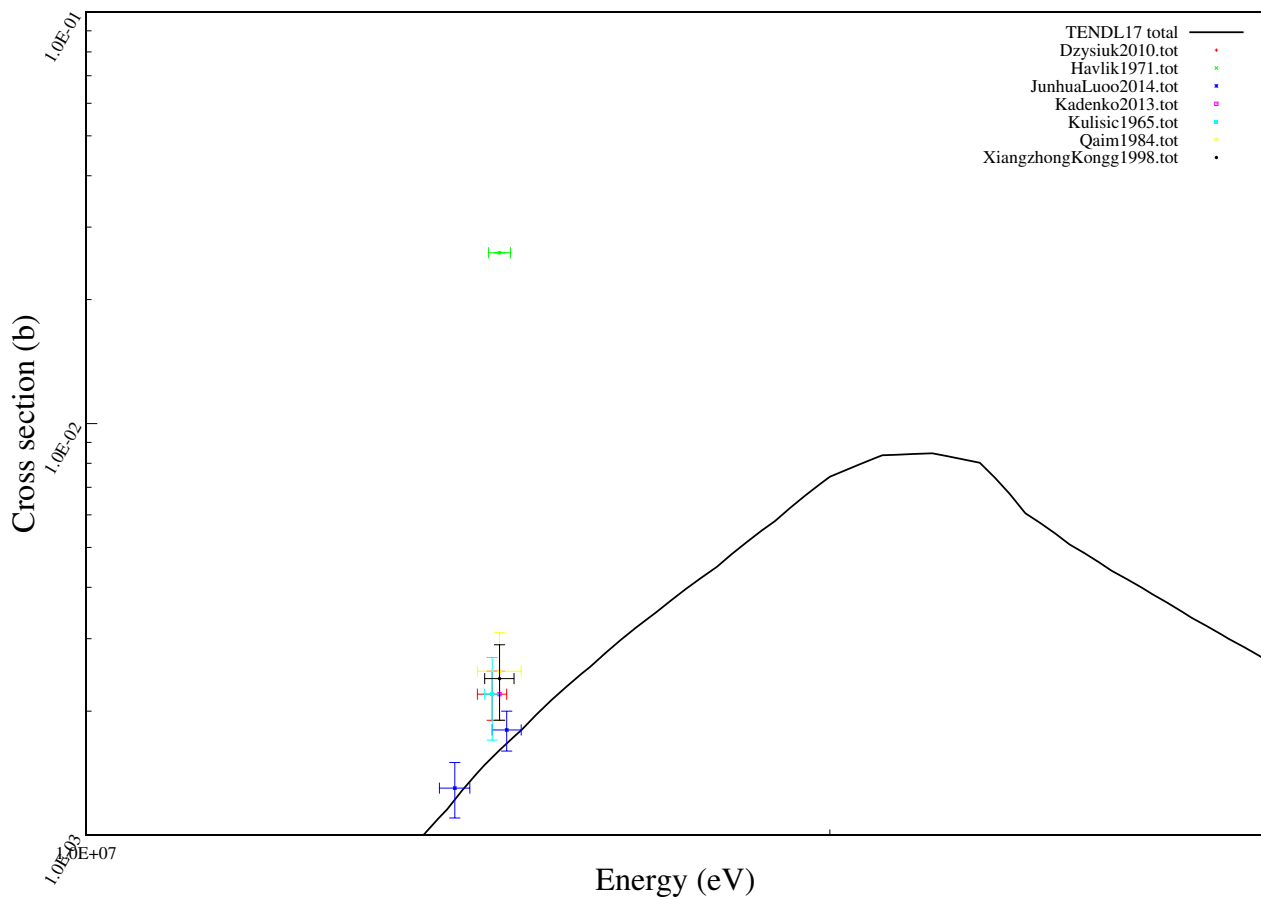
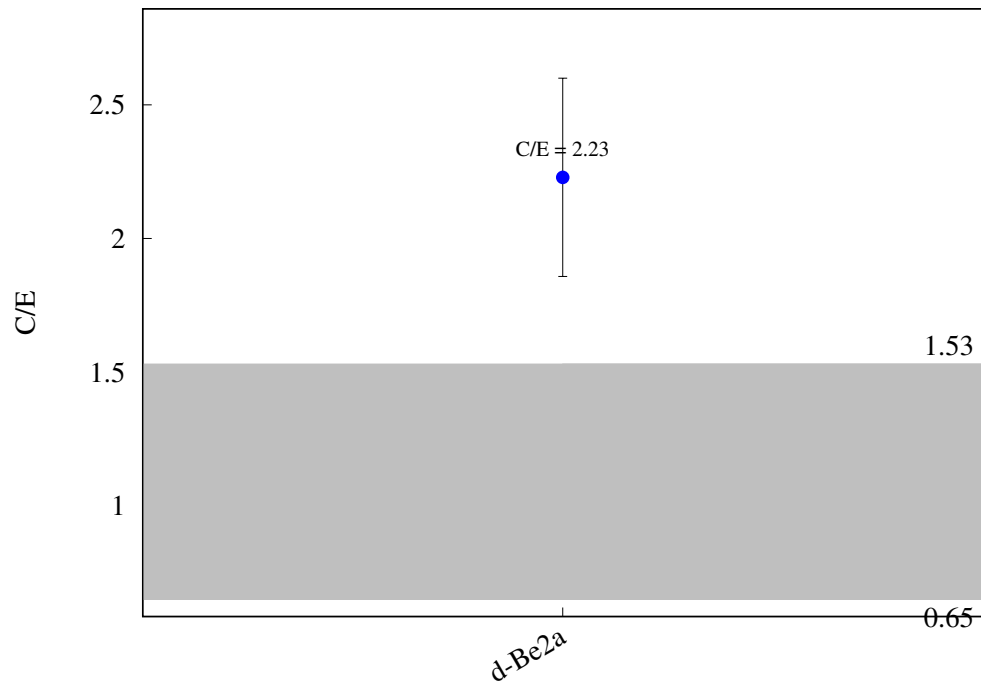
^{160}Gd (n,g) ^{161}Gd 

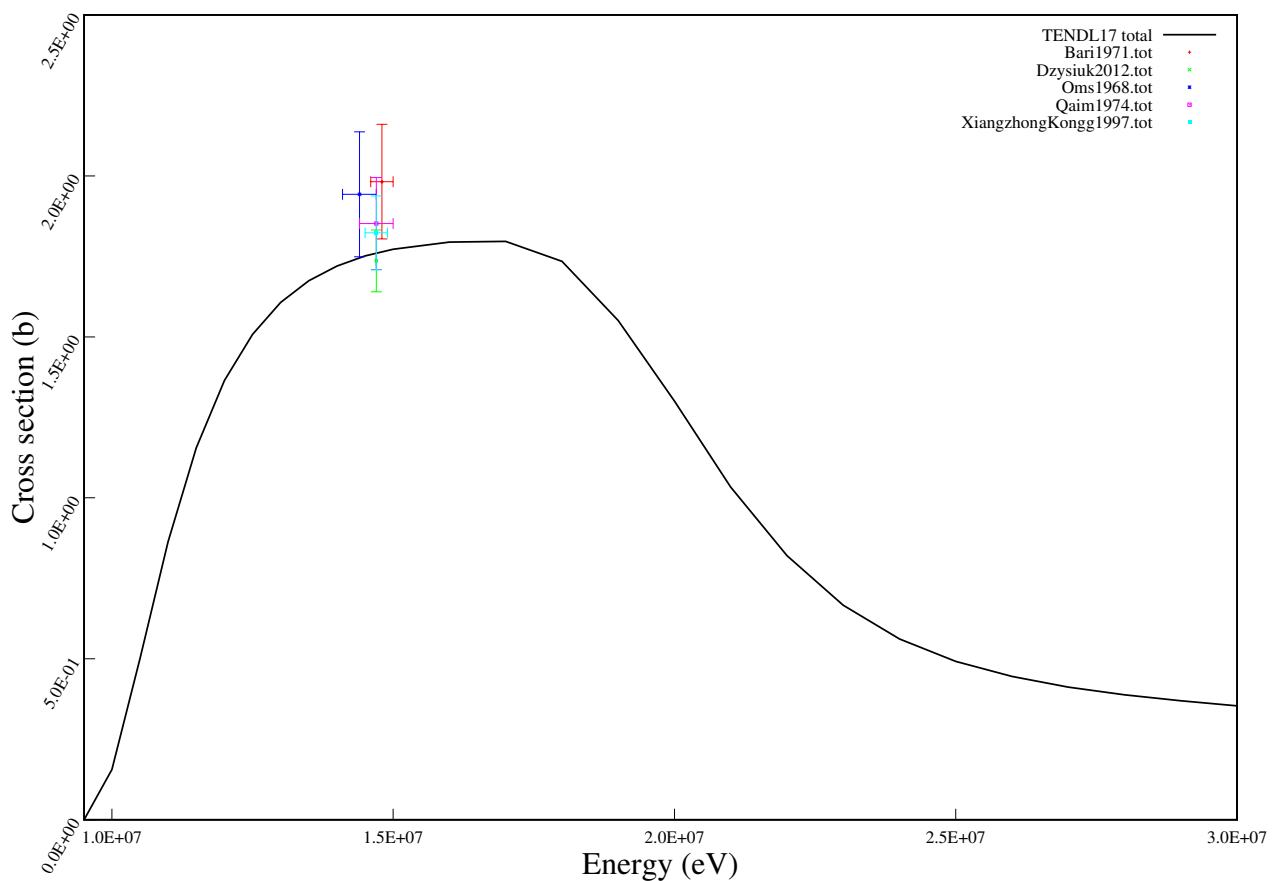
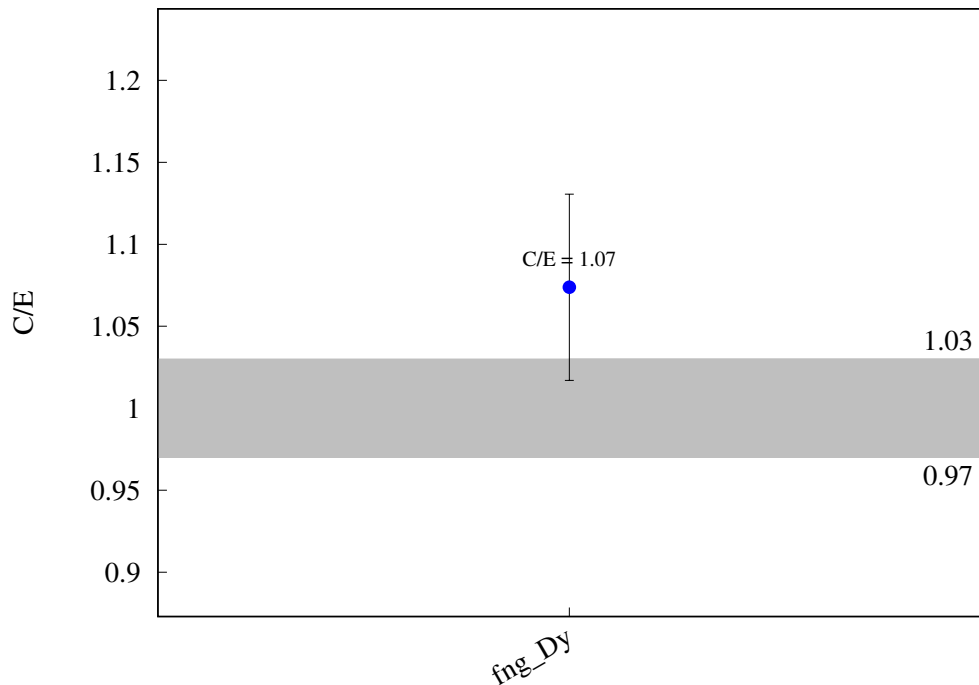
^{160}Gd (n,p) ^{160}Eu 

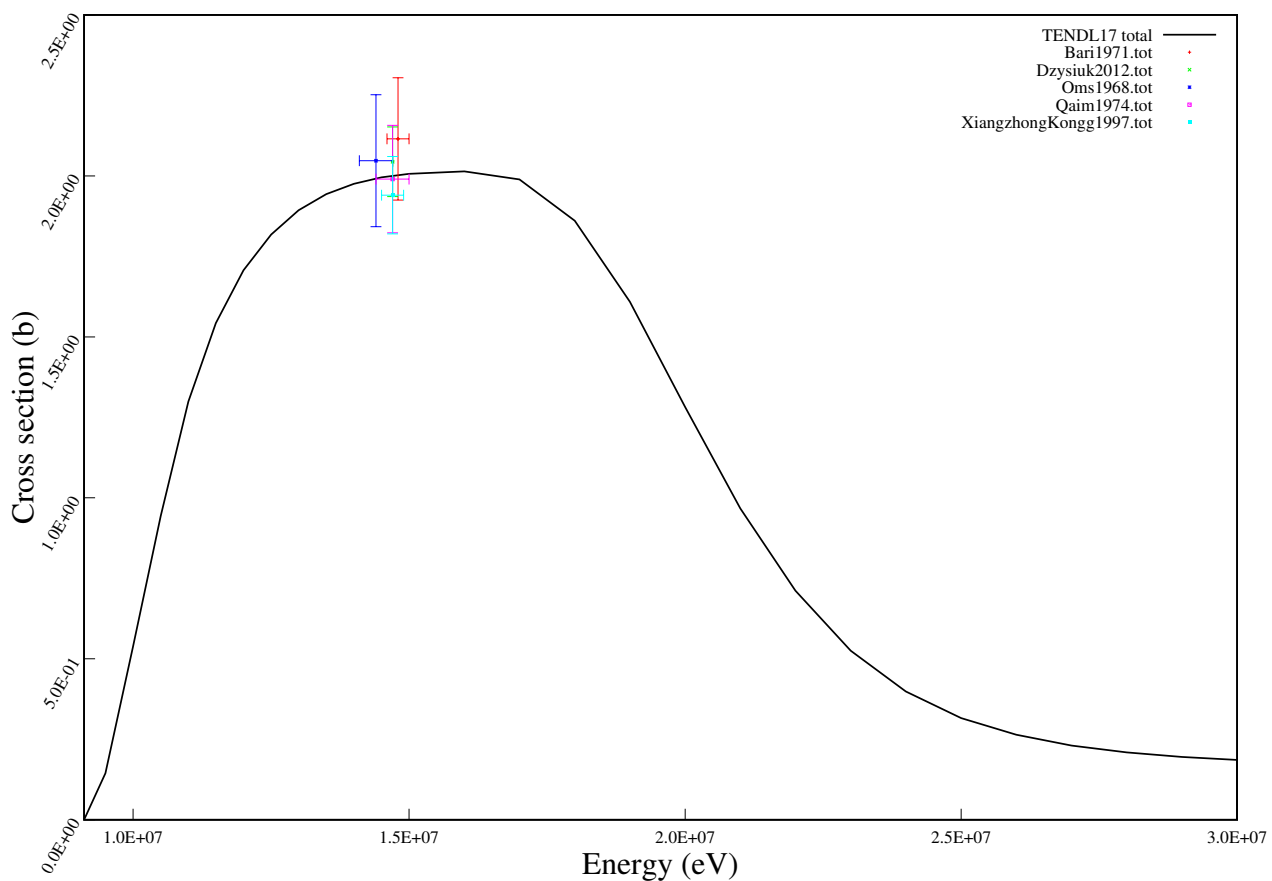
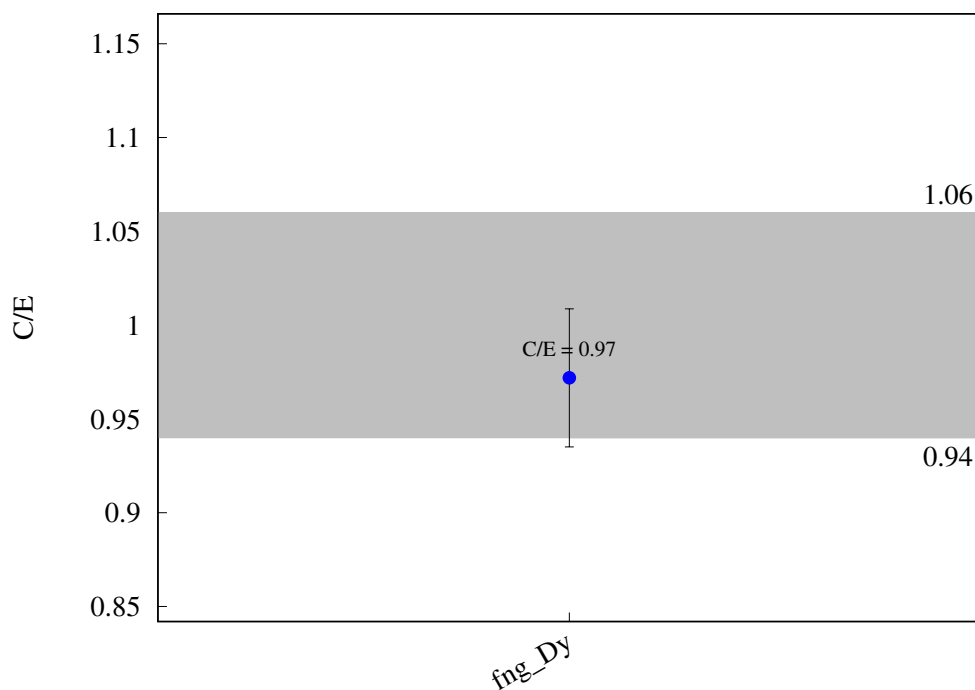
^{159}Tb ($n,2n$) $^{158\text{m}}\text{Tb}$ 

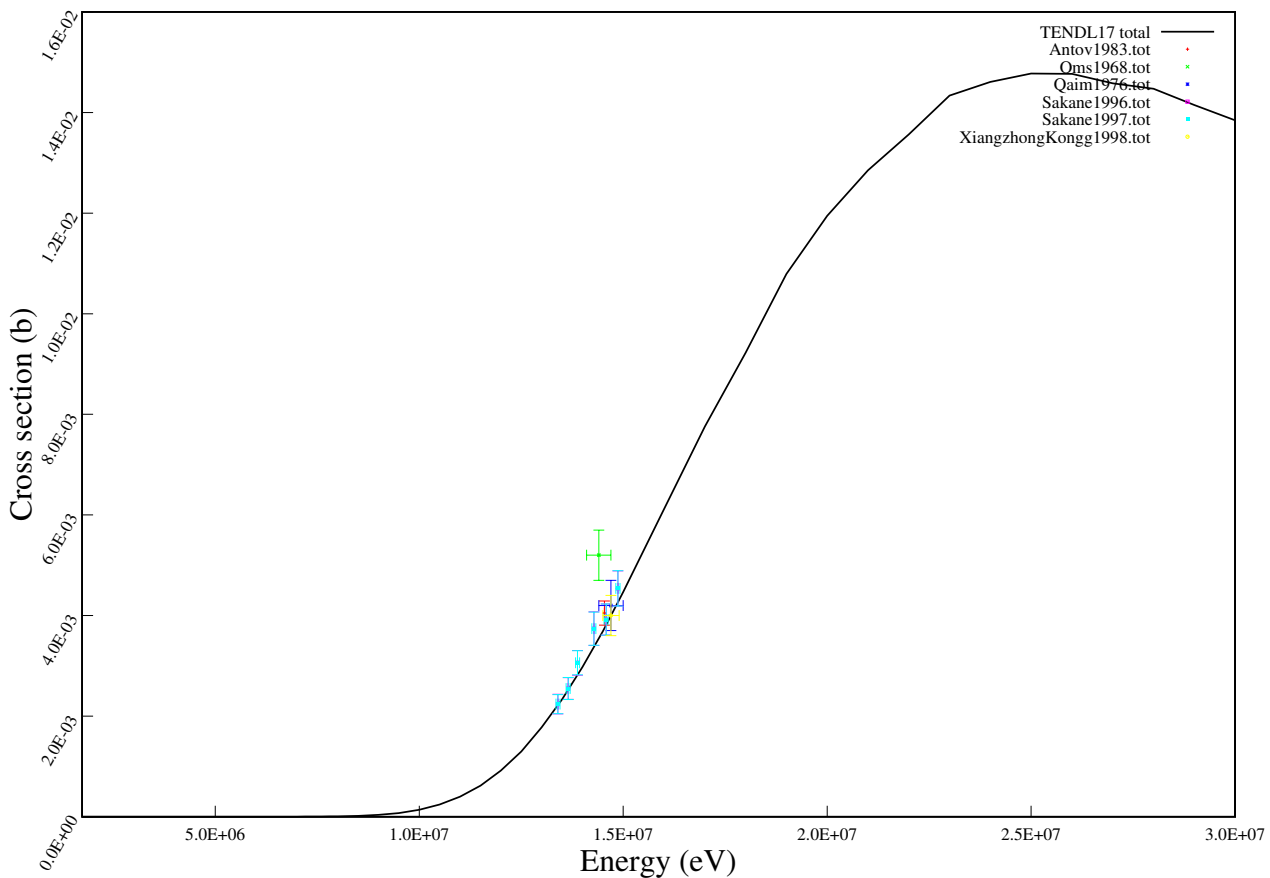
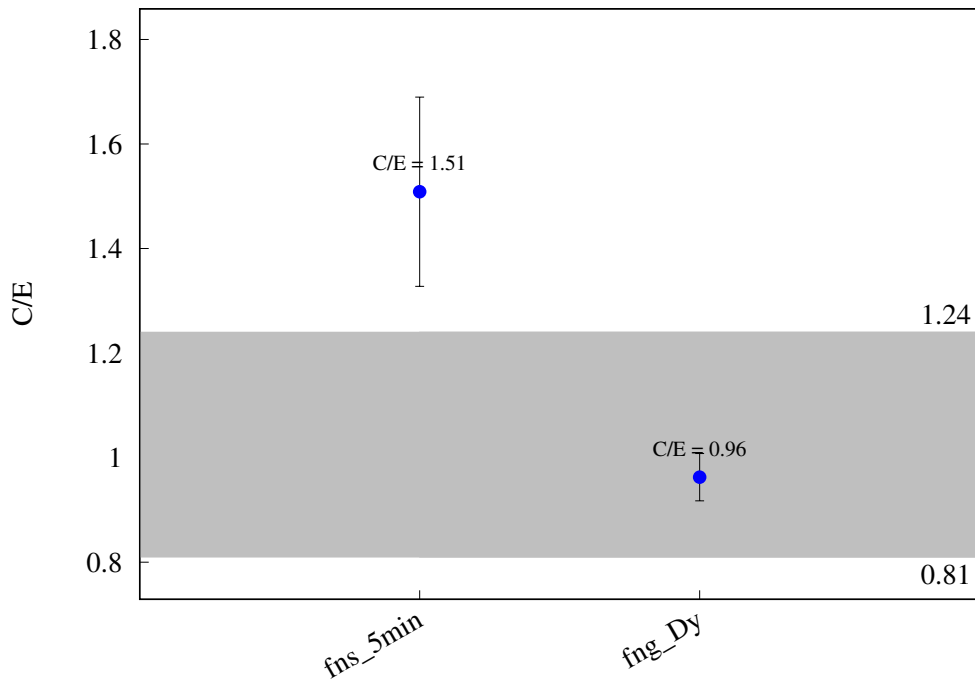
$^{159}\text{Tb} (\text{n},\text{p}) ^{159}\text{Gd}$ 

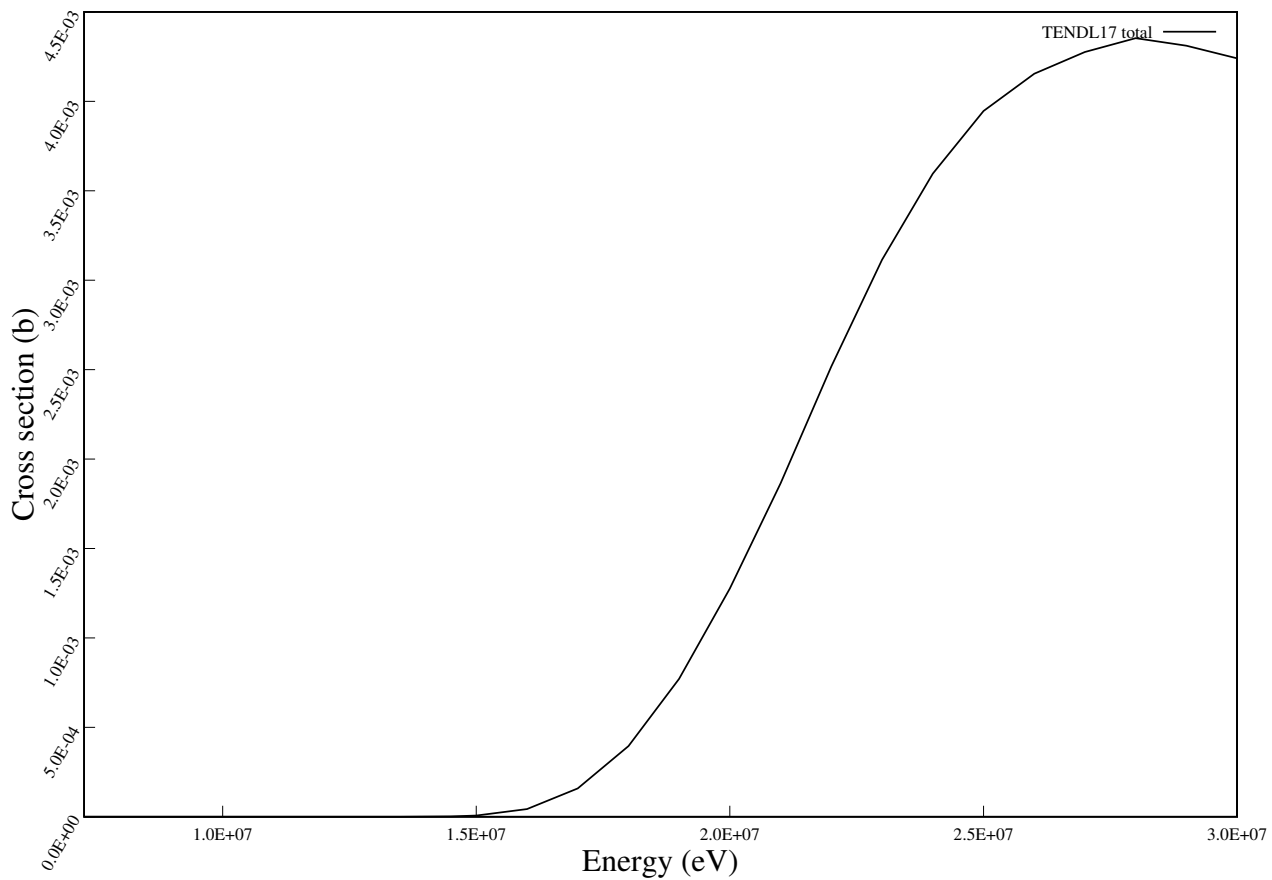
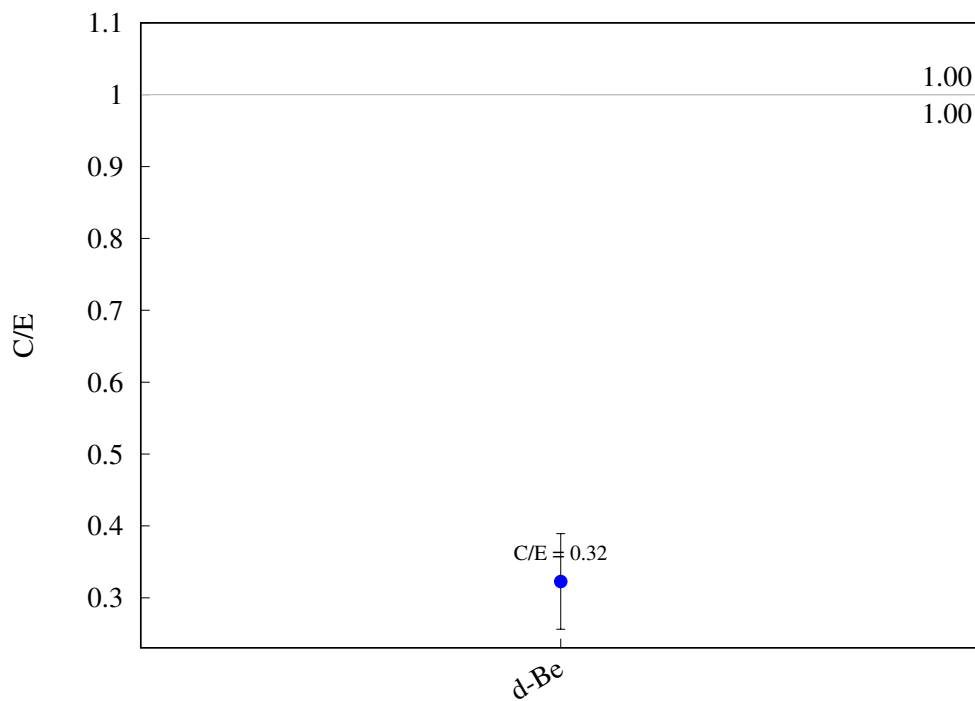
$^{159}\text{Tb} (\text{n},\text{t}) ^{157}\text{Gd}$ 

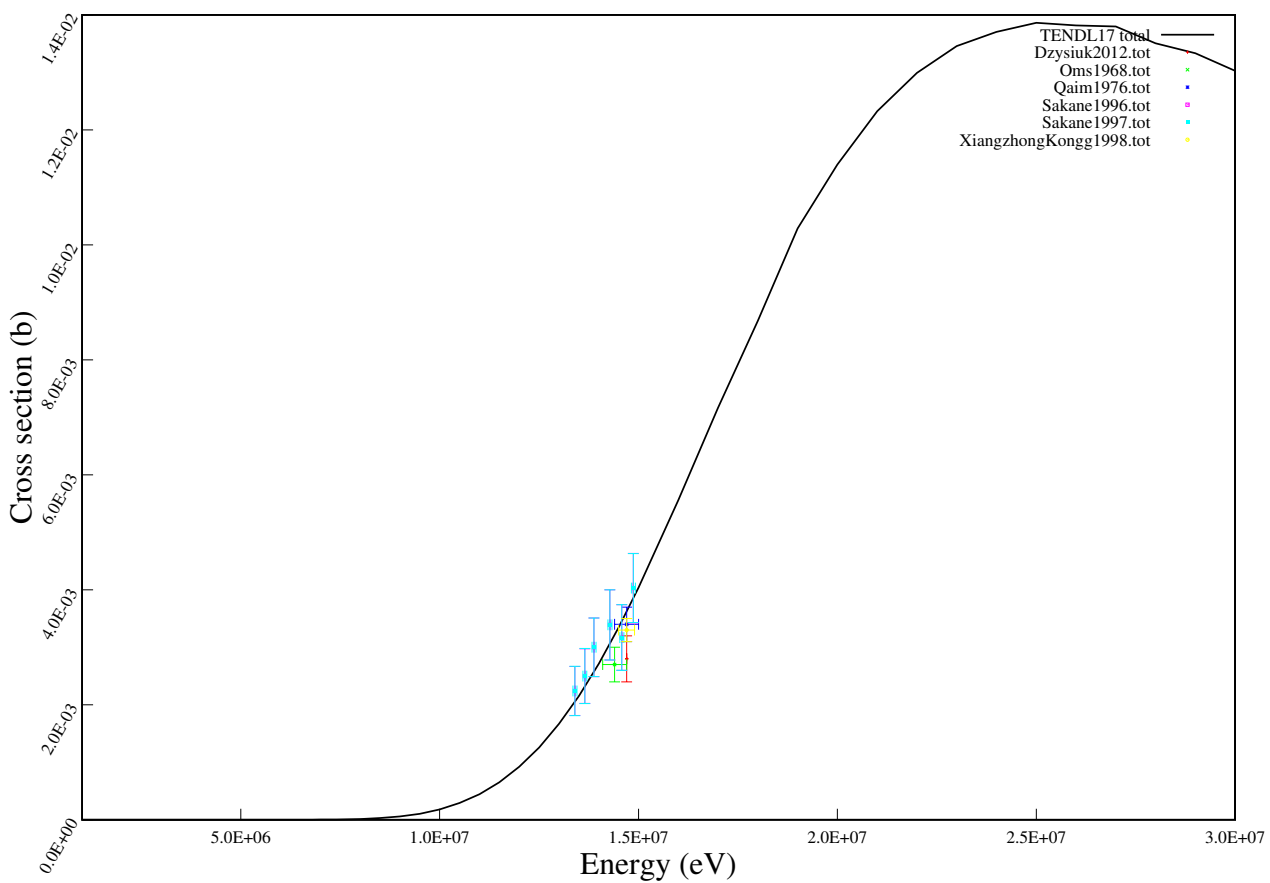
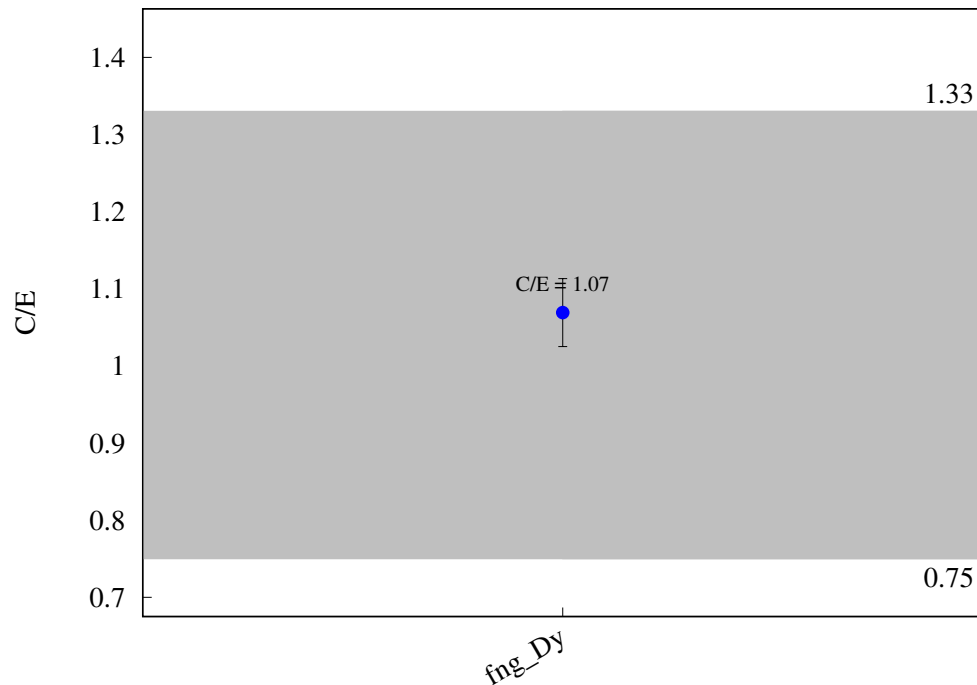
$^{159}\text{Tb} (\text{n,a}) ^{156}\text{Eu}$ 

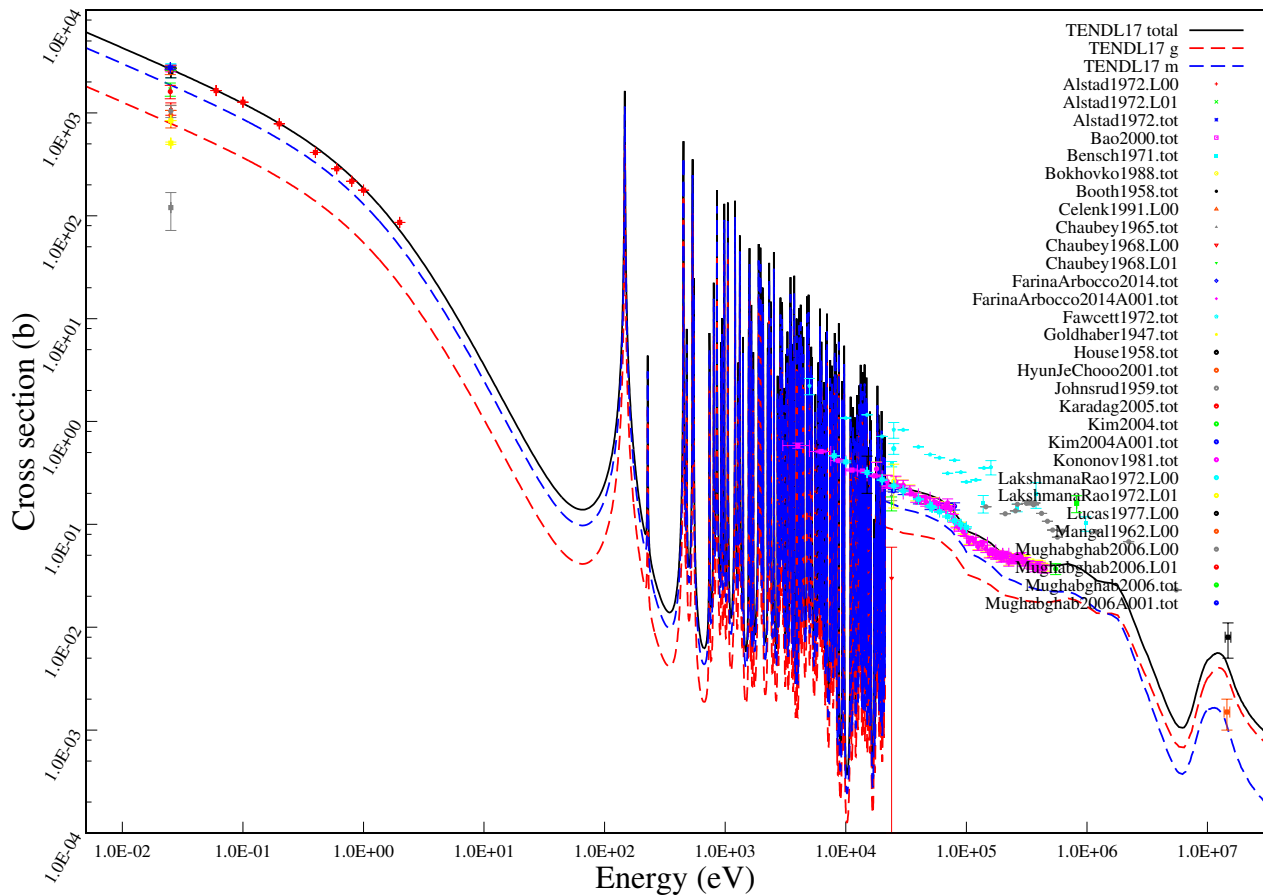
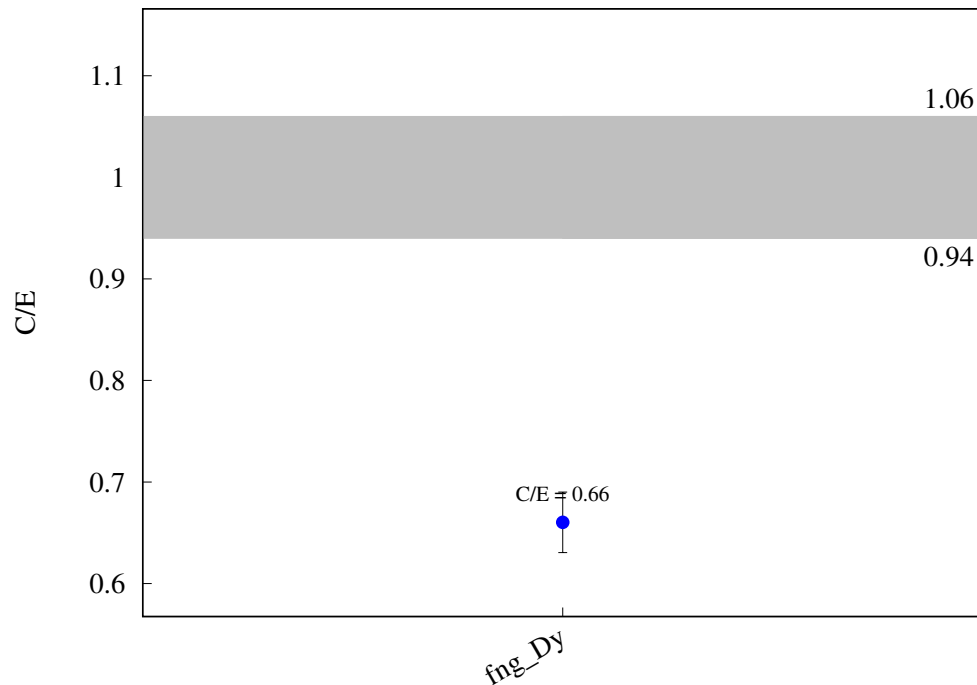
^{156}Dy (n,2n) ^{155}Dy 

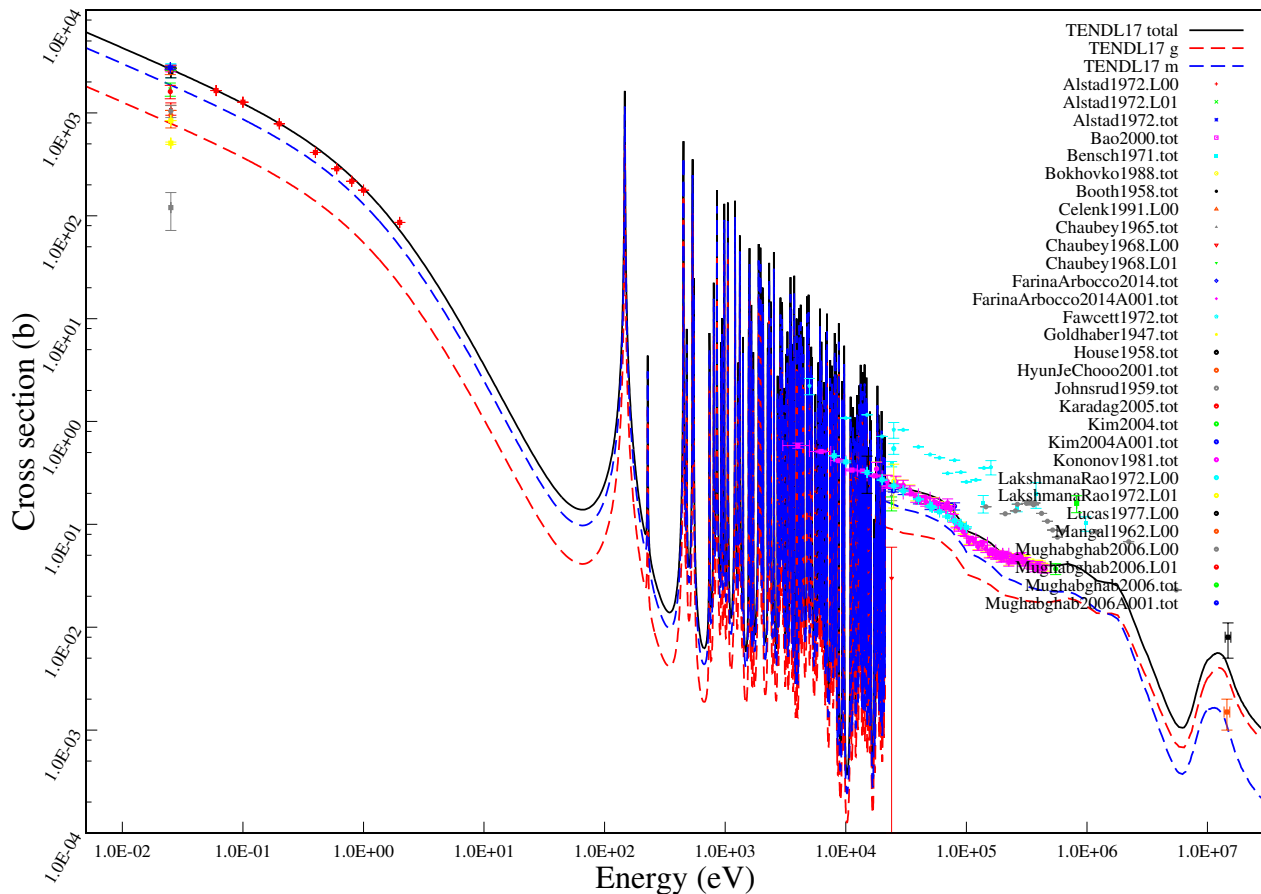
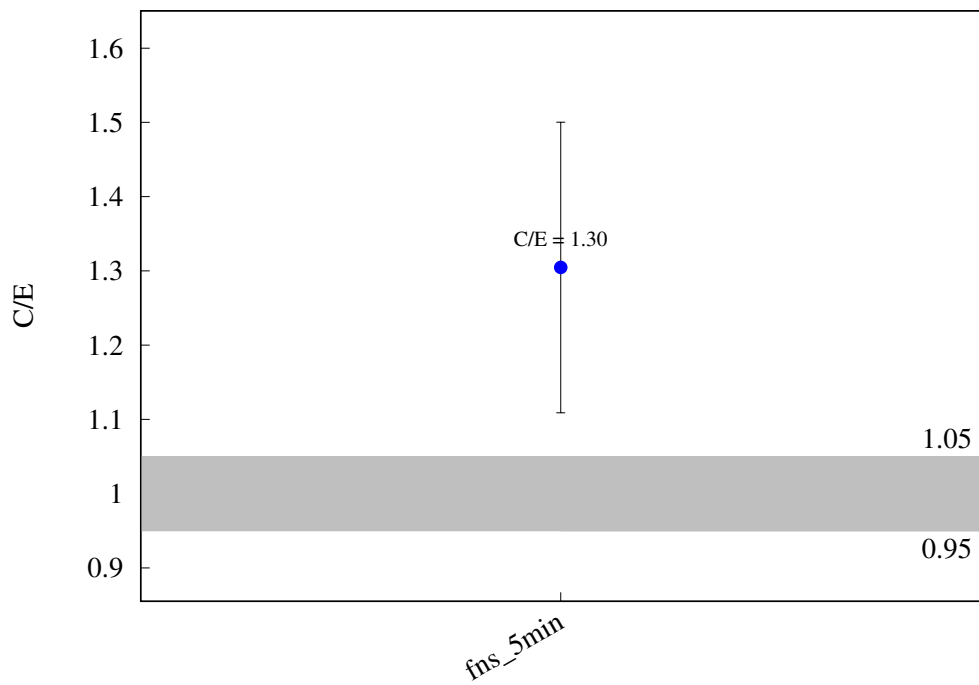
^{158}Dy (n,2n) ^{157}Dy 

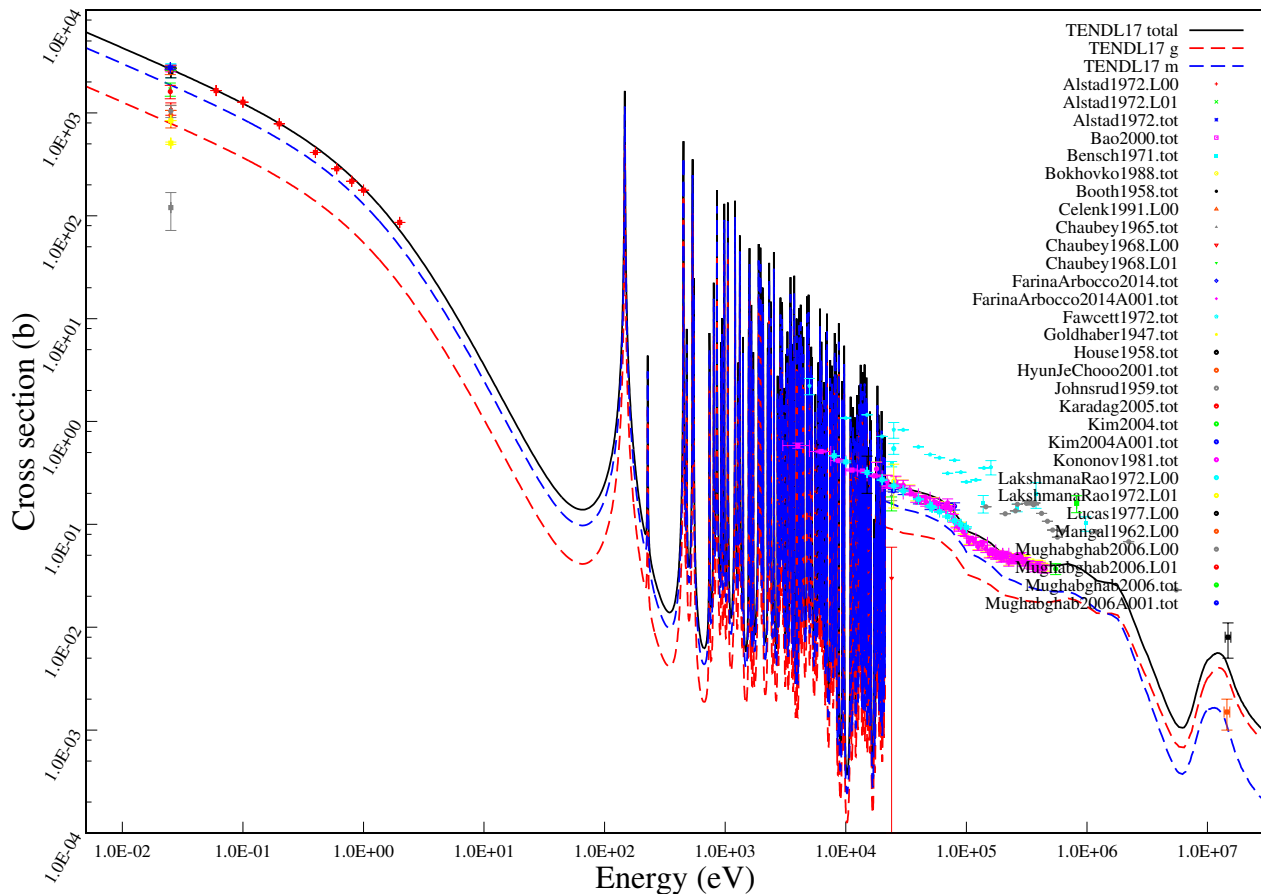
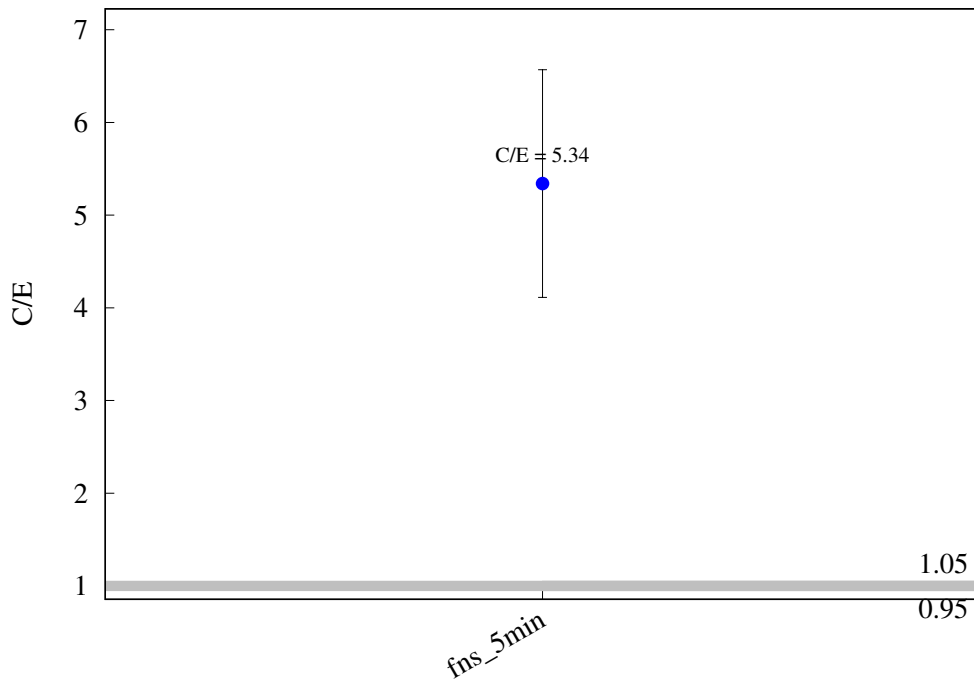
^{162}Dy (n,p) ^{162}Tb 

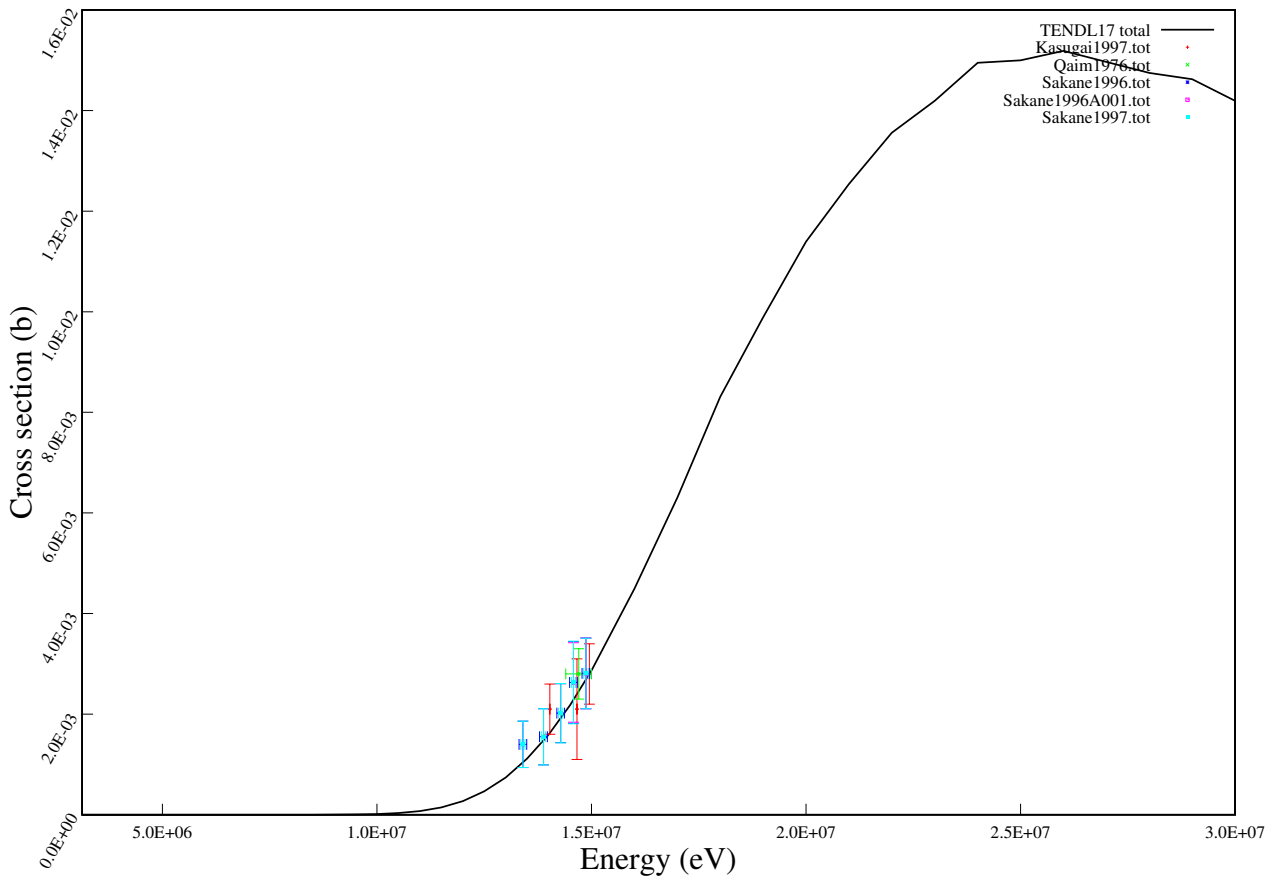
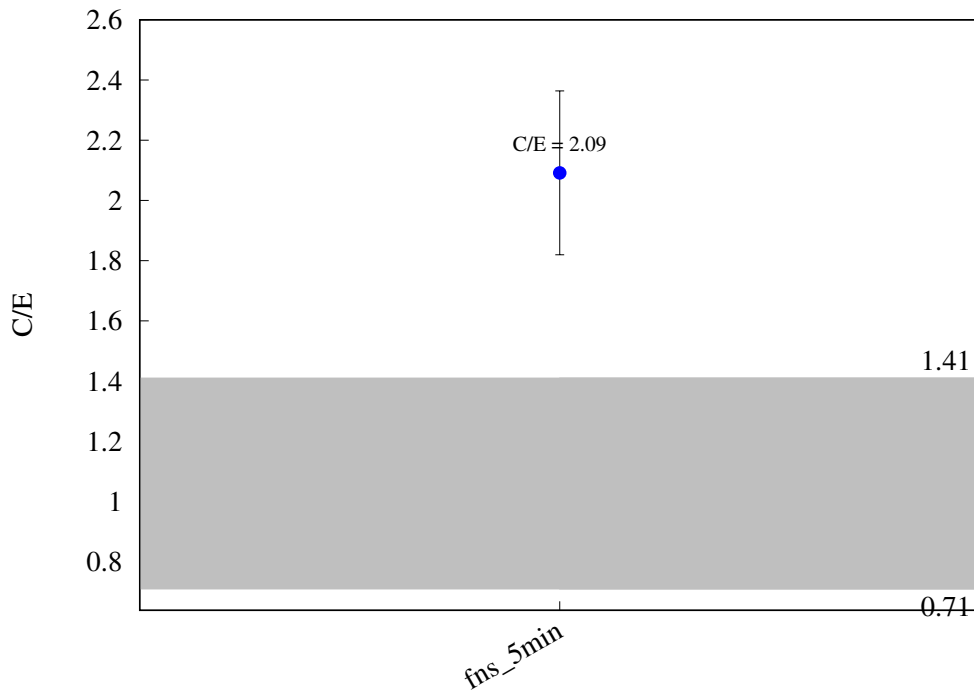
$^{162}\text{Dy} (\text{n},\text{t}) ^{160}\text{Tb}$ 

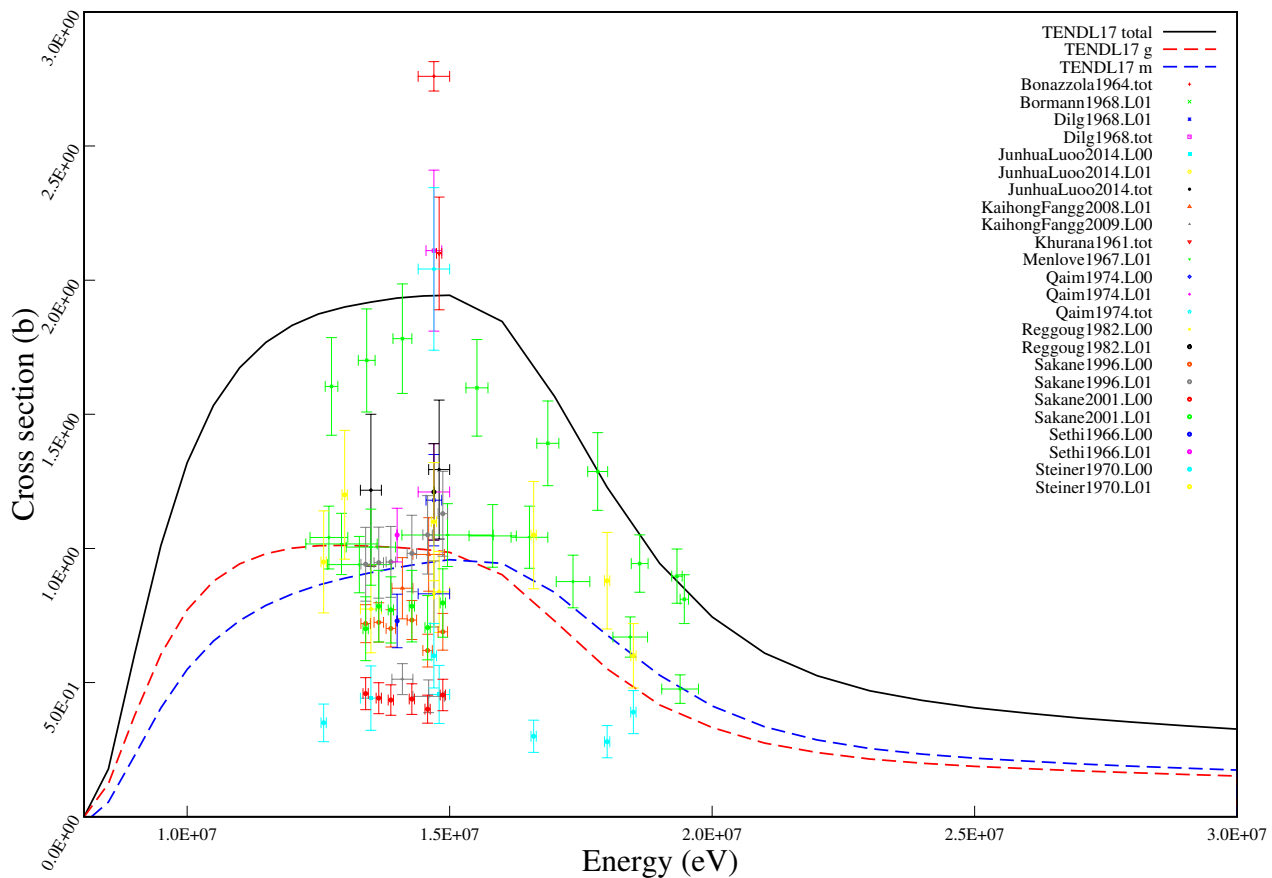
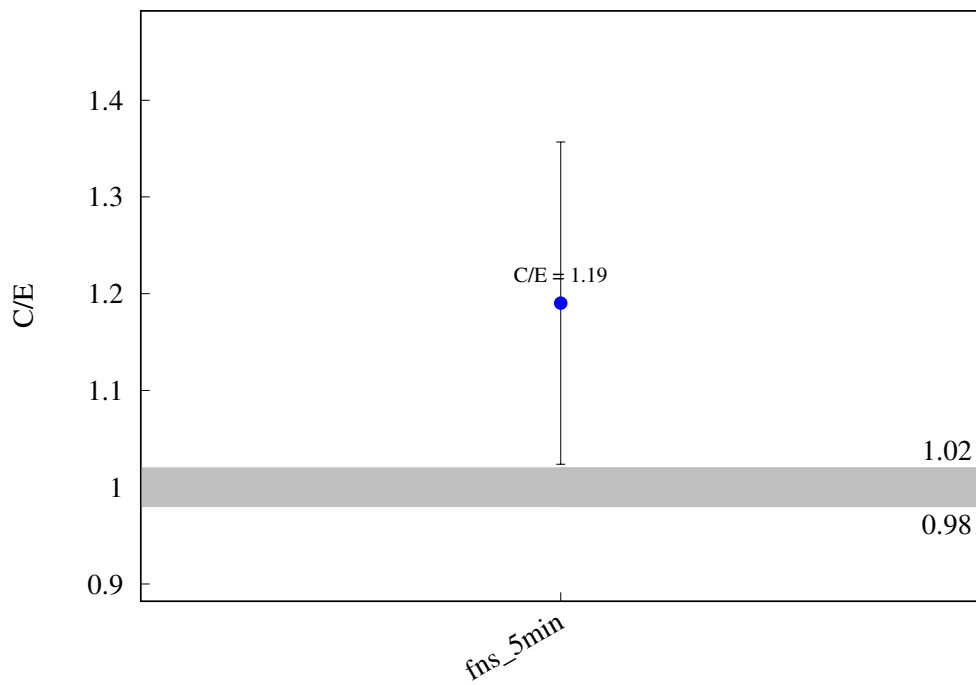
$^{163}\text{Dy} (\text{n},\text{p}) ^{163}\text{Tb}$ 

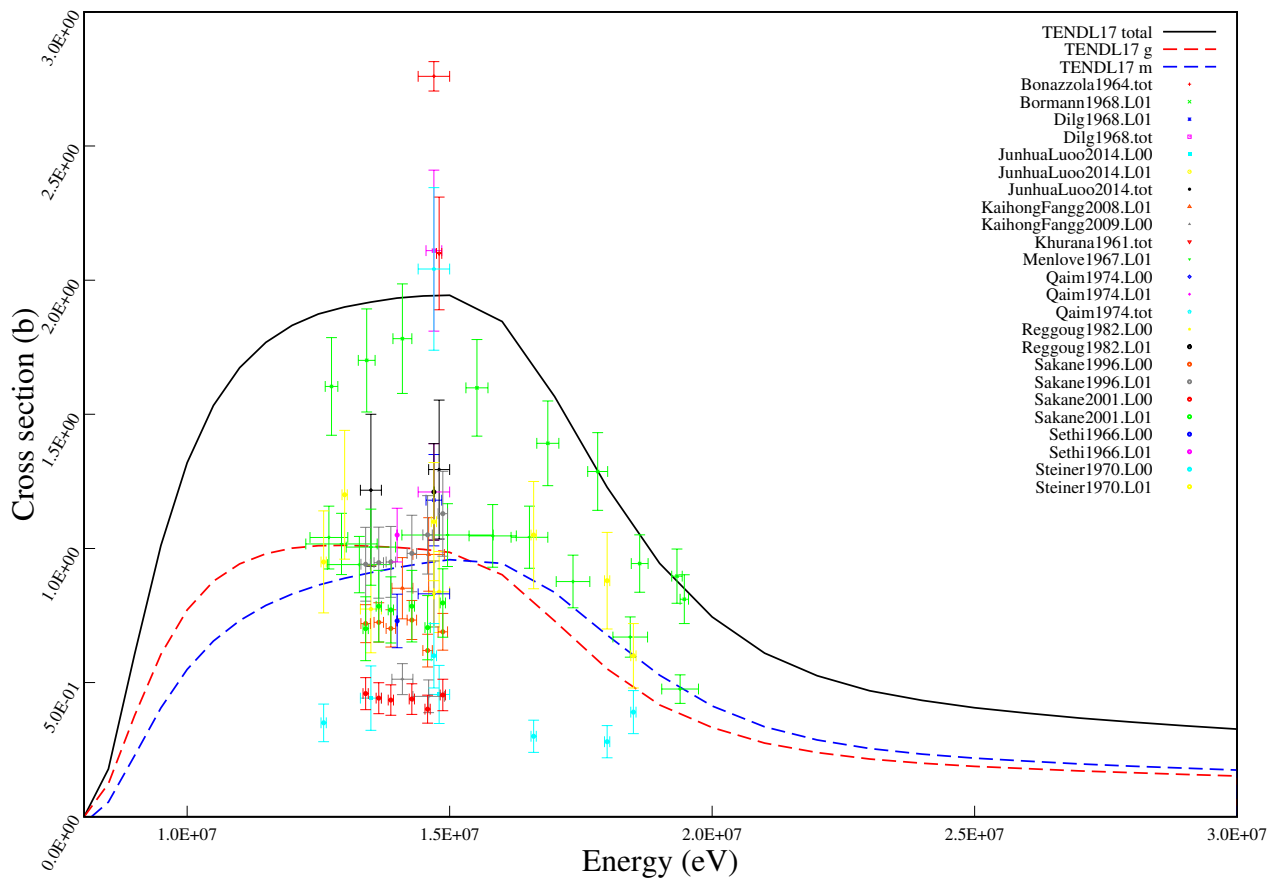
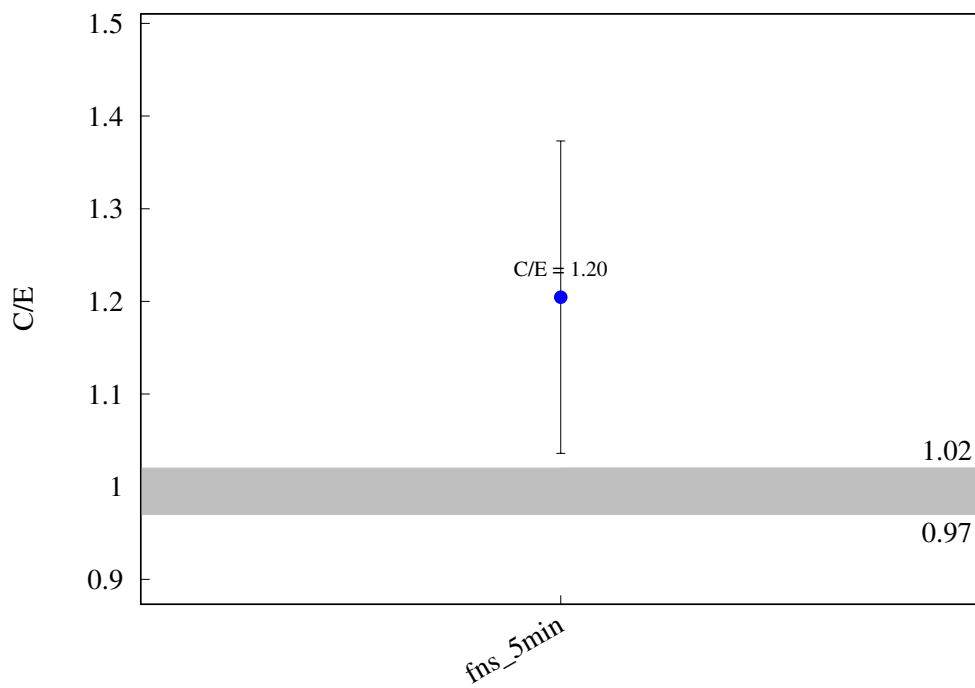
^{164}Dy (n,g) ^{165}gDy 

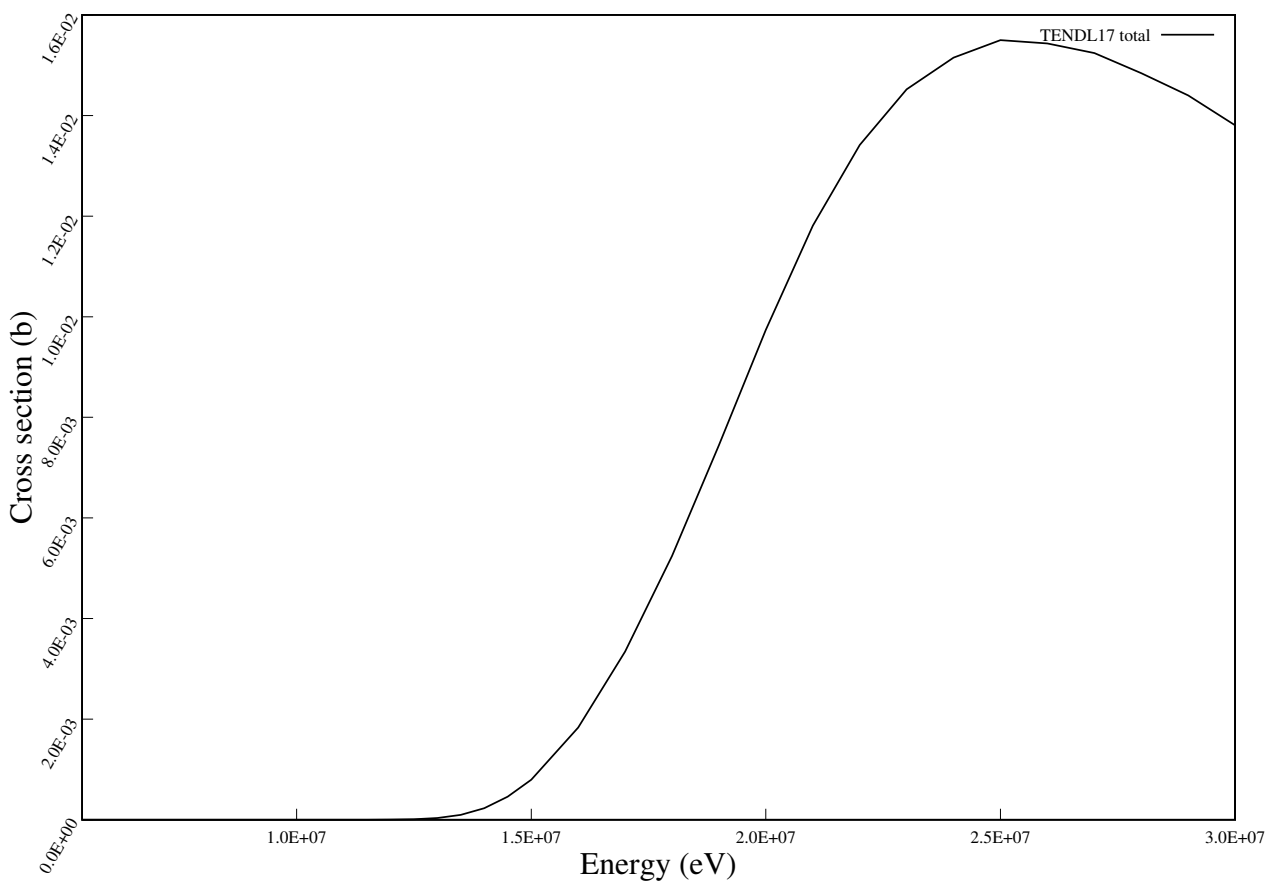
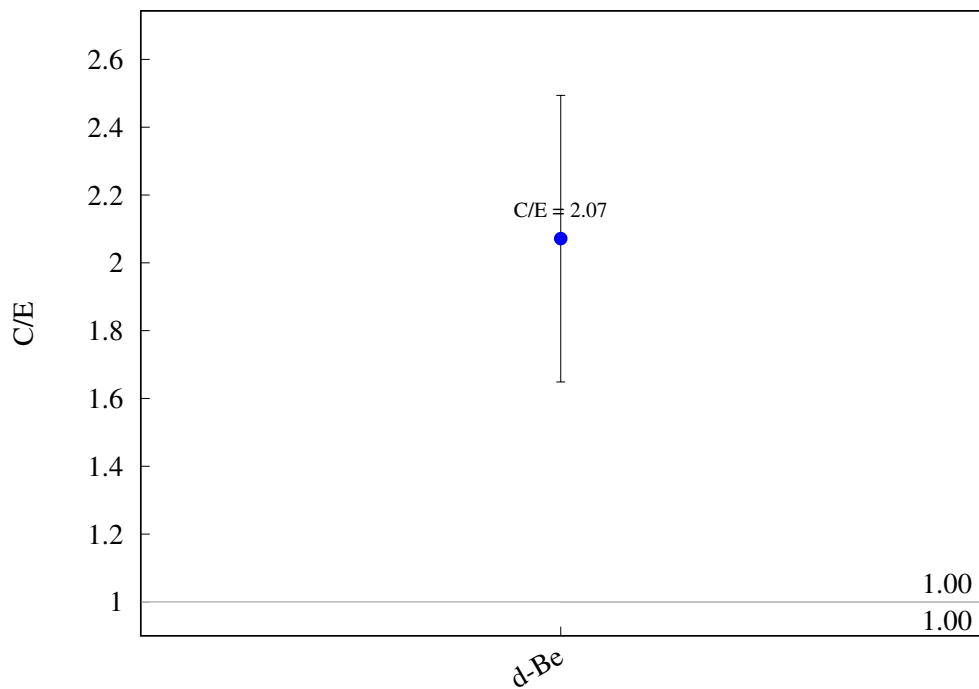
^{164}Dy (n,g) ^{165m}Dy 

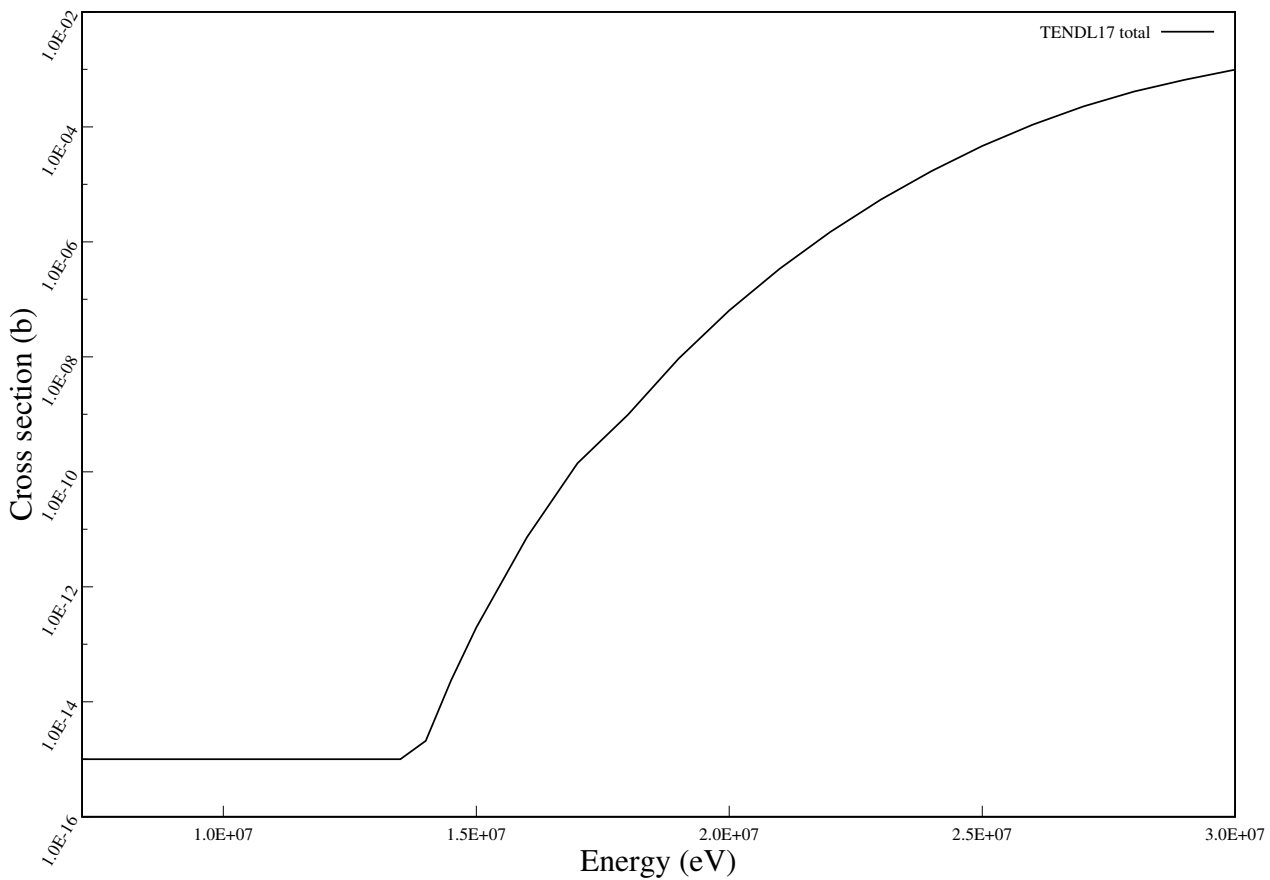
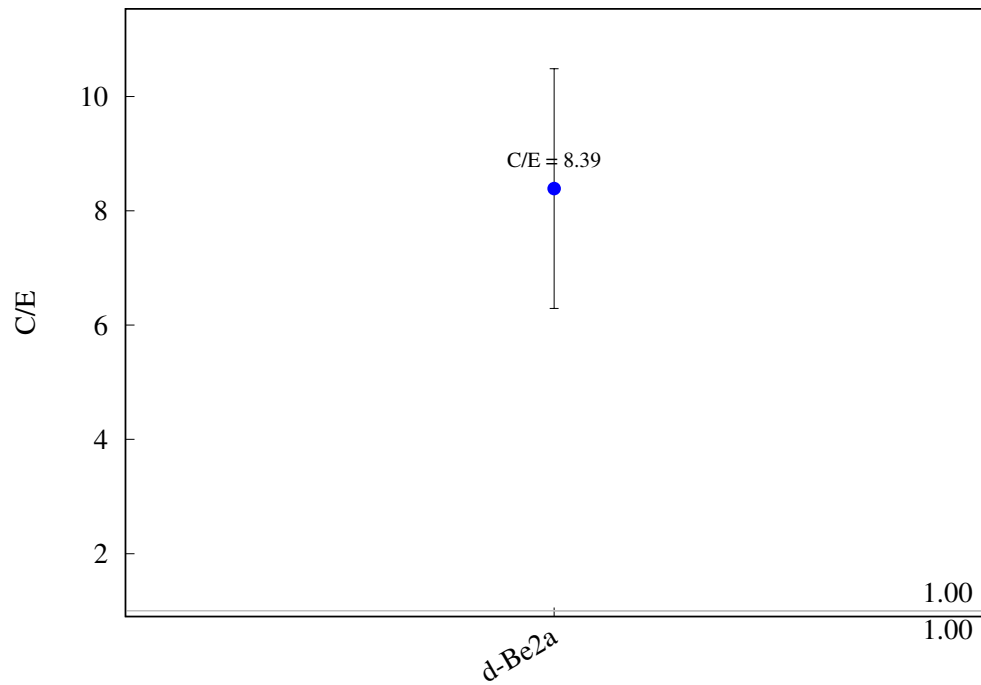
^{164}Dy (n,g) ^{165}Dy 

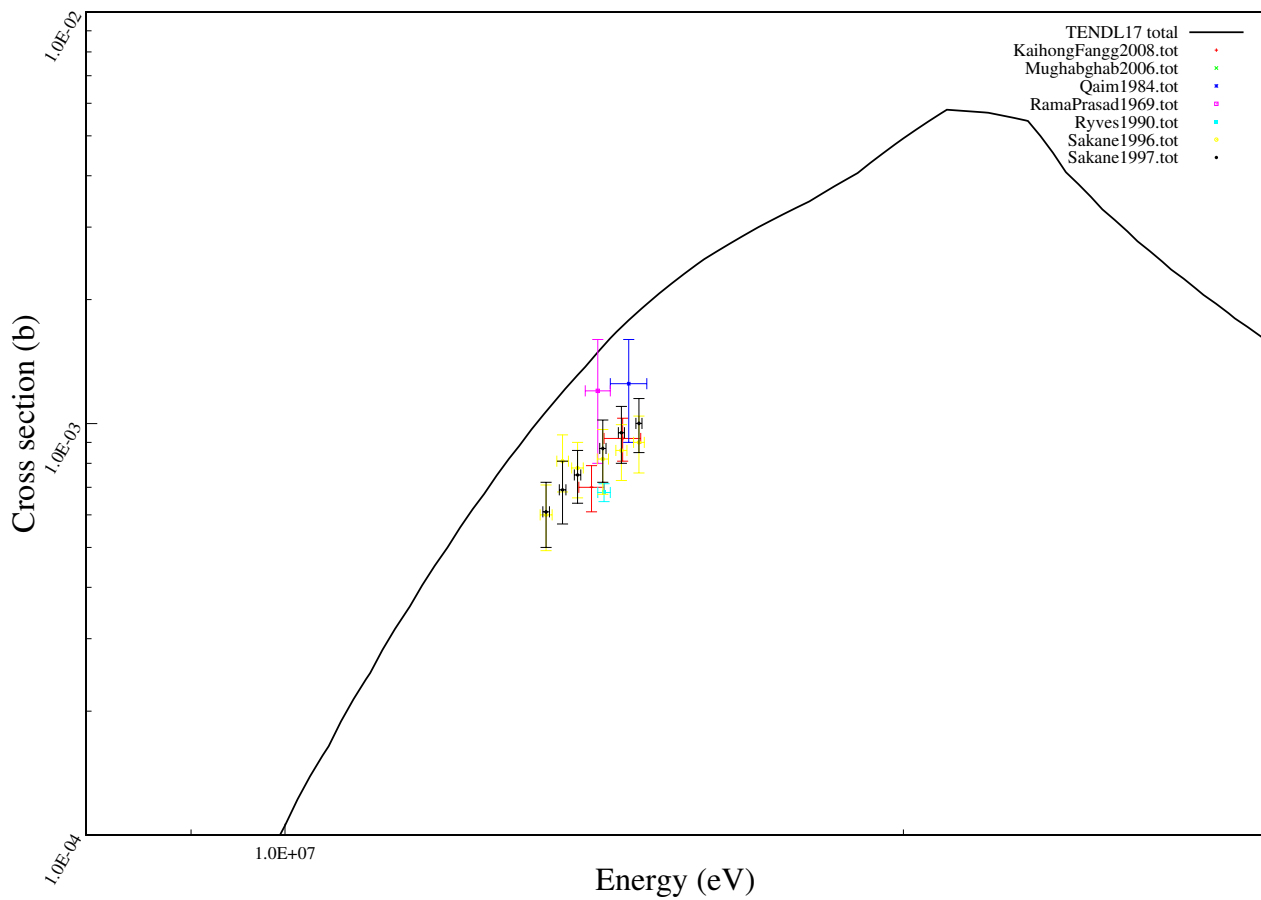
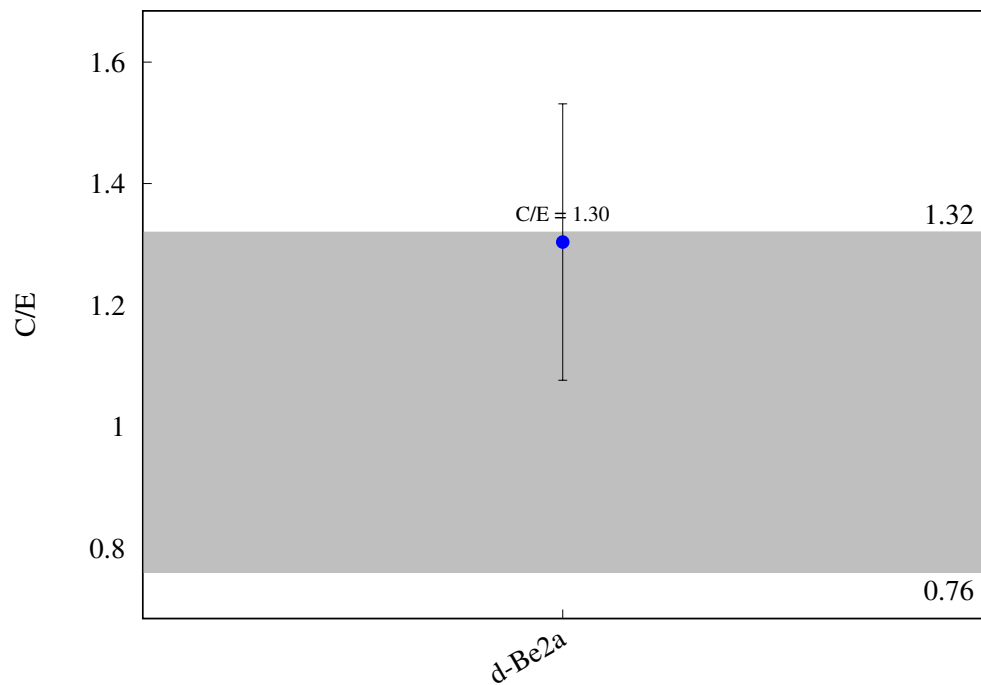
^{164}Dy (n,p) ^{164}Tb 

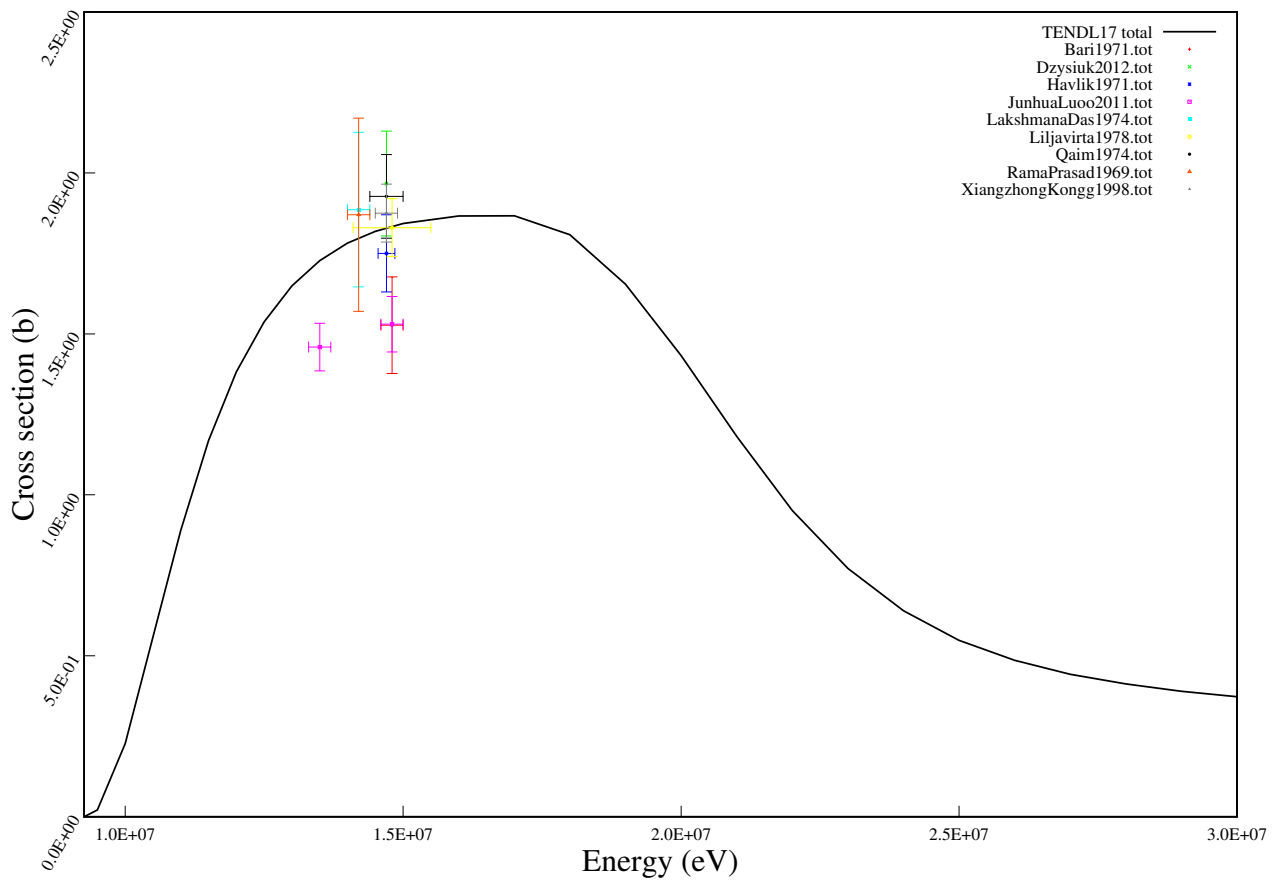
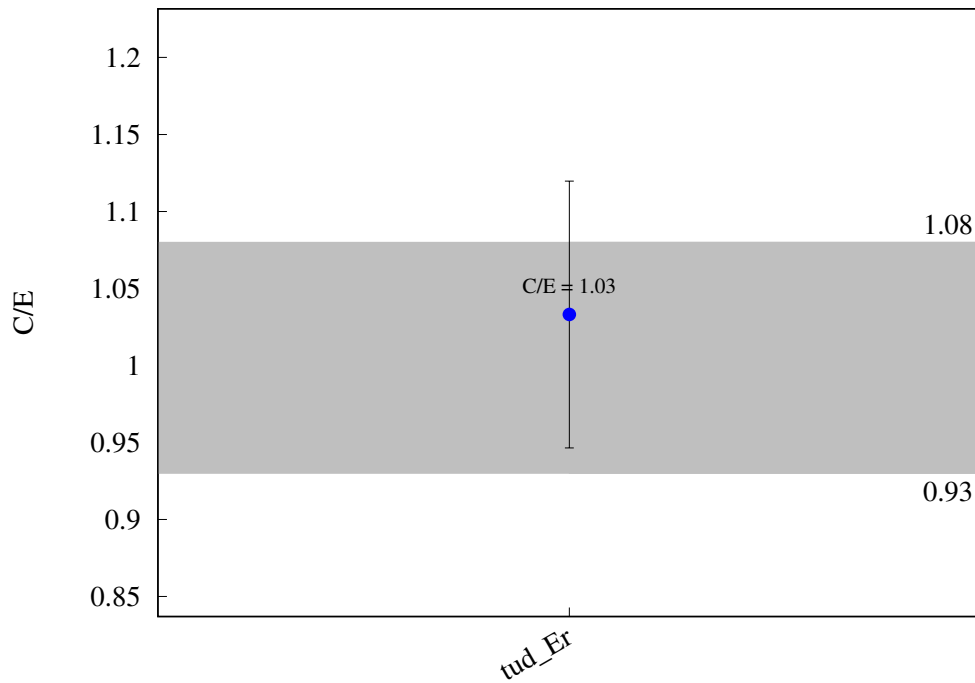
^{165}Ho (n,2n) $^{164\text{m}}\text{Ho}$ 

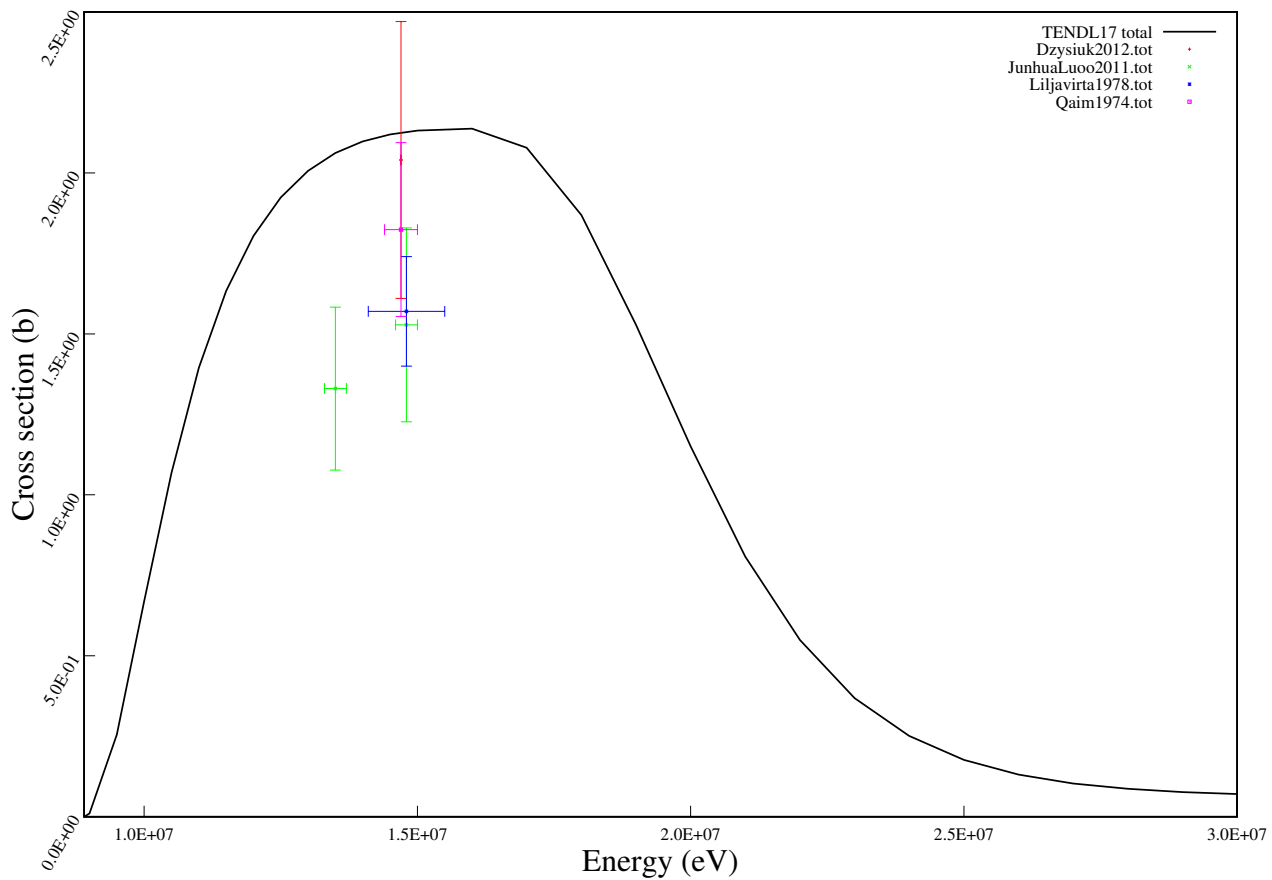
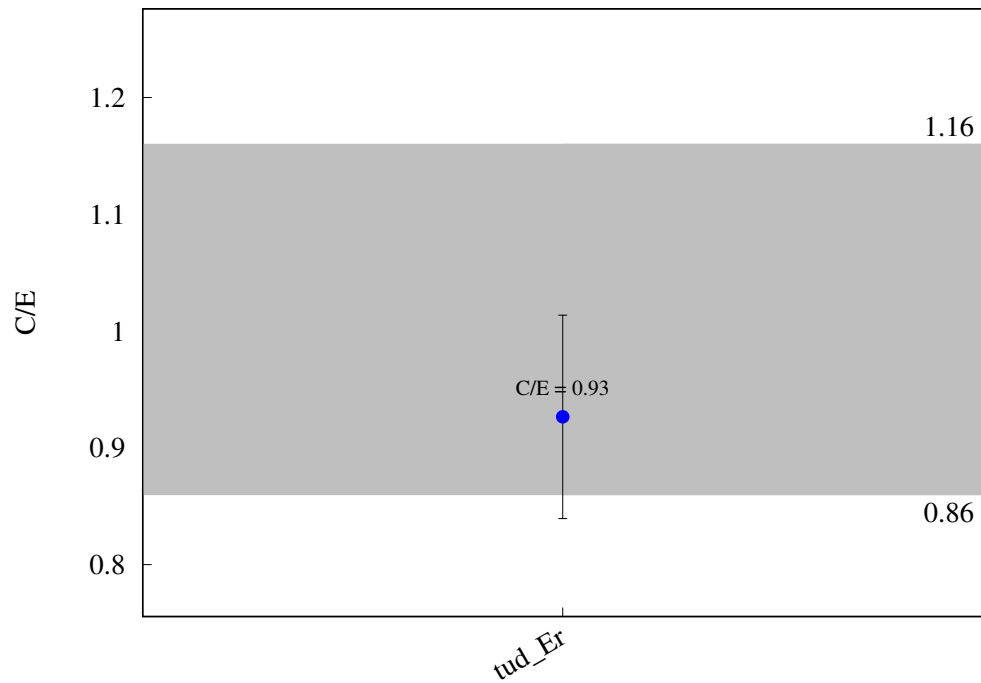
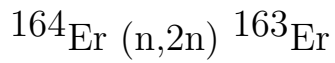
^{165}Ho (n,2n) ^{164}Ho 

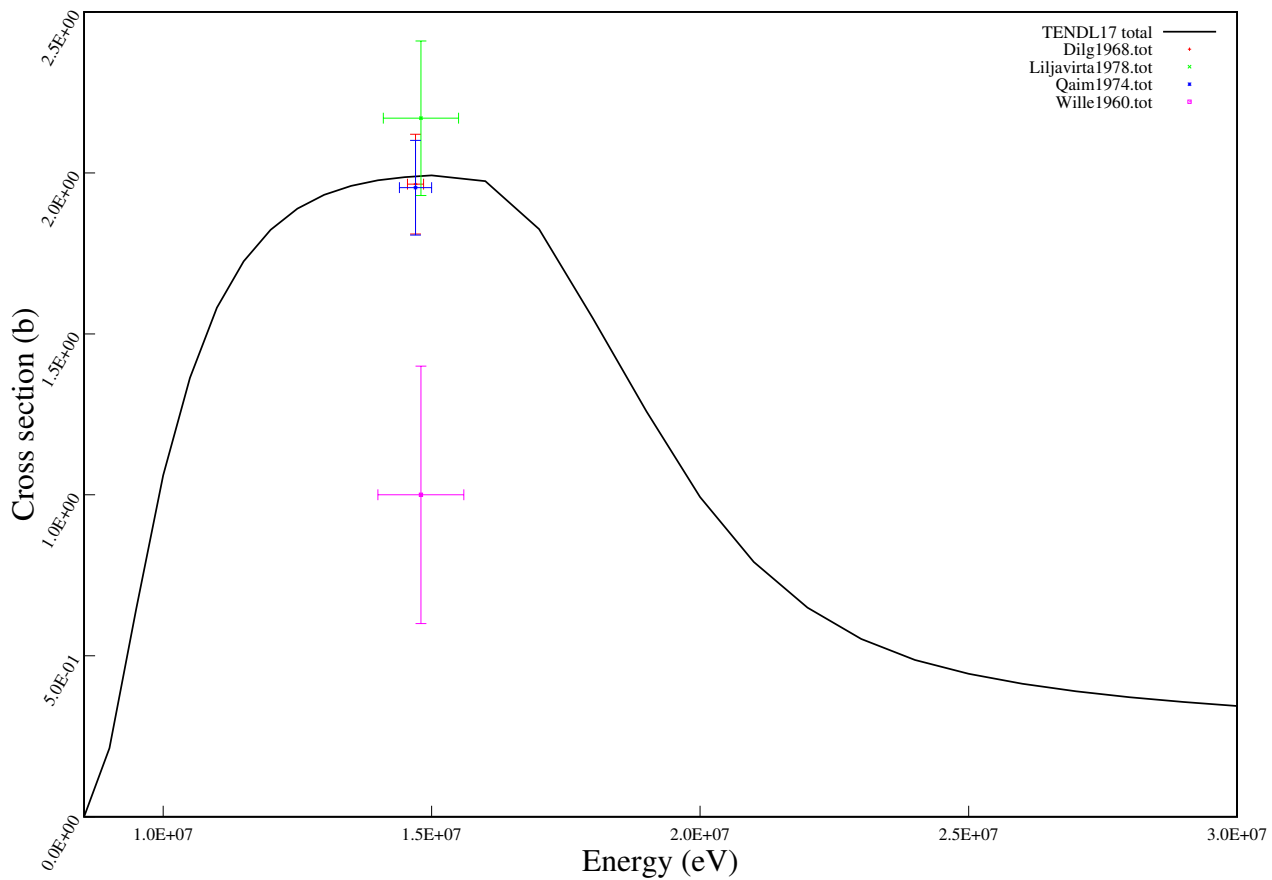
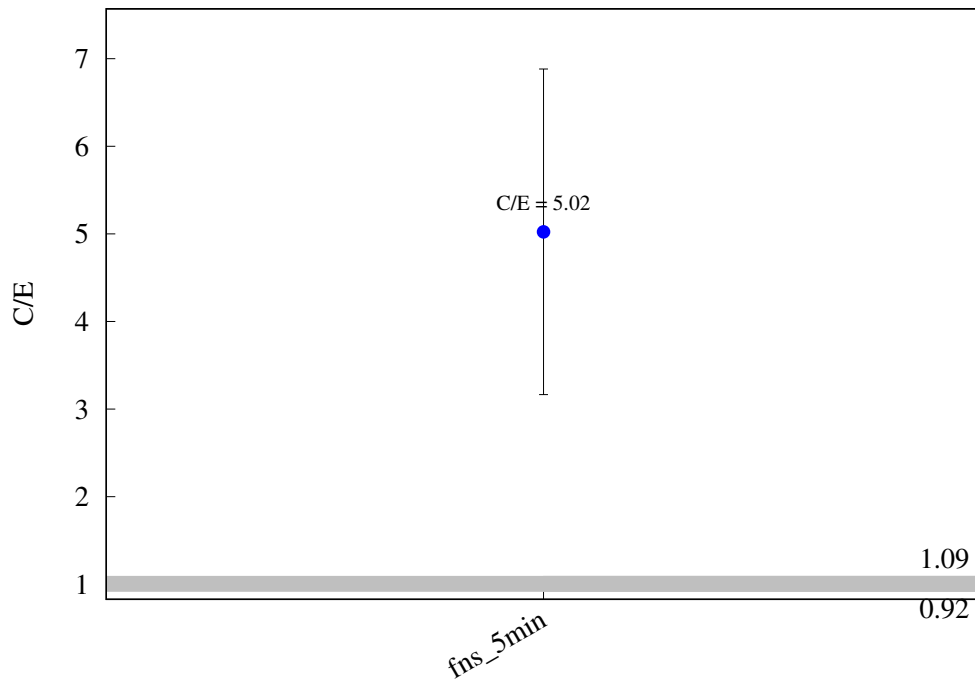
^{165}Ho (n,t) ^{163}Dy 

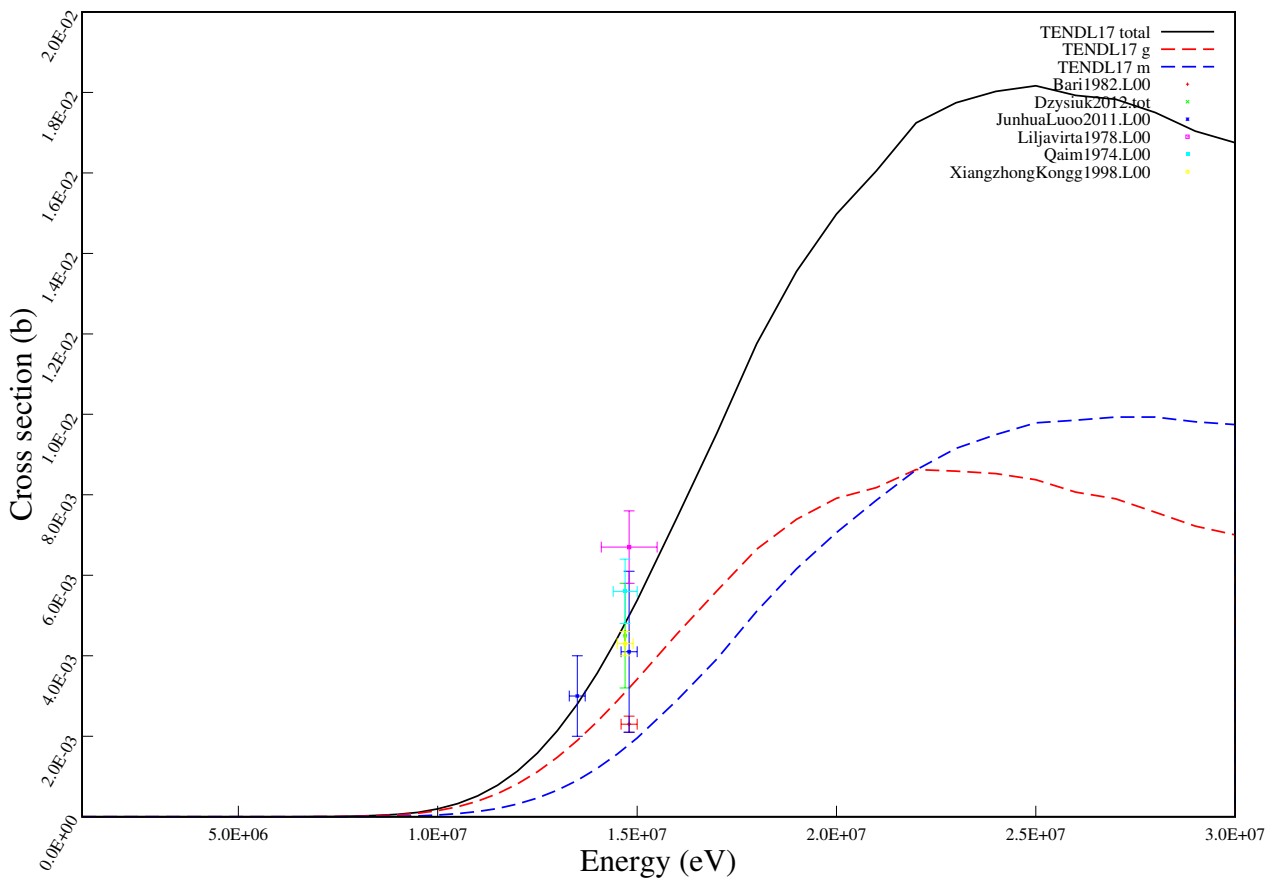
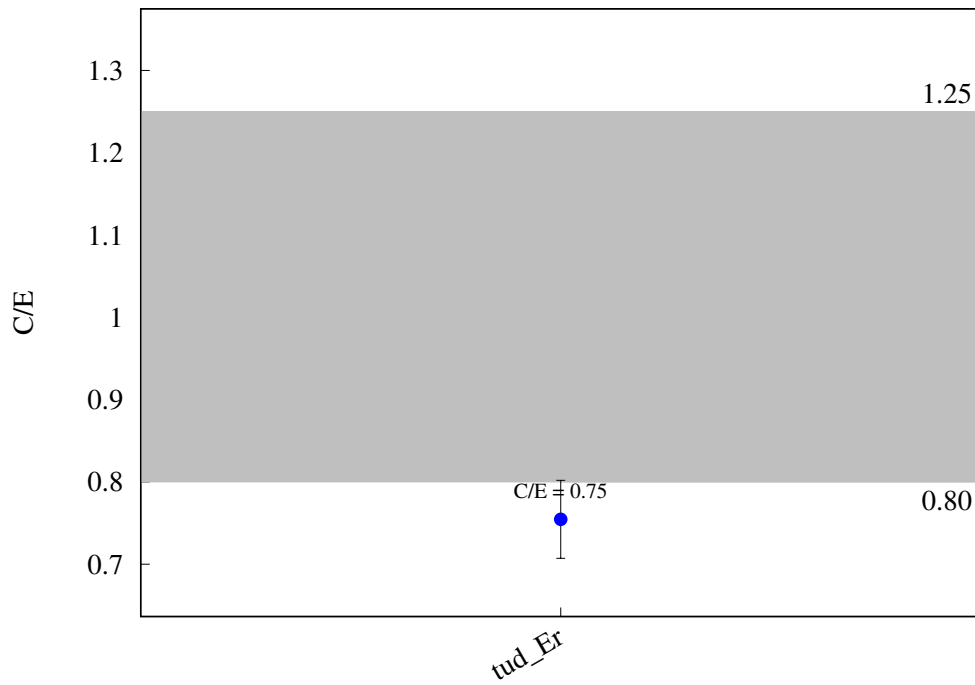
^{165}Ho (n,h) ^{163}Tb 

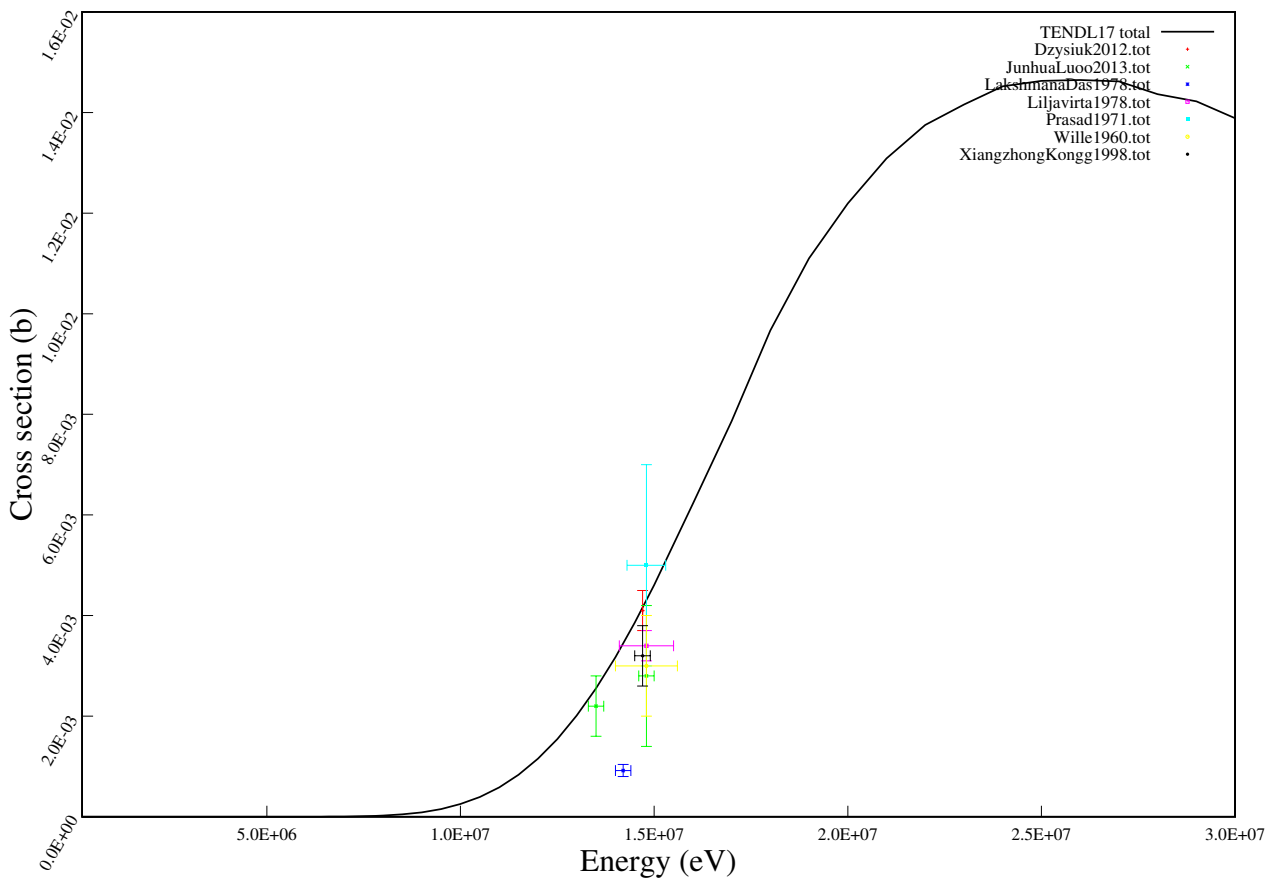
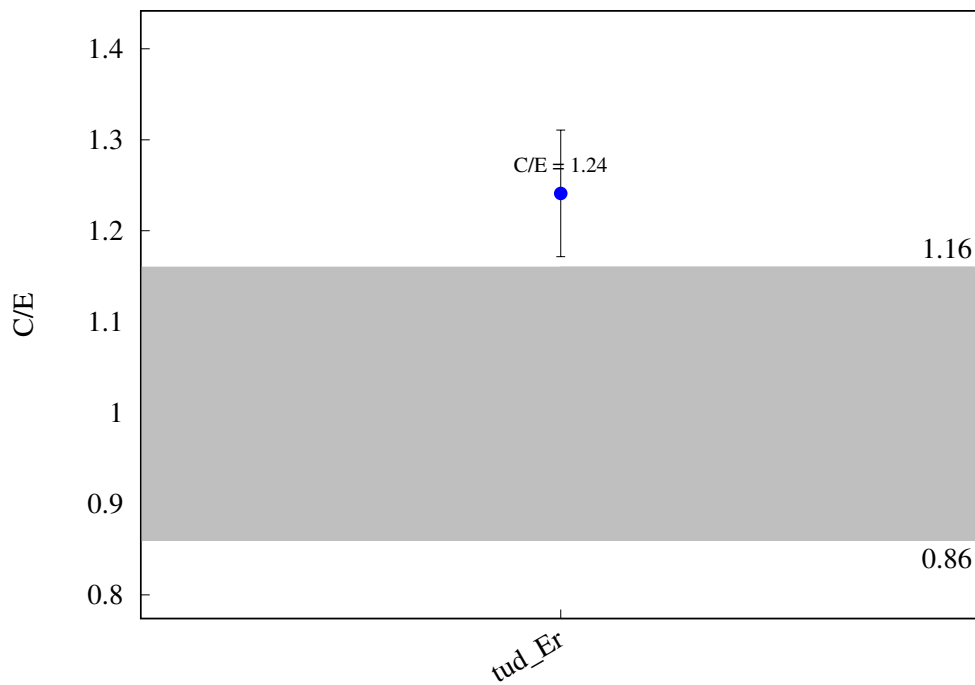
^{165}Ho (n,a) ^{162}Tb 

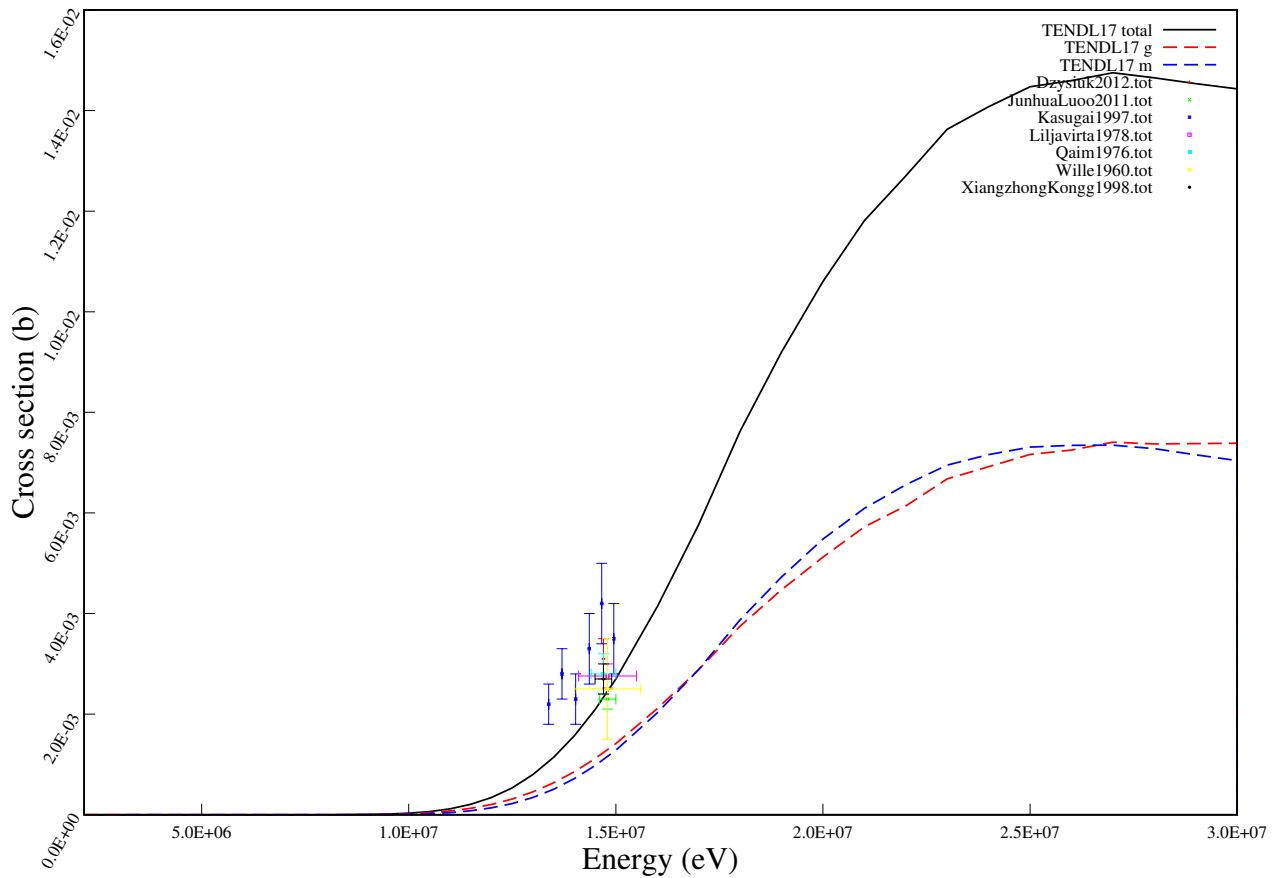
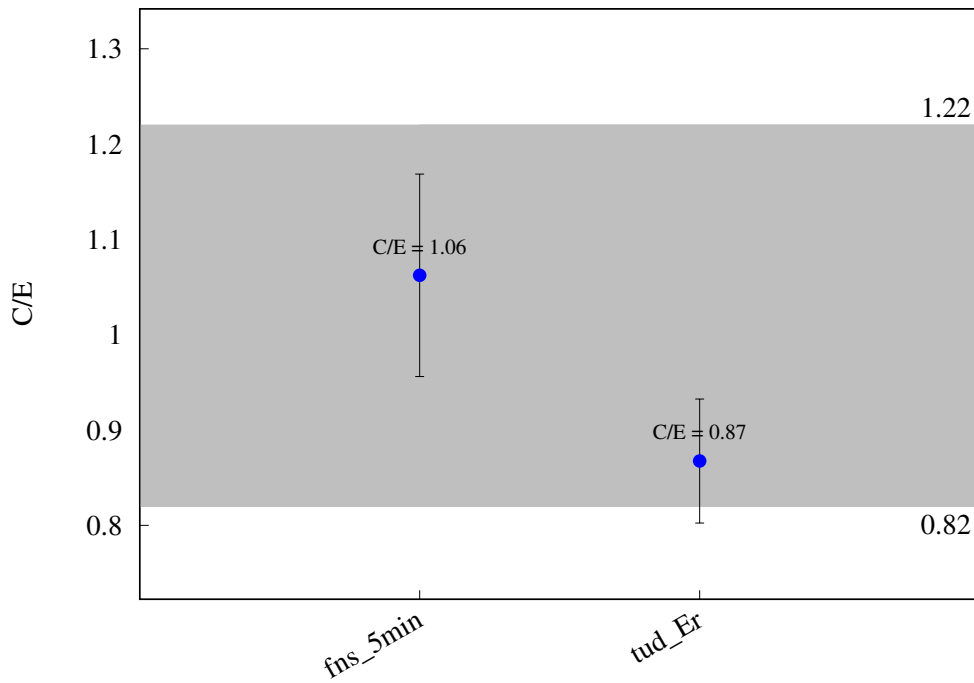
^{162}Er (n,2n) ^{161}Er 

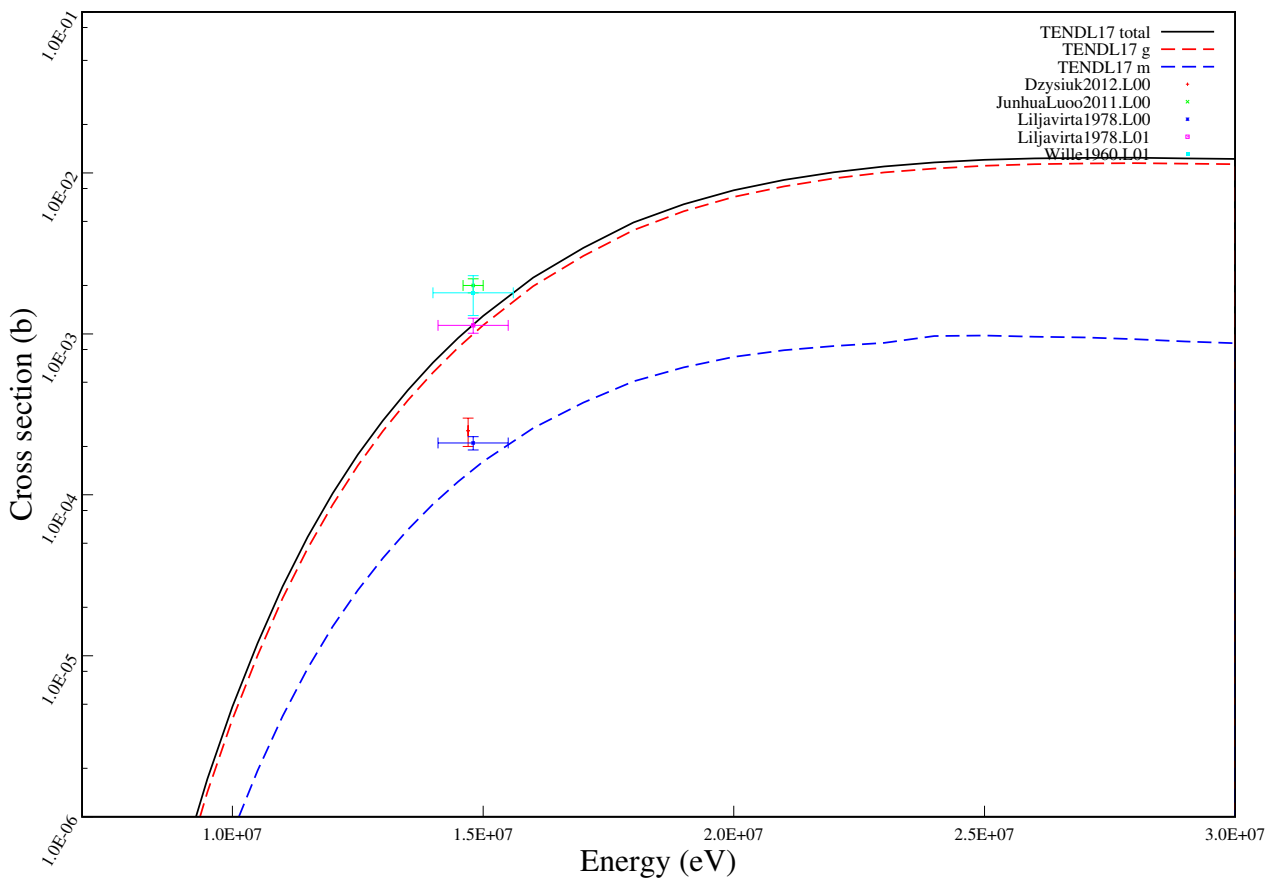
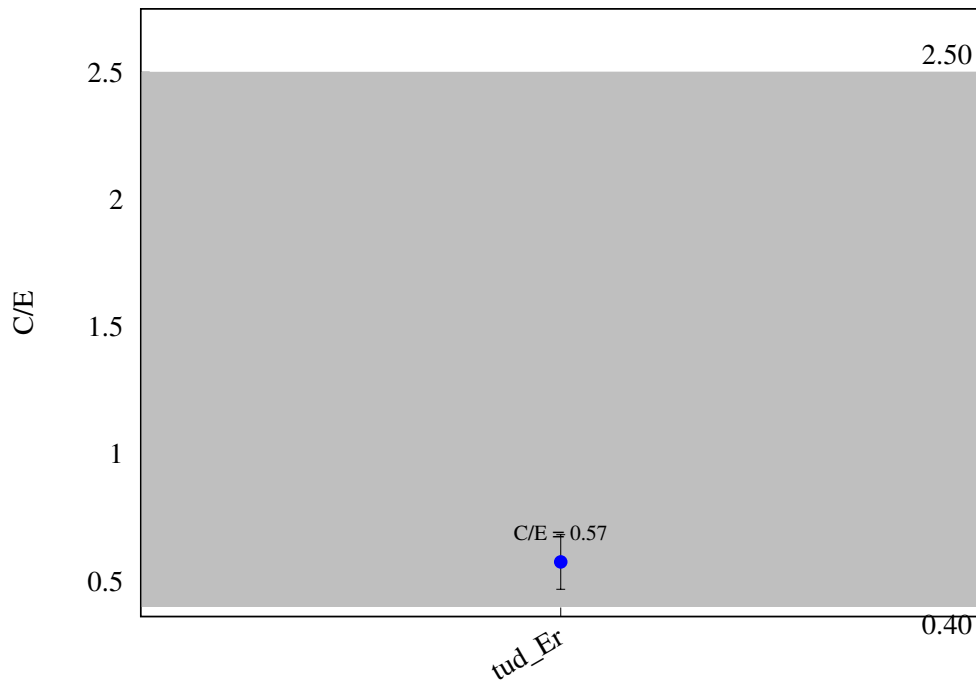


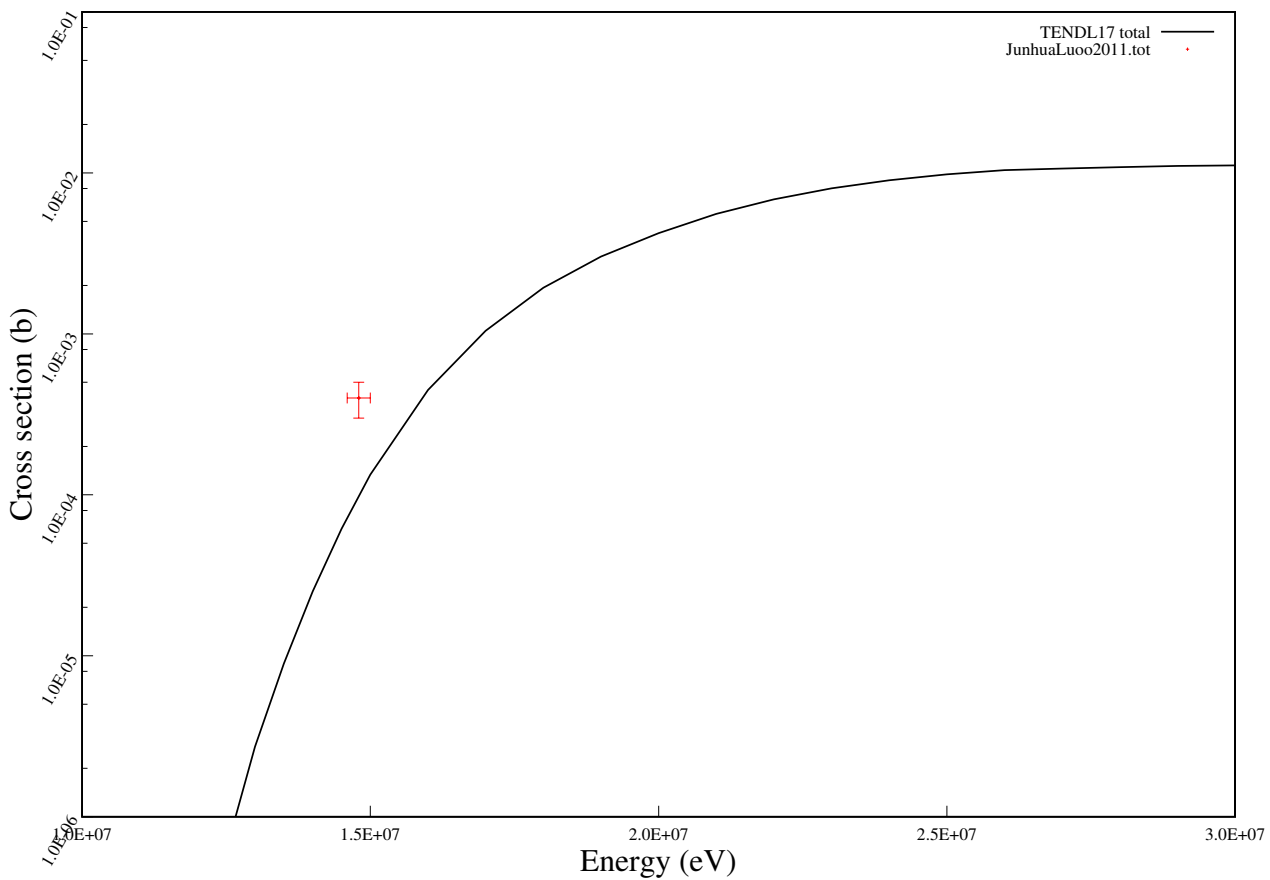
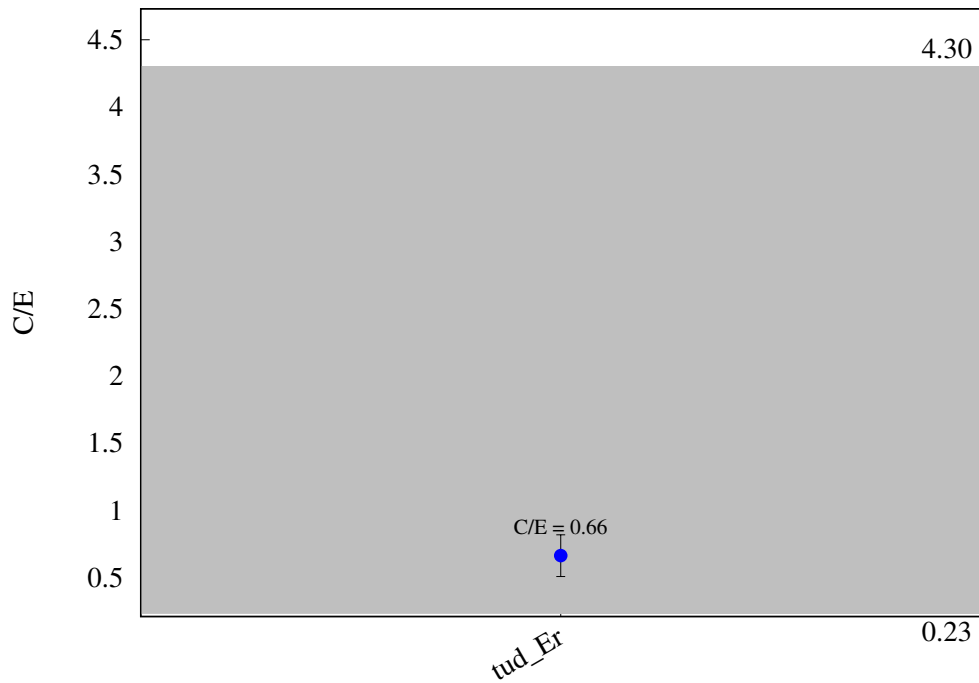
^{166}Er (n,2n) ^{165}Er 

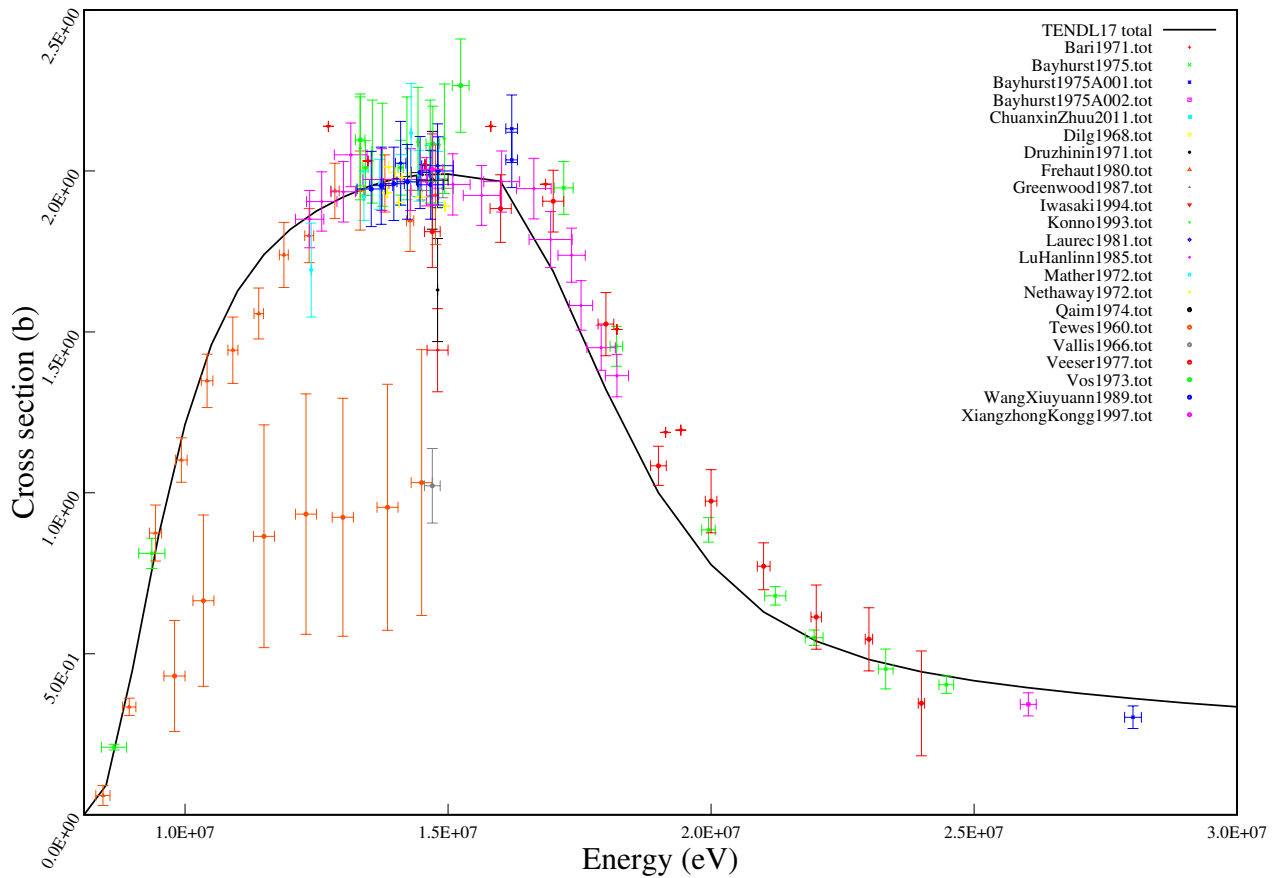
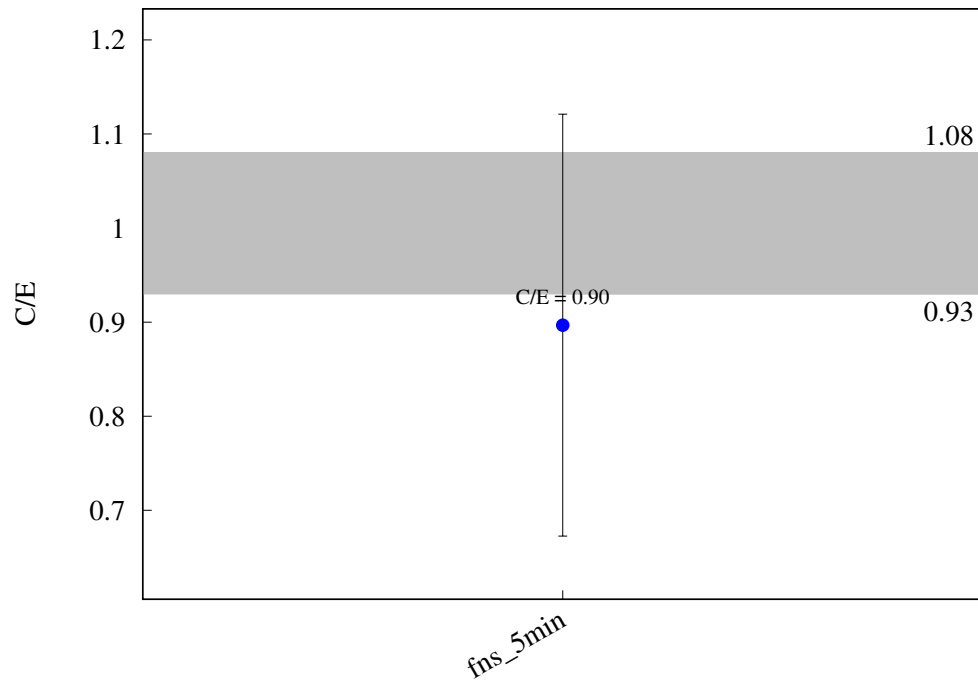
^{166}Er (n,p) ^{166}gHo 

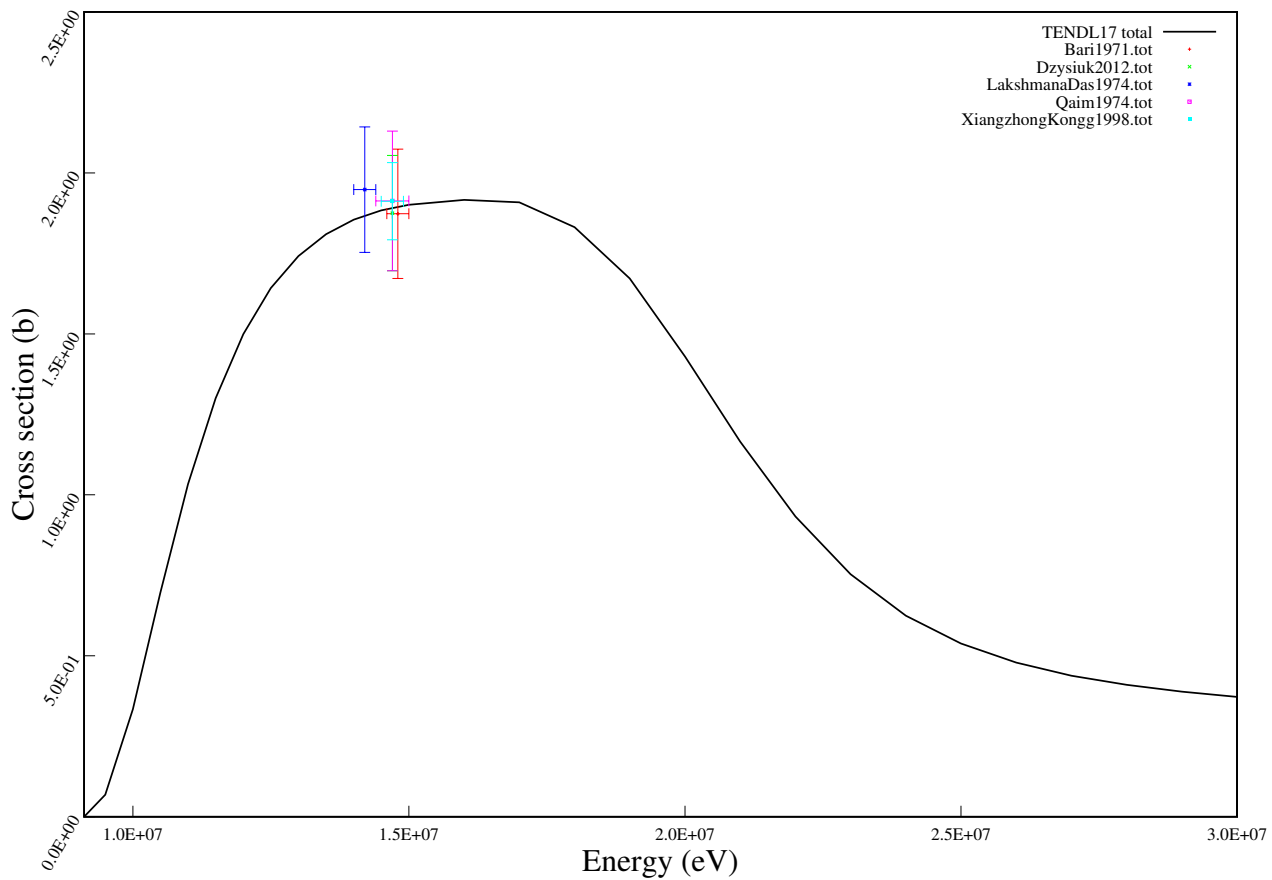
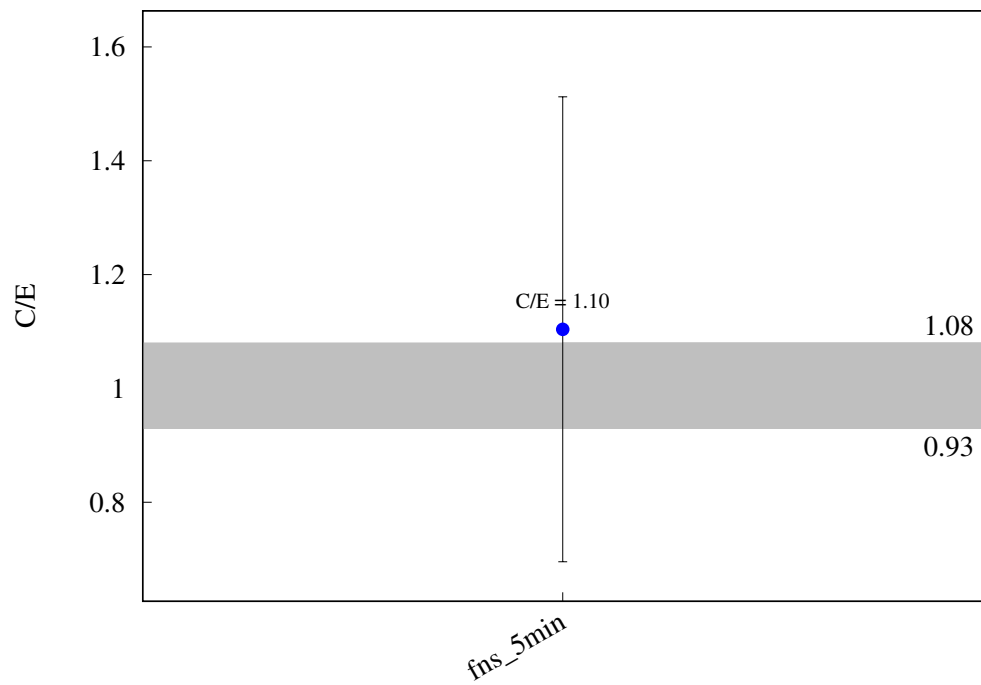
^{167}Er (n,p) ^{167}Ho 

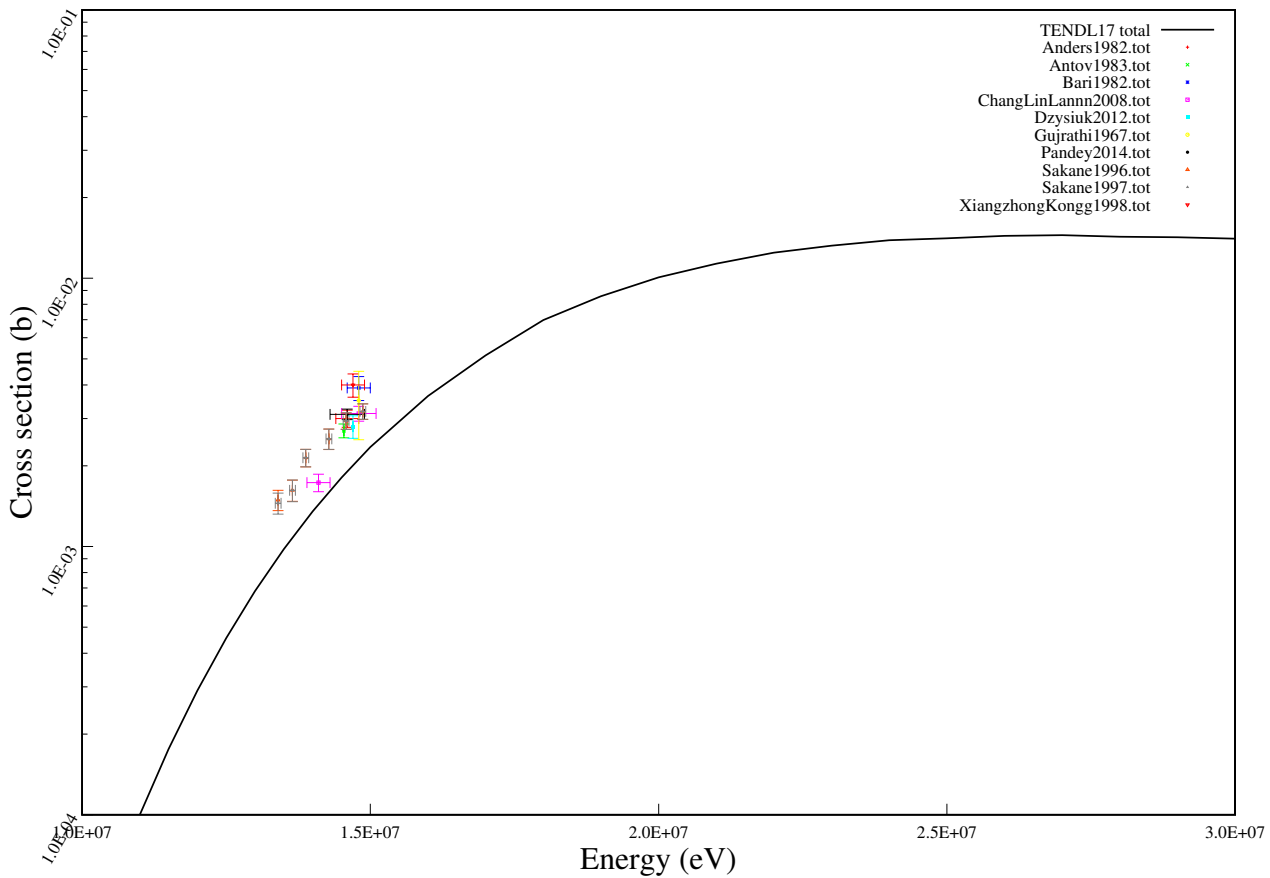
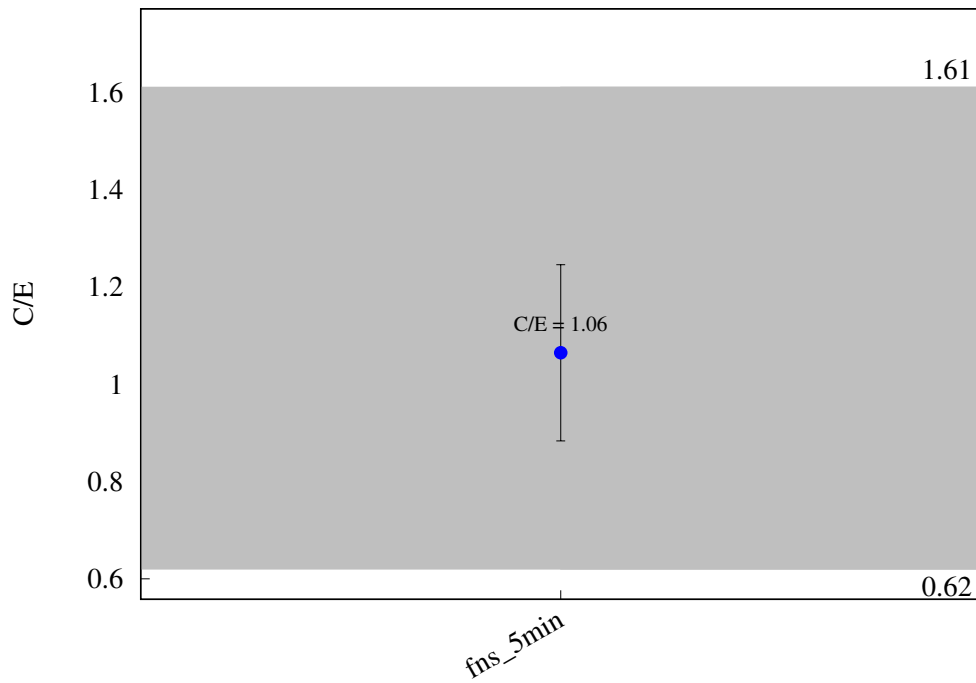
^{168}Er (n,p) ^{168}Ho 

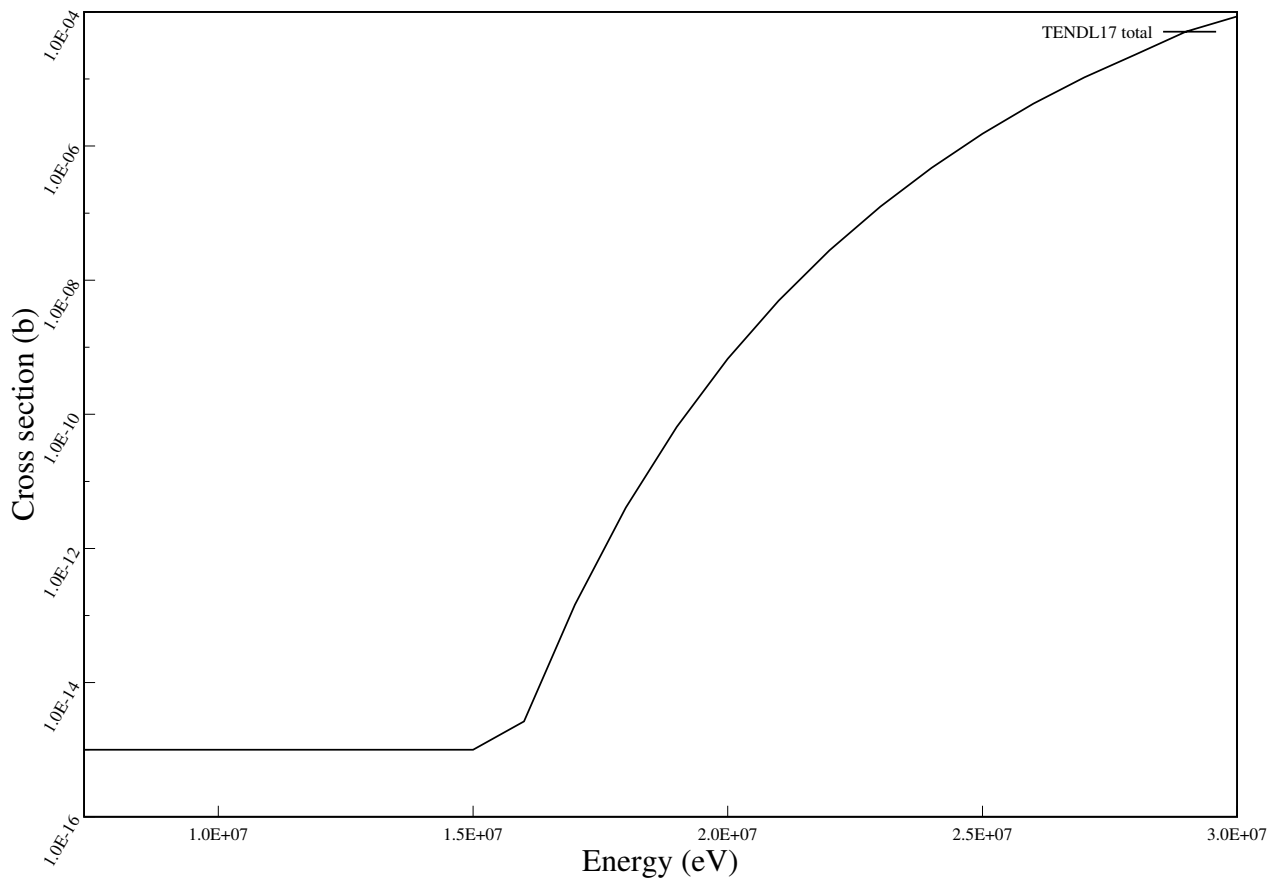
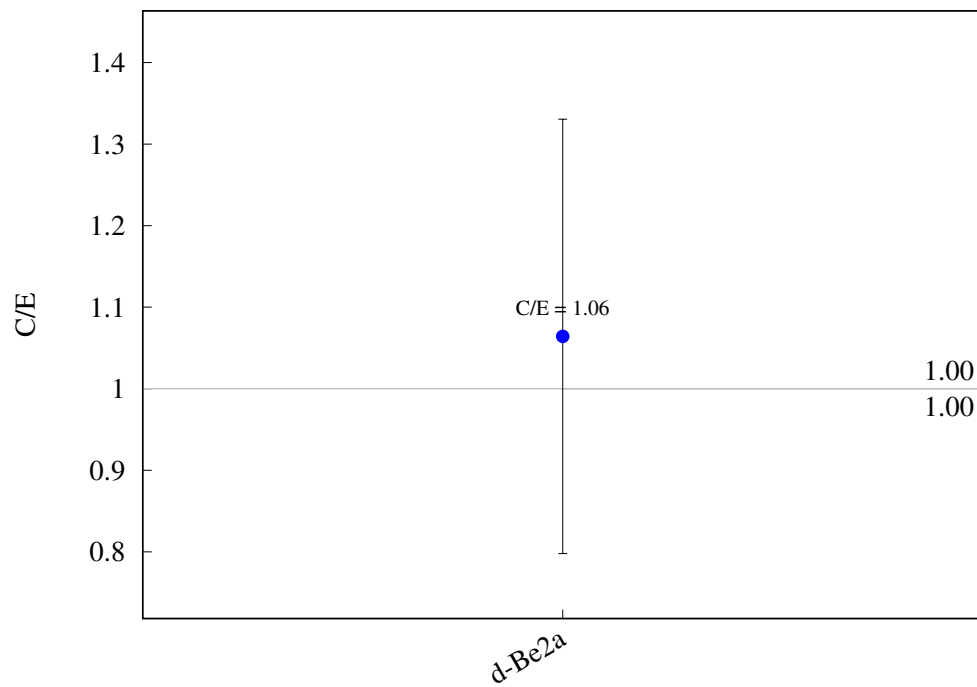
^{170}Er (n,p) ^{170}gHo 

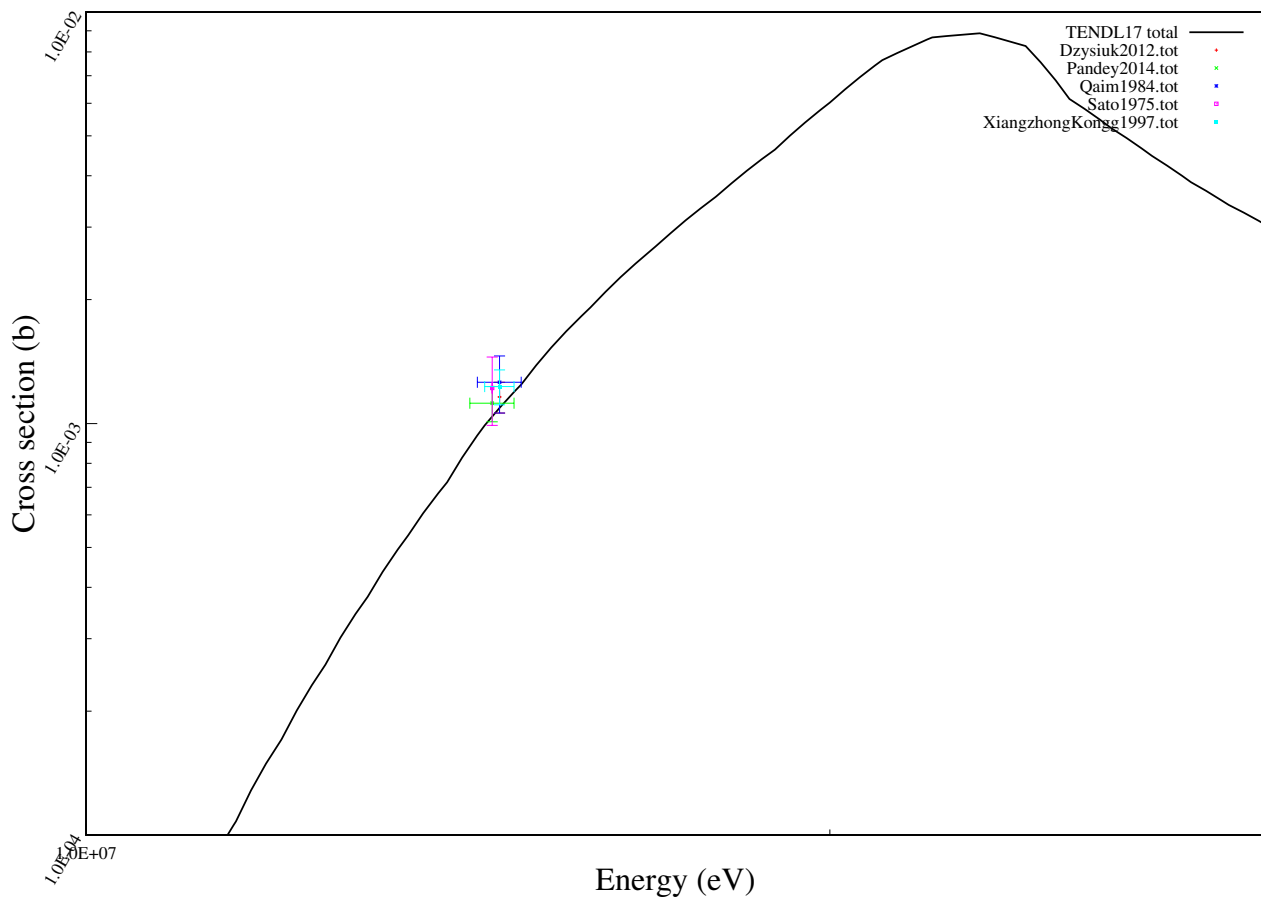
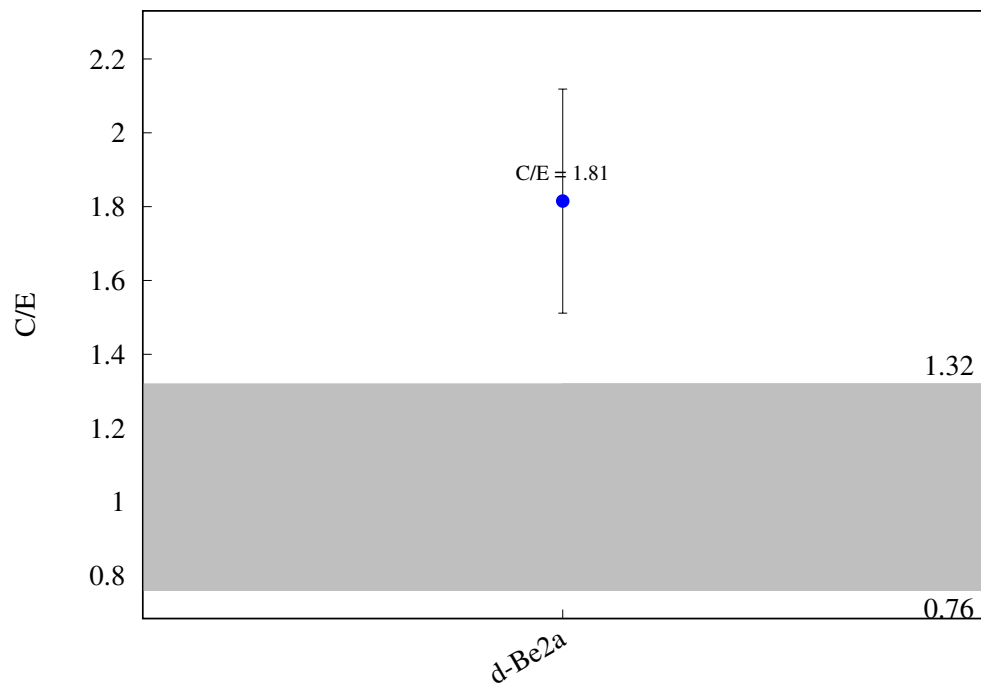
^{170}Er (n,d) ^{169}Ho 

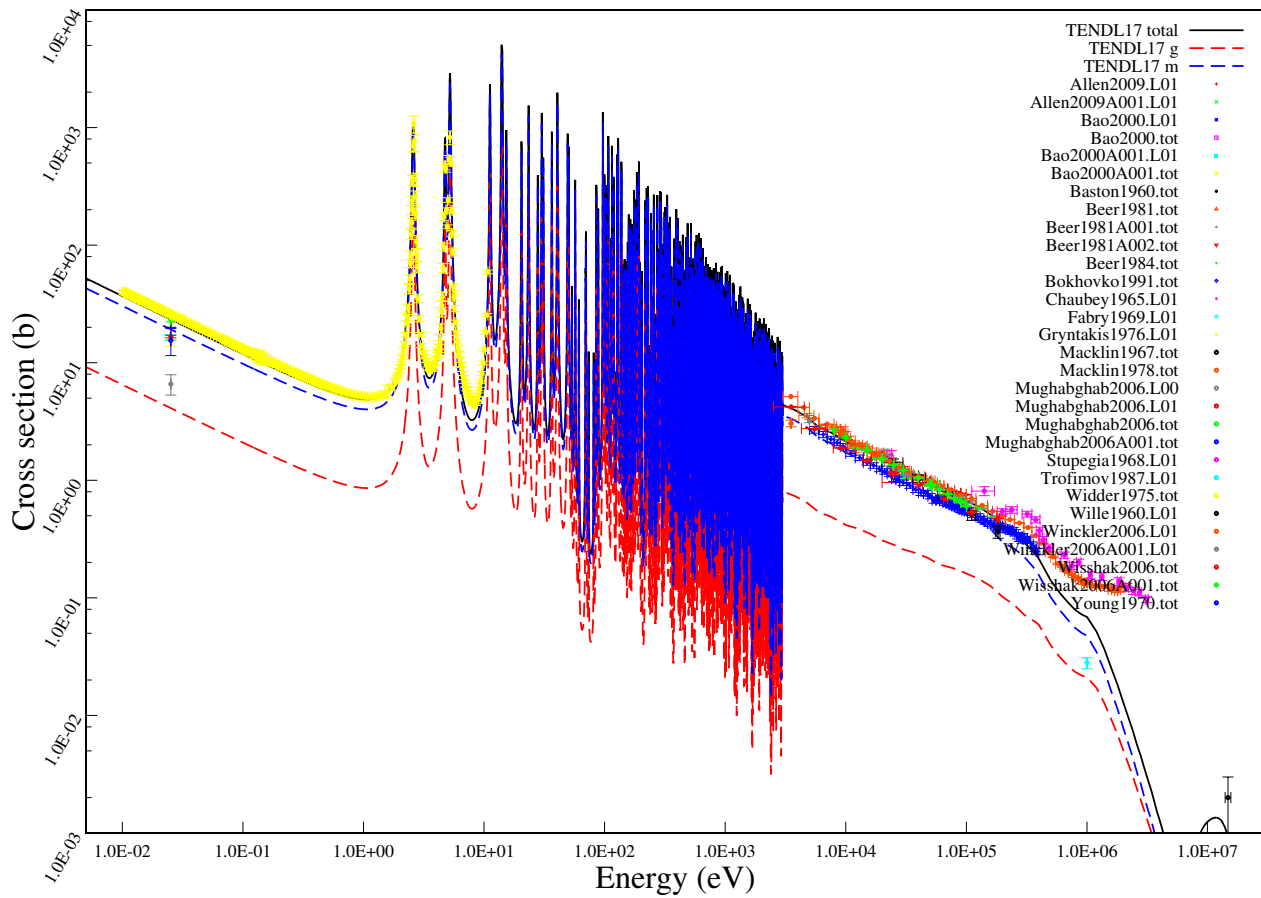
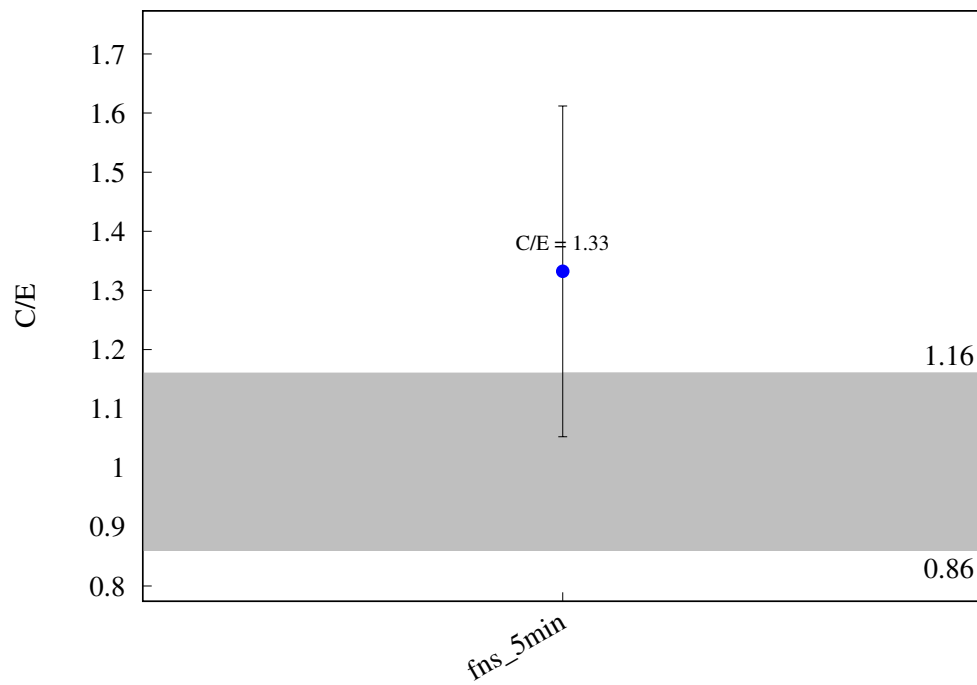
^{169}Tm (n,2n) ^{168}Tm 

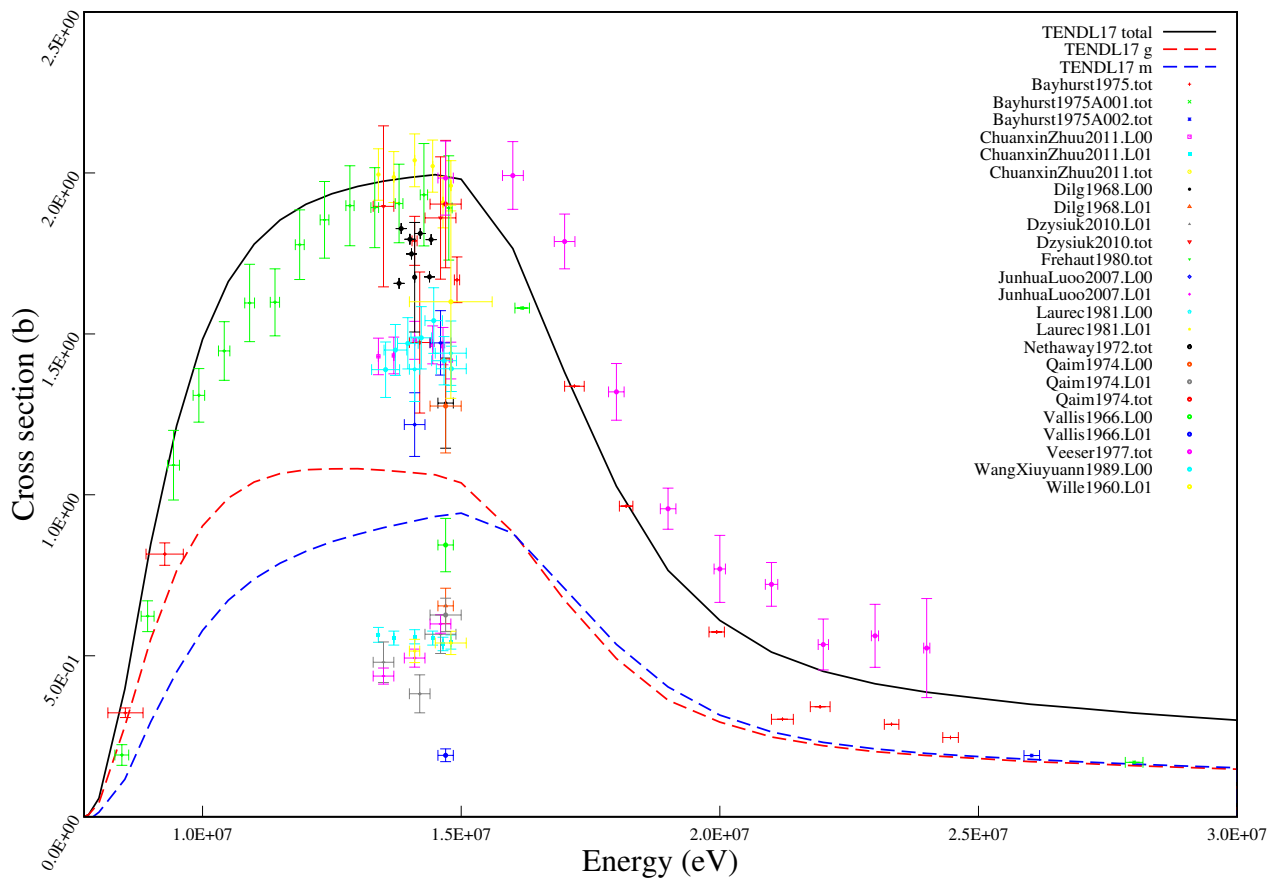
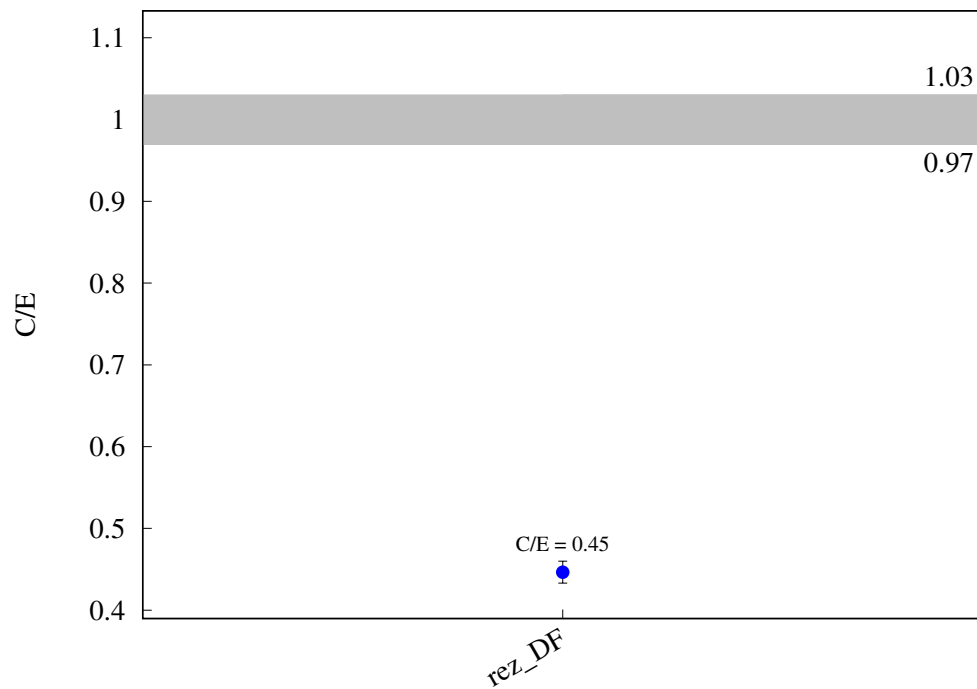
^{168}Yb (n,2n) ^{167}Yb 

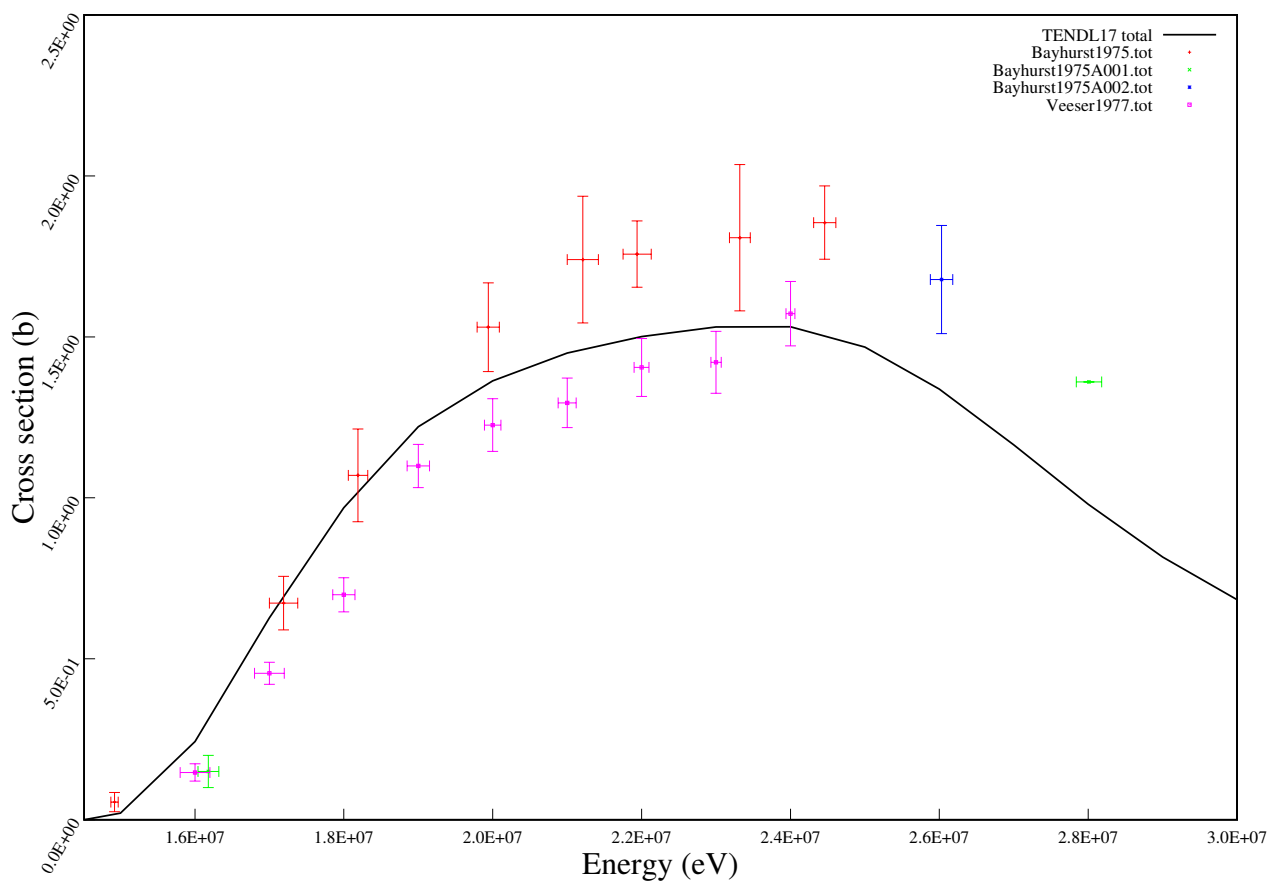
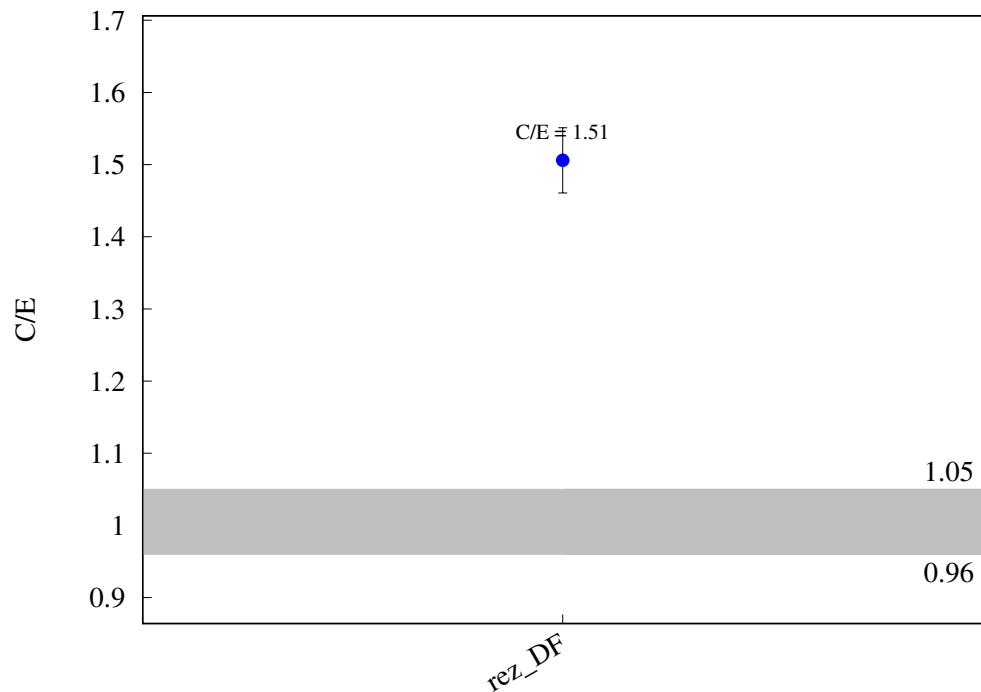
$^{174}\text{Yb} (\text{n},\text{p}) ^{174}\text{Tm}$ 

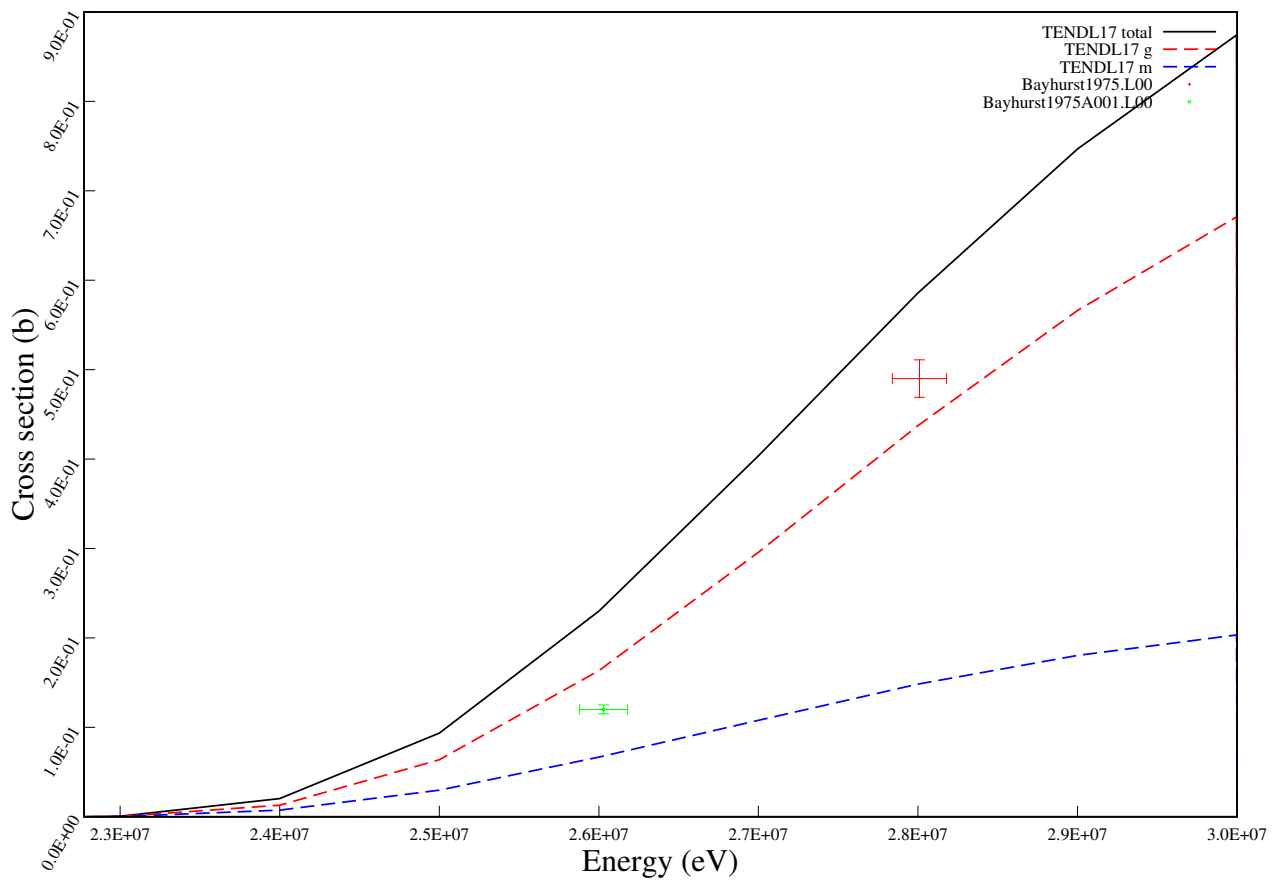
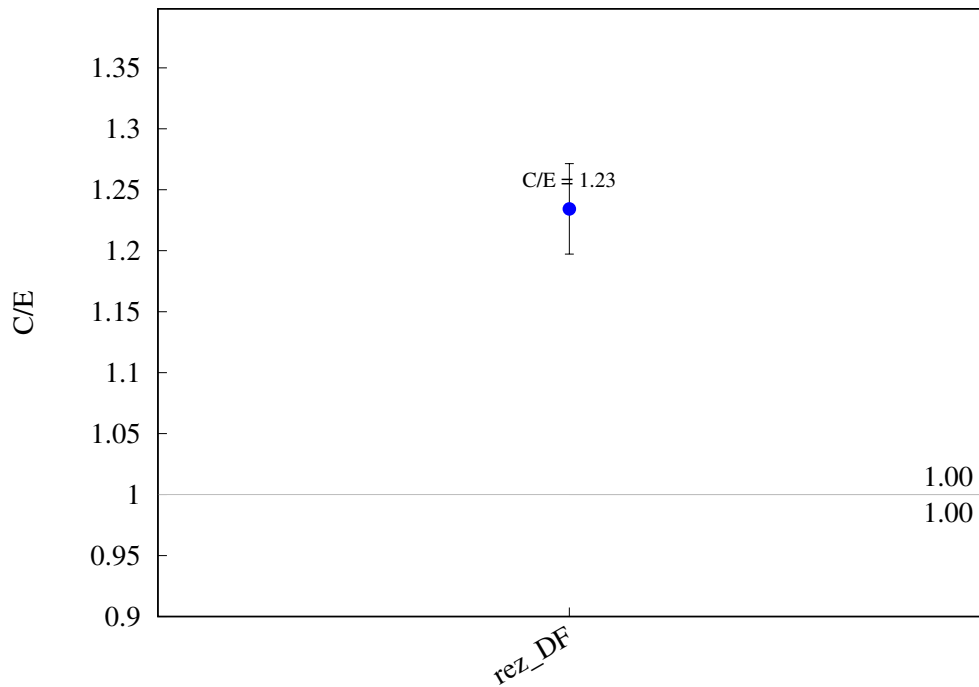
^{174}Yb (n,h) ^{172}Er 

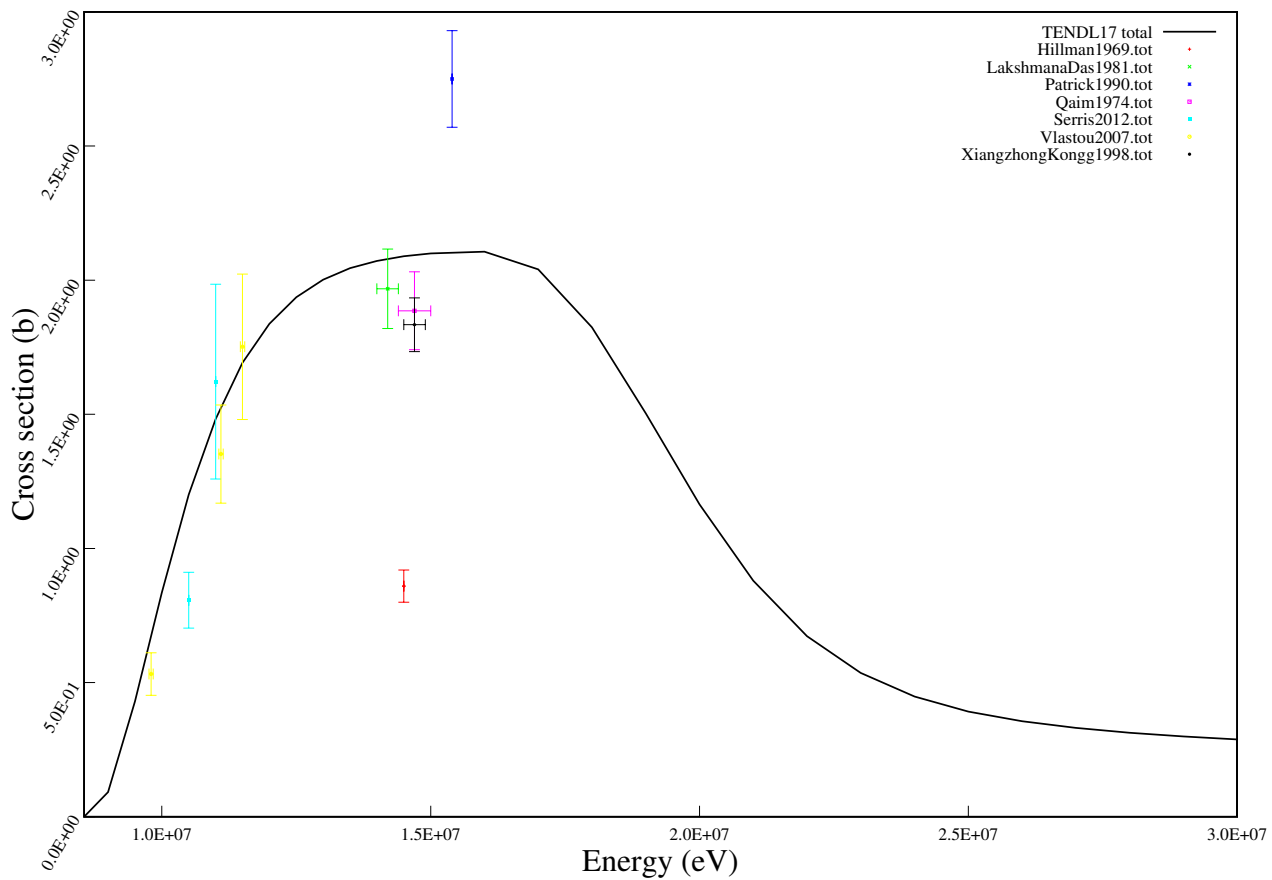
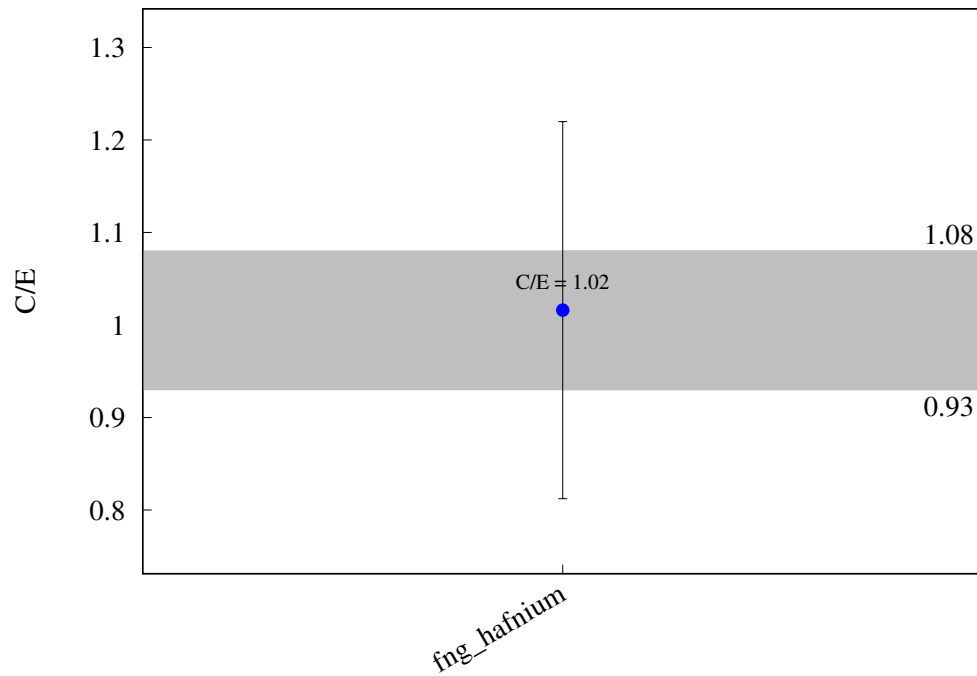
$^{174}\text{Yb} (\text{n},\text{a}) ^{171}\text{Er}$ 

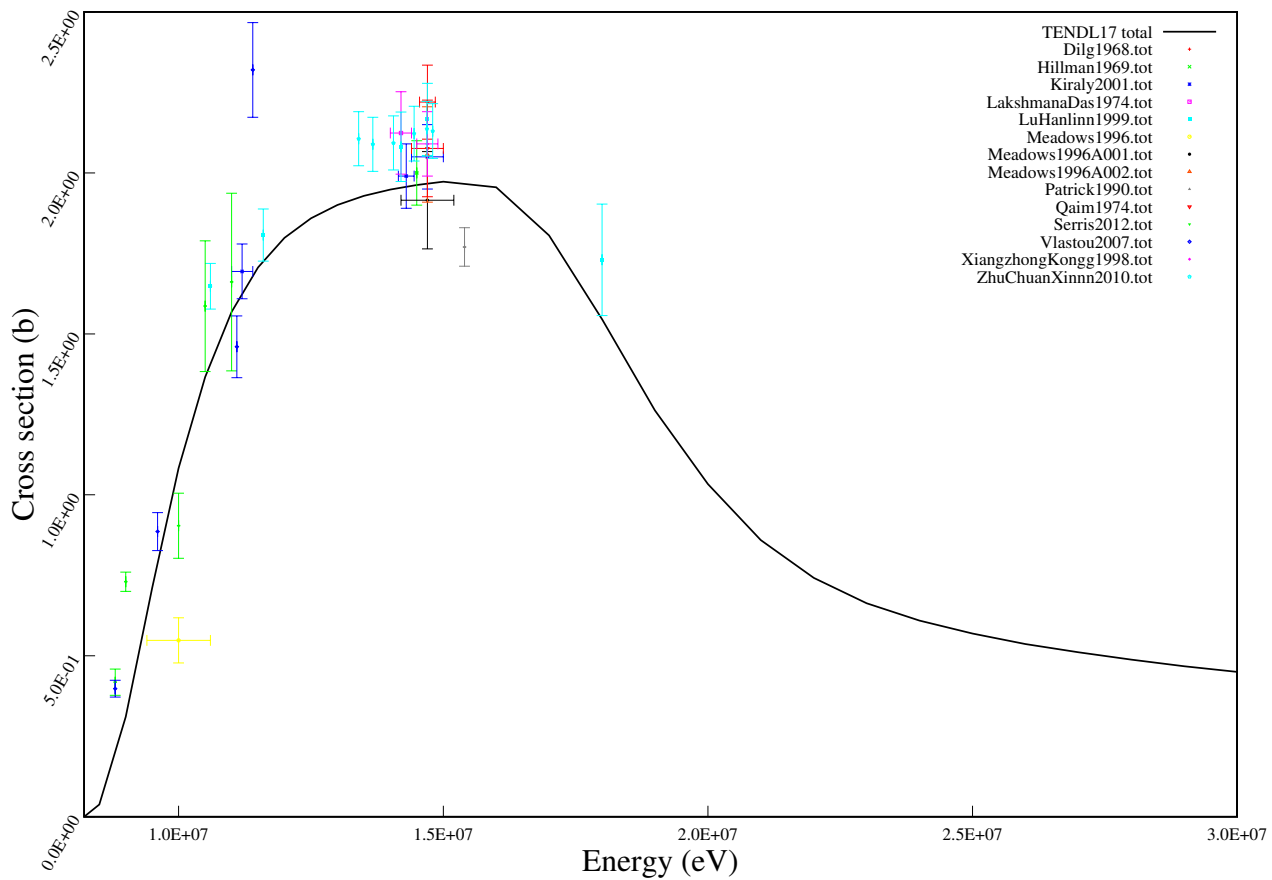
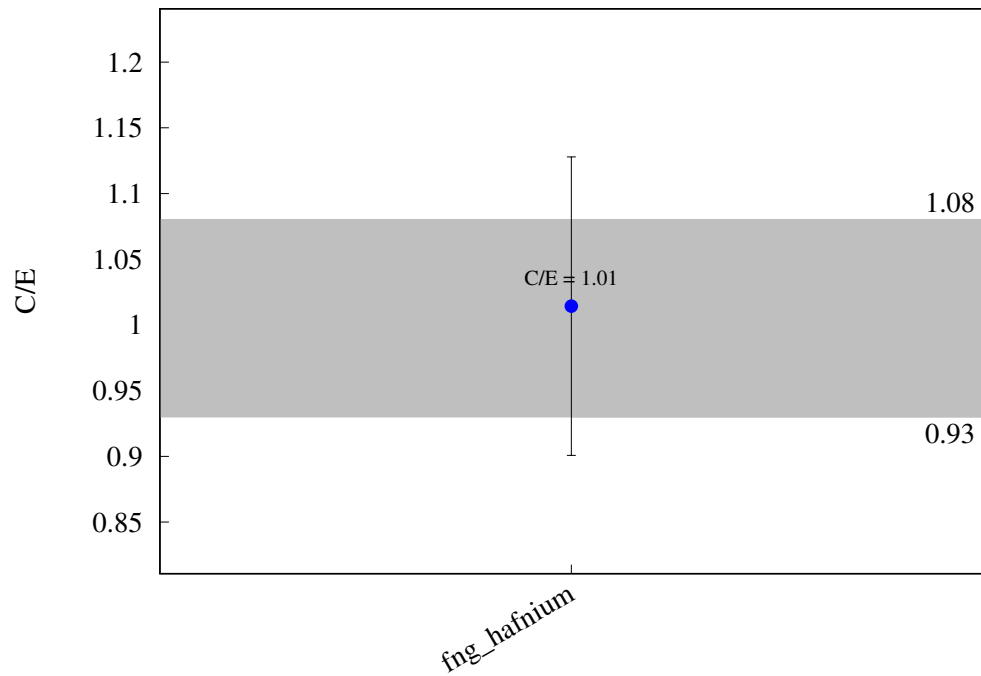
^{175}Lu (n,g) $^{176\text{m}}\text{Lu}$ 

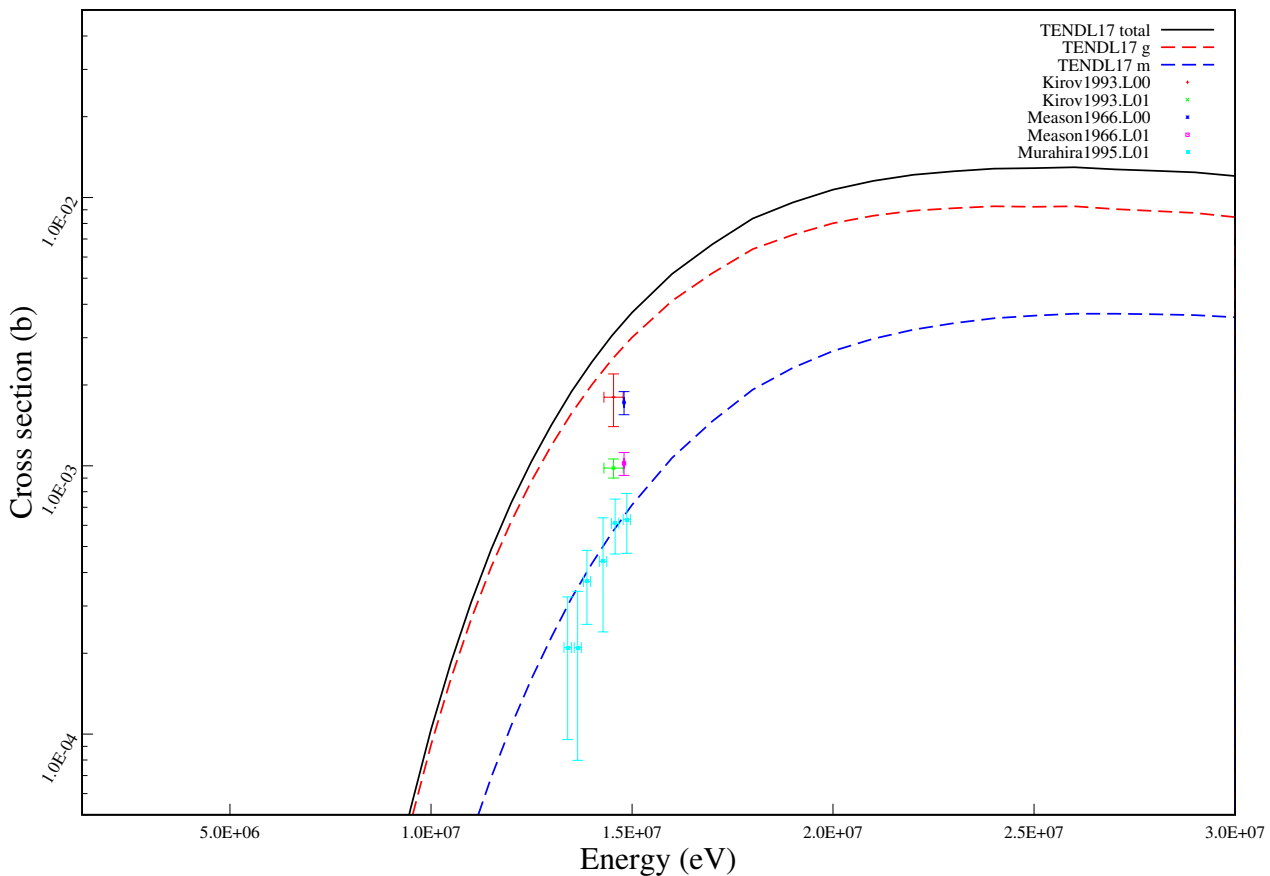
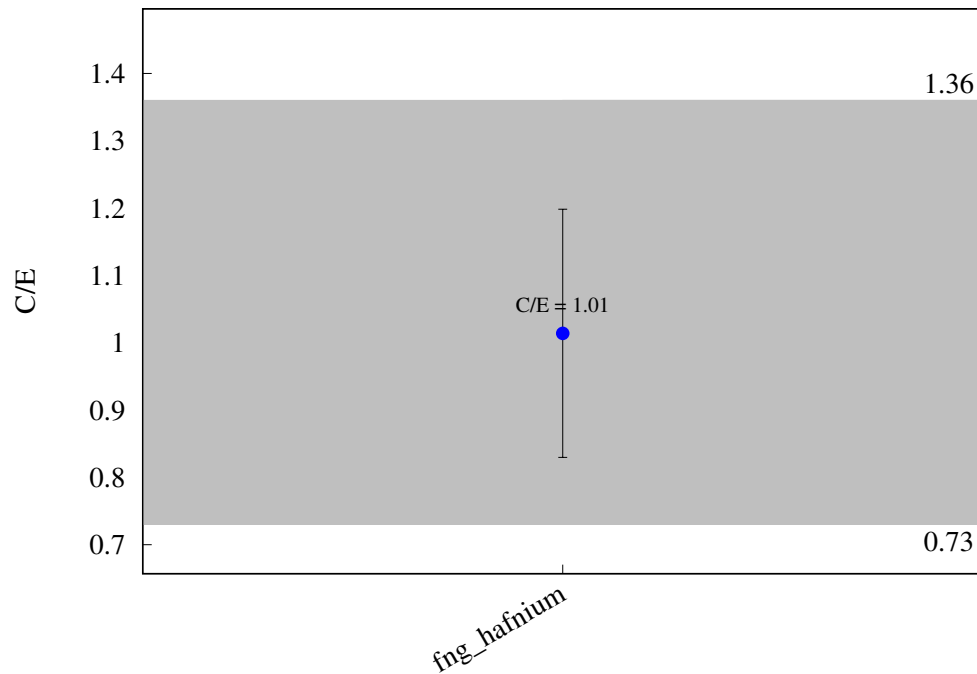
^{175}Lu (n,2n) ^{174}gLu 

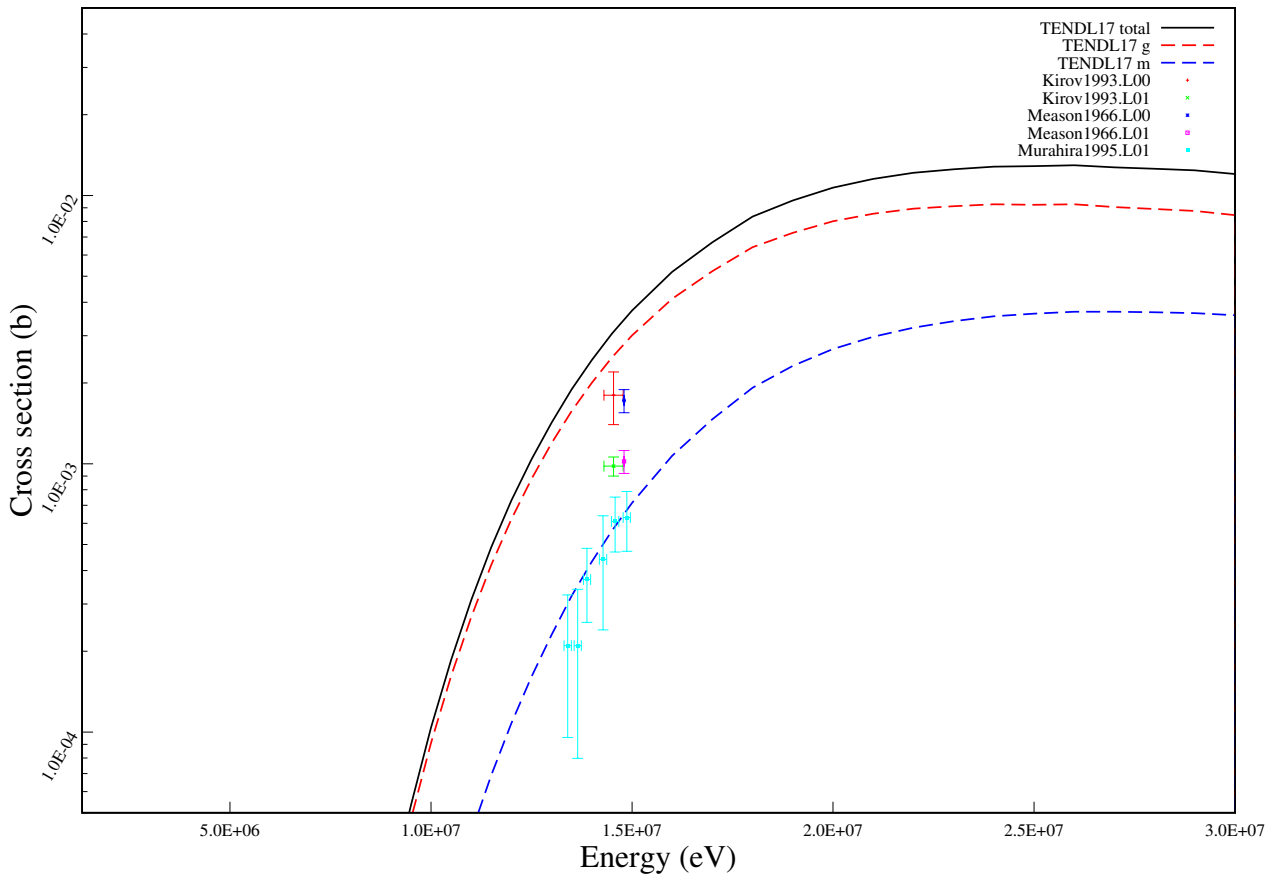
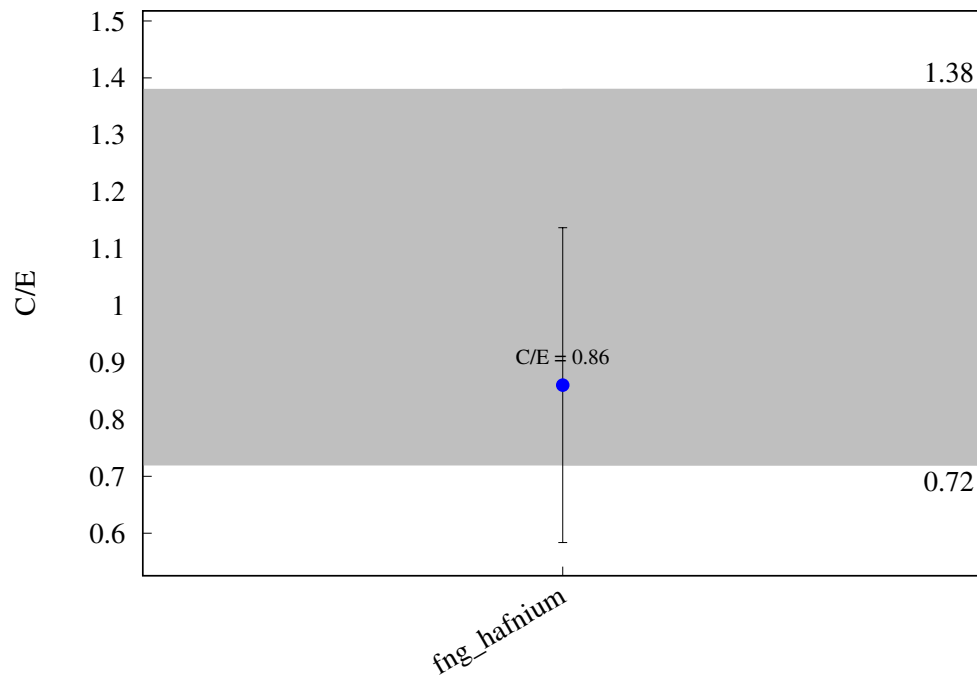
^{175}Lu (n,3n) ^{173}Lu 

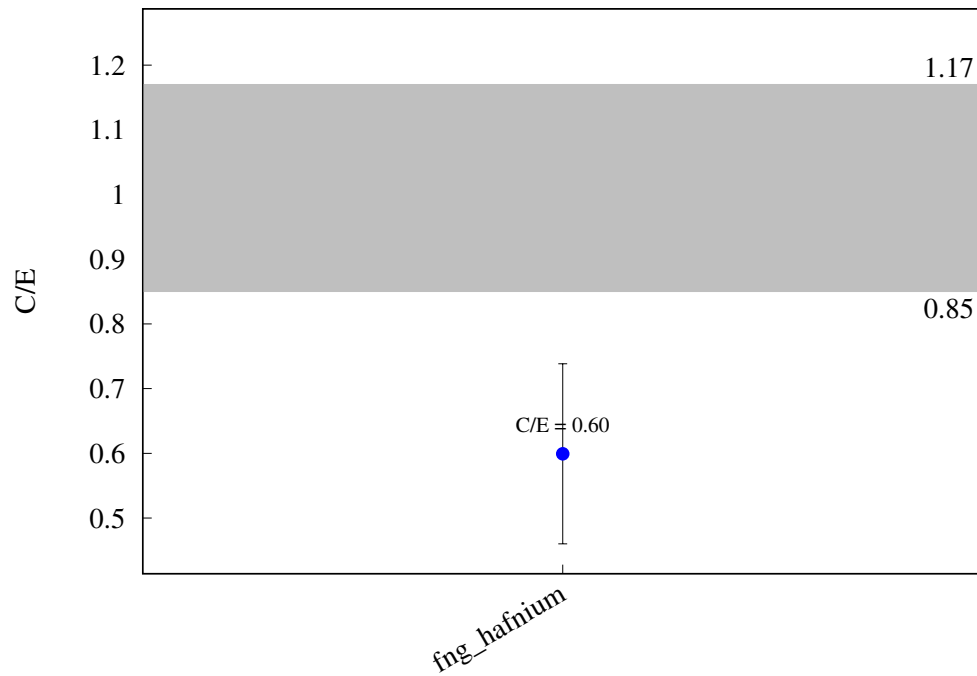


^{174}Hf (n,2n) ^{173}Hf 

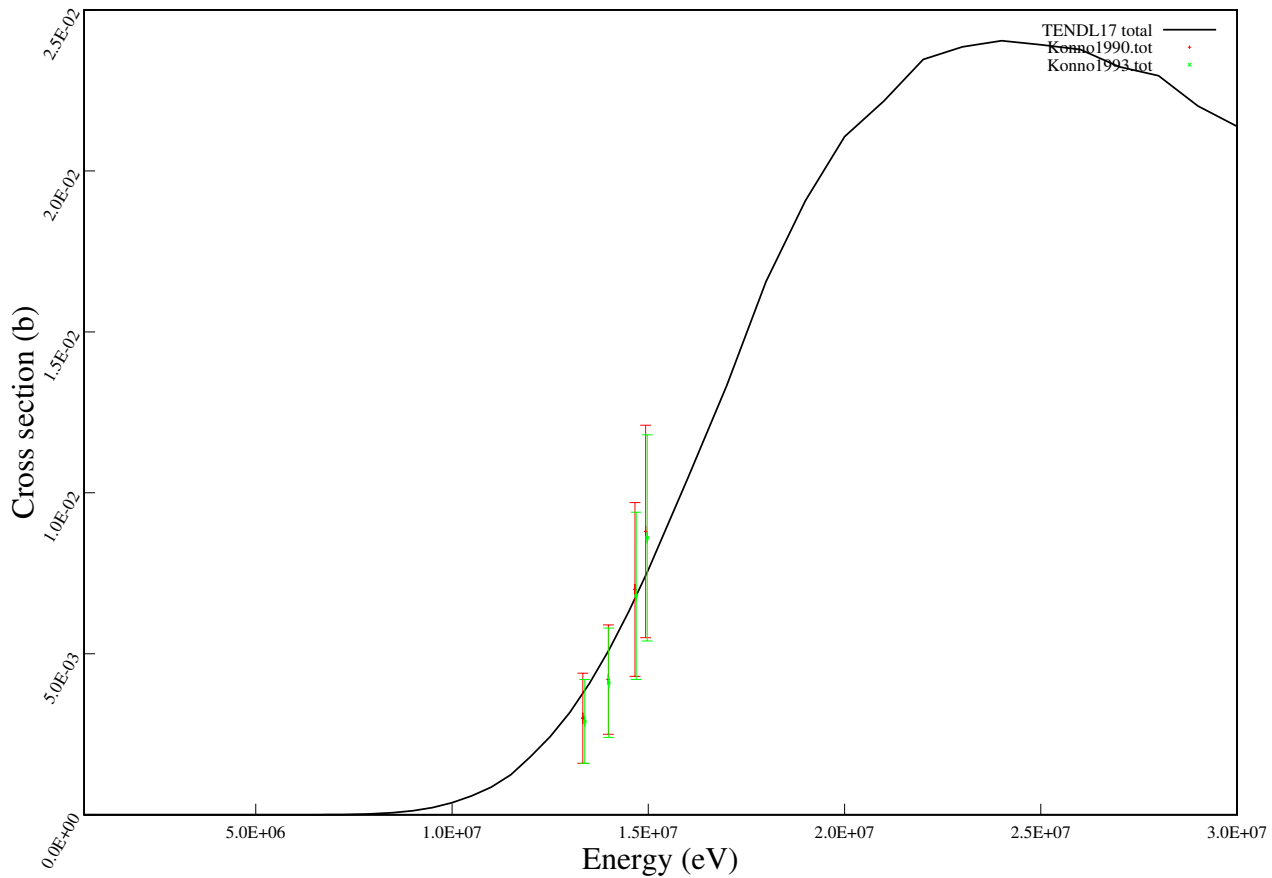
^{176}Hf (n,2n) ^{175}Hf 

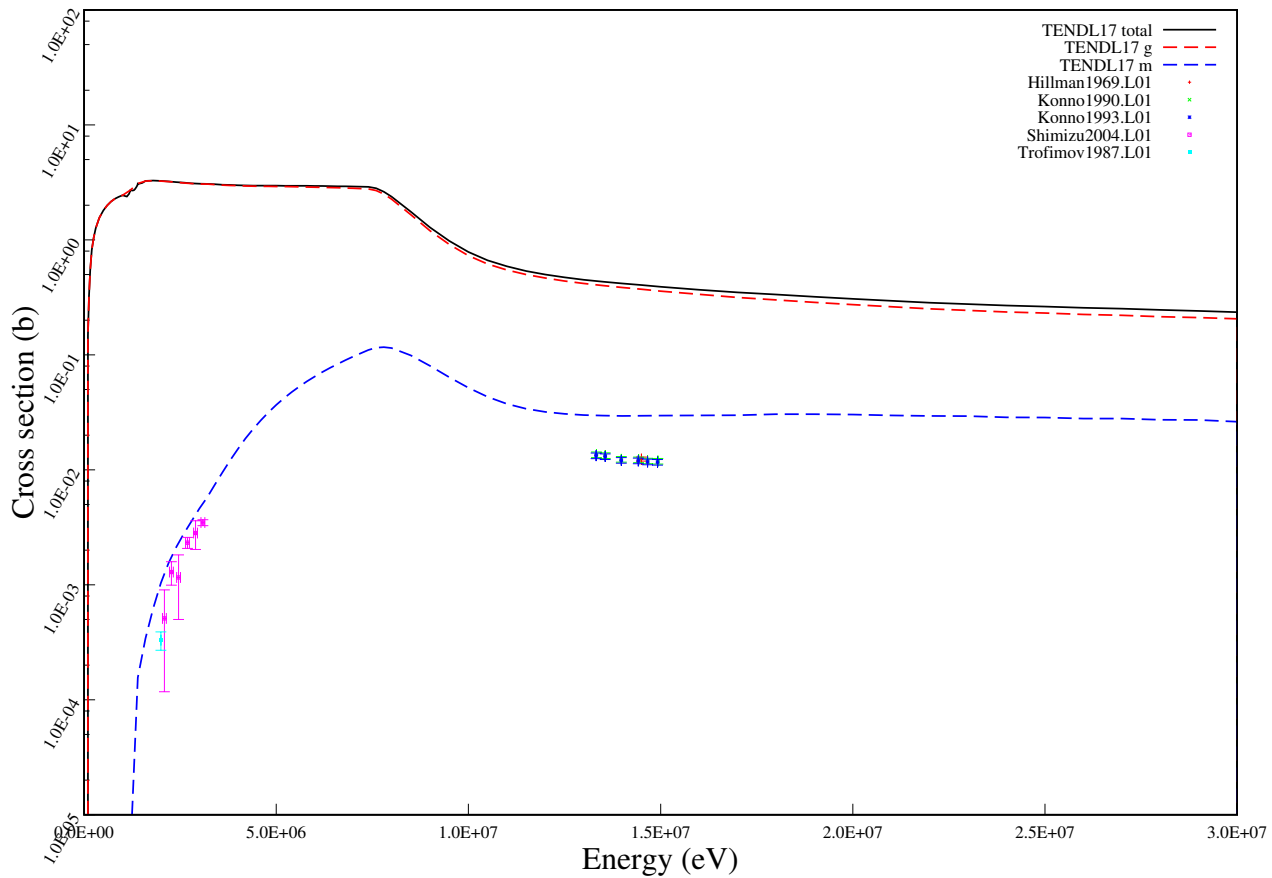
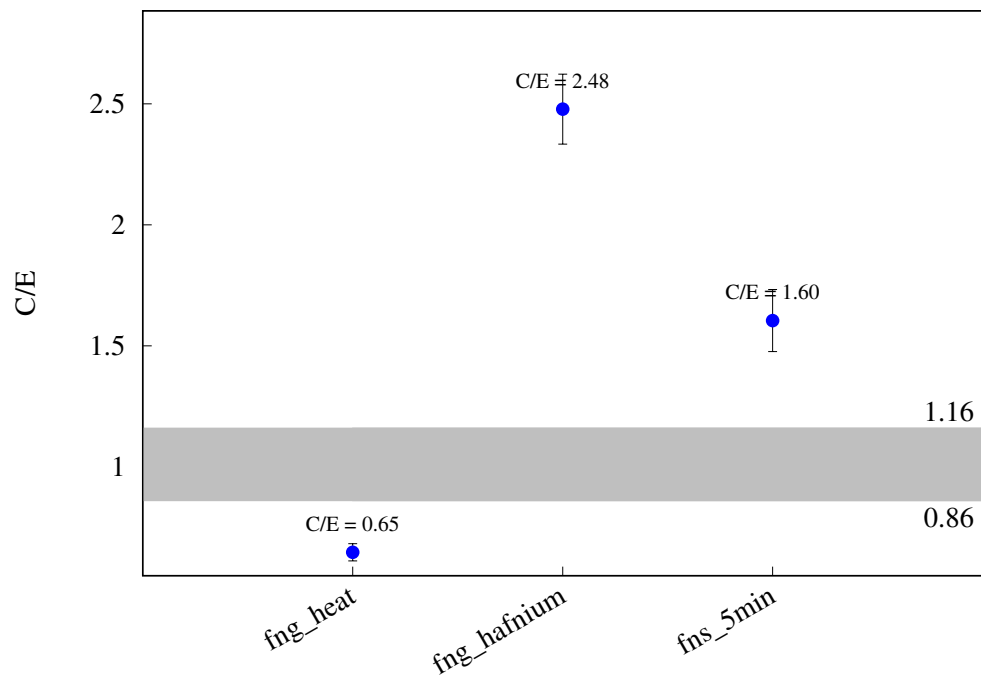
$^{178}\text{Hf} (\text{n},\text{p}) ^{178m}\text{Lu}$ 

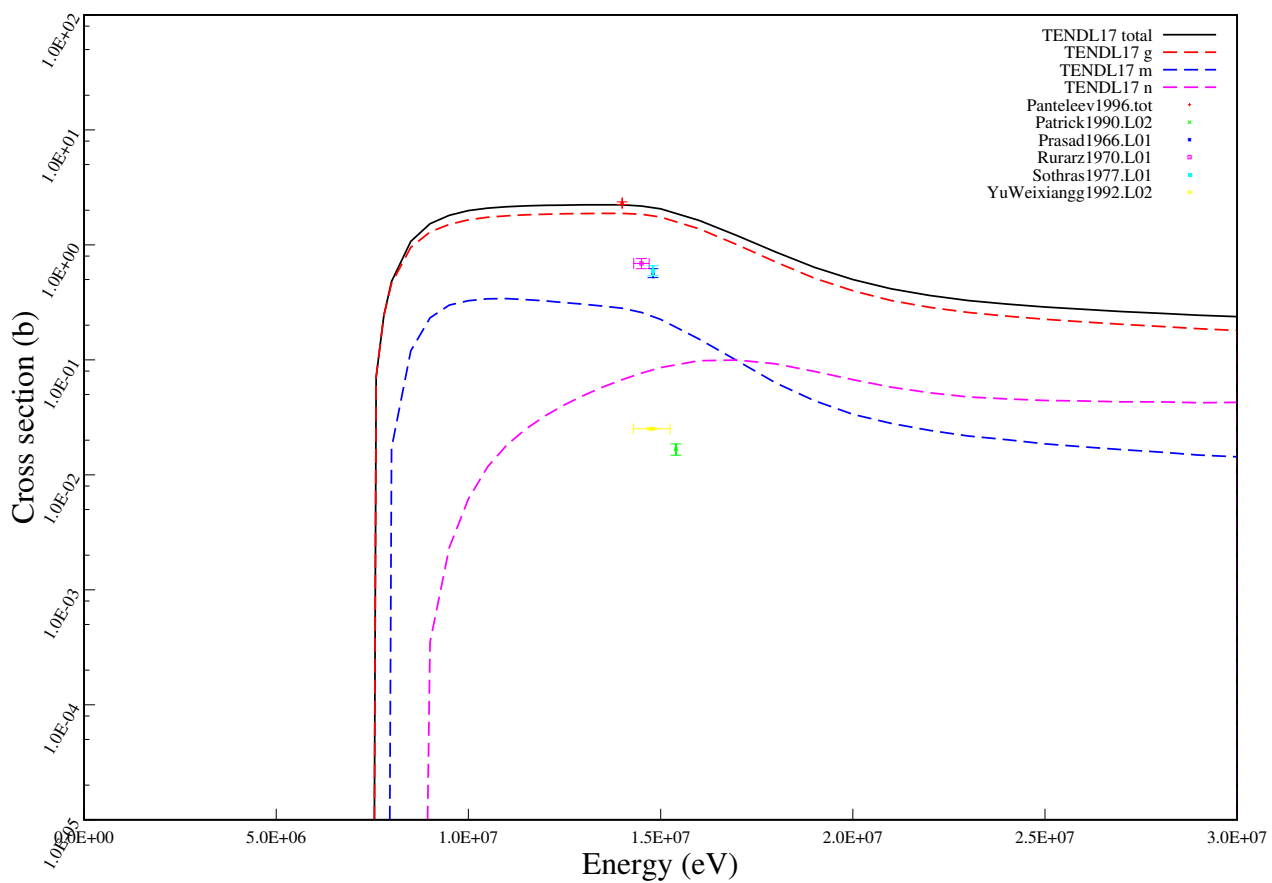
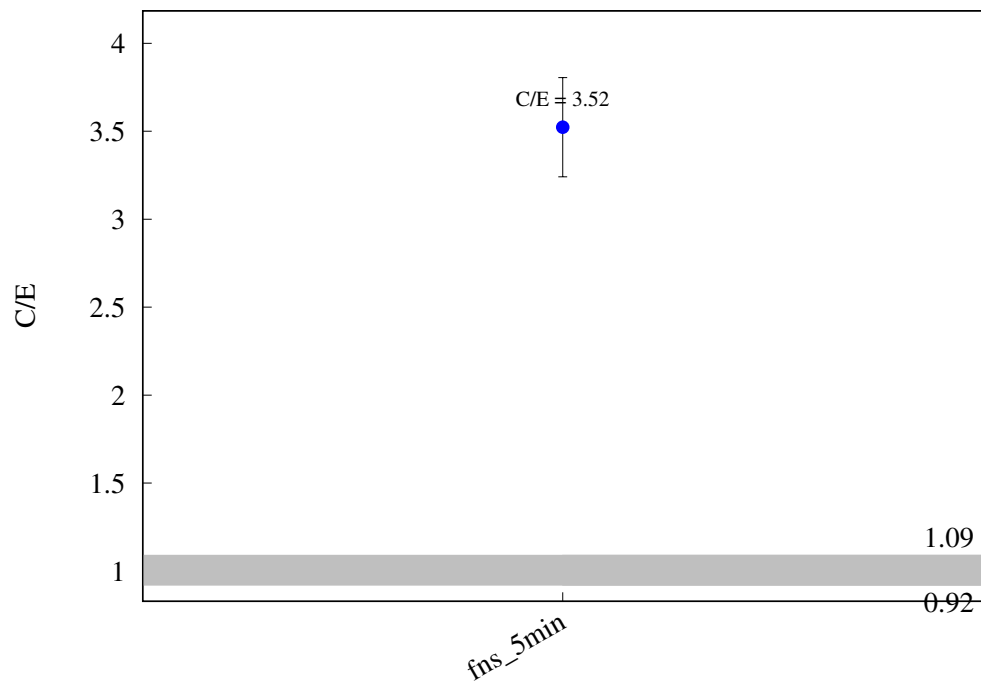
$^{178}\text{Hf} (\text{n},\text{p}) ^{178}\text{Lu}$ 

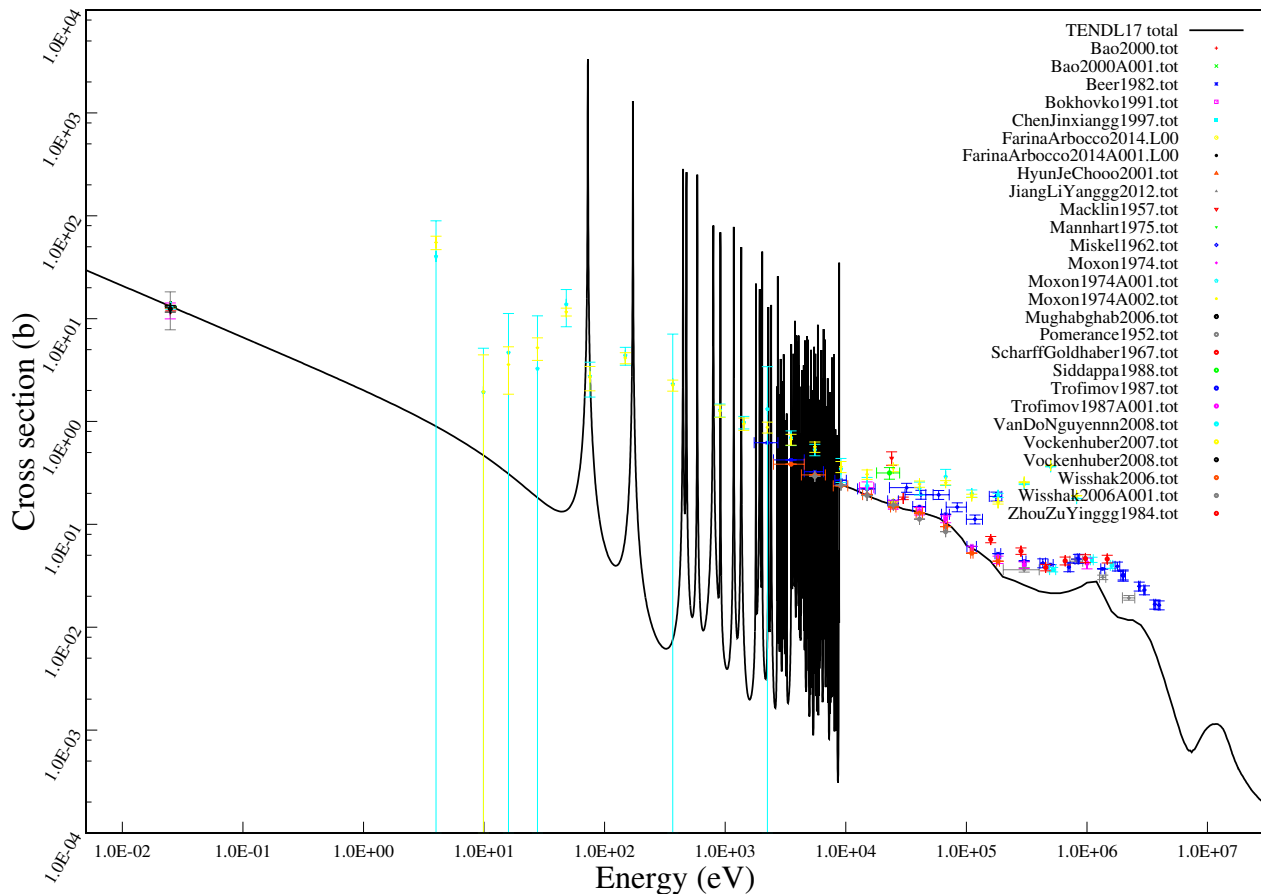
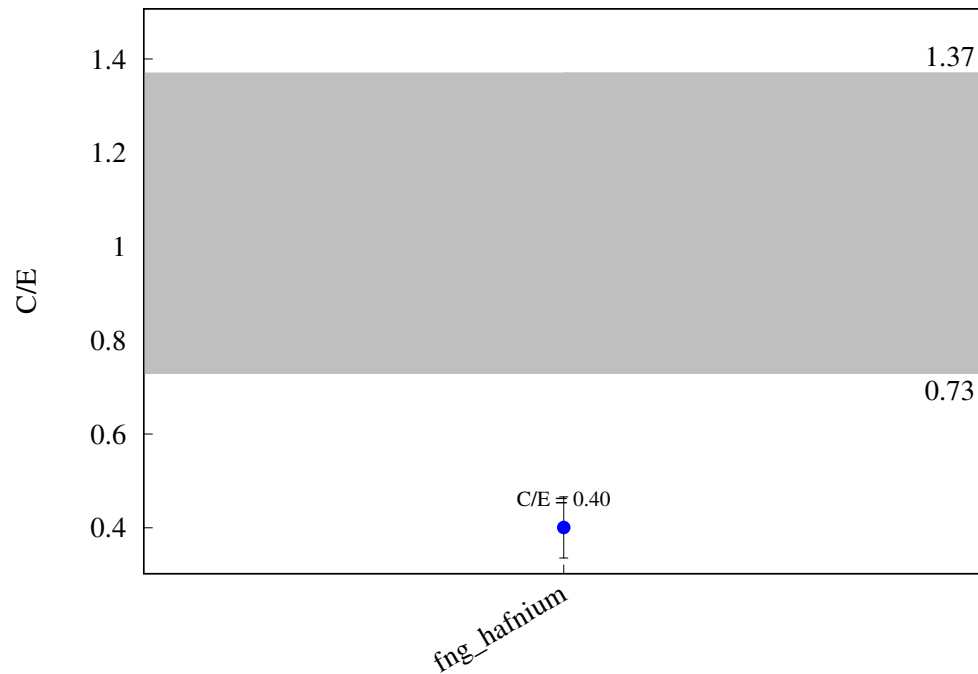
$^{179}\text{Hf} (\text{n},\text{p}) ^{179}\text{Lu}$ 

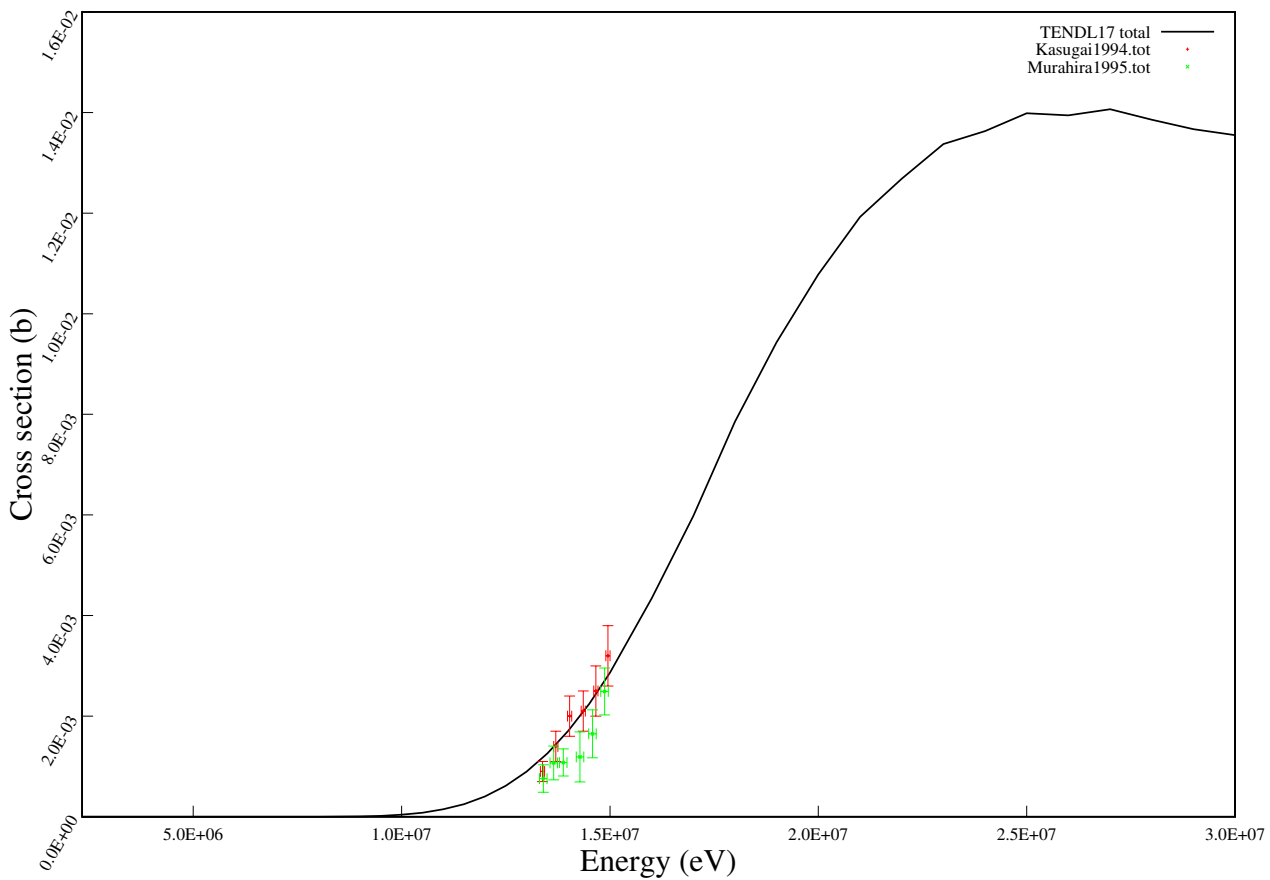
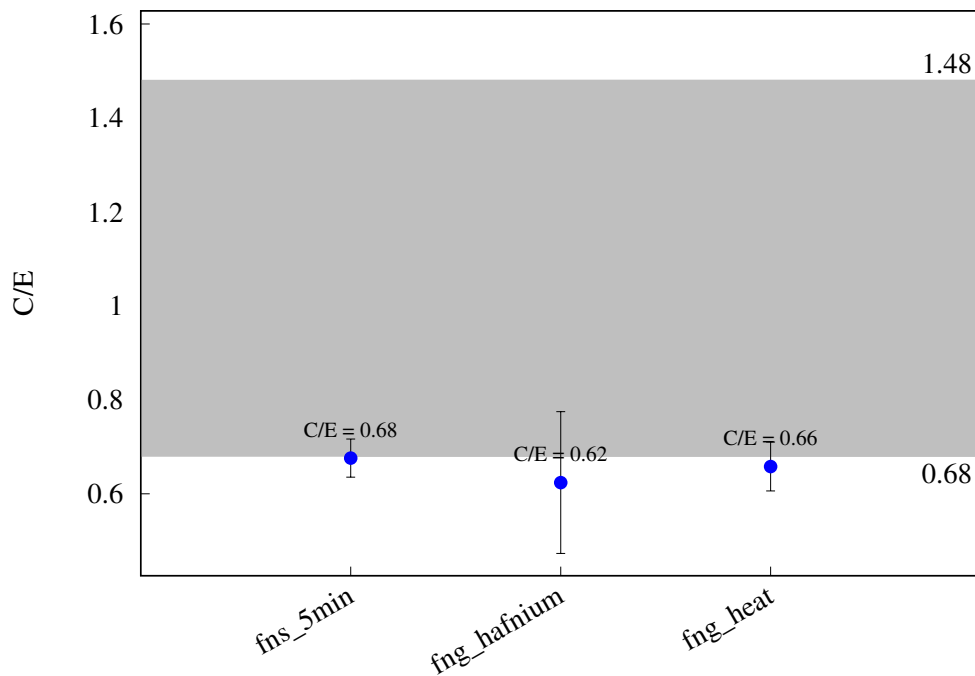
fng_hafnium

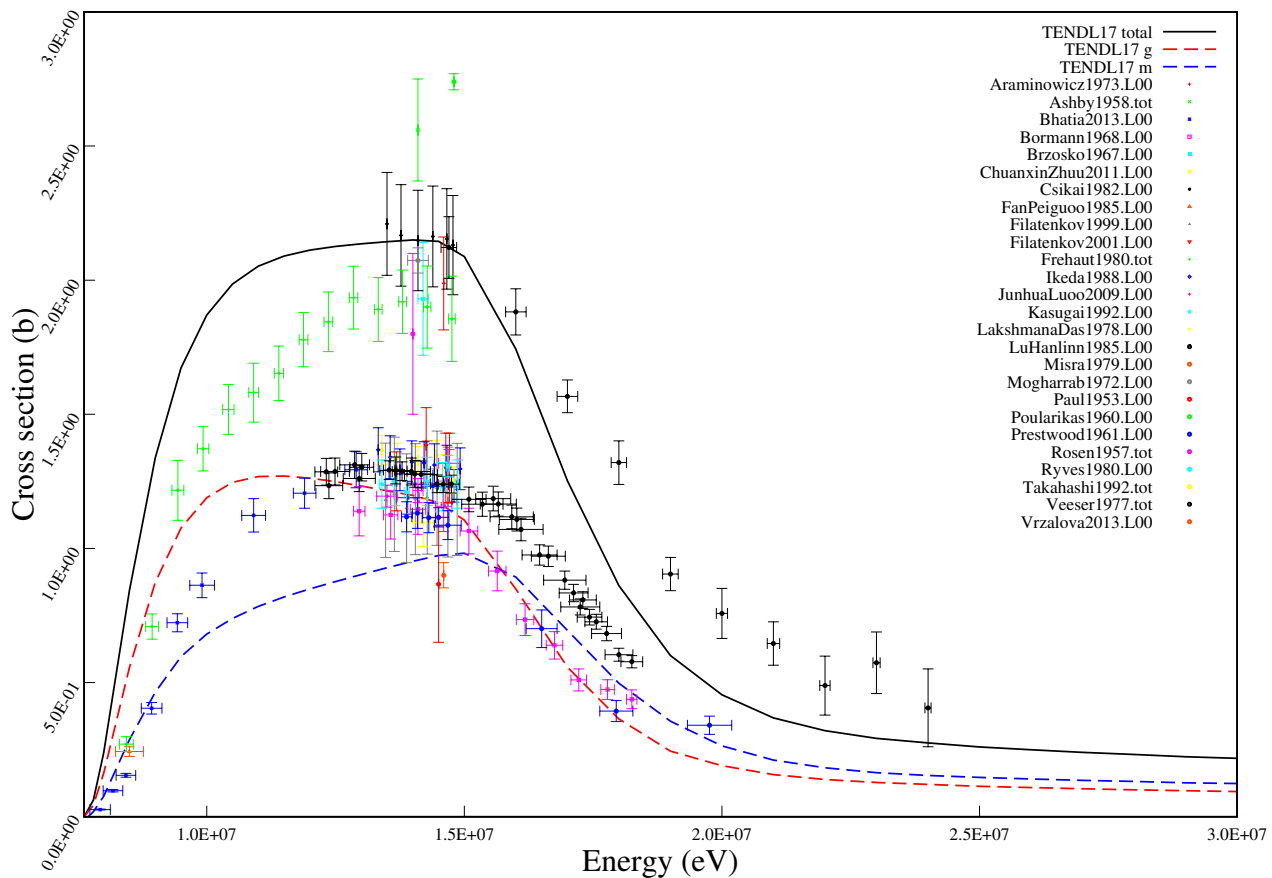
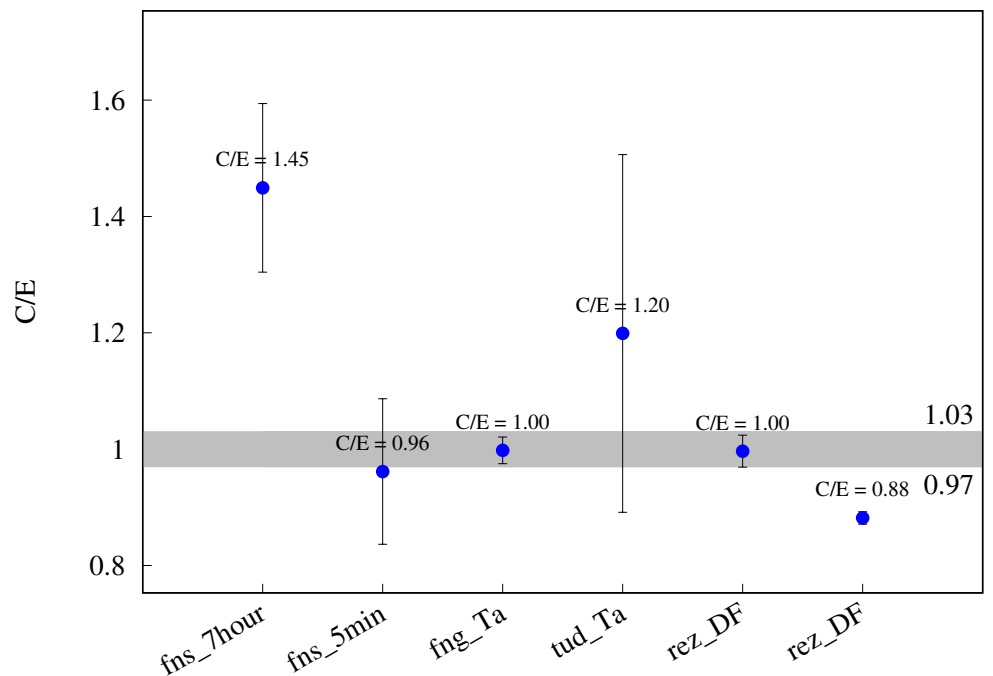


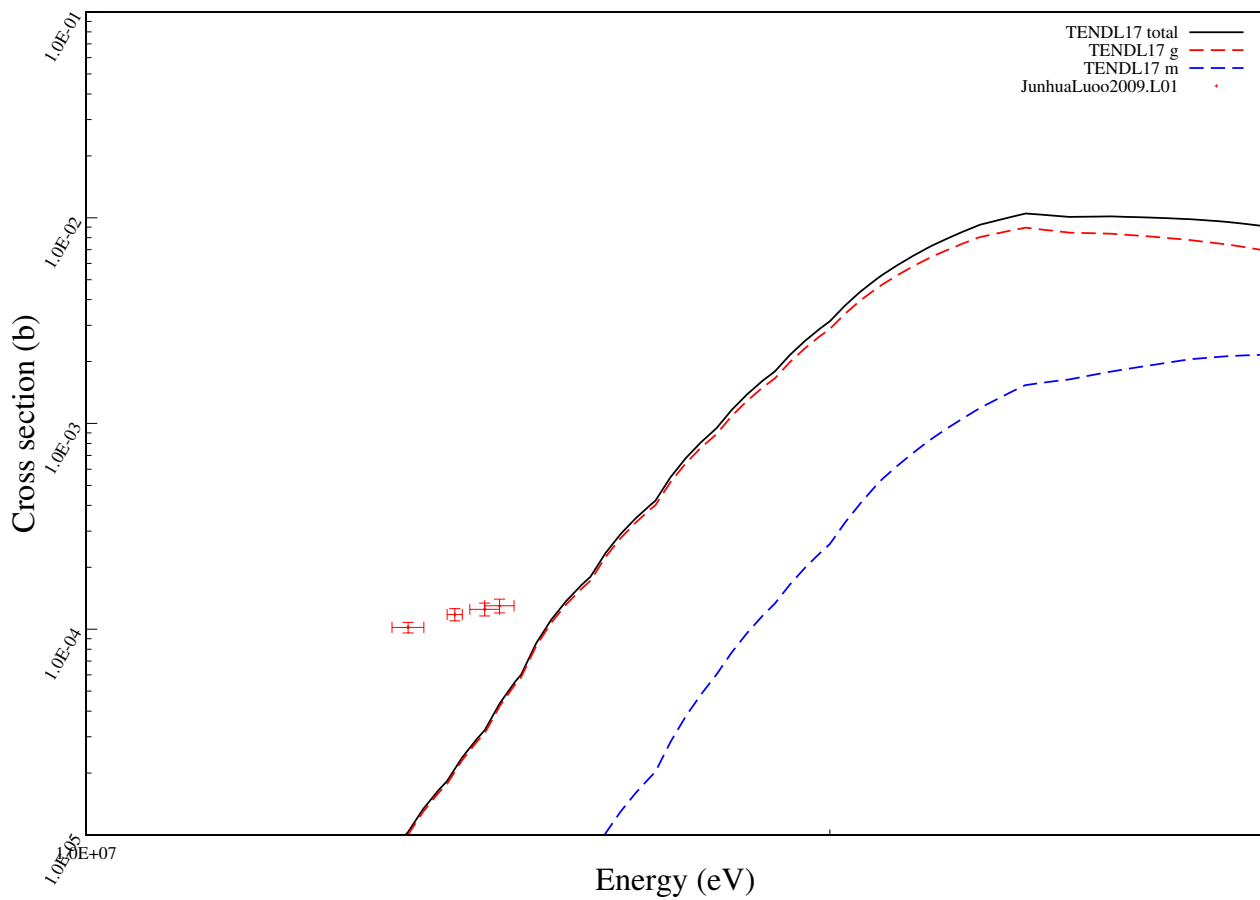
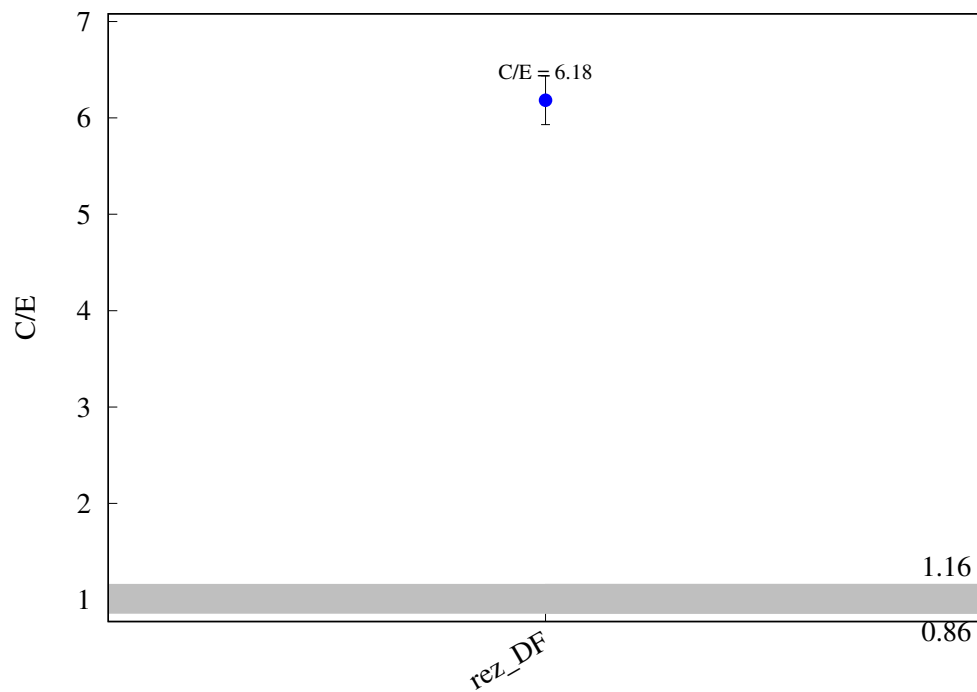
^{180}Hf (n,n) $^{180\text{m}}\text{Hf}$ 

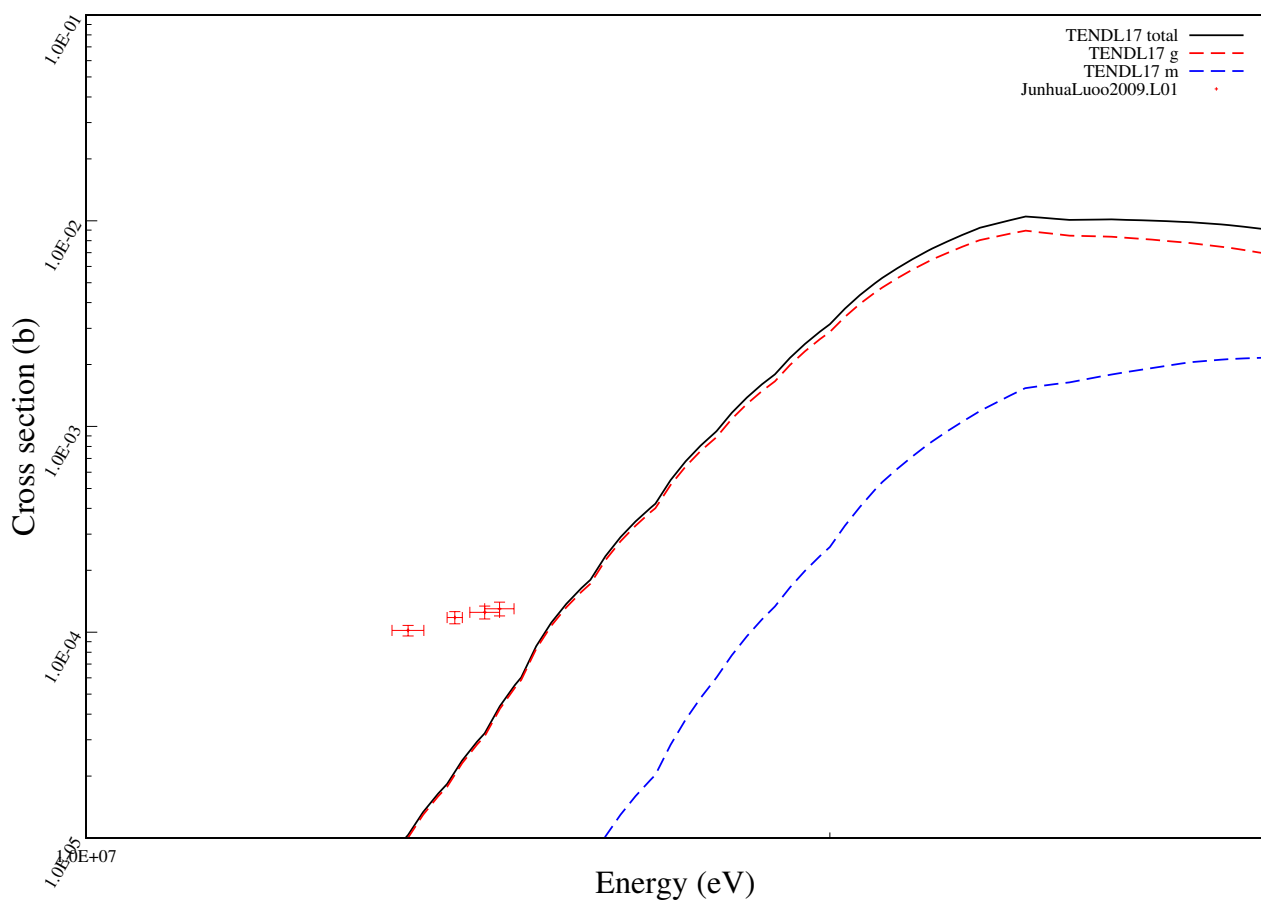
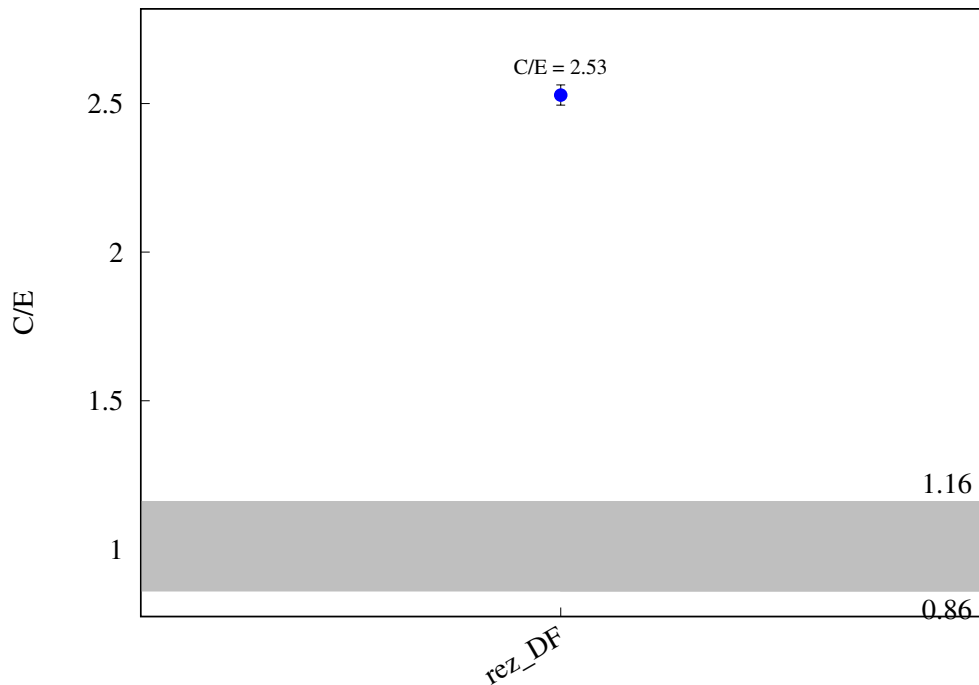
^{180}Hf (n,2n) ^{179m}Hf 

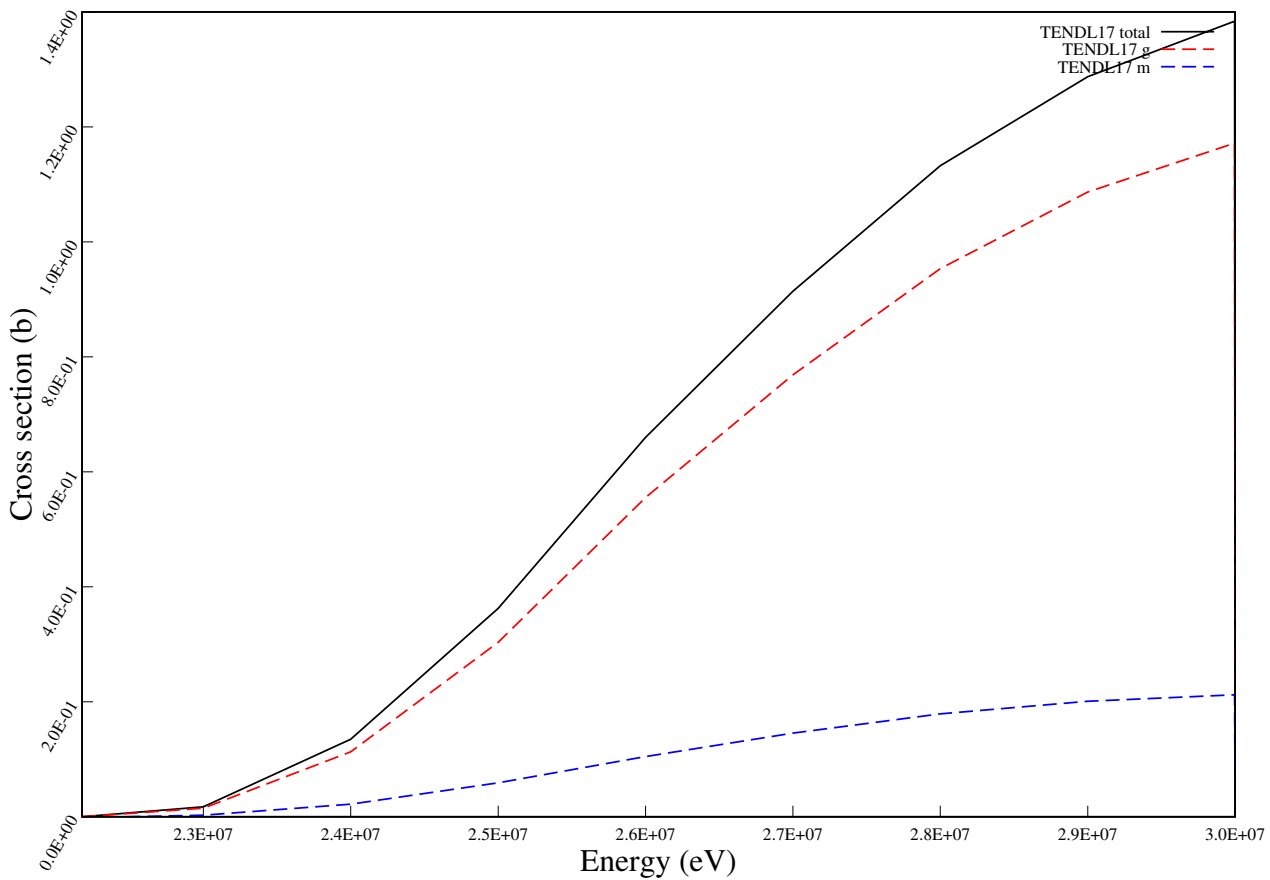
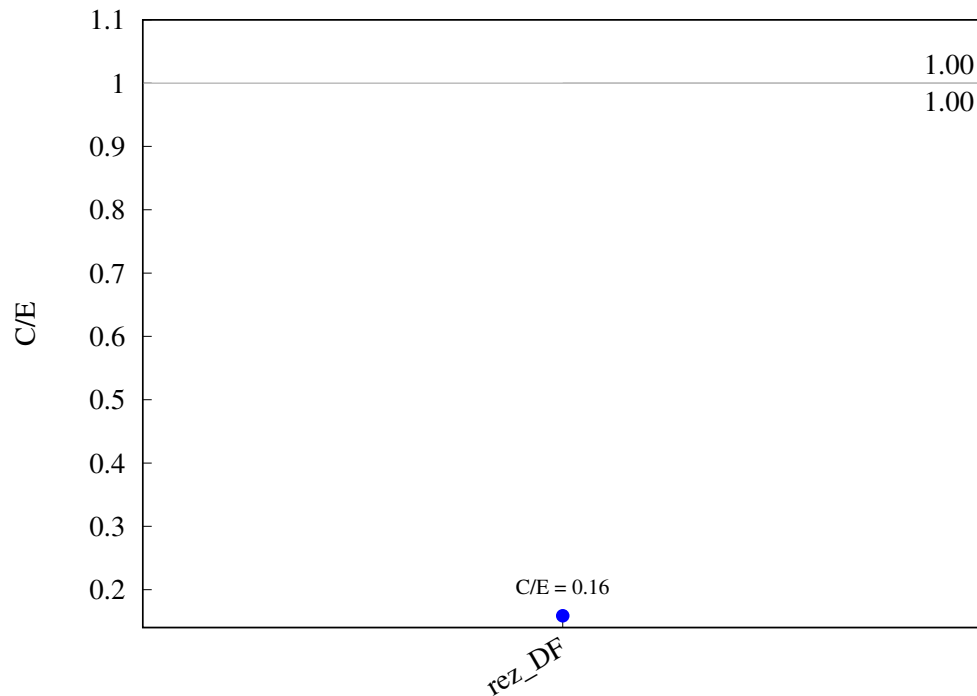
^{180}Hf (n,g) ^{181}Hf 

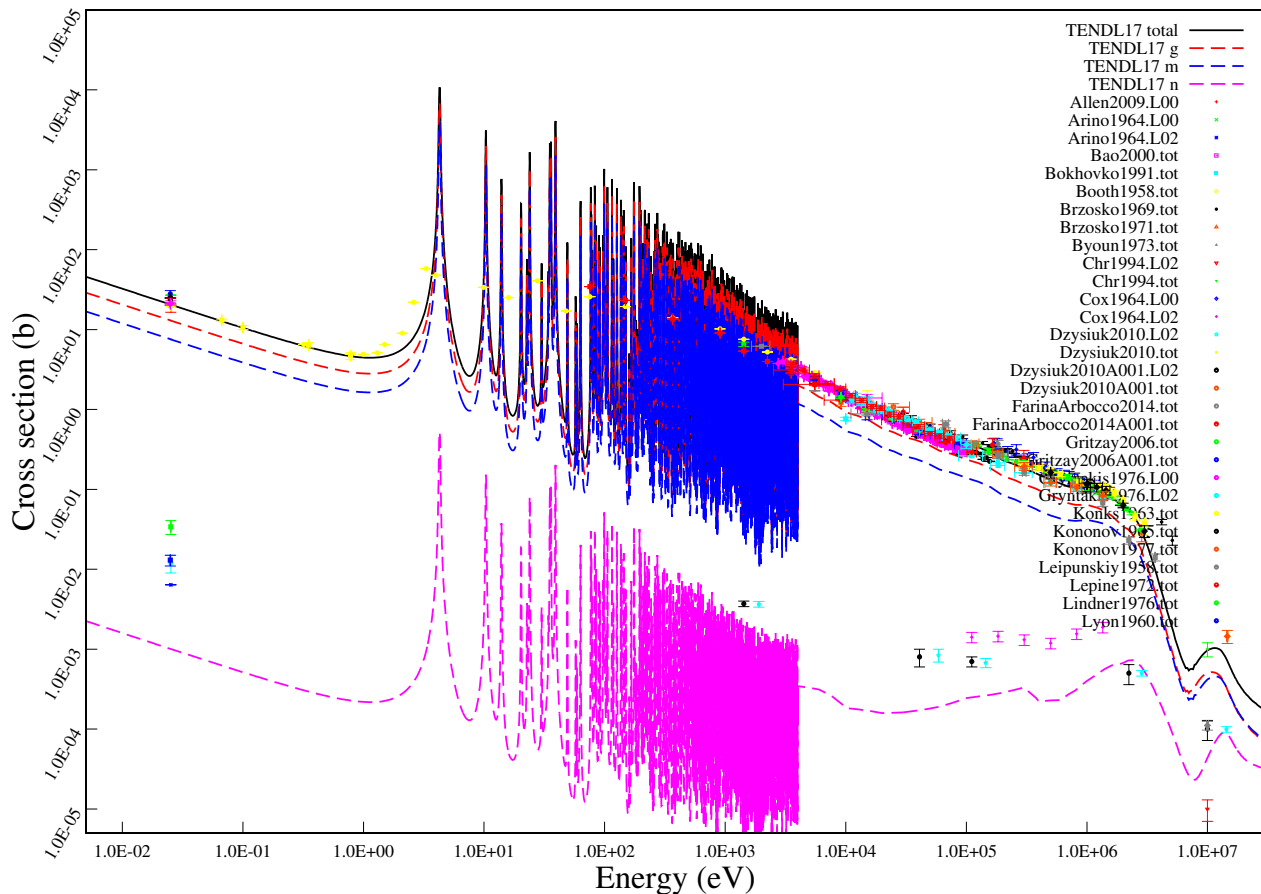
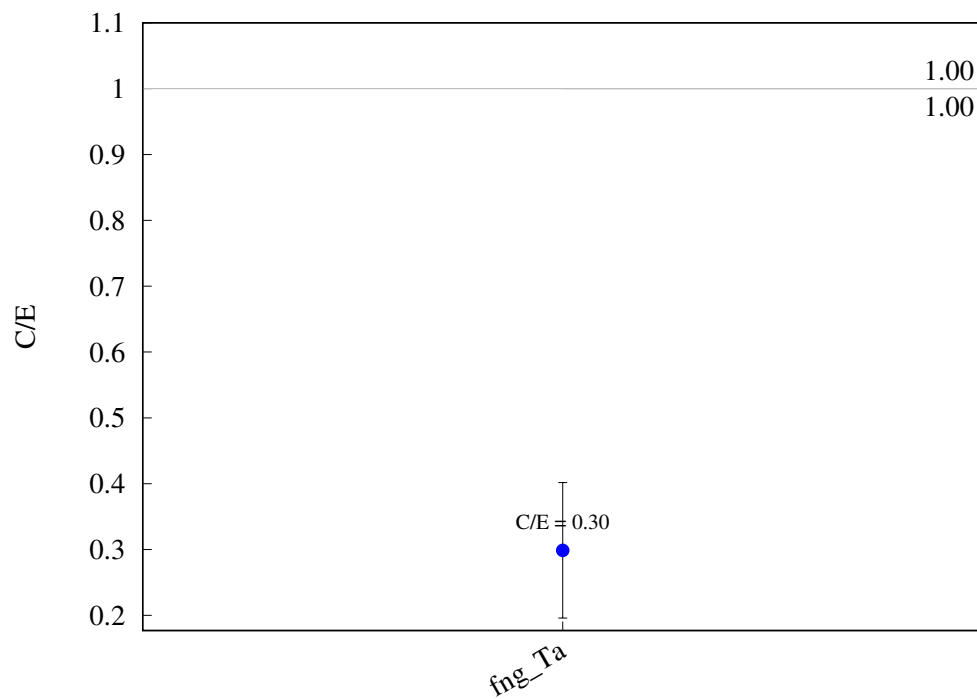
$^{180}\text{Hf} (\text{n},\text{p}) ^{180}\text{Lu}$ 

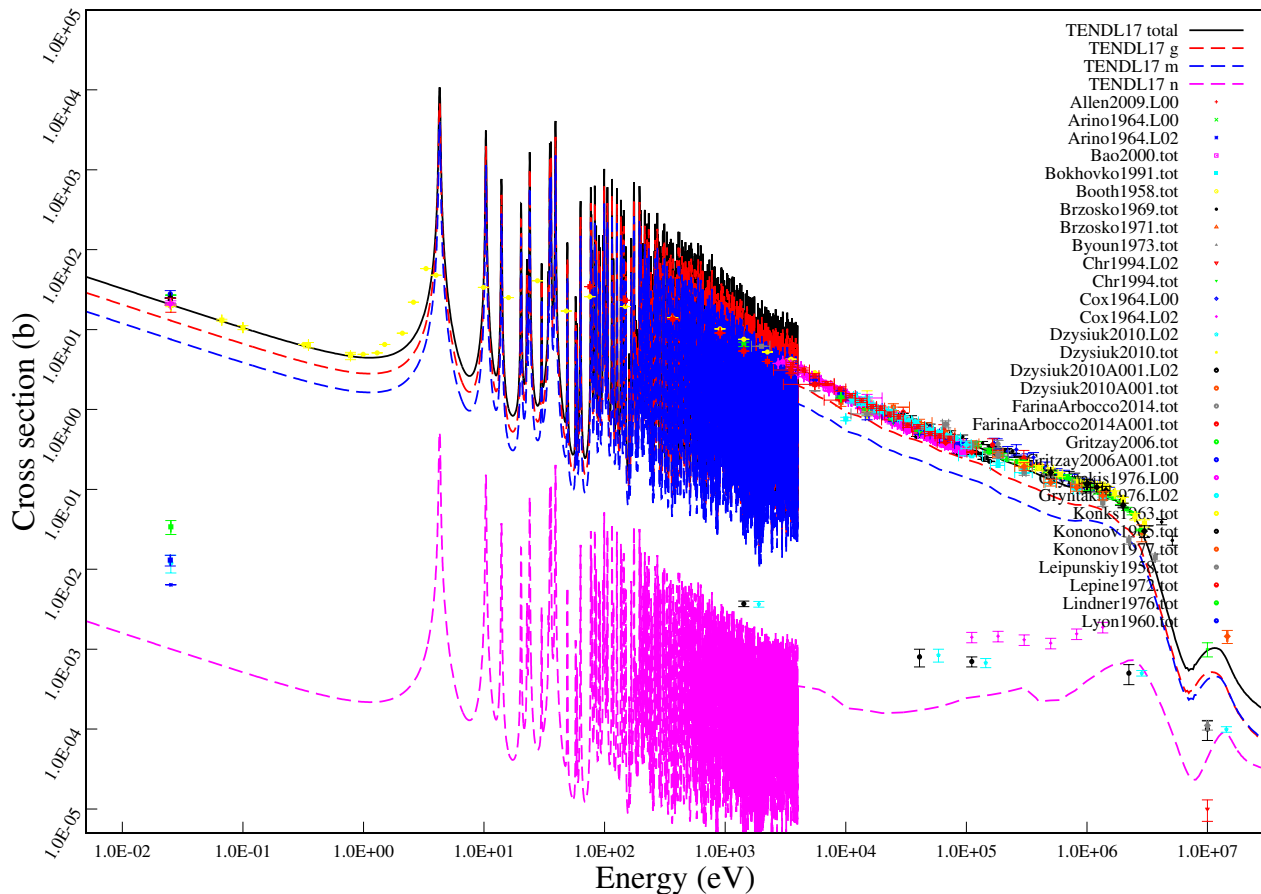
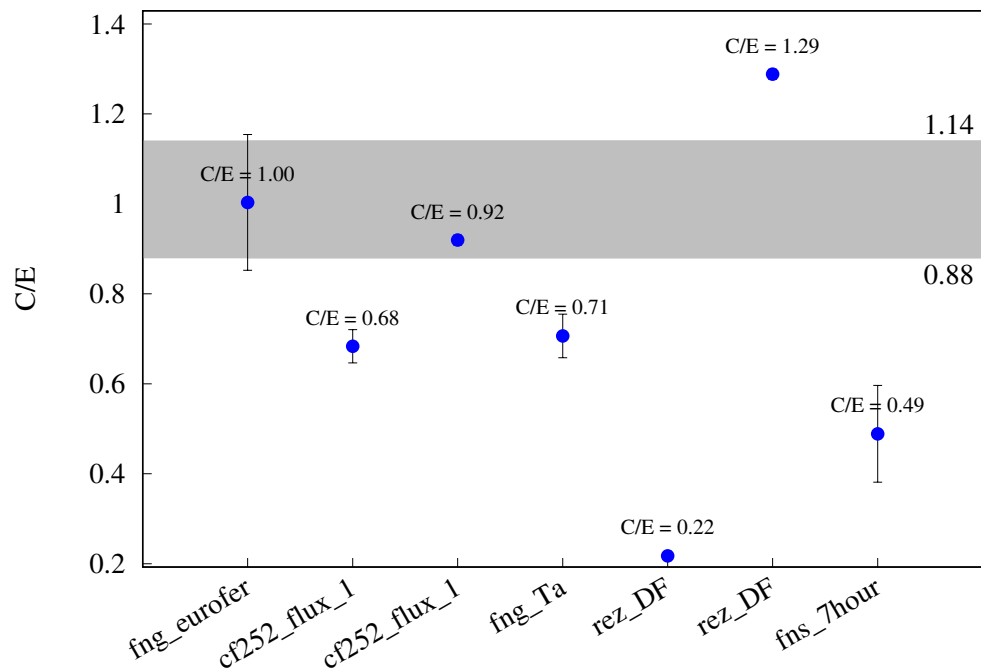
^{181}Ta (n,2n) ^{180}gTa 

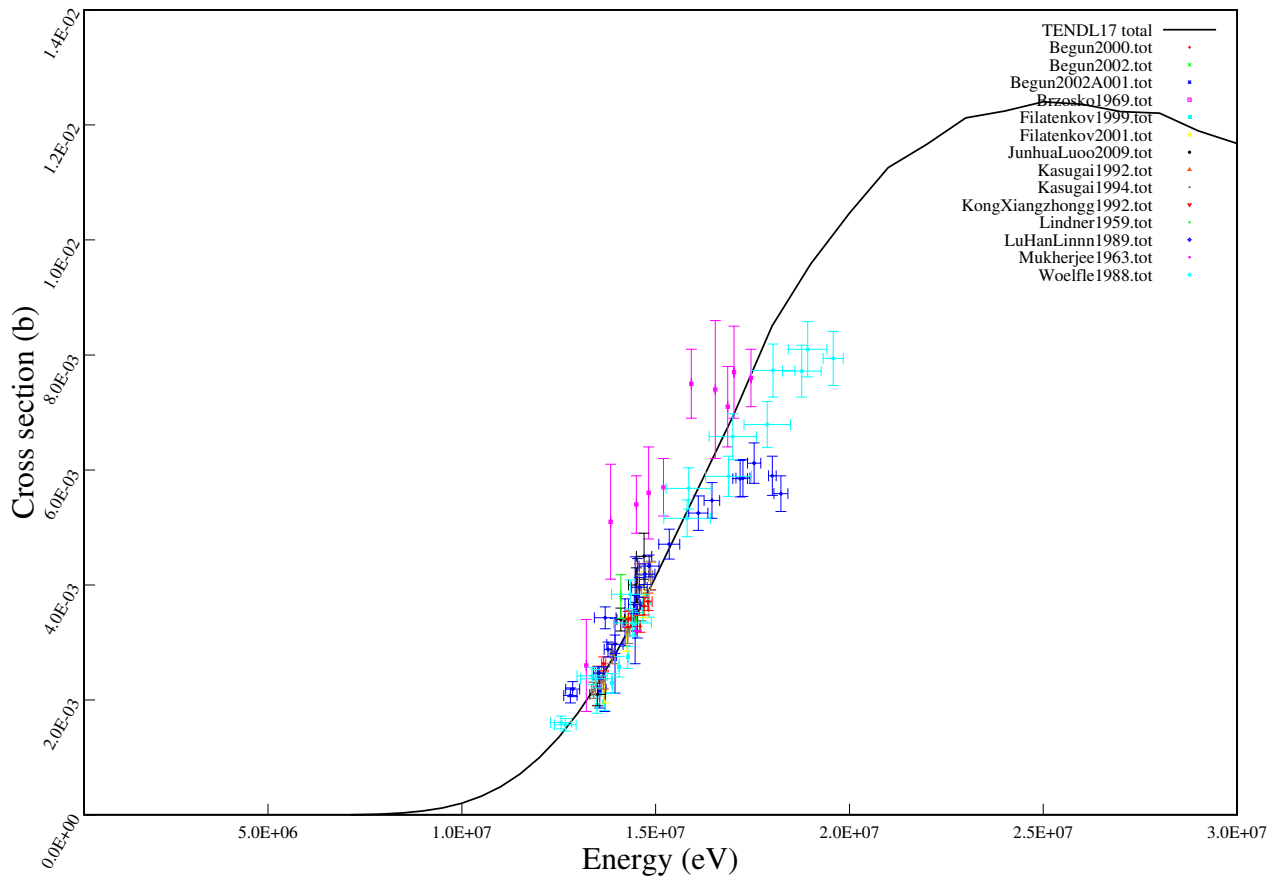
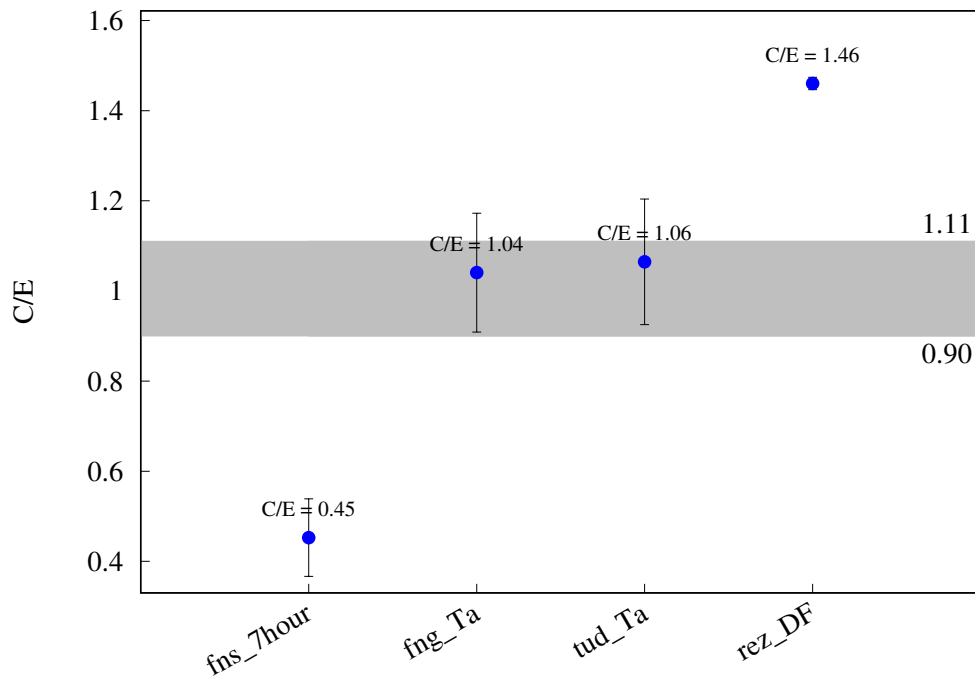
^{181}Ta (n,na) $^{177\text{m}}\text{Lu}$ 

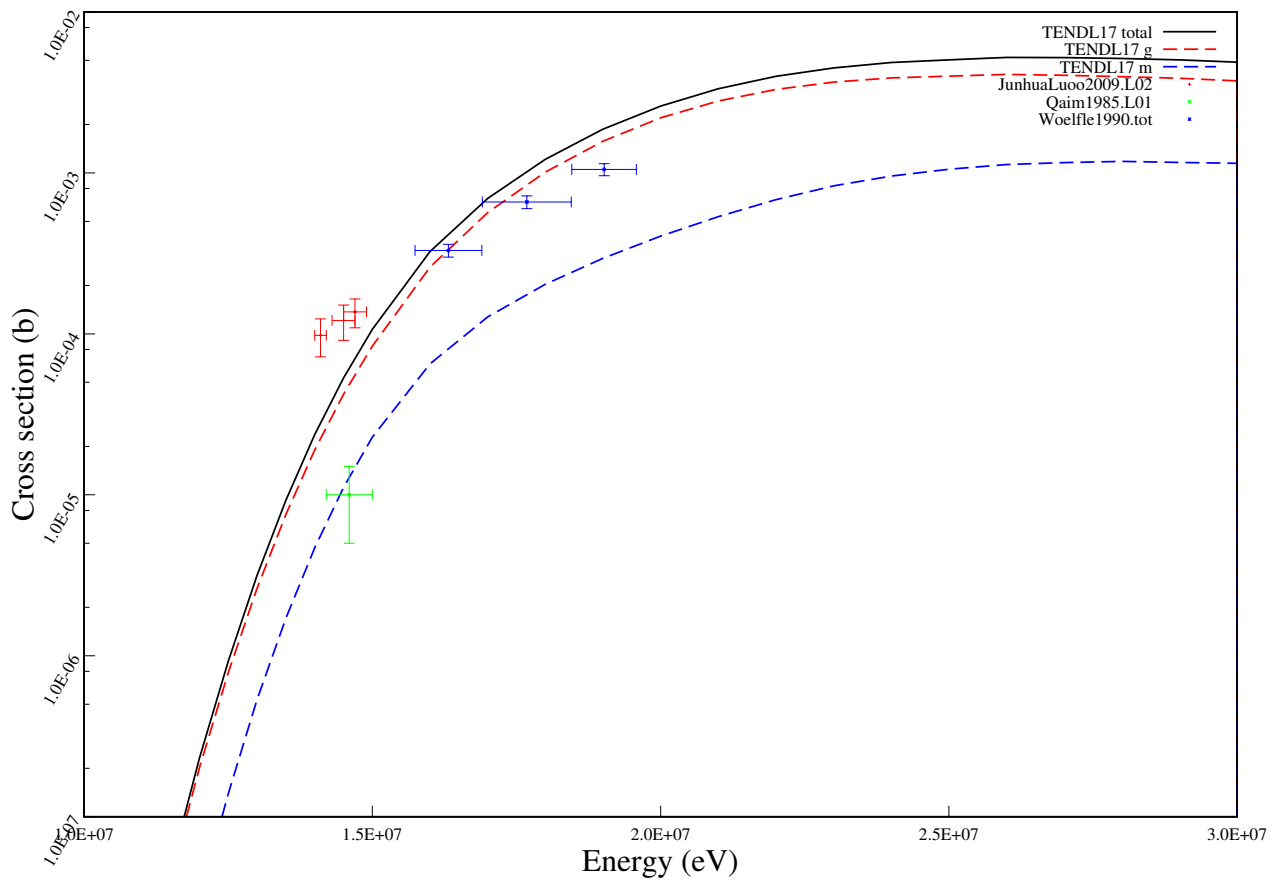
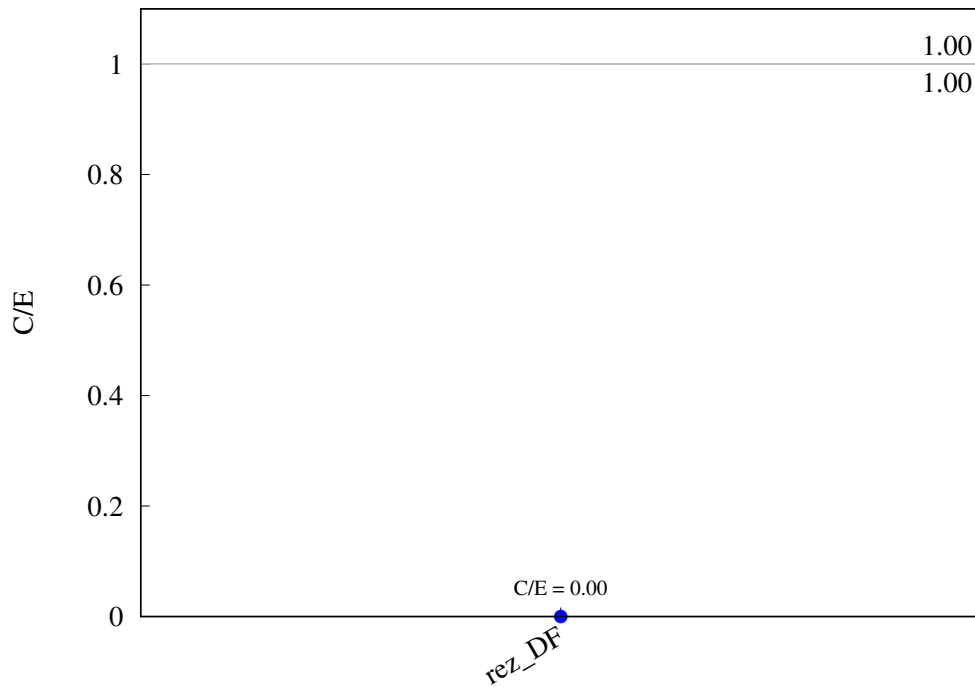
^{181}Ta (n,na) ^{177}Lu 

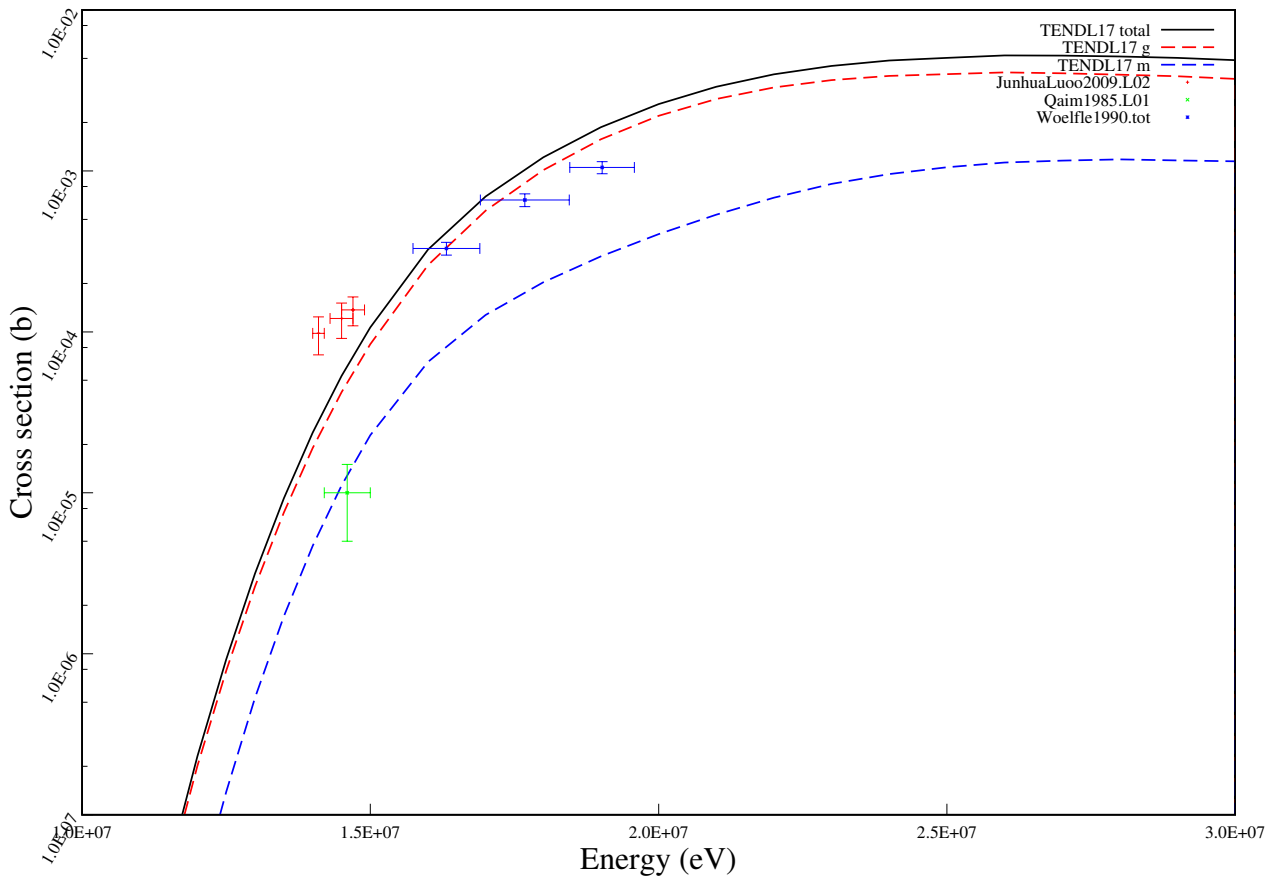
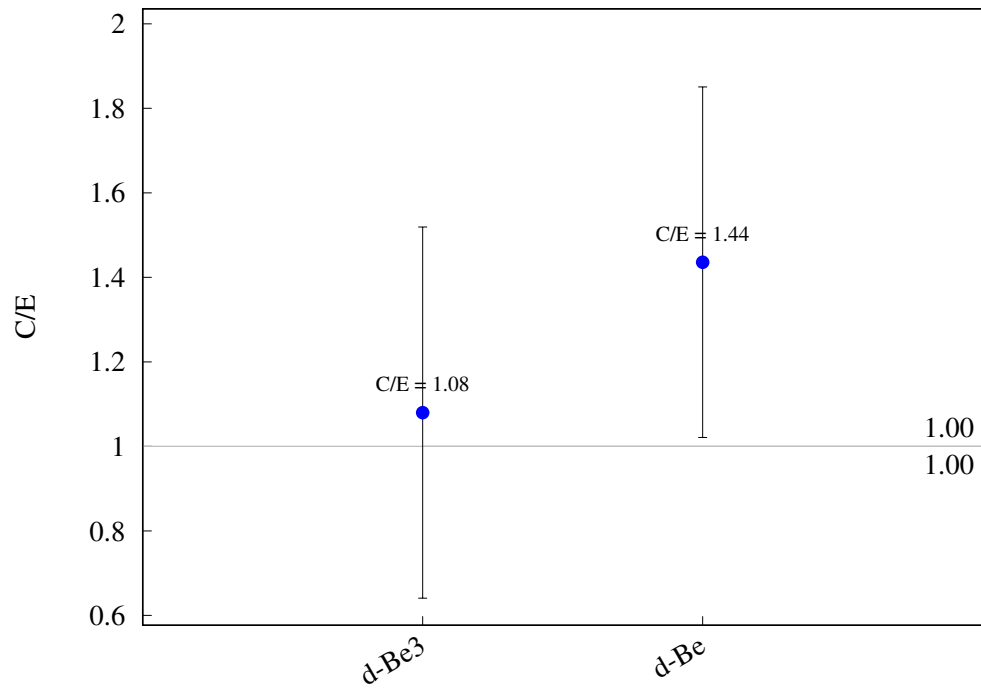
^{181}Ta (n,4n) $^{178\text{m}}\text{Ta}$ 

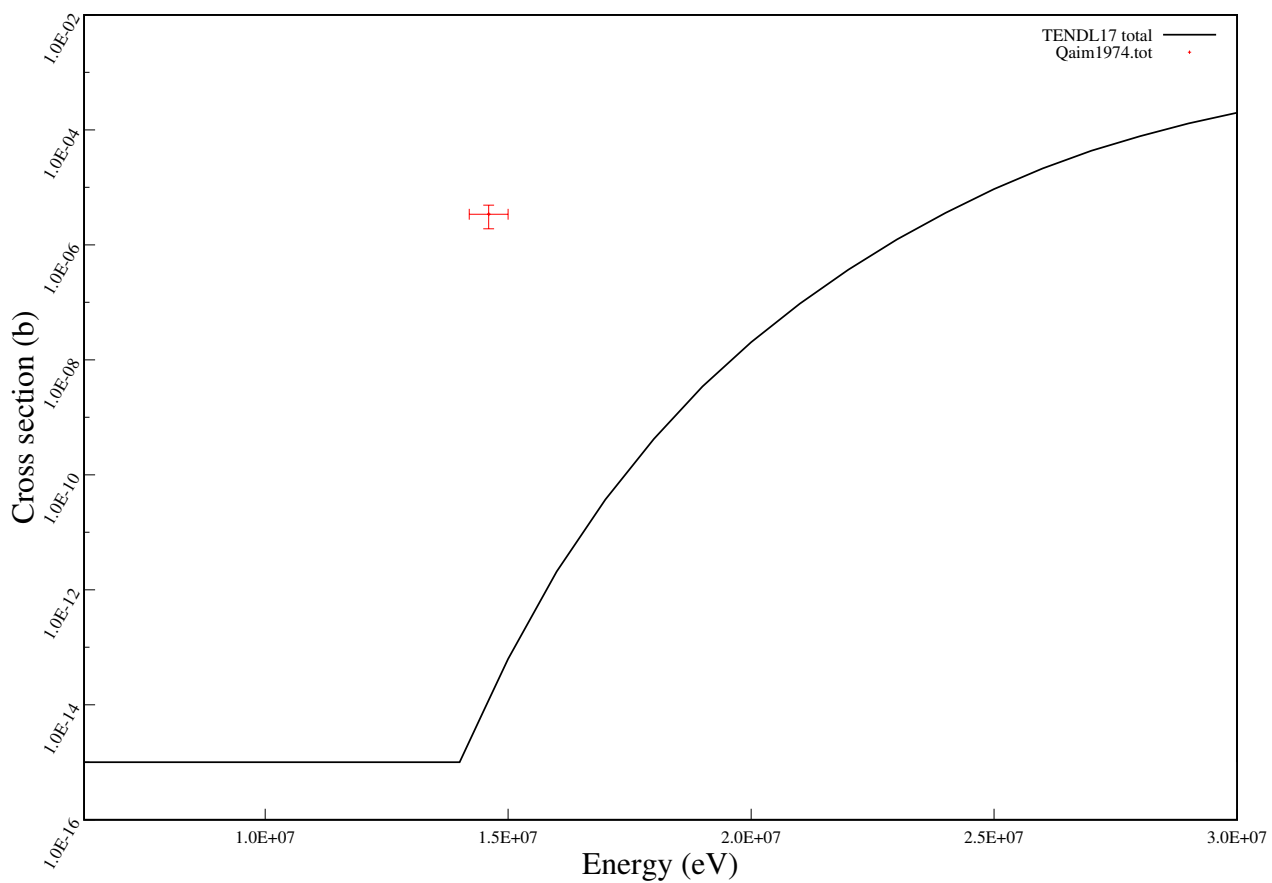
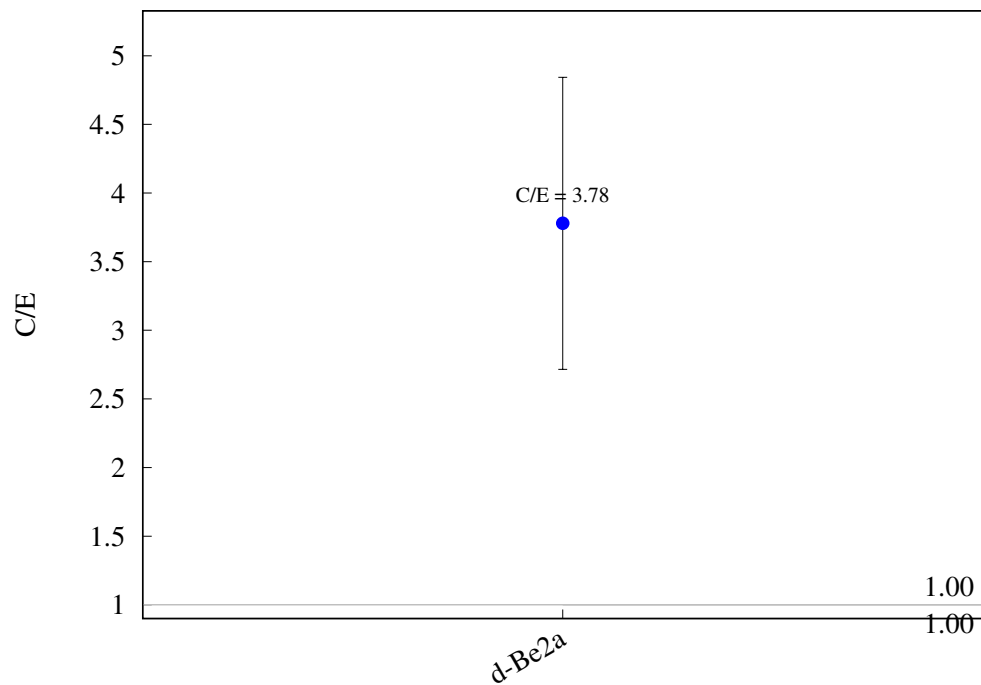
^{181}Ta (n,g) ^{182}nTa 

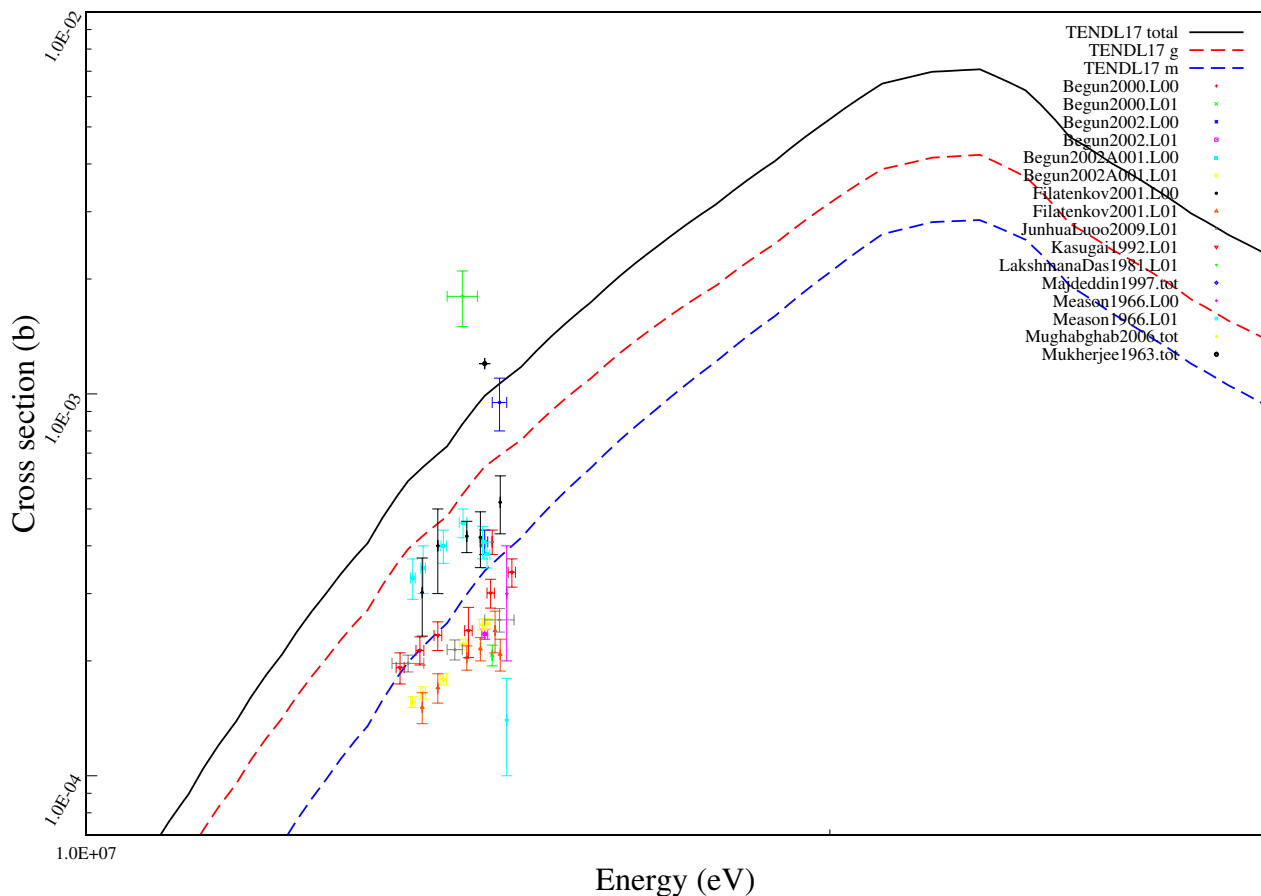
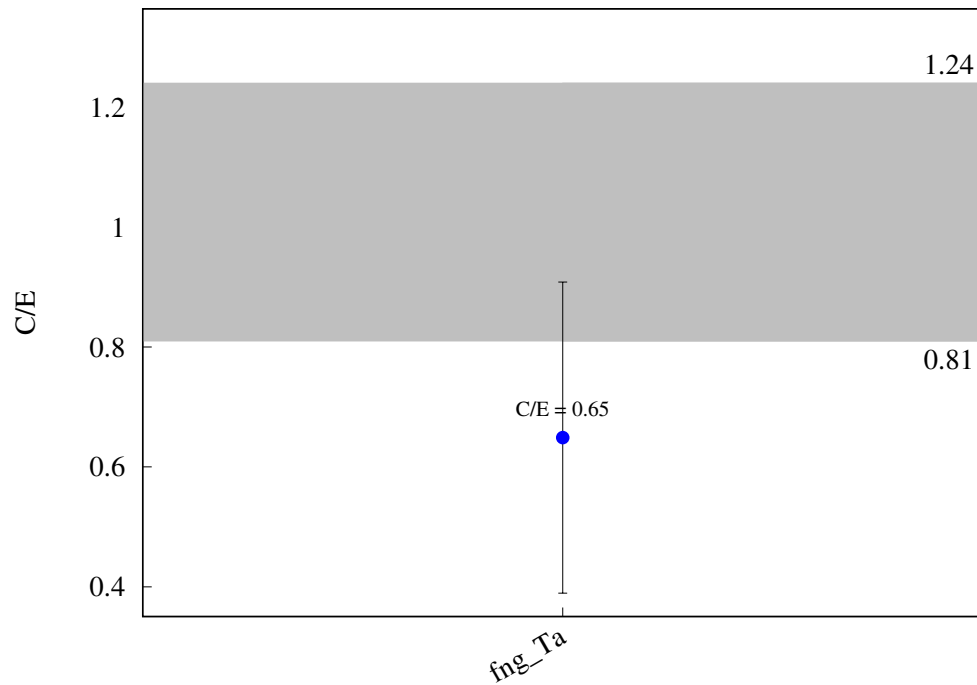
^{181}Ta (n,g) ^{182}Ta 

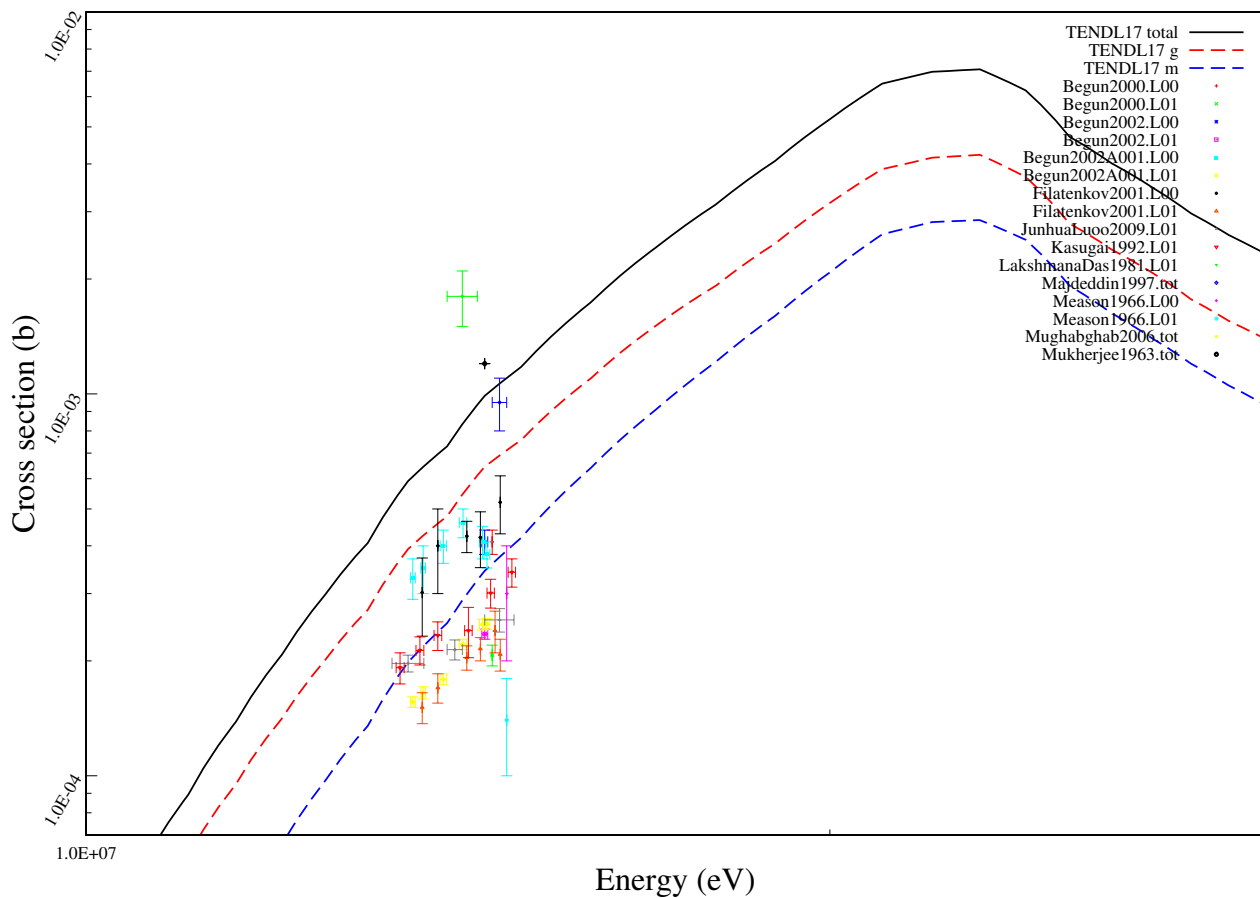
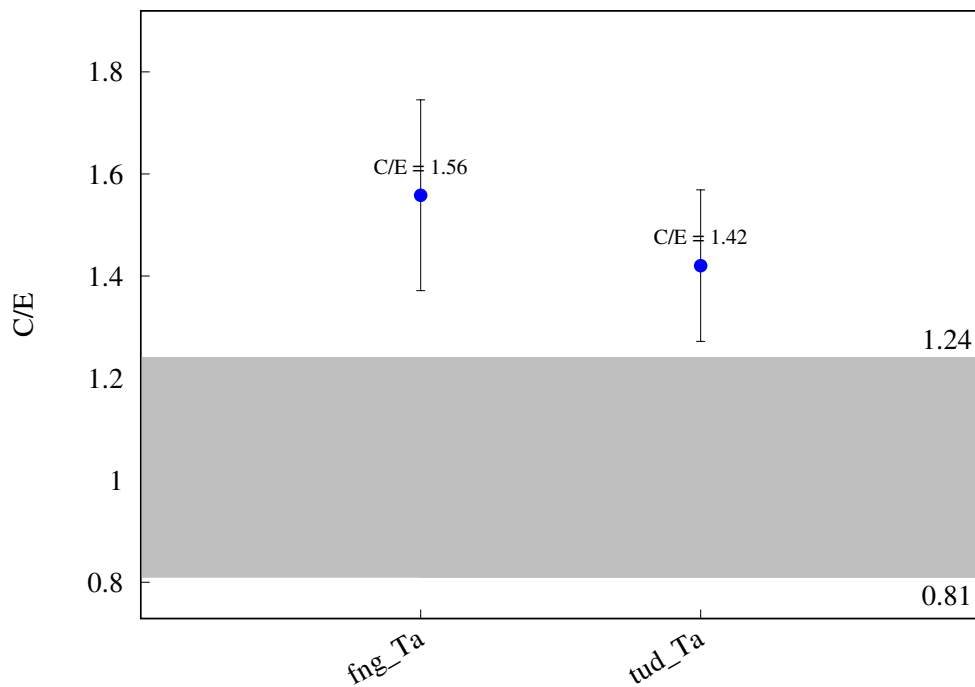
^{181}Ta (n,p) ^{181}Hf 

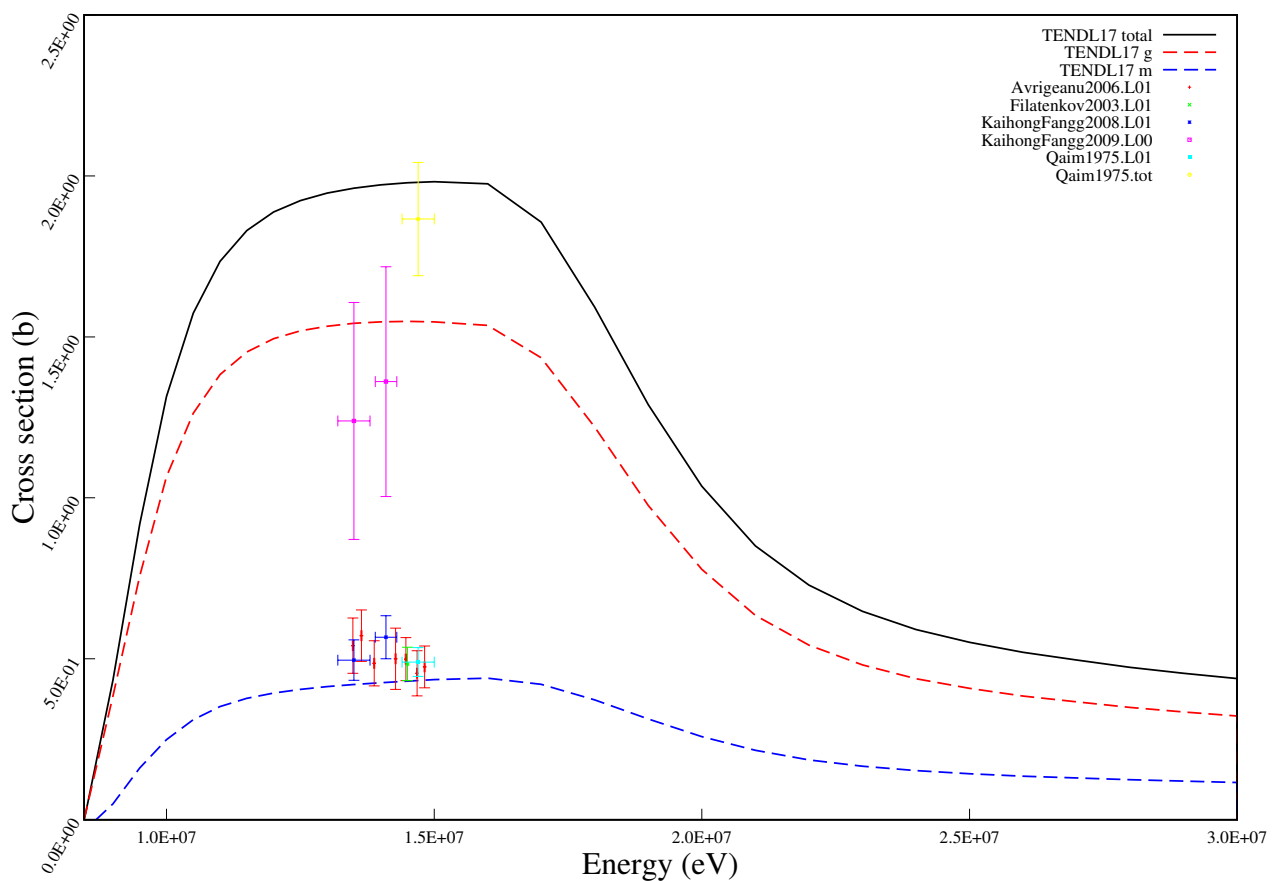
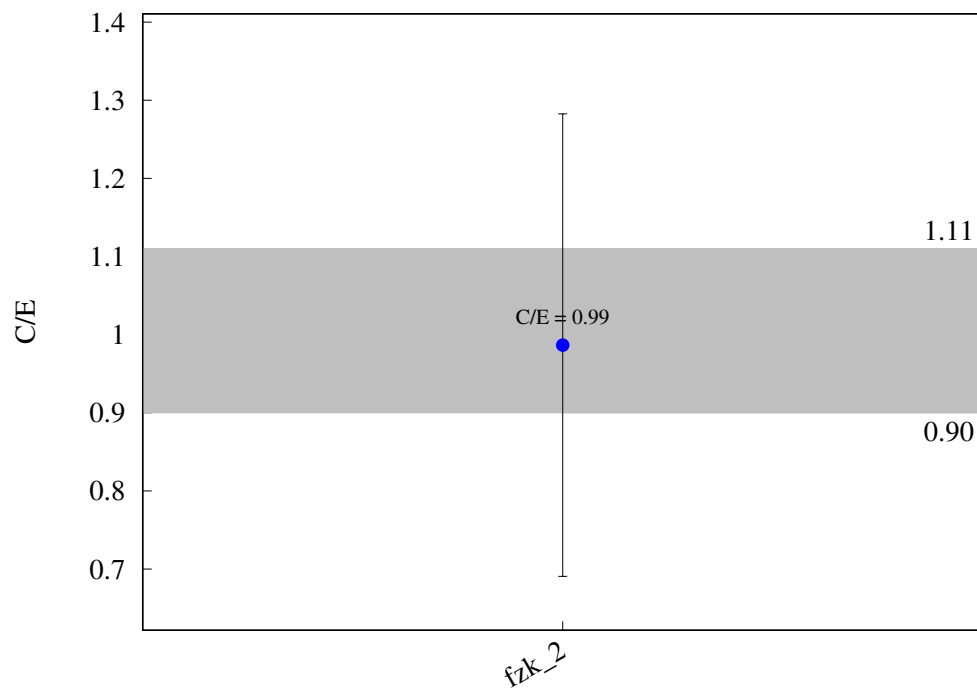
^{181}Ta (n,t) ^{179}nHf 

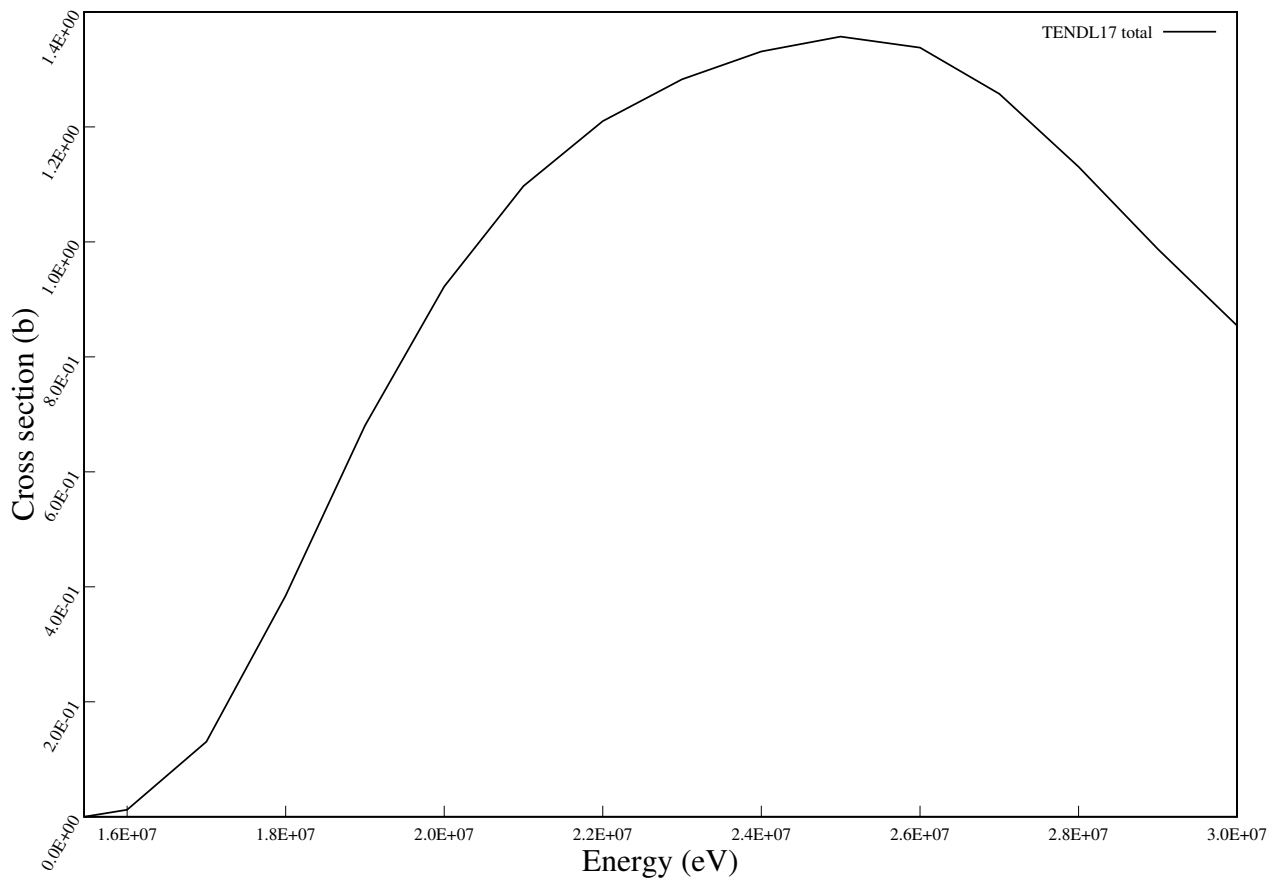
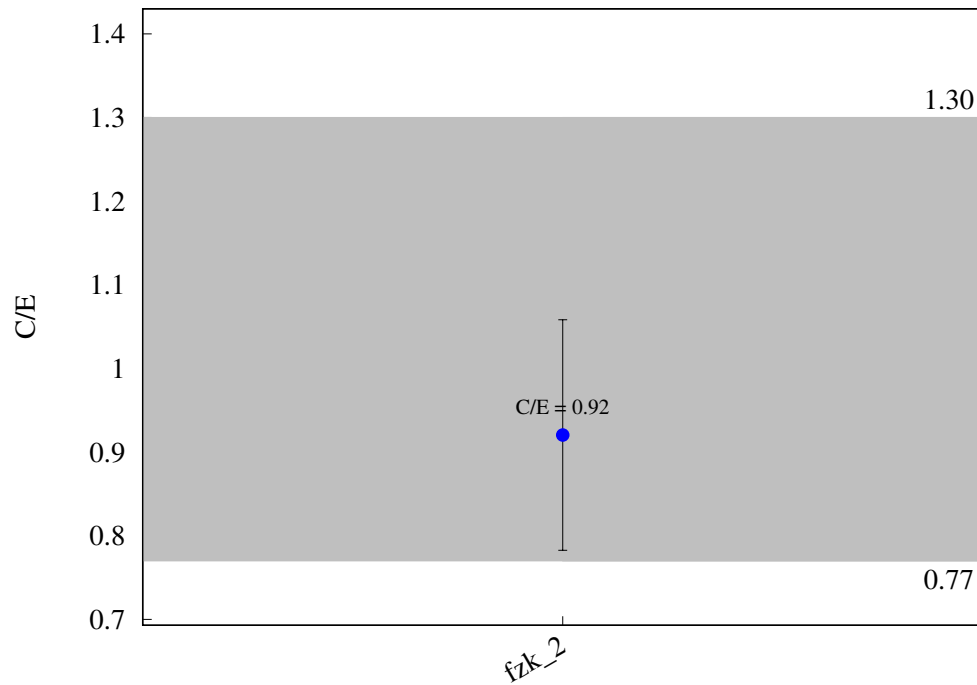
$^{181}\text{Ta} (\text{n},\text{t}) ^{179}\text{Hf}$ 

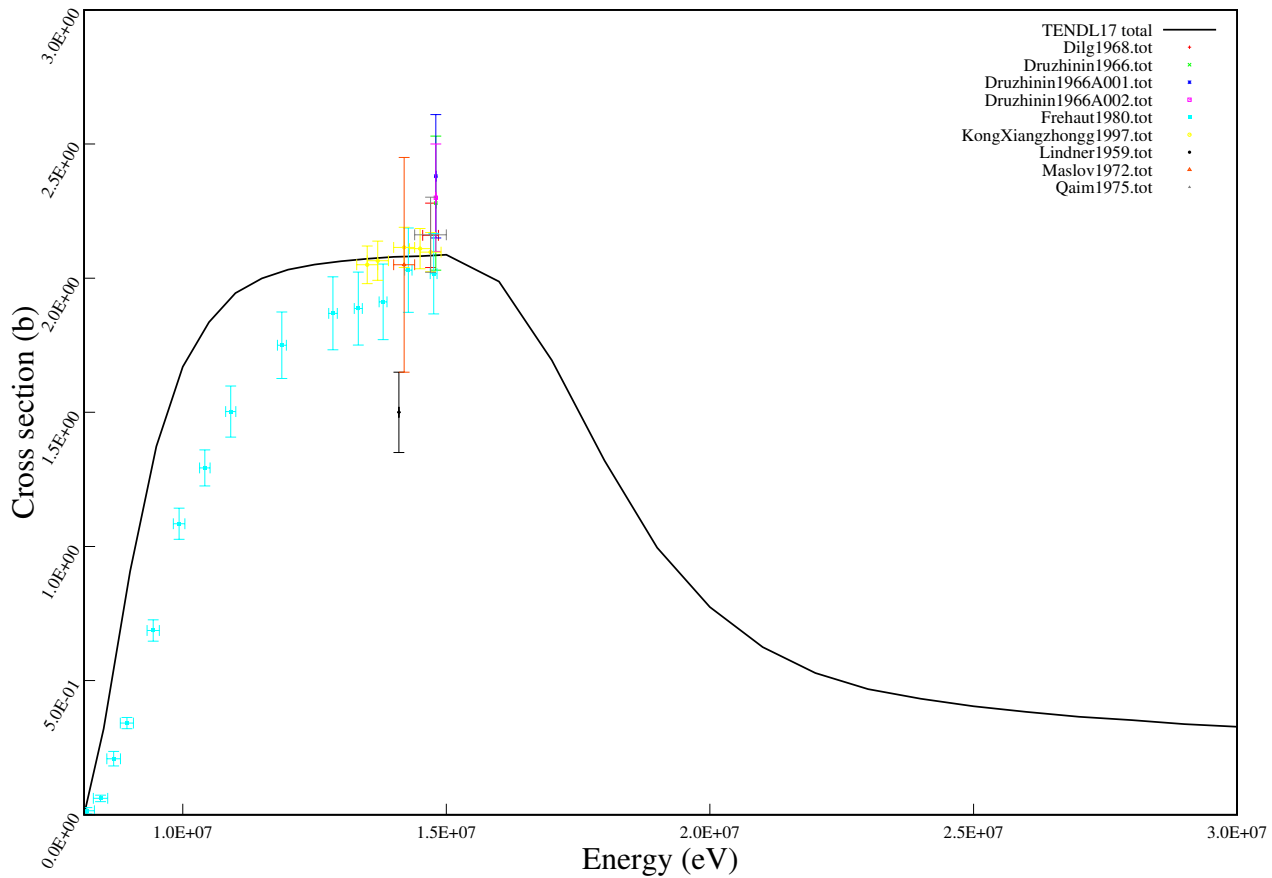
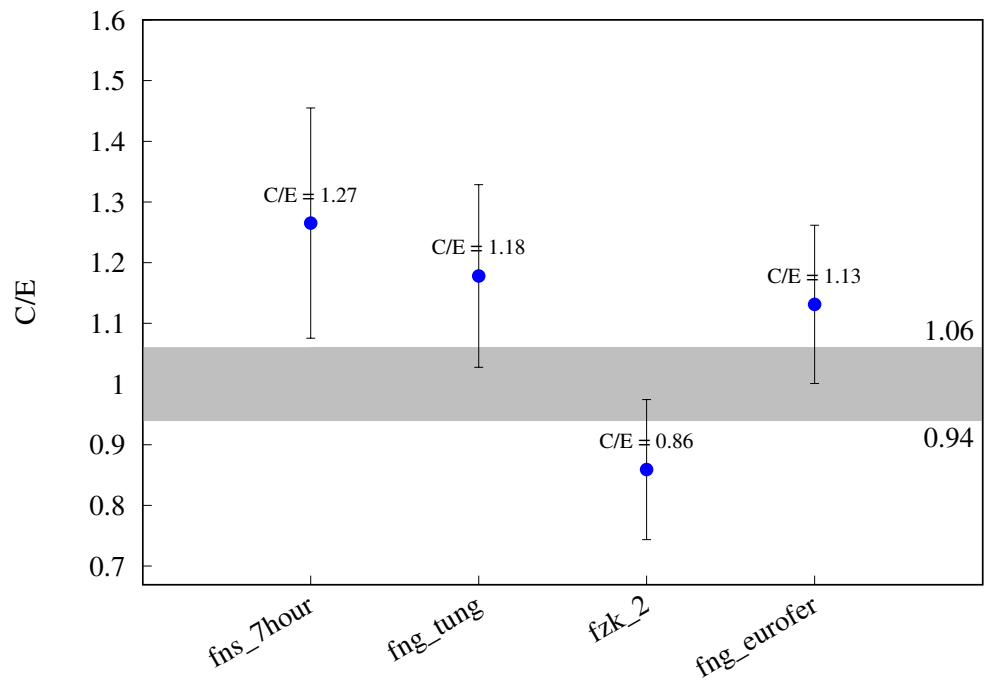
$^{181}\text{Ta} (\text{n},\text{h}) ^{179}\text{Lu}$ 

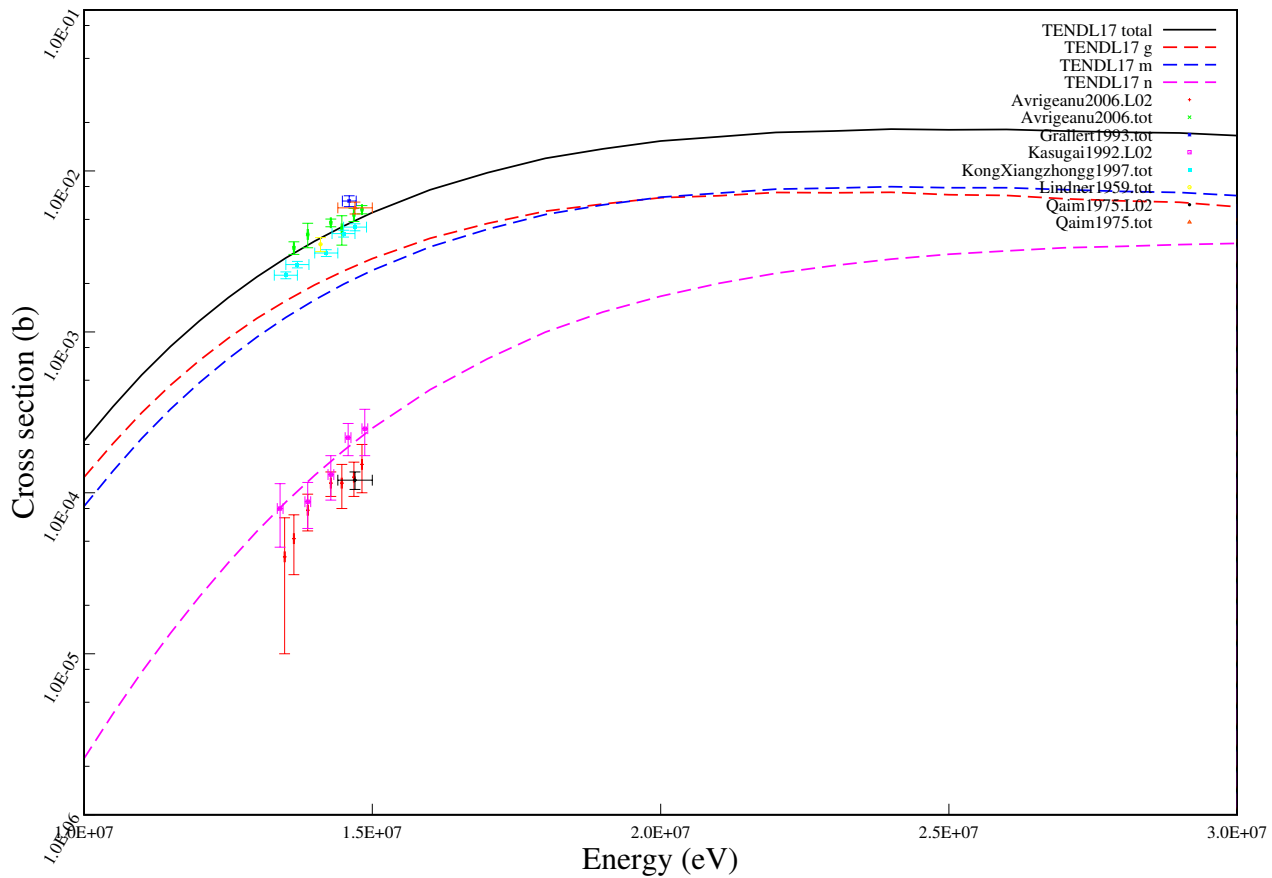
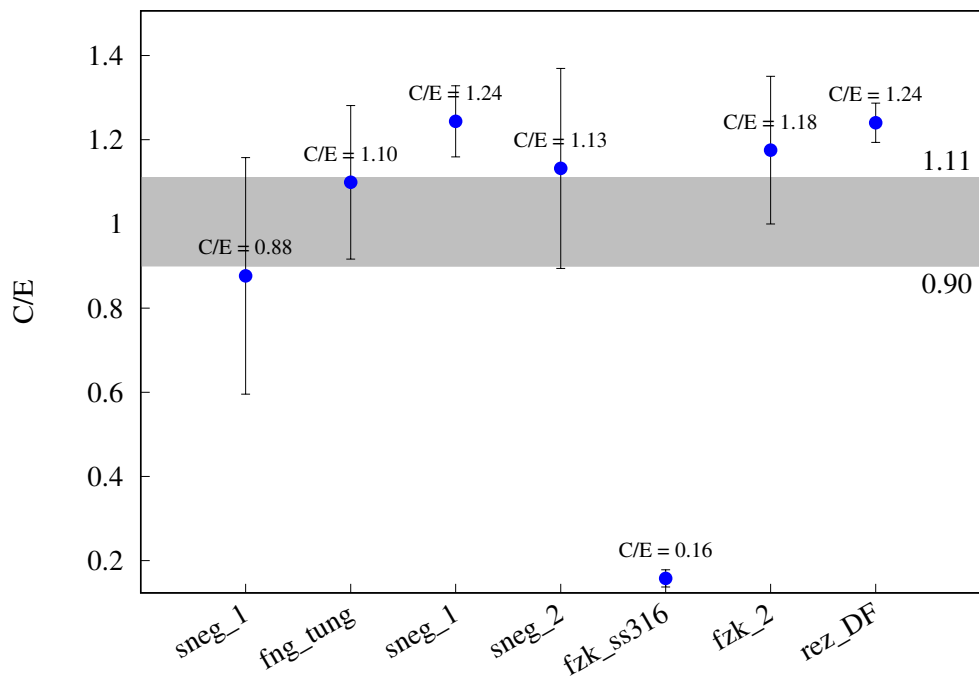
^{181}Ta (n,a) ^{178}gLu 

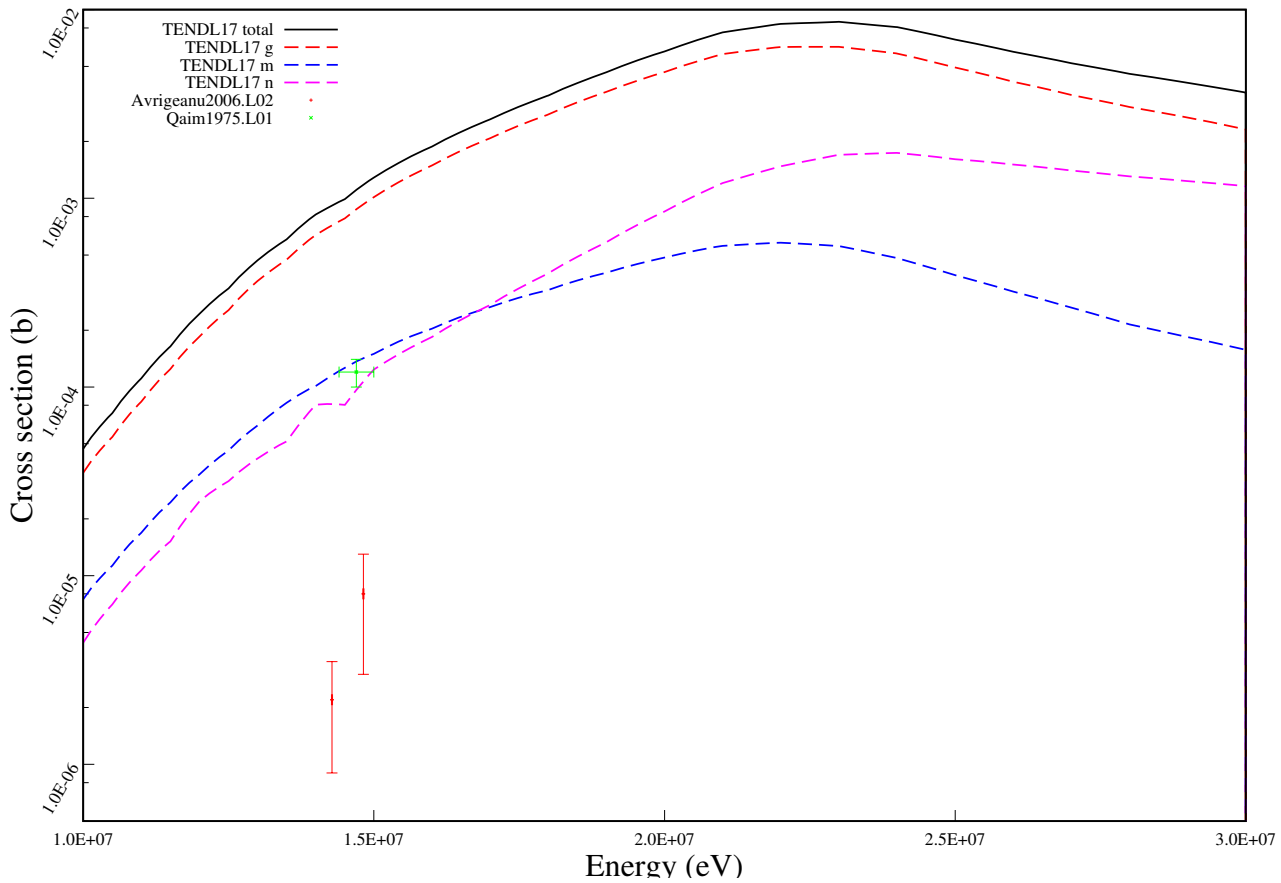
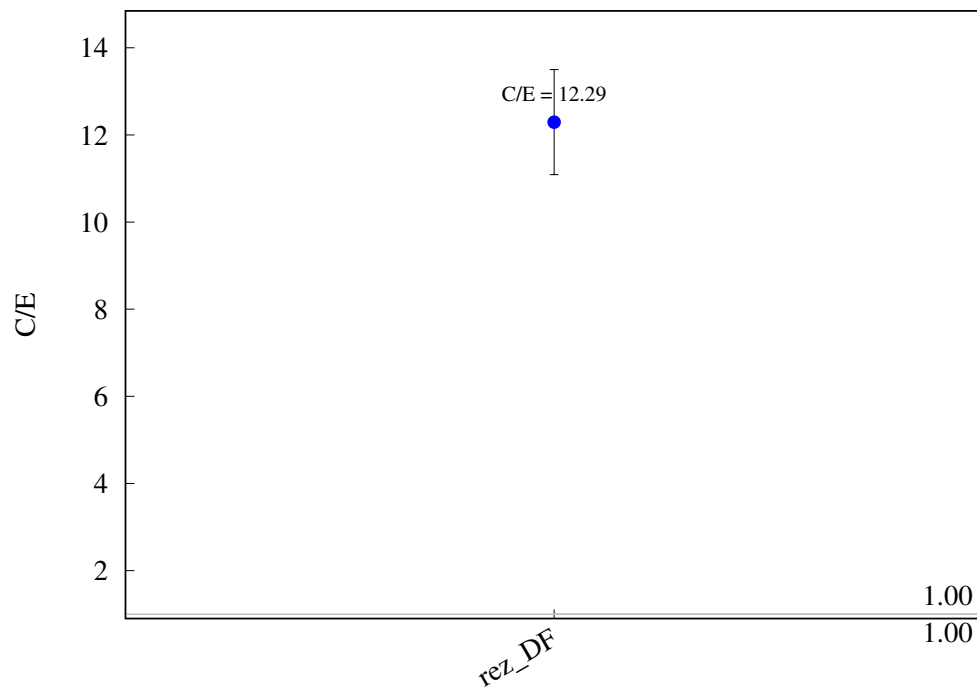
^{181}Ta (n,a) $^{178\text{m}}\text{Lu}$ 

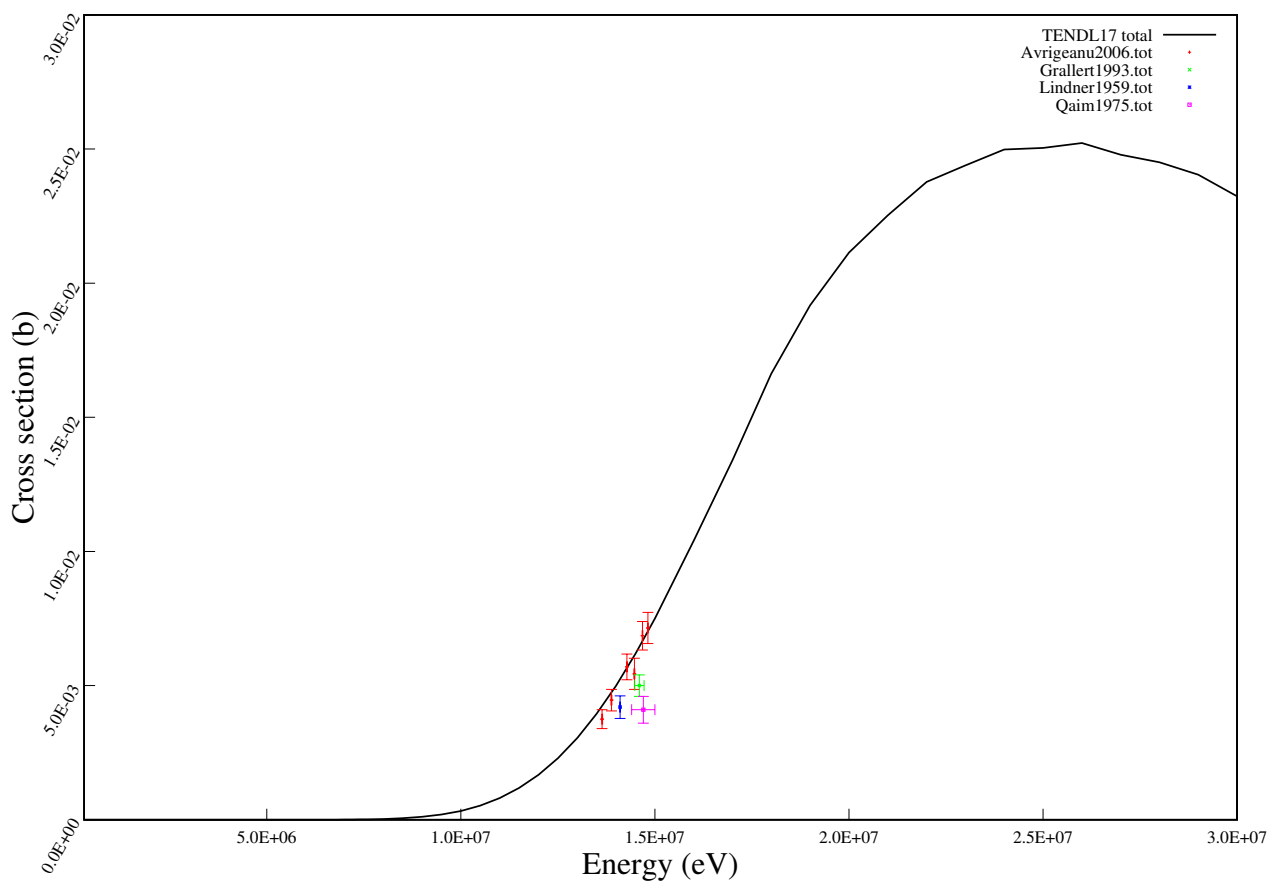
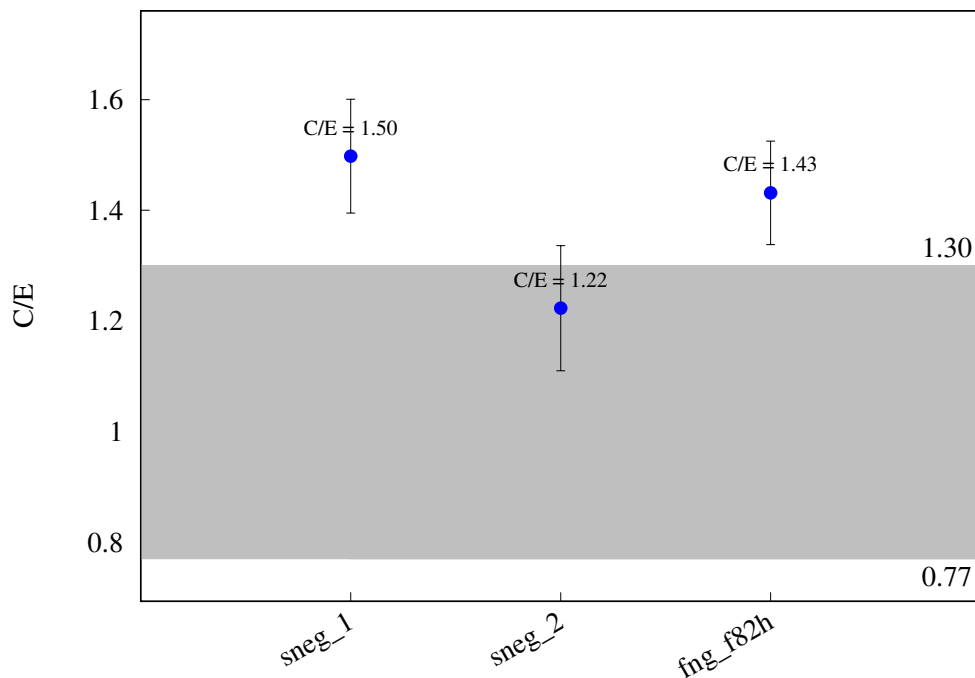
^{180}W ($n,2n$) ^{179m}W 

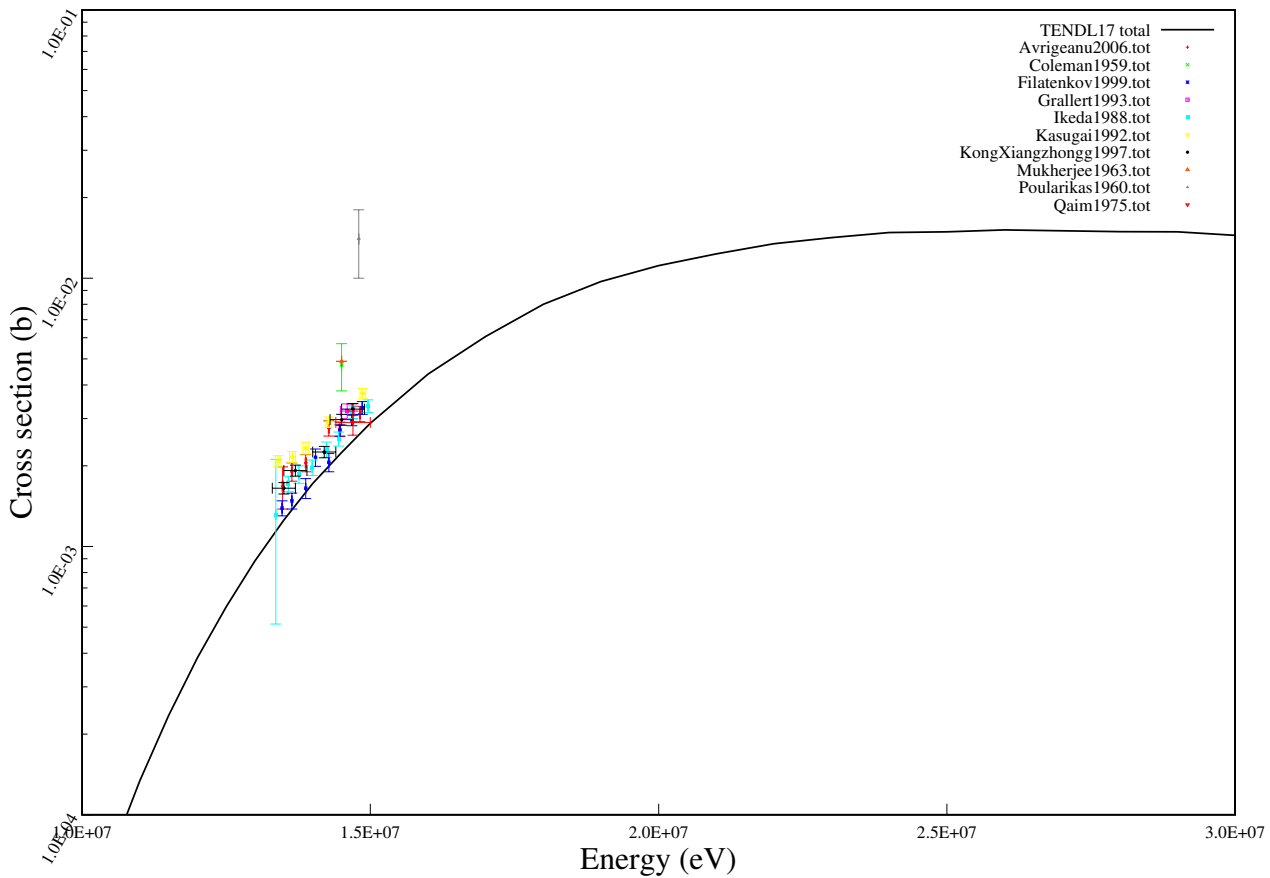
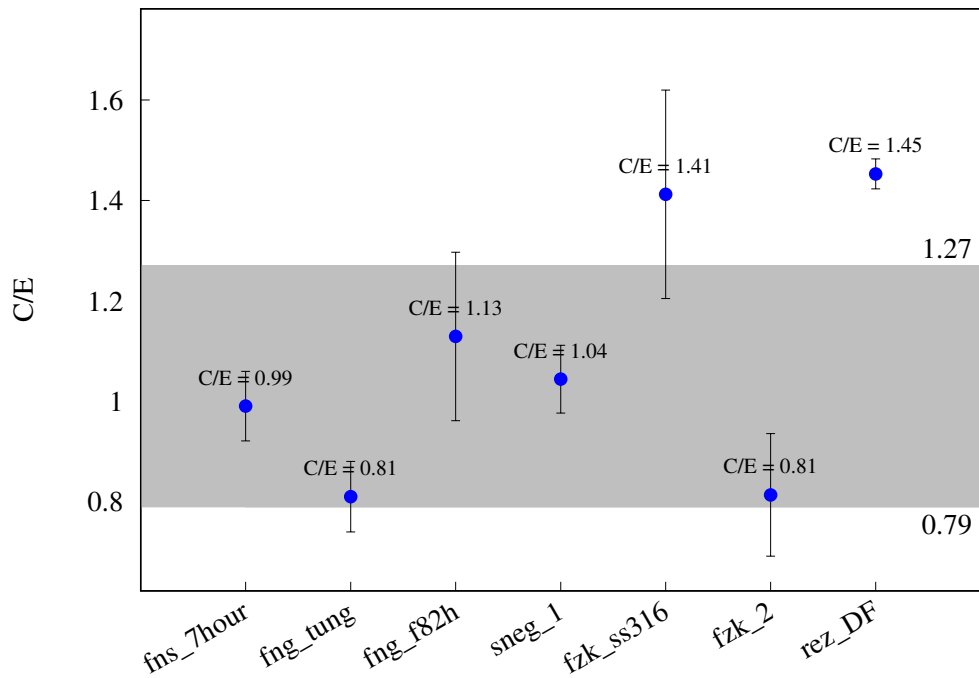
^{180}W (n,3n) ^{178}W 

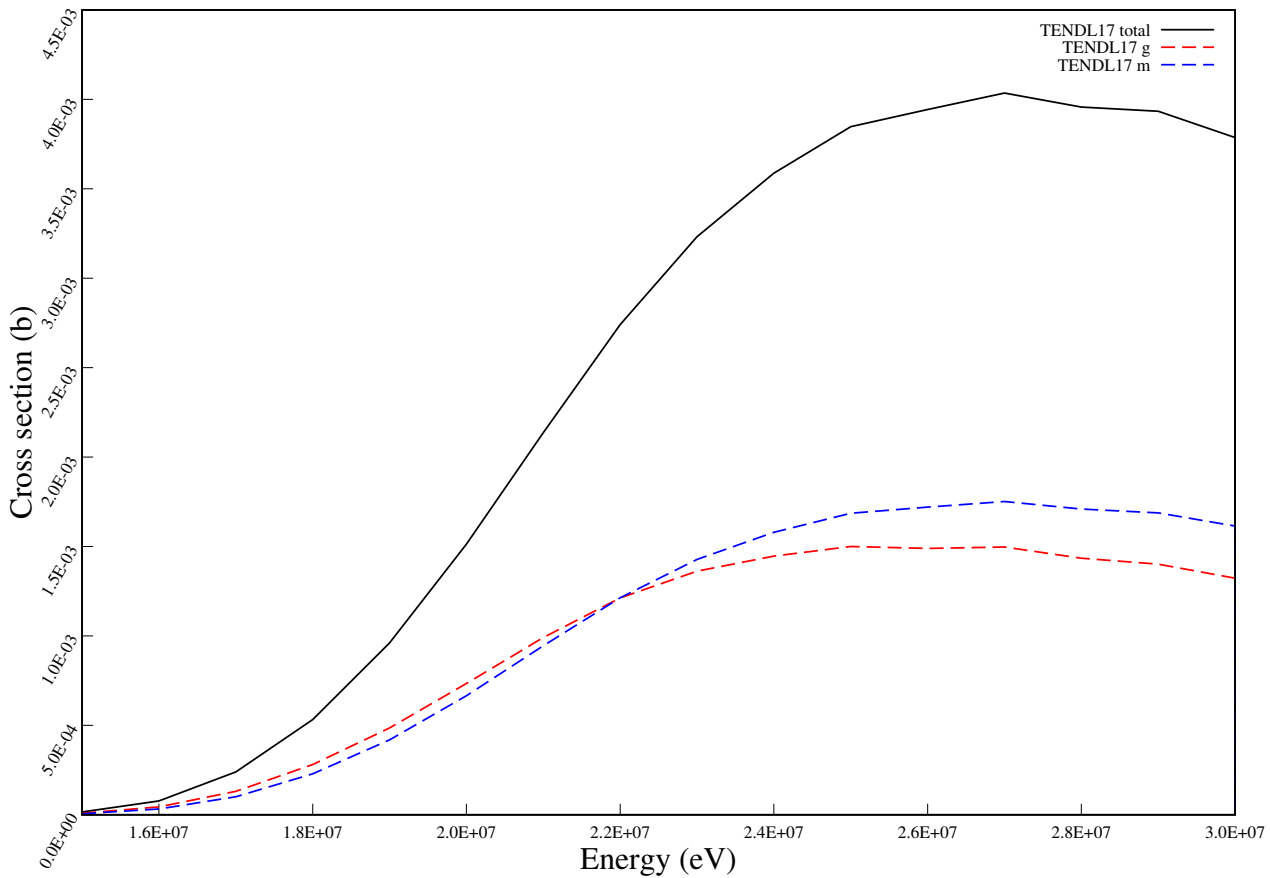
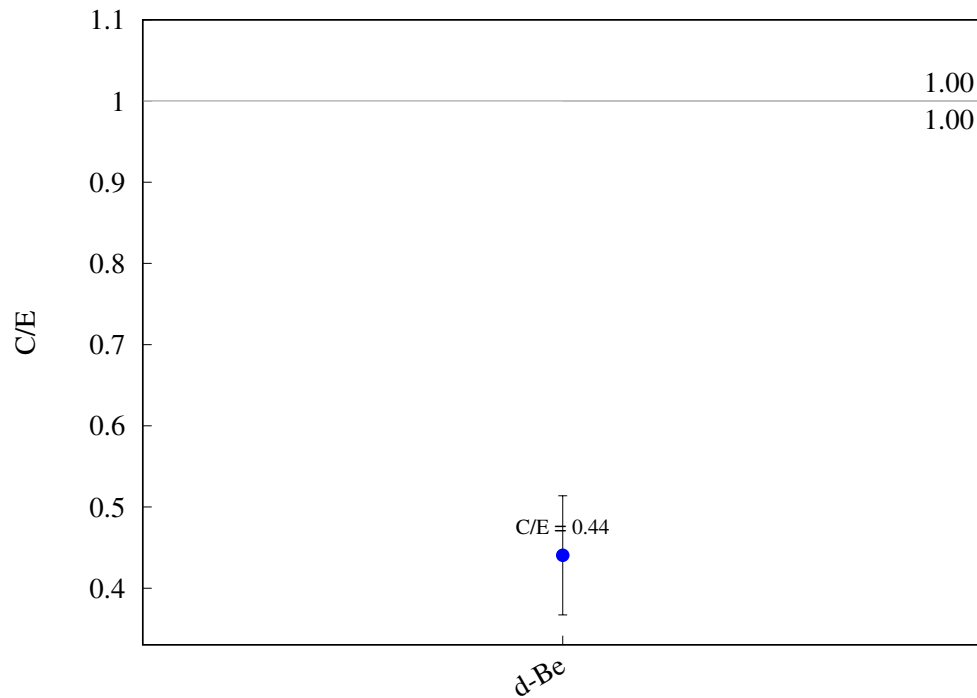
^{182}W (n,2n) ^{181}W 

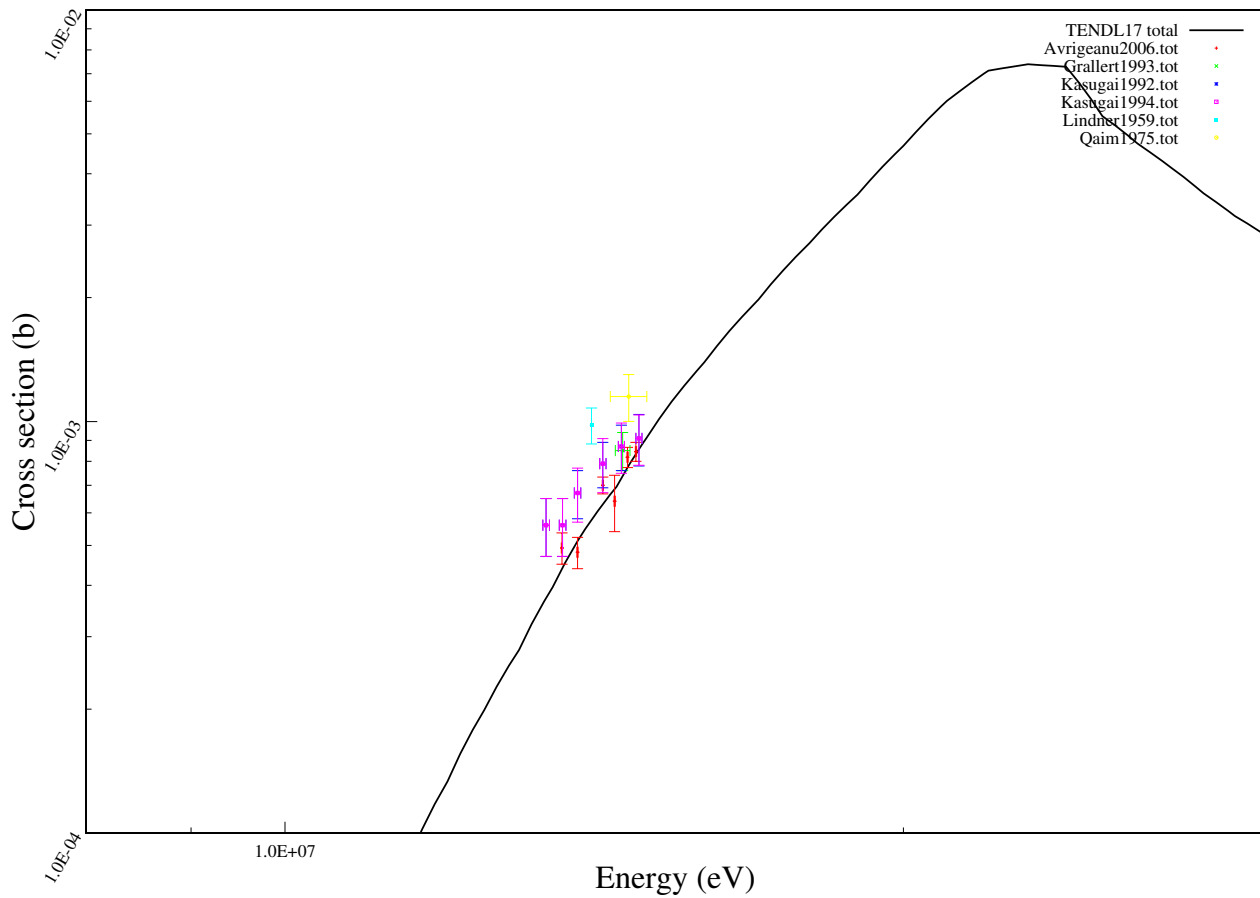
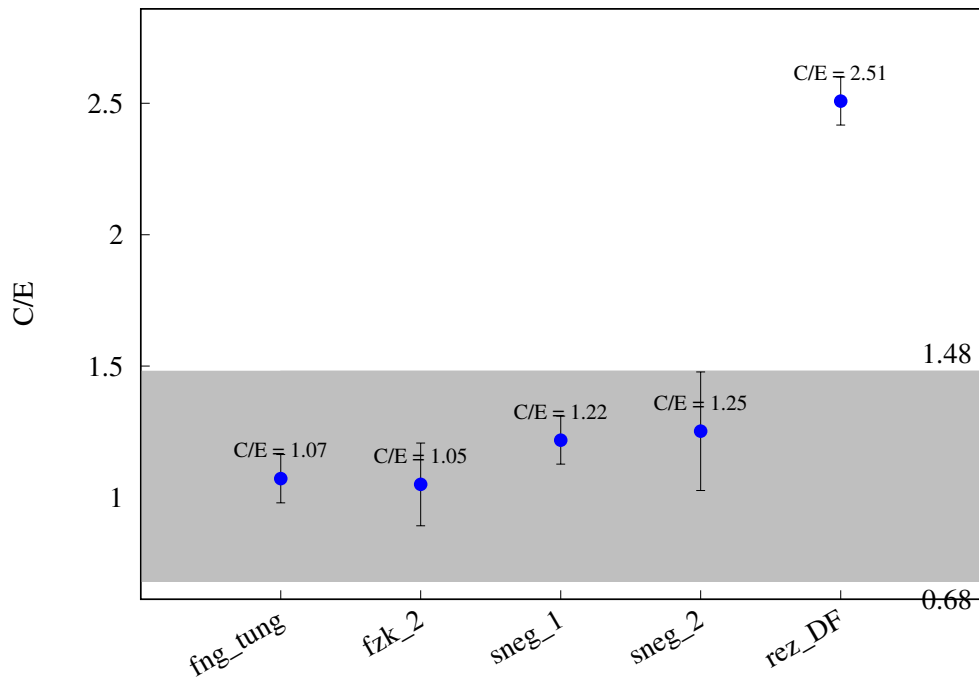
^{182}W (n,p) ^{182}Ta 

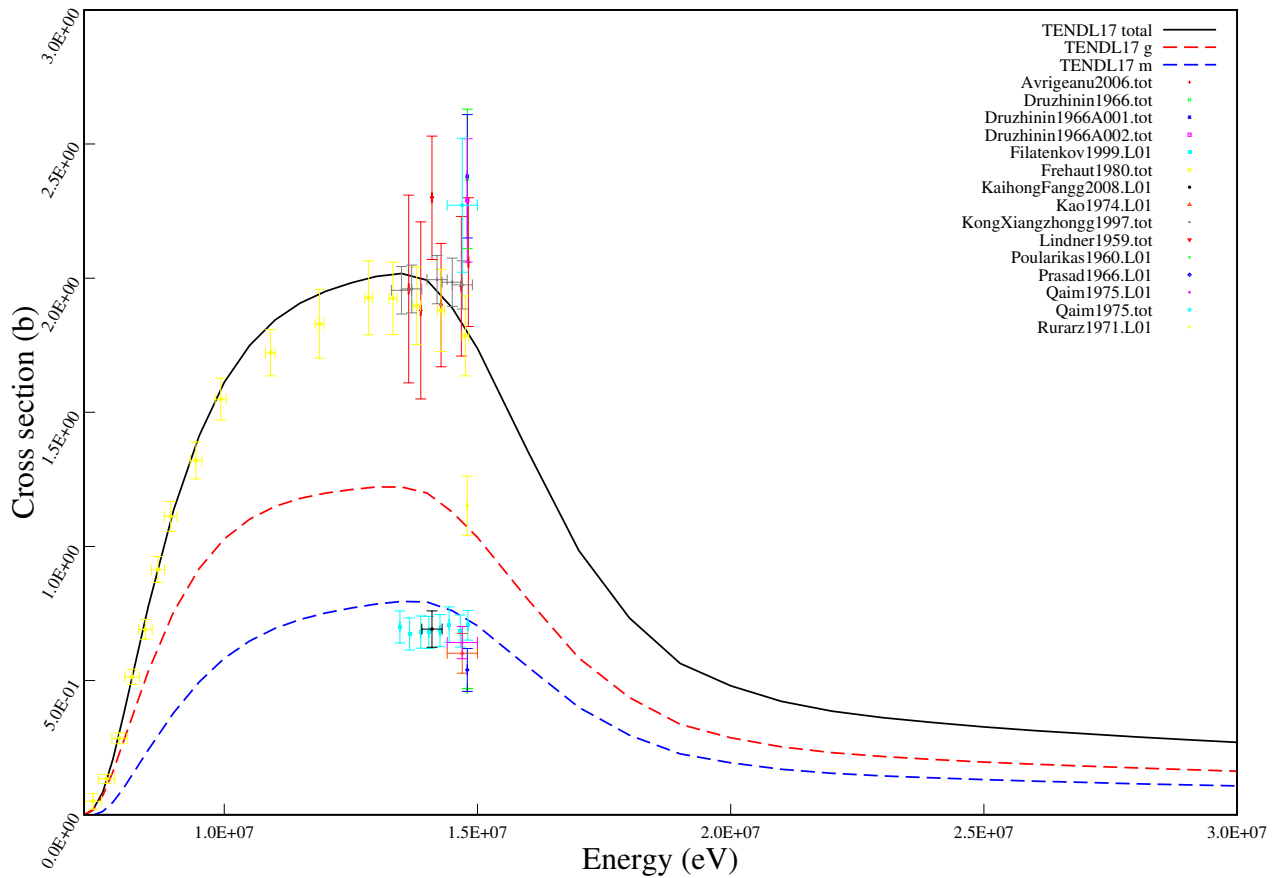
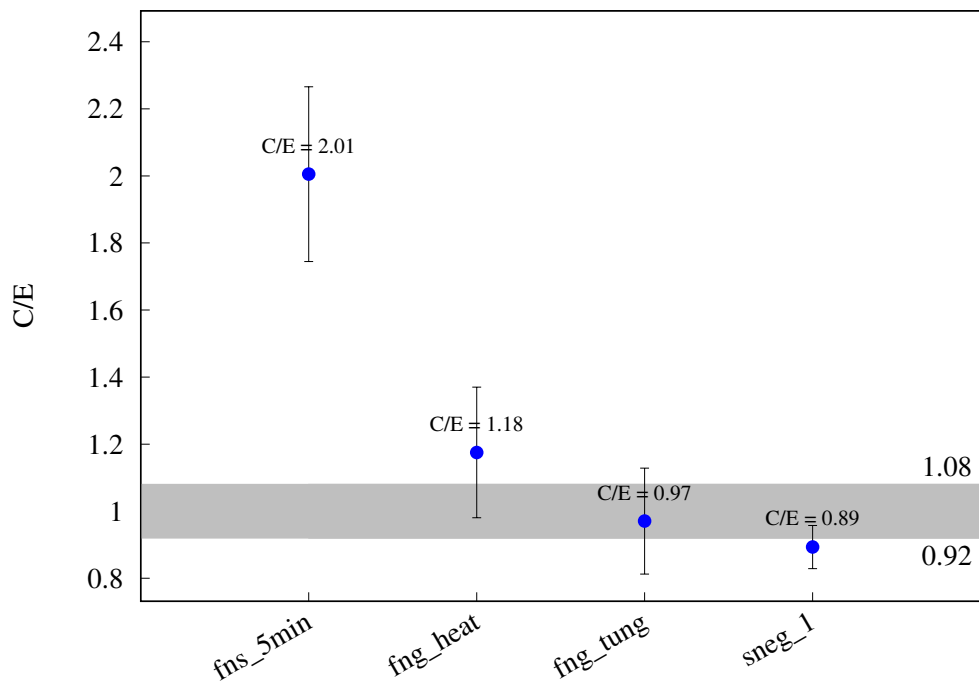
^{182}W (n,a) ^{179}nHf 

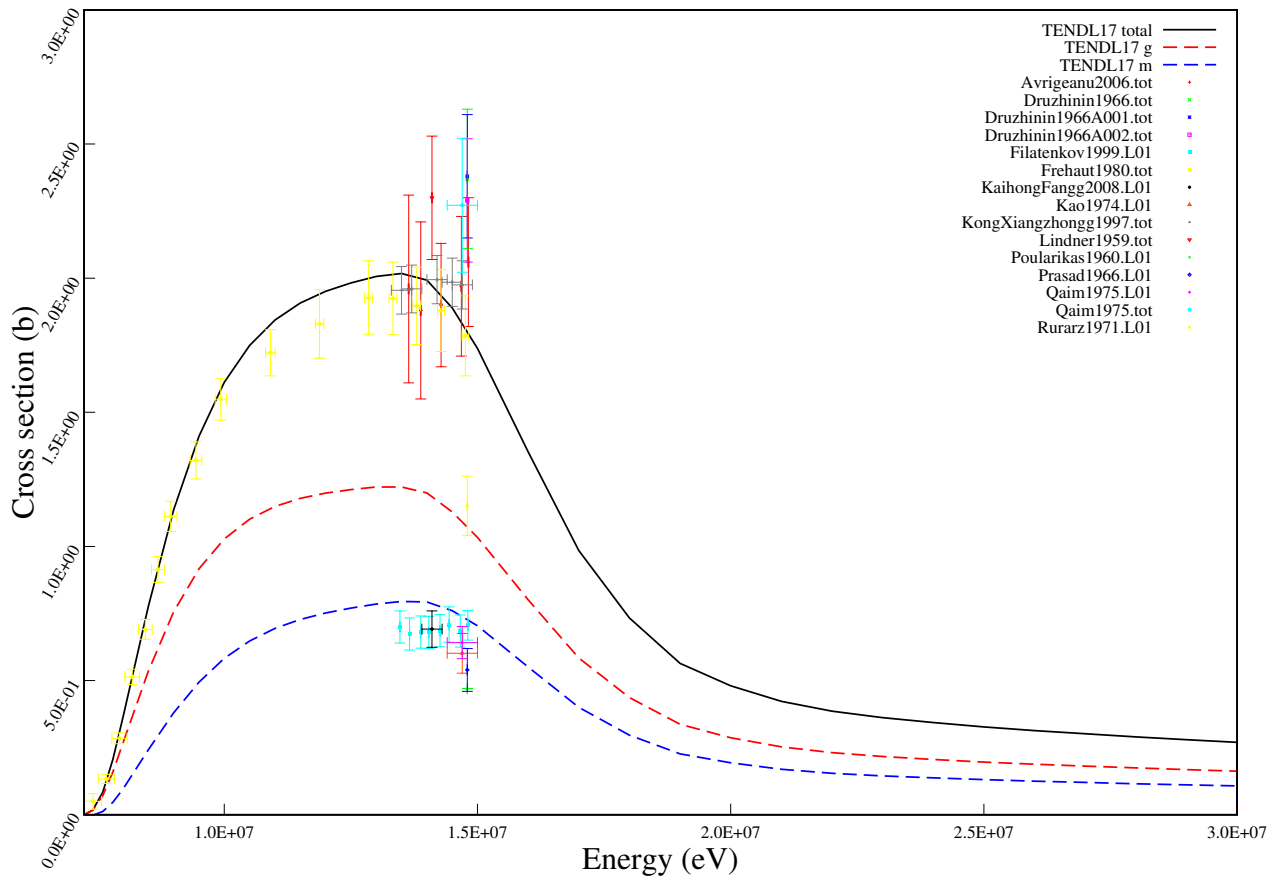
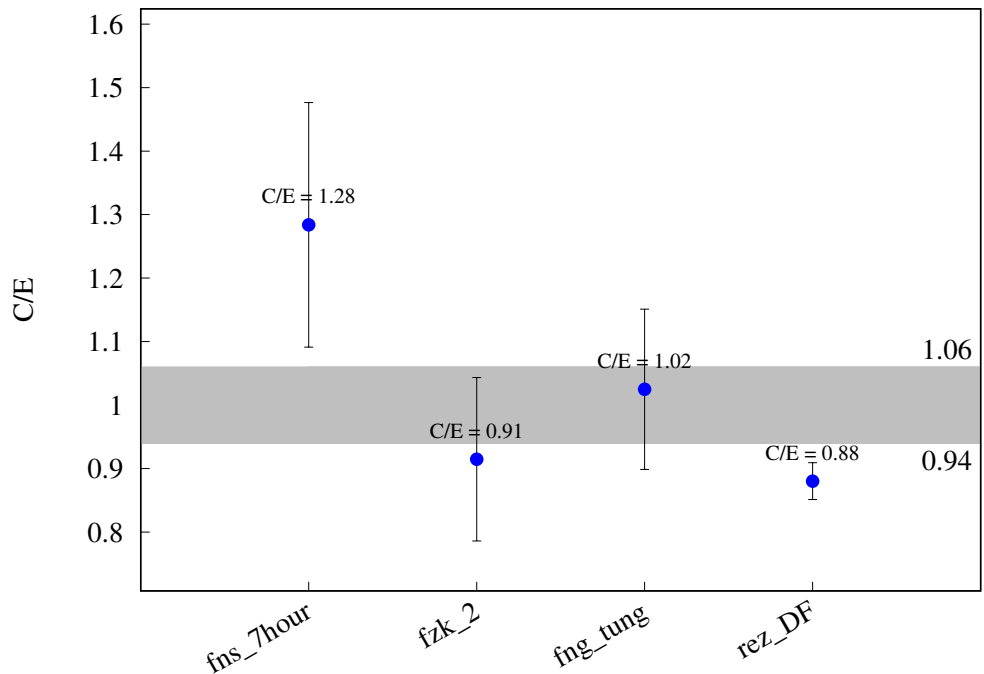
$^{183}\text{W} (\text{n},\text{p}) ^{183}\text{Ta}$ 

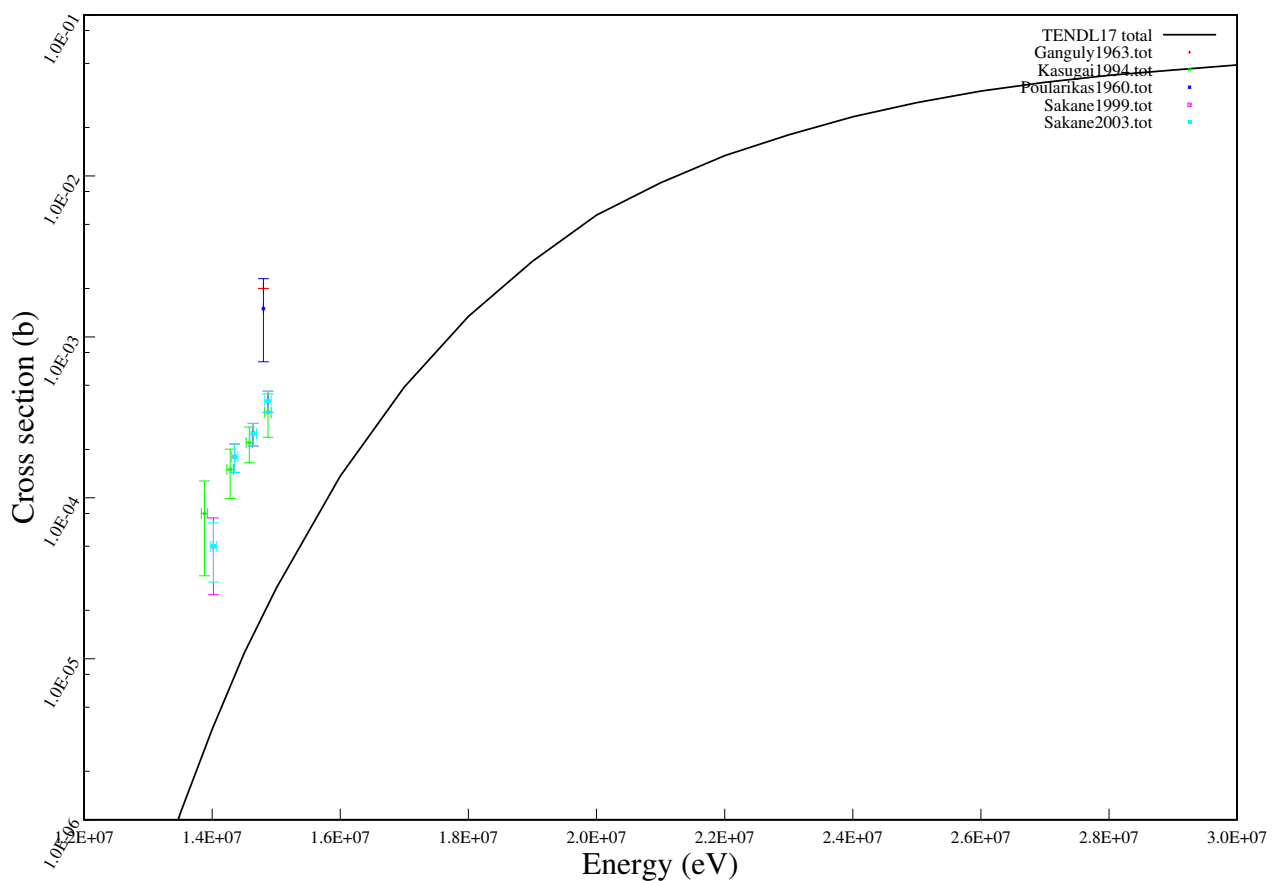
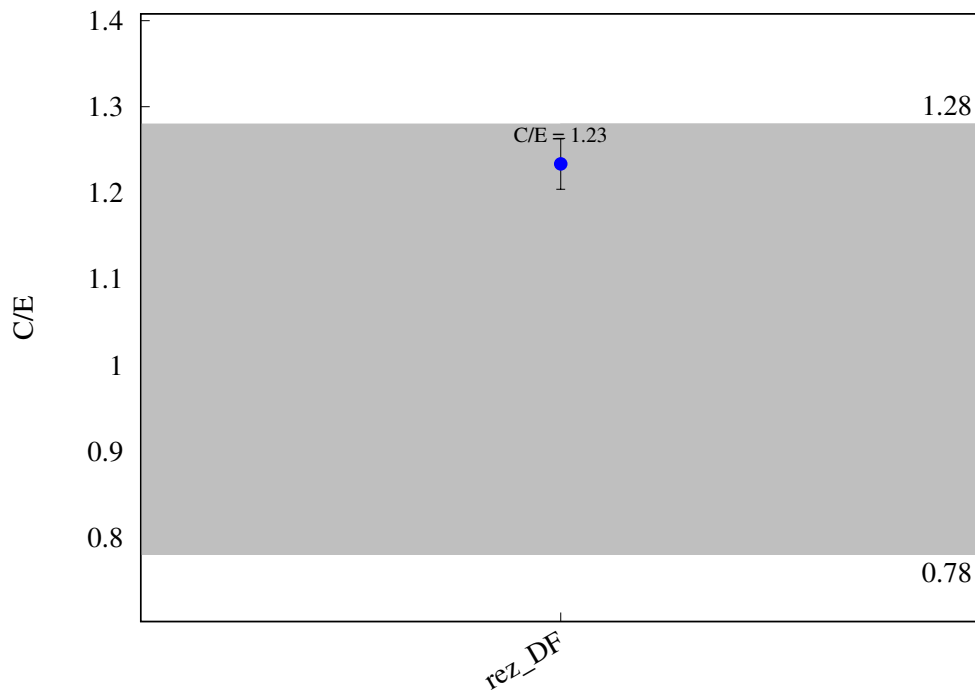
$^{184}\text{W} (\text{n},\text{p}) ^{184}\text{Ta}$ 

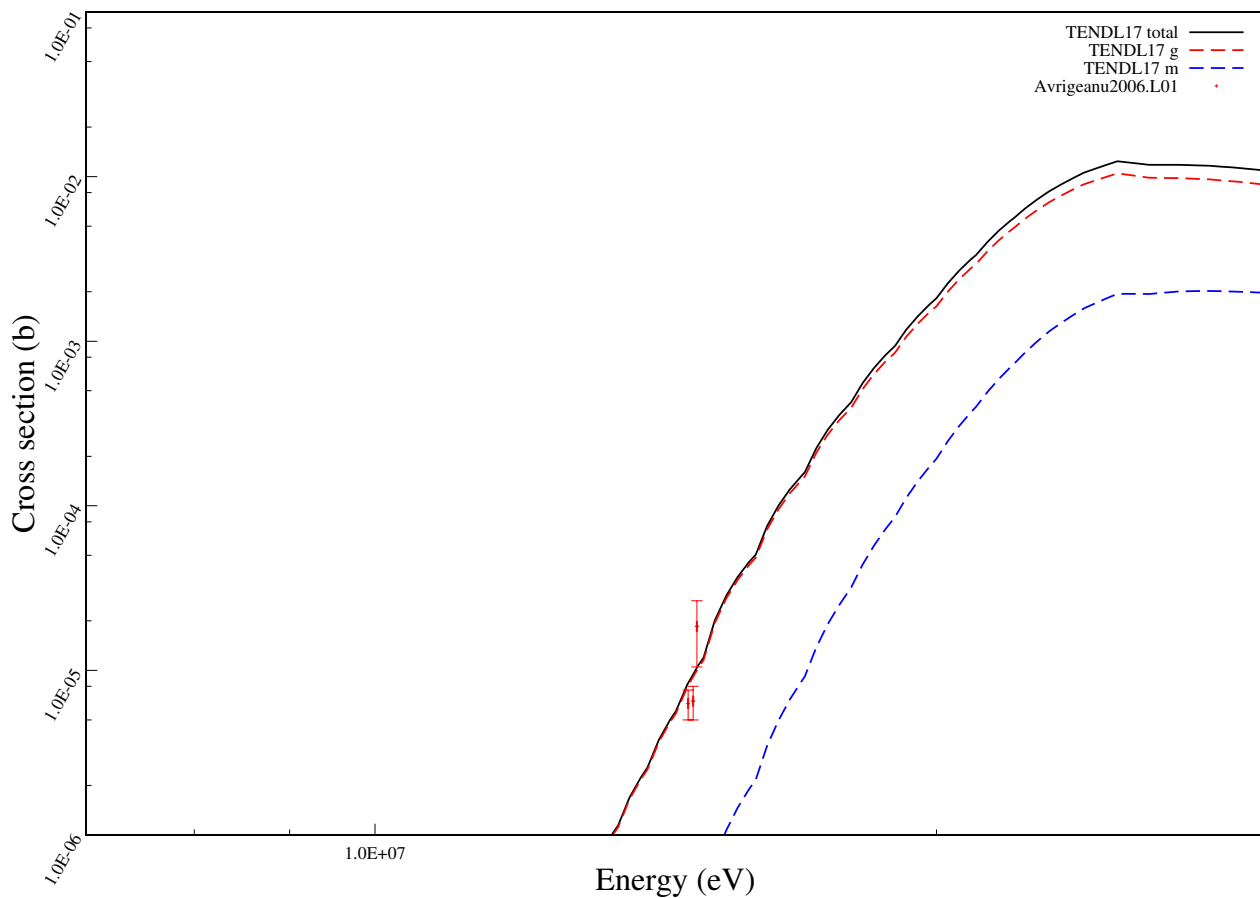
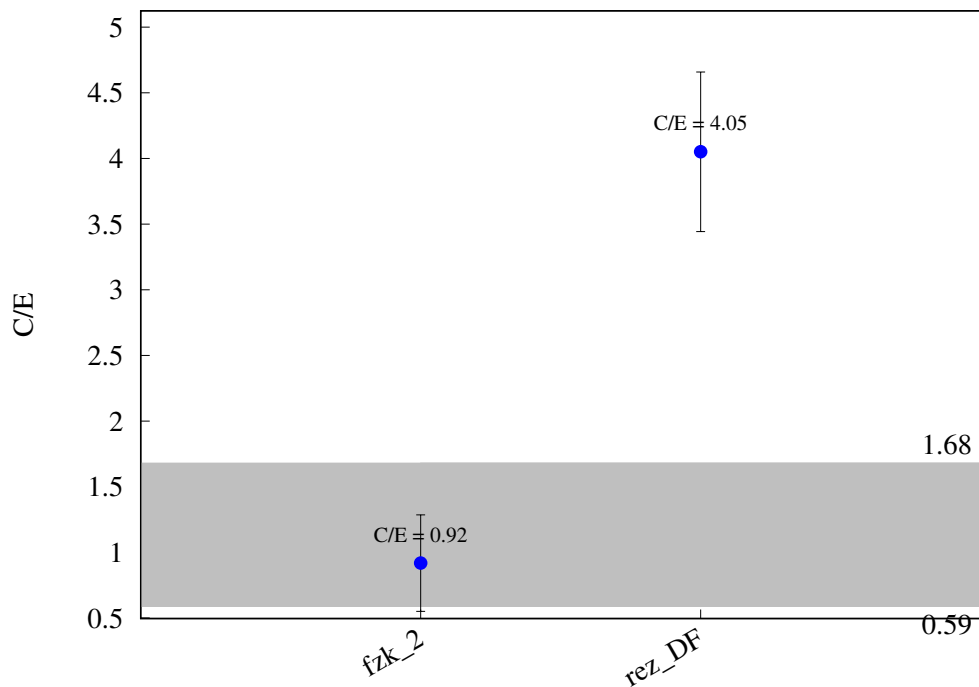
$^{184}\text{W} (\text{n},\text{t}) ^{182}\text{Ta}$ 

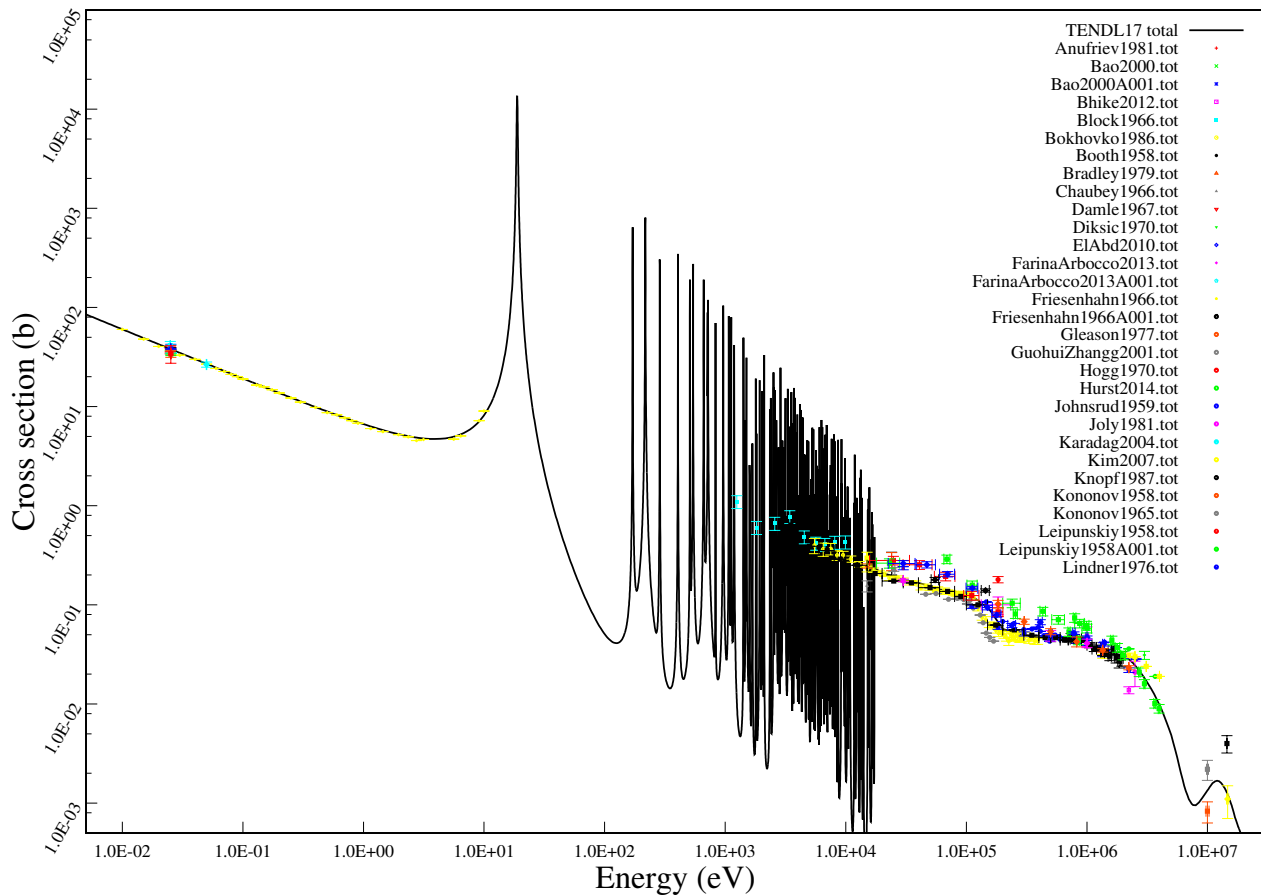
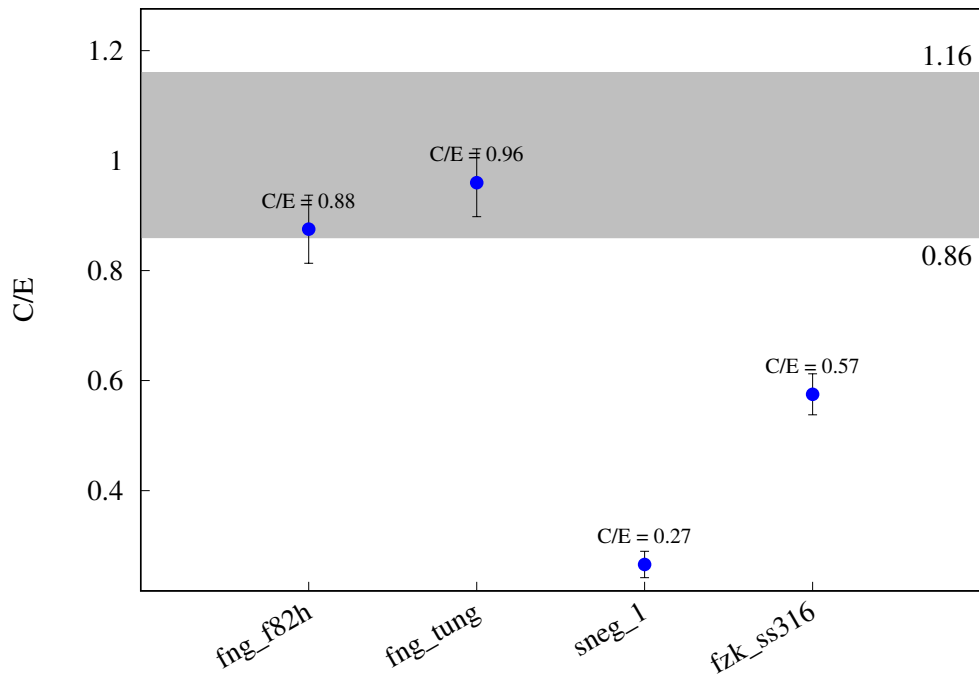
^{184}W (n,a) ^{181}Hf 

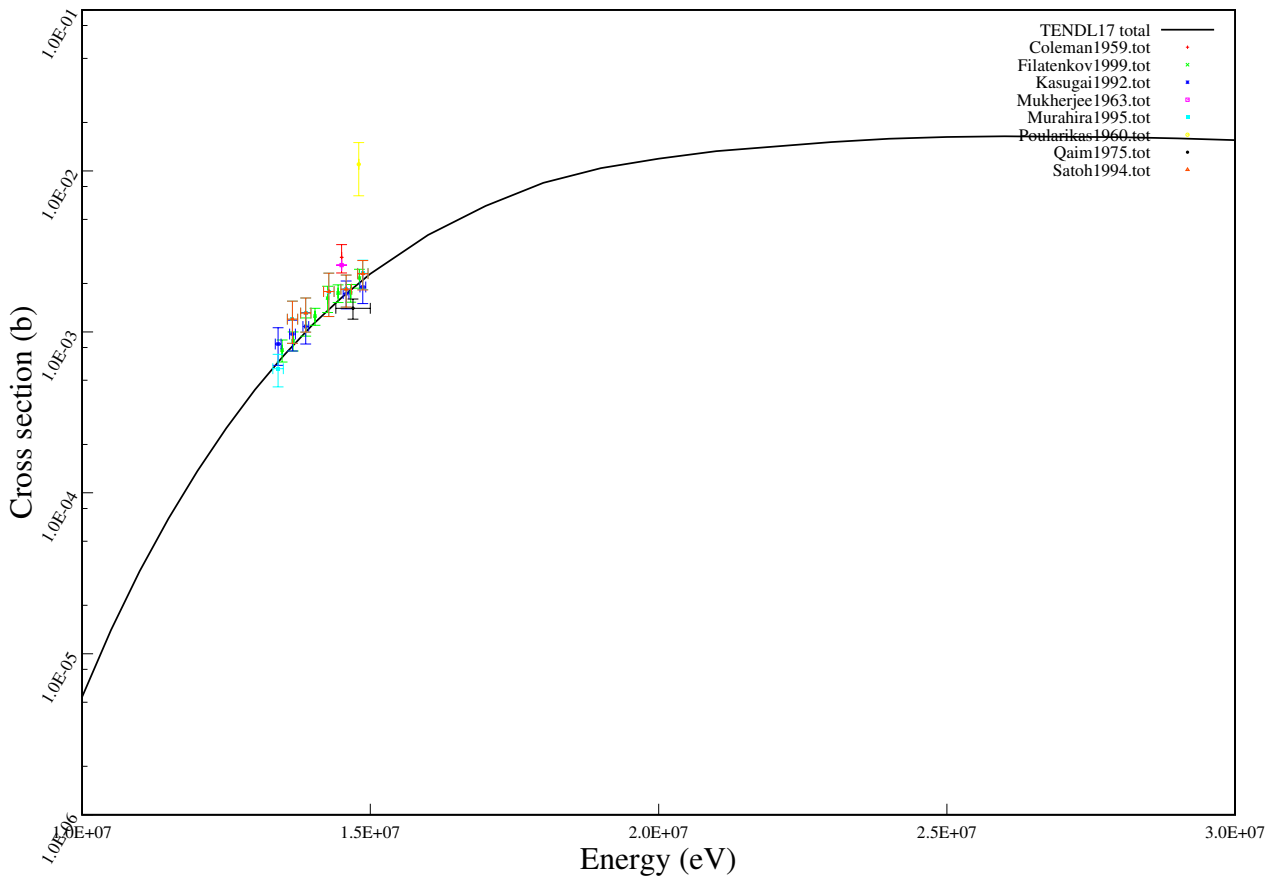
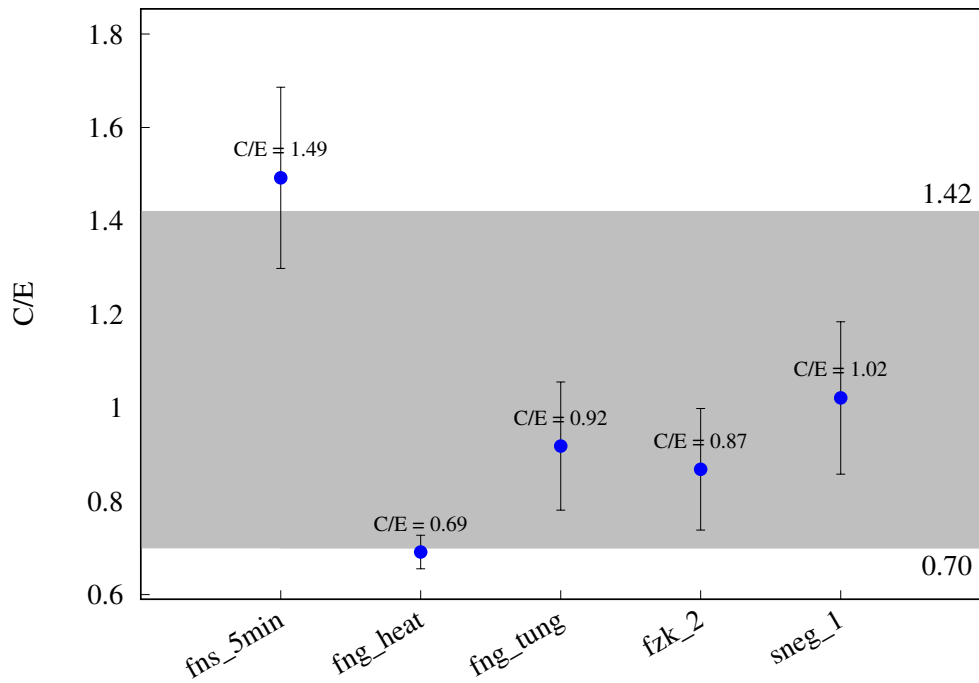
^{186}W (n,2n) ^{185}mW 

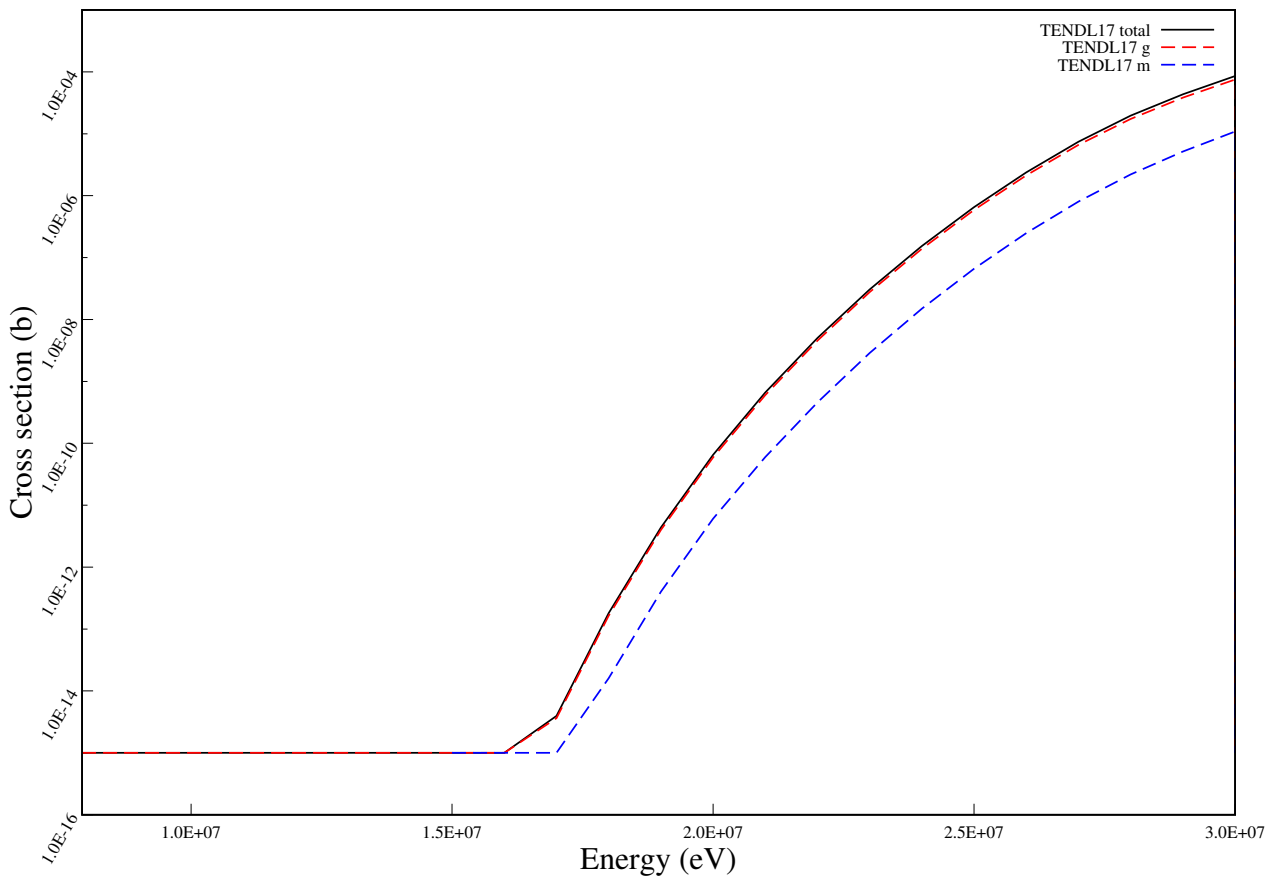
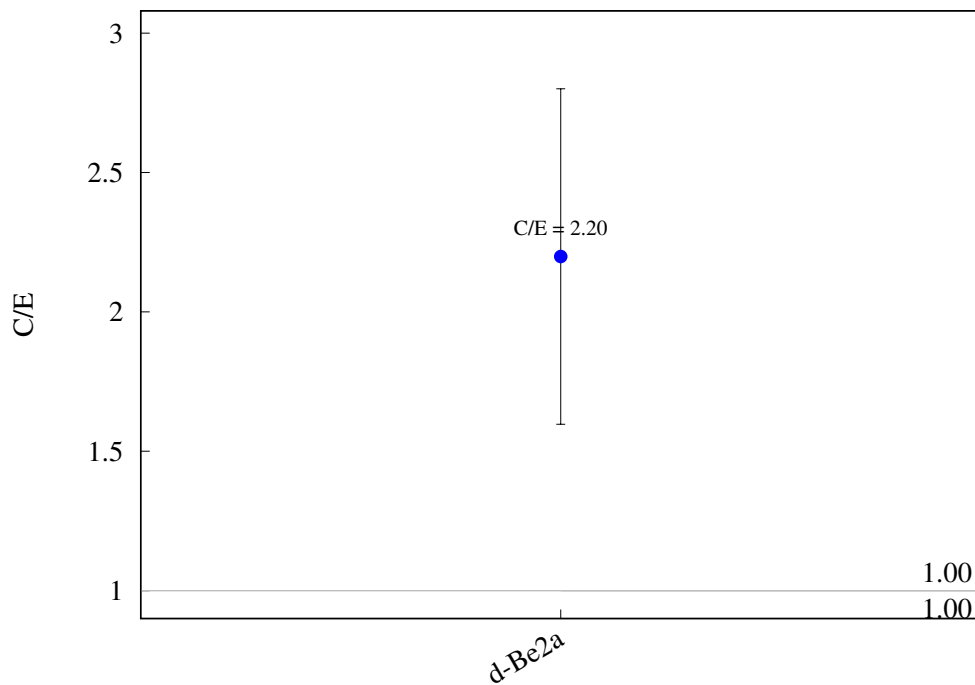
^{186}W (n,2n) ^{185}W 

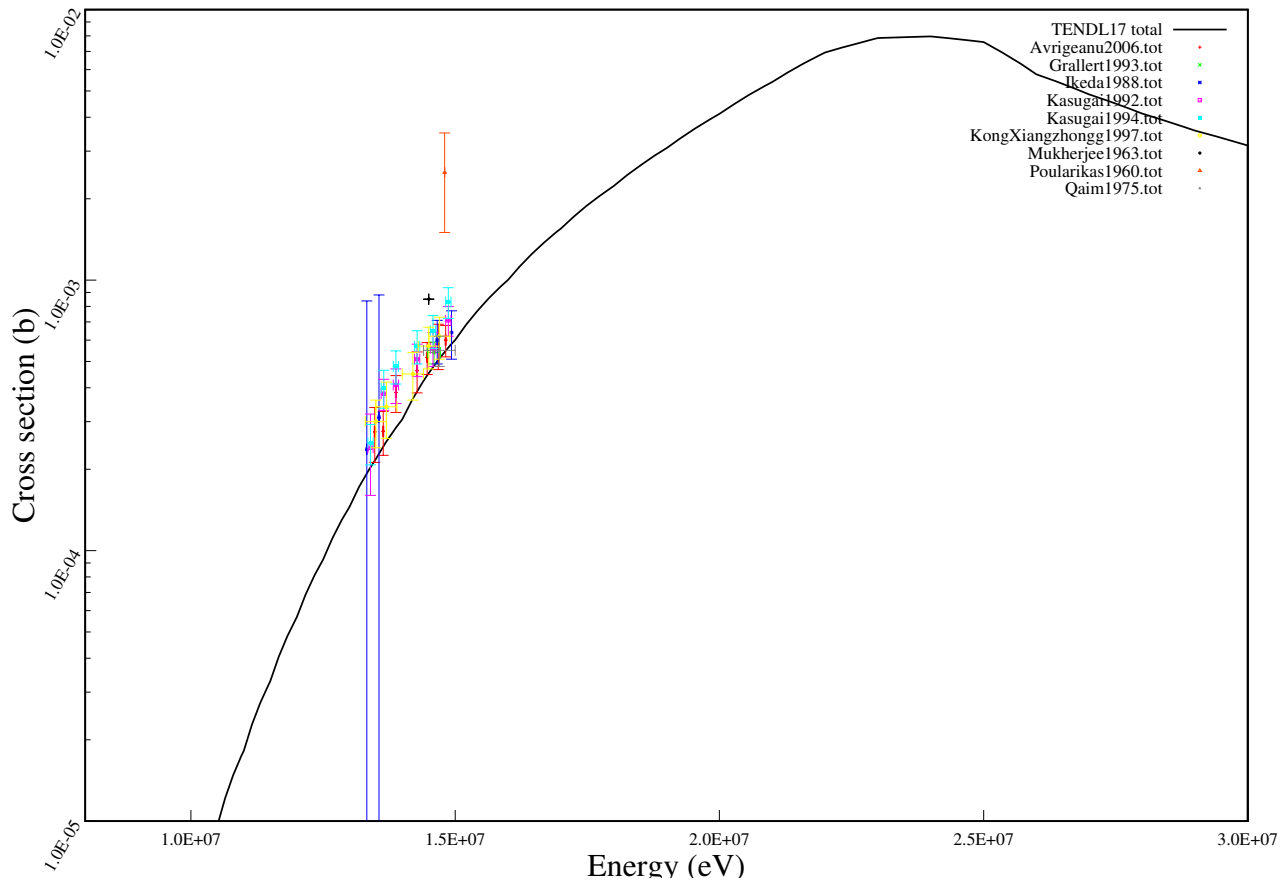
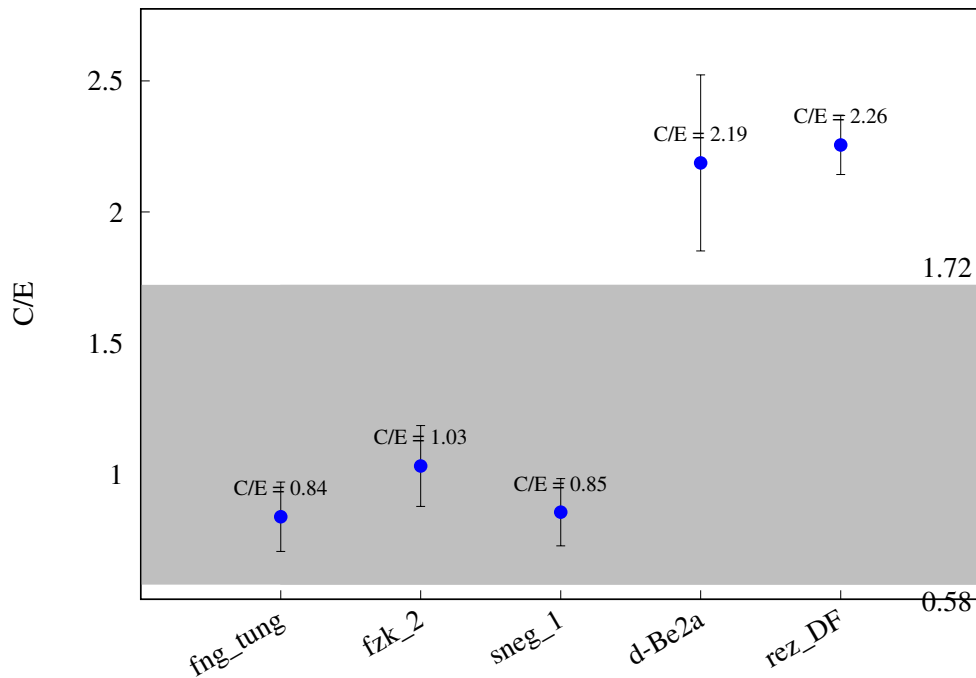
^{186}W (n,np) ^{185}Ta 

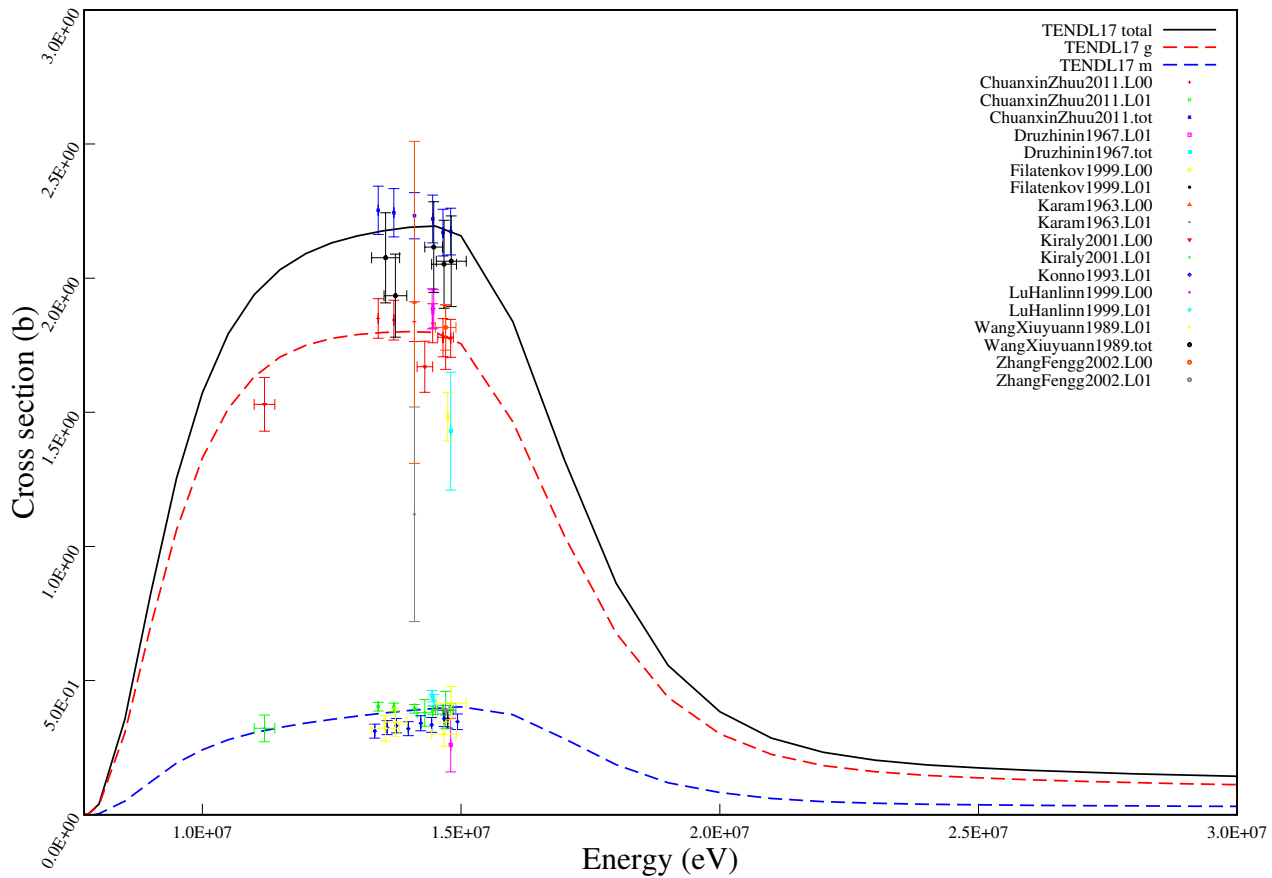
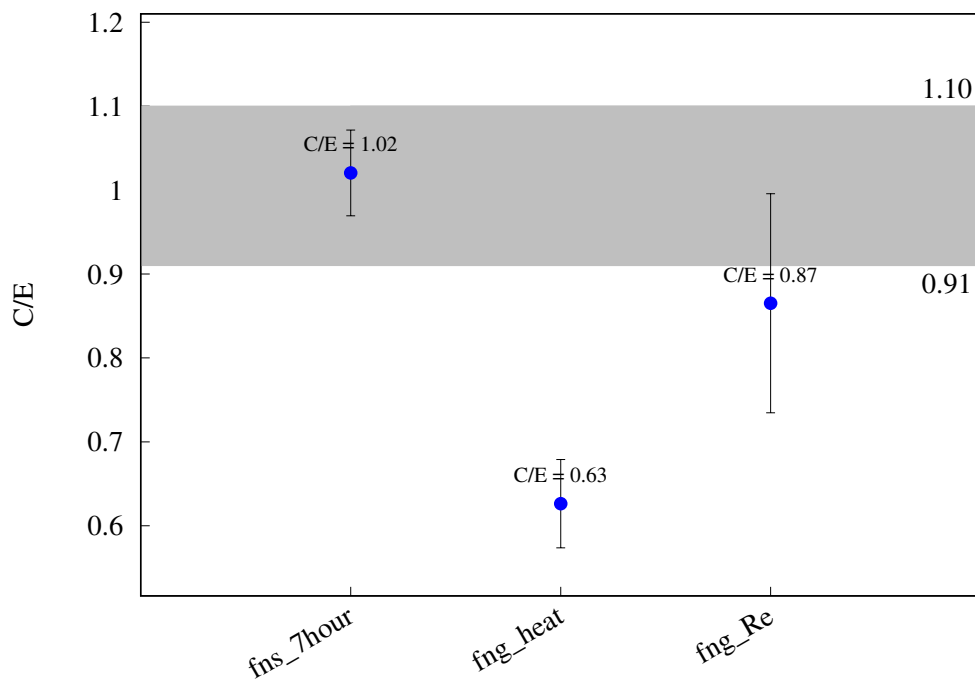
^{186}W (n,na) $^{182\text{m}}\text{Hf}$ 

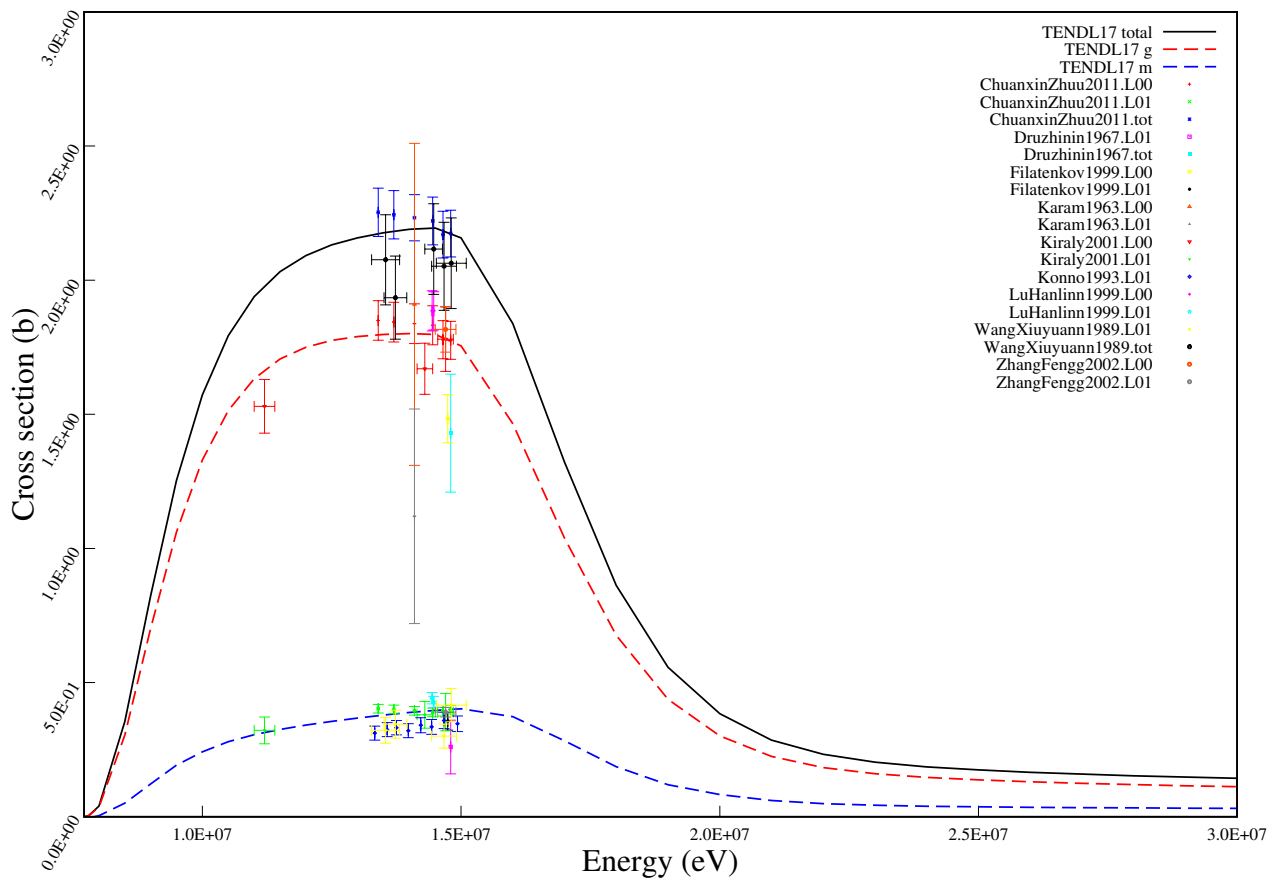
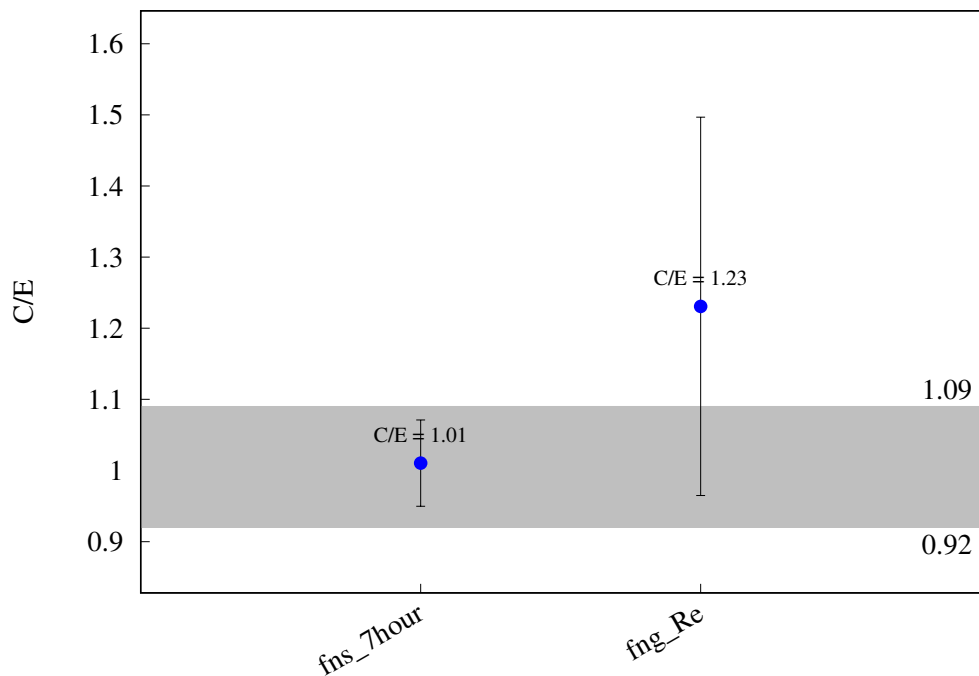
^{186}W (n,g) ^{187}W 

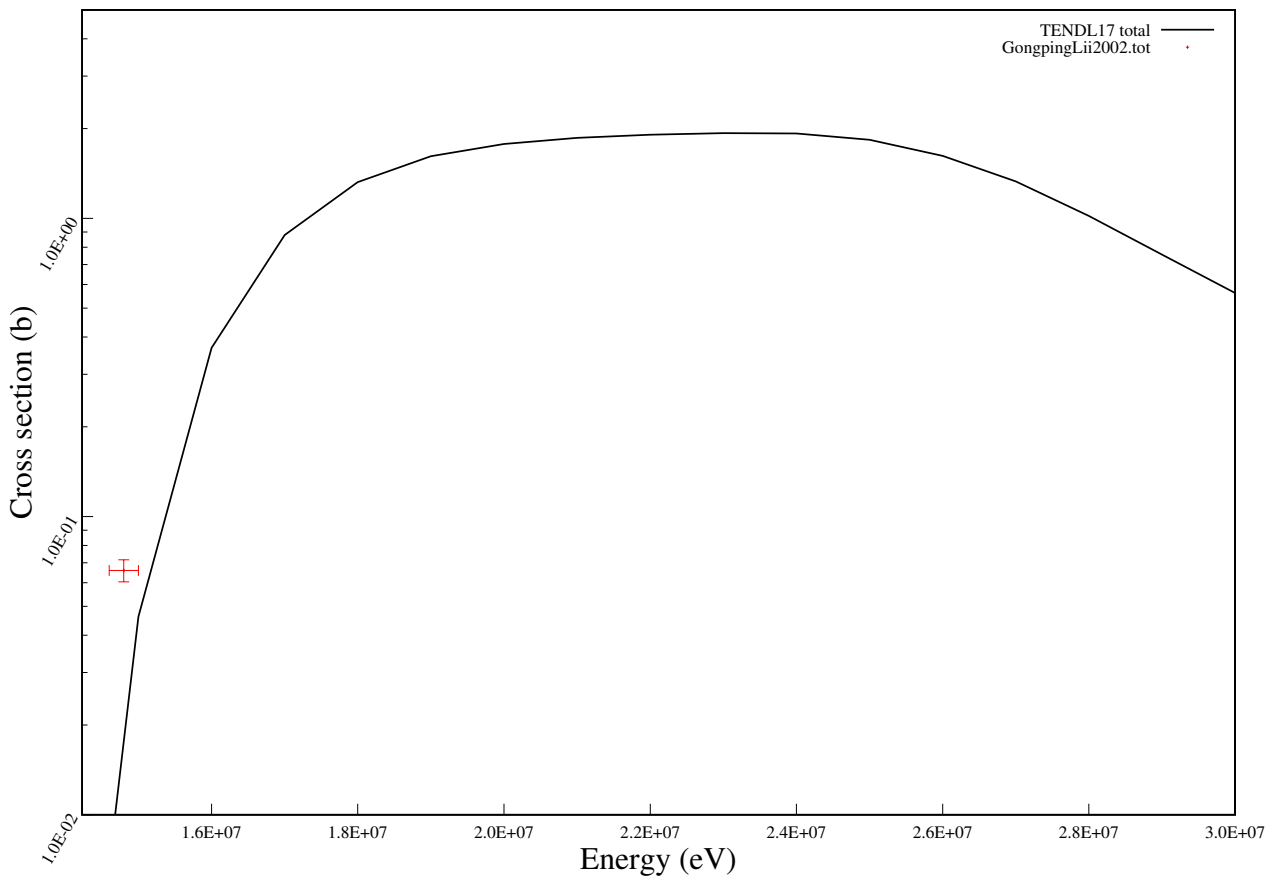
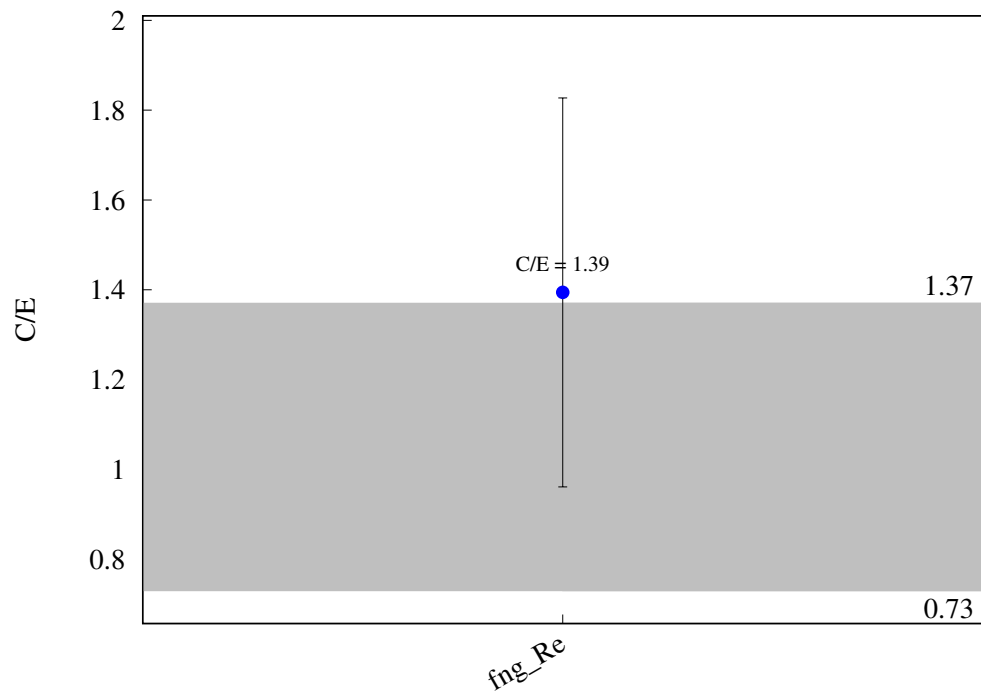
$^{186}\text{W} (\text{n},\text{p}) ^{186}\text{Ta}$ 

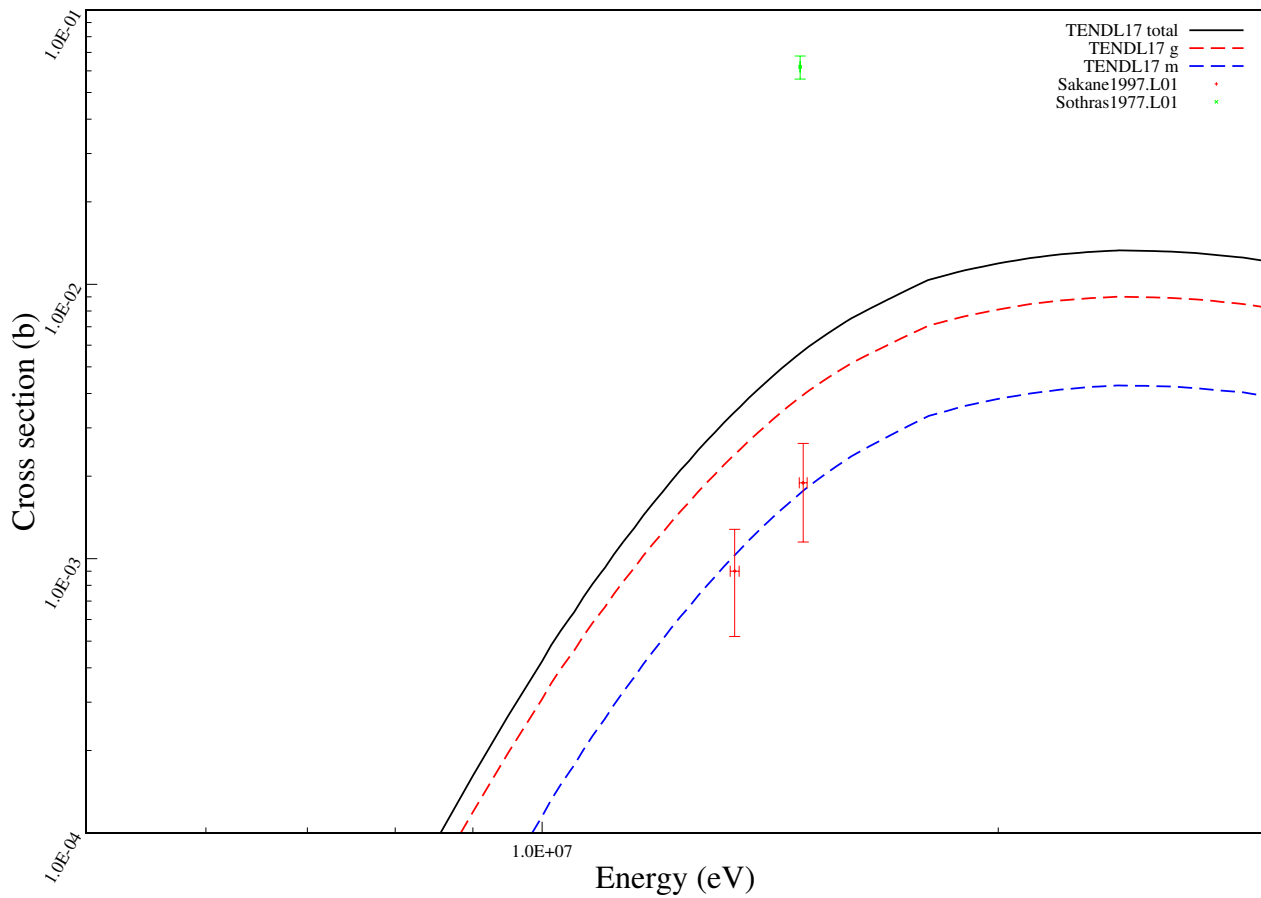
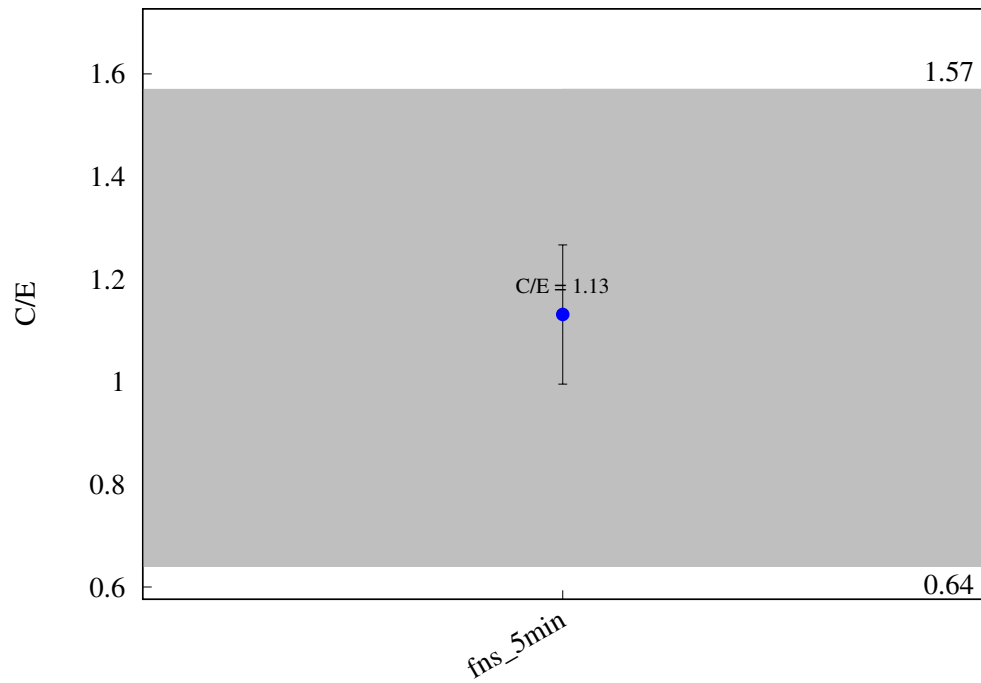
^{186}W (n,h) ^{184}Hf 

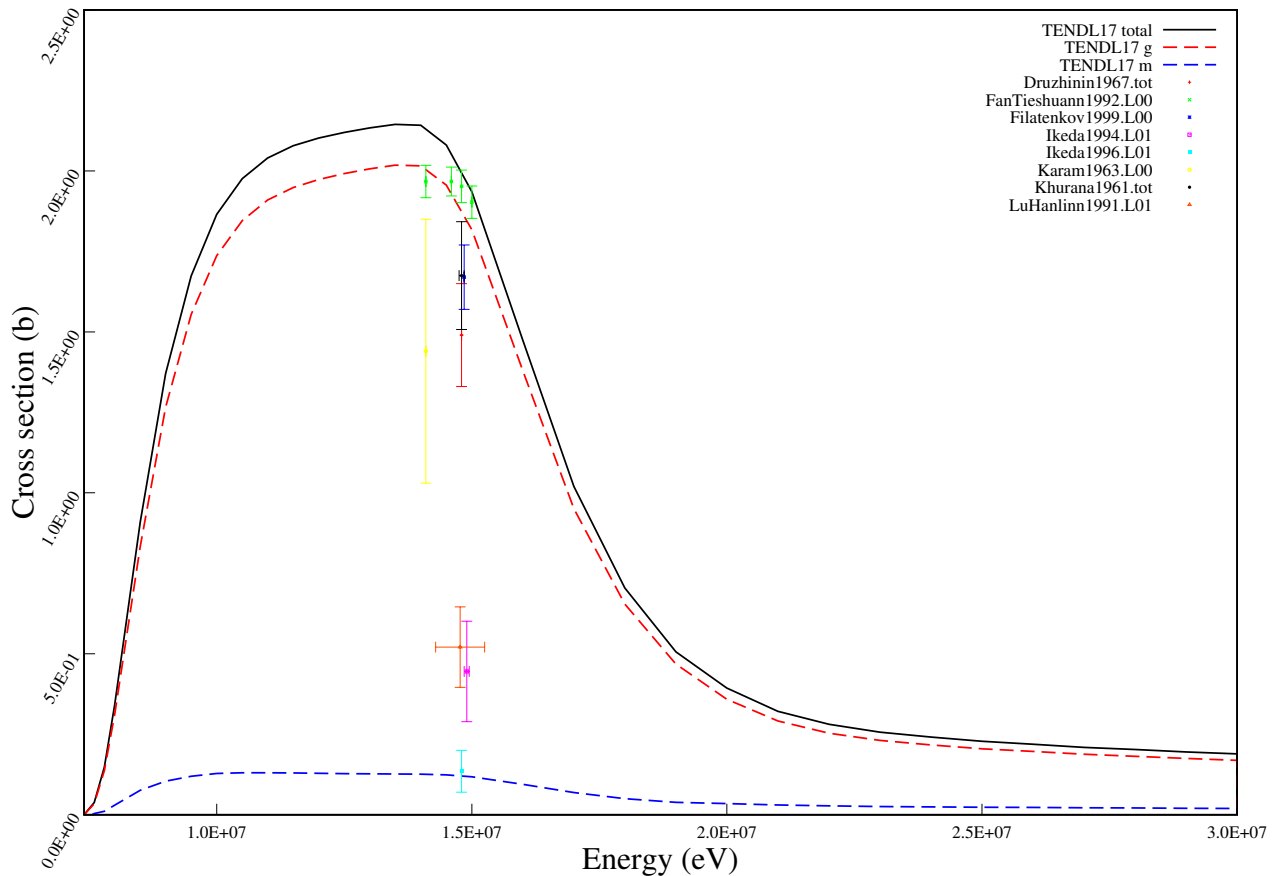
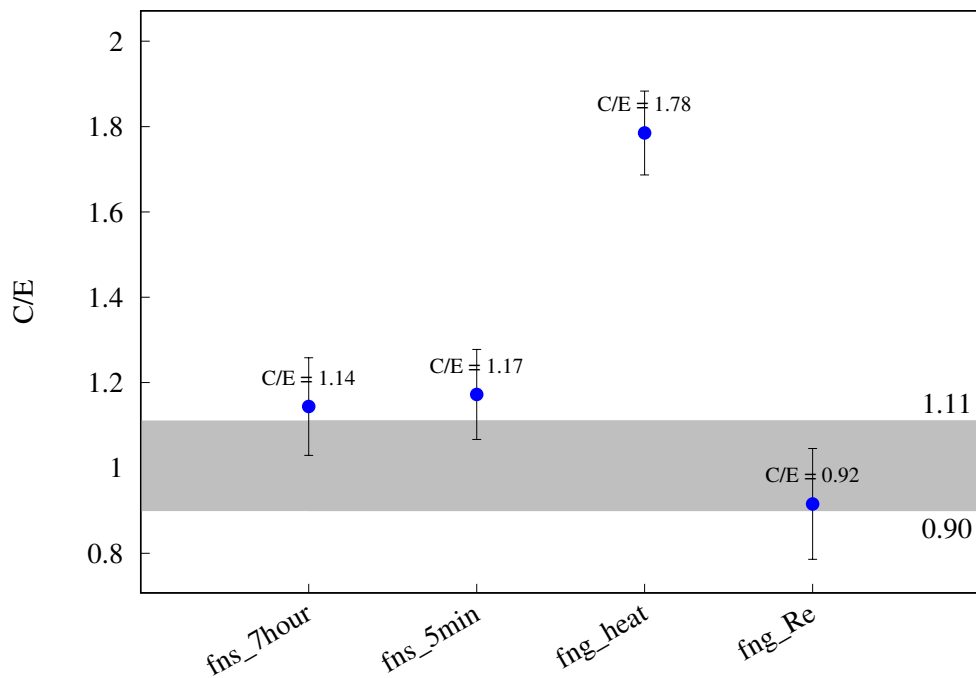
^{186}W (n,a) ^{183}Hf 

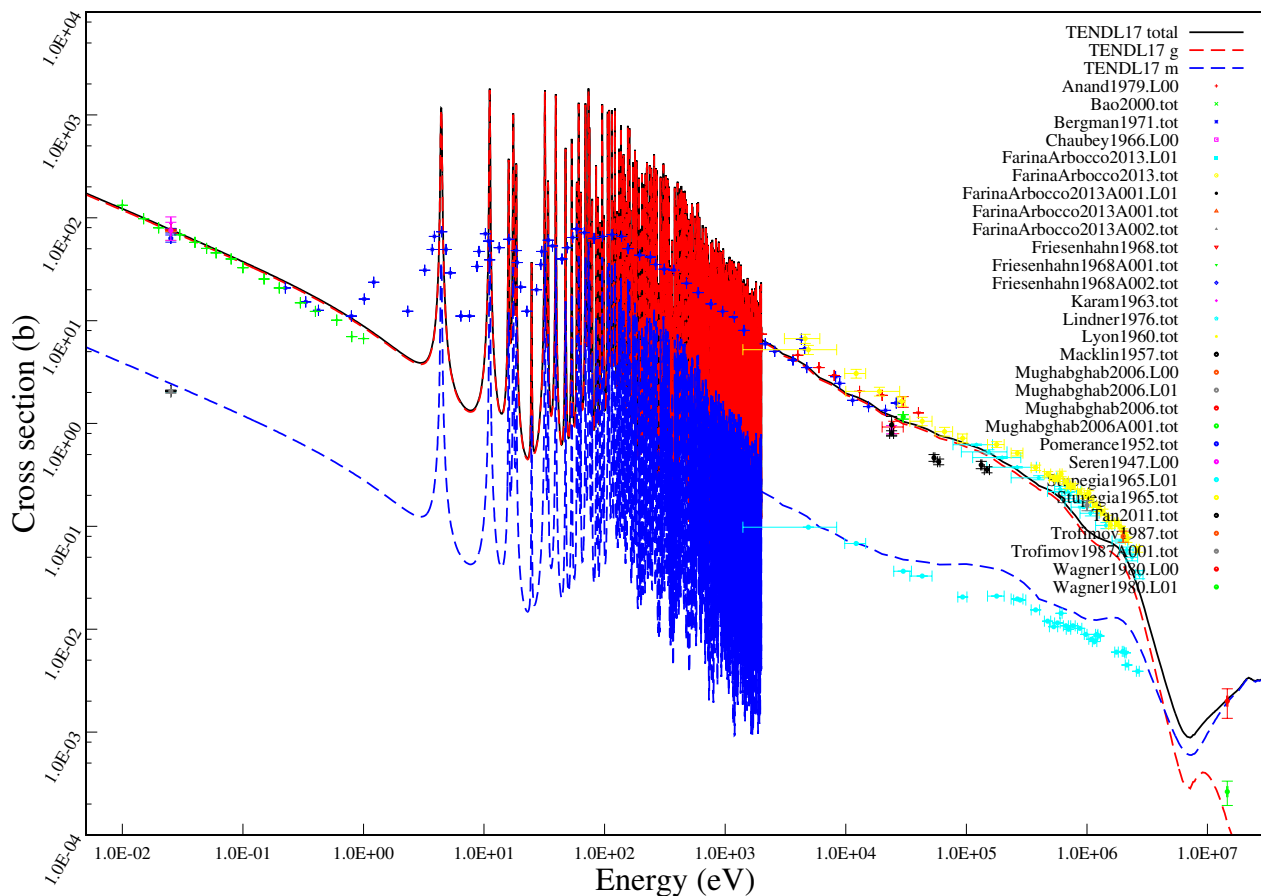
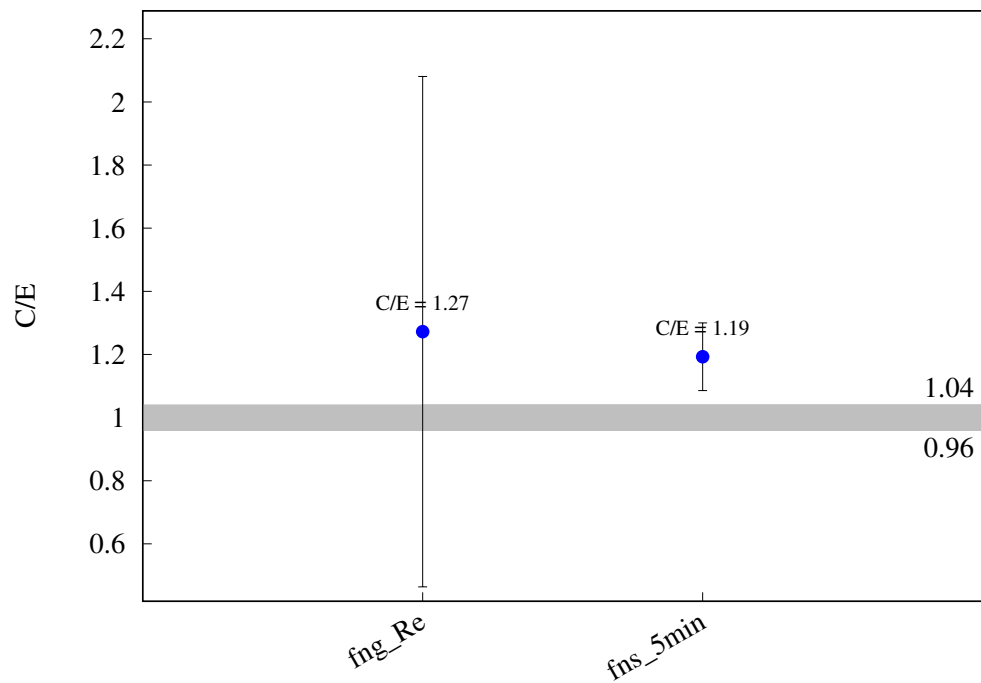
^{185}Re (n,2n) ^{184}gRe 

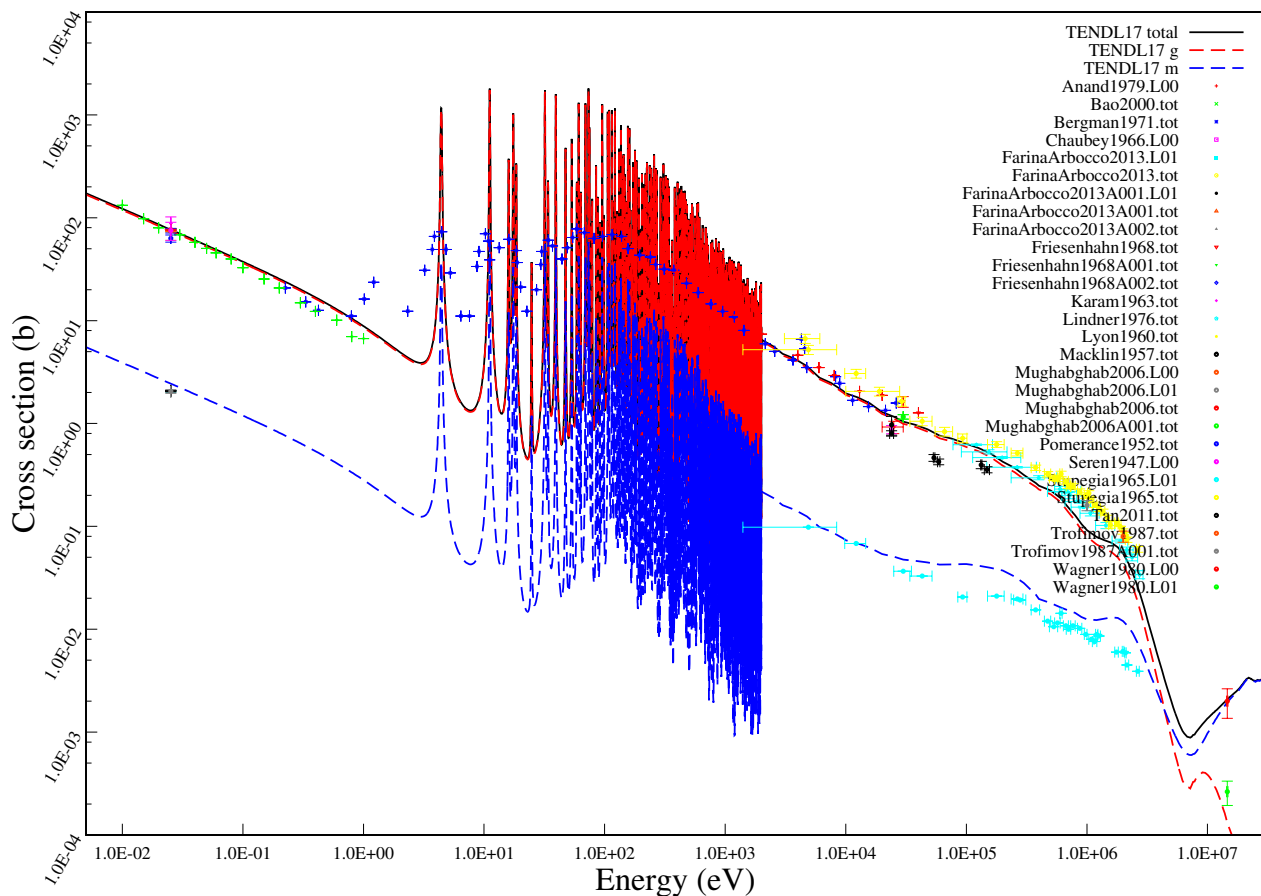
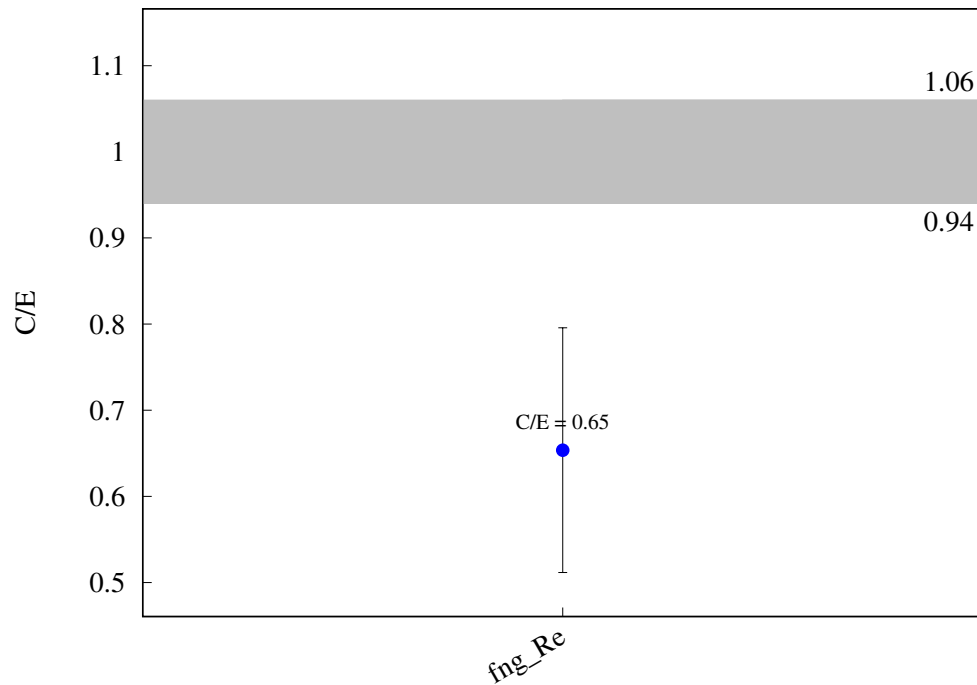
^{185}Re (n,2n) $^{184\text{m}}\text{Re}$ 

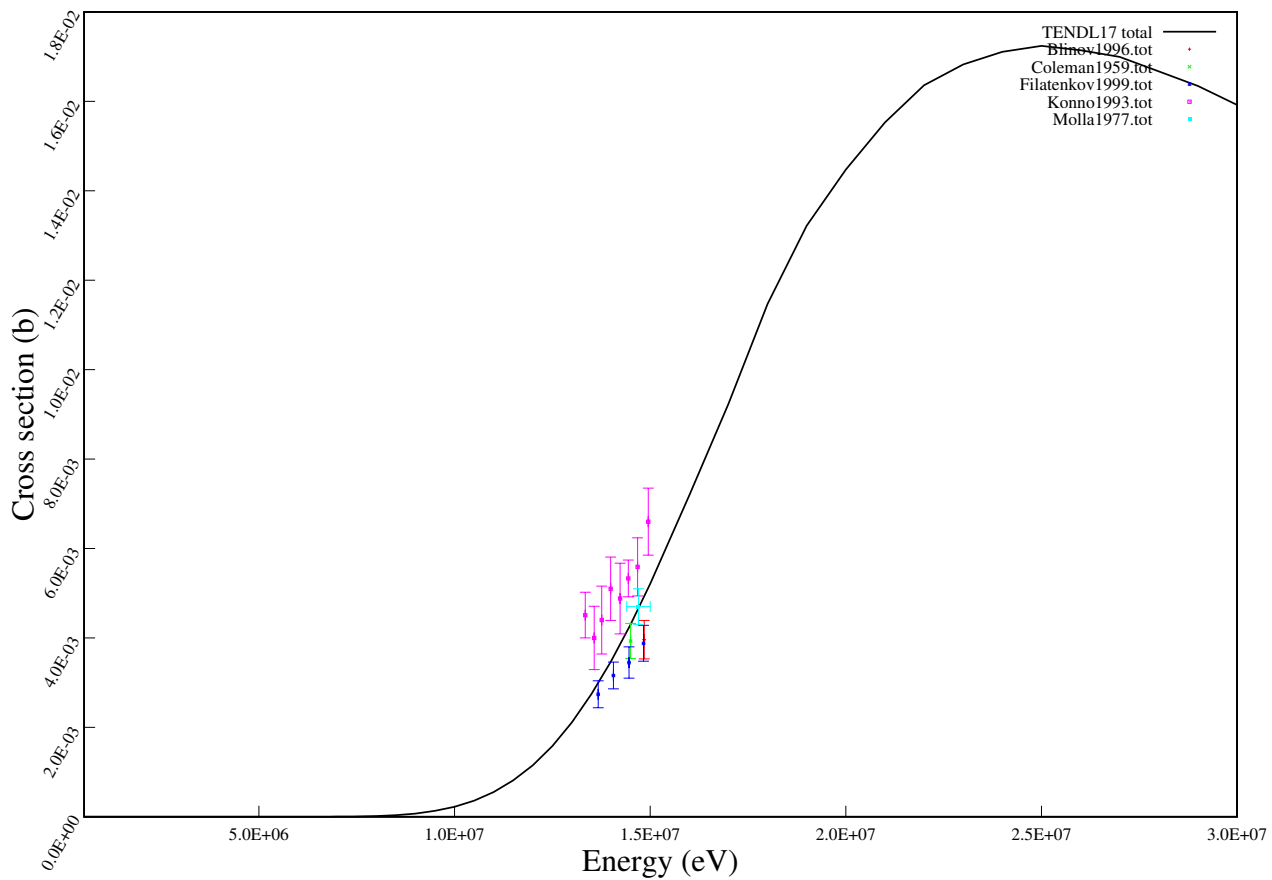
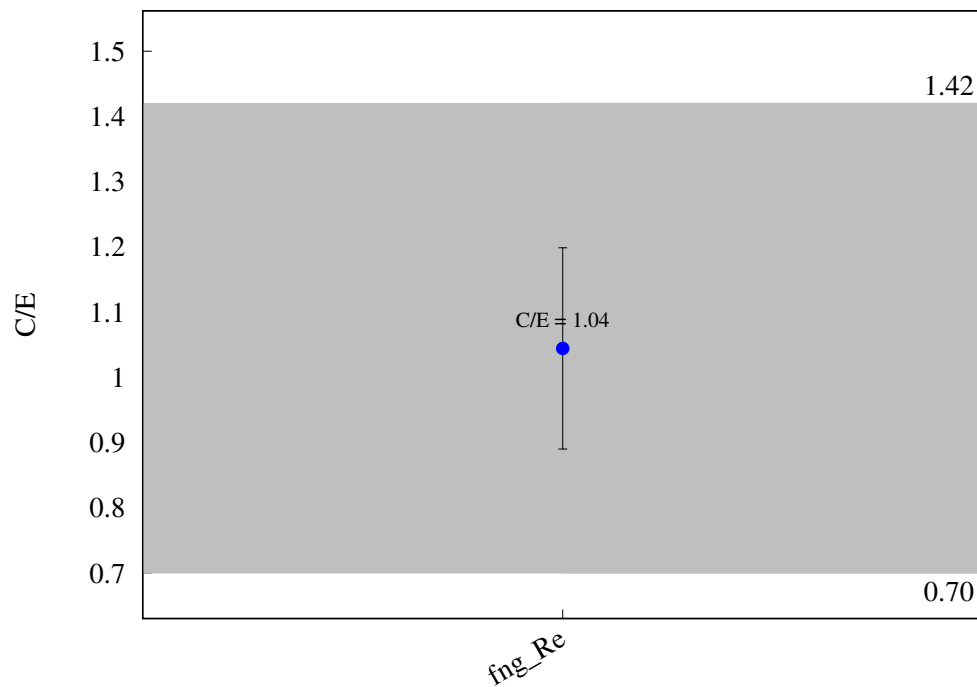
^{185}Re (n,3n) ^{183}Re 

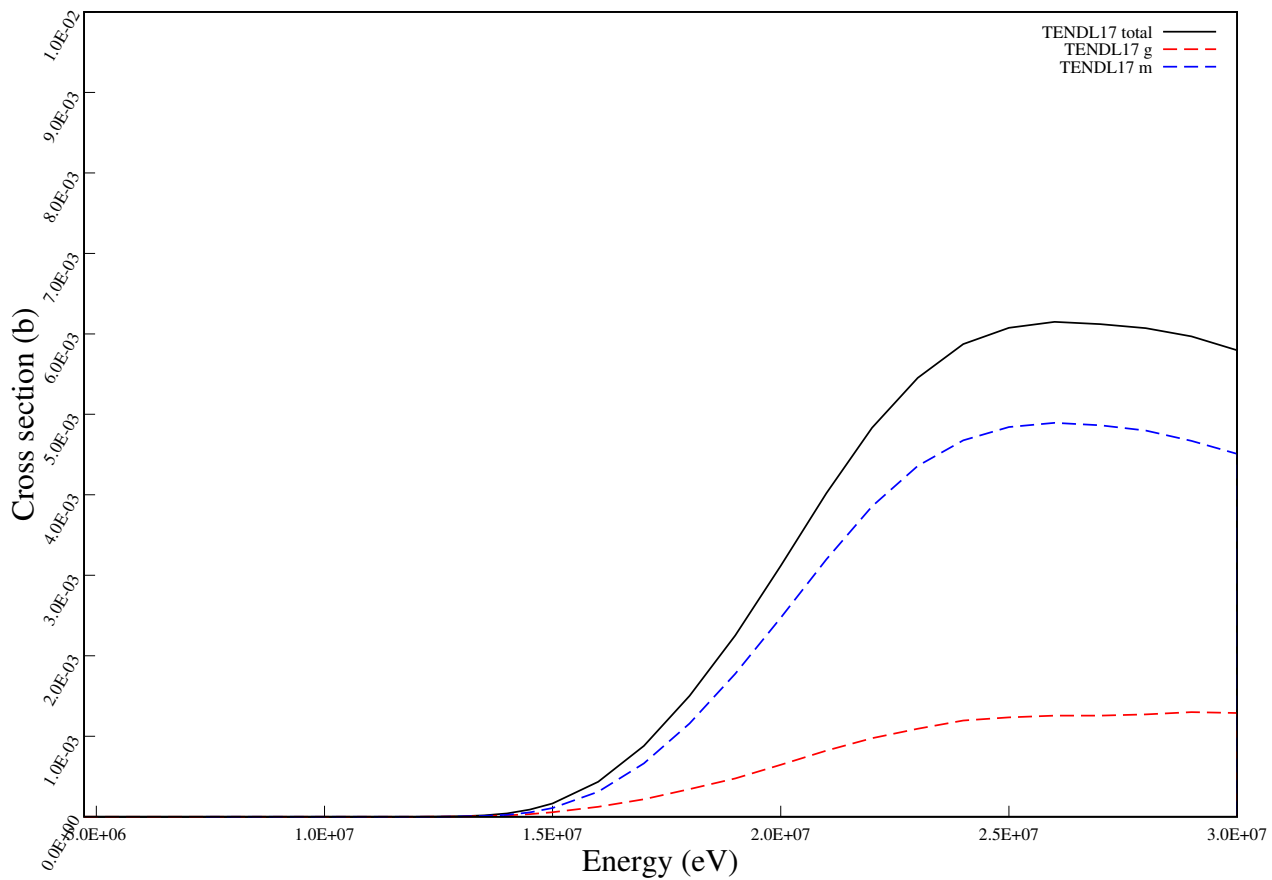
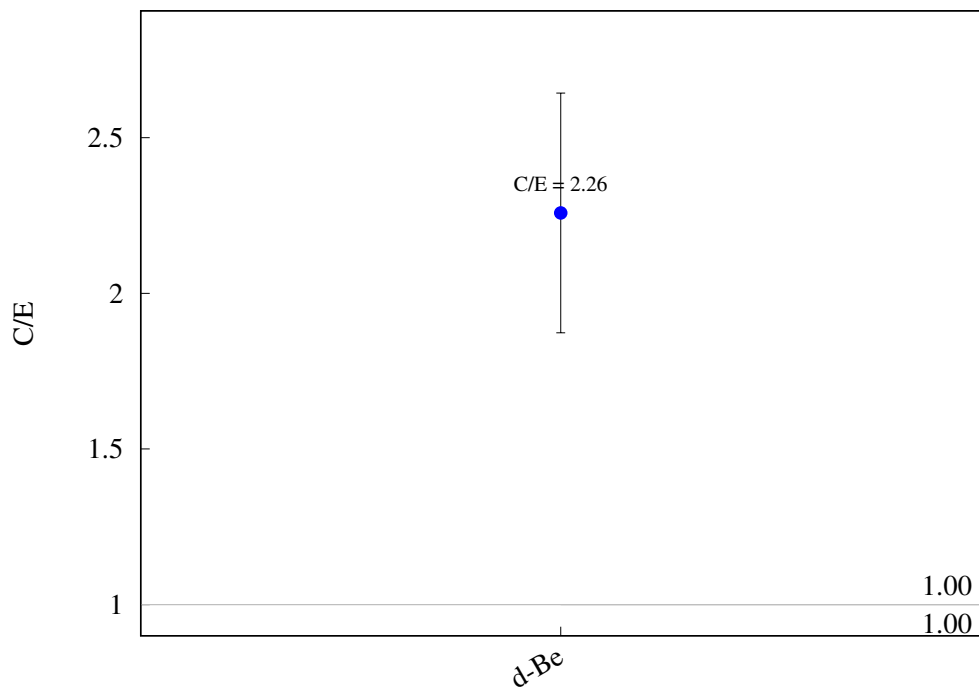
^{185}Re (n,p) $^{185\text{m}}\text{W}$ 

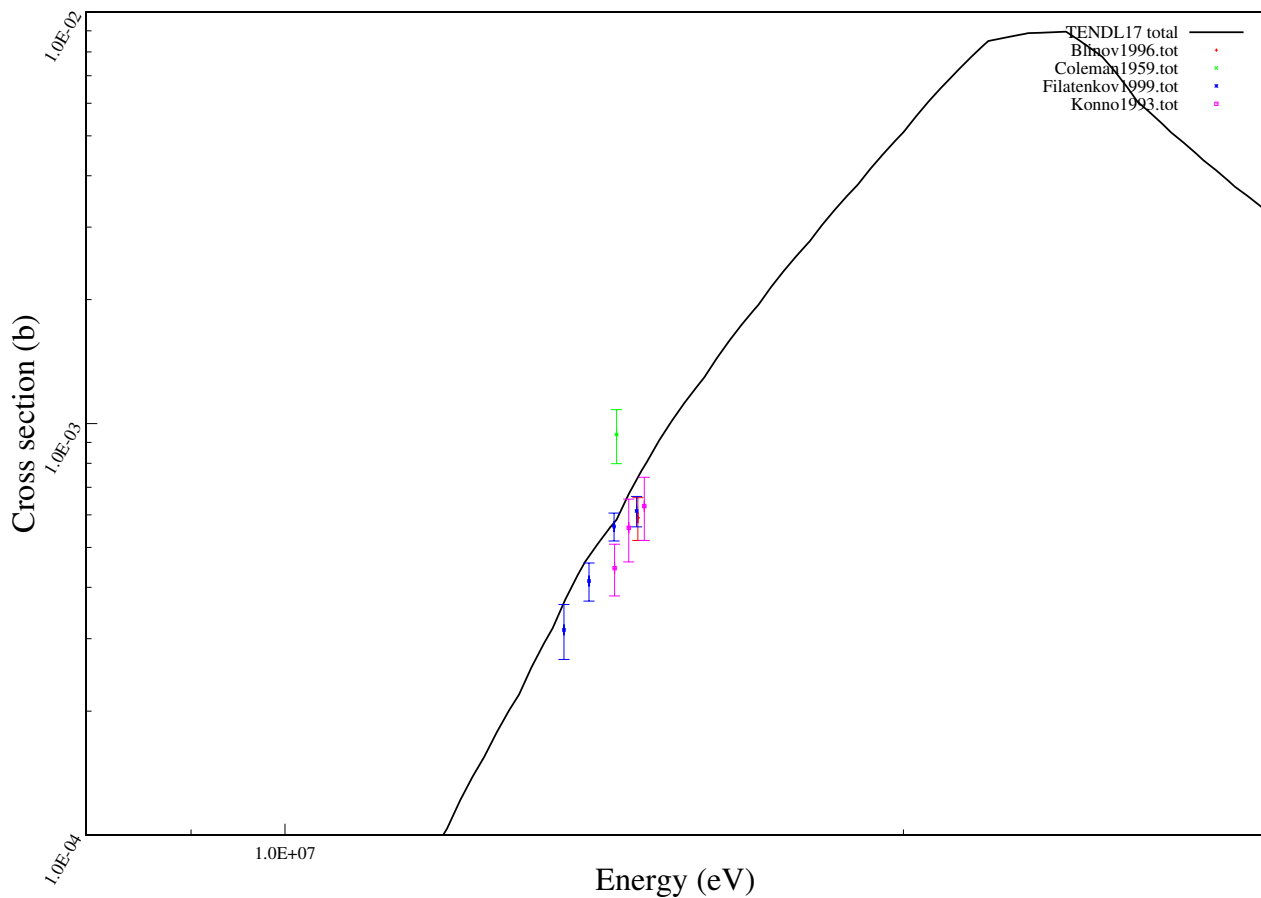
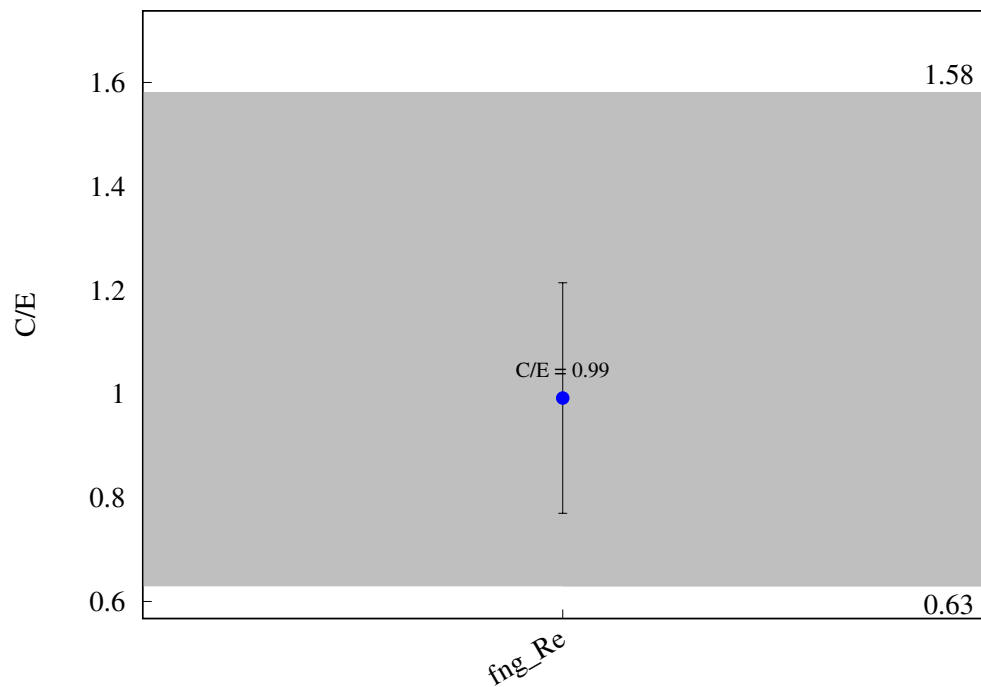
^{187}Re (n,2n) ^{186}gRe 

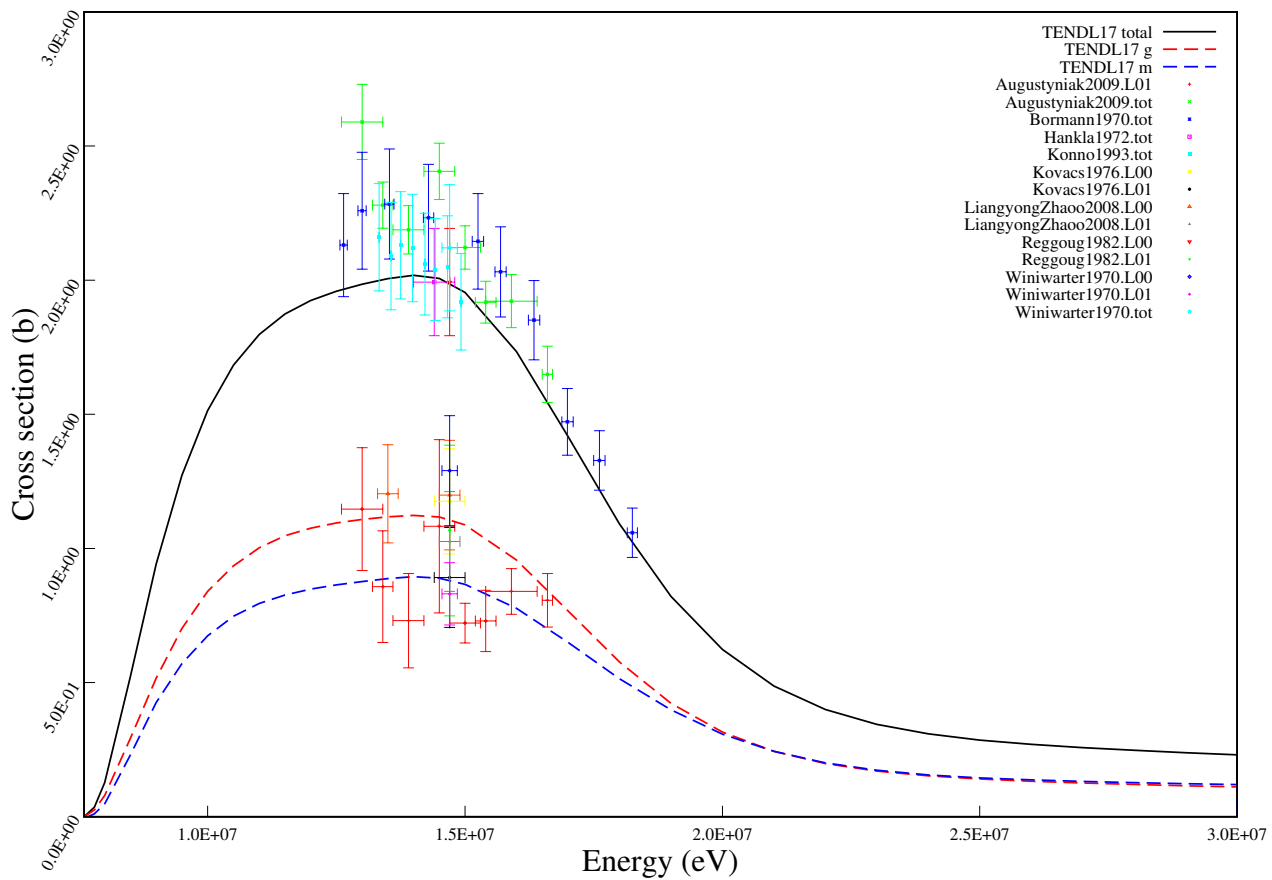
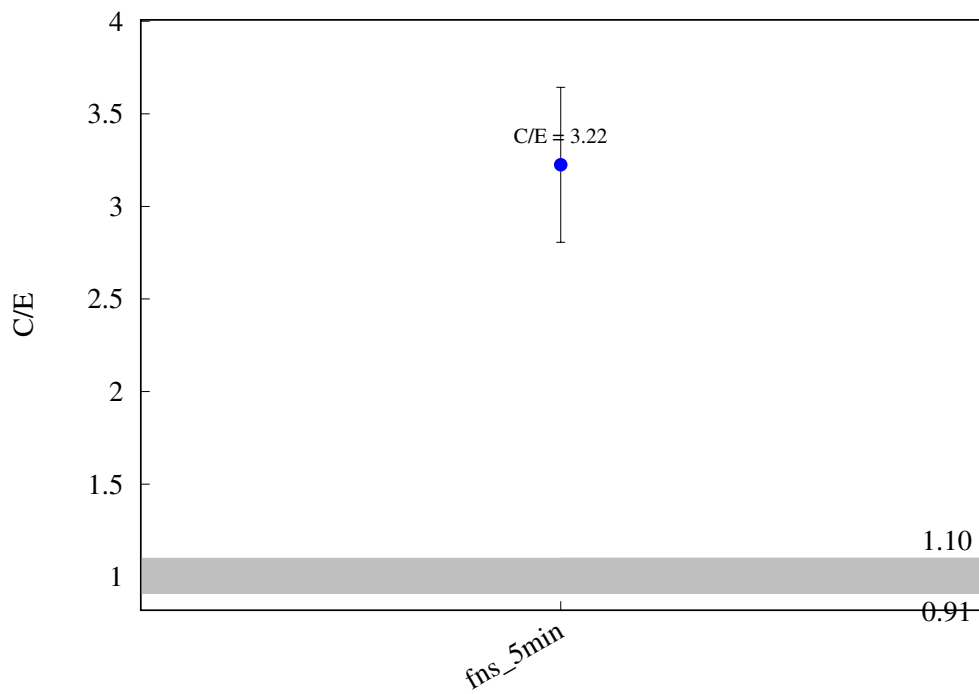
^{187}Re (n,g) $^{188\text{m}}\text{Re}$ 

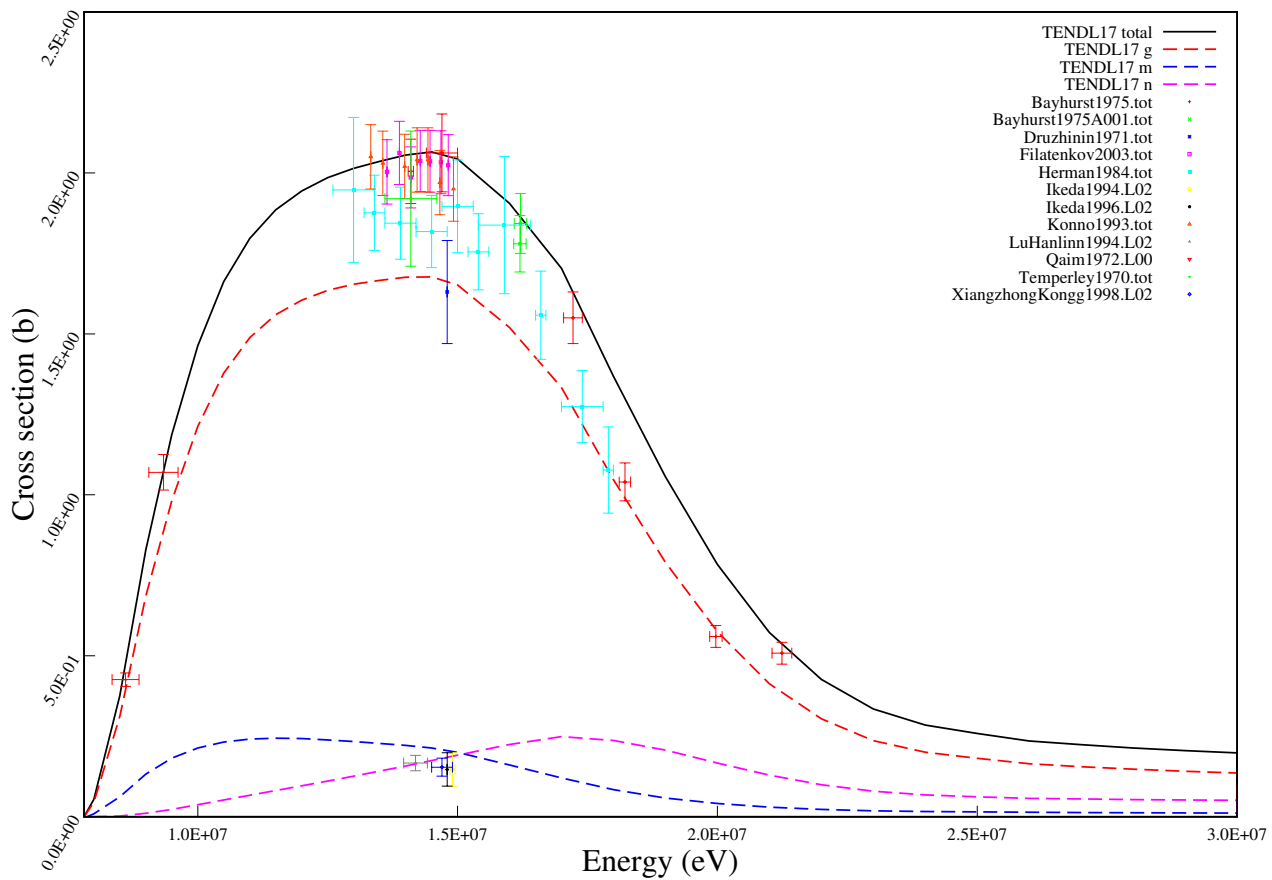
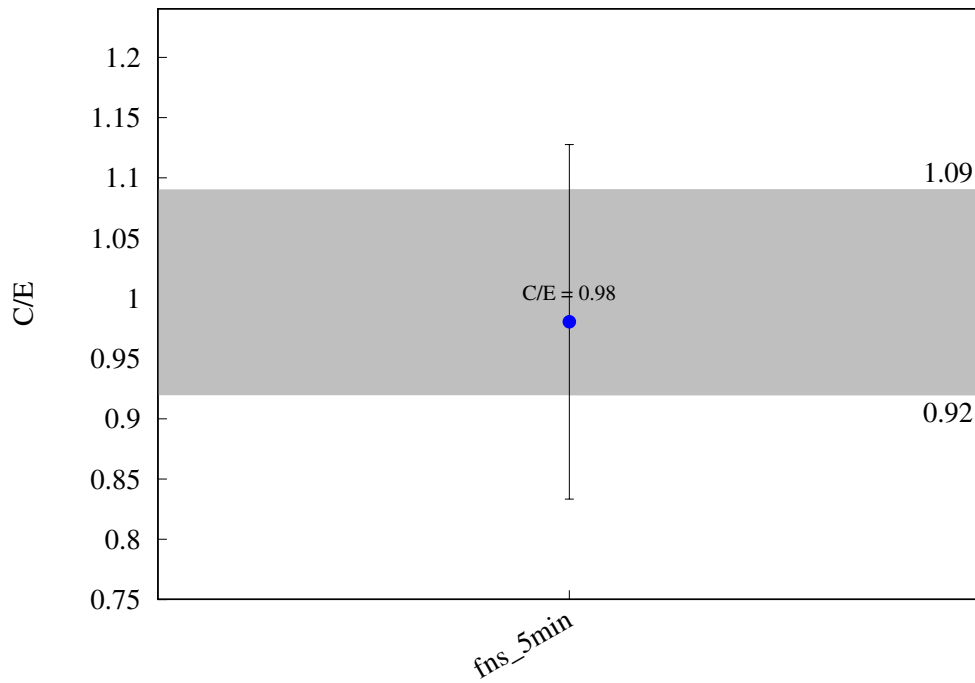
^{187}Re (n,g) ^{188}Re 

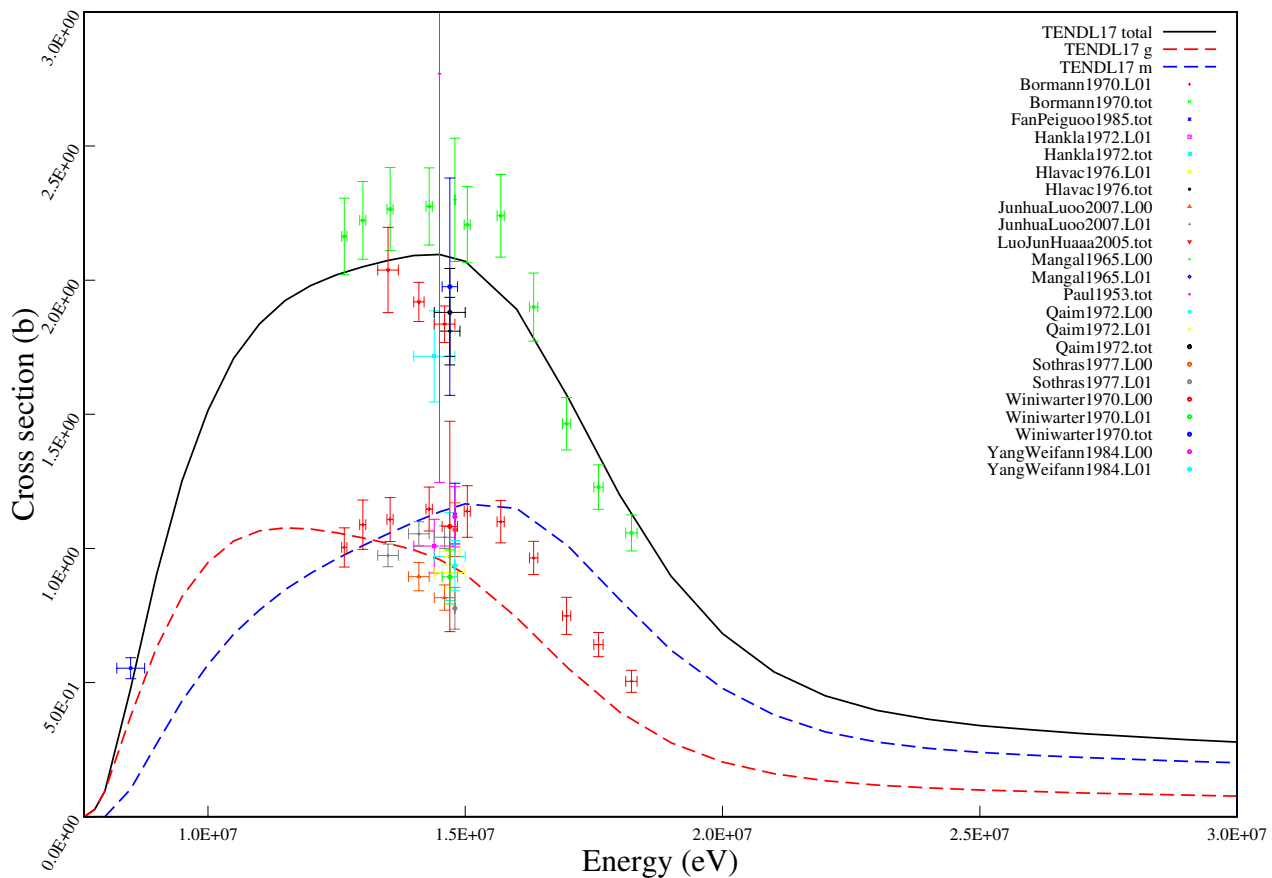
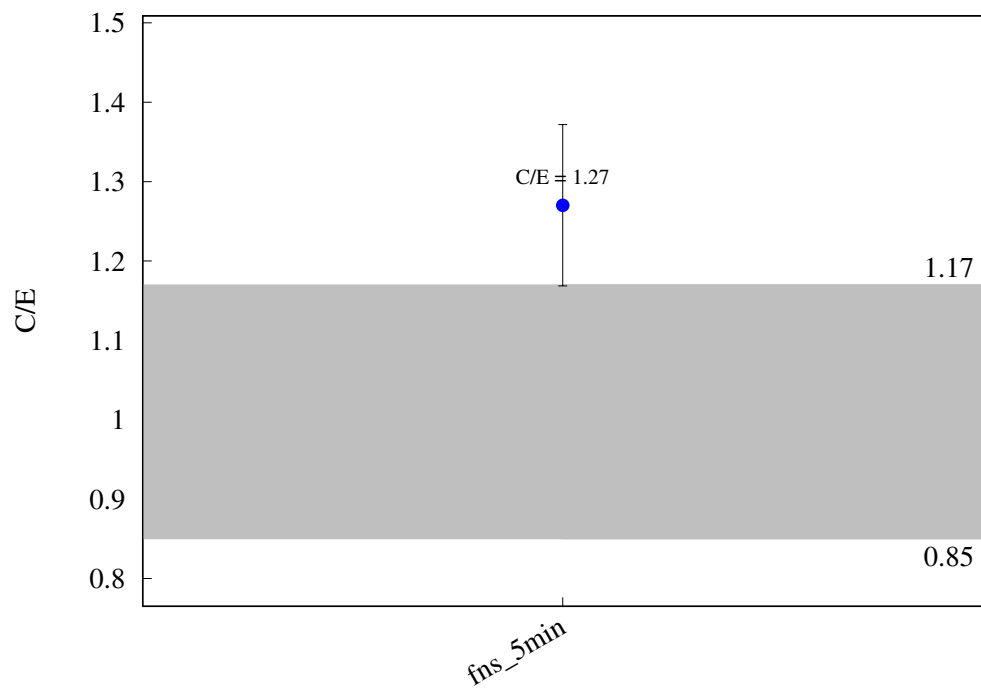
^{187}Re (n,p) ^{187}W 

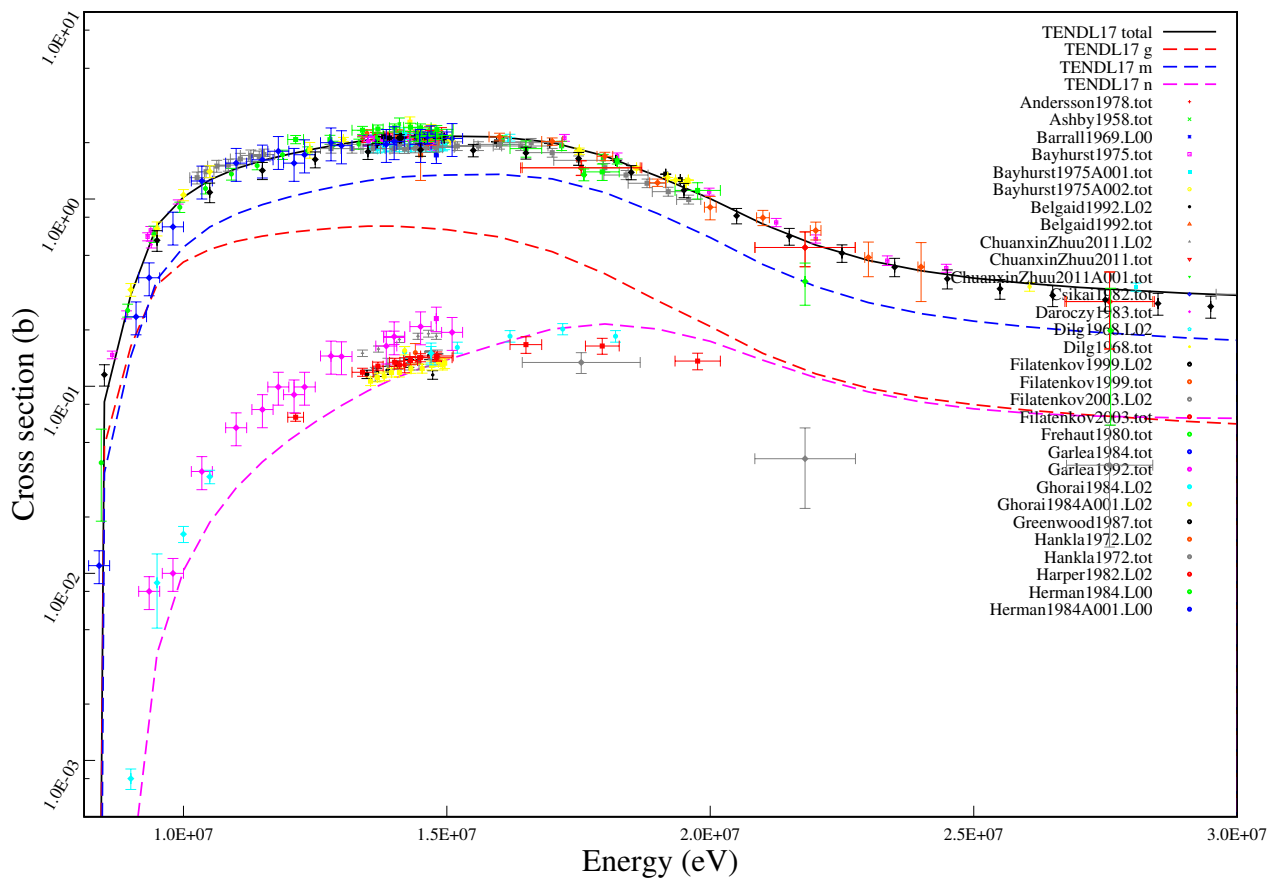
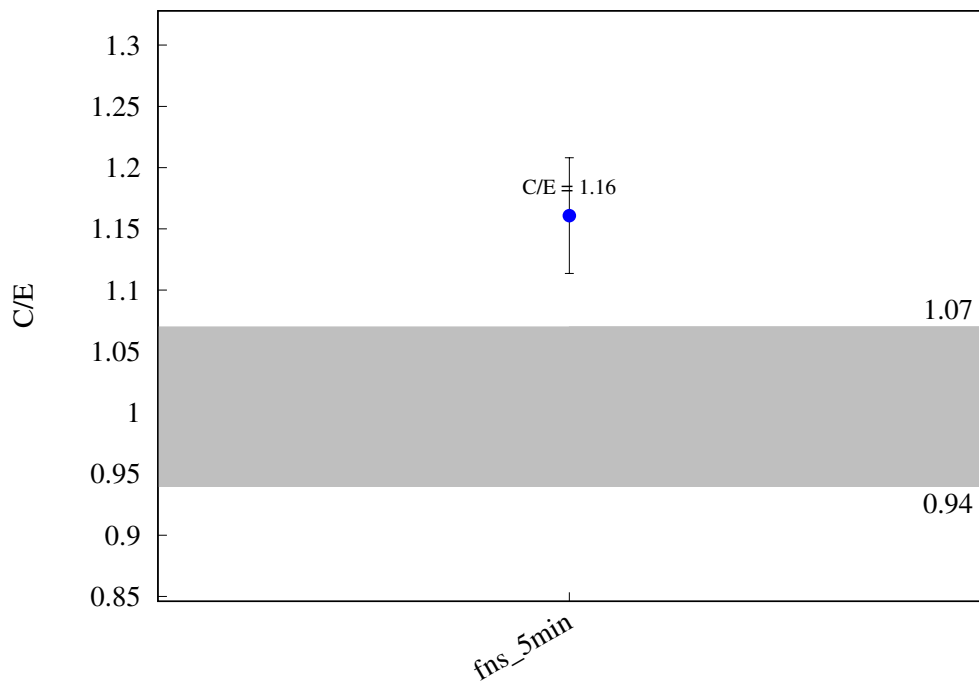
$^{187}\text{Re} (\text{n},\text{t}) ^{185}\text{W}$ 

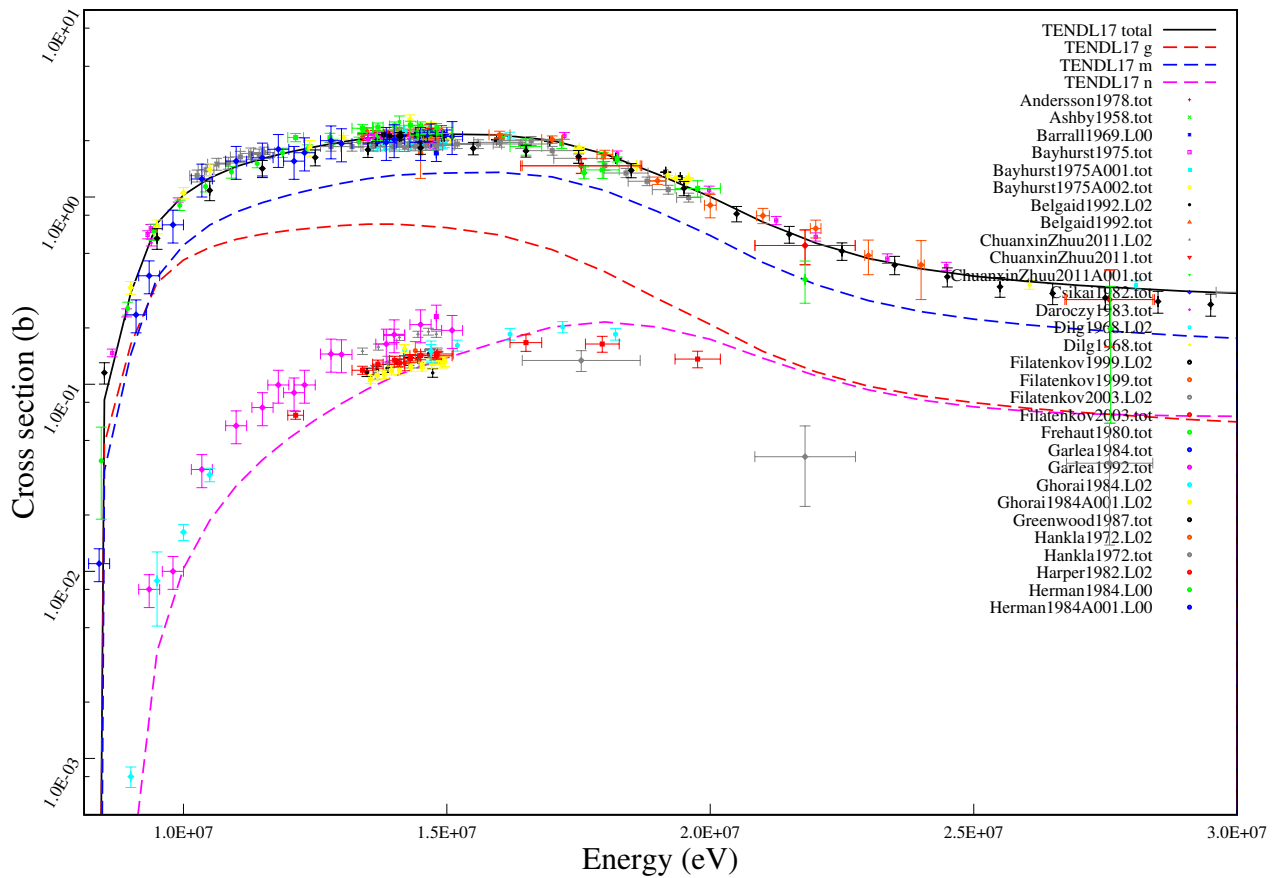
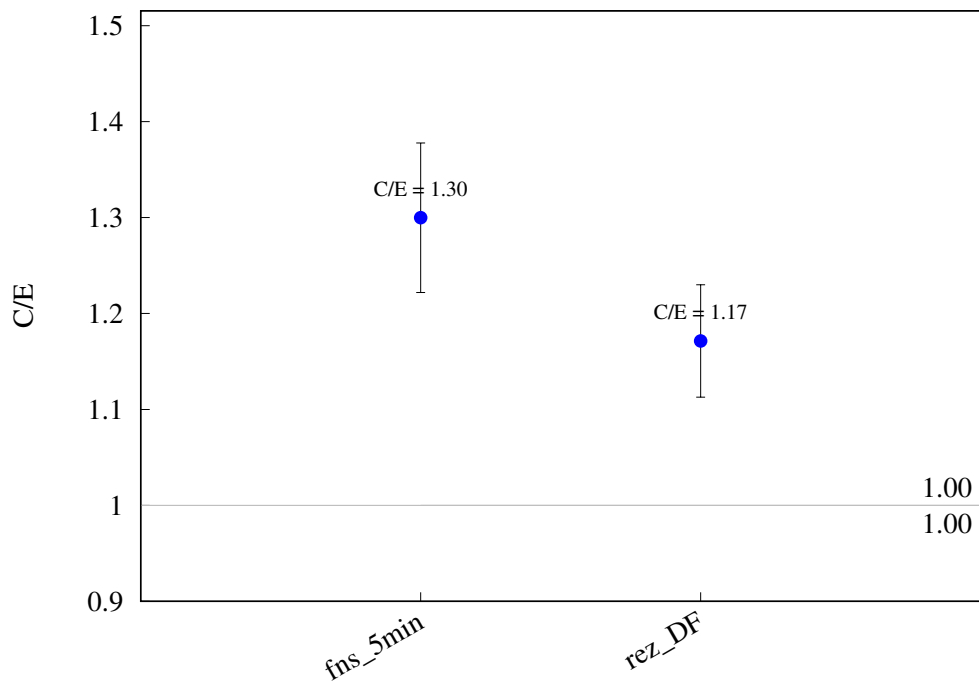
^{187}Re (n,a) ^{184}Ta 

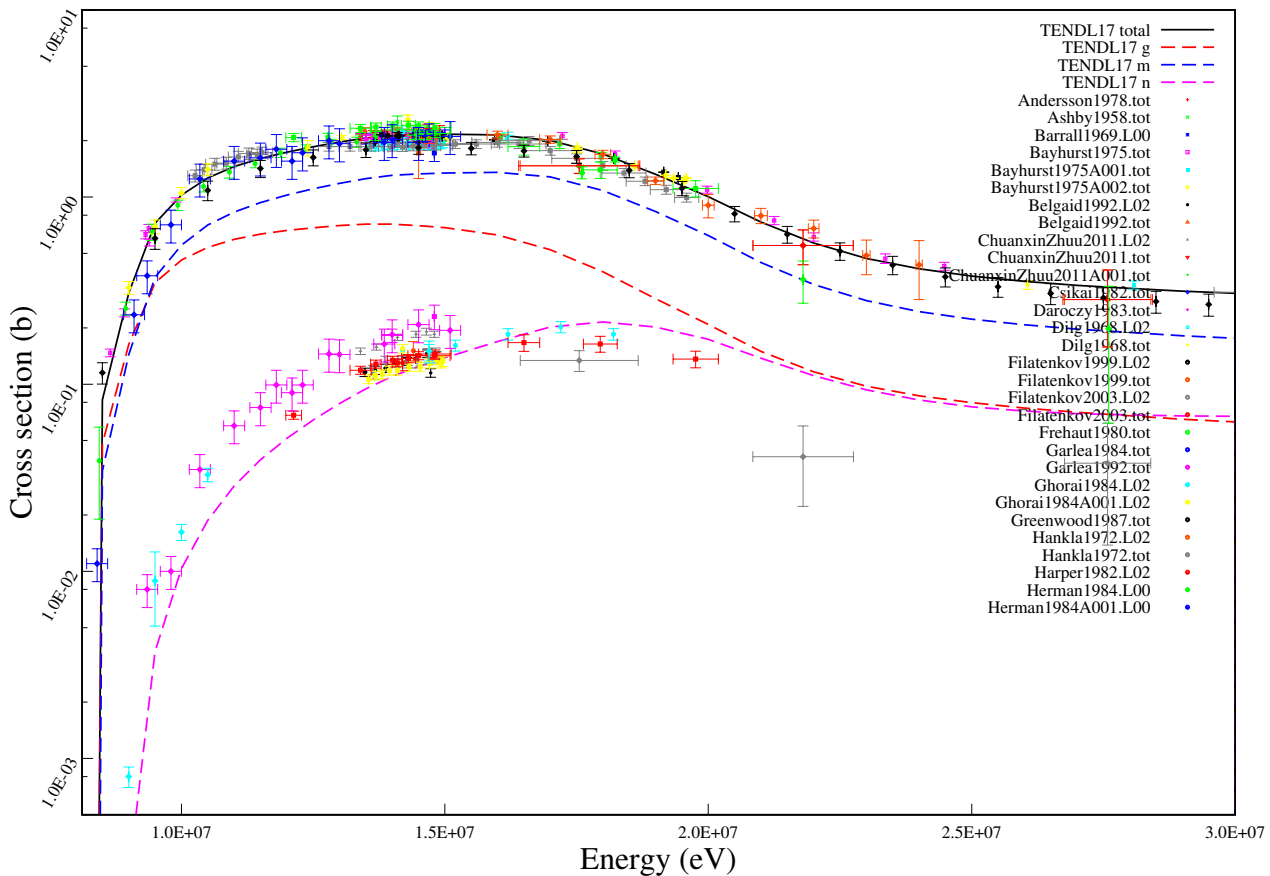
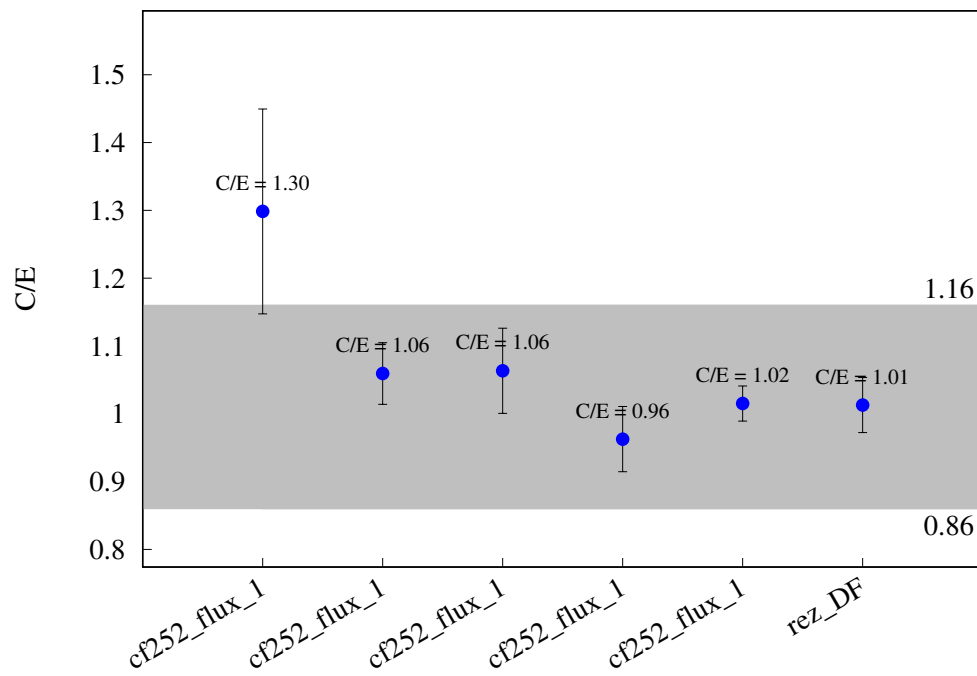
^{192}Os (n,2n) $^{191\text{m}}\text{Os}$ 

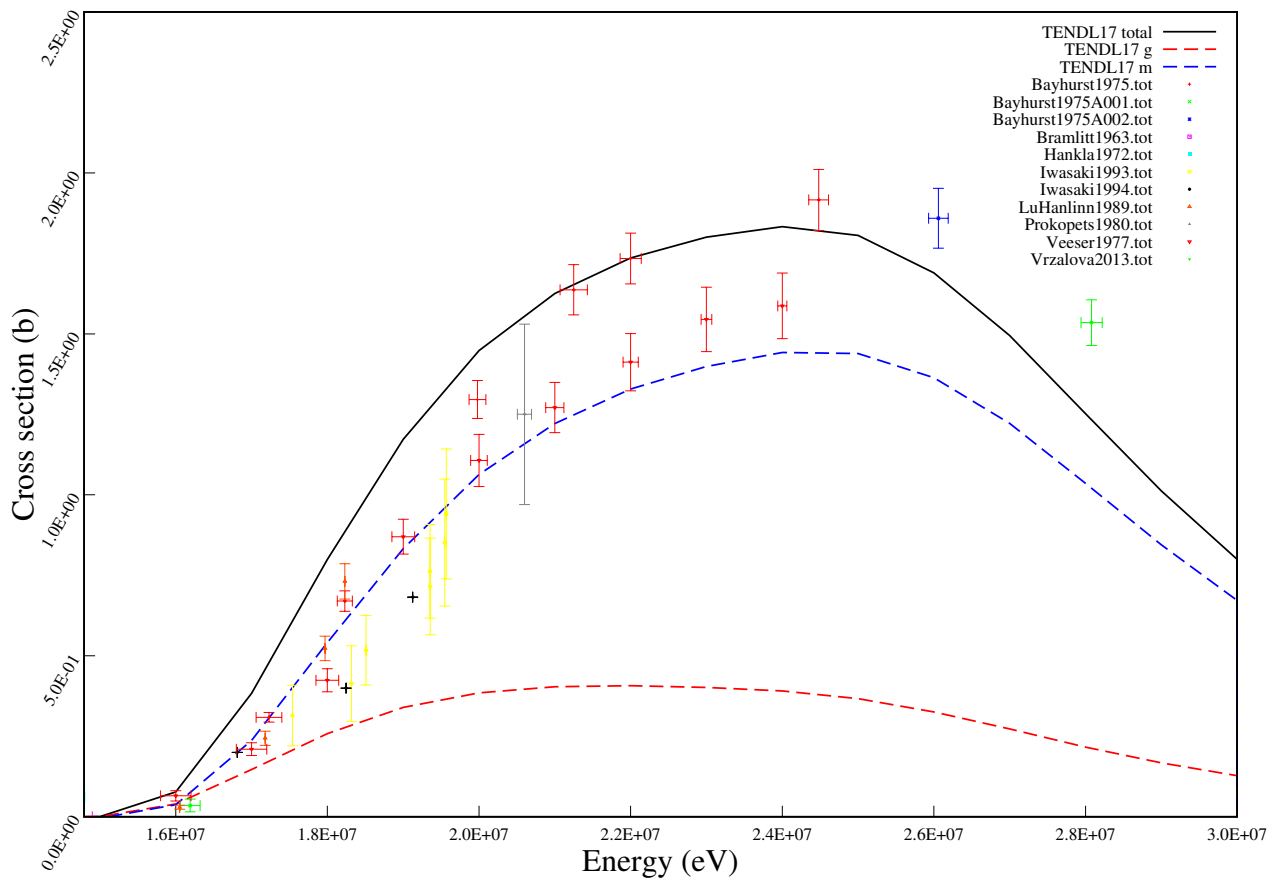
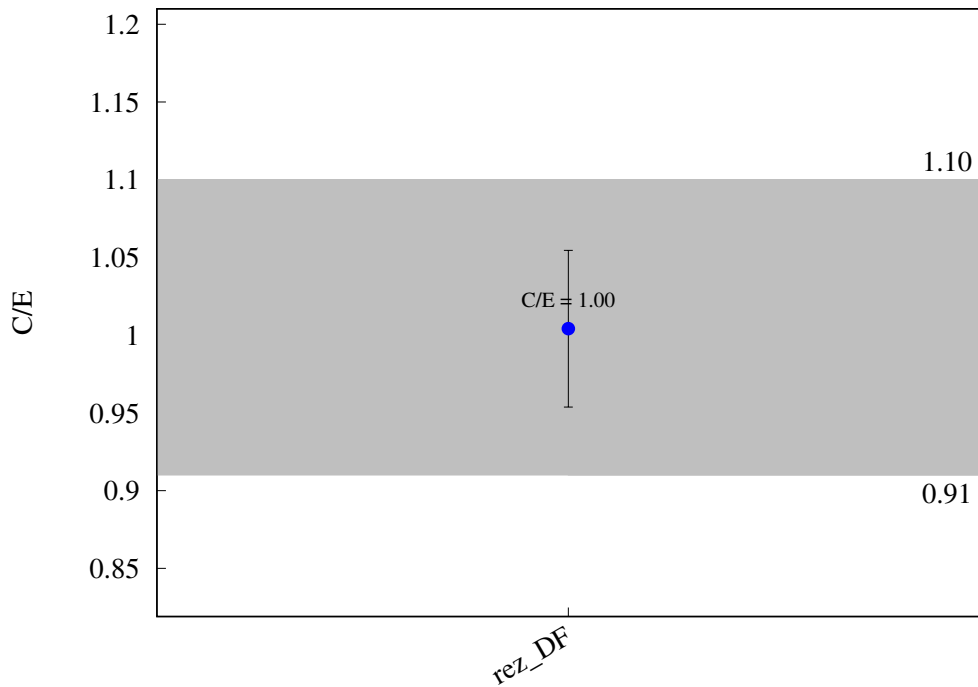
^{193}Ir (n,2n) $^{192\text{m}}\text{Ir}$ 

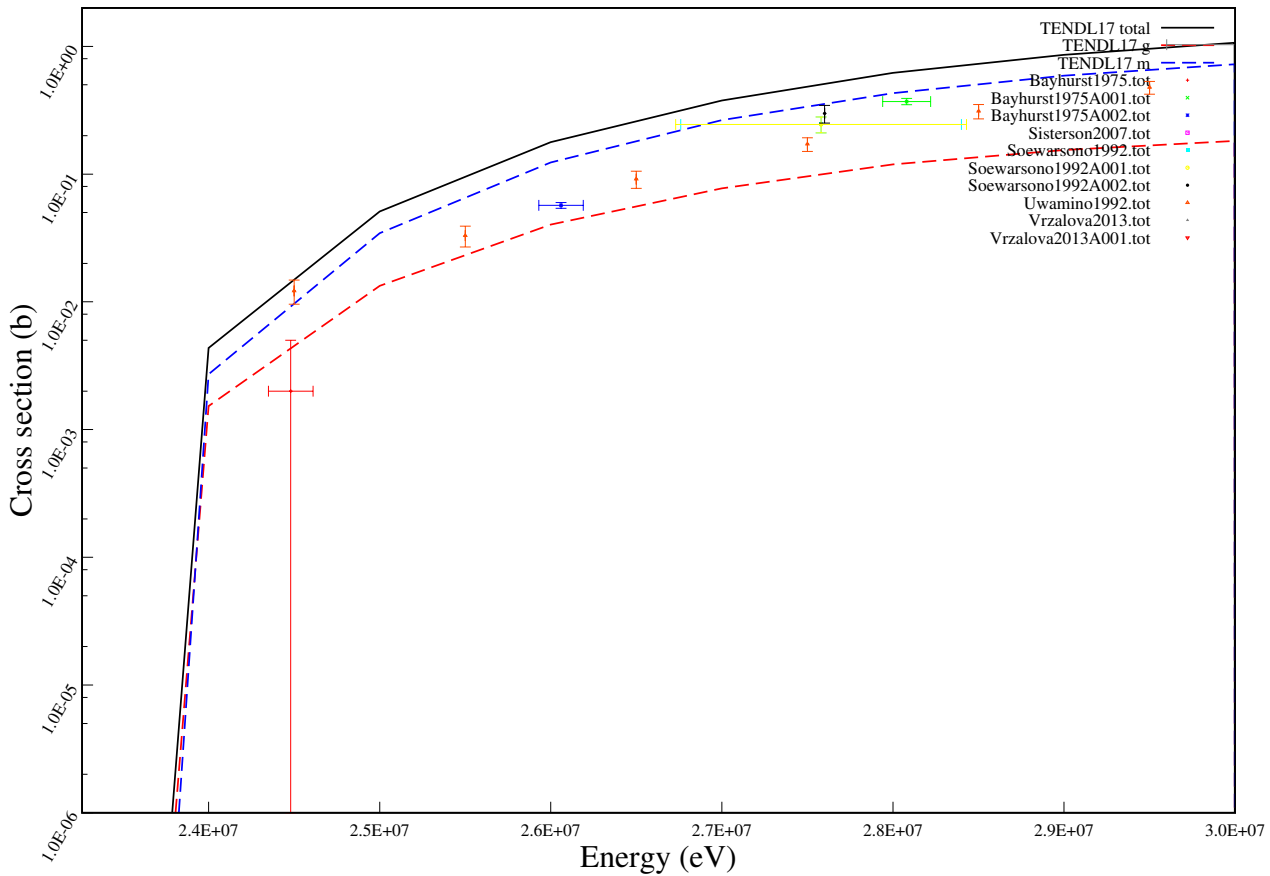
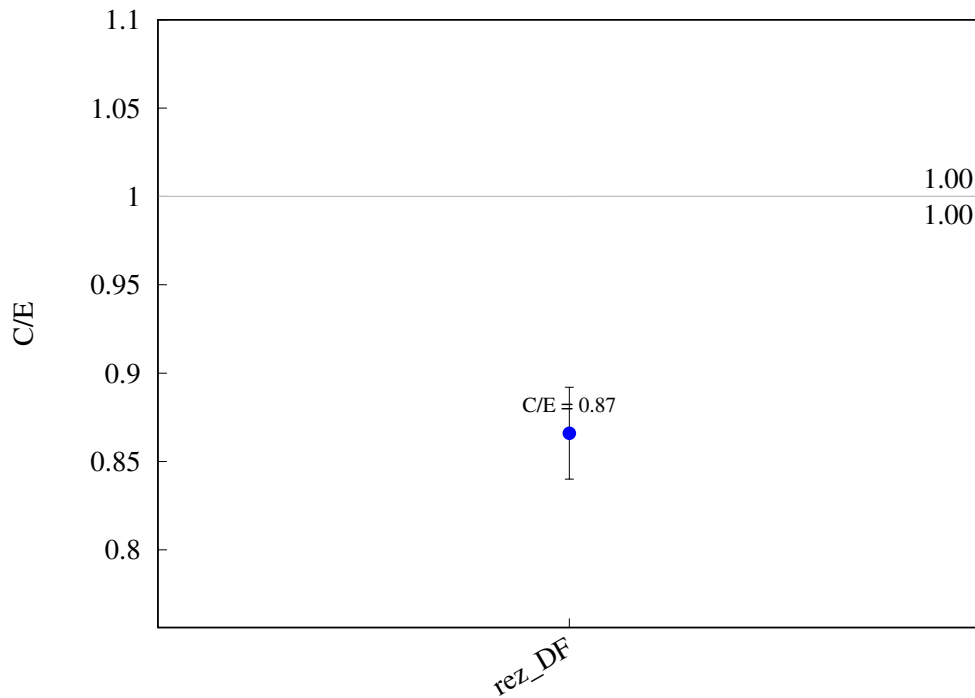
^{198}Pt (n,2n) $^{197\text{m}}\text{Pt}$ 

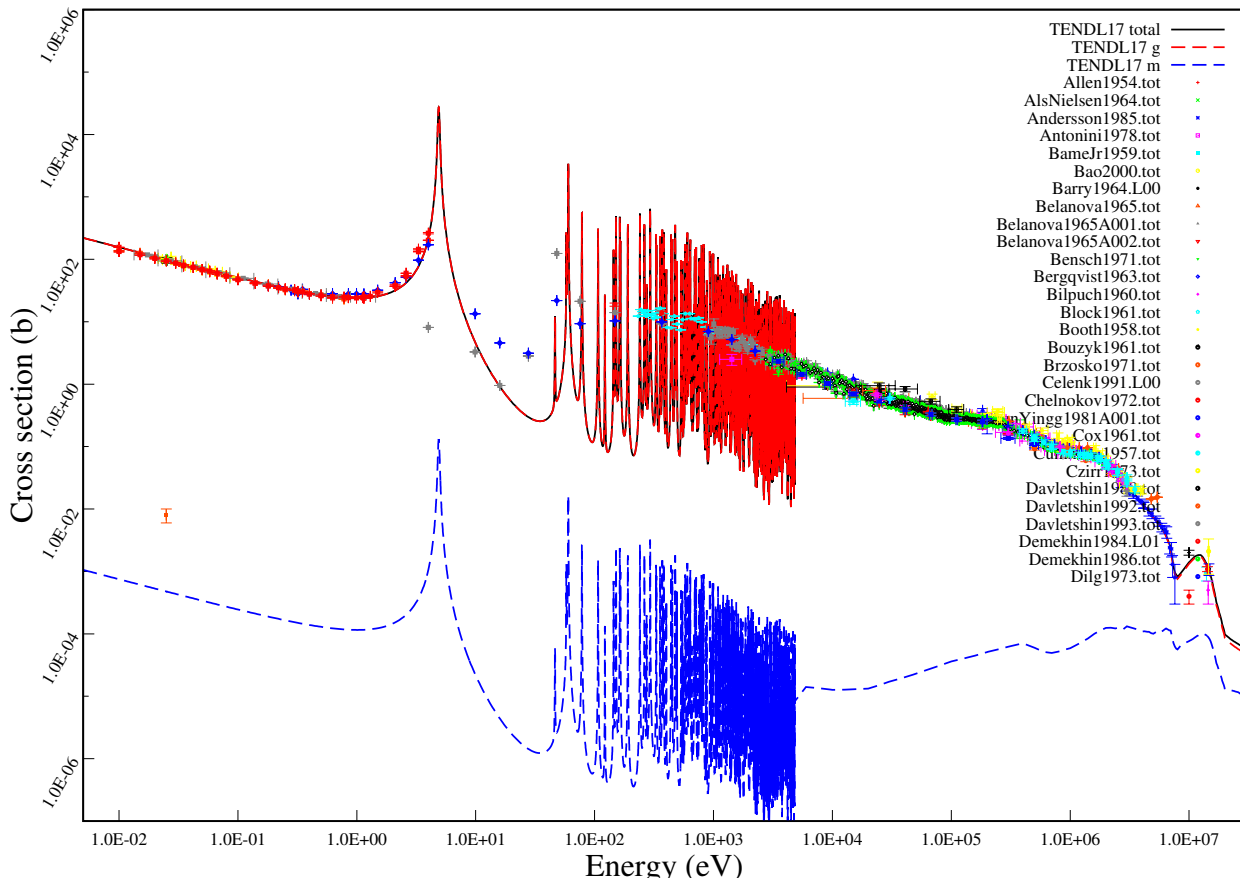
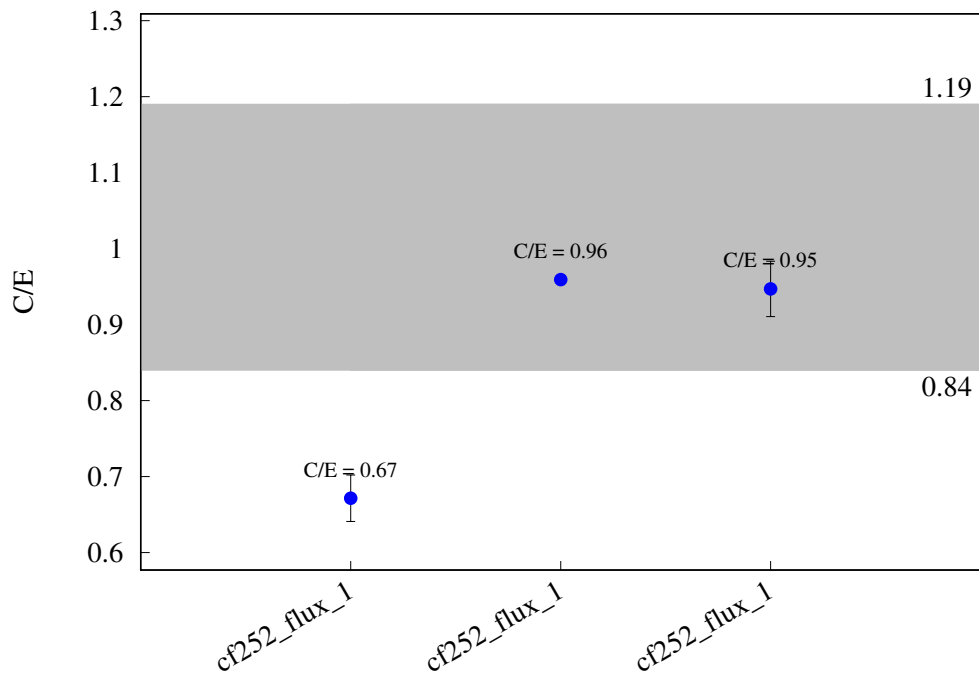
^{197}Au (n,2n) $^{196\text{m}}\text{Au}$ 

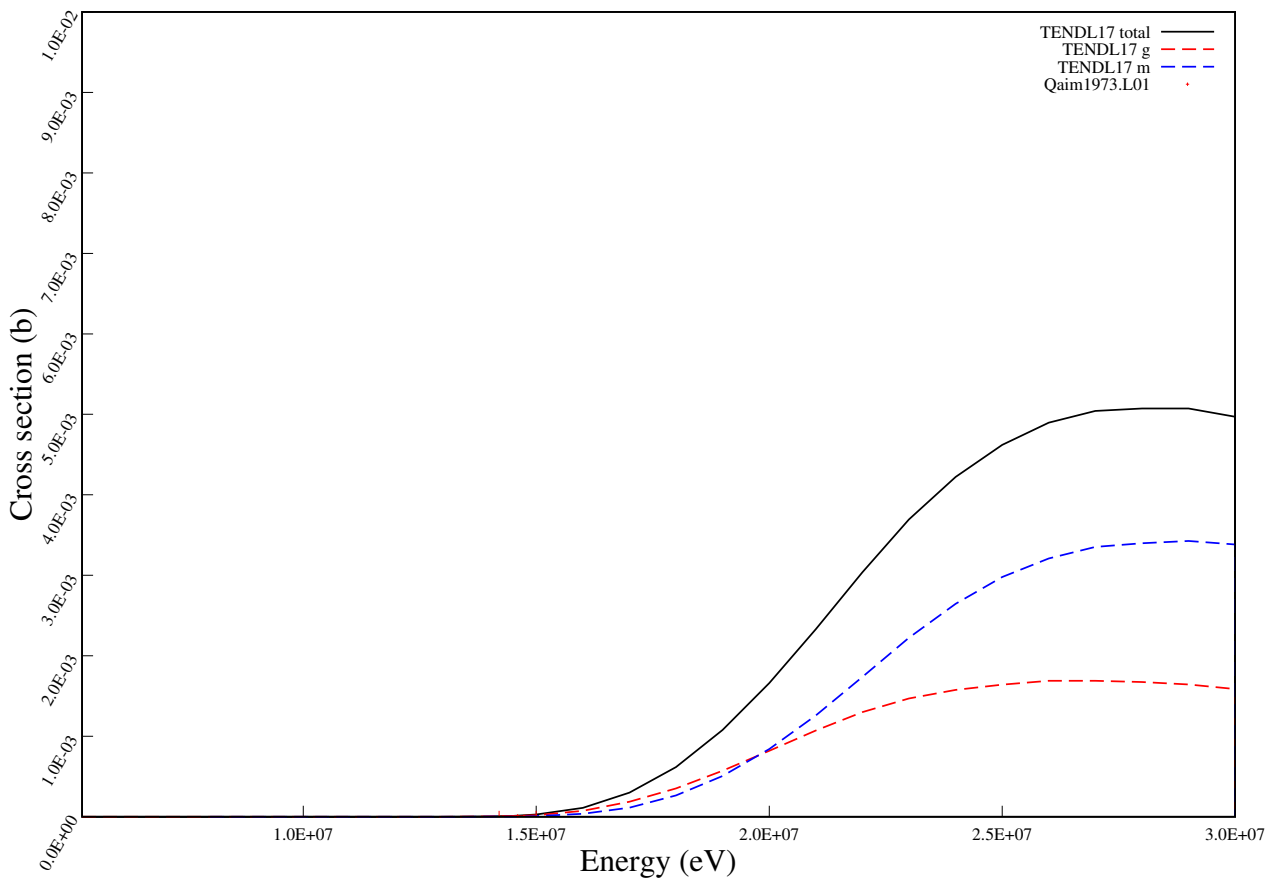
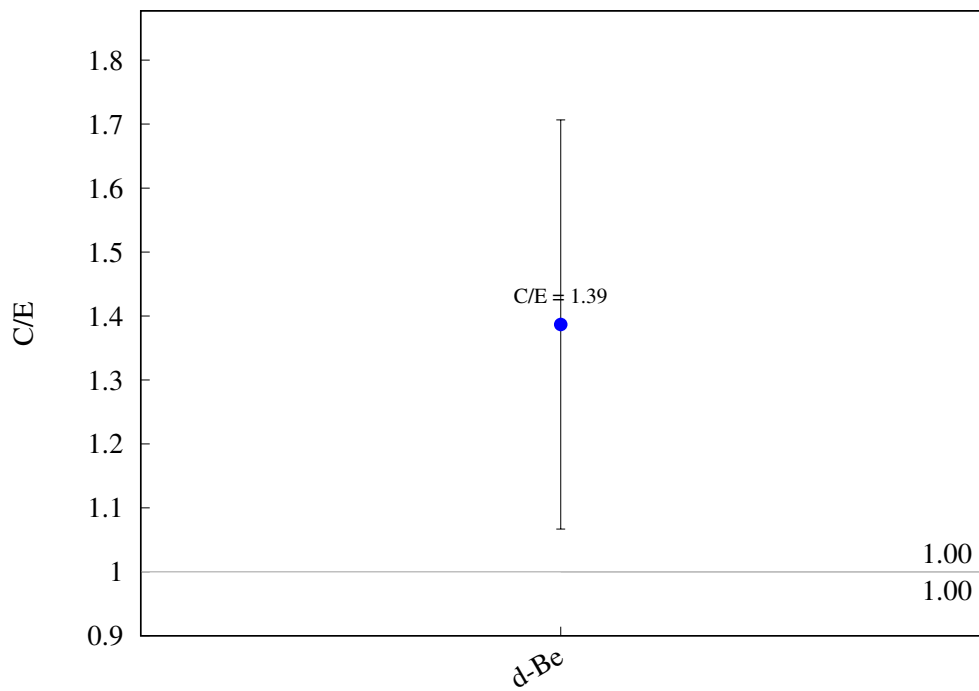
^{197}Au (n,2n) ^{196}n Au 

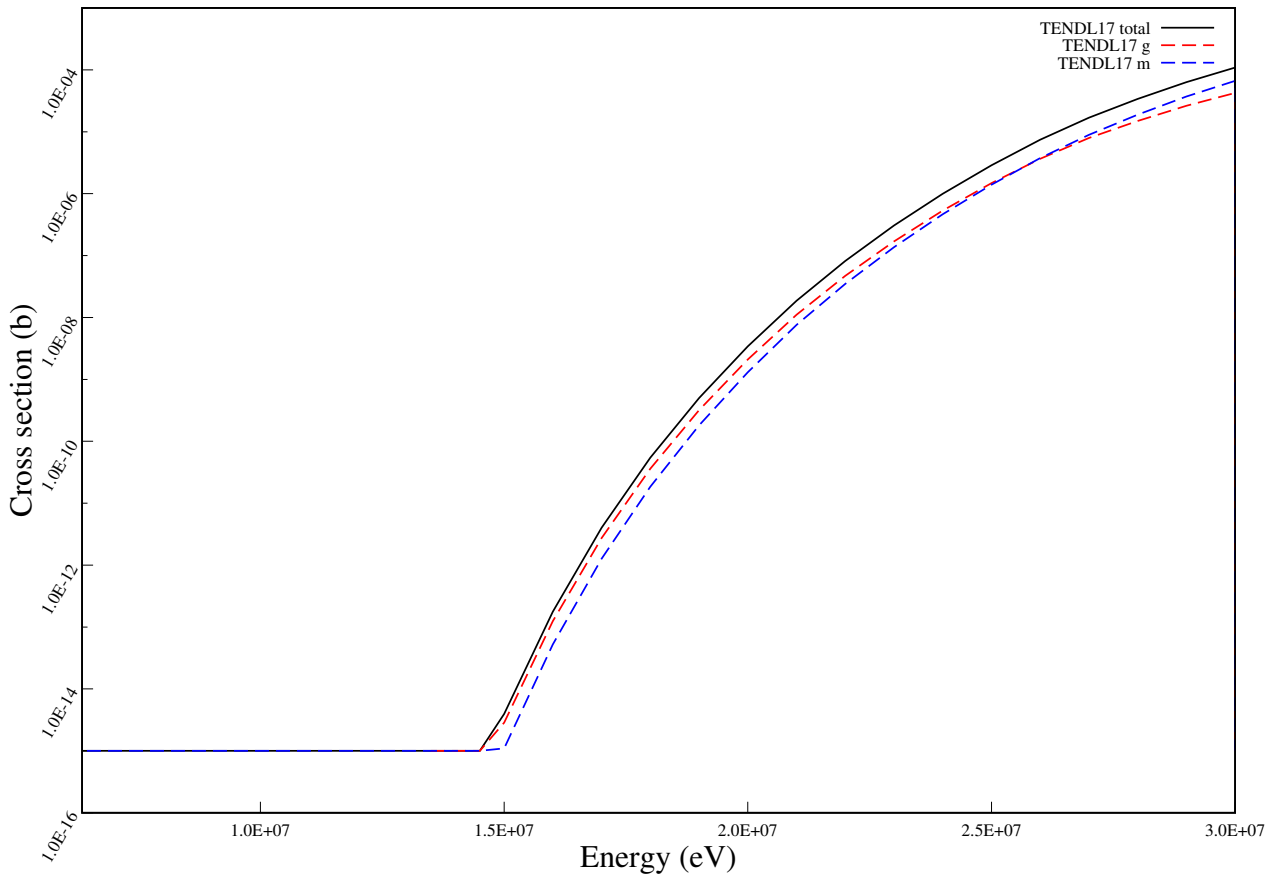
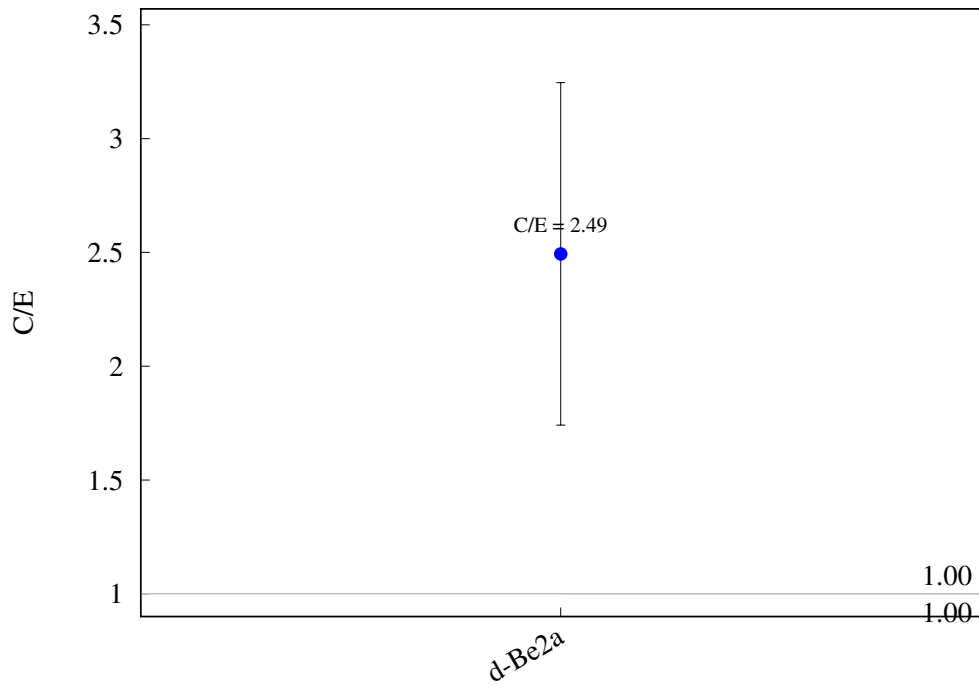
^{197}Au (n,2n) ^{196}Au 

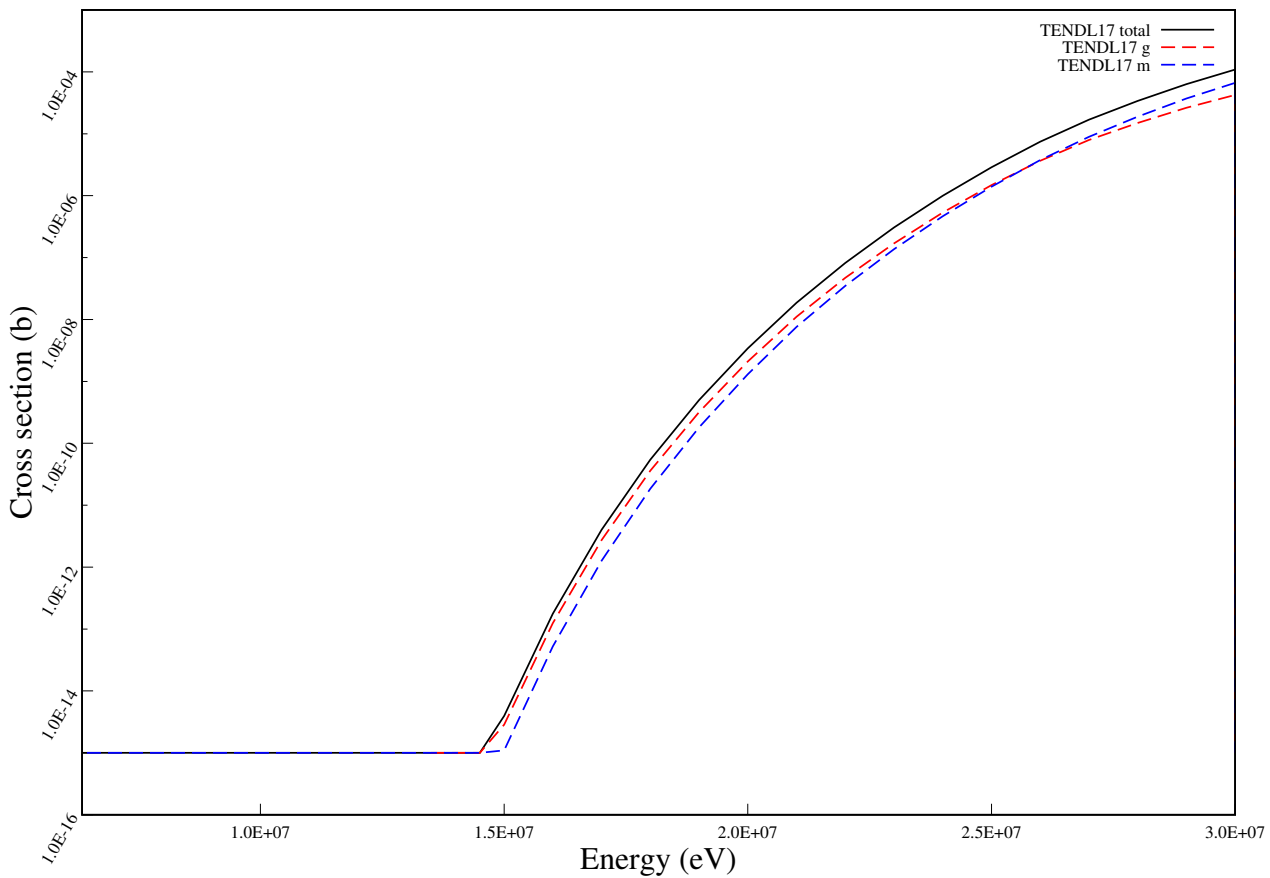
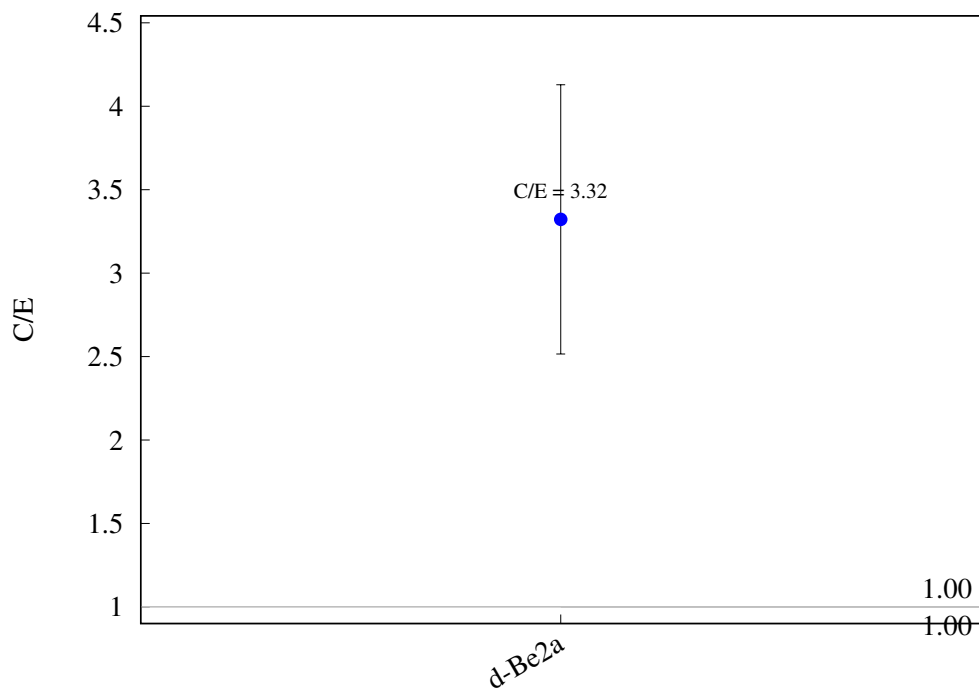
^{197}Au (n,3n) ^{195}Au 

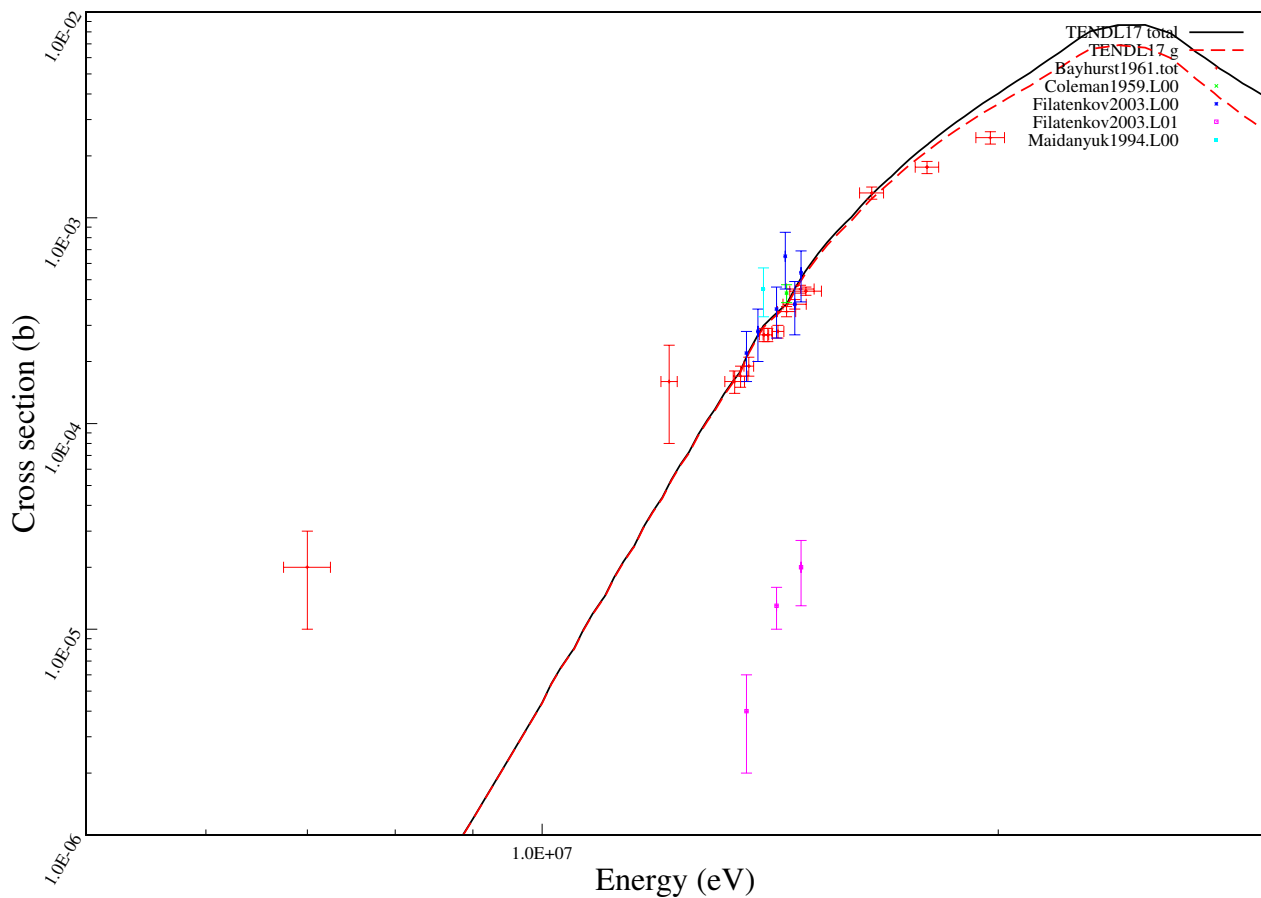
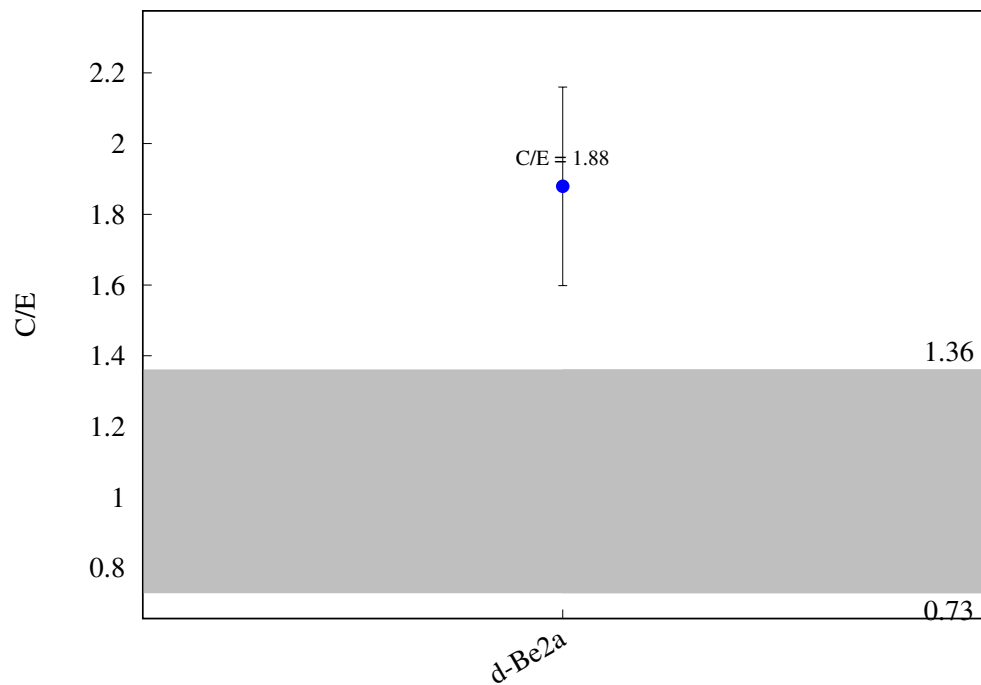
^{197}Au (n,4n) ^{194}Au 

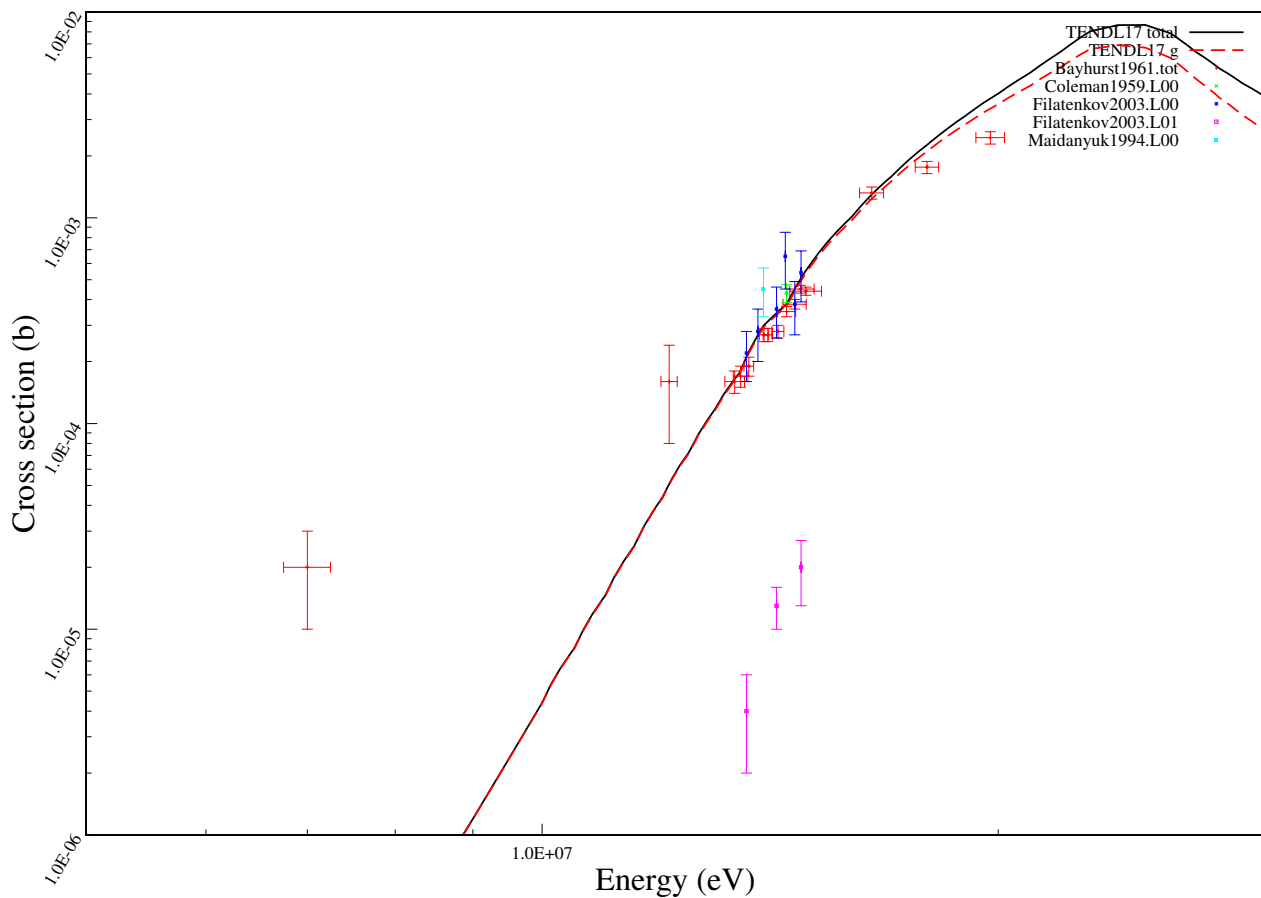
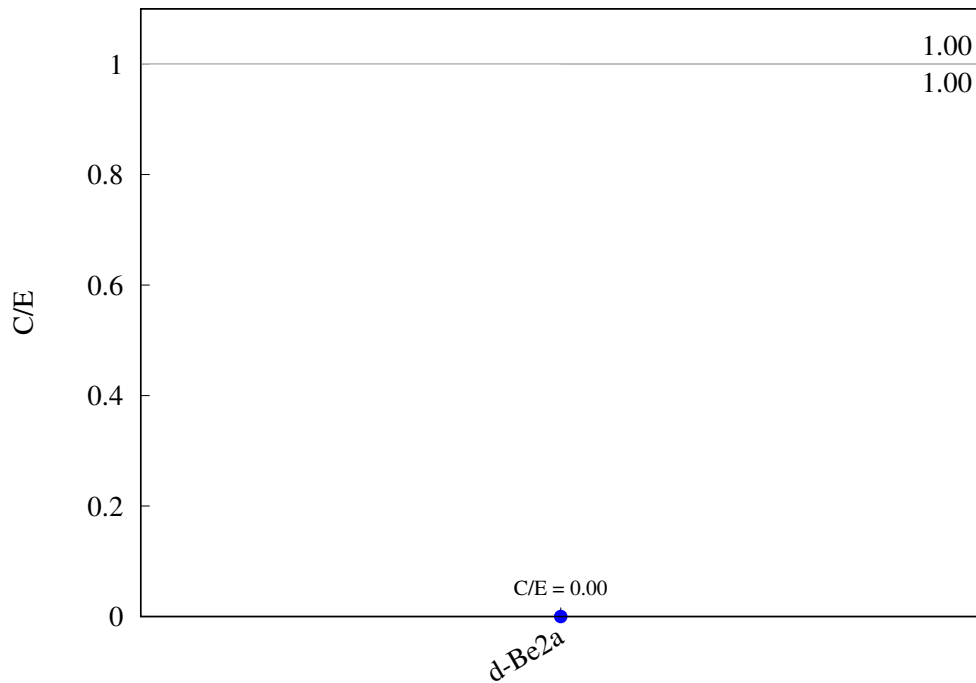
^{197}Au (n,g) ^{198}Au 

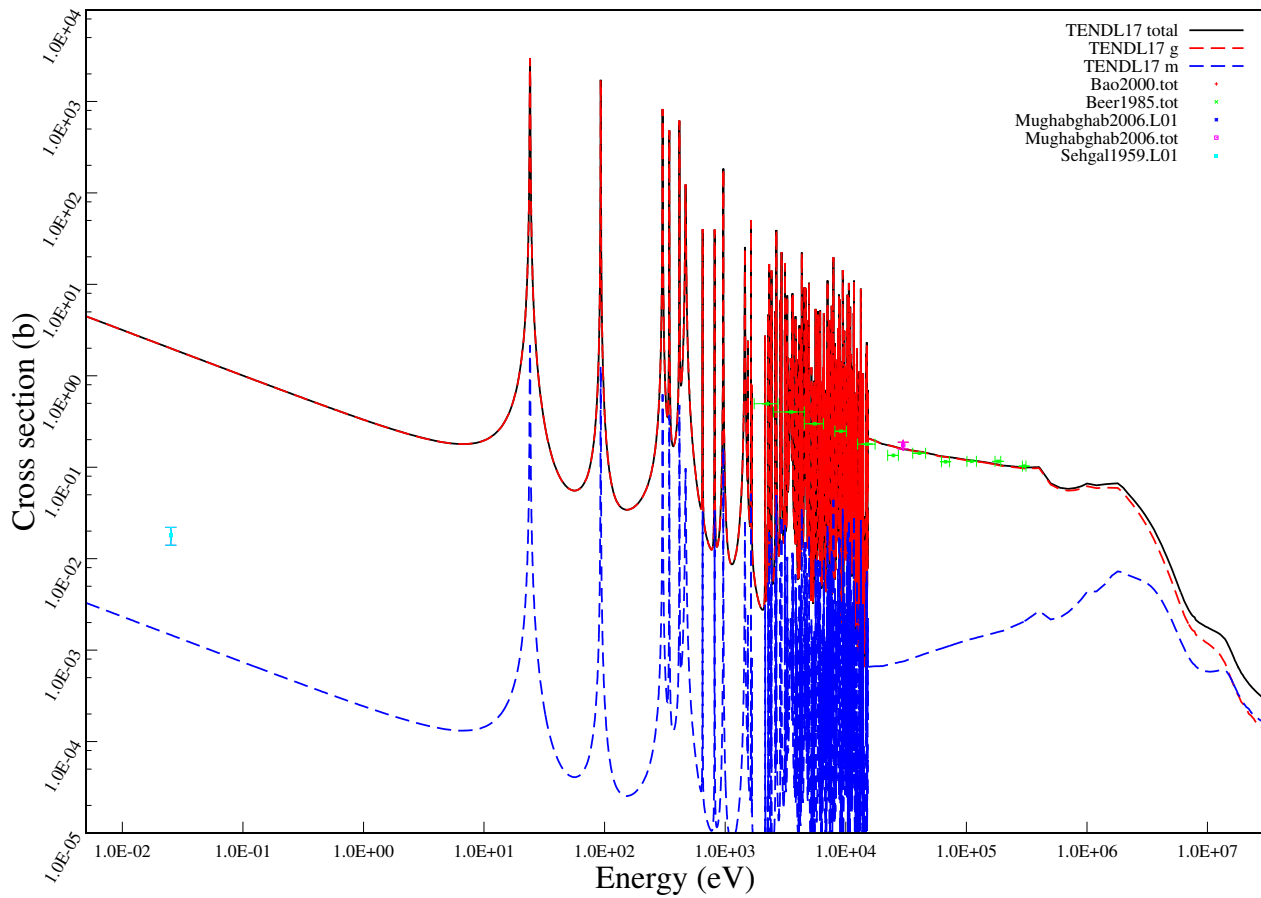
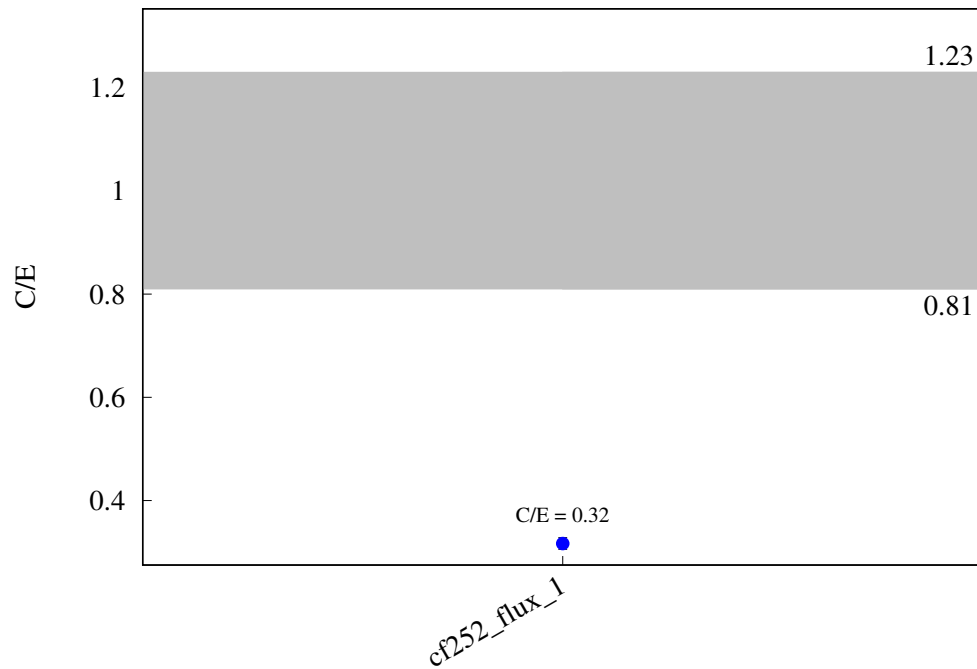
$^{197}\text{Au} (\text{n},\text{t}) ^{195}\text{Pt}$ 

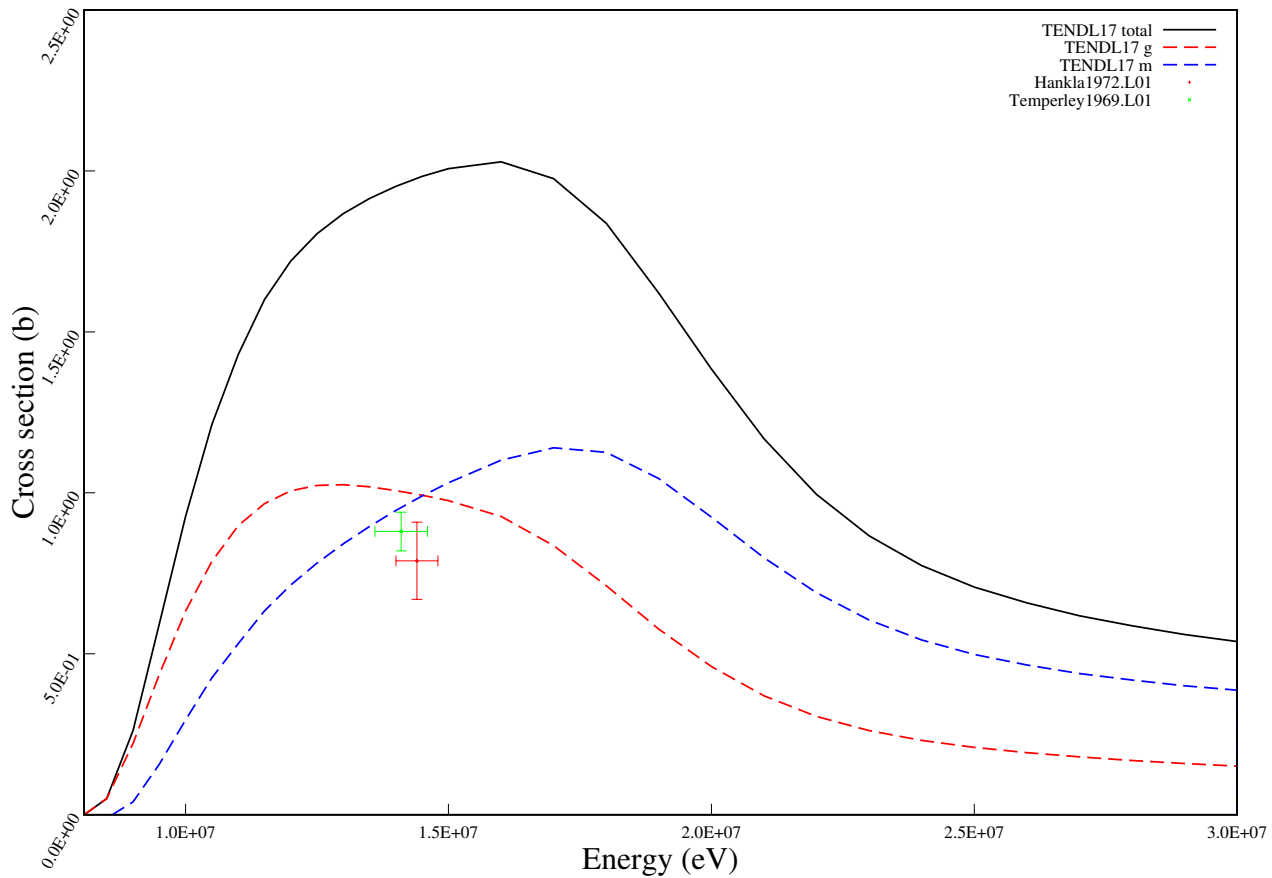
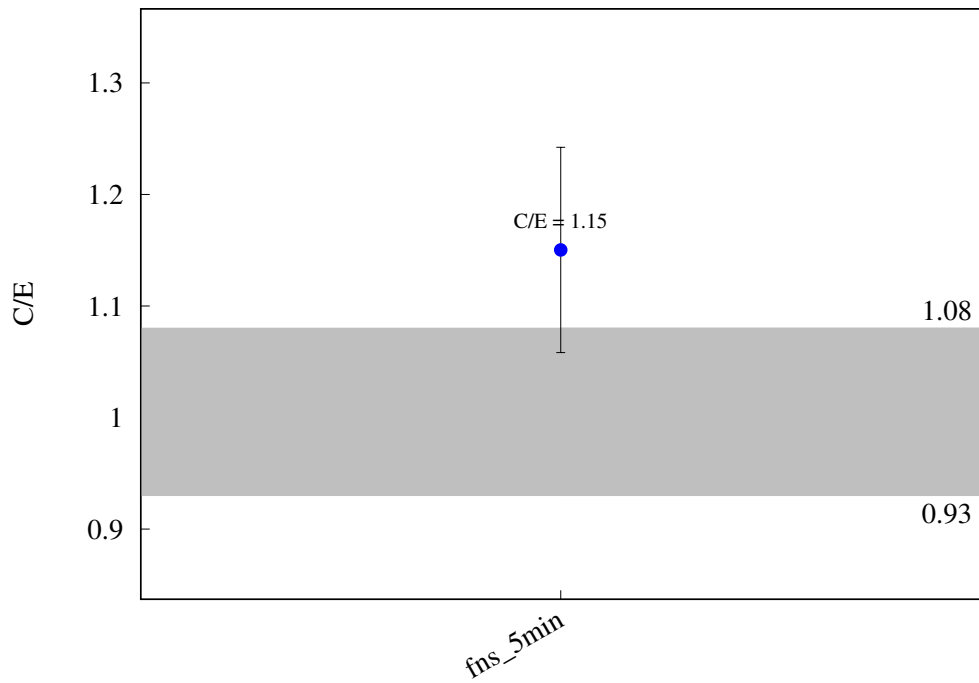
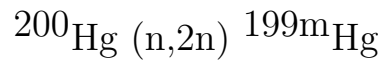
^{197}Au (n,h) ^{195}gIr 

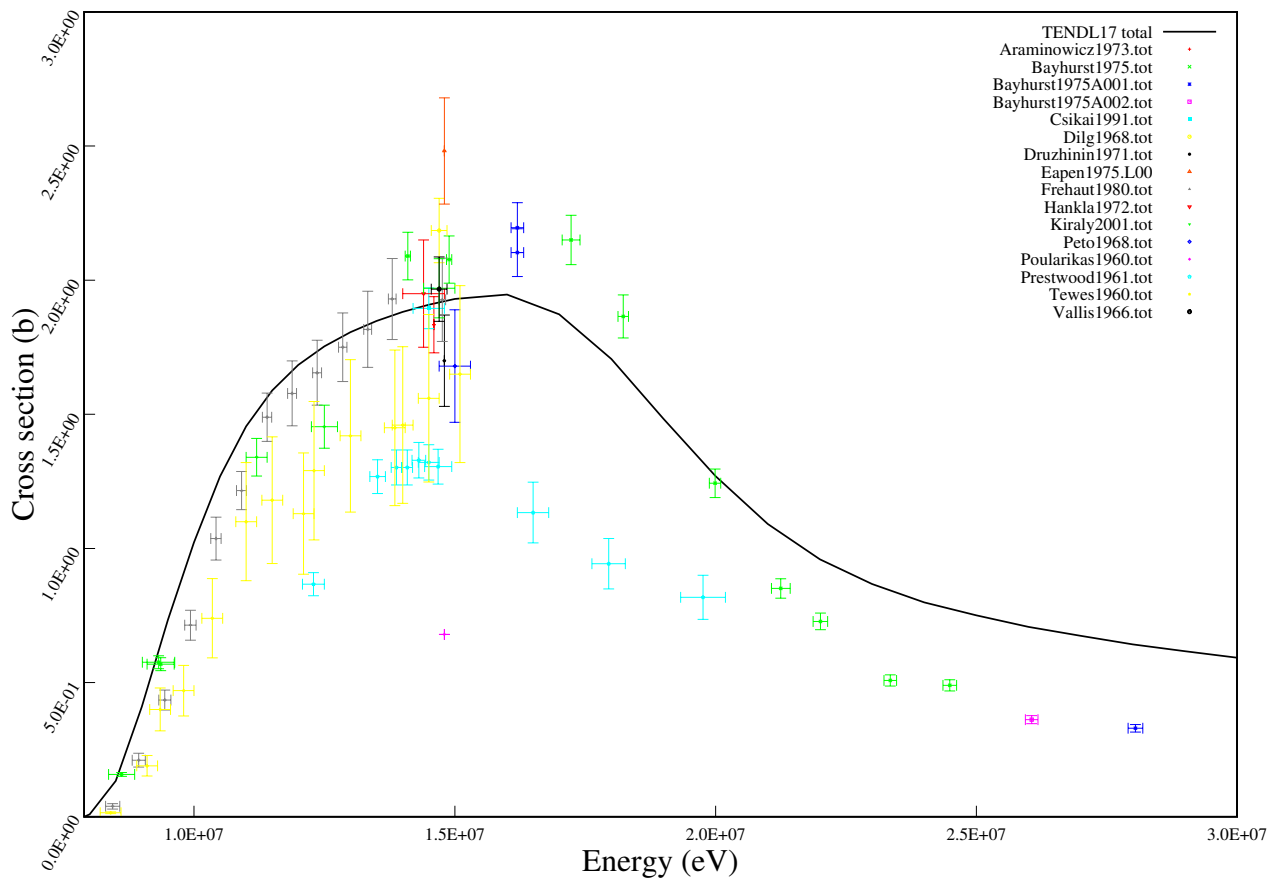
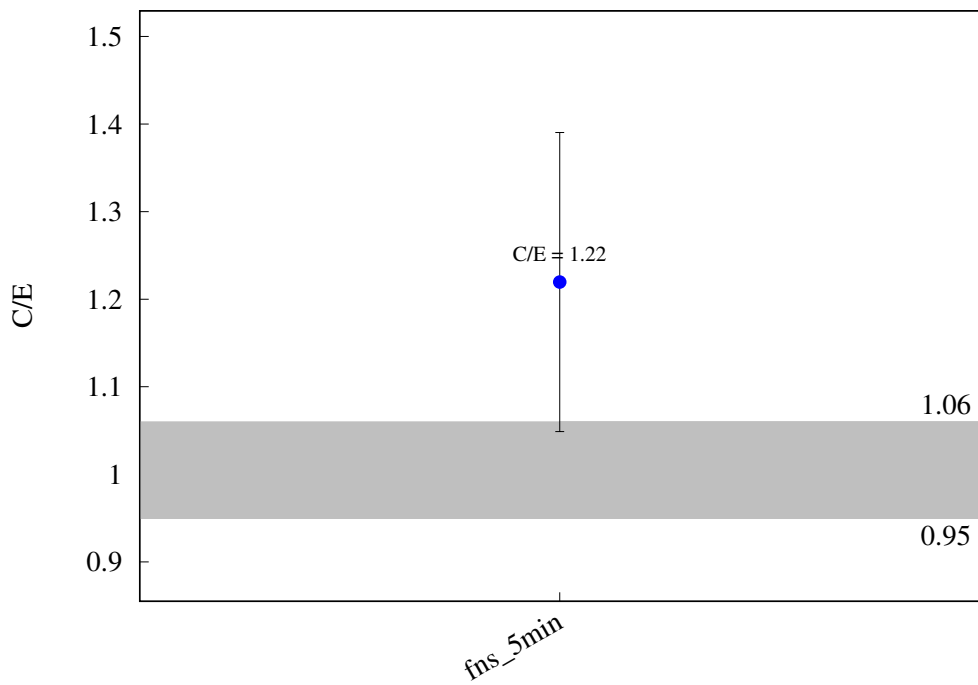
$^{197}\text{Au} (\text{n},\text{h}) ^{195}\text{Ir}$ 

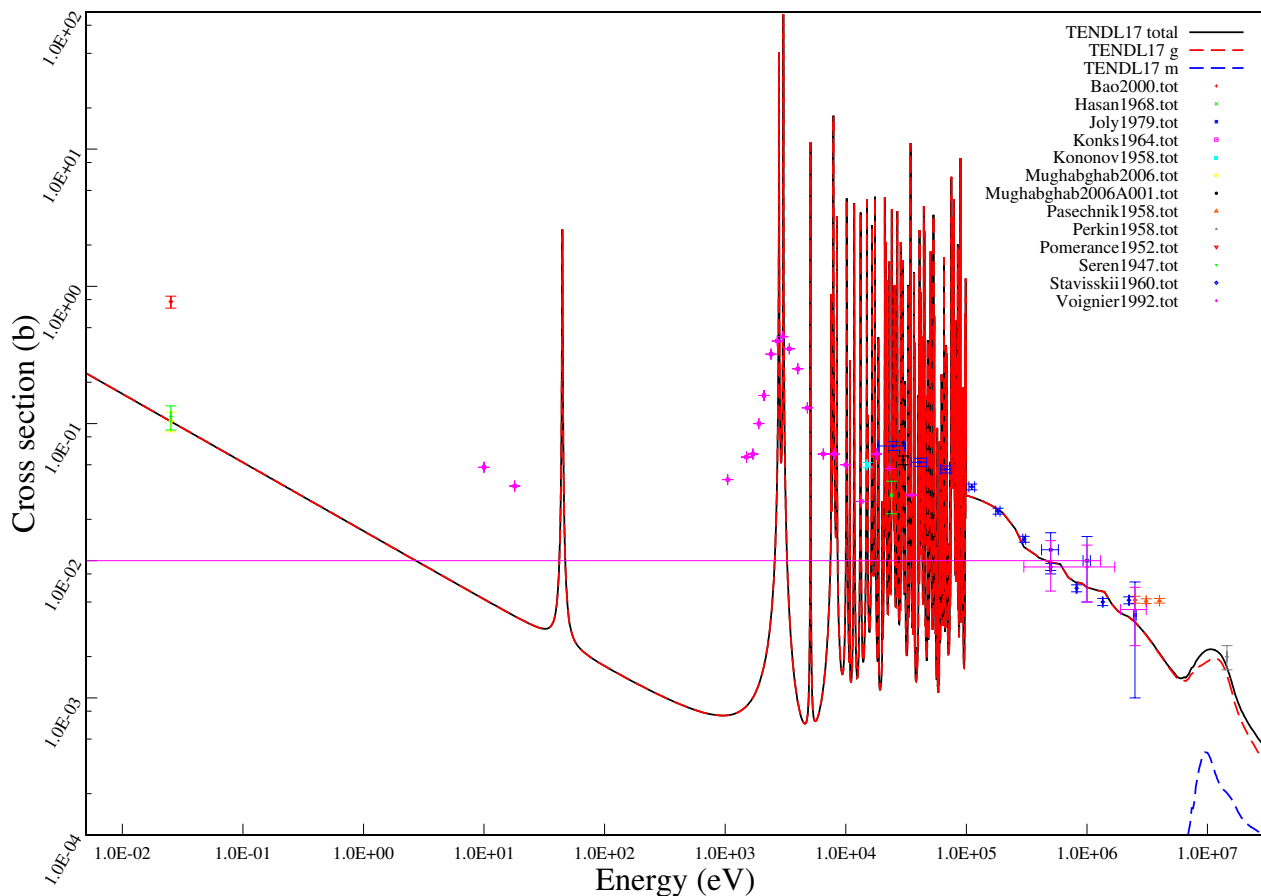
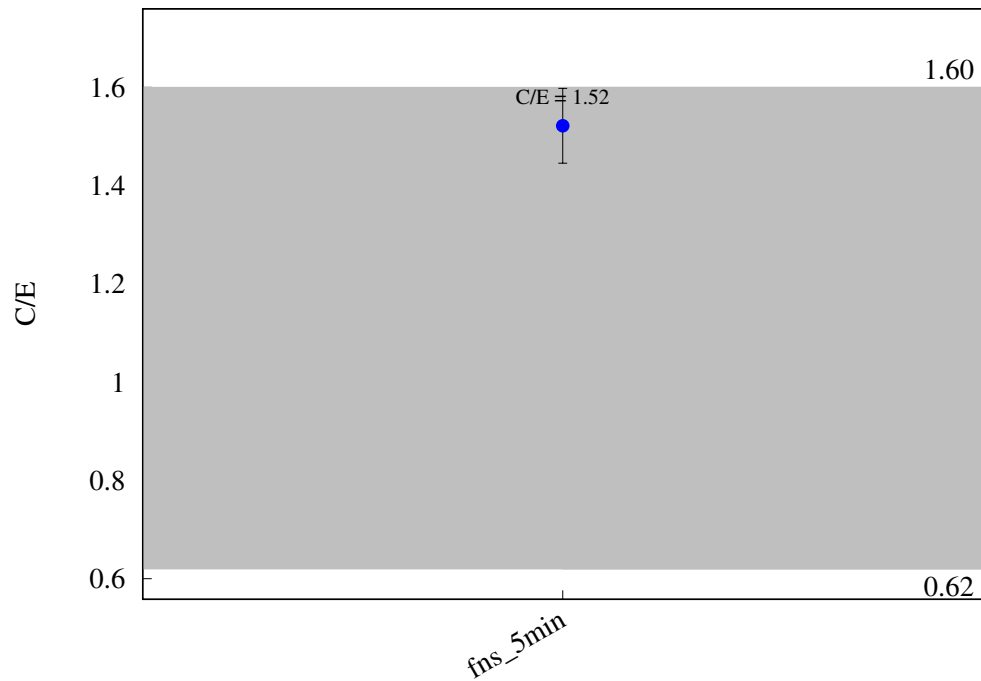
^{197}Au (n,a) ^{194}gIr 

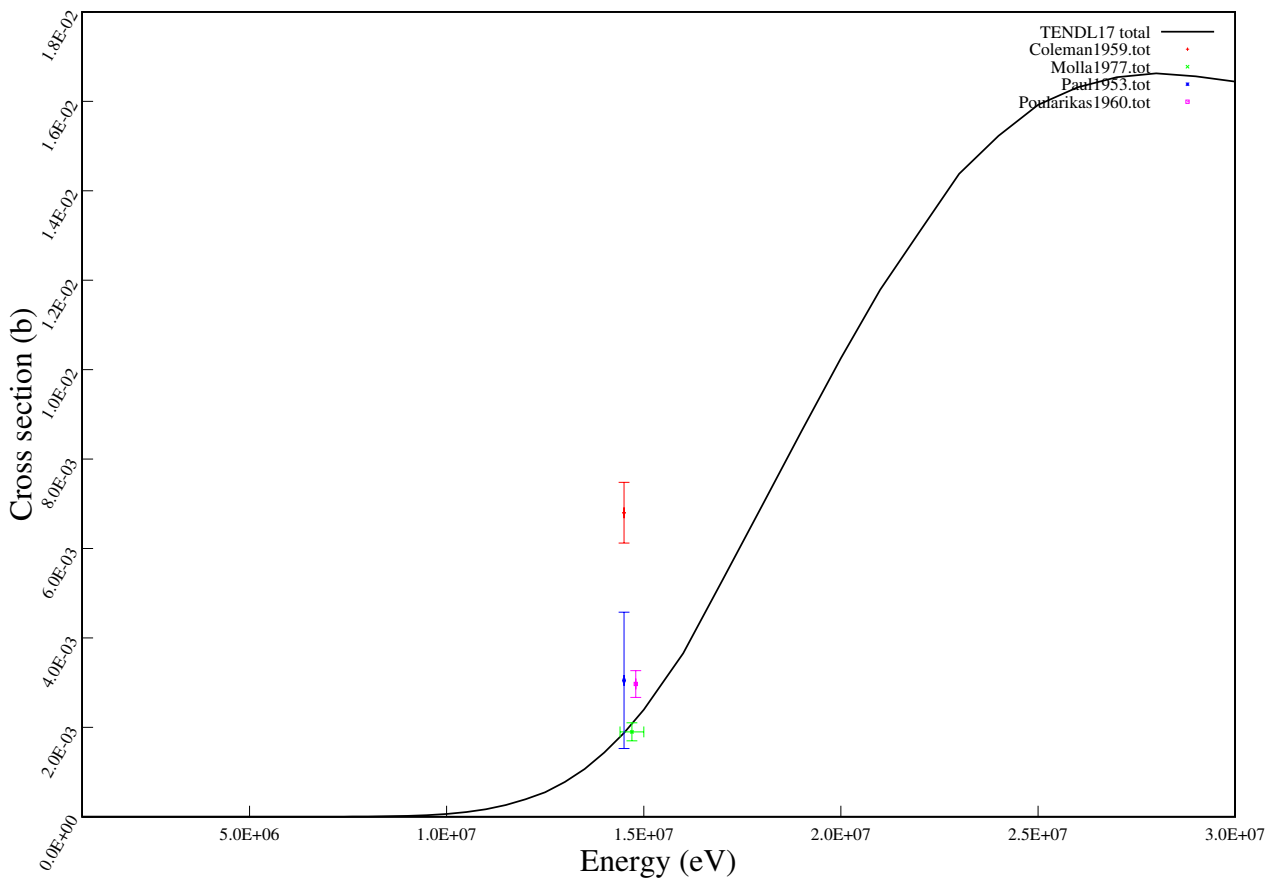
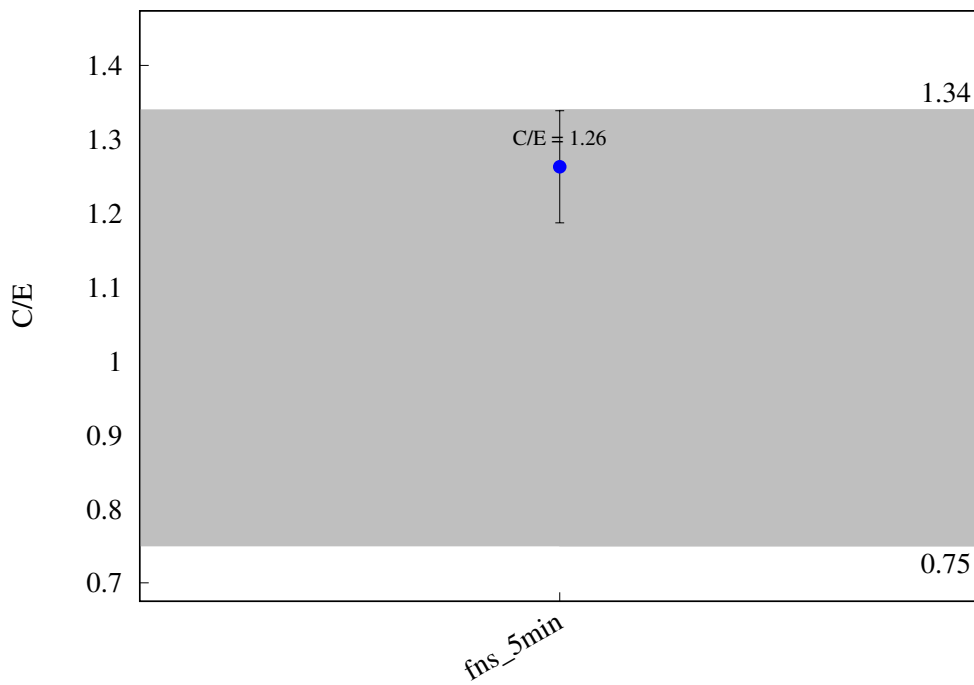
^{197}Au (n,a) $^{194\text{m}}\text{Ir}$ 

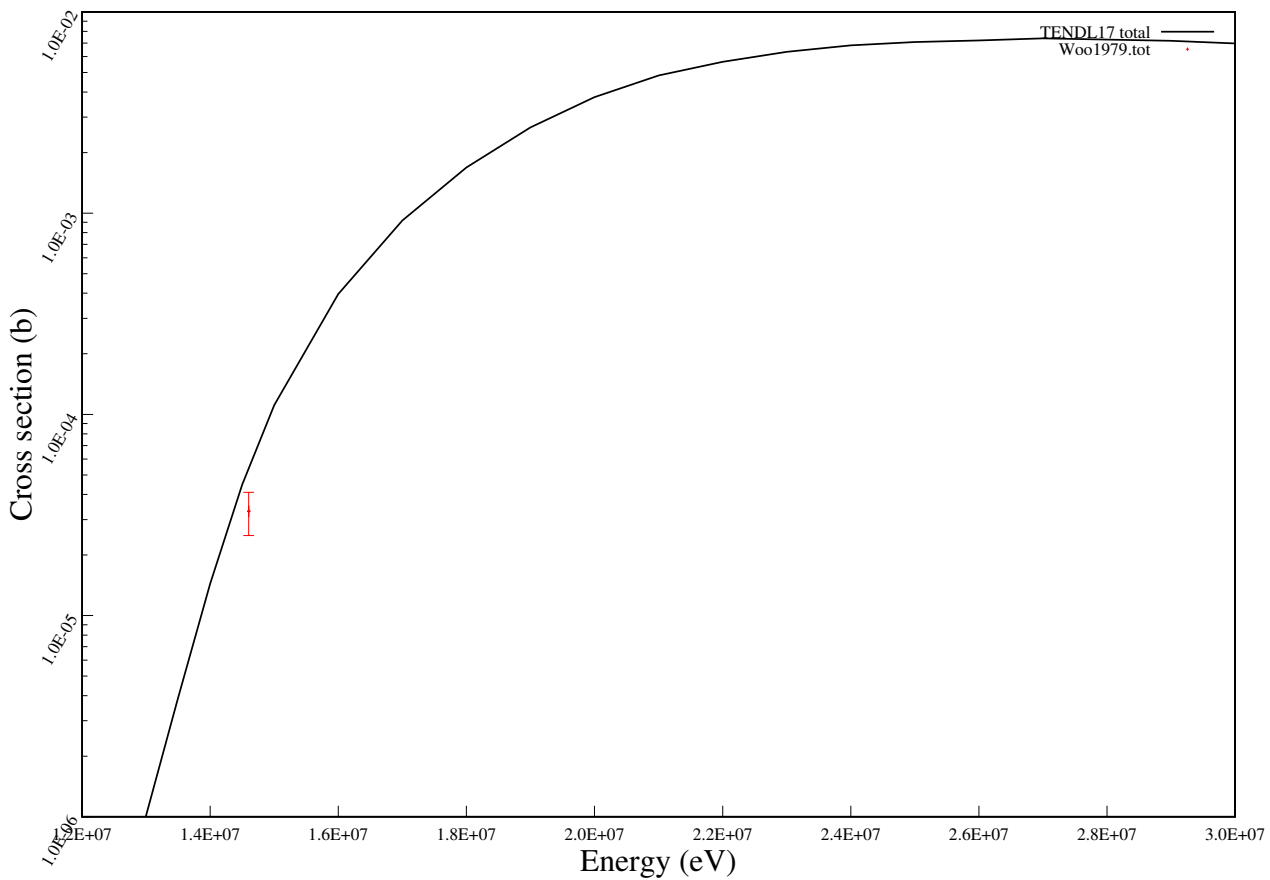
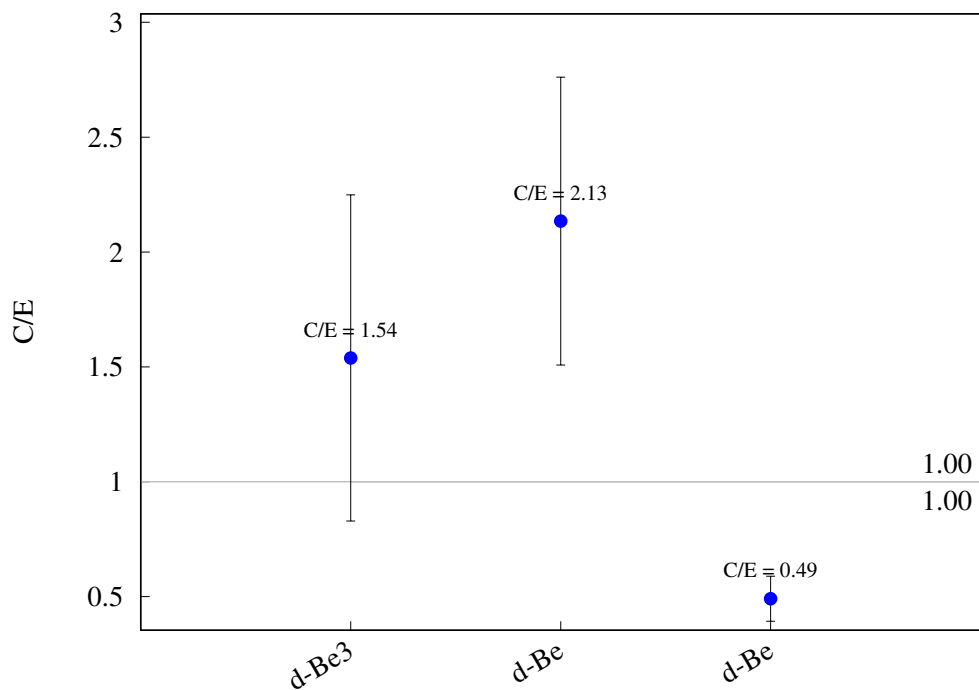
^{198}Hg (n,g) ^{199}Hg 

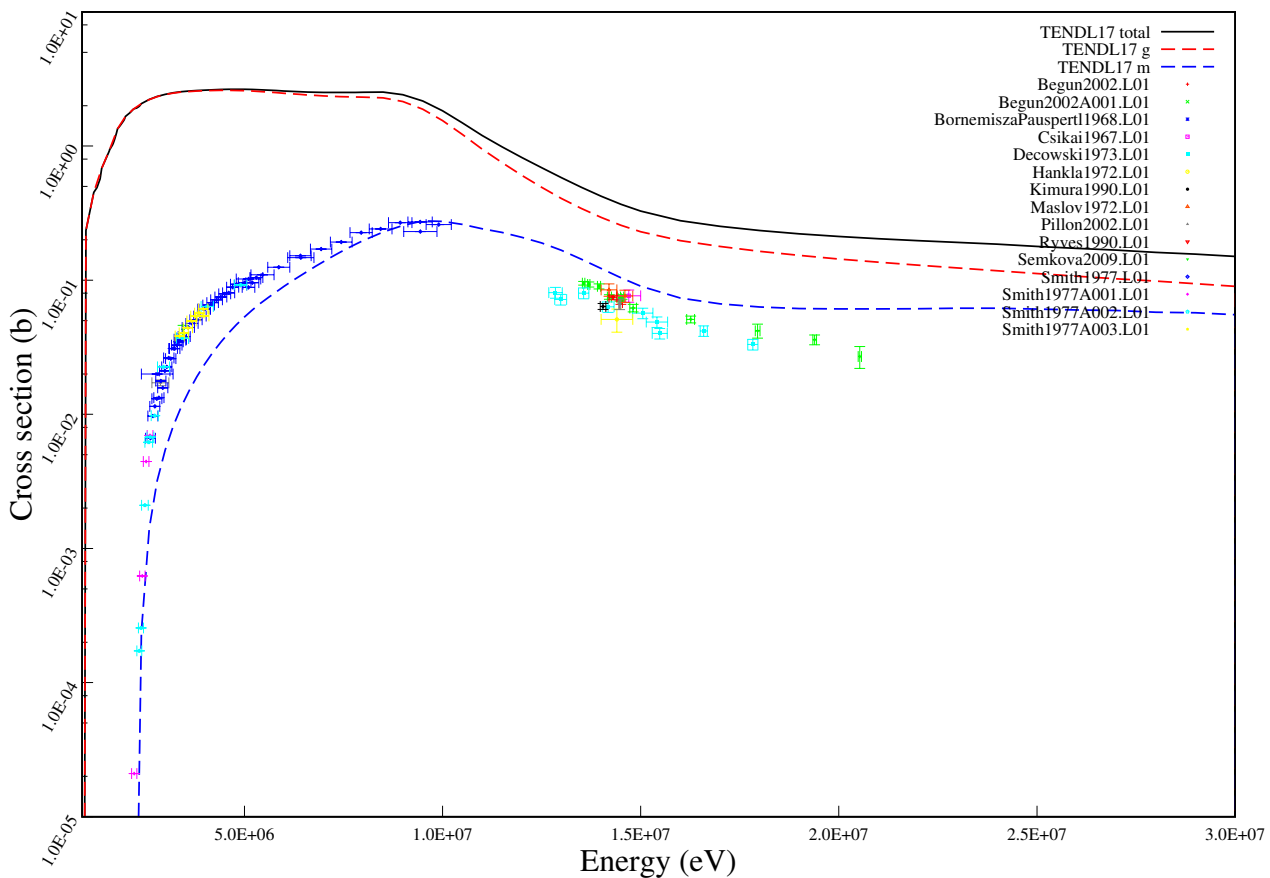
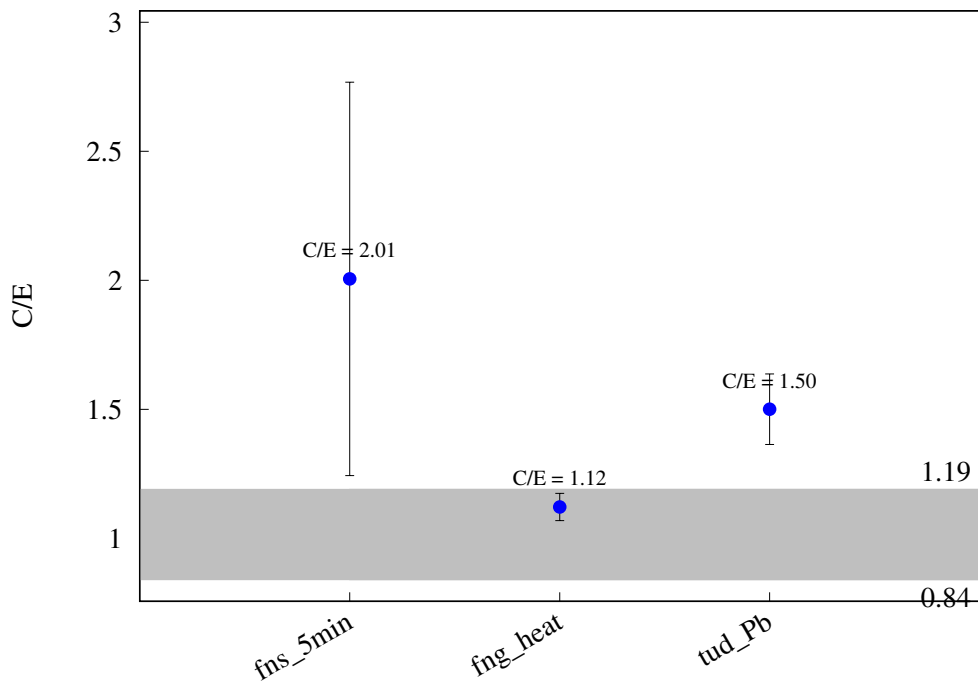


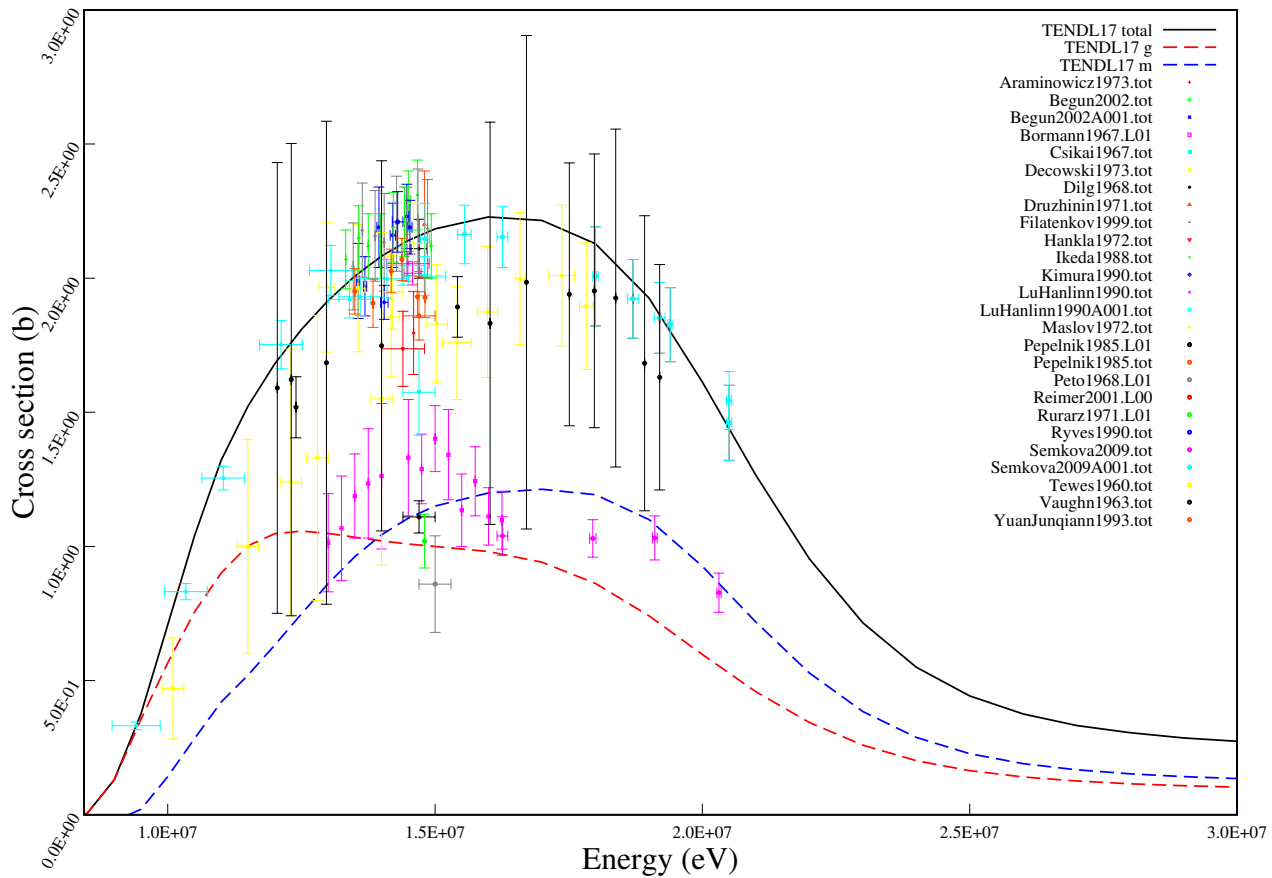
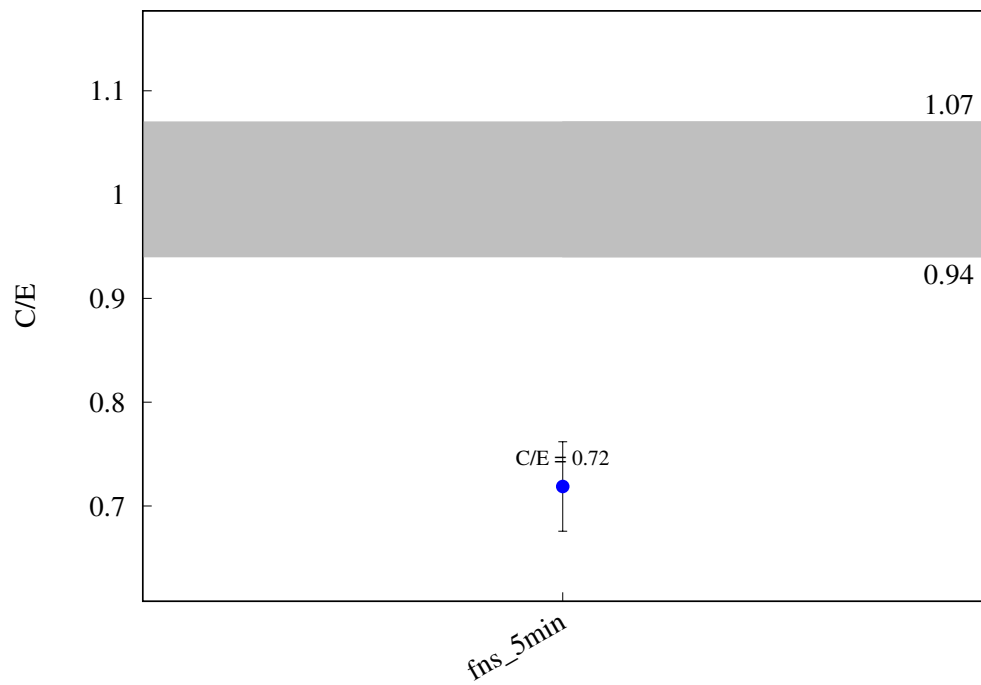
^{203}Tl (n,2n) ^{202}Tl 

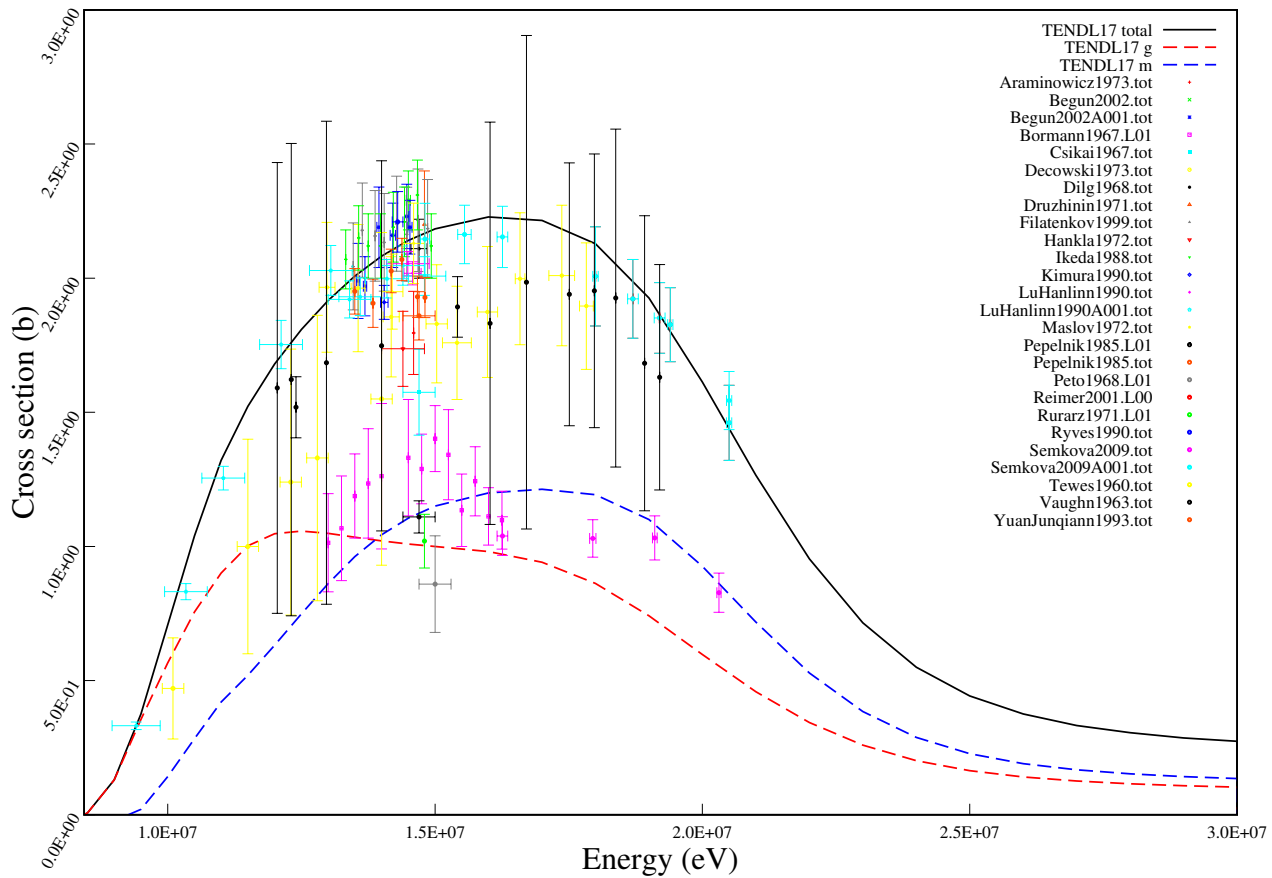
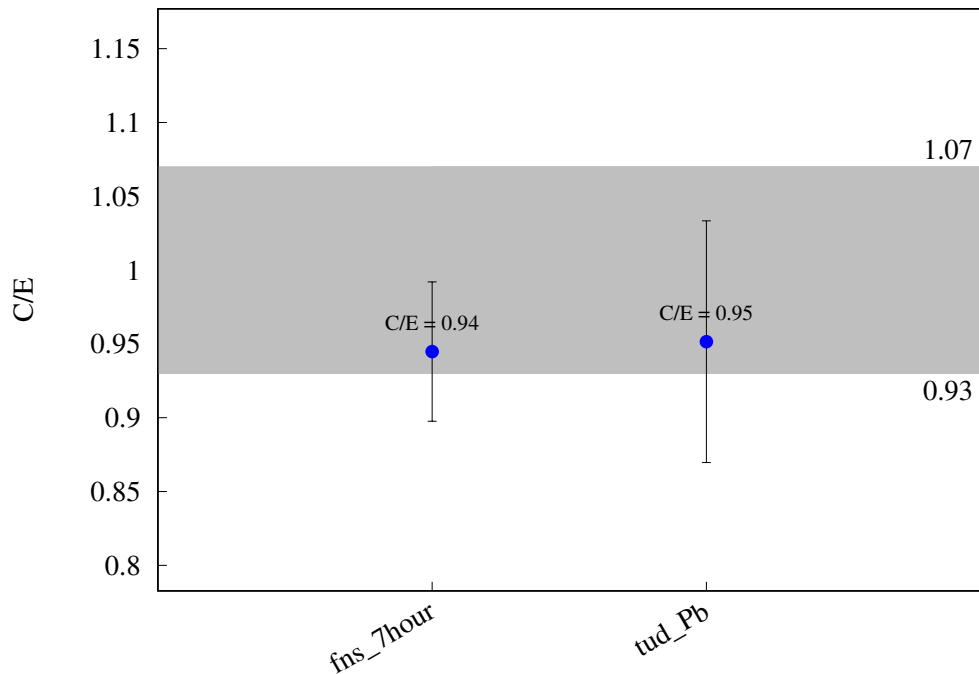
^{205}Tl (n,g) ^{206}Tl 

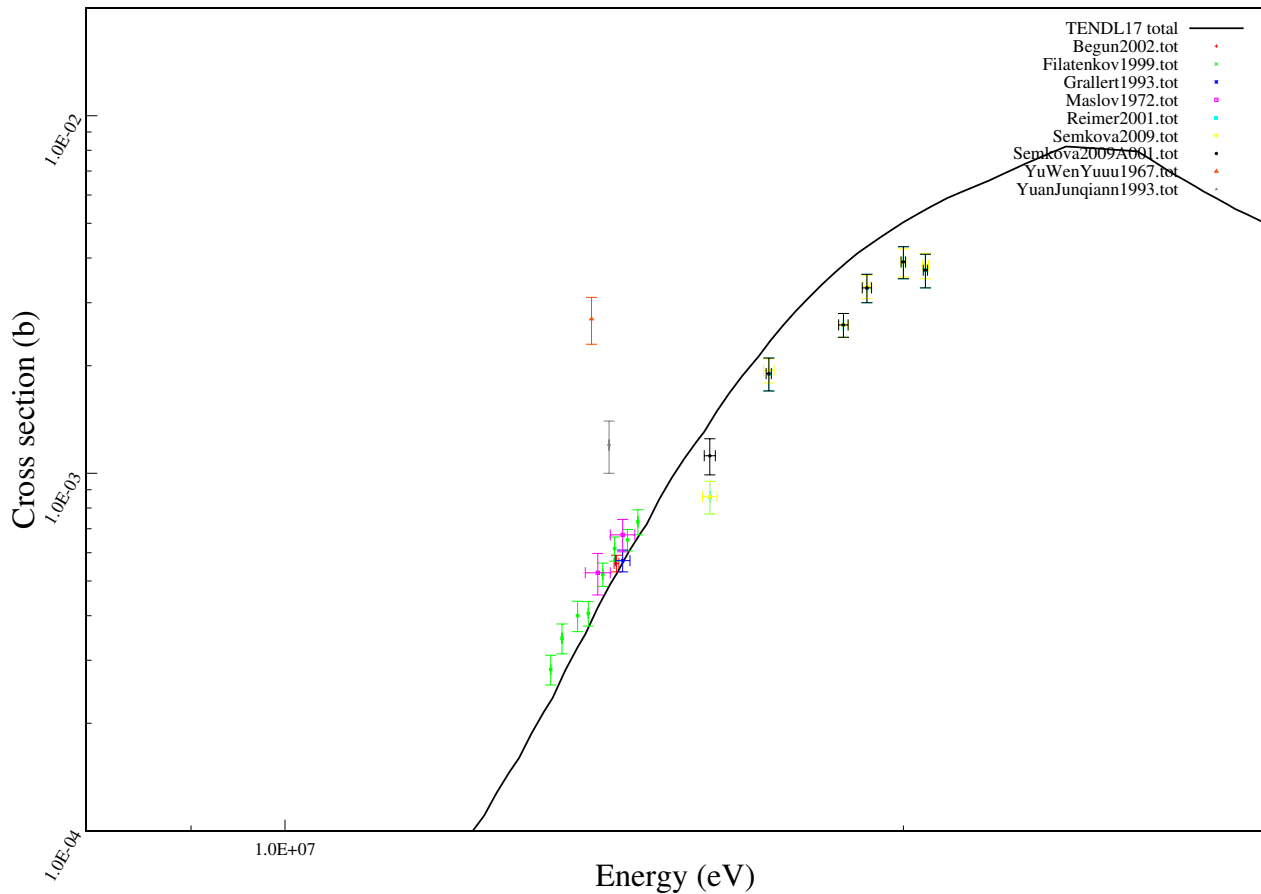
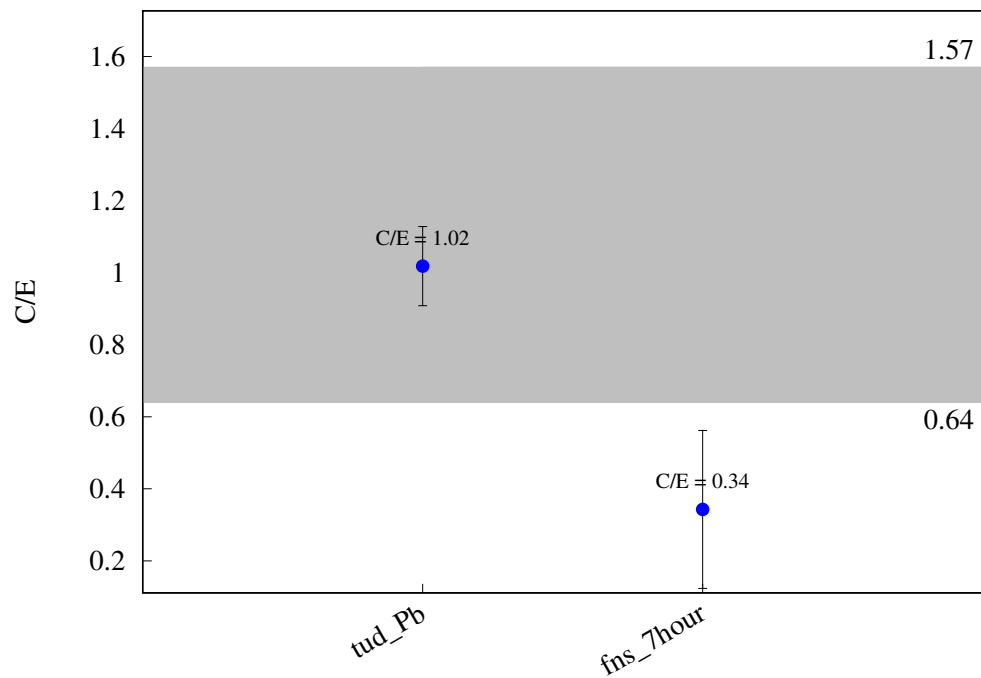
^{205}Tl (n,p) ^{205}Hg 

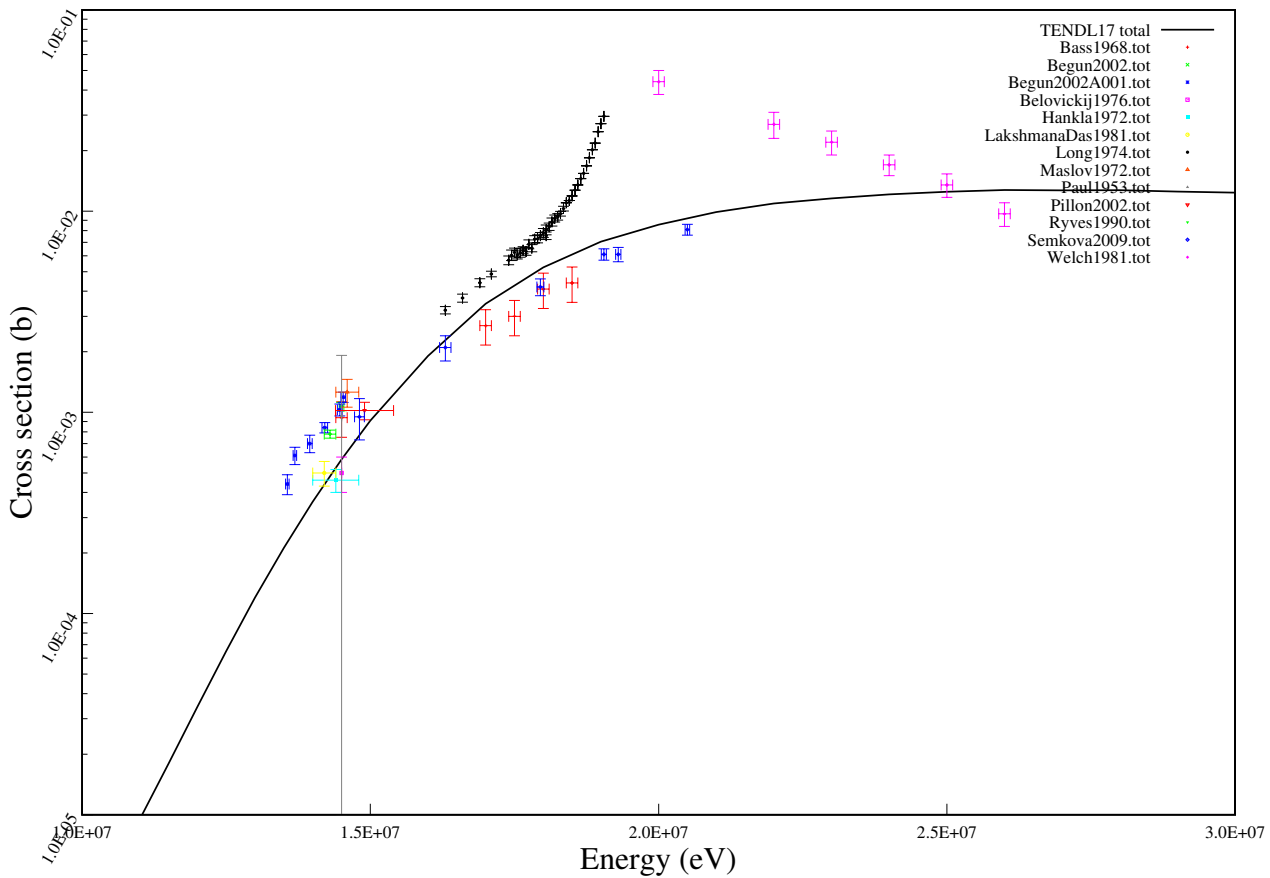
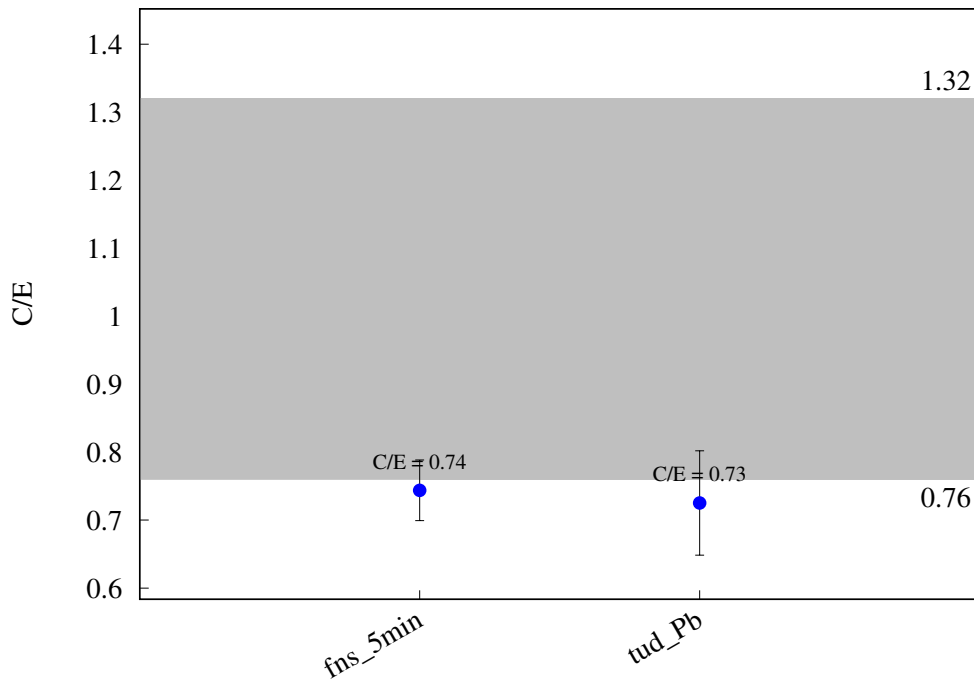
$^{205}\text{Tl} (\text{n},\text{t}) ^{203}\text{Hg}$ 

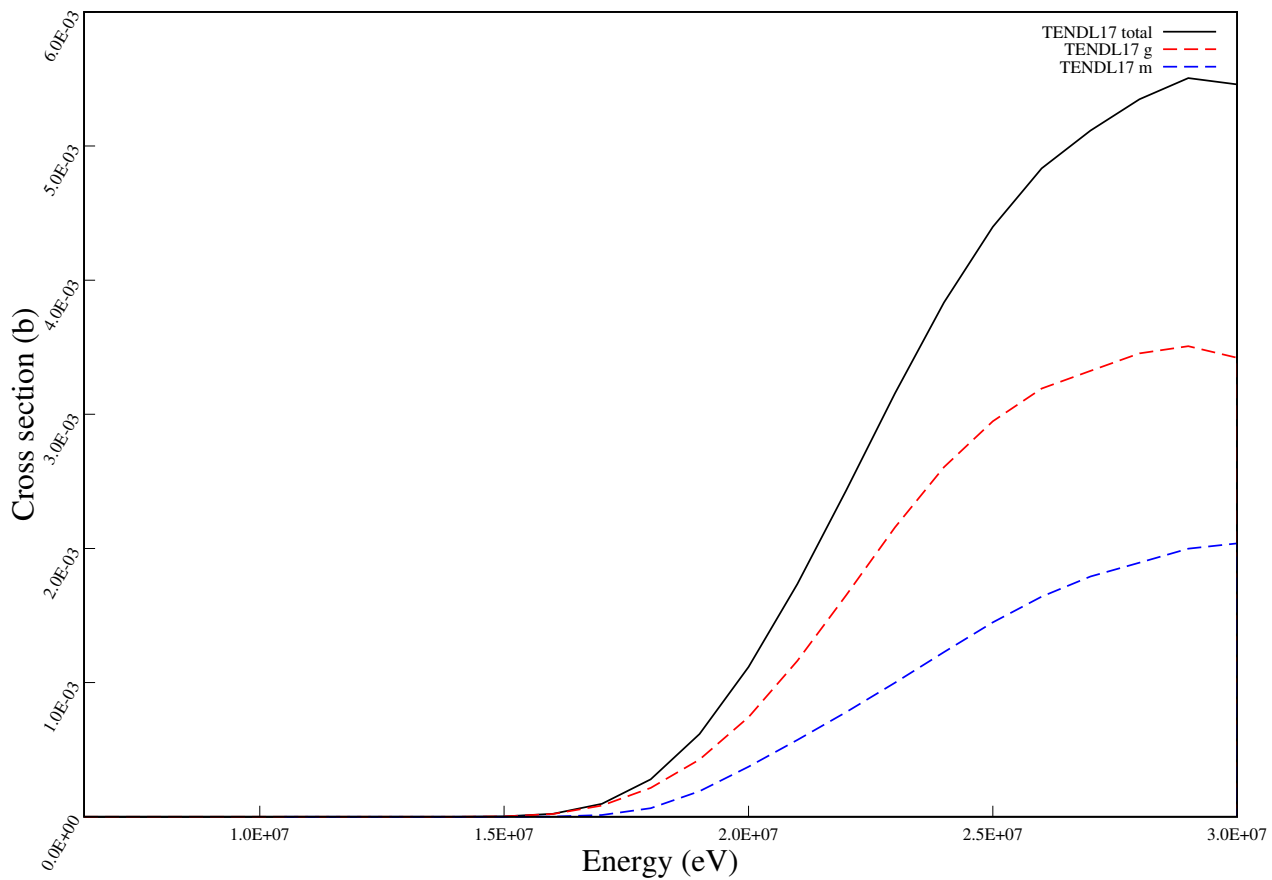
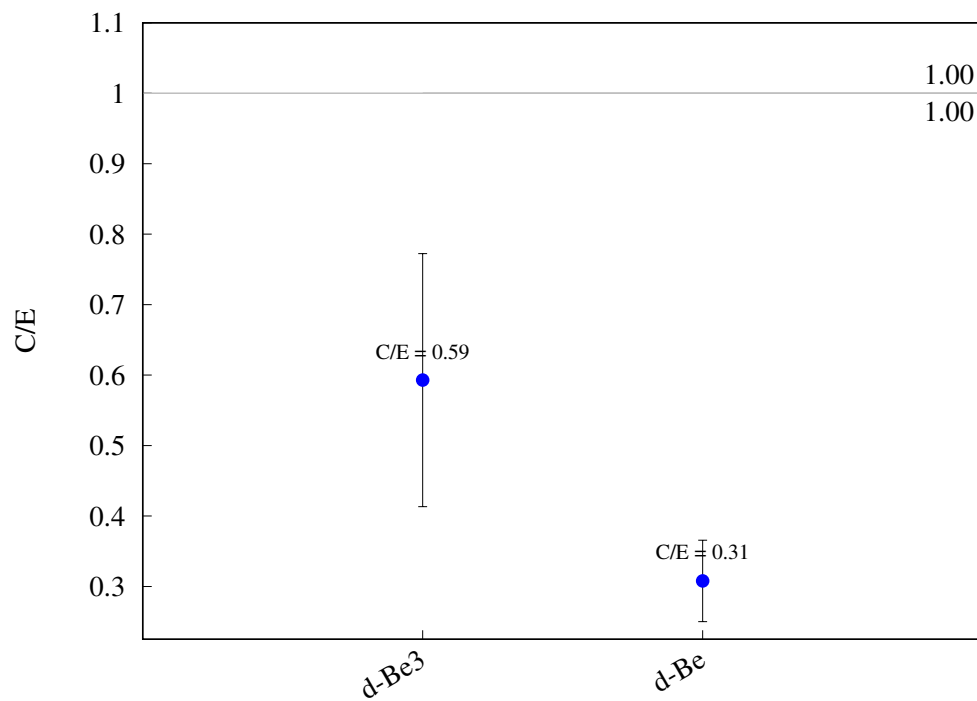
^{204}Pb (n,n) $^{204\text{m}}\text{Pb}$ 

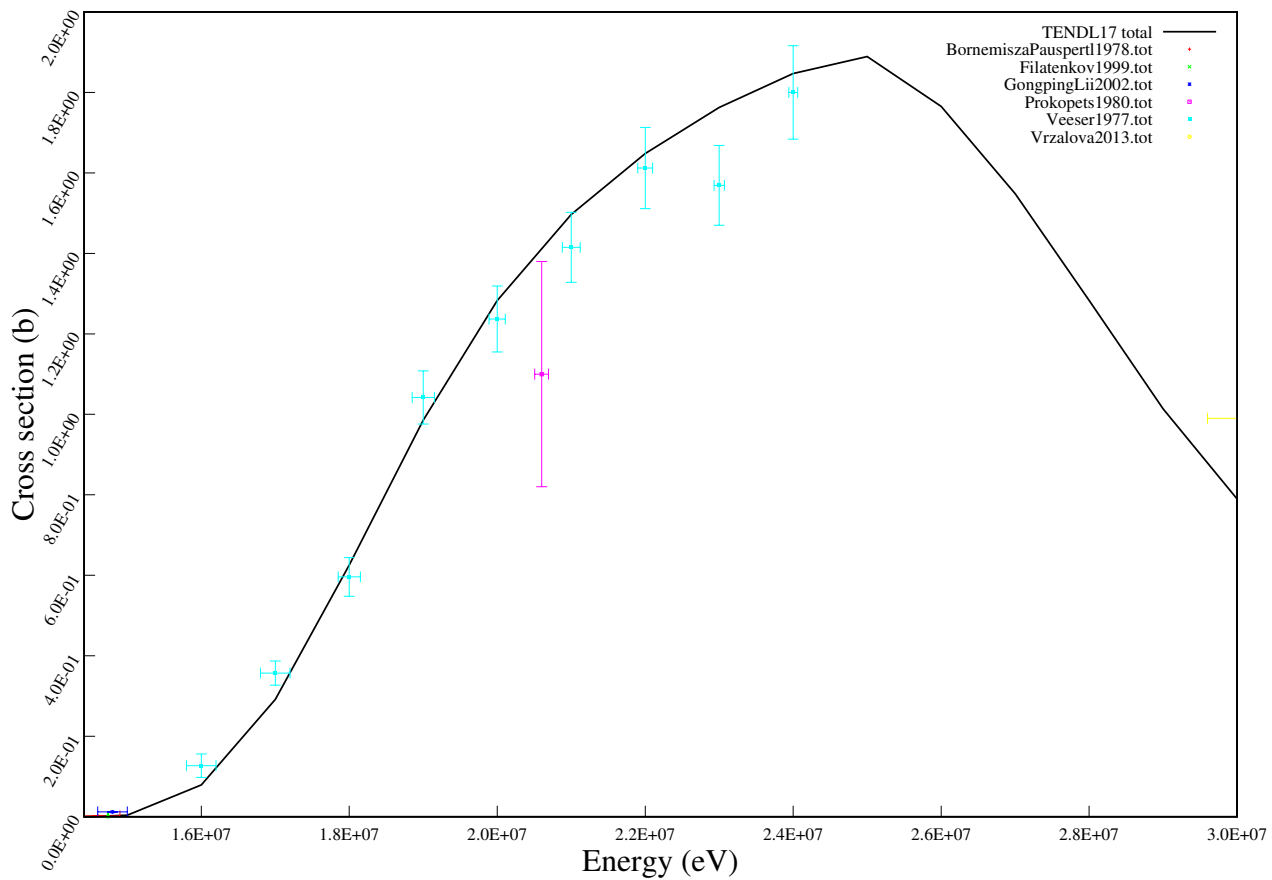
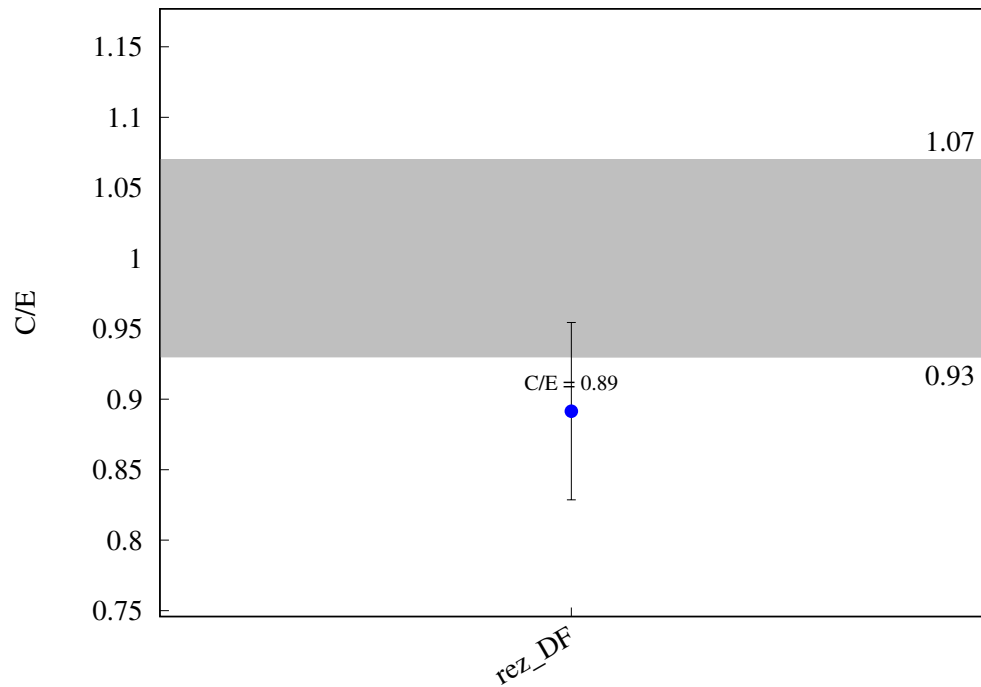
^{204}Pb ($n,2n$) $^{203\text{m}}\text{Pb}$ 

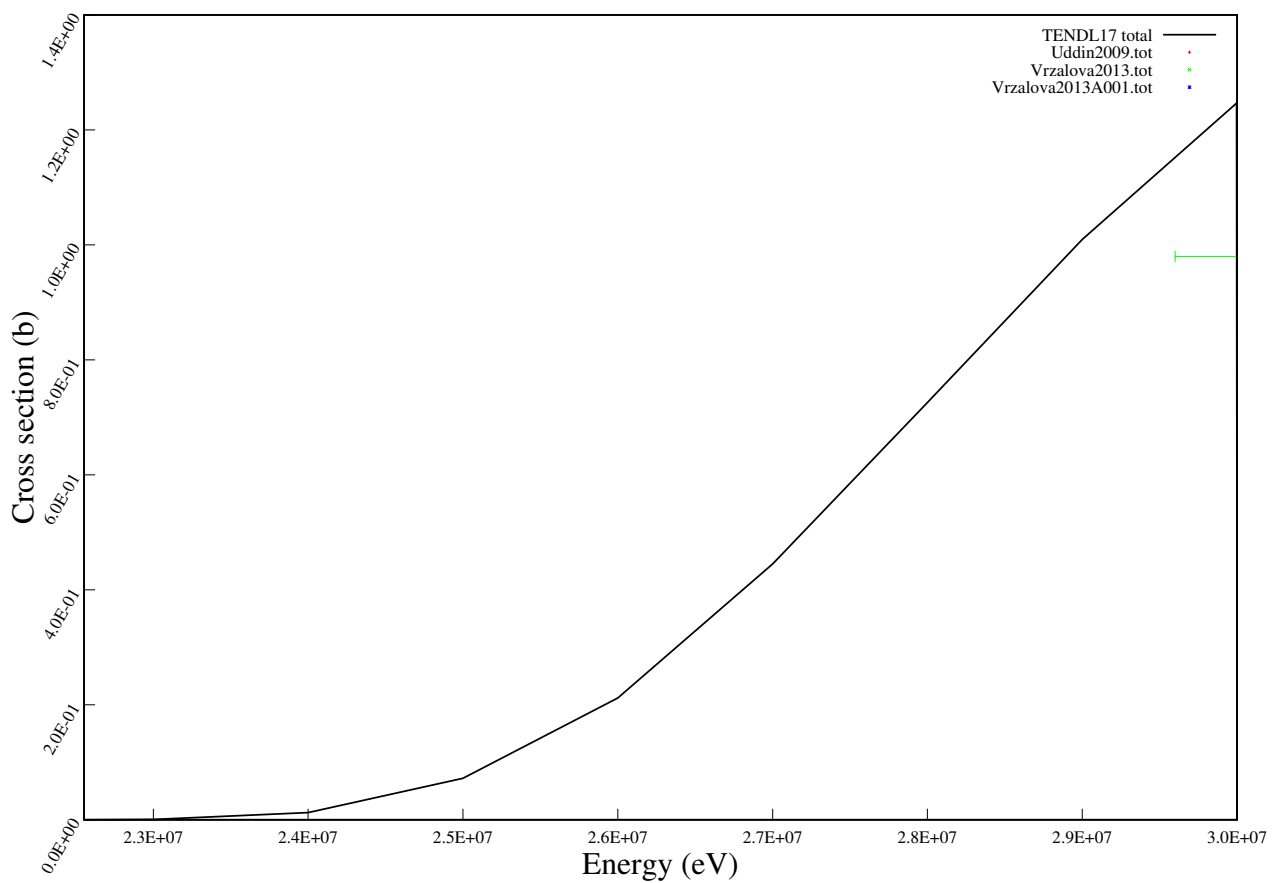
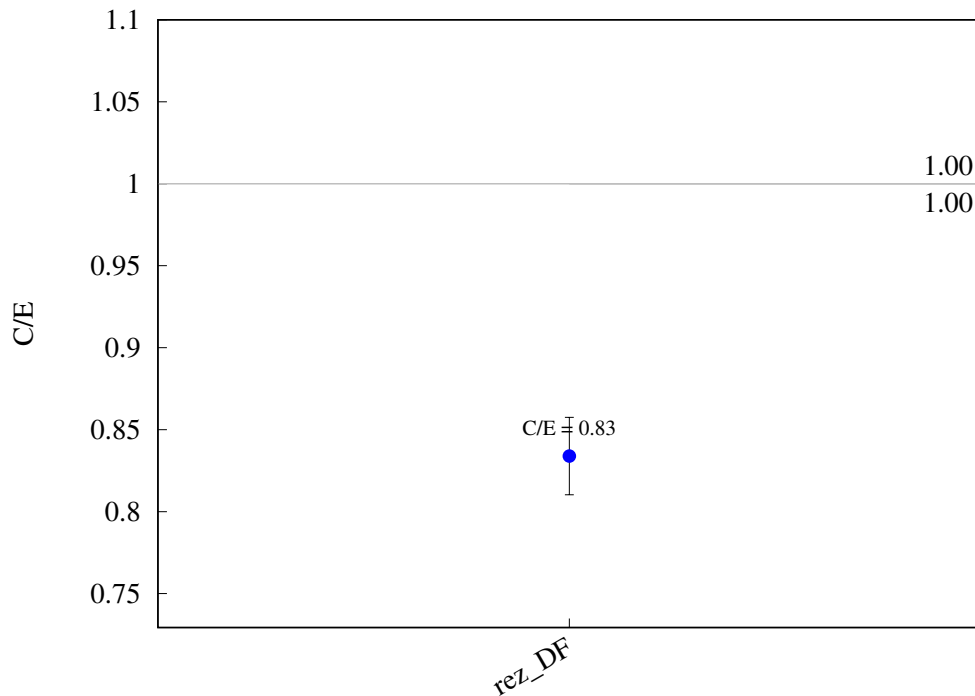
^{204}Pb (n,2n) ^{203}Pb 

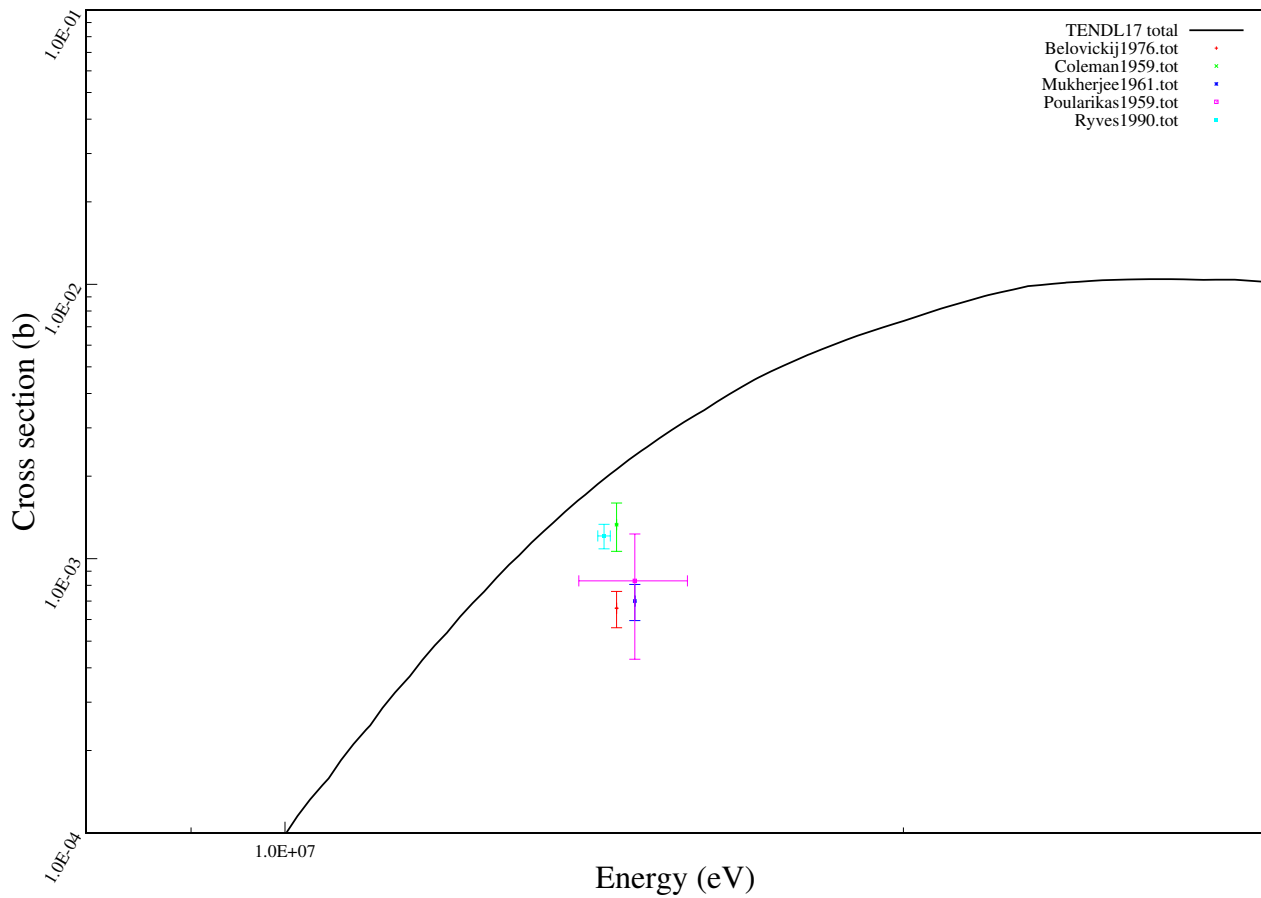
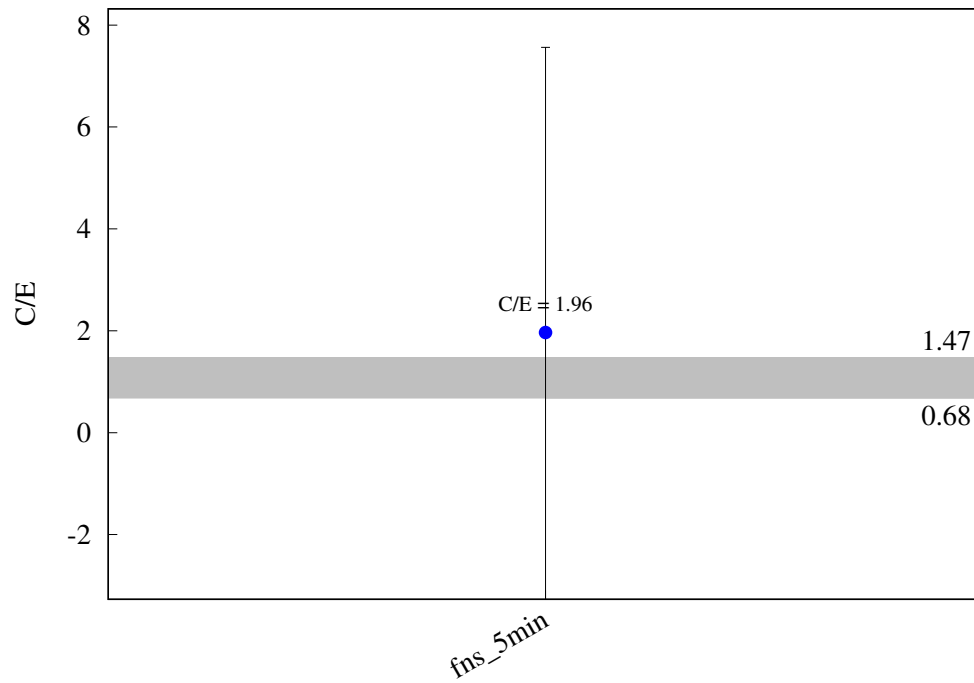
^{206}Pb (n,a) ^{203}Hg 

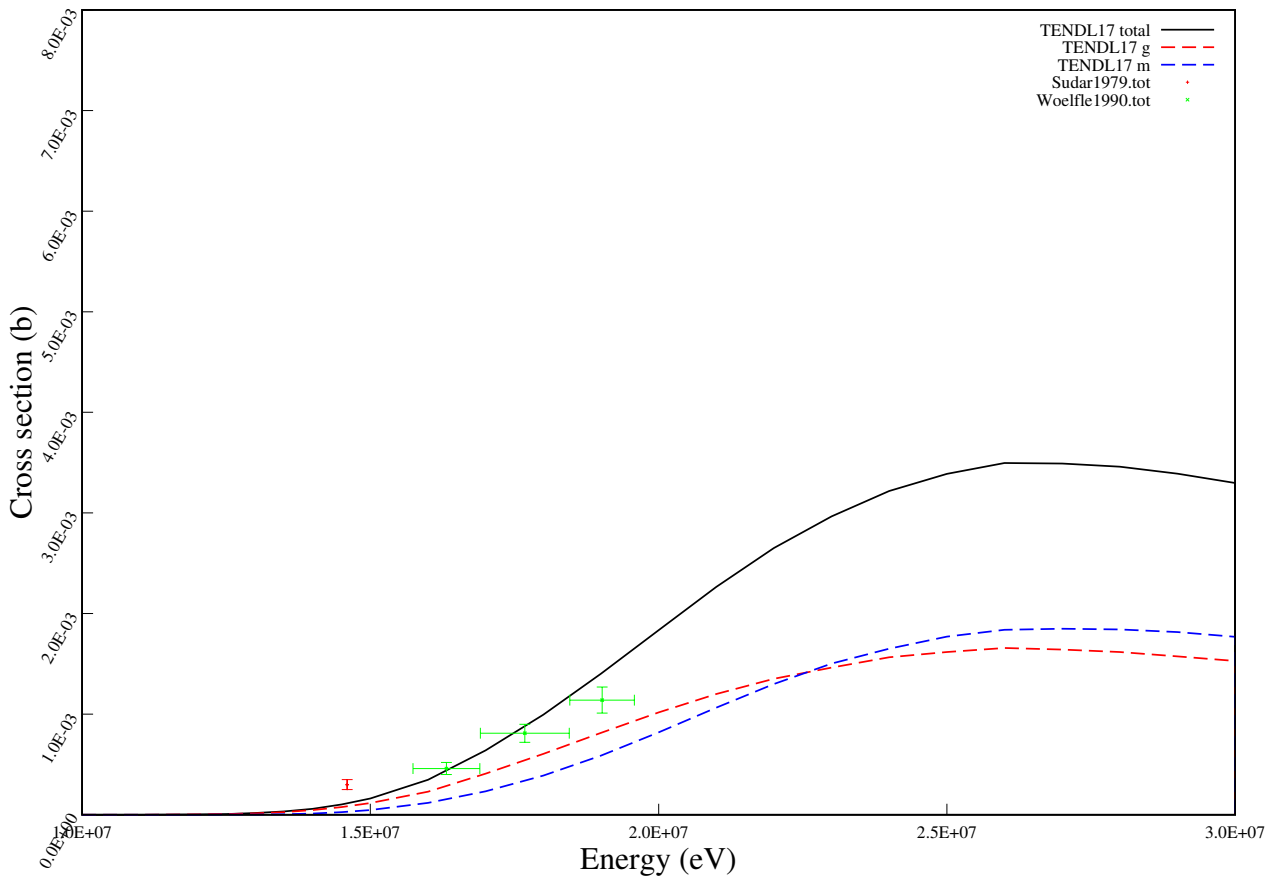
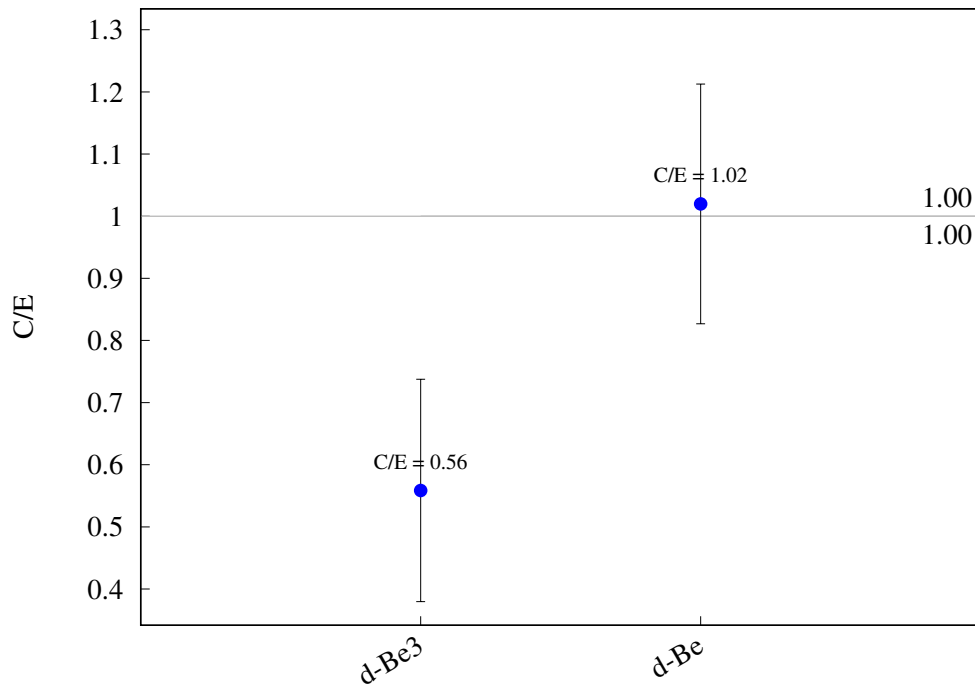
^{208}Pb (n,p) ^{208}Tl 

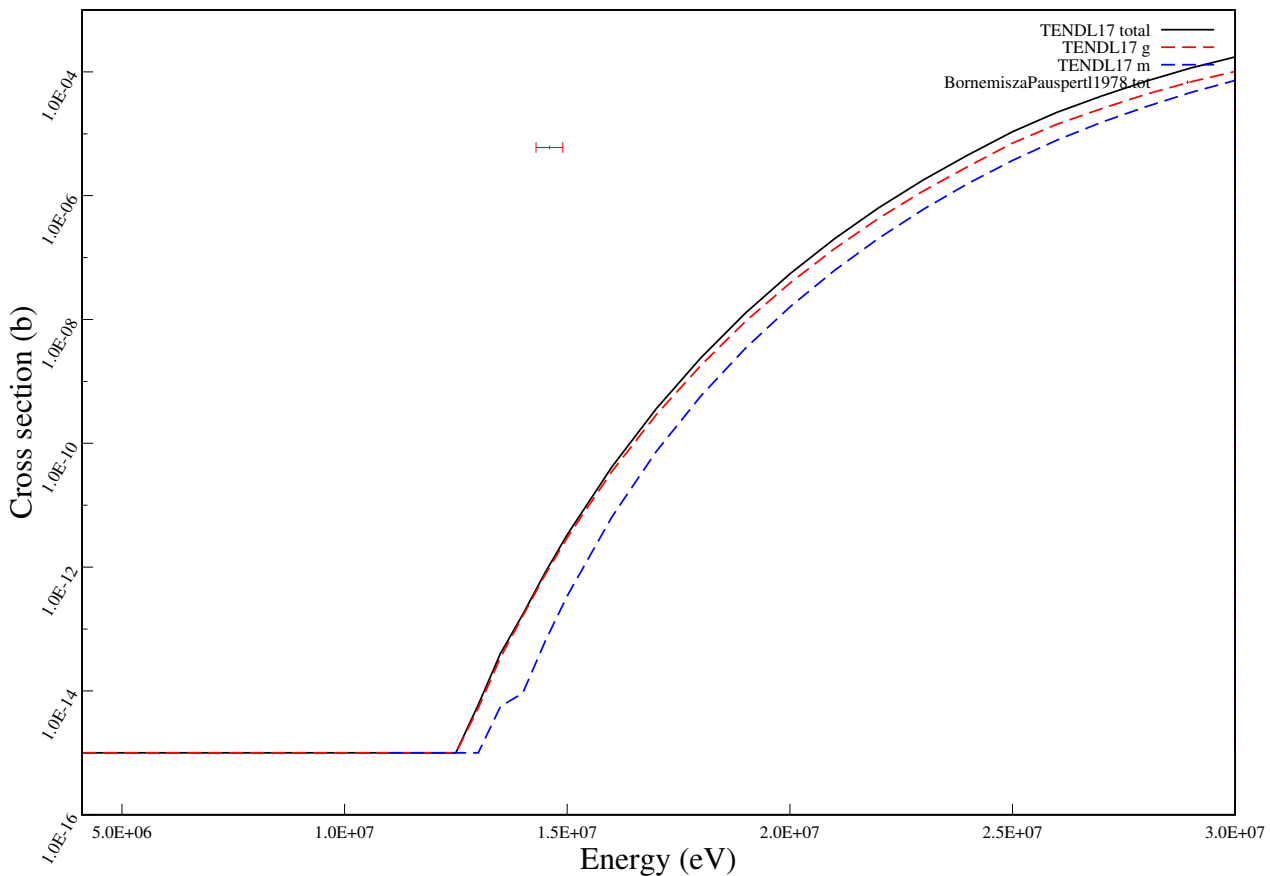
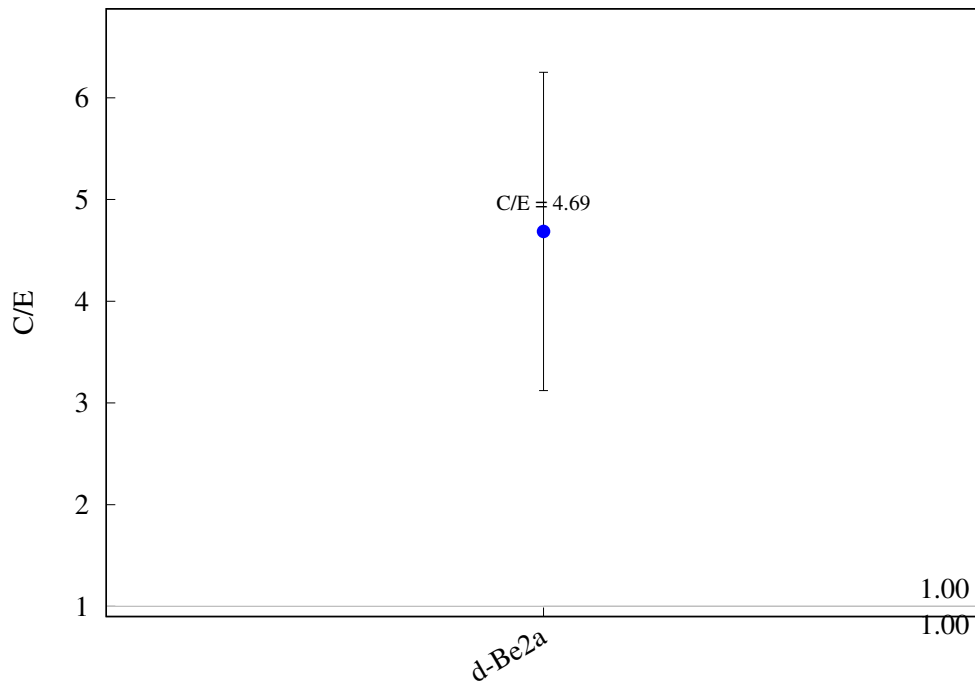
$^{208}\text{Pb} (\text{n},\text{t}) ^{206}\text{Tl}$ 

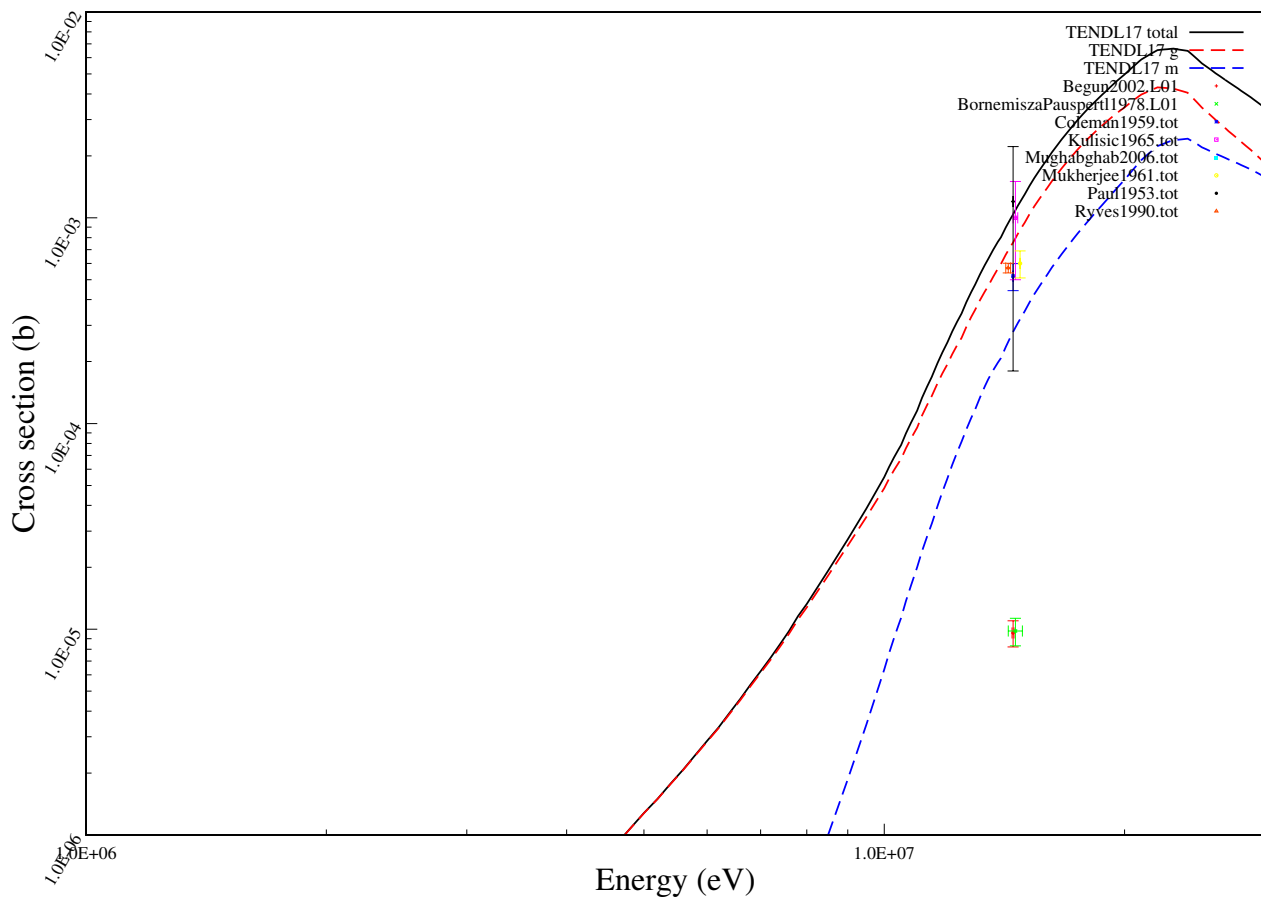
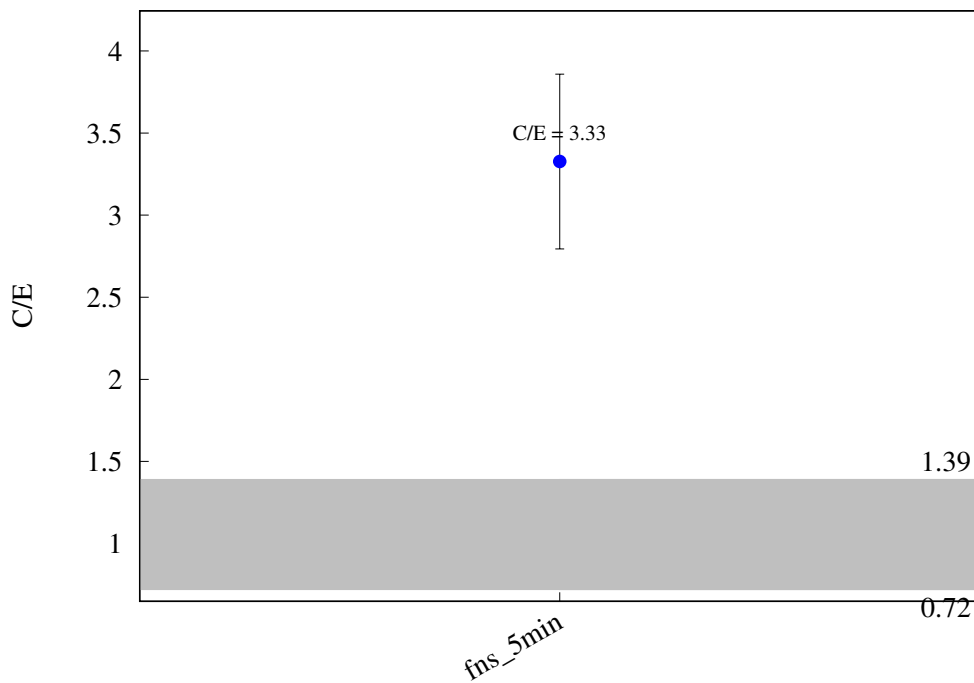
^{209}Bi (n,3n) ^{207}Bi 



^{209}Bi (n,p) ^{209}Pb 

$^{209}\text{Bi} (\text{n},\text{t}) ^{207}\text{Pb}$ 

^{209}Bi (n,h) ^{207}Tl 

^{209}Bi (n,a) ^{206}Tl 

6 Discussion

The experiments considered in this report span several neutron spectra of considerably different physical systems, including a standard spontaneous fission source and deuteron accelerators producing d-T, d-Be and d-Li reactions. The measurements are made with a mix of spectroscopic techniques or total heat measurements with the majority of the data provided as effective cross-sections based on the simulation tools used at the time of the experiment. Care must be taken when claiming that a reaction has been ‘validated’, since the detailed structure of a cross-section is not fully probed (even with multiple experiments using complementary spectra) and a new experiment using a different spectrum could find discrepant results. Aside from the differences in experimental design, there is tremendous deviation in the quality of the spectral characterisations, simulation tools used to calculate data (ultimately including the effective cross section) and reporting of measurement methodologies. Many of the experimental data are exclusively available within JEFF/EFF-DOCs and have never been published in peer-reviewed journals. Even for experiments which have found their way to the peer-reviewed literature, essential details to assess the quality of the measurements are often missing. For example, the $^{93}\text{Nb}(\text{n},\text{a})^{90g}\text{Y}$ reported in [89] has no description of the methodology for identification of that nuclide. The authors of that report have kindly provided the experimental measurements which have been used to re-analyse the data, but only the FNS and FNG heat measurements have received this level of scrutiny in this report.

As the JAEA FNS decay heat measurements have the largest number of high-quality, comparable data sets, it is illustrative to isolate only these values, as shown in Figures 10 and 11. While in previous iterations the TENDL values experienced more fluctuation between releases, the continuity between 2014-2017 is significant. Some few improvements have been made with detailed re-evaluation of input TALYS parameters, while some small number of discrepancies persist. Those highlighted in the figures are the remaining concerns for fusion decay heat analyses – so far as experimental data exist.

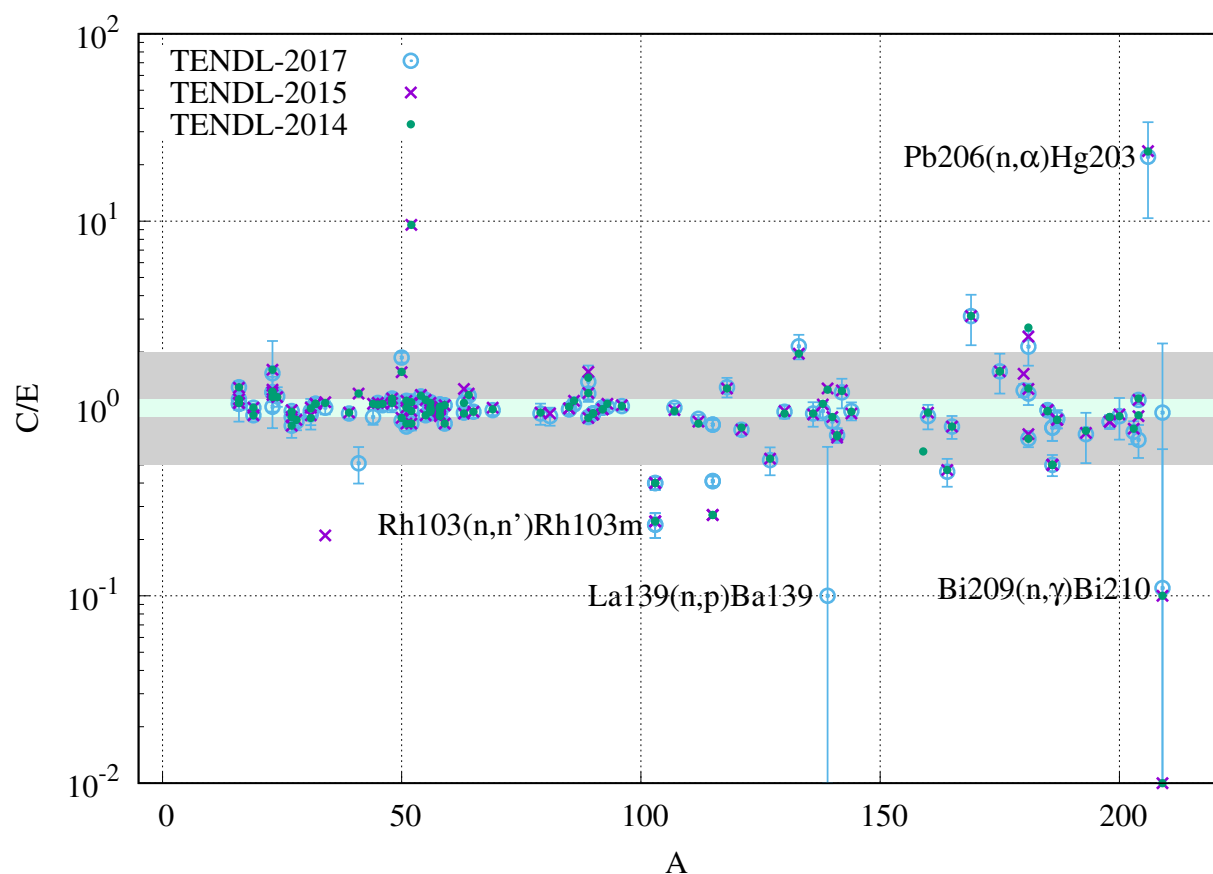


Figure 10: Comparison of all TENDL-2017,-2015,-2014 C/E values for dominant radionuclide cross sections in FNS decay heat measurements.

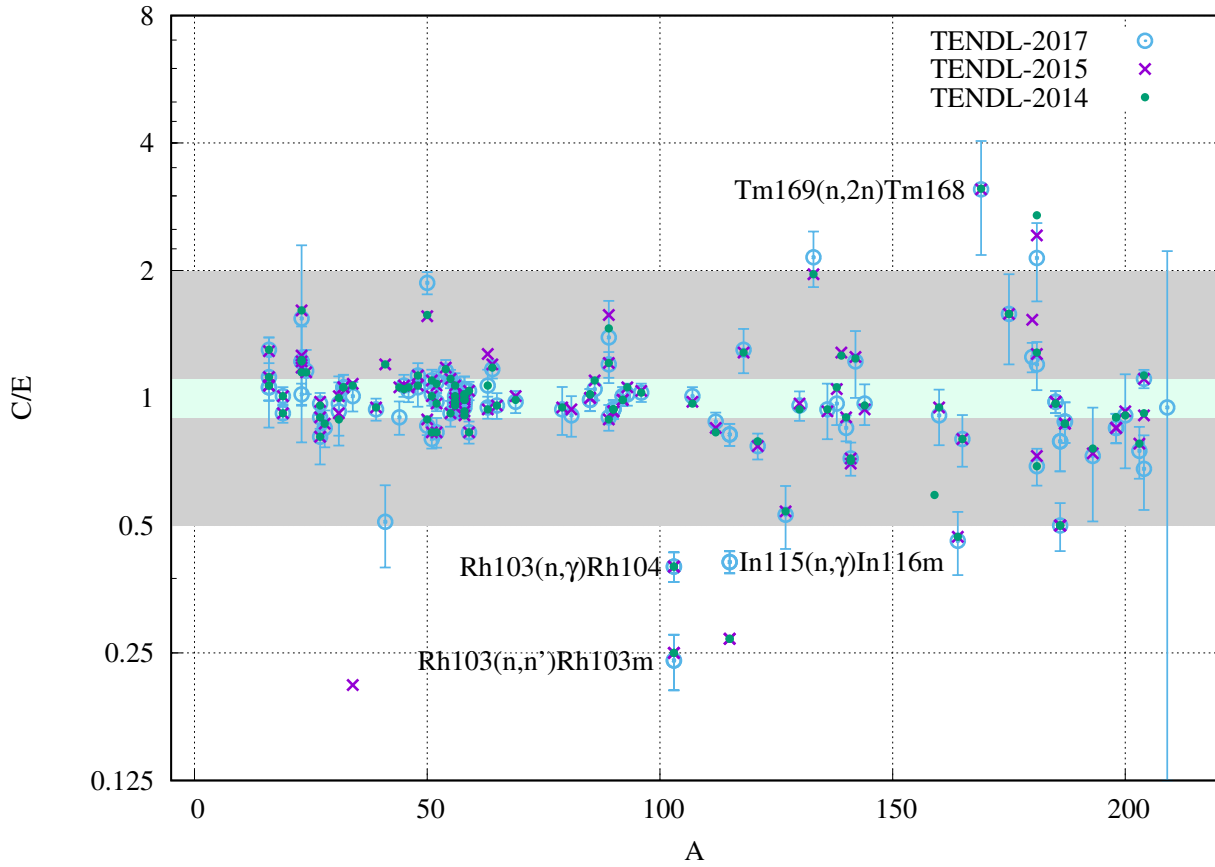


Figure 11: Comparison of all TENDL-2017,-2015,-2014 C/E values for dominant radionuclide cross sections in FNS decay heat measurements. Values more than one order of magnitude have been excluded for detail on the remaining values.

The data presented here can however point toward reactions which are less well characterised. Differential data may not be available for some reactions or not available in the various energy regions which are required. Substantial discrepancy in integral values may be used to direct the next experimental campaigns and lead to long-term nuclear data improvement. Whether or not one integral measurement on a relatively poorly known cross section (for example, many (n,t) or (n,h) reactions) is worthy of renormalising TALYS outputs is the concern of evaluators. It is the responsibility of the interested reader to delve into the details of the measurements when considering any of these reactions and absence from this table should not be considered an implicit claim that the reaction has been validated.

Whatever limitations exist within the set of experimental data, nuclear simulations will be carried out using a suitable nuclear data library and comparisons between the available data sources can provide useful information for analysts. Taking the same set

of reactions with both TENDL-2017 and the previous EAF-2010 data, the distribution of C/E values is shown in Figure 12. Note that the x -axis is shown in equal log(C/E) intervals, which gives a symmetric visualisation of the distribution.

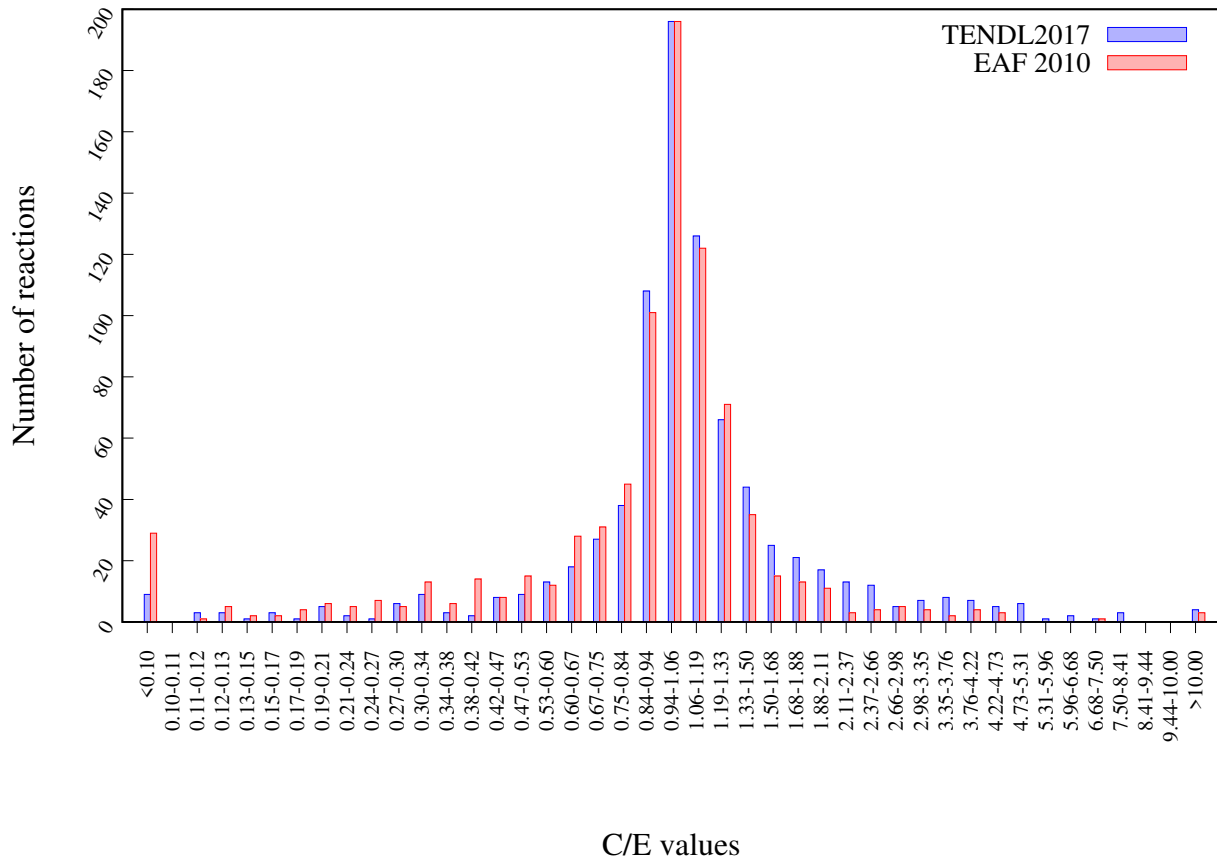


Figure 12: C/E distribution for TENDL-2017 and EAF-2010 given in equal log(C/E) spacing.

The distributions show a generally similar, but slightly better agreement for TENDL-2017. The log-mean $\overline{C/E}$ value,

$$\text{Log} \left(\overline{C/E} \right) = \frac{1}{n} \sum_{i=1}^n \text{Log} (C_i/E_i), \quad (8)$$

for TENDL-2017 is 1.046, while the EAF-2010 data yields a surprising 0.850. This can be intuitively seen in the skewed EAF distribution of C/E values, indicating a systematic under-prediction for the integral values of this report. The fact that TENDL provides a more symmetric distribution should not be surprising; the data is derived

from physical parameters which globally govern the production of reaction information. In comparison, the asymmetry of EAF belies its methodology, where pathways are included depending on an evaluator's judgement. As a result, pathways are missing or under-represented and result in an overall under-prediction for nuclide production.

Two reactions which has been reportedly measured for the production of isomers are not included in the TENDL-2017 library: $^{181}\text{Ta}(\text{n},\text{t})^{179n}\text{Hf}$ and $^{197}\text{Au}(\text{n},\text{a})^{194m}\text{Ir}$. The original reports for these measurements have been checked, which describe measurements of the specific gamma lines which correspond with levels in the RIPL database [90]. Both reactions additionally has differential EXFOR entries which support the integral measurement and the inelastic certainly produces this isomer, which should be present in the library. The tantalum case was previously reported [12], while the gold reaction channel is due to a error in the MF=9 of the ^{197}Au file, which is missing the second entry for the isomer.

Of the remaining seven reactions with C/E less than 0.10, six come from the more dubious d-Be (n,t) or ^{252}Cf (n,g) reactions. The last comes from the $^{100}\text{Mo}(\text{n},\text{a})$ from the FZK d-Li experiment, where TENDL shows reasonable agreement with all of the modern differential data. Of the two cases with C/E greater than 10, one is the $^{182}\text{W}(\text{n},\text{a})^{179n}\text{Hf}$, where the recent differential experiments support the integral measurement and suggest an over-estimation from TENDL.

Note the TALYS format errors in MF=9 production that were documented in a previous report [12] have been corrected. The mis-allocation of branching ratios for $^{92}\text{Mo}(\text{n},\text{p})$ and $^{115}\text{In}(\text{n},\text{g})$ were isolated errors, but in particular for the ^{115}In case the correction significantly improves agreement with experiment.

It should be noted that the EAF library was constructed and modified with knowledge of these integral measurements, which were used as justification for renormalisations leading to better agreement with the experiments. That TENDL-2017 *blindly* predicts these effective cross-sections, using physical parameters, with greater accuracy than a library tuned by renormalisations is quite remarkable.

When the standard international libraries are used to calculate the effective cross-sections considered the distribution shows a tremendous lack of data, as depicted in Figure 13. The most notable difference here is that approximately *one third of the C/E values are less than 0.1*, with a large majority of these being precisely zero due to missing reactions. This is not unexpected, since these libraries do not contain the data required for activation-transmutation simulations and should not be relied upon or trusted for such analysis. However, it is troublesome since it is often claimed that those libraries are validated for various applications that require these (and many other) reactions.

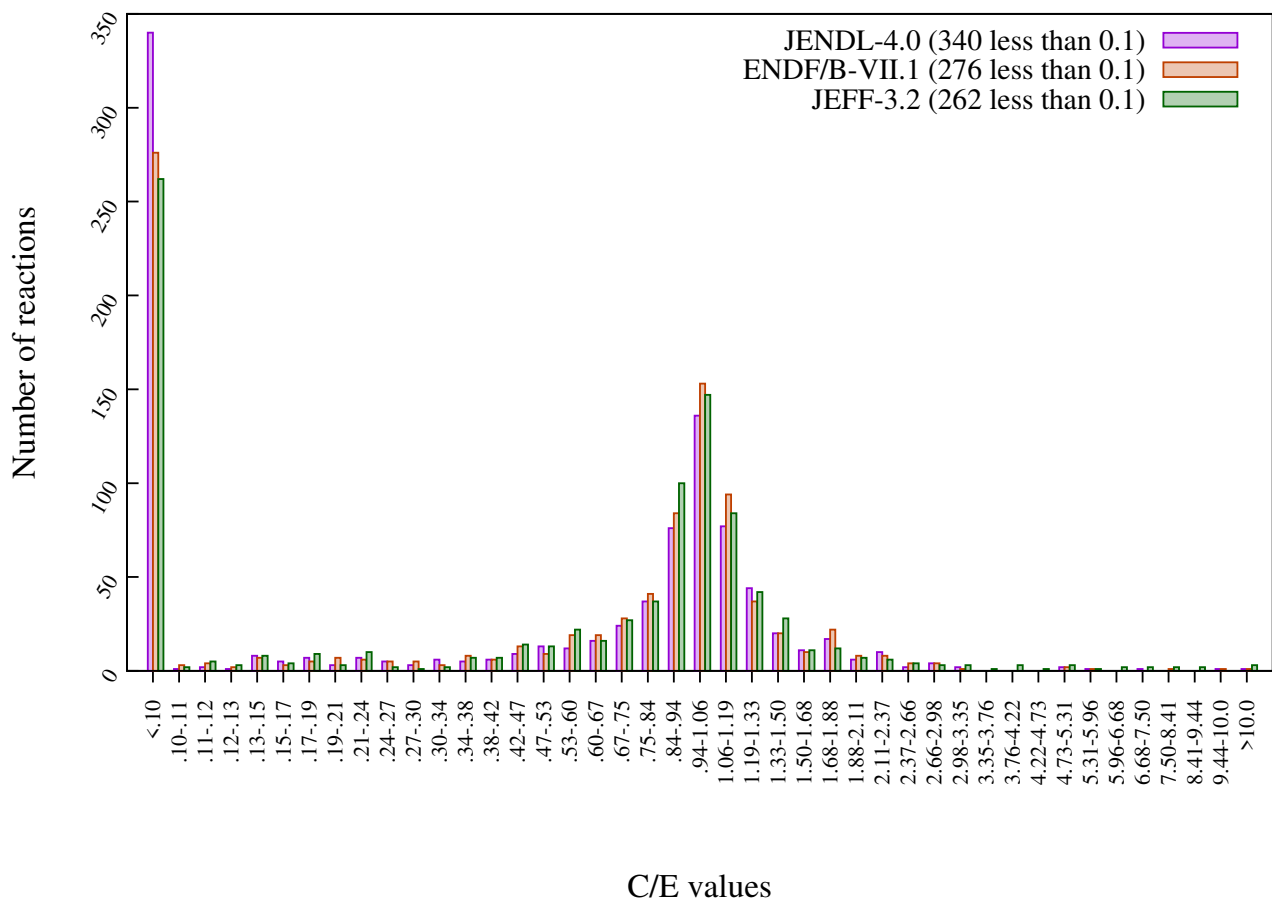


Figure 13: C/E distribution for JENDL-4.0, ENDFB/VII.1 and JEFF3.2 in equal log(C/E) spacing.

References

- [1] A. Koning and D. Rochman, "Modern Nuclear Data Evaluation with the TALYS Code System," *Nuclear Data Sheets*, vol. 113, no. 12, pp. 2841 – 2934, 2012. Special Issue on Nuclear Reaction Data.
- [2] A. J. Koning, D. Rochman, *et al.*, "TENDL-2017." Release Date: December 29, 2017. Available from https://tendl.web.psi.ch/tendl_2017/tendl2017.html.
- [3] Rochman, D., Koning, A.J., Sublet, J.Ch., Fleming, M., Bauge, E., Hilaire, S., Romain, P., Morillon, B., Duarte, H., Goriely, S., van der Marck, S.C., Sjstrand, H., Pomp, S., Dzysiuk, N., Cabellos, O., Ferroukhi, H., and Vasiliev, A., "The TENDL library: Hope, reality and future," *EPJ Web Conf.*, vol. 146, p. 02006, 2017.
- [4] M. Fleming, T. Stainer, and M. Gilbert, "FISPACT-II User Manual," Tech. Rep. UKAEA-R(18)001, UKAEA, Jan. 2018.
- [5] J.-Ch. Sublet, J. Eastwood, J. Morgan, M. Gilbert, M. Fleming, and W. Arter, "FISPACT-II: An Advanced Simulation System for Activation, Transmutation and Material Modelling," *Nuclear Data Sheets*, vol. 139, pp. 77 – 137, 2017. Special Issue on Nuclear Reaction Data.
- [6] J.-Ch. Sublet and F. Maekawa, "Decay Power: A Comprehensive Experimental Validation," Tech. Rep. CEA-R-6213, ISSN 0429 - 3460, CEA, 2009. Alternative Energies and Atomic Energy Commission.
- [7] M. Gilbert and J-Ch.. Sublet, "Decay heat validation, FISPACT-II & TENDL-2017, JEFF-3.3, ENDF/B-VIII.0, EAF2010, and IRDFF-1.05 nuclear data libraries," Tech. Rep. UKAEA-CCFE-R(18)002, CCFE, 2018.
- [8] R. Forrest, M. Pillon, U. v. Moellendorff, and K. Seidel, "Validation of EASY-2001 using integral measurements," Tech. Rep. UKAEA-FUS-467, United Kingdom, 2001.
- [9] R. Forrest, M. Pillon, U. v. Moellendorff, K. Seidel, J. Kopecky, and J.-C. Sublet, "Validation of EASY-2003 using integral measurements," Tech. Rep. UKAEA-FUS-500, United Kingdom, 2003.
- [10] R. Forrest, M. Pillon, U. v. Moellendorff, K. Seidel, J. Kopecky, P. Bém, M. Honusek, and E. Šimecková, "Validation of EASY-2005 using integral measurements," Tech. Rep. UKAEA-FUS-526, United Kingdom, 2006.
- [11] R. Forrest, M. Pillon, J. Kopecky, A. Klix, S. P. Simakov, J.-C. Sublet, P. Bém, M. Honusek, and E. Šimecková, "Validation of EASY-2007 using integral measurements," Tech. Rep. UKAEA-FUS-547, United Kingdom, 2008.
- [12] M. Fleming, J-Ch.. Sublet, and J. Kopecky, "Integro-Differential Verification and Validation, FISPACT-II & TENDL-2014, nuclear data libraries," Tech. Rep. CCFE-R(15)27, CCFE, Mar. 2015.

- [13] A. J. Koning, D. Rochman, *et al.*, “TENDL-2014.” Release Date: December 11, 2014. Available from <ftp://ftp.nrg.eu/pub/www/talys/tendl2014/tendl2014.html>.
- [14] J. Kopecky, “Validation of FENDL-3/A Library using Integral Measurements,” Tech. Rep. INCD(NED)-011, JUKO, August 2012.
- [15] J. Kopecky, “Validation of activation cross sections in large libraries,” Tech. Rep. JEF/DOC-1575, JUKO, April 2014.
- [16] J. Kopecky, “Final verification and validation of JEFF-3.2,” Tech. Rep. JEF/DOC-1590, JUKO, November 2014.
- [17] M. Fleming and J-Ch.. Sublet, “Maxwellian-Averaged Neutron-Induced Cross Sections for kT=1 keV to 100 keV, KADoNiS, TENDL-2017,-2014, ENDF/B-VIII.0,-VII.1, JEFF-3.3,-3.2, JENDL-4.0u, and EAF-2010 nuclear data,” Tech. Rep. UKAEA-R(18)005, UKAEA, feb 2018.
- [18] EXFOR: Experimental Nuclear Reaction Data, www-nds.iaea.org/exfor/.
- [19] P. Reimer, V. Avrigeanu, S. V. Chuvaev, A. A. Filatenkov, T. Glodariu, A. Koning, A. J. M. Plomp, S. M. Qaim, D. L. Smith, and H. Weigmann, “Reaction mechanisms of fast neutrons on stable Mo isotopes below 21 MeV,” vol. 044617, pp. 1–20, 2005.
- [20] H. Sakane, Y. Kasugai, M. Shibata, H. Takeuchi, and K. Kawade, “Measurements of the (n, np+d) activation cross sections with 13.4-14.9 MeV neutrons using a fusion neutronics source/JAERI,” *Annals of Nuclear Energy*, vol. 30, no. 18, pp. 1847 – 1862, 2003.
- [21] F. Maekawa, C. Konno, Y. Kasugi, Y. Oyama, and Y. Ikeda, “Data collection of fusion neutron benchmark experiments conducted at FNS/JAERI,” Tech. Rep. JAERI-Data/Code 98-021, FNS/JAERI, 1998.
- [22] F. Maekawa, M. Wada, and Y. Oyama, “Compilation of benchmark results for fusion related Nuclear Data,” Tech. Rep. JAERI-Data/Code 989-024, FNS-JAERI, 1998.
- [23] F. Maekawa, M. Wada, and Y. Ikeda, “Decay heat experiment and validation of calculation code system for fusion reactor,” Tech. Rep. JAERI-Data/Code 98-055, FNS/JAERI, 1999.
- [24] F. Maekawa and Y. Ikeda, “Decay heat experiment on thirty-two fusion reactor relevant materials irradiated by 14-MeV neutrons,” *Fusion Engineering and Design*, vol. 47, no. 4, pp. 377 – 388, 2000.
- [25] F. Maekawa, K.-i. Shibata, Y. Ikeda, H. Takeuchi, and M. Wada, *Comprehensive activation experiment with 14-MeV neutrons covering most of naturally existing elements 5 minutes irradiation experiment*. Japan: Atomic Energy Society of Japan, 2002.

- [26] V. D. Kovalchuk, A. V. Krasilnikov, V. M. Bagaev, S. I. Bobrovnik, V. D. Kovalchuk, and V. I. Trotsik, "Neutron generator sneg-13: neutron and photon field characteristics," Tech. Rep. IAE-5589/8, Russian Research Centre 'Kurchatov Institute', Moscow, 1992.
- [27] K. Seidel, R. A. Forrest, H. Freiesleben, V. D. Kovalchuk, D. V. Markovskij, D. Richter, V. I. Tereshkin, and S. Unholzer, "Measurement and analysis of radioactivity induced by 14-MeV neutrons in steels and vanadium alloys," Tech. Rep. TUD-IKTP/99-02, TUD, 1999.
- [28] H. Freiesleben, D. Richter, K. Seidel, and S. Unholzer, "Activation of steels and vanadium alloys," Tech. Rep. EFF DOC-617, 1997.
- [29] H. Freiesleben, V. Kovalchuk, D. Markovskij, K. Seidel, V. Tereshkin, and S. Unholzer, "Experimental investigation of radioactivities induced in fusion reactor materials by 14-MeV neutrons," *Fusion Engineering and Design*, vol. 42, pp. 337–341, Sept. 1998.
- [30] K. Seidel, R. Forrest, H. Freiesleben, V. Kovalchuk, D. Markovskij, D. Richter, V. Tereshkin, and S. Unholzer, "Experimental investigation of radioactivity induced in the fusion power plant structural material SiC and in the breeder material Li₄SiO₄ by 14-MeV neutrons," *Fusion Engineering and Design*, vol. 58-59, pp. 585–590, Nov. 2001.
- [31] K. Seidel, "Activation experiment in the 14 MeV fusion peak neutron spectrum," Tech. Rep. EFF-DOC-739, 2000.
- [32] K. Seidel, R. Eichin, R. Forrest, H. Freiesleben, S. Goncharov, V. Kovalchuk, D. Markovskij, D. Maximov, and S. Unholzer, "Activation experiment with tungsten in fusion peak neutron field," *Journal of Nuclear Materials*, vol. 329-333, pp. 1629–1632, Aug. 2004.
- [33] R. Eichin, R. A. Forrest, H. Freiesleben, S. A. Goncharov, V. D. Kovalchuk, D. V. Markovskij, D. V. Maximov, K. Seidel, and S. Unholzer, "Measurement and analysis of induced activation in CuCrZr irradiated in fusion peak neutron field," Tech. Rep. EFF-DOC-858, 2003.
- [34] R. Eichin, R. A. Forrest, H. Freiesleben, K. Seidel, and S. Unholzer, "Validation experiment of gamma activities of yttrium irradiated in fusion peak neutron field," Tech. Rep. TUD-IKTP/02-03, TUD, 2003.
- [35] R. Eichin, R. A. Forrest, H. Freiesleben, K. Seidel, and S. Unholzer, "Validation experiment of gamma activities of tantalum irradiated in fusion peak neutron spectrum," Tech. Rep. TUD-IKTP/01-05, TUD, 2003.
- [36] R. Eichin, R. A. Forrest, H. Freiesleben, K. Seidel, and S. Unholzer, "Validation experiment of gamma activities of pb irradiated in fusion peak neutron field," Tech. Rep. TUD-IKTP/01-04, TUD, 2004.

- [37] A. Klix, R. A. Forrest, H. Freiesleben, K. Schomburg, K. Seidel, and S. Unholzer, “Validation experiment of gamma activities of la and er irradiated in a fusion peak neutron spectrum,” Tech. Rep. EFF-DOC-971, 2006.
- [38] A. Klix, R. A. Forrest, H. Freiesleben, K. Schomburg, K. Seidel, and S. Unholzer, “Validation experiment of gamma activities of erbium irradiated in fusion peak neutron spectrum,” Tech. Rep. TUD-IKTP/01-2008, 2008.
- [39] K. Seidel, R. A. Forrest, H. Freiesleben, A. Klix, K. Schomburg, and S. Unholzer, “Validation experiment of gamma activities of lanthanum irradiated in fusion peak neutron spectrum,” Tech. Rep. TUD-IKTP/02-06, 2006.
- [40] F. Maekawa, U. von Möllendorff, P. P. H. Wilson, and Y. Ikeda, “Determination of a deuteron-beryllium neutron source spectrum by multifoil activation,” *Fusion Science and Technology*, vol. 36, no. 2, pp. 165–172, 1999.
- [41] U. V. Möllendorff, H. Giese, and F. Maekawa, “Integral activation experiments on fusion relevant materials using a white fast-neutron field,” Tech. Rep. FZKA-6684, Forschungszentrum Karlsruhe, 2002.
- [42] F. Maekawa, U. von Möllendorff, M. Wada, P. Wilson, and Y. Ikeda, “Determination of neutron spectra formed by 40-MeV deuteron bombardment of a lithium target with multi-foil activation technique,” *Fusion Engineering and Design*, vol. 51, no. 0, pp. 815 – 820, 2000.
- [43] U. von Möllendorff, F. Maekawa, H. Giese, and P. Wilson, “Experimental test of structural materials activation in the IFMIF neutron spectrum,” *Fusion Engineering and Design*, vol. 51, pp. 919 – 924, 2000.
- [44] U. von Möllendorff, H. Giese, H. Feuerstein, and F. Maekawa, “A nuclear simulation experiment for the international fusion materials irradiation facility (ifmif),” Tech. Rep. FZKA-6764, Germany, 2002.
- [45] M. Pillon, M. Angelone, P. Batistoni, R. Forrest, and J. C. Sublet, “Benchmark Experiments of Fusion Neutron Induced Gamma-Ray Radioactivity in Various Structural Materials,” *Journal of Radioanalytical and Nuclear Chemistry*, vol. 244, pp. 441–445, 05 2000.
- [46] M. Pillon and M. Angelone, “Status report on irradiation of F82H steel,” Tech. Rep. EFF-DOC-591, 1997.
- [47] M. Pillon, “Final report on irradiation of f82h steel,” Tech. Rep. EFF-DOC-609, 1997.
- [48] M. Pillon, “Further measurements on EUROFER-97 using low background HPGe detector,” Tech. Rep. EFF-DOC-778, 2001.
- [49] M. Pillon and M. Angelone, “1st intermediate report on irradiation of sic/sic composite,” Tech. Rep. EFF-DOC-437, 1995.

- [50] M. Pillon, "Status report on irradiation of sic/sic composite," Tech. Rep. EFF-DOC-495, 1996.
- [51] M. Pillon, "Final report on irradiation of tungsten," Tech. Rep. EFF-DOC-671, 1999.
- [52] M. Pillon, "First results about irradiation of chromium samples," Tech. Rep. EFF-DOC-793, 2001.
- [53] M. Pillon, "Measurements of nuclear decay heat and gamma activation in hafnium samples," Tech. Rep. EFF-DOC-794, 2001.
- [54] M. Pillon, "Measurement and analysis of nuclear decay heat in cucrzs," Tech. Rep. EFF-DOC-838, 2002.
- [55] M. Pillon, M. Angelone, and R. A. Forrest, "Development of a spectrometer to measure photon and electron decay heat from radionuclides," (Tsukuba, Japan), International Conference on Nuc. Data Sci. Tech., 2001.
- [56] M. Pillon, "Measurements of Nuclear Decay Heat and Gamma Activation in Hafnium Samples," Tech. Rep. EFF-DOC-794, 2001.
- [57] M. Pillon, "Measurements of decay heat and validation of the European activation code system for fusion power plant applications," Tech. Rep. EFF-DOC-812, 2002.
- [58] M. Pillon, "Preliminary measurements and analysis of nuclear decay heat in sc, sm, gd and dy," Tech. Rep. EFF-DOC-862, 2003.
- [59] M. Pillon, "Nuclear decay heat in yttrium, revised measurements and analysis," Tech. Rep. EFF-DOC-903, 2004.
- [60] M. Pillon, "Decay heat in molybdenum irradiated in a first-wall like neutron spectrum. measurement and analyses," Tech. Rep. FUS-TN-MA-NE-R-13, ENEA, December 2005.
- [61] M. Pillon, "Decay heat in tantalum irradiated in a first-wall like neutron spectrum. measurement and analyses," Tech. Rep. FUS-TN-MA-NE-R-11, ENEA, 2005.
- [62] M. Pillon, "Measurements of nuclear decay heat in Rhenium and comparison with EASY-2007 predictions," Tech. Rep. EFF-DOC-1025, 2007.
- [63] M. Pillon, "Measurements of decay heat in tin," Tech. Rep. EFF-DOC-962, 2006.
- [64] M. Pillon, "Measurements of decay heat in tin irradiated in a first-wall like neutron spectrum. measurement and analyses," Tech. Rep. FUS-TN-MA-NE-R-20, ENEA, 2006.
- [65] S. Qaim, R. Wölfle, and G. Stöcklin, "Fast neutron induced $[(n,t) + (n,n't)]$ reaction cross-sections in the medium and heavy mass regions," *Journal of Inorganic and Nuclear Chemistry*, vol. 36, no. 12, pp. 3639 – 3642, 1974.

- [66] S. Qaim and R. Wölfle, "Triton emission in the interactions of fast neutrons with nuclei," *Nuclear Physics A*, vol. 295, no. 1, pp. 150 – 162, 1978.
- [67] C. Wu, R. Wölfle, and S. Qaim, "Activation and mass spectrometric study of ${}^3\text{He}$ particle emission in the interactions of fast neutrons with medium mass nuclei," *Nuclear Physics A*, vol. 329, no. 1, pp. 63 – 72, 1979.
- [68] S. M. Qaim, S. Khatun, and R. Woelfle, "Integral cross section measurements on (n,x) reactions induced by 30 MeV d(Be) break-up neutrons on FRT wall and structural materials," Tech. Rep. DOE/NDC-21/L(Vol2), United States, 1980.
- [69] S. Qaim, C. Wu, and R. Wölfle, " ${}^3\text{He}$ particle emission in fast neutron induced reactions," *Nuclear Physics A*, vol. 410, no. 3, pp. 421 – 428, 1983.
- [70] R. Wölfle, S. Khatun, and S. Qaim, "Triton-emission cross sections with 30 MeV d(Be) break-up neutrons," *Nuclear Physics A*, vol. 423, no. 1, pp. 130 – 138, 1984.
- [71] R. Wölfle, S. Sudár, and S. M. Qaim, "Determination of Excitation Function of Triton Emission Reaction on Aluminum from Threshold up to 30 MeV via Activation in Diverse Neutron Fields and Unfolding Code Calculations," *Nuclear Science and Engineering*, vol. 91, pp. 162–172, October 1985.
- [72] A. Mannan, I. H. Qureshi, M. Z. Iqbal, R. Woelfle, and S. M. Qaim, "Integral tests of differential cross sections for (n, α) and (n,2n) reactions on niobium," vol. 51, no. 2, pp. 49 – 53, 1990.
- [73] R. Wölfle, A. Suhaimi, and S. M. Qaim, "Determination of the Excitation Function of the (n,xt) Process on Beryllium via Activation in Diverse Neutron Fields and Unfolding Code Calculations," *Nuclear Science and Engineering*, vol. 115, pp. 71–75, September 1993.
- [74] L. Oláh, A. El-Megrab, A. Fenyvesi, A. Majdeddin, R. Dóczsi, V. Semkova, S. Qaim, and J. Csikai, "Investigations on neutron fields produced in ${}^2\text{H}(\text{d},\text{n}){}^3\text{He}$ and ${}^9\text{Be}(\text{d},\text{n}){}^{10}\text{B}$ reactions," *Nuclear Instruments and Methods in Physics Research Section A: Accelerators, Spectrometers, Detectors and Associated Equipment*, vol. 404, no. 2, pp. 373 – 380, 1998.
- [75] M. I. Majah, A. Chiadli, S. Sudár, and S. Qaim, "Cross sections of (n,p), (n, α) and (n,2n) reactions on some isotopes of zirconium in the neutron energy range of 10 MeV and integral tests of differential cross section data using a 14meV d(Be) neutron spectrum," *Applied Radiation and Isotopes*, vol. 54, no. 4, pp. 655 – 662, 2001.
- [76] I. Spahn, H. H. Coenen, and S. M. Qaim, "Enhanced production possibility of the therapeutic radionuclides ${}^{64}\text{Cu}$, ${}^{67}\text{Cu}$ and ${}^{89}\text{Sr}$ via (n,p) reactions induced by fast spectral neutrons," vol. 92, no. 3, pp. 183–186, 2004.
- [77] G. Schweimer, "Fast neutron production with 54 MeV deuterons," *Nuclear Physics A*, vol. 100, no. 3, pp. 537 – 544, 1967.

- [78] J. P. Meulders, P. Leleux, P. C. Macq, and C. Pirart, "Fast neutron yields and spectra from targets of varying atomic number bombarded with deuterons from 16 to 50 MeV (for radiobiology and radiotherapy)," *Physics in Medicine and Biology*, vol. 20, no. 2, p. 235, 1975.
- [79] P. Bém, V. Burjan, M. Götz, M. Honusek, U. Fischer, V. Kroha, U. von Möllendorff, J. Novák, S. Simakov, and E. Šimečková, "Activation of Eurofer in an IFMIF-like neutron field," *Fusion Engineering and Design*, vol. 75-79, pp. 829–833, Nov. 2005.
- [80] P. Bém, V. Burjan, U. Fischer, M. Honusek, M. Götz, V. Kroha, J. Novák, S. P. Simakov, and E. Šimečková, "Experimental determination of the NPI p-D₂O neutron source spectrum for activation benchmark tests," Tech. Rep. EFF-DOC-944, 2005.
- [81] P. Bém, V. Burjan, M. Götz, M. Honusek, V. Kroha, J. Novák, E. Šimečková, B. Esposito, M. Angelone, A. Pensa, and S. P. Simakov, "Testing of Dosimetry Foils in the IFMIF-like Neutron field, Report on the EFDA task TWO-TTMN-003, D8C," Tech. Rep. EXP(EFDA)-08/2004, NPI Řež, 2004.
- [82] P. Bém, V. Burjan, M. Götz, M. Honusek, U. Fischer, V. Kroha, U. v. Möllendorff, J. Novák, S. P. Simakov, and E. Šimečková, "Experiments for the validation of cross-sections up to 55 MeV in an IFMIF-like neutron spectrum: Activation experiment on Eurofer & neutron transport benchmark on iron," Tech. Rep. EXP(EFDA)-04/2004, NPI Řež, 2004.
- [83] P. Bém, V. Burjan, M. Götz, M. Honusek, U. Fischer, V. Kroha, J. Novák, and E. Šimečková, "Activation experiment on tungsten in the npi p-d₂o neutron field," Tech. Rep. EXP(EFDA)-09/2004, NPI Řež, 2004.
- [84] P. Bém, V. Burjan, M. Götz, M. Honusek, U. Fischer, V. Kroha, J. Novák, S. P. Simakov, and E. Šimečková, "Activation experiment on tantalum in the NPI p-D₂O neutron field," Tech. Rep. EXP(EFDA)-01/2005, NPI Řež, 2005.
- [85] P. Bém, V. Burjan, M. Götz, M. Honusek, U. Fischer, V. Kroha, J. Novák, S. Simakov, and E. Šimečková, "Activation experiment on chromium in the NPI p-D₂O neutron field," Tech. Rep. EFDA-TW6-TTMN-002-D06, NPI Řež, 2007.
- [86] S. Simakov, U. Fischer, P. Bém, V. Burjan, M. Götz, M. Honusek, V. Kroha, J. Novák, and E. Šimečková, "Pre- and post-analysis of the validation experiments for Cr activation cross sections up to 55 MeV in an IFMIF-like neutron spectrum," tech. rep., FZK, 2007.
- [87] W. Mannhart, "Evaluation of the Cf-252 Fission Neutron Spectrum between 0 MeV and 20 MeV," Tech. Rep. IAEA-TECDOC-410, IAEA, Vienna, 1987.
- [88] A. Koning, "Statistical Verification and Validation of the EXFOR database: (n,n'), (n,2n), (n,p), (n,a) and other neutron-induced threshold reaction cross-sections," Tech. Rep. NEA/DB/DOC(2014)3, OECD NEA Data Bank, September 2014.

- [89] M. Pillon, M. Angelone, and R. A. Forrest, “Measurements of decay heat and validation of the european activation code system for fusion power plant applications,” *Fusion Engineering and Design*, vol. 63-64, no. 0, pp. 101 – 106, 2002.
- [90] R. Capote, M. Herman, P. Obložinský, P. Young, S. Goriely, T. Belgya, A. Ignatyuk, A. Koning, S. Hilaire, V. Plujko, M. Avrigeanu, O. Bersillon, M. Chadwick, T. Fukahori, Z. Ge, Y. Han, S. Kailas, J. Kopecky, V. Maslov, G. Reffo, M. Sin, E. Soukhovitskii, and P. Talou, “RIPL Reference Input Parameter Library for Calculation of Nuclear Reactions and Nuclear Data Evaluations,” *Nuclear Data Sheets*, vol. 110, no. 12, pp. 3107 – 3214, 2009. Special Issue on Nuclear Reaction Data.

A Pathway analysis

This section contains a summary of all pathway analysis performed using FISPACT-II and the TENDL-2017 nuclear data library. Brief experimental descriptions and references to the original data sources are provided in section 3. The neutron spectra used in the calculations are displayed in each table caption and all paths which contribute at least 1% of the total pathway for the target nuclide are shown. Note that this analysis is required to accurately determine what fraction of the experimental observation (heat or activity) can be attributed to a specific reaction.

In comparison with the previous EASY/EAF integral data validation reports [8, 9, 10, 11], there are in many cases several reaction pathways available in TENDL which were not included in EAF. This has allowed corrections for measurements such as the Fe59 of FZK copper foil irradiation. The EAF validation report included a C/E of 0.006 for a 99% Co59(n,p) attributed to known Co impurities. TENDL includes the dominant Cu63(n,pa) pathway at 97.88%. Other additions include (n,O) reactions which represent reactions above 30 MeV. Note that these specifically *do not* declare the pathways responsible and the emitted particles, but only list the parent and residual nuclides. A large number of pathways become available at these energies and identifying the breakdown becomes a rather dubious process. Instead, when it is determined that (n,O) reactions are responsible for production of a target nuclide the report refrains from selecting an apportionment of sub-paths and leaves the reaction out of the validation. The (n,O) data can be found in MF=3 MT=5 as a lumped total, while the yields are found in MF=10 broken down by ejected particle.

A.1 Technische Universität Dresden data

Table 4: TUD (SNEG-13) pathways for V3Ti1Si (short irradiation) using spectrum sneg_1

Product	Pathway(s)	%
Al28	Si28(n,p)Al28	99.5
Ti51	V51(n,p)Ti51	99.1
V52	V51(n,g)V52	99.3

Table 5: TUD (SNEG-13) pathways for V4Ti4Cr (short irradiation) using spectrum sneg_1

Product	Pathway(s)	%
Ti45	Ti46(n,2n)Ti45	100.0
V52	V51(n,g)V52	35.3
	Cr52(n,p)V52	62.2
	Cr53(n,np)V52	1.5

Table 6: TUD (SNEG-13) pathways for V5Ti2Cr (short irradiation) using spectrum sneg_1

Product	Pathway(s)	%
V52	V51(n,g)V52	50.7
	Cr52(n,p)V52	47.9
Sc46	Ti46(n,p)Sc46	57.4
	Ti46(n,p)Sc46m(IT)Sc46	19.6
	Ti47(n,np)Sc46	18.1
	Ti47(n,d)Sc46	1.5
	Ti47(n,np)Sc46m(IT)Sc46	2.9
Sc47	Ti47(n,p)Sc47	37.1
	Ti48(n,np)Sc47	35.4
	Ti48(n,d)Sc47	13.9
	V50(n,a)Sc47	8.9
	V51(n,na)Sc47	4.7
Sc48	Ti48(n,p)Sc48	12.6
	V51(n,a)Sc48	87.4

Table 7: TUD (SNEG-13) pathways for V5Ti2Cr (long irradiation) using spectrum sneg_1

Product	Pathway(s)	%
V52	V51(n,g)V52	50.7
	Cr52(n,p)V52	47.9
Sc46	Ti46(n,p)Sc46	57.2
	Ti46(n,p)Sc46m(IT)Sc46	19.9
	Ti47(n,np)Sc46	18.0
	Ti47(n,d)Sc46	1.5
	Ti47(n,np)Sc46m(IT)Sc46	3.0
Sc47	Ti47(n,p)Sc47	37.2
	Ti48(n,np)Sc47	35.4
	Ti48(n,d)Sc47	13.9
	V50(n,a)Sc47	8.9
	V51(n,na)Sc47	4.7
Sc48	Ti48(n,p)Sc48	12.6
	V51(n,a)Sc48	87.9

Table 8: TUD (SNEG-13) pathways for V5Ti2Cr (long irradiation) using spectrum sneg_2

Product	Pathway(s)	%
V52	V51(n,g)V52	48.1
	Cr52(n,p)V52	51.3
Sc46	Ti46(n,p)Sc46	62.5
	Ti46(n,p)Sc46m(IT)Sc46	22.3
	Ti47(n,np)Sc46	12.2
	Ti47(n,np)Sc46m(IT)Sc46	1.6
Sc47	Ti47(n,p)Sc47	56.9
	Ti48(n,np)Sc47	18.0
	Ti48(n,d)Sc47	12.9
	V50(n,a)Sc47	12.1
Sc48	Ti48(n,p)Sc48	13.9
	V51(n,a)Sc48	86.7

Table 9: TUD (SNEG-13) pathways for Li₄SiO₄ using spectrum sneg_1

Product	Pathway(s)	%
Mg27	Al27(n,p)Mg27	2.6
	Si30(n,a)Mg27	96.4
Al28	Si28(n,p)Al28	99.4
Al29	Si29(n,p)Al29	97.7

Table 10: TUD (SNEG-13) pathways for SiC using spectrum sneg_1

Product	Pathway(s)	%
Mg27	Al27(n,p)Mg27	6.6
	Si30(n,a)Mg27	92.7
Al28	Si28(n,p)Al28	99.4
Al29	Si29(n,p)Al29	97.9

Table 11: TUD (SNEG-13) pathways for Eurofer97 (short irradiation) using spectrum sneg_1

Product	Pathway(s)	%
Mn56	Fe56(n,p)Mn56	99.4
Cr51	Cr52(n,2n)Cr51	87.9
	Fe54(n,a)Cr51	12.0
Mn54	Mn55(n,2n)Mn54	21.8
	Fe54(n,p)Mn54	78.2
Sc48	Ti48(n,p)Sc48	5.1
	V51(n,a)Sc48	94.9
Na24	Al27(n,a)Na24	100.0
Al28	Si28(n,p)Al28	99.2
Ti51	V51(n,p)Ti51	67.3
	Cr54(n,a)Ti51	32.6
V52	Cr52(n,p)V52	95.1
	Cr53(n,np)V52	2.3
	Mn55(n,a)V52	1.9
V53	Cr53(n,p)V53	98.6
Mn57	Fe57(n,p)Mn57	98.7
Fe53	Fe54(n,2n)Fe53	100.0

Table 12: TUD (SNEG-13) pathways for Eurofer97 using spectrum sneg_1

Product	Pathway(s)	%
Mn56	Fe56(n,p)Mn56	98.8
Cr51	Cr52(n,2n)Cr51	88.0
	Fe54(n,a)Cr51	12.0
Mn54	Mn55(n,2n)Mn54	21.8
	Fe54(n,p)Mn54	78.2
Sc48	Ti48(n,p)Sc48	5.1
	V51(n,a)Sc48	95.0
Na24	Al27(n,a)Na24	100.0
Al28	Si28(n,p)Al28	99.6
Ti51	V51(n,p)Ti51	67.3
	Cr54(n,a)Ti51	32.7
V52	Cr52(n,p)V52	95.3
	Cr53(n,np)V52	2.3
	Mn55(n,a)V52	1.9
V53	Cr53(n,p)V53	99.2
Mn57	Fe57(n,p)Mn57	99.4
Fe53	Fe54(n,2n)Fe53	100.0

Table 13: TUD (SNEG-13) pathways for Eurofer97 using spectrum sneg_2

Product	Pathway(s)	%
Mn56	Fe56(n,p)Mn56	99.0
Cr51	Cr52(n,2n)Cr51	85.4
	Fe54(n,a)Cr51	14.6
Mn54	Mn55(n,2n)Mn54	18.7
	Fe54(n,p)Mn54	81.3
Sc48	Ti48(n,p)Sc48	5.7
	V51(n,a)Sc48	94.5
Na24	Al27(n,a)Na24	100.0
Al28	Si28(n,p)Al28	99.8
Ti51	V51(n,p)Ti51	69.3
	Cr54(n,a)Ti51	30.7
V52	Cr52(n,p)V52	97.0
	Mn55(n,a)V52	1.8
V53	Cr53(n,p)V53	99.8

Product	Pathway(s)	%
Mn57	Fe57(n,p)Mn57	99.8
Fe53	Fe54(n,2n)Fe53	100.0

Table 14: TUD (SNEG-13) pathways for SS316 using spectrum sneg_1

Product	Pathway(s)	%
Fe59	Co59(n,p)Fe59	26.2
	Ni62(n,a)Fe59	72.5
Co57	Ni58(n,np)Co57	96.0
	Ni58(n,d)Co57	2.8
Co58	Ni58(n,p)Co58	59.2
	Ni58(n,p)Co58m(IT)Co58	37.9
Co60	Ni60(n,p)Co60m(IT)Co60	55.4
	Ni60(n,p)Co60	42.7
Ni57	Ni58(n,2n)Ni57	100.0
Zr89	Mo92(n,a)Zr89	75.0
	Mo92(n,a)Zr89m(IT)Zr89	25.2
Nb95	Mo95(n,p)Nb95	77.3
	Mo96(n,np)Nb95	8.8
	Mo96(n,d)Nb95	11.6
Nb96	Mo96(n,p)Nb96	91.9
	Mo97(n,np)Nb96	3.8
	Mo97(n,d)Nb96	4.6
Mo99	Mo100(n,2n)Mo99	100.0

Table 15: TUD (SNEG-13) pathways for F82H using spectrum sneg_1

Product	Pathway(s)	%
Na24	Al27(n,a)Na24	99.9
Sc48	V51(n,a)Sc48	98.7
Cr51	Cr52(n,2n)Cr51	85.8
	Fe54(n,a)Cr51	14.2
Mn54	Mn55(n,2n)Mn54	8.0
	Fe54(n,p)Mn54	92.0
Mn56	Fe56(n,p)Mn56	99.5
Ta182	W182(n,p)Ta182	48.6
	W182(n,p)Ta182m(IT)Ta182	41.3

Product	Pathway(s)	%
	W182(n,p)Ta182n(IT)Ta182m(IT)Ta182	4.3
	W183(n,d)Ta182	1.8
Ta183	W183(n,p)Ta183	78.8
	W184(n,np)Ta183	2.6
	W184(n,d)Ta183	6.4
	W186(n,a)Hf183(b-)Ta183	12.2
W187	W186(n,g)W187	100.0

Table 16: TUD pathways for yttrium using spectrum tud_Y

Product	Pathway(s)	%
Y88	Y89(n,2n)Y88	100.0
Y90m	Y89(n,g)Y90m	100.0

Table 17: TUD pathways for CuCrZr using spectrum tud_CuCrZr

Product	Pathway(s)	%
Cr51	Cr52(n,2n)Cr51	100.0
Co60	Cu63(n,a)Co60m(IT)Co60	52.0
	Cu63(n,a)Co60	48.0
Co61	Cu65(n,na)Co61	100.0
Co62m	Cu65(n,a)Co62m	99.7
Ni65	Cu65(n,p)Ni65	100.0
Cu62	Cu63(n,2n)Cu62	99.2
Cu64	Cu65(n,2n)Cu64	99.7
Zr89	Zr90(n,2n)Zr89	83.2
	Zr90(n,2n)Zr89m(IT)Zr89	16.9

Table 18: TUD pathways for lead using spectrum tud_Pb

Product	Pathway(s)	%
Hg203	Pb206(n,a)Hg203	96.3
	Pb207(n,na)Hg203	3.7
Pb203	Pb204(n,2n)Pb203m(IT)Pb203	51.8
	Pb204(n,2n)Pb203	46.9

Product	Pathway(s)	%
Pb204m	Pb204(n,n)Pb204m	100.0
Tl208	Pb208(n,p)Tl208	96.9

Table 19: TUD pathways for erbium using spectrum tud_Er

Product	Pathway(s)	%
Er161	Er162(n,2n)Er161	100.0
Ho167	Er167(n,p)Ho167	81.7
	Er168(n,np)Ho167	1.6
	Er168(n,d)Ho167	4.2
	Er170(n,a)Dy167(b-)Ho167	12.9
Ho168	Er168(n,p)Ho168	46.5
	Er168(n,p)Ho168m(IT)Ho168	43.6
Ho170	Er170(n,p)Ho170	96.0
Er163	Er164(n,2n)Er163	99.9
Ho169	Er170(n,np)Ho169	10.7
	Er170(n,d)Ho169	80.2
Ho166	Er166(n,p)Ho166	97.0
	Er167(n,d)Ho166	2.2

Table 20: TUD pathways for tantalum using spectrum tud_Ta

Product	Pathway(s)	%
Lu178m	Ta181(n,a)Lu178m	99.1
Hf180m	Ta181(n,np)Hf180m	37.0
	Ta181(n,d)Hf180m	62.3
Hf181	Ta181(n,p)Hf181	100.0
Ta180	Ta181(n,2n)Ta180	100.0
Ta182	Ta181(n,g)Ta182	61.9
	Ta181(n,g)Ta182m(IT)Ta182	37.7
Ta182n	Ta181(n,g)Ta182n	97.4

A.2 Forschungszentrum Karlsruhe data

Table 21: FZK pathways for V3Ti1Si using spectrum fz_k_1

Product	Pathway(s)	%
Sc46	Ti46(n,p)Sc46	62.4
	Ti46(n,p)Sc46m(IT)Sc46	28.9
	Ti47(n,np)Sc46	6.3
Sc47	Ti47(n,p)Sc47	26.2
	Ti48(n,np)Sc47	17.0
	Ti48(n,d)Sc47	3.6
	V50(n,a)Sc47	3.8
	V51(n,na)Sc47	49.3
Cr51	Cr52(n,2n)Cr51	46.9
	Fe54(n,a)Cr51	52.9
Mn54	Fe54(n,p)Mn54	98.8
Co57	Ni58(n,np)Co57	95.1
	Ni58(n,d)Co57	2.9
	Ni58(n,2n)Ni57(b+)Co57	1.9
Co58	Ni58(n,p)Co58	66.0
	Ni58(n,p)Co58m(IT)Co58	34.1
Co60	Ni60(n,p)Co60m(IT)Co60	63.3
	Ni60(n,p)Co60	35.9
Zr95	Zr94(n,g)Zr95	5.2
	Zr96(n,2n)Zr95	94.1
Nb92m	Nb93(n,2n)Nb92m	78.1
	Mo92(n,p)Nb92m	21.9
Nb95	Zr96(n,2n)Zr95(b-)Nb95	25.7
	Mo95(n,p)Nb95	52.7
	Mo95(n,p)Nb95m(IT)Nb95	2.4
	Mo96(n,np)Nb95	9.0
	Mo96(n,d)Nb95	7.6

Table 22: FZK pathways for V5Ti2Cr using spectrum fz_k_2

Product	Pathway(s)	%
Sc46	Ti46(n,p)Sc46	62.5
	Ti46(n,p)Sc46m(IT)Sc46	28.9
	Ti47(n,np)Sc46	6.4
Cr51	Cr52(n,2n)Cr51	99.6
Mn54	Mn55(n,2n)Mn54	4.2
	Fe54(n,p)Mn54	95.6

Product	Pathway(s)	%
Co57	Ni58(n,np)Co57	95.1
	Ni58(n,d)Co57	2.9
	Ni58(n,2n)Ni57(b+)Co57	2.0
Co58	Ni58(n,p)Co58	66.0
	Ni58(n,p)Co58m(IT)Co58	34.1
Co60	Ni60(n,p)Co60m(IT)Co60	63.3
	Ni60(n,p)Co60	35.9

Table 23: FZK pathways for Eurofer-97 using spectrum fz_k_2

Product	Pathway(s)	%
Sc46	Ti46(n,p)Sc46	61.4
	Ti46(n,p)Sc46m(IT)Sc46	28.4
	Ti47(n,np)Sc46	6.3
Sc47	Ti47(n,p)Sc47	19.1
	Ti48(n,np)Sc47	12.5
	Ti48(n,d)Sc47	2.6
	V50(n,a)Sc47	4.6
	V51(n,na)Sc47	61.1
V48	Cr50(n,t)V48	100.0
Cr51	Cr52(n,2n)Cr51	76.7
	Fe54(n,a)Cr51	23.0
Mn52	Fe54(n,t)Mn52	97.7
	Fe54(n,t)Mn52m(IT)Mn52	2.3
Mn54	Mn55(n,2n)Mn54	3.4
	Fe54(n,p)Mn54	96.5
Fe59	Fe58(n,g)Fe59	74.5
	Co59(n,p)Fe59	24.8
Co57	Ni58(n,np)Co57	95.6
	Ni58(n,d)Co57	3.0
Co58	Co59(n,2n)Co58m(IT)Co58	5.9
	Co59(n,2n)Co58	5.0
	Ni58(n,p)Co58	61.2
	Ni58(n,p)Co58m(IT)Co58	28.0
Co60	Co59(n,g)Co60m(IT)Co60	5.1
	Co59(n,g)Co60	4.2
	Ni60(n,p)Co60m(IT)Co60	49.6
	Ni60(n,p)Co60	28.2
	Cu63(n,a)Co60m(IT)Co60	7.3
	Cu63(n,a)Co60	5.0
Nb92m	Nb93(n,2n)Nb92m	95.0

Product	Pathway(s)	%
	Mo92(n,p)Nb92m	5.0
Hf181	Ta181(n,p)Hf181	61.3
	W184(n,a)Hf181	38.7
Ta182	Ta181(n,g)Ta182	57.9
	Ta181(n,g)Ta182m(IT)Ta182	36.6
	W182(n,p)Ta182	2.0
	W182(n,p)Ta182m(IT)Ta182	1.8
Ta183	W183(n,p)Ta183	62.9
	W184(n,np)Ta183	10.5
	W184(n,d)Ta183	13.7
	W186(n,a)Hf183(b-)Ta183	12.8
W181	W182(n,2n)W181	96.0
	W183(n,3n)W181	3.9
W185	W184(n,g)W185	4.8
	W186(n,2n)W185	59.4
	W186(n,2n)W185m(IT)W185	35.5

Table 24: FZK pathways for nickel using spectrum fzк_2 (1 of 2)

Product	Pathway(s)	%
Fe59	Ni60(n,2p)Fe59	3.6
	Ni62(n,a)Fe59	96.4
Co56	Ni58(n,t)Co56	100.0
Co57	Ni58(n,np)Co57	96.9
	Ni58(n,d)Co57	3.0
Co58	Ni58(n,p)Co58	95.4
	Ni58(n,p)Co58m(IT)Co58	4.6
Co60	Ni60(n,p)Co60m(IT)Co60	60.4
	Ni60(n,p)Co60	38.9
Co61	Ni61(n,p)Co61	67.5
	Ni62(n,np)Co61	24.4
	Ni62(n,d)Co61	5.9
	Ni64(n,a)Fe61(b-)Co61	1.9
Ni57	Ni58(n,2n)Ni57	100.0
Ni65	Ni64(n,g)Ni65	99.9

Table 25: FZK pathways for copper using spectrum fzк_2 (1 of 2)

Product	Pathway(s)	%
Fe59	Cu63(n,pa)Fe59	99.5
Co58m	Co59(n,2n)Co58m	40.0
	Ni58(n,p)Co58m	60.0
Co60	Cu63(n,a)Co60m(IT)Co60	56.0
	Cu63(n,a)Co60	44.0
Co61	Cu65(n,na)Co61	99.1
Ni65	Cu65(n,p)Ni65	99.9
Cu64	Cu63(n,g)Cu64	7.7
	Cu65(n,2n)Cu64	92.3

Table 26: FZK pathways for tungsten using spectrum fzк_2 (1 of 2)

Product	Pathway(s)	%
Hf180m	Hf180(n,n)Hf180m	1.5
	W183(n,a)Hf180m	72.3
	W184(n,na)Hf180m	26.1
Hf182m	W186(n,na)Hf182m	99.6
Hf183	W186(n,a)Hf183	99.6
Ta182m	W182(n,p)Ta182m	72.9
	W182(n,p)Ta182n(IT)Ta182m	10.5
	W183(n,np)Ta182m	6.8
	W183(n,d)Ta182m	5.5
	W184(n,t)Ta182m	2.3
Ta184	W184(n,p)Ta184	96.5
	W186(n,t)Ta184	3.5
Ta185	W186(n,np)Ta185	40.3
	W186(n,d)Ta185	59.2
Ta186	W186(n,p)Ta186	99.8
W179m	W180(n,2n)W179m	100.0
W187	W186(n,g)W187	100.0

Table 27: FZK pathways for tungsten using spectrum fz_k_2
(2 of 2)

Product	Pathway(s)	%
Hf179n	W182(n,a)Hf179n	94.8
	W183(n,na)Hf179n	4.7
Hf181	W184(n,a)Hf181	100.0
Ta178	W180(n,3n)W178(b+)Ta178	97.7
	W180(n,t)Ta178	2.3
Ta182	W182(n,p)Ta182	41.4
	W182(n,p)Ta182m(IT)Ta182	36.6
	W182(n,p)Ta182n(IT)Ta182m(IT)Ta182	5.2
	W183(n,np)Ta182	3.6
	W183(n,d)Ta182	3.3
	W183(n,np)Ta182m(IT)Ta182	3.4
	W183(n,d)Ta182m(IT)Ta182	2.7
Ta183	W183(n,p)Ta183	62.9
	W184(n,np)Ta183	10.5
	W184(n,d)Ta183	13.7
	W186(n,a)Hf183(b-)Ta183	12.8
W181	W182(n,2n)W181	96.0
	W183(n,3n)W181	3.9
W185	W184(n,g)W185	4.8
	W186(n,2n)W185	59.4
	W186(n,2n)W185m(IT)W185	35.5

Table 28: FZK pathways for Li4SO4 using spectrum fz_k_1

Product	Pathway(s)	%
Mg27	Al27(n,p)Mg27	31.0
	Si30(n,a)Mg27	68.1
Mg28	Si29(n,2p)Mg28	99.5
Al28	Si28(n,p)Al28	99.7
Al29	Si29(n,p)Al29	97.6
	Si30(n,np)Al29	1.7
Na22	Na23(n,2n)Na22	99.9
Na24	Mg24(n,p)Na24	3.6
	Al27(n,a)Na24	95.7
Ca47	Ca48(n,2n)Ca47	58.5
	Ti50(n,a)Ca47	41.2
Sc46	Ti46(n,p)Sc46	62.7
	Ti46(n,p)Sc46m(IT)Sc46	29.0
	Ti47(n,np)Sc46	6.4

Product	Pathway(s)	%
Sc47	Ti47(n,p)Sc47	55.8
	Ti48(n,np)Sc47	36.2
	Ti48(n,d)Sc47	7.6
Sc48	Ti48(n,p)Sc48	98.9
Cr51	Cr52(n,2n)Cr51	57.1
	Fe54(n,a)Cr51	42.7
Mn54	Mn55(n,2n)Mn54	11.4
	Fe54(n,p)Mn54	88.4
Zr89	Zr90(n,2n)Zr89	82.1
	Zr90(n,2n)Zr89m(IT)Zr89	17.9

Table 29: FZK pathways for SS-316 using spectrum fzk_ss316

Product	Pathway(s)	%
Sc48	Ti48(n,p)Sc48	52.2
	Ti49(n,np)Sc48	2.5
	Cr52(n,pa)Sc48	19.6
	Cr52(n,O)Sc48	20.8
V48	Cr50(n,nd)V48	6.0
	Cr50(n,2np)V48	21.8
	Cr50(n,t)V48	5.3
	Cr50(n,O)V48	63.3
	Cr52(n,O)V48	2.3
Cr48	Cr50(n,3n)Cr48	20.3
	Cr50(n,O)Cr48	77.3
	Fe54(n,O)Cr48	2.1
Cr49	Cr50(n,2n)Cr49	84.9
	Cr50(n,O)Cr49	8.4
	Cr52(n,O)Cr49	3.5
	Fe54(n,O)Cr49	2.7
Cr51	Cr52(n,2n)Cr51	89.3
	Cr52(n,O)Cr51	3.5
	Fe54(n,a)Cr51	4.2
Mn52	Mn55(n,O)Mn52	2.8
	Fe54(n,O)Mn52	60.5
	Fe54(n,nd)Mn52	4.6
	Fe54(n,2np)Mn52	22.3
	Fe54(n,t)Mn52	6.1
	Fe56(n,O)Mn52	1.8
Mn54	Mn55(n,2n)Mn54	22.2
	Fe54(n,p)Mn54	39.8
	Fe56(n,nd)Mn54	2.3

Product	Pathway(s)	%
	Fe56(n,2np)Mn54	9.5
	Fe56(n,t)Mn54	2.1
	Fe56(n,O)Mn54	20.9
	Ni58(n,pa)Mn54	1.9
Mn56	Fe56(n,p)Mn56	94.9
	Fe56(n,O)Mn56	2.7
	Fe57(n,np)Mn56	1.7
Fe52	Fe54(n,O)Fe52	78.3
	Fe54(n,3n)Fe52	20.4
Fe59	Fe58(n,g)Fe59	3.0
	Co59(n,p)Fe59	8.4
	Ni60(n,2p)Fe59	39.6
	Ni60(n,O)Fe59	5.7
	Ni62(n,a)Fe59	38.5
Co55	Ni58(n,nt)Co55	3.8
	Ni58(n,O)Co55	96.2
Co56	Ni58(n,nd)Co56	6.1
	Ni58(n,2np)Co56	37.9
	Ni58(n,t)Co56	3.0
	Ni58(n,O)Co56	52.9
Co57	Ni58(n,np)Co57	91.7
	Ni58(n,d)Co57	4.3
	Ni58(n,O)Co57	3.7
Co58	Ni58(n,p)Co58	92.4
	Ni58(n,p)Co58m(IT)Co58	4.9
Co60	Ni60(n,p)Co60m(IT)Co60	52.6
	Ni60(n,p)Co60	38.9
	Ni61(n,np)Co60	2.3
	Ni61(n,np)Co60m(IT)Co60	1.6
Co61	Ni61(n,p)Co61	19.8
	Ni62(n,np)Co61	54.2
	Ni62(n,d)Co61	11.7
	Ni62(n,O)Co61	10.4
Ni56	Ni58(n,3n)Ni56	35.4
	Ni58(n,O)Ni56	64.6
Ni57	Ni58(n,2n)Ni57	93.1
	Ni58(n,O)Ni57	6.9
Y87m	Mo92(n,O)Y87m	47.3
	Mo92(n,npa)Y87m	2.2
	Mo92(n,O)Zr87(b+)Y87m	47.6
	Mo92(n,O)Zr87m(IT)Zr87(b+)Y87m	1.7
Y87	Mo92(n,O)Y87	74.2
	Mo92(n,npa)Y87	5.7
	Mo92(n,O)Y87m(IT)Y87	10.6

Product	Pathway(s)	%
	Mo92(n,O)Zr87(b+)Y87m(IT)Y87	7.5
Y88	Nb93(n,O)Y88	1.7
	Mo92(n,pa)Y88	78.3
	Mo92(n,O)Y88	16.4
Zr86	Mo92(n,O)Zr86	100.0
Zr88	Mo92(n,na)Zr88	84.9
	Mo92(n,O)Zr88	14.8
Zr89	Mo92(n,O)Zr89	6.9
	Mo92(n,a)Zr89	67.8
	Mo92(n,a)Zr89m(IT)Zr89	18.0
	Mo92(n,O)Nb89(b+)Zr89	2.2
	Mo94(n,O)Zr89	2.0
Zr97	Mo100(n,a)Zr97	95.8
	Mo100(n,O)Zr97	4.1
Nb90	Mo92(n,O)Nb90	39.4
	Mo92(n,nd)Nb90	2.4
	Mo92(n,2np)Nb90	28.5
	Mo92(n,t)Nb90	3.0
	Mo92(n,O)Nb90m(IT)Nb90	13.0
	Mo92(n,2np)Nb90m(IT)Nb90	8.2
	Mo92(n,t)Nb90m(IT)Nb90	1.7
	Mo92(n,O)Mo90(b+)Nb90	1.9
Nb92m	Nb93(n,2n)Nb92m	4.2
	Mo92(n,p)Nb92m	83.0
	Mo94(n,O)Nb92m	3.6
	Mo94(n,2np)Nb92m	3.3
	Mo95(n,O)Nb92m	3.1
Nb95	Mo95(n,O)Nb95	1.8
	Mo95(n,p)Nb95	31.4
	Mo96(n,O)Nb95	8.4
	Mo96(n,np)Nb95	30.0
	Mo96(n,d)Nb95	15.3
	Mo97(n,O)Nb95	3.7
	Mo97(n,2np)Nb95	1.7
	Mo97(n,t)Nb95	1.5
	Mo98(n,O)Nb95	4.4
Nb95m	Mo95(n,O)Nb95m	2.0
	Mo95(n,p)Nb95m	47.0
	Mo96(n,O)Nb95m	5.7
	Mo96(n,np)Nb95m	21.3
	Mo96(n,d)Nb95m	17.0
	Mo97(n,O)Nb95m	2.2
	Mo98(n,O)Nb95m	1.6
Mo90	Mo92(n,3n)Mo90	29.0

Product	Pathway(s)	%
	Mo92(n,O)Mo90	71.0
Mo93m	Mo94(n,O)Mo93m	2.6
	Mo94(n,2n)Mo93m	33.1
	Mo95(n,O)Mo93m	14.2
	Mo95(n,3n)Mo93m	41.2
	Mo96(n,O)Mo93m	7.8
Mo99	Mo98(n,g)Mo99	4.2
	Mo100(n,2n)Mo99	92.6
	Mo100(n,O)Mo99	1.6
Tc99m	Mo98(n,g)Mo99(b-)Tc99m	4.2
	Mo100(n,2n)Mo99(b-)Tc99m	92.8
	Mo100(n,O)Mo99(b-)Tc99m	1.6

Table 30: FZK pathways for F82H using spectrum fzк_ss316

Product	Pathway(s)	%
Sc46	Ti46(n,p)Sc46	8.4
	Ti46(n,p)Sc46m(IT)Sc46	3.5
	Ti47(n,np)Sc46	4.2
	Ti48(n,O)Sc46	3.3
	V51(n,O)Sc46	22.4
	V51(n,O)Sc46m(IT)Sc46	3.7
	Cr50(n,O)Sc46	9.7
	Cr50(n,pa)Sc46	16.9
Sc47	Ti47(n,p)Sc47	1.7
	Ti48(n,np)Sc47	9.8
	Ti48(n,d)Sc47	1.7
	V51(n,na)Sc47	40.7
	V51(n,O)Sc47	7.7
	Cr52(n,O)Sc47	35.7
Sc48	Ti48(n,p)Sc48	8.1
	V51(n,a)Sc48	46.2
	V51(n,O)Sc48	1.8
	Cr52(n,pa)Sc48	20.1
	Cr52(n,O)Sc48	21.3
V48	V51(n,O)V48	2.7
	Cr50(n,nd)V48	5.7
	Cr50(n,2np)V48	20.7
	Cr50(n,t)V48	5.0
	Cr50(n,O)V48	59.9
	Cr52(n,O)V48	2.1
	Fe54(n,O)V48	3.7

Product	Pathway(s)	%
Cr48	Cr50(n,3n)Cr48	19.5
	Cr50(n,O)Cr48	74.0
	Fe54(n,O)Cr48	6.2
Cr49	Cr50(n,2n)Cr49	80.2
	Cr50(n,O)Cr49	7.9
	Cr52(n,O)Cr49	3.3
	Fe54(n,O)Cr49	8.0
Cr51	Cr52(n,2n)Cr51	79.8
	Cr52(n,O)Cr51	3.1
	Fe54(n,a)Cr51	11.9
	Fe56(n,O)Cr51	3.1
Mn52	Fe54(n,O)Mn52	63.0
	Fe54(n,nd)Mn52	4.8
	Fe54(n,2np)Mn52	23.2
	Fe54(n,t)Mn52	6.4
	Fe56(n,O)Mn52	1.8
Mn54	Mn55(n,2n)Mn54	1.9
	Fe54(n,p)Mn54	52.1
	Fe56(n,nd)Mn54	3.0
	Fe56(n,2np)Mn54	12.5
	Fe56(n,t)Mn54	2.8
	Fe56(n,O)Mn54	27.3
Mn56	Fe56(n,p)Mn56	95.1
	Fe56(n,O)Mn56	2.7
	Fe57(n,np)Mn56	1.7
Fe52	Fe54(n,O)Fe52	79.3
	Fe54(n,3n)Fe52	20.7
Co56	Ni58(n,nd)Co56	6.0
	Ni58(n,2np)Co56	37.4
	Ni58(n,t)Co56	3.0
	Ni58(n,O)Co56	52.1
Co57	Co59(n,3n)Co57	2.1
	Ni58(n,np)Co57	88.7
	Ni58(n,d)Co57	4.1
	Ni58(n,O)Co57	3.5
Co58	Co59(n,2n)Co58	17.3
	Co59(n,2n)Co58m(IT)Co58	2.2
	Ni58(n,p)Co58	73.7
	Ni58(n,p)Co58m(IT)Co58	3.9
Co60	Co59(n,g)Co60m(IT)Co60	2.5
	Co59(n,g)Co60	2.3
	Ni60(n,p)Co60m(IT)Co60	37.0
	Ni60(n,p)Co60	27.3
	Ni61(n,np)Co60	1.6

Product	Pathway(s)	%
	Cu63(n,a)Co60m(IT)Co60	12.1
	Cu63(n,a)Co60	10.8
Ni57	Ni58(n,2n)Ni57	93.1
	Ni58(n,O)Ni57	6.9
Ta183	W183(n,p)Ta183	23.5
	W183(n,O)Ta183	2.6
	W184(n,np)Ta183	29.3
	W184(n,d)Ta183	14.4
	W184(n,O)Ta183	18.3
	W186(n,O)Ta183	5.9
	W186(n,a)Hf183(b-)Ta183	4.2
Ta184	W184(n,p)Ta184	53.3
	W184(n,O)Ta184	7.3
	W186(n,nd)Ta184	3.3
	W186(n,2np)Ta184	4.6
	W186(n,t)Ta184	7.6
	W186(n,O)Ta184	23.8
W187	W186(n,g)W187	100.0

Table 31: FZK pathways for vanadium using spectrum fzks316

Product	Pathway(s)	%
Ca47	V51(n,pa)Ca47	55.2
	V51(n,O)Ca47	44.8
Sc46	V51(n,O)Sc46	81.6
	V51(n,2na)Sc46	3.0
	V51(n,O)Sc46m(IT)Sc46	13.3
Sc47	V51(n,na)Sc47	83.7
	V51(n,O)Sc47	15.9
Sc48	V51(n,a)Sc48	96.3
	V51(n,O)Sc48	3.7
V48	V50(n,3n)V48	2.9
	V50(n,O)V48	2.3
	V51(n,O)V48	94.8
Nb92m	Nb93(n,O)Nb92m	2.2
	Nb93(n,2n)Nb92m	92.5
	Mo92(n,p)Nb92m	4.6

Table 32: FZK pathways for vanadium alloy using spectrum fz_k_ss316

Product	Pathway(s)	%
Ca47	Ti48(n,2p)Ca47	11.9
	Ti48(n,O)Ca47	24.8
	Ti50(n,a)Ca47	24.6
	V51(n,pa)Ca47	20.0
	V51(n,O)Ca47	16.2
Sc43	Ti46(n,nt)Sc43	5.2
	Ti46(n,O)Sc43	92.8
	Ti47(n,O)Sc43	1.8
Sc44	Ti46(n,O)Sc44	53.3
	Ti46(n,nd)Sc44	4.2
	Ti46(n,2np)Sc44	10.0
	Ti46(n,t)Sc44	21.9
	Ti47(n,O)Sc44	5.9
	V51(n,O)Sc44	1.9
Sc44m	Ti46(n,O)Sc44m	57.0
	Ti46(n,nd)Sc44m	4.2
	Ti46(n,2np)Sc44m	13.0
	Ti46(n,t)Sc44m	13.0
	Ti47(n,O)Sc44m	6.6
	Ti48(n,O)Sc44m	1.6
	V51(n,O)Sc44m	3.6
Sc46	Ti46(n,p)Sc46	13.3
	Ti46(n,p)Sc46m(IT)Sc46	5.5
	Ti47(n,np)Sc46	6.6
	Ti48(n,O)Sc46	5.2
	V51(n,O)Sc46	49.9
	V51(n,2na)Sc46	1.8
	V51(n,O)Sc46m(IT)Sc46	8.1
Sc47	Ti47(n,p)Sc47	2.0
	Ti48(n,np)Sc47	11.8
	Ti48(n,d)Sc47	2.0
	V51(n,na)Sc47	69.0
	V51(n,O)Sc47	13.1
Sc48	Ti48(n,p)Sc48	10.6
	V51(n,a)Sc48	84.9
	V51(n,O)Sc48	3.3
V48	V50(n,3n)V48	2.8
	V50(n,O)V48	2.3
	V51(n,O)V48	92.1
	Cr50(n,O)V48	1.8
Cr49	Cr50(n,2n)Cr49	87.2

Product	Pathway(s)	%
	Cr50(n,O)Cr49	8.6
	Cr52(n,O)Cr49	3.6
Cr51	Cr52(n,2n)Cr51	94.6
	Cr52(n,O)Cr51	3.7
Mn52	Fe54(n,O)Mn52	63.1
	Fe54(n,nd)Mn52	4.8
	Fe54(n,2np)Mn52	23.2
	Fe54(n,t)Mn52	6.4
	Fe56(n,O)Mn52	1.8
Nb92m	Nb93(n,O)Nb92m	2.3
	Nb93(n,2n)Nb92m	95.2
	Mo92(n,p)Nb92m	2.2

A.3 Frascati Neutron Generator data

Table 33: FNG pathways for V4Cr4Ti using spectrum fng_vanad

Product	Pathway(s)	%
Na24	Al27(n,a)Na24	100.0
Ca47	Ti50(n,a)Ca47	100.0
Sc46	Ti46(n,p)Sc46	58.8
	Ti46(n,p)Sc46m(IT)Sc46	20.9
	Ti47(n,np)Sc46	16.0
	Ti47(n,np)Sc46m(IT)Sc46	2.5
Sc47	Ti47(n,p)Sc47	41.1
	Ti48(n,np)Sc47	30.4
	Ti48(n,d)Sc47	12.9
	V50(n,a)Sc47	11.3
	V51(n,na)Sc47	4.6
Sc48	Ti48(n,p)Sc48	10.8
	V51(n,a)Sc48	89.8
Cr49	Cr50(n,2n)Cr49	100.0
Ti51	V51(n,p)Ti51	99.9
V52	V51(n,g)V52	97.0
	Cr52(n,p)V52	2.9
Cr51	Cr50(n,g)Cr51	3.7
	Cr52(n,2n)Cr51	96.4
Mn54	Fe54(n,p)Mn54	99.8
Mn56	Fe56(n,p)Mn56	100.0
Co57	Ni58(n,np)Co57	97.0
	Ni58(n,d)Co57	2.7
Co58	Ni58(n,p)Co58	83.8
	Ni58(n,p)Co58m(IT)Co58	14.5
Co60	Ni60(n,p)Co60m(IT)Co60	17.1
	Ni60(n,p)Co60	13.5
	Cu63(n,a)Co60m(IT)Co60	35.9
	Cu63(n,a)Co60	33.2
Nb92m	Nb93(n,2n)Nb92m	88.8
	Mo92(n,p)Nb92m	11.3
Nb95	Mo95(n,p)Nb95	80.3
	Mo96(n,np)Nb95	8.0
	Mo96(n,d)Nb95	11.0
Tc99m	Mo98(n,g)Mo99(b-)Tc99m	3.9
	Mo100(n,2n)Mo99(b-)Tc99m	87.4

Table 34: FNG pathways for F82H using spectrum fng_F82H

Product	Pathway(s)	%
Na24	Al27(n,a)Na24	100.0
Sc48	Ti48(n,p)Sc48	1.8
	V51(n,a)Sc48	98.2
Cr51	Cr52(n,2n)Cr51	84.0
	Fe54(n,a)Cr51	15.3
Mn54	Mn55(n,2n)Mn54	7.1
	Fe54(n,p)Mn54	92.9
Mn56	Fe56(n,p)Mn56	99.0
Ni57	Ni58(n,2n)Ni57	100.0
Fe59	Fe58(n,g)Fe59	88.0
	Co59(n,p)Fe59	11.1
Co57	Ni58(n,np)Co57	97.1
	Ni58(n,d)Co57	2.7
Co58	Co59(n,2n)Co58	33.2
	Co59(n,2n)Co58m(IT)Co58	9.1
	Ni58(n,p)Co58	49.3
	Ni58(n,p)Co58m(IT)Co58	8.5
Co60	Co59(n,g)Co60m(IT)Co60	30.7
	Co59(n,g)Co60	19.6
	Ni60(n,p)Co60m(IT)Co60	22.4
	Ni60(n,p)Co60	17.6
	Cu63(n,a)Co60m(IT)Co60	4.8
	Cu63(n,a)Co60	4.4
Ta182	Ta181(n,g)Ta182	44.7
	Ta181(n,g)Ta182m(IT)Ta182	26.1
	W182(n,p)Ta182	14.5
	W182(n,p)Ta182m(IT)Ta182	12.2
Ta183	W183(n,p)Ta183	83.2
	W184(n,np)Ta183	2.2
	W184(n,d)Ta183	5.6
	W186(n,a)Hf183(b-)Ta183	9.1
Ta184	W184(n,p)Ta184	99.6
W187	W186(n,g)W187	100.0

Table 35: FNG pathways for Eurofer-97 using spectrum fng_eurofer

Product	Pathway(s)	%
Cr51	Cr50(n,g)Cr51	3.2
	Cr52(n,2n)Cr51	84.5

Product	Pathway(s)	%
	Fe54(n,a)Cr51	12.3
Mn54	Mn55(n,2n)Mn54	19.6
	Fe54(n,p)Mn54	80.4
Fe59	Fe58(n,g)Fe59	95.5
	Co59(n,p)Fe59	4.2
Co57	Ni58(n,np)Co57	97.0
	Ni58(n,d)Co57	2.7
Co58	Co59(n,2n)Co58	37.3
	Co59(n,2n)Co58m(IT)Co58	10.7
	Ni58(n,p)Co58	44.3
	Ni58(n,p)Co58m(IT)Co58	7.8
Co60	Co59(n,g)Co60m(IT)Co60	52.8
	Co59(n,g)Co60	33.5
	Ni60(n,p)Co60m(IT)Co60	6.8
	Ni60(n,p)Co60	5.3
Ta182	Ta181(n,g)Ta182	62.7
	Ta181(n,g)Ta182m(IT)Ta182	36.5
W181	W182(n,2n)W181	98.7

Table 36: FNG pathways for silicon carbide using spectrum fng_SiC

Product	Pathway(s)	%
Mg27	Si30(n,a)Mg27	100.0
Al28	Si28(n,p)Al28	99.7
Al29	Si29(n,p)Al29	99.0

Table 37: FNG pathways for niobium using spectrum fng_SiC

Product	Pathway(s)	%
Nb92m	Nb93(n,2n)Nb92m	100.0
Y90m	Nb93(n,a)Y90m	100.0

Table 38: FNG pathways for yttrium using spectrum fng_Y

Product	Pathway(s)	%
Y88	Y89(n,2n)Y88	100.0
Y90m	Y89(n,g)Y90m	96.6
	Zr90(n,p)Y90m	4.5
Zr89	Zr90(n,2n)Zr89	85.0
	Zr90(n,2n)Zr89m(IT)Zr89	15.0
Rb86	Y89(n,a)Rb86	69.5
	Y89(n,a)Rb86m(IT)Rb86	30.5
Ta180	Ta181(n,2n)Ta180	100.0
Y89m	Y89(n,n)Y89m	100.0
Rb86m	Y89(n,a)Rb86m	100.0

Table 39: FNG pathways for tungsten (1 of 2) using spectrum fng_tung

Product	Pathway(s)	%
Hf181	W184(n,a)Hf181	100.0
Hf183	W186(n,a)Hf183	99.8
Ta182	W182(n,p)Ta182	49.8
	W182(n,p)Ta182m(IT)Ta182	42.1
	W182(n,p)Ta182n(IT)Ta182m(IT)Ta182	3.0
	W183(n,d)Ta182	1.7
Ta184	W184(n,p)Ta184	99.6
Ta185	W186(n,np)Ta185	17.6
	W186(n,d)Ta185	82.2
Ta186	W186(n,p)Ta186	99.3
W181	W182(n,2n)W181	98.6
W185	W184(n,g)W185	4.7
	W186(n,2n)W185	57.6
	W186(n,2n)W185m(IT)W185	37.7
W185m	W186(n,2n)W185m	99.9
W187	W186(n,g)W187	100.0

Table 40: FNG pathways for tungsten (2 of 2) using spectrum fng_tung

Product	Pathway(s)	%
Hf181	W184(n,a)Hf181	100.0

Product	Pathway(s)	%
Hf183	W186(n,a)Hf183	100.0
Ta182	W182(n,p)Ta182	49.4
	W182(n,p)Ta182m(IT)Ta182	41.7
	W182(n,p)Ta182n(IT)Ta182m(IT)Ta182	3.8
	W183(n,d)Ta182	1.7
Ta184	W184(n,p)Ta184	99.8
Ta185	W186(n,np)Ta185	17.6
	W186(n,d)Ta185	82.4
Ta186	W186(n,p)Ta186	99.8
W181	W182(n,2n)W181	98.6
W185	W184(n,g)W185	4.6
	W186(n,2n)W185	57.2
	W186(n,2n)W185m(IT)W185	38.1
W185m	W186(n,2n)W185m	99.9
W187	W186(n,g)W187	100.0

Table 41: FNG pathways for chromium using spectrum fng_Cr

Product	Pathway(s)	%
Cr49	Cr50(n,2n)Cr49	100.0
Cr51	Cr52(n,2n)Cr51	100.0
V52	Cr52(n,p)V52	97.7
	Cr53(n,np)V52	2.0

Table 42: FNG pathways for CuCrZr using spectrum fng_CuCrZr

Product	Pathway(s)	%
Cr51	Cr52(n,2n)Cr51	100.0
Co60	Cu63(n,a)Co60m(IT)Co60	51.7
	Cu63(n,a)Co60	48.3
Co61	Cu65(n,na)Co61	98.9
Cu64	Cu65(n,2n)Cu64	99.3
Ni65	Cu65(n,p)Ni65	99.3
Co62m	Cu65(n,a)Co62m	99.7
Zr89	Zr90(n,2n)Zr89	83.1
	Zr90(n,2n)Zr89m(IT)Zr89	16.8

Table 43: FNG pathways for hafnium using spectrum fng_hafnium

Product	Pathway(s)	%
Lu178	Hf178(n,p)Lu178	94.0
	Hf179(n,np)Lu178	1.5
	Hf179(n,d)Lu178	3.4
Lu178m	Hf178(n,p)Lu178m	76.3
	Hf179(n,np)Lu178m	8.2
	Hf179(n,d)Lu178m	13.8
Lu179	Hf179(n,p)Lu179	89.3
	Hf180(n,np)Lu179	4.1
	Hf180(n,d)Lu179	6.5
Lu180	Hf180(n,p)Lu180	100.0
Hf173	Hf174(n,2n)Hf173	100.0
Hf175	Hf176(n,2n)Hf175	98.3
	Hf177(n,3n)Hf175	1.6
Hf179n	Hf179(n,n)Hf179n	9.6
	Hf180(n,2n)Hf179n	90.4
Hf180m	Hf180(n,n)Hf180m	98.9
Hf181	Hf180(n,g)Hf181	100.0

Table 44: FNG pathways for molybdenum (short) using spectrum fng_Mo

Product	Pathway(s)	%
Zr89	Mo92(n,a)Zr89	75.2
	Mo92(n,a)Zr89m(IT)Zr89	25.1
Nb92m	Mo92(n,p)Nb92m	100.0
Nb95m	Mo95(n,p)Nb95m	80.1
	Mo96(n,np)Nb95m	5.1
	Mo96(n,d)Nb95m	14.7
Nb95	Mo95(n,p)Nb95	80.4
	Mo96(n,np)Nb95	8.0
	Mo96(n,d)Nb95	11.0
Nb96	Mo96(n,p)Nb96	93.2
	Mo97(n,np)Nb96	3.4
	Mo97(n,d)Nb96	4.2
Tc99m	Mo100(n,2n)Mo99(b-)Tc99m	88.2
Mo99	Mo100(n,2n)Mo99	99.8

Table 45: FNG pathways for molybdenum using spectrum fng_Mo

Product	Pathway(s)	%
Zr89	Mo92(n,a)Zr89	75.2
	Mo92(n,a)Zr89m(IT)Zr89	25.1
Nb92m	Mo92(n,p)Nb92m	100.0
Nb95m	Mo95(n,p)Nb95m	80.1
	Mo96(n,np)Nb95m	5.1
	Mo96(n,d)Nb95m	14.7
Nb95	Mo95(n,p)Nb95	80.4
	Mo96(n,np)Nb95	8.0
	Mo96(n,d)Nb95	11.0
Nb96	Mo96(n,p)Nb96	93.2
	Mo97(n,np)Nb96	3.4
	Mo97(n,d)Nb96	4.2
Tc99m	Mo100(n,2n)Mo99(b-)Tc99m	88.2
Mo99	Mo100(n,2n)Mo99	99.8

Table 46: FNG pathways for tantalum using spectrum fng_Ta

Product	Pathway(s)	%
Lu178	Ta181(n,a)Lu178	97.7
Lu178m	Ta181(n,a)Lu178m	98.3
Hf180m	Ta181(n,np)Hf180m	38.2
	Ta181(n,d)Hf180m	61.4
Hf181	Ta181(n,p)Hf181	100.0
Ta180	Ta181(n,2n)Ta180	100.0
Ta182	Ta181(n,g)Ta182	62.3
	Ta181(n,g)Ta182m(IT)Ta182	37.4
Ta182n	Ta181(n,g)Ta182n	99.9

Table 47: FNG pathways for dysprosium using spectrum fng_Dy

Product	Pathway(s)	%
Dy155	Dy156(n,2n)Dy155	100.0
Dy157	Dy158(n,2n)Dy157	99.5

Product	Pathway(s)	%
Tb162	Dy162(n,p)Tb162	97.6
	Dy163(n,np)Tb162	2.4
	Dy163(n,d)Tb162	5.6
Tb163	Dy163(n,p)Tb163	100.0
	Dy164(n,np)Tb163	1.9
	Dy164(n,d)Tb163	6.2
Dy165	Dy164(n,g)Dy165m(IT)Dy165	67.0
	Dy164(n,g)Dy165	35.6

Table 48: FNG pathways for rhenium using spectrum fng_Re

Product	Pathway(s)	%
Re184	Re185(n,2n)Re184	100.0
Re184m	Re185(n,2n)Re184m	100.0
Re183	Re185(n,3n)Re183	100.0
Re186	Re185(n,g)Re186	12.9
	Re187(n,2n)Re186	87.2
Re188	Re187(n,g)Re188	98.1
	Re187(n,g)Re188m(IT)Re188	2.0
Re188m	Re187(n,g)Re188m	100.0
Ta184	Re187(n,a)Ta184	100.0
W187	Re187(n,p)W187	100.0

Table 49: FNG pathways for tin using spectrum fng_Sn

Product	Pathway(s)	%
Sn111	Sn112(n,2n)Sn111	100.0
Sn113	Sn114(n,2n)Sn113m(IT)Sn113	69.4
	Sn114(n,2n)Sn113	28.5
Sn113m	Sn114(n,2n)Sn113m	100.0
In116	Sn116(n,p)In116	97.1
	Sn117(n,np)In116	1.7
In115m	Sn115(n,p)In115m	6.8
	Sn116(n,np)In115m	37.4
	Sn116(n,d)In115m	53.7
	Sn117(n,t)In115m	2.1
In117	Sn117(n,p)In117	87.3
	Sn118(n,np)In117	6.9
	Sn118(n,d)In117	3.8

Product	Pathway(s)	%
In117m	Sn117(n,p)In117m	78.2
	Sn118(n,np)In117m	3.7
	Sn118(n,d)In117m	16.4
	Sn120(n,a)Cd117(b-)In117m	1.7
Sn117m	Sn117(n,n)Sn117m	5.3
	Sn118(n,2n)Sn117m	94.6
Cd115	Sn118(n,a)Cd115	99.7
Cd117	Sn120(n,a)Cd117	100.0
Cd117m	Sn120(n,a)Cd117m	100.0
Sn123	Sn124(n,2n)Sn123	99.9
Sn123m	Sn124(n,2n)Sn123m	100.0

Table 50: FNG pathways for scandium using spectrum fng_ScSmGd

Product	Pathway(s)	%
Sc44	Sc45(n,2n)Sc44	100.0
Sc44m	Sc45(n,2n)Sc44m	100.0
K42	Sc45(n,a)K42	100.0

Table 51: FNG pathways for samarium using spectrum fng_ScSmGd

Product	Pathway(s)	%
Pm150	Sm150(n,p)Pm150	100.0
Nd149	Sm152(n,a)Nd149	100.0
Sm153	Sm152(n,g)Sm153	1.6
	Sm154(n,2n)Sm153	98.4

Table 52: FNG pathways for gadolinium using spectrum fng_ScSmGd

Product	Pathway(s)	%
Eu158	Gd158(n,p)Eu158	100.0
Sm155	Gd158(n,a)Sm155	100.0
Gd159	Gd160(n,2n)Gd159	99.9

Table 53: FNG pathways for spectroscopic heat measurements using spectrum fng_heat

Product	Pathway(s)	%
Na24	Mg24(n,p)Na24	99.2
Na25	Mg25(n,p)Na25	100.0
	Mg26(n,d)Na25	3.8
Mg27	Al27(n,p)Mg27	100.0
Na24	Al27(n,a)Na24	100.0
Sc48	Ti48(n,p)Sc48	99.4
Sc49	Ti49(n,p)Sc49	97.6
	Ti50(n,np)Sc49	2.3
	Ti50(n,d)Sc49	1.9
Sc50	Ti50(n,p)Sc50m(IT)Sc50	60.0
	Ti50(n,p)Sc50	45.0
Co60	Ni60(n,p)Co60	68.5
	Ni60(n,p)Co60m(IT)Co60	24.4
Co62	Ni62(n,p)Co62	100.0
Co62m	Ni62(n,p)Co62m	100.0
Cu62	Cu63(n,2n)Cu62	99.6
Zr89m	Zr90(n,2n)Zr89m	100.0
Y94	Zr94(n,p)Y94	100.0
Mo91	Mo92(n,2n)Mo91	100.0
	Mo92(n,2n)Mo91m(IT)Mo91	4.9
Y90	Nb93(n,a)Y90	91.8
	Nb93(n,a)Y90m(IT)Y90	8.2
Nb92m	Nb93(n,2n)Nb92m	100.0
Ag106	Ag107(n,2n)Ag106	100.0
Ag108	Ag107(n,g)Ag108	1.9
	Ag109(n,2n)Ag108	100.0
Cd111m	Cd111(n,n)Cd111m	12.5
	Cd112(n,2n)Cd111m	90.3
Sn123m	Sn124(n,2n)Sn123m	100.0
Hf180m	Hf180(n,n)Hf180m	99.1
Lu180	Hf180(n,p)Lu180	100.0
Re184	Re185(n,2n)Re184	100.0
W185	W186(n,2n)W185	61.8
	W186(n,2n)W185m(IT)W185	37.8
Ta186	W186(n,p)Ta186	100.0
Re186	Re187(n,2n)Re186	98.8
Pb204m	Pb204(n,n)Pb204m	100.0

A.4 Japan Atomic Energy Agency data

Table 54: JAEA pathways for 5 minute irradiation samples using spectrum fns.5min

Product	Pathway(s)	%
N13	N14(n,2n)N13	100.0
N16	O16(n,p)N16	100.0
O19	F19(n,p)O19	99.8
F18	F19(n,2n)F18	100.0
Ne23	Na23(n,p)Ne23	100.0
Ne23	Mg26(n,a)Ne23	100.0
Na24	Na23(n,g)Na24	100.0
Na24	Mg24(n,p)Na24	99.1
Na25	Mg25(n,p)Na25	96.8
	Mg26(n,d)Na25	3.4
Mg27	Al27(n,p)Mg27	99.9
Mg27	Si30(n,a)Mg27	99.9
Al28	Si28(n,p)Al28	98.1
Al28	P31(n,a)Al28	100.0
Al29	Si29(n,p)Al29	98.8
Si31	S32(n,2p)Si31	25.5
	S34(n,a)Si31	74.5
P34	S34(n,p)P34	100.0
P34	Cl37(n,a)P34	99.8
S35	K39(n,pa)S35	100.0
S37	Cl37(n,p)S37	100.0
Cl34m	Cl35(n,2n)Cl34m	100.0
Cl38	K41(n,a)Cl38	72.6
	K41(n,a)Cl38m(IT)Cl38	25.9
K38	K39(n,2n)K38	100.0
K44	Ca44(n,p)K44	100.0
Ar41	K41(n,p)Ar41	100.0
Sc44	Sc45(n,2n)Sc44	100.0
Sc48	Ti48(n,p)Sc48	99.4
Sc50	Ti50(n,p)Sc50m(IT)Sc50	56.8
	Ti50(n,p)Sc50	42.4
Ti51	V51(n,p)Ti51	99.9
V52	Mn55(n,a)V52	100.0
V52	Cr52(n,p)V52	97.7
	Cr53(n,np)V52	2.0
Cr49	Cr50(n,2n)Cr49	100.0
Cr55	Mn55(n,p)Cr55	100.0
Mn56	Mn55(n,g)Mn56	100.0

Product	Pathway(s)	%
Mn56	Fe56(n,p)Mn56	99.5
Mn56	Co59(n,a)Mn56	100.0
Co60m	Ni60(n,p)Co60m	99.4
Co62	Ni62(n,p)Co62	98.7
Co62m	Ni62(n,p)Co62m	100.0
Cu62	Cu63(n,2n)Cu62	100.0
Zn63	Zn64(n,2n)Zn63	100.0
Ga68	Ga69(n,2n)Ga68	100.0
Ga70	Ga71(n,2n)Ga70	99.0
Ga74	Ge74(n,p)Ga74	80.9
	Ge74(n,p)Ga74m(IT)Ga74	19.1
Ge75	Ge76(n,2n)Ge75m(IT)Ge75	66.3
	Ge76(n,2n)Ge75	33.2
Ge75	As75(n,p)Ge75m(IT)Ge75	57.3
	As75(n,p)Ge75	42.9
Ge75m	Ge76(n,2n)Ge75m	98.5
Ge75m	As75(n,p)Ge75m	99.4
Se77m	Se77(n,n)Se77m	13.6
	Se78(n,2n)Se77m	86.1
Se81	Se80(n,g)Se81	2.5
	Se82(n,2n)Se81	88.8
	Se82(n,2n)Se81m(IT)Se81	8.6
Br78	Br79(n,2n)Br78	99.8
Br80	Br79(n,g)Br80	6.0
	Br81(n,2n)Br80	93.1
Rb84	Rb85(n,2n)Rb84	94.4
	Rb85(n,2n)Rb84m(IT)Rb84	5.6
Rb86m	Rb87(n,2n)Rb86m	99.7
Rb86m	Y89(n,a)Rb86m	100.0
Rb88	Sr88(n,p)Rb88	100.0
Y88	Y89(n,2n)Y88	100.0
Y89m	Y89(n,n)Y89m	100.0
Y89m	Nb93(n,na)Y89m	99.9
Y90m	Nb93(n,a)Y90m	100.0
Y94	Zr94(n,p)Y94	100.0
Zr89m	Zr90(n,2n)Zr89m	100.0
Nb94m	Nb93(n,g)Nb94m	99.7
Mo91	Mo92(n,2n)Mo91	95.8
	Mo92(n,2n)Mo91m(IT)Mo91	4.3
Mo91m	Mo92(n,2n)Mo91m	100.0
Tc100	Ru100(n,p)Tc100	83.0
	Ru101(n,np)Tc100	12.8
	Ru101(n,d)Tc100	4.3

Product	Pathway(s)	%
Tc102m	Ru102(n,p)Tc102m	100.0
Ru95	Ru96(n,2n)Ru95	100.0
Rh103m	Rh103(n,n)Rh103m	100.0
Rh104	Rh103(n,g)Rh104 Rh103(n,g)Rh104m(IT)Rh104	96.4 2.8
Rh108m	Pd108(n,p)Rh108m	99.9
Pd107m	Pd108(n,2n)Pd107m	99.6
Pd109	Pd108(n,g)Pd109 Pd110(n,2n)Pd109 Pd110(n,2n)Pd109m(IT)Pd109	5.9 83.5 10.5
Pd109m	Pd110(n,2n)Pd109m	99.0
Ag106	Ag107(n,2n)Ag106	100.0
Ag108	Ag107(n,g)Ag108 Ag109(n,2n)Ag108	4.8 94.9
Ag114	Cd114(n,p)Ag114	100.0
Cd111m	Cd111(n,n)Cd111m Cd112(n,2n)Cd111m	13.3 86.7
In114	In115(n,2n)In114	99.2
In116m	In115(n,g)In116m In115(n,g)In116n(IT)In116m	79.4 20.6
In118m	Sn118(n,p)In118m Sn118(n,p)In118n(IT)In118m	88.0 10.8
In120m	Sn120(n,p)In120m	98.6
Sn123m	Sn124(n,2n)Sn123m	99.9
Sb120	Sb121(n,2n)Sb120	100.0
Te129	Te130(n,2n)Te129	99.7
I128	I127(n,g)I128	100.0
Cs132	Cs133(n,2n)Cs132	100.0
Cs136m	Ba136(n,p)Cs136m Ba137(n,d)Cs136m	83.3 14.9
Cs138	Ba138(n,p)Cs138 Ba138(n,p)Cs138m(IT)Cs138	83.1 17.1
Ba137m	Ba137(n,n)Ba137m Ba138(n,2n)Ba137m	3.3 95.8
Ba137m	Ce140(n,a)Ba137m	99.3
Ba139	La139(n,p)Ba139	100.0
La142	Ce142(n,p)La142	100.0
Ce139m	Ce140(n,2n)Ce139m	98.8
Pr140	Pr141(n,2n)Pr140	99.5
Nd141m	Nd142(n,2n)Nd141m	98.6
Nd149	Nd150(n,2n)Nd149	99.5
Sm143	Sm144(n,2n)Sm143 Sm144(n,2n)Sm143m(IT)Sm143	62.2 38.0

Product	Pathway(s)	%
Sm143m	Sm144(n,2n)Sm143m	98.5
Eu152m	Eu151(n,g)Eu152m	64.3
	Eu153(n,2n)Eu152m	35.7
Eu160	Gd160(n,p)Eu160	98.5
Gd159	Gd160(n,2n)Gd159	98.9
Gd159	Tb159(n,p)Gd159	100.0
Gd161	Gd160(n,g)Gd161	99.4
Tb158m	Tb159(n,2n)Tb158m	100.0
Tb162	Dy162(n,p)Tb162	92.3
	Dy163(n,np)Tb162	2.2
	Dy163(n,d)Tb162	5.3
Tb164	Dy164(n,p)Tb164	99.2
Dy165	Dy164(n,g)Dy165m(IT)Dy165	59.5
	Dy164(n,g)Dy165	41.0
Dy165m	Dy164(n,g)Dy165m	98.3
Ho164	Ho165(n,2n)Ho164	95.8
	Ho165(n,2n)Ho164m(IT)Ho164	4.2
Ho164m	Ho165(n,2n)Ho164m	100.0
Ho168	Er168(n,p)Ho168	66.5
	Er168(n,p)Ho168m(IT)Ho168	34.4
Er165	Er166(n,2n)Er165	99.7
Tm168	Tm169(n,2n)Tm168	100.0
Tm174	Yb174(n,p)Tm174	99.6
Yb167	Yb168(n,2n)Yb167	100.0
Lu176m	Lu175(n,g)Lu176m	90.1
	Lu176(n,n)Lu176m	9.9
Lu180	Hf180(n,p)Lu180	100.0
Hf179m	Hf178(n,g)Hf179m	28.0
	Hf179(n,n)Hf179m	7.2
	Hf180(n,2n)Hf179m	64.8
Ta180	Ta181(n,2n)Ta180	100.0
Ta186	W186(n,p)Ta186	100.0
W185m	W186(n,2n)W185m	98.2
W185m	Re185(n,p)W185m	91.2
	Re187(n,t)W185m	8.8
Re186	Re185(n,g)Re186	4.8
	Re187(n,2n)Re186	95.2
Os191m	Os192(n,2n)Os191m	99.1
Ir192m	Ir191(n,g)Ir192m	31.7
	Ir193(n,2n)Ir192m	67.1
Pt197m	Pt198(n,2n)Pt197m	100.0
Au195m	Au197(n,3n)Au195m	100.0
Au196m	Au197(n,2n)Au196m	99.9

Product	Pathway(s)	%
Au196n	Au197(n,2n)Au196n	100.0
Au197m	Au197(n,n)Au197m	100.0
Hg199m	Hg199(n,n)Hg199m Hg200(n,2n)Hg199m	12.4 87.5
Hg205	Tl205(n,p)Hg205	99.7
Tl202	Tl203(n,2n)Tl202	100.0
Tl206	Tl205(n,g)Tl206 Tl205(n,g)Tl206m(IT)Tl206	96.9 2.6
Tl206	Bi209(n,a)Tl206 Bi209(n,a)Tl206m(IT)Tl206	92.7 13.2
Tl208	Pb208(n,p)Tl208	100.0
Pb203m	Pb204(n,2n)Pb203m Pb204(n,2n)Pb203n(IT)Pb203m	97.4 2.6
Pb204m	Pb204(n,n)Pb204m	100.0
Pb209	Bi209(n,p)Pb209	100.0

Table 55: JAEA pathways for 7 hour irradiation samples using spectrum fns_7hour

Product	Pathway(s)	%
Na22	Na23(n,2n)Na22	100.0
Na24	Na23(n,g)Na24	99.9
Na24	Al27(n,a)Na24	99.9
P32	S32(n,p)P32	99.5
K42	K41(n,g)K42	99.9
K42	Ca42(n,p)K42 Ca43(n,np)K42	98.0 1.6
Ca47	Ca48(n,2n)Ca47	100.0
Sc46	Ti46(n,p)Sc46 Ti46(n,p)Sc46m(IT)Sc46 Ti47(n,np)Sc46 Ti47(n,np)Sc46m(IT)Sc46	60.9 21.7 13.8 2.0
Sc48	Ti48(n,p)Sc48	99.6
Sc48	V51(n,a)Sc48	100.0
Cr51	Cr52(n,2n)Cr51	100.0
Mn54	Fe54(n,p)Mn54	100.0
Mn56	Mn55(n,g)Mn56	99.3
Mn56	Fe56(n,p)Mn56	98.6
Co57	Ni58(n,np)Co57 Ni58(n,d)Co57	97.1 2.6
Co58	Ni58(n,p)Co58	80.0

Product	Pathway(s)	%
	Ni58(n,p)Co58m(IT)Co58	20.0
Co58	Co59(n,2n)Co58	71.9
	Co59(n,2n)Co58m(IT)Co58	28.2
Co58m	Co59(n,2n)Co58m	99.8
Co60	Cu63(n,a)Co60m(IT)Co60	52.8
	Cu63(n,a)Co60	47.2
Ni57	Ni58(n,2n)Ni57	100.0
Cu64	Cu65(n,2n)Cu64	99.5
Sr83	Sr84(n,2n)Sr83	84.3
	Sr84(n,2n)Sr83m(IT)Sr83	15.7
Sr85	Sr86(n,2n)Sr85	80.5
	Sr86(n,2n)Sr85m(IT)Sr85	19.5
Sr87m	Sr87(n,n)Sr87m	2.3
	Sr88(n,2n)Sr87m	97.1
Y88	Y89(n,2n)Y88	100.0
Zr89	Zr90(n,2n)Zr89	84.0
	Zr90(n,2n)Zr89m(IT)Zr89	16.0
Zr95	Zr96(n,2n)Zr95	99.5
Zr95	Mo98(n,a)Zr95	100.0
Nb91m	Mo92(n,np)Nb91m	92.3
	Mo92(n,d)Nb91m	3.9
	Mo92(n,2n)Mo91m(b+)Nb91m	3.7
Nb92m	Nb93(n,2n)Nb92m	100.0
Nb92m	Mo92(n,p)Nb92m	100.0
Nb95	Mo95(n,p)Nb95	83.2
	Mo96(n,np)Nb95	6.4
	Mo96(n,d)Nb95	9.7
Mo99	Mo100(n,2n)Mo99	99.6
Sn117m	Sn117(n,n)Sn117m	5.1
	Sn118(n,2n)Sn117m	94.8
Sn119m	Sn119(n,n)Sn119m	6.1
	Sn120(n,2n)Sn119m	93.8
Sn123	Sn124(n,2n)Sn123	99.9
Ba131	Ba132(n,2n)Ba131m(IT)Ba131	59.2
	Ba132(n,2n)Ba131	39.6
Ba133m	Ba134(n,2n)Ba133m	100.0
Ba135m	Ba135(n,n)Ba135m	10.6
	Ba136(n,2n)Ba135m	89.3
Hf181	Ta181(n,p)Hf181	100.0
Ta180	Ta181(n,2n)Ta180	99.7
Ta182	Ta181(n,g)Ta182	59.3
	Ta181(n,g)Ta182m(IT)Ta182	38.9
	Ta181(n,g)Ta182n(IT)Ta182m(IT)Ta182	1.8

Product	Pathway(s)	%
Ta184	W184(n,p)Ta184	99.6
W181	W182(n,2n)W181	99.8
W185	W186(n,2n)W185 W186(n,2n)W185m(IT)W185	59.8 40.0
Re184	Re185(n,2n)Re184	100.0
Re184m	Re185(n,2n)Re184m	100.0
Re186	Re187(n,2n)Re186	99.7
Pb203	Pb204(n,2n)Pb203m(IT)Pb203 Pb204(n,2n)Pb203	51.7 47.1
Hg203	Pb206(n,a)Hg203 Pb207(n,na)Hg203	96.2 3.8

A.5 Jülich Nuclear Physics Group data

The various papers cited in section 3.5 provide effective cross-section data and experimental information. Elements with multiple isotopes isolated the nuclide with the dominant reaction and scaled by isotopic fraction. Note that the results from these experiments often contain total production cross-sections such as (n,Xt) and $^3\text{He}/^4\text{He}$ production ratios which are used to calculate (n,h) cross-sections. An approximate d-Be neutron spectrum was produced, as outlined in section 3.5, and effective cross-sections are computed from collapse with nuclear data.

A.6 National Physics Institute Řež data

Table 56: NPI Řež pathways for aluminium using spectrum rez_DF

Product	Pathway(s)	%
Na22	Al27(n,2na)Na22	37.7
	Al27(n,O)Na22	62.3
Na24	Al27(n,a)Na24	99.5

Table 57: NPI Řež pathways for titanium using spectrum rez_DF

Product	Pathway(s)	%
Sc46	Ti46(n,p)Sc46	41.6
	Ti46(n,p)Sc46m(IT)Sc46	17.8
	Ti47(n,np)Sc46	18.8
	Ti47(n,d)Sc46	2.3
	Ti47(n,np)Sc46m(IT)Sc46	4.2
	Ti48(n,O)Sc46	2.2
	Ti48(n,nd)Sc46	4.5
	Ti48(n,2np)Sc46	3.0
	Ti48(n,t)Sc46	1.8

Table 58: NPI Řež pathways for cobalt using spectrum rez_DF

Product	Pathway(s)	%
Mn56	Co59(n,a)Mn56	99.2
Fe59	Co59(n,p)Fe59	99.5
Co57	Co59(n,3n)Co57	91.9
	Co59(n,O)Co57	8.1
Co58	Co59(n,2n)Co58	65.5
	Co59(n,2n)Co58m(IT)Co58	33.9
Co58m	Co59(n,2n)Co58m	99.2

Table 59: NPI Řež pathways for zirconium using spectrum rez_DF

Product	Pathway(s)	%
Zr89	Zr90(n,2n)Zr89	79.8
	Zr90(n,2n)Zr89m(IT)Zr89	16.2
	Zr91(n,3n)Zr89	2.8

Table 60: NPI Řež pathways for yttrium using spectrum rez_DF

Product	Pathway(s)	%
Y87	Y89(n,O)Y87	6.0
	Y89(n,3n)Y87	60.5
	Y89(n,O)Y87m(IT)Y87	3.5
	Y89(n,3n)Y87m(IT)Y87	30.1
Y88	Y89(n,2n)Y88	99.4

Table 61: NPI Řež pathways for niobium using spectrum rez_DF

Product	Pathway(s)	%
Nb90	Nb93(n,O)Nb90	78.4
	Nb93(n,4n)Nb90	5.1
	Nb93(n,O)Nb90m(IT)Nb90	15.7
Nb91m	Nb93(n,O)Nb91m	4.3
	Nb93(n,3n)Nb91m	95.7
Nb92m	Nb93(n,2n)Nb92m	99.5

Table 62: NPI Řež pathways for rhenium using spectrum rez_DF

Product	Pathway(s)	%
Ru103	Rh103(n,p)Ru103	99.4
Rh100	Rh103(n,O)Rh100m(IT)Rh100	40.5
	Rh103(n,4n)Rh100m(IT)Rh100	25.3
	Rh103(n,O)Rh100	20.6
	Rh103(n,4n)Rh100	13.6

Product	Pathway(s)	%
Rh101m	Rh103(n,O)Rh101m	3.3
	Rh103(n,3n)Rh101m	96.7
Rh102	Rh103(n,2n)Rh102	99.8

Table 63: NPI Řež pathways for lutetium using spectrum rez_DF

Product	Pathway(s)	%
Lu172	Lu175(n,O)Lu172	13.1
	Lu175(n,4n)Lu172	61.5
	Lu175(n,O)Lu172m(IT)Lu172	3.8
	Lu175(n,4n)Lu172m(IT)Lu172	21.7
Lu173	Lu175(n,3n)Lu173	98.3
Lu174	Lu175(n,2n)Lu174	98.7

Table 64: NPI Řež pathways for gold using spectrum rez_DF

Product	Pathway(s)	%
Au194	Au197(n,O)Au194m(IT)Au194	13.7
	Au197(n,4n)Au194m(IT)Au194	54.9
	Au197(n,O)Au194	3.3
	Au197(n,4n)Au194	15.6
	Au197(n,O)Au194n(IT)Au194	3.5
	Au197(n,4n)Au194n(IT)Au194	9.0
Au195	Au197(n,3n)Au195m(IT)Au195	75.6
	Au197(n,3n)Au195	23.3
Au196	Au197(n,2n)Au196m(IT)Au196	63.8
	Au197(n,2n)Au196	33.5
	Au197(n,2n)Au196n(IT)Au196m(IT)Au196	2.5
Au196n	Au197(n,2n)Au196n	99.5

Table 65: NPI Řež pathways for bismuth using spectrum rez_DF

Product	Pathway(s)	%
Bi206	Bi209(n,4n)Bi206	79.3
	Bi209(n,O)Bi206	20.7

Product	Pathway(s)	%
Bi207	Bi209(n,3n)Bi207	98.8

Table 66: NPI Řež pathways for Eurofer-97 using spectrum rez_DF

Product	Pathway(s)	%
Na24	Al27(n,a)Na24	79.4
	Si28(n,pa)Na24	17.6
	Si28(n,O)Na24	1.7
Sc46	Ti46(n,p)Sc46	8.5
	Ti46(n,p)Sc46m(IT)Sc46	3.7
	Ti47(n,np)Sc46	3.8
	V51(n,O)Sc46	4.7
	V51(n,2na)Sc46	2.7
Sc47	Ti48(n,np)Sc47	6.2
	V51(n,na)Sc47	87.0
	V51(n,O)Sc47	3.6
Sc48	Ti48(n,p)Sc48	3.5
	V51(n,a)Sc48	60.0
	Cr52(n,pa)Sc48	30.9
	Cr52(n,O)Sc48	4.9
V48	Cr50(n,nd)V48	15.0
	Cr50(n,2np)V48	53.7
	Cr50(n,t)V48	12.6
	Cr50(n,O)V48	18.2
Cr48	Cr50(n,3n)Cr48	74.4
	Cr50(n,O)Cr48	25.5
Cr51	Cr52(n,2n)Cr51	86.1
	Fe54(n,a)Cr51	11.2
Mn52	Fe54(n,O)Mn52	17.4
	Fe54(n,nd)Mn52	11.7
	Fe54(n,2np)Mn52	55.4
	Fe54(n,t)Mn52	14.7
Mn54	Mn55(n,2n)Mn54	6.3
	Fe54(n,p)Mn54	65.7
	Fe56(n,nd)Mn54	3.9
	Fe56(n,2np)Mn54	16.3
	Fe56(n,t)Mn54	3.4
	Fe56(n,O)Mn54	4.3
Mn56	Fe56(n,p)Mn56	96.8
	Fe57(n,np)Mn56	1.6

Product	Pathway(s)	%
Fe52	Fe54(n,O)Fe52	29.1
	Fe54(n,3n)Fe52	70.6
Fe59	Fe58(n,g)Fe59	71.2
	Co59(n,p)Fe59	26.2
Co56	Ni58(n,nd)Co56	11.3
	Ni58(n,2np)Co56	70.2
	Ni58(n,t)Co56	5.1
	Ni58(n,O)Co56	13.5
Co57	Co59(n,3n)Co57	3.3
	Ni58(n,np)Co57	90.5
	Ni58(n,d)Co57	4.4
Co58	Co59(n,2n)Co58	14.2
	Co59(n,2n)Co58m(IT)Co58	8.8
	Ni58(n,p)Co58	60.6
	Ni58(n,p)Co58m(IT)Co58	15.4
Ni57	Ni58(n,2n)Ni57	98.6
Hf180m	Ta181(n,O)Hf180m	2.9
	Ta181(n,np)Hf180m	32.0
	Ta181(n,d)Hf180m	15.4
	W183(n,a)Hf180m	12.5
	W184(n,O)Hf180m	1.8
	W184(n,na)Hf180m	34.7
Ta180	Ta181(n,2n)Ta180	98.9
Ta182	Ta181(n,g)Ta182	43.0
	Ta181(n,g)Ta182m(IT)Ta182	26.8
	W182(n,p)Ta182m(IT)Ta182	5.3
	W182(n,p)Ta182	5.2
	W183(n,np)Ta182m(IT)Ta182	4.1
	W183(n,np)Ta182	3.8
Ta183	W183(n,p)Ta183	27.2
	W184(n,np)Ta183	38.4
	W184(n,d)Ta183	17.9
	W184(n,O)Ta183	3.3
	W186(n,a)Hf183(b-)Ta183	10.0
	W186(n,nt)Ta183	2.0
W187	W186(n,g)W187	99.9

Table 67: NPI Řež pathways for tungsten using spectrum rez_DF

Product	Pathway(s)	%
Hf179n	W182(n,O)Hf179n	1.6

Product	Pathway(s)	%
	W182(n,a)Hf179n	72.6
	W183(n,na)Hf179n	18.0
	W184(n,O)Hf179n	1.7
	W184(n,2na)Hf179n	4.6
Hf180m	W183(n,a)Hf180m	25.3
	W184(n,O)Hf180m	3.7
	W184(n,na)Hf180m	70.3
Hf181	W184(n,a)Hf181	89.8
	W186(n,2na)Hf181	7.0
	W186(n,O)Hf181	2.0
Hf182m	W186(n,O)Hf182m	4.5
	W186(n,na)Hf182m	94.8
Hf183	W186(n,a)Hf183	98.3
Ta182	W182(n,p)Ta182m(IT)Ta182	18.2
	W182(n,p)Ta182	18.0
	W182(n,p)Ta182n(IT)Ta182m(IT)Ta182	4.3
	W183(n,np)Ta182m(IT)Ta182	14.1
	W183(n,d)Ta182m(IT)Ta182	3.9
	W183(n,np)Ta182	13.1
	W183(n,d)Ta182	4.0
	W183(n,np)Ta182n(IT)Ta182m(IT)Ta182	3.7
	W184(n,2np)Ta182m(IT)Ta182	2.2
	W184(n,t)Ta182m(IT)Ta182	2.8
	W184(n,2np)Ta182	1.9
	W184(n,t)Ta182	2.6
Ta183	W183(n,p)Ta183	28.6
	W184(n,np)Ta183	40.4
	W184(n,d)Ta183	18.8
	W184(n,O)Ta183	3.5
	W186(n,a)Hf183(b-)Ta183	5.4
	W186(n,nt)Ta183	2.1
Ta184	W184(n,p)Ta184	71.3
	W184(n,O)Ta184	1.8
	W186(n,nd)Ta184	5.2
	W186(n,2np)Ta184	7.1
	W186(n,t)Ta184	11.0
	W186(n,O)Ta184	3.5
Ta185	W186(n,np)Ta185	66.0
	W186(n,d)Ta185	27.6
	W186(n,O)Ta185	5.7
W181	W182(n,2n)W181	74.6
	W183(n,3n)W181	17.4
	W184(n,4n)W181	6.7
W185	W184(n,g)W185	4.4

Product	Pathway(s)	%
	W186(n,2n)W185	58.8
	W186(n,2n)W185m(IT)W185	35.8
W187	W186(n,g)W187	100.0

Table 68: NPI Řež pathways for tantalum using spectrum rez_DF

Product	Pathway(s)	%
Lu177m	Ta181(n,O)Lu177m	5.1
	Ta181(n,na)Lu177m	94.9
Lu177	Ta181(n,O)Lu177	2.7
	Ta181(n,na)Lu177	97.3
Hf179n	Ta181(n,2n)Ta180(b+)Hf180(n,O)Hf179n	72.8
	Ta181(n,3n)Ta179(n,p)Hf179n	10.9
	Ta181(n,np)Hf180(n,2n)Hf179n	2.9
	Ta181(n,d)Hf180(n,2n)Hf179n	1.7
	Ta181(n,np)Hf180m(n,2n)Hf179n	2.4
	Ta181(n,p)Hf181(n,3n)Hf179n	3.0
Hf180m	Ta181(n,O)Hf180m	5.7
	Ta181(n,np)Hf180m	63.6
	Ta181(n,d)Hf180m	30.5
Hf181	Ta181(n,p)Hf181	98.0
	Ta181(n,O)Hf181	2.0
Ta178m	Ta181(n,O)Ta178m	11.0
	Ta181(n,4n)Ta178m	88.8
Ta180	Ta181(n,2n)Ta180	99.6
Ta182	Ta181(n,g)Ta182	61.3
	Ta181(n,g)Ta182m(IT)Ta182	38.3

Table 69: NPI Řež pathways for chromium (long irradiation) using spectrum rez_DF

Product	Pathway(s)	%
Sc46	Cr50(n,O)Sc46	6.8
	Cr50(n,pa)Sc46	80.2
	Cr50(n,pa)Sc46m(IT)Sc46	11.9
Sc48	Cr52(n,pa)Sc48	86.2
	Cr52(n,O)Sc48	13.8
V48	Cr50(n,nd)V48	15.1

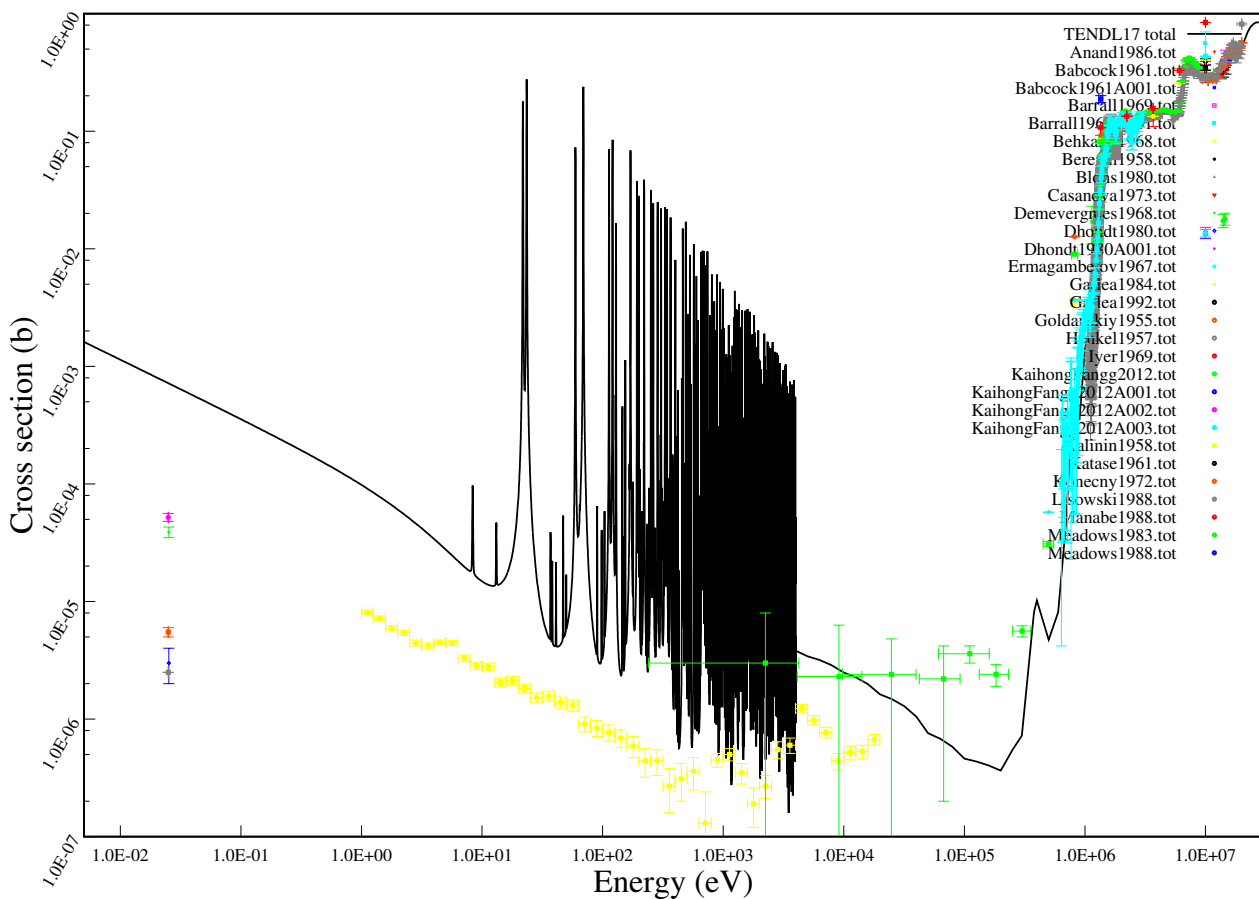
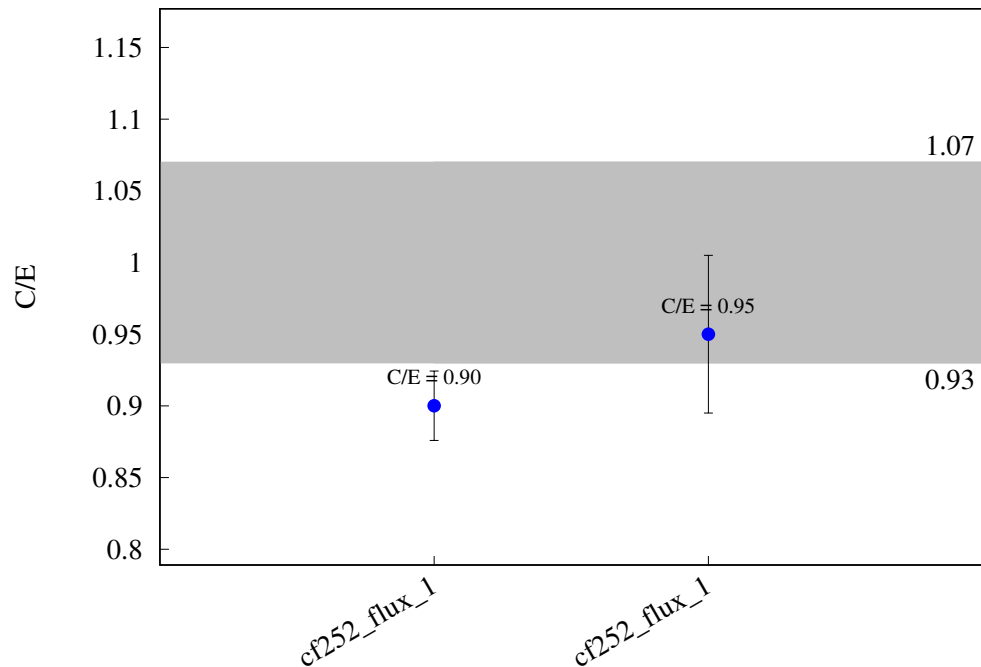
Product	Pathway(s)	%
	Cr50(n,2np)V48	54.0
	Cr50(n,t)V48	12.7
	Cr50(n,O)V48	18.3
Cr48	Cr50(n,3n)Cr48	74.5
	Cr50(n,O)Cr48	25.5
Cr49	Cr50(n,2n)Cr49	98.2
	Cr50(n,O)Cr49	1.8
Cr51	Cr52(n,2n)Cr51	97.5

Table 70: NPI Řež pathways for chromium (short irradiation)
using spectrum rez_DF

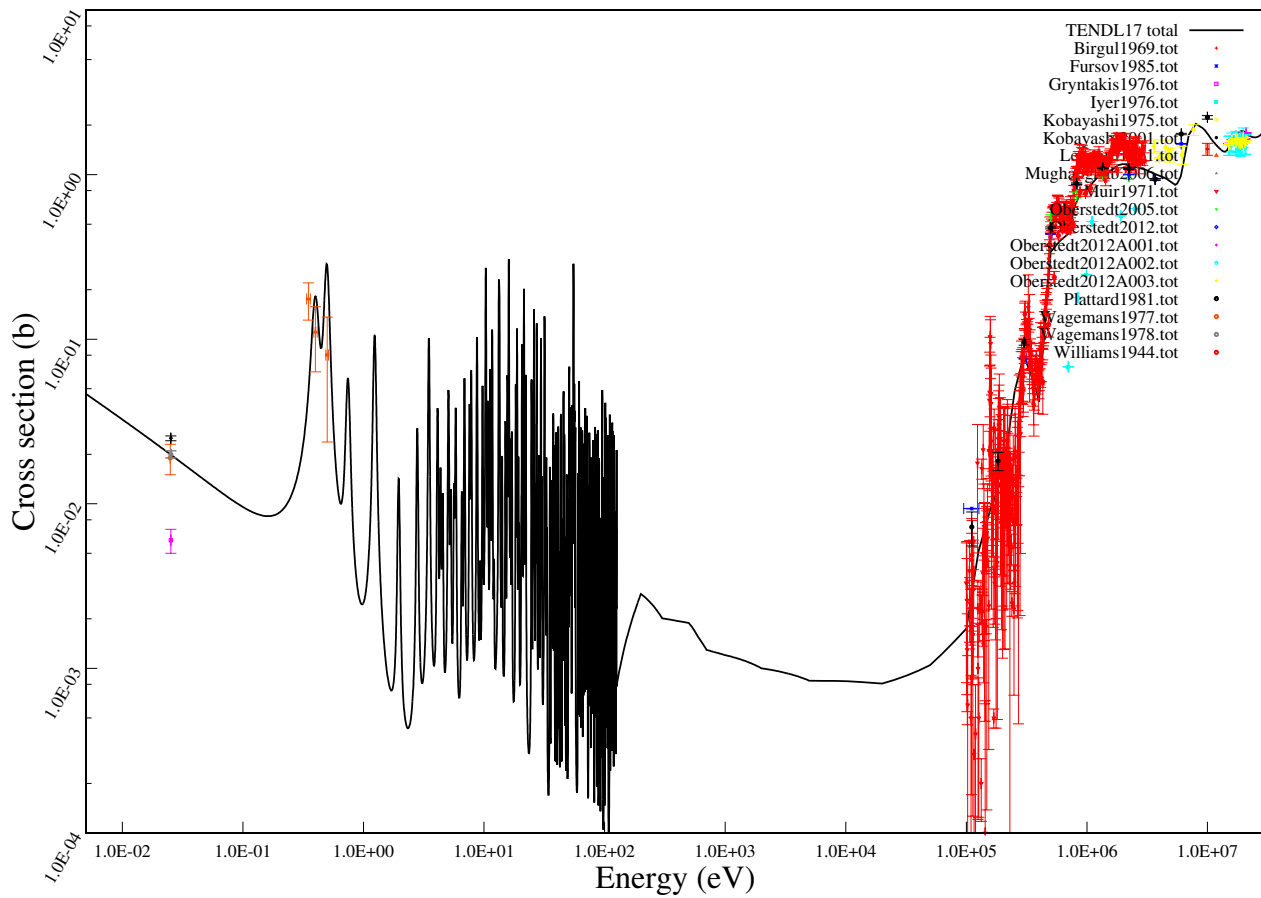
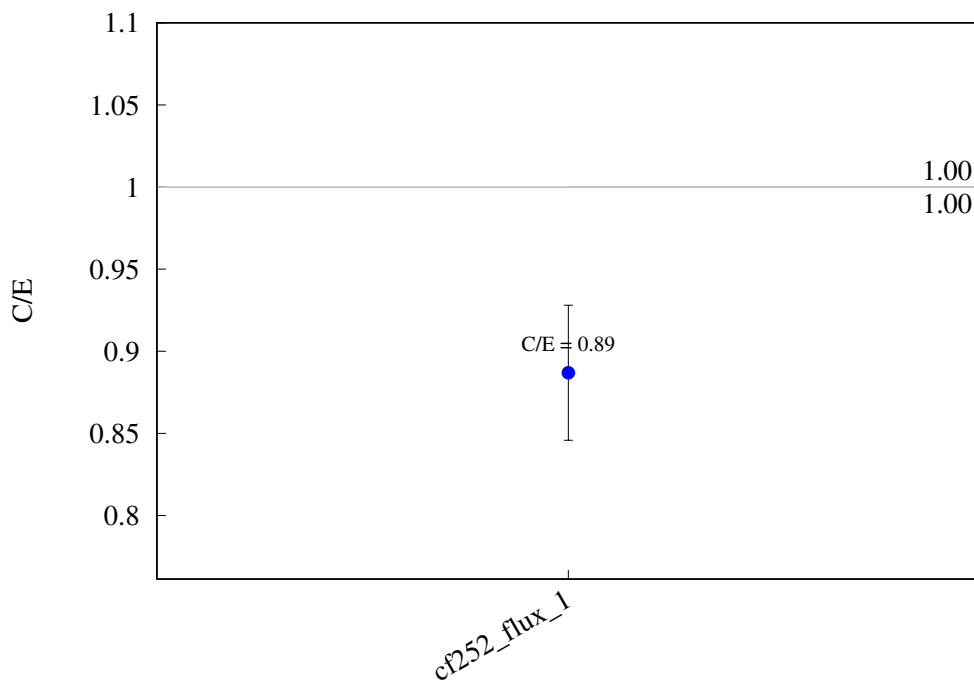
Product	Pathway(s)	%
Sc48	Cr52(n,pa)Sc48	86.2
	Cr52(n,O)Sc48	13.8
Ti51	Cr52(n,2p)Ti51	54.1
	Cr52(n,O)Ti51	2.8
	Cr53(n,h)Ti51	6.7
	Cr54(n,a)Ti51	35.0
V52	Cr52(n,p)V52	88.1
	Cr53(n,np)V52	9.9
V53	Cr53(n,p)V53	76.3
	Cr54(n,np)V53	18.8
	Cr54(n,d)V53	4.4
Cr48	Cr50(n,3n)Cr48	74.5
	Cr50(n,O)Cr48	25.5
Cr49	Cr50(n,2n)Cr49	98.2
	Cr50(n,O)Cr49	1.8
Cr51	Cr52(n,2n)Cr51	97.5

B Actinide data

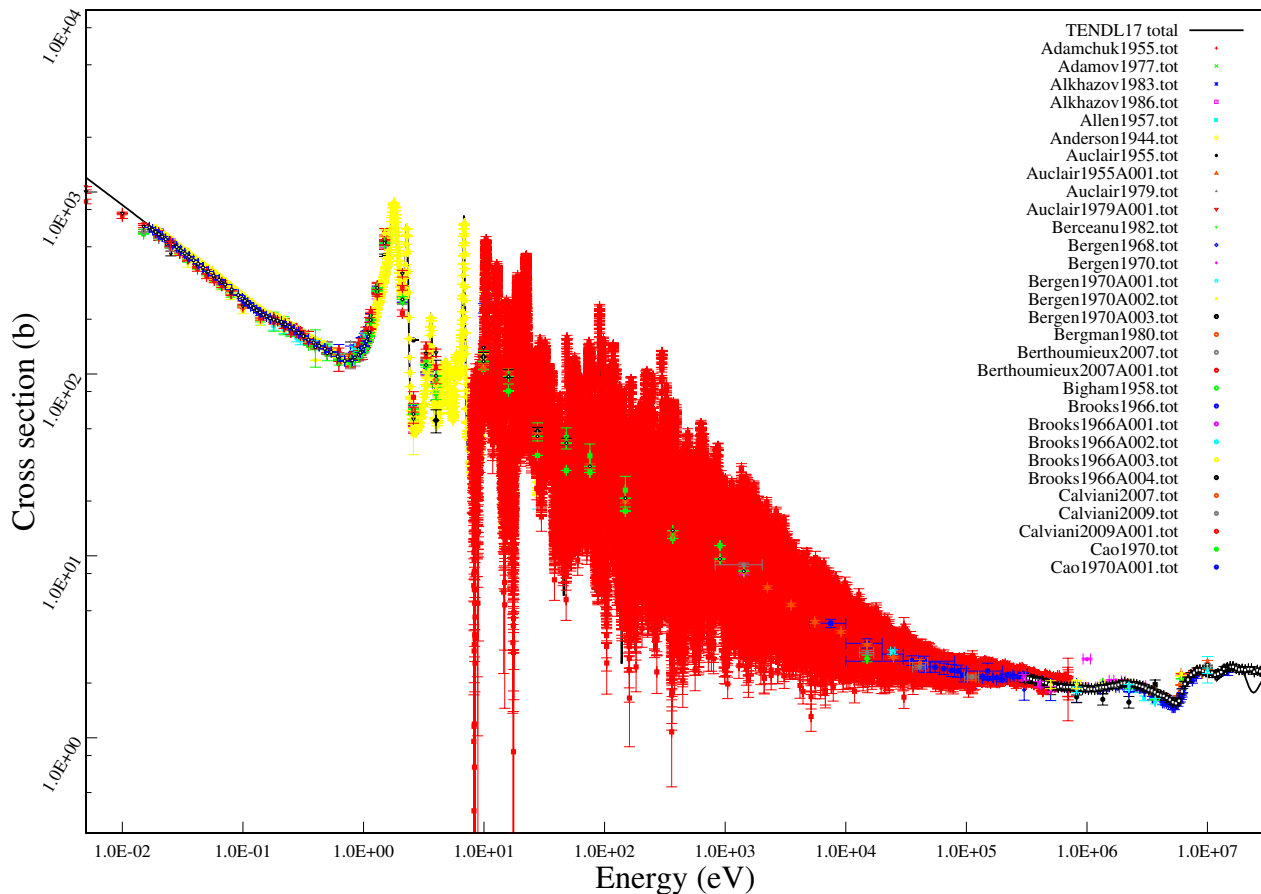
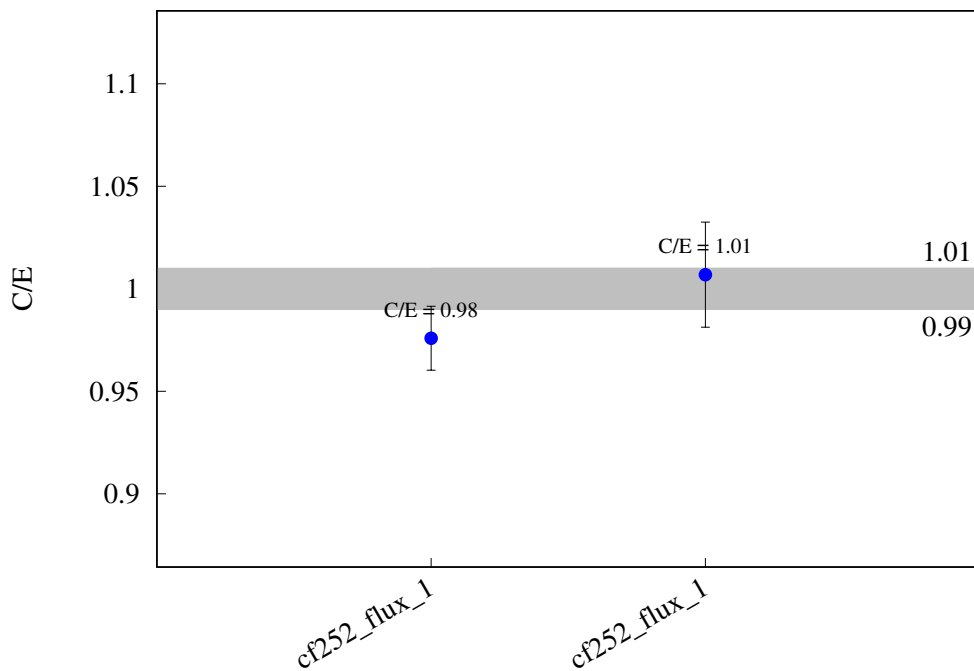
^{232}Th (n,f)



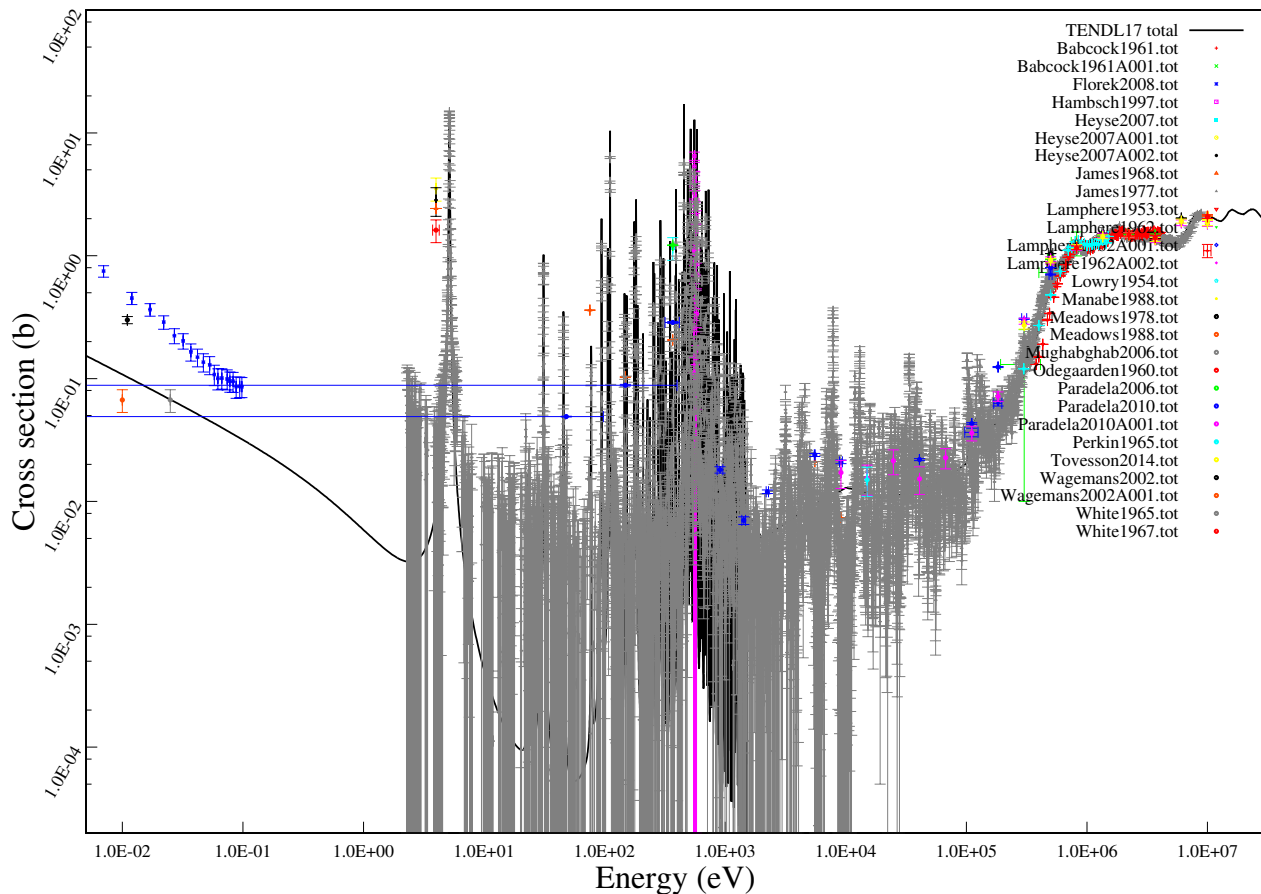
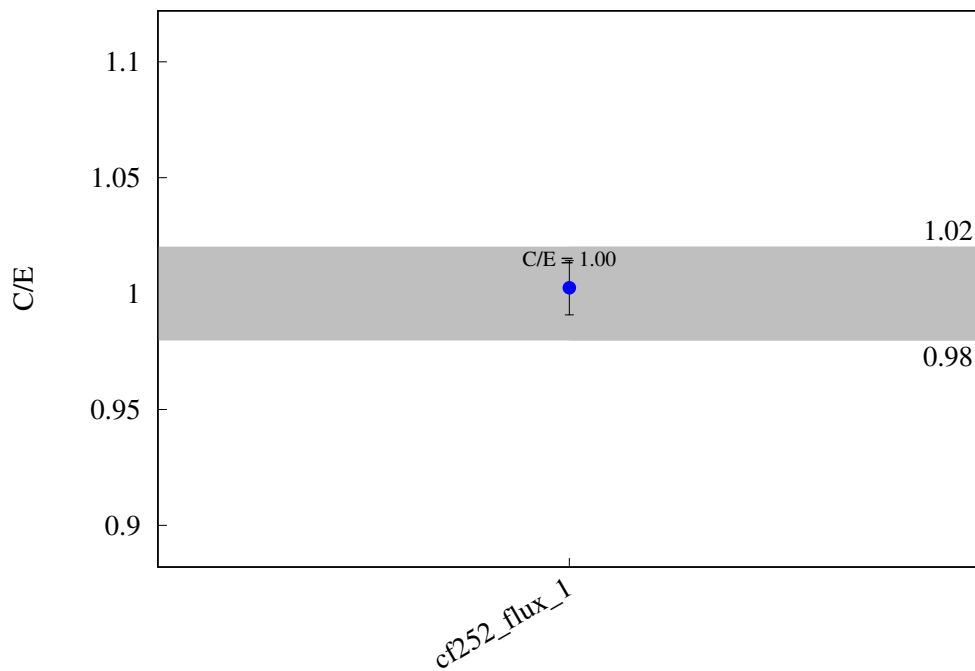
^{231}Pa (n,f)



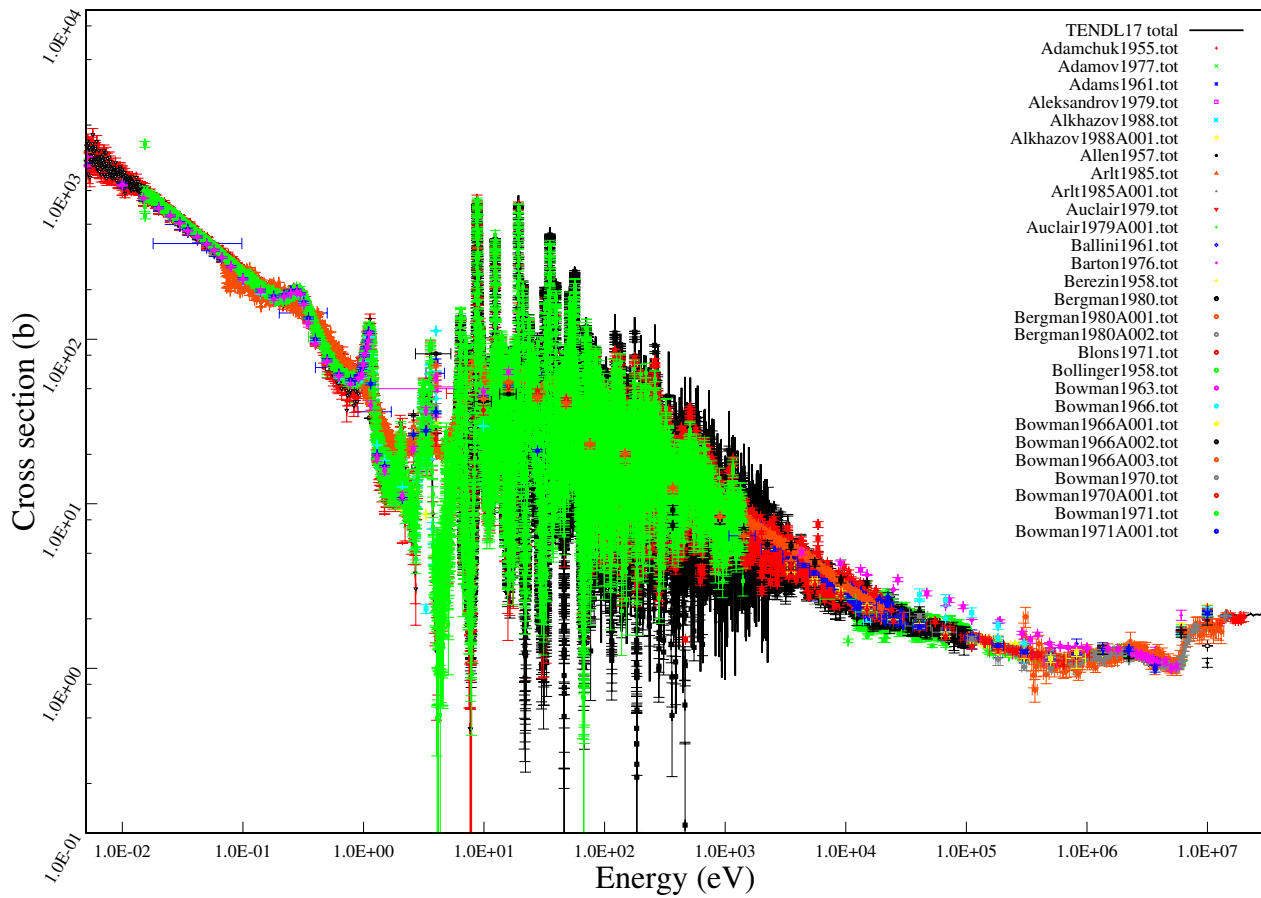
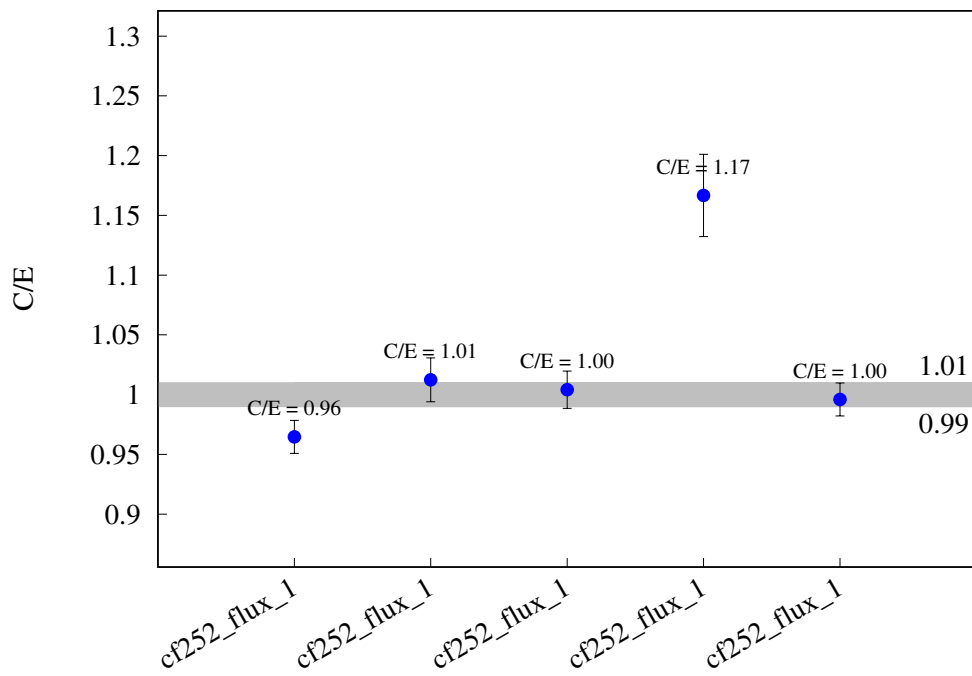
^{233}U (n,f)



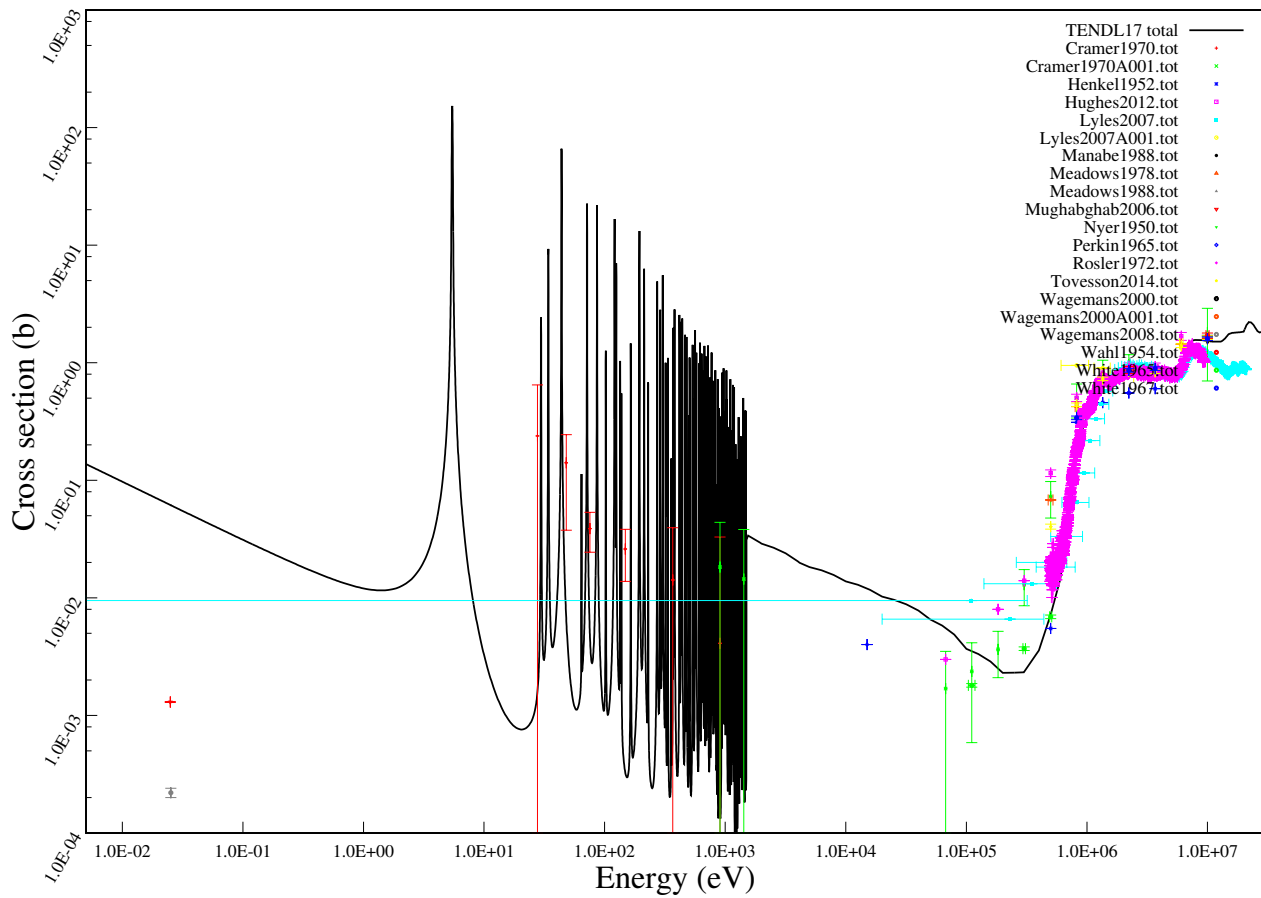
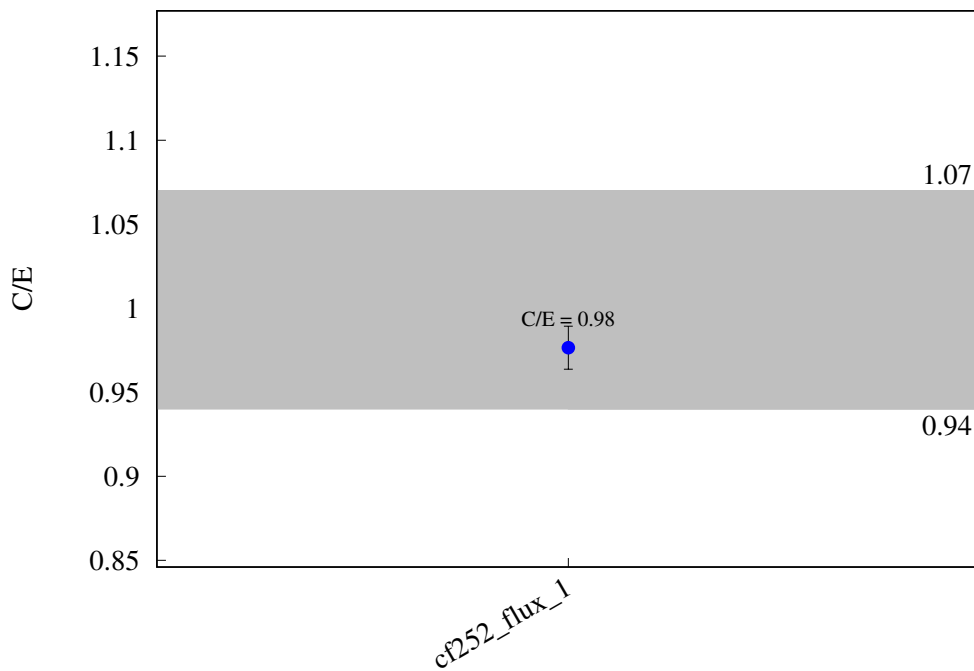
^{234}U (n,f)



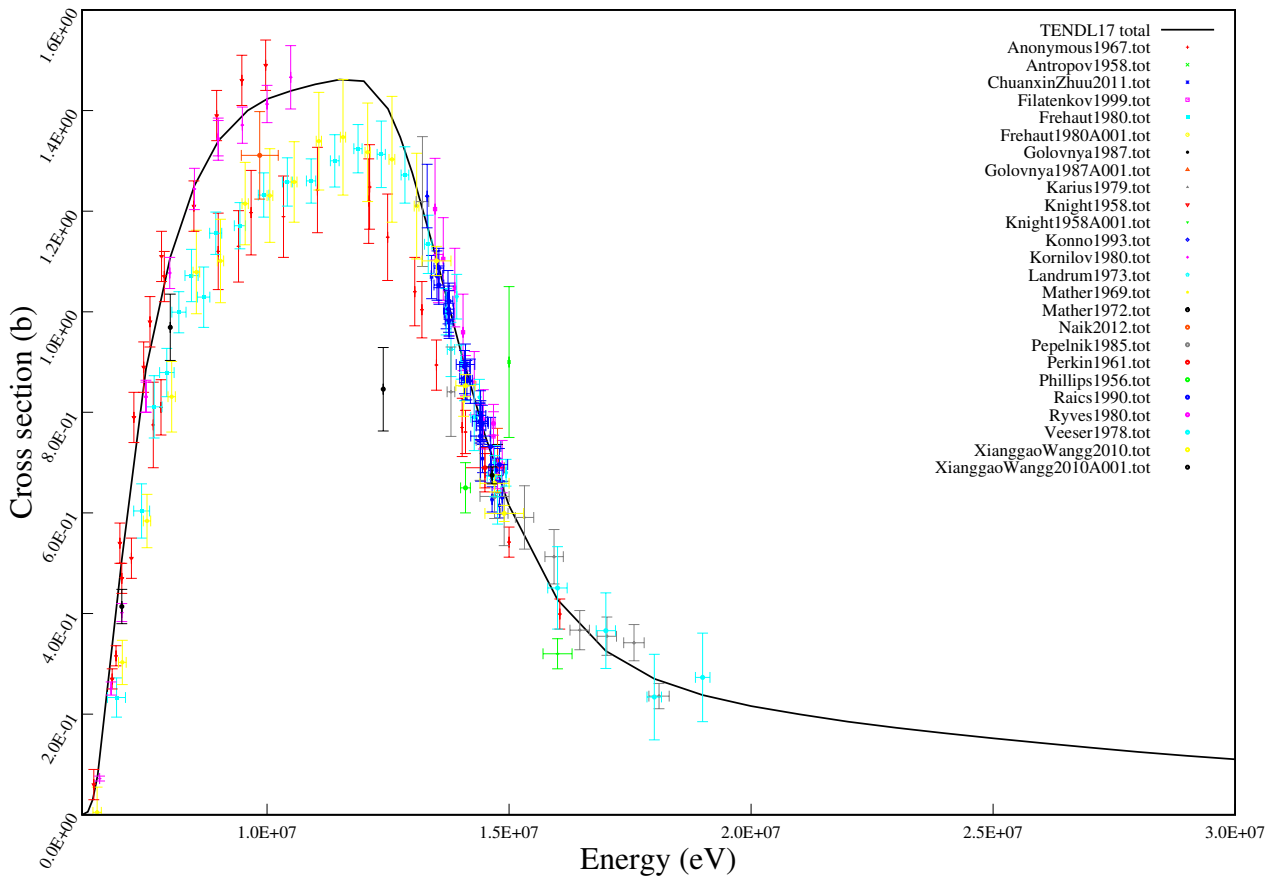
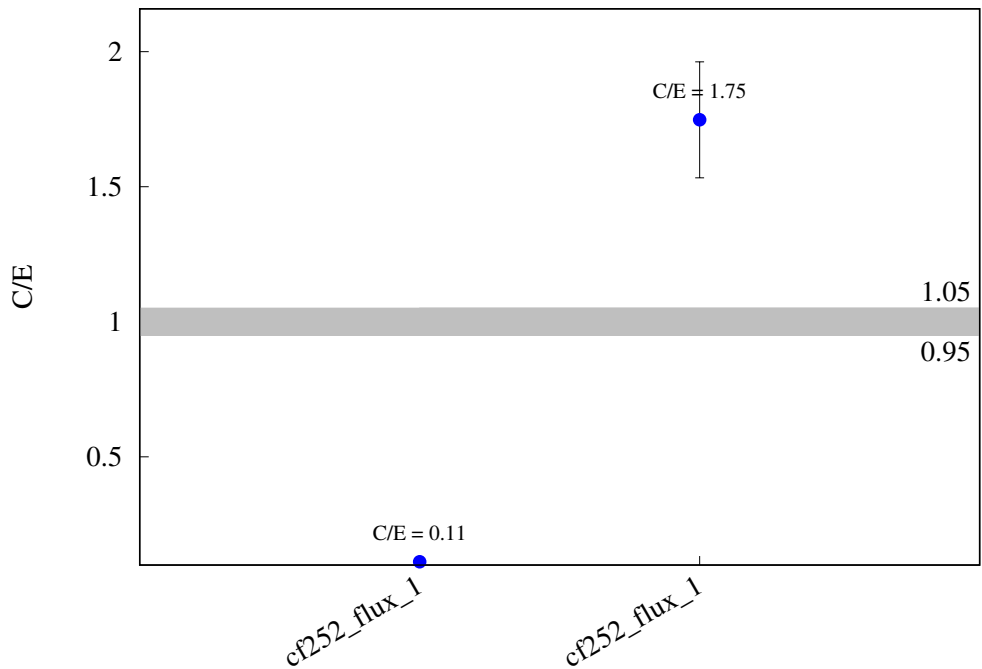
^{235}U (n,f)



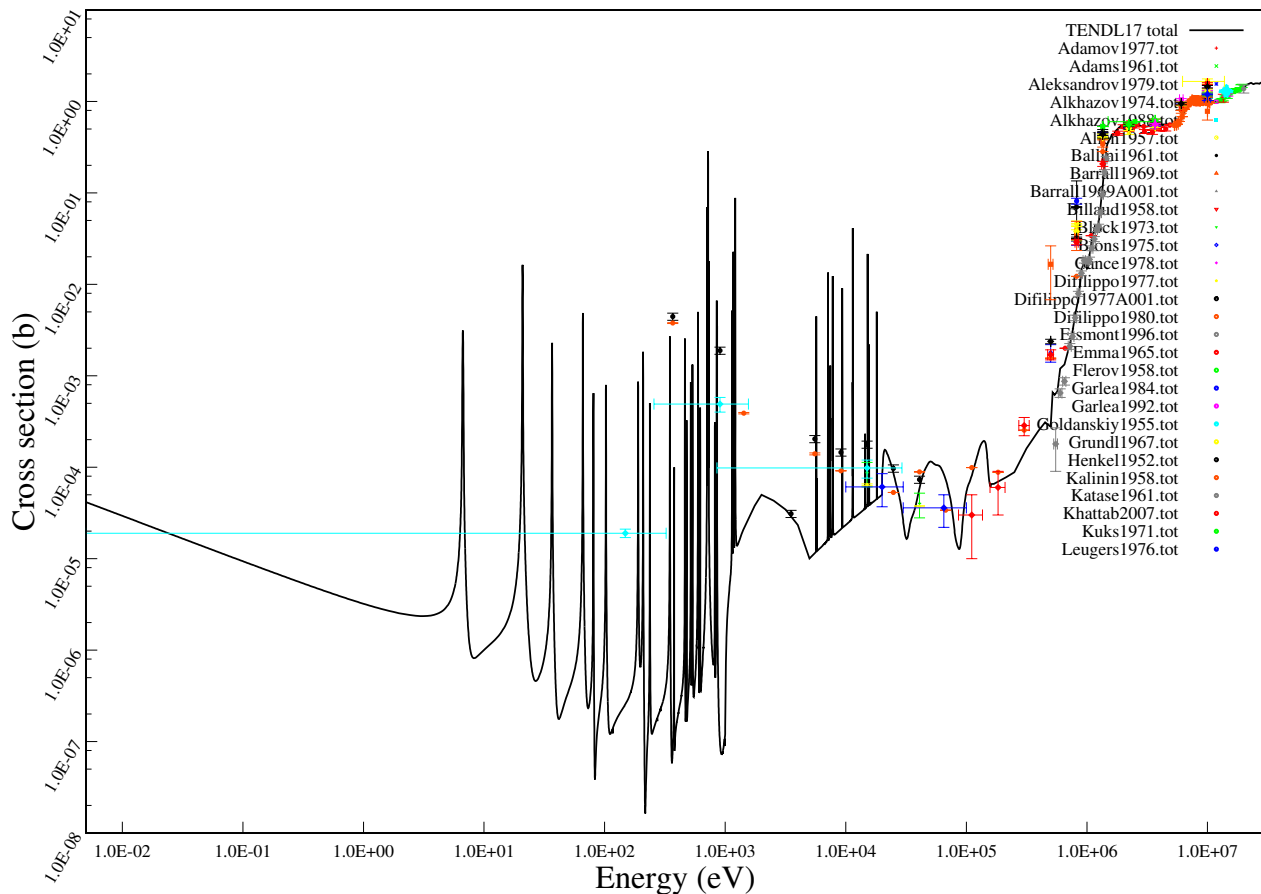
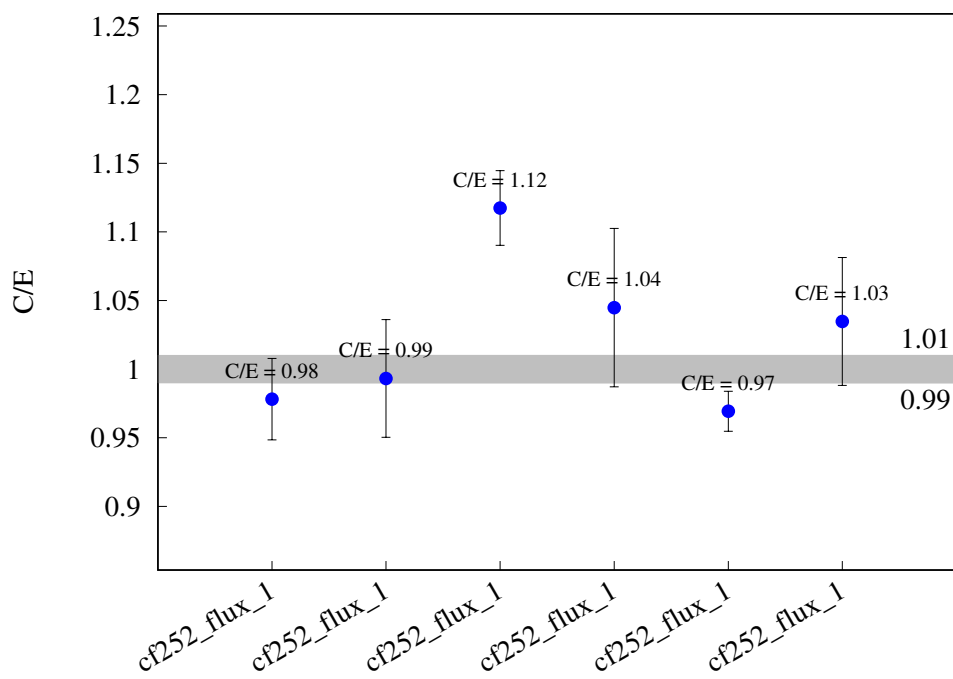
^{236}U (n,f)



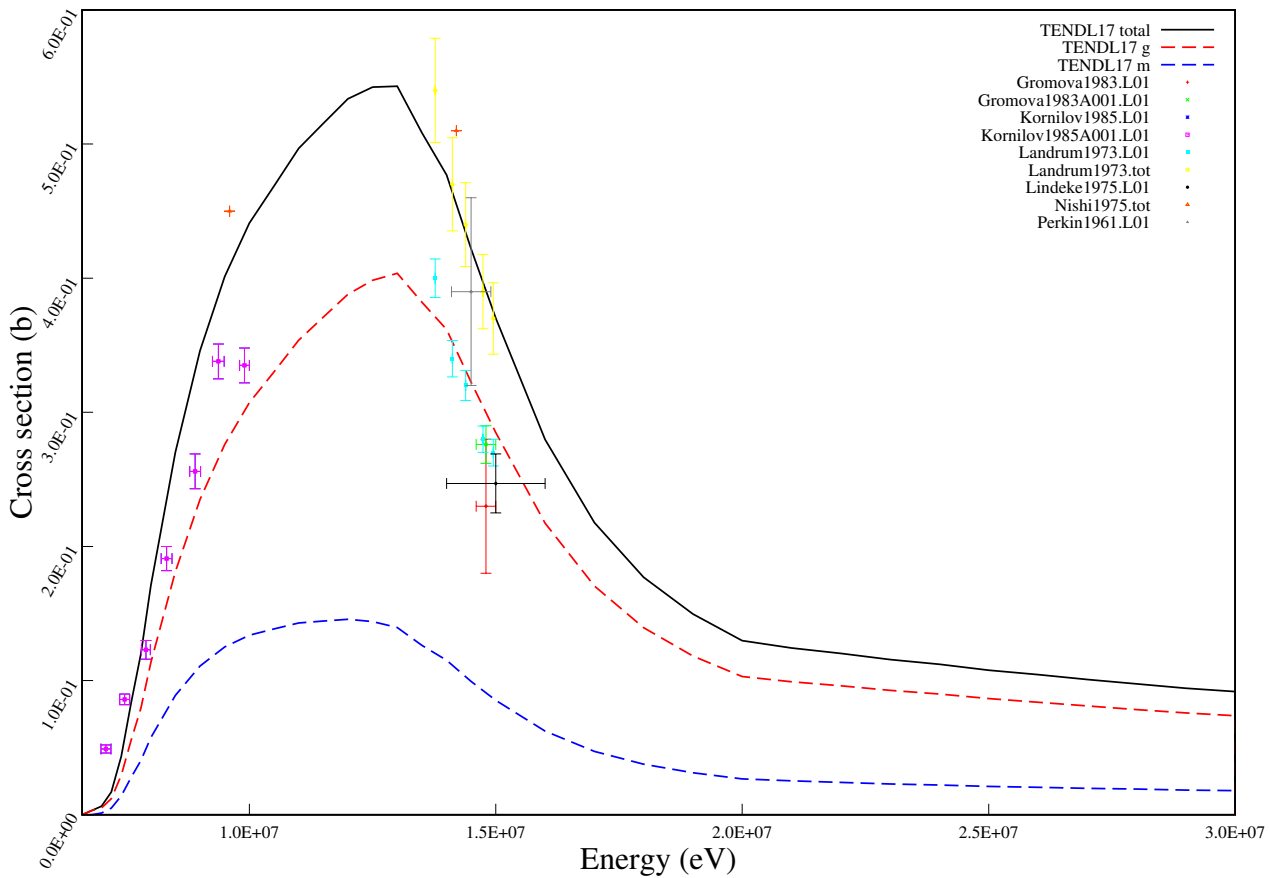
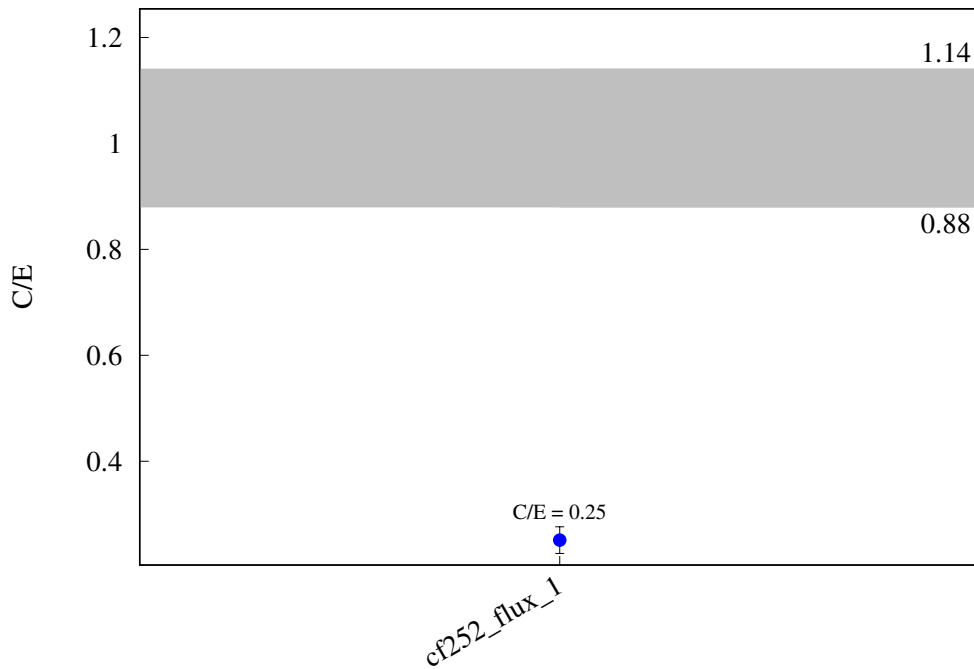
^{238}U (n,2n) ^{237}U



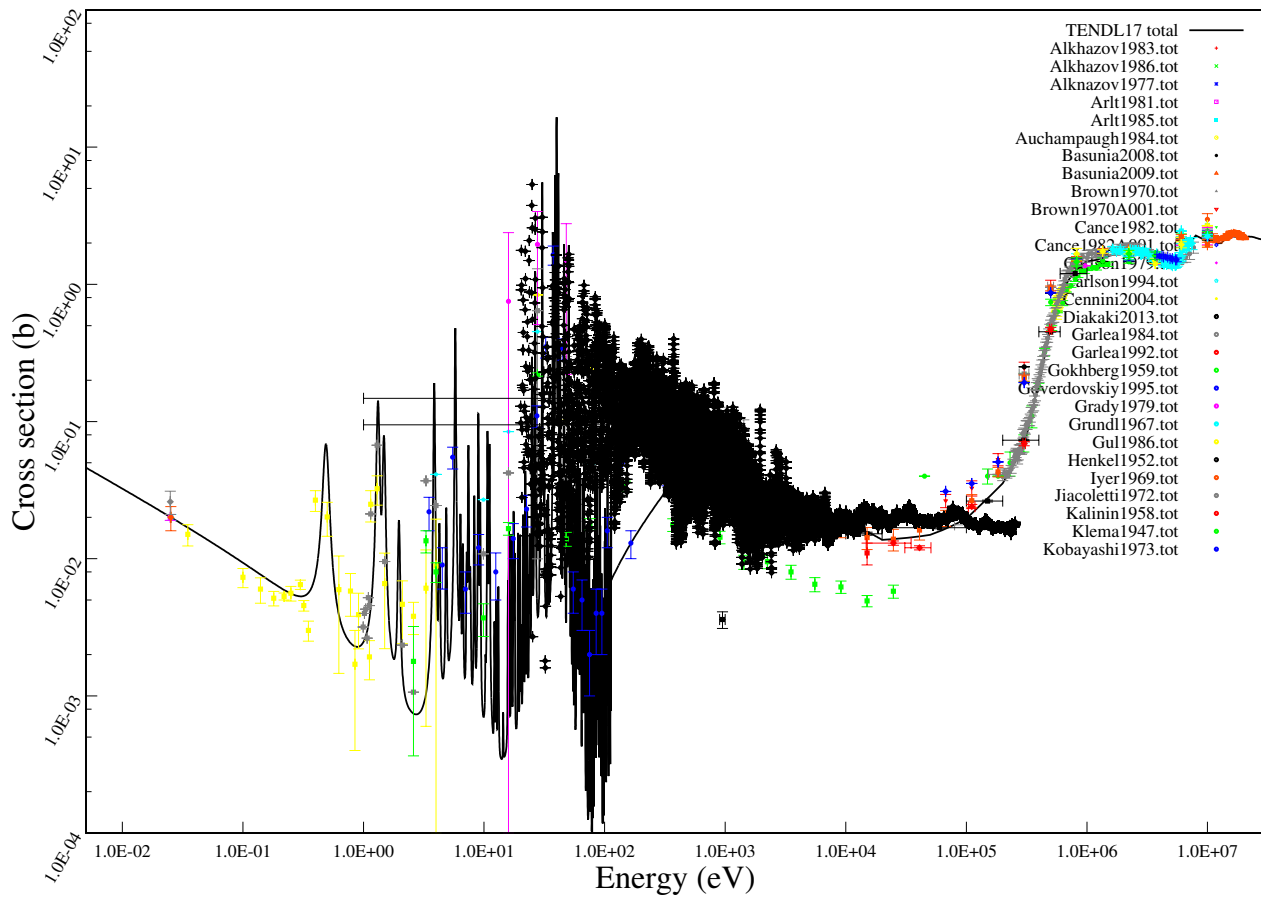
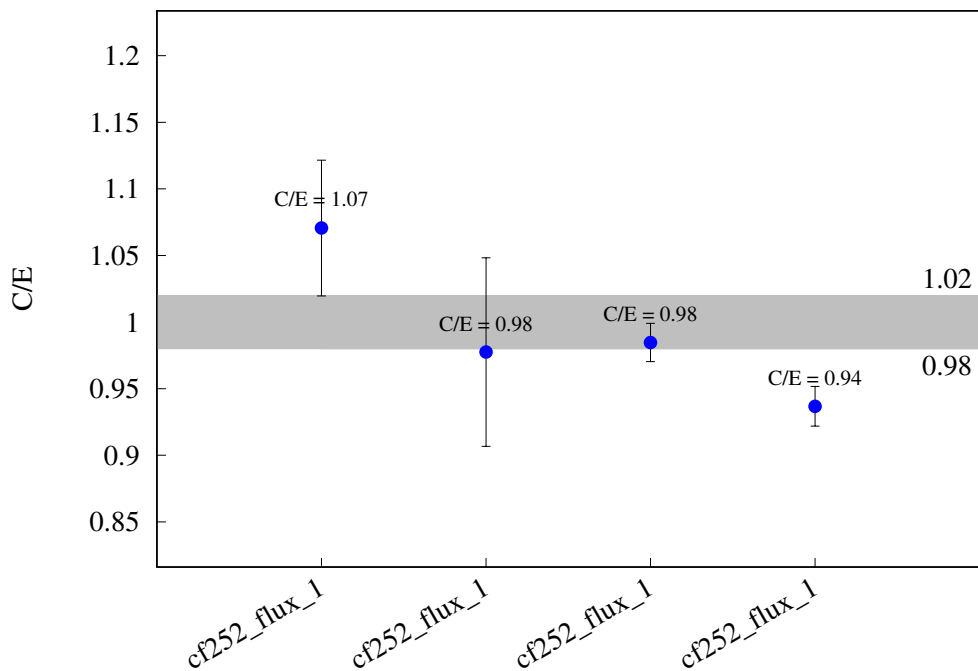
^{238}U (n,f)



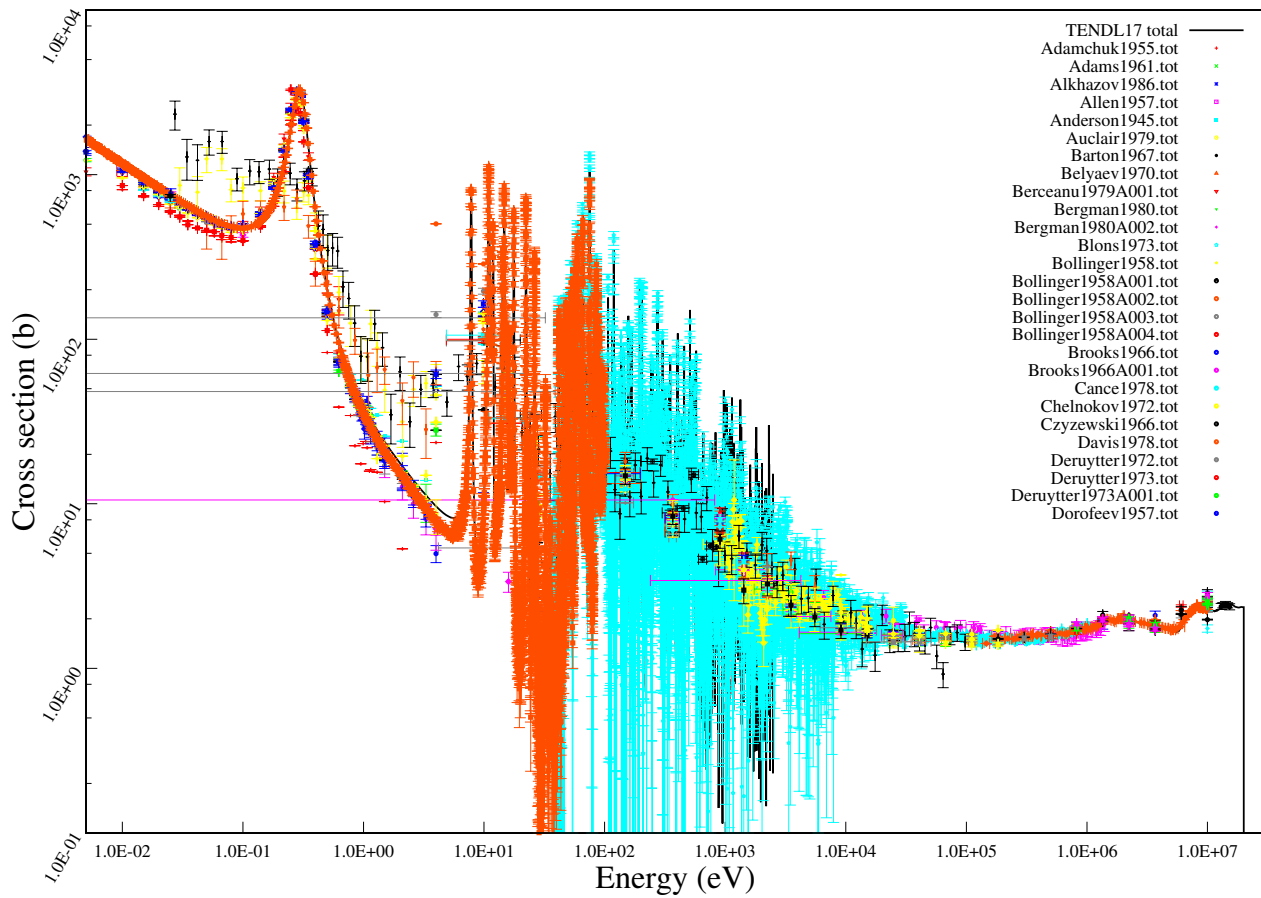
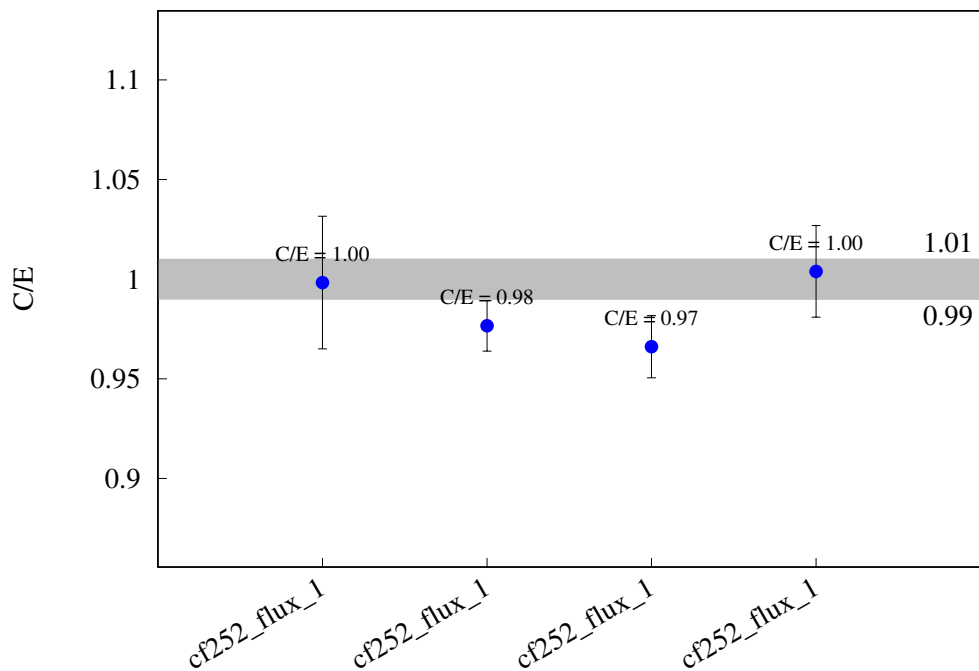
^{237}Np (n,2n) ^{236m}Np



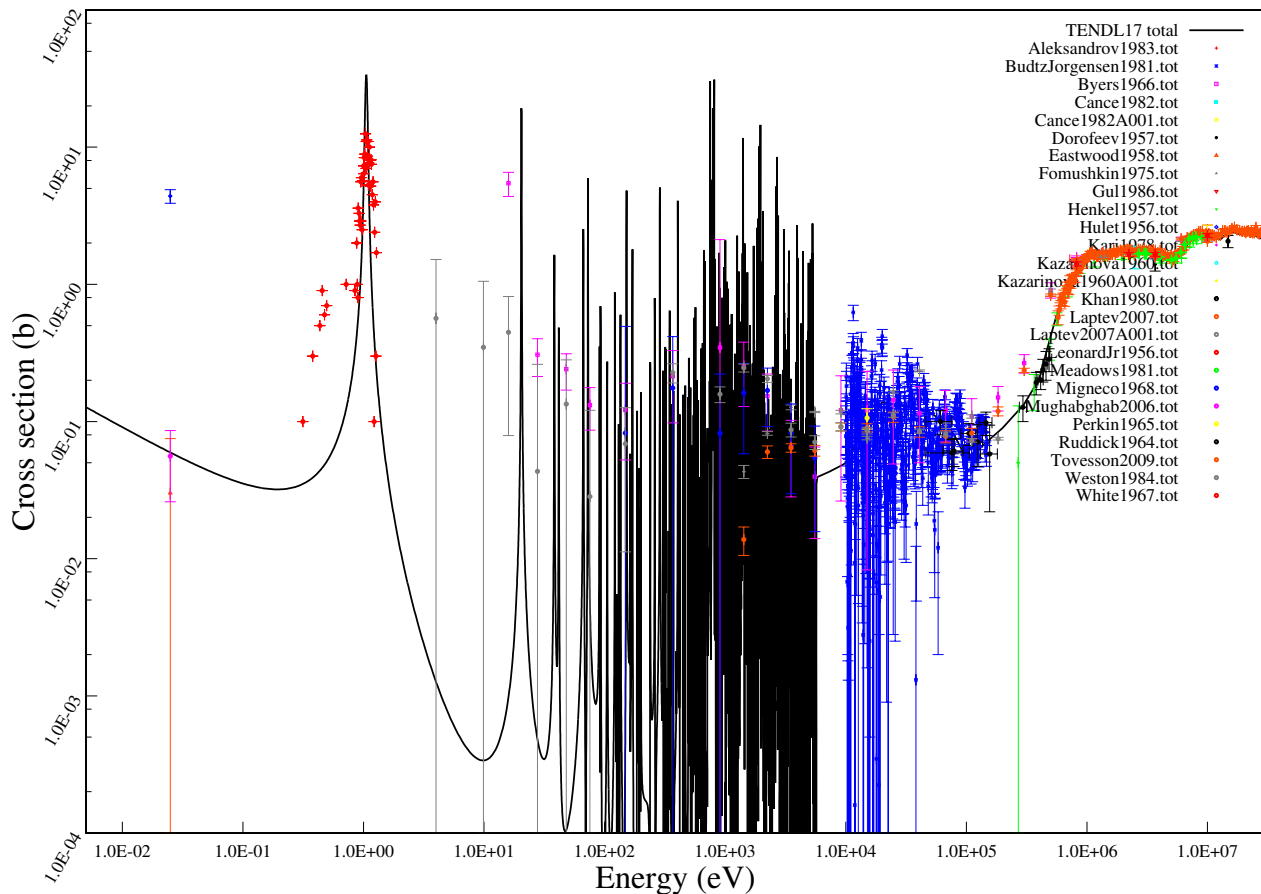
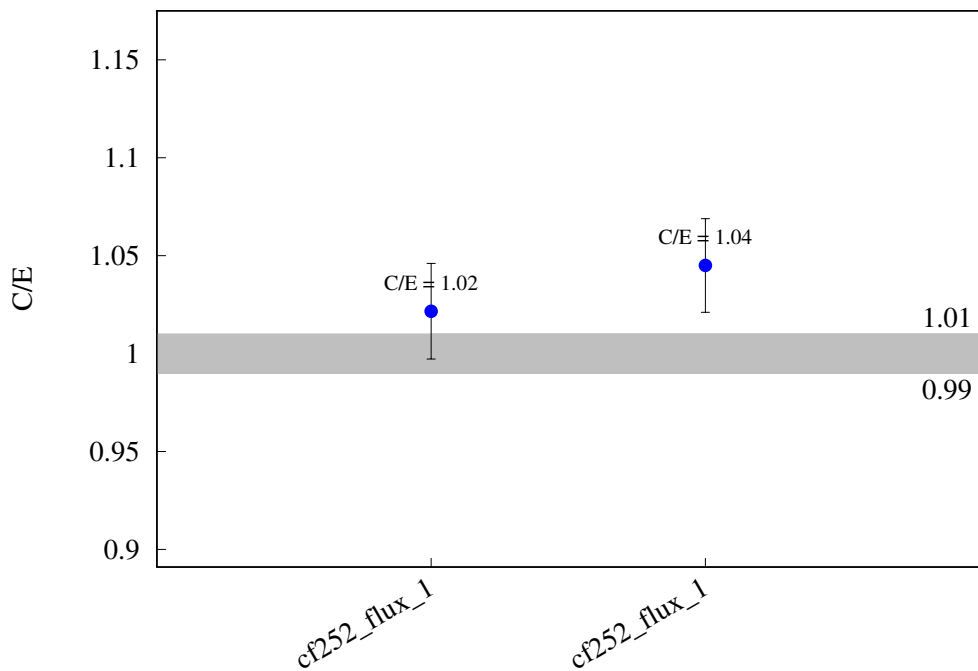
^{237}Np (n,f)



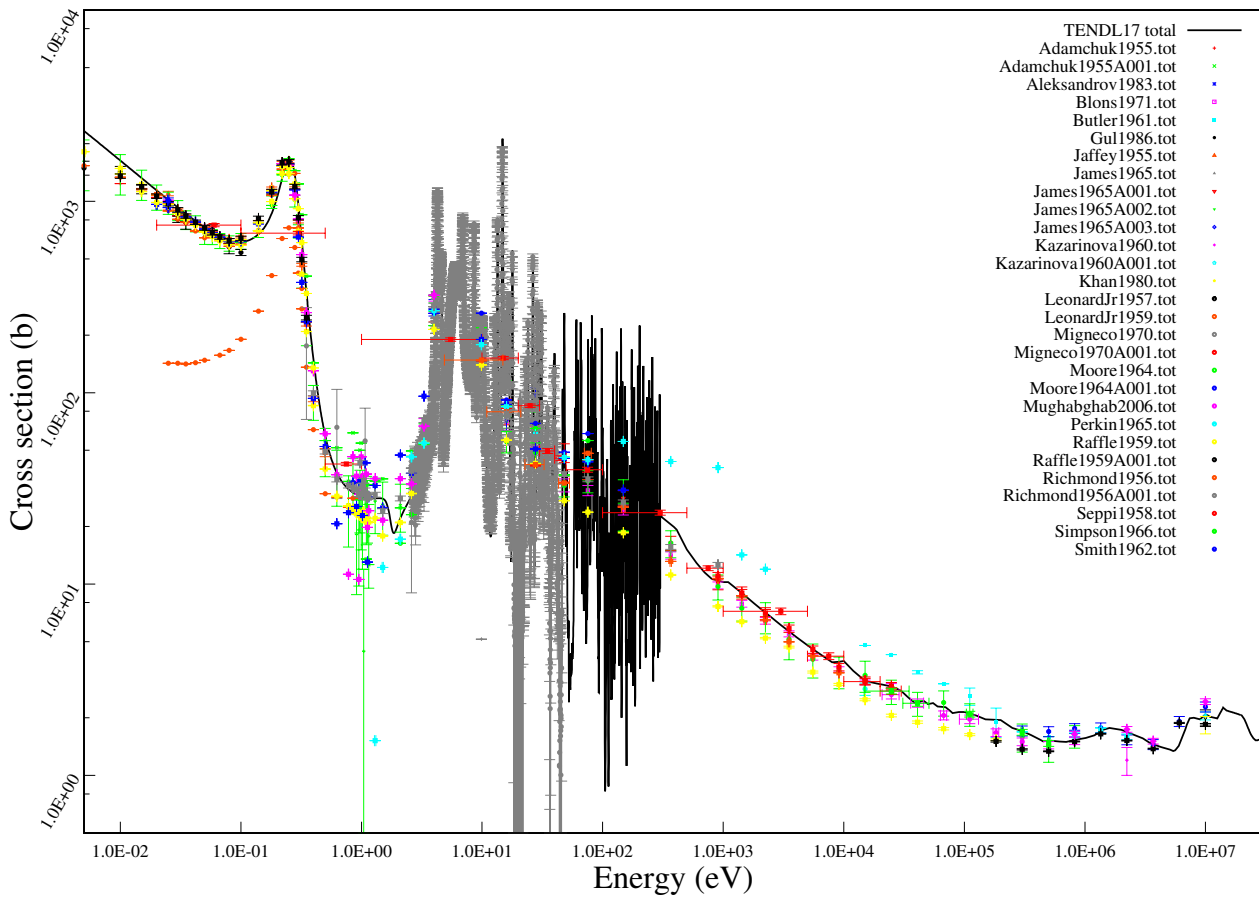
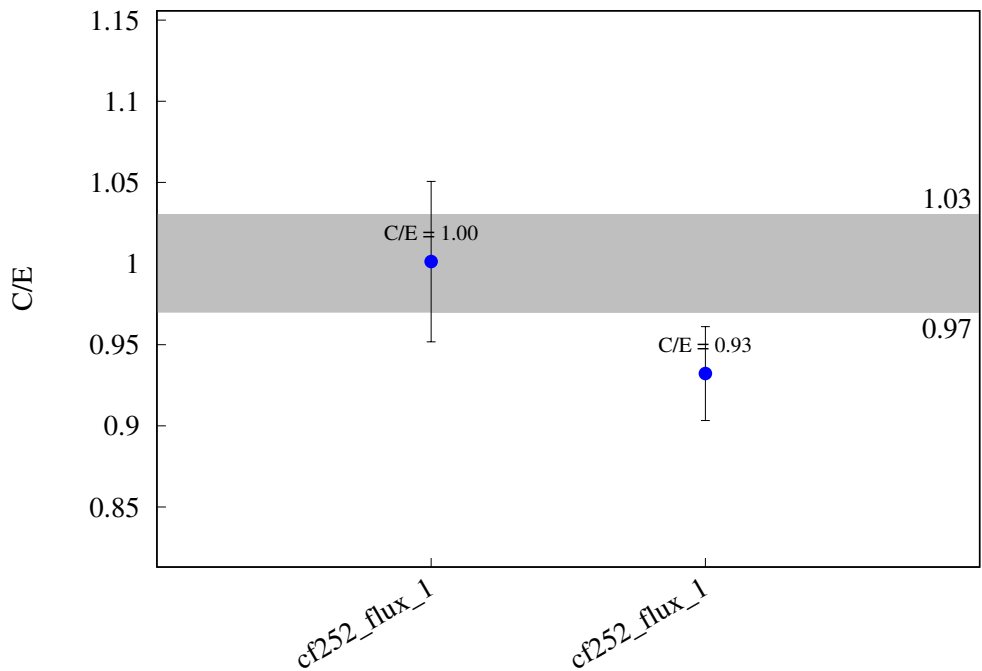
^{239}Pu (n,f)



^{240}Pu (n,f)



^{241}Pu (n,f)



^{243}Am (n,f)

